



GEOLOGICAL FIELDWORK 2006

A Summary of Field Activities and Current Research



Report 2007-1

**Ministry of Energy, Mines
and Petroleum Resources**
British Columbia Geological Survey

Paper 2007-1

Ministry of Energy, Mines and Petroleum Resources Mining and Minerals Division British Columbia Geological Survey

Parts of this publication may be quoted or reproduced if source and authorship is acknowledged.
The following is the recommended format for referencing individual works contained in this publication:

Alldrick, D.J., MacIntyre, D.G. and Villeneuve, M.E. (2007): Geology, Mineral Deposits and Exploration Potential of the Skeena Group, Central BC; in Geological Fieldwork 2006, *British Columbia Ministry of Energy, Mines and Petroleum Resources*, Paper 2007-1 and *Geoscience BC*, Report 2007-1, pp 1-18.

This publication is also available, free of charge, as colour digital files, in Adobe Acrobat PDF format, from the BC Ministry of Energy, Mines and Petroleum Resources internet website at:

http://www.em.gov.bc.ca/Mining/Geosurv/Publications/catalog/cat_fldwk.htm

COVER PHOTO: *Photo of Chilcotin basalts with well-developed columnar jointing, near Quesnel, which are typical of the plateau basalts in central British Columbia. These basalts are the focus of much recent geoscience research as geoscientists attempt to better understand their character, distribution and thickness, particularly in the interior plateau region most affected by the Mountain Pine Beetle epidemic.*

British Columbia Cataloguing in Publication Data

Main entry under title:

Geological Fieldwork: - 1974 -

Annual.

Issuing body varies

Vols. For 1978-1996 issued in series: Paper / British Columbia. Ministry of Energy, Mines and Petroleum Resources; vols for 1997- 1998, Paper / British Columbia. Ministry of Employment and Investment; vols for 1999- , Paper / British Columbia Ministry of Energy and Mines; vols for 2006- , Paper / British Columbia Ministry of Energy, Mines and Petroleum Resources.

Includes Bibliographical references.

ISSN 0381-243X=Geological Fieldwork

1. Geology - British Columbia - Periodicals. 2. Mines and mineral resources - British Columbia - Periodicals. 3. Geology - Fieldwork - Periodicals. 4. Geology, Economic - British Columbia - Periodicals. 5. British Columbia. Geological Survey Branch - Periodicals. I. British Columbia. Geological Division. II. British Columbia. Geological Survey Branch. III. British Columbia. Geological Survey Branch. IV. British Columbia. Dept. of Mines and Petroleum Resources. V. British Columbia. Ministry of Energy, Mines and Petroleum Resources. VI. British Columbia. Ministry of Employment and Investment. VII. British Columbia Ministry of Energy and Mines. VIII. Series: Paper (British Columbia. Ministry of Energy, Mines and Petroleum Resources). IX. Series: Paper (British Columbia. Ministry of Employment and Investment). X. Series: Paper (British Columbia Ministry of Energy and Mines). XI. Series: Paper (British Columbia Ministry of Energy, Mines and Petroleum Resources).

VICTORIA
BRITISH COLUMBIA
CANADA

JANUARY 2007

FOREWORD

Geological Fieldwork 2006

The **British Columbia Geological Survey** (BCGS) presents the results of 2006 geoscience surveys and studies in this thirty-second edition of *Geological Fieldwork*. Most of the articles within the first half of this volume are contributions from Survey staff who have worked extensively throughout the province on geology, geochemistry and mineral deposits. In previous years the results of similar field surveys and the provision of geoscience data has led to claim staking and increased mineral exploration expenditures. These are the first steps towards the development of new mines which benefit British Columbians, particularly those living in regional communities.

The second part of this volume consists of articles provided by **Geoscience BC**, an industry-focused, not-for-profit society that works with industry, academia, government, First Nations and communities to attract mineral and oil and gas investment to British Columbia. These articles span a wide spectrum from geochemical and geophysical surveys and mineral deposit studies to new exploration tools. For details of the Geoscience BC program, see their program review and project reports in this volume.

BC Geological Survey Successes

- British Columbia Geological Survey geological database was ranked number one globally by the Fraser Institute Survey.
- Staff are key contributors to the volume titled “*Paleozoic Evolution and Metallogeny of Pericratonic Terranes at the Ancient Pacific Margin of North America*” published by the Geological Association of Canada, Special Paper 45.
- Over 95% of industry assessment reports have been published to the Survey website to improve access to this critical exploration database. This is part of an ongoing responsibility to act as the custodian for the province’s mineral and coal geoscience data.
- Rift model published pointing out key locations for exploration for Eskay Creek-type Au-Ag deposits.
- MapPlace continues to be used by the exploration community from around the world and to attract exploration investment to the province with more than 6 million visits during 2006.
- Systematic geology and geophysical surveys completed for the Toodoggone mining camp with new insights into the metallogeny of the porphyry and epithermal deposits.
- An evaluation of the Quaternary volcanic cover rocks in the Interior Plateau suggests that they are thinner and less extensive than previously thought, which opens up new exploration potential.
- Survey staff, including those based in Vancouver and Ministry regional offices, contributed their expertise to assist in government decisions, respond to client inquiries in confidence and report on industry activity in the province.
- Survey staff continue to train and mentor geology students as they prepare for their careers.

2006 Field Surveys and Publications

Articles in this volume include reports on British Columbia Geological Survey programs in the Smithers-Hazelton, Canim Lake, Rock Creek, northeast coalfield, northern Vancouver Island and Terrace areas. The Survey has recognized the impact of the Mountain Pine Beetle infestation in the central interior of the province and initiated a new survey to complement existing projects in this area to attract mineral exploration. Despite excellent mineral potential, the central interior has been under-explored due to widespread glacial till and young, volcanic cover rocks. Geoscience could provide one option to help alleviate the economic downturn in forestry by attracting mineral exploration and possibly mine development. Studies continued at the provincial scale on industrial minerals and geochemistry. British Columbia’s largest metal deposits, porphyries, continued to be the focus of a joint partnership with several companies and university researchers.

Many BCGS programs involved cooperative partnerships with universities, other government agencies, First Nations and industry. The Survey continued its tradition of working with the Geological Survey of Canada on British Columbia projects providing technical and financial assistance to the Targeted Geoscience Initiative in southern British Columbia. The new agency, Geoscience BC, is another key partner.

Over the past year the Geological Survey Branch published *Geological Fieldwork 2005*, *Exploration and Mining in British Columbia 2005*, 14 Open File map and reports, 7 Geoscience Maps, 12 GeoFile maps, reports and data and 5 Information Circulars. All geoscience publications are routinely posted to the Ministry of Energy, Mines and Petroleum Resources website. MapPlace, one of the world’s premier geoscience internet-map systems, continues to improve with the additional data layers and improved tools. Clients can now access more than 95% of the company mineral assessment reports from the ARIS database over the internet. Survey staff played active roles as presenters and organizers at numerous conferences and events to market British Columbia’s mineral potential, including trade missions to Toronto and China, international conferences in Toronto and Vancouver, and numerous meetings and workshops around the province.

This Fieldwork volume is made possible by the hard work and expertise of numerous authors who have contributed their insight to improve our understanding of British Columbia’s geology and mineral deposits. The articles have been improved by peer and supervisor review. The quality services of RnD Technical are acknowledged for helping to put the volume together. However, it is Brian Grant, the editor, who deserves special commendation for being the key person in so many ways in producing *Geological Fieldwork*. This is his 19th year at the helm.

*D.V. Lefebure
Chief Geologist
British Columbia Geological Survey*

www.empr.gov.bc.ca/Geology

CONTENTS

BC GEOLOGICAL SURVEY

- Aldrick, D.J., MacIntyre, D.G. and Villeneuve, M.E.:** Geology, Mineral Deposits and Exploration Potential of the Skeena Group, Central BC 1
- Ash, C.H., Reynolds, P.H., Creaser, R.A. and Mihalynuk, M.G.:** ^{40}Ar - ^{39}Ar and Re-O Isotopic Ages for Hydrothermal Alteration and Related Mineralization at the Highland Valley Cu-Mo Deposit, Southwestern BC 19
- Demerse, D.K., Kennedy, L.A. and Hopkins J.J.:** Pootlass High-Strain Zone near Bella Coola, West-Central BC: Preliminary Observations 25
- Hora, Z.D., Langrova, A. and Pivec, E.:** Rhodonite from the Bridge River Assemblage, Downton Creek, Southwestern BC 39
- Jones, L.D., Desjardins, P.J., Hancock, K.D., Wilcox, A.F., de Groot, L.L. and McArthur, J.G.:** Update of the British Columbia Geological Survey Geospatial Databases and Applications 45
- Jonnes, S. and Logan, J.M.:** Bedrock Geology and Mineral Potential of Mouse Mountain, Central BC 55
- Legun, A.S.:** Mapping and Review of Coal Geology in the Wolverine River Area, Peace River Coalfield, Northeastern BC 67
- Lett, R.E. and Bluemel, B.:** Multimedia Geochemical Surveys in the Lillooet and McLeod Lake Map Sheets, Central BC 77
- Lett, R.E., Ferbey, T., Roberts, M. and Bluemel, B.:** Orientation Geochemical Survey over the Jake Gold Prospect, Clearwater, South-Central BC 87
- Logan, J.M., Mihalynuk M.G., Ullrich, T and Friedman, R.M.:** U-Pb Ages of Intrusive Rocks and ^{40}Ar - ^{39}Ar Plateau Ages of Copper-Gold-Silver Mineralization Associated with Alkaline Intrusive Centres at Mount Polley and the Iron Mask Batholith, Southern and Central BC. 93
- Massey, N.W.D.:** Boundary Project: Rock Creek area, Southern BC 117
- Massey, N.W.D.:** Lexington Porphyry Revisited, Southern BC 129
- Mihalynuk, M.G.:** Evaluation of Mineral Inventories and Mineral Exploration Deficit of the Interior Plateau Beetle Infested Zone (BIZ), South-Central BC 137
- Mihalynuk, M.G.:** Neogene and Quaternary Chilcotin Group Cover Rocks in the Interior Plateau, South-Central BC: A Preliminary 3-D Thickness Model 143
- Nelson, J. and Kennedy, R.:** Terrace Regional Mapping Project Year 2: New Geological Insights and Exploration Targets (NTS 1031/16S, 10W), West-Central BC. 149
- Nixon, G.T. and Orr, A.J.:** Recent Revisions to the Early Mesozoic Stratigraphy of Northern Vancouver Island and Metallogenic Implications. 163
- Schiarizza, P. and Macauley, J.:** Geology and Mineral Occurrences of the Hendrix Lake Area, South-Central BC 179
- Simandl, G.J.:** Selected Industrial Minerals Trends in British Columbia, 2006. 203
- Simmons, A.T., Tosdal, R.M., Awmack, H.J., Wooden, J.L. and Friedman, R.M.:** Early Triassic Stuhini Group and Tertiary Sloko Group Magmatism, Northwestern BC: New U-Pb Geochronological Results 211

GEOSCIENCE BC

- Anglin, C.D.:** Geoscience BC Program Activities 2006 . . 227
- Andrews, G.D.M. and Russell, J.K.:** Mineral Exploration Potential Beneath the Chilcotin Group, South-Central BC: Preliminary Insights from Volcanic Facies Analysis. . 229
- Arehart, G.B., Smith, J.L. and Pinsent, R.:** New Models for Mineral Exploration in BC: Is there a Continuum between Porphyry Molybdenum Deposits and Intrusion-Hosted Gold Deposits? 239
- Best, M.E. and Lakings, J.:** Preliminary Results from a Microseismic Noise Test Utilizing Passive Seismic Transmission Tomography, Nechako Basin, South-Central BC 243
- Breitsprecher, K., Scoates, J.S., Anderson, R.G. and Weis, D.:** Geochemistry of Mesozoic Intrusions, Quesnel and Stikine Terranes, South-Central BC: Preliminary Characterization of Sampled Suites 247
- Chamberlain, C.M., Jackson, M., Jago, C.P., Pass, H.E., Simpson, K.A., Cooke, D.R. and Tosdal, R.M.:** Toward an Integrated Model for Alkalic Porphyry Copper Deposits in BC 259
- Gagnon, J-F., Loogman, W., Waldron, J.W.F., Cordey, F. and Evenchick, C.A.:** Stratigraphic Record of Initiation of Sedimentation in the Bowser Basin, Northwestern BC 275
- Gordee, S., Andrews, G., Simpson, K.A. and Russell J.K.:** Subaqueous Channel-Confined Volcanism within the Chilcotin Group, Bull Canyon Provincial Park, South-Central BC 285
- Hart, C.J.R. and Goldfarb, R.J.:** Geochronological and Regional Metallogenic Investigations in the Bralorne – Bridge River Mining District, Southwestern BC: Project Rationale. 291
- Hollis, L., Blevings, S.K., Chamberlain, C.M., Hickey, K.A. and Kennedy, L.A.:** Mineralization, Alteration and Structure of the Tsaeko Lakes Region, Southwestern BC: Preliminary Analysis 297
- Jackaman, W.:** Mountain Pine Beetle Infestation Area, Central BC: Regional Geochemical Data Repository Project 307

- Jackaman, W. and Balfour, J.S.:** South Nechako Basin and Cariboo Basin Lake Sediment Geochemical Survey, Central BC 311
- Kilby, W.E. and Kilby, C.E.:** ASTER Multispectral Satellite Imagery and Product Coverage, BC – Phase 2 315
- Larocque, J. and Canil, D.:** Ultramafic Rock Occurrences in the Jurassic Bonanza Arc near Port Renfrew, Southern Vancouver Island 319
- Loogman, W., Gagnon, J-F., Waldron, J.W.F. and Evenchick, C.A.:** Structural Overprinting in the Northwestern Skeena Fold Belt, Northwestern BC. 325
- MacIntyre, D.:** Geology and Mineral Deposits of the Skeena Arch, West-Central BC: Update on a Geoscience BC Digital Data Compilation Project 333
- Mahoney, J.B., Haggart, J.W., Hooper, R.L., Snyder, L.D., Woodsworth, G.J. and Friedman, R.M.:** New Geological Mapping and Implications for Mineralization Potential in the Southern and Western Whitesail Lake Map Area, Southwestern BC 341
- Marshall, D., Street, E., Ullrich, T., Xue, G., Close, S. and Fecova, K.:** Geology and Mineral Potential Update for the Muchalat-Hesquiat Region, Vancouver Island. 355
- McCurdy, M.W., Smith, I.R., Plouffe, A., Bednarski, J., Day, S.J.A., Friske, P.W.B., McNeil, R.J., Kjarsgaard, I.M., Ferbey, T., Levson, V.M., Hickin, A.S., Trommelen, M. and Demchuk, T.E.:** Indicator Mineral Content and Geochemistry of Stream and Glacial Sediments from the Etsho Plateau Region as an Aid to Kimberlite and Base Metal Exploration, Northeastern BC 361
- Miles, W.F., Dumont, R. and Lowe, C.:** Aeromagnetic Survey over the Jennings River Map Area, Northern BC 373
- Miles, W.F., Shives, R.B.K., Carson, J., Buckle, J., Dumont, R. and Coyle, M.:** Airborne Gamma-Ray Spectrometric and Magnetic Surveys over the Bonaparte Lake Area, South-Central BC 375
- Mustard, P.S. and Mahoney, J.B.:** Stratigraphic Analysis of Cretaceous Strata Flanking the Southern Nechako Basin, BC: Constraining Basin Architecture and Reservoir Potential 377
- Ruks, T. and Mortensen, J.K.:** Geological Setting of Volcanogenic Massive Sulphide Occurrences in the Middle Paleozoic Sicker Group of the Southeastern Cowichan Lake Uplift, Southern Vancouver Island 381
- Spratt, J.E., Craven, J., Jones, A.G., Ferri, F. and Riddell, J.:** Utility of Magnetotelluric Data in Unravelling the Stratigraphic-Structural Framework of the Nechako Basin, South-Central BC, from a Re-Analysis of 20-Year-Old Data 395

Geology, Mineral Deposits and Exploration Potential of the Skeena Group (NTS 093E, L, M; 103I), Central British Columbia

by D.J. Aldrick, D.G. MacIntyre¹ and M.E. Villeneuve²

KEYWORDS: Skeena Group, mid-Cretaceous, Rocky Ridge Formation, basalt, rhyolite, Equity Silver mine, mineral exploration

INTRODUCTION

Extending from Berriasian to Cenomanian time, the Skeena Group is a 3.5 km thick succession of mixed clastic sedimentary rocks with minor intercalated basalt and rhyolite flows that record 50 million years (143–93 Ma) of Early to mid-Cretaceous sedimentation and volcanism in central British Columbia (Fig 1). Volcanic strata are age-equivalent to the Spences Bridge and Crowsnest volcanics in southern BC and to the Mount Nansen and South Fork volcanics in the Yukon (Fig 8 in Bassett and Kleinspehn, 1996). Sedimentary strata are age-equivalent with units of the Bowser Lake Group and overlap in time with the generally younger successions of the Kasalka Group of central BC and the Nanaimo Group of Vancouver Island.

Previous Geological Work

Skeena Group strata are widely distributed through central BC and have been studied for 125 years as part of regional mapping projects. A comprehensive bibliography is included at the end of this report.

Major steps in the evolution of stratigraphic nomenclature of the Skeena Group are shown in Figure 2. Dawson (1881) first included the strata now recognized as Skeena Group as a part of the larger 'Porphyrite Group'. Leach (1910) divided the Porphyrite Group into two units, the lower Hazelton Group and an upper Skeena series, and Hanson (1924b) and Jones (1925) raised the latter unit to formation status.

The differentiation between Hazelton Group and Skeena Formation strata was challenging because both units are characterized by clastic sedimentary rocks near their contact. Consequently, Armstrong (1944a, 1944b) merged both of these units into a larger Hazelton Group, which combined the clastic sedimentary rocks near the top of the earlier-defined Hazelton Group and the clastic sedimentary rocks of the Skeena Formation, into a single unit called the Upper Sedimentary Division. Sutherland Brown (1960b) continued with this system, formally naming

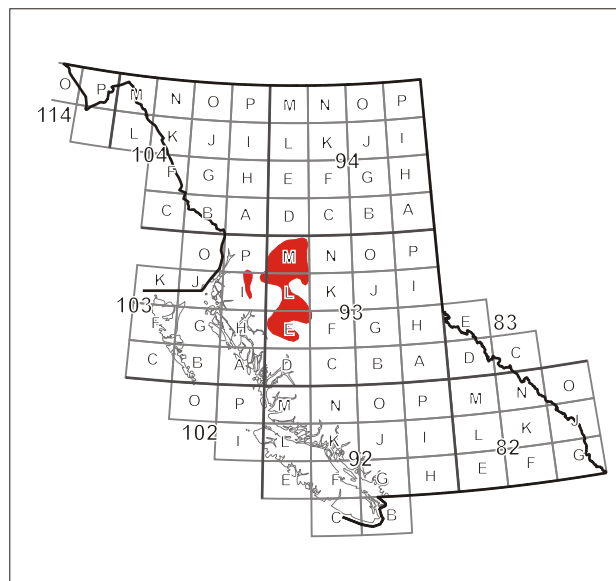


Figure 1. Distribution of Skeena Group rocks in BC.

Armstrong's 'Upper Jurassic to Lower Cretaceous Sedimentary Division' the 'Red Rose Formation'.

Following Roddick's (1970) informal usage of the term 'Bowser Group' for a regionally extensive clastic sedimentary succession exposed around Bowser Lake, Duffell and Souther (1964, p 27–33) proposed the name Bowser Group for a thick section of Late Jurassic to Early Cretaceous clastic sedimentary rocks in the Terrace area. This step created a major new unit in the midst of Armstrong's (1944a, 1944b) thickened Early Jurassic to mid-Cretaceous Hazelton Group. Working farther to the east where all rock units are exposed, Tipper and Richards (1976) addressed this problem by redefining the Hazelton Group as an Early to Middle Jurassic sequence, the Bowser Lake Group as a Middle to Late Jurassic sequence and resurrecting the name Skeena Group for the Early to mid-Cretaceous succession of sedimentary and volcanic rocks. Tipper and Richards (1976) also recognized the Late Cretaceous to Eocene Sustut Group as the unit that immediately overlies the northeast part of the Skeena Group strata. In the southeast part of the Skeena Group area, MacIntyre (1985) defined the Late Cretaceous Kasalka Group, which regionally overlies the Skeena Group at an angular unconformity.

Figure 3 presents the evolution of the internal stratigraphic subdivisions of Skeena Group. Leach (1909, p 62) described the Skeena series as a sequence of non-marine shale, sandstone and coal. Armstrong (1944a, 1944b) subdivided this rock sequence into a Sedimentary Division and an overlying Volcanic Division at the top of his larger

¹ D.G. MacIntyre and Associates Ltd., Victoria, BC

² Geological Survey of Canada, Ottawa, ON

This publication is also available, free of charge, as colour digital files in Adobe Acrobat® PDF format from the BC Ministry of Energy, Mines and Petroleum Resources website at http://www.em.gov.bc.ca/Mining/GeolSurv/Publications/catalog/cat_fldwk.htm

Dawson (1881) Leach (1908,1909)	Leach (1910)	Hanson (1924) Jones (1925)	Armstrong (1944a, 1944b)	Sutherland Brown (1960)	Tipper and Richards (1976)	
Porphyrite Group	Skeena Series	Skeena Formation	Hazelton Group	Volcanic Division	Brian Boru Formation	
				Sedimentary Division	Red Rose Formation	
					Bowser Lake Group	
				Hazelton Group		Upper Sedimentary Division
	Upper Volcanic Division	Volcanic Division	Nilkitwa Formation			
	Lower Sedimentary Division	Sedimentary Division	Telkwa Formation			
	Lower Volcanic Division	Volcanic Division				

Figure 2. Development of regional stratigraphic subdivisions and nomenclature (modified from Ferri et al., 2005).

Tipper and Richards (1976)	Richards (1980)	Richards (1990)	Bassett and Kleinspehn (1996)	Bassett and Kleinspehn (1997)	MacIntyre (2001a)	This Study (2007)	
	Brian Boru Formation	Kasalka Group				Sustut / Kasalka Group	
	Sustut Group	Sustut Group	Sustut Group	Sustut Group	Sustut Group		
Skeena Group	Brian Boru Formation	Red Rose Formation	Red Rose Formation	Rocher Deboule Formation	Rocher Deboule Formation	Rocher Deboule Formation	
							Albian black shale
	Rocky Ridge volcanic rocks	Hanawald conglomerate	Bulkley Canyon Formation	Bulkley Canyon Formation	Bulkley Canyon Formation		
	Kitsuns Creek sediments					Kitsumkalum shale	Kitsuns Creek Member
	black shale	Kitsuns Creek Formation	Couture Formation	Laventie Formation	Laventie Formation		
	conglomerate						
	Red Rose Formation						
	Bowser Lake Group	Bowser Lake Group	Bowser Lake Group	Bowser Lake Group	Bowser Lake Group	Bowser Lake Group	Bowser / Hazelton Group

Figure 3. Development of Skeena Group subdivisions and nomenclature.

Hazelton Group succession. Sutherland Brown (1960b) formalized these same two stratigraphic divisions as the Red Rose and Brian Boru formations, respectively. Richards (1980) introduced six subdivisions for the Skeena Group and separated the Brian Boru Formation as a younger unit. Further refinement created five formal subdivisions for the Skeena Group (Richards, 1990). The first study to focus entirely on Skeena Group rocks was the PhD research program of Bassett (1995), which is also available as two publications (Bassett and Kleinspehn, 1996, 1997). They first interpreted Skeena Group stratigraphy as four formations (Bassett and Kleinspehn, 1996), but modified the nomenclature slightly in the second paper (Bassett and Kleinspehn, 1997). Subsequent targeted studies have been completed by Tackaberry (1998), MacIntyre (2001b) and MacIntyre *et al.* (2004). In the latter report, Skeena Group stratigraphy is simplified further into three main formations. In this report, the Skeena Group is divided into the same four formations and one member used by Bassett and Kleinspehn (1997), but the Kitsuns Creek Member is now combined with the Rocky Ridge Formation.

Mineral deposits hosted by Skeena Group rocks are discussed by Fleet Robinson (1911), Malloch (1914), Galloway (1914, 1916), O'Neill (1919), Jones (1925), Lang (1929), Kerr (1936), Kindle (1940, 1954), Stevenson (1947), Sutherland Brown (1960b), Wojdak and Sinclair (1984), Cyr *et al.* (1984), Church (1984, 1986), MacIntyre (1985a, 1985b, 2001b, 2006), Church and Barakso (1990), Leitch *et al.* (1990), Gaba *et al.* (1992), Church and Klein (1998), Wojdak and Ethier (2000), MacIntyre and Villeneuve (2001a), Fingler (2004) and MacIntyre *et al.* (2004) in addition to summary property descriptions available from MINFILE and comprehensive data provided in exploration assessment reports.

Current Project

A new research project was launched to examine the widespread exposures of Skeena Group volcanic units over the full extent of these rocks and to study all the metallic mineral occurrences hosted by Skeena Group strata.

In addition to documenting new mineral discoveries, existing mineral deposits will be reassessed and a series of recently proposed metallogenic models for the Skeena Group will be evaluated. The bimodal volcanic units of the Skeena Group have recently been interpreted as evidence for a caldera setting (MacIntyre, 2001a), which is the optimal setting for the formation and preservation of alkaline epithermal mineral deposits (Hedenquist and Sillitoe, 2003; Hedenquist and White, 2005). Previously, these same volcanic rocks were identified as products of rifting (Barrett and Kleinspehn, 1996), which is the optimal setting for the development of subaerial Bonanza-type epithermal deposits and subaqueous exhalative mineralization (Hedenquist and White, 2005). Overall, the regional depositional environment for the Skeena Group is interpreted as a continental margin or fore arc tectonic setting (Barrett and Kleinspehn, 1997), similar to the interpreted setting for the world's greatest VMS district, the Devonian-Mississippian Iberian Pyrite Belt (White, 1999).

Only one geological setting and metallogenic interpretation can be the best fit. The BC Geological Survey field program was developed to evaluate these contrasting interpretations through study of the volcanic strata and examination of the mineral deposits. Results will identify the

model with the best correlation to field and laboratory evidence and will help focus exploration efforts. Work in the 2006 field season concentrated on readily accessible exposures in the Babine Lake, Rocky Ridge and Francois Lake areas adjacent to the Smithers – Houston – Burns Lake corridor (Fig 4).

REGIONAL GEOLOGICAL SETTING AND SKEENA GROUP GEOLOGY

Overall, the regional depositional environment for the Skeena Group is a continental margin setting along western North America. In detail, Skeena Group strata record three distinct paleogeographic stages, reflecting contrasting tectonic phases. The summary below is *modified from* Bassett and Kleinspehn (1997) and Ferri *et al.* (2005).

In the first paleogeographic stage, Berriasian to Aptian (143–115 Ma), Skeena strata is represented as two contrasting rock types that grade laterally (Fig 4, 5). Coal-bearing micaceous sandstone and siltstone of the lower Bulkley Canyon Formation are interpreted as sediment accumulation in a series of coal-swamp deltas. The lower Bulkley Canyon Formation hosts the important Telkwa coalfields. Marine black shale, and lesser siltstone and sandstone, of the lower Laventie Formation are interpreted as deposits accumulated in restricted tidal basins adjacent to the deltas. These Early Cretaceous rock types correlate to the north with the deep basinal deposits of the McEvoy Formation of the Bowser Lake Group, which record the final filling of the Bowser foredeep produced by Jurassic accretion of the Intermontane Belt to North America.

The second paleogeographic stage is recorded by early Albian to early Cenomanian (115–95 Ma) deeper water marine sedimentation and coeval interbasinal volcanism. Southeastward marine transgression is recorded as finer grained sedimentary rocks of the upper Laventie Formation. The upper Bulkley Canyon Formation is preserved at the southern limit of Skeena Group exposures as more micaceous, fossil-poor, coal-absent tidal sandstone–siltstone sequences interpreted as shallow-water delta-front or delta-plain deposits. The contemporaneous Rocky Ridge Formation includes several widely scattered eruptive centres of volcanic rocks that record a period of minor crustal extension in the subsiding basin. Adjacent to the volcanic flows, volcanic detritus is incorporated in the sedimentary stratigraphy. These distinctive sedimentary rocks rich in volcanic clasts comprise the Kitsuns Creek Member of the Rocky Ridge Formation. Individual volcanic centres vary from subaerial to submarine. The peripheral volcanoclastic Kitsuns Creek Member grades laterally outward into either upper Laventie Formation or upper Bulkley Canyon Formation sedimentary strata. These Early to mid-Cretaceous rock types correlate with the magmatism in the Omineca Belt to the east, with ongoing arc volcanism of the upper Gambier group to the west and continued sedimentation of the upper McEvoy Formation of the Bowser Lake Group to the north. The upper McEvoy Formation hosts minor distal volcanic ash.

The third paleogeographic stage records a brief episode (early to mid-Cenomanian; 95–92 Ma) marked by the accumulation of subaerial fluvial and deltaic conglomerate, sandstone and siltstone of the Rocher Debole Formation. Coarse clastic debris is dominated by chert pebbles, with local volcanic clasts eroded from the underlying Rocky

Ridge Formation. The mid-Cretaceous conglomerate correlates to the north with fluvial chert-pebble conglomerate and sandstone of the Devil's Claw Formation of the Bowser Lake Group. These rocks record the final filling of the Bowser foredeep produced by the Jurassic accretion of the Intermontane Belt to North America. Within the area of the Rocher Debole Formation, the fluvial conglomerate is conformably overlain by fluvial chert-granite conglomerate, sandstone and mudstone of the Tango Creek Formation of the Sustut Group. To the south, Rocher Debole strata correlate with the red basal conglomerate of the Kasalka Group, which unconformably overlies lower Skeena Group rocks in the Tahtsa Lake area (MacIntyre, 1985a).

The Devil's Claw Formation (Bowser Lake Group), the lower member of the Tango Creek Formation (Sustut Group), the basal conglomerate of the Kasalka Group and the Rocher Debole Formation (Skeena Group) are all roughly coeval and are all composed of fluvial chert-clast-rich conglomerate and sandstone. Bassett and Kleinspehn (1997) conclude that all four formations are laterally equivalent units of the same progradational chert-rich unit and predict that these similar, coeval units will ultimately be consolidated into a single formation.

Geology of the Rocky Ridge Formation

The volcanic rocks of the Skeena Group were named the Rocky Ridge volcanics by Richards (1980) and formalized as the Rocky Ridge Formation by Richards (1990). These two maps also recognized the associated volcanoclastic sedimentary strata as the Kitsuns Creek Member (Richards, 1980) and then the Kitsuns Creek Formation (Richards, 1990). All of these strata have been further described in a series of maps and reports, including MacIntyre (1985a, 1998, 2001a, 2001b, 2006), Bassett (1991, 1995), Bassett and Kleinspehn (1996, 1997), Richards *et al.* (1997), Tackaberry (1998), MacIntyre *et al.* (2001a, 2001b, 2004) and MacIntyre and Villeneuve (2007). The most comprehensive studies of this volcanic strata are reports by Bassett and Kleinspehn (1996) and Tackaberry (1998) and the most recent geochronological results for the Rocky Ridge volcanics are tabulated in MacIntyre and Villeneuve (2007).

Rocky Ridge volcanics occur in isolated geographic areas within the otherwise continuous clastic sedimentary deposition of the Skeena Group (Fig 6; Bassett and Kleinspehn, 1996). Prior to 1998, the Rocky Ridge Formation was defined as a sequence of mafic volcanic flows, associated fragmental facies and minor intercalated volcanoclastic sedimentary rocks. In all reports and maps completed from 1998 onwards, the Rocky Ridge Formation is described as a package of bimodal volcanic rocks and related sedimentary facies. New radiometric dates (MacIntyre and Villeneuve, 2007) establish that the felsic and mafic volcanic units differ by 10 million years in age. New fieldwork reveals that felsic and mafic volcanic rocks of the Skeena Group are stratigraphically separated by hundreds of metres of clastic sedimentary rocks. Consequently, these contrasting volcanic units are described separately in this report, although both rock types are still included as parts of the Rocky Ridge Formation.

FELSIC VOLCANIC ROCKS OF THE ROCKY RIDGE FORMATION

Rounded, equidimensional intrusive 'rhyolite plugs' are widespread throughout Skeena Group rocks. These

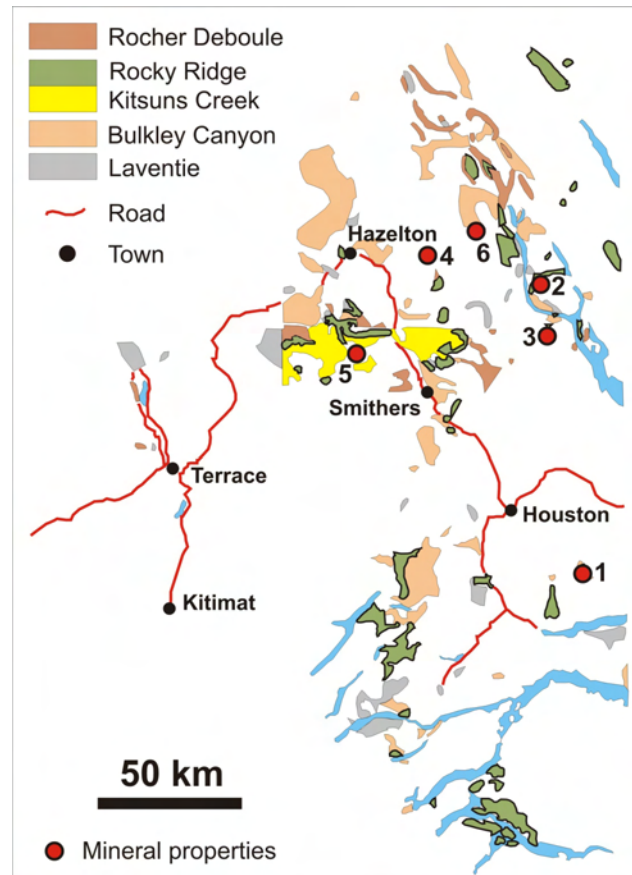


Figure 4. Geology map of the Skeena Group (modified from Bassett and Kleinspehn, 1997). Numbers show mineral properties from Table 2.

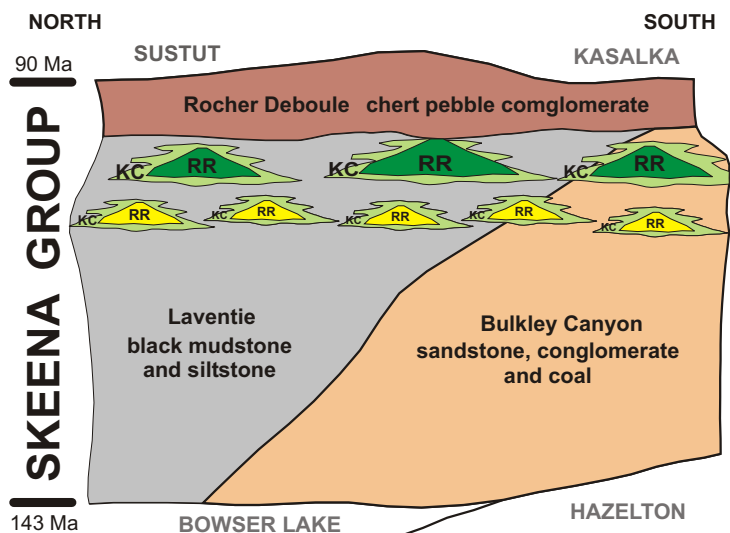


Figure 5. Schematic stratigraphy of Skeena Group (modified from Bassett and Kleinspehn, 1997). Abbreviations: RR, Rocky Ridge Formation; KC, Kitsuns Creek Member.

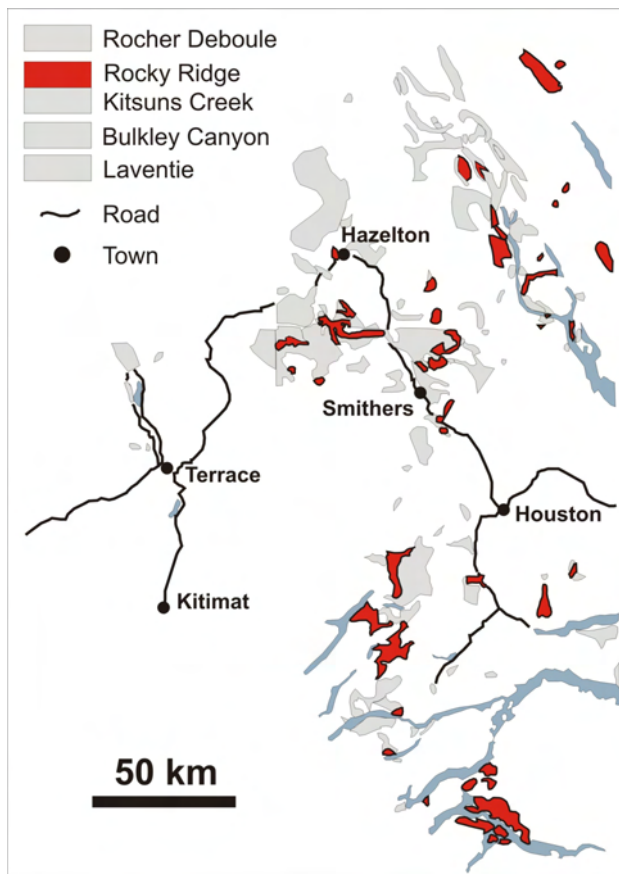


Figure 6. Geological map of volcanic units of the Skeena Group (modified from Bassett and Kleinspehn, 1997).

bodies were initially mapped as a series of Eocene stocks ('EBr'; Richards, 1980). Textures and field relationships evident in subsequent mapping by MacIntyre indicated that rhyolite bodies close to the Granisle and Bell mines in central Babine Lake were extrusive rhyolite domes or cryptodomes (MacIntyre, 1998). Subsequent reassessment of the field data (Tackaberry, 1998; MacIntyre, 2001b) lead to the conclusion that the ring of 14 rhyolite domes north and west of Old Fort Mountain were mid-Cretaceous, and therefore also extrusive bodies. New U-Pb dating (MacIntyre and Villeneuve, 2007) shows that felsic volcanic rock exposed along the walls of the main pit road at the Equity Silver mine are also mid-Cretaceous, confirming that the ore-hosting succession of sedimentary and volcanic rocks at the mine are Skeena Group rocks.

West Morrison Rhyolite

Felsic volcanic rocks within the Skeena Group are exposed in outcrop in a series of 14 small rhyolite domes north and west of Old Fort Mountain and adjacent to north-central Babine Lake.

Eleven discrete outcrop areas of Skeena Group rhyolite are exposed along the West Morrison logging road network, north and west of Old Fort Mountain, northern Babine Lake. These rocks are best described in a BSc thesis by Tackaberry (1998). The white to pale grey rhyolite domes are enveloped in a black matrix lapilli tuff containing clasts of the rhyolite and dacite (Fig 7). Also preserved within this black matrix lapilli tuff are small lenses of fine-

grained, dark grey orthoclase and plagioclase-porphyrific dacite. Due to the dark colouring, these outcrops were originally misidentified as basalt, giving rise to the identification of a 'bimodal' basalt-rhyolite succession for the Rocky Ridge volcanics in this area.

Bell Mine Dacite

A similar massive dacite rock collected southeast of the Bell mine yielded a U-Pb age of 107.9 ± 0.2 Ma (MacIntyre and Villeneuve, 2001b). A crosscutting basalt dike from this same outcrop, dated by the $^{40}\text{Ar}/^{39}\text{Ar}$ method at 104.8 ± 1.2 Ma, provides a minimum age for the felsic volcanic rock (MacIntyre and Villeneuve, 2001b).

Kitseguecla Lake Rhyolite

A 10 km long rhyolite lens is well exposed as a prominent resistant ridge along the north side of the Kitseguecla Lake road and adjacent logging roads to the north. Initially mapped by Richards (1980) as an Eocene sill, MacIntyre *et al.* (2004) speculated that this rock unit might be another extrusive rhyolite dome, cryptodome or subvolcanic sill, similar to the West Morrison rhyolite domes. Samples from this unit have not yielded enough zircons for a radiometric date (MacIntyre and Villeneuve, 2007).

Knoll Rhyolite

This large mineralized rhyolite dome is correlated to other rhyolite domes that are part of the Rocky Ridge Formation (MacIntyre, 2001b; MacIntyre *et al.*, 2004). This unit has not yielded enough zircon for an age determination (MacIntyre and Villeneuve, 2007).

Equity Silver Mine Dacite

Felsic lapilli tuff exposed in the east ramp of the Main Zone pit was collected in 2003 by MacIntyre and Villeneuve as part of a Rocks to Riches-funded project (MacIntyre *et al.*, 2004; Villeneuve, 2004; MacIntyre and Villeneuve, 2007). The rock was collected from a stratigraphic package called the Pyroclastic Division, which is described as a sequence of welded to non-welded coarse-grained lapilli tuff and ash tuff, volcanic breccia and minor intercalated, very fine grained tuff or dust tuff (Cyr *et al.*, 1984). Rocks of the Pyroclastic Division are primarily dacite. This sample has yielded an age of $113.5 +4.5/-7.2$ Ma, which firmly establishes the hostrock succession of interbedded volcanic and sedimentary rocks at the Equity Silver mine as Skeena Group strata.

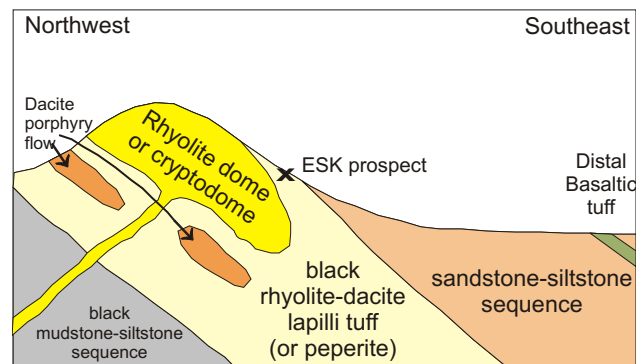


Figure 7. Schematic cross-section through a rhyolite dome along the West Morrison logging road (modified from Tackaberry, 1998).

INTERMEDIATE VOLCANIC ROCKS OF THE ROCKY RIDGE FORMATION

Equity Silver Mine Andesite

On the mine property, the fragmental dacite described above is overlain by a succession of andesite and dacite flows called the Volcanic Flow Division (unit 3a on Fig 8; unit 4 of Cyr *et al.*, 1984). This demonstrates that volcanic rocks with intermediate composition are also preserved in the Skeena Group. A K-Ar date of 58.5 ± 2.0 Ma was obtained from sericite alteration superimposed on these volcanic flow rocks (Wetherell, 1979; Cyr *et al.*, 1984); however, this is interpreted as a reset sericite date reflecting the proximity of the multiphase Eocene monzonite-diorite-gabbro intrusion, which crops out a few tens of metres to the east (Cyr *et al.*, 1984).

Mount Ney Volcanics

Extensive outcrops of mid-Cretaceous Mount Ney volcanics form scattered mound-like exposures in the forest-covered region of the central and northeast Newcombe Lake map area (NTS 093E/14), where this informal unit was first introduced as unit IKv (Diakow and Drobe, 1989a). The current name appeared first in Geoscience Map 2006-5 (Diakow, 2006). Mount Ney volcanics are predominantly lava flows that range in composition from basaltic andesite to andesite (Diakow and Drobe, 1989b, p 184, *under* 'Lower Cretaceous'). Flows exhibit amygdaloidal and more commonly porphyritic texture defined by felted fine-grained plagioclase laths and pyroxene grains. Except for one large exposure of pillow lava, indicating submarine deposition, they generally form massive unstructured outcrops.

MAFIC VOLCANIC ROCKS OF THE ROCKY RIDGE FORMATION

The Rocky Ridge Formation was defined by Richards (1980, 1990) for the thick succession of porphyritic basalt flows and intercalated volcanoclastic sediments exposed along the length of Rocky Ridge, 25 km northwest of Smithers. Additional basalt units, now correlated with Skeena Group, have been mapped by Woodsworth (1980) in the Morice Lake – Tahtsa Lake – Whitesail Lake – Eutsuk Lake region. North of Rocky Ridge, Richards (1990) mapped small bands of Rocky Ridge basalt within the main Rocher Deboile range. Farther northeast, similar mafic volcanic rocks were mapped through a large region 25 km northwest of Nilkitkwa Lake, and over a similarly large area 25 km north-northwest of Bulkley House at the north end of Takla Lake (Richards, 1990).

All of these mafic volcanic rocks are alkaline and porphyritic (Tackaberry, 1998), although phenocrysts vary between pyroxene, plagioclase and hornblende. Most flows are vesicular, with infillings of calcite or zeolite. Basalt exposures are mainly subaerially deposited; however, outcrops near Tahtsa Lake show a thin accumulation of pillowed flows at the base of a sequence that grades upward into massive flows. Lava flows are interbedded with pyroclastic flows, tuff breccia, siltstone and peperite.

Fossil suites collected from sedimentary units below, above and interbedded with these basalt successions constrain the age of the flows to early Albian (110 Ma) in the south and to mid-Albian to mid-Cenomanian (105–93 Ma) in the north (Bassett and Kleinspehn, 1996). Dating by $^{40}\text{Ar}/^{39}\text{Ar}$ on hornblende crystals from the uppermost flows

exposed on the Rocky Ridge gives an age of 95.6 ± 1.6 Ma (Bassett and Kleinspehn, 1996, p 731). A whole rock $^{40}\text{Ar}/^{39}\text{Ar}$ age of 93.0 ± 2.3 Ma was obtained from a basalt flow in the same area (MacIntyre and Villeneuve, 2007). A basalt dike sampled south of the Bell mine (MacIntyre and Villeneuve, 2001b) yields an $^{40}\text{Ar}/^{39}\text{Ar}$ whole rock age of 104.8 ± 1.2 Ma. In summary, combined fossil and geochronology studies constrain the age of the basaltic units of the Rocky Ridge Formation to 110 Ma in the south and from 105 to 93 Ma in the north.

Rocky Ridge Basalt

Bassett and Kleinspehn (1996, p 733) provide the most comprehensive description of this unit at its type area 25 km northwest of Smithers. Strata consist of interbedded alkaline basaltic lava flows and pyroclastic flows averaging 10 to 20 m in thickness. Flows display large (4–8 mm) pyroxene phenocrysts with rare plagioclase or hornblende phenocrysts. Most flows are highly vesicular. The subaerial features of the lava, pyroclastic flows and the presence of vesicular basalt clasts in distal interbedded fluvial deposits indicates that this volcanic complex was emergent, had high relief and was a source of sediment.

Black shale with interbedded sandstone crops out around the coeval volcanoclastic deposits, indicating a tidally dominated shallow-marine setting around the volcanic edifices (Bassett and Kleinspehn, 1996).

GEOLOGY OF THE KITSUNS CREEK MEMBER

Rocks of the Kitsuns Creek Member are fine-grained or medium-grained clastic sedimentary rocks characterized by fine to coarse, monolithic volcanic clasts. They represent volcanoclastic debris shed into medium-grained sedimentary rocks of the deltaic Bulkley Canyon Formation or into black, fine-grained basinal sedimentary rocks of the Laventie Formation. These rocks can only form adjacent to volcanic rock units of the Rocky Ridge Formation. Consequently the Kitsuns Creek Member is classified here as a facies of the Rocky Ridge Formation rather than a facies of the clastic sedimentary formations of the Skeena Group.

There are four contrasting 'end-members' of Kitsuns Creek rock types: massive black mudstone with rhyolite clasts, massive black mudstone with basalt clasts, sandstone or grit with rhyolite clasts and sandstone or grit with basalt clasts. Sedimentary units hosting clasts of intermediate volcanic composition are also described from the Equity mine succession (Cyr *et al.*, 1984).

These rock types are important because they may be first field indicators that volcanic units of the Rocky Ridge Formation exist nearby. At the Knoll property, mineralization is hosted by the volcanic unit; but at the ESK property, the sedimentary rocks rich in volcanic clasts or reworked lapilli tuff of the Kitsuns Creek Member host the vein network with elevated base and precious metal values.

The black matrix breccia exposed in many locations along the West Morrison logging road envelopes the ring of 14 prominent rhyolite domes that are exposed in this area. These black matrix breccia form both the immediate footwall and hangingwall rocks to the rhyolite bodies. Initially mapped as basalt conglomerate (with rhyolite clasts), the petrochemical analysis of these rocks by Tackaberry (1998) showed an overall composition of dacite, leading to

a classification as dacitic lapilli tuff. An alternative interpretation, based on field textures, is that these rocks are peperite generated by the flow of rhyolite lava, or by the emplacement of a rhyolite cryptodome, into unconsolidated black silt and mud of the Laventie Formation.

GEOLOGICAL AND TECTONIC HISTORY

Skeena Group rocks accumulated on the western continental margin of North America from Early to mid-Cretaceous time. These shallow-water strata grade laterally to the north and northwest into deeper water, basinal sedimentary rocks of the Bowser Lake Group; to the south and southeast, Skeena Group sedimentary rocks pinch out against the subaerially exposed micaceous continental rocks that provided the sediment.

Bassett and Kleinspehn (1996, 1997) describe the evolution of the geological setting of these strata. In the Early Cretaceous, the depositional setting is a series of shallow-water to locally emergent deltas (Bulkley Canyon Formation) adjacent to restricted tidal basins where black shale accumulated (Laventie Formation).

In the mid-Cretaceous, the subsidence of the continental margin was recorded by southeastward marine transgression and more widespread accumulation of the basinal black shale (Laventie Formation). This was accompanied by intermittent volcanism (Rocky Ridge Formation) from widely scattered, subaerial and submarine volcanic centres that evolved over 10 to 15 million years from calcalkaline felsic to alkaline mafic compositions. Bassett and Kleinspehn (1996) conclude that Rocky Ridge volcanic rocks may have accumulated along a rift. MacIntyre (2001a) concluded that the felsic volcanic centres represent caldera complexes.

Toward the end of mid-Cretaceous time, the seafloor rebounded and rebedded chert-pebble conglomerate found in a shallow-water to subaerial fluvial environment (Rocher Deboule Formation) prograded northwestward. Northwest of this advancing shoreline, the depositional environments were once again tidal deltas.

Over the 50-million-year span of Skeena Group time, these strata record the evolution from moderately extensional to moderately compressive tectonics affecting the continental margin.

Although the paleotopographic setting is clear, the tectonic setting for this part of the continental margin of North America in Early to mid-Cretaceous time is uncertain. The area of Skeena Group sedimentation and volcanism and Bowser Basin sedimentation immediately to the northwest has been identified by various researchers as a fore arc, back arc, extensional basin or foreland setting (Evenchick and Thorkelson, 2005). The existence of the Gambier arc off to the west throughout the Early and mid-Cretaceous (Souther, 1991) suggests that Skeena Group volcanism could record the onset of back arc extension. MacIntyre *et al.* (2004) interpret the scattered volcanic centres of the Rocky Ridge Formation as a nascent (or incipient) volcanic arc, with the individual volcanic centres representing caldera complexes. Bassett and Kleinspehn (1996, Fig 5) interpret the locus for the Rocky Ridge volcanic centres as a north-northeast-trending rift.

MINERAL DEPOSITS

All mineral occurrences hosted by Skeena Group strata are listed in Table 1, where individual occurrences are sorted into alphabetical order. In Table 2, the ten coal deposits are removed from this initial list, three broad alteration zones that lack elevated base and precious metal values are also removed from the initial list and the Mount Cronin mine is removed from the list because a new radiometric date (MacIntyre and Villeneuve, 2007) reveals that

TABLE 1. MINERAL OCCURRENCES HOSTED BY THE SKEENA GROUP.

Name	Property	MINFILE	Status
1600 Zone	Fireweed	093M 151	deposit
Anomalous Zone	Equity Silver	093L 001	showing
Beamont station			alteration
BQ			prospect
Cabinet Creek			past producer
Chisholm Lake		093L 159	showing
Denys Creek			
East Zone	Fireweed	093M 151	deposit
ESK	Old Fort Mountain		showing
Far East Zone	Fireweed	093M 151	deposit
Far West Zone	Fireweed	093M 151	deposit
Gaul	Equity Silver	093L 001	prospect
Goathorn Creek		093L 156	past producer
Hematite	French Peak	093M 015	past producer
Hope	Equity Silver	093L 001	prospect
Jan	Fireweed	093M 151	deposit
Kathlyn Lake			deposit
Knoll		093M 100	prospect
Main	Equity Silver	093L 001	past producer
MN	Fireweed	093M 151	deposit
Mt. Cronin		093L 127	deposit
North Zone	Equity Silver	093L 001	prospect
Owen Creek			deposit
Rio	French Peak	093M 015	past producer
Seeley Lake		093M 150	
South Zone	Fireweed	093M 151	deposit
Southern Tail	Equity Silver	093L 001	past producer
Sphalerite	Fireweed	093M 151	deposit
Superstition	Equity Silver	093L 001	prospect
Tadinlay	Old Fort Mountain		alteration
Telkwa River		093L 156	past producer
Thautil River		093L 158	showing
Ute	French Peak	093M 015	past producer
Waterline	Equity Silver	093L 001	past producer
West Morrison	Old Fort Mountain		alteration
West Zone	Fireweed	093M 151	deposit
Zest	Equity Silver	093L 001	showing
Zymoetz River		093L 154	
3200 Zone	Fireweed	093M 151	deposit

TABLE 2. METALLIC MINERAL OCCURRENCES HOSTED BY THE SKEENA GROUP, SORTED BY

Map no.	Property	MINFILE	Status
1	Equity Silver	093L 001	past producer
2	Old Fort Mountain		showing
3	Fireweed	093M 151	deposit
4	Knoll	093M 100	prospect
5	BQ		prospect
6	French Peak	093M 015	past producer

the Mount Cronin deposit is hosted by Kasalka Group rocks. All the remaining prospects from Table 1 were then resorted and grouped according to their individual properties in Table 2, revealing that there are just six areas with metallic mineralization within Skeena Group rocks. Four of these areas have been discovered within the last 20 years.

Equity Silver Mine (MINFILE 093L 001)

The Equity Silver mine produced silver, copper, gold, antimony and arsenic from complex sulphide ores between 1980 and 1994. Open pit and underground workings at four adjacent orebodies (Fig 8; North zone, Waterline, Main zone and Southern Tail) yielded a total of 33.8 Mt of ore at an average grade of 64.9 g/t Ag, 0.4% Cu and 0.46 g/t Au. South of the Southern Tail orebody, the Hope, Superstition and Gaul mineral prospects lie along the south-southwest extension of this same trend. Mineralogy of the ore zones and peripheral alteration zones are summarized in Table 3.

The mine property is underlain by a mixed sedimentary-volcanic succession (Cyr *et al.*, 1984). Basal conglomerate and minor argillite (Clastic Division; units 1a and 1b on Fig 8) is conformably overlain by a sequence of intercalated subaerial tuff breccia and minor reworked pyroclastic debris (Pyroclastic Division; units 2a and 2b) that hosts the orebodies. This package is conformably overlain by bedded andesite to dacite flows (Volcanic Flow Division; unit 3a) and an onlapping sequence of interbedded volcanic conglomerate, sandstone and tuff (Sedimentary-Volcanic Division; unit 3b).

At different times, these rocks have been correlated with Hazelton Group, Skeena Group and Kasalka Group strata. New U-Pb zircon geochronology results (MacIntyre and Villeneuve, 2007) from a sample of felsic lapilli tuff collected from the east ramp of the Main zone pit give an age of 113.5 ± 4.5/-7.2 Ma. This confirms that the hostrock volcanic succession (unit 2 on Fig 8) at Equity Silver mine is mid-Cretaceous Skeena Group strata. Underlying chert-pebble conglomerate and carbonaceous siltstone of unit 1 (Coarse Clastic Division) may be part of the Bowser Lake Group.

The ore deposits are hosted within rocks of the pyroclastic division and lie between two intrusive stocks. West of the mine, the 58 ± 2 Ma quartz monzonite stock has unaltered and altered zones; the eastern kaolin-sericite-chlorite-pyrite-altered portion hosts weak porphyry-style copper-molybdenum mineralization. East of the mine, the 48 ± 2 Ma gabbro-monzonite intrusion has five mappable, sequential phases (gabbro, intermediate phase, diorite, monzonite and hypabyssal monzonite) all cut by late felsite dikes termed 'quartz latite'. Since the orebodies lie between these two intrusions, published genetic models relate ore formation at the Equity Silver Mine to these distinctly different intrusions. Cyr *et al.* (1984) and Wojdak and Sinclair (1984) conclude that the ore is epigenetic and epithermal in character and associated with the emplacement of the older western stock that hosts the porphyry Cu-Mo-style mineralization. Church (1984) and Church and Barakso (1990) conclude that the multiple ore zones are epigenetic and associated with intrusion of the younger eastern polyphase intrusion (Fig 9).

In addition to the two main genetic models summarized above, Wojdak and Sinclair (1984) discussed the possibility that the ore may have formed penecontemporan-

eously with its host volcanic rocks, as a late-stage epithermal vein system (Fig 9). Panteleyev (1995) proposes similar timing for the formation of the Equity Silver ores as a 'transitional' ore deposit, which form at moderate depths

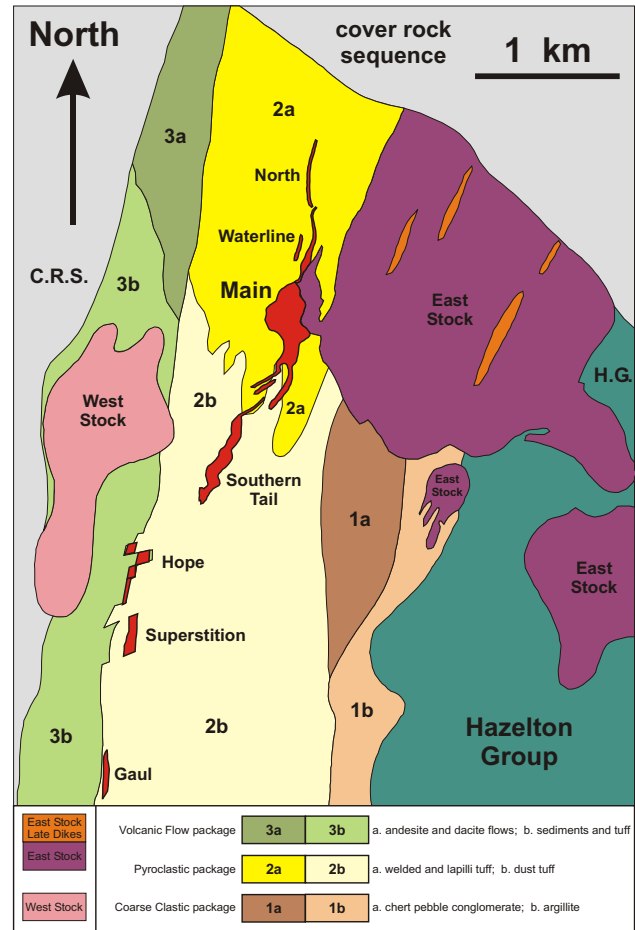


Figure 8. Geology map of the Equity Silver mine area (modified from company plans). Abbreviation: C.R.S., cover rock sequence.

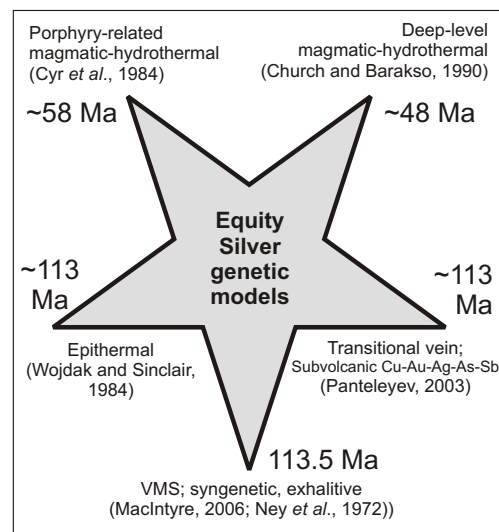


Figure 9. Schematic summary of five genetic models for ore formation at the Equity Silver mine.

(2–3 km), shallower than the setting for conventional porphyry copper deposits, but deeper than the setting for epithermal ore deposits (Fig 9).

In contrast, Ney *et al.* (1972) initially regarded the deposits as syngenetic volcanogenic massive sulphide deposits that were later deformed and recrystallized by the gabbro-monzonite intrusion (Fig 9). As an evolution from this early genetic model, MacIntyre (2001b) considered the largest individual ore zone (Main zone, 22 Mt) as the remains of an initially larger syngenetic, exhalative volcanogenic massive sulphide lens, which accumulated within the 113.5 Ma dacitic pyroclastic volcanic facies (Fig 10a). A portion of the syngenetic sulphide minerals of the Main zone were intruded by the western edge of the gabbro-monzonite intrusive complex and the sulphide minerals were remobilized and extensively redistributed both northward and southward along a north-northeast-trending fault zone that is parallel to the orientation of the late, planar, hypabyssal monzonite intrusive phase of the younger gabbro-monzonite intrusive complex (Fig 10b).

The following list restates all these proposed genetic models in light of the mid-Cretaceous age now established for the hostrocks volcanics at the mine (*see also* Fig 9):

- synvolcanic exhalative mineralization related to mid-Cretaceous volcanism, with later recrystallization and remobilization caused by the intrusion of the eastern Eocene stock;
- penecontemporaneous epithermal mineralization related to mid-Cretaceous volcanism, with later recrystallization and remobilization caused by the intrusion of the eastern Eocene stock;
- penecontemporaneous transitional (porphyry-epithermal transition) mineralization related to mid-Cretaceous volcanism, with later recrystallization and remobilization caused by the intrusion of the eastern Eocene stock;
- Eocene epigenetic mineralization related to the emplacement of the 58 Ma western quartz monzonite stock; and
- Eocene epigenetic mineralization related to the emplacement of the 48 Ma eastern gabbro-monzonite stock.

TABLE 3. MINERALOGY OF EQUITY SILVER ORE AND ALTERATION ZONES (FROM CYR ET AL., 1984).

Mineral ¹	Main	Southern Tail	Waterline	Cu-Mo Porphyry	Tourmaline
Pyrite	XXXXX	XXXXX	XXXXX	XXXX	XXXXX
Rutile	X	X	X	X	
Ilmenite	X	X			
Magnetite	XXXX	XXX	XXX	X	XX
Pyrrhotite	XXXX		XX		
Molybdenite		X	X	XXX	X
Specular hematite	XXXX	XX	XXX		X
Arsenopyrite	XX	XXXXX	X		
Sphalerite	XXX	XXX	XXX		XX
Chalcopyrite	XXXXX	XXXX	XXXX	XX	XX
Tetrahedrite	XXXX	XXXXX	XX	X	X
Gold	XX	X	XX		
Galena	XX	XX	XX		XX
Sulfosalts	XX	XX	X		
Marcasite	XXX		X		
Chalcocite	X	X		X	
Covellite	X	X			
Scheelite			X		
Wolframite		X			
Stibnite	X				
Corundum	XX				
Andalusite	XX	XX	XX		
Tourmaline	XXXX	X	XX	X	XXXXX
Dumortierite	XX				X
Scorzalite	XXX	X	XX		
Spinel	XX				
Chlorite	XXXX	XXXX	XXX	XX	XX

¹ listed in approximate order of paragenesis

XXXXX, very abundant; XXXX, abundant; XXX, moderate; XX, minor; X, trace

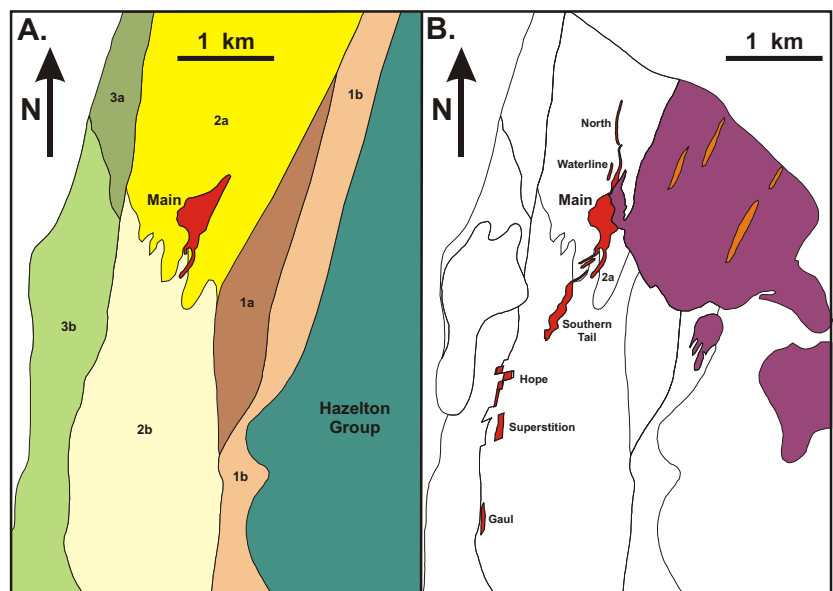


Figure 10. Two-stage genetic model for the formation of the Equity Silver deposits; a) mid-Cretaceous VMS deposit formed at Main zone; b) Eocene pluton intrudes, recrystallizes and remobilizes Main zone sulphide minerals along one of a series of fracture zones; see legend for Fig 8.

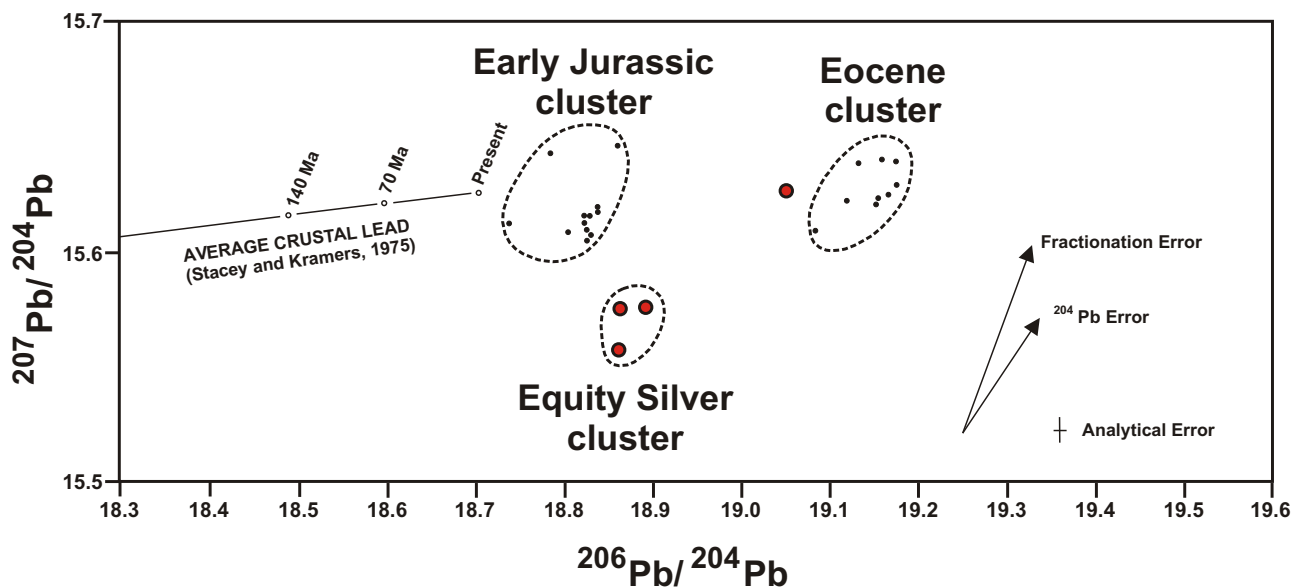


Figure 11. Galena Pb isotope data from the Equity Silver mine (data from Godwin *et al.*, 1988; chart from Alldrick, 1993).

Galena Pb isotope analyses of seven samples collected from different ore zones at the Equity Silver mine show a tight cluster of lead isotope ratios from three samples (Fig 11). This ‘Equity Silver’ cluster represents significantly older lead than the well-established lead analyses from several types of Eocene ore deposits (Fig 11; Alldrick, 1993). It is also younger than the lead isotope signatures obtained from many Early Jurassic ore deposits hosted by Hazelton Group island arc rocks (Fig 11; Alldrick, 1993). Since only Early Jurassic, mid-Cretaceous and Eocene rocks are present in the mine area, the data cluster from the three Equity Silver samples is interpreted as a mid-Cretaceous age. This means the lead initially crystallized in galena that was syngenetic with, or penecontemporaneous with, the mid-Cretaceous Skeena Group volcanic hostrocks (genetic models 1, 2 or 3 above). A single data point lies in the direction of the younger Eocene-age data cluster (Fig 11). This result suggests that, for this sample only, the primary mid-Cretaceous mineralization was likely remobilized by a later magmatic, hydrothermal and structural event that contributed some new lead to the mid-Cretaceous galena crystals in two of the analysis samples. This later event was most likely the intrusion of the large multiphase gabbro-monzonite intrusion that intrudes and displaces the Main zone orebody along its northeastern margin (Fig 10b). Remobilized sulphide minerals were displaced into north-northeast-trending fractures and/or faults that accompanied the later hypabyssal monzonite stage of emplacement of the multistage intrusion (Fig 10b).

Cyr *et al.* (1984) recognized that different parts of the Equity Silver ore zones and their different associated alteration suites have chemistry, mineralogy and textures that are characteristic of either epithermal or exhalative styles of ore deposits (Table 3). This is a consequence of sulphide deposition in and around a shallow-water volcanic edifice constructed on sediments of a deltaic sedimentary succession. Historically, epithermal and exhalative deposit types have been regarded as mutually exclusive mineralizing systems, but many years of detailed studies at the Eskay Creek gold mine (Roth, 2002) reveal that epithermal, exhalative

and even clastic sedimentary ore deposits can be deposited around the same long-lived hydrothermal system as the structural controls and the depositional environment change with time.

Fireweed (MINFILE 093M 151)

Sulphide minerals were discovered in outcrop at the Mn (manganese) and sphalerite (zinc) showings in 1987. Ongoing exploration work has defined 10 mineralized zones (Table 1) with a drill-indicated resource at the West Zone of 580 544 t grading 342 g/t silver, 2.22% zinc and 1.34% lead. The property geology is described in a recent comprehensive report by Price (2006).

Bedrock exposures are limited on the property. Extensive drilling reveals that the host strata is a succession of mudstone, siltstone and fine to coarse sandstone. Conglomerate and volcanic units are conspicuously absent. In this report, these strata are correlated with the Bulkley Canyon Formation of the Skeena Group.

Sedimentary rocks are cut by dikes or sills of felsic volcanic rock, variously termed ‘latite’, ‘quartz latite’ and ‘rhyolite’ in earlier reports. The dikes are light grey, fine-grained rhyolite porphyry with fine plagioclase phenocrysts and quartz eyes (Howell, pers comm, 2006). These intrusive rocks have previously been correlated with Eocene biotite-feldspar porphyritic intrusions and andesitic volcanic rocks of the Mount Newman Formation that crop out along the southern edge of the property (Price, 2006; MacIntyre, 2001a). MacIntyre *et al.* (2004) reinterpreted these felsic dike rocks as possible feeders to the mid-Cretaceous Rocky Ridge rhyolite domes mapped to the north. Three kilometres north of the Fireweed property, a large dome of Rocky Ridge rhyolite underlies the eastern half of McKendrick Island. A new age determination from a rhyolite dike collected from drillcore at the Fireweed property gives an age of 103.4 ± 0.4 Ma, confirming this correlation (MacIntyre and Villeneuve, 2007).

On the Fireweed property, the presence of these mid-Cretaceous subvolcanic rhyolite feeder dikes, the absence

of rhyolite domes and flows of the Rocky Ridge Formation and the absence of volcanoclastic conglomerate of the Kitsuns Creek Member, all support the interpretation that the sedimentary strata on the property are a section of the Bulkley Canyon Formation lying somewhere stratigraphically below the time-horizon of Rocky Ridge volcanics and Kitsuns Creek Member conglomerate of the upper Skeena Group.

Mineralization is polymetallic with variable amounts of silver, lead, zinc, copper and gold. The zones also have anomalous concentrations of manganese, cadmium, arsenic, tungsten and antimony. In order of abundance, sulphide minerals identified on the property are pyrite, pyrrhotite, sphalerite, chalcopyrite, galena, marcasite and tetrahedrite. The three main types of mineralization are

- breccia zones: fractured or brecciated sedimentary rock infilled with fine to coarse-grained massive pyrite-pyrrhotite and lesser sphalerite, chalcopyrite and galena.
- disseminated sulphide minerals: fine to very fine grains of pyrite, marcasite, sphalerite, galena and minor tetrahedrite are interstitial to sand grains in coarser-grained sandstone.
- massive sulphide minerals: fine-grained, commonly banded, massive sulphide minerals contain rounded quartz grains and fine fragments of sedimentary rocks, and form distinct bands within fine-grained sedimentary rocks. Composed of alternating bands of pyrite and pyrrhotite, with minor chalcopyrite, sphalerite and galena, these bands are typically associated with the breccia zones and are commonly sandwiched between the altered dikes. The term 'massive sulphide' does not imply any genetic process, *i.e.*, this style of mineralization does not necessarily indicate syngenetic or exhalative volcanogenic massive sulphide mineralization.

Knoll (MINFILE 093M 100)

The Knoll prospect is located 60 km north of Smithers, along the east bank of Harold Price Creek. Massive to flow-banded rhyolite crops out as a prominent dome (Wojdak and Ethier, 2000; MacIntyre, 2001b). This unit is locally spherulitic and is intercalated with rhyolite breccia and volcanoclastic conglomerate. Beyond this resistant dome, the surrounding strata is a sequence of feldspathic sandstone, carbonaceous mudstone and siltstone and thinly bedded felsic ash tuff. All these units are interpreted as part of the Skeena Group; the rhyolite is interpreted as Rocky Ridge Formation and is similar to the rhyolite domes exposed along the West Morrison logging road, north of Old Fort Mountain.

Discovered in 1983, mineralization consists of disseminations and veinlets of pyrite, sphalerite and galena hosted by the massive rhyolite, rhyolite breccia and lapilli tuff. Disseminated pyrite is widespread in the rocks of the rhyolite dome. Grab samples collected from outcrop returned high assays for lead, zinc and arsenic, elevated silver and cadmium, and anomalous levels of gold and copper. Seven holes were drilled on induced polarization targets in 1988. The best intersection was 1 m grading 0.51% Pb, 1.32% Zn, 9.58% As, 30 ppm Ag and 1610 ppb Au. In 2006, a soil sampling program was completed over the property.

ESK

ESK is a new sulphide discovery hosted by the black felsic fragmental unit that envelops the series of prominent rhyolite domes near the West Morrison logging road, northern Babine Lake. At this showing on the south side of the rhyolite ring, the distinctive black-matrix, white-rhyolite-clast volcanic breccia stratigraphically overlies the massive white rhyolite domes (Fig 7). The same breccia texture is also well exposed, stratigraphically underlying the same rhyolite domes, along the north side of the ring of rhyolite domes. Mineralization consists of 2 to 4% fine disseminated sulphide minerals in clast-rich rhyolite breccia to crackle breccia of flow-banded rhyolite. Best assays are 172 ppm Zn, 14 ppm Pb, 5 ppm Cu, 278 ppb Ag, 6 ppb Au, 77 ppm As and 1116 ppb Hg.

BQ

BQ was discovered by prospecting in 1994, but saw little work until 2006 when trenching, geophysical surveying (induced polarization) and two drill programs were completed. Sediment-hosted sulphide mineralization is localized along steep fractures adjacent to dikes of locally flow-banded quartz-feldspar porphyritic rhyolite and aphanitic rhyolite (Watkins, 2005). Sedimentary strata exposed in the local area include micaceous sandstone and grit, black carbonaceous siltstone and shale. Sulphide minerals form individual veins, vein networks, replacement zones and scattered blebs of pyrite, arsenopyrite, pyrrhotite, sphalerite and chalcopyrite distributed over a 400 m long zone of fracturing, adjacent to a prominent rhyolite dike. A broad sericite-quartz-carbonate-clay alteration zone is overprinted on the fractured to locally brecciated sedimentary hostrock. Best assay intervals from 11 drillholes completed to date include 7.31 g/t Au over 1.3 m, 0.776 g/t Au over 233.05 m and 4.18% Zn over 1.0 m.

The age of this fracture-hosted mineralization and the adjacent felsic dike has not been determined; a sample collected by MacIntyre and Villeneuve (2007) produced insufficient zircons for dating. The dike is texturally similar to a 10 km long rhyolite sill that crops out as a prominent ridge along the north side of the Kitseguella Lake Road. The northern edge of this sill crops out just 500 m south of the main roadside showing on the BQ prospect. This large sill locally displays tiny quartz eyes, hosts minor very fine disseminated pyrite, shows distinctive flow-banding along its northern margin that trends north (perpendicular to the east-west trend of the main sill) and closely resembles the rhyolite exposed in the string of rhyolite domes along the West Morrison logging road.

French Peak (MINFILE 093M 015)

The French Peak deposits include the Ute, Rio, Mud and Hematite prospects. Mineralization consists of quartz-siderite veins and mineralized shear zones hosting tetrahedrite, galena, chalcopyrite, sphalerite and pyrite. A resource of 2630 t grading 411 g/t Ag, 2.4 g/t Au, 14% Pb and 5% Cu was calculated for the property. The 2006 exploration program completed 11 drillholes totalling 1445 m on the Ute and Rio showings.

The rhyolite, dacite, andesite and basalt hostrocks, termed 'French Peak volcanics', have previously been classified as Kasalka Group rocks, but a new $^{40}\text{Ar}/^{39}\text{Ar}$ date of 99.3 ± 2.3 Ma (MacIntyre and Villeneuve, 2007) on augite-

phyric basalt shows that these rocks are volcanics of the Rocky Ridge Formation, Skeena Group.

CURRENT EXPLORATION

Exploration programs within Skeena Group volcanic rocks during 2006 included initial drilling on the BQ claims northeast of Kitsegucla Lake, follow-up drilling on the Fireweed property southeast of Smithers Landing and on the French Peak property west-northwest of Fort Babine, a soil sampling grid over the Knoll property and prospecting on the ESK claims northwest of Old Fort Mountain (Fig 4). The Superstition Creek prospect, just south of the Equity Silver mine (Fig 8), was drilled in 2004.

METALLOGENIC MODELS

The bimodal volcanic units of the Skeena Group have recently been interpreted as evidence for a caldera setting (MacIntyre, 2001b), which is the optimal setting for the formation and preservation of alkaline epithermal mineral deposits (Fig 12; Hedenquist and White, 2005). Previously, these same volcanic rocks were identified as products of rifting (Barrett and Kleinspehn, 1996), which is the optimal setting for the development of subaerial Bonanza-type epithermal deposits and subaqueous exhalative mineralization (Sillitoe, 2002; Sillitoe and Hedenquist, 2003; Hedenquist and White, 2005). On a larger scale, the tectonic setting for the Skeena Group was interpreted as an active continental margin (fore arc) tectonic setting (Barrett and Kleinspehn, 1997), similar to the world's greatest VMS district, the Devonian-Mississippian Iberian Pyrite Belt (White, 1999). These contrasting metallogenic models are summarized in Table 4.

DISCUSSION

A bimodal volcanic succession must display a simple or complex alternating sequence of basalt and rhyolite flows in close association. Andesite and dacite units should be conspicuously absent. There is no exposure of bimodal volcanic rocks *sensu stricto* in any of the Rocky Ridge volcanic sections examined in the field this season or presented in the literature. This term may have evolved when the black, carbonaceous dacitic lapilli tuff that envelops the rhyolite domes along West Morrison logging road were misidentified as 'basalt' during the initial mapping program (unit lKvb in MacIntyre *et al.*, 1997a). A close spatial association between rhyolite and basalt flows is exposed in outcrops southeast of the pit at the Bell mine, but the rhyolite and basalt units are juxtaposed across a major fault break. There are basalt flows and tuff exposed several hundred metres stratigraphically above the rhyolite 'domes' exposed along the West Morrison (Fig 7) and Kitsegucla Lake roads. However, the intervening strata are thick successions of fine to coarse clastic sedimentary rocks of the

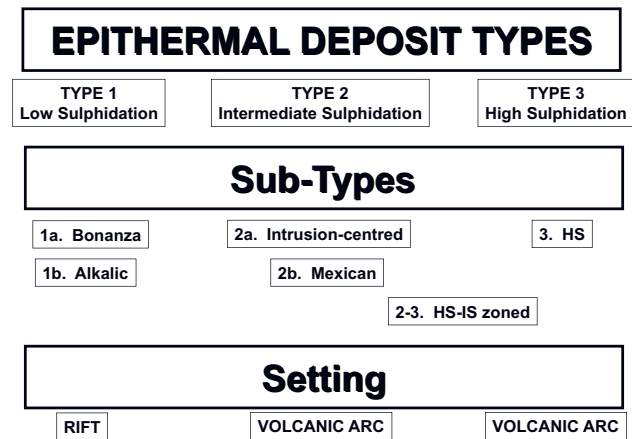


Figure 12. Classification system for epithermal ore deposits (Hedenquist and White, 2005).

upper Skeena Group, indicating a substantial passage of time between volcanic eruptions.

Volcanic rocks that accumulate in caldera settings are characteristically bimodal and alkaline, while the upper, younger, basalt units of the Rocky Ridge Formation are alkaline, underlying rhyolite, andesite and dacite units are consistently calcalkaline (Tackaberry, 1998). Taken together, these points indicate that none of Rocky Ridge volcanism erupted in a caldera setting.

Volcanic rocks that accumulate in rift settings are also characteristically bimodal (Sillitoe, 2002) and are usually preserved as thick successions of complexly interlayered basalt, rhyolite and siltstone. There are no volcanic intervals anywhere within Skeena Group strata that resemble typical rift-fill successions or distribution patterns (thick, linear, volcanic-filled troughs).

The points above indicate that it is unlikely that the geological setting for the deposition of the volcanic rocks within the Skeena Group is either a caldera or rift structure.

Other possible settings are within a fore arc, in a back arc rift (marginal basin) or within an intracratonic rift. Fore arc volcanism is extremely rare and is characterized by linear arrays of volcanic centres (Cees van Staal, pers comm, 2006). Intercontinental rifts are characterized by bimodal volcanic rocks and often provide the setting for abundant exhalative (volcanogenic massive sulphide) mineralization (*e.g.*, the Iberian Pyrite Belt). Since these characteristic features are not in evidence in the volcanic strata of the Rocky Ridge Formation, these two tectonic settings are also considered unlikely.

In contrast to the above models, the concept of a nascent, continental margin volcanic arc that does not fully develop (MacIntyre *et al.*, 2004) is a good fit with the documented features of Rocky Ridge volcanism. The early onset of differentiated calcalkaline andesite, dacite and rhyolite volcanism from widely scattered volcanic centres was fol-

TABLE 4. METALLOGENIC MODELS PROPOSED FOR THE SKEENA GROUP.

Tectonic model	Proposed by	Associated deposit types	Reference
Caldera	MacIntyre, 2001b	Alkaline epithermal	Hedenquist and White (2005)
Rift	Bassett and Kleinspehn, 1996	Epithermal and VMS	Sillitoe (2002)
Continental margin, fore arc	Bassett and Kleinspehn, 1996	VMS	White (1999)

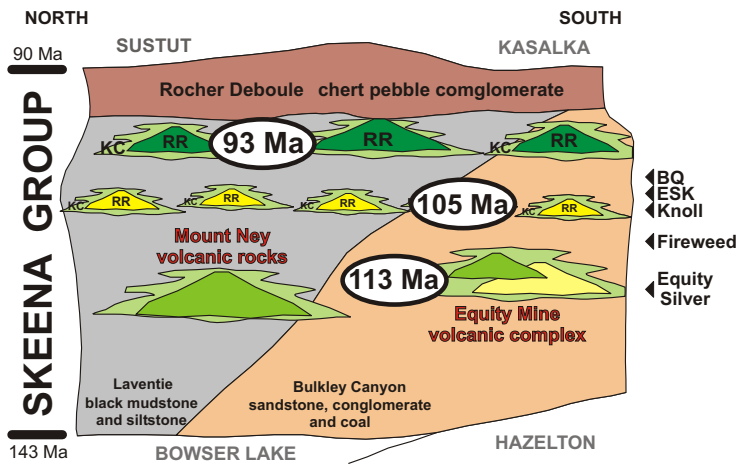


Figure 13. Schematic stratigraphy of Skeena Group (modified from Bassett and Kleinspehn, 1997), showing the relative position of the Equity Mine and Mount Ney volcanic complexes and relative stratigraphy position of key mineral prospects. Abbreviations: RR, Rocky Ridge Formation; KC, Kitsuns Creek Member.

lowed by an episode of alkaline basaltic volcanism. Then, all volcanic activity terminated during the period of deposition of the Rocher Deboule Formation. In the Late Devonian volcanic succession of the Finlayson Lake district of the Yukon Territory, Piercey *et al.* (2002) attribute the change from initial felsic calcalkaline to younger mafic alkaline volcanism to the interruption of an initial period of typical subduction by subduction hinge roll-back, which triggered back arc rifting. Within the Skeena Group, the onset of alkaline basalt volcanism near the end of Rocky Ridge Formation time may have marked the initiation of back arc rifting, but further rifting and its associated volcanism ceased abruptly about 93 Ma.

The other tectonic and metallogenic model that may apply puts the entire mid-Cretaceous Rocky Ridge volcanic succession in an incipient back arc rift setting, lying east of the Gambier volcanic arc, which remained active throughout the Early and mid-Cretaceous.

CONCLUSIONS

Toward the end of Skeena Group sedimentation, a 20-million-year period (113–93 Ma) of intermittent volcanism evolved from intermediate to felsic to alkaline mafic composition. Most volcanic piles were built on deltaic alluvial fans and were locally emergent, with the base of each volcano submerged and the surrounding volcanoclastic debris apron deposited in shallow marine settings. The youngest (93 Ma) mafic volcanic units have no associated mineralization (Fig 13). The intermediate age (108–104 Ma) rhyolite volcanic rocks have minor to significant mineralization associated with subvolcanic feeder dikes, sills and cryptodomes. The oldest (113 Ma) andesitic to dacitic volcanic piles have associated economic concentrations of silver, copper and gold.

The Equity Silver deposit is poorly exposed in outcrop. Its discovery was the result of the follow-up of multiphase geochemical surveys and boulder tracing (Ney *et al.*, 1972). Within the Skeena Group, the Mount Ney volcanics are a broad expanse of intermediate composition volcanic sequences with similar age as the Equity Silver mine volcanics (Fig 14). A strategy committed to systematic, sequential reconnaissance and follow-up exploration programs through this region would be necessary to zero in on a similar target.

BIBLIOGRAPHY

- Alldrick, D.J. (1993): Geology and metallogeny of the Stewart mining camp, northwestern BC; *BC Ministry of Energy, Mines and Petroleum Resources*, Bulletin 85, 105 pages.
- Armstrong, J.E. (1944a): Preliminary map, Smithers, British Columbia; *Geological Survey of Canada*, Paper 44-23, scale 1:126 720.
- Armstrong, J.E. (1944b): Preliminary map, Hazelton, British Columbia; *Geological Survey of Canada*, Paper 44-24, scale 1:126 720.
- Armstrong, J.E. and Kindle, K.D. (1952): Preliminary map, Hazelton, British Columbia; *Geological Survey of Canada*, Paper 44-24 (revised), scale 1:126 720.

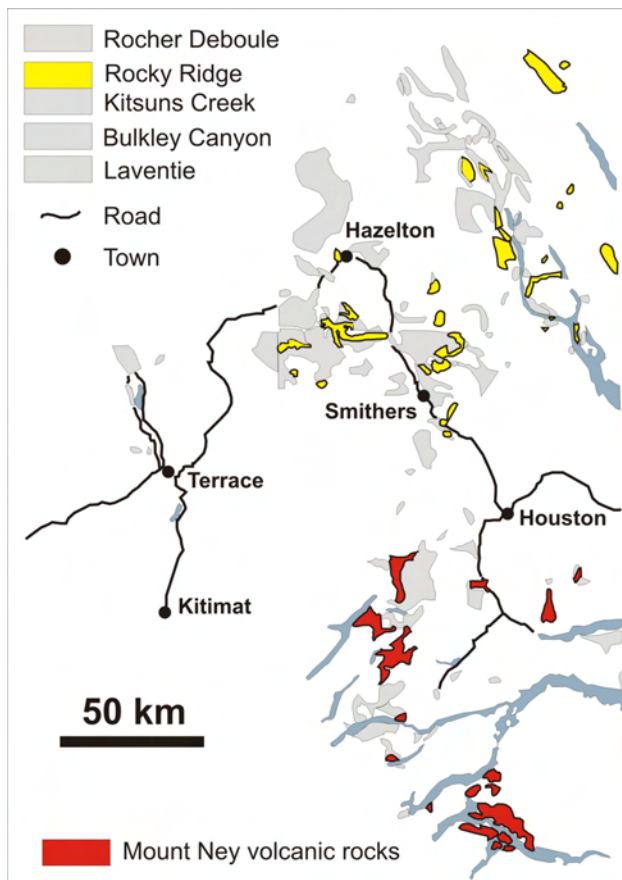


Figure 14. Distribution of the younger Rocky Ridge (rhyolite-basalt) and older Mount Ney (andesite-dacite) volcanic packages of the Skeena Group (modified from Bassett and Kleinspehn, 1997; Diakow, 2006).

- Bassett, K.N. (1991): Preliminary results of the sedimentology of the Skeena Group in west-central British Columbia; in Current Research, Part A, *Geological Survey of Canada*, Paper 91-1A, pages 131–141.
- Bassett, K.N. (1995): A basin analysis of the lower to mid-Cretaceous Skeena Group, west-central British Columbia – implications for regional tectonics and terrane accretion; *University of Minnesota*, unpublished PhD thesis, 413 pages.
- Bassett, K.N. and Kleinspehn, K.L. (1996): Mid-Cretaceous transtension in the Canadian Cordillera – evidence from the Rocky Ridge volcanics of the Skeena Group; *Tectonics*, Volume 15, pages 727–746.
- Bassett, K.N. and Kleinspehn, K.L. (1997): Early to middle Cretaceous paleogeography of north-central British Columbia – stratigraphy and basin analysis of the Skeena Group; *Canadian Journal of Earth Sciences*, Volume 34, pages 1664–1669.
- Church, B.N. (1973): Geology of the Owen Lake, Parrott Lakes, Goosly Lake area, Omineca Mining Division, British Columbia; *BC Ministry of Energy, Mines and Petroleum Resources*, Preliminary Map No. 13A, scale 1:50 000.
- Church, B.N. (1984): Update on the geology and mineralization in the Buck Creek area – the Equity Silver mine revisited; in Geological Fieldwork 1984, *BC Ministry of Energy, Mines and Petroleum Resources*, Paper 1985-1, pages 175–188.
- Church, B.N. (1986): The Bob Creek gold-silver prospect (93L); in Geological Fieldwork 1985, *BC Ministry of Energy, Mines and Petroleum Resources*, Paper 1986-1, pages 121–124.
- Church, B.N. (1990): Geology of the Buck Creek Tertiary outlier; *BC Ministry of Energy, Mines and Petroleum Resources*, coloured map included in Paper 1990-2, scale 1:100 000.
- Church, B.N. and Barakso, J.J. (1990): Geology, lithochemistry and mineralization in the Buck Creek area, British Columbia; *BC Ministry of Energy, Mines and Petroleum Resources*, Paper 1990-2, 95 pages.
- Church, B.N. and Klein, G.H. (1998): The Allin property and Equity-type mineralization, central British Columbia; in Geological Fieldwork 1997, *BC Ministry of Energy, Mines and Petroleum Resources*, Paper 1998-1, pages 23-1–23-10.
- Cook, S., Levson, V., Jackaman, W., Law, D. and Douville, M. (2000): Regional geochemical compilation – Babine porphyry belt (NTS 1040/13); *BC Ministry of Energy, Mines and Petroleum Resources*, Open File 2000-24, 9 map sheets, scale 1:100 000.
- Cyr, J.B., Pease, R.B. and Schroeter, T. (1984): Geology and mineralization at Equity Silver mine; *Economic Geology*, Volume 79, pages 947–968.
- Dawson, G.M. (1881): On the geology of the region between the 54th and 56th parallels, from the Pacific Coast to Edmonton; in Report on an Exploration from Port Simpson on the Pacific Coast, to Edmonton on the Saskatchewan, Embracing a Portion of the Northern Part of British Columbia, and the Peace River country; *Geological Survey of Canada*, Report on Progress 1879–1880, pages 99B–142B.
- Desjardins, P. and Arksey, R. (1991): Geology of the Lamprey Creek area; *BC Ministry of Energy, Mines and Petroleum Resources*, Open File 1991-1, scale 1:50 000.
- Desjardins, P., Arksey, R.L. and MacIntyre, D.G. (1991): Geology of the Lamprey Creek mapsheet (NTS 93L/03); in Geological Fieldwork 1990, *BC Ministry of Energy, Mines and Petroleum Resources*, Paper 1991-1, pages 111–119.
- Desjardins, P., Lyons, L., Pattenden, S., MacIntyre, D.G. and Hunt, J. (1990a): Geology of the Thautil River area; *BC Ministry of Energy, Mines and Petroleum Resources*, Open File 1990-5, scale 1:50 000.
- Desjardins, P., MacIntyre, D.G., Hunt, J., Lyons, L. and Pattenden, S. (1990b): Geology of the Thautil River map area (NTS 93L/06); in Geological Fieldwork 1989, *BC Ministry of Energy, Mines and Petroleum Resources*, Paper 1990-1, pages 91–99.
- Diakow, L.J. (1990): Geology of Nanika Lake map area (NTS 93E/13); in Geological Fieldwork 1989, *BC Ministry of Energy, Mines and Petroleum Resources*, Paper 1990-1, pages 83–89.
- Diakow, L.J. (2006): Geology of the Tahtsa Ranges between Eutsuk Lake and Morice Lake, Whitesail Lake map area, west-central British Columbia; *BC Ministry of Energy, Mines and Petroleum Resources*, Geoscience Map 2006-5, scale 1:150 000.
- Diakow, L.J. and Drobe, J. (1989a): Geology and mineral occurrences in north Newcombe Lake mapsheet; *BC Ministry of Energy, Mines and Petroleum Resources*, Open File 1989-1, scale 1:50 000.
- Diakow, L.J. and Drobe, J. (1989b): Geology and mineral occurrences in north Newcombe Lake mapsheet (NTS 93E/14); in Geological Fieldwork 1988, *BC Ministry of Energy, Mines and Petroleum Resources*, Paper 1989-1, pages 183–188.
- Diakow, L.J. and Koyanagi, V. (1988): Stratigraphy and mineral occurrences of the Chikamin Mountain and Whitesail Reach map areas (NTS 93E/06, 10); in Geological Fieldwork 1987, *BC Ministry of Energy, Mines and Petroleum Resources*, Paper 1988-1, pages 155–168.
- Diakow, L.J. and Mihalynuk, M. (1987): Geology of Whitesail Reach and Troitsa Lake map areas (NTS 93E/10W, 11E); in Geological Fieldwork 1986, *BC Ministry of Energy, Mines and Petroleum Resources*, Paper 1987-1, pages 171–179.
- Duffell, S. and Souther, J.G. (1964): Geology of Terrace map area, British Columbia (NTS 1031 east half); *Geological Survey of Canada*, Memoir 329, 117 pages.
- Evenchick, C.A., Mustard, P.S., Woodsworth, G.J. and Ferri, F. (2004): Compilation of geology of Bowser and Sustut Basins draped on shaded relief map, north-central British Columbia; *Geological Survey of Canada*, Open File 4638, scale 1:500 000.
- Evenchick, C.A. and Thorkelson, D.J. (2005): Geology of the Spatsizi River map area, north-central British Columbia; *Geological Survey of Canada*, Bulletin 577, 276 pages.
- Ferri, F., Mustard, P.S., McMechan, M., Ritcey, D., Smith, G.T., Boddy, M. and Evenchick, C.A. (2005): Skeena and Bowser Lake Groups, west half Hazelton map area (NTS 93M); in Summary of Activities 2005, *BC Ministry of Energy, Mines and Petroleum Resources*, URL <<http://www.em.gov.bc.ca/subwebs/oilandgas/pub/reports/summary2005.htm>>, pages 113–131.
- Fingler, J. (2004): Silver Hope project surface geology map; in Report on the 2004 diamond drilling program–Silver Hope property; *BC Ministry of Energy, Mines and Petroleum Resources*, AR27862, scale 1:10 000.
- Gaba, R.G., Desjardins, P. and MacIntyre, D.G. (1992): Mineral potential investigations in the Babine mountains recreation area (NTS 93L/14E, 15W; 93M/2W); in Geological Fieldwork 1991, *BC Ministry of Energy, Mines and Petroleum Resources*, Paper 1992-1, pages 93–101.
- Galloway, J.D. (1914): Rocher Deboule camp; *BC Ministry of Energy, Mines and Petroleum Resources*, Minister of Mines Annual Report, pages 184–193.
- Galloway, J.D. (1916): Rocher Deboule camp; *BC Ministry of Energy, Mines and Petroleum Resources*, Minister of Mines Annual Report, pages 106–119.
- Godwin, C.I., Gabites, J.E. and Andrew, A. (1988): Leadtable – a galena lead isotope database for the Canadian Cordillera; *BC Ministry of Energy, Mines and Petroleum Resources*, Paper 1988-4, 188 pages.

- Hanson, G. (1924a): Driftwood Creek map area, Babine Mountains; *Geological Survey of Canada*, Summary Report 1924, Part A, pages 19–37.
- Hanson, G. (1924b): Prince Rupert to Burns Lake; *Geological Survey of Canada*, Summary Report 1924, Part A, pages 38–43.
- Hanson, G. (1925): Reconnaissance in the Zymoetz River area; *Geological Survey of Canada*, Summary Report 1925, Part A, pages 100–119.
- Hedenquist, J.W. and White, N.C. (2005): Epithermal gold-silver ore deposits – characteristics, interpretation and exploration; *Prospectors and Developers Association of Canada*, Short course notes, March 2005, 378 pages.
- Hedenquist, J.W. and Sillitoe, R.H. (2003): Alteration, degradation, and slope failure of volcanoes; abstract, *Geological Society of America Annual Meeting*, Seattle, Washington, 2–5 November 2003, Program with Abstracts, Volume 33.
- Hunt, J.A. (1992): Stratigraphy, maturation and source rock potential of Cretaceous strata in the Chilcotin – Nechako region of British Columbia; *The University of British Columbia*, unpublished MSc thesis, 447 pages.
- Jones, R.H.B. (1925): Geology and ore deposits of Hudson Bay Mountain; *Geological Survey of Canada*, Summary Report 1925, Part A, pages 120–143.
- Kerr, F.A. (1936): Mineral resources along the Canadian National Railway between Prince Rupert and Prince George; *Geological Survey of Canada*, Paper 36–20.
- Kindle, K.D. (1954): Mineral resources, Hazelton and Smithers areas, Cassiar and Coast districts, British Columbia; *Geological Survey of Canada*, Memoir 223, 148 pages.
- Koo, J. (1984): Telkwa coalfield, west-central British Columbia (NTS 93L); in *Geological Fieldwork 1982*, *BC Ministry of Energy, Mines and Petroleum Resources*, Paper 1983-1, pages 113–121.
- Koo, J. (1984): The Telkwa, Red Rose and Klappan coal measures in northwestern British Columbia (NTS 93L, 93M, 104H); in *Geological Fieldwork 1983*, *BC Ministry of Energy, Mines and Petroleum Resources*, Paper 1984-1, pages 81–90.
- Lang, A.H. (1929): Owen Lake mining camp, British Columbia; *Geological Survey of Canada*, Summary Report 1928, Part A, pages 62A–93A.
- Lang, A.H. (1940): Houston map area, British Columbia; *Geological Survey of Canada*, Paper 40–18.
- Lang, A.H. (1942): Houston area, British Columbia; *Geological Survey of Canada*, Map 671A.
- Leech, W.W. (1907): The Telkwa River and vicinity, British Columbia; *Geological Survey of Canada*, Publication 988.
- Leech, W.W. (1909): Bulkley valley and vicinity; *Geological Survey of Canada*, Summary Report 1908, pages 41–45.
- Leech, W.W. (1910): Skeena River District; *Geological Survey of Canada*, Summary Report 1909, pages 61–68.
- Leech, W.W. (1911): Skeena River District; *Geological Survey of Canada*, Summary Report 1910, pages 91–101.
- Leitch, C.H.B., Hood, C.T., Cheng, X. and Sinclair, A.J. (1990): Geology of the Silver Queen mine area, Owen Lake, central British Columbia (NTS 93L); in *Geological Fieldwork 1989*, *BC Ministry of Energy, Mines and Petroleum Resources*, Paper 1990-1, pages 287–295.
- Levson, V.M., Cook, S.J., Hobday, J., Huntley, D.H., O'Brien, E.K., Stumpf, A.J. and Weary, G.W. (1997): Till geochemistry of the Old Fort Mountain map area, north central British Columbia (NTS 93M/011); *BC Ministry of Energy, Mines and Petroleum Resources*, Open File 1997-10a, 3 data tables.
- MacIntyre, D.G. (1985a): Geology and mineral deposits of the Tahtsa Lake district, west-central British Columbia; *BC Ministry of Energy, Mines and Petroleum Resources*, Bulletin 75, 82 pages.
- MacIntyre, D.G. (1985b): Geology of the Dome Mountain gold camp; in *Geological Fieldwork 1984*, *BC Ministry of Energy, Mines and Petroleum Resources*, Paper 1985-1, pages 193–213.
- MacIntyre, D.G. (1998): Babine porphyry belt project – bedrock geology of the Nakinilerak Lake map sheet (93M/8), British Columbia; in *Geological Fieldwork 1997*, *BC Ministry of Energy, Mines and Petroleum Resources*, Paper 1998-1, pages 2-1–2-18.
- MacIntyre, D.G. (2001a): Geological compilation map – Babine porphyry copper district, central British Columbia (NTS 93L/09,16; 93M/01,02E,07E,08); *BC Ministry of Energy, Mines and Petroleum Resources*, Open File 2001-3, scale 1:100 000.
- MacIntyre, D.G. (2001b): The mid-Cretaceous Rocky Ridge Formation – a new target for subaqueous hot-spring deposits (Eskay Creek type) in central British Columbia; in *Geological Fieldwork 2000*, *BC Ministry of Energy, Mines and Petroleum Resources*, Paper 2001-1, pages 253–268.
- MacIntyre, D.G. (2006): Geology and mineral deposits of the Skeena arch, west-central British Columbia – a Geoscience BC digital data compilation project; in *Geological Fieldwork 2005*, *BC Ministry of Energy, Mines and Petroleum Resources*, Paper 2006-1, pages 303–312.
- MacIntyre, D.G., Ash, C.H., Britton, J.B., Kilby, W. and Grunsky, E. (1995): Mineral potential assessment of the Skeena-Nass area (NTS 93E, 93L, 93M, 94D, 103G, 103H, 103I, 103J, 103O, 103P, 104A, 104B); in *Geological Fieldwork 1994*, *BC Ministry of Energy, Mines and Petroleum Resources*, Paper 1995-1, pages 459–468.
- MacIntyre, D.G., Brown, D., Desjardins, P. and Mallett, P. (1987a): Geology of the Dome Mountain area (NTS 93L10/15); *BC Ministry of Energy, Mines and Petroleum Resources*, Open File 1987-1, scale 1:20 000.
- MacIntyre, D.G., Brown, D., Desjardins, P. and Mallett, P. (1987b): Babine project; in *Geological Fieldwork 1986*, *BC Ministry of Energy, Mines and Petroleum Resources*, Paper 1987-1, pages 201–222.
- MacIntyre, D.G. and Desjardins, P. (1988a): Geology of the Silver King – Mount Cronin area, Babine Range, west-central British Columbia (NTS 93L15); *BC Ministry of Energy, Mines and Petroleum Resources*, Open File 1988-20, scale 1:20 000.
- MacIntyre, D.G. and Desjardins, P. (1988b): Babine project; in *Geological Fieldwork 1987*, *BC Ministry of Energy, Mines and Petroleum Resources*, Paper 1988-1, pages 181–193.
- MacIntyre, D.G., Desjardins, P. and Tercier, P. (1989a): Jurassic stratigraphic relationships in the Babine and Telkwa ranges (NTS 93L/10, 11, 14, 15); in *Geological Fieldwork 1988*, *BC Ministry of Energy, Mines and Petroleum Resources*, Paper 1989-1, pages 195–208.
- MacIntyre, D.G., Desjardins, P., Tercier, P. and Koo, J. (1989b): Geology of the Telkwa River area (NTS 93L/11); *BC Ministry of Energy, Mines and Petroleum Resources*, Open File 1989-16, scale 1:50 000.
- MacIntyre, D.G., McMillan, R.H. and Villeneuve, M.E. (2004): The mid-Cretaceous Rocky Ridge Formation – important host rocks for VMS and related deposits in central British Columbia; in *Geological Fieldwork 2003*, *BC Ministry of Energy, Mines and Petroleum Resources*, Paper 2004-1, pages 231–247.
- MacIntyre, D.G., Schiarizza, P. and Struik L.C. (1998): Preliminary bedrock geology of the Tochcha Lake map area, British Columbia (NTS 93K/13); in *Geological Fieldwork 1997*, *BC Ministry of Energy, Mines and Petroleum Resources*, Paper 1998-1, pages 3-1–3-13.

- MacIntyre, D.G. and Struik, L.C. (1997): Nechako Natmap Project – 1996; in *Geological Fieldwork 1996, BC Ministry of Energy, Mines and Petroleum Resources*, Paper 1997-1, pages 39–45.
- MacIntyre, D.G. and Struik, L.C. (1999): Nechako NATMAP project, central British Columbia – 1998 overview; in *Geological Fieldwork 1998, BC Ministry of Energy, Mines and Petroleum Resources*, Paper 1999-1, pages 1–13.
- MacIntyre, D.G. and Struik, L.C. (2000): Nechako NATMAP project, central British Columbia – 1999 overview; in *Geological Fieldwork 1999, BC Ministry of Energy, Mines and Petroleum Resources*, Paper 2000-1, pages 7–13.
- MacIntyre, D.G. and Villeneuve, M.E. (2001): Geochronology of mid-Cretaceous to Eocene magmatism, Babine porphyry copper district, central British Columbia; *Canadian Journal of Earth Sciences*, Volume 38, pages 639–655.
- MacIntyre, D.G. and Villeneuve, M.E. (2007): Geochronology of the Rocky Ridge volcanics, Skeena Group, British Columbia; *BC Ministry of Energy Mines and Petroleum Resources*, Geofile 2007-4.
- MacIntyre, D.G., Villeneuve, M.E. and Schiarizza, P. (2001a): Timing and tectonic setting of Stikine Terrane magmatism, Babine – Takla lakes area, central British Columbia; *Canadian Journal of Earth Sciences*, Volume 38, pages 579–601.
- MacIntyre, D.G., Webster, I.C.L. and Bellefontaine, K.A. (1996a): Babine porphyry belt project – bedrock geology of the Fulton Lake map area, north-central British Columbia (NTS 93L/16); *BC Ministry of Energy, Mines and Petroleum Resources*, Open File 1996-29, scale 1:50 000.
- MacIntyre, D.G., Webster, I.C.L. and Bellefontaine, K.A. (1996b): Babine porphyry belt project – bedrock geology of the Fulton Lake map area, British Columbia (NTS 93L/16); in *Geological Fieldwork 1995, BC Ministry of Energy, Mines and Petroleum Resources*, Paper 1996-1, pages 11–35.
- MacIntyre, D.G., Webster, I.C.L. and Desjardins, P. (1997a): Bedrock geology of the Old Fort Mountain area, northwestern British Columbia (NTS 93M/1); *BC Ministry of Energy, Mines and Petroleum Resources*, Open File 1997-10, scale 1:50 000.
- MacIntyre, D.G., Webster, I.C.L. and Villeneuve, M. (1997b): Babine porphyry belt project – bedrock geology of the Old Fort Mountain area (93M/1), British Columbia; in *Geological Fieldwork 1996, BC Ministry of Energy, Mines and Petroleum Resources*, Paper 1997-1, pages 47–67.
- Malloch, G.S. (1914): Metalliferous deposits in the vicinity of Hazelton; *Geological Survey of Canada*, Summary Report 1912, pages 102–107.
- McConnell, R.G. (1914): Geological section along the Grand Trunk Pacific Railway from Prince Rupert to Aldermere, British Columbia; *Geological Survey of Canada*, Summary Report 1912, pages 55–62.
- MINFILE (2005): MINFILE BC mineral deposits database; *BC Ministry of Energy, Mines and Petroleum Resources*, URL <<http://www.em.gov.bc.ca/Mining/Geosurv/Minfile/>> [December 2006].
- Ney, C.S., Anderson, J.M. and Panteleyev, A. (1972): Discovery, geological setting and style of mineralization, Sam Goosly deposit, British Columbia; *Canadian Institute of Mining and Metallurgy Bulletin*, Volume 65, Number 723, pages 53–64.
- O'Neill, J.J. (1919): Preliminary report on the economic geology of Hazelton district, British Columbia; *Geological Survey of Canada*, Memoir 110, 50 pages.
- Palsgrove R.J. and Bustin, R.M. (1990): Stratigraphy and sedimentology of the lower Skeena Group, Telkwa coalfield, central British Columbia (NTS 93L/11); in *Geological Fieldwork 1989, BC Ministry of Energy, Mines and Petroleum Resources*, Paper 1990-1, pages 449–454.
- Panteleyev, A. (1995): Subvolcanic Cu-Au-Ag-As-Sb; *BC Ministry of Energy, Mines and Petroleum Resources*, Mineral Deposit Profiles, Number L01, 4 pages.
- Piercey, S.J., Mortensen, J.K., Murphy, D.C., Paradis, S. and Creaser, R.A. (2002): Geochemistry and tectonic significance of alkalic mafic magmatism in the Yukon-Tanana Terrane in the Finlayson Lake region, Yukon, Canada; *Canadian Journal of Earth Sciences*, Volume 40, pages 77–97.
- Piercey, S.J., Paradis, S., Murphy, D.C. and Mortensen, J.K. (2001): Geochemistry and paleotectonic setting of felsic volcanic rocks in the Finlayson Lake volcanic-hosted massive sulphide district, Yukon, Canada; *Economic Geology*, Volume 96, pages 1877–1905.
- Price, B.J. (2006): Technical report on the Fireweed silver-lead-zinc deposit; *BC Ministry of Energy, Mines and Petroleum Resources*, AR28161, 71 pages.
- Richards, T.A. (1980): Geology of Smithers map area (NTS 93L); *Geological Survey of Canada*, Open File 351, scale 1:126 720.
- Richards, T.A. (1990): Geology of Hazelton map area (NTS 93M); *Geological Survey of Canada*, Open File 2322, scale 1:250 000.
- Richards, T.A., Woodsworth, G.J. and Tipper, H.W. (1997): Geology of Hazelton map area (NTS 93M), British Columbia; *Geological Survey of Canada*, Map 1852A (unpublished), scale 1:250 000.
- Robertson, W.F. (1911): Mineral claims in the Hazelton district; *BC Ministry of Energy, Mines and Petroleum Resources*, Minister of Mines Annual Report, pages 95–99.
- Roddick, J.A. (1970): Douglas Channel – Hecate Strait map area (103H, 103G E half), British Columbia; *Geological Survey of Canada*, Paper 70-41.
- Roth, T. (1993): Geology, alteration and mineralization in the Eskay Creek 21A zone, northwestern British Columbia, Canada; *The University of British Columbia*, unpublished MSc thesis, 230 pages.
- Roth, T. (2002): Physical and chemical constraints on mineralization in the Eskay Creek deposit, northwestern British Columbia – evidence from petrography, mineral chemistry and sulfur isotopes; *The University of British Columbia*, unpublished PhD thesis, 401 pages.
- Ryan, B.D. (1991): Deposits of coal from the Telkwa coal property, northwestern British Columbia (NTS 93L/11); in *Geological Fieldwork 1990, BC Ministry of Energy, Mines and Petroleum Resources*, Paper 1991-1, pages 399–406.
- Ryan, B.D. (1992): Coal rank variations in the Telkwa coalfield, central British Columbia (NTS 93L/11); in *Geological Fieldwork 1991, BC Ministry of Energy, Mines and Petroleum Resources*, Paper 1992-1, pages 451–460.
- Ryan, B.D. (1993): Geology of the Telkwa coalfield, British Columbia (NTS 93L/11,14); *BC Ministry of Energy, Mines and Petroleum Resources*, Open File 1993-21, scale 1:20 000.
- Ryan, B.D. and Dawson, M.F. (1994): Potential coal and coalbed methane resource of the Telkwa coalfield, central British Columbia (NTS 93L/11); in *Geological Fieldwork 1993, BC Ministry of Energy, Mines and Petroleum Resources*, Paper 1994-1, pages 225–243.
- Schiarizza, P. and MacIntyre, D.G. (1999): Geology of the Babine Lake – Takla Lake area, central British Columbia (NTS 93K/11, 12, 13, 14; 93N/03,04,05,06); in *Geological Fieldwork 1998, BC Ministry of Energy, Mines and Petroleum Resources*, Paper 1999-1, pages 33–68.
- Sillitoe, R.H. (1999): Styles of high-sulphidation gold, silver and copper mineralization in the porphyry and epithermal environments; in *PacRim '99 Congress Proceedings*, Bali, Indonesia, Weber, G., Editor, *Australasian Institute of Mining and Metallurgy*, pages 29–44.

- Sillitoe, R.H. (2002): Rifting, bimodal volcanism, and bonanza gold veins; *Society of Economic Geologists*, Newsletter, Number 48, pages 24–26.
- Sillitoe, R.H. and Hedenquist, J.W. (2003): Linkages between volcanotectonic settings, ore-fluid compositions, and epithermal precious-metal deposits; in *Understanding Crustal Fluids – Roles and Witnesses of Processes Deep within the Earth*, Giggenbach Memorial Volume, Simmons, S.F., Editor, *Society of Economic Geologists and Geochemical Society*, Special Publication 10, pages 315–343.
- Smith, G.T. and Mustard, P.S. (2005): The southern contact of the Bowser Lake and Skeena Groups – unconformity or transition?; in *Summary of Activities 2005, BC Ministry of Energy, Mines and Petroleum Resources*, URL <<http://www.em.gov.bc.ca/subwebs/oilandgas/pub/reports/summary2005.htm>>, pages 152–156.
- Souther, J.G. (1991): Volcanic Regimes; Chapter 14; in *Geology of the Cordilleran Orogen in Canada*, Gabrielse, H. and Yorath, C.J., Editors, *Geological Survey of Canada*, Geology of Canada, Number 4, pages 457–490.
- Stacey, J.S. and Kramers, J.D. (1975): Approximation of terrestrial lead isotope evolution by a two-stage model; *Earth and Planetary Science Letters*, Volume 26, pages 207–221.
- Stevenson, J.S. (1947): Red Rose mine; *Economic Geology*, Volume 42, pages 433–464.
- Struik, L.C., MacIntyre, D.G. and Hastings, N.L. (2001a): Geochemistry data – Nechako NATMAP project; *BC Ministry of Energy, Mines and Petroleum Resources*, Open File 2001-9.
- Struik, L.C. and MacIntyre, D.G. (2001b): Introduction to the special issue of the *Canadian Journal of Earth Sciences* – the Nechako NATMAP project of the central Canadian Cordillera; *Canadian Journal of Earth Sciences*, Volume 38, pages 485–494.
- Sutherland Brown, A. (1960a): Geological map of the Rocher de Boule range, Hazelton Mountains, British Columbia; *BC Ministry of Energy, Mines and Petroleum Resources*, coloured map to accompany Bulletin 43, scale 1:63 360.
- Sutherland Brown, A. (1960b): Geological map of the Rocher de Boule range, Hazelton Mountains, British Columbia; *BC Ministry of Energy, Mines and Petroleum Resources*, Bulletin 43, 86 pages.
- Tackaberry, D.M. (1998): Petrography, litho-geochemistry and VMS potential of mid-Cretaceous Rocky Ridge volcanics, Babine Lake area, central British Columbia; unpublished BSc thesis, *University of Victoria, School of Earth and Ocean Sciences*, 73 pages.
- Tipper, H.W. (1976): Smithers, British Columbia (NTS 93L); *Geological Survey of Canada*, Open File 35.
- Tipper, H.W. and Richards, T.A. (1976): Jurassic stratigraphy and history of north-central British Columbia; *Geological Survey of Canada*, Bulletin 270, 73 pages.
- Villeneuve, M.E. (2004): Preliminary report – $^{40}\text{Ar}/^{39}\text{Ar}$ and U-Pb geochronology for Rocky Ridge volcanics, British Columbia; unpublished report prepared for D. MacIntyre, November 2004, 17 pages.
- Watkins, J.J. (2005): Evaluation report of the mineral potential of the BQ property, Omineca mining district; *BC Ministry of Energy, Mines and Petroleum Resources*, AR27943, 45 pages.
- Wetherell, D.G. (1979): Geology and ore genesis of the Sam Goosly copper-silver-antimony deposits, British Columbia; unpublished MSc thesis, *The University of British Columbia*, 208 pages.
- White, N.C. (1999): Convergent evolution and ore deposits; *Society of Economic Geologists*, SEG Video/DVD Series, Thayer Lindsay Lecture Number 4B.
- Woodsworth, G.J. (1979): Geology of Whitesail Lake map area, British Columbia; *Geological Survey of Canada*, Current Research–Part A, Paper 79-1A, pages 25–29.
- Woodsworth, G.J. (1980): Geology of Whitesail Lake map area, British Columbia (NTS 93E); *Geological Survey of Canada*, Open File 708, scale 1:250 000.
- Woodsworth, G.J., Hill, M.L. and van der Heyden, P. (1985): Preliminary geologic map of Terrace map area, British Columbia (NTS 103I east half); *Geological Survey of Canada*, Open File 1136, scale 1:250 000.
- Wojdak, P.J. and Ethier, D. (2000): Geologic setting of the Knoll property – an Eskay Creek target in Cretaceous rhyolite; in *Exploration and Mining in BC 1999, BC Ministry of Energy, Mines and Petroleum Resources*, pages 79–84.
- Wojdak, P.J. and Sinclair, A.J. (1984): Equity Silver silver-copper-gold deposit – alteration and fluid inclusion studies; *Economic Geology*, Volume 79, pages 969–990.

$^{40}\text{Ar}/^{39}\text{Ar}$ and Re-O Isotopic Ages for Hydrothermal Alteration and Related Mineralization at the Highland Valley Cu-Mo Deposit (NTS 092I), Southwestern British Columbia

by C.H. Ash, P.H. Reynolds¹, R.A. Creaser² and M.G. Mihalynuk

KEYWORDS: Quesnellia, Highland Valley deposit, Cu-Mo porphyry, geochronology, $^{40}\text{Ar}/^{39}\text{Ar}$, Re-Os

INTRODUCTION

The Highland Valley Cu (Mo, Ag, Au) deposit is located roughly 200 km northeast of Vancouver and 75 km southwest of Kamloops, in southern British Columbia (Fig 1). It is the largest operating base metal mine in Canada. Production began in 1962 from several separate mines, which were amalgamated in 1986 to form Highland Valley Copper, a subsidiary of Teck Cominco Limited. Recorded metal production from the Highland Valley deposit to 2005 exceeds 3.33 billion kilograms of copper (average grade of 0.43%), 44 million kilograms of molybdenum (average grade of 0.03%), 1 billion grams of silver and 7 million grams of gold.

The age of mineralization at Highland Valley has been inferred, on the basis of its syngenetic porphyry character, to be more or less coeval with the Late Triassic magmatic history of the host Guichon Creek batholith (Osatenko and Jones, 1976; Casselman *et al.*, 1995). Uranium-lead zircon dating of the batholith suggests an age within the range 213 to 207 Ma (210 ± 3 Ma; Mortimer *et al.*, 1990; Fig 1). However, conventional K-Ar isotopic analysis of sericite from the ore mineral assemblage has yielded ages that are significantly younger than the crystallization age of the intrusion. For example, a 202 ± 8 Ma (recalculated with modern decay constants from data reported in Jones, 1975; *cf.* Breitsprecher and Mortensen, 2004) and 198 ± 12 Ma (recalculated with modern decay constants from data reported in Blanchflower, 1971; *cf.* Breitsprecher and Mortensen, 2004), and 191.3 ± 4 Ma (recalculated with modern decay constants from data reported in Wanless *et al.*, 1973; *cf.* Breitsprecher and Mortensen, 2004). At the lower limit of error, all three of these ages are younger than the 200 Ma base of the Jurassic epoch. At their upper limit of error, the first two analyses are both 210 Ma (Late Triassic), equivalent to the best crystallization age for the batholith

(Mortimer *et al.*, 1990). The Wanless *et al.* (1973) date remains Early Jurassic at its upper limit of error (195.3 Ma).

Ore mineral assemblages were resampled with the aim of subjecting them to more precise geochronological dating techniques. Samples were collected by the first author during a three-day field visit to the Valley pit in 1999. Sericite and biotite were collected for $^{40}\text{Ar}/^{39}\text{Ar}$ age determination, and molybdenite was collected for application of the Re-Os chronometer. If successful, the new dating would eliminate the ambiguity raised by the overlapping magmatic and hydrothermal ages from the deposit that existed at the time. This field examination was intended as reconnaissance for a detailed mapping project of the Highland Valley deposit. Unfortunately, the project did not proceed beyond this preliminary stage and geological relationships between the units dated were not established.

SAMPLE DESCRIPTIONS

Three distinct mineral assemblages were collected from the 1025 m level of the Valley pit (Fig 2). Sample CAS99-HV1 is molybdenite from a massive, 8 to 10 cm wide, steeply dipping vein on the southeastern corner of the pit along the bench wall. The molybdenite vein cut dark to light grey biotite-quartz diorite in which quartz is coarse grained relative to the medium-grained matrix feldspar and biotite. This unit is representative of the Bethsaida phase of the Guichon Creek batholith (McMillan, 1978).

Sample CAS99-HV2 consists of medium-grained sericite from Cu-Mo-mineralized quartz stockwork collected from a well-washed portion of the mining bench. Sericite constitutes up to several percent of the dark grey quartz vein material, but is mostly concentrated as envelopes along the vein margins. Quartz veins at this locality range from 2 to 10 mm thick and form a stockwork that makes up between 5 and 15% of the bench exposures. The plutonic host rock in this area is mineralogically and texturally consistent with that hosting the massive molybdenite vein described above.

The third dated sample is of biotite collected from a texturally distinctive plutonic phase occurring near the centre of the pit. In contrast to the typical Bethsaida phase, this rock is much more leucocratic. It has a coarse to very coarse grained, white, quartzofeldspathic matrix with very coarse (2–4 cm), euhedral, black biotite books. It contains no observable sulphide mineralization. Contacts with the Bethsaida phase were not established.

¹ Department of Earth Sciences, Dalhousie University, Halifax, NS B3H 3J5

² Department of Earth and Atmospheric Sciences, University of Alberta, Edmonton, AB T6G 2E3

This publication is also available, free of charge, as colour digital files in Adobe Acrobat® PDF format from the BC Ministry of Energy, Mines and Petroleum Resources website at http://www.em.gov.bc.ca/Mining/Geolsurv/Publications/catalog/cat_fldwk.htm

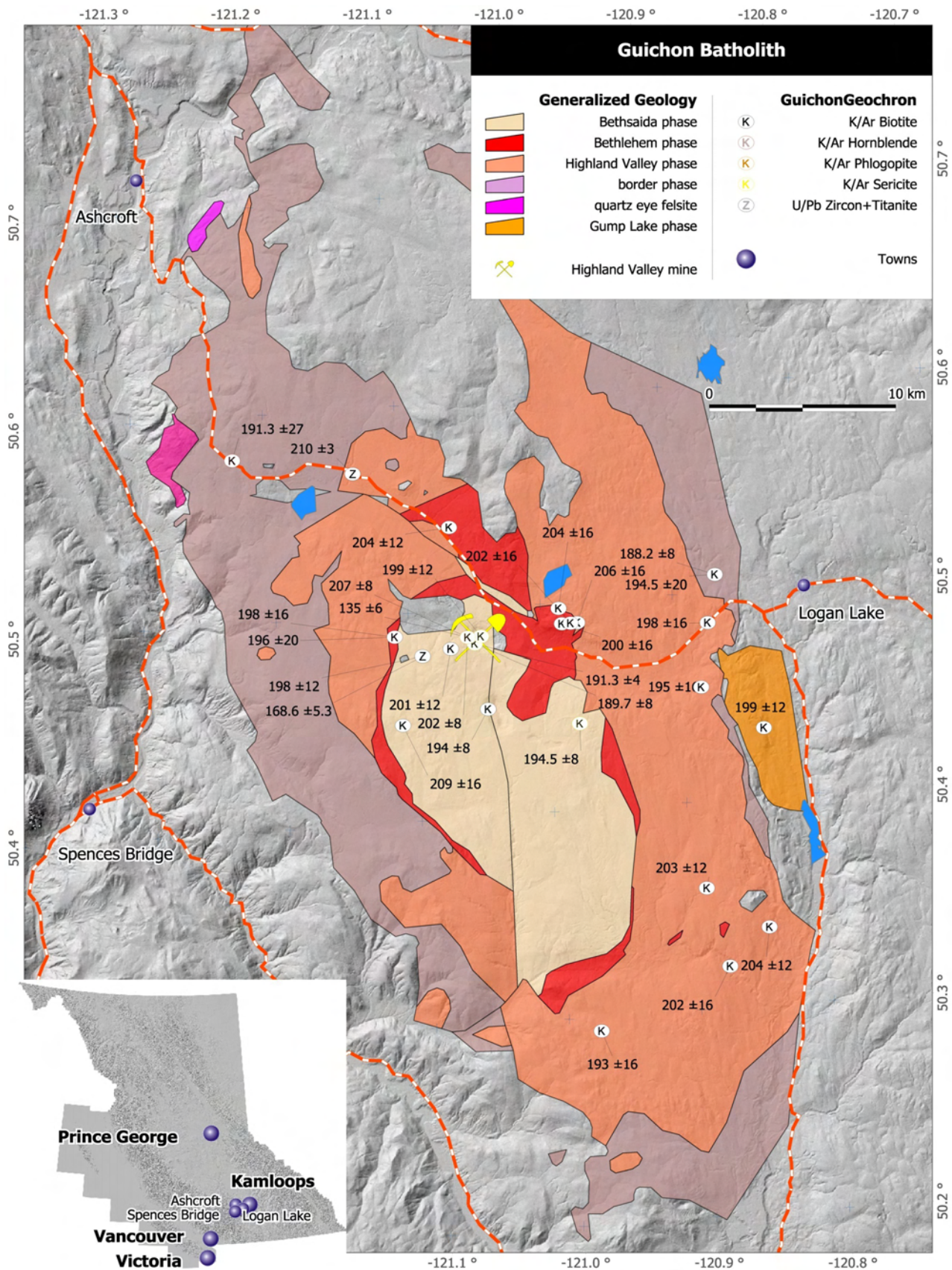


Figure 1. Location and generalized geology of the Guichon batholith. Also shown is the distribution of geochronological data from the batholith and the location of the Highland Valley mine, the collection site of the samples analyzed for this study. Major units and geological contacts are from the compilation of Massey *et al.* (2005); geochronological data are from the compilation of Breitsprecher and Mortensen (2004; 'unreliable' data omitted).

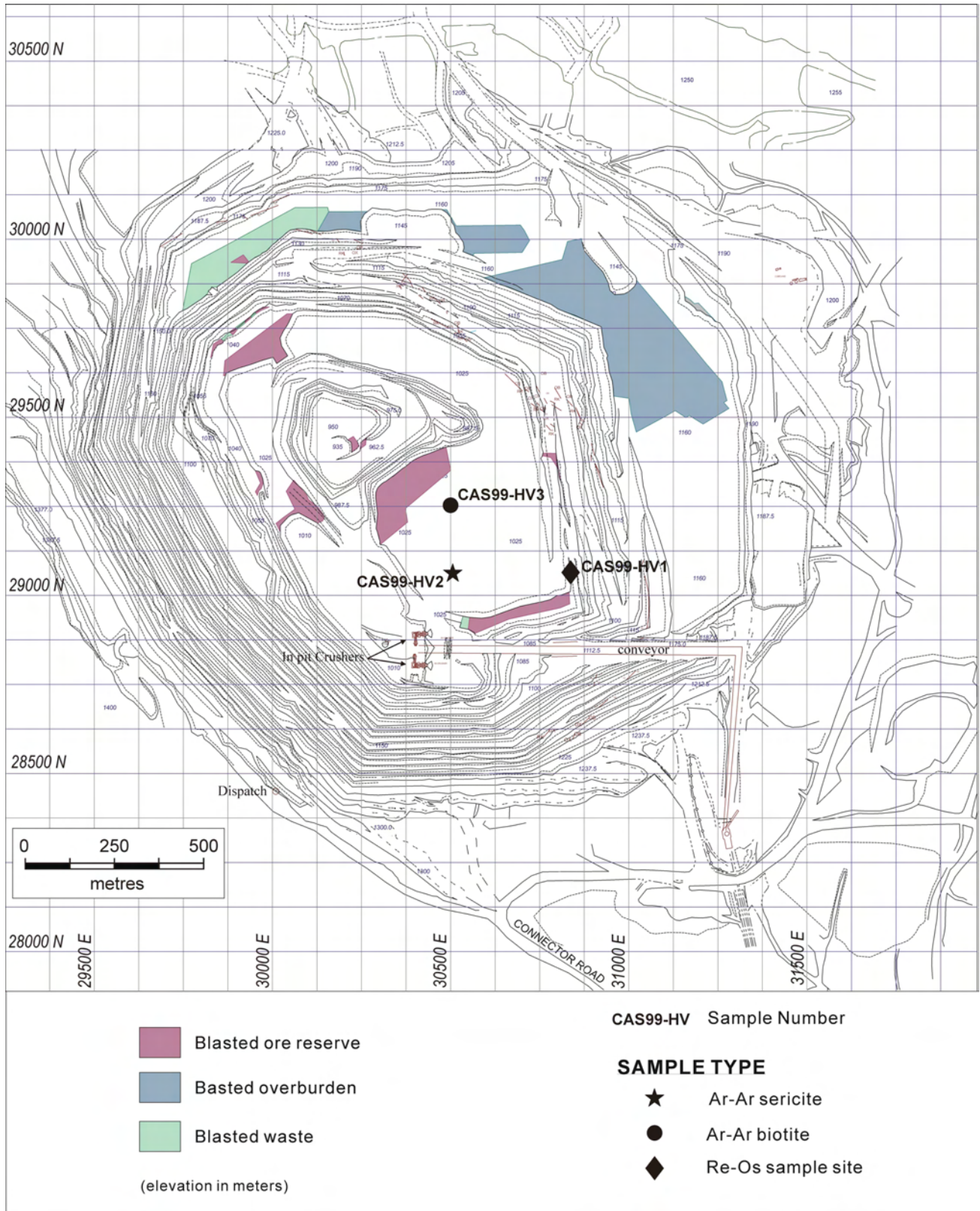


Figure 2. Valley pit, indicating locations of the individual samples dated.

TABLE 1. RE-OS ISOTOPIC DATA FOR AGES FOR MOLYBDENITE, VALLEY PIT, HIGHLAND VALLEY CU-MO DEPOSIT.

Sample	Re (ppm)	¹⁸⁷ Re (ppm)	¹⁸⁷ Os (ppb)	Age, with 2σ uncertainty (Ma)
CAS99-HV1a	112.5	70.708	243.92	206.7 ± 1.5
CAS99-HV1b	155.81	97.932	336.36	205.8 ± 1.5

Uncertainty is 2σ (95% confidence). All known sources of uncertainty which affect the age have been fully propagated to calculate the uncertainty estimates, which includes a value of ±0.31% uncertainty for the half-life of ¹⁸⁷Re. Age calculated using the decay constant λ¹⁸⁷Re = 1.666 × 10⁻¹¹ y⁻¹ (Smoliar et al., 1996).

TABLE 2. ⁴⁰AR-³⁹AR ANALYTICAL DATA FOR MICAS, VALLEY PIT, HIGHLAND VALLEY CU-MO DEPOSIT.

T°C	mV 39	39%	Age (Ma) ±1σ	% ATM	37/39	36/40	39/40	% IIC
600	40.7	2.5	140.9 ± 1.9	23.8	0.04	0.000806	0.023733	0.01
650	78.3	5.0	200 ± 1.4	9.3	0.01	0.000318	0.01956	0
700	12.2	0.7	206.5 ± 4.5	3.1	0.01	0.000106	0.020226	0
750	4.9	0.3	203.4 ± 6.9	2.3	0.01	0.000079	0.020739	0
800	70.5	4.5	205.8 ± 1.2	0.3	0	0.000012	0.020868	0
850	69.0	4.4	206.9 ± 1.2	0.6	0	0.000021	0.020693	0
900	67.0	4.2	207.9 ± 1.2	0.8	0	0.000027	0.020552	0
950	104.6	6.6	210.9 ± 1.1	0.5	0	0.000019	0.020288	0
1000	269.7	17.2	208.3 ± 1	0.3	0	0.000012	0.0206	0
1050	369.7	23.6	206.5 ± 1	0.3	0	0.000013	0.020793	0
1100	306.2	19.5	205.7 ± 1	0.6	0.01	0.000023	0.020805	0
1250	160.4	10.2	206 ± 1	2.8	0.06	0.000096	0.020334	0.01
1450	11.9	0.7	201.7 ± 7.6	49.5	0.33	0.001675	0.010807	0.07

Mean age (800°C - 1450°C) = 206.9 ± 2.1 Ma (2σ uncertainty, including error in J)

J = 0.002532 ± 0.000025 (0.9 %)

37/39, 36/40 and 39/40 Ar ratios are corrected for mass spectrometer discrimination, interfering isotopes and system blanks

% IIC, interfering isotopes correction

T°C	mV 39	39%	Age (Ma) ±1σ	% ATM	37/39	36/40	39/40	% IIC
550	1.5	0	129 ± 29.5	9.9	0.22	0.00034	0.030773	0.07
575	3.1	0.1	144.8 ± 13.1	10.7	0.18	0.000366	0.027037	0.05
600	6.9	0.2	178.2 ± 7.1	6.0	0.35	0.000207	0.022902	0.08
625	12.3	0.4	198.5 ± 4.9	4.5	0.68	0.000155	0.020767	0.15
650	19.4	0.6	197 ± 2.7	3.1	0.66	0.000108	0.021234	0.15
675	30	1	196 ± 1.9	3.3	0.25	0.000114	0.021311	0.05
700	36.5	1.2	197.5 ± 1.7	5.4	0.02	0.000185	0.020685	0
725	47.9	1.6	201.2 ± 1.5	3.9	0	0.000133	0.020607	0
750	62.6	2.1	203 ± 1.3	1.8	0	0.000062	0.020859	0
800	243.6	8.5	204.1 ± 1	2.3	0	0.00008	0.020629	0
850	716.5	25.1	204.3 ± 0.9	0.6	0	0.000021	0.020978	0
875	406	14.2	204.4 ± 0.9	0.5	0	0.000017	0.020989	0
900	277.4	9.7	203.9 ± 1	0.6	0	0.000022	0.021008	0
925	189.1	6.6	203.9 ± 1	0.9	0	0.000032	0.020951	0
950	139.1	4.8	204.1 ± 1	0.8	0	0.000029	0.020945	0
975	118.9	4.1	204 ± 1	0.8	0	0.000027	0.020969	0
1000	114.6	4	204.2 ± 1	0.7	0	0.000025	0.020957	0
1050	191.5	6.7	205.6 ± 1	0.5	0	0.000017	0.020853	0
1100	188.3	6.6	205.9 ± 1	0.0	0	0.000003	0.020914	0
1250	37.9	1.3	209.5 ± 1.8	9.6	0.01	0.000325	0.01858	0
1450	2.2	0	346.6 ± 70.4	66.7	0.1	0.002258	0.00398	0.01

Mean age (800°C - 1100°C) = 204.4 ± 2 Ma (2σ uncertainty, including error in J)

J = 0.002532 ± 0.000025 (0.9 %)

37/39, 36/40 and 39/40 Ar ratios are corrected for mass spectrometer discrimination, interfering isotopes and system blanks

% IIC, Interfering isotopes correction

RE-OS DATING OF MOLYBDENITE

Two separate fractions of the Valley pit molybdenite sample (CAS99-HV1a and b) were analyzed at the University of Alberta Radiogenic Isotope Facility in Edmonton, under the supervision of R.A. Creaser. Methods used for molybdenite analysis are described in detail by Selby and Creaser (2001a). The ^{187}Re and ^{187}Os concentrations in molybdenite were determined by isotope dilution mass spectrometry using Carius-tube, solvent extraction, anion chromatography and negative thermal ionization mass spectrometry techniques. Isotopic analysis was made using a Micromass Sector 54 mass spectrometer by Faraday collector. Total procedural blanks for Re and Os are less than 15 and 2 pg ($<25\text{ fg }^{187}\text{Os}$), respectively. These procedural blanks are insignificant in comparison to the Re and Os concentrations in molybdenite. The Chinese molybdenite powder HLP-5 (Markey *et al.*, 1998), which is used as an in-house 'control sample' by AIRIE, Colorado State University, is also routinely analyzed at the University of Alberta. This 'control sample' yielded an average Re-Os date of $220.5 \pm 0.5\text{ Ma}$ ($\pm 0.45\%$ at the 2σ level, $n = 17$). This Re-Os age is identical to a $221.0 \pm 1\text{ Ma}$ ($\pm 0.4\%$ at the 1σ level, $n = 19$) age determined by alkaline fusion (Markey *et al.*, 1998) and two Carius-tube ages of 219.8 ± 0.7 and $221.0 \pm 0.8\text{ Ma}$ (H. Stein, pers comm, 2000).

Re-Os Results

The analytical data and calculated ages for both the initial and repeat analyses of molybdenite sample CAS99-HV1 (a and b) are shown in Table 1. Sample CAS99-HV1a yielded an initial calculated age of $206.7 \pm 1.5\text{ Ma}$. This is slightly older than the repeat analysis age of $205.8 \pm 1.5\text{ Ma}$, but is equivalent within the stated limits of error.

AR-AR DATING OF MICAS

Two different mica samples, one of sericite (CAS99-HV2) from Cu-Mo-bearing quartz stockwork and a second of coarse, euhedral magmatic biotite (CAS99-HV3), were analyzed at Dalhousie University by the conventional $^{40}\text{Ar}/^{39}\text{Ar}$ step-heating method under the supervision of P.H. Reynolds.

Individual grains were hand-picked from each of the samples. These grains were wrapped in aluminum foil and interspersed with three to five aliquots of the flux monitor (the hornblende standard MMhb-1, with an assumed age of $520 \pm 2\text{ Ma}$; Samson and Alexander, 1987). The entire package was irradiated in the McMaster University nuclear reactor.

An internal tantalum resistance furnace of the double-vacuum type was used to carry out the step-heating. All isotopic analyses were made in a VG 3600 mass spectrometer.

Ar/Ar Results

The results of the sericite (CAS99-HV2) and magmatic biotite (CAS99-HV3) analyses are given in Tables 2a and b. The sericite sample produced a uniform release spectrum, as shown in Figure 3a. A plateau age of $204 \pm 2\text{ Ma}$ is defined by 10 steps representing approximately 90% of the total gas released (age uncertainty given is at the 95% confi-

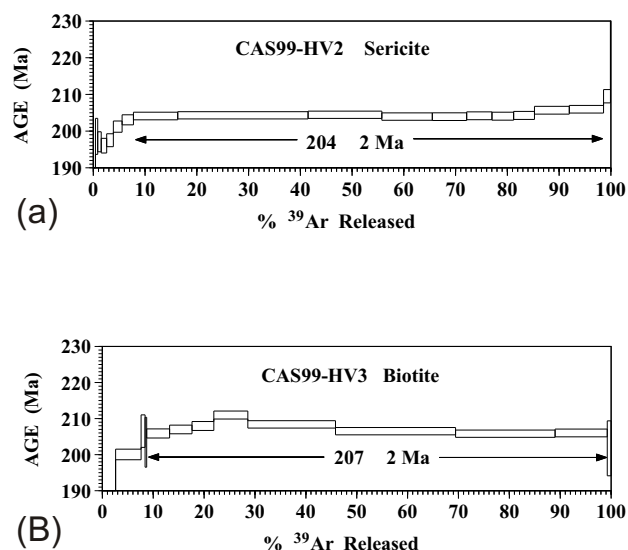


Figure 3. $^{40}\text{Ar}/^{39}\text{Ar}$ age spectra plots for a) hydrothermal sericite from Cu-Mo-mineralized quartz stockwork (CAS99-HV1), and b) very coarse grained euhedral biotite from leucocratic quartz diorite of the Guichon Creek batholith (CAS99-HV2).

dence limit and includes the uncertainty in the irradiation parameter, J).

The spectral plot for the biotite sample is shown in Figure 3b. A plateau age of $207 \pm 2\text{ Ma}$ is defined by eight steps representing approximately 90% of the total gas released (age uncertainty given is at the 95% confidence limit and includes the uncertainty in the irradiation parameter, J).

DISCUSSION

Rhenium-osmium dating laboratories continue to demonstrate the remarkable robustness of the Re-Os geochronometer. Not only can it withstand post-ore hydrothermal metamorphism (Selby and Creaser, 2001b), but also granulite-facies temperatures (Bingen and Stein, 2002). Therefore, the Re-Os isotopic age determined from the molybdenite veins should record their age of formation, not the age of some later disturbance. The age for molybdenum mineralization at the Highland Valley deposit is indistinguishable from the magmatic crystallization age based

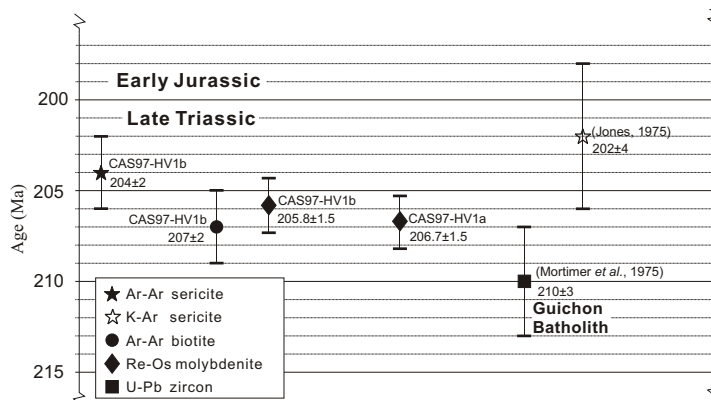


Figure 4. Summary of selected isotopic ages reported for the Highland Valley Cu-Mo deposit. Error bars indicate 2σ uncertainty.

upon the U-Pb zircon data of Mortimer *et al.* (1990; 210 ± 3 Ma). Both are Late Triassic, with error envelopes overlapping between 207 and 207.2 Ma (Fig 4). However, at the outer error limits, molybdenite mineralization could be as much as 8.7 m.y. younger than the crystallization age. The age at which the crystallized body cooled through the biotite closure temperature (~350°C for a rapidly cooling body; Harrison *et al.*, 1985) is recorded by the magmatic biotite sample as 207 ± 2 Ma. Error limits permit a range of interpretations of the time required to cool through the biotite closure temperature: from instantaneous to approximately 8 m.y. Clearly, more precise geochronometric analyses are required before a definitive history of magmatic crystallization and mineralization can be constructed. In particular, a precise crystallization age for the Bethsaida phase, which hosts the Highland Valley deposit, needs to be determined. It is the youngest of four major intrusive pulses, whereas the crystallization age determination of Mortimer *et al.* (1990) is from a sample of the Highland Valley phase, the second oldest major phase within the Guichon Creek batholith.

When considered in isolation, these new age data constrain the timing of mineralization within the Valley pit to within 3 m.y., between 205 and 207 Ma (age range increases to 6.2 m.y. at the outer limits of the error envelopes). The calculated ages for each of the newly dated minerals appear to follow a sequence that is consistent with the observed textural and crosscutting relationships. Magmatic biotite gives the oldest calculated cooling age (207 ± 2 Ma). Molybdenite from veins that crosscut the plutonic host is next in the sequence (206.7 ± 1.5 Ma, 205.8 ± 1.5 Ma). Sericite is inferred to have formed latest in the magmatic history of the batholith, and returned the youngest age determination (204 ± 2 Ma).

Mineralization at the Highland Valley mine, herein dated as between *ca.* 204 and *ca.* 207 Ma, can now be considered as nearly contemporaneous with the *ca.* 204 Ma mineralization in the Iron Mask batholith (60 km to the east), as reported by Logan *et al.* (2007).

ACKNOWLEDGMENTS

The authors express their appreciation to both Alan Galley (Geological Survey of Canada, Ottawa) and Bill McMillan (previously with British Columbia Geological Survey, now retired) for their enthusiastic insights during the three-day field visit to the Highland Valley mine. Loren Bond, with Highland Valley Copper at the time of the field visit, is graciously acknowledged for providing a tour of the Valley pit that enabled direct observation and sampling of ore-grade material for isotopic dating. Completion of this paper would not have been possible without the efforts of Ron Graden with Highland Valley Copper in providing digital pit maps and related information.

REFERENCES

- Bingen, B. and Stein, H.J. (2002): Molybdenite Re-Os dating of biotite dehydration melting: the Rogaland granulites, S Norway; *12th Annual V.M. Goldschmidt Conference*, Davos, Switzerland, page A78.
- Blanchflower, J.D. (1971): Isotopic dating of copper mineralization at Alwin and Valley properties, Highland Valley, British Columbia; unpublished BSc. thesis, *University of British Columbia*, Vancouver, BC.
- Breitsprecher, K. and Mortensen, J.K. (2004): BC Age 2004A-1: a database of isotopic age determinations for rock units from British Columbia; *BC Ministry of Energy, Mines and Petroleum Resources*, Open File 2004-3, URL <<http://www.em.gov.bc.ca/Mining/Geosurv/Publications/OpenFiles/OF2004-03/toc.htm>> [December 2006].
- Casselman, M.J., McMillan, W.J. and Newman, K.M. (1995): Highland Valley porphyry copper deposit near Kamloops, British Columbia: a review and update with emphasis on the Valley deposit; in *Porphyry Deposits of the Northwestern Cordillera of North America*, *Canadian Institute of Mining, Metallurgy and Petroleum*, Special Volume 46, pages 161-191.
- Harrison, T.M., Duncan, I. and McDougall, I. (1985): Diffusion of ⁴⁰Ar in biotite: temperature, pressure and compositional effects; *Geochimica et Cosmochimica Acta*, volume 49, pages 2461-2468.
- Jones, M.B. (1975): Hydrothermal alteration and mineralization of the Valley Copper deposit, Highland Valley, BC; unpublished Ph.D. thesis, *Oregon State University*, Corvallis, Oregon.
- Logan, J.M., Mihalynuk M.G., Ullrich, T and Friedman, R.M. (2007): U-Pb ages of intrusive rocks and ⁴⁰Ar/³⁹Ar plateau ages of copper-gold-silver mineralization associated with alkaline intrusive centres at Mount Polley and the Iron Mask batholith, southern and central British Columbia; in *Geological Fieldwork, 2006*, *BC Ministry of Energy, Mines and Petroleum Resources*, Paper 2007-1 and *Geoscience BC*, Report 2007-1, pages 93-116.
- Markey, R.J., Stein, H.J. and Morgan, J.W. (1998): Highly precise Re-Os dating of molybdenite using alkaline fusion and NTIMS; *Talanta*, volume 45, pages 935-946.
- Massey, N.W.D., MacIntyre, D.G., Desjardins, P.J. and Cooney, R.T. (2005): Digital geology map of British Columbia: whole province; *BC Ministry of Energy, Mines and Petroleum Resources*, GeoFile 2005-1, URL <<http://www.em.gov.bc.ca/Mining/Geosurv/Publications/GeoFiles/Gf2005-1/toc.htm>> [June 2006].
- McMillan, W.J. (1978): Geology of the Guichon Creek Batholith (NTS 921); *BC Ministry of Energy Mines and Petroleum Resources*, notes and legend to accompany Preliminary Map 30, 17 pages.
- Mortimer, N., Van Der Heyden, P. Armstrong, R.L. and Harakal, J. (1990): U-Pb and K-Ar dates related to timing of magmatism and deformation in the Cache Creek Terrane and Quesnellia, southern British Columbia; *Canadian Journal of Earth Sciences*, volume 27, pages 117 to 123.
- Osatenko, M.J. and Jones, M.B. (1976): Valley Copper; in *Porphyry Copper Deposits of the Canadian Cordillera*, Sutherland Brown, A., Editor, *Canadian Institute of Mining and Metallurgy*, Special Volume 15, pages 130-143.
- Samson, S.D. and Alexander, E.C., Jr. (1987): Calibration of the interlaboratory ⁴⁰Ar/³⁹Ar dating standard MMhb-1; *Chemical Geology*, volume 66, pages 27-34.
- Selby, D., and Creaser, R.A. (2001a): Late- and Mid-Cretaceous mineralization in the northern Canadian Cordillera: constraints from Re-Os molybdenite dates; *Economic Geology*, volume 96, pages 1461-1467.
- Selby, D. and Creaser, R.A. (2001b): Re-Os geochronology and systematics in molybdenite from the Endako porphyry molybdenum deposit, British Columbia, Canada; *Economic Geology*, volume 96, pages 197-204.
- Smoliar, M.I., Walker, R.J. and Morgan, J.W. (1996): Re-Os isotope constraints on the age of Group IIA, IIIA, IVA, and IVB iron meteorites; *Science*, volume 271, pages 1099-1102.
- Wanless, R.K., Stevens, R.D., Lachance, G.R. and Delabio, R.N. (1973): Age determinations and geological studies, Ar-Ar and K-Ar isotopic ages, Report 11; *Geological Survey of Canada*, Paper 73-2.

Pootlass High-Strain Zone near Bella Coola (NTS 093D/02, 07), West-Central British Columbia: Preliminary Observations

by D.K. Demerse¹, L.A. Kennedy¹ and J.J. Hopkins¹

KEYWORDS: transpression, terrane-boundary tectonics, strain partitioning, sinistral shear zone, Bella Coola, Mount Pootlass

INTRODUCTION

The Pootlass high-strain zone (PHSZ) was first recognized by Mahoney *et al.* (2002) as a part of the Targeted Geoscience Initiative to map the Bella Coola map sheet (NTS 093D) and was referred to as the Jump Across shear zone. The PHSZ lies to the east of the Coast shear zone, a continental-scale zone interpreted to have accommodated significant dextral translation in the late Cretaceous and represents the boundary between the Intermontane and Insular Belts at this latitude (Hollister and Andronicos, 2006). The width, lateral extent, kinematics, timing and tectonic significance of the PHSZ are not well known. This report presents field data collected during the first of two planned field seasons near Bella Coola, BC (Fig 1), and is part of a two-year MSc degree undertaken by the first author. The purpose of this research is to constrain the timing, kinematics, extent and significance of the PHSZ and to place it in a regional geological and tectonic context.

REGIONAL GEOLOGY

The Bella Coola area lies within the Intermontane Belt, close to the boundary with the Insular Belt, which is located just to the west of the field area (Fig 1). Results from a Targeted Geoscience Initiative (Struik *et al.*, 2002; Struik and Veljkovic, 2001) divide the Bella Coola map sheet into two northwest-trending parallel belts of island arc volcanic and sedimentary rocks (Haggart *et al.*, 2003; Haggart *et al.*, 2006). The eastern belt is mostly early to mid-Jurassic in age and is composed of volcanic and sedimentary rocks belonging to the Hazelton Group (Haggart *et al.*, 2004). The western belt, which includes the focus area of this paper, is mostly early to mid-Cretaceous in age and consists predominantly of volcanic and sedimentary rocks of the Monarch assemblage, with some volcanic and sedimentary rocks of the Salloomt assemblage and Hazelton Group (Haggart *et al.*, 2004; Struik *et al.*, 2002). Obscuring these two panels is a diverse suite of plutonic rocks ranging in age from Jurassic to Eocene (Haggart *et al.*, 2004). The volume



Figure 1. Location map of the field area near Bella Coola, south-western BC.

of plutonic rock intruding crustal units increases to the west (Haggart *et al.*, 2003; Fig 2).

A well-developed system of northeast-trending, northeast-verging folds and some thrust faults occur in the eastern portion of the Bella Coola map sheet (Mahoney *et al.*, 2002). The folds vary in their geometry from close to isoclinal and occur at the outcrop and map scale. Axial planar cleavages are well developed in slaty units. Mahoney *et al.* (2002) correlate this fold system to the Late Cretaceous regional-scale Waddington fold and thrust belt (Rusmore and Woodsworth, 2000). The western part of the Bella Coola map sheet is dominated by high-angle shear zones, the largest of which is the focus of this report.

2006 FIELDWORK PROGRAM

Fieldwork, conducted during July and August 2006, consisted of geological mapping with a focus on structural features associated with the Pootlass high-strain zone. The purpose of the fieldwork was to characterize the geometry and kinematics of the Pootlass high-strain zone, to deter-

¹Department of Earth and Ocean Sciences, University of British Columbia, Vancouver, BC

This publication is also available, free of charge, as colour digital files in Adobe Acrobat® PDF format from the BC Ministry of Energy, Mines and Petroleum Resources website at http://www.em.gov.bc.ca/Mining/Geosurv/Publications/catalog/cat_fldwk.htm

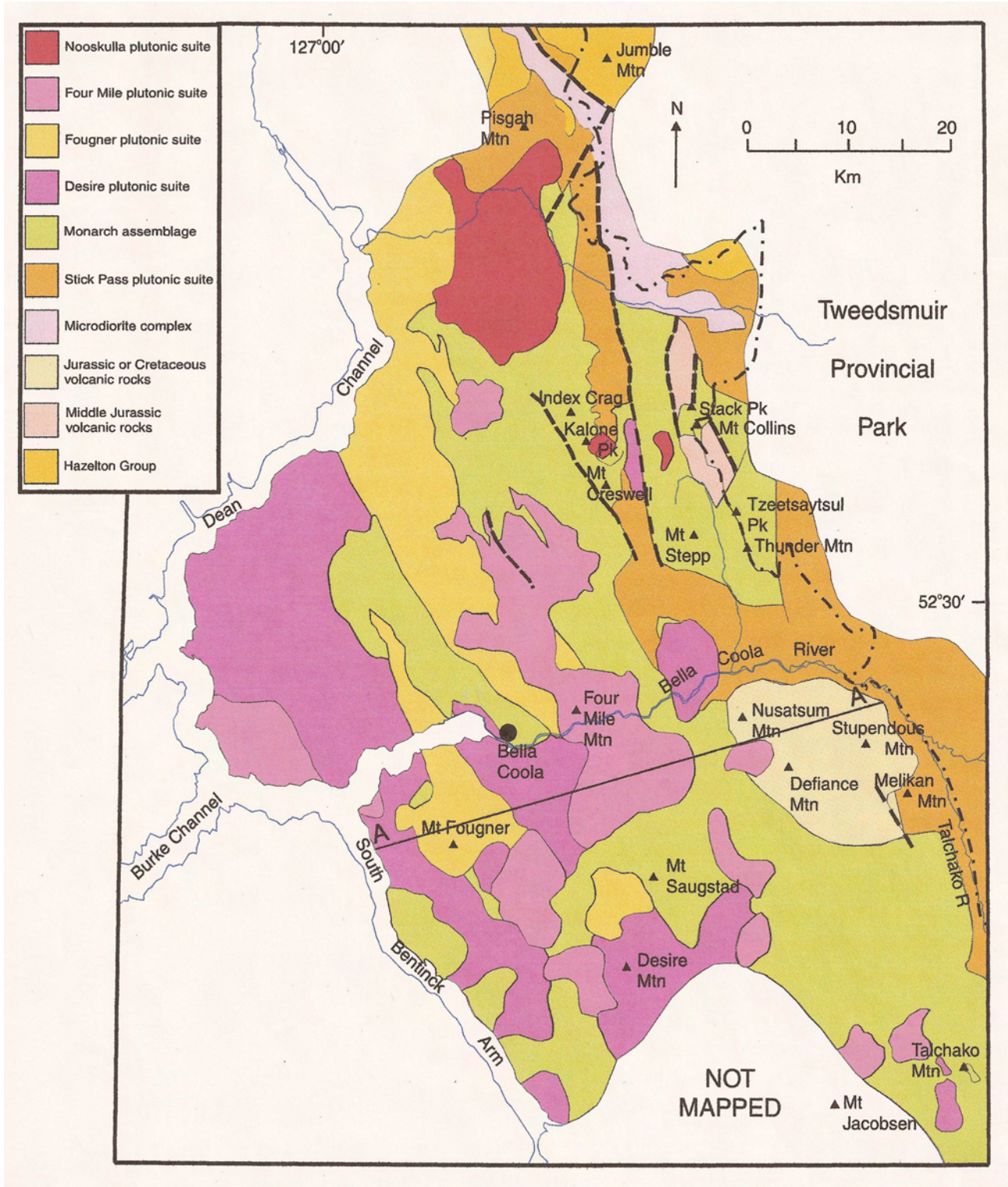


Figure 2. Regional geology of the Bella Coola area, southwestern BC.

mine the distributions of rock types and to determine the extent of deformation within the zone. Three areas of the high-strain zone were mapped at a 1:10 000 scale: Mount Pootlass, Falls Camp and Snootli Peak. The areas were accessed via helicopter out of Bella Coola. Oriented samples were collected for structural analyses, petrology and age dating.

MOUNT POOTLASS

Two ridges leading up to the summit of Mount Pootlass were mapped. The eastern ridge is characterized by strongly foliated and folded, sheeted layers of granodiorite, alternating with foliation-parallel and folded, sheeted mafic layers (Fig 3, 4). The southern ridge is dominated by laminated and strongly folded and sheared metasedimentary rocks, with local intrusions of deformed plutonic rocks (Fig 4).

The peak of Mount Pootlass is composed entirely of plutonic rocks, most of which are deformed granodiorite and diorite with sheeted mafic intrusions. The plutonic rocks on Mount Pootlass are interpreted to be a part of the 119 ± 2 Ma Desire plutonic suite (Gehrels and Boghossian, 2000).

Eastern Ridge: Lithology and Structural Features

The granodiorite that characterizes most of the eastern ridge of Mount Pootlass is composed of quartz, feldspar, biotite and hornblende, with sparse fine-grained garnet. Toward the eastern end of the ridge, the granodiorite includes interlayered felsic and mafic layers that are separated by abrupt contacts. Mafic plutonic layers are medium to fine grained, rich in biotite and hornblende and show some evidence of chilled margins. The felsic layers are medium to fine grained and contain predominantly quartz and feldspar. These felsic and mafic layers are foliation-parallel sheeted intrusions with thicknesses ranging from approximately 0.15 to 1.5 m. One relatively small (30 m wide) package of fine-grained, finely laminated metasedimentary rocks interlayered with granodiorite occurs near the middle of the eastern ridge. At the eastern end of the eastern ridge, the PHSZ is truncated by an undeformed, coarse-grained pluton composed of quartz, feldspar, muscovite and biotite, which is interpreted by Haggart *et al.* (2004) as part of the 68 Ma Fougner plutonic suite. At the juncture of the eastern and southern ridges on Mount Pootlass, a small plug of coarse-grained amphibole-rich magnetic gabbro is in intrusive contact with the granodiorite to the east and the metasedimentary rocks to the west.

All rocks of the eastern ridge, excluding the undeformed pluton, exhibit a dominant subvertical foliation striking approximately 300° (Fig 5).

The dominant foliation is compositional, here termed a transposition foliation, F_T (*see below*), with layers defined by alternating mafic (biotite and amphibole) and felsic (quartz and feldspar) minerals. In addition, protomylonite and mylonite fabrics were also identified within the foliation, defined by aligned and elongated biotite, amphibole and feldspar grains, with alignment and elongation being more pronounced and better developed toward the eastern end of the eastern ridge. The predominant foliation exhibits a very slight gradual rotation from north-northwest to north along the eastern ridge.



Figure 3. Looking to the south. Foliated, folded and sheeted granodiorite and felsic and mafic layers; eastern ridge, Mount Pootlass, Bella Coola, southwestern BC.

Mineral lineations are stretching lineations, defined by elongate (rodged) quartz and feldspar grains (Fig 6) in granodiorite, and are well developed near the peak of Mount Pootlass, as well as near the eastern end of the ridge. Mineral lineations trend approximately 140° and plunge very slightly to the south (Fig 7).

The ‘sheeted’ intrusive rocks on the eastern ridge are polydeformed. The most well-developed and dominant folds are upright, isoclinal folds that trend roughly toward 130° and plunge toward the south at approximately 25° (Fig 7, 8). These isoclinal folds are southwest-verging, with subvertical western limbs and steeply eastward-dipping eastern limbs. The isoclinal folds are refolded into Type 3 interference patterns (Ramsay and Huber, 1983), generally associated with progressive deformation and interpreted here as F_1 and F_2 folds (Fig 9).

The axial surfaces of the dominant folds are subparallel to foliation; therefore, the foliation may be a composite of two foliations (S_T). The F_1 and F_2 folds are overprinted by gently undulating folds (F_3) with wavelengths on the order of several metres and near-vertical fold axes with a subvertical axial surface orientation of roughly 215° . In some localities, the F_3 folds are observed folding the limbs and the hinges of the F_T folds.

Abundant boudinage of mafic layers within the granodiorite occurs throughout the eastern ridge and attests a significant component of flattening. The boudinage are formed within the main foliation (S_T) but are deformed by F_3 . Quartz and feldspar-rich felsic bands form the neck folds.

On horizontal surfaces, perpendicular to the foliation, ductile shear-sense indicators in the granodiorite provide evidence for both dextral and sinistral senses of movement at the eastern end of the eastern ridge; however, to the west, kinematic indicators show a predominantly sinistral sense of shear. Shear-sense indicators observed consist of dragfolds in quartz and feldspar stringers, brittle-ductile extensional shear bands and asymmetric foliation orientations. Further detailed mapping must be completed at the eastern end of the ridge to produce a more detailed recording of the kinematics.

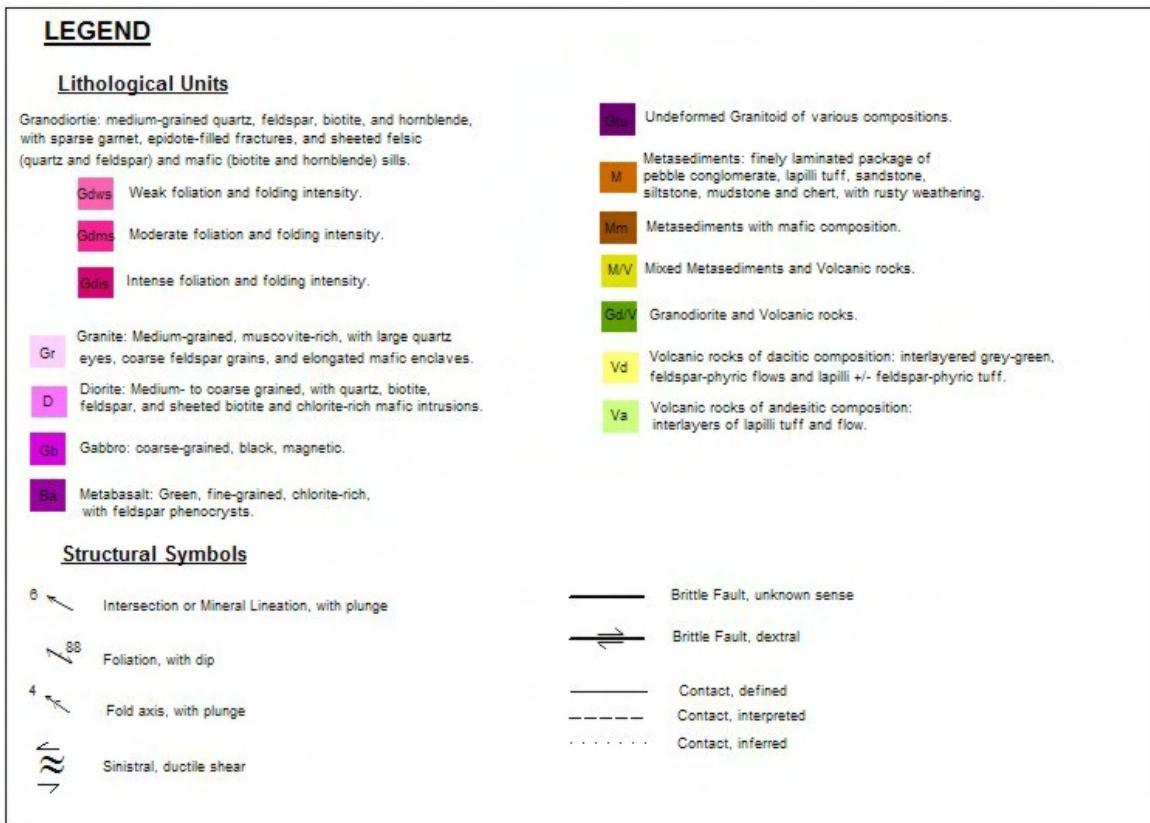
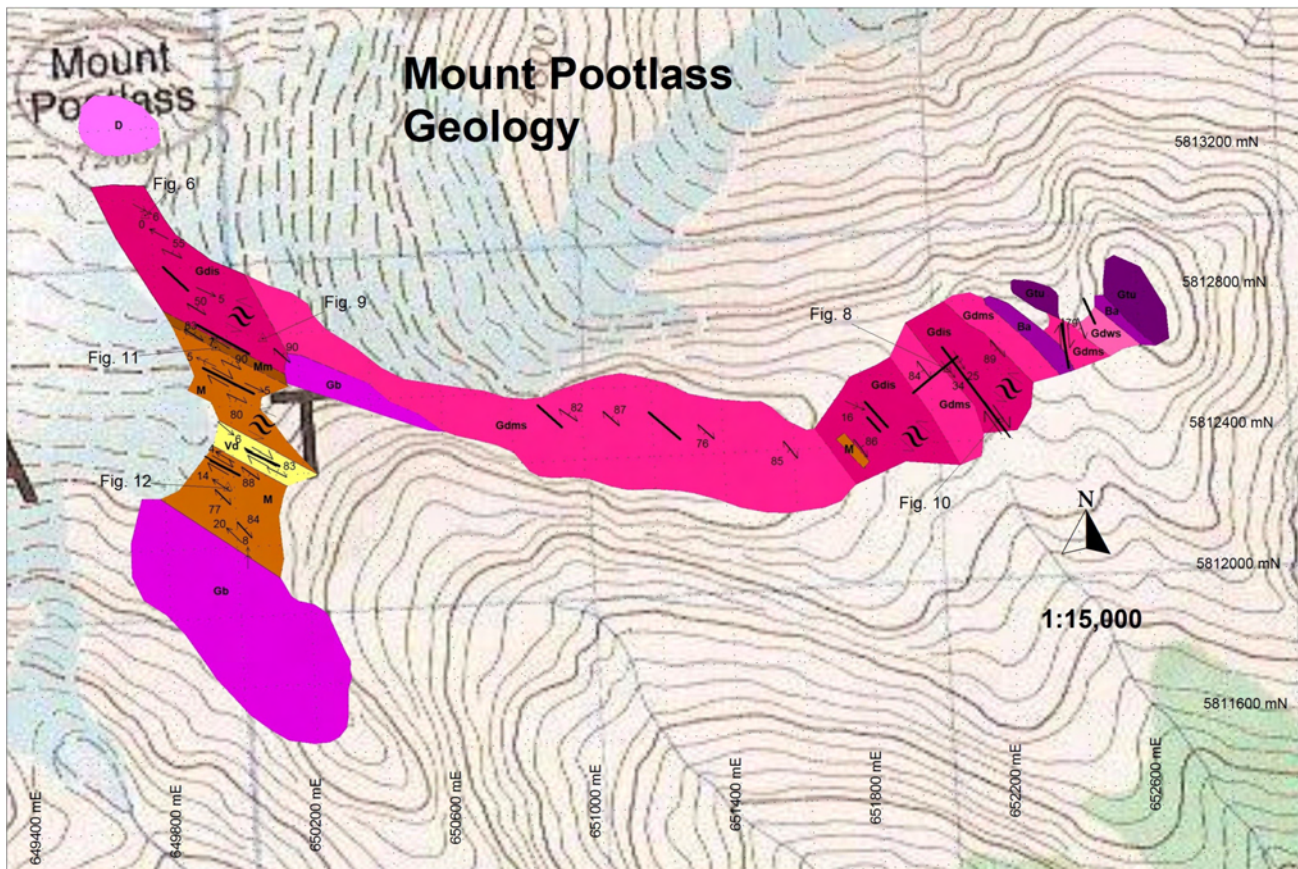


Figure 4. Geology of eastern and southern ridges of Mount Pootlass, Bella Coola, southwestern BC, 1:15 000 scale.

Brittle faults are common and contain dextral fabrics typically associated with light to dark green mafic sills that are composed almost entirely of platy foliated chlorite and often juxtaposed against a very fine grained and competent felsic layer that is composed predominantly of quartz and feldspar with sparse garnet (Fig 10).

The felsic unit has a well-developed foliation defined by bands of slight variation in colour and/or translucency of the rock. Both the mafic chlorite-rich unit and the felsic unit are each generally between 0.1 and 1 m in width. Brittle faults are oriented parallel to the dominant foliation and occur within plutonic and metasedimentary units.

Southern Ridge: Lithology and Structural Features

The southern ridge of Mount Pootlass is dominated by a succession of finely laminated, well-foliated and isoclinally folded metasedimentary rocks, with interlayers of dacitic to andesitic lapilli tuff and flows. The metasedimentary rocks consist of pebble conglomerate, sandstone, siltstone and mudstone as well as more tightly laminated siltstone, mudstone and chert. Garnet is rare in the metasedimentary layers. The metasedimentary package is interlayered with very felsic, fine-grained, highly strained rocks, possibly rhyolite, and with amphibole-rich mafic dikes and sills that are folded with the rest of the sedimentary package.

A large undeformed pluton ranging from diorite to gabbro with abundant enclaves, including two large (10 by 20 m) rotated metasedimentary rafts, is located at the south end of the southern ridge. This pluton is interpreted to be a part of the 119 ± 2 Ma Desire plutonic suite (Gehrels and Boghossian, 2000).

The sedimentary package on Mount Pootlass reached a maximum of amphibolite facies metamorphism, as indicated by the abundant hornblende in more mafic rocks. Pelitic rocks are composed mostly of quartz, chlorite, muscovite and garnet and may represent greenschist facies. Detailed petrological analyses will be completed in the coming year.

Toward the peak of Mount Pootlass, the metasedimentary rocks are in sharp contact with the pluton, where many fractures are infilled with epidote. At the contact, the felsic layers in the metasedimentary rocks are abundant and have brittle-ductile dextral dragfolds and fractures, a succession of very tight isoclinal folds and mafic chlorite-rich fault-related material (possibly cataclasite). The granodiorite includes many felsic and mafic sheets near the contact with the metasedimentary rocks, as described for the eastern ridge section above. The peak of Mount Pootlass is composed of a coarse-grained diorite.

The plutonic rocks have a well-developed subvertical foliation striking 310° , which is very similar to that described for the eastern ridge (Fig 5). The foliation is especially well developed, as exhibited by pronounced mineral alignment and elongations, in the granodiorite near the contact with the metasedimentary rocks, as well as in an area 250 to 350 m from the summit. An L-tectonite also occurs

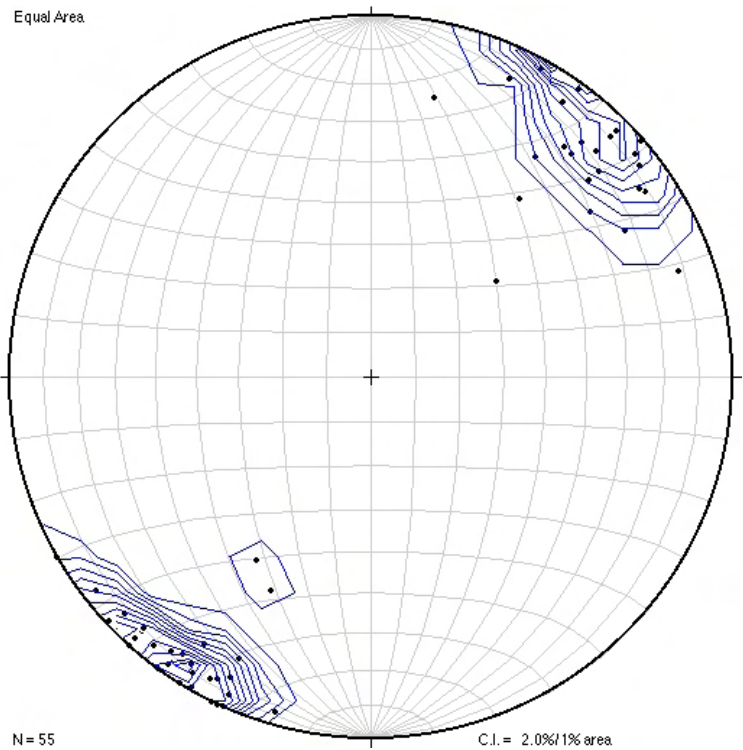


Figure 5. Stereonet diagram showing poles to foliation; Mount Pootlass, Bella Coola, southwestern BC. Abbreviation: C.I., contour interval.

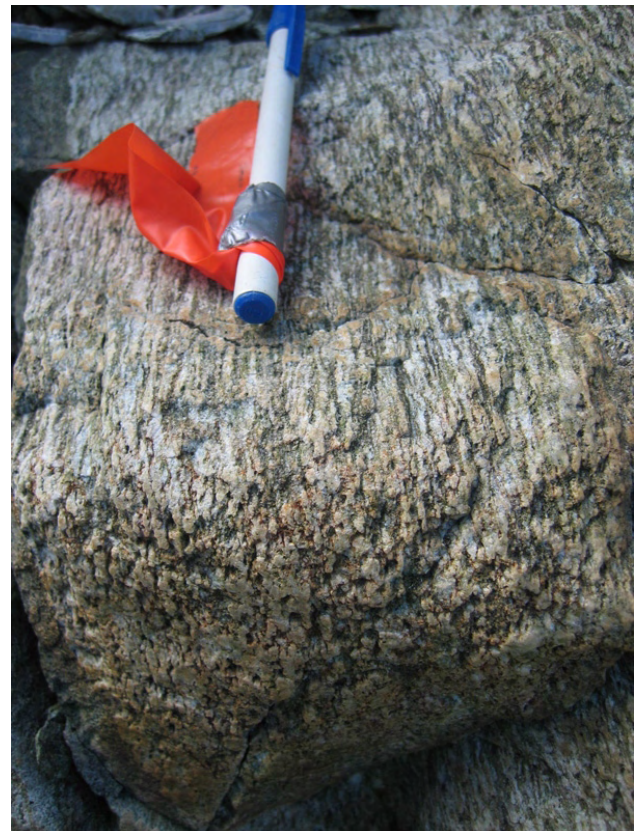


Figure 6. Pen points toward 300° . Elongated (rodged) quartz and feldspar in granodiorite; junction of southern and eastern ridges, Mount Pootlass.

in this zone, as indicated by rodded quartz and feldspar grains and a lack of foliation in the granodiorite (Fig 6), and many mafic layers that display sinistral shearing as indicated by dragfolds in felsic stringers. Near the junction between the eastern and southern ridges of Mount Pootlass, the plutonic rocks exhibit melt injection textures and passive folding and shearing, indicating that the intrusive activity is likely syndeformational (Fig 11).

The bedding of the metasedimentary package is difficult to discern due to the strong foliation. Intersection lineations between bedding and the dominant cleavage foliation (F_T) are widespread, with values averaging a trend of 130° and a subhorizontal plunge (Fig 7).

Metasedimentary and intrusive rocks are isoclinally folded, with axial planes parallel to the dominant foliation. Isoclinal fold axes trend toward approximately 310° and are subhorizontal (Fig 7). Folding on this ridge is similar to the eastern ridge in that fold hinges exhibit refolding along the same trend, indicating progressive refolding, with F_2 folds folding F_1 and with fold axes for F_1 and F_2 being subparallel. Furthermore, a gentle overprinting folding episode (F_3) is also exhibited in the metasedimentary sequence with a subvertical fold axis trending roughly 245° .

Flattening is indicated by boudinage of the mafic layers within the metasedimentary package and the granodiorite. Boudinage is not as common on the southern ridge of Mount Pootlass as it is on the eastern ridge.

Sinistral ductile shear-sense indicators occur in both the metasedimentary and plutonic rocks. Shear-sense indicators used include 1) metasedimentary rock layers dragfolded in a ductile manner (Fig 12) and 2) felsic stringers elongated oblique to the dominant foliation in mafic, amphibole-rich dikes, similar to those seen at Falls Camp (Fig 17).

Brittle faults are distributed along the southern ridge and up toward the summit of Mount Pootlass. Similar to the eastern ridge, the brittle faults typically occur within mafic layers that are altered to chlorite and adjacent to a fine-grained felsic unit that is composed predominantly of quartz and feldspar with sparse garnet. A dextral strike-slip shear sense is provided by Reidel fault geometries located on the horizontal surface perpendicular to the foliation (Fig 10). The foliation is defined by platy chlorite.

FALLS CAMP

Lithology and Structural Features

The Falls Camp area is characterized by interlayered and laminated metasedimentary rocks and dacitic to andesitic flows and tuff with rare basaltic flows, as well as granodiorite (Fig 13).

Volcanic rocks comprise fine-grained, very competent, grey-green flows and elongated lapilli and/or feldsparphyric tuff. Recrystallized quartz eyes and feldspar laths occur in some localities. Dacite tuff is composed predominantly of fine-grained quartz and muscovite=amphibole,

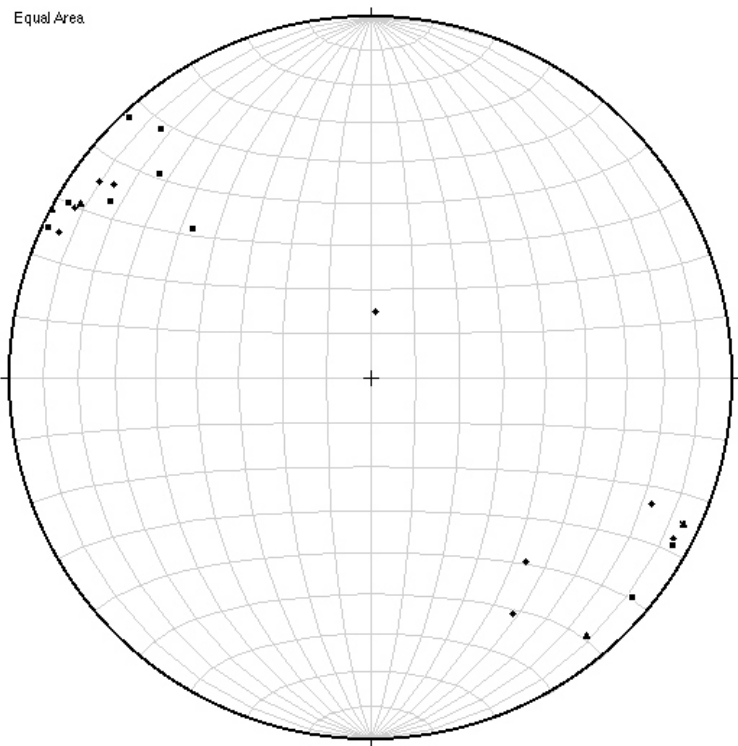


Figure 7. Stereonet diagram showing F_T fold axes (diamonds), intersection lineations (squares) and mineral lineations (triangles); Mount Pootlass, Bella Coola, southwestern BC.

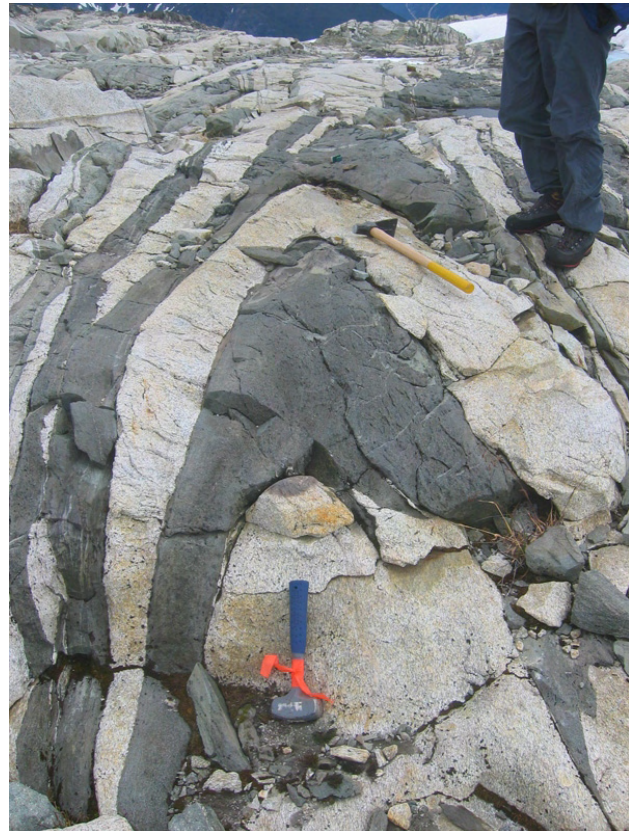


Figure 8. Looking north. West-verging, isoclinally folded (F_T) felsic and mafic sheets in granodiorite. Fold width approximately 2 m; eastern ridge, Mount Pootlass, Bella Coola, southwestern BC.



Figure 9. Refolded F_{1-2} fold in granodiorite indicating progressive deformation; eastern ridge, Mount Pootlass, Bella Coola, southwestern BC.



Figure 10. North is to the left. Felsic stringer in a mafic layer of a brittle fault exhibiting dextral shear sense; eastern ridge, Mount Pootlass, Bella Coola, southwestern BC.



Figure 11. Hammer to the northwest. Passive, high-temperature folding in granodiorite near to junction of southern and eastern ridges; Mount Pootlass, Bella Coola, southwestern BC.

biotite and trace to 1% pyrite. Volcanic units are on average moderately foliated, defined by the alignment of mica, feldspar and amphibole, and some are segregated into felsic and mafic bands with layer thicknesses averaging from 5 to 25 cm. Metasedimentary rocks are finely laminated and fissile with a slaty cleavage. The metasedimentary rocks vary in composition and grain size from chert to mudstone and siltstone, with sparse garnet. Layers are mostly dark with rusty weathering and vary in thickness from approximately 1 to 10 cm.

The potential metamorphic grade of the sedimentary package in the Falls Camp area is interpreted as greenschist facies because of the quartz, chlorite, muscovite and sparse garnet assemblage; however, it may reach amphibolite facies, as indicated by abundant hornblende in more mafic rocks.

The granodiorite at the Falls Camp area is characterized by many quartz and biotite stringers and veins. The granodiorite includes felsic and mafic sheeted dikes. Sheeted sills of granodiorite with thicknesses of approximately 0.1 to 1 m occur within the dacitic to andesitic flows and tuff.

An undeformed pluton, interpreted by Haggart *et al.* (2004) as being part of the 63.3 ± 0.3 Ma Four Mile plutonic suite (van der Heyden, 2004), occurs at the northeast end of the Falls Camp area, with very coarse grained and equigranular quartz, feldspar and biotite. Felsic sills within the metasedimentary package appear to increase in frequency with proximity to this pluton, and therefore may be related melt injections.

Bedding in the metasedimentary rocks is subparallel with the main foliation. Intersection lineations between bedding and foliation are widespread, trending roughly 315° with a plunge of between 10 and 20° (Fig 14, 15). All rock units in the Falls Camp area, except for the undeformed pluton, exhibit a subvertical dominant foliation striking approximately 330° (Fig 16). This foliation is marked by aligned feldspar, amphibole and mica in the granodiorite and volcanic rocks. In metasedimentary rocks,



Figure 12. Pen points toward 300° . Sinistral ductile dragfold in metasedimentary rocks; southern ridge, Mount Pootlass, Bella Coola, southwestern BC.

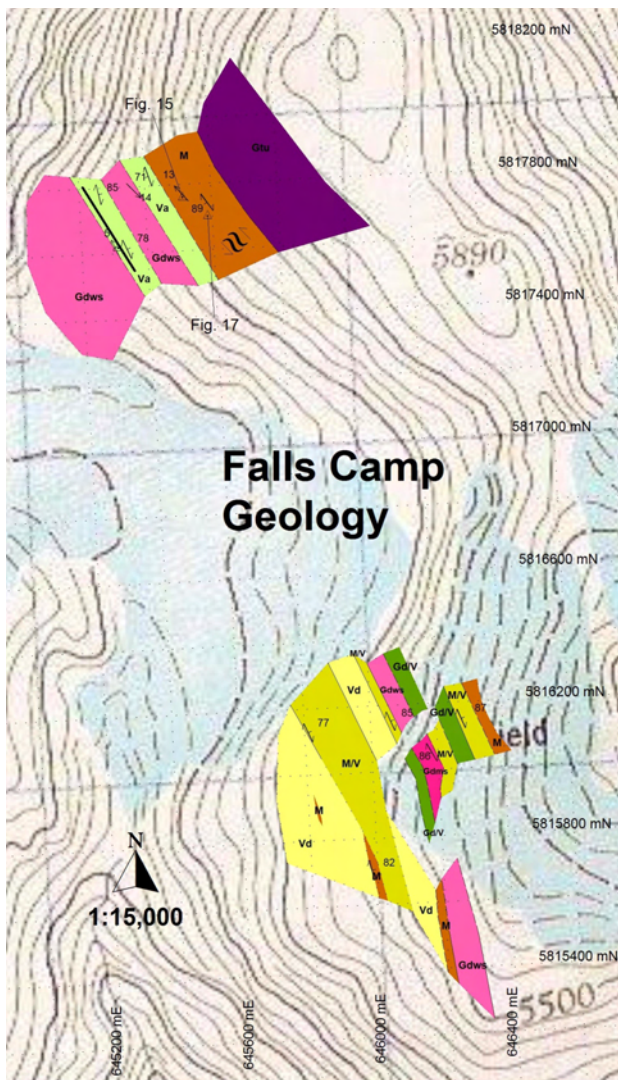


Figure 13. Geology of Falls Camp, Bella Coola, southwestern BC., 1:15 000. See Figure 4 for map legend.

the foliation is compositional with laminated layers cleaving along the dominant foliation direction. The foliation is weakly to moderately well developed compared to the foliation on Mount Pootlass. All rocks are also isoclinally folded with subhorizontal fold axes trending 330° (Fig 14).

Folds are southwest-verging, upright and often show brittle extensional fractures in fold hinges, especially in the granodiorite sheets. Gentle, undulating folds overprint the upright folds in metasedimentary rocks, with a subvertical fold axis orientation of roughly 215° . One sheath fold was spotted in the metasedimentary rocks, indicating a very high strain regime. Flattening in the area is indicated by boudinage of the mafic layers in the metasedimentary rocks.

Although folding and cleavage development dominate, there are areas where sinistral shearing is apparent, especially in mafic dikes with felsic minerals elongate on an angle oblique to the dominant foliation (Fig 17). Ductile sinistral shear bands and lapilli with a sinistral sense of shear also occur in volcanic tuff.

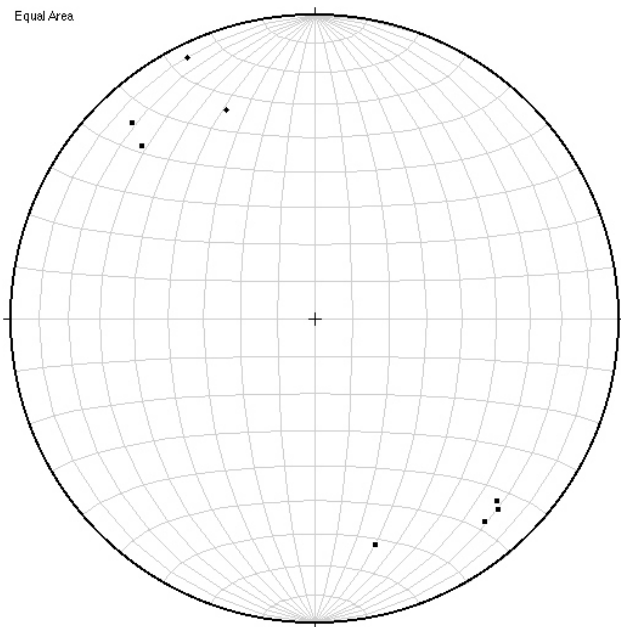


Figure 14. Stereonet diagram showing F_T fold axes (diamonds) and intersection lineations (squares); Falls Camp, Bella Coola, southwestern BC.

There is a roughly 4 m wide, recessively weathered brittle fault in volcanic rocks in the northwest end of the Falls Camp area. The fault is aligned with the dominant foliation ($\sim 330^\circ$) and the sense of movement is unclear.

SNOOTLI PEAK

Lithology and Structural Features

The Snootli Peak zone includes plutonic rocks ranging from granite to diorite to gabbro, metasedimentary rocks, as well as andesitic and basaltic volcanic rocks (Fig 18). Toward the eastern end of the mapped area, a well-foliated, medium-grained, muscovite-rich granite exhibits large quartz eyes and feldspar grains, some of which are elon-



Figure 15. Arrow points toward approximately 330° and indicates the orientation of the intersection lineation in metasedimentary rocks between bedding and cleavage; Falls Camp, Bella Coola, southwestern BC.

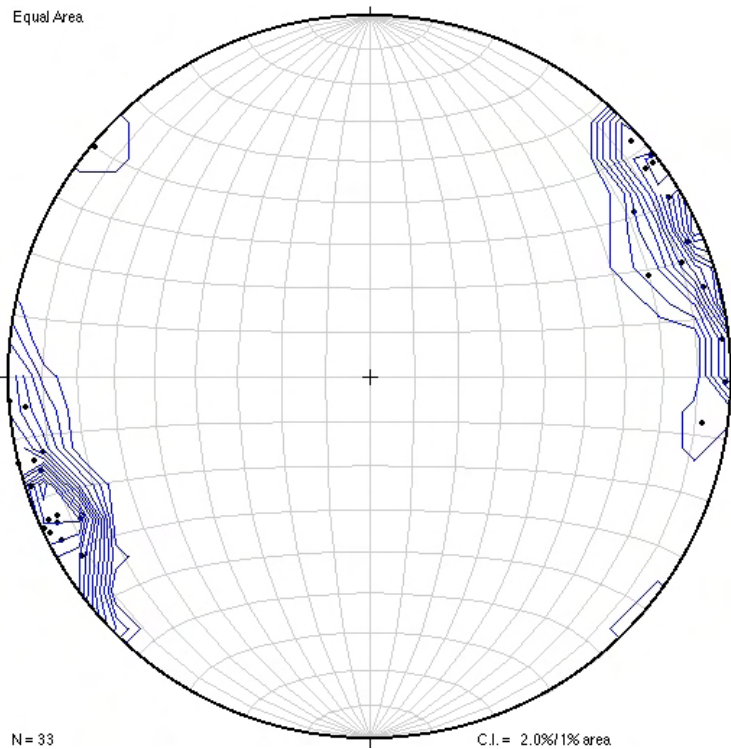


Figure 16. Stereonet diagram showing poles to foliation; Falls Camp, Bella Coola, southwestern BC. Abbreviation: C.I., contour interval.

gated. Mafic enclaves formed predominantly of chlorite are also elongated. Very fine-grained felsic layers (20–30 cm wide) occur within the granite, as well as mafic sills (0.05–1 m thick) composed of green fine-grained chlorite with quartz and feldspar phenocrysts. Mafic sills are commonly boudinaged. Dark grey to black, very coarse to medium-grained, undeformed, magnetic gabbro occurs in two localities with magnetite, epidote and trace to 1% pyrite.

A well-foliated diorite outcrops across a significant proportion of the centre of the mapped area. This unit is



Figure 17. Pen points toward approximately 330° along compositional foliation in metasedimentary rocks. Orange pencil indicates felsic stringers in mafic layer that are oblique to the foliation and indicate sinistral shear sense; Falls Camp, Bella Coola, southwestern BC.

composed predominantly of fairly coarse grained biotite, elongated quartz and feldspar with some epidote-rich patches. A fine-grained dark green unit, comprising approximately 10% of the area mapped as diorite, has biotite ‘books’ and fine, elongated feldspar grains.

Metasedimentary rocks in the Snootli Peak area have a very intense rusty weathering colour and consist of very fine-grained and very finely laminated mudstone and siltstone, with minor pebble conglomerate and lapilli tuff. Amphibole and biotite-rich mafic layers are interspersed throughout the metasedimentary rocks. Toward the western end of the mapped area, the sedimentary rocks are finely laminated and very siliceous, with an abundance of chert along with mudstone, siltstone and pebble conglomerate. The abundance of biotite and chlorite in the metasedimentary rocks indicate that they reached greenschist facies metamorphic conditions.

Most of the volcanic packages observed are andesitic in composition and are composed of lapilli tuff and flows, with thin fine-grained green, mafic interlayers. Volcanic rocks are fractured, leached and pervasively altered, with many randomly oriented quartz stringers near to a faulted contact with a metasedimentary package that occurs near the centre of the mapped area.

Volcanic rocks that outcrop at the eastern end of the mapped area are andesitic to basaltic in composition, with interlayers of lapilli tuff and flows averaging in thickness from 0.02 to 3 m. Many sills and dikes, ranging in composition from aplite to diabase, crosscut the volcanic package. A brittle deformation zone occurs to the east of the mafic volcanic package in a mafic chlorite-rich unit and is very similar to faults described for the Pootlass area. The deformation zone is approximately 5 m wide and extends along the dominant foliation for at least 200 m. Any sense of movement is unclear.

All rock units in the Snootli Peak area exhibit a dominant foliation, striking approximately 340° and dipping between 40 and 70° (Fig 19).

West-verging, upright, tightly spaced, isoclinal folds are common. Fold axes in the central mapped area generally trend toward the south, with southerly plunges ranging from 10 to 30°. However, in the spectacularly folded metasedimentary rocks toward the western end of the mapped area, folds have a northerly trend and plunge approximately 20° toward the north (Fig 20, 21). Fold hinges in the diorite are commonly composed of a fine-grained green mafic unit with biotite ‘books’ and parasitically folded felsic stringers. Gently undulating F_3 folds are well developed in the metasedimentary rocks (Fig 22). The F_3 fold axes trend toward approximately 060° with a plunge ranging from 70 to 80° (Fig 21).

Bedding in the metasedimentary package is subparallel to the dominant foliation and intersection lineations between the two generally trend toward 150° with southward plunges ranging from 5 to 30° (Fig 21). Toward the western end of the mapped ridge, intersection lineations in the metasedimentary rocks have a northerly trend and a plunge of approximately 5° (Fig 21).

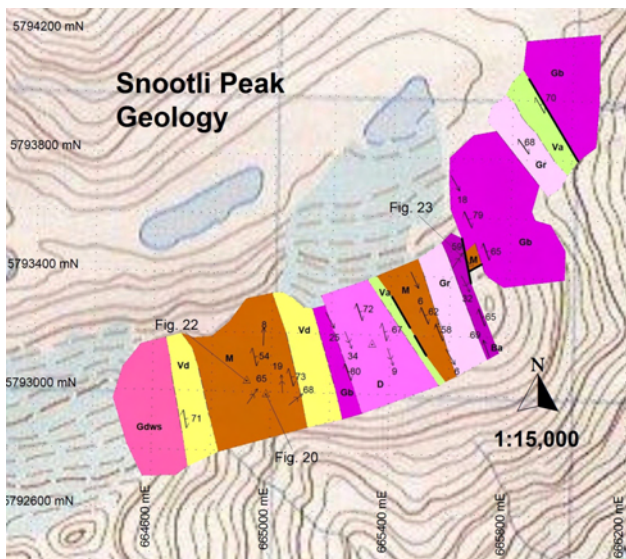


Figure 18. Geology of Snootli Peak, Bella Coola, southwestern BC; scale 1:15 000. See Figure 4 for map legend.

Metasedimentary and volcanic rocks include boudinage of mafic layers with wavelengths of approximately 1 m. Flattening is also indicated in metasedimentary rocks by conjugate kink bands (Fig 23).

Macroscopic evidence of ductile shearing is very rare in the Snootli Peak area. One small, ductile sinistrally sheared felsic dragfold in the metasedimentary package was identified, but the area is generally characterized by folding and cleavage development (*i.e.*, flattening).

Brittle faults of unknown movement sense are oriented parallel to the dominant foliation (340°) and occur between metasedimentary packages and volcanic rocks.

DISCUSSION

Metasedimentary rocks at Mount Pootlass, Falls Camp and Snootli Peak are interpreted as part of the same formation due to their lithological similarities and location along strike. At all localities, mudstone, siltstone, sandstone, pebble conglomerate, lapilli tuff and mafic amphibole-rich layers dominate. This sedimentary package corresponds to the description of the Monarch assemblage that outcrops between the Noosgulch River and the Dean Channel, by Mahoney *et al.* (2002): olive green dacite to andesite flows and associated breccia and tuff breccia dominate the succession, with intercalated sedimentary rocks, including volcanoclastic sandstone and slate, forming continuous stratigraphic sections up to several hundred metres in thickness. Mahoney *et al.* (2002) also report that stratigraphy within this sedimentary sequence is complex, complicated by abrupt lateral facies changes and structural deformation, as is seen on the southern ridge of Mount Pootlass. The base of the Monarch assemblage overlies a quartz diorite pluton that yields a 134 ± 0.3 Ma U-Pb zircon age (van

der Heyden, 1991). Regionally, the Monarch assemblage is interpreted to be Valanginian in age, partially on the basis of sparse ammonites noted by Struik *et al.* (2002).

The Hazelton Group of lower to mid-Jurassic sedimentary and volcanic rocks also has been reported to occur regionally (Haggart *et al.*, 2004). This sedimentary package includes massively bedded basalt and basaltic andesite flows intercalated with crudely stratified fragmental rocks such as coarse-grained volcanic lithic arenite, arkosic sandstone, conglomerate, and minor, medium to thick-bedded calcareous sandstone and sandy limestone that are locally rich in fossils — gastropods, bivalves and ammonites (Haggart *et al.*, 2003). More work is required, in particular age dating, in order to determine to which formation this package of deformed and metamorphosed sedimentary rocks belongs.

A previous structural analysis of the Bella Coola map sheet has been presented by Mahoney *et al.* (2002), who report several distinct deformational phases recording extension, contraction and transpression. Early east-west extension resulted in the deposition of Hazelton Group and Monarch assemblage volcanic and sedimentary rocks, as well as the injection of north-trending andesite dikes that cut plutonic rocks (Mahoney *et al.*, 2002). Contraction in the Bella Coola region formed a northwest-trending, northeast-vergent and shallowly plunging fold system that is best developed in the Monarch assemblage. Folds vary from close to tight, asymmetric to recumbent and are locally isoclinal (Mahoney *et al.*, 2002). Fold axial planes strike northwest and dip southwest throughout the eastern Bella Coola map area (Mahoney *et al.*, 2002). This folding system is interpreted by Mahoney *et al.* (2002) to be part of the Waddington fold and thrust belt, based on similarities in structural style, including northwest-trending folds and

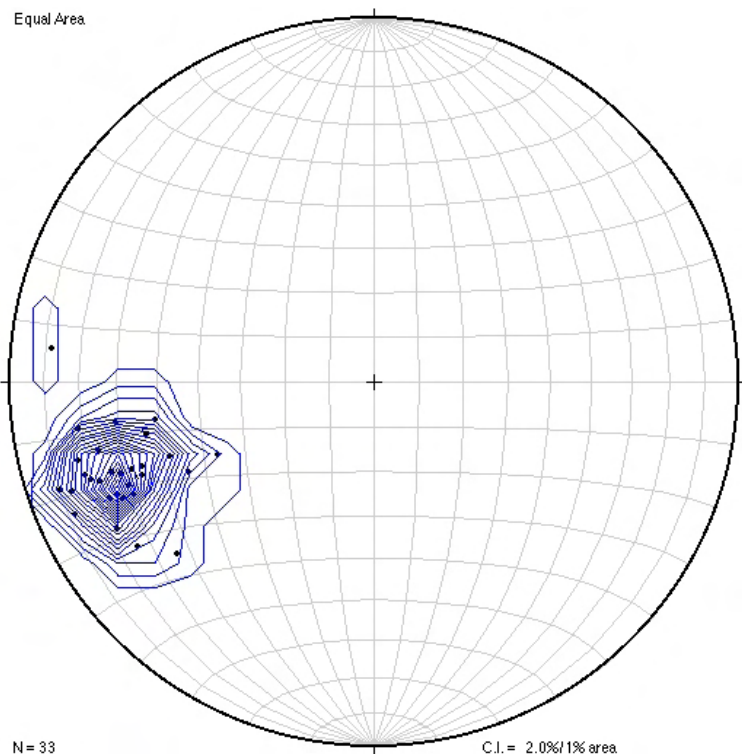


Figure 19. Stereonet diagram showing poles to foliation; Snootli Peak, Bella Coola, southwestern BC. Abbreviation: C.I., contour interval.



Figure 20. Looking north. West-verging F_1 fold hinge in metasedimentary rocks at the western end of mapped area; Snootli Peak, Bella Coola, southwestern BC.



Figure 22. North is to the left. The GPS unit is in the fold hinge of a gentle F_3 fold. Below the GPS unit in outcrop is an F_1 fold hinge folded by the F_3 fold; Snootli Peak, Bella Coola, southwestern BC.

thrusts, northeast vergence and projection along strike. Mahoney *et al.* (2002) suggest that field evidence indicates that this episode of contractional deformation is Early Cretaceous to Tertiary in age.

Transpression of the Bella Coola map sheet area is evidenced by northwest-trending, steeply dipping ductile shear zones occurring between Mount Pootlass and Mount Saunders (north of Falls Camp) that involve Jurassic and Cretaceous plutonic rocks and the Monarch assemblage (Mahoney *et al.*, 2002). Mahoney *et al.* (2002) describe mineral lineations defined by rodded quartz that indicate significant stretch and moderate to intense flattening is indicated by boudinage of mafic layers in plutonic and metasedimentary rocks on Mount Pootlass, similar to the structure reported here.

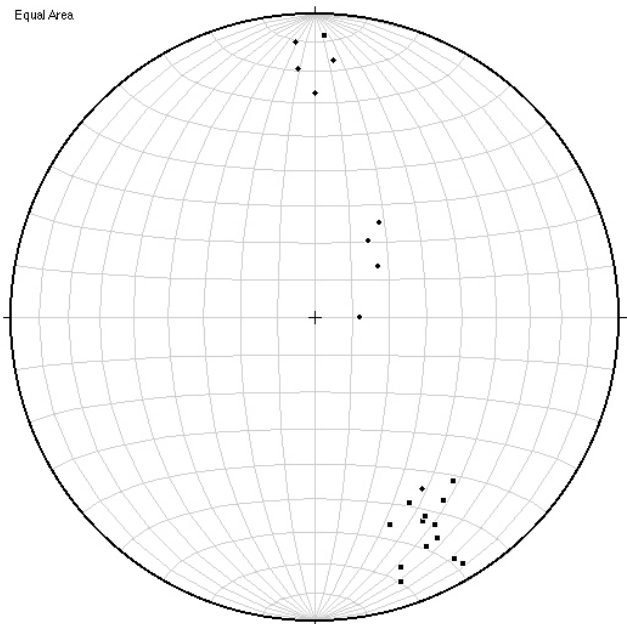


Figure 21. Stereonet diagram showing F_1 fold axes (diamonds), F_3 fold axes (circles) and intersection lineations (squares); Snootli Peak, Bella Coola, southwestern BC.

The major folding phase reported in this paper (F_{1-2}) occurs on Mount Pootlass, at Falls Camp and at Snootli Peak, and is characterized by isoclinal west to southwest-verging upright and tightly spaced folds displayed in plutonic, volcanic and metasedimentary rocks. Fold axes of this episode are mostly subhorizontal or slightly southerly plunging. The major folding episode is most evident in intrusive sheets at the eastern end of the eastern Mount Pootlass ridge (Fig 8) and in metasedimentary rocks at the western end of the Snootli Peak area (Fig 20). A west to southwest-verging orientation for this folding episode in the study area presented in this paper contrasts with the northeast-verging direction presented by Mahoney *et al.* (2002). This indicates that whereas the northeast-verging folds described by Mahoney *et al.* (2002) have been attributed to the Waddington thrust belt, the major folding event (F_{1-2}) presented in this paper is likely related to the mid-Cretaceous contraction of the Coast Belt that has been reported to have been accommodated primarily by the development of southwest-verging thrust faults that were active



Figure 23. Pen points to approximately 330° along the dominant foliation in the metasedimentary rocks. Conjugate kink bands indicate flattening. Green pencil trends toward 342° , yellow pencil trends toward 012° ; Snootli Peak, Bella Coola, southwestern BC.

between 100 and 91 Ma (Journeay and Friedman, 1993; Umhoefer and Miller, 1996).

High-temperature sinistral shearing is best developed on Mount Pootlass in metasedimentary layers (Fig 12) and many felsic stringers in plutonic rocks. The high intensity of non-coaxial strain on Mount Pootlass may be related to magmatism during deformation that promoted strain softening (*i.e.*, strain localization) in the rocks and led to more intense shearing. The presence of L-tectonite in this area suggests that the rocks were very weak during deformation, which is likely a result of syntectonic magmatism.

High-temperature sinistral shear was also noted in metasedimentary rocks at Falls Camp, whereas the Snootli Peak area shows F_{1-2} and F_3 folds with no structures recording non-coaxial strain. The Snootli Peak area is interpreted as recording pre-shearing structures with no strike-slip overprint and attests to the along-strike variation in the PHSZ.

Sinistral shear in the Taseko Lakes has also been documented by Israel *et al.* (2006), who report brittle and ductile sinistral structures in several fault zones in the Tchaikazan River area. Israel *et al.* (2006) suggest that the major Tchaikazan fault was the locus of significant sinistral displacement prior to its reactivation as part of a Late Cretaceous to Eocene dextral fault system.

Low-temperature, foliation-parallel brittle faults are observed in all three areas and cut through all rock types. Several of these late brittle faults show dextral strike-slip movement. These faults are likely to have formed during a Cretaceous to Eocene dextral strike-slip event that affected the entire southeastern Coast Belt (McLaren, 1990; Schiarizza *et al.*, 1997; Andronicos *et al.*, 1999). At the east end of the eastern ridge on Mount Pootlass, these faults may represent a dextral brittle reactivation of an earlier localization of sinistral ductile deformation.

FUTURE RESEARCH

In order to constrain the ages of contraction and transpression, Ar-Ar and U-Pb dating will be conducted on folded and sheared felsic and mafic interlayers in the plutonic and metasedimentary rocks. Thin sections will be used for a petrographic analysis of microstructures that may further identify the kinematic sense of shearing. Fieldwork is scheduled for the summer of 2007 that will focus on other along-strike locations of the high-strain zone and involve a more regional component to put the PHSZ into a regional context.

ACKNOWLEDGMENTS

This research was made possible by a Discovery grant to L.A. Kennedy from the National Sciences and Engineering Research Council of Canada. The authors would like to thank the wonderful crew at the West Coast Helicopters base in Bella Coola, BC for their unwavering support and hospitality. We thank J.B. Mahoney and his team for sharing their knowledge and advice and J. Haggart for supplying us with an up-to-date map of the Bella Coola area. We would also like to thank the people of the Bella Coola Valley for welcoming us into their community.

REFERENCES

- Andronicos, C.L., Hollister, L.S., Davidson, C. and Chardon, D. (1999): Kinematics and tectonic significance of transpressive structures within the Coast Plutonic Complex, British Columbia; *Journal of Structural Geology*, volume 21, pages 229–243.
- Gehrels, G.E. and Boghossian, N.D. (2000): Reconnaissance geology and U-Pb geochronology of the west flank of the Coast Mountains between Bella Coola and Prince Rupert, coastal British Columbia; in *Tectonics of the Coast Mountains, southeastern Alaska and British Columbia*, Stowell, H.H. and McClelland, W.C., Editors, *Geological Society of America*, Special Paper 343, pages 61–75.
- Haggart, J.W., Mahoney, J.B., Woodsworth, G.J., Diakow, L.J., Gordee, S.M., Rusmore, M. and Struik, L.C. (2006): Geology, Bella Coola region (93D/01, /07, /08, /10, /15 and parts of 93D/02, 03, /06, /09, /11, /14, /16 and 92M/15 and /16), British Columbia; Geological Survey of Canada, Open File 5385, scale 1:100 000.
- Haggart, J.W., Diakow, L.J., Mahoney, J.B., Struik, L.C., Woodsworth, G.J. and Gordee, S.M. (2004): Geology, Bella Coola area (parts of 93D/01, D/02, D/06, D/07, D/08, D/09, D/11, D/15 and D/16), British Columbia; *Geological Survey of Canada*, Open File 4639 and *BC Ministry of Energy, Mines and Petroleum Resources*, Open File 2004-13, scale 1:150 000.
- Haggart, J.W., Mahoney, J.B., Diakow, L.J., Woodsworth, G.J., Gordee, S.M., Snyder, L.D., Poulton, T.P., Friedman, R.M. and Villeneuve, M.E. (2003): Geological setting of the eastern Bella Coola map area, west-central British Columbia; *Geological Survey of Canada*, Current Research 2003-A4, 9 pages.
- Hollister, L.S. and Andronicos, C.L. (2006): Formation of new continental crust in western British Columbia during transpression and transtension; *Earth and Planetary Science Letters*, volume 249, pages 29–38.
- Israel, S., Schiarizza, P., Kennedy, L.A., Friedman, R.M. and Villeneuve, M. (2006): Evidence for Early to Late Cretaceous sinistral deformation in the Tchaikazan River area, southwestern British Columbia: Implications for the tectonic evolution of the southern Coast Belt; in *Paleogeography of the North American Cordillera: Evidence For and Against Large-Scale Displacements*, Haggart, J.W., Enkin, R.J. and Monger, J.W.H., Editors, *Geological Association of Canada*, Special Paper 46, pages 329–348.
- Journeay, J.M. and Friedman, R.M. (1993): The Coast Belt thrust system: evidence of Late Cretaceous shortening in southwest British Columbia; *Tectonics*, volume 12, number 3, pages 756–775.
- Mahoney, J.B., Struik, L.C., Diakow, L.J., Hruday, M.G. and Woodsworth, G.J. (2002): Structural geology of eastern Bella Coola map area, southwest British Columbia, *Geological Survey of Canada*, Current Research 2002-A10, 9 pages.
- McLaren, G.P. (1990): A mineral resource assessment of the Chilko Lake planning area; *BC Ministry of Energy, Mines and Petroleum Resources*, Bulletin 81, 117 pages.
- Ramsay, J.G. and Huber, M.I. (1987): *The Techniques of Modern Structural Geology*; volume 2, *Folds and Fractures*, Academic Press, 700 pages.
- Rusmore, M.E., Woodsworth, G.J. and Gehrels, G.E. (2000): Late Cretaceous evolution of the eastern Coast Mountains, Bella Coola, British Columbia: tectonics of the Coast Mountains, southeastern Alaska and British Columbia; *Geological Society of America*, Special Paper 343, pages 89–105.
- Schiarizza, P., Gaba, R.G., Glover, J.K., Garver, J.I. and Umhoefer, P.J. (1997): Geology and mineral occurrences of the Taseko

- Bridge River area; *BC Ministry of Energy, Mines and Petroleum Resources*, Bulletin 100, 291 pages.
- Struik, L.C., Mahoney, J.B., Hrudey, M.G., Diakow, L.J., Woodsworth, G.J., Haggart, J.W., Poulton, T.P., Sparks, H.A. and Kaiser, E.A. (2002): Lower Cretaceous stratigraphy and tectonics of eastern Bella Coola map area, southwest British Columbia; *Geological Survey of Canada*, Current Research 2002-A11, 10 pages.
- Struik, L.C. and Veljkovic, V. (2001): Geology, Bella Coola, British Columbia; *Geological Survey of Canada*, Open File 4018, scale 1:250 000.
- Umhoefer, P.J. and Miller, R.B. (1996): Mid-Cretaceous thrusting in the southern Coast Belt, British Columbia and Washington, after strike-slip fault reconstruction; *Tectonics*, volume 15, pages 545–565.
- van der Heyden, P. (2004): Uranium-lead and potassium-argon ages from eastern Bella Coola and adjacent parts of Anahim Lake and Mount Waddington map area, west-central British Columbia; *Geological Survey of Canada*, Current Research, 2004-A2, 16 pages.
- van der Heyden, P. (1991): Preliminary U-Pb dates and field observations from the eastern Coast Belt near 52°N, British Columbia; *Geological Survey of Canada*, Current Research, Part A, Paper 91-1E, pages 79–84.

Rhodonite from the Bridge River Assemblage, Downton Creek (NTS 092J/09), Southwestern British Columbia

by Z.D. Hora¹, A. Langrova² and E. Pivec³

KEYWORDS: industrial minerals, rhodonite, sedimentary manganese minerals, chert, rhodochrosite, kutnohorite, cobaltite, gersdorffite, ullmannite, tucekite, replacement mineralization

INTRODUCTION

A new rhodonite occurrence was discovered in the Downton Creek area, about 20 km west of Lillooet (Fig 1). Prospector G. Polischuk of Lillooet made the discovery while carrying out work between 1996 and 1999, under a 1995–1996 Prospector's Grant. Float in Downton Creek was traced to an outcrop in a small unnamed northern tributary, and subsequent staking of two mineral claims, Southern Gem 1 and 2, covered the rhodonite outcrops.

Samples of Downton Creek rhodonite differ from those studied from similar showings in British Columbia (Nelson *et al.*, 1990; Simandl and Church, 1996; Hora *et al.*, 2005). Hydrothermal replacement of the Downton Creek rhodonite has completely destroyed its original banded structure.

Based upon petrographic textures, it appears that rhodonite grains first recrystallized into automorphic shapes and, during later hydrothermal alteration, were replaced by Mn carbonates and finally quartz. Veinlets rich in Ni-Co-Sb-As sulphides, together with a Bi-Te mineral, indicate a fluid contribution from a source other than the Mn protolith.

ANALYTICAL PROCEDURES

Analytical procedures were similar to those reported in Hora *et al.* (2005). The only difference is that, in order to study the base metal minerals, a beam diameter of approximately 2 μm , an accelerating potential of 20 KeV and a beam current 10 nA was used. Nine new standards were

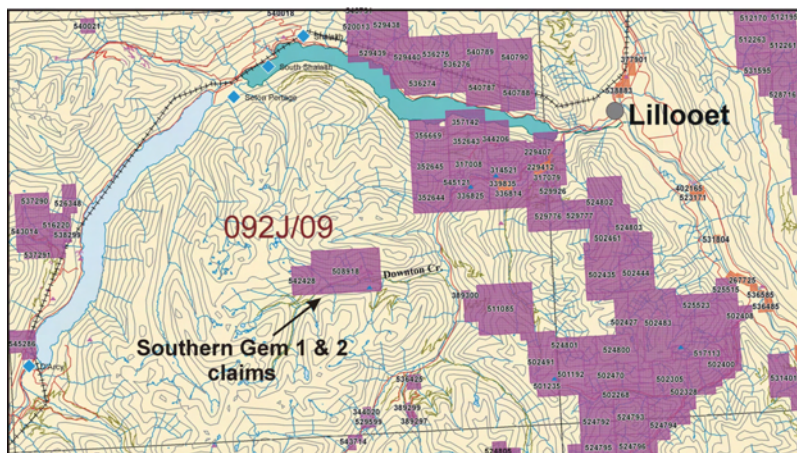


Figure 1. Location of rhodonite occurrence on Downton Creek, near Lillooet.

used: marcasite, GaAs, Ni, Co, Mn_3O_4 , Ag, Bi_2SO_3 , pyrite and stibnite.

GEOLOGY

The Downton Creek rhodonite occurrence is located along the Downton Creek fault in the central Cayoosh Range. It occurs within the Eastern assemblage of the Bridge River Complex (Journey and Northcote, 1992), which consists primarily of sheared greenstone, serpentinite, chert and fine-grained volcanoclastic rocks (Journey, 1993).

Rhodonite occurs in slabs of up to 30 cm^2 in association with cherty quartzite and greenstone (G. Polischuk, pers comm, 2006). Quartz veining with arsenopyrite, pyrite and chalcopyrite is common along faults and shear zones that are exposed in logging-road cuts (Polischuk, 1999).

Between the Duffy Lake road and Anderson Lake, the northwest-trending Downton Creek fault marks the boundary between two facies of the Bridge River assemblage, a coherent greenstone-chert argillite in the west and sheared greenstone-chert mélangé in the east. The fault cuts the overturned limb of a regional southwest-verging syncline and associated thrust faults in the Downton Creek headwater region (Journey *et al.*, 1992).

MINERALOGY

The dominant mineral in the samples studied is typically pink rhodonite. Compared to similar samples from Arthur Point, near Bella Coola, it is coarser grained (up to 1 mm) with frequent automorphic-shaped pinacoidal crystals (Fig 2, 3).

¹British Columbia Geological Survey (retired)

²Geological Institute, Academy of Sciences of the Czech Republic, Prague, Czech Republic

³Geological Institute, Academy of Sciences of the Czech Republic, Prague, Czech Republic (retired)

This publication is also available, free of charge, as colour digital files in Adobe Acrobat® PDF format from the BC Ministry of Energy, Mines and Petroleum Resources website at http://www.em.gov.bc.ca/Mining/Geosurv/Publications/catalog/cat_fldwk.htm

The crystals grow into the cavities, which were later filled with vein quartz (Fig 4, 5). Quartz replaces rhodonite crystals so that, in some samples, only fragments of the original columnar rhodonite crystals remain (Fig 6, 7, 8). The chemical composition of rhodonite is almost pure MnSiO_3 (Table 1), except for Ca, which may constitute from 1 to 7 wt. % of the mineral formula (as CaO). Taken together, the remaining elements form less than 1 wt%. Elevated Zn (0.11%) is common in rhodonite associated with chert (Crerar *et al.*, 1982) and correlates positively with FeO .

The second most common mineral in Downton Creek rhodonite samples is quartz, which is the latest hydrothermal mineral, replacing all other mineral phases. Quartz veinlets cut along cleavage and pressure fractures in rhodonite crystals (Fig 4, 5) and display undulatory extinction (Fig 9). Whether the quartz is a product of the transformation of rhodonite to rhodochrosite, or a product of some other hydrothermal event, has not been established.



Figure 2. Automorphic rhodonite crystals in quartz-filled vugs, with quartz partially replacing rhodonite; cross-polarized light.

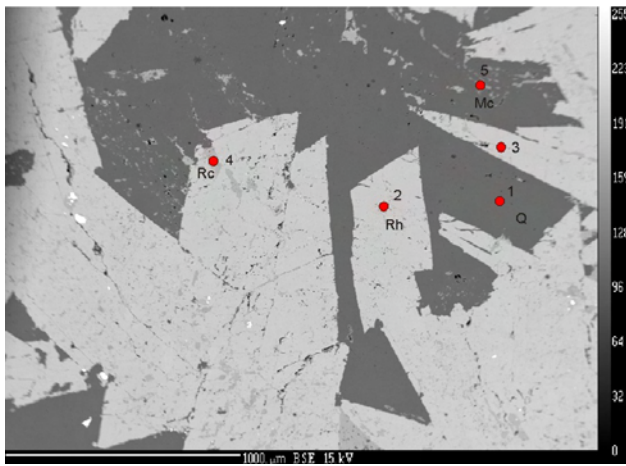


Figure 3. Same as Figure 2, showing rhodonite (Rh) being replaced by rhodochrosite (Rc) and successively by quartz (Q); white grains are ore minerals (sulphides of the niccolite-cobaltite-skutterudite group); back-scattered electron image with location of microprobe tests.

A relatively common component of the sample is kutnohorite $\text{Ca}(\text{Mn, Mg, Fe})(\text{CO}_2)_2$ (see x-ray diffraction record, Fig 10) which is present as greyish pink aggregates of xenomorphic grains approximately 0.05 mm in diameter (Fig 11, 12). Compared to the kutnohorite from a classical occurrence (Fron del and Bauer, 1955; Trdlička and Ševců, 1968), the Downton Creek samples have lower contents of MgO and FeO (Table 1). Their unusual composition may be explained by formation via replacement of rhodonite.

Veinlets and aggregates of kutnohorite (Fig 11, 12) penetrate into rhodonite along cleavage and boundaries of adjacent crystals. In some samples, kutnohorite is replaced by quartz (Fig 5). Rhodochrosite occurs in veinlets and aggregates up to 100 μm in size (Fig 13, 14), locally with manganocalcite. Both are later than rhodonite, but earlier than kutnohorite and quartz. Relics of manganocalcite and rhodochrosite (Fig 3) within quartz and along rims of rhodonite suggest that rhodonite was originally replaced by both, followed by quartz replacement.

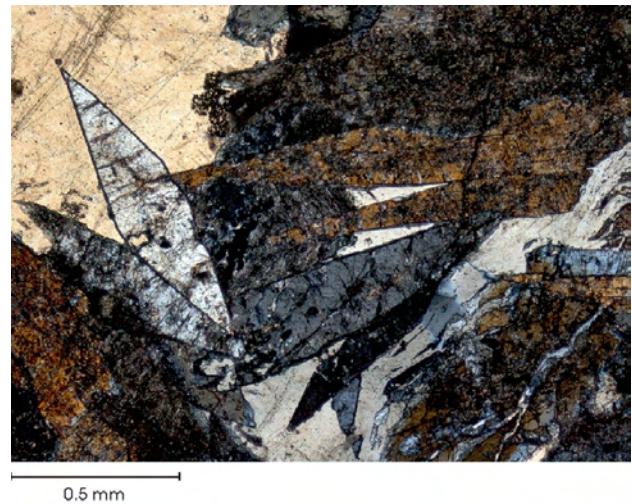


Figure 4. Automorphic crystals of rhodonite (1 mm in size) in quartz filled vug; quartz also penetrates rhodonite along fractures and cleavage planes; cross-polarized light.

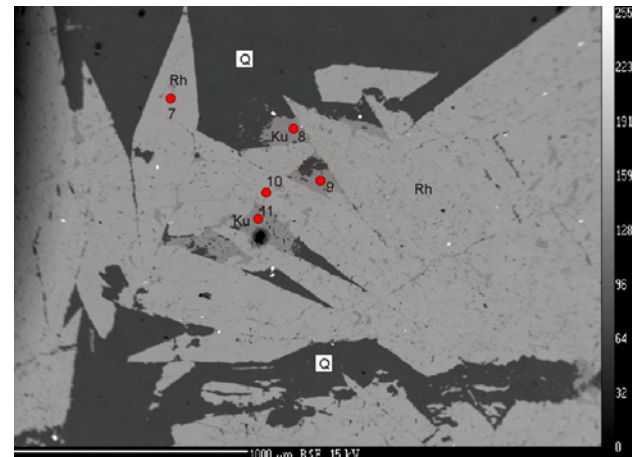


Figure 5. Same as Figure 4, with rhodonite (Rh) being replaced by kutnohorite (Ku); ore minerals (white grains) are irregularly dispersed, mainly in rhodonite; back-scattered electron image with location of microprobe tests.

Cobaltite (CoAsS), gersdorffite (NiAsS), ullmannite (NiSbS) and tučekite (Ni₉Sb₂S₈) all occur as tiny grains (up

to 2 μm) along fractures in rhodonite and less commonly in quartz (Table 2; Fig 2, 5). Some grains exhibit zoning (Fig 15).

A grey metallic mineral containing 48.69% Bi, 36.58% Te, 2.91% Ni and 0.21% Se could not be identified with certainty due to its tiny grain size (less than 2 μm). Its chemical composition is suggestive of tetradymite affinity.

TABLE 1. SELECTED ANALYSES OF MINERALS FROM DOWNTON CREEK RHODONITE OCCURRENCE.

Element (wt%)	Cobaltite		Gersdorffite		Ullmannite	Tučekite	
Fe	0.05	0.19	0.09	0.22	0.01	0.85	0.10
Ni	2.49	5.63	35.10	31.00	27.57	48.74	46.34
Co	31.50	28.96	0.20	3.80	0.26	2.15	4.75
Sb	0.17	0.49	3.91	4.50	52.20	22.37	17.11
Mn	0.44	1.89	0.91	0.80	0.57	1.31	2.14
Ag	0.44	0.00	0.00	0.00	0.02	0.00	0.00
Bi	0.00	0.00	0.06	0.00	0.19	0.06	0.00
As	42.21	43.67	41.65	40.08	4.26	0.62	2.73
S	20.48	19.80	18.96	19.39	15.24	24.84	25.82
Total	97.78	100.63	100.88	99.79	100.32	100.94	98.99



Figure 6. Skeletal arrangement of rhodonite crystals partially replaced by quartz; cross-polarized light.



Figure 7. Same as Figure 6, in plane-polarized light.



Figure 9. Rhodonite replaced by quartz with undulatory extinction; cross-polarized light.

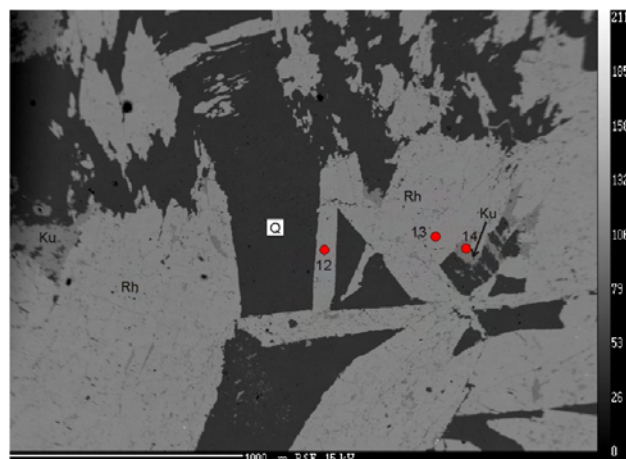


Figure 8. Same as Figures 6 and 7, with quartz (Q) replacing rhodonite (Rh) and kutnohorite (Ku); back-scattered electron image with locations of microprobe tests.

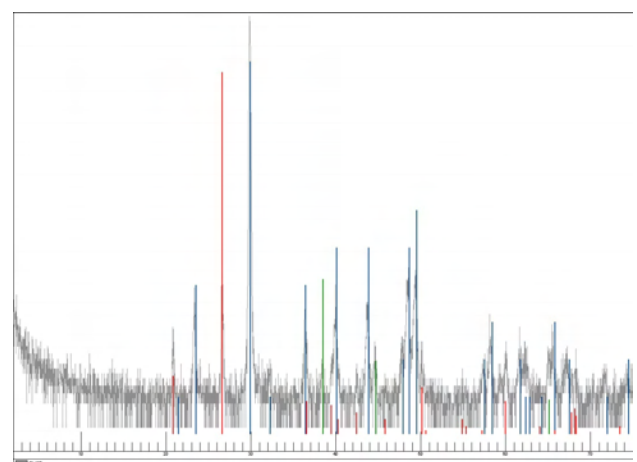


Figure 10. X-ray diffraction record of calcian kutnohorite (blue, kutnohorite; red, quartz; green, alumina holder).

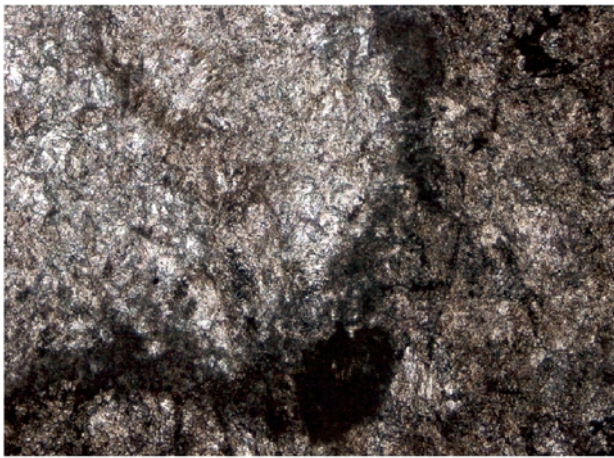


Figure 11. Fine-grained rhodonite (darker) is replaced by rhodochrosite (lighter); boundary between the two is formed by quartz; plane-polarized light.

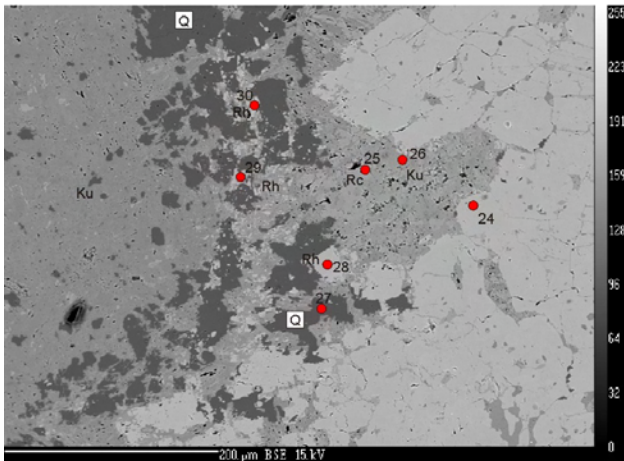


Figure 12. Same view as in Figure 11, showing the manganese carbonates rhodochrosite (Rc) and kutnohorite (Ku) replacing rhodonite (Rh), which results in the silica component being freed from the rhodonite as quartz (Q); back-scattered electron image with location of microprobe tests.



Figure 13. Ladder arrangement of partially replaced rhodonite crystals in a quartz vein; plane polarized light.

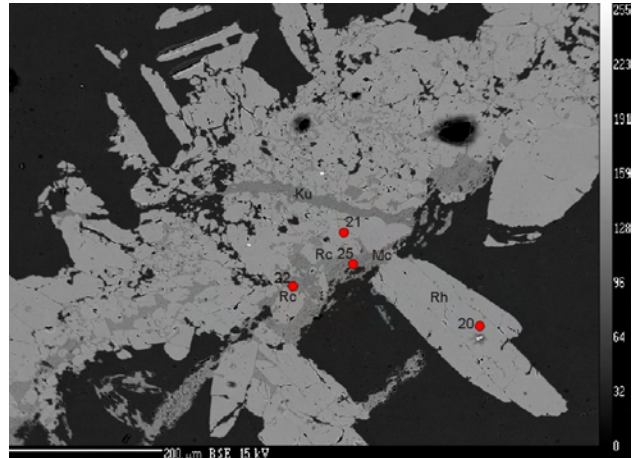


Figure 14. Rhodonite 'ladder' arrangement in detail: rhodonite (Rh), rhodochrosite (Rc), kutnohorite (Ku) and Mn calcite (Mc) are replaced by quartz (Q); back-scattered electron image with location of microprobe tests.

SUMMARY

The rhodonite sample from Downton Creek is significantly distinct from material described earlier from Arthur Point. Extensive hydrothermal replacement of the Downton Creek rhodonite has destroyed all original banding within the protolith. Rhodonite was recrystallized into idiomorphic grains, and was subsequently replaced by Mn carbonate and finally by quartz.

The occurrence of Ni-Co-Sb-As minerals together with Bi-Te minerals is unusual in rhodonite deposits. The Bi-Te minerals are common accessory minerals in mesothermal lode gold deposits and are known from the Bridge River camp (Cairnes, 1937). Free gold has also been recovered from the adjacent Raven claims (G. Polischuk, pers comm, 2006). Similar associations of minerals of Ni and Co are known as coproducts of serpentinization, occurring as veins within rodingite rims of serpentinite bodies in both Morocco (Leblanc and Billaud, 1982) and the Italian Alps (Castelli and Rosetti, 1994). The proximity of this rhodonite showing to a major fault and its association with greenstone-serpentine mélangé suggest that the Ni-Co minerals were mobilized from the oceanic crust and mantle facies of the Bridge River assemblage.

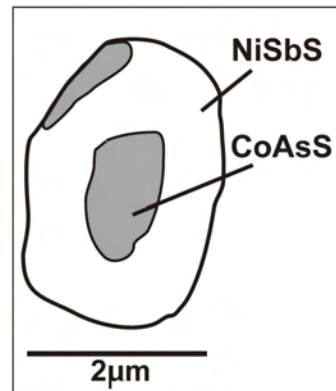


Figure 15. Example of zoning in ore mineral, with cobaltite surrounded by ullmannite.

TABLE 2. SELECTED ANALYSES OF DISSEMINATED ORE MINERALS FROM DOWNTON CREEK RHODONITE OCCURRENCE.

	Rhodonite			Rhodochrosite			Kutnohorite		Mn calcite	
Sample	1	1	2	1	2	2	1	1	1	1
Text figure	3	5	11	3	13	11	5	8	3 (ni)	13
Analyses	2	7	24	4	22	25	8	14	5	18
Oxide (wt%):										
SiO ₂	46.97	47.40	46.73	0.08	0.00	0.01	0.00	0.01	0.13	0.03
TiO ₂	0.00	0.02	0.02	0.00	0.00	0.00	0.02	0.00	0.00	0.00
Al ₂ O ₃	0.02	0.00	0.03	0.00	0.03	0.02	0.00	0.04	0.00	0.01
Cr ₂ O ₃	0.00	0.03	0.00	0.06	0.00	0.00	0.03	0.04	0.12	0.00
FeO	0.60	0.36	0.22	0.06	0.00	0.00	0.00	0.12	0.00	0.10
MgO	0.67	0.22	0.37	0.55	0.49	0.38	0.22	0.24	0.22	0.43
MnO	43.28	43.75	45.48	52.28	50.28	48.60	44.60	46.78	24.26	38.22
CaO	7.17	7.43	7.17	6.24	8.22	9.80	12.69	12.86	36.00	18.99
ZnO	0.11	0.00	0.01	0.00	0.00	0.00	0.00	0.09	0.00	0.00
BaO	0.00	0.00	0.07	0.00	0.00	0.00	0.02	0.00	0.00	0.00
Na ₂ O	0.00	0.00	0.03	0.00	0.01	0.01	0.01	0.00	0.00	0.00
K ₂ O	0.00	0.02	0.00	0.00	0.03	0.00	0.01	0.00	0.00	0.01
Total	98.82	99.23	100.13	59.27	59.06	58.82	57.60	60.18	60.73	57.79

Abbreviation: ni, not included

ACKNOWLEDGMENTS

The authors wish to thank Gary Polischuk for bringing this discovery to their attention and for providing samples for this study. J. Pávková and Z. Korblová provided technical assistance; J. Brožek, V. Šrein and B. Šreinová helped with photo-documentation; and J. Dobrovolný helped with X-ray records. Constructive comments and editorial improvements were provided by Brian Grant, Mitch Mihalynuk and Paul Schiarizza.

REFERENCES

- Cairnes, C.E. (1937): Geology and mineral deposits of Bridge River mining camp, British Columbia; *Geological Survey of Canada*, Memoir 213, 140 pages.
- Castelli, D. and Rossetti, P. (1994): Sulphide-arsenide mineralization in rodingite from the Balangero mine (Italian western Alps): hydrothermalism related to metamorphic fluids; *Giornata di studio in ricordo del Prof. Stefano Zucchetti*, Politecnico di Torino, pages 103–110.
- Crerar, D.A., Namson, J., Chyi, M.S., Williams, L. and Feigenson, M.D. (1982): Manganiferous cherts of the Franciscan Assemblage: I. General geology, ancient and modern analogues, and implications for hydrothermal convection at oceanic spreading centers; *Economic Geology*, volume 72, pages 519–540.
- Frondele C. and Bauer L.H. (1955): Kutnohorite: a manganese dolomite; *American Mineralogist*, volume 40, pages 748–759.
- Hora, Z.D., Langrova, A. and Pivec, E. (2005): Contribution to the mineralogy of the Arthur Point rhodonite deposit, southwestern British Columbia; in *Geological Fieldwork 2004*, BC Ministry of Energy, Mines and Petroleum Resources, Paper 2005-1, pages 177–185.
- Journeay, J.M. (1993): Tectonic assemblages of the eastern Coast Belt, southwestern British Columbia: implications for the history and mechanisms of terrane accretion; in *Current Research, Part A*, *Geological Survey of Canada*, Paper 93-1A, pages 221–233.
- Journeay, J.M. and Northcote, B.R. (1992): Tectonic assemblages of the eastern Coast Belt, southwest British Columbia; in *Current Research, Part A*, *Geological Survey of Canada*, Paper 92-1A, pages 215–224.
- Journeay, J.M., Sanders, C., Van-Konijnenburg, J.H. and Jaasma, M. (1992): Fault systems of the eastern Coast Belt, southwest British Columbia; in *Current Research, Part A*, *Geological Survey of Canada*, Paper 92-1A, pages 225–235.
- Leblanc, M. and Billaud, P. (1982): Cobalt arsenide orebodies related to an Upper Proterozoic ophiolite, Bou Azzer (Morocco); *Economic Geology*, volume 77, pages 162–175.
- Nelson, J.A., Hora, Z.D. and Harvey-Kelly, F. (1990): A new rhodonite occurrence in the Cassiar area, northern British Columbia (104P/5); in *Geological Fieldwork 1989*, BC Ministry of Energy, Mines and Petroleum Resources, Paper 1990-1, pages 347–350.
- Polischuk, G. (1999): Prospecting assessment report on the Sam mineral claim, Lillooet Mining Division, Canada; *BC Ministry of Energy, Mines and Petroleum Resources*, Assessment Report 26987, 18 pages.
- Simandl, G.J. and Church, B.N. (1996): Clearcut pyroxmangite/rhodonite occurrence, Greenwood area, southern British Columbia (82E/E2); in *Geological Fieldwork 1995*, BC Ministry of Energy, Mines and Petroleum Resources, Paper 1996-1, pages 219–222.
- Trdlička, Z. and Ševců, J. (1968): Chemisches und roentgenographisches Studium des Kutnohorits von Kutna Hora; *Acta Universitatis Carolinae*, Geologica, volume 3, pages 175–189.

Update of British Columbia Geological Survey Geospatial Databases and Applications

by L.D. Jones, P.J. Desjardins, K.D. Hancock, A.F. Wilcox, L.L. de Groot and J.G. McArthur

KEYWORDS: MINFILE, Property File, MapPlace, ARIS, Geospatial Data, MapPlace2Go, Geological Publications, Exploration Assistant, Geological Databases

INTRODUCTION

The Fraser Institute's Annual Survey of Mining Companies 2005/2006 recognized British Columbia as having the top-ranked geological database in the world. More than 300 mining, exploration and consulting companies responded and rated BC's attractiveness for investment in mineral exploration and mine development. In 2005, these mining companies invested approximately \$2 billion in exploration worldwide. In BC, the industry invested approximately \$200 million in the same period. This ranking, in comparison with 64 jurisdictions, is a strong indicator of the competitive advantage that results from a superior geological database as well as the opportunity to attract a larger share of worldwide expenditures.

The BC geological database includes geological knowledge produced and recorded for over 110 years by a diverse range of geoscientists. These include those who have worked in industry, academia and government, as well as independent, entrepreneurial prospectors and miners. The exceptional value of this database is that a high percentage of the geological work carried out in BC has been documented and is easily accessible, using state-of-the-art information management technology.

The BC Geological Survey (BCGS) is only one of several key organizations that contribute annually to this body of knowledge. The BCGS's main map and database access tool is called the MapPlace. The strength of this Internet-based system lies in its ability to retrieve geological and mineral-related data from our own corporate datasets as well as data and map information from other sources, both within and outside of BC.

The BCGS databases are continually evolving with the addition of new data and improvements to accessibility and functionality. The purpose of this paper is to provide an update on the status of the following corporate databases:

- MINFILE, the provincial mineral inventory with over 12 300 mineral, coal and industrial mineral occurrence records compiled over the past 35 years;

- The Property File, an *ad hoc* collection of hardcopy reference materials supporting the descriptions of occurrences in MINFILE;
- ARIS, the Mineral Assessment Report Indexing System with over 28 000 reports submitted, documenting the results of industry exploration investments in BC since 1947, and;
- The MapPlace, an Internet-based, interactive GIS tool for viewing, analyzing and interpreting BC's geological database in the broadest sense, including MINFILE, COALFILE, ARIS and numerous internal and external geoscience-related datasets.

The BC geological database should be considered an integral component of the infrastructure fabric that supports the province, its economic and resource development and the protection of its physical environment. The above databases are of strategic importance to the provincial mandate to manage the stewardship of its mineral and coal resources.

The right tools, such as interactive maps, appropriate downloads and scanned reports, can help effectively and efficiently retrieve mineral-related information to develop exploration investment strategies, conduct geoscience research, evaluate the resource potential of an area or plan for land-related decisions.

MINFILE ENHANCEMENTS

MINFILE/www is an internet-based mineral inventory database system for over 12 300 metallic mineral, coal and industrial mineral occurrences in BC. MINFILE/www is recognized internationally as an exceptional geoscience information system. The system is a 'desktop prospecting' tool used for planning exploration programs, investment, resource management, policy planning, land use planning, teaching and research. The site is located at <http://www.MINFILE.ca>.

The 2005 system upgrades to MINFILE/www included rewriting the DOS-based MINFILE system — the first in 20 years — and establishing it as an SQL database accessed through the Internet. While the database formats have changed, the fundamental, underlying data architecture has remained the same. This aspect has maintained the overall robustness of the original MINFILE system. MINFILE/www was optimized for Microsoft® Internet Explorer® (IE) 6; however, it will work on IE 7 and Netscape®. MINFILE/www searches can be used with dial-up connections, but better performance is achieved with higher bandwidth connections.

MINFILE/www is interconnected with other Ministry database interfaces. Location information is linked to the MapPlace by clicking on the latitude-longitude link, which

This publication is also available, free of charge, as colour digital files in Adobe Acrobat® PDF format from the BC Ministry of Energy, Mines and Petroleum Resources website at http://www.em.gov.bc.ca/Mining/Geosurv/Publications/catalog/cat_fldwk.htm

opens a new window with an interactive map. The resulting linked window shows the series of layers turned on and the occurrence at the centre of the map. MINFILE/www is also linked to the ARIS (Assessment Report Index System) data interface. Clicking on an assessment report number link in the MINFILE bibliography connects to the ARIS Summary Report with a link to the PDF report. This interconnection structure has been designed to increase the accessibility of our data. Part of the system upgrade focused on the ability to crosslink all three of these data interfaces so it is possible to reach any one from another.

The new MINFILE/www system has a user-friendly interface with Online Help throughout (Fig 1). The layout has thematic tabs grouped by Identification/Location, Mineral Occurrence, Host Rock, Geological Setting, Inventory, Production and Capsule Geology/Bibliography. Searches can be done using input text, including partial text strings, drop-down pick lists and check boxes. Significant improvements include free-text searches on all comment fields and the Capsule Geology and Bibliography fields. Searches can be stacked to refine a series of results to very specific criteria. The default Basic Search has a link to the Advanced Search, which includes more fields and allows for complex searches around Boolean logic operators.

Initial search results are delivered in tabular format, showing several key fields. Clicking on the MINFILE number links to a summary page and further links connect to the full MINFILE detailed report, as well as production and inventory reports, if available. At all stages of the search, download information is available, differing in type depending on the depth within the search result stack. Download formats include PDF documents, Microsoft Word documents, plain-text files and Microsoft Excel spreadsheets.

Other features include the 'Import Numbers' tab, MINFILE/pc and the online MINFILE Coding Card. The Import Numbers tab allows a user to manually input individual MINFILE numbers to search. The numbers can be input from a previously developed search where the result-

ing MINFILE numbers were downloaded, a text file list developed by a user or typed directly into a special window in the search application. This feature allows searches to be 'saved' for future use or to have user-specific requirements met, such as a client's property portfolio.

MINFILE/pc is a user-friendly, Microsoft Access application that is downloadable for offline use. It has an interface similar to MINFILE/www and consists of Basic/Advanced searches, on-screen occurrence summary data and other reports and downloads. MINFILE/pc provides a portable extract of the MINFILE database, along with search forms and printable reports. This is useful for those that want to take the full database into the field. The data can be updated simply by connecting to the Internet and downloading again.

The online MINFILE Coding Card allows clients to update existing or report new descriptions of mineral occurrences. It is similar to the search pages and is supplied with many drop-down lists, pick boxes and automated fill fields designed to make coding convenient. Once an addition is made and approved, the update is immediately available online. Those wishing to do online coding must contact the BCGS for access and more information.

The upgraded MINFILE system software and reports provides convenient and comprehensive access to the MINFILE database. The move to an Internet-based system makes it accessible from anywhere in the world. The enhancements have increased the variety and sophistication of searches that can be done. Downloadable products and interconnectivity with other Ministry applications make MINFILE/www a world leader in geological search and retrieval data systems.

MINFILE Database

The first computerized database of mineral occurrence information for BC began at The University of British Columbia in the early 1970s and was known as MINDEP. It

Figure 1. MINFILE/www search screen.

soon migrated to the BC Geological Survey as a mainframe application and database that became known as MINFILE. In 1986, after the advent of minicomputers, MINFILE was completely restructured for the smaller platform and rewritten as a relational database. Since 1984, the information in the MINFILE database has undergone extensive expansion. The data has been updated by experienced geologists to ensure that the information available is factual, concise and high quality. By June 1990, MINFILE had 4950 occurrences updated and released, which represented 48% of the provincial total. As of April 1995, 85% of MINFILE had been updated. By January 2002, MINFILE had 12 098 occurrences and by the end of 2005, all 12 300 occurrences were completed to the standard set in 1986. Challenges still exist to maintain currency of the data and add new occurrences. The recent focus has been to update the major exploration projects and mines.

PROPERTY FILE PROJECT

Property File is an *ad hoc* collection of documents that have been acquired over the years by Ministry staff as well as donations from the mining industry and academic institutions. Property File currently contains over 90 linear metres of reports and maps that are generally unavailable elsewhere. These documents can be extremely valuable to researchers. It comprises, but is not limited to unpublished reports; theses and papers; field notes; company prospectuses and pamphlets; historical information; geology, geochemistry, geophysics and drill information; claim maps, sketches of workings; photographs; memos; letters; news clippings and articles, all from as far back as the late 1800s. The documents vary in size, from small notes and newspaper 'clippings' through to 4' by 6' drawing sheets. The bulk of the contents are original documents, with photocopies typically of news-type items such as trade papers and trade/technical journals. Property File also contains general, regional, geological and mineral deposit information on mineral occurrences in BC, the National Mineral Inventory data cards, topographic maps and some work histories. In addition, Property File has been a location for placing miscellaneous information (such as promotional material), which may have little or no technical importance, but provides background material to specific mineral occurrences or camps. Many of the documents are unique and have historical (archival) relevance. Property File also has several special collections that were donated by mineral exploration and mining companies. These sizable collections are currently housed in offsite storage. The uniqueness and age of the information contained make Property File a valuable research tool, yet it is greatly underused due to limited access and its lack of a comprehensive, centralized index.

In 2005, the Property File project was initiated to make this material Internet accessible. Property File documents will be scanned and indexed in a metadata catalogue and made fully searchable. The documents will be linked to MINFILE/www and the MapPlace. Upon completion of a pilot project to determine the most effective way to scan and index the wide variety of documents, the project will start with the Ministry's collection in the Library. Following that, our other collections of donated files will be incorporated into the database. As well, other collections in the regional offices including Cranbrook, Kamloops, Prince George and Smithers will be reviewed for inclusion. The data structure and metadata catalogue are currently in the

development stage. As the project proceeds, depending on annual funding, scanned documents and metadata will be posted to the Internet. This project will be ongoing, similar to the mineral assessment reports being made available online. The BC Geological Survey will be pleased to receive additional donations of company or personal geoscience documents to add to the Property File collection. Donations will be acknowledged as part of the database and will be posted on the Property File web page (<http://www.em.gov.bc.ca/mining/Geolsurv/Minfile/propfile.htm>).

COALFILE

Coal is the second-most important resource exported from BC, next to wood products. The Ministry maintains a library of 828 coal assessment reports. These reports have been scanned as PDF documents. Partial versions are available for download from the web or full versions are available on DVD at a cost of \$20 per report. An online COALFILE search application allows searches on COALFILE Number, Report Year, Coal Field and NTS Map (<http://webmap.em.gov.bc.ca/mapplace/coal/search.asp>). Results include links to Coal Assessment Reports, Boreholes, Bulk Samples, Trenches, MINFILE, MapPlace and Google Earth.

ARIS (ASSESSMENT REPORT INDEXING SYSTEM)

Results of mineral and placer exploration and development programs are required to be submitted to the Ministry in the form of an assessment report and reviewed for compliance with the *Mineral Tenure Act* (MTA) Regulations. The reports are indexed in the ARIS (Assessment Report Indexing System) Assessment work comprises approximately 40% of the overall mineral exploration carried out in the province. Of this 40%, about 75% is filed to maintain claims and 25% is filed in portable credit accounts (PAC).

The Assessment Report Library contains over 28 000 reports describing exploration work valued at over \$1 billion. After the one-year confidential period, all reports are scanned for distribution on CD-ROM/DVD and the Assessment Report home page. A total of 26 250 reports (96%) are currently scanned and available for free downloading.

The ARIS database can be accessed through ARIS/www, an online search tool (Fig 2), and the MapPlace. The electronic distribution of mineral assessment reports enhances our current Internet service and eliminates the production of microfiche. Benefits of this project are faster access to data for 'desktop prospecting', improved user friendliness and worldwide access for prospective investors.

Brief History of ARIS

The assessment report system was introduced in 1947 to archive information collected by the mineral exploration industry. These reports are used by prospectors and exploration companies to facilitate the discovery of new mines. It also plays an important role in mineral resource assessments by governments.

ARIS Assessment Report Database

Search on any combination of fields:

New Search Import Reports Help

AR Number	<input type="text"/>	Latitude	<input type="text"/> <input type="text"/> <input type="text"/>	To	<input type="text"/> <input type="text"/> <input type="text"/>
Affidavit Date	<input type="text"/> To <input type="text"/>	Longitude	<input type="text"/> <input type="text"/> <input type="text"/>	To	<input type="text"/> <input type="text"/> <input type="text"/>
<i>Dates must be in the format YYYYMMDD.</i>					
Claim Name	<input type="text"/>	Mining Camp		<input type="text"/>	
Property Name	<input type="text"/>	Keywords		<input type="text"/>	
Individual Name	<input type="text"/>	General Work		<input type="checkbox"/> Drilling <input type="checkbox"/> Geochemical	
<input type="checkbox"/> Operators <input type="checkbox"/> Owners <input type="checkbox"/> Authors		Specific Work		<input type="checkbox"/> Geological <input type="checkbox"/> Geophysical	
Mining Division	<input type="text"/>	Physical		<input type="checkbox"/> Prospecting	
NTS Map Number	<input type="text"/>	Becker Hammer		<input type="text"/>	
BCGS Map Number	<input type="text"/>	Churn		<input type="text"/>	
MINFILE Number	<input type="text"/>				

Search on All 27,789 Assessment Reports (Approved or Under Review)

Figure 2. ARIS search screen.

The Assessment Report Library ceased microfilming the assessment reports in 1999 and switched to scanning the reports as PDF (Adobe Acrobat™ portable document files). This began through a partnership with Abitibi Mining Corp., Black Bull Resources Inc., Eagle Plains Resources Ltd, Kennecott Canada Exploration Inc. and Klondike Gold Corp. Since that time, the BC Geological Survey has entered into several other major partnerships. The following companies are acknowledged for their contribution in helping scan portions of the reports: Heritage Explorations Ltd., International Wayside Gold Ltd., St. Andrew Goldfields, Ram Explorations, SYMC Resources Limited and Geoinformatics Exploration Ltd.

ARIS MapBuilder

The ARIS MapBuilder was created to quickly produce location and claim maps of properties to partially fulfill assessment reporting requirements. Users simply enter the property name and all associated Tenure ID Numbers in the online form and click a Create Map button. A Tenure Report button creates a list of tenures on the property with links to details from Mineral Titles Online. The resulting index map of the property, the claim map (Fig 3), and a list of all the claims can then be included in an assessment report. This saves the author time in drafting the map or looking for the required information. The site also creates a Keyhole Markup Language (KML) file to show claims in viewers such as Google Earth.

NEW AND UPDATED MAPPLACE DATA LAYERS AND TOOLS FOR THE PROSPECTOR

Overview

The MapPlace (www.mapplace.ca) uses the Internet to provide interactive access to an extensive array of

geospatial map information related to BC bedrock and surficial geology, terrain information, mineral resources, mineral exploration and onshore/offshore energy resources. The site is hosted by the BC Ministry of Energy, Mines and Petroleum Resources and has been in operation since 1995. The award-winning site (BC & Yukon Chamber of Mines Award 2000 and Service to the Public Award 2001) has proven very successful in providing easy access to current information and a number of spatial analysis capabilities.

The MapPlace has over 50 maps, many with theme data and some with interactive tools. Data themes available on the MapPlace cover a broad range of spatial data in vector and attribute form, including bedrock geology; geochemical surveys; mineral occurrences; exploration assessment reports; and mineral, coal and petroleum tenure locations. These data can be combined with other base data, including administrative boundaries, topographic features and raster images such as Landsat images and aeromagnetics. User-defined map views can then be printed or pasted into common graphics packages (e.g., Microsoft PowerPoint®, CorelDraw™). Many individual map objects are linked to valuable attribute data or to a separate website, allowing further search and retrieval capabilities. All geospatial data maintained by the BCGS is available for free download in shape or Microsoft Access™ formats.

Each map has a 'More Details' link to provide further information, such as unique layers, special instructions to view certain features and links to additional information. The MapPlace website has pages for online help, FAQs, links to workshop notes, site updates, geospatial downloads, metadata summaries and an extensive list of links to other data and maps.

Main Maps

The Main Maps page has links to 11 maps. The British Columbia Geological Survey Geoscience Map accesses

most of the geospatial datasets. The Exploration Assistant map features eight analysis tools, including the Image Analysis Tool, to display information based on query selections. The Mineral Titles map has additional title layers and a split screen to view reports. Two maps, the MapperWrapper and MapBuilder, offer different approaches to annotate and save maps. The MapPlace Lite WMS Viewer displays the main geoscience data, such as geology, mineral occurrences, assessment reports and mineral tenure, without the use of the MapGuide® Viewer. It has limited functionality, but has a WMS service which can be used in other WMS compliant viewers. The UTM Zone maps display BC, projected for each of the five UTM zones in the province.

EXPLORATION ASSISTANT WITH REMOTE SENSING IMAGE ANALYSIS

The Exploration Assistant map offers mineral exploration clients GIS tools and data to enhance their research capabilities in planning new exploration programs. Clients can use the new location tools (Fig 4) to search, display and Zoom Goto Indian Reserves, Latitude-Longitude Co-ordinates, Mapsheet, Municipality, Place Name, Scale or UTM Co-ordinates. The Discovery Potential tool displays where deposit types are likely found (based on the Mineral Resource Assessment program). The MINFILE database can be searched and displayed by commodity, deposit type, name, Mining Division or NTS Map. Clients can display geology by age, lithology and terrane. Tools are also available to search and display Mineral Titles by Name, Owner ID, Anniversary Date and Acquired Date. The Geochemistry Element section features the selection of 38 elements,

from the Regional Geochemical Survey program, for display as provincial or map sheet thresholds; symbols can also be resized. The Search Publications section, described below, features searches on the BCGS publications by Author, Title, Keyword, Abstract, Year, Scale, Series, Publication ID, Map Extent and All Fields. The Layer Finder helps locate any of the over 500 layers using keywords.

The Exploration Assistant supports a set of Image Analysis Tools (IAT), providing sophisticated analysis capabilities to be performed on geopositioned multiband and hyperspectral imagery. The site now includes 68 Landsat and 239 ASTER images to analyze. The site is supported with a tutorial manual and video tutorials. For details on the IAT, see the 2004 to 2007 papers by Kilby *et al.* in the Bibliography and More Information section.

The following recent geochemical datasets were added as separate layers to the Exploration Assistant: Geofile 2006-12, Golden, Brazeau Lake, Canoe River and Mount Robson; Geofile 2006-9, Re-analysis of samples from the McLeod Lake area; Geofile 2006-11, Anahim Lake – Nechako River; RGS 57, Fort Fraser; RGS 58, Bowser Lake and Spatsizi River. The data from these surveys will be integrated into the provincial geochemical database of the RGS layers of over 50 000 samples.

MAPPERWRAPPER AND MAPBUILDER

An online mapping application called the ‘MapperWrapper’ allows users to build on existing MapPlace maps by adding new layers and map objects of their own and saving the resulting custom map. The MapperWrapper also features the ‘UnPluggger’, which al-

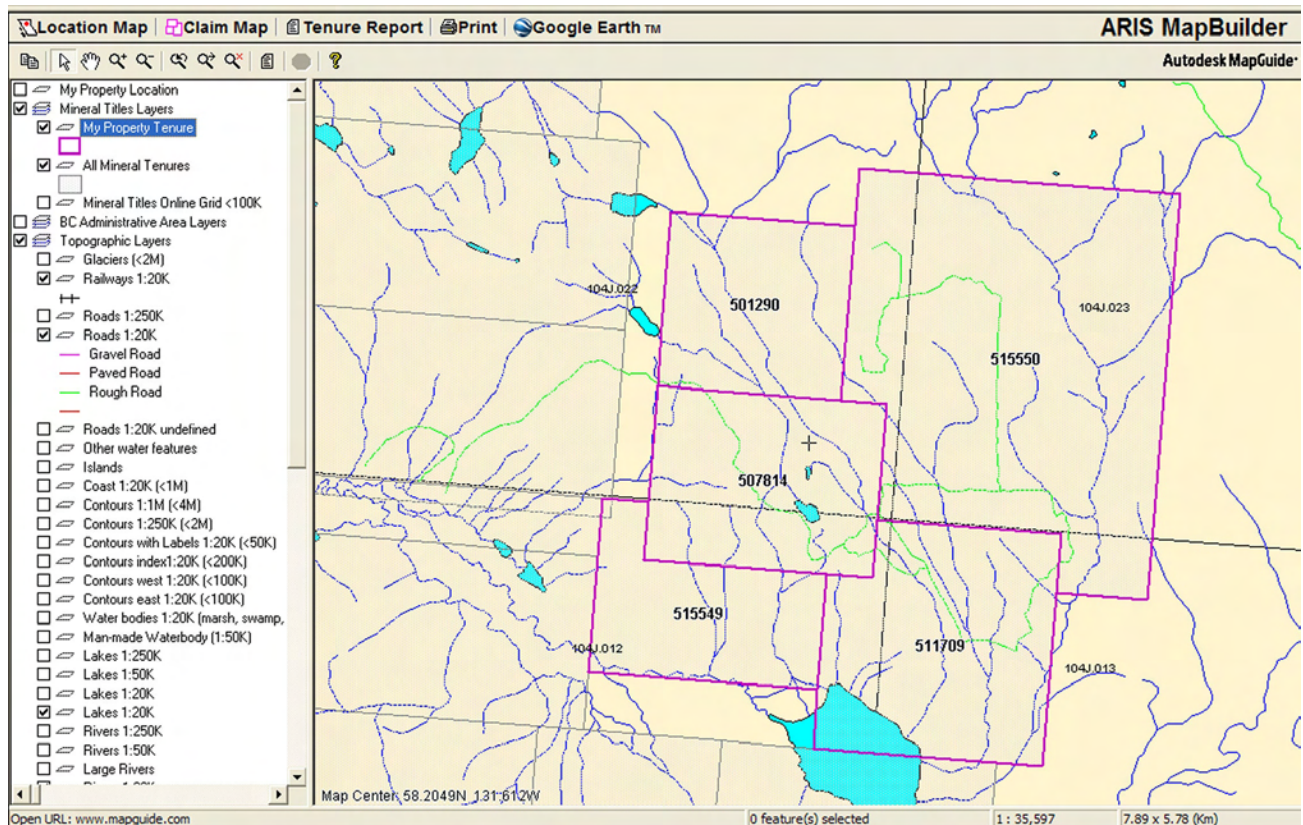


Figure 3. ARIS Map Builder tenure location map.

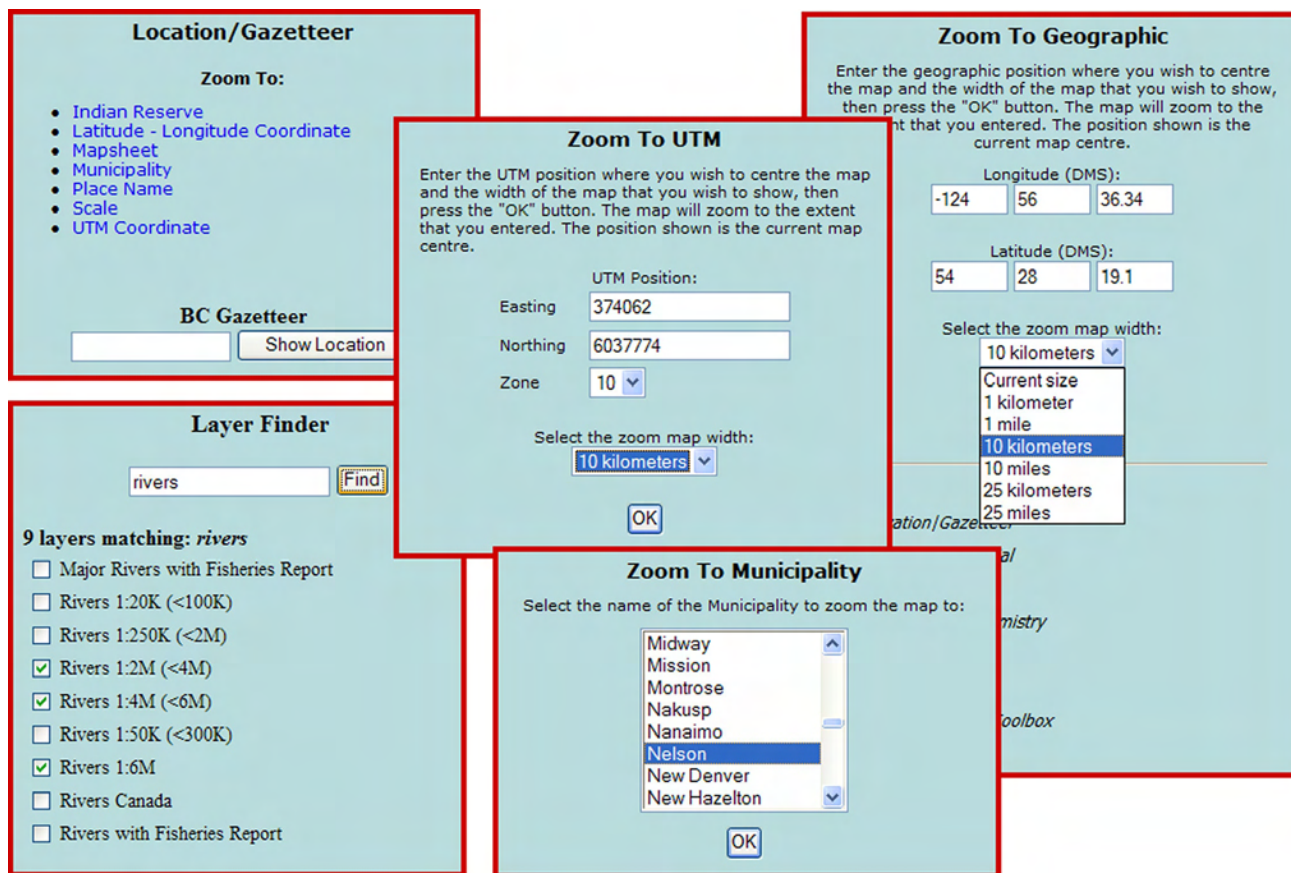


Figure 4. New Exploration Assistant tools.

allows users to create maps for offline viewing. For example, an exploration geologist could create a project map embedded with a limited number of data themes, such as Landsat, topography, hydrology, roads, MINFILE and geology. Once this map is saved, the geologist could disconnect the laptop from the internet, travel to the field and, by using MapperWrapper tool, view the maps with saved layers.

As a complement to the ARIS MapBuilder described above, the MapBuilder was built to quickly create and mark up claim location maps. Here, users can annotate the maps with symbols, lines, polygons and text. Mark-up preferences allow the user to define the colour, size and style of mark-up features added. Users can also adjust layer position and delete layers. The 'Highlight Tenure' button allows a customized tenure layer to be built. Users can also save a map created to their computer that can be opened and edited later.

PUBLICATION SEARCH APPLICATION

The Publication Search application (Fig 5) quickly displays area footprints for many of the over 3300 BCGS publications. It has been redesigned with enhanced searches by Author, Title, Keyword, Abstract, Year, Scale, Series and Map Extent. Users can refine searches with additional criteria. The Map Extent option will return all publications completely enclosed by the current map view. Results of the publication search can either be displayed on the map or as a table in a new window. If available, the map footprint links to the online publication, as does the report summary. An abstract report is also available with the Select and Re-

port tools. The BCGS publication catalogue can be downloaded as a Microsoft Access database.

Thematic Maps

The Thematic Maps page has over 30 maps. The General BC Map section includes three general purpose maps: a map that can be used to display base map features with minimal geoscience data; data in KML format that can be added to viewers such as Google Earth; and the new MapPlace2Go map, designed for non-technical users. Other theme-based maps include Petroleum Tenure & Wells, Offshore Map Gallery (Oil and Gas), various coal maps, Publication Index, Aggregate Potential, Terrain & Soils Digital Map library (funded by Forest Renewal BC from 1996–2002), Geophysical, Detailed Geology and Mining Economy maps.

MAPPLACE2GO

The new MapPlace2Go map (Fig 6) is designed for simple use, to quickly navigate, zoom and produce high-quality, page-size prints for reports and meetings. Limited data themes (Table 1) include Base Map, Mining, Exploration Projects, Tenure, First Nations, Administrative and Environmental Assessment Projects. Some themes include a 'Zoom GoTo' feature that provides the ability to narrow the view to the immediate surroundings of a desired location/item. This feature is accessed by clicking on a magnifying glass button to the right of the layer. A legend tab displays the active layers in a legend.

There are reports associated with all the mining related layers, tenure, First Nations' Aboriginal Communities layer, Federal Electoral Boundaries layer and Environmental Assessment for Mining and Energy projects. To activate the reports, double-click on the desired object on the map.

A 'Project Record Summary' report is generated from the mining-related layers. This report delivers the project status, for example: 'Operating' or 'Significant Exploration', and company contact information, including their website if it is available. From this report, there are links to a KML file for Google Earth display, MINFILE, Notice of Work summary and Environmental Assessment information. Tenure can be viewed at a 1:1 million scale and is linked to the Mineral Titles Online viewer report. The Federal Electoral Boundaries layers link to the Voter Information Service site for the selected district. The Environment Assessment layer links the Environmental Assessment Office (EAO) Project Information Centre (e-PIC) site.

MINERAL PROPERTIES AVAILABLE IN BC MAP

In partnership with the Association for Mineral Exploration British Columbia (AME BC), the Ministry developed a 'mineral properties for sale/option' map within BC. Clients use an interactive submission form to identify properties, their location and the contact information for the owner. Approved submissions are displayed on the MapPlace map with a linked report for details. The new submissions appear as a separate layer at the top of the legend in the map. Hardcopy and PDF provincial-scale maps

were published in January 2005, May 2005 and January 2006. The map will be updated annually.

NEW GEOLOGICAL AND GEOPHYSICAL MAPS

All maps on the MapPlace now display the 2005 geological compilation as the provincial Digital Bedrock Geology. The BCGS Geoscience map has a button to display a coloured legend for the screen view and includes bounding box co-ordinates and the NTS sheets. Layers displayed include quaternary geology, faults and geology contacts, bedrock geology with map unit labels, basins and terrane information, and ocean mask.

Two new geology and metallogenic map compilations were built for MapPlace. The first was created as part of the federal-provincial geological surveys' Targeted Geoscience Initiative (TGI) program and the other was completed through a grant from Geoscience BC to D. MacIntyre. The Geoscience BC – funded map is of the Skeena Arch area, West Central BC and the TGI map is of the Belt-Purcell Basin, southeast BC. For details on these maps, see MacIntyre (2007) in the Bibliography and Additional Information section.

The Geological Survey of Canada released multisensor (gamma ray spectrometric and magnetic) airborne geophysical information for 10 areas of central BC: Indata Lake, Sylvester Creek, Wittichica Creek, Taltapin Lake, Cottonwood, Wells, Hydraulic, Lac La Hache, Eagle (Murphy) Lake and McKinley Creek. These surveys are shown on the 2005 Geophysics Surveys map. Geophysical

Publications Search

Author: hoy
 Title: rossland
 Keyword:
 Abstract:
 Year:
 Scale: No Scale
 Map Extents: Completely Encloses

Add Criterion Delete Criterion

Show Footprints
 Show Results

Click "Show Footprints" to display your search results on the map, or click "Show Results" to display a table of results.

You can refine your search with additional criteria by clicking the "Add Criterion" button. The "Delete

BC Geological Survey Publications

Issue ID	Author	Title	Year	Scale 1:	NTS
B102	T. Hoy and K.P.E. Dunne	Late Jurassic Rossland Group	1997	082F/4	
EXP1988-04	Andrew, K.P.E., Hoy, T.	The Shaft Showing, Elise Formation, Rossland Group	1989	082F	
EXP1989-01	Andrew, K.P.E., Hoy, T.	Geology and Exploration of the Rossland Group in the Swift Creek Area	1990	082F	
P1989-01-04	Hoy, T., Andrew, K.P.E.	The Rossland Group, Nelson Map Area, Southeastern British Columbia	1989	082F/4	
P1990-01-01	Hoy, T., Andrew, K.P.E.	Geology of the Rossland Group, Mount Kelly-Helloaring Creek Area, Southeastern B.C.	1990	082F/4	
P1990-01-02	Andrew, K.P.E., Hoy, T., Drobe, J.R.	Stratigraphy and Tectonic Setting of the Archibald and Elise Formations, Rossland Group	1990	082F/4	
P1991-01-01	Andrew, K.P.E., Hoy, T.	Geology of the Rossland Group in the Erie Lake Area, with Emphasis on Stratigraphy and Structure of the Hall Formation, Southeastern British Columbia	1991	082F/4	
P1991-01-02	Hoy, T., Andrew, K.P.E.	Geology of the Rossland Area, Southeastern British Columbia	1991	082F/4	

Figure 5. Publication Search application with search results.

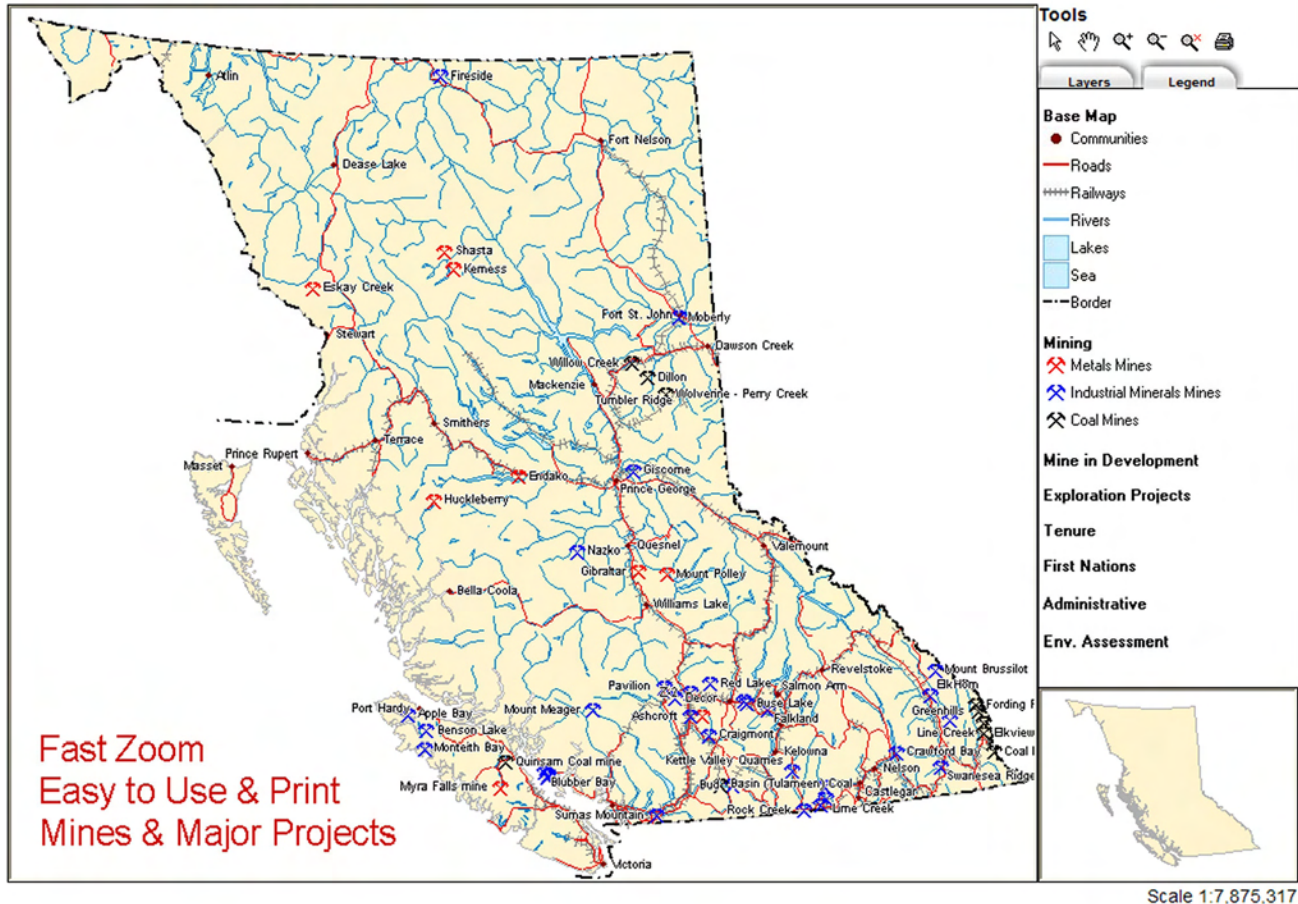


Figure 6. MapPlace2Go map.

surveys on the MapPlace now total 20, with more to come this year.

A Google Earth Data page includes links for MINFILE, ARIS, Faults, Terranes and Project and ASTER examples in KML format for use in viewers such as Google Earth.

Recent Additions of Non-Mineral/Geological Data Layers and Downloads

These new data layers are available on the Main Maps: BCGS Geoscience, Exploration Assistant, Mineral Titles and some of the Thematic Maps:

- Digital Road Atlas visible below 1:250 000 scale, with Street Name labels visible below 1:20 000 scale;
- Forestry Roads, in Topographic Layers group, visible at 1:250 000 scale;
- Environmental Assessment Office Layer group with EAO Projects separated into Mining and Energy themes;
- Wildlife Layers group with Wildlife Habitat Area, Ungulate Winter Range and Guide Outfitter Areas layers and reports;
- Survey Layers (Tantalus) group with Crown Grants, Survey Parcels, Survey Parcel Right of Ways, Sur-

veyed Transport, Integrated Cadastral Fabric (ICI), No Staking Reserve and Placer Reserves Sites. Survey Parcels are available at 1:100 000 scale and ICI at 1:20 000 scale. The layers are linked to reports with Legal Descriptions and PIN Number. See Metadata on Survey Parcels, with link to Tantalus GATOR System for more information;

- Public layers from the government Land and Resource Data Warehouse (LRDW) using FME Provider for MapGuide. This technology from Safe Software allows access to current spatial data such as mineral titles, that are updated nightly; and

TABLE 1. MAPPLACE2GO DATA LAYERS.

Category	Data Layers
Basemap data	Communities, roads, railways, rivers, lakes, seas and borders
Mining data	Mines, major projects and exploration projects for metals, industrial minerals and coal
Tenure	Mineral and placer tenure
First Nations	Aboriginal Communities, Indian Reserves, Statement of Intent areas
Administrative	Provincial electoral boundaries, Federal electoral boundaries, Mining regions, Regional districts
Environmental Assessment	Mining projects, energy projects

Zoom Goto features are available for Communities, Producing Mines, Major Projects, Exploration Projects, and Statement of Intent areas.

- Shape file downloads for MiDA and MTO available on Geospatial Data Downloads page.

MapPlace Technology Details

The MapPlace uses Autodesk® MapGuide 6.5 to provide free access to the extensive array of information related to BC geology, mineral exploration and energy resources. The MapPlace server acts as an agent for other MapGuide websites and provides a WMS service.

- Autodesk MapGuide 6.5 Server is used to deliver over 400 data layers through over 50 maps in the MapPlace application.
- Autodesk MapGuide Author is used to create, modify and publish maps that users can view with the free Autodesk MapGuide Viewer.
- Autodesk MapGuide LiteView Server is used to deliver Open Geospatial Consortium Inc. (OGC) compliant data through the MapPlace Lite WMS Viewer with Web Map Service (WMS) available at <http://webmap.em.gov.bc.ca/mapplacewms/wmsviewer.htm>. The WMS service requests (GetCapabilities) can be used in other WMS-compliant viewers.
- ColdFusion® Server 4.5 is used to report and distribute data using CFM scripts. Supporting scripts are written in HTML, JavaScript, ASP and KML (for Google Earth use).
- Safe Software FME® Provider for MapGuide provides access to external spatial data sources such as the ARC SDE Land and Resource Data Warehouse (LRDW) of Land Information BC.
- RSI IDL ION – Script 6.1 server is used to process and analyze imagery with the Image Analysis Toolbox in the Exploration Assistant.
- Client-side software required or recommended: Microsoft Internet Explorer 6 or higher, Autodesk MapGuide 6.5 Viewer, Adobe Acrobat Reader 6 or higher, Microsoft Excel® 2003, Microsoft PowerPoint 2003, Microsoft Word 2003, Cute PDF™, CorelDraw 12 and ARC™ Explorer 9.1.
- Database management: Microsoft Access 2000, Oracle® and SQL.
- Spatial and raster formats: SHP, SDF, DWF, TIFF, JPG, SID and ECW.
- Autodesk MapGuide Enterprise and Open Source are currently being evaluated as a complement to the site.
- Application server licenses are less than \$6300 per year. Server maintenance and data backup is assisted by Workplace Technology Services (WTS) staff.
- Microsoft FrontPage® is used to develop and maintain documentation, metadata and marketing on MapPlace and associated databases.

Brief History of MapPlace

The driving force to create this website was the need to distribute the results of provincial geoscience information and the compilation of mineral potential estimates through a graphical user interface that could easily deliver spatial

data and related information. The second major incentive was to create a means to house and deliver the digital library of terrain and soils maps funded by Forest Renewal BC.

In 1995, the server was a desktop Pentium and the original software was Argus MapGuide, by Argus Technologies in Calgary, Alberta, which was acquired by Autodesk in 1996. In 1997, the Exploration Assistant theme map was developed and provided more interaction for the user. Subsequently, new hardware was provided to more efficiently deliver the information and to house very large datasets. The initial development was within the BC Geological Survey, by W. Kilby. The site is currently maintained by two staff members, L. Jones and P. Desjardins, with periodic assistance from students and consultants. MapPlace also partners with other MapGuide sites, such as the Communities Mapping Network (www.cmnbc.ca).

In 2000, MapPlace recorded over 190 000 website hits per year and in 2001, it recorded over 880 000 hits, a 450% increase. In 2002, the website had over 1.2 million hits and over 2500 users had visited the site 4 times or more. By 2005, hits reached over 6 million per year and there were 5600 users with 4 or more visits.

The MapPlace has proven useful to diverse agencies and stakeholders, such as explorationists, land planners, environmental consultants, native groups and university students. Users have save time in research and analysis as well as experiencing the reduction of data costs. See the MapPlace in action at www.MapPlace.ca.

ACKNOWLEDGMENTS

The following are acknowledged for their contributions. Ryan Cooney designed and programmed MapPlace2Go, ARIS MapBuilder, MapBuilder, Publication Search application, KML generation, Exploration Assistant tools and the rewrite of ARIS search code in ASP. Spot Solutions Ltd. built the new MINFILE/www, MINFILE/pc and Property File applications. Cal Data Ltd. created the Image Analysis Tools (IAT) application and carried out special processing of satellite imagery, Natural Resources Canada's geophysical data and BCGS's Regional Geochemical data, so it could all be posted to the MapPlace. Nicole Robinson contributed to the design of the Property File data model and application. Sarah Meredith-Jones did rigorous testing of the MINFILE search application. Karl Flower captured metadata for the publications catalogue. Don MacIntyre is the original developer of the Offshore Map Gallery in MapPlace.

Significant Internet Links

BC Geological Survey: www.em.gov.bc.ca/mining/Geosurv/default.htm

MINFILE: www.em.gov.bc.ca/mining/Geosurv/Minfile/default.htm or www.minfile.ca

Property File: www.em.gov.bc.ca/mining/Geosurv/Minfile/PropFile.htm

COALFILE: www.em.gov.bc.ca/mining/Geosurv/coal/default.htm

ARIS: www.em.gov.bc.ca/mining/Geosurv/Aris/default.htm

MapPlace: www.em.gov.bc.ca/mining/Geosurv/MapPlace/default.htm or www.MapPlace.ca

MapPlace Online Help and Documents: www.em.gov.bc.ca/mining/Geosurv/MapPlace/onlineHelp.htm

IAT: www.em.gov.bc.ca/mining/Geosurv/MapPlace/MoreDetails/IAT.htm

Publication Search: www.em.gov.bc.ca/mining/Geosurv/MapPlace/MoreDetails/geolindx.htm

MapperWrapper: www.em.gov.bc.ca/mining/Geosurv/MapPlace/MoreDetails/mapperWrapper.htm

MapPlace2Go: www.em.gov.bc.ca/mining/Geosurv/MapPlace/MoreDetails/map2go.htm

Mineral Titles Online (MTO): www.mtonline.gov.bc.ca/

Natural Resource Information Centre (NRIC): www.nric.ca/

Land & Resource Data Warehouse: lrdw.ca/

Sensitive Habitat Inventory and Mapping (SHIM): www.shim.bc.ca/

Community Mapping Network (CMN): www.cmnb.ca/

BIBLIOGRAPHY AND ADDITIONAL INFORMATION

Fraser Institute Annual Survey of Mining Companies 2005/2006 (2006); URL <<http://www.fraserinstitute.ca>> [March 2006].

Google (2006): Google Earth, Global internet viewer of imagery and vector information; URL <<http://earth.google.com>> [November 2006].

Jones, L.D. (1998): A guide to locating mineral-related information in BC; in *Exploration and Mining in British Columbia 1998*, BC Ministry of Energy, Mines and Petroleum Resources, pages E-1–E-9.

Jones, L.D., MacIntyre, D.G. and Desjardins, P.J. (2002): The MapPlace – an Internet-based mineral exploration tool; in

Geological Fieldwork 2001, BC Ministry of Energy, Mines and Petroleum Resources, Paper 2002-1, pages 409–420.

Kilby, W.E. (2005): MapPlace.ca Image Analysis Toolbox – Phase 2; in *Geological Fieldwork 2004*, BC Ministry of Energy, Mines and Petroleum Resources, Paper 2005-1, pages 231–235.

Kilby, W.E. and Kilby, C.E. (2006): ASTER imagery for BC – an online exploration resource; in *Geological Fieldwork 2005*, BC Ministry of Energy, Mines and Petroleum Resources, Paper 2006-1, pages 287–294.

Kilby, W.E. and Kilby, C.E. (2006): Examining ASTER imagery with the MapPlace Image Analysis Toolbox—a tutorial manual; BC Ministry of Energy, Mines and Petroleum Resources, GeoFile 2006-8 and *Geoscience BC* Report 2006-3, 41 pages.

Kilby, W.E. and Kilby, C.E. (2007): ASTER multispectral satellite imagery and product coverage, British Columbia – Phase 2; in *Geological Fieldwork 2006*, BC Ministry of Energy, Mines and Petroleum Resources, Paper 2007-1 and *Geoscience BC*, Report 2007-1, pages 315-318.

Kilby, W.E., Jones, L.D. and Desjardins, P.J. (2004): MapPlace client-mapping tools; in *Geological Fieldwork 2003*, BC Ministry of Energy, Mines and Petroleum Resources, Paper 2004-1, pages 217–218.

Kilby, W.E., Kliparchuk, K. and McIntosh, A. (2004): Image Analysis Toolbox and enhanced satellite imagery integrated into the MapPlace; in *Geological Fieldwork 2003*, BC Ministry of Energy, Mines and Petroleum Resources, Paper 2004-1, pages 209–215

MacIntyre, D.G. (2007): Belt-Purcell Metallogenic Data and Map; BC Ministry of Energy, Mines and Petroleum Resources, GeoFile 2007-2.

MacIntyre, D.G. (2007): Skeena Arch Metallogenic Data and Map; BC Ministry of Energy, Mines and Petroleum Resources, in preparation.

Bedrock Geology and Mineral Potential of Mouse Mountain (NTS 093G/01), Central British Columbia

by S. Jonnes^{1,2} and J.M. Logan

KEYWORDS: Intermontane Belt, Quesnellia, alkaline copper-gold porphyry, monzonite intrusion, Valentine zone, chalcopyrite, malachite

INTRODUCTION

Mouse Mountain is situated 70 km northwest of Mount Polley and 200 km southeast of Mount Milligan, two alkaline, intrusive-related copper-gold porphyry deposits hosted within the Quesnel Terrane of central British Columbia. In this belt, the Quesnel Terrane is characterized by Triassic to Early Jurassic volcanic and sedimentary arc rocks and high-level, comagmatic alkaline intrusions. Complex, multiple intrusive centres define the axis of the arc and occur systematically every 13 km along its length. Mouse Mountain is interpreted to represent one of these Late Triassic intrusive centres.

On the eastern flank of Mouse Mountain is an area known as the Valentine zone, which shows classic alkalic porphyry attributes centred on a composite monzonite intrusion: potassium metasomatism enveloped by peripheral propylitic alteration and stockwork breccia copper-gold mineralization. The extent of mineralization within the monzonite-syenite intrusive complex has been a subject of debate for over 50 years. The current study is designed to test whether the mineralization/alteration at the Valentine zone represents the tail of an elephant or the body of a mouse.

This report describes the preliminary results of a detailed bedrock geology study conducted over the Mouse Mountain property. Exploration and mapping began on the May 20, 2006, and was carried out by the senior author and one assistant until the end of August 2006. The area mapped covers approximately 16 km² of generally subdued topography on the eastern margin of the low-lying Fraser Plateau. Previous bedrock maps of the area are based on reconnaissance-scale mapping carried out by Teck in 1992 and Sanguinetti in 1989. The bedrock geology map created in 2006 builds on these previous works and benefits from petrographic studies of the major rock units on the property.

¹ Richfield Ventures Corporation, Quesnel, BC

² Earth and Ocean Sciences Department, University of Victoria, Victoria, BC

This publication is also available, free of charge, as colour digital files in Adobe Acrobat® PDF format from the BC Ministry of Energy, Mines and Petroleum Resources website at http://www.em.gov.bc.ca/Mining/GeolSurv/Publications/catalog/cat_fldwk.htm

Background and History

Mouse Mountain is situated 9 km east-northeast of Quesnel in the Quesnel River area of central British Columbia at latitude 53°02'N, longitude 122°19'W, or UTM 545094E, 5876965N, in zone 10 (NAD 83). The Mouse Mountain property is wholly owned by Richfield Ventures Corporation (RVC), a private company with offices in Quesnel, BC.

Mineral exploration at Mouse Mountain has focused on copper-gold-porphyry-style mineralization, with the earliest work dating from the 1950s. At this time, 20 tonnes of hand-sorted ore grading 1.55 g/t Au, 15.5 g/t Ag and 5.6% Cu was produced from open pits and shipped to the Tacoma smelter (Sutherland Brown, 1957). In 1967, Euclid Mining Corporation tried to heap leach copper from the old workings, but abandoned the project without success. Subsurface exploration followed in the 1970s when Bethlehem Copper Corp. and DuPont of Canada Limited carried out preliminary percussion drilling programs. Soil geochemical and geophysical surveys were conducted over the property by a number of companies, but it was Placer Dome Inc. using a total field ground magnetic survey that recognized the large magnetic anomaly under Mouse Mountain. Teck Exploration Ltd. drilled several short diamond-drill holes in 1991 with the best intersection including 6.1 m of 0.31% Cu and 123 ppb Au. In 2003, Richfield Ventures Corp. acquired the Mouse Mountain property and began an extensive exploration program comprising soil sampling, induced polarization, geological mapping, prospecting and trenching.

REGIONAL GEOLOGICAL SETTING

The Quesnel Terrane, or Quesnellia, defines the eastern margin of the Intermontane Belt close to its tectonic boundary with the Omineca Belt (Fig 1, 2). Quesnellia extends from north-central BC to south of the United States border and comprises the Stuhini, Takla, Nicola and Rossland Groups, respectively. These Middle Triassic to Early Jurassic volcanic, sedimentary and plutonic assemblages formed in an island arc setting outboard or marginal to the ancestral North American continental margin (Bailey, 1988; Panteleyev *et al.*, 1996; Rees, 2005). Major porphyry copper deposits generated by Early Mesozoic, calcalkalic or alkalic island-arc magmatism within Quesnellia include: Highland Valley, Copper Mountain, Afton-Ajax, Mount Milligan and Mount Polley (Logan and Bath, 2005; Rees 2005).

At the latitude of the study area, Quesnellia is fault-bounded, juxtaposed on the west (fore-arc) with Paleozoic and Mesozoic rocks of the Cache Creek subduction-accretionary complex, and on the east by Paleozoic and

older metasedimentary, metavolcanic and metaplutonic rocks of the pericratonic Kootenay Terrane. The western terrane boundary is marked by high-angle, strike-slip faults, which is probably the southern extension of the Pinchi fault system (Bailey, 1988). Along the eastern margin, rocks of the Quesnel belt are structurally coupled and tectonically emplaced by the Eureka thrust onto the Snowshoe Group of the Barkerville subterrane (Struik, 1983, 1988). Intensely deformed and variably metamorphosed Proterozoic and Paleozoic rocks of the Barkerville subterrane are characteristic components of the western limits of the Omineca Belt (Struik, 1986).

In the central Quesnel belt, Mesozoic strata of the Nicola Group consist of a basal unit of Middle Triassic argillite and fine clastic sedimentary rocks, and an overlying thick sequence of Late Triassic shoshonitic alkali volcanic and volcanoclastic rocks (Panteleyev *et al.*, 1996; Rees, 2005). Toward the top of the sedimentary unit, mafic volcanic debris becomes common within the sedimentary rocks, suggesting that early mafic volcanism and late sedimentation were contemporaneous (Panteleyev *et al.*, 1996). Unconformably overlying the Late Triassic submarine to subaerial volcanic sequence are Early Jurassic sedimentary and epiclastic rocks.

Intrusive rocks in this part of Quesnellia record alkaline and calcalkaline arc episodes of magmatism during the Late Triassic and calcalkaline magmatism in the Early Jurassic, Middle Jurassic and mid-Cretaceous. Small isolated alkaline feeders to the widespread Tertiary continental volcanism record the youngest magmatic activity in the area (Logan *et al.*, 2007).

The structural geology and regional metamorphism of the central Quesnel Belt records the Middle Jurassic collision and amalgamation of Quesnellia arc rocks with rocks of the Omineca Belt to the east (Bailey, 1988; Panteleyev *et al.*, 1996; Rees, 2005). Most faults are normal or strike-slip and trend either north or north-northwest (Rees, 2005). Complicating these arc-parallel structures are orthogonal, east and northeast-trending block faults related to a later period of crustal extension (Bailey, 1988). Regional metamorphism is low grade, typical of zeolite or lower greenschist facies. Contact metamorphic aureoles (biotite hornfels) are developed around several isolated plutons (Bailey, 1988).

The central Quesnel belt hosts a wide variety of mineral deposits, including surficial gold placers, precious and base metal veins and industrial minerals, but copper-gold porphyry comprises the most economically important exploration targets (Bailey, 1988; Panteleyev *et al.*, 1996; Tempelman-Kluit, 2006). The Mount Polley open pit copper-gold mine is the largest alkaline porphyry system in this belt, with proven and probable reserves for the Wight, Bell, Springer and Southeast open pits totalling 40.9 million tonnes grading 0.448% copper and 0.31 g/t gold (Imperial Metals Corporation, 2006). However, almost all Late Triassic alkalic stocks intruding the volcanic rocks are mineralized. In the Swift River area, copper mineralization is known in stocks south of Benson Lake, at Cantin Creek and at Mouse Mountain (Bailey, 1988). Magnetite is also ubiquitous and magnetic patterns are important indicators of the

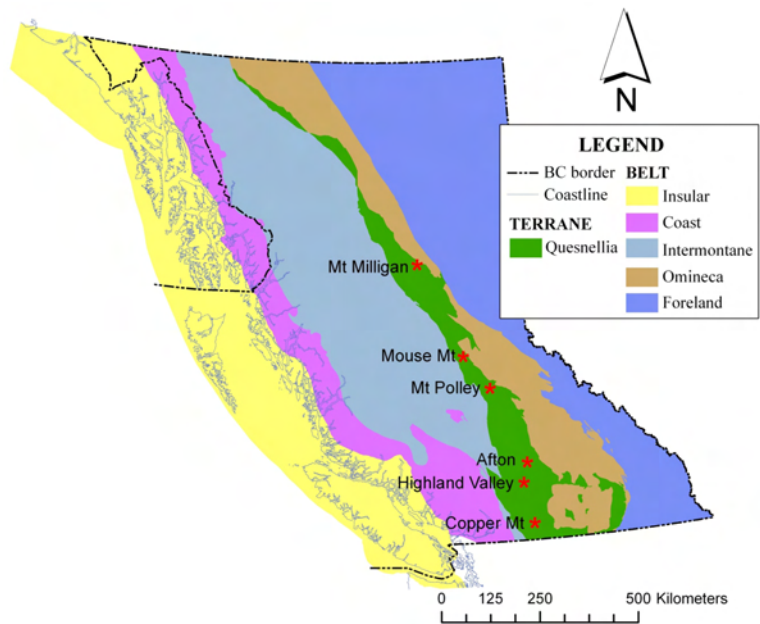


Figure 1. Map of British Columbia, showing the location of the study area in relation to other alkaline porphyry copper deposits in Quesnellia.

presence of stocks in overburden-covered areas. Copper is invariably chalcopyrite with minor bornite and occasional chalcocite. Mineralization is coupled with hydrothermal alteration of the intrusive bodies and hostrocks (Panteleyev *et al.*, 1996). The mineral showings consist of stockworks, veinlets and disseminations of copper minerals, associated with alteration minerals such as K-feldspar, magnetite, albite, actinolite, pyrite and sericite and surrounded by a propylitic halo containing chlorite, epidote and carbonate (Bailey, 1988; Panteleyev *et al.*, 1996).

PROPERTY STRATIGRAPHY

Stratigraphy for the Mouse Mountain area follows the stratigraphic relationships established by Bailey (1988) for the Swift River area and Panteleyev *et al.* (1996) for the Quesnel River – Horsefly map area. Figure 3 shows these relationships schematically. Absolute ages for the rocks in the study area are unknown; however, correlative units at Mount Polley are intruded by plutons having Late Triassic crystallization ages (204.7 ± 3 Ma; Mortensen *et al.*, 2005) using the time scale of Palfy *et al.* (2000). Physiographic features of the area and the distribution of rock types are shown on the property geology map (Fig 4).

Lower Sedimentary Rocks

SILTSTONE (UNIT 1)

Black siltstone outcrops in the far northeast portion of the property (Fig 5). It dips steeply to the southwest and may be traced as far south as Fallen Log Lake, where a small section of black siltstone was also found. Bedding surfaces or bases were not exposed, although the unit exceeds 7 m in thickness. The unit is dominated by dark to medium grey beds that are approximately 10 cm thick, with interbedded leucocratic laminations. Although the matrix is weakly calcareous, no fossils were observed. This unit correlates with the sedimentary package mapped by Bailey

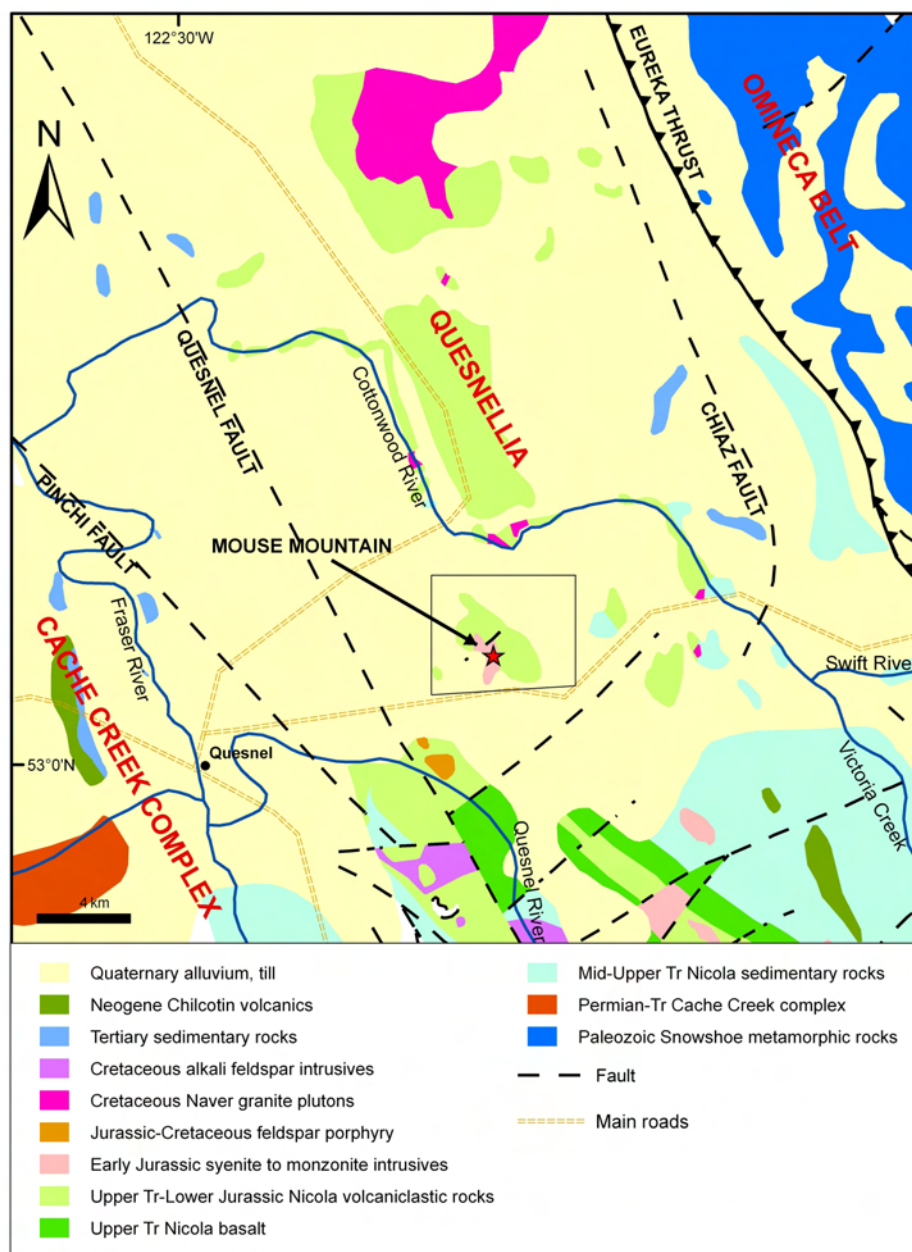


Figure 2. Regional geology map of the Quesnel belt around Mouse Mountain, showing the property outline. Compiled from www.mapplace.ca (BC Geological Survey, 2006) and Bailey (1988).

(1988) and dated as Carnian by Struik (1988) as the oldest recognized part of the Quesnel belt stratigraphy. Sediments of unit 1 probably underlie the volcanic succession seen on the property, although field relations are not directly evident.

Lower Volcanic and Volcaniclastic Rocks

AUGITE PORPHYRY FLOWS (UNIT 2)

Volcanic rocks of unit 2 (Fig 6) underlie the northeastern half of the map area in a continuous belt extending from the southeast corner of the property to the northwest corner. Augite porphyry also occupies areas to the west and south-east of the main showings, where it forms north to north-

west-trending ridges. The areal distribution of the basalt is extensive at the property scale; however, the unit thickness is unknown.

The basalt is green-grey and maroon and forms monolithic tuff breccia and autobrecciated flows. Phenocrysts of augite comprise up to 10 to 35% and are approximately 2 to 3 mm in size. Less abundant phenocrysts of intermediate plagioclase are ubiquitous. The groundmass is aphanitic, grey-green, weakly hematite-stained and composed of fine-grained pyroxene and plagioclase. The unit appears to be mainly intact and unaltered, except for weak saussurite alteration. Accessory magnetite and pyrite were also noted. Quartz and calcite-filled amygdules are common in the northern outcrops of unit 2. These amygdules constitute approximately 10% of the mode and are approximately 1 cm

Late Triassic to Early Jurassic
Nicola Group
 Mouse Mountain Area

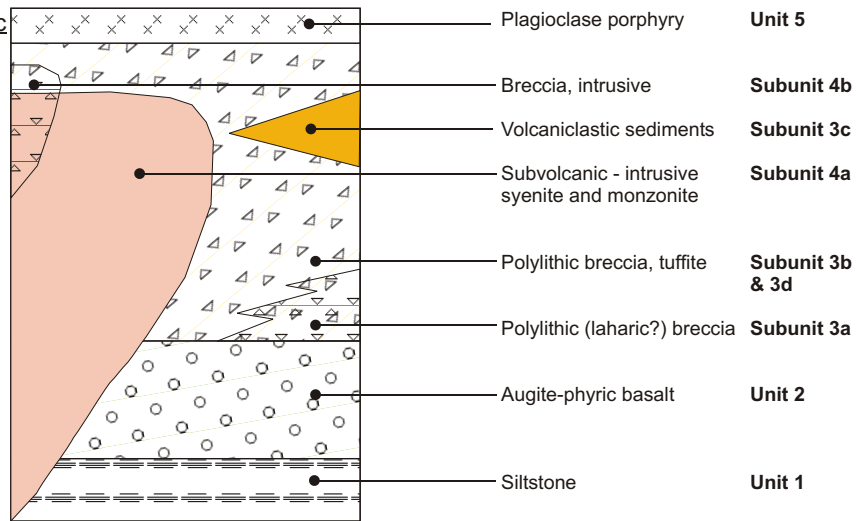


Figure 3. Schematic stratigraphy diagram for the Mouse Mountain area.

in size, spherical oblate and weakly flattened. In thin section, these basalts show well-developed trachytic flow textures.

Contact relationships are not obvious because Quaternary deposits mask large tracts of land on the Mouse Mountain property. However, unit 2 is believed to be equivalent to unit 2 in Bailey (1988) and is therefore the oldest and most widespread unit of volcanic rocks found in the

Quesnel belt. The age of the unit is interpreted as early Norian (Late Triassic; Bailey, 1988).

Upper Clastic Volcanic Rocks

The majority of the property is underlain by a variety of massive, clastic volcanic rocks, which for the most part are heterolithic and show evidence of reworking. Clast compositions have been used to subdivide the rocks into

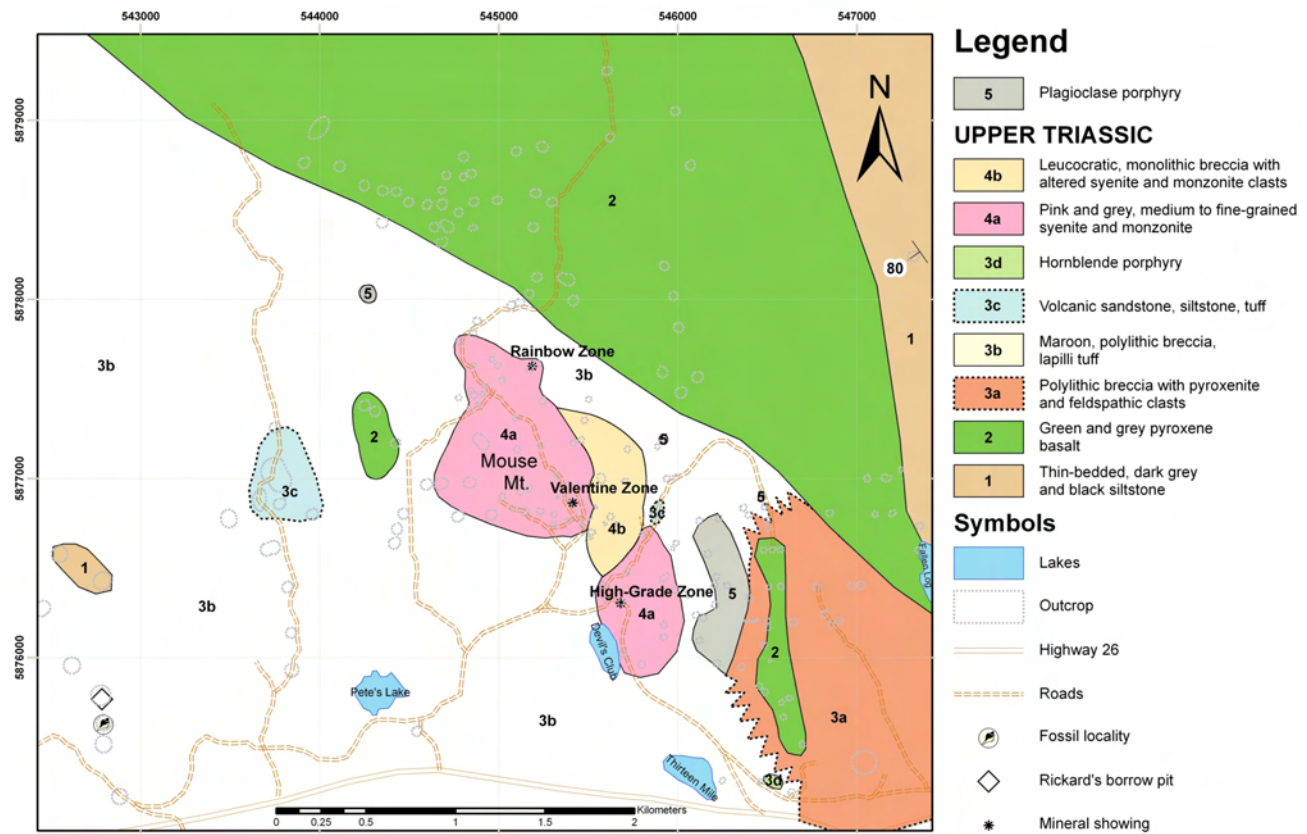


Figure 4. Mouse Mountain property geology map.



Figure 5. Finely laminated steeply dipping siltstone of unit 1, north-east of the Mouse Mountain peak.

four subunits. Definitive evidence for tuffaceous components (*i.e.*, pumice or fiamme) is lacking, although fresh pyroxene and plagioclase crystal-rich matrices to the breccia and conglomerate suggest limited reworking.

EPICLASTIC BRECCIA (SUBUNIT 3A)

Due east of Thirteen Mile Lake are metre-thick outcrops of laharic (?) breccia (Fig 4, 7). Subunit 3a is an unsorted, matrix-supported (locally clast-supported), polymictic breccia with coarse intrusive, feldspathic and lapilli-sized mafic volcanic clasts (hornblendite and pyroxenite). Hornblende-plagioclase-phyric lapilli fragments dominate the clast population. The variable-coloured, rounded and subangular clasts, some as large as 15 to 20 cm, occupy an aphanitic, hematite-stained, maroon matrix. The fine ash and crystal matrix consists of reworked plagioclase and hornblende crystals. Subunit 3a consists of mixed pyroclasts (?) and epiclasts, which are subangular and subrounded, respectively. In thin section, it is apparent that both the clasts and the matrix of subunit 3a are weakly potassium altered and sericitized. Soft sediment deformation features drape the breccia in places and possibly correspond to periods of quiescence in volcanic activity.

A late-stage plagioclase porphyry dike crosscuts subunit 3a on the western margin of the property. Subunit 3a is correlated with maroon heterolithic breccia mapped by Bailey (1988) and Panteleyev *et al.* (1996), to stratigraphically overlie mafic volcanic units similar to unit 2. Their work suggested this contact was an angular

unconformity and interpreted the breccia to be Sinemurian in age (Lower Jurassic).

CRYSTAL-RICH LAPILLI VOLCANICLASTIC TUFFITE (SUBUNIT 3B)

Subunit 3b is the dominant lithology in the map area, occurring around the intrusive rocks of Mouse Mountain peak and to the west of the property (Fig 4). This heterolithic breccia (to crystal-lithic tuff) is provisionally distinguished by having volcanic components, particularly augite-phyric basalt clasts that reach up to 50 cm in size, and felsic hypabyssal clasts. Subunit 3b is generally green to grey, matrix-supported (but locally clast-supported), with subangular to subrounded clasts. This subunit is distinguished from subunit 3a on the basis of three observations: better sorting, better rounding and the lack of ultramafic clasts. The matrix, evident from thin section analysis, consists of mature crystals and reworked lapilli.

Stratigraphically, this breccia may be related to subunit 3a in the south, and grades laterally into finer-grained volcaniclastic rocks of subunits 3c and 3d. In general, subunit 3b is not altered or mineralized, although weak metamorphism of this unit has caused pervasive sericitization. Lithologically, this breccia correlates with subunit 3b mapped and characterized by Bailey (1988), to contain felsic rocks as well as basaltic debris derived from underlying units. Originally, this subunit was believed to be Sinemurian in age (Lower Jurassic), but isotopic dating by Mortensen *et al.* (1995) indicate these maroon volcaniclastic rocks are intruded by Late Triassic intrusive rocks at Mount Polley and therefore cannot be Jurassic in age.

A fossil-bearing horizon in granule conglomerate and reworked volcaniclastic rocks of subunit 3b was recognized in the southwest portion of the map area (Fig 4, 8b). The subunit is massive and bedding is not obvious, but a repetitive attitude of 270°/60° is assumed to indicate depositional layering. Macrofossil imprints and moulds of bivalves, gastropods and solitary corals are most common, although soft body fragments replaced by black calcite and pyritized nodules that are approximately 5 cm in diameter



Figure 6. Basaltic rock of unit 2, with megacrystic augite phenocrysts. The scale is in centimetres.



crystals in an otherwise aphanitic groundmass. These rocks are interpreted as distal deposits and probably represent reworked crystal tuff.

HORNBLLENDE-PORPHYRY (SUBUNIT 3D)

Situated in the southeast portion of the map area, enveloped in subunit 3b, is a small outcrop of hornblende-plagioclase porphyry (Fig 4, 10). Hornblende phenocrysts are approximately 5 mm in size and constitute 30 to 40% of the mode; interstitial plagioclase crystals are 1 mm in length and occur in an aphanitic matrix that is abundant with blebby magnetite. With the exception of flow banding, this unit has extrusive flow features, such as monomictic autobrecciation textures on weathered surfaces and scattered centimetre-sized mafic rip-up clasts. Subunit 3d is either a small flow or ignimbrite unit. It may be related to the late-stage volcanic event that led to the formation of unit 5.



Figure 7. a) Laharic (?) breccia of subunit 3a, from the southeast part of the property, with a large ultramafic xenolith; b) breccia, with mixed clasts in soft sediment 'slump' structure.

were also observed. Samples have been collected for macrofossil and conodont analysis and sent to P. Smith of the Paleontology department of the University of British Columbia, Vancouver, and results are pending. The fossil assemblage was probably deposited in a high-energy beach environment.

VOLCANICLASTIC SEDIMENTS (SUBUNIT 3C)

Two small exposures of fine-grained, dark greyish-green, volcanic-derived siltstone and feldspathic sandstone occur on the east and west side of the Mouse Mountain peak (Fig 4, 9). This unit has gradational contacts and similar mineralogy to subunit 3b and is interpreted to be a finer-grained facies equivalent. Graded bedding and load structures (oriented at 165°/68°) indicate overturned bedding at one locale, which is interpreted to reflect soft sediment slumping rather than tectonic inversion. Thin section analysis of subunit 3c shows a few scattered broken plagioclase

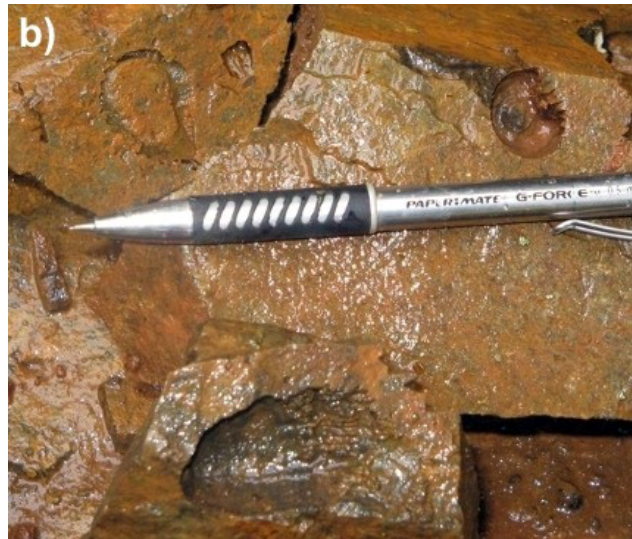


Figure 8. Variable texture of subunit 3b, that is a) dominated by augite-phyric clasts and b) fossiliferous.



Figure 9. Volcanic sedimentary rock of subunit 3c, with white plagioclase crystals. The scale is in centimetres.

Intrusive Rocks

MONZONITE-SYENITE (SUBUNIT 4A)

Intrusive rocks underlie the main area of Mouse Mountain, encompassing an area of approximately 1.3 km² (Fig 4, 11). The intrusive rocks are felsic and typically weather off-white or a deep rusty brown where pyrite is present. When fresh, the rocks are creamy grey or pink in colour. In hand sample, the rocks are fine grained, microporphyritic and appear more like high-level subvolcanic bodies than plutons or stocks with well-developed equigranular texture. Subunit 4a varies compositionally and texturally from the top of Mouse Mountain toward the Valentine zone. At the peak of the mountain, the subunit is characterized by coarse potassium-feldspar megacrysts and a nepheline-normative syenite composition. Along the eastern margin of the intrusion at the Valentine zone, the monzonite is a microporphyr monzonite. Pyroxene and lesser biotite comprise the mafic minerals at both locales.

The monzonite of subunit 4a is flanked by and presumably intrudes maroon tuffite and volcanoclastic subunit 3b,

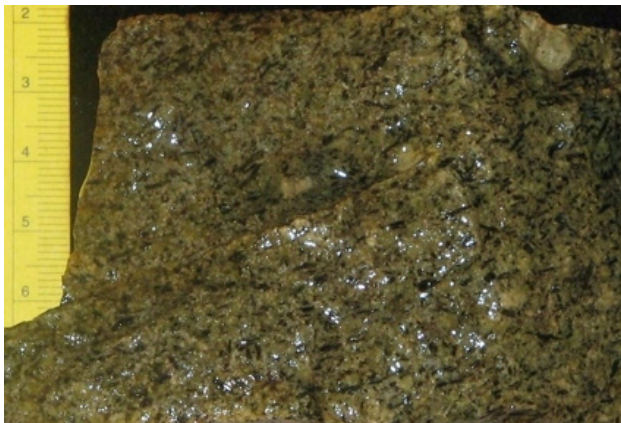


Figure 10. Hornblende porphyry of subunit 3d, east of Thirteen Mile Lake.

although intrusive contacts were not recognized in the field. All known significant pyrite-chalcopyrite mineralization on the property is associated with monzonite bodies that occur within 1 or 2 km of the Mouse Mountain peak.

The monzonite stocks at Mouse Mountain correlate with subunit 7a of Bailey (1988). They are similar in composition, regional distribution and temporal relationships to the suite of Latest Triassic alkaline intrusive rocks that define the medial arc axis and magmatic centres at Mount Polley, the Quesnel River deposit (QR) and Cantin Creek, where they are associated with alteration and copper-gold mineralization. Most of subunit 4a probably represents subvolcanic dikes, sills and stocks, which have intruded the Triassic volcanic stratigraphy (Panteleyev *et al.*, 1996).

BRECCIA, INTRUSIVE (SUBUNIT 4B)

Separating the monzonite due east of the Mouse Mountain peak is a distinctive breccia subunit consisting primarily of pink-weathering (felsic) intrusive clasts in a white-creamy rock flour matrix (Fig 4, 12). subunit 4b is essentially monolithic with subangular potassic altered monzonite and syenite clasts (except for the occasional ma-



Figure 11. a) Nepheline syenite from the Mouse Mountain peak, subunit 4a, stained with Na-cobaltinitrate to distinguish potassium minerals; b) Altered and mineralized fine-grained monzonite from the Valentine zone.



Figure 12. Monolithic breccia of subunit 4b, with a) rock flour matrix and b) the occasional maroon volcanic clast.

roon volcanic clast) that range in size from 1 to 10 cm. The breccia is clast-supported (locally matrix-supported), massive and unsorted. Contact relationships between the monzonite and the maroon, heterolithic volcaniclastic unit are unknown. In addition, small isolated breccia zones are known to occur in the main monzonite stock to the west of the Valentine zone. Alteration is limited to the matrix of these breccia subunits and is characterized by magnetite and/or albite replacement.

The breccia contains occasional potassium-altered clasts (orthoclase, magnetite and biotite) and clasts of copper (malachite and/or pyrite) mineralization. These clasts represent primary hypogene mineralization and suggest that brecciation may have accompanied or postdated early potassium-copper mineralization. Albite, epidote and late chlorite alteration of the rock flour matrix represents the waning stages of the hydrothermal system. Multistage breccia events are common in high-level hydrothermal systems and particularly so in the alkaline systems of BC (Copper Mountain, Iron Mask, Mount Polley and Galore Creek). This subunit may represent a hydrothermal breccia or eruptive diatreme located near the top of the intrusive pile. Equivalent units elsewhere in the Quesnel belt have been used successfully in regional exploration to outline erup-

tive volcanic centres (Fox, 1975) that are underlain by high-level intrusive bodies (Panteleyev *et al.*, 1996).

Volcanic Rocks

PLAGIOCLASE PORPHYRY (UNIT 5)

Plagioclase-dominated porphyry crops out in the southeast corner of the map, east of Devils Club Lake. Here, plagioclase-porphyrific volcanic rocks and subvolcanic intrusions, possibly feeders to the flows, underlie a broad crescent around the east-southeast limits of Mouse Mountain, encompassing an area of approximately 0.25 km² (Fig 4, 13). The unit is grey-greenish with off-white (locally crowded) plagioclase laths in an aphanitic dark grey groundmass. The plagioclase phenocrysts are euhedral, up to 1 cm, form 20 to 30% of the mode and typically do not show any flow alignment. Subordinate hornblende occurs as minor phenocrysts or in the groundmass. Unit 5 is generally fresh and unaltered, andesitic in composition and contains minor amounts of hydrous minerals (hornblende and lesser biotite). The plagioclase porphyry is considered to be late, crosscutting and overlying the augite porphyry and volcaniclastic units.

SURFICIAL GEOLOGY

The Mouse Mountain property lies in a region affected by extensive glacial erosion and deposition. Unconsolidated Pleistocene glacial, glaciofluvial, till and organic material covers much of the map area. In low-lying areas, swamps, bogs and glaciolacustrine deposits are common, whereas till and glaciofluvial deposits occupy the elevated slopes and ridges. A thin veneer of till typically drapes the underlying bedrock, but in river valleys south of the property, thicknesses of greater than 150 m are attained. Glacial striations and the trend of bedrock ridges are commonly between 330 and 350°, which reflect the major direction of glacial transport (Bailey, 1988).

STRUCTURE

The structural geology of the Mouse Mountain property is poorly constrained due to limited exposure and the



Figure 13. Plagioclase porphyry of unit 5; Mouse Mountain, central BC.

massive nature of the volcanic units. In general, contacts and structures trend northwesterly parallel to the dominant regional tectonic grain. The few faults, fractures and slickensides that were observed are disorderly and unrelated. Bedding in the northeast corner of the map area dips and faces southwesterly, consistent with the eastern flank of the Quesnel belt (Panteleyev *et al.*, 1996).

A major east-striking fault zone oriented 280°/78°N crops out approximately 3 km west of Mouse Mountain in Rickard's borrow pit. This 2.5 m wide zone of crushed rock, fault gouge and sandy infill corresponds to a splay of the Chiaz fault (Bailey, 1988). The fault is shown to transect the monzonite at Mouse Mountain (Fig 2); however, evidence for the structure or displacement of the monzonite could not be substantiated in outcrop.

METAMORPHISM

The metamorphic grade of the rocks of the Mouse Mountain property is for the most part sub-greenschist facies. Primary textures and fabrics are preserved, except where the rocks have been affected by faulting or hydrothermal alteration. The metavolcanic rocks of unit 2 and unit 3 occur within the chlorite metamorphic isograd, with the characteristic metamorphic minerals being chlorite+epidote±clinozoisite. In unit 3, the saussuritization of plagioclase varies from slight to complete replacement by fine-grained epidote, calcite and sericite. The dark green to dark grey pyroxene basalts of unit 2 contain mafic crystals with only slightly chloritized rims, although the plagioclase is universally turbid and saussuritized. Amygdules within the vesicular portion of the flows contain calcite and lesser quartz. Locally, zones of more intense replacement of the greenschist assemblage are interpreted to be products of propylitic alteration related to the nearby intrusion.

ALTERATION AND MINERALIZATION

Three separate zones of copper-gold mineralization and associated alteration occur in the vicinity of the Mouse Mountain peak (Fig 14). These zones are aligned and distributed along a north-northwest-trending strike length of 3 km. They include, from north to south: the Rainbow, Valentine and High-grade zones.

Geochemistry

Table 1 presents the results of geochemical analyses of rock samples collected from the Rainbow, Valentine and High-grade zones. The samples prefaced with SJ06 were collected and analyzed for Au, Pd and Pt by fire assay and for 28 elements by ICP-MS, by Eco-Tech Laboratories Limited in Kamloops, BC. The remaining samples prefaced with 06JLO were steel milled at the BC Geological Survey Laboratory in Victoria. Splits were shipped for analyses to ACME Analytical Laboratories Ltd., Vancouver, for trace-element analyses using inductively coupled plasma emission spectrometry (ICP-ES) and Activation Laboratories Ltd., Ancaster, Ontario for Au analyses using instrumental neutron activation (INAA).

Rainbow Zone

The Rainbow zone is a small, poorly exposed area of altered monzonite situated at the northwest end of the min-

eralized corridor approximately 1 km north-northwest of the Valentine zone. The intrusive rocks in this area are generally fine-grained, pink-orange-yellow in colour and silicified. This zone is characterized by pervasive, texturally destructive quartz-carbonate and fuchsite-mariposite alteration. In thin section, ankerite is the dominant carbonate mineral present, with calcite occurring only in late-stage crosscutting veinlets. Chalcedonic quartz, characterized by numerous fluid inclusions, occurs in veins and blebs. Where the carbonate alteration is strongest, sulphides and copper carbonates have been leached out of the rock. Locally, however, unaltered monzonite has fresh biotite phenocrysts.

Mineralization at the Rainbow zone occurs as disseminations and microveins of pyrite, chalcopyrite, malachite and azurite. Negligible amounts of fluorite, sphalerite and bornite were also observed. Chalcopyrite mineralization estimated at 0.5% occupies the core of the Rainbow zone and is enveloped by a pyrite-only mineralized margin. A couple of grab samples of chalcopyrite mineralization returned low copper (~0.25%) and gold (100 ppb) values (SJ06-051, 196; *see* Table 1).

Valentine Zone

The Valentine zone is located due east of the Mouse Mountain peak. It occupies an east-facing hillslope that was stripped in 1987 and comprises a well-exposed 100 m by 100 m outcrop area of variably altered and mineralized microporphyrific monzonite. Mineralization, alteration and structure of the Valentine zone are the focus of ongoing studies by the senior author. The following summarizes preliminary work to date.

The Valentine zone is developed close to the eastern margin of the Mouse Mountain monzonite, which at the Valentine zone is a nepheline-normative micromonzonite. This zone exhibits classic alkalic porphyry-style alteration zonation comprising propylitic-phyllitic-potassic with limited supergene enrichment, from the fringe to the core. In the outer margins of the study area and in the surrounding country rock, a mineral assemblage of chlorite+epidote+carbonate defines the propylitic alteration zone. Stockworks of sericite, quartz and pyrite are common on the periphery of the Valentine zone, delineating a phyllic halo. In the potassic core, an assemblage of potassium feldspar+magnetite+biotite+chlorite+diopside±actinolite hosts disseminations and stockworks of pyrite and chalcopyrite. Discrete zones of pervasive iron-carbonate alteration overprint the alkalic alteration assemblage. These zones are structurally controlled (north and east-trending), texturally destructive and can dilute copper-gold grades of the monzonite-related mineralization. An assemblage of dolomite, pyrite, calcite, quartz and sericite characterizes this late-stage event. Zones of iron-carbonate alteration are characterized by elevated arsenic, antimony and molybdenum values (SJ06-196, 06JLO8-86, SJ06-104; *see* Table 1). At the top of the deposit, supergene processes have leached sulphides from the cap rock and precipitated iron oxide, malachite and azurite on fracture surfaces; this is the most noticeable evidence of the copper mineralization.

There are three main fault sets that crosscut the Valentine zone. These trend 040°, 220° and 310° and all dip moderately to steeply. Hypogene mineralization consists of early pyrite replaced by magnetite and chalcopyrite. Miner-

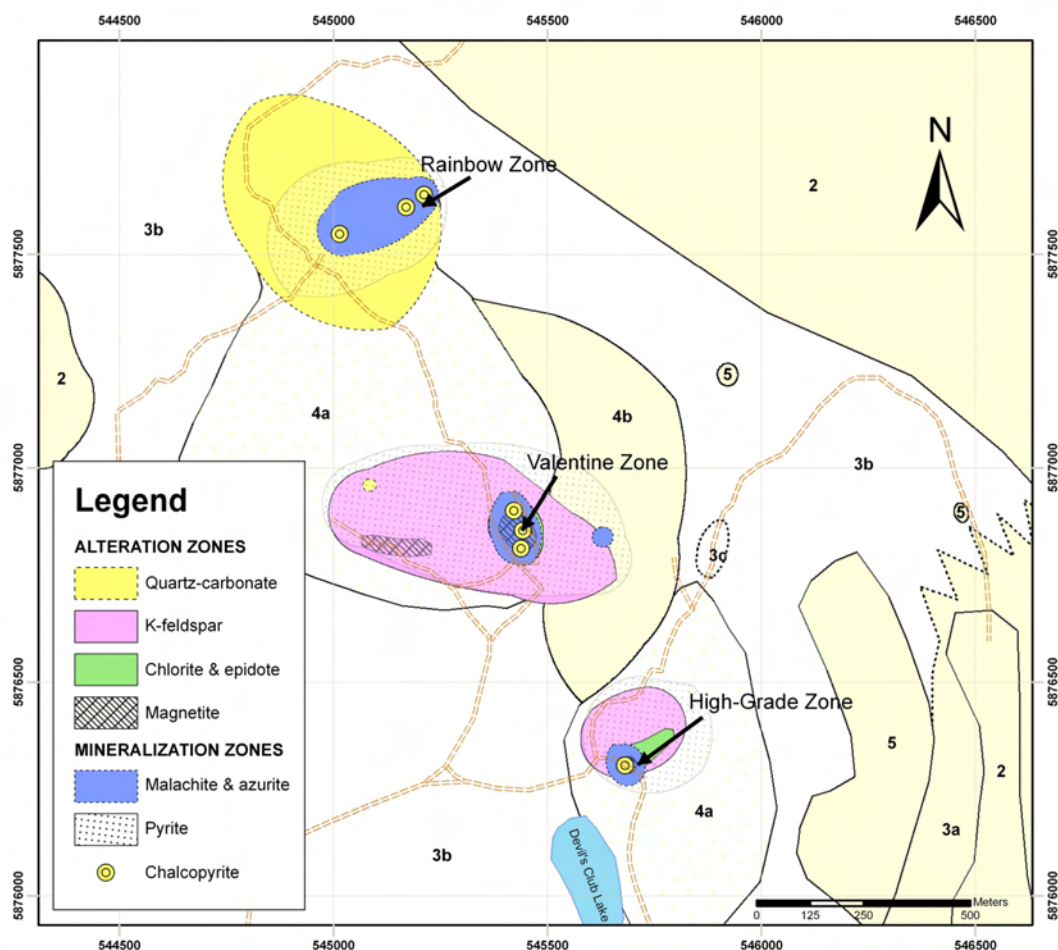


Figure 14. Alteration and mineralization zones on the Mouse Mountain property..

alization occupies anastomosing and coalescing series of fractures and breccia that appear to postdate some of the potassium alteration. The highest assay results from grab samples collected on the Valentine zone returned 0.6056% Cu and 455 ppb Au. Palladium shows slightly elevated values in sulphide-rich samples from the Valentine and High-grade zones (SJ06-133 and 149).

High-Grade Zone

Two hundred metres north of Devils Club Lake and 750 m south of the Valentine zone is a small mineralized outcrop known as the High-grade zone. The entire zone is approximately 3 m by 2 m and is exposed in the wall of a flooded pit, presumably the source of early production. The hostrock to the mineralization is fine to medium grained, grey-pink in colour and resembles monzonite from the Valentine zone. Compositionally, however, monzonite from the High-grade zone is distinct on two accounts: clinopyroxene is more abundant (~25% of the mode) and nepheline is not present. Alteration is similar to that at the Valentine zone: fine-grained magnetite and potassium alteration flood the monzonite replacing the matrix and altering the clinopyroxene to biotite, epidote and chlorite assemblages. Younger potassium alteration occurs in veins with coarse crystalline magnetite. Cockscomb calcite occupies open fractures. Copper mineralization consists of cop-

per carbonates and chalcopyrite. The highest assay results from grab samples collected at the High-grade zone returned 1.38% Cu and 1.23 g/t Au (SJ06-149; see Table 1).

CONCLUSION

The 2006 summer mapping program has successfully mapped and described a variety of lithological units on the Mouse Mountain property, and for the first time applied thin section analyses to validate these descriptions. Nicola Group rocks underlie the Mouse Mountain property and can be correlated along strike with volcanoclastic units and porphyritic subvolcanic monzonite intrusions, which are spatially and temporally associated with mineralization at Mount Polley. Heterolithic, maroon volcanoclastic rocks that are Late Triassic or Early Jurassic (?) in age, underlie the majority of the Mouse Mountain property. In general, the volcanic succession consists of subaqueous pyroxenophytic basalt flows and breccia, an overlying sequence of pyroclastic and epiclastic volcanic deposits, and shallow-water sedimentary rocks that overlap and flank the volcanic accumulations. Late Triassic alkaline intrusions intrude the volcanoclastic succession, producing high-level breccia by steam-blasted disintegration. At Mouse Mountain, there are multiple events of hydrothermal alteration, brecciation

TABLE 1. ICP-ES AND FIRE ASSAY RESULTS FROM SELECTED MINERALIZED SAMPLES, MOUSE MOUNTAIN.

			Element	Ag	Al	As	Au	Ba	Bi	Ca	Cd	Ce	Co	Cr	Cu	Fe	Hf	K	La	Li	Mg	Mn	Mo			
			Units	ppm	%	ppm	ppb	ppm	ppm	%	ppm	ppm	ppm	ppm	ppm	%	ppm	%	ppm	ppm	%	ppm	ppm			
			Method	TICP	TICP	TICP	FA	TICP	TICP	TICP	TICP	TICP	TICP	TICP	TICP	TICP	TICP	TICP	TICP	TICP	TICP	TICP	TICP			
Station Number	Easting	Northing																								
Rainbow Zone																										
SJ06-051	544960	5877660	<0.2	0.66	5	10	180	<5	2.78	<1	-	18	22	92	4.31	-	-	<10	-	1.14	1354	<1				
SJ06-198	545016	5877544	0.2	0.35	985	100	190	<5	1.7	6	-	23	41	2510	1.92	-	-	<10	-	0.38	405	10				
Valentine Zone																										
06JLO2-12	545433	5876857	0.5	8.62	14	325	1092	0.2	3.04	0.1	18	14.6	68.5	2944	5.63	1.1	3.65	8.4	25.7	1.49	748	2.5				
06JLO8-86	545476	5876810	0.9	8.47	434	9	1077	0.2	3.28	0.1	16	15.1	34.5	3269	5.86	0.6	4.66	6.8	1.8	0.13	825	7.5				
06JLO9-85	545453	5876847	0.5	8.53	12	356	1248	0.1	2.93	0.1	18	18.5	68.3	2059	6.06	1.2	3.32	8.1	20.1	1.47	818	7.3				
06JLO9-87	545453	5876856	0.7	8.5	14	307	1007	0.1	3.49	0.1	19	16.9	71.6	2275	5.86	1	4.48	8.2	27.9	1.69	873	3.4				
06JLO9-88	545311	5876796	<.1	9.21	21	253	1288	<.1	3.33	0.1	12	8.8	23.8	30.9	3.72	2	4.15	5.6	18	0.93	714	1.8				
SJ06-104	545402	5876896	0.2	0.19	215	165	935	<5	6.1	<1	-	15	56	1305	4.09	-	-	<10	-	1	1160	5				
SJ06-109	545453	5876840	1.3	0.92	35	455	270	<5	1.34	<1	-	32	40	6056	6.8	-	-	<10	-	1.23	848	9				
SJ06-131	545423	5876862	<0.2	0.25	50	40	250	<5	4.47	<1	-	12	33	341	4.64	-	-	<10	-	0.61	750	14				
SJ06-132	545457	5876870	0.5	1.04	10	255	35	<5	1.2	<1	-	26	49	2658	7.76	-	-	<10	-	1.64	870	7				
SJ06-133	545477	5876809	0.7	0.23	110	460	140	<5	5.97	<1	-	28	17	3543	5.14	-	-	<10	-	1.88	1084	8				
SJ06-134	545438	5876818	<0.2	1.41	5	15	60	<5	3.73	<1	-	24	<1	202	7.33	-	-	<10	-	2.04	2302	2				
High-Grade Zone																										
06JLO2-11	545685	5876296	0.3	8.82	11	277	1100	0.6	5.99	<.1	22	29.6	57.3	5466	7.9	1.2	2.91	12.6	43.3	2.9	1142	2.6				
SJ06-149	545682	5876305	1.3	2.1	20	>1000	65	<5	5.76	<1	-	34	60	>10000	8.23	-	-	<10	-	0.38	405	10				
Std CANMET WPR1			0.6	1.55	-1	45	19	0.1	1.61	0.2	5	174	2370.6	1692	10.96	0.5	0.09	1.9	4.6	18.57	1352	0.3				
Recommended			0.7	1.64	1.4	42.2	22	0.19	1.43	0.43	6	180	3300	1640	9.93	0.61	0.165	2.2	4.2	18.69	1549	0.9				
% Difference			3.8	1.4	300.0	1.3	3.7	15.5	3.0	18.3	4.5	0.8	8.2	0.8	2.5	5.0	14.7	3.7	2.3	0.2	3.4	25.0				
			Element	Na	Nb	Ni	P	Pb	Pd	Rb	S	Sb	Sc	Sn	Sr	Th	Ti	U	V	W	Y	Zn	Zr			
			Units	%	ppm	ppm	%	ppm	ppb	ppm	%	ppm	ppm	ppm	ppm	ppm	%	ppm	ppm	ppm	ppm	ppm	ppm			
			Method	TICP	TICP	TICP	TICP	FA	TICP	FA	TICP	TICP	TICP	TICP	TICP	TICP	TICP	TICP	TICP	TICP	TICP	TICP	TICP			
Station Number	Easting	Northing																								
Rainbow Zone																										
SJ06-051	544960	5877660	0.04	-	11	1770	6	<5	-	-	<5	-	<20	138	-	0.05	<10	119	<10	18	44	-				
SJ06-198	545016	5877544	0.07	-	8	1590	6	<5	-	-	10	-	<20	71	-	<0.01	<10	41	<10	10	31	-				
Valentine Zone																										
06JLO2-12	545433	5876857	3.777	2.6	18.9	0.105	4.1	16	55.8	0.2	1.1	12	1.5	596	1.5	0.299	1	206	0.4	13.1	33	30.2				
06JLO8-86	545476	5876810	3.233	2.4	14.7	0.132	6	<2	62.7	0.1	26.6	10	1.5	337	1.2	0.297	0.9	250	2.2	9.7	48	16.6				
06JLO9-85	545453	5876847	2.819	3	16.9	0.117	4.9	22	43.6	0.2	0.7	14	1.7	661	1.6	0.316	1.1	246	0.6	16	40	31.6				
06JLO9-87	545453	5876856	2.751	2.6	19	0.11	5	42	63.1	0.2	0.7	13	1.5	407	1.5	0.298	1	219	0.4	14.7	38	26.9				
06JLO9-88	545311	5876796	3.908	2.8	3.2	0.125	4.7	10	61.6	<.1	1.1	7	0.7	686	1.5	0.317	1.4	192	0.8	15.2	36	62.2				
SJ06-104	545402	5876896	<0.01	-	9	1020	14	15	-	-	335	-	<20	165	-	<0.01	<10	58	<10	6	38	-				
SJ06-109	545453	5876840	0.02	-	25	1150	24	25	-	-	<5	-	<20	40	-	0.09	<10	216	<10	13	48	-				
SJ06-131	545423	5876862	0.01	-	11	1060	8	<5	-	-	30	-	<20	75	-	<0.01	<10	72	<10	9	25	-				
SJ06-132	545457	5876870	0.02	-	22	1010	20	15	-	-	<5	-	<20	28	-	0.15	<10	249	<10	6	42	-				
SJ06-133	545477	5876809	0.01	-	18	1030	14	60	-	-	<5	-	<20	103	-	<0.01	<10	134	<10	18	35	-				
SJ06-134	545438	5876818	0.02	-	21	2160	18	<5	-	-	<5	-	<20	39	-	0.03	<10	256	<10	20	77	-				
High-Grade Zone																										
06JLO2-11	545685	5876296	2.644	2.1	14.7	0.284	3.7	53	61.1	0.3	0.6	25	1.2	968	1.1	0.444	1	358	0.6	19	47	26.7				
SJ06-149	545682	5876305	0.03	-	22	3660	62	70	-	-	<5	-	<20	158	-	0.17	30	308	<10	17	70	-				
Std CANMET WPR1			0.017	1.8	3151	0.018	5.7	277	3.8	0.8	0.7	11	0.7	6	0.3	0.204	0.1	72	0.1	4.3	94	14.2				
Recommended				2.4	2900	0.013	6	285	5	0.9	0.9	12	1.1	7	0.4	0.179	0.2	65			95	18				
% Difference			50.0	7.1	2.1	8.1	1.3	0.7	6.8	2.9	6.3	2.2	11.1	3.8	7.1	3.3	16.7	2.6	50.0	50.0	0.3	5.9				

06JLO: TICP= Four acid digestion - inductively coupled plasma emission/mass spectrometry analysis. FA - Lead collection fire assay - ICPES Finish. Acme Analytical, Vancouver
 SJ06: TICP = Aqua regia digestion - inductively coupled plasma emission/mass spectrometry analysis, FA= fire assay. Eco Tech Laboratory, Kamloops

and mineralization associated with the invasion of stocks and sills into the country rock.

Limited rock geochemical sampling and analyses indicates a Triassic mineral assemblage of copper-gold-palladium associated with alkaline magmatism and a younger, possibly Middle Jurassic or Cretaceous metal assemblage of molybdenum-arsenic-antimony associated with iron-carbonate-silica alteration. Ongoing studies of the mineralization, alteration and intrusive paragenesis at the Valentine zone is designed to understand the processes contributing to mineral deposition within an alkaline magmatic centre and permit assessment of other potential magmatic centres in the Quesnel belt.

ACKNOWLEDGMENTS

The authors extend their thanks to Dirk Tempelman-Kluit for his guidance and support throughout the mapping project. Geological discussions with Mitch Mihalyuk and Lee Ferreira were informative and appreciated. Lee Dearing is gratefully acknowledged for her capable assistance in the field. David Nelles is also thanked for kindly loaning the senior author his petrographic microscope.

REFERENCES

- Bailey, D.G. (1988): Geology of the central Quesnel belt, Swift River, south-Central British Columbia (93B/16, 93A/12, 93G/1); in *Geological Fieldwork 2005, BC Ministry of Energy, Mines and Petroleum Resources*, Paper 1989-1, pages 167–172.
- BC Geological Survey (2006): MapPlace GIS internet mapping system; *BC Ministry of Energy, Mines and Petroleum Resources*, MapPlace website, URL <<http://www.MapPlace.ca>> [November 2006].
- Donkersloot, P. (1992): Geophysical, geological and drill report on the Mouse Mountain Property, Cariboo Mining Division; unpublished report for Teck Exploration Ltd., July 15, 1992, pages 1–21.
- Fox, P.E. (1975): Alkaline rocks and related mineral deposits of the Quesnel Trough, British Columbia (abstract); *Geological Association of Canada*, Program with Abstracts, page 12.
- Imperial Metals Corporation (2006): Imperial reports production statistics and updated Mount Polley Resource: Imperial Metals Corporation, Press release, January 23, 2006, URL <http://www.imperialmetals.com/s/News-2006.asp?ReportID=127260&_Type=News-Release-2006&_Title=Imperial-Reports-Production-Statistics-and-Updated-Mount-Polley-Resource> [November 2006].
- Logan, J.M. and Bath, A.B. (2005): Geochemistry of Nicola Group basalt from the central Quesnel Trough at the latitude of Mount Polley (NTS 093A/5, 6, 11, 12), central BC; in *Geological Fieldwork 2005, BC Ministry of Energy, Mines and Petroleum Resources*, Paper 2006-1, pages 83–98.
- Logan, J.M., Mihalyuk, M.G., Ullrich, T. and Friedman, R.M. (2007): U-Pb ages of intrusive rocks and ^{40}Ar - ^{39}Ar plateau ages of copper-gold-silver mineralization associated with alkaline intrusive centres at Mount Polley and the Iron Mask batholith, southern and central British Columbia; in *Geological Fieldwork 2006, BC Ministry of Energy, Mines and Petroleum Resources*, Paper 2007-1 and *Geoscience BC*, Report 2007-1, pages 93–116.
- Mortensen, J.K., Ghosh, D.K. and Ferri, F. (1995): U-Pb geochronology of intrusive rocks associated with copper gold porphyry deposits in the Canadian Cordillera; in *Porphyry Deposits of the northwestern Cordillera of North America*, Schroeter, T.G., Editor, *Canadian Institute of Mining, Metallurgy and Petroleum*, Special Volume 46, pages 142–158.
- Palfy, J., Smith, P.L. and Mortensen, J.K. (2000): A U-Pb and ^{40}Ar - ^{39}Ar time scale for the Jurassic; *Canadian Journal of Earth Sciences*, volume 37, pages 923–944.
- Panteleyev, A., Bailey, D.G., Bloodgood, M.A. and Hancock, K.D. (1996): Geology and mineral deposits of the Quesnel River – Horsefly map area, central Quesnel Trough, British Columbia; *BC Ministry of Energy, Mines and Petroleum Resources*, Bulletin 97, 156 pages.
- Rees, C. (2005): Geological Report on the Mount Polley Property and Summary of Exploration in 2003-2004; unpublished report for Imperial Metals Corporation, pages 1–211.
- Sanguinetti, M.H. (1989): Report on the Mouse Mountain Property, Quesnel River area, Cariboo Mining Division, British Columbia; unpublished report for Quesnel Mines Limited, Sanguinetti Engineering Ltd., November 8, 1989, pages 1–35.
- Sutherland Brown, A. (1957): Mouse Mountain (53° 122° S.E.); in *Minister of Mines, Annual Report 1956, BC Ministry of Energy, Mines and Petroleum Resources*, page 33.
- Struik, L.C. (1983): Bedrock geology of Spanish Lake (93A/11) and parts of adjoining map areas, central British Columbia; *Geological Survey of Canada*, Open File Map 920, scale 1:50 000.
- Struik, L.C. (1986): Imbricated terranes of the Cariboo gold belt with correlations and implications for tectonics in southeastern British Columbia; *Canadian Journal of Earth Sciences*, volume 23, pages 1047–1061.
- Struik, L.C. (1988): Regional imbrication within Quesnel Terrane, central British Columbia, as suggested by conodont ages; *Canadian Journal of Earth Sciences*, volume 25, pages 1608–1617.
- Tempelman-Kluit, D.J. (2006): Geological Report on the Quesnel Trough project including the G-South, Mouse Mountain, Blackstone, Chubby Bear, Quesnel River Area, Cariboo Mining Division, British Columbia; unpublished report for Richfield Ventures Corporation, May 8, 2006, pages 1–88.

Mapping and Review of Coal Geology in the Wolverine River Area, Peace River Coalfield (NTS 093P/03), Northeastern British Columbia

by A.S. Legun

KEYWORDS: Peace River coalfield, coal exploration, geological mapping, Gates Formation, Gething Formation, Bullmoose thrust fault, Mesa thrust fault, J seam, E seam, D seam

INTRODUCTION

This report discusses a compilation of coal geology in the Wolverine River area, west of the town of Tumbler Ridge, in northeastern British Columbia as illustrated in Figure 1. This is an area of old, new and potential coal-pit developments within the Peace River coalfield. New developments include Perry Creek of Western Canada Coal Corporation (WCCC). Potential pits include Hermann North and EB (also WCCC). Old pits, now reclaimed, include the Wolverine (originally known as Frame), Deputy, McConkey, Mesa, Mesa North and Mesa North Extension pits of Quintette Coal Ltd. (Quintette). This area of developed infrastructure, with power, rail and road, has the potential for surface coal and coal gas in the shallow subsurface and natural gas in Paleozoic reservoirs at depth.

The project objectives are to produce a map at 1:25 000 scale, improve understanding of the geological framework and suggest new areas for exploration. Geological linework, pit development locations and a line of section in the Gates Formation coal measures are included in Figure 2.

Existing maps, varying in scale from 1:50 000 to 1:5000, were reviewed prior to fieldwork. In addition, numerous coal assessment reports (COALFILE, 2006), available on the ministry's MapPlace website (BC Geological Survey, 2006), were accessed. The area was the focus of rapid development during the early 1980s with pits of Teck-Bullmoose Coal Inc. and Quintette coming online. Outlying areas underlain by coal measures received little additional scrutiny. Both these mines closed a few years ago and it is timely to step back and look again at the prospective ground. There is scope for new discoveries and this is facilitated by better definition of faults and folds affecting the coal measures.

Access is fairly good within the area and includes forestry, coal exploration, logging and petroleum-well access roads, together with numerous recent cutlines for seismic surveys. The level of exposure varies from excellent, in the alpine, to poor at lower elevations with gentler slope and in some drift-filled valley bottoms.

This publication is also available, free of charge, as colour digital files in Adobe Acrobat® PDF format from the BC Ministry of Energy, Mines and Petroleum Resources website at http://www.em.gov.bc.ca/Mining/Geolsurv/Publications/catalog/cat_fldwk.htm

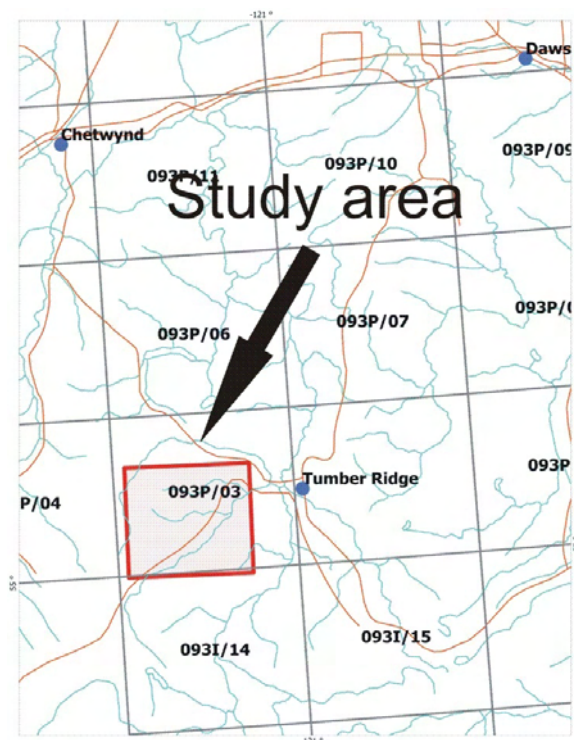


Figure 1. Location of study area, northeastern BC.

The current geological mapping complements previous work on the Gates Formation coal measures (Legun, 2006). That work focused on the relationships of marine tongues and nearshore deposits with coal measures in the area of Wolverine River.

A description of undrilled resource targets in the Gates Formation has been included in this paper. It is also suggested that Gething Formation coal measures, a target of early exploration in the area, deserve renewed scrutiny. The reported results are preliminary and subject to further ground examinations.

METHODOLOGY

Numerous maps from coal assessment reports were copied from digital assessment files and georegistered into Manifold project space. Bedding data was digitized from the maps and the compilation of a large database of structural data is in progress. Fieldwork was facilitated by stereopairs of colour airphotos flown in 2005, and orthophoto images provided control for linework. Digital elevation models (DEM) were brought into Manifold GIS

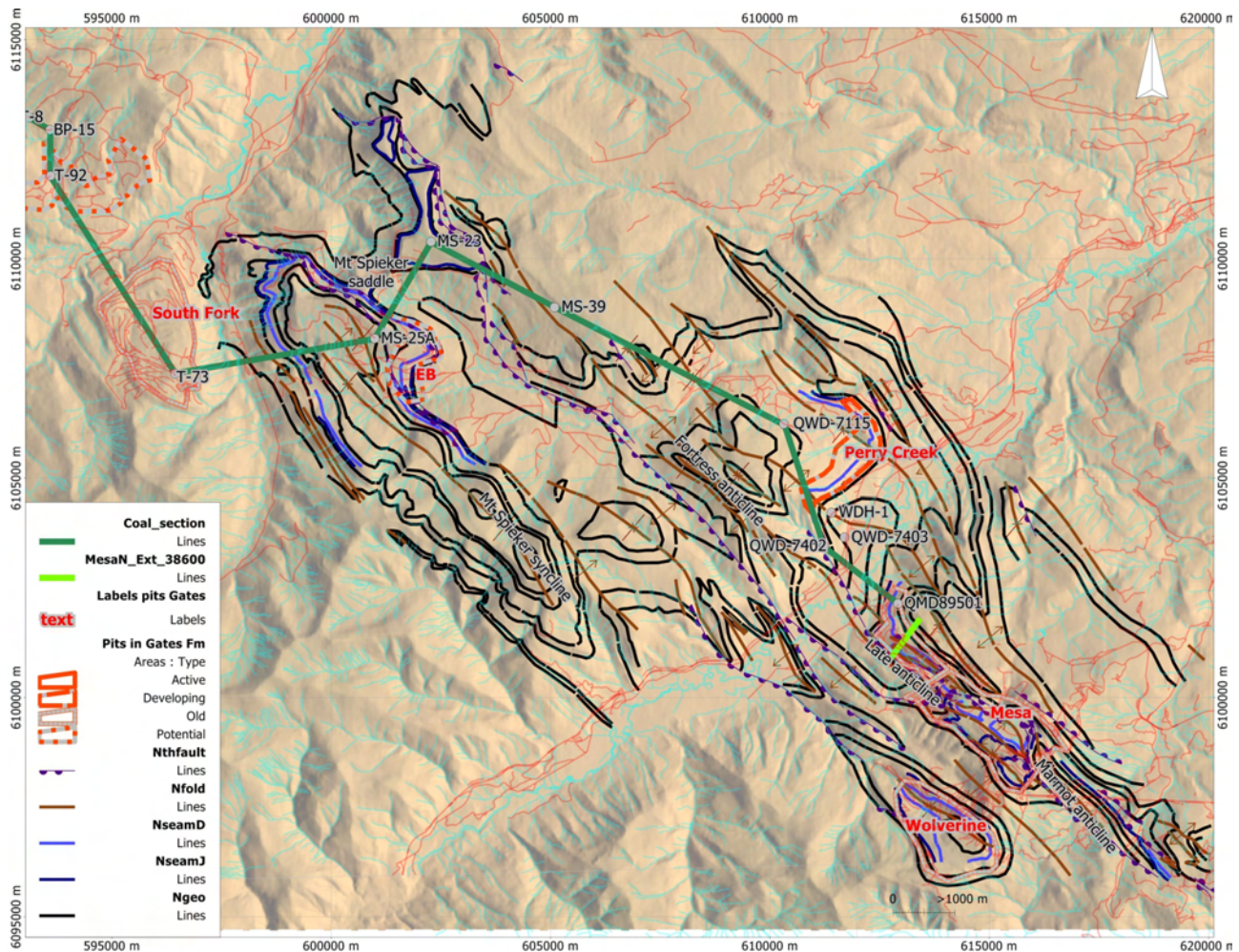


Figure 2. Some elements of the geological compilation in the Wolverine River area, Peace River coalfield, northeastern BC.

software as surfaces. The latter provide a sense of relief to orthophotos (when overlain as a transparency) and assist in the correct placement of contacts affected by topography.

The surface trace of two seam intervals, D and E at the top and J at the base of the middle Gates Formation, were digitized from various reports, which covered the Mesa, Hermann North, Mt. Spieker and Perry Creek areas. These two seams have considerable lateral extent and are the primary economic seams of interest in the Wolverine River area.

Approximately four weeks were spent in the field, with student assistance provided by A. Stephenson of the University of Victoria. Traverses were concentrated in peripheries of old and new pits, areas of limited data (Fortress Mt.) and in chasing major structures, such as the Bullmoose fault.

PREVIOUS WORK

Early exploration interest was in the Gething Formation coals, pursuing trends from the Sukunka property immediately to the north (MINFILE 093P 014; MINFILE, 2006). The focus then switched to Gates Formation coal, with intercepts of thick clean coal of metallurgical quality in the Gates interval within the Wolverine River area. Addi-

tional drilling indicated good continuity of the individual seams. Mapping in the northern part of the work area by Ranger Oil Ltd. resulted in a detailed map of the Mt. Spieker area being produced in the late 1970s (COALFILE 557). Quintette produced a series of 1:5000 scale maps in the south focusing on the Gates Formation (COALFILE 607, 615). Gilchrist and Flynn (1978) published a compilation prior to Quintette's development of a mine south of the Wolverine river and Kilby and Wrightson (1987) published during the main phase of mining. Industry continued mapping as the pit developed. However, some areas (e.g., near the Frame pit) did not seem to receive much follow-up and this is one area where contacts below the Gates Formation remain unresolved.

REGIONAL STRATIGRAPHY

The mapped interval is Early Cretaceous with the Gething Formation coal measures ranging from Aptian to early Albian (Gibson, 1992), while the Gates Formation is limited entirely to the Albian. The following summary encompasses the stratigraphy from the Gething Formation to the Hulcross Formation shale. Related data can be found in summary tables of Quintette reports (e.g., COALFILE 746, Table 3.1).

Hulcross Formation

The Hulcross Formation is a rusty marine sequence of shale and siltstone containing a thin ferruginous pebble zone, locally, at the base. The thin-bedded sequence occupies a recessive notch below Boulder Creek sandstone and conglomerate. The formation averages approximately 100 m in thickness in the area. The Hulcross Formation is similar to the Moosebar Formation but lacks the glauconitic zones towards the base as well as pure mudstone.

Gates Formation

The Gates Formation comprises basal, sheet sandstone (lower Gates member), a middle sequence rich in coals (middle Gates member) and an upper sequence (upper Gates member) usually comprising upward-coarsening deposits of marine origin capped by thin coals and silty beds. This division into members is informal and follows terminology in assessment reports covering the area from Wolverine River to the Alberta border. There is a broad transition zone at the base of the formation. Table 1 shows the stratigraphic correspondence of various unit names. A line of section relates the succession near the Bullmoose mine to that at the Quintette's Mesa pit (Fig 3).

The Gates Formation is 200 to 230 m thick within the field area. The value differs from that reported by Quintette due to a different pick for the base of the formation (*see* discussion following).

UPPER GATES MEMBER

The upper Gates member is defined by Quintette as the top of D seam to the base of the Hulcross Formation shale. In the area of interest, there is no economic coal in the upper Gates member. The member corresponds to the "major marine tongue" and overlying "silty member" of Duff and Gilchrist (1981). The marine tongue is known as the Notikewan in subsurface and the Babcock Member in surface coalfield terminology. Usually it is an upward-coarsening sequence with a characteristic gamma signature on geophysical logs. However, at Quintette Mesa pit a basal

conglomerate, known as the caprock conglomerate, is in erosional contact with the top of D seam.

Carmichael (1988) ascribed much of the Babcock Member to an environment of estuarine shoals. The upper Gates member is approximately 120 m thick at the Mesa North pit. At Perry Creek, up to 100 m of upper Gates member is preserved within the core of Perry syncline. This must be almost a complete section, the Hulcross Formation contact is not noted in a WCCC correlation chart (Western Canada Coal Corporation, 2004, Fig 2.03-07). The Fortress Mt. unit shown on that chart is equivalent to Babcock/Notikewan and should be included in the upper Gates member.

MIDDLE GATES MEMBER

The middle Gates member was defined by the Quintette geologists as the base of J seam to the top of D seam. In the south, this includes some additional strata below J seam to K seam. The middle Gates member comprises the main coal-bearing interval within the Gates Formation. At Mesa pit, the member encompassed up to 18 m of coal in 60 m of section. Trends and details of the middle Gates member stratigraphy are discussed later.

LOWER GATES MEMBER

The lower Gates member has not been consistently defined. Quintette considered the base of the first thick sandstone (COALFILE 746, p 3-4) in the transition zone from Moosebar Formation shale as the base. Duff and Gilchrist (1981) also placed the contact low in the transition and defined a sandy 'Spieker' Member within the Gates Formation. Both definitions translate to a lower Gates member that is a non-coal bearing interval, which is more than 100 m thick. The base of the Gates Formation, however, has been formally defined (McLean, 1982) as the first sandstone not having significant shale above it. This definition often moves the contact to a stratigraphically higher sandstone unit, often within approximately 25 m of J seam.

The top of the lower Gates member is dominated by sheet sandstone, which forms a strandplain (Leckie, 1986).

TABLE 1. NOMENCLATURE OF COAL SEAMS AND LITHOLOGICAL UNITS, GATES FORMATION, WOLVERINE RIVER AREA, BC.

Gates Formation	Lithology	West Fork deposit	Teck-Bullmoose mine (reclaimed)	Perry Creek pit	Quintette Mesa pit (reclaimed)	Subsurface (oil and gas wells)	Carmichael (1983) regional study
Upper	interbeds sandstone/ conglomerate unit			Fortress Mt. unit	Babcock Member	Notikewan	Babcock Member
Middle	coal	(E)	(E)	D seam	D seam		
	interbeds coal sandstone/ conglomerate unit	(D)	(D)	E, F seams Wolverine unit	E seam E conglomerate	Fahler C	
	coal interbeds sandstone/ conglomerate unit	(C)	(C)	G seam	G seam		
	coal sandstone/ conglomerate unit	unnamed conglomerate		J conglomerate		Fahler D	
Lower	coal sandstone unit	A, B seams	A, B seams	J (plies 1 to 3) Quintette sandstone ("Torrens")	J seam (plies 1 to 3) Quintette sandstone ("Torrens")	Fahler F	Sheriff Member
	sandstone unit					Fahler G	Torrens Member

Notes: brackets indicate comparable stratigraphic position; Torrens is an informal term for a unit of massive sandstones at base of J seam.

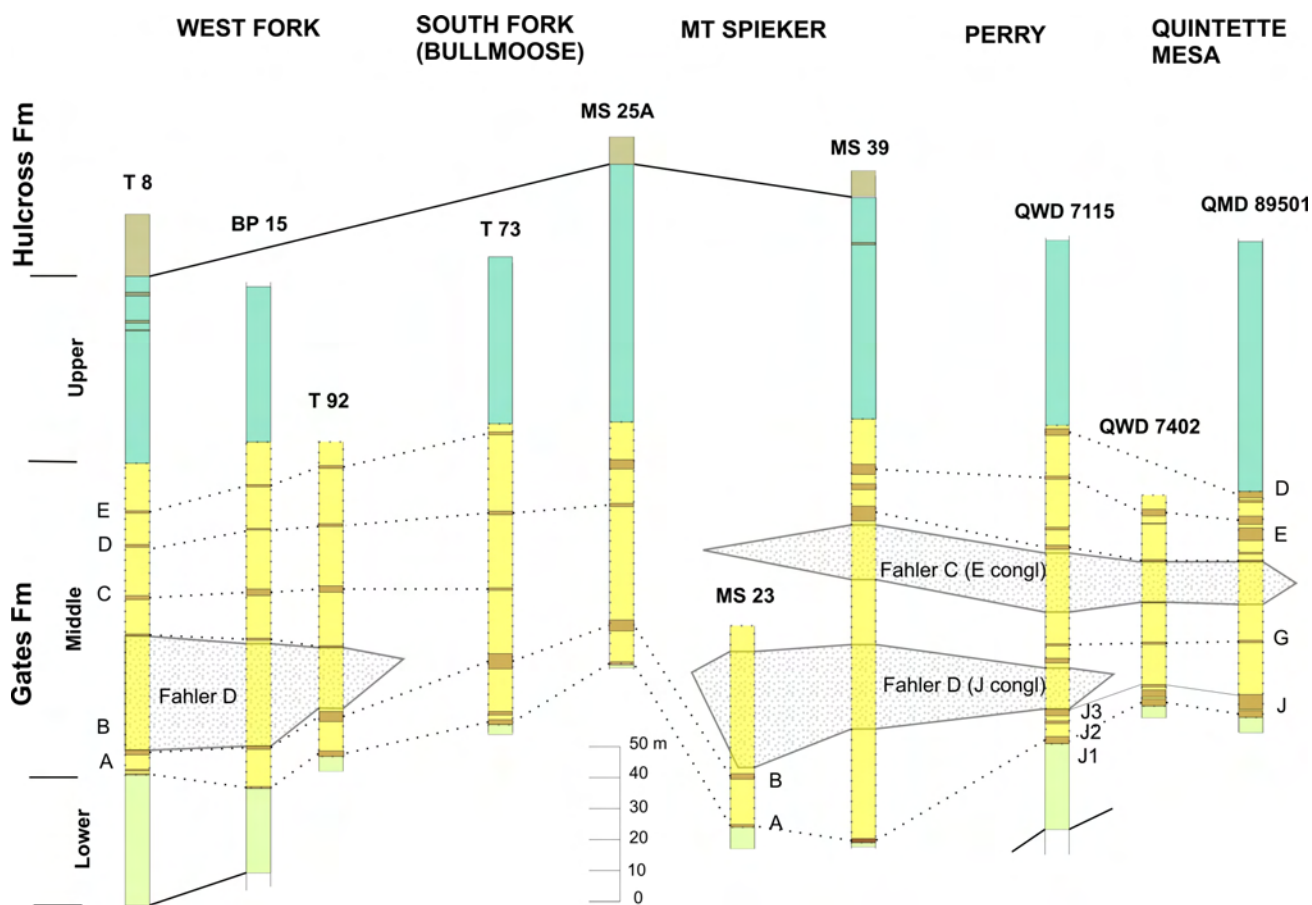


Figure 3. Line of section West Fork to Quintette's Mesa pit, illustrating the position of coal seams in the middle Gates member, northeastern British Columbia.

Moosebar Formation

The Moosebar Formation comprises approximately 80 m of dark marine shale followed by 70 to 95 m of interbedded, flaggy sandstone and shale. Quintette geologists restricted the formation to shale units. Using the formal definition of Gates Formation, the interbedded zone should be part of the Moosebar Formation and not the Gates Formation.

The thickness between the Gething Formation top and J seam is approximately 200 m in the area. This is composed of 175 m of Moosebar Formation followed by 25 m of the lower Gates member, according to the formal definition.

Gething Formation

The Gething Formation is divided into three members: a coal-bearing deltaic facies (Chamberlain Member), an underlying sequence of marine shale (Bullmoose Member) and a basal deltaic coal-bearing sequence of regional extent (Gaylard Member). The Chamberlain Member is 40 to 50 m thick in the Wolverine River area and shows some features of a wave-dominated delta. For example, it has a clean and widespread basal strandplain sandstone, which is the floor to a seam known as the Chamberlain seam. Lateral equivalents of the Skeeter and Bird seams found to the north (Sukunka area) are also present. The underlying sequence,

of approximately the same thickness, comprises shale that coarsens upward to flaggy interbedded sandstone and shale. This 40 to 50 m thick interval is the Bullmoose Member and foreshadows, in its facies transitions, the younger and depositionally thicker Moosebar Formation to Gates Formation transition. The shale of the Bullmoose Member abruptly overlies sandy glauconitic beds of the lower Gething Formation or Gaylard Member. The Gaylard Member, approximately 120 m thick, has a coal interval approximately 45 m from the top, known as the middle coals.

The total thickness of Gething Formation strata is approximately 207 m in the Perry Creek area based on drillhole correlations (*see* COALFILE 597). Farther south, thickness is difficult to assess as the transition to the underlying Cadomin Formation conglomerate is gradual.

STRUCTURE

The area of study lies within the inner foothills characterized by broad, open synclines and box anticlines interspersed with tight folds of short wavelength. Tight folds include east-verging asymmetric anticlines related to thrusts. Both north and south-plunging fold structures are present. Open synclines, and straight fold limbs paralleling topographic slope, are the favoured ground for developing coal open pits.

Workers have noted that folding at the structural level of the Gething and Cadomin formations is tighter than in the overlying Gates Formation. Structures evident in the Gething Formation die at the level of the Moosebar Formation (COALFILE 556) and many long, tight synclines are confined to the Moosebar Formation. Moosebar Formation strata form the hangingwall over a considerable strike length within a number of thrust panels. These features suggest detachment occurs within the Moosebar Formation strata.

Fieldwork in 2006 indicated asymmetric anticlines with eastern, overturned limbs are more common than previously identified. Examples include the major anticline crossing Perry Creek valley, near the pit access road, and the Marmot anticline crossing the line of the Quintette conveyor belt.

Bullmoose Thrust Fault

The Bullmoose thrust fault is a major fault in the area. The fault cuts the eastern flank of the flat-top Mt. Spieker at a shallow dip of 10 to 15°. The fault steepens as it is traced to the valley side of Perry Creek. It includes mappable fault slices of Moosebar Formation shale. It is represented in the valley bottom of Perry Creek near Fortress Mt. by a complex zone of steeply dipping beds, faults and disharmonic folds involving Gates and Moosebar formation beds. A sequence of overturned beds (Moosebar Formation-Gates Formation transition), exposed to the west, forms the hanging wall. The fault parallels a low marshy and drift-filled linear valley west of Fortress Mt. Its exact trace is unknown but is constrained by Gething and Hulcross formation rocks facing each other across the valley. The fault crosses the Wolverine River Road east of tight folds involving Gething and Cadomin formation beds but west of roadside exposures of Moosebar Formation.

The hanging wall in this segment is believed to be Gething Formation strata. Between Mt. Spieker and Wolverine, the footwall ranges from the Gates Formation to the Hasler Formation.

The trace to the south is uncertain. Displacement may be spread on several splays, one of which is the Mesa thrust fault in the Quintette pit area. Farther south, a single major fault cuts the Transfer syncline with a stratigraphic displacement of approximately 350 m (COALFILE 753, cross-section 30000, Transfer area).

Mesa Thrust Fault and Fortress Mt. Anticline

An anticline, exposing Gething Formation rocks in the eroded core and Moosebar and Gates formation rocks at a higher structural and topographic level, extends across the Wolverine River. It is exposed as a prominent

anticlinal arch on the higher slopes of Fortress Mt. (Fig 4). The east limb steepens and is locally overturned near the level of the Wolverine River.

On the south side of the river, the fold appears contiguous with the Late and Marmot anticlines in the Mesa-McConkey pit areas. The fold is overridden by the Mesa fault (a probable splay of the Bullmoose thrust fault) at the Quintette pits. It is underlain by a fault that brings Moosebar Formation strata over the middle Gates member, as exposed in a mine section at Perry Creek pit.

Incipient Triangle Zone Geometry (?)

Reverse faults with opposing dips and sense of vergence are noted in the Hermann North and Quintette Mesa areas. The general geological setting is illustrated in Figure 5, a view that is partly cross-sectional due to topographic relief. A drill section at the Mesa North Extension pit provides a more detailed view along strike (Fig 6).

This style continues along strike, well to the north. West-verging folds have been noted north of the map area by Hunter and Cunningham (1991). This pattern of paired reverse faults may mark an incipient triangle zone at the east margin of the coal belt.

DETAILS OF MIDDLE GATES MEMBER COAL STRATIGRAPHY

Middle Gates Member Trends

The middle Gates member thickens northward due to intrastratal bodies of marine sandstone and conglomerate. At the Mesa pit, there is 60 m of middle Gates member rock which expands to 75 m in the Mesa North pit (diamond-drill hole [ddh] QMD 89501 on Fig 3) due to an interval of E

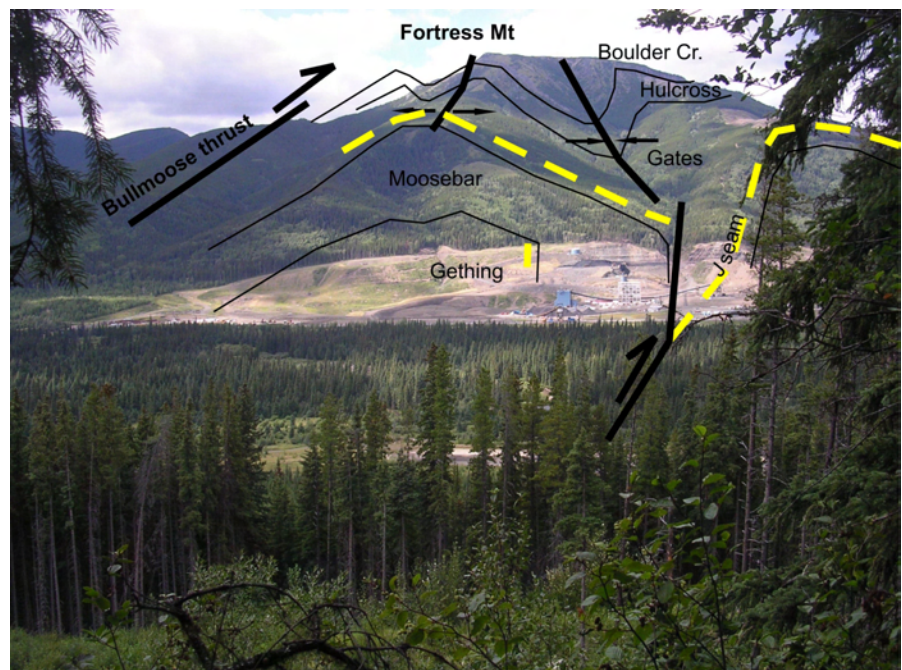


Figure 4. The Fortress Mt. anticline, outlined by a resistant arch of lower Gates member behind the Perry Creek plant site, northeastern BC. Note the faults bounding the anticline on east and west flanks.

conglomerate (Fahler C). This increases to over 100 m in the Perry Creek area (ddh QWD 7115 on Fig 3) and includes a second conglomerate wedge (J conglomerate or Fahler D). It reaches 125 m northeast of the Perry pit area (ddh QWD 7401) and even thicker to the northwest (approximately 136 m in ddh MS 39 on Fig 3). In these northern holes, the total coal in section is greatly reduced compared to the south.

The middle Gates member is approximately 85 to 90 m thick to the northwest, in the EB pit area, and 80 m thick at the former Bullmoose mine. Marine conglomerate reappears in the West Fork resource area north of Bullmoose and the middle Gates member correspondingly thickens.

Two significant coal intervals (J and E and D seam intervals) lie at the top and base of the middle Gates member and are extensive. The G seam at the Quintette pit (and roughly equivalent C seam at Bullmoose mine) is also a widespread coal interval which formed during the interval between Fahler D and C marine incursions.

J SEAM

At Quintette's Mesa pit, J seam averages over 5.5 m in thickness. Remnants of J seam within the pit lie within approximately 10 cm of a hard competent floor of shallow marine sandstone, which is part of the lower Gates Forma-

tion. J seam developed on a strandplain behind barriers of a wave-dominated delta (Kalkreuth and Leckie, 1989). It is overlain by lacustrine deposits with nonmarine unionid bivalves (Carmichael, 1983, p 39).

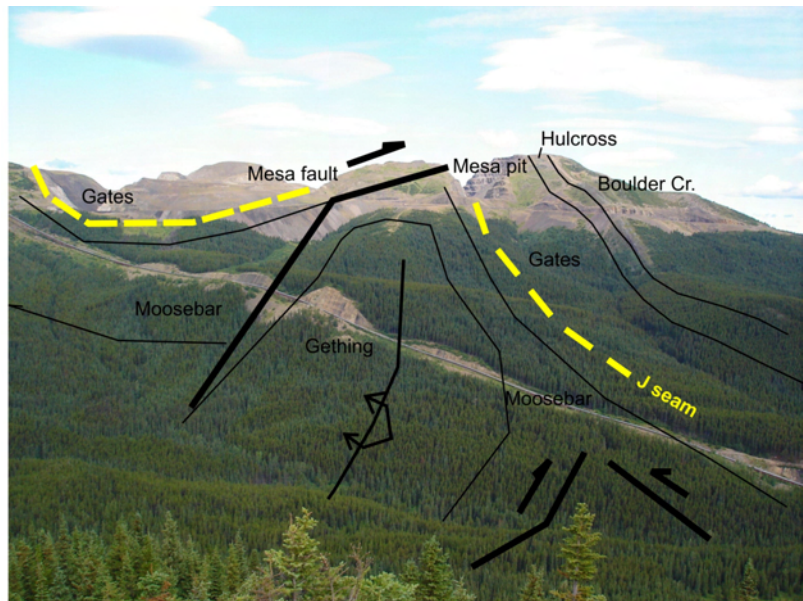


Figure 5. General cross-sectional view to the south side of Quintette Mesa pit from the Hermann North property, northeastern BC.

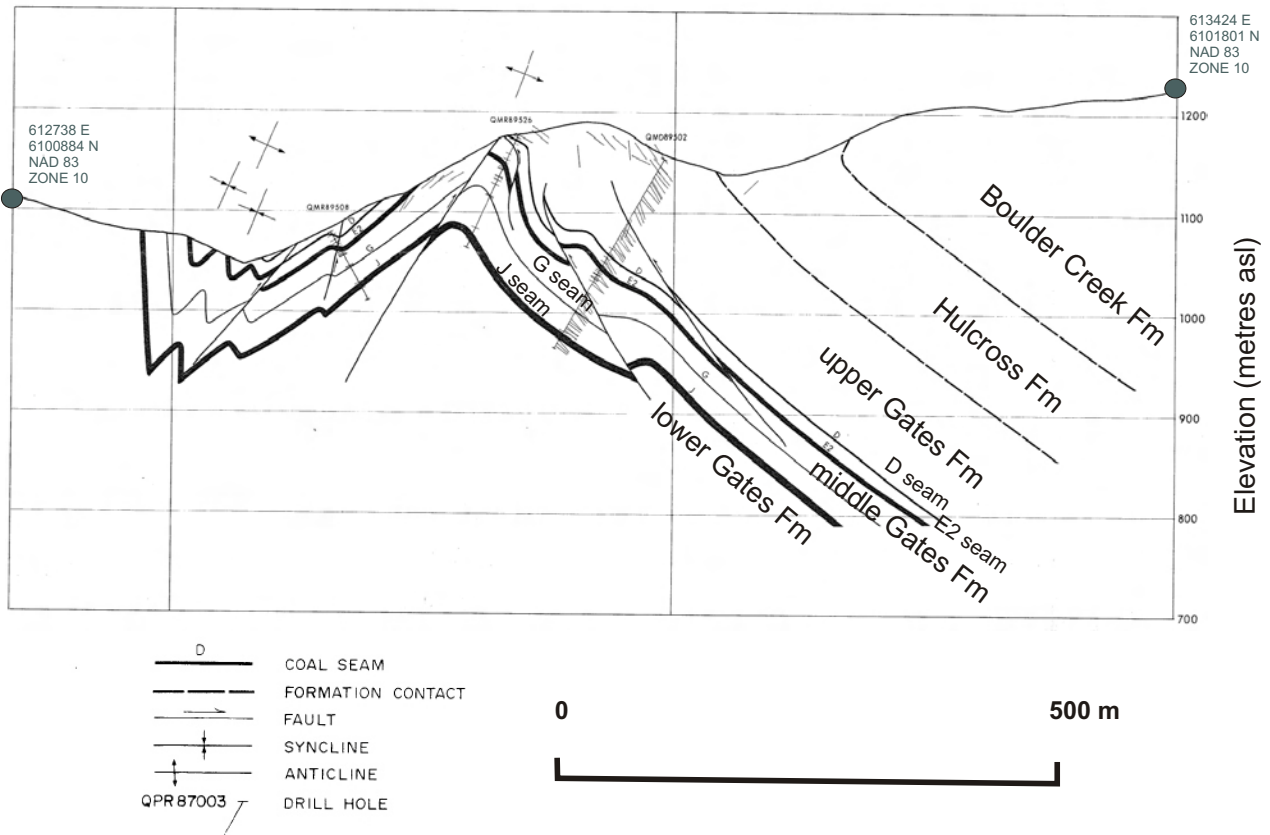


Figure 6. Drill section 38600 Mesa North Extension, northeastern BC.

North of Mesa pit, J seam splits into three plies (J1, 2, 3), the interseam interval thickens with indications of marine influence. In the Perry Creek pit area, the massive J conglomerate (Fahler D) overlies the northward thinning seam. In exposures along Perry Creek, the J seam is covered with a thin lag deposit of pebbles, followed by the massive marine sandstone of Fahler D.

The J seam thins westward with reduced thickness noted in Quintette's mined Wolverine (Frame) pit (average 3.5 m) and at the west end of Perry Creek pit. At the west margin of Mt. Spieker syncline (UTM Zone 10, 600909E, 6105026N, NAD 83), in exposures obscured by colluvium, the interval (approximately 3 m thick) is overlain by several metres of laminated papery shale.

The seam is present in the subsurface to the east and can be recognized in logs of wells (well authorization numbers 3403, 3319 and 15372, BC Oil and Gas Commission, 2006), as well as in deep drillhole Dupont Wolverine 79-2 (COALFILE 515).

The seam persists to the northwest. J seam may be correlated to the A, B seams at Bullmoose based on stratigraphic position relative to the Fahler D conglomerate above (Fig 3).

E AND D SEAM INTERVAL

The second major coal interval spans E and D seams at the Quintette pit and lies between Fahler C and the upper Gates Formation (Fig 3). It comprises numerous coal plies (E1 to E4, D3 and D4 at Quintette Mesa pit) separated by mudstone rich in plant impressions. The top of D seam shows marine influence in the Quintette pit area, documented in the coal petrography by Lamberson *et al.* (1991). The interval persists to the Perry Creek area and to the Mt. Spieker EB pit area, where a coal ply may be up to 4 m thick. At Bullmoose mine, a similar shale-rich interval with coal is present below the upper Gates Formation and includes D and E seams, using the local nomenclature. These

seams are 2 m or less thick and were mined selectively at Bullmoose (Drozd, 1985).

Areas of Exploration Interest, Middle Gates Formation

Gates Formation coal measures are preserved in folded strata lying between Quintette's Mesa pit and WCCC's Perry Creek developments (Fig 7). The folds are on strike with folds across the river in the Perry Creek area. It appears that folds on the north side plunge to the south, while folds on the south side plunge to the north, resulting in a canoe-shaped configuration of geological units. Folds are tighter on the south side of the river. The area was identified as a resource in the early 1970s but was not examined subsequently. Several traverses were run in this area. Although the basal J seam is close to river level at the limit of mining in the Mesa North pit, it is above the river in the anticlinal structure facing the Perry Creek anticline.

An area of possible exploration interest lies on the access road to the Perry Creek pit. The subvertical limbs of a tight anticline intersect the access road and Gates Formation coal is sporadically exposed in the areas of roadside culverts.

The E and D coal interval may be present in areas east and northeast of the Mt. Spieker mesa. It was intersected in drillhole MS39 (Fig 3) east of the Bullmoose fault and included a 4 m coal interval at 265 m depth. This is the only drillhole in the area and it was spudded in the Boulder Creek Formation. There is potential for this seam to underlie the area at much shallower depths. The Gates Formation comes to surface in an anticlinal arch northeast of the mesa toward Bullmoose Creek. The area is not covered by coal licenses.

GETHING FORMATION TRENDS AND AREAS OF INTEREST

Trends in the Gething Formation are compiled in Legun (1990) and Gibson (1992). Gething coals show strong thickness variations within the area, reaching 6 m on WCCC's Hermann Gething property, just south of the study area. Gething coals are usually slightly higher in rank (medium to low volatile) than the Gates coals immediately above them in the section. Gething coals display a more variable free swelling index (FSI) and are generally of lower metallurgical quality than the Gates coals, but they tend to wash cleaner than the Gates coal (Ryan, 1997).

Coals of the Chamberlain Member

TREND MINE AREA

Northern Energy and Mining Inc. (NEMI) is exploiting Chamberlain Member coals on their Trend property south of the study area. An aggregate thickness of up to 8.1 m is

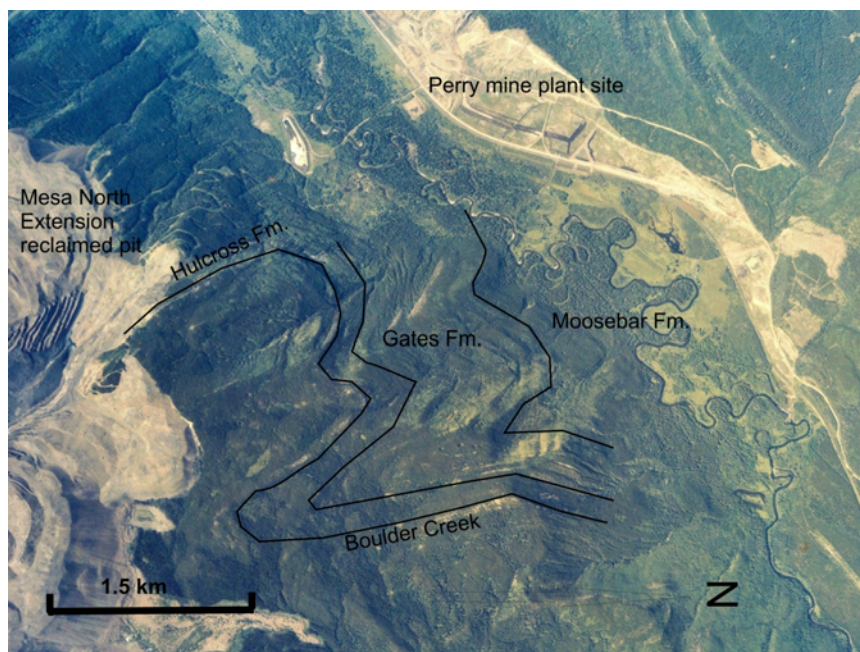


Figure 7. Fold structures between Quintette's reclaimed Mesa North pit and WCCC's Perry Creek pit, northeastern BC. North is to the right.

present in 3 to 4 closely spaced seams over a 15 m stratigraphic interval with a clean sandstone at the base and the Moosebar Formation shale above. These seams, where unoxidized, are mined as metallurgical coal and supply approximately 15% of the total tonnage of coal mined at the Trend mine, at a lower stripping ratio than for the Gates Formation seams (Norwest Corporation, 2005).

PERRY CREEK PIT AREA

A sloughed coal zone, extending for over 5 m of section, is exposed in a roadside bank (UTM Zone 10, 611063E, 6103077N, NAD 83). The zone is overlain by a rusty conglomerate and there are exposures of Moosebar Formation shale nearby. The coal seam is near the top of the Gething Formation, possibly correlating with the Skeeter and Chamberlain seams (also overlain by conglomerate) intersected in drillhole WDH1 approximately 1 km away (Fig 2). In that hole, the Skeeter seam is approximately 3 m in thickness and the Chamberlain seam is 2.6 m thick with a 1.4 m rock parting of mudstone and coaly shale. A correlation chart of the interval is available in COALFILE 606. The interval appears to thin northeast of WDH1 toward QWD 7115. Its development to the west could be tested by some trenching and drilling.

MESA AREA

Quintette drilled an upper coal zone within the Gething Formation at the edge of the Mesa North pit area. The company recognized three rather ashy coal seams with an average thickness of 2 m (COALFILE 842). These seams probably correspond to the Chamberlain Member.

Coals of the Gaylard Member

The middle coals in the area southwest of Perry Creek pit have been related to the Moosebar Formation contact via the deep drillhole QWD 7115 as well as QWD 7112 (see correlation chart in COALFILE 606). In ddh WDH1 (Fig 2), approximately 4.6 m of bright coal occur within an interval of 8.1 m. Diamond-drill hole QWD 7403 (Fig 2) has the thickest single seam at 2.4 m. The seams are approximately 135 m below the top of the Gething Formation and 45 m below the top of the Bullmoose Member (*i.e.*, below the marine tongue of the Gething Formation). These seams match seams GT1 and 2 at the Hermann Gething property (hole QHD 86010).

CONCLUSIONS AND FURTHER WORK

Ongoing compilation mapping at a 1:25 000 scale will help improve the understanding of the geological framework of this part of the northeastern coalbelt. Two major coal intervals in the Gates Formation are of wide extent in the Wolverine River area (J and E and D). Some secondary targets remain in the Gates Formation – an area of folded Gates Formation strata between the Perry Creek pit and Quintette's pits is a modest target for drilling. There is unknown potential for the E and D coal interval in the area east of the Mt. Spieker area and the Bullmoose thrust fault. Gates coal is present below the access road to Perry Creek pit, where the steep limb of a fold crosses the road.

The Gething Formation, an early exploration target for coal, merits a review on the ground. It is mined as supplementary metallurgical coal at the Trend mine south of the

study area. Coals of the Chamberlain Member and Gaylard Member middle coals are stratigraphic drill targets.

ACKNOWLEDGMENTS

Andrew Stephenson provided reliable assistance in the field, followed good safety procedures, and was quick in data input. Al Kangas of Quintette Coal Ltd. facilitated access to the Quintette pits and the old map files in the office. A tour of the Perry Creek pit by Gary Gould of Western Canada Coal Corporation and the Trend mine by Kevin Sharman of Northern Energy and Mining Inc. was helpful. Support by the BC Ministry of Energy, Mines and Petroleum Resources, manager Brian Grant and chief geologist Dave Lefebure is gratefully acknowledged.

REFERENCES

- BC Oil and Gas Commission (2006): Public internet site; *BC Ministry of Energy, Mines and Petroleum Resources*, URL <<http://www.ogc.gov.bc.ca>> [December 2006].
- Carmichael, S.M. (1983): Sedimentology of the Lower Cretaceous Gates and Moosebar formations, northeast coalfields, British Columbia; unpublished PhD thesis, *University of British Columbia*, 285 pages.
- Carmichael, S.M. (1988): Linear estuarine conglomerate bodies formed during a mid-Albian marine transgression; "upper Gates" Formation, Rocky Mountain foothills of northeastern British Columbia; in *Sequences, Stratigraphy, Sedimentology: Surface and Subsurface*, James, D.P. and Leckie, D.A., Editors, *Canadian Society of Petroleum Geologists*, Memoir 15, pages 49–62.
- COALFILE (2006): COALFILE BC Peace River NE BC coal assessment reports; *BC Ministry of Energy, Mines and Petroleum Resources*, URL <http://webmap.em.gov.bc.ca/mapplace/terrain/reports_pr.htm> [December 2006].
- Drozdz, R. (1985): The Bullmoose mine project; in *Coal in Canada, Canadian Institute of Mining and Metallurgy*, Special Volume 31, pages 263–268.
- Duff, P.McL.D. and Gilchrist, R.D. (1981): Correlation of Lower Cretaceous coal measures, Peace River coalfield, British Columbia; *BC Ministry of Energy, Mines and Petroleum Resources*, Paper 1981-3, 31 pages.
- Gibson, D.W. (1992): Stratigraphy, sedimentology, coal geology and depositional environments of the Lower Cretaceous Gething Formation, northeastern British Columbia and west-central Alberta; *Geological Survey of Canada, Bulletin* 431, 127 pages.
- Gilchrist, R.D. and Flynn, B.P. (1978): Coal resources, Peace River coalfield, northeastern British Columbia; *BC Ministry of Energy, Mines and Petroleum Resources*, Preliminary Map 33 (sheets 2,3).
- Hunter, D.J. and Cunningham, J.M. (1991): Burnt River mapping and compilation project; in *Geological Fieldwork 1990, BC Ministry of Energy, Mines and Petroleum Resources*, Paper 1991-1, pages 407–414.
- Kalkreuth, W. and Leckie, D.A. (1989): Sedimentological and petrographical characteristics of Cretaceous strandplain coals: a model for coal accumulation from the North American western interior seaway; in *Peat and Coal: Origin, Facies and Depositional Models*, Lyons, P.C. and Alpern, B., Editors, *International Journal of Coal Geology*, Volume 12, pages 381–424.
- Kilby, W. and Wrightson, C.B. (1987): Bedrock geology of the Bullmoose Creek area (93P/3); *BC Ministry of Energy, Mines and Petroleum Resources*, Open File 87-6.

- Lamberson, M.N., Bustin, R.M. and Kalkreuth, W. (1991): Lithotype (maceral) composition and variation as correlated with paleo-wetland environments, Gates Formation, north-eastern British Columbia, Canada; *International Journal of Coal Geology*, Volume 18, pages 87–124.
- Leckie, D.A. (1986): Rates, controls, and sand-body geometries of transgressive-regressive cycles: Cretaceous Moosevale and Gates formations, British Columbia; *American Association of Petroleum Geologists*, Bulletin, Volume 70, pages 516–535.
- Legun, A. (1990): Stratigraphic trends in the Gething Formation; *BC Ministry of Energy, Mines and Petroleum Resources*, Open File 1990-33.
- Legun, A.S. (2006): The Gates Formation in the Wolverine River area, northeastern British Columbia; in Geological Fieldwork 2005, *BC Ministry of Energy, Mines and Petroleum Resources*, Paper 2006-1 and *Geoscience BC*, Report 2006-1, pages 73–82.
- McLean, J.R. (1982): Lithostratigraphy of the Lower Cretaceous coal-bearing sequence, Foothills of Alberta; *Geological Survey of Canada*, Paper 80-29, 46 pages.
- MINFILE (2006): MINFILE BC mineral deposits database; *BC Ministry of Energy, Mines and Petroleum Resources*, URL <<http://www.em.gov.bc.ca/Mining/Geolsurv/Minfile/>> [December 2006].
- Norwest Corporation (2005): Technical report 05-2173 on the Trend Full mine feasibility; *Norwest Corporation*, URL <http://www.nemi-energy.com/i/pdf/TR_TFM_Feasibility.pdf> unpublished company report, 116 pages [December 2006].
- Ryan, B.D. (1997): Coal quality variations in the Gething Formation, northeast British Columbia (93 O, J, I); in Geological Fieldwork 1996, *BC Ministry of Energy, Mines and Petroleum Resources*, Paper 1997-1, pages 373–397.
- Western Canada Coal Corporation (2004): Environmental assessment supplementary information report for the Wolverine project, Volume 2; *BC Environmental Assessment Office*, URL <http://www.eao.gov.bc.ca/epic/output/html/deploy/epic_document_162_18907.html>, Additional Information Report - Figures, Part 1 [December 2006].

roadcuts for elements by aqua regia digestion – ICP-MS and INAA

- analysis of the –200 mesh (<0.070 mm) fraction of rock samples collected from outcrop for elements by aqua regia digestion – ICP-MS and INAA
- analysis of filtered (0.45 micron) acidified water samples for Al, B, Ag, As, Ba, Be, Ca, Cd, Ce, Co, Cr, Cs, Cu, Dy, Er, Eu, Fe, Ga, Gd, Ge, Hf, Ho, In, K, La, Li, Lu, Mg, Mn, Mo, Na, Nd, Ni, P, Pb, Pr, Rb, Re, S, Sb, Sc, Se, Si, Sm, Sn, Sr, Ta, Tb, Te, Ti, Tl, Tm, U, V, Y, W, Zn and Zr, by ICP-MS and for Ca, K and Na by inductively coupled plasma emission spectroscopy (ICP-ES). The water samples will be analyzed later for sulphate and fluoride
- collection of bulk drainage sediment samples for preparation of a heavy mineral concentrate. The heavy mineral concentrate will be used for mineralogical examination and for geochemical analysis

Water sample preservation was carried out in the field; sediment and rock samples were prepared in the BC Geological Survey Laboratory, Victoria. Pre-preparation (*i.e.*, in the field) and post-preparation duplicate samples and standard reference materials were included with samples sent for analysis to commercial laboratories. The drainage sediment, moss sediment, glacial sediment and soil and rock samples were analyzed by aqua regia digestion – ICP-MS at Acme Analytical Laboratories Ltd., Vancouver, and by INAA at Activation Laboratories, Ancaster, Ontario. Water samples were analyzed by the Environmental Geochemistry Laboratory, Geological Survey of Canada, Ottawa, Ontario.

Field and analytical duplicate samples and standard reference materials were analyzed with routine samples to generate the data for assessing accuracy and precision. The percent difference for analytical duplicates was less than 5% for most elements and below 10% for field replicates. Precision at the 95% confidence limit calculated from replicate analyses of a BCGS standard was less than $\pm 15\%$ for most elements. Larger variations between replicate samples and precision more than $\pm 15\%$ were measured for Au and Sb.

LILLOOET AREA

Description

Geochemical samples were collected in a 400 km² area west of Ward Creek and French Bar Creek. Topography of this area ranges from deep valleys occupied by creeks that flow through the rugged Camelsfoot Range into the Fraser River to a more subdued upland relief characteristic of the dissected Fraser Plateau. This plateau was formed by the erosion of flat-lying Miocene volcanic and associated sedimentary rocks (Holland, 1964). The Fraser River valley forms the eastern boundary of the area surveyed. Climate and vegetation of the area reflect a transitional environment from that of the Coast Ranges to the Fraser Plateau. Annual rainfall is less than 280 mm and temperatures range from -1°C in winter to above 40°C in summer. Vegetation in the Camelsfoot Range is mainly Interior Douglas fir, Montane spruce and Engelmann spruce. Much of the mature timber has been harvested and the remaining stands are heavily damaged by mountain pine beetle. Closer to the Fraser River and on the Fraser Plateau vegetation is typically

steppe or bunchgrass prairie with sagebrush and scattered Ponderosa pine or Douglas fir. Ward Creek and French Bar Creek flow east from the uplands into the Fraser River through deeply incised valleys. Commonly, there is a dense alder and willow growth in the valleys. Moore Lake, the source of Ward Creek, is supplied by water flowing through an aqueduct that crosses the watershed and intersects an upper reach of French Bar Creek 20 km to the west.

Alpine glaciers increased in size at higher elevations during the early stages of the Fraser Glaciation. Ice flowed northeast and southwest from a dispersal centre in the Camelsfoot Range forming glaciers that filled the major northeast and east-trending valleys (*e.g.*, French Bar Creek). Eventually the valley glaciers coalesced to block the Fraser River resulting in the formation of a large, proglacial lake. Sand and gravel deposits are common along the Fraser River and up to 300 m of lacustrine, glaciofluvial and fluvial sediment may have been deposited in the Fraser River valley during the Pleistocene. Debris flows, crossbedding and climbing ripples reflect the deposition of sediment into the river valley from braided streams, glacial lakes and alluvial fans. Huntley and Broster (1993) infer the presence of an ice divide separating north and south-flowing ice near Ward Creek and French Bar Creek from the orientation of cirques in the Camelsfoot Range. Broster and Huntley (1992) have identified massive matrix-supported, massive clast-supported and stratified diamict units in the area. Locally, surficial sediments range from a sandy till deposited on the uplands to talus and colluvium covering steeper hill slopes. Ice melt-out features and glaciofluvial deposits in the area include eskers and gravel terraces along valleys. An example of an esker in the French Bar Creek area is shown in Figure 2.

Rocks of the Lower Cretaceous Jackass Mountain Group, an Eocene volcanic assemblage and the Chilcotin Group outcrop in the surveyed area. The northwest-trending Slok Creek fault, a splay of the Fraser fault system, separates Eocene volcanic rocks in the northeast from the predominantly sedimentary Jackass Mountain Group in the southwest. Cathro *et al.* (1998) describe the Jackass Mountain Group as a southwest-dipping assemblage of volcanoclastic sedimentary rocks deposited during the Cretaceous as a submarine fan complex in the Tyaughton Ba-



Figure 2. Winding east-trending esker near French Bar Creek. The esker is approximately 2 km in length.

sin. South and west of Moore Lake, outcropping Jackass Mountain rocks range from massive sandstone to polymictic conglomerate (Hickson *et al.*, 1994). Eocene rocks are typically green to maroon andesite and dacite with minor banded rhyolite that most likely are representative of unit Evd mapped by Read (1988). The Eocene volcanic rocks in the area have been described in detail by Hickson *et al.* (1994). Chilcotin Group rocks are mainly vesicular and amygdaloidal basalt flows.

No precious or base-metal mineralization has been found in the surveyed area, but there are several Au-vein occurrences south of Moore Lake in the Watson Bar Au belt. These occurrences are spatially associated with a cluster of porphyry bodies that have intruded the Jackass Mountain Group. At the largest mineral occurrence, the Watson Bar deposit (MINFILE 092O 051), a shallow southwest-dipping thrust (Zone 5) contains an estimated 136 962 tonnes grading 14.33 g/t Au. Other styles of Au mineralization found in the Watson Bar Au belt are Fe carbonate silica alteration zones enriched in Au, As, Sb and Hg; quartz-sulphide veins related to quartz-feldspar porphyry sills, high-angle quartz-sulphide vein stockworks and conformable Au-rich zones in the sediments (Cathro *et al.*, 1998). Northwest of the Watson Bar deposit are several

smaller Au prospects such as the MAD (MINFILE 092O 092), Buster (MINFILE 092O 055), Astonisher (MINFILE 092O 054) and GB (MINFILE 092O 060). The GB, an epithermal low-sulphur Au-mineralized vein with elevated Hg, Sb, Pb and Zn, is close to the headwaters of Roderick Creek immediately south of the surveyed area. Between the Watson Bar deposit and the Fraser River is the Big Bar (MINFILE 092O 091) epithermal Au prospect. Quartz-carbonate veins in a Late Cretaceous andesite contain chalcopyrite, sphalerite and arsenopyrite with up to 2.17 ppm Au. Read (1988) mapped several perlite, volcanic glass and bentonite mineral occurrences in the surveyed area, such as the French Bar Creek (MINFILE 092O 106) and Moore Lake (MINFILE 092O 103).

Results

Results of the 1992 RGS, shown in Figure 3, reveal that sediment from French Bar Creek below the confluence with Boiler Creek has more than 95 ppb Au. The analysis of 100 samples collected at 50 sites in the same area during 2006 identifies several additional stream sediment, moss sediment and till multi-element anomalies. Site locations, sample types and the numbered anomalies with their multi-

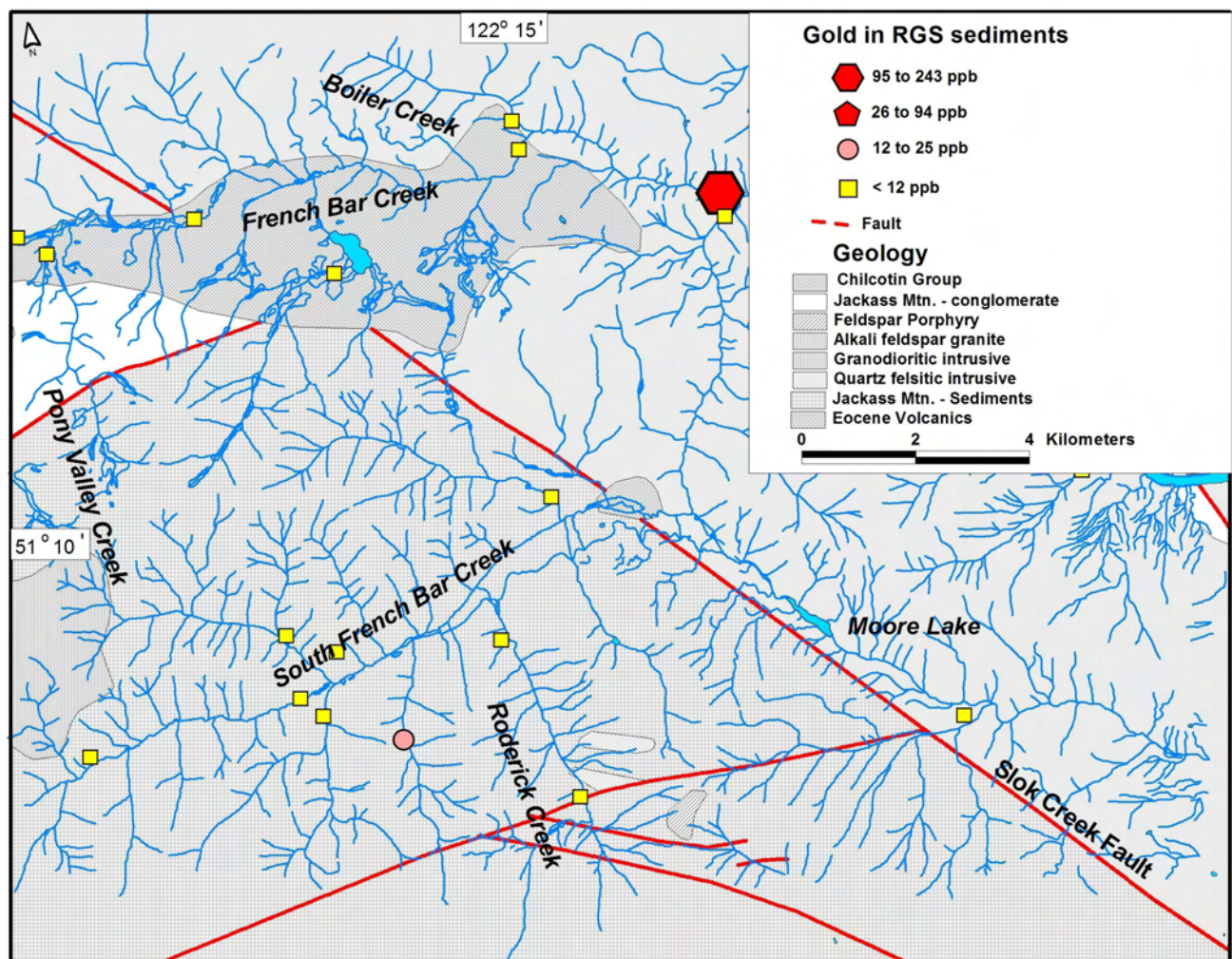


Figure 3. Distribution of regional geochemical survey (RGS) Au values in the French Bar Creek – Ward Creek survey area. Symbols represent intervals at the 90th, 95th and 98th percentiles from data previously published by Jackaman *et al.* (1992).

element signature are shown on Figure 4. Median, third quartile and maximum values for ore indicator and pathfinder elements representing each sample type and listed in Table 1. Third quartile values have been used as an anomaly threshold.

Anomaly 1 in moss sediment from a stream flowing into Pony Valley Creek, a tributary of French Bar Creek, has up to 10.4 ppb Au (by ICP-MS) with anomalous Zn, Ag and Se. This stream flows through a marshy area and the anomalous levels could reflect the effect of higher organic matter (17% LOI) in the sediment. However, there is a similar Au content (9.7 ppb) in sediment from Pony Valley Creek downstream from the confluence with the anomalous tributary. Colluvium overlying a steeply dipping fracture zone filled with Fe-carbonate and hematite in a conglomerate exposure on a road 500 m east of Pony Valley Creek has anomalous Zn, Cu, Fe, As, Sb, Hg and V.

Sediment from a tributary of Boiler Creek contains 420 ppb Au by aqua regia – ICP-MS, a value confirmed by an INAA analysis of 367 ppb (Anomaly 2). In addition to the anomalous Au value, only high Mn (>2800 ppm) was detected in the sample. Slightly alkaline (pH 7.8) streamwater contains elevated Al, Zn, Si and rare earth elements;

this signature could be explained by the weathering of clay minerals in rhyolite bedrock. A sample from Boiler Creek about 3 km to the west also has elevated levels of the rare earth elements La, Ce, Nd, Sm, Eu, Tb, Yb and Lu in the stream sediment and the water, although Au is not anomalous (Anomaly 3). The weathering of clay minerals may also be the reason for the elevated rare earth elements in the sediment.

Up to 85 ppm As with anomalous Mo, Mn, Hg and V and a trace (3.9 ppb) of Au were found in organic (*i.e.*, 70% LOI) sediment from a small creek flowing east through a swampy valley into the Fraser River (Anomaly 4). High organic matter content and observed colloidal iron-hydroxide precipitate in the sediment could partially explain the elevation of metal values caused by adsorption to the organic matter and iron hydroxide.

Moss sediment from south French Bar Creek has 110 ppb Au (INAA), but only anomalous Pb (6 ppm) in the corresponding steam sediment (Anomaly 5). Till from a road exposure on the south side of the valley near the stream site contains anomalous Cu and Ag levels. The most likely cause for the Au anomaly is the capture of Au grains by moss from the suspended sediment load, but the source of

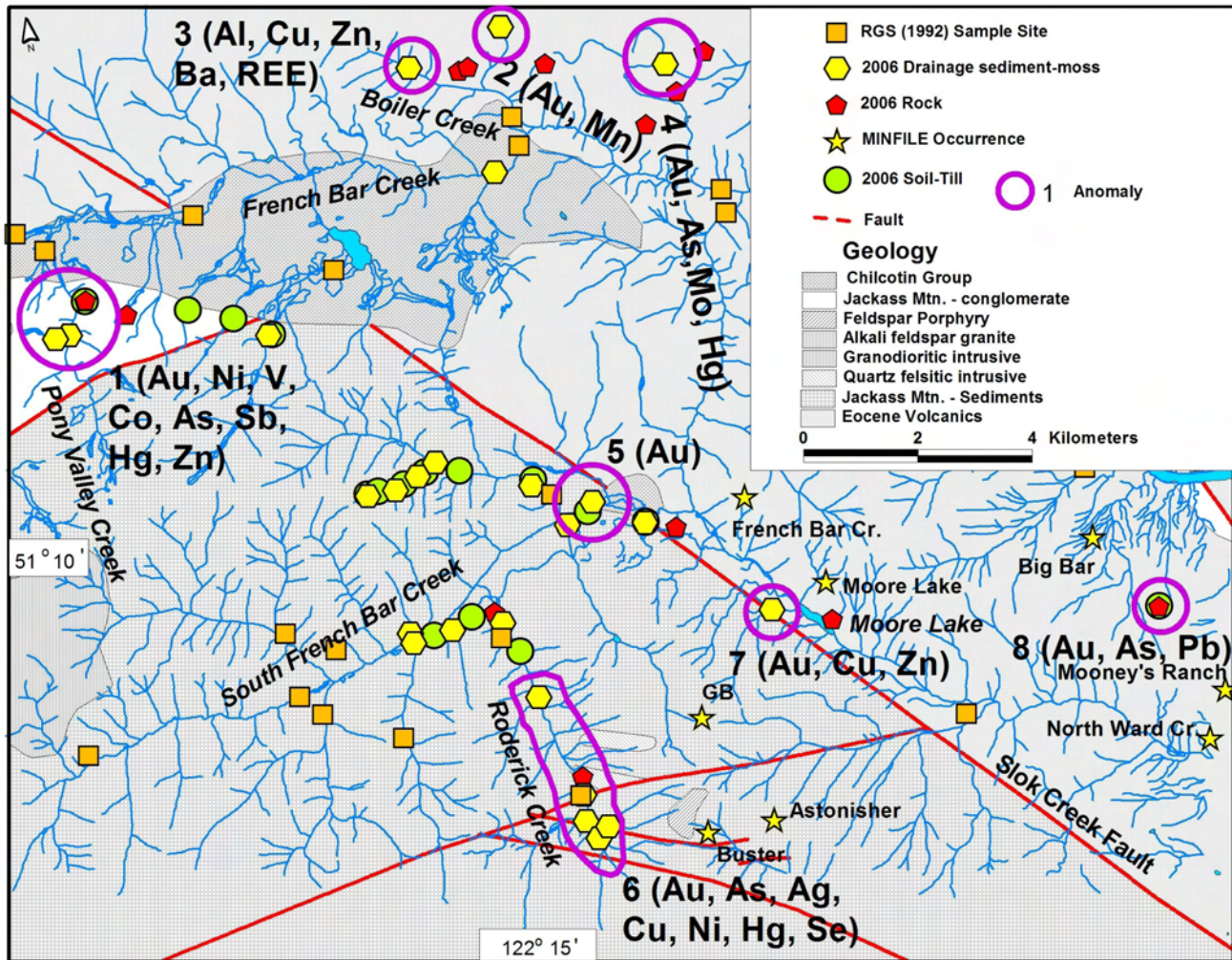


Figure 4. Location of samples in the French Bar Creek – Ward Creek survey area. Bedrock geology, mineral occurrences and major faults are shown on the map. Sample types are distinguished by symbols and numbered anomalies with their geochemical signature are described in the text. Geology is based on digital data published by Massey *et al.* (2006a).

the Au in the sediment cannot be determined precisely because of a large catchment basin upstream from the sample site.

Up to 220 ppb Au (ICP-MS) in moss sediment occurs along a 2 km reach of Roderick Creek (Anomaly 6). Anomalous Ag, Ni and As values occur with Au, but no other elements are above the threshold in stream sediment. A stream draining from the east into the upper basin of Roderick Creek has anomalous Ag, As, Ni, Hg, Se and Zn in sediment with 4.3 ppb As in streamwater, but no detectable Au. This creek meanders across an inclined, swampy valley floor that has been disturbed by logging and the high (*i.e.*, 27% LOI) sediment organic content could explain the elevated metals. However, the creek drains an area where there are several known epithermal Au-Ag-As-Sb-Hg mineral occurrences (*e.g.*, Buster) and this type of mineralization could be a likely source for the sediment-water multi-element anomaly.

Sediment from a stream draining a ridge underlain by the Jackass Mountain Group south of Moore Lake has an Au content of 101 ppb by INAA and 28.5 ppb by aqua regia – ICP-MS with anomalous Cu and Zn (Anomaly 7). This sample site is almost directly over the surface projection of the Slok Creek fault and Au mineralization associated with this structure or in Jackass Mountain Group rocks upstream could explain the elevated Au, Cu and Zn.

Colluvial till from an exposure on the West Pavilion Road roughly 4 km south of the Big Bar ferry contains 28 ppb Au by INAA and 26.5 ppb Au by aqua regia – ICP-MS with anomalous As and Pb values (Anomaly 8). No Au or other anomalous metal could be detected in a dark brown, clay-rich sedimentary or volcanoclastic rock outcropping beneath the colluvium. The source of this anomaly may be epithermal Au mineralization similar to that reported at the Big Bar occurrence (MINFILE 0920 091).

MCLEOD LAKE

Description

Geochemical samples were collected in an area around Great Beaver Lake in the western part of the McLeod Lake map sheet (NTS 093J/05, 06, 11, 12). A predominantly rolling to hilly land surface reflects the effects of extensive glaciation across the Fraser Basin, a physiographic subdivision of the Interior Plateau. The highest feature of the

TABLE 1. MEDIAN, THIRD QUARTILE AND MAXIMUM VALUES FOR ELEMENTS IN STREAM SEDIMENT (SED; 25 SAMPLES), MOSS SEDIMENT (MOSS; 10 SAMPLES) AND TILL (TILL; 17 SAMPLES); ABBREVIATIONS: ICP, AQUA REGIA – ICP-MS; INA, NEUTRON ACTIVATION; N.D., NOT DETERMINED.

Analytical parameter	Moss			Stream sediments			Till		
	Median	Third quartile	Maximum	Median	Third quartile	Maximum	Median	Third quartile	Maximum
Ag (ppb; ICP)	63	73.8	199	54	71	169	130	91	359
Al (%; ICP)	1.82	1.96	2.27	1.81	1.97	2.61	3.28	2.83	5.03
As (ppm; ICP)	6.0	9.4	45.1	6.0	8.2	72.8	15.75	7.50	93.2
As (ppm; INA)	9	13.75	57.3	9.3	11.5	85.4	21.28	10.75	111
Au (ppb; ICP)	1.2	2.9	220.0	0.7	1.2	420.4	4.03	1.90	26.6
Au (ppb; INA)	2	8.5	198	2	2	367	8.00	5.00	37
Ba (ppm; INA)	505	535	640	580	613	760	680	615	770
Bi (ppm; ICP)	0.07	0.08	0.09	0.06	0.07	0.12	0.12	0.11	0.2
Br (ppm; INA)	15	24.8	72.1	11.9	19.8	92.3	2.80	1.50	6
Ca (%; ICP)	1.11	1.22	1.82	1.16	1.61	6.23	1.42	0.97	11.42
Cd (ppm; ICP)	0.1	0.2	0.3	0.13	0.17	0.6	0.15	0.10	0.3
Co (ppm; ICP)	12.3	13.9	17.4	11.8	13.5	24.8	21.08	15.75	31.1
Co (ppm; INA)	16	17	19	15	16	25	21.50	17.00	28
Cr (ppm; ICP)	43.3	48.3	56.9	33.0	44.2	76	57.98	47.10	64.6
Cr (ppm; INA)	166	210	276	106	151	220	120	106	146
Cu (ppm; ICP)	24.3	29.2	53.3	21.86	25.38	59.41	56.45	50.12	124.37
Fe (%; INA)	4.03	4.40	4.69	3.84	4.02	5.34	5.00	4.77	9.47
Hg (ppb; ICP)	43	50	208	37	49	234	74.75	52.50	191
La (ppm; INA)	16.6	18.2	21.8	14.6	15.2	27.5	20.55	17.95	31.5
LOI (%)	12.35	19	33.8	14.1	23.2	71.8	n.d.	n.d.	n.d.
Mn (ppm; ICP)	569	626	3099	631	1401	4102	759.25	531.50	1301
Mo (ppm; ICP)	0.62	0.74	1.87	0.57	0.81	3.02	0.63	0.54	2.02
Ni (ppm; ICP)	33.9	37.6	46.5	31.7	36.3	65.6	48.03	45.80	57.9
P (%; ICP)	0.084	0.098	0.114	0.074	0.083	0.46	0.09	0.08	0.099
Pb (ppm; ICP)	5.74	5.88	7.62	5.02	5.97	8.84	7.70	6.72	13.15
Sb (ppm; INA)	1	1.6	3.1	0.8	1.2	3.4	1.93	1.25	5.1
Se (ppm; ICP)	1.0	1.425	2.8	0.9	1.3	3.5	0.20	0.10	0.5
V (ppm; ICP)	83	91	95	76	84	238	102.25	88.00	233
Zn (ppm; ICP)	63.3	65.8	81.5	60.0	66.5	87.3	69.73	64.90	136.4

Abbreviation: n.d., not determined

undulating landscape is Mount Prince southwest of Great Beaver Lake, which is drained by the Salmon River into the Fraser River. Smaller streams, while clearly marked on 1:20 000 scale maps, are commonly dry or have minimal water flow. Vegetation, dominated by White spruce, reflects a cold, dry climate and basic soils. Locally, there are stands of Black spruce and Lodgepole pine favouring better-drained, acid soils. Tamarack is common on organic soils in valleys formed by meltwater and Trembling aspen favours soils with a higher base saturation or where the area has been disturbed by logging (Dawson, 1989).

A till blanket deposited by an ice sheet advancing from the Coast Mountains onto the Interior Plateau during the later stages of the Fraser Glaciation (15 Ka) covers much of the area. Southwest to northeast ice advances deposited the till and formed surface features such as glacial grooves and numerous cigar and egg-shaped drumlins that are up to 30 m high (Clague *et al.*, 1987). A dark grey-brown, dense, calcareous till is the most common glacial deposit forming the drumlins. West and south of Great Beaver Lake there are extensive lacustrine varved clay, silt and sand deposited into a large glacial lake that extended into the Nechako Plateau. Locally, the lacustrine sediments are fluted and mounded by minor ice re-advances into drumlins. Glaciofluvial sand, silt, clay and gravel, locally up to 70 m thick, were deposited around Great Beaver Lake and along the Salmon River valley indicating a significant meltwater channel. Luvisolic soil has developed on well-drained glacial

cial sediments, whereas gleysolic and organic have formed in poorly drained areas (Dawson, 1989).

Struik (1989) mapped several distinct, fault-bounded assemblages within the McLeod Lake map sheet. Mainly Precambrian to early Paleozoic carbonate and clastic sedimentary rocks were deposited in the eastern half of the map sheet. The western half of the map sheet is composed of late Paleozoic to Triassic basalt, diorite, gabbro, limestone, greywacke and chert of the Slide Mountain, Cache Creek and Takla Groups. The Wolverine complex, which consists mainly of quartz-feldspathic paragneiss and granitic plutonic rocks with smaller postdeformational granite, tonalite, syenite and granodiorite intrusions, forms the another assemblage in the north-central part of the map sheet.

Pennsylvanian to Triassic Cache Creek rocks are predominantly massive blue-grey recrystallized limestone with minor bedded limestone, marble chert, argillite and greenstone. The Cache Creek Group is in fault contact with volcanic and sedimentary rocks of the Upper Triassic Takla Group. Locally, Cache Creek rocks have been subdivided into the Pope and Sowchea successions. Great Beaver Lake

is partly underlain by a northwest-trending belt of Takla Group mudstone, siltstone and fine sedimentary rocks in fault contact to the southwest with calalkaline volcanic flows, agglomerate and breccia. To the northwest, the Takla Group has been intruded by small granodiorite and ultramafic bodies and is partly covered by flat-lying vesicular, columnar-jointed olivine basalt flows of the Chilcotin Group. The basalt erupted from centres such as Teapot Mountain and Coffeepot Mountain to the east of the surveyed area.

Northwest, north and northeast-trending strike-slip and extensional faults cross the McLeod Lake map sheet and are believed to reflect two distinct plate-motion configurations between the North American and the Kula-Pacific plates. The Pinchi Fault crossing the southwest corner of the area is one example of a major northwest-trending structure that forms the Cache Creek – Takla contact.

Only two mineral occurrences, the Mount Prince Southeast (MINFILE 093J 010) and the Mount Prince Northwest (MINFILE 093J 011), have been reported in the area surveyed. The few known occurrences most likely re-

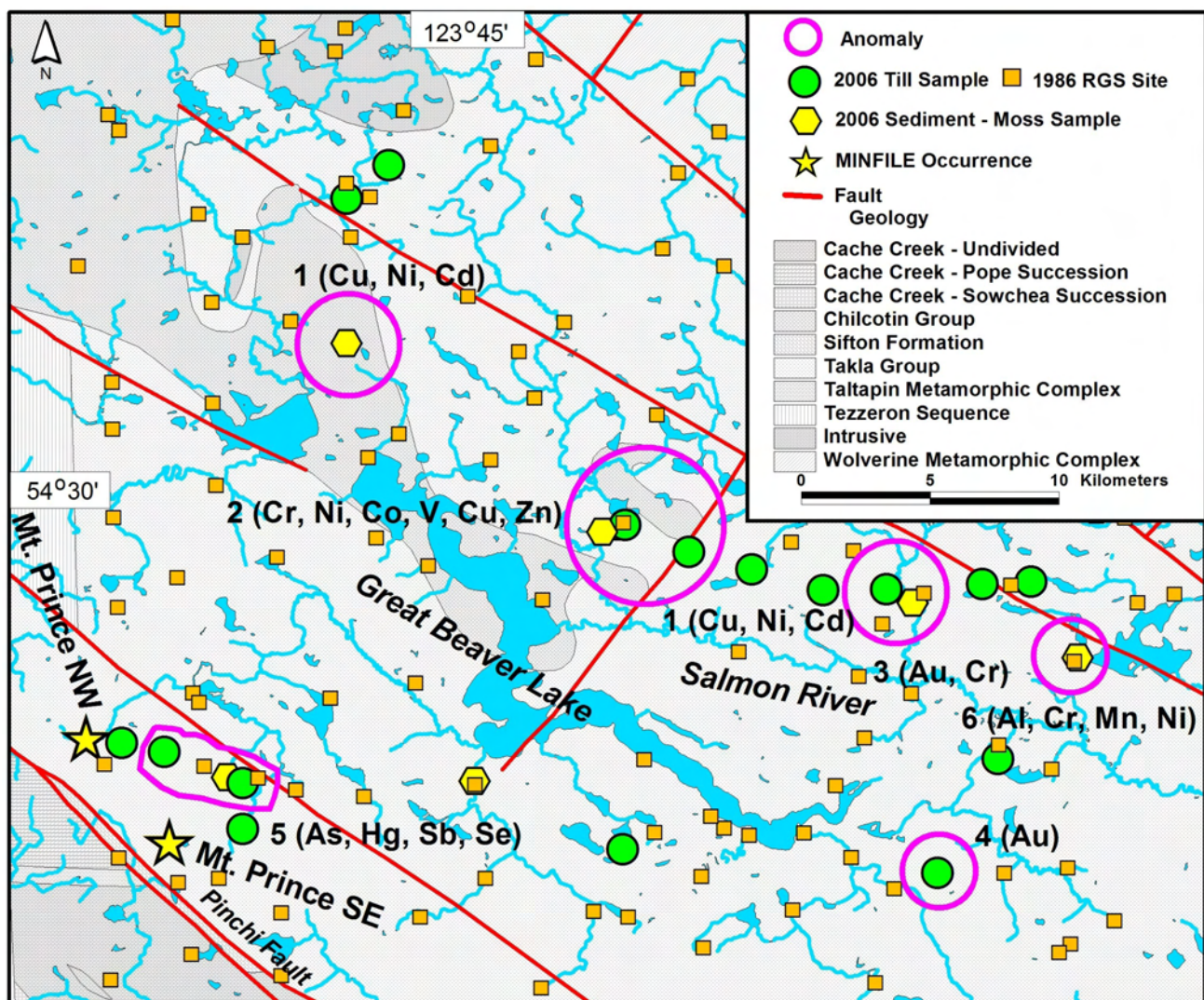


Figure 5. Location of samples in the McLeod Lake survey area. Bedrock geology, mineral occurrences and major faults are shown on the map. Sample types are distinguished by symbols and numbered anomalies with their geochemical signature are described in the text. Geology is based on digital data published by Massey *et al.* (2006b).

flect the problem of prospecting in an area covered by thick, almost continuous overburden. Mount Prince Southeast and Northwest are Hg prospects where minor cinnabar occurs in carbonatized, sheared Takla Group mafic volcanic rocks close to the Pinchi Fault. North of the area surveyed is the Windy (MINFILE 093J 024), described as an example of alkalic porphyry Cu-Au mineralization. This showing is underlain by poorly exposed Takla Group augite porphyry flows and minor tuffaceous rocks to the north and an extensively chloritized and sheared diorite intrusion to the south. Chalcopyrite with minor pyrite with up to 0.57 ppm Au and 1.25 ppm Pd occurs disseminated and in veinlets in the diorite.

Results

The location of stream sediment, moss sediment and till geochemical anomalies revealed by the analysis of 40 samples collected at 22 sites around Great Beaver Lake are shown on Figure 5. Median, third quartile (threshold) and maximum values for Au and selected elements in till and stream sediment are listed in Table 2. Till statistics were calculated from data for the 17 samples collected during the present survey, whereas the stream sediment statistics were calculated using the results of the reanalysis of regional survey samples previously reported by Lett and Bluemel (2006).

Anomaly 1 reflects increased Mo (2.06 ppm), Cu (61 ppm), Ni (117 ppm) and Cd (1.76 ppm) values in sediment from a small, dry creek northwest of Great Beaver Lake. The anomalous metals could reflect adsorption of metal to organic matter because the sediment from this creek has high organic matter content (*i.e.*, LOI = 30%). Faulkner (1987) commented on the frequency of highly organic RGS sediment samples in the McLeod Lake map sheet. Previously published regional geochemical survey data from the region northwest of Great Beaver Lake revealed high Cr and Ni values in stream sediment (BC Ministry of Energy, Mines and Petroleum Resources, 1986). Anomaly 2 outlines part of the same area where several samples of a dense, calcareous till from sites over an 8 km distance have anomalous Cr, Ni, V, Co, Cu and Zn. While Cu values in the till are less than 100 ppm, Cr and Ni exceed 200 ppm. Similar Cu and V levels (up to 700 ppm) have been reported by Lett and Jackaman (2000) in till down-ice from the Samatosum Cu-Pb-Zn-Au-Ag massive sulphide deposit where mafic rocks in the mineralized zone contain the Cr-rich mica, fuchsite. The source for the Cr-Ni-V-rich till cannot be confirmed, but the southwest to northeast ice flow suggested that the metal-rich till may have originated from the basin presently occupied by Great Beaver Lake. Moss sediment from a dry creek within 30 m of one anomalous till site also has elevated Cr and over 900 ppb Hg. The corresponding stream sediment also has anomalous Cr, but background Hg values and the high Hg concentration in the moss could reflect sample contamination.

Sediment from a creek draining into the Salmon River from a large catchment basin to the north had up to 289 ppb Au (INAA), 441 ppm Cr and 2213 ppm Mn (Anomaly 3). The presence of Au is confirmed by an 82.8 ppb value by aqua regia – ICP-MS in a split of the prepared sediment sample. A regional geochemical survey sample from the Salmon River about 4 km to the south of the anomalous site recorded 63 ppb Au in the sediment (Lett and Bluemel, 2006). The source of the anomalous Au cannot be determined for certain except that the higher Cr associated with

TABLE 2. MEDIAN, THIRD QUARTILE AND MAXIMUM VALUES FOR ELEMENTS IN STREAM SEDIMENT (1152 SAMPLES) AND TILL (17 SAMPLES). ABBREVIATIONS: ICP, AQUA REGIA – ICP-MS; INA, NEUTRON ACTIVATION; N.D., NOT DETERMINED.

Analytical parameter	Till			Stream sediments		
	Median	Third quartile	Maximum	Median	Third quartile	Maximum
Ag (ppb; ICP)	106	114	245	111	194	2571
Al (%; ICP)	1.67	1.86	2.06	1.15	1.50	4.23
As (ppm; ICP)	9.50	12	14.0	3.7	5.5	91.8
As (ppm; INA)	13.60	14.90	20.5	n.d.	n.d.	n.d.
Au (ppb; ICP)	2.10	3.70	121	1.1	1.7	147.5
Au (ppb; INA)	2	6	101	n.d.	n.d.	n.d.
Ba (ppm; INA)	1020	1100	1310	n.d.	n.d.	n.d.
Bi (ppm; ICP)	0.13	0.15	0.18	0.09	0.13	0.73
Br (ppm; INA)	0.5	0.5	1.3	n.d.	n.d.	n.d.
Ca (%; ICP)	2.23	2.78	3.54	0.57	0.83	6.8
Cd (ppm; ICP)	0.67	0.77	1.37	0.32	0.53	8.97
Co (ppm; ICP)	21.1	15.8	31.1	10.4	13.5	24.8
Co (ppm; INA)	19	23	28	n.d.	n.d.	n.d.
Cr (ppm; ICP)	83.80	101.80	131.9	37.1	55.6	175.3
Cr (ppm; INA)	190	211	256	n.d.	n.d.	n.d.
Cu; (ppm; ICP)	55.8	66.2	72.8	21.3	30.5	107.0
Fe (%; INA)	3.50	3.68	4.04	2.20	2.73	12.98
Hg (ppb; ICP)	136	195	229	92	151	4437
La (ppm; INA)	12.40	13.40	18.2	12.6	16.9	96.2
LOI (%)	n.d.	n.d.	n.d.	8.2	18.4	92.4
Mn (ppm; ICP)	770	871	1051	544	838	7832
Mo (ppm; ICP)	1.14	1.34	2.71	0.71	1.13	21.39
Ni (ppm; ICP)	122.4	160.1	210.8	31.0	47.0	293.4
P (%; ICP)	0.088	0.096	0.120	0.085	0.104	0.353
Pb (ppm; ICP)	8.08	9.06	16.9	6.44	9.02	32.8
Sb (ppm; INA)	0.61	0.72	1.65	0.28	0.40	4.35
Se (ppm; ICP)	0.3	0.3	0.5	0.4	0.8	19.6
V (ppm; ICP)	69	75	85	40	56	156
Zn (ppm; ICP)	91.30	114.90	191.5	66.6	87.6	922.8

Abbreviation: n.d., not determined

the Au may reflect stream sediment that has been largely derived from Cr-rich till.

Anomaly 4 is represented by an Au value of 1010 ppb (INAA) in a till sample from a site east of Great Beaver Lake. Analysis of a second split of the sample determined a value of 121 ppb Au by aqua regia and ICP-MS. No other elements are anomalous in the sample and a possible source for the Au is most likely concealed in bedrock to the southwest. East of Mount Prince, several till sites have samples containing anomalous Ba, As, Hg, Sb and Se. Anomaly 5, for example, has 229 ppb Hg and the most likely source for the metal is Hg mineralization along the Pinchi Fault similar to that reported at the Mount Prince occurrences.

Most of the water samples collected are weakly alkaline and have no detectable or very low metal contents. One water sample, however (Anomaly 6), has several ppb of Al, Mn, Co, Ni and Y. The stream flows through a swampy area and the elevated metals could be explained by natural complexes formed with dissolved organic matter. There are no anomalous metals in stream sediment at the site.

CONCLUSIONS

- Detailed geochemical surveys north of Lillooet and in the McLeod Lake map sheet have identified new Au and base-metal anomalies.
- In the French Bar Creek – Ward Creek area, a possible source for the high Au values with anomalous Hg and As in stream and moss sediment from

Roderick Creek is epithermal Au-Ag-As-Hg mineralization.

- There is no obvious source for high Au values in sediment from Boiler Creek draining Eocene volcanic rocks north of French Bar Creek. Elevated rare earth element and Al in water may be caused by the weathering of the Eocene volcanic rocks. Similarly, there is no known mineralization to explain Au and trace-element anomalies in the Pony Creek valley area. More detailed stream sediment sampling and prospecting should be carried out in both areas.
- While there is no clear source for the Au anomalies in stream sediment and till around Great Beaver Lake in the McLeod Lake map sheet, the high Cr, Ni and V in till indicates the presence of mafic and/or ultramafic rocks. Ice flow indicators suggest that these rocks are concealed beneath the lake or south of the lake.
- An absence of active first-order drainages in both areas limits more detailed follow-up stream sediment sampling. Moss sediment is often more effective than drainage sediment for detecting Au where there are streams. However, moss is not always present in low-relief areas and therefore cannot be used for routine geochemical sampling. Moss sampling is most effective in mountainous, high-rainfall areas where drainage samples are commonly depleted in fine-textured sediment. An abundance of lakes in the McLeod Lake map sheet suggests that a lake sediment survey would be a good follow-up strategy for the RGS stream-sediment anomalies.
- Basal till (*i.e.*, a first derivative of bedrock), is very effective for stream sediment anomaly follow-up. Well-developed basal or lodgment till in Great Beaver Lake area should be sampled as part of a regional till survey to identify the source of the Au and base-metal anomalies. Ideally, in combination with collecting basal till samples, the ice flow history of the area would have to be established by surficial mapping so that the transport direction of the till, and ultimately the trace-element chemistry, could be more accurately interpreted. A mineralogical examination of till heavy mineral concentrates in addition to geochemical analysis should be a routine component of a till survey.
- A sandy till in the French Bar Creek – Ward Creek area suggests a predominantly ice melt-out sediment derived from a relatively large source area. Till or soil geochemistry would be less effective for stream sediment anomaly follow-up because melt-out till, unlike basal till, is a less well-defined source of anomalous metal. However, systematic prospecting and colluvium sampling would be better follow-up techniques because of the greater bedrock exposure.
- Highly organic sediment and soil can lead to spuriously elevated trace element values (*e.g.*, Cu, Pb, Zn and Hg) in stream sediment and soil. Field recording of sample site characteristics and loss on ignition (LOI) analysis of samples are simple ways for interpreting spurious anomalies caused by the presence of organic matter.

ACKNOWLEDGMENTS

We would like to thank R. Durfeld for very generously allowing us to stay at his camp near Watson Bar Creek. B. Madu and M. Cathro kindly provided background information on the regional geology of the Lillooet area. G. Hall, Head of the Environmental Geochemistry Laboratory, Geological Survey of Canada, Ottawa, Ontario, very kindly analyzed the water samples.

REFERENCES

- BC Ministry of Energy, Mines and Petroleum Resources (1986): National Geochemical Reconnaissance 1:250 000 Map Series McLeod Lake (NTS 93J); *BC Ministry of Energy, Mines and Petroleum Resources*, RGS 15 and *Geological Survey of Canada*, Open File 1216, 106 pages.
- Broster, B.E. and Huntley, D.H. (1992): Quaternary stratigraphy in the east-central Taseko Lakes area, British Columbia, in *Current Research, Part A; Geological Survey of Canada*, Paper 1992-1A; pages 237–241.
- Cathro, M.S., Durfeld, R.M. and Ray, G.E. (1998): Epithermal mineralization on the Watson Bar property (92/01E), Clinton Mining Division, southern BC; in *Geological Fieldwork 1997, BC Ministry of Energy, Mines and Petroleum Resources*, Paper 1998-1, pages 21-1–21-13.
- Clague, J.J., Evans, S.G., Faulton, R.J., Ryder, J.M. and Stryd, A.H. (1987): Quaternary geology of the southwest Canadian Cordillera; *International Union of Quaternary Research (INQUA 87)*, Excursion Guide Book A-18, 67 pages.
- Dawson, A.B. (1989) Soils of the Prince George – McLeod Lake area; *BC Ministry of Environment*, Report 23, 219 pages.
- Faulkner, E.L. (1987): British Columbia Regional Geochemical Survey Release – An Assessment (93G, 93H and 93J); in *Geological Fieldwork 1986, BC Ministry of Energy, Mines and Petroleum Resources*, Paper 1987-1, pages 385–386.
- Hickson, C.J., Mahoney, J.B. and Read, P. (1994): Geology of Big Bar map area, British Columbia: facies distribution in the Jackass Mountain Group; in *Current Research, Paper 1994-A; Geological Survey of Canada*, pages 143–150.
- Holland, S.S. (1964): Landforms of British Columbia; *BC Ministry of Energy, Energy and Petroleum Resources*, Bulletin 48, 138 pages.
- Huntley, D.H. and Broster, B.E. (1993): Glacier flow patterns in the Cordilleran Ice Sheet during the Fraser Glaciation, Taseko Lakes map area, British Columbia; in *Current Research, Part A; Geological Survey of Canada*, Paper 1993-1A; pages 167–172.
- Jackaman, W. Matysek, P.F. and Cook, S.J. (1992): British Columbia Regional Geochemical Survey NTS 92O – Taseko Lakes, *BC Ministry of Energy, Mines and Petroleum Resources*, RGS 35, URL <<http://www.em.gov.bc.ca/Mining/Geolsurv/Geochinv/rgs/sheets/92O1.htm>> [November 2006]
- Massey, N.W.D., MacIntyre, D.G., Desjardins, P.J. and Cooney, R.T. (2005a): Digital Map of British Columbia: Tile NM 10 Southwest BC; *BC Ministry of Energy, Mines and Petroleum Resources*, Geofile 2005-03.
- Massey, N.W.D., MacIntyre, D.G., Desjardins, P.J. and Cooney, R.T. (2005b): Digital Map of British Columbia: Tile NN 10 Central BC; *BC Ministry of Energy, Mines and Petroleum Resources*, Geofile 2005-63.
- MINFILE (2006): MINFILE BC mineral deposit database; *BC Ministry of Energy, Mines and Petroleum Resources*, RGS 35, URL <<http://www.em.gov.bc.ca/Mining/Geolsurv/Minfile/>> [November 2006].

- Lett, R.E.W. (2006): Geochemical Surveys in the Lillooet Area (NTS areas 92J, 92I, 92O, 92P), Southwest British Columbia; in *Geological Fieldwork 2005, BC Ministry of Energy, Mines and Petroleum Resources*, Paper 2006-1, pages 63–71.
- Lett, R.E.W. and Bluemel, B. (2006): Reanalysis of regional geochemical survey stream sediment samples from the McLeod Lake area, NTS 93J; *BC Ministry of Energy, Mines and Petroleum Resources*, Geofile 2006-09, 13 pages.
- Lett, R.E.W. and Jackaman, W. (2000): Geochemical exploration models, south central British Columbia; *BC Ministry of Energy, Mines and Petroleum Resources*, Open File 2000-31, 33 pages.
- Read, P.B. (1988): Tertiary stratigraphy and industrial minerals Fraser River to Gang Ranch, southwestern British Columbia (92I/5, 92I/12, 92I/13, 92J/16, 92O/1, 92O/8, 92 P/4); *BC Ministry of Energy, Mines and Petroleum Resources*, Open File 1988-29, map and notes.
- Schroeter, T., Cathro, M., Grieve, D., Lane, R., Pardy, J. and Wojdak, P (2006): Exploration and mining in British Columbia; *BC Ministry of Energy, Mines and Petroleum Resources*, pages 61–62.
- Struik, L.C. (1989): Regional geology of the McLeod Lake map area, British Columbia; in *Current Research, Part E; Geological Survey of Canada*; Paper 89-1E, pages 109–114.

Orientation Geochemical Survey over the Jake Gold Prospect, Clearwater (NTS 092J/09), South-Central British Columbia

by R.E. Lett, T. Ferbey, M. Roberts¹ and B. Bluemel²

KEYWORDS: geochemistry, stream sediments, moss sediments, soil geochemistry, gold occurrence

INTRODUCTION

Mineral deposits in British Columbia usually have a complex surface geochemical expression reflecting bedrock geology, the style of mineralization, the type of surficial sediment and characteristics of the secondary environment such as drainage, topography and climate. Orientation surveys are therefore necessary to assess how these factors control element dispersion. Past case histories have shown localities where geochemical surveys may have been unable to detect mineralization because the influence of the near-surface environment on element migration was not fully appreciated. For example, at a mineral property on Vancouver Island, the high clay content of a consolidated till inhibited Cu and Zn dispersion in B-horizon soil from buried sulphide mineralization, giving rise to a sporadic pattern of B-horizon soil anomalies which were unrelated to the bedrock source. However, more coherent Cu and Zn B-horizon soil anomalies were formed over a more permeable till (Smee, 1987). An orientation geochemical survey was carried out by the authors in 2006 in an area west of Clearwater, BC, around the Jake prospect, to identify

- the main types of glacial sediment and their distribution,
- geochemical sample media most suitable for detecting mineralization, and
- the source of regional stream sediment – water geochemical anomalies.

Preliminary results of the orientation survey are reported in this paper.

SURVEY AREA

Topography and Surface Environment

The orientation survey was carried out within mineral claims covering an area of roughly 300 km² along the Mann Creek valley west of Clearwater, BC (Fig 1). Topography is



Figure 1. Location of the Jake prospect.

typical of the Shuswap Highland and is characterized by undulating, gently to moderately sloping uplands dissected by steep sided valleys and major rivers (Holland, 1964). Elevations range from about 360 m ASL along the floor of the Thompson River valley near Clearwater to over 2000 m on Grizzly Cub Mountain. Mann Creek, flowing south into the North Thompson River, drains the mineral claims. Upstream, the creek meanders across a broad, often marshy valley, but closer to the North Thompson River, the creek descends by several waterfalls where the channel has eroded flat-lying basalt that is partially infilling the valley. Lakes and small marshy depressions are relatively common through the area, including a small wetland just west of the Jake prospect.

Vegetation on better-drained soils is predominantly subalpine fir, Engelmann spruce, western hemlock and western red cedar, typical of the Interior Wet Belt Region (Gough, 1988). Willow and alder grow along valley floors and in wetlands. The area around the prospect has been logged and mountain pine beetle has damaged much of the timber being harvested.

Undisturbed soil formed on better-drained glacial deposits and colluvium is typically luvisolic with a developed, leached Ae horizon and a pH that is greater than 5.5. Depending on the parent material, soil texture ranges from sandy to gravelly loam. Organic soils (loss-on-ignition [LOI] >30%) and gleysolic soils have formed in poorly drained depressions, such as the marshy area just west of the Jake prospect. The marsh is typical of many small hillside wetlands where there is a thick understorey of cedar, alder and devils club.

¹Rimfire Minerals, Vancouver, BC

²University of Victoria, Victoria, BC

This publication is also available, free of charge, as colour digital files in Adobe Acrobat® PDF format from the BC Ministry of Energy, Mines and Petroleum Resources website at http://www.em.gov.bc.ca/Mining/GeolSurv/Publications/catalog/cat_fldwk.htm

Surficial Geology

Gough (1988) mapped surficial deposits along the Mann Creek valley, including the area around the Jake prospect, as predominantly till with lesser colluvium. A closer examination of surficial geology in the immediate vicinity of the prospect, during the present survey, revealed that colluvium (*i.e.*, sediment transported downslope by gravity) appears to be the dominant surficial sediment. Field observations confirm Gough's mapping that till (*i.e.*, sediment deposited by a glacier or debris-rich ice) also occurs in the immediate vicinity of the prospect. However, the sandy matrix and lack of fines (silt-clay), the high clast content and the abundance of large boulders (0.75 to >1 m) at the surface all suggest that this till is likely an ablation or melt-out deposit. This material was likely released from the melting of stagnant/dead ice, not by mechanisms active at the ice/substrate contact, such as lodgment processes, that produce material types such as basal till. Figure 2 shows a typical sandy diamicton at the Jake prospect, interpreted here as a colluvium.

Near the Jake prospect, weathered bedrock appears to be close to surface, sometimes within 1 m, and is directly overlain by colluvium. Given the irregular topography, relative changes in elevation and observed bedrock outcropping locally in the area, bedrock is likely within metres (approx. 1–10 m) of the surface beneath the hill where the showing is located and under the hill west of the swampy depression. Bedrock might be more deeply buried down-ice from the showing or in the lee of the high point of land where a greater thickness of till may have been deposited. Local ice-flow directions were not investigated during the present fieldwork, but Paulen *et al.* (2000) report that regional ice-flow was toward the south to southeast.

Basal till does occur in the region. One basal till sample, collected directly north of the Jake prospect near Clearwater Peak, has abundant volcanic rock clasts of the Fennell Formation. Other basal till samples were collected in the northwest part of the mineral property and, in contrast, have a higher content of granitic clasts.

Bedrock Geology and Mineralization

The geology of the area surrounding the Jake prospect has been mapped and described by Schiarizza *et al.* (2002a, b). Much of the mineral claim area, including the Jake prospect, is underlain by pillowed and massive basalt with lesser chert and gabbro representing the upper structural division of the Carboniferous to Permian Fennell Formation. To the east, a lower division of the Fennell Formation has a greater abundance of metasedimentary rocks in the volcanic sequence. Phyllite and slate, interbedded with quartzite and siltstone lamellae representing the Lemieux Creek succession of the Middle and Upper Triassic Nicola Group, outcrop west of the Fennell Formation. The Lemieux Creek fault forms a contact between the Fennell Formation to the east and the Lemieux Creek succession to the west. Further west, sedimentary units within the Lemieux Creek succession are separated from Nicola Group volcanic breccia, tuff, basalt, sandstone and conglomerate by the Taweel Lake fault. Partially infilling the Mann Creek valley and outcropping north of the Jake prospect are flat-lying Quaternary alkaline olivine basalt flows. North and east of Surprise Lake is Jurassic to Cretaceous granite and granodiorite forming part of the Raft batholith.

The Jake property consists of 21 000 ha of contiguous mineral claims, wholly owned by Rimfire Minerals Corporation, centred on the Jake prospect. Rimfire optioned the prospect from M. Kaufman, the prospector who made the original discovery in 2005. Kaufman was alerted to the showing by the gossanous nature of the soils and weathered bedrock exposed in a new forestry access road. In March of 2006, Rimfire excavated trenches centred on the discovery outcrop and oriented parallel to the established road on the basis of the existing exploration permit. The north-south oriented trench cut across multiple steeply dipping veins over a trench length of 75 m. Bedrock in the trench consists of chlorite-altered, pillowed basaltic flows and lapilli tuff and contains 1 to 3% disseminated pyrrhotite and pyrite. Veins have average widths of approximately 50 cm, but swell to widths of up to 100 cm. Individual veins are composed of quartz, pyrite, pyrrhotite, chalcopyrite and bismuthinite. Significant Au mineralization occurs in three separate clusters of quartz veins over a 36 m length of trench (approximately 20 m true thickness). As an example of mineralization, four composite samples across veining over a 4 m strike length returned an arithmetic average of 9.9 g/t Au over an average width of 0.8 m (Rimfire press release, 2006). Up to 10 ppm Au was detected in grab samples of the vein material collected as part of the orientation survey.

There is no record of regional scale exploration for discrete Au-quartz vein deposits in the Fennell Formation within the Jake property, although several Cu-Zn mineralized quartz vein occurrences have been noted on the property, *i.e.*, Mann Creek (MINFILE 092P 029) and CP (MINFILE 092P 116, 117, 118). The most similar style of Au mineralization to the Jake prospect in the region is the Windpass deposit east of the North Thompson River and approximately 24 km south of Clearwater. At Windpass, mineralization occurs within relatively shallowly dipping, north-striking Au-bearing quartz veins (typically about 40 cm wide) hosted by rocks of the Fennell Formation. Vein mineralization contains variable amounts of pyrite, chalcopyrite, bismuth sulphide, free Au, magnetite and Au tellurides. Mining between 1934 and 1939 extracted 93 425 t of rock yielding 1 071 684 g of Au, 53 469 g of Ag and 78 906 kg of Cu. The Windpass deposit is considered a proximal intrusion-related Au deposit associated with the Baldy batholith (Logan, 2001).



Figure 2. Sandy deposit exposed in a trench at the Jake prospect. The deposit is interpreted as colluvium.

The Cam-Gloria Au prospect, a pyrrhotite-pyrite quartz vein occurrence, is located 9 km from the southeast margin of the Baldy batholith (Cathro *et al.*, 2000). The vein has a Au-Bi-Cu-Pb-Mo-Te-W-As geochemical association resembling the Windpass deposit suggesting that the Baldy batholith could be a driver for mid-Cretaceous intrusion-related Au systems (Logan, 2002).

SAMPLE COLLECTION AND ANALYSIS

Overburden (till, colluvium and soil), stream sediment, moss and streamwater samples were collected during a visit to the Jake property in June 2006. Overburden samples were collected from vertical profiles along the south side of a trench crossing the main showing, from a wetland on the north side of the trench and from roadcuts north and northwest of the showing. Stream sediment, moss sediment and streamwater samples were taken from drainages within the property (Fig 3). Bulk stream sediment for heavy mineral concentration was taken from several of the streams. Water sample preservation was carried out in the field; sediment and rock samples were prepared in the BC Geological Survey Laboratory, Victoria, BC. Water samples were analyzed for elements by the Geological Survey of Canada Methods Development Laboratory, Ottawa, Ontario. Pre-preparation (*i.e.*, field) and post-preparation duplicate samples and standard reference materials were included with the samples sent for analysis to commercial laboratories. The -230 (<0.063 mm) fraction of overburden samples was analyzed at ASL Chemex for Au by lead collection fire assay – ICP-ES (inductively coupled plasma emission spectroscopy) and for trace elements by aqua regia digestion – ICP-MS (inductively coupled plasma mass spectrometry). The -80 (<0.177 mm) fraction of stream sediment and moss sediment samples was analyzed for Au and trace metals by the same methods as overburden samples. There is less than 10% difference between pathfinder element (*e.g.*, Cu, As and Bi) analyses of duplicate field and duplicate analytical samples. Gold, arsenic, bismuth and silver analyses of a standard reference material differ by less than 25% of the recommended value for the standard.

RESULTS

Stream Sediment, Moss Sediment and Water Geochemistry

Most Au and pathfinder element (*e.g.*, As, Sb, Hg, Cu, Pb and Zn) values in moss and sediment samples collected as part of the present orientation survey are below thresholds calculated at the 95 percentile from regional stream sediment data for NTS 092P map sheet RGS (Matysek *et al.*, 1992). Values at the 95 percentile are commonly used to define anomaly thresholds for larger datasets, whereas quartiles are more realistic for small sample groups. The third quartile value thresholds (Table 1) calculated from the moss and stream sediment data generated from the present geochemical sampling reveal several subtle multi-element anomalies. Most elements (*e.g.*, Au, Ag, As, Bi, Cd, Cu, Pb, V, and Zn) are higher in moss sediment compared to stream sediment. This enhancement could reflect discrete silicate, oxide or sulphide grains rather than the adsorption of metals to clay-sized minerals and/or secondary oxides. Heavier grains would be captured preferentially from the suspended load in a stream by moss, thereby depleting the sediment in

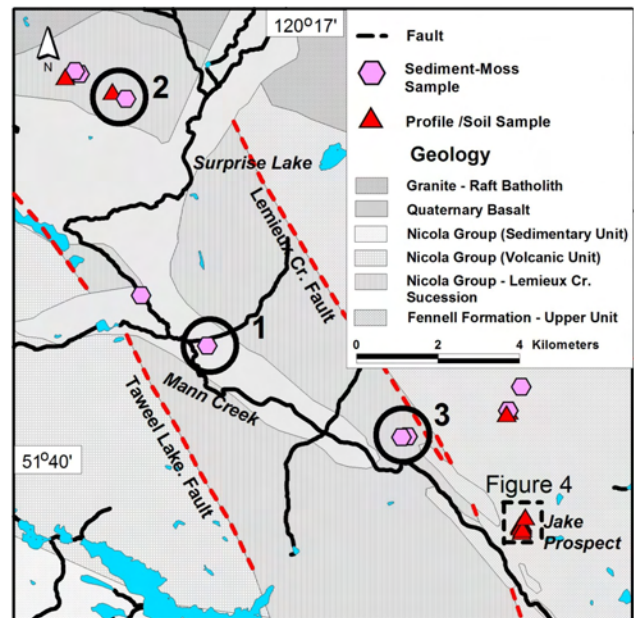


Figure 3. Regional geology, prospect location and geochemical sample locations. Bedrock geology has been summarized from the digital map published by Massey *et al.* (2005).

smaller, heavier grains. This might explain the presence of a moss sediment Au anomaly and the absence of Au in drainage sediment at the same site. While moss sediment clearly increases Au anomaly contrast, the routine use of this media for geochemical surveys is limited by the absence of moss in some streams. Previous drainage surveys on Vancouver Island and in the Adams Lake area have demonstrated the advantages of moss sediment geochemistry for Au (Matysek and Day, 1988; Lett *et al.*, 2000).

Element anomalies are identified by number on Figure 3. The highest Au value (762 ppb) detected is in moss sediment from a stream draining the area south of Surprise Lake (Anomaly 1). No other anomalous elements occur in either the moss or stream sediment at this site and no visible Au grains were identified in a heavy mineral concentrate prepared from a bulk sediment sample. Other sites with lower Au in drainage sediment and moss sediment have elevated levels of associated pathfinder elements. For example, a stream draining the area underlain by the Raft batholith in the northwest part of the mineral claims has anomalous Au (24 ppb), As, Sb, Bi, Cd, Se, V and Zn in moss with a similar multi-element signature in sediment (Anomaly 2). The streamwater has elevated Cu (3.9 ppb) and Rb. Till exposed in a roadcut near the stream has elevated Bi, Be, Rb, Sr and U, suggesting that the source of the anomalous metal in till and sediment is the granite. Closer to the Jake prospect, a creek draining from the north has detectable, but background Au in sediment and moss with anomalous As, Cd, Cu, Ni, Sb, Se, Tl and Zn (Anomaly 3). There is no obvious source for the anomaly, but the multi-element association could reflect vein-type mineralization in the drainage basin.

Till, Colluvium and Soil Samples

Median value thresholds have been used to identify Au and pathfinder elements in till, colluvium and soil. Median

TABLE 1. MEDIAN, 3RD QUARTILE (QUART) AND MAXIMUM (MAX) VALUES FOR ELEMENTS DETERMINED BY AQUA REGIA DIGESTION – ICP-MS AND AU BY LEAD COLLECTION FIRE ASSAY – ICP-MS IN STREAM SEDIMENT (10 SAMPLES) AND MOSS SEDIMENT (8 SAMPLES). ABBREVIATION: SED, STREAM SEDIMENT.

Element	Sediments			Moss		
	Median	Quartile	Maximum	Median	Quartile	Maximum
Au (ppb)	9	11	22	13	20	762
Ag (ppb)	20	25	33	31	36	49
Al (%)	1.54	1.72	1.99	1.65	1.83	1.92
As (ppm)	6.20	6.90	11.40	7.05	9.35	16.20
Ba (ppm)	100.00	110.00	140.00	75.00	102.50	150.00
Be (ppm)	0.56	0.61	0.84	0.53	0.68	0.94
Bi (ppm)	0.13	0.37	0.50	0.16	0.25	0.58
Ca (%)	0.53	0.68	0.75	0.80	0.90	1.40
Cd (ppm)	0.46	0.56	2.88	0.61	0.95	4.90
Ce (ppm)	31.50	42.70	58.20	26.90	42.18	52.50
Co (ppm)	8.00	12.20	21.30	10.70	13.73	15.30
Cr (ppm)	27.00	31.00	51.00	26.00	30.00	42.00
Cs (ppm)	2.06	2.53	3.06	2.01	2.74	3.21
Cu (ppm)	22.5	35.6	39.6	30.1	49.1	65.3
Fe (%)	1.78	2.25	2.88	2.06	2.41	2.71
Ga (ppm)	3.51	4.53	5.15	3.56	4.24	5.10
Hg (ppb)	50	70	90	90	10	130
K (%)	0.05	0.14	0.16	0.09	0.11	0.21
La (ppm)	18.60	28.90	39.10	17.75	27.75	44.30
Li (ppm)	10.40	17.00	18.80	10.15	14.88	18.70
Mg (%)	0.38	0.42	1.00	0.41	0.51	0.79
Mn (ppm)	543	613	1320	741	866	968
Mo (ppm)	2.33	2.92	6.37	0.96	2.08	6.94
Nb (ppm)	2.04	2.32	2.46	1.64	2.60	2.85
Ni (ppm)	18.20	22.80	39.40	17.90	30.35	36.60
P (ppm)	720	780	1290	1020	1070	1140
Pb (ppm)	6.40	8.00	10.20	6.55	8.35	11.40
Rb (ppm)	5.90	19.70	26.00	7.30	11.93	30.80
S (%)	0.04	0.06	0.07	0.10	0.12	0.13
Sb (ppm)	0.26	0.31	1.01	0.35	0.49	1.32
Sc (ppm)	2.90	3.30	4.70	2.85	3.18	3.90
Se (ppm)	1.10	1.30	3.10	1.60	3.08	5.70
Sr (ppm)	25.20	29.00	49.30	33.25	50.93	57.20
Te (ppm)	0.02	0.02	0.03	0.02	0.02	0.04
Th (ppm)	3.60	4.60	7.40	1.85	2.83	6.50
Ti (%)	0.08	0.10	0.17	0.08	0.08	0.17
Tl (ppm)	0.13	0.20	0.30	0.14	0.28	0.46
U (ppm)	1.98	3.16	6.63	2.48	3.26	5.53
V (ppm)	49.00	59.00	74.00	44.50	57.50	77.00
W (ppm)	0.97	1.80	5.83	0.20	1.35	3.52
Y (ppm)	9.50	12.30	15.25	13.15	16.76	21.30
Zn (ppm)	49.00	58.00	146.00	53.00	70.50	140.00

values are those reported by Paulen *et al.* (2000) from data for a regional till geochemical survey in the Chu Chua – Clearwater area. The survey covered a region immediately south of the Jake prospect. Thresholds are 36 ppb Au; 28 ppm As; 1 ppm Bi; 111 ppm Cu; 30 ppb Hg; 1.2 ppm Sb; 1.2 ppm Se; 0.2 ppm Tl; and 89 ppm V. Till samples taken at sites remote from the Jake prospect are shown on Figure 3. Two of the samples have detectable background levels of Au and in the northwest part of the mineral property the till has elevated Bi, Be, Rb, Sr and U.

Locations of vertical sediment profiles east and west of the Jake prospect are shown on Figure 4. Element variations down the vertical profiles reveal that high Au (10 ppm), As (36 ppm), Ag (2.5 ppm), Bi (823 ppm) and Cu (2250 ppm) in quartz vein material are reflected in anomalous metal values in colluvium immediately above the bedrock surface. Increased Se, Tl and V accompany the high metal values, but there are no anomalous elements in the overlying B-horizon soil. Only V is elevated in the deeper sediments from Profile 2, located 20 m to the south of Profile 1, but there are anomalous Au, As, Bi and V in deeper

sediments from Profile 4, located 50 m south of Profile 1. The only anomaly present in bedrock and deeper colluvium from Profile 3, located 100 m south of Profile 1, is V and there are no anomalous elements in the overlying B-horizon soil. At Profile 5, located 200 m north of Profile 1, a lower, clay-rich, more dense diamicton (possibly basal till) has anomalous Au, As, Cu and V. Again, these higher values are not reflected in the overlying more sandy sediment or the B-horizon soil. The Au-As-Cu-V association in the lower sediments could reflect another more remote, mineralized source to the north, since Profile 5 may be up-ice relative to Au-Bi-Cu-Ag-As mineralization at the Jake prospect. The absence of Bi, but anomalous V, in the till from Profile 5 could reflect a mineralized source that is different from the Jake prospect.

The spatial variation of elements in soil and glacial sediment over mineralized bedrock at the Jake prospect is summarized in Figure 5 by a series of block prisms. Anomalous element associations down each profile distinguish between Au, As, Bi and V in profiles south of the prospect, compared to Au, As, V to the north. All of the profiles show that anomalous element concentrations are confined to the sediment immediately above the bedrock and that they decrease sharply within more shallow soils.

Wetland Samples

Only the surface, fibrous layer on the wetland just west of the Jake Showing has been sampled and only Se is anomalous in the material. The presence of anomalous Se can be explained by the higher S content of the organic matter. No elements appear to have accumulated in the organic sediment.

CONCLUSIONS

- Much of the Mann Creek valley, including the area of the Jake prospect, is covered by sandy glacial

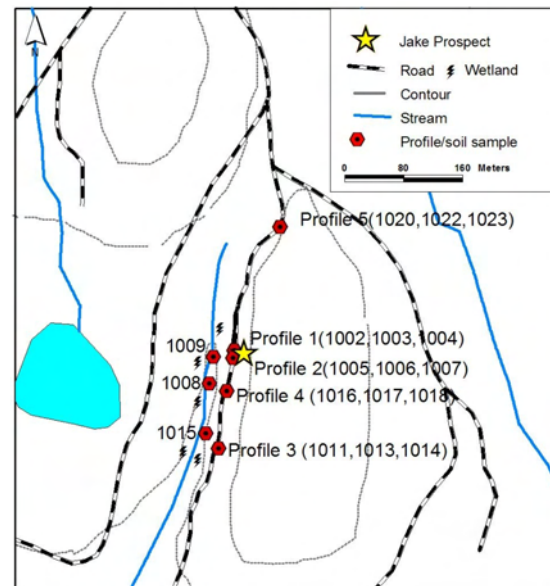


Figure 4. Vertical sediment profile locations around the Jake prospect.

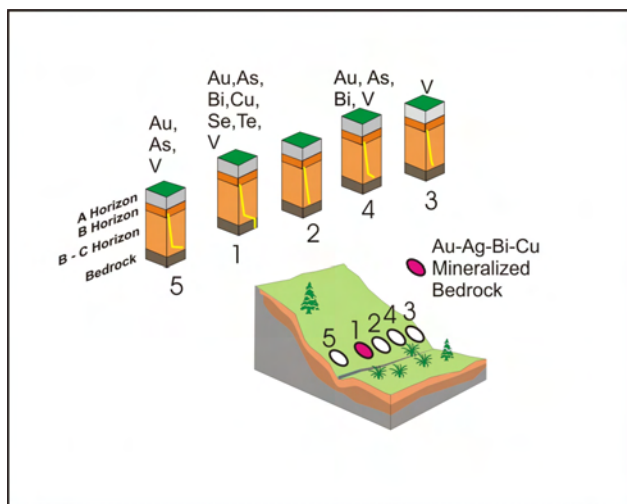


Figure 5. Model showing variation of metals in soil profiles around the Jake prospect.

sediment interpreted as colluvium with perhaps a minor component of melt-out till. Basal till appears to be a common glacial deposit at higher elevations and more stable, less steep slopes in the valley. Element variations in vertical sediment profiles over Au-Bi-Ag-Cu mineralization demonstrate that only samples collected close to bedrock would identify the presence of mineralization. Since basal till (typically a first derivative of bedrock) is the target sediment type for a till geochemical survey, the colluvium and soil (and possibly melt-out till) occurring at the Jake prospect would not be effective media for geochemical surveys. However, basal till surveys could be conducted at a more regional scale. Ideally, in combination with collecting basal till samples, the ice-flow history of the area would have to be investigated so that the transport direction of basal till, and ultimately trace element determinations, could be more accurately interpreted.

- Moss sediment is generally more effective for detecting Au, especially in steeper, high-energy streams where the amount of fine-textured bottom sediment is small. However, the significance of high Au in moss sediment combined with the absence of other typical Au pathfinder elements (e.g., As) in both moss sediment and steam sediment should be treated with caution. One creek northwest of the Jake prospect containing anomalous Au, Ag, As, Sb, Bi, Cd, Se, V and Zn in moss and stream sediment with higher metal in nearby till could indicate vein-type Au mineralization in the granite of the Raft batholith.

ACKNOWLEDGMENTS

The authors very much appreciate the assistance and support from Rimfire Minerals during fieldwork on the Jake prospect and with the subsequent sample analysis. Paul Schiarizza very kindly provided advice on geology of the area around the Jake prospect and identified clast types in the till samples. Gwendy Hall, head of the Environmental Geochemistry Laboratory, Geological Survey of Canada, Ottawa, is sincerely thanked for analyzing the water samples.

REFERENCES

- Cathro, M.S. and Lefebure, D.V. (2000): Several new plutonic related gold, bismuth and tungsten occurrences in southern British Columbia; in *Geological Fieldwork 2001, BC Ministry of Energy, Mines and Petroleum Resources*, Paper 1999-1, pages 207–224.
- Gough, N.A. (1988): Soils of the Bonaparte River–Canim Lake map area (92P East Half); *BC Ministry of Environment and Parks*, BC Soil Survey Report 24, 229 pages.
- Holland, S.S. (1964): Landforms of British Columbia; *BC Ministry of Energy, Mines and Petroleum Resources*, Bulletin 48, 138 pages.
- Lett, R.E.W., Jackaman, W. and Englund, L. (2000): Stream sediment exploration for pluton related quartz-vein gold deposits in southern British Columbia; *BC Ministry of Energy, Mines and Petroleum Resources*, Open File 2000-23, 34 pages.
- Logan, J.M. (2002): Intrusion-related gold mineral occurrences of the Bayonne magmatic belt; in *Geological Fieldwork 2001, BC Ministry of Energy, Mines and Petroleum Resources*, Paper 2002-1, pages 237–246.
- Logan, J.M. (2001): Prospective areas for intrusion-related gold-quartz veins in southern BC; in *Geological Fieldwork 2000, BC Ministry of Energy, Mines and Petroleum Resources*, Paper 2001-1, pages 231–252.
- Massey, N.W.D., MacIntyre, D.G., Desjardins, P.J. and Cooney, R.T. (2005): Digital map of British Columbia: tile NM 10 southwest BC; *BC Ministry of Energy, Mines and Petroleum Resources*, Geofile 2005-03.
- Matysek, P.F. and Day, S.J. (1988): Geochemical orientation surveys: northern Vancouver Island, fieldwork and preliminary results; in *Geological Fieldwork 1987, BC Ministry of Energy, Mines and Petroleum Resources*, Paper 1988-1, pages 493–502.
- Matysek, P.F., Jackaman, W. and Cook, S.J. (1992): British Columbia Regional Geochemical Survey–Bonaparte Lake (NTS 92P); *BC Ministry of Energy, Mines and Petroleum Resources*, RGS 36.
- MINFILE (2005): MINFILE BC mineral deposit database; *BC Ministry of Energy, Mines and Petroleum Resources*, RGS 35, URL <<http://www.em.gov.bc.ca/Mining/Geosurv/Minfile/>> [November 2006]
- Paulen, R.C., Bobrowsky, P.T., Lett, R.E., Jackaman, W., Bichler, A.J. and Wingerter, C. (2000): Till geochemistry of the Chu Chua – Clearwater area, BC (parts of NTS 92P/8 and 92P/9); *BC Ministry of Energy, Mines and Petroleum Resources*, Open File 2000-17, 233 pages.
- Rimfire (2006): Jake Trenching Exposes Gold Mineralization; Further Exploration Planned; Rimfire Minerals press release, May 24, 2006.
- Schiarizza, P., Heffernan, S. and Zuber, J. (2002a): Geology of the Slide Mountain Terranes, west of Clearwater, south-central British Columbia (92P/9,10,15,16); in *Geological Fieldwork 2001, BC Ministry of Energy, Mines and Petroleum Resources*, Paper 2002-1, pages 83–108.
- Schiarizza, P., Heffernan, S., Israel, S. and Zuber, J. (2002b): Geology of the Clearwater – Bowers Lake area; *BC Ministry of Energy, Mines and Petroleum Resources*, Open File 2002-15.
- Smee, B.W. (1987): Soil sampling strategies in an area with alpine glaciation, British Columbia, Canada; in *Practical Problems in Exploration Geochemistry*, Levinson, A.A., Bradshaw, P.M.D. and Thomson, I. Editors, *Applied Publishing Limited*, pages 78–82.

U-Pb Ages of Intrusive Rocks and $^{40}\text{Ar}/^{39}\text{Ar}$ Plateau Ages of Copper-Gold-Silver Mineralization Associated with Alkaline Intrusive Centres at Mount Polley and the Iron Mask Batholith, Southern and Central British Columbia

by J.M. Logan, M.G. Mihalynuk, T. Ullrich¹ and R.M. Friedman¹

KEYWORDS: U-Pb zircon isotopic age, $^{40}\text{Ar}/^{39}\text{Ar}$ plateau cooling age, alkaline, porphyry copper-gold, mineralization, Afton, Ajax, Mount Polley, Northeast zone, hydrothermal breccia

INTRODUCTION

Porphyry deposits in British Columbia have produced more than \$27 billion worth of copper and gold. They formed during two distinct periods in the development of the Cordillera: the first in the Late Triassic to Early Jurassic and the second in the Cretaceous to Eocene. Most porphyry production has come from the southern part of Quesnel Terrane, where two cycles of calcalkaline through alkaline magmatism are recognized in the Late Triassic and Early Jurassic. The reason for the *ca.* 10 Ma cycle of early calcalkaline and later alkaline volcanism, plutonism and mineralization is not fully resolved, but the same pattern repeated in the central and northern parts of the terrane suggest a feature fundamental to the Quesnel Arc genesis.

British Columbia alkaline porphyry deposits are associated with small, complex, either nepheline or leucite-normative intrusions and contain almost no quartz. The deposits comprise multiple, high-grade (0.5–1.0% Cu, 0.5–1.0 g/t Au) centres, each generally less than 150 million tonnes in size. Vein and stockwork development is insignificant and hydrothermal breccia-centred systems dominate. Mineralization is focused near the volcanic-plutonic interface, presumably as a result of late-stage magma devolatilization of highly oxidized (magnetite, hematite and anhydrite), primarily magmatic, high-salinity fluids. Late Triassic BC deposits are unique end-members of a continuum of porphyry deposits associated with calcalkaline, high-K calcalkaline or alkaline systems. Understanding the conditions of alkaline porphyry formation and the distinction between barren and fertile alkaline intrusions are important criteria for the evaluation of the Intermontane arc terranes and their economic potential in BC.

In 2004, the BC Ministry of Energy, Mines and Petroleum Resources, Abacus Mining and Exploration Corporation, Imperial Metals Corporation and Spectrum Gold Inc. (now NovaGold Resources) initiated a geoscience partner-

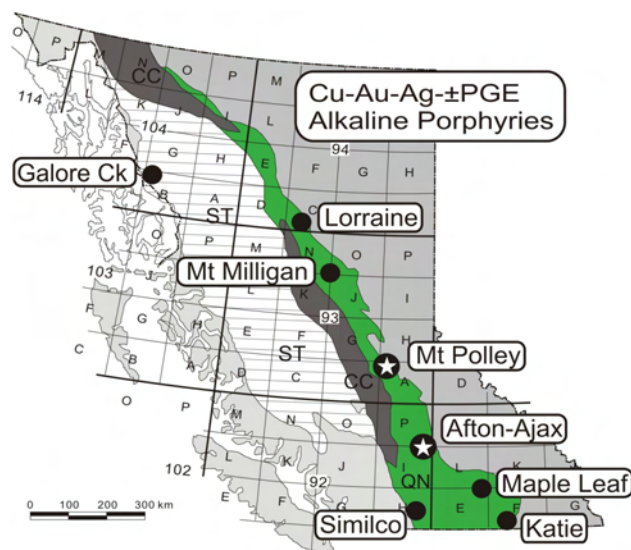


Figure 1. Location of BC Cu-Au-Ag±PGE alkaline porphyry deposits; green band indicates the Quesnel Terrane and the grey band indicates the Cache Creek Terrane. Abbreviation: ST, Stikine Terrane.

ship agreement focused on refining the alkaline Cu-Au porphyry exploration model as it applies to the Iron Mask, Mount Polley and Galore Creek alkaline magmatic centres (Fig 1). Recent deposit and regional-scale geological mapping have established a better understanding of the stratigraphic and tectonic framework that hosts these alkaline Cu-Au mineral systems, their geochemistry and their ages of formation (Logan and Mihalynuk, 2005a, b; Bath and Logan, 2006; Logan and Bath, 2006).

This report presents 17 new U-Pb and $^{40}\text{Ar}/^{39}\text{Ar}$ age determinations that have become available since the study began, for the Iron Mask batholith and the Mount Polley Cu-Au mine area. Data from Galore Creek and Copper Mountain will be presented separately.

GEOLOGICAL SETTING

The study area lies along the eastern margin of the Intermontane Belt close to its tectonic boundary with the Omineca Belt, in south-central BC (Fig 1). At this latitude, the Intermontane Belt is underlain mainly by Late Paleozoic to Early Mesozoic arc volcanic, plutonic and sedimentary rocks of the Quesnel Terrane. Farther west are coeval rocks of the oceanic Cache Creek Terrane. The southern Quesnel Terrane consists of an isotopically and

¹ University of British Columbia, Vancouver, BC

This publication is also available, free of charge, as colour digital files in Adobe Acrobat® PDF format from the BC Ministry of Energy, Mines and Petroleum Resources website at http://www.em.gov.bc.ca/Mining/Geosurv/Publications/catalog/cat_fldwk.htm

geochemically primitive Late Triassic to Early Jurassic magmatic arc complex, which formed above an east-dipping subduction zone (Mortimer, 1987). The Cache Creek Terrane, with its Late Triassic (Paterson and Harakal, 1974; Ghent *et al.*, 1996) blueschist-facies rocks, represents the remnants of this subduction-accretionary complex (Travers, 1977; Mihalynuk *et al.*, 2004). Quesnellia is fault-bounded, juxtaposed on the west with Paleozoic and Mesozoic rocks of the Cache Creek Complex and on the east by Mesozoic to Paleozoic and older metasedimentary, metavolcanic and metaplutonic rocks of the pericratonic Kootenay 'terrene'. Slide Mountain Terrane rocks have been interpreted to represent the remnants of a Late Paleozoic marginal basin (Scharizza, 1989; Roback *et al.*, 1994), which separated Quesnellia from North America until its closure in the Early Jurassic. By Middle Jurassic time, Stikinia had collided with Quesnellia, resulting in the demise of the Cache Creek subduction zone (173 Ma) and the stitching of the boundary in the northern Cordillera by ca. 172 Ma plutons (Mihalynuk *et al.*, 2004). At the same time, the Quesnellia, Slide Mountain, Barkerville and Cariboo subterrains were imbricated and thrust eastward onto the North American craton (Nixon *et al.*, 1993). Cretaceous intrusions, Tertiary volcanic rocks and feeder dikes of the Eocene Kamloops and Miocene Chilcotin groups are the youngest rocks in the region (Mathews, 1989).

Quesnel Arc magmatism and associated porphyry mineralization migrated eastward with time, beginning in the west, ca. 210 to 215 Ma, with the emplacement of plutons and the development of calcalkaline Cu-Mo±Au deposits at Highland Valley and Gibraltar. New data suggests that mineralization at Highland Valley postdates the intrusion of the Guichon batholith by up to 4 Ma (*see* Ash *et al.*, 2007). East of Gibraltar, in the central axis of the arc, are alkaline intrusions and 205 Ma, Cu-Au mineralization at Mount Polley. A chain of similar deposits extends the length of the Intermontane Belt (Barr *et al.*, 1976; Fig 1). In the south, they are associated with the Iron Mask batholith (Afton, Ajax and Crescent) and Copper Mountain intrusive rocks (Copper Mountain, Ingerbelle) and to the north, with the Hogem batholith (Lorraine). Uplift and erosion of the fore arc produced sub-Jurassic unconformities as magmatism shifted east and culminated with the intrusion of calcalkaline composite plutons consisting of quartz monzodiorite (ca. 202 Ma) and granodiorite (193–195 Ma) phases (Scharizza and Macauley, 2007) in the south (Takomkane, Thuya, Wild Horse and Pennask) and deposition of distal volcanoclastic and younger sedimentary rocks across the terrane. A temporally unrelated, ca. 183 Ma syn-accretionary pulse of alkaline magmatism and Cu-Au mineralization is recognized at Mount Milligan, 275 km northwest of Mount Polley. Post-accretion plutons in the central Quesnel belt include a Middle Jurassic (ca. 163 Ma) alkali leucogranite associated with Cu-Mo mineralization at Gavin Lake, and the ca. 104 Ma, mid-Cretaceous Bayonne suite plutons associated with Mo mineralization at Boss Mountain deposit and the Anticlimax showing.

GEOCHRONOLOGY

First attempts at determining the ages of Cu-Au mineralization within the Iron Mask batholith by Cockfield (1948) and Northcote (1977) and at Mount Polley by Campbell (1978) and Bailey (1978) used stratigraphic and paleontological constraints. Subsequent K-Ar isotopic dat-

ing of intrusions and alteration assemblages associated with mineralization were reported by Preto *et al.* (1979) for the Iron Mask batholith and by Panteleyev *et al.* (1996) and Bailey and Archibald (1990) for various intrusions in the Mount Polley region. On the basis of the K-Ar age data and alkaline compositions, most of these intrusions were included in the Early and Middle Jurassic Copper Mountain suite by Woodsworth *et al.* (1991).

Prior to the widespread application of U-Pb techniques to date intrusions, the majority of the age data for Cordilleran porphyry systems consisted of K-Ar and Rb-Sr cooling or isotopic disturbance ages (R.L. Armstrong, UBC data file) rather than crystallization ages. In areas of protracted magmatism or subsequent thermal/hydrothermal overprinting, common in porphyry deposits, neither the K-Ar nor the Rb-Sr technique can provide a reliable crystallization age. Using the U-Pb age dating technique, Mortensen *et al.* (1995) was able to resolve two discrete episodes of alkaline magmatism associated with copper-gold mineralization in the Canadian Cordillera: 210 Ma to 200 Ma and 183 Ma. Armed with the revised time scale of Palfy *et al.* (2000), subsequent workers were able to determine that the older episode, including intrusive phases at the Iron Mask batholith (204 ± 3 Ma) and at Mount Polley (204.7 ± 3 Ma), falls entirely within the Late Triassic, while the younger episode is Early Jurassic in age. Our geochronological work was aimed at establishing a finer temporal resolution for magmatic-hydrothermal events at existing deposits, as well as evaluating whether compositionally similar intrusions in the belt are coeval with the important 204 Ma Cu-Au metallogenic event.

ANALYTICAL TECHNIQUES

All U-Pb and $^{40}\text{Ar}/^{39}\text{Ar}$ sample preparation and analytical work was conducted at the Pacific Centre for Isotopic and Geochemical Research (PCIGR) at the Department of Earth and Ocean Sciences, University of British Columbia. Analytical results determined by U-Pb methods are listed in Tables 1 and 2. Step-heating gas release plots for $^{40}\text{Ar}/^{39}\text{Ar}$ analyses and concordia plots for U-Pb analyses are shown in Figures 3, 6, 9 and 11.

U-Pb-Thermal Ionization Mass Spectrometry

Zircon was separated from samples using conventional crushing, grinding and Wilfley table techniques, followed by final concentration using heavy liquids and magnetic separations. For this study, coarse titanite was disaggregated directly from hand samples with no additional mineral separation necessary. Zircon fractions were selected on the basis of grain quality, size, magnetic susceptibility and morphology. All zircon fractions were air abraded prior to dissolution to minimize the effects of post-crystallization Pb loss, using the technique of Krogh (1982). Mineral fractions were dissolved in sub-boiled 48% HF and 14 M HNO₃ (ratio of ~10:1, respectively) in the presence of a mixed ^{233}U - ^{235}U - ^{205}Pb tracer; zircons for 40 hours at 240°C in 300 µL PTFE or PFA microcapsules contained in high-pressure vessels (Parr™ acid digestion vessels with 125 mL PTFE liners) and titanite on a hotplate in 7 mL screw-top PFA beakers for at least 48 hours at ~130°C. Sample solutions were then dried to salts at ~130°C. Zircon residues were re-dissolved in ~100 µL of

sub-boiled 3.1 M HCl for 12 hours at 210°C in high-pressure vessels and titanite residues on a hotplate in ~1 mL of sub-boiled 6.2 M HCl in the same 7 mL screw-top PFA beakers for at least 24 hours at ~130°C. Titanite solutions were again dried to salts and were again re-dissolved on a hotplate, in the same beakers, in 1 mL of sub-boiled 3.1 M HCl at ~130°C for at least 24 hours. For single-grain zircon fractions E, F and G, sample JLO-05-6-27 3.1 M HCl was transferred to 7 mL PFA beakers, dried to a small droplet after the addition of 2 µL of 1 M H₃PO₄ and loaded directly on to Re filaments for analysis, as described below. For all other zircon and titanite fractions, the separation and purification of Pb and U employed ion exchange column techniques modified slightly from those described by Parrish *et al.* (1987). Lead and uranium were sequentially eluted into a single beaker; U from titanite solutions was purified by passing through columns a second time. Elutants were dried in 7 mL screw-top PFA beakers on a hotplate at ~120°C in the presence of 2 µL of ultra-pure 1 M phosphoric acid (H₃PO₄). Samples were then loaded on single, degassed zone refined Re filaments in 5 µL of a silica gel (SiCl₄) phosphoric acid emitter. Isotopic ratios were measured using a modified single collector VG-54R thermal ionization mass spectrometer equipped with an analogue Daly photomultiplier. Measurements were done in peak-switching mode on the Daly detector. Analytical blanks during the course of this study were <1 pg for U and for Pb in the range of 1 to 3 pg for no chemistry fractions and 2 to 10 pg for zircons passed through columns and titanite. Uranium fractionation was determined directly on individual runs using the ²³³⁻²³⁵U tracer and Pb isotopic ratios were corrected for the fractionation of 0.32 to 0.37%/amu, based on replicate analyses of the NBS-982 Pb standard and the values recommended by Thirlwall (2000). Reported precisions for Pb/U and Pb/Pb dates were determined by numerically propagating all analytical uncertainties through the entire age calculation using the technique of Roddick (1987). Standard concordia diagrams were constructed and regression intercepts calculated with Isoplot v. 3.00 (Ludwig, 2003). Unless otherwise noted, all errors on interpreted ages are quoted at the 2σ level.

U-Pb thermal ionization mass spectrometry (TIMS) analytical results are presented in Table 1. Discussion of results in a geological context follow in these sections: 'Iron Mask', 'Mount Polley', 'Shiko Lake Stock', 'Woodjam Property' and 'Gavin Lake'.

Laser Ablation Inductively Coupled Plasma Mass Spectrometry

Laser ablation inductively coupled plasma mass spectrometry (LA-ICP-MS) dating has recently been established as a routine procedure at the PCIGR. Zircons are separated from their hostrocks using conventional mineral separation methods and sectioned in an epoxy grain mount along with grains of internationally accepted standard zircon (FC-1, a *ca.* 1100 Ma zircon standard), and brought to a very high polish. The grains are examined using a stage-mounted cathodoluminescence imaging set-up that makes it possible to detect the presence of altered zones or inherited cores within the zircon. The highest-quality portions of each grain, free of alteration, inclusion or cores, are selected for analysis. The surface of the mount is then washed for ~10 minutes with dilute nitric acid and rinsed in ultra-clean water. Analyses are carried out using a New Wave 213 nm Nd-YAG laser coupled to a Thermo Finnigan

Element2 high-resolution ICP-MS. Ablation takes place within a New Wave 'Supercell' ablation chamber, which is designed to achieve very high efficiency entrainment of aerosols into the carrier gas. Helium is used as the carrier gas for all experiments and gas flow rates, and together with other parameters, such as torch position, are optimized prior to beginning a series of analyses. We typically use a 25 µm spot with 60% laser power, and do line scans rather than spot analyses in order to avoid within-run elemental fractions. Each analysis consists of a 7 second background measurement (laser off) followed by a ~28 second data acquisition period with the laser firing. A typical analytical session consists of four analyses of the standard zircon, followed by four analyses of unknown zircons, two standard analyses, four unknown analyses, etc. and finally four standard analyses. Data are reduced using the GLITTER software developed by the Geochemical Evolution and Metallogeny of Continents (GEMOC) group at Macquarrie University, which can subtract background measurements, propagate all analytical errors and calculate isotopic ratios and ages. This application generates a time-resolved record of each laser shot. Final ages for contiguous populations of relatively young (Phanerozoic) zircons are based on a weighted average of the calculated ²⁰⁶Pb/²³⁸U ages for 10 to 15 individual analyses. Interpretation and plotting of the analytical results employs Isoplot v. 3.00 software (Ludwig, 2003).

The LA-ICP-MS analytical results are presented in Table 2. A discussion of results in a geological context follow in these sections: 'Iron Mask', 'Mount Polley', 'Shiko Lake Stock', 'Woodjam Property' and 'Gavin Lake'.

Ar/Ar

Mineral separates were hand-picked, washed in nitric acid, rinsed in de-ionized water, dried, wrapped in aluminum foil and stacked in an irradiation capsule with similar-aged samples and neutron flux monitors (Fish Canyon tuff sanidine, 28.02 Ma; Renne *et al.*, 1998). The samples were irradiated on February 15 to 17, 2006 at the McMaster Nuclear Reactor in Hamilton, Ontario, for 90 MWh, with a neutron flux of approximately 3 by 10¹⁶ neutrons/cm²/s. Analyses (n = 57) of 19 neutron flux monitor positions produced errors of <0.5% in the J value.

The samples were analyzed at the Noble Gas Laboratory, Pacific Centre for Isotopic and Geochemical Research, The University of British Columbia, Vancouver. The mineral separates were step-heated at incrementally higher powers in the defocused beam of a 10 W CO₂ laser (New Wave Research MIR10) until fused. The gas evolved from each step was analyzed by a VG5400 mass spectrometer equipped with an ion-counting electron multiplier. All measurements were corrected for total system blank, mass spectrometer sensitivity, mass discrimination, radioactive decay during and subsequent to irradiation, as well as interfering Ar from atmospheric contamination and the irradiation of Ca, Cl and K (isotope production ratios: [⁴⁰Ar/³⁹Ar]_K=0.0302 ±0.00006; [³⁷Ar/³⁹Ar]_{Ca}=1416.4 ±0.5; [³⁶Ar/³⁹Ar]_{Ca}=0.3952 ±0.0004, Ca/K=1.83 ±0.01[³⁷Ar_{Ca}/³⁹Ar_K]).

The plateau and correlation ages were calculated using Isoplot v. 3.00 (Ludwig, 2003). Errors are quoted at the 2σ (95% confidence) level and are propagated from all sources except mass spectrometer sensitivity and age of the flux

TABLE 1. U-PB THERMAL IONIZATION MASS SPECTROMETRY (TIMS) ANALYTICAL DATA.

Fraction ¹	Wt (mg)	U ² (ppm)	Pb ³ (ppm)	²⁰⁶ Pb ⁴ / ²⁰⁴ Pb	Pb ⁵ (pg)	Th/U ⁶	Isotopic ratios (1σ, %) ⁷			Apparent ages (2σ, Ma) ⁷		
							²⁰⁶ Pb/ ²³⁸ U	²⁰⁷ Pb/ ²³⁵ U	²⁰⁷ Pb/ ²⁰⁶ Pb	²⁰⁶ Pb/ ²³⁸ U	²⁰⁷ Pb/ ²³⁵ U	²⁰⁷ Pb/ ²⁰⁶ Pb
JLO-04-2-14												
T1, 3	179	42	1.5	65	308	0.87	0.03103 (0.78)	0.2107 (3.3)	0.04925 (2.9)	197.0 (3.0)	194 (12)	160 (130/141)
T2, 5	214	41	1.4	65	370	0.67	0.03130 (1.1)	0.2169 (3.9)	0.05027 (3.3)	198.7 (4.4)	194 (14)	208 (144/158)
T3, 2	181	70	2.4	90	354	0.66	0.03154 (0.74)	0.2132 (2.7)	0.04901 (2.2)	200.2 (2.9)	196.2 (9.4)	148 (101/107)
JLO04-21-84												
A, 6	34	573	19.6	4457	8.0	0.97	0.02918 (0.11)	0.2009 (0.25)	0.04994 (0.20)	185.4 (0.4)	185.4 (0.4)	192.0 (9.4/9.5)
B, 7	27	899	42.6	6179	7.3	2.54	0.02959 (0.23)	0.2038 (0.37)	0.04994 (0.27)	188.0 (0.9)	188.3 (1.3)	192 (13)
C, 8	21	818	32.2	5035	6.4	1.55	0.02956 (0.10)	0.2035 (0.24)	0.04992 (0.19)	187.8 (0.4)	188.1 (0.8)	191.3 (8.9/9.0)
D, 10	9	674	19.3	1869	5.9	2.25	0.02938 (0.17)	0.2023 (0.54)	0.04994 (0.49)	186.7 (0.6)	187.1 (1.8)	192 (23)
E, 10	13	343	19.0	2149	3.9	3.41	0.03013 (0.19)	0.2073 (0.47)	0.04990 (0.43)	191.3 (0.7)	191.3 (1.6)	190 (20)
JLO04-24-111												
A, 3	4	1597	66.7	2656	4.8	1.40	0.03246 (0.20)	0.2266 (0.57)	0.05063 (0.54)	205.9 (0.8)	207.4 (2.2)	224 (25)
B, 7	7	1230	49.5	2927	6.0	1.25	0.03224 (0.10)	0.2239 (0.35)	0.05038 (0.31)	204.6 (0.4)	205.2 (1.3)	213 (14/15)
C, 11	5	1403	55.8	5303	2.7	1.19	0.03227 (0.15)	0.2246 (0.28)	0.05048 (0.24)	204.7 (0.6)	205.8 (1.1)	217 (11)
D, 14	6	1093	45.9	5904	2.3	1.43	0.03245 (0.10)	0.2267 (0.25)	0.05066 (0.21)	205.9 (0.4)	207.5 (0.9)	225.4 (9.7/9.8)
E, ~30	12	837	34.2	9533	2.2	1.31	0.03234 (0.14)	0.2260 (0.22)	0.05067 (0.18)	205.2 (0.6)	206.9 (0.8)	226.1 (8.5)
JLO-04-50-510												
B, 2	42	197	6.6	4478	3.7	0.49	0.03229 (0.09)	0.2238 (0.20)	0.05027 (0.15)	204.9 (0.4)	204.9 (0.7)	207.3 (6.9/7.0)
D, 2	47	784	31.9	33080	2.2	1.31	0.03227 (0.09)	0.2239 (0.16)	0.05032 (0.09)	204.7 (0.4)	205.1 (0.6)	209.7 (4.1/4.2)
E, 4	57	286	9.7	2793	11.5	0.52	0.03235 (0.10)	0.2230 (0.59)	0.04999 (0.55)	205.2 (0.4)	204.4 (2.2)	195 (25/26)
MMI04-26-18												
A, 2	144	73	2.3	3147	6.3	0.38	0.03085 (0.10)	0.2126 (0.31)	0.04997 (0.26)	195.9 (0.4)	195.7 (1.1)	194 (12)
B, 4	201	55	1.7	4231	5.0	0.41	0.03065 (0.09)	0.2115 (0.26)	0.05006 (0.21)	194.6 (0.4)	194.9 (0.9)	198 (10)
D, 5	189	89	2.8	4657	6.8	0.40	0.03100 (0.31)	0.2136 (0.33)	0.04997 (0.31)	196.8 (1.2)	196.5 (1.2)	194 (14/15)
E, 6	222	57	1.8	3585	6.7	0.44	0.03071 (0.19)	0.2129 (0.32)	0.05029 (0.30)	195.0 (0.7)	196.0 (1.2)	209 (14)
JLO05-6-27												
A, 2	23	187	7.6	435	26.1	0.33	0.04094 (0.17)	0.2913 (1.2)	0.05160 (1.1)	258.7 (0.9)	259.6 (5.4)	268 (50/52)
B, 3	12	314	10.5	129	71.3	0.31	0.03395 (0.44)	0.2341 (2.2)	0.05001 (1.9)	215.2 (1.9)	213.5 (8.3)	195 (88/93)
C, 4	12	260	8.1	362	17.7	0.28	0.03165 (0.17)	0.2252 (2.0)	0.05160 (1.9)	200.9 (0.7)	206.2 (7.5)	268 (86/91)
D, 4	11	200	7.3	392	13.3	0.34	0.03670 (0.18)	0.2626 (2.4)	0.05191 (2.3)	232.3 (0.8)	237 (10)	281 (101/108)
E, 1	6	333	9.4	975	3.8	0.19	0.02940 (0.14)	0.2031 (0.60)	0.05011 (0.57)	186.8 (2.1)	187.7 (2.1)	200 (26/27)
F, 1	5	484	15.6	951	5.2	0.29	0.03276 (0.18)	0.2324 (0.54)	0.05145 (0.49)	207.8 (2.1)	212.2 (2.1)	261 (22/23)
G, 1	4	188	6.2	1056	1.5	0.26	0.03353 (0.19)	0.2340 (0.95)	0.05062 (0.89)	212.6 (3.6)	213.5 (3.6)	224 (41/42)

¹ All zircon grains selected for analysis were air abraded prior to dissolution. Fraction ID (capital letter - zircon A, B, etc.; titanite: T1, T2, etc.), followed by the number of grains

² U blank correction of 1pg ±20%; U fractionation corrections were measured for each run with a double²³³U-²³⁶U spike.

³Radiogenic Pb

⁴Measured ratio corrected for spike and Pb fractionation of 0.32-0.37amu ± 20% (Daly collector) which was determined by repeated analysis of NBS Pb 982 standard throughout the course of this study.

⁵Total common Pb in analysis based on blank isotopic composition.

⁶Model Th/U derived from radiogenic ²⁰⁶Pb and the ²⁰⁷Pb/²⁰⁶Pb age of fraction

⁷Blank and common Pb corrected; Pb procedural blanks were ~1.5-5 pg and U <1 pg. Common Pb concentrations are based on Stacey-Kramers model Pb at the interpreted age of the rock or the ²⁰⁷Pb/²⁰⁶Pb age of the rock (Stacey and Kramers, 1975).

monitor. The best statistically justified plateau and plateau age were picked based on the following criteria:

- three or more contiguous steps comprising more than 30% of the ³⁹Ar;
- the probability of fit of the weighted mean age greater than 5%;
- the slope of the error-weighted line through the plateau ages equals zero at 5% confidence;
- the ages of the two outermost steps on a plateau are not significantly different from the weighted-mean plateau age (at 1.8σ, six or more steps only); and
- the outermost two steps on either side of a plateau must not have nonzero slopes with the same sign (at 1.8σ, nine or more steps only).

Analytical results for ⁴⁰Ar/³⁹Ar are presented in Table 3. A discussion of results in a geological context follow

in these sections: 'Iron Mask', 'Mount Polley', 'Shiko Lake Stock', 'Woodjam Property' and 'Gavin Lake'.

IRON MASK BATHOLITH

The Iron Mask batholith is a northwest-trending, diorite-monzonite complex that intruded Carnian to Norian volcanic and sedimentary rocks of the eastern Nicola Group (Preto, 1979; Mortimer, 1987). It consists of two separate bodies: the 22 km long by 5 km wide Iron Mask batholith (Fig 2) in the southeast and the smaller, 5 km by 5 km Cherry Creek pluton in the northwest (Preto 1967, 1972; Northcote, 1974). The two are separated by an east-trending graben filled with Eocene Kamloops Group volcanic and sedimentary rocks. Snyder and Russell (1993, 1995) have described the various phases of the batholith and studied the petrogenetic relationships between them, as

Potassium-argon biotite cooling ages for samples of the Hybrid and Cherry Creek phases and hydrothermal alteration associated with mineralization (Preto *et al.*, 1979) range from 201 to 209 Ma (mean 204 ± 12 Ma). The U-Pb age data for samples of the Pothook, Hybrid and Cherry Creek phases of the batholith (Mortensen *et al.*, 1995) are 204 ± 3 Ma. Sugarloaf diorite is the youngest phase of the Iron Mask batholith. According to Ross *et al.* (1995), it is responsible for albitic alteration and copper-gold mineralization. Attempts to extract zircon from this unit have hitherto been unsuccessful.

Samples of the Iron Mask were collected from five separate sites along the southwestern margin of the batholith (Fig 2). Sampling includes a pegmatitic variety of the Iron Mask Hybrid phase, foliated augite crystal tuff of the Nicola Group, two hornblende diorite samples of the Sugarloaf phase and hydrothermal titanite from a mineralized vein in the Ajax West pit. Sample descriptions and data interpretation are below.

Iron Mask Hybrid (MMI-04-4-1A)

The Iron Mask Hybrid phase is a xenolith-rich, heterogeneous unit that comprises approximately 45% of the Iron Mask batholith (Fig 2). Hybrid rocks mark the contact zones between individual phases (*i.e.*, Pothook, Cherry Creek and Sugarloaf) within the batholith, as well as the contact zones between the margin of the batholith and the volcanic country rock. A xenolith-poor intrusive breccia occupies a northerly trending belt, extending from the Ajax deposit to Coal Hill. Here, it is fine-grained to pegmatitic with local trachytic segregations of clinopyroxene, plagioclase, hornblende and magnetite. North of the Ajax deposit, the hybrid rocks possess a consistent east-trending magmatic foliation and pegmatitic mineral growth direction is perpendicular to the magmatic foliation, probably parallel to the direction of dilatancy (Fig 10; Logan and Mihalynuk, 2005b).

Coarse-grained hornblende crystals that define this well-developed mineral lineation were selected and dated with $^{40}\text{Ar}/^{39}\text{Ar}$ step-heating techniques to constrain the timing of crystal growth and cooling history (hornblende closure temperature of 550°C ; Harrison, 1981). The hornblende separate (MMI-04-4-1A) yields a good 206.9 ± 2.2 Ma age spectrum with a strong plateau representing 97.7% of the total ^{39}Ar released (Fig 3a). The inverse isochron plot gave an atmospheric intercept of 285 ± 25 Ma and an isochron age of 207.1 ± 1.3 Ma, which agrees within error to the calculated plateau age. Preto *et al.* (1979) reported a biotite K-Ar age for a sample of the Iron Mask Hybrid phase from a similar location with a cooling age of 204 ± 12 Ma, equivalent within the limits of error.

Foliated Pyroxene-Porphyrific Basalt (JLO-04-17a)

On the south side of the Ajax west pit decline, foliated, carbonate-altered augite crystal tuff, augite porphyry basalt and picrite are intruded by a 1.2 m thick Sugarloaf dike. Both the foliation and the dike are warped by a gentle upright fold. The foliation and the fold axial plane average $120^\circ/60^\circ$ mineral elongation lineation developed around pyroxene porphyroblasts in the adjacent picrite trend $10^\circ/115^\circ$.

The foliated augite tuff was collected and a sample of sericite that defines the fabric (Fig 4) was dated using $^{40}\text{Ar}/^{39}\text{Ar}$ step-heating techniques to constrain the timing of foliation generation. The age spectra are complicated and the four-point inverse isochron plot is unusable. The heating data indicates probable excess argon in the low-temperature steps (1–5) and high Ca/K ratios indicative of contamination in the high-temperature steps (11–16). The four-step plateau age of 205.6 ± 1.3 Ma is defined by 37% of the total ^{39}Ar (Fig 3b). In spite of the high Ca/K ratios, the last 4 high-temperature steps yield a *ca.* 189 Ma age with 20% of the ^{39}Ar . An accurate assessment of the metamorphic age cannot be derived from these data, but a Late Triassic to Early Jurassic age for crystallization of the sericite is indicated.

Sugarloaf Hill Monzodiorite (JLO-04-6-67)

The Sugarloaf Hill stock is one of the lenticular north-west-trending intrusions of Sugarloaf monzodiorite that are dispersed primarily along the western margin of the batholith. These stocks are associated with Cu-Au porphyry mineralization at the past-producing Ajax East deposit and at the Rainbow deposit, which has drill-indicated resources from the #2 and #22 zones of 21.9 million tonnes grading 0.464% Cu and 0.106 g/t Au (0.30% Cu cut-off; Abacus Mining and Exploration Corporation, 2006). The Rainbow property is located on the eastern slopes of Sugarloaf Hill, close to the Leemac fault. The #1 and #17 zones are hosted in Sugarloaf hornblende porphyry; the #2 and #22 zones in Pothook/Sugarloaf hybrid and metavolcanic rock, respectively (Logan and Mihalynuk, 2005b). All mineralization is fracture or breccia-controlled and consists of chalcopyrite±magnetite accompanied with pyrite and alteration mineralogy.

According to Oliver (1995), Sugarloaf Hill is underlain by three mappable stocks: hornblende diorite, albite-phyrific monzodiorite and a microphyric hornblende diorite. Snyder and Russell (1993) interpreted the radial distribution of hornblende porphyry dikes around Sugarloaf Hill as evidence that the stock was a subvolcanic intrusive centre. The stocks intrude picrite and volcanoclastic units of the Nicola Group. On their northeast margin, the Sugarloaf Hill stocks are faulted and structurally interleaved along the Leemac fault with the Hybrid and Pothook phases.

A sample of least altered, medium-grained hornblende-porphyrific monzodiorite was collected from the southeastern end of the stock (Fig 2) for chemical and age determination. The diorite is characterized by 1 to 3 mm euhedral hornblende (20%) and plagioclase (35%) phenocrysts in a fine-grained groundmass of plagioclase, clinopyroxene, magnetite and potassium feldspar. Accessory minerals include apatite, sphene, magnetite, pyrite and traces of quartz. Minor alteration products include actinolite, sericite and calcite.

A hornblende separate was dated by $^{40}\text{Ar}/^{39}\text{Ar}$ step-heating techniques to constrain the cooling age of the intrusion. Analyses of hornblende from JLO-04-6-67 gave a good age spectrum, showing some Ar loss in the early heating stages and a cooling age of 200.1 ± 2.5 Ma using 6 of 11 steps and 89.2% of the ^{39}Ar (Fig 3c). The inverse isochron plot gave an atmospheric intercept of 263 ± 84 Ma and an isochron age of 202.2 ± 6.1 Ma, which agrees within error to the calculated plateau age.

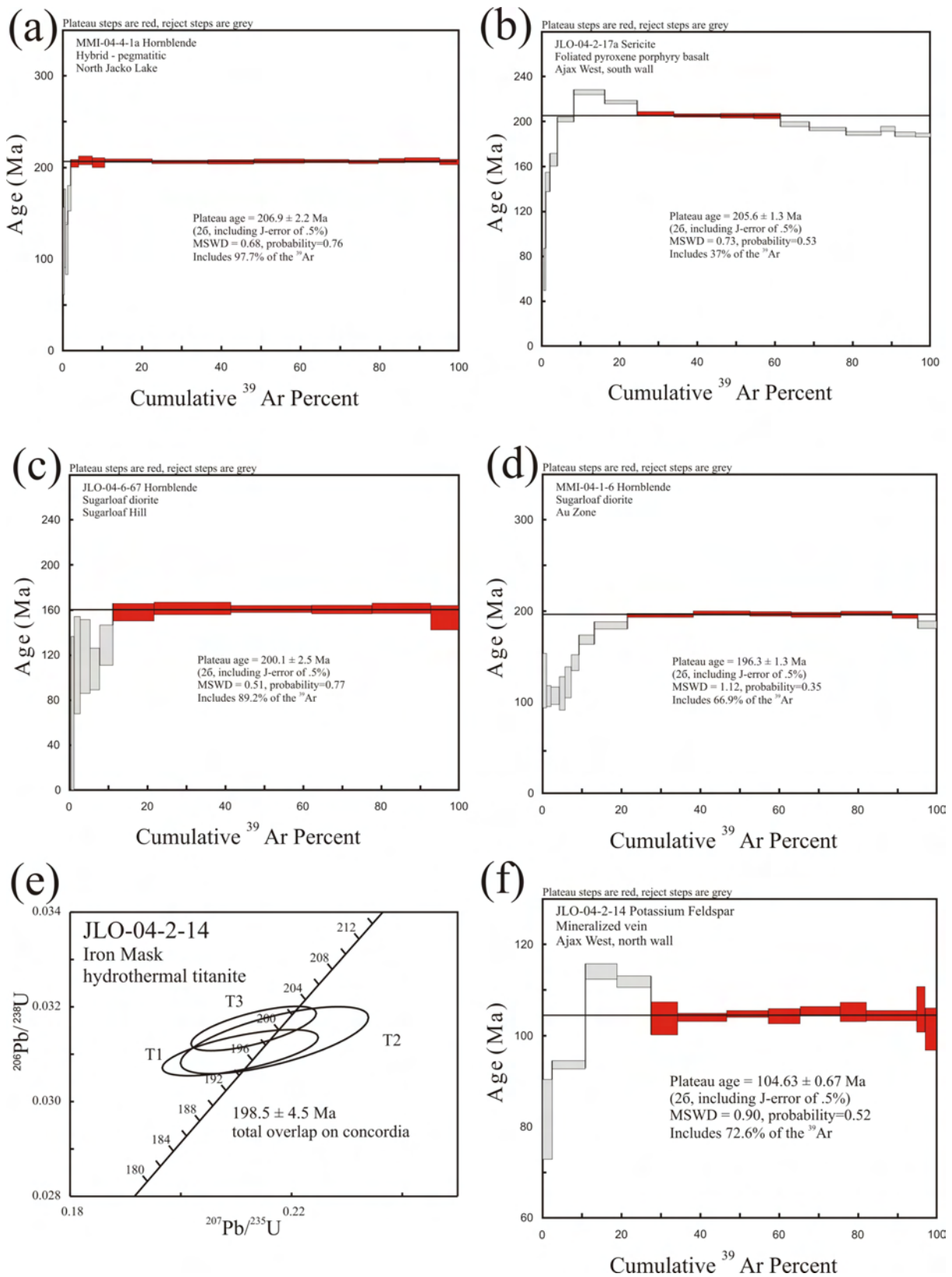


Figure 3. Step-heating gas release plots for $^{40}\text{Ar}/^{39}\text{Ar}$ analyses for a) hornblende sample MMI-04-4-1a from North Jacko Lake; b) sericite sample JLO-04-2-17a from Ajax West, south wall; c) hornblende sample JLO-04-6-67 from Sugarloaf Hill; d) concordia plot of U-Pb thermal ion mass spectrometry (TIMS) data for samples from the Iron Mask batholith; e) step-heating gas release plots for $^{40}\text{Ar}/^{39}\text{Ar}$ analysis for potassium feldspar sample JLO-04-2-14 from Ajax West, north wall; T1, T2 and T3 correspond to fraction numbers in Table 1. All errors are displayed as 2σ level of uncertainty.

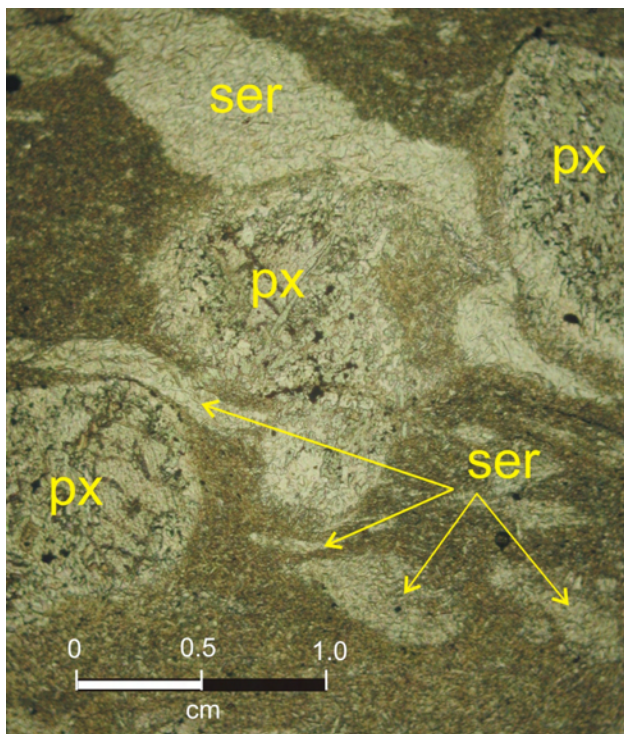


Figure 4. Photomicrograph of foliated and weakly crenulated sericite porphyroblastic augite crystal tuff (JLO-04-17a); plane-polarized light. Abbreviations: px, pyroxene; ser, sericite.

Gold Zone, Sugarloaf Dike (MMI-04-1-6)

Gold-rich, copper-poor mineralization occurs in two northwest-trending zones (Gold and East) that are located immediately southwest of the Pothook pit (Fig 2). The Gold zone was first recognized by Teck Cominco in the 1990s at the structurally complicated contact between the Pothook and Cherry Creek phases and the Nicola Group country rocks. Another feature of the Gold zone is a northwesterly swarm of Sugarloaf diorite dikes at the southern margin of the broad propylitic alteration zone, which extends to the northern Afton pit, where it is an important part of the mineralizing system.

Sugarloaf dikes in the Gold zone are weakly trachytic, hornblende-porphyrific diorite with a moderate to strong albitic and propylitic overprint. An ICP-MS analysis of one of the dikes that returned 480 ppb Au and 161 ppm Cu. Reported drill intersections of >0.2% Cu and >0.2 g/t Au characterize the mineralized zone, with higher-grade intersections up to 3.0 g/t Au (Evans, 1992). Grab samples from the southeast end of the East zone returned gold-rich assays of 6.36 g/t Au, 0.83 g/t Pd and 1.0% Cu (Abacus News Release, Dec 17, 2002).

A sample of one of the least-altered Sugarloaf dikes was collected from the Gold zone to establish the crystallization age and to provide constraints on the cooling history for the hydrothermal mineralizing system responsible for the gold-rich, copper-poor mineralization. Although the age spectrum shows Ar loss in the early heating steps and a slightly hump-shaped pattern, a good plateau is defined by five steps representing more than 66% of the total ^{39}Ar released (Fig 3d). The 196.3 ± 1.3 Ma hornblende cooling age is interpreted to represent the magmatic crystallization age.

Hydrothermal Titanite and Potassium Feldspar (JLO-04-2-14)

The Ajax West and Ajax East deposits are located on the southwest side of the Iron Mask batholith at the contact between medium to coarse-grained Iron Mask Hybrid diorite and Sugarloaf diorite (Fig 2). Mineralization occurs as disseminated and veinlet chalcopyrite in propylitic, albitic and potassic-altered Sugarloaf diorite. In the west deposit, a core of intense albitic alteration diminishes outward to less pervasive peripheral propylitic alteration (chlorite, epidote, calcite±pyrite; Ross *et al.*, 1995). Outside the ore shell, but within the propylitic alteration zone in the north wall of the West pit, *en échelon* northwest-striking ($300^\circ/62^\circ$) salmon-pink potassium feldspar veins (10–50 cm) cut Iron Mask Hybrid rocks. These veins have a margin of magnetite intergrown with biotite±chlorite and a core of a vuggy intergrown aphyric matrix of potassium feldspar and albite with calcite, chalcopyrite, pyrite and coarse euhedral crystals of titanite-filling fractures and interconnected vugs (Fig 18; Logan and Mihalynuk, 2005b).

Titanite was separated from the hydrothermal vein assemblage and analyzed using U-Pb TIMS geochronological techniques to provide a maximum age limit on the chalcopyrite mineralization hosted within the vein set. One large (~0.5 cm), pale yellow, clear to slightly cloudy, striated titanite grain was removed from a vug and broken into fragments. Three of the clearest of these were analyzed and gave concordant and overlapping results. A crystallization age of 198.5 ± 4.5 Ma is based on the total range of $^{206}\text{Pb}/^{238}\text{U}$ ages and associated 2σ errors for the three results (Fig 3e, Table 1).

In addition to titanite, potassium feldspar was separated from the vein assemblage and dated with $^{40}\text{Ar}/^{39}\text{Ar}$ step-heating techniques to constrain the cooling history of the hydrothermal vein mineralization. The potassium feldspar has a complex age spectra with older apparent ages in the low-temperature steps (Fig 3f). A plateau age of 104.63 ± 0.67 Ma calculated from the final 72.6% of the ^{39}Ar provides a good cooling age, which is interpreted as the hydrothermal crystallization age of the feldspar. An inverse isochron plot gave an isochron age of 103.6 ± 2.9 Ma, which agrees within error to the calculated plateau age.

CENTRAL QUESNEL BELT

The Nicola Group of the central Quesnel belt consists of a two-fold subdivision: a lower fine-grained Middle to Upper Triassic sedimentary succession and an upper 'alkalic or shoshonitic' sequence of Upper Triassic calcalkaline arc volcanic deposits, which are gradational with and conformably overlie the sedimentary package. Lower to Middle Jurassic sedimentary and less common volcanic rocks unconformably overlie the Nicola Group (Logan and Mihalynuk, 2005a, b). A number of small composite granitic bodies intrude the area. Data from this study and others (Breitsprecher and Mortensen, 2004) indicate the presence of at least five intrusive suites: Late Triassic (Granite Mountain suite, *ca.* 212 Ma), latest Late Triassic (Mount Polley intrusive suite, *ca.* 205 Ma), Early Jurassic (Takomkane-Thuya suite, *ca.* 193 Ma), Middle Jurassic (Gavin Lake suite, *ca.* 163 Ma) and mid-Cretaceous (Naver suite, *ca.* 106 Ma).

An axis of alkalic intrusions and related mineralization occupies the eastern part of the Quesnel Arc in central British Columbia (Fig 8 in Panteleyev *et al.*, 1996). Fewer and more widely spaced mineral occurrences associated with calcalkaline intrusions are located on the western margin of Quesnellia.

In the area surrounding Mount Polley, there are a number of small, high-level composite intrusions composed of diorite through monzonite to syenite compositions. These are interpreted to have been emplaced into the upper levels of the arc and are often hosted by coarse, extrusive-facies volcanic rocks that indicate individual eruptive centres (*i.e.*, Mount Polley, Bailey and Hodgson, 1979; Shiko Lake, Panteleyev *et al.*, 1996). An extensive program of geological mapping and geochronology was conducted over the eastern Intermontane Belt in the Quesnel and Quesnel River areas by Bailey (1988, 1990), Panteleyev (1987, 1988) and Panteleyev *et al.* (1996). Geochronological samples were collected from the Mount Polley area as part of a regional mapping program in the Quesnel Lake (Fig 5) and Horsefly Lake (Fig 10) map areas in 2004 and 2005. Samples from the immediate vicinity of the Mount Polley mine include two from pyroxene monzonite satellite stocks, a potassium feldspar megacrystic dike, a quartzphyric andesite and hydrothermal biotite from the Cariboo pit and the Northeast zone. Additional sampling was carried out at Shiko Lake (quartz syenite), Woodjam property (hornblende-quartz monzonite and quartz-feldspar porphyry) and Gavin Lake (quartz-porphyrific monzogranite). Sample descriptions and data interpretation are below.

MOUNT POLLEY INTRUSIVE COMPLEX (MPIC)

The Mount Polley alkalic intrusive complex is a north to northwest elongated, composite centre located in a large (40 by 17 km) regional aeromagnetic anomaly. This high-level intrusive complex is 5.5 by 4 km in size and comprised primarily of fine-grained porphyritic monzodiorite and monzonite, plagioclase porphyry and syenite stocks and dikes with abundant screens of metavolcanic rock and hydrothermal breccia (Fraser, 1994, 1995; Hodgson *et al.*, 1976), features characteristic of a subvolcanic environment (Fig 5). It is separated from another northwest-elongated composite intrusive body to the southwest across a ~1 km thick panel of volcanic strata. Known as the Bootjack stock, this second body is 2.3 by 7 km, is characterized by an unusual orbicular pseudoleucite syenite (Bath and Logan, 2006) and lacks subvolcanic textures.

Published geochronology from the Bootjack stock includes a hornblende $^{40}\text{Ar}/^{39}\text{Ar}$ plateau age of 203.1 ± 2.0 Ma from the coarse-grained syenite phase (Bailey and Archibald, 1990), a U-Pb zircon age from the orbicular syenite (202.7 ± 7.1 Ma; Mortensen *et al.*, 1995) and a Pb-Pb titanite age from pseudoleucite syenite (200.7 ± 2.8 Ma; Mortensen *et al.*, 1995). Uranium-lead ages from two intrusive phases from the MPIC (201.7 ± 4 Ma zircon from diorite and 204.7 ± 3 Ma zircon from plagioclase porphyry) are similar, within error, to ages from the Bootjack stock (Mortensen *et al.*, 1995). Fraser (1995), however, infers that the Bootjack stock is younger than the MPIC on the basis of diorite xenoliths present within the nepheline pseudoleucite and orbicular syenite units. Such an age relationship can be accommodated by the error envelopes on

the geochronological data from the MPIC and Bootjack stock.

Satellite Monzonite Stock (JLO-04-24-111)

A northwest-trending hypabyssal stock (1 km by 3 km) of pyroxene monzonite crops out northwest of Bootjack Lake. It consists of holocrystalline plagioclase-pyroxene-phyric monzodiorite and pink pyroxene monzonite. Rounded xenoliths of pyroxene porphyry and diorite are common. The stock is fine-grained, equigranular or microporphyritic and weakly trachytic. Petrographic observations reveal that both phases have the same modal mineralogy: sericitized plagioclase laths (45%, 1 mm), potassium feldspar (40%, <1 mm laths and matrix material) and euhedral pyroxene crystals (10–15%, 0.5–1 mm). Accessory minerals include magnetite, apatite and zircon. Potassium alteration is pervasive, flooding the matrix and as overgrowths on feldspar phenocrysts. Late-stage deuteric alteration has produced isolated patches of chlorite and calcite.

In places, the weathered surfaces of fine-grained monzonite display a crackle or autobrecciated texture. At its southern margin, the breccia is pink with clasts defined by a tight, anastomosing network of chlorite fractures. Nearer its centre, the stock is dominated by a potassic albite-altered breccia resembling the hydrothermal breccia at the Springer zone and on Mount Polley (Logan and Mihalynuk, 2005a).

A 20 kg sample was collected from a borrow pit located in the centre of the stock. This sample yielded clear, colourless, euhedral stubby zircon prisms and more commonly broken pieces. Five air-abraded multigrain fractions ranging from 3 to ~30 complete or broken grains were analyzed using the TIMS technique. Results indicate minor inheritance. An age estimate of $203.1 +1.6/-12.7$ Ma (mean standard weighted deviate = 0.42) is based on the lower intercept of a five-point regression (Fig 6a). Due to very limited data dispersion near the low end of the regression line, the precision of the upper intercept is a very poor $1284 +1300/-872$ Ma. This value gives an estimate for the average age of inheritance in analyzed grains.

Polley Lake Road, Monzonite (JLO-04-20-70b)

A small (<1 km²), hypabyssal monzonite stock crops out north of the Polley Lake Road approximately 500 m east of the Frypan Road junction (Fig 5). The rock is a microporphyritic plagioclase-pyroxene-phyric monzonite, similar to the stock located northwest of Bootjack Lake (JLO-04-24-111). It is composed of roughly equal amounts of plagioclase (3–5 mm tabular laths), potassium feldspar (subhedral 2–3 mm grains and matrix material), 10 to 15% tabular euhedral pyroxene (0.7–1.5 mm) and trace hornblende and biotite. Accessory minerals include magnetite, sphene and apatite. Potassium alteration has created a turbid matrix and has replaced most of the feldspar phenocrysts. Late deuteric alteration caused chloritization of hornblende and biotite, but had little effect on pyroxene.

The stock intrudes altered breccia and clastic rocks of the Mount Polley intrusive complex very close to the erosional top of the Triassic section. Early Jurassic bedded volcanoclastic rocks, tuff (MMI-04-26-18) and conglomerate unconformably overlie the MPIC at this locality and al-

ity of concordance = 0.071; Ludwig, 2003). We consider this to be the crystallization age for the potassium-feldspar-porphyrific dike.

Cariboo Pit, Hydrothermal Biotite (MMI-04-24-1)

Mineralization at Mount Polley is hosted by a variety of hydrothermal breccia that cut a high-level multiphase dioritic-monzonitic intrusive sequence. Alteration and mineralization are interpreted to be related to a single hydrothermal centre (Hodgson *et al.*, 1976; Bailey and Hodgson, 1979) modified by faulting (Fraser, 1994). The breccia and hydrothermal alteration, however, imposed on them display sufficient zonal variation to warrant subdivision into the West (Springer), Central (Cariboo and Bell), Northeast and Southeast zones (Fig 16; Logan and Mihalynuk, 2005a).

Work by Fraser (1994, 1995) in the Central and West zones resulted in the subdivision of the potassic core into three subzones defined on the basis of the dominant alteration mineral: biotite, actinolite or potassium feldspar albite. The biotite and actinolite subzones overprint the Central zone east of the Mount Polley fault; the potassium feldspar albite zone occurs west of the fault in a northwest-

trending belt west of Mount Polley (West zone). Farther west still is the actinolite zone.

A sample of coarse hydrothermal biotite was collected from the east wall of the Cariboo pit in the biotite subzone of the potassic core zone (Fraser, 1995). This zone is characterized by coarse, secondary biotite developed within the matrix of mineralized hydrothermal breccia in the core of the Central zone.

The biotite separate yielded a normal diffusive loss profile in the low-temperature steps. Apparent ages increase over the initial 45% of the ³⁹Ar released. The remainder of the spectra is fairly constant and gave a weighted mean age of 220.8 ± 1.3 Ma (Fig 6d). The inverse isochron plot gave an atmospheric intercept of 280 ± 31 Ma and an isochron age of 221.4 ± 1.6 Ma, which agrees, within error to the calculated plateau age. The biotite plateau age for sample MMI-04-24-1 predates the intrusion of the alkaline MPIC rocks by approximately 15 Ma, and is herein considered suspect.

Northeast Zone, Hydrothermal Biotite and Orthoclase (WB-05-209)

The Northeast zone is a 150 by 500 m northwest-trending, steeply dipping tabular zone of Cu-Au-Ag miner-

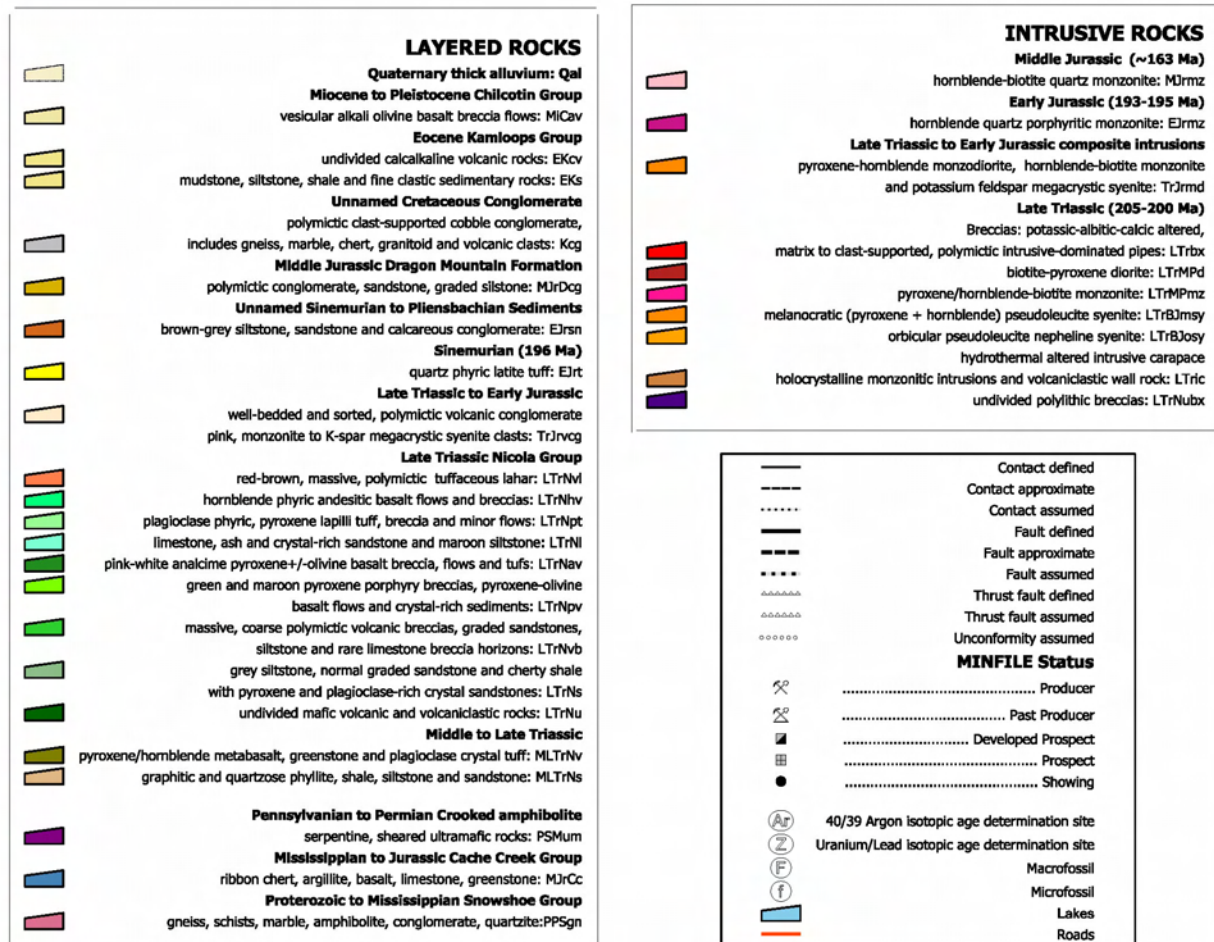


Figure 5. Regional geology map of the Mount Polley area with the location of geochronological samples. Inset shows the detailed area of the Mount Polley intrusive complex (MPIC); modified from Logan *et al.* (2007).

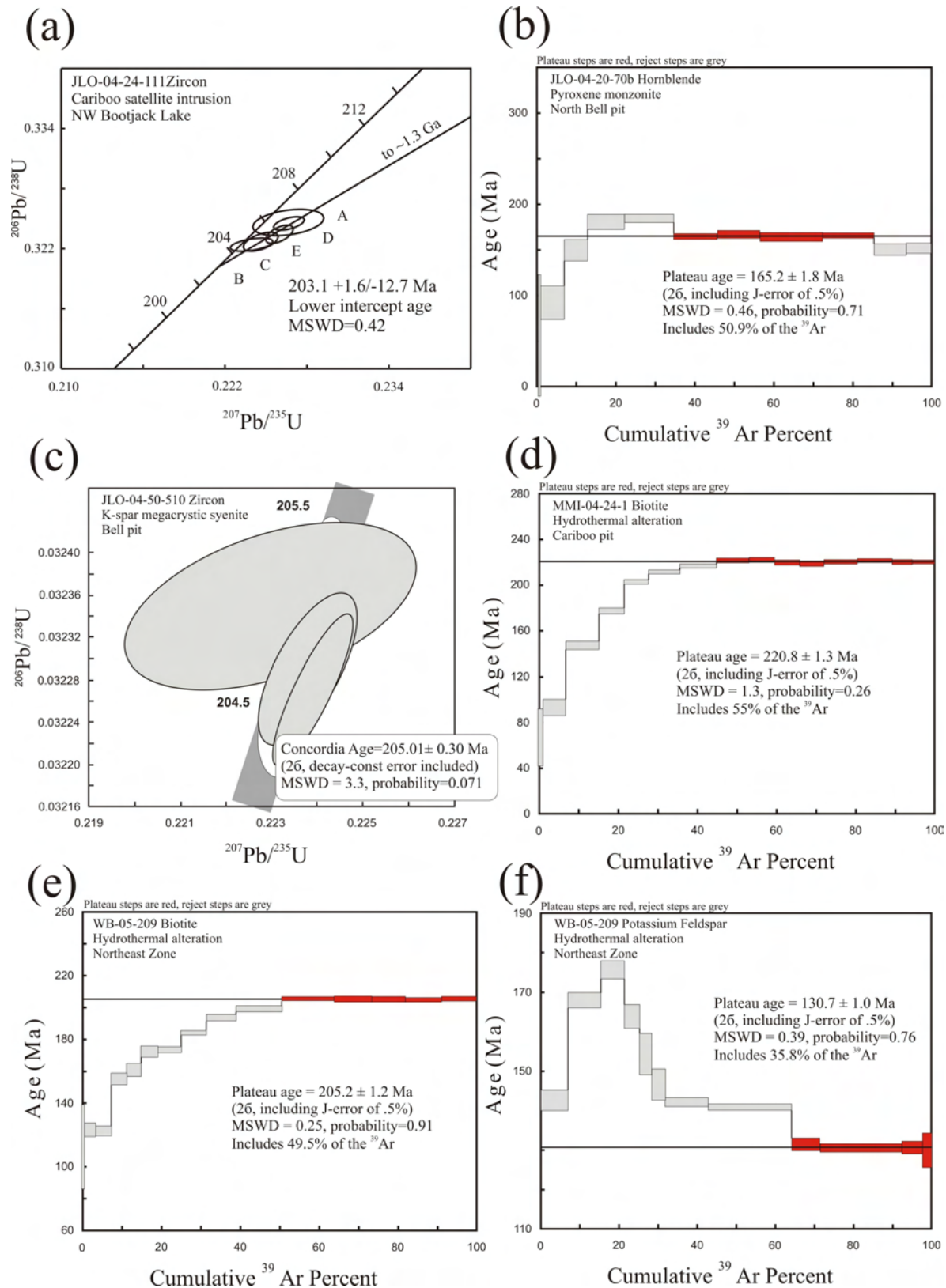


Figure 6. a) Concordia plot of U-Pb thermal ion mass spectrometry (TIMS) data for zircon samples JLO-04-24-111 from northwest Bootjack Lake; A, B, C, D and E correspond to fraction numbers in Table 1; b) step-heating gas release plot for ⁴⁰Ar/³⁹Ar analyses for hornblende samples JLO-04-20-70b from the North Bell pit; c) concordia plot of U-Pb TIMS data for zircon samples JLO-04-50-510 from the Bell pit; d) step-heating gas release plot for ⁴⁰Ar/³⁹Ar analyses for biotite samples MMI-04-24-1 from the Cariboo pit; e) step-heating gas release plot for ⁴⁰Ar/³⁹Ar analyses for biotite samples WB-05-209 from the Northeast zone; f) step-heating gas release plot for ⁴⁰Ar/³⁹Ar analyses for potassium feldspar samples WB-05-209 from the Northeast zone.

alized breccia located close to the northern margin of the MPIC. Alteration at the Northeast zone is similar to that present at the Central and West zone (1.5 km southwest). There are, however, subtle differences, plus mineralization is higher-grade overall with higher Cu: Au ratios, higher silver and bornite content, lower magnetite and higher copper grades, which make it an important exploration target.

A comprehensive petrographic study, augmented by SEM work on the mineralogy at the Northeast zone was completed by Ross (2004) in an unpublished report for Imperial Metals (summarized in Logan and Mihalynuk, 2005a). Ongoing research on the Northeast zone includes melt inclusion studies by A. Bath, carbonate geochemistry by H. Pass (both at CODES, University of Tasmania) and breccia genesis and alteration mineralogy by M. Jackson (MDRU, University of British Columbia).

Biotite is not a common alteration mineral in the Northeast zone, but a mineralized sample containing biotite was sampled from a 7 cm section of split drillcore from 289 m below the collar of diamond drill hole WB-05-209 (kindly contributed by L. Ferreira, Imperial Metals Corporation). The section sampled consists of pervasive potassium-flooded, salmon-pink microporphyritic plagioclase monzonite breccia. The rock is crackle brecciated and variably replaced and veined by chalcopyrite and coarse biotite (1.5–2 mm books). Chalcopyrite and biotite are intimately intergrown and believed to be coeval (Fig 7). Both biotite and potassium feldspar were separated from this sample and analyzed to constrain the cooling history of the alteration and mineralizing system in the Northeast zone (Fig 6e, f).

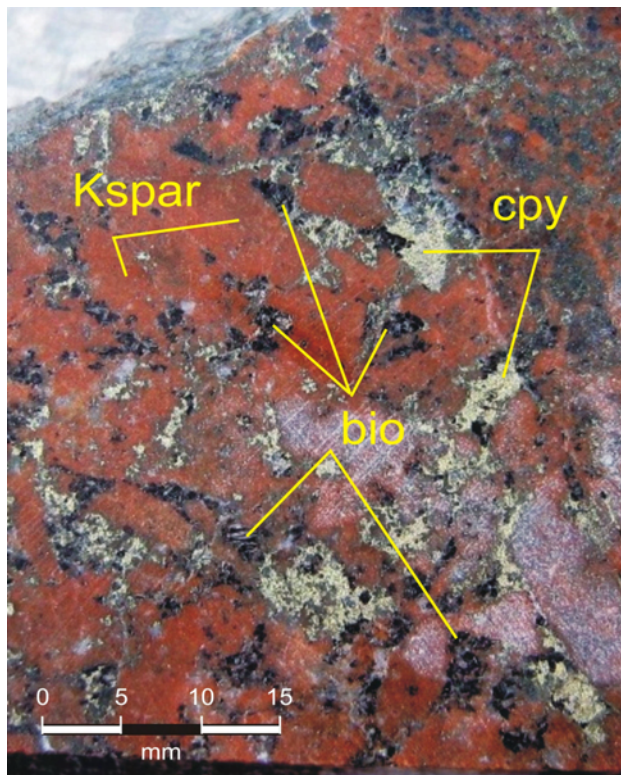


Figure 7. Diamond drill core sample (WB-05-209 at 289 m) of potassic-altered Northeast zone monzonite, showing coarse intergrowths of chalcopyrite and large books of secondary biotite sampled for $^{40}\text{Ar}/^{39}\text{Ar}$ age determination; abbreviations: cpy, chalcopyrite; kspar, potassium feldspar.

The increasing apparent ages displayed in the initial 50.5% of the biotite age spectrum represents a normal diffusion loss profile. A plateau age of 205.2 ± 1.2 Ma calculated from the final 49.5% of the ^{39}Ar provides a good cooling age, which is interpreted as the crystallization age of the biotite. Potassium feldspar separated from the same sample has a complex age spectrum. A plateau age, using 35.8% of the ^{39}Ar in the last 5 heating steps, yielded 130.7 ± 1.0 Ma. The potassium feldspar plateau age yields the same age, as do the lowest temperature steps of the biotite spectrum.

Quartz-Phyric Mauve Andesite (MMI-04-26-18)

Dense, quartz-phyric, white to mauve-weathering lapilli tuff is exposed in two outcrops between Bootjack and northern Polley lakes (Fig 3; Logan and Mihalynuk, 2005a). We used the field term 'mauve dacite' for this unit, but the SiO_2 content (<60%) indicates it is an andesite. It is crystal-rich, composed of tabular and broken plagioclase laths (40%, <3 mm), hornblende (3% altered 2–3 mm prisms), light grey quartz eyes (up to 1% and 5 mm diameter) and biotite (<1%, altered 2–3 mm booklets). The andesite contains undigested accidental fragments, shard-like crystal fragments, broken vesicular clasts and a devitrified glassy matrix (Fig 8). A vague compaction fabric is preserved locally, but clear evidence of collapsed pumice fragments or welding is absent. Possible collapsed pumice blocks are displayed in one outcrop below the Polley Lake road. For these reasons, we maintain that an extrusive origin (*i.e.*, ash flow) best accounts for the formation of this unit.

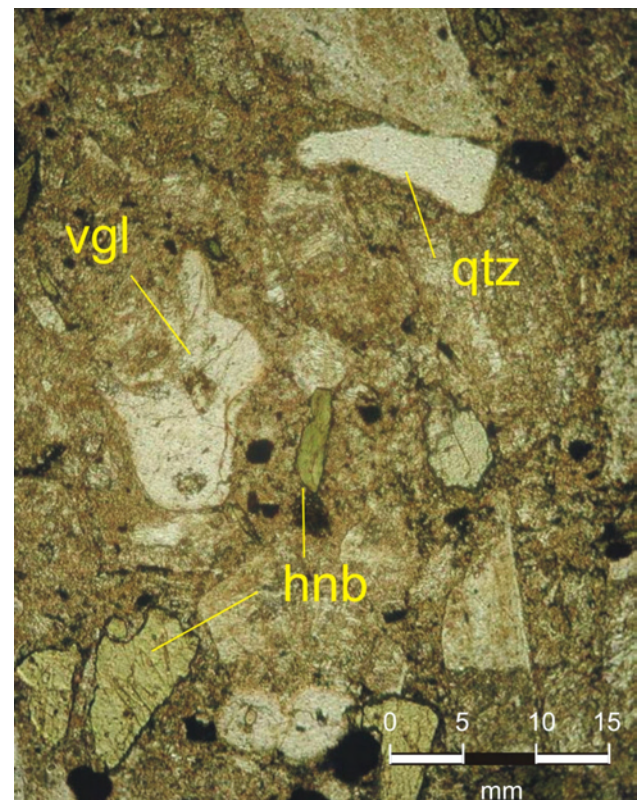


Figure 8. Quartz-phyric mauve andesite tuff. Note the devitrified glassy matrix, curvilinear fragments of vesicular glass (vgl) and crystal shards of hornblende (hnb) and quartz (qtz).

Bedding orientations of enclosing strata are parallel with the trend of the mauve andesite unit. A poorly exposed, probable gradational southern contact with the maroon laharic conglomerate is consistent with a pyroclastic origin and not a hypabyssal intrusion. This volcanic and epiclastic succession is unmineralized; it apparently overlaps mineralized breccia of the MPIC, thereby constraining the maximum age of mineralization.

Approximately 25 kg of the mauve andesite was collected for U-Pb analyses and a determination of a magmatic crystallization age to provide an age limit on the host volcanic stratigraphy. Abundant zircons were recovered from the sample. Zircons are vivid pink, stubby prismatic grains with abundant clear inclusions. Approximately 25 of the coarsest crystals were air abraded and run as 4 multigrain fractions of 2–6 grains each. The interpreted age of 196.7 ± 1.3 Ma is based on two concordant ellipses on concordia (Fig 9a, d). Slightly younger U/Pb results for fractions B and E are attributed to minor Pb loss (Fig 9a).

SHIKO LAKE STOCK

A high-level alkalic stock intrudes Early Jurassic arc strata 15 km southeast of Mount Polley mine, near Shiko Lake (Fig 5). Three separate intrusive phases comprise the stock. These are, from oldest to youngest: a melanocratic, medium-grained, equigranular, biotite-pyroxene monzodiorite; a pink trachytic, medium to coarse-grained, potassium-feldspar-phyric syenite and a leucocratic alkali feldspar quartz syenite. The quartz syenite truncates a well-developed west-striking, 30° north-dipping trachytic fabric in the potassium feldspar megacrystic syenite, which veins and engulfs the earlier diorite. All phases contain mafic xenoliths of olivine-pyroxene-phyric basalt, fine-grained metasedimentary rocks and subvolcanic diorite to monzonite. Xenoliths increase in abundance toward the contact of the stock (Logan and Mihalynuk, 2005a).

Chalcopyrite and minor bornite occur as veins and disseminated clots within all three intrusive phases. Veins cutting the stock are intergrowths of actinolite, potassium feldspar, sphene, magnetite, and pyrite±chalcopyrite. Potassic overgrowths on feldspars and the replacement of hornblende by actinolite and biotite by chlorite are attributed to late deuteric alteration.

Potassium-argon biotite cooling dates on samples from the monzonitic core are reported by Panteleyev *et al.* (1996) as 192 ± 10 Ma and 182 ± 6 Ma, and from a hornblende porphyry dike cutting the stock as 196 ± 7 Ma. A number of macrofossil identifications from the sedimentary rocks intruded by the Shiko stock are Early Jurassic (GSC-C-118687, probable Sinemurian; GSC-C-118685, Lower Sinemurian or possibly Hettangian; GSC-C-118686, Lower Sinemurian, lower Pliensbachian; Tipper, *in* Panteleyev *et al.*, 1996). Panteleyev *et al.* (1996) describe volcanic and intrusive breccia along the southern contact of the stock, which they interpreted to represent the vent zone of an intrusive centre.

Leucocratic Quartz Syenite (JLO-04-21-84)

The leucocratic quartz syenite is a medium to fine-grained equigranular rock characterized by quartz-filled miarolitic cavities and a negligible magnetic susceptibility. It is composed of interlocking tabular plagioclase laths (30%, <1 mm), equant orthoclase crystals (50%, 1–

1.5 mm), interstitial vitreous quartz (18%), rare chloritic hornblende (3%, <1 mm) and biotite (<1%, altered <1 mm booklets). Accessory minerals include zircon, present as crystal aggregates or small euhedral crystals, apatite, calcite and pyrite.

A 20 kg sample of leucocratic quartz syenite was collected from a quarry at the western end of the stock for an age determination. It was selected because it is demonstratively the youngest mineralized phase. In addition, it is quartz saturated and possibly unrelated to other mineralized alkaline bodies in the Quesnel belt. The sample yielded clear, amber, euhedral to subhedral broken zircon crystals and a smaller population of complete grains of zircon. Approximately 30 of the best-quality grains (pieces and available complete crystals) were selected for analysis (*see* photo) and were strongly air abraded. During this process, much of the material was broken along internal fractures, ending up as smaller subrounded pieces. The clearest of these fragments ($n = 6–10$ per fraction) were selected for analysis. Uranium-lead results for the five analyzed fractions reflect minor Pb loss only; results are 0 to 3.5% discordant. The age estimate of 191.6 ± 5.3 Ma is based on the calculated $^{207}\text{Pb}/^{206}\text{Pb}$ weighted mean, which is equivalent to the upper intercept of a regression anchored through 0 m.y. and all five fractions, as shown on standard concordia plot for this sample (Fig 9b).

WOODJAM PROPERTY

The Woodjam property is located approximately 35 km southeast of the Mount Polley copper-gold mine. It is underlain by hornfelsed Late Triassic Nicola Group volcanic and related sedimentary rocks within the contact metamorphic aureole of the Early Jurassic Takomkane batholith; a composite, quartz-saturated calcalkaline intrusion composed of hornblende monzodiorite to hornblende-biotite monzogranite. Intrusive rocks dominate the eastern portion of the property and to the west, Miocene to Pleistocene alkali olivine flood basalt of the Chilcotin Group overlie Nicola Group volcanic rocks (Wetherup, 2000; Peters, 2005). Three zones of porphyry Cu-Au mineralization (Megabuck, Takom and Spellbound) are reported for the property (Fig 10).

The Megabuck zone (400 m by 350 m) occurs within crowded plagioclase and hornblende-plagioclase-porphyrific volcanic breccia, tuff and fine-grained reworked clastic rocks and possibly coeval intrusive rocks. Mineralization consists of an early quartz-magnetite-chalcopyrite±gold stockwork system overprinted by carbonate±chalcopyrite-pyrite veinlets and surrounded by a pyritic halo. At the centre of the zone where veinlet intensity is highest, the volcanoclastic sequence is flooded with potassium feldspar and replaced by blebs of quartz, magnetite/hematite and chalcopyrite intergrowths. Quartz veinlets and stockworks contain chalcopyrite, lesser bornite and rare pyrite. Gold values show good correlation with copper, and gold is assumed to occur as microscopic inclusions within chalcopyrite grains.

The Takom zone is located 2.5 km south of the Megabuck zone. The Spellbound zone is located 2.5 km east of the Megabuck zone. Both zones are characterized by a weak quartz-chalcopyrite stockwork developed in weak to strong epidote±tourmaline hornfelsed volcanoclastic units situated adjacent to the north-trending contact of the Takomkane batholith. Quartz-carbonate vein stockworks

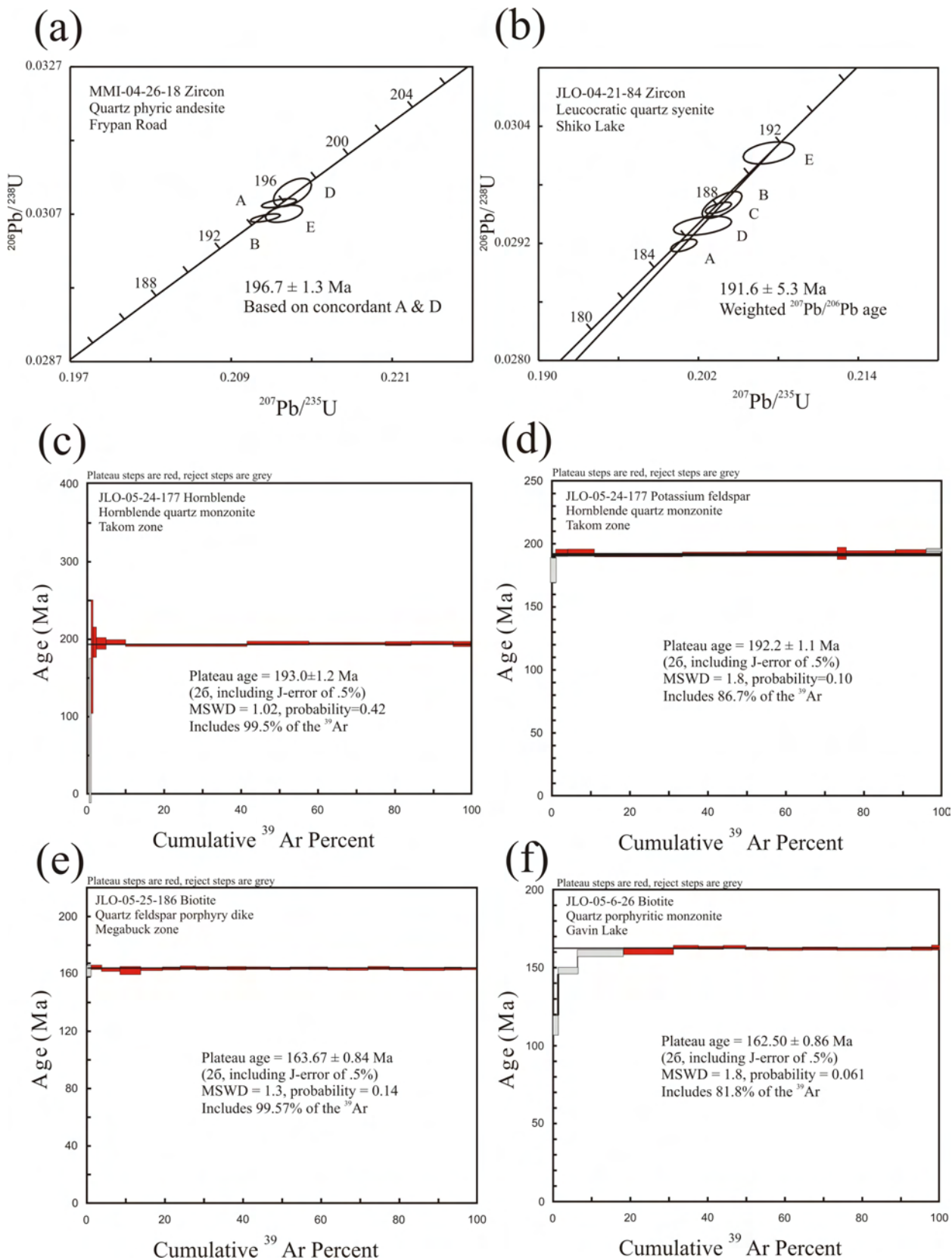


Figure 9. a) Concordia plots of U-Pb thermal ion mass spectrometry (TIMS) data for zircon samples MMI-04-26-18 from Frypan Road; A, B, C, D and E correspond to fraction numbers in Table 1; b) concordia plots of U-Pb TIMS data for zircon samples JLO-04-21-84 from Shiko Lake; A, B, C, D and E correspond to fraction numbers in Table 1; c) step-heating ^{39}Ar release plots for $^{40}\text{Ar}/^{39}\text{Ar}$ analyses from hornblende samples JLO-05-24-177 from the Takom zone; d) step-heating ^{39}Ar release plots for $^{40}\text{Ar}/^{39}\text{Ar}$ analyses for potassium feldspar samples JLO-05-24-177 from the Takom zone; e) step-heating ^{39}Ar release plots for $^{40}\text{Ar}/^{39}\text{Ar}$ analyses from biotite samples JLO-05-25-186 from the Megabuck zone; f) step-heating ^{39}Ar release plots for $^{40}\text{Ar}/^{39}\text{Ar}$ analyses for biotite samples JLO-05-6-26 from Gavin Lake. All errors are displayed as 2σ level of uncertainty.

at the Takom zone cut bleached, clay-altered pyroxene and feldspar porphyry flows and tuff where hornblende monzodiorite and quartz diorite apophyses of the Takomkane batholith intrude the sequence.

Absolute ages of the hornblende and feldspar crystal tuff, breccia and subvolcanic rocks that host mineralization on the Woodjam property were not previously known. Cannon and Pentland (1983) and Panteleyev *et al.* (1996) con-

cluded that they are Eocene in age; Wetherup (2000), Lane (2006) and this study believe that they are Late Triassic Nicola Group – equivalent units. The tuff and volcanic breccia exhibit weak to strong epidote alteration and hornfels that increases in intensity with proximity to the Early Jurassic Takomkane batholith and supports an older Mesozoic age; however, podiform epidote replacements, potassium feldspar and tourmaline, sericite, pyrite, quartz

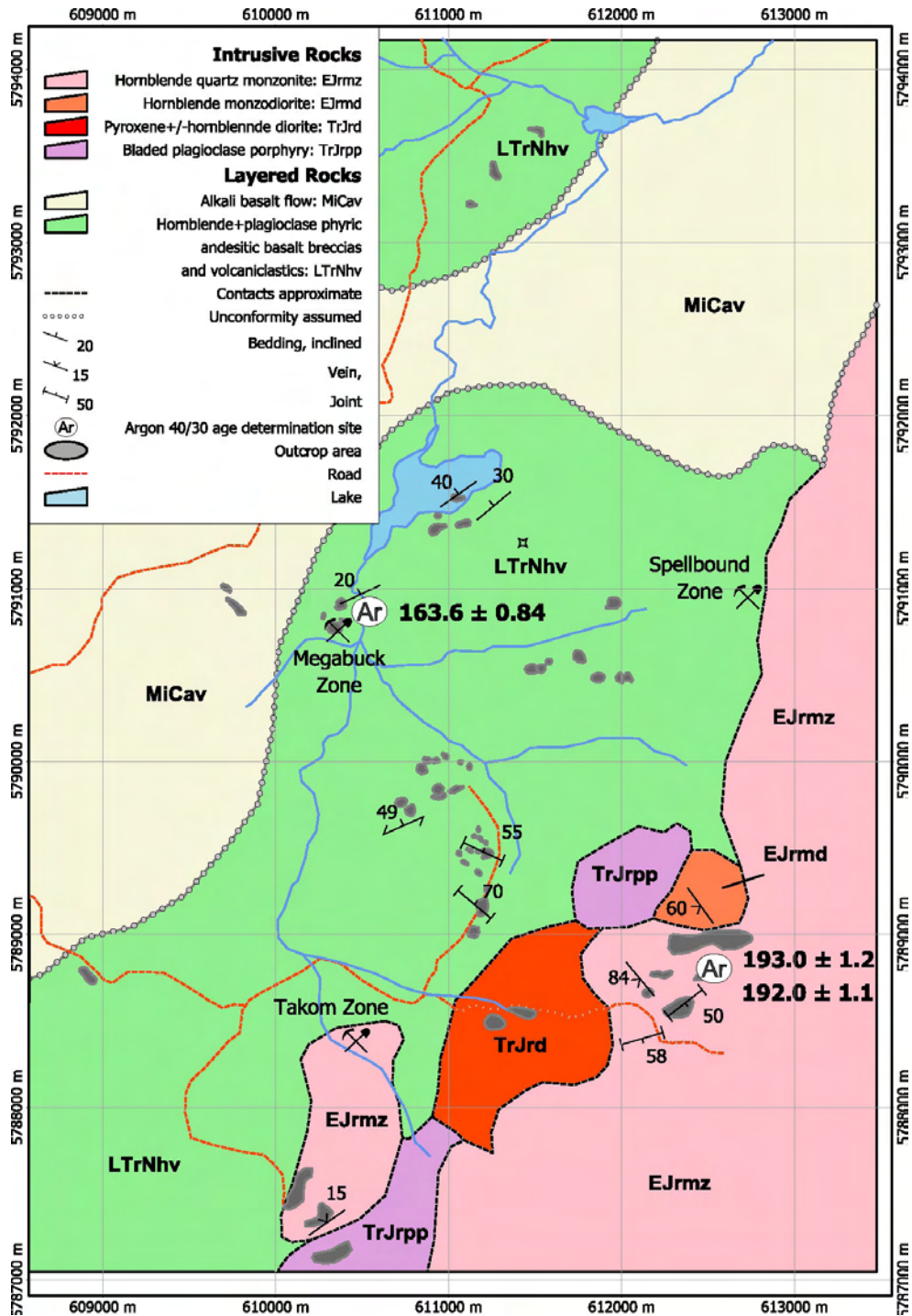


Figure 10. Compilation map of the Woodjam property showing the locations of $^{40}\text{Ar}/^{39}\text{Ar}$ isotopic age determination sites and analytical results. Incorporates unpublished assessment work by Wetherup (2000).

stockwork alteration affects both the Early Jurassic intrusion and host country rocks, and could be related to a younger event. Analogy with the Mount Polley Mine has been suggested, but the Quesnel belt alkaline Cu-Au porphyry is typically quartz undersaturated, not characterized by quartz stockwork, and they are Late Triassic in age. A better analogy might be the mineralization at the Mount Milligan deposit. It comprises four zones situated within and adjacent to the west-dipping Early Jurassic MBX stock (Sketchley *et al.*, 1995). East of the stock, in the footwall, is the copper-gold MBX, which to the south passes into the gold-rich, copper-poor 66 zone. To the west, in the hangingwall of the stock, are the WBX and DWBX zones, where chalcopyrite and gold mineralization is associated with quartz veins. Woodjam mineralization is most similar to the WBX and DWBX zones.

To better understand the relationships between the silica-rich hydrothermal mineral system at the Megabuck zone and the Takomkane batholith, $^{40}\text{Ar}/^{39}\text{Ar}$ age dating was undertaken. Two samples were collected: one from the main phase of the Takomkane batholith and the other from a post-mineralization quartz-feldspar porphyry (QFP) dike that cuts Cu-Au mineralization at the Megabuck zone.

Hornblende Quartz Monzonite (05JLO-24-177)

A medium to coarse-grained equigranular hornblende±biotite quartz monzonite comprises the main phase of the Takomkane batholith, where it crops out along the eastern side of the Woodjam property. The batholith contact trends north-northeast and is characterized by a mixed border phase that includes hornblende quartz diorite, pyroxene monzodiorite and distinctive bladed feldspar porphyry (Wetherup, 2000). Regional aeromagnetic patterns suggest that the batholith border may underlie the hornblende-plagioclase porphyritic breccia, tuff and volcanoclastic rocks on the western portion of the Woodjam property.

A sample was collected from the main medium-grained, equigranular quartz monzonite exposed approximately 1 km east of the Takom zone (Fig 10). The monzonite is massive, homogeneous and unaltered. Locally, it contains ovoid epidote+plagioclase+tourmaline nodules (1–2 cm) or is cut by centimetre-wide potassium feldspar veins. Both of these features were avoided during sample collection. The collected sample contains hornblende (8–10%, 1–1.3 cm), biotite (1%, 1–2 mm), feldspar (3–6 mm) and subrounded quartz (19%) with accessory amounts of tourmaline, magnetite, apatite, epidote and pyrite.

Hornblende and potassium feldspar were separated from the quartz monzonite and analyzed separately to constrain the cooling history of the unit (Fig 9c, d). The age for the hornblende separate gave 193.0 ± 1.2 Ma, with only minor Ar loss displayed in the earliest heating step. The plateau age includes 99.59% of the ^{39}Ar and provides a good undisturbed cooling age that is interpreted as the crystallization age. Potassium feldspar from this same sample gave a well-defined Ar/Ar plateau age of 192.2 ± 1.1 Ma, represented by 86.7% of the ^{39}Ar . This is essentially identical within error; hornblende and potassium feldspar plateau ages for this sample support an undisturbed cooling age of ca. 193 Ma.

Quartz-Feldspar Porphyry Dike (05JLO-25-186)

A quartz-feldspar porphyry dike intrudes hornblende-phyric metavolcanic rocks at the Megabuck showing on the Woodjam property. The dike was intersected over a 12 m interval near the bottom of diamond drillhole WJ04-37. The dike contains stubby white plagioclase laths (40%, 3 mm), light grey quartz eyes (up to 5% and 5 mm diameter) and biotite (<1%, fresh 2–3 mm booklets), in a fine-grained altered matrix of quartz, plagioclase and potassium feldspar. Five 2 m assay samples collected across the dike returned mean values of 0.001% Cu and 0.01 g/t Au (Peters, 2005). The dike is unmineralized and is assumed to post-date mineralization. The footwall contact to the dike is faulted, and below this fault, some of the better copper and gold grades were encountered (2.05 m of 0.496% Cu and 0.205 g/t Au, and 1.74 m of 1.805% Cu and 2.204 g/t Au; Peters, 2005).

Biotite was separated from the QFP dike and analyzed to constrain the age of mineralization. Although the dike is friable and the groundmass is altered to pale, chalky clay minerals, the euhedral biotite phenocrysts are very fresh. The biotite returned an age of 163.67 ± 0.84 Ma, with only minor Ar loss displayed in the earliest two heating steps (Fig 9e). The plateau age includes 99.57% of the ^{39}Ar and provides a good undisturbed cooling age for the quartz-feldspar porphyry dike that crosscuts host volcanic rocks and mineralization at the Megabuck zone.

GAVIN LAKE

The western portion of the Quesnel belt at this latitude is well defined by the north-northwest-trending edge of the Mount Polley aeromagnetic anomaly. Volcanic rocks in the belt are intruded by metre to decimetre-wide quartz porphyritic monzogranite dikes (Fig 5). The dikes consist of a fine-grained leucocratic matrix, variable amounts of finely disseminated pyrite and up to 10% euhedral quartz phenocrysts. Biotite, to several percent, and rare hornblende is present, but both are commonly completely replaced by sericite and carbonate. Weathering produces a distinctive limonitic, pinkish, fine-grained massive rock with conspicuous (2–8 mm) quartz phenocrysts. The largest concentration of these intrusive rocks occur at Gavin Lake, where a coalescing swarm of east-trending dikes and small quartz monzonite porphyry plugs intrude volcanic sedimentary rocks in an area approximately 1 km by 4 km immediately north of the lake (Logan and Bath, 2005). Sparse chalcopyrite and molybdenite mineralization is associated with quartz and potassium feldspar stockwork veining in the dikes. A similar swarm of carbonate-altered quartz-eye porphyritic monzogranite intrusions crop out along the Quesnel River, 80 km northwest of Gavin Lake, at the Kate showing. There, Cu, Au and Mo mineralization occupies narrow quartz and quartz-carbonate stockwork veinlets in the monzogranite. Pyrite dominates, with less abundant chalcopyrite, and assays return a distinctive metal assemblage elevated in bismuth, antimony, arsenic and silver values. Bailey (1978) and Panteleyev *et al.* (1996) correlate these quartz-bearing calcalkaline intrusions with hornblende-biotite monzogranite of the Nyland Lake stock and include them in the Cretaceous, Naver plutonic suite (Woodsworth *et al.*, 1991).

Quartz-Plagioclase-Porphyrific Monzogranite (05JLO-06-26)

A sample of least-altered, porphyritic quartz-plagioclase monzogranite was collected from an exploration trench located north of the east end of Gavin Lake. The rock has conspicuous euhedral plagioclase (25%, 2–3 mm), subhedral to rounded vitreous quartz phenocrysts (10%, 2–6 mm) and fresh euhedral black books of biotite (3–4%, 1 mm) in a fine-grained groundmass (55–60%) of potassium feldspar, plagioclase, quartz and opaque minerals. It is cut by narrow (0.5–1 cm wide) sheeted quartz veins mineralized with variable amounts of pyrite and chalcopyrite.

Igneous biotite was separated from the porphyritic monzogranite and analyzed to constrain the cooling history for this calcalkaline episode of magmatism and provide a minimum age for alteration and mineralization. Steps 4 through 14 of the ^{39}Ar release spectrum represent 81.4% of the total ^{39}Ar and yield a plateau age of 162.5 ± 0.86 Ma. Minor Ar loss is displayed in the earliest low-temperature heating steps (Fig 9f). The plateau age is slightly too old due to the presence of excess argon. An inverse isochron plot, based on 11 points, yielded a correlation age of 161.77 ± 0.99 Ma (mean standard weighted deviate = 1.13), which agrees within error with the calculated plateau age. The integrated (or total gas) age of 160.46 ± 0.53 Ma is also similar to the correlation age because the sample is so highly radiogenic that the excess argon makes little difference to the calculated age.

Quartz-Plagioclase-Porphyrific Monzogranite (05JLO-06-27)

A 20 kg sample of quartz-plagioclase-porphyrific monzogranite was collected from an outcrop located north of the Gavin Lake Road, midway along the length of Gavin Lake. Zircons are clear to slightly cloudy, subhedral (slightly rounded and resorbed) prisms with cores that are evident in plane light. Cathodoluminescence (CL) imaging reveals that most grains are dominated by cores with relatively narrow rims. Some grains feature irregularly shaped rims that extend well into the interior, indicating that significant resorption occurred during magmatism (Fig 11b). Uranium-lead TIMS results for seven multigrain fractions and single grains that lie between about 185 Ma and 260 Ma are interpreted as mixtures of rim and core material or for the older grains, possibly a record of the age of the core. It is likely that for these latter grains, the narrow cores may have been completely removed during air abrasion. The youngest TIMS result at ca. 187 Ma is considered as a maximum age constraint (Fig 11a).

Laser ablation ICP-MS U-Pb dating was undertaken in order to better isolate the ages of cores and rims. The data are listed in Table 2. Figure 11c is a concordia plot of the laser ablation U-Pb data, highlighting the difference between core and rim ages. Cores are mainly ca. 200 to 240 Ma and rims are ca. 160 Ma. A composite rim age of 160.0 ± 2.3 Ma, based on a weighted average of eight $^{206}\text{Pb}/^{238}\text{U}$ dates (Fig 11d), is thought to record a minimum crystallization age for the intrusion. At the 2σ level of uncertainty, this date is statistically equivalent to the biotite Ar/Ar date of 162.5 ± 0.9 Ma.

INTERPRETATION AND DISCUSSION

Geochronological results from the Iron Mask batholith and Mount Polley studies corroborate earlier work and also provide new age constraints on the limits of alkaline and calcalkaline-related porphyry mineralization in the central Quesnel Terrane. Applied regionally, these results help clarify the Mesozoic metallogenic evolution of this part of the Quesnel Terrane (52.5°N). Geochronological results from this study are summarized in Table 3.

Mineral exploration and property assessment are assisted by deposit models. The recognition of the most appropriate deposit model and, in the case of BC alkaline Cu-Au porphyry deposits, the correct magmatic suite, is important for the early stage of deposit evaluation. The recognition of alkaline versus calcalkaline alteration and mineral zonation patterns are important steps to the evaluation of nascent mineral exploration targets. This is particularly true in areas with limited exposure, like many parts of the Intermontane Belt.

Iron Mask Batholith

The ages reported here for plutonic rocks and hydrothermal titanite from the Iron Mask batholith include the first cooling ages obtained for the Sugarloaf diorite. They support the stratigraphy proposed by Snyder (1994) and Snyder and Russell (1995). The U-Pb crystallization ages for samples of the Pothook, Hybrid and Cherry Creek phases of the Iron Mask batholith (Mortensen *et al.*, 1995) fall within the age range of 204 ± 3 Ma. The Sugarloaf diorite is the youngest phase (from crosscutting relationships) but eludes U-Pb techniques due to low zircon content. The $^{40}\text{Ar}/^{39}\text{Ar}$ cooling age determinations for hornblende from two samples of Sugarloaf diorite give ages of 200.1 ± 2.5 Ma and 196.3 ± 1.3 Ma. The young $^{40}\text{Ar}/^{39}\text{Ar}$ ages for the Sugarloaf diorite are consistent with, and overlap the error envelope of the titanite cooling age for the Ajax hydrothermal assemblage. Mineralization at both the Rainbow and Gold zones is hosted by Sugarloaf hybrid units and altered hornblende porphyry phases of Sugarloaf diorite, and are likely related to late-stage fluids generated from these same phases.

Magmatic foliation in the hybrid phase is consistently oriented $\sim 280^\circ$, suggesting tectonic control on the emplacement and cooling of the Iron Mask batholith. The timing of deformation is further constrained by a single 206.9 ± 2.2 Ma cooling age for lineated pegmatitic hornblende segregations (MMI-04-4-1a) of hybrid rocks from north of Jacko Lake. The cooling age is older, but within error of the crystallization age (204.6 ± 2.6 Ma) reported by Mortensen *et al.* (1995) for the hybrid phase. Schistosity is well developed within carbonate porphyroblastic augite tuff and sericitic metasediment near the south rim of the Ajax West Pit. There, Sugarloaf dike rocks are also weakly foliated. Sericite from a foliated augite tuff (JLO-04-2-17a) yielded a complex spectra with a plateau age of 205.6 ± 1.3 Ma, coeval within error with hornblende having a preferred orientation within the Hybrid phase, but predates the cooling/crystallization ages of the two Sugarloaf diorite samples (JLO-04-6-67 and MMI-04-1-6). The age spectra also contain evidence for a younger (ca. 189 Ma) cooling event in the high-temperature steps, probably reflecting known regional Early Jurassic magmatism.

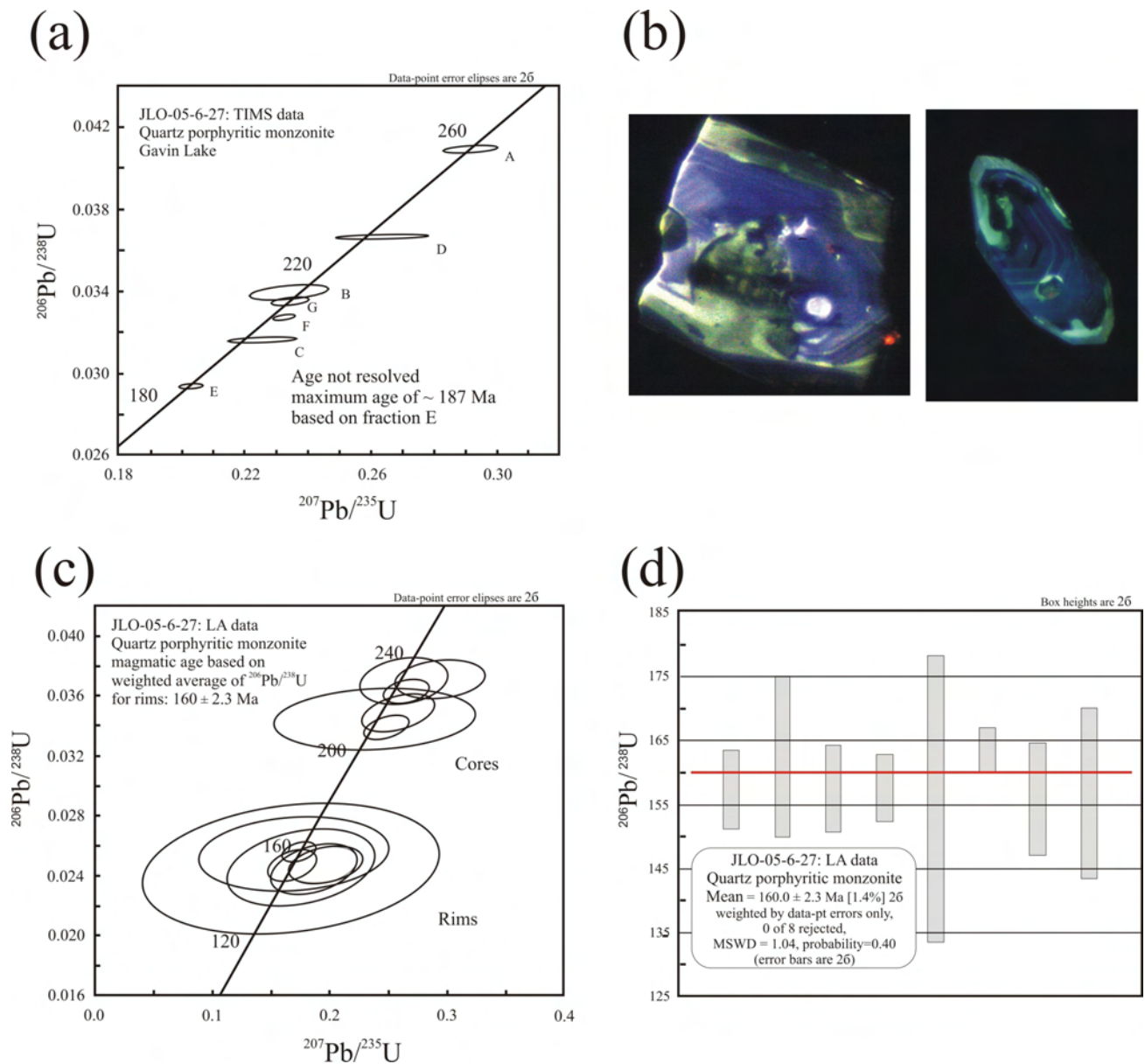


Figure 11. U-Pb concordia plots for thermal ionization mass spectrometry (TIMS); a) and laser ablation; A, B, C, D, E, F and G correspond to 7 multigrain fractions in Table 1; b) two cathodoluminescence images of single zircon grains show complex core-rim geometry and fine-scale igneous zoning in their cores. Dark lines are laser tracks across greenish rim (right image) and blue core material (right side of left image). The length of the crystals is ~0.2 mm; c) U-Pb concordia plots for TIMS data for zircon fractions from Gavin Lake porphyritic quartz monzonite; d) crystallization age based on a weighted average of eight $^{206}\text{Pb}/^{238}\text{U}$ dates from laser ablation data of zircon rims. All errors are displayed at the 2 σ level of uncertainty.

The crystallization age of 198.5 ± 4.5 Ma for hydrothermal titanite is assumed to represent the age of vein mineralization hosted in the Iron Mask Hybrid unit. The geometry of the vein and *en échelon* tension gash system is consistent with tops-to-the-southeast sense of motion at the time of mineralization. The 104.6 ± 0.67 Ma $^{40}\text{Ar}/^{39}\text{Ar}$ cooling age for potassium feldspar separate from the vein suggests that the system was susceptible to a low-temperature thermal overprint until the mid-Cretaceous.

Mount Polley Area

The U-Pb and $^{40}\text{Ar}/^{39}\text{Ar}$ ages reported here are similar within error to previously published crystallization and cooling ages for intrusive rocks and alteration assemblages in the central Quesnel belt (Bailey, 1988, 1990; Panteleyev, 1986, 1987; Mortensen *et al.*, 1995; Panteleyev *et al.*, 1996). Geochronological data for plagioclase porphyry, pyroxene monzonite, potassium megacrystic syenite and

TABLE 3. SUMMARY OF U-PB AND ⁴⁰AR/³⁹AR ANALYSES.

Sample no	Location	Unit ^a	Method	Mineral ^b	Age ±2σ error (Ma)	Age interpretation
Iron Mask						
MMI-04-4-1a	Jacko Lake	Hybrid - pegmatitic	Ar/Ar	HRNBLD	206.9 ±2.2	Plateau age taken as crystallization age
JLO-04-2-17a	Ajax W, S wall	Foliated augite tuff	Ar/Ar	SERICITE	205.6 ±1.3	Complex plateau, Ar recoil effects
JLO-04-6-67	Sugarloaf Hill	Sugarloaf diorite	Ar/Ar	HRNBLD	200.1 ±2.5	Plateau age taken as crystallization age
MMI-04-1-6	Au zone	Sugarloaf diorite	Ar/Ar	HRNBLD	196.3 ±1.3	Plateau age taken as crystallization age
JLO-04-2-14	Ajax W, N wall	Mineralized vein	Ar/Ar	KSPAR	104.6 ±0.67	Plateau age taken as crystallization age
JLO-04-2-14	Ajax W, N wall	Mineralized vein	U/Pb	TITANITE	198.5 ±4.5	3 concordant, overlapping fractions taken as crystallization age
Mount Polley						
JLO04-24-111	Satellite stock	Pyroxene monzonite	U/Pb	ZIRCON	203.1 +1.6/-12.7	Lower intercept age of 5 point regression
JLO04-20-70b	N Bell pit	Pyroxene monzonite	Ar/Ar	HRNBLD	165.2 ±1.8	Possible pyroxene contamination & Ar recoil
JLO04-50-510	Bell pit	Kspar megacrystic monz	U/Pb	ZIRCON	205.01 ±0.3	Combined errors on three concordant fractions
MMI04-24-1	Cariboo	Hydrothermal alteration	Ar/Ar	BIOTITE	220.8 ±1.3	Plateau age taken as crystallization age
WB-05-209	NE zone	Hydrothermal alteration	Ar/Ar	BIOTITE	205.2 ±1.2	Plateau age taken as crystallization age
WB-05-209	NE zone	Hydrothermal alteration	Ar/Ar	KSPAR	130.7 ±1.0	Complex plateau, contamination or excess Ar
MMI04-26-18	Fry Pan Road	Quartz-phyric andesite	U/Pb	ZIRCON	196.7 ±1.3	Crystallization age based on two concordant fractions as crystallization age
JLO04-21-84	Shiko Lake	Quartz syenite	U/Pb	ZIRCON	191.6 ±5.3	Weighted mean ²⁰⁷ Pb/ ²⁰⁶ Pb age, minor Pb loss
JLO 24-177	Takome zone	Hornblende quartz monz	Ar/Ar	HRNBLD	193.0 ±1.2	Plateau age taken as crystallization age
JLO 24-177	Takome zone	Hornblende quartz monz	Ar/Ar	KSPAR	192.2 ±1.1	Plateau age taken as crystallization age
JLO 25-186	Megabuck zone	Quartz-feldspar porphyry	Ar/Ar	BIOTITE	163.6 ±0.84	Plateau age taken as crystallization age
JLO 6-26	Gavin Lk	Quartz phyric monz	Ar/Ar	BIOTITE	162.5 ±0.86	Plateau age taken as crystallization age
JLO 6-27	Gavin Lk	Quartz phyric monz	U/Pb	ZIRCON	160.0 ±2.3	Weighted average ²⁰⁶ Pb/ ²³⁸ U age for rims taken as crystallization age

^a Kspar, potassium feldspar; monz, monzonite

^b KSPAR, potassium feldspar; HRNBLD, hornblende

diorite phases of the Mount Polley intrusive complex range between 204.7 ±3 Ma (Mortensen *et al.*, 1995; this study) and *ca.* 197 Ma. The youngest *ca.* 197 Ma age limit is defined by quartz-phyric andesite tuff that apparently overlaps the mineralized Mount Polley Igneous Complex (MPIC) and was deposited following local emergence and incision of the arc. Quartz-bearing andesite tuff, volcanic conglomerate and interbedded hornblende-phyric volcanoclastic rocks unconformably (?) overlie the MPIC north of Polley Lake Road. The sequence is unmineralized and characterized by low-temperature white and pink zeolite assemblages but not potassic, albitic or calcisilicate hypogene alteration assemblages. Stratigraphic and petrographic relationships support an extrusive origin for the tuff and a change from quartz-undersaturated to quartz-saturated magmatism and isolated volcanism.

In this study, ⁴⁰Ar/³⁹Ar age determinations for biotite associated with chalcopyrite mineralization from the Northeast zone (Wight Pit) gave a date of 205.2 ±1.2 Ma, which we regard as the age of mineralization. This age is indistinguishable from the U-Pb crystallization age of a potassium feldspar megacrystic dike in the Bell pit (205.01 ±0.3 Ma) and consistent with high-level emplacement and rapid cooling of the intrusive complex. Map relations in the pits and drillcore show that alteration and brecciation followed the intrusion of the megacrystic dike phase because fragments of this unit are present in the Northeast zone breccia. Mineralization postdates breccia formation that was restricted to a single, main event, due to the paucity of clasts of breccia within breccia zones. Northeast zone copper mineralization, however, appears to have been introduced in two stages. First-stage chalcopyrite, as an interconnected network of fractures and veinlets, is overprinted by later bornite, rimming and replacing chalcopyrite, and focused in steep northwest-trending centimetre-thick sheeted veins.

Pervasive potassic alteration precedes breccia formation and mineralization at Mount Polley; therefore, the 130.7 ±1.0 Ma potassium feldspar plateau age for WB-05-209 must reflect a much younger, probably local, thermal overprint. Young, low-temperature (*i.e.*, below the Ar closure temperature for biotite, 300–350°C) hydrothermal event(s) could reset the *ca.* 205 Ma mineralizing event in the potassium feldspar. Plutonic potassium feldspar has Ar closure temperatures of 200 to 225°C (Foland, 1994) or as low as 150°C (McDougall and Harrison, 1999). Evidence for a *ca.* 130 Ma magmatic or thermal event in this part of the Quesnel belt has not been previously documented, although Mortimer *et al.* (1990) report a 130 Ma date from lamprophyre dikes that crosscut Quesnel Terrane Nicola Group rocks east of Kamloops.

Biotite cooling ages (below 350°C) for the MPIC include the 205.2 ±1.2 Ma plateau age from the Northeast zone (WB-5-209) and the 220.8 ±1.3 Ma plateau age from coarse hydrothermal alteration assemblages associated with hypogene mineralization in the Cariboo pit (MMI-04-24-1). The relatively undisturbed age spectrum for biotite associated with hypogene mineralization in the Northeast zone contrasts sharply with the biotite cooling ages from the Cariboo pit. The biotite plateau age for Cariboo pit sample MMI-04-24-1 predates crystallization ages of the MPIC rocks by approximately 15 Ma. We believe this age to be erroneous. Cooling ages calculated for hornblende (203.1 ±2.0 Ma) and titanite (200.7 ±2.8 Ma) from the Bootjack stock (Bailey and Archibald, 1990; Mortensen *et al.*, 1995) indicate variable but considerably slower cooling (below 600–550°C) for this intrusion (*i.e.*, younger ages for minerals with higher closure temperatures).

Satellite plugs of pyroxene monzonite crop out peripheral to the MPIC. Sample JLO-04-24-111 has a U-Pb zircon crystallization age of 203.1 +1.6/-12.7 Ma, which overlaps within error the U-Pb zircon crystallization age range of the

MPIC. Sample JLO-04-20-70b is mineralogically identical to other Late Triassic pyroxene monzonite, but has a Middle Jurassic $^{40}\text{Ar}/^{39}\text{Ar}$ plateau age (165.2 ± 1.8 Ma). This age is interpreted to reflect a Middle Jurassic thermal overprint and is complicated by excess argon and recoil related to contamination. Petrographic analysis of this sample shows that the hornblende is chloritic and makes up a much smaller component of the monzonite than initially assumed, thus, it is probable that the hornblende separated for $^{40}\text{Ar}/^{39}\text{Ar}$ dating included a significant proportion of pyroxene.

The leucocratic quartz syenite that cuts monzodiorite and trachytic feldspar porphyry syenite of the Shiko Lake stock has a U-Pb zircon crystallization age of 191.6 ± 5.3 Ma. This provides a minimum age for copper-gold mineralization that is hosted in all three units. It is possible, however, that the intrusion of the younger quartz-bearing syenite incorporated and remobilized earlier mineralization associated with the quartz-undersaturated monzodiorite and porphyritic syenite phases. Mineral assemblages in these earlier alkaline phases (actinolite, potassium feldspar, magnetite, pyrite and chalcopyrite) are similar to those in the Cariboo pit at Mount Polley.

Copper and gold quartz stockwork mineralization at the Woodjam property is hosted in epidote-magnetite-pyrite±tourmaline hornfelsed hornblende-plagioclase-phyrical andesitic breccia, bedded volcanoclastic rocks and apophyses of the Takomkane batholith. The Takomkane is a complex batholith that apparently spans the Late Triassic to Early Jurassic boundary (*ca.* 202–193 Ma; Schiarizza and Macauley, 2007), the main phase in the vicinity of the Woodjam property is Early Jurassic (193 Ma). An unmineralized quartz-feldspar-biotite porphyry dike that crosscuts mineralization at the Megabuck zone is herein dated as 163 Ma, providing a minimum age constraint on mineralization (*i.e.*, not Tertiary as previously proposed). The quartz stockwork style of Cu-Au mineralization at the Megabuck is dissimilar to the Late Triassic alkaline centres in the area (*i.e.*, Mount Polley, Shiko Lake and QR) and cuts an Early Jurassic hornfels related to the Takomkane batholith. We interpret the age of the mineralization at the Woodjam property to be Early Jurassic, *ca.* 193 Ma. It is similar in style to *ca.* 183 Ma mineralization at Mount Milligan, ~275 km to the northwest.

Copper and molybdenum quartz stockwork mineralization at Gavin Lake is associated with a quartz-phyrical calcalkaline dike swarm. Geochronology indicates Middle to Late Triassic xenocrystic zircons mantled by Middle Jurassic zircon rims that give concordant ages of *ca.* 160.0 Ma and are interpreted as the age of intrusion. The xenocrystic zircons have originated from either the source region or the wallrocks in the path of ascent, and possess no evidence for any extensive interaction with older North American crust. Regional correlative stocks and dikes are characteristically iron-carbonate altered, pyritic high-level siliceous leucogranite intrusions.

CONCLUSIONS

Magmatic, tectonic and geochronological features of the Iron Mask and Mount Polley areas support the following conclusions:

- intrusion of the main phases of these alkaline intrusive complexes occurred over a short time span in the Late Triassic (204 ± 3 Ma)
- probably in a shallow or subvolcanic environment
- mineralization was focused over a relatively short time interval(s) from 205 to 200 Ma at the Triassic–Jurassic boundary (Woodjam is calcalkaline type and Early Jurassic in age)
- ductile deformation accompanied the intrusion and cooling of the early phases of the Iron Mask batholith

ACKNOWLEDGMENTS

This work was made possible through the financial support of our corporate partners, Abacus Mining and Exploration Corporation and Imperial Metals Corporation. Geochronological sample analyses were conducted in partnership with the Pacific Centre for Isotopic and Geochemical Research at the Department of Earth and Ocean Sciences, The University of British Columbia. We thank Brian Grant and Paul Schiarizza for their careful review of the manuscript.

REFERENCES

- Abacus Mining and Exploration Corporation (2006): Afton Area Properties – Rainbow and DM/Audra/Crescent Resource Summary; *Abacus Mining and Exploration Corporation*, Press release, July 6, 2006, URL <http://www.amemining.com/s/NewsReleases.asp?ReportID=111406&_Type=News-Releases&_Title=Afton-Area-Properties-Rainbow-and-DMAudraCrescent-Resource-Summary> [December 2006].
- Ash, C.H., Reynolds, P.H., Creaser, R.A. and Mihalyuk, M.G. (2007): ^{40}Ar - ^{39}Ar and Re-O isotopic ages for hydrothermal alteration and related mineralization in the Highland Valley Cu-Mo deposit, SW BC; in *Geological Fieldwork 2006, BC Ministry of Energy, Mines and Petroleum Resources*, Paper 2007-1 and *Geoscience BC*, Report 2007-1, pages 19–24.
- Bailey, D.G. (1978): The Geology of the Morehead Lake Area; unpublished PhD thesis, *Queen's University*, 198 pages.
- Bailey, D.G. (1988): Geology of the Hydraulic Map Area, NTS 93A/12; *BC Ministry of Energy, Mines and Petroleum Resources*, Preliminary Map 67, scale 1:50 000.
- Bailey, D.G. (1990): Geology of the Central Quesnel Belt, British Columbia; *BC Ministry of Energy, Mines and Petroleum Resources*, Open File 1990-31, 1:100 000 map with accompanying notes.
- Bailey, D.G. and Archibald, D.A. (1990): Age of the Bootjack Stock, Quesnel Terrane, south-central British Columbia (93A); in *Geological Fieldwork 1989, BC Ministry of Energy, Mines and Petroleum Resources*, Paper 1990-1, pages 79–82.
- Bailey, D.G. and Hodgson, C.J. (1979): Transported altered wall rock in laharic breccias at the Cariboo-Bell Cu-Au porphyry deposit, British Columbia; *Economic Geology*, Volume 74, pages 125–128.
- Barr, D.A., Fox, P.E., Northcote, K.E. and Preto, V.A. (1976): The Alkaline Suite Porphyry Deposits: A Summary; in *Porphyry Deposits of the Canadian Cordillera*, Sutherland Brown, A., Editor, *Canadian Institute of Mining and Metallurgy*, Special Volume 15, pages 359–367.
- Bath, A.B. and Logan, J.M. (2006): Petrography and geochemistry of the Late Triassic Bootjack Stock, south-central British

- Columbia; in Geological Fieldwork 2005, *BC Ministry of Energy, Mines and Petroleum Resources*, Paper 2006-1.
- Breitsprecher, K. and Mortensen, J.K. (2004): BC Age 2004A-1: A database of isotopic age determinations for rock units from British Columbia; *BC Ministry of Energy, Mines and Petroleum Resource*, Open File 2004-03.
- Campbell, R.B. (1978): Quesnel Lake (93A) map-area; *Geological Survey of Canada*, Open File Map 574.
- Cannon, R. and Pentland, W.S. (1983): A geological, geophysical and geochemical report on the Horsefly property; *BC Ministry of Energy, Mines and Petroleum Resources*, AR11379.
- Cockfield, W.E. (1948): Geology and mineral deposits of Nicola map area, British Columbia; *Geological Survey of Canada*, Memoir 249, 164 pages.
- Evans, G. (1992): Property geology map covering the northwest margin of the Iron Mask Batholith in the vicinity of the Pothook pit; *Teck Exploration Ltd*, unpublished 1:2500 map.
- Foland, K. A. (1994): Argon diffusion in feldspars; in *Feldspars and Their Reactions*, Parsons, I., Editor, *Kluwer*, pages 415–447.
- Fraser, T.M. (1994): Hydrothermal breccias and associated alteration of the Mount Polley copper-gold deposit; in *Geological Fieldwork 1993*, *BC Ministry of Energy, Mines and Petroleum Resources*, Paper 1994-1, pages 259–267.
- Fraser, T.M. (1995): Geology, Alteration and the Origin of Hydrothermal Breccias at the Mount Polley Alkaline Porphyry Copper-Gold Deposit, South-Central British Columbia; unpublished MSc thesis, *The University of British Columbia*, 259 pages.
- Fraser, T.M., Stanley, C.R., Nikic, Z.T., Pesalj, R. and Gorc, D. (1995): The Mount Polley Copper-Gold Alkaline Porphyry Deposit, South-Central British Columbia; in *Porphyry Deposits of the Northern Cordillera*, Schroeter, T.G., Editor, *Canadian Institute of Mining and Metallurgy*, Special Volume 46, pages 609–622.
- Ghent, E.D., Erdmer, P., Archibald, D.A. and Stout, M.Z. (1996): Pressure-temperature and tectonic evolution of Triassic lawsonite – aragonite blueschists from Pinchi Lake, British Columbia; *Canadian Journal of Earth Sciences*, Volume 33, pages 800–810.
- Harrison, T.M. (1981): Diffusion of ^{40}Ar in hornblende; *Contributions to Mineralogy and Petrology*, Volume 78, pages 324–331.
- Hodgson, C.J., Bailes, R.J. and Versoza, R.S. (1976): Cariboo-Bell; in *Porphyry Deposits of the Canadian Cordillera*, Sutherland Brown, A., Editor, *Canadian Institute of Mining and Metallurgy*, Special Volume 15, pages 388–396.
- Krogh, T.E. (1982): Improved accuracy of U-Pb ages by the creation of more concordant systems using an air abrasion technique; *Geochimica et Cosmochimica Acta*, Volume 46, pages 637–649.
- Kwong, Y.T.J. (1987): Evolution of the Iron Mask batholith and its associated copper mineralization; *BC Ministry of Energy, Mines and Petroleum Resources*, Bulletin 77, 55 pages.
- Lane, B. (2006): Central Region; in *Exploration and Mining in British Columbia 2005*, *BC Ministry of Energy, Mines and Petroleum Resources*, pages 41–52.
- Lang, J.R. and Stanley, C.R. (1995): Contrasting styles of alkaline porphyry copper-gold deposits in the northern Iron Mask batholith, Kamloops, British Columbia; in *Porphyry Deposits of the Northwestern Cordillera of North America*, Schroeter, T.G., Editor, *Canadian Institute of Mining, Metallurgy and Petroleum*, Special Volume 46.
- Lang, J.R., Lueck, B., Mortensen, J.K., Russell, J.K., Stanley, C.R. and Thompson, J.F.H. (1995): Triassic-Jurassic silica-undersaturated and silica-saturated intrusions in the Cordillera of British Columbia: implications for arc magmatism; *Geology*, Volume 23, pages 451–454.
- Logan, J.M. and Bath, A.B. (2006): Geochemistry of Nicola Group basalt from the central Quesnel trough at the latitude of Mount Polley (NTS 093A/5, 6, 11, 12), central British Columbia; in *Geological Fieldwork 2005*, *BC Ministry of Energy, Mines and Petroleum Resources*, Paper 2006-1, pages 83–98.
- Logan, J.M. and Mihalynuk, M.G. (2005a): Regional geology and setting of the Cariboo, Bell, Springer and Northeast Porphyry Cu-Au zones at Mount Polley, south-central British Columbia; in *Geological Fieldwork 2004*, *BC Ministry of Energy, Mines and Petroleum Resources*, Paper 2005-1, pages 249–270.
- Logan, J.M. and Mihalynuk, M.G. (2005b) Porphyry Cu-Au deposits of the Iron Mask batholith, southeastern British Columbia; in *Geological Fieldwork 2004*, *BC Ministry of Energy, Mines and Petroleum Resources*, Paper 2005-1, pages 271–290.
- Logan, J.M., Mihalynuk, M.G., Ullrich, T.D. and Friedman, R. (2006): Geology of the Iron Mask Batholith; *BC Ministry of Energy, Mines and Petroleum Resources*, Open File Map 2006-11.
- Logan, J.M., Bath, A.B., Mihalynuk, M.G., Ullrich, T.D. and Friedman, R. (2007): Regional Geology of the Mount Polley area, central British Columbia; *BC Ministry of Energy, Mines and Petroleum Resources*, Geoscience Map 2007-1.
- Ludwig K.R. (2003): Isoplot 3.00, a geochronological toolkit for Microsoft Excel; *University of California at Berkeley*, Berkeley Geochronology Center, Special Publication No. 4.
- Mathews, W.H. (1989): Neogene Chilcotin basalts in south-central British Columbia: geology, ages, and geomorphic history; *Canadian Journal of Earth Sciences*, Volume 26, pages 969–982.
- McDougall, I. and Harrison, T.M. (1999): Geochronology and Thermochronology by the $^{40}\text{Ar}/^{39}\text{Ar}$ Method; *Oxford University Press*, 269 pages.
- Mihalynuk, M.G., Erdmer, P., Ghent, E.D., Cordey, F., Archibald, D.A., Friedman, R.M. and Johannson, G.G. (2004): Coherent French Range blueschist: Subduction to exhumation in <2.5 m.y.?; *Geological Society of America*, Bulletin, Volume 116, No. 7/8, pages 910–922.
- Mortensen, J.K., Ghosh, D.K. and Ferri, F. (1995): U-Pb geochronology of intrusive rocks associated with copper-gold porphyry deposits in the Canadian Cordillera; in *Porphyry Deposits of the Northwestern Cordillera of North America*, Schroeter, T.G., Editor, *Canadian Institute of Mining, Metallurgy and Petroleum*, Special Volume 46, pages 142–158.
- Mortimer, N. (1987): The Nicola Group: Late Triassic and Early Jurassic subduction-related volcanism in British Columbia; *Canadian Journal of Earth Sciences*, Volume 24, pages 2521–2536.
- Mortimer, N., van der Heyden, P., Armstrong, R.L. and Harakal, J. (1990): U-Pb and K-Ar dates related to the timing of magmatism and deformation in the Cache Creek Terrane and Quesnellia, southern British Columbia; *Canadian Journal of Earth Sciences*, Volume 27, pages 117–123.
- Nixon, G.T., Archibald, D.A. and Heaman, L.M., (1993): $^{40}\text{Ar}/^{39}\text{Ar}$ and U-Pb geochronometry of the Polaris Alaskan-type complex, British Columbia; precise timing of Quesnellia – North America interaction; in *Geological Association of Canada – Mineralogical Association of Canada Annual Meeting, Program with Abstracts, Joint Annual Meeting*, *Geological Association of Canada*, page 76.
- Northcote, K.E. (1974): Geology of the northwest half of the Iron Mask Batholith; in *Geological Fieldwork 1974*, *BC Ministry of Energy, Mines and Petroleum Resources*, Paper 1975-1, pages 22–26.
- Northcote, K.E. (1977): Preliminary Map No. 26 (Iron Mask Batholith) and accompanying notes; *BC Ministry of Energy, Mines and Petroleum Resources*, 8 pages.

- Oliver, J.L. (1995): Report on the 1994 exploration program Rainbow property; *BC Ministry of Energy, Mines and Petroleum Resources*, AR23917.
- Palfy, J., Smith, P.L. and Mortensen, J.K. (2000): A U-Pb and $^{40}\text{Ar}/^{39}\text{Ar}$ time scale for the Jurassic; *Canadian Journal of Earth Sciences*, Volume 37, pages 923–944.
- Panteleyev, A. (1987): Quesnel Gold belt – alkalic volcanic terrane between Horsefly and Quesnel lakes (93A/6); in *Geological Fieldwork 1986, BC Ministry of Energy, Mines and Petroleum Resources*, Paper 1987-1, pages 125–133.
- Panteleyev, A. (1988): Quesnel mineral belt – The central volcanic axis between Horsefly and Quesnel Lakes (93A/5E, 6W); in *Geological Fieldwork 1987, BC Ministry of Energy, Mines and Petroleum Resources*, Paper 1988-1, pages 131–137.
- Panteleyev, A. and Hancock, K.D. (1989a): Quesnel mineral belt: summary of the geology of the Beaver Creek – Horsefly River map area; in *Geological Fieldwork 1988, BC Ministry of Energy, Mines and Petroleum Resources*, Paper 1989-1, pages 159–166.
- Panteleyev, A., Bailey, D.G., Bloodgood, M.A. and Hancock, K.D. (1996): Geology and mineral deposits of the Quesnel River–Horsefly map area, central Quesnel Trough, British Columbia (NTS 93A/5, 6, 7, 11, 12, 13; 93B/9, 16; 93G/1; 93H/4); *BC Ministry of Energy, Mines and Petroleum Resources*, Bulletin 97, 156 pages.
- Parrish, R., Roddick, J.C., Loveridge, W.D. and Sullivan, R.W. (1987): Uranium lead analytical techniques at the geochronology laboratory, Geological Survey of Canada; in *Radiogenic Age and Isotopic Studies*, Report 1, *Geological Survey of Canada*, Paper 87-2, pages 3–7.
- Paterson, I. and Harakal, J. (1974): Potassium-argon dating of blueschists from Pinchi Lake, central British Columbia; *Canadian Journal of Earth Sciences*, Volume 11, pages 1007–1011.
- Peters, L.J. (2005): Summary technical report on the Woodjam claims, Cariboo Mining District; unpublished report, *Fjordland Exploration Inc.*, 115 pages.
- Preto, V.A. (1967): Geology of the eastern part of the Iron Mask Batholith; in *BC Minister of Mines Annual Report 1967, BC Ministry of Energy, Mines and Petroleum Resources*, pages 137–147.
- Preto, V.A. (1972): Report on Afton, Pothook; in *Geology, Exploration and Mining 1972, BC Ministry of Energy, Mines and Petroleum Resources*, pages 209–220.
- Preto, V.A. (1979): Geology of the Nicola Group between Merritt and Princeton, British Columbia; *BC Ministry of Energy, Mines and Petroleum Resources*, Bulletin 69, 90 pages.
- Preto, V.A., Osatenko, M.J., McMillan, W.J. and Armstrong, R.L. (1979): Isotopic dates and strontium isotopic ratios for plutonic and volcanic rocks in the Quesnel trough and Nicola belt, south-central British Columbia; *Canadian Journal of Earth Sciences*, Volume 16, pages 1658–1672.
- Renne, P.R., Swisher, C.C., III, Deino, A.L., Karner, D.B., Owens, T. and DePaolo, D.J. (1998): Inter-calibration of standards, absolute ages and uncertainties in $^{40}\text{Ar}/^{39}\text{Ar}$ dating; *Chemical Geology*, Volume 145, Numbers 1–2, pages 117–152.
- Roback, R.C., Sevigny, J.H. and Walker, N.W. (1994): Tectonic setting of the Slide Mountain Terrane, southern British Columbia; *Tectonics*, Volume 13, pages 1242–1258.
- Roddick, J.C. (1987): Generalized numerical error analysis with application to geochronology and thermodynamics; *Geochimica et Cosmochimica Acta*, Volume 51, pages 2129–2135.
- Ross, K.V. (1993): Geology of the Ajax East and West, silica-saturated, alkali copper-gold porphyry deposits, Kamloops, south-central British Columbia; unpublished MSc thesis, *The University of British Columbia*, Vancouver, 210 pages.
- Ross, K.V. (2004): Alteration study of the Northeast zone, Mount Polley mine, British Columbia; unpublished report, *Imperial Metals Corporation*, 84 pages.
- Ross, K.V., Godwin, C.I., Bond, L. and Dawson, K.M. (1995): Geology, alteration and mineralization in the Ajax East and Ajax West deposits, southern Iron Mask batholith, Kamloops, British Columbia; in *Porphyry Deposits of the Northwestern Cordillera of North America*, Schroeter, T.G., Editor, *Canadian Institute of Mining, Metallurgy and Petroleum*, Special Volume 46, pages 565–580.
- Schiarizza, P. (1989): Structural and stratigraphic relationships between the Fennel Formation and Eagle Bay Assemblage, western Omineca Belt, south-central British Columbia: implications for Paleozoic tectonics along the paleocontinental margin of western North America; unpublished MSc thesis, *University of Calgary*, Calgary, Alberta, 343 pages.
- Schiarizza, P. and Macauley, J. (2007): Geology and mineral occurrences of the Hendrix Lake area, south-central British Columbia (93A/02); in *Geological Fieldwork 2006, BC Ministry of Energy, Mines and Petroleum Resources*, Paper 2007-1 and *Geoscience BC*, Report 2007-1, pages 179–202.
- Sketchley, D.A., Rebagliati, C.M. and Delong, C. (1995): Geology, alteration and zoning patterns of the Mt. Milligan copper-gold deposits; in *Porphyry Deposits of the Northwestern Cordillera of North America*, Schroeter, T.G., Editor, *Canadian Institute of Mining, Metallurgy and Petroleum*, Special Volume 46, pages 650–665.
- Stacey, J.S. and Kramers, J.D. (1975): Approximation of terrestrial lead isotope evolution by a two-stage model; *Earth and Planetary Science Letters*, Volume 26, pages 207–221.
- Snyder, L.D. (1994): Petrological studies within the Iron Mask batholith, south-central British Columbia; unpublished MSc thesis, *The University of British Columbia*, Vancouver, 192 pages.
- Snyder, L.D. and Russell, J.K. (1993): Field constraints on diverse igneous processes in the Iron Mask Batholith (92L/9); in *Geological Fieldwork 1992, BC Ministry of Energy, Mines and Petroleum Resources*, Paper 1993-1, pages 281–286.
- Snyder, L.D. and Russell, J.K. (1994): Petrology and stratigraphic setting of the Kamloops Lake picritic basalts, Quesnellia Terrane, South-central B.C.; in *Geological Fieldwork 1993, BC Ministry of Energy, Mines and Petroleum Resources*, Paper 1994-1, pages 297–309.
- Snyder, L.D. and Russell, J.K. (1995): Petrogenetic relationships and assimilation processes in the alkalic Iron Mask batholith, south-central British Columbia; in *Porphyry Deposits of the Northwestern Cordillera of North America*, Schroeter, T.G., Editor, *Canadian Institute of Mining, Metallurgy and Petroleum*, Special Volume 46, pages 593–608.
- Stanley, C.R. (1994): Geology of the Pothook alkalic copper-gold porphyry deposit, Afton Mining Camp, British Columbia (92I/9, 10); in *Geological Fieldwork 1993, BC Ministry of Energy, Mines and Petroleum Resources*, Paper 1994-1, pages 275–284.
- Struik, L.C., Parrish, R.R. and Gerasimoff, M.D. (1992): Geology and age of the Naver and Ste Marie plutons, central British Columbia; in *Radiogenic age and isotopic studies: Report 5; Geological Survey of Canada*, Paper 91-2, pages 155–162.
- Thirlwall, M.F. (2000): Inter-laboratory and other errors in Pb isotope analyses investigated using a ^{207}Pb – ^{204}Pb double spike; *Chemical Geology*, Volume 163, pages 299–322.
- Travers, W.B. (1977): Overturned Nicola and Ashcroft strata and their relations to the Cache Creek Group, southwestern Intermontane Belt, British Columbia; *Canadian Journal of Earth Sciences*, Volume 15, pages 99–116.
- Wetherup, S. (2000): Diamond drilling report on the Woodjam Property; *BC Ministry of Energy, Mines and Petroleum Resources*, AR26242.

Woodsworth, G.J., Anderson, R.G. and Armstrong, R.L. (1991):
Plutonic Regimes: Chapter 15; *in* Geology of the
Cordilleran Orogen in Canada, Gabrielse, H. and Yorath,

C.J., Editors, *Geological Association of Canada*, Geology
of Canada, Volume 4, pages 491–531.

Boundary Project: Rock Creek Area (NTS 082E/02W, 03E), Southern British Columbia

by N.W.D. Massey

KEYWORDS: Quesnellia, Knob Hill Complex, Anarchist schist, Brooklyn Formation, Rock Creek

INTRODUCTION

The Boundary Project was initiated in 2005 with the purpose of better characterizing the lithological and geochemical variations within and between the various Paleozoic sequences in the southern Okanagan region along the Canada-United States border. These occur within Quesnel Terrane, which is dominated by Paleozoic mafic volcanic and pelitic rocks, unconformably overlain by Triassic and Jurassic volcanic and sedimentary rocks. In the Boundary District, such sequences include the Knob Hill Complex, Attwood Formation, Kobau Group and the Anarchist schist. These are exposed between downfaulted blocks of Tertiary volcanic and sedimentary cover preserved in structural keels between gneissic domes (Fig 1). In 2006, fieldwork was concentrated in the Rock Creek and Johnstone Creek areas, south and west of the Kettle River valley (NTS 082E/02W, 03E).

Six weeks of fieldwork in 2006 were primarily conducted in the area south of Rock Creek and in the Johnstone Creek area, west of the Kettle River and as far north as Conkle Lake. Sampling for geochemistry and geochronology was also carried out in the Greenwood area. Fieldwork was focused on

- new mapping in Rock Creek and Johnstone Creek areas in order to produce a new geological map of the southern Kettle River valley area and to contribute to a compilation map for the Greenwood sheet (Massey, 2007);

- collecting geochemical samples from volcanic rocks in the Knob Hill Complex and Anarchist schist;

- identifying and collecting suitable materials for geochronological age determinations of the Paleozoic sequences and Jurassic intrusions;

- investigating the use of litho-geochemistry to characterize and discriminate the various Paleozoic and Jurassic argillaceous sequences.

PREVIOUS WORK

The Rock Creek area has a mining history dating from the first discoveries of placer gold in the 1860s and lode de-

posits in the 1880s. The first geological report was that of Bauerman (1885) as part of the Boundary Commission Expedition of 1859 to 1861. Regional mapping has been undertaken by Brock (1902, 1903, 1905a, b), Daly (1912), Cairnes (1940), Little (1957, 1961, 1983), Monger (1968), Church (1980), Templeman-Kluit (1989a, b) and Fyles (1990). Adjacent areas in Washington State have been mapped by Umpleby (1911), Fox (1970, 1978), Pearson (1967) and Stoffel (1990), and mineral deposits reviewed by Moen (1980).

PALEOZOIC SEQUENCES OF THE ROCK CREEK AREA

Paleozoic rocks underlie two separate areas, the Rock Creek and Johnstone Creek areas, each with distinct characteristics. Previous workers included all these rocks within the Anarchist schist (Daly, 1912; Cairnes, 1940; Little, 1957). However, mafic volcanic flows and cherts in the Johnstone Creek area are contiguous with similar outcrops of the Knob Hill Complex on the east side of the Kettle River valley (Fyles, 1990; Massey, 2006). It is thus proposed to extend the Knob Hill Complex designation to these rocks. The term Anarchist schist is retained for the sequence of metasedimentary rocks and metabasalts south of Highway 3, between Osoyoos and Rock Creek. Though the rock units of the Anarchist schist are similar to those of the Knob Hill Complex, the Anarchist schist is distinguished in being more argillaceous and more complexly deformed. It is also proposed to apply the Anarchist schist designation to similar rocks in the Greenwood area, which Fyles (1990) and Massey (2006) had included in the Knob Hill Complex.

The ages of the Anarchist schist and Knob Hill Complex are still poorly determined. No paleontological or geochronological data are available for the Anarchist schist in the study area. Rubidium-strontium geochronology in the Osoyoos area only records Tertiary metamorphic ages (Ryan, 1973). A Carboniferous to Permian age was assigned to the Knob Hill Complex by Little based on a single macrofossil locality (Little, 1983, locality F7, p 12). However, this same limestone bed has yielded conodonts of Late Devonian, Frasnian age (Orchard, 1993). Determinable radiolarian are rare in the cherts of the Knob Hill Complex, though one sample has yielded a Late Pennsylvanian to earliest Permian age (Table 1). Church (1986) reported a K-Ar whole rock age of 258 ± 10 Ma (Permian) for unalitized gabbro from the Winnipeg mine. However, the reliability of such K-Ar whole rock ages is very suspect and it is doubtful that this is recording a crystallization age. A coarse-grained gabbro sample, also from the Winnipeg mine area, has yielded a small amount of zircon. Preliminary analyses of 16 of the best quality zircons by Mortensen (pers comm, 2006) suggest ages that range between 390 and 340 Ma,

This publication is also available, free of charge, as colour digital files in Adobe Acrobat® PDF format from the BC Ministry of Energy, Mines and Petroleum Resources website at http://www.em.gov.bc.ca/Mining/Geolsurv/Publications/catalog/cat_fldwk.htm

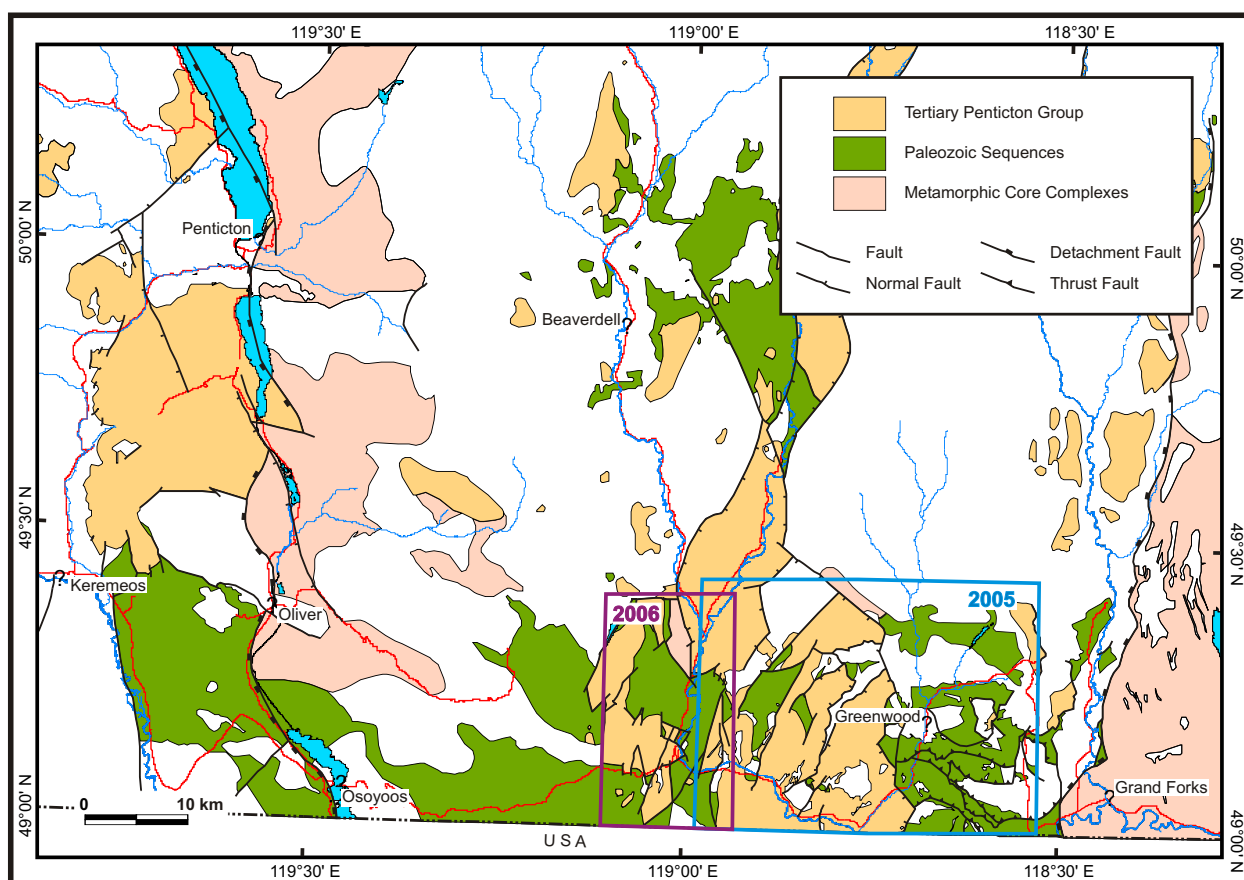


Figure 1. Distribution of Paleozoic Quesnellian rock suites in the Boundary District (south-central part of NTS 082E), southern BC, amended from the digital geology map of British Columbia (Massey *et al.*, 2005).

TABLE 1: RADIOLARIA DETERMINATIONS FROM CHERT OF THE KNOB HILL COMPLEX, BC. DETERMINATIONS MADE BY CORDEY (2006).

	Sample number 05NMA-16-007	Sample number 05NMA-22-014
Location	Lee Main road, approximately 1/2 km north of Matthews Lake	Riverside Road, approximately 2 km southeast of Zamora
Coordinates		
Lat/Long	49.127866°N, 118.863477°W	49.139180°N, 118.963673°W
UTM (zone 11)	5443342N, 364053E	5444784N, 356777E
Geological unit	Knob Hill Complex	Knob Hill Complex
Lithology	black chert, pyrite	light green chert
Occurrence of radiolarians	confirmed	confirmed
Preservation	poor to moderate	poor to moderate
Radiolarian taxa	<i>Entactinia</i> sp. <i>?Latentibifistula</i> sp. <i>Schaferbergia</i> sp.	<i>Entactinia</i> sp. <i>Latentibifistula</i> sp. <i>Schaferbergia</i> sp. <i>Pseudoalbaillella bulbosa</i> Ishiga
Other	silica fragment (matrix), a few pyrite aggregates, rare sponge spicules (undiagnostic)	silica fragment (matrix), a few pyrite aggregates
Age	Carboniferous - Permian	Late Pennsylvanian - Earliest Permian (Kashimovian - Asselian)
Comment	range is based on the common occurrence of quoted genera, no further precision is possible	range is based on the common occurrence of <i>Pseudoalbaillella bulbosa</i> Ishiga

middle Devonian to early Mississippian. Further processing of this sample, and new samples collected in 2006, is continuing.

Knob Hill Complex

The Knob Hill Complex is composed of chert, argillite, basalt, gabbro and serpentinite that constitute a disrupted ophiolite (Little, 1983; Dostal *et al.*, 2001). Stratigraphic relationships between map units are not always clear in the Greenwood area. However, in the area north of Rock Creek and east of the Kettle River valley, gabbro and serpentinite

pass northwards, and probably upwards, into greenstone, mixed greenstone and chert and finally into chert and argillite. This pattern is repeated on the west side of the valley in the Johnstone Creek area, although disrupted by north-northeast-trending Tertiary faults.

SERPENTINITE AND GABBRO UNITS

Intrusive components of the complex are limited to the Highway 33 and Hulme Creek areas. Serpentinite is typically black to bright green. It is often phyllitic to schistose but may show boudinaged kernels of hard coherent serpentinite in the foliated matrix. Cores of relict pyroxenite occur, though rarely. Calcite veining is common. Listwanite is exposed in outcrops along Highway 33. The carbonate-rich rock is pale buff on fresh surfaces but typically bright orange on weathered surfaces with white quartz veins.

Gabbro is composed of white plagioclase and green to black pyroxenes extensively replaced by hornblende. Chlorite is common on fractures and in shears. The gabbro is generally coarse grained and massive but can show a characteristic variable and patchy texture, with coarse-grained gabbro phases grading into finer microgabbro or even coarser pegmatitic phases.

GREENSTONE UNIT

Basaltic greenstones are mostly massive flows; medium grey to green and aphyric, though rare feldspar, pyroxene and magnetite are seen. Alteration is variable and can be quite extensive. Chlorite, epidote, calcite and quartz are common alteration minerals in veins, fractures and within the rock. Pillow structures are rare though irregular chloritic bands appear to be selvages (Fig 2). Minor breccia, agglomerate, tuff and chlorite schist occur between flows (Fig 3) as do chert, cherty argillite and rare grey limestone beds. Chert beds can be significant enough in some areas to designate as a mixed greenstone-chert unit transitional to the chert-argillite unit.

Geochemical studies of the Knob Hill Complex greenstone are still ongoing. Preliminary interpretation of new and published (Dostal *et al.*, 2001) data from the Greenwood area suggests the presence of three distinct magma suites within the lavas: a) a typical mid-ocean ridge basalt (MORB) suite, b) an enriched MORB suite and c) an island-arc tholeiite (IAT) suite (Fig 4, 5, 6). Further geochemistry is underway to enhance the database and determine if there are



Figure 2. Chloritic pillow selvages in Knob Hill Complex greenstone; arrows point to selvages. Hammer for scale (06NM24-05, UTM zone 11, 5443064N, 351166E, NAD 83).

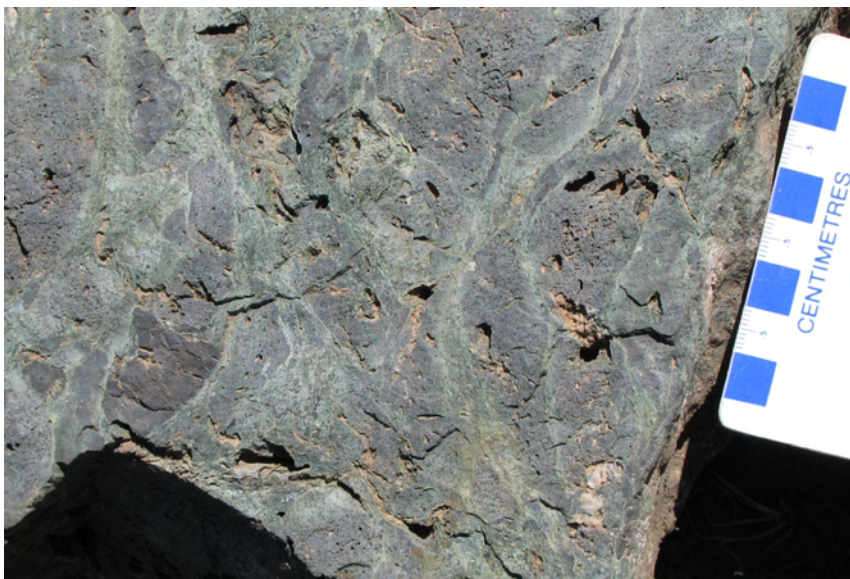


Figure 3. Basalt volcanic breccia, Knob Hill Complex (06NMA19-01-03, UTM zone 11, 5443064N, 351240E, NAD 83).

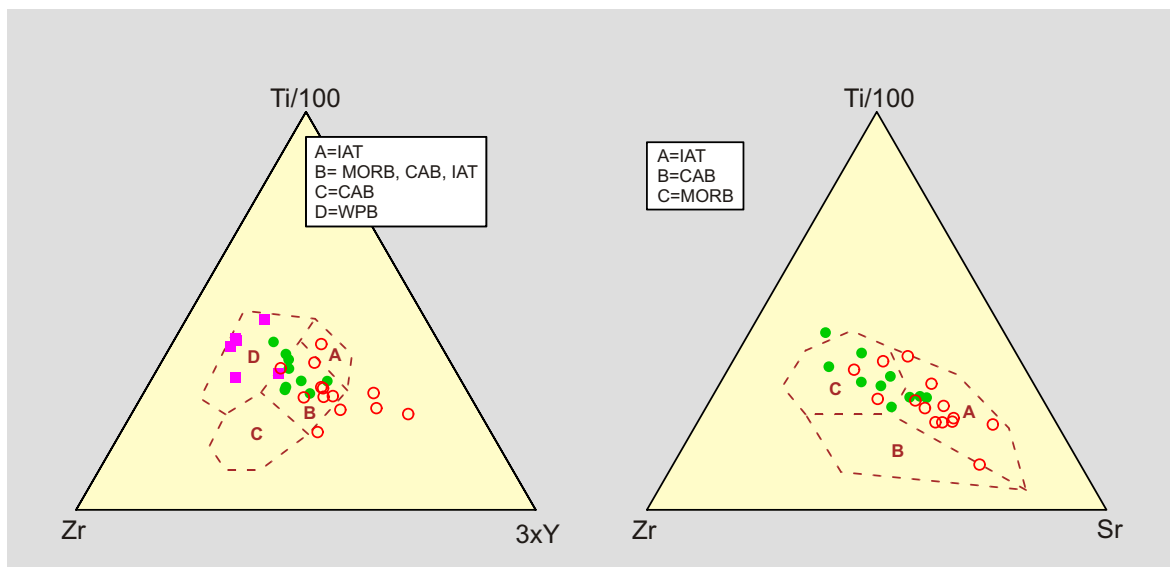


Figure 4. Discriminant triangle plots, Ti-Zr-Y and Ti-Zr-Sr, for Knob Hill Complex greenstone; petrotextonic fields (after Pearce and Cann, 1973). Abbreviations: IAT, island-arc tholeiite; MORB, mid-ocean ridge basalt; CAB, calcalkaline basalt; WPB, within-plate basalt. Filled circles: MORB suite samples; filled squares: enriched MORB suite samples; open circles: IAT suite

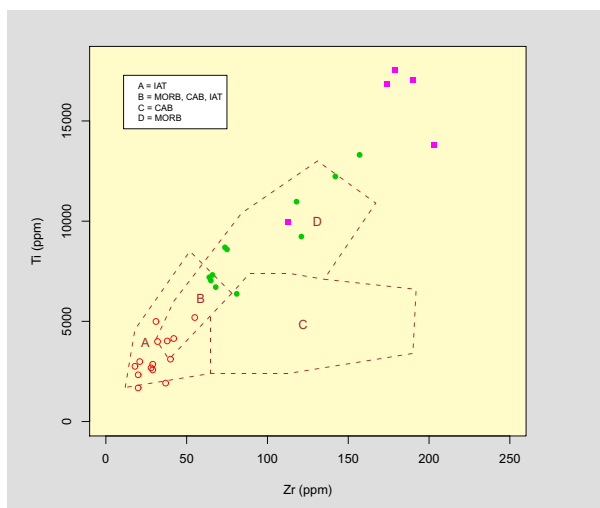


Figure 5. Discriminant plot, Ti-Zr, for Knob Hill Complex greenstone; petrotextonic fields (after Pearce and Cann, 1973). Abbreviations: IAT, island-arc tholeiite; MORB, mid-ocean ridge basalt; CAB, calcalkaline basalt. Filled circles: MORB suite samples; filled squares: enriched MORB suite samples; open circles: IAT suite samples.

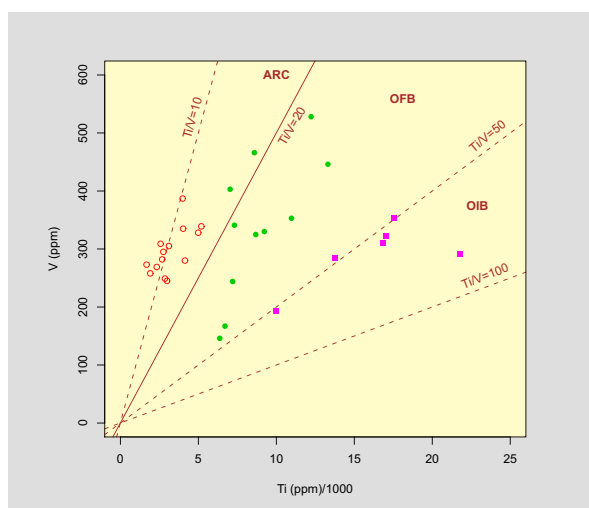


Figure 6. Discriminant plot, Ti-V, for Knob Hill Complex greenstone; petrotextonic fields (after Shervais, 1982). Abbreviations: ARC, island-arc tholeiite; OFB, ocean-floor basalt; OIB, ocean-island basalt and alkalic basalt. Filled circles: MORB suite samples; filled squares: enriched MORB suite samples; open circles: IAT suite samples.

any spatial or stratigraphic controls on the distribution of these suites.

CHERT-ARGILLITE UNIT

Sedimentary rocks in the Knob Hill Complex are typically fine grained, mainly grey to white cherts interbedded with grey to black argillites, black siliceous argillites and occasional chert breccia. Cherts are highly fractured and jointed, tend to be massive to thickly bedded and only rarely show ribbon structures (Fig 7). The cherts are variably recrystallized producing a fine to medium-grained

saccharoidal texture and destroying any radiolaria. Chert breccias contain angular to subrounded clasts of chert and cherty tuff in a siliceous matrix and are usually associated with unbroken chert.

Anarchist Schist

The Anarchist schist can be subdivided into a metasedimentary unit and a metavolcanic unit, delineated on the dominant lithologies within them. Stratigraphic relationship between the units is uncertain. Deformation of the



Figure 7. Ribbon chert of the Knob Hill Complex. Hammer for scale (06NMA22-04, UTM zone 11, 5445398N, 352228E, NAD 83).

schists is much higher than observed in the Knob Hill Complex, involving at least two phases of deformation. Schistosity generally trends east-southeast with medium to steep northerly dips. Several areas, however, are marked by northeasterly trending schistosity with steep or moderate northwesterly dips. Secondary spaced cleavages in quartzites also trend north to northeast. However, lack of distinctive marker beds makes tracing of folds almost impossible.

METASEDIMENTARY UNIT

The metasedimentary unit is dominated by quartzite, argillaceous quartzite and meta-argillites with minor metabasalt and limestone. The quartzite and metachert are typically white to pale grey or darker bluish grey. Beds are usually 1 to 2 m thick but can reach up to 10 m. They may show a knobby or irregular weathered surface. They are variably recrystallized with a fine to medium-grained sugary texture. They may be massive or show dark and light laminations and banding (Fig 8a, b). Ribbon bedding is occasionally preserved.

Phyllitic to schistose argillaceous metasedimentary rocks are darker, with fine-grained black chlorite or biotite schist layers interlayered with lighter quartz-rich layers (Fig 8c). The schistosity is commonly crenulated and contorted, and quartz veining may also be contorted and augened (Fig 8d). Some thicker, less siliceous meta-argillites are carbonaceous. White, sulphurous-smelling barite beds and pods are found interbedded with meta-argillite on the Lapin property (MINFILE 082ESW 256; MINFILE, 2006) west of Budy Creek (Fig 9).

Minor limestone beds vary from 1 to 10 m thick. They are white to grey, fine to medium grained and recrystallized.

METAVOLCANIC UNIT

The metavolcanic unit comprises greenstone flows with minor breccia and tuff and minor metasedimentary rocks. Greenstone flows are massive, medium to dark grey or black. They are fine grained and generally aphyric, though rare feldspar crystals are seen. Chlorite±epidote alteration is common, along with veining of quartz±chlorite±calcite. The flows may be magnetic, with magnetite present in rock and veins. Tuffaceous interbeds are altered to green quartz-chlorite±sericite schist.

THE MIGHTY WHITE DOLOMITE

A thick dolomite unit occurs at the Mighty White dolomite mine (MINFILE 082ESE 200), south of Rock Creek. This is a fine to equigranular, medium-grained, white crystalline dolomite. It is massive, with no apparent bedding, and intruded by dark grey-green chloritic dikes. Chlorite-epidote skarn is apparent around the margins of the dikes.

The relationship of the dolomite to the rest of the Anarchist schist is enigmatic. It is much thicker than the minor limestone seen elsewhere, and unique in being dolomitic. It is underlain by a distinctive foliated greenstone (Fig 10) that passes down into more usual massive greenstone. The gneissic-like foliation dips moderately to shallowly to the east and could possibly be mylonitic resulting from the structural emplacement of the dolomite on top of the basalt. No indicators of sense of motion were apparent though, nor is there any obvious source of origin nor correlatives for the dolomite.

OTHER PRE-JURASSIC ROCKS OF THE ROCK CREEK AREA

Proterozoic (?) Orthogneiss

Orthogneiss forms an inlier in the Ed James Lake area, lying structurally beneath the Knob Hill Complex, though



Figure 8. Typical rock types of the Anarchist schist metasedimentary unit: a) laminated quartzite (metachert) (06NMA09-05, UTM zone 11, 5433188N, 354076E, NAD 83); b) laminated quartzite with spaced cleavage (s_2) (06NMA08-11, UTM zone 11, 5432800N, 353609E, NAD 83); c) argillaceous metasedimentary rocks (06NMA02-11, UTM zone 11, 5431735N, 355263E, NAD 83); d) deformed quartz vein in meta-argillite (06NMA09-16, UTM zone 11, 5433145N, 354173E, NAD 83).

the bounding fault is not exposed. Schistosity within the gneiss is flat to dipping moderately to the east, matching that in the overlying Knob Hill Complex rocks, and suggests an easterly dipping extensional fault. A subvertical normal fault bounds the gneiss to the east, putting it in contact with Tertiary volcanic and sedimentary rocks. The gneiss is tentatively correlated with gneiss of the Proterozoic Grand Forks Gneiss Complex, which shares a similar structural relation to the Knob Hill Complex in the Grand Forks area (Höy and Jackaman, 2005), or with the Vaseaux gneiss of the Okanagan Valley.

A variety of orthogneiss is seen. A grey biotite-feldspar-quartz gneiss is most common (Fig 11a). It is coarse grained and well foliated, with schistosity resulting from the alignment of biotite porphyroblasts. White feldspar porphyroblasts (Fig 11b) range up to 5 mm in size, forming small augens. Biotite forms large clots, up to 2 cm in diameter, within the foliation plane giving a spotted appearance to the rock when broken appropriately. Variation in mineral proportions results in colour banding (Fig 11c) and a variation from diorite to granodiorite in composition. A distinctive coarse-grained, pink augen gneiss is also common (Fig 11d). Large pink potassium-feldspar augens are scattered in a foliated biotite-feldspar-quartz groundmass.

The gneiss is intruded by an unfoliated leucogranite (Fig 11a). This is a medium to coarse-grained rock, generally white on both weathered and fresh surfaces, but occasionally showing a pinkish hue on fresh surfaces. The rock is composed predominantly of white feldspar and quartz with minor biotite; colour index is less than 5. Pegmatitic phases contain pink potassium-feldspar.

Brooklyn Formation

Conglomerate and limestone of the Middle Triassic Brooklyn Formation have previously been included in the Anarchist schist (*e.g.*, Little, 1961). They form scattered outcrops in the Johnstone Creek area and more extensive outcrops in the area south of Rock Creek, between Budy Creek and the Bridesville-Rock Creek Road. These units unconformably overlie the Anarchist schist and Knob Hill Complex rocks.

Sharpstone conglomerate is polymictic though dominated by angular to subrounded clasts of a variety of cherts and cherty argillites in a chert-rich matrix. Minor greenstone and argillite clasts are also seen. Commonly the clasts are granule to pebble size. Limestone clasts are seen in the area east of Budy Creek, but are notably lacking in the Johnstone Creek area. Where present, the limestone clasts are larger than other clasts and may be up to 15 cm in size. Interbeds



Figure 9. Barite interbedded with meta-argillite (b) of the Anarchist schist (a), Lapin property. Hammer for scale.



Figure 10. Foliated (possibly mylonitized) greenstone in the footwall of the Mighty White dolomite (06NMA02-04, UTM zone 11, 5431791N, 356073E, NAD 83).

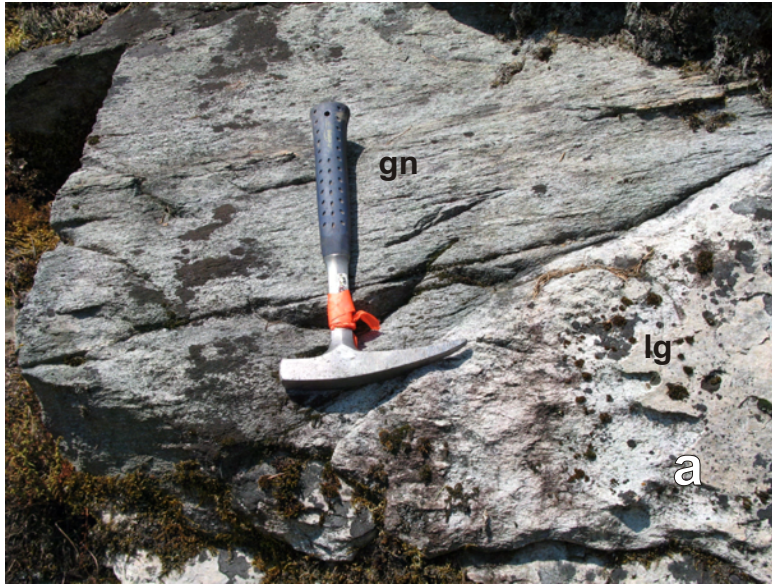


Figure 11. Varieties of gneiss from the Ed James Lake area: a) grey biotite-feldspar-quartz gneiss (gn) intruded by leucogranite (lg) (06NMA22-12, UTM zone 11, 5446243N, 352916E, NAD 83); b) feldspar porphyroblasts in biotite-feldspar gneiss (06NMA23-07, UTM zone 11, 5444280N, 353711E, NAD 83); c) compositional banding in grey gneiss (06NMA22-17, UTM zone 11, 5446621N, 352437E, NAD 83); d) potassium-feldspar augen gneiss (06NMA22-14, UTM zone 11, 5446634N, 353223E, NAD 83).

of gritty sandstone and argillite can occur with the conglomerate.

Limestone overlies the sharpstone conglomerate in the Budy Creek area. Limestone is massive and poorly bedded, white to grey on fresh surfaces with pale buff to grey weathered surfaces. Though some of the limestone is fine grained and powdery, it is more commonly medium to coarse grained, equigranular and sparry in texture. Recrystallization and skarning is evident along the margins of the Jurassic diorite. Monolithic limestone breccias may have resulted from paleokarstification (Fig 13). Other limestone conglomerate contains rounded to subrounded pebbles of cherty argillite, chert and limestone in a medium-grained calcareous matrix.

Volcanic rocks of the Brooklyn Formation are limited to the area adjacent to the Washington border, south of the Bridesville-Rock Creek Road. Greenstone flows are grey to green, fine grained, aphyric or sparsely pyroxene and magnetite-phyric. Chlorite and epidote are common as alteration and in veins. Flows are massive, though rare varioles may suggest some pillow flows (Fig 14). Tuff, breccia, chlorite schist and quartz-chlorite schist also occur.

STRUCTURAL RELATIONSHIP OF PALEOZOIC UNITS

The Paleozoic rocks of the Greenwood-Rock Creek area are preserved in a series of northward-dipping thrust sheets (Fig 15). Many of the bounding thrusts are marked by serpentine layers or pods. Tertiary extensional faulting has disrupted and modified the thrust sheets and makes correlation difficult between the Greenwood and Rock Creek areas. Detailed descriptions of the thrust sheets in the Greenwood map area have been provided by Fyles (1990) and summarized by Massey (2006).

The sheets are informally numbered from south to north, structurally from bottom to top (Fig 15). Only thrust sheets 2 and 5 appear to continue into the Rock Creek area. These are occupied by the Anarchist schist and Knob Hill Complex, respectively. Fyles (1990) suggested the presence of thrust sheet 1 in the Myers Creek area. In the Greenwood area, this thrust sheet is underlain by argillites ascribed to the Attwood Formation, with overlying Triassic Brooklyn Formation volcanic rocks. However, the correlation of the argillites south of the No 7 fault is debatable and these may be Jurassic (*see* discussion in Massey [2007]). Furthermore, south of Rock Creek, the Myers Creek quartz diorite stock is found in contact, either faulted (Fig 16) or intrusive, with quartzite and



Figure 12. Sharpstone conglomerate with gritstone interbeds, Middle Triassic Brooklyn Formation. Hammer for scale (06NMA21-18, UTM zone 11, 5441144N, 348947E, NAD 83).



Figure 13. Limestone breccia, Middle Triassic Brooklyn Formation. Coin for scale (06NMA14-20, UTM zone 11, 5430277N, 348449E, NAD 83).

metasedimentary rocks of the Anarchist schist not Attwood Formation argillite.

ACKNOWLEDGMENTS

The author is much indebted to Jim Fyles and Neil Church for all their invaluable help and advice during the planning stages of this project and since. The collaboration, support and ready welcome of the Boundary District exploration community continues to be exceptional. Ranchers



Figure 14. Variolites in possibly pillowed basalt, Middle Triassic Brooklyn Formation (06NMA15-11, UTM zone 11, 5430006N, 350332E, NAD 83).

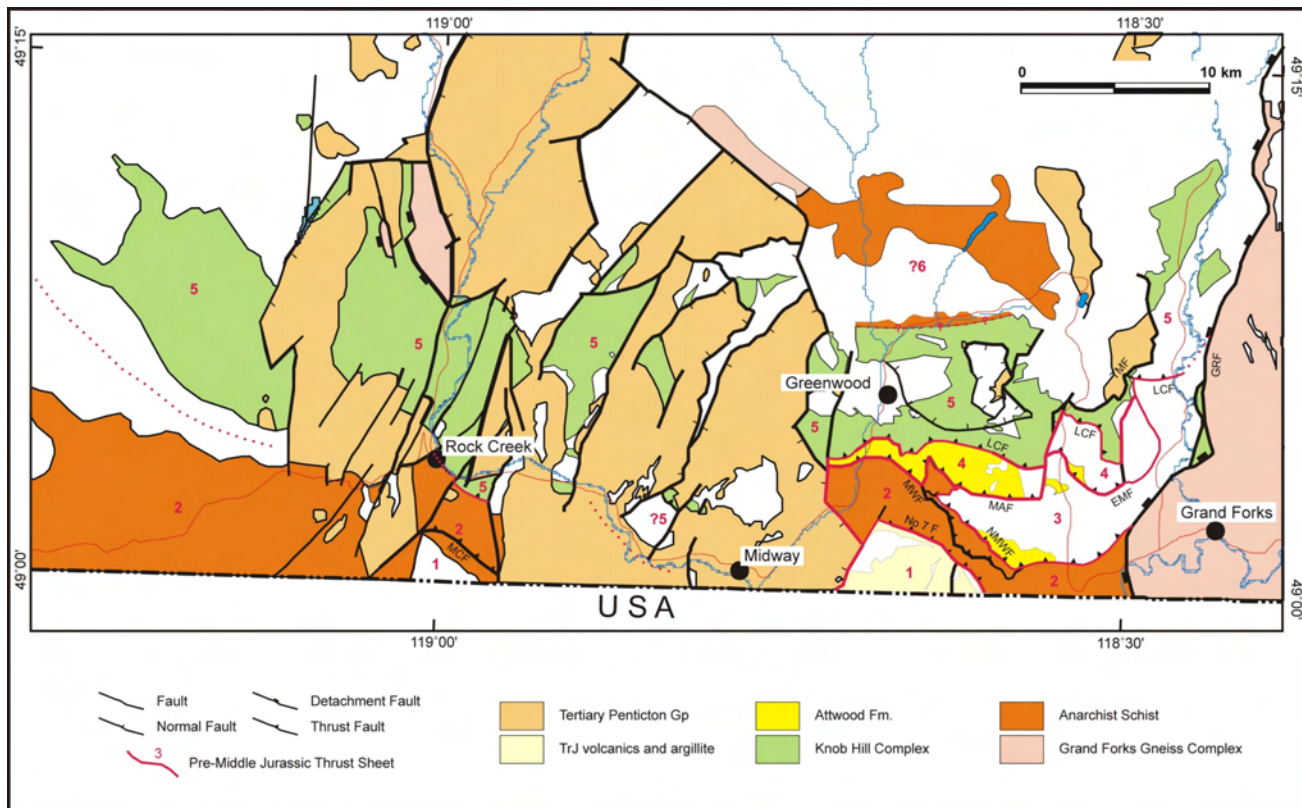


Figure 15. Main structural elements of the Greenwood-Rock Creek area, outlining the major thrust sheets (numbered 1–6) containing the Paleozoic and Mesozoic sequences (*modified from Fyles, 1990*). Abbreviations: No 7 F, Number 7 fault; MWF, Mount Wright fault; NMWF, North Mount Wright fault; MAF, Mount Attwood fault; LCF, Lind Creek fault; EMF, Eagle Mountain fault; TMF, Thimble Mountain fault; GRF, Granby River fault.

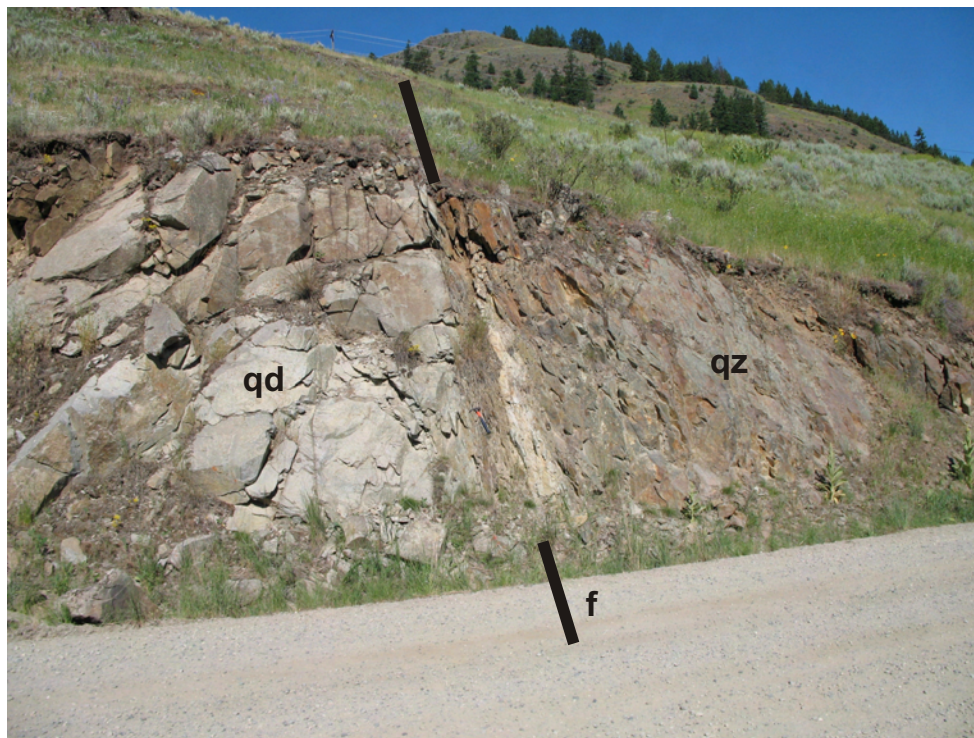


Figure 16. Faulted contact (f) between the Myers Creek quartz diorite (qd) and quartzite of the Anarchist schist (qz) exposed in a roadcut adjacent to Myers Lake, BC (06NMA05-01, UTM zone 11, 5431245N, 352934E, NAD 83).

and landowners in the Myers Creek area and along Highway 33 graciously allowed access to their properties. The author also acknowledges the indispensable assistance of Eric Westberg during fieldwork and in the office.

REFERENCES

- Bauerman, H. (1885): Geology of the country near the forty-ninth parallel of north latitude, west of the Rocky Mountains; *Geological Survey of Canada*, Report of Progress 1882-83-84, pages 5B-42B.
- Brock, R.W. (1902): The Boundary Creek district, British Columbia; *Geological Survey of Canada*, Summary Report 1901, Volume XIV, pages 51A-69A.
- Brock, R.W. (1903): Preliminary report on the Boundary Creek district, British Columbia; *Geological Survey of Canada*, Summary Report 1901, Volume XV, pages 92A-138A.
- Brock, R.W. (1905a): Geological and topographical map of Boundary Creek mining district, British Columbia; *Geological Survey of Canada*, Map 828, scale 1:63 360.
- Brock, R.W. (1905b): Topographical map of Boundary Creek mining district (economic minerals and glacial striae), British Columbia; *Geological Survey of Canada*, Map 834, scale 1:63 360.
- Cairnes, C.E. (1940): Kettle River (west half), British Columbia; *Geological Survey of Canada*, Map 538 A, scale 1:253 440.
- Church, B.N. (1980): Geology of the Rock Creek Tertiary outlier; *BC Ministry of Energy, Mines and Petroleum Resources*, Preliminary Map 41.
- Church, B.N. (1986): Geological setting and mineralization in the Mount Attwood – Phoenix area of the Greenwood mining camp; *BC Ministry of Energy, Mines and Petroleum Resources*, Paper 1986-2, 65 pages.
- Cordey, F. (2006): Report on radiolarians; unpublished consultant's report, Report No. FC2006-BCGSB-2.
- Daly, R.A. (1912): Geology of the North American Cordillera at the forty-ninth parallel; *Geological Survey of Canada*, Memoir 38.
- Dostal, J., Church, B.N. and Höy, T. (2001): Geological and geochemical evidence for variable magmatism and tectonics in the southern Canadian Cordillera: Paleozoic to Jurassic suites, Greenwood, southern British Columbia; *Canadian Journal of Earth Sciences*, Volume 38, pages 75-90.
- Fox, K.F., Jr. (1970): Geologic map of the Oroville quadrangle, Okanogan County, Washington; *United States Geological Survey*, Open-File Report 70-128, 3 sheets, scale 1:62 500.
- Fox, K.F., Jr. (1978): Geologic map of the Mt. Bonaparte quadrangle, Okanogan County, Washington; *United States Geological Survey*, Open File Report 78-732, 2 sheets, scale 1:48 000.
- Fyles, J.T. (1990): Geology of the Greenwood – Grand Forks area, British Columbia, NTS 82E/1, 2; *BC Ministry of Energy, Mines and Petroleum Resources*, Open File 1990-25, 19 pages.
- Höy, T. and Jackaman, W. (2005): Geology of the Grand Forks map sheet (082E/01); *BC Ministry of Energy, Mines and Petroleum Resources*, Geoscience Map 2005-1, scale 1:50 000.
- Little, H.W. (1957): Kettle River (east half), British Columbia; *Geological Survey of Canada*, Map 6-1957, scale 1:253 440.
- Little, H.W. (1961): Kettle River (west half), British Columbia; *Geological Survey of Canada*, Map 15-1961, scale 1:253 440.
- Little, H.W. (1983): Geology of the Greenwood map-area, British Columbia; *Geological Survey of Canada*, Paper 79-29, 37 pages.
- Massey, N.W.D. (2006): Boundary Project: reassessment of Paleozoic rock units of the Greenwood area (NTS 82E/02), southern British Columbia; in *Geological Fieldwork 2005*,

- BC Ministry of Energy, Mines and Petroleum Resources, Paper 2006-1 and *Geoscience BC*, Report 2006-1, pages 99–107.
- Massey, N.W.D. (2007): Lexington porphyry revisited (NTS 082E/02), southern British Columbia; in Geological Fieldwork 2006, *BC Ministry of Energy, Mines and Petroleum Resources*, Paper 2007-1 and *Geoscience BC*, Report 2007-1, pages 129–136.
- Massey, N.W.D., MacIntyre, D.G., Desjardins, P.J. and Cooney, R.T. (2005): Digital geology map of British Columbia; *BC Ministry of Energy, Mines and Petroleum Resources*, Open File 2005-2, DVD.
- MINFILE (2006): MINFILE BC mineral deposits database; *BC Ministry of Energy, Mines and Petroleum Resources*, URL <<http://www.em.gov.bc.ca/Mining/Geolsurv/Minfile/>> [November 2006].
- Moen, W.S. (1980): Myers Creek and Wauconda mining districts of northeastern Okanogan County, Washington; *Washington Division of Geology and Earth Resources*, Bulletin 73, 96 pages.
- Monger, J.W.H. (1968): Early Tertiary stratified rocks, Greenwood map-area (82E/2) British Columbia; *Geological Survey of Canada*, Paper 67-42, 39 pages.
- Orchard, M.J. (1993): Report on conodonts and other microfossils, Penticton (82E); *Geological Survey of Canada*, Report Number OF-1993-19.
- Pearce, J.A. and Cann, J.R. (1973): Tectonic setting of basic volcanic rocks determined using trace element analyses; *Earth and Planetary Science Letters*, Volume 19, pages 290–300.
- Pearson, R.C. (1967): Geologic map of the Bodie Mountain quadrangle, Ferry and Okanogan counties, Washington; *United States Geological Survey*, Geologic Quadrangle Map GQ-636, scale 1:62 500.
- Ryan, B.D. (1973): Structural geology and Rb-Sr geochronology of the Anarchist Mountain area, southcentral British Columbia; unpublished PhD thesis, *University of British Columbia*.
- Shervais, J.W. (1982): Ti-V plots and the petrogenesis of modern and ophiolitic lavas; *Earth and Planetary Science Letters*, Volume 59, pages 101–118.
- Stoffel, K.L. (1990): Geologic map of the Republic 1:100 000 quadrangle, Washington; *Washington Division of Geology and Earth Resources*, Open File Report 90-10, 62 pages, 1 map.
- Templeman-Kluit, D.J. (1989a): Geological map with mineral occurrences, fossil localities, radiometric ages and gravity field for Penticton map area (NTS 82/E), southern British Columbia; *Geological Survey of Canada*, Open File 1969.
- Templeman-Kluit, D.J. (1989b): Geology, Penticton, British Columbia; *Geological Survey of Canada*, Map 1736A, scale 1:250 000.
- Umpleby, J.B. (1911): Part I—geology and ore deposits of the Myers Creek mining district; Part II—geology and ore deposits of the Oroville-Nighthawk mining district; *Washington Geological Survey*, Bulletin 5, 111 pages.

Lexington Porphyry Revisited (NTS 082E/02), Southern British Columbia

by N.W.D. Massey

KEYWORDS: economic geology, porphyry, Lexington, Jurassic, volcanic, geochemistry, Elise Formation

INTRODUCTION

The Lexington mining camp is located 10 km to the south-southeast of Greenwood (Fig 1). It comprises up to 11 copper-gold-porphyry and vein deposits in BC and Washington, hosted by the Lexington porphyry within the No 7 fault zone. The mineralization stretches in a linear belt from the No 7 mine in the northwest to the Lone Star mine, in Washington, in the southeast. In Washington, the No 7 fault is offset northward to the Danville area where it hosts the Morning Star deposit. Exploration and development in the Lexington camp first started in 1890 and continues to this day. Important reviews of mineralization and historical development are provided by Church (1970, 1986) and Seraphim *et al.* (1995).

The No 7 fault is marked by a thick serpentinite sheet along its length from McCarren Creek to the international border. Along Goosmus Creek, the serpentinite is apparently split in two by the intrusion of a quartz porphyry body known as the Lexington porphyry (Church, 1992). High-grade copper-gold sulphide mineralization forms a series of stacked lenses in the porphyry just above the footwall serpentinite (Merit Mining Corp., 2006). The Gidon Creek porphyry, a quartz-feldspar porphyry body found in the footwall of the No 7 fault to the west of the Lexington camp (Fig 1), has been correlated with the Lexington quartz porphyry. This quartz-feldspar porphyry is, however, marked by large pink K-feldspar phenocrysts that are absent from the type Lexington porphyry, which raises doubts about their correlation.

Several authors have mapped areas of andesitic to dacitic volcanoclastic rocks around some of the mines within the Lexington camp (*e.g.*, Fig 9 in Church, 1986) and equivalents in Washington (*e.g.*, Morning Star deposit; Caron, pers comm, 2005; Cheney, 2004). Dacitic volcanoclastic rocks that host mineralization are also reported by company geologists in drillcore from the area (Butler, 1997; Cowley, 2004). Seraphim *et al.* (1995), however, assert that these units at Lexington are not original volcanic rocks but the result of cataclasis of the porphyry within the fault zone, though they do allow for “the presence of xenoliths and screens of old volcanic rocks in the intrusion.”

During the summer of 2005, a series of samples were collected from outcrops and selected drillcore from both the massive dacitic porphyry and possible volcanoclastic rocks within the Lexington porphyry of Merit Mining Corporation's Grenoble property. This paper reports petrological and petrochemical studies on these samples.

LXINGTON PORPHYRY

The Lexington porphyry was observed in outcrops along the Gidon Creek – City of Paris Road on the northwest side of Goosmus Creek as well as drillcore samples from the Grenoble property. A range of rock types is present, suggesting that several different porphyry bodies may be present in the sequence, though these have never been mapped out. Typically, the porphyry is light to medium grey in colour, though can be apple green with increased propylitic alteration. It is massive to weakly foliated, foliation being defined by aligned sericite in the groundmass. Phenocrysts are predominantly white to grey feldspar, euhedral to subhedral lath shapes and usually 2 to 4 mm in diameter, occasionally up to 6 mm (Fig 2). Alteration of the phenocrysts to sericite±calcite is common and may be complete in the most severely altered samples. Quartz is present in most, though not all, outcrops. When present, the quartz eyes may be more apparent on weathered surfaces than the less distinct feldspars even though they are much less abundant. They are commonly 1 to 2 mm in diameter, ranging up to 6 to 8 mm. Mafic phenocrysts are absent from the typical feldspar porphyry, but more quartz dioritic samples have tabular to elongate hornblende, which may vary up to 6 mm and up to 20% of the phenocrysts (Fig 3). They are altered to chlorite with lesser sulphide. Groundmass comprises finer-grained feldspar, quartz and occasional mafic minerals but is usually altered to sericite-chlorite-quartz±calcite..

Volcanoclastic fabrics have been observed in some outcrops and in drillcore. Mineralogically, most tuff is similar to the massive porphyry, comprising feldspar and quartz crystals in a finer groundmass. However, there is often a pronounced alignment of feldspar crystals and any mafic minerals present. Some samples also show dark, wispy to elongate, lithic clasts (Fig 4, 5), which vary from a few millimetres up to several centimetres in size. Darker grey to reddish fine-grained units are also seen bedded with the lighter-coloured crystal tuff (Fig 6). Most tuff shows a weak to good schistosity; however, there is no evidence of comminution of crystals and no mylonitization was observed.

GIDON CREEK PORPHYRY

The Gidon Creek porphyry is well exposed in roadcuts in the Norwegian Creek and Gidon Creek areas. It is a leucocratic quartz-feldspar porphyry (Fig 7). Pink K-feld-

This publication is also available, free of charge, as colour digital files in Adobe Acrobat® PDF format from the BC Ministry of Energy, Mines and Petroleum Resources website at http://www.em.gov.bc.ca/Mining/Geosurv/Publications/catalog/cat_fldwk.htm

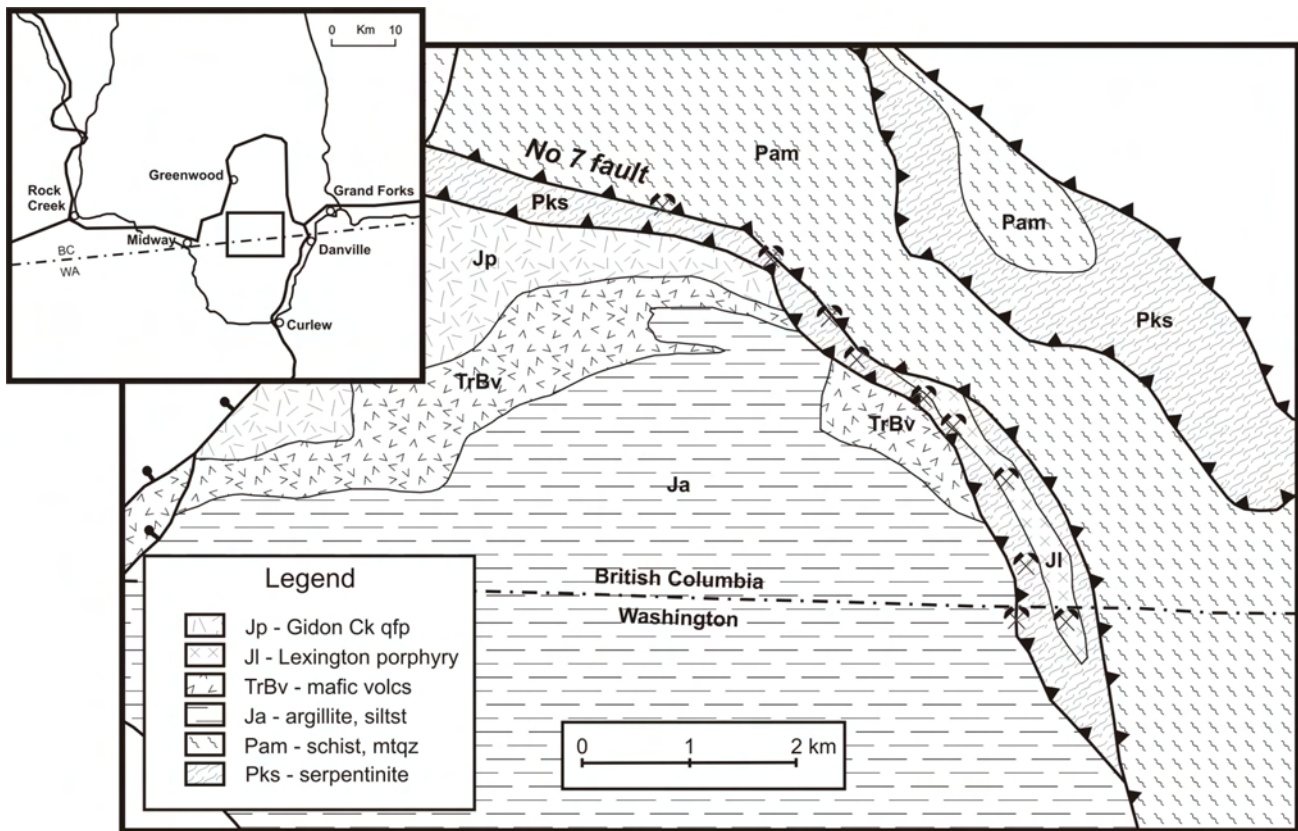


Figure 1. Simplified geological map of the Lexington Camp; individual occurrences indicated by crossed hammer symbol. Inset shows the location of the map to the south-southeast of Greenwood (abbreviations: qfp, quartz-feldspar porphyry; volcs, volcanic rocks; siltst, siltstone; mtqz, metaquartzite).

spar megacrysts are subhedral to subrounded, about 1 cm in diameter, though ranging up to 2 cm. They are perthitic and show simple twinning in thin sections. Plagioclase phenocrysts are also observed, though smaller than the K-feldspar, showing albitic and cross-twinning in thin section. Quartz eyes are rounded, commonly 3 to 5 mm in size but ranging up to 10 mm. The groundmass is a white to pale pink, finer-grained mosaic of quartz, K-feldspar and plagioclase crystals. Mafic minerals are sparse, with colour index (CI) often <5%, and mostly consists of biotite replaced by chlorite. Epidote is seen in the groundmass in thin

section along with minor sphene, opaque minerals and secondary sericite.

The porphyry is seen to intrude Triassic Brooklyn Formation metavolcanic rocks in the Norwegian Creek area. The margins of the porphyry are sheared; foliation varying from trachytic to mylonitic in appearance (Fig 8). Where they are still preserved, phenocrysts are either broken and form augen or are strung out along the foliation. Quartz shows strained extinction in thin sections. Feldspar grains are completely altered to sericite, epidote and chlorite.

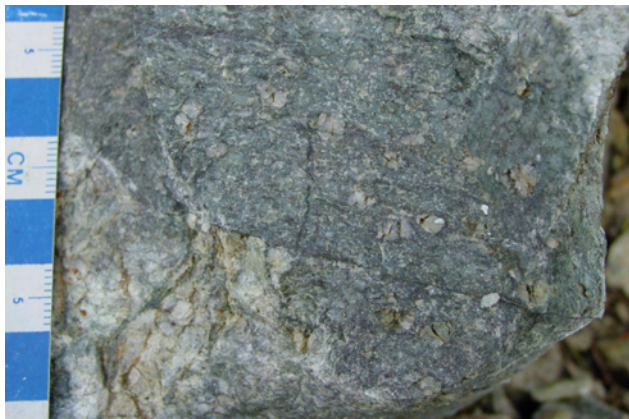


Figure 2. Typical Lexington feldspar porphyry (05NMA25-09, UTM zone 11, 5429300N, 382397E NAD 83).

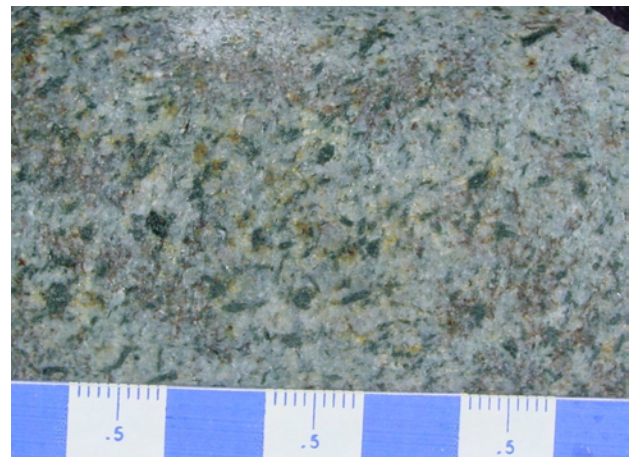


Figure 3. Hornblende phenocrysts in the quartz dioritic phase of porphyry (DHL-05-44-75, Grenoble Property)

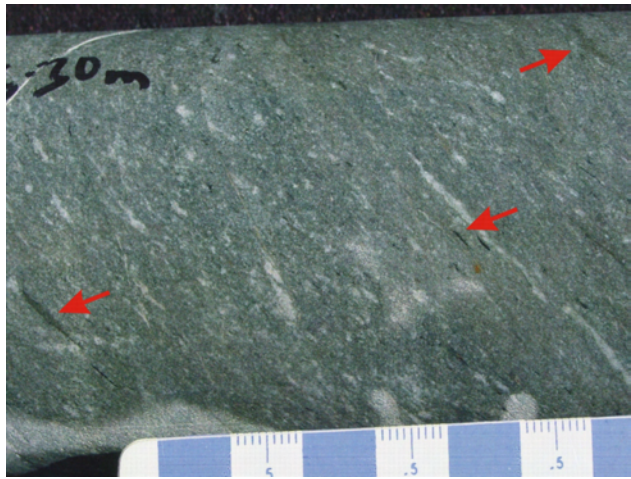


Figure 4. Feldspar-quartz crystal tuff with dark, wispy to elongate, lithic clasts (DHL05-48-195, Grenoble property).

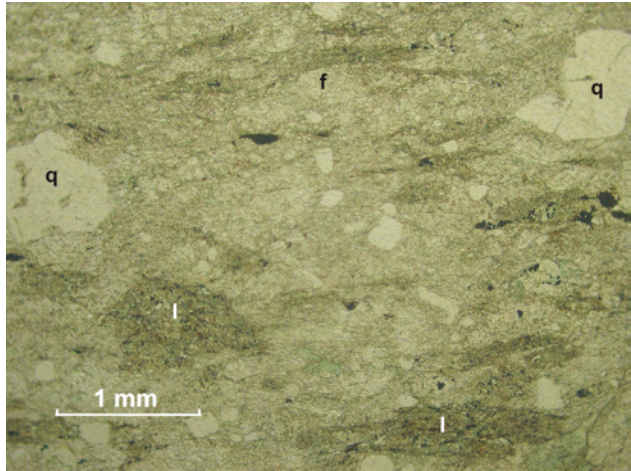


Figure 5. Photomicrograph (plane-polarized light) of feldspar-quartz crystal lithic tuff. Note the weakly foliated texture with the alignment of elongate lithic fragments (l) and feldspar phenocrysts (f). Also note embayments in rounded, clear quartz (q) (DHL 04-08-91, Grenoble property).

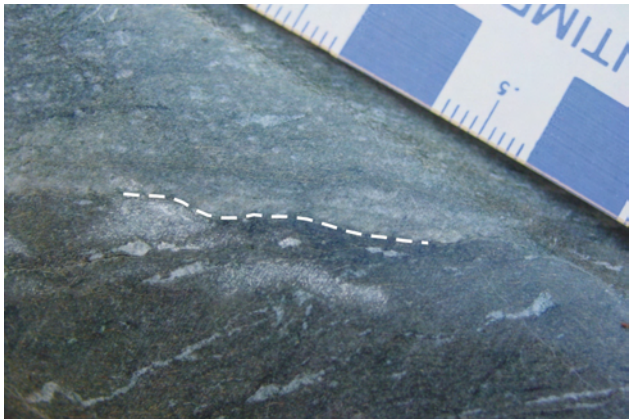


Figure 6. Bedding between light grey crystal tuff and dark grey fine-grained tuff (DHL 05 48-195, Grenoble property).



Figure 7. Typical Gidon Creek quartz-feldspar porphyry (05NMA25-03, UTM zone 11, 5431227N, 377351E NAD 83).

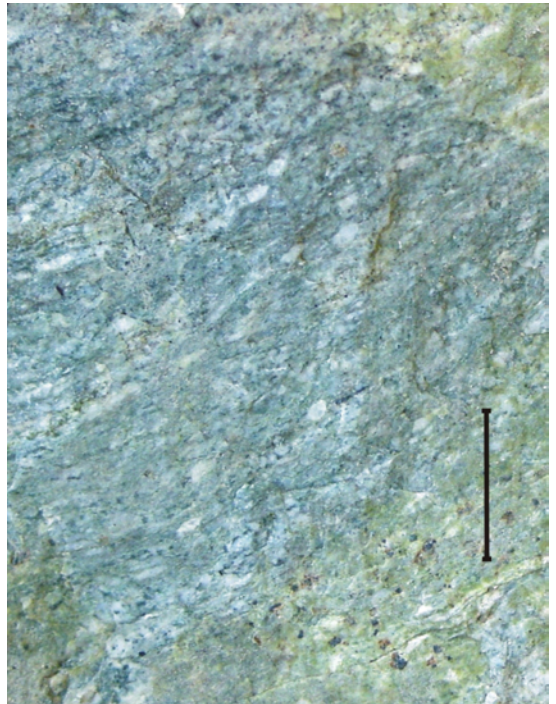


Figure 8. Sheared margin of Gidon Creek quartz-feldspar porphyry. Scale approximately 1 cm (05NMA25-01, UTM zone 11, 5429810N, 376039E NAD 83).

Such marginal shearing is typical of synkinematic intrusions of the Rosslund area (Dunne and Höy, 1992).

GEOCHEMISTRY

Geochemical analyses were performed on 15 samples from Lexington porphyry and volcanoclastic rocks and two samples of Gidon Creek porphyry. Major, minor and trace element data are reported in Table 1.

All Lexington samples are typical calcalkaline rocks of generally dacite to rhyolite composition (Fig 9, 10) and of typical volcanic arc affinity (Fig 11). Crystal tuff and massive dacite porphyry are similar in chemistry and appear to be comagmatic. Mafic tuff, however, differs significantly from its felsic cohort in high field-strength elements (HFSE) and rare earth elements (REE; Fig 12) and, despite being coeval, must be derived from a different magmatic source.

The Gidon Creek porphyry is also calcalkaline and of volcanic arc affinity (Fig 9, 10, 11) but differs from the Lexington dacite rocks in being more enriched in Ta, Nb (Fig 11b, d) and light rare earth elements (LREE; Fig 12). Along with lithological differences, this suggests that the Gidon Creek porphyry is not directly correlatable with the Lexington porphyry.

GEOCHRONOLOGY

The Lexington porphyry was previously ascribed a Cretaceous or Tertiary age (Little, 1983). Church (1992) and Dostal *et al.* (2001) have reported U-Pb zircon data for a quartz porphyry sample collected from the City of Paris mine area. This sample yielded zircons with variable inheritance from a Proterozoic source (2445 Ma old), though one concordant fraction suggested an age of 199.4 ± 1.4 Ma.

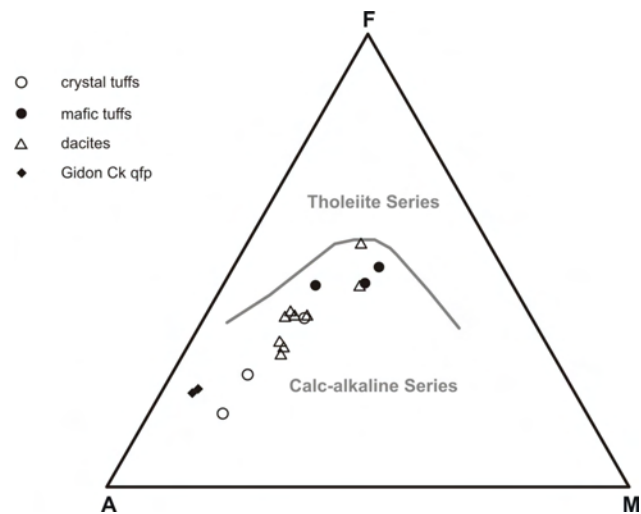


Figure 9. AFM diagram for Lexington and Gidon Creek samples; abbreviations: A, Na₂O + K₂O; M, MgO; F, FeO(t) + MnO; qfp, quartz-feldspar porphyry. Tholeiite-calcalkaline discriminant line after Irvine and Baragar (1971).

Ages of the volcanoclastic rocks have not been determined, though geochemical data would suggest that the crystal tuff is comagmatic and coeval.

A sample of Gidon Creek porphyry collected in 2005 from the Norwegian Creek area has also yielded zircons with considerable Proterozoic inheritance. A preliminary interpretation of the data by Mortensen (pers comm, 2006) suggests a date of 175 to 180 Ma, which is younger than the Lexington porphyry.

TABLE 1. MAJOR, MINOR AND TRACE ELEMENT ANALYSES FOR SAMPLES FROM THE GIDON CREEK AND LEXINGTON PORPHYRY DEPOSITS. ABBREVIATIONS: FSP, FELDSPAR; HB, HORNBLLENDE; MEGAXST, MEGACRYST; QZ, QUARTZ; XST, CRYSTAL.

Sample	Lab No	Suite	Description	SiO ₂ wt %	TiO ₂ wt %	Al ₂ O ₃ wt %	Fe ₂ O _{3t} wt %	MnO wt %	MgO wt %	CaO wt %	Na ₂ O wt %	K ₂ O wt %	P ₂ O ₅ wt %	LOI wt %	Total wt %
05NMA25-01B	59134	Gidon Creek	Quartz-eye, K-feldspar megaXst porphyry	66.62	0.34	16.28	2.73	0.07	0.77	3.19	4.74	3.38	0.12	0.92	99.23
05NMA25-03A	59135	Gidon Creek	Quartz-eye, K-feldspar megaXst porphyry	66.03	0.32	16.60	2.61	0.07	0.68	3.46	4.50	3.73	0.18	1.04	99.30
05NMA25-08A	59136	Lexington	dacite	61.11	0.55	18.91	5.07	0.01	2.38	2.33	2.52	2.66	0.32	3.92	99.83
05NMA25-08B	59137	Lexington	qz-fsp xst tuff ?	68.86	0.33	17.38	1.81	0.01	1.44	0.65	5.19	1.84	0.15	1.99	99.67
05NMA25-09	59138	Lexington	qz-fsp xst tuff ?	64.36	0.36	17.54	3.10	0.01	1.67	1.92	4.19	2.66	0.14	3.49	99.49
DHL04-01-99	59139	Lexington	dacite	60.46	0.35	17.14	4.29	0.02	2.35	3.05	2.70	3.69	0.14	4.39	98.64
DHL04-08-91A	59140	Lexington	?xst tuff	46.49	0.73	16.45	9.19	0.05	4.77	7.98	2.88	1.19	0.17	9.72	99.64
DHL04-08-91B	59141	Lexington	xst tuff	61.02	0.49	17.41	5.03	0.02	2.32	2.84	2.68	2.62	0.19	4.64	99.30
DHL04-08-126	59142	Lexington	qz-fsp-?hb dacite	61.64	0.16	16.60	4.39	0.34	2.35	3.81	2.60	0.05	2.64	4.59	99.21
DHL04-39-110	59143	Lexington	tuff	51.02	0.88	15.09	7.71	0.13	2.80	7.63	4.87	1.08	0.44	7.56	99.25
DHL05-44-75	59144	Lexington	?hb-qz-fsp dacite	64.27	0.16	17.81	3.95	0.43	2.32	1.57	6.38	0.03	0.39	2.11	99.60
DHL05-44-102	59145	Lexington	qz-fsp porphyry	61.66	0.19	17.28	5.41	0.41	1.99	4.93	2.14	0.10	1.48	3.51	99.15
DHL05-45-88	59146	Lexington	fsp-?hb-qz porphyry	60.40	0.39	16.28	5.21	0.01	1.95	3.75	3.37	2.57	0.15	4.46	98.59
DHL05-45-112	59147	Lexington	qz-fsp porph dacite	61.81	0.38	16.62	4.35	0.02	2.13	3.24	4.81	1.45	0.14	4.11	99.09
DHL05-48-195	59148	Lexington	?fsp xst tuff/schist	45.13	0.94	12.44	8.61	0.21	4.63	10.91	3.80	1.01	0.42	10.92	99.11
DHL05-53-165	59149	Lexington	fsp-qz(-hb) porph dacite	55.93	0.37	14.60	4.61	0.04	1.90	7.91	2.64	2.37	0.20	6.96	97.56
DHL05-55-154	59150	Lexington	qz-fsp-?hb porph dacite	60.53	0.33	16.33	5.53	0.02	2.05	3.39	3.81	2.07	0.22	4.83	99.16
			Reported detection limit	0.01	0.01	0.01	0.01	0.01	0.01	0.01	0.01	0.01	0.01	0.01	
			Analytical method	XRF1	XRF1	XRF1	XRF1	XRF1	XRF1	XRF1	XRF1	XRF1	XRF1	FUS	

XRF1 = Fused Disc - X-ray fluorescence
XRF2 = Pressed pellet - X-ray fluorescence
FUS = Loss on Ignition by fusion @1100 C
PIMS = Peroxide fusion-ICPMS

DISCUSSION

Petrological and lithological studies demonstrate that volcanoclastic rocks are included with massive dacite porphyry in the package known as the Lexington porphyry. Lithologically and geochemically, the intermediate to felsic crystal lithic tuff is very similar to the dacitic porphyry and is believed to be comagmatic. The massive rock types may be either shallow-level intrusions or flows. Mafic tuff interbedded in the sequence is coeval, though derived from a different magmatic source. The recognition of these units as true volcanic rocks could have significant implications not only for regional correlation and tectonic history, but also for the possible potential for VMS deposits such as the Lamfoot deposit (Cheney, 2004; Cheney *et al.*, 1994).

Similar felsic volcanoclastic rocks are not found in the immediate Lexington area and correlative equivalents are not recognized in the overall Boundary region. An age of 199 Ma would suggest a correlation of the Lexington package with the Lower Jurassic Elise Formation of the Rosslund Group. Höy and Andrew (1989) report a U-Pb zircon age of 197.1 ± 0.5 Ma for a feldspar crystal tuff approximately in the middle of the Elise Formation succession. Like the Lexington sample, this also has Proterozoic inheritance. Felsic volcanic rocks overlying the stratabound Lamfoot copper-gold deposit in Washington have been previously correlated with the Paleozoic Attwood Group (Cheney *et al.*, 1994). However, Rasmussen (2000) reported an Ar/Ar plateau age of 195 Ma on sericite

from these volcanic rocks and suggested correlation with the Elise Formation. Similar correlations are made for felsic volcanic rocks at the Morning Star mine (Cheney, 2004; Caron, pers comm, 2005). In the Rosslund area itself, however, the type Elise Formation comprises dominantly mafic

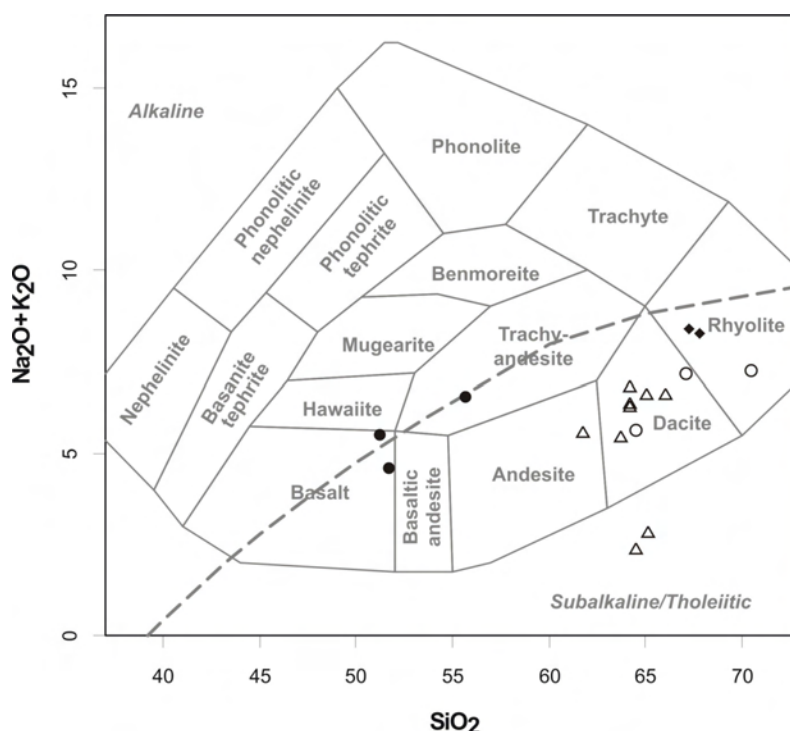


Figure 10. Total alkali-silica diagram for Lexington and Gidon Creek samples (symbols as for Fig 9). Classification after Cox *et al.* (1979).

TABLE 1 (CONTINUED)

Sample	Rb	Sr	Ba	Cs	V	Y	Zr	Hf	Nb	Ta	Th	La	Ce	Pr	Nd	Sm	Eu	Gd	Tb	Dy	Ho	Er	Tm	Yb	Lu
	ppm	ppm	ppm	ppm	ppm	ppm	ppm	ppm	ppm	ppm	ppm	ppm	ppm	ppm	ppm	ppm	ppm	ppm							
05NMA25-01B	80	1062	751	-3	63	21	144	3.428	18.646	1.014	4.405	19.798	35.702	4.225	16.687	3.124	0.850	2.825	0.400	2.437	0.540	1.584	0.240	1.565	0.240
05NMA25-03A	106	1087	836	-3	61	10	146	3.068	20.360	1.142	4.701	18.209	34.140	4.037	16.161	3.043	0.818	2.716	0.398	2.362	0.524	1.514	0.232	1.558	0.232
05NMA25-08A	84	391	500	-3	131	16	84	2.274	4.228	0.240	1.319	8.229	17.498	2.412	11.624	2.745	0.925	2.954	0.435	2.703	0.599	1.734	0.255	1.706	0.247
05NMA25-08B	72	314	241	-3	71	5	73	1.473	3.518	0.209	0.865	3.629	6.554	0.986	4.540	1.113	0.309	1.222	0.195	1.216	0.277	0.847	0.131	0.912	0.134
05NMA25-09	85	226	455	5	87	5	65	1.941	2.814	0.169	1.060	5.346	10.024	1.387	6.143	1.371	0.429	1.574	0.209	1.225	0.247	0.724	0.104	0.738	0.113
DHL04-01-99	114	195	556	-3	100	12	67	1.717	3.781	0.208	1.053	6.651	12.669	1.556	6.666	1.352	0.422	1.537	0.230	1.468	0.316	0.955	0.148	1.007	0.152
DHL04-08-91A	48	302	215	-3	249	15	52	1.491	2.570	0.129	1.122	7.752	16.135	2.211	10.378	2.449	1.098	3.062	0.464	2.997	0.635	1.858	0.280	1.830	0.242
DHL04-08-91B	74	255	388	-3	132	10	74	2.275	4.614	0.243	1.352	7.694	16.081	2.141	9.188	2.056	0.672	2.276	0.330	2.078	0.435	1.312	0.196	1.355	0.202
DHL04-08-126	105	209	575	4	110	11	58	1.776	3.777	0.206	1.072	4.998	9.731	1.219	5.214	1.186	0.375	1.464	0.226	1.439	0.312	0.953	0.147	0.972	0.149
DHL04-39-110	36	419	370	-3	245	12	116	3.275	16.026	1.008	3.373	17.063	33.569	4.220	17.950	3.702	1.153	4.182	0.590	3.580	0.723	2.060	0.299	1.999	0.276
DHL05-44-75	70	180	260	-3	122	27	76	2.232	3.991	0.250	1.620	41.443	70.440	7.442	26.214	4.427	0.960	4.225	0.688	4.334	0.861	2.454	0.362	2.391	0.321
DHL05-44-102	138	136	967	5	90	12	83	1.882	4.263	0.220	1.400	8.026	16.313	2.118	9.132	2.012	0.724	2.100	0.334	2.093	0.435	1.328	0.195	1.348	0.202
DHL05-45-88	83	281	555	3	120	3	60	1.778	3.811	0.181	0.968	4.694	9.191	1.174	5.082	1.201	0.446	1.390	0.225	1.484	0.327	0.991	0.146	1.007	0.153
DHL05-45-112	53	382	346	-3	103	14	61	1.333	3.644	0.175	0.920	5.083	10.032	1.269	5.367	1.224	0.387	1.354	0.217	1.379	0.286	0.856	0.130	0.927	0.135
DHL05-48-195	36	481	961	-3	255	24	92	2.648	15.033	0.856	2.411	15.393	30.877	4.010	17.411	3.896	1.195	4.016	0.596	3.549	0.690	1.916	0.272	1.785	0.249
DHL05-53-165	74	284	278	-3	94	13	57	1.419	2.942	0.137	0.774	6.207	11.934	1.540	6.797	1.563	0.638	1.648	0.252	1.558	0.320	0.966	0.144	0.980	0.146
DHL05-55-154	79	405	459	-3	101	4	61	1.911	2.430	0.124	0.942	5.137	10.025	1.254	5.375	1.299	0.440	1.425	0.203	1.340	0.261	0.776	0.119	0.830	0.137
	3	3	3	3	3	3	3	0.011	0.004	0.010	0.005	0.004	0.003	0.002	0.027	0.010	0.004	0.013	0.003	0.009	0.001	0.005	0.001	0.007	0.003
	XRF2	PIMS	PIMS	PIMS	PIMS	PIMS	PIMS	PIMS	PIMS	PIMS	PIMS	PIMS	PIMS	PIMS	PIMS	PIMS	PIMS	PIMS	PIMS						

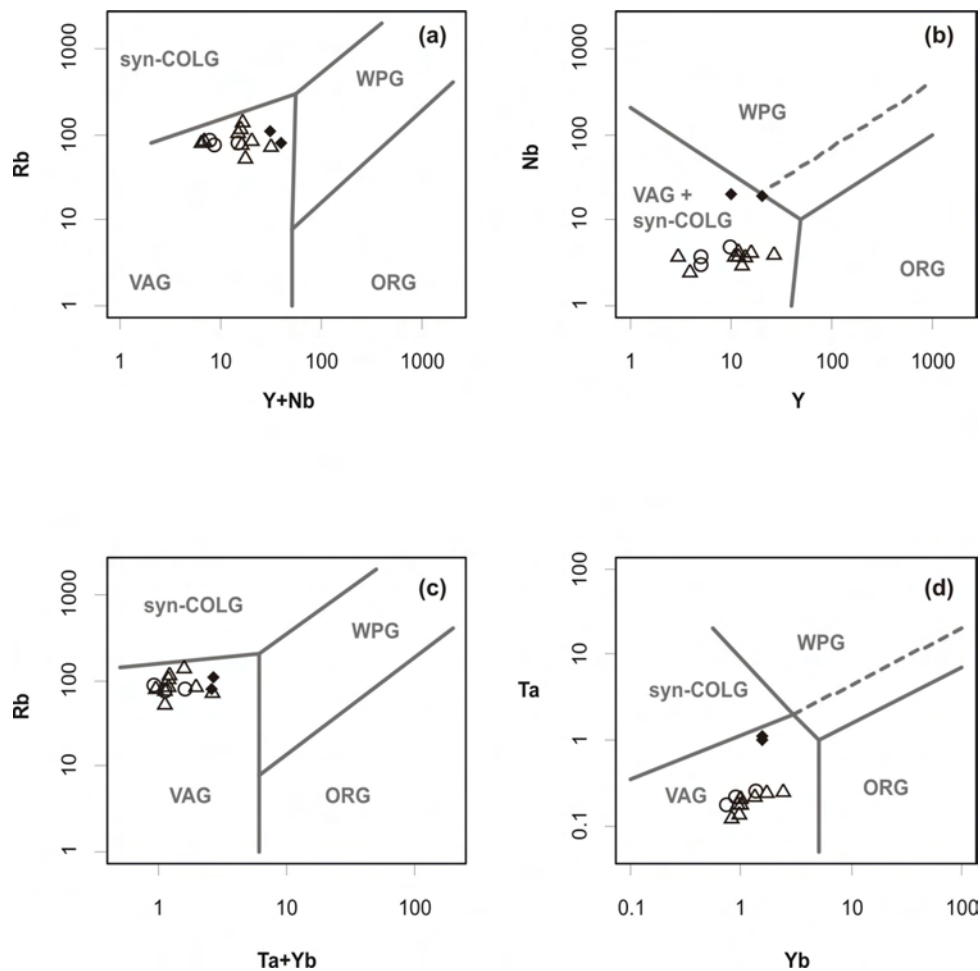


Figure 11. Tectonic discrimination diagrams for Lexington and Gidon Creek samples (symbols as for Fig 9), after Pearce *et al.* (1984); a) Y+Nb vs. Rb; b) Y vs. Nb; c) Ta+Yb vs. Rb; d) Yb vs. Ta. Abbreviations: ORG, ocean-ridge granite; WPG, within-plate granite; VAG, volcanic arc granite; syn-COLG, syn-collision granite.

to andesitic volcanic rocks and lacks significant felsic rocks (Höy and Andrew, 1989; Andrew *et al.*, 1990; Höy and Dunne, 1997).

The correlation of the Lexington porphyry rocks with the Elise Formation may shed some light on the age of sedimentary rocks in the footwall of the No 7 Fault. Black argillite, fine-grained dark grey siltstone or quartz wacke, with minor pebble conglomerate crop out around Mount McLaren and Rusty Mountain. This unit was assumed to be Jurassic by Little (1983) and to rest conformably on volcanic flows of the Triassic Brooklyn Formation to the north. However, the argillite was included in the Attwood Formation by Church (1986) and Fyles (1990). Similar argillite rocks, in a similar structural position in the footwall of the No 7 fault, and also associated with possible Elise Formation volcanic rocks, are found around the Morning Star deposit in Washington, where they are correlated with the Lower Jurassic Archibald Formation of the Rossland Group (Cheney, 2004; Caron, pers comm, 2005). Such a correlation can also be suggested for the Mount McLaren area.

The Gidon Creek quartz-feldspar porphyry is lithologically and chemically distinct from the Lexington porphyry. It is also younger and may correlate with the sim-

ilarly aged 178 to 182 Ma Silver King intrusions of the Rossland area. These synkinematic intrusions show similar intensely sheared margins to the Gidon Creek porphyry but lack the K-feldspar megacrysts (Dunne and Höy, 1992). Significantly, the Silver King intrusions and other synorogenic intrusions such as the Aylwin Creek and Cooper Creek stocks host copper-gold-silver mineralization, though no such mineralization has yet been reported in the Gidon Creek porphyry.

ACKNOWLEDGMENTS

The author is much indebted to Jim Fyles and Neil Church for all their invaluable help and advice during every stage of the Boundary project. The collaboration, support and ready welcome of the Boundary District exploration community were exceptional and, in particular, many thanks are extended to Bruce Laird of Merit Mining Corp. for his co-operation and invaluable assistance in sampling drillcore from the Grenoble property. The author also acknowledges the indispensable assistance of Ashley Dittmar and Eric Westberg during fieldwork. JoAnne Nelson read and provided valuable comments on an earlier version of this paper.

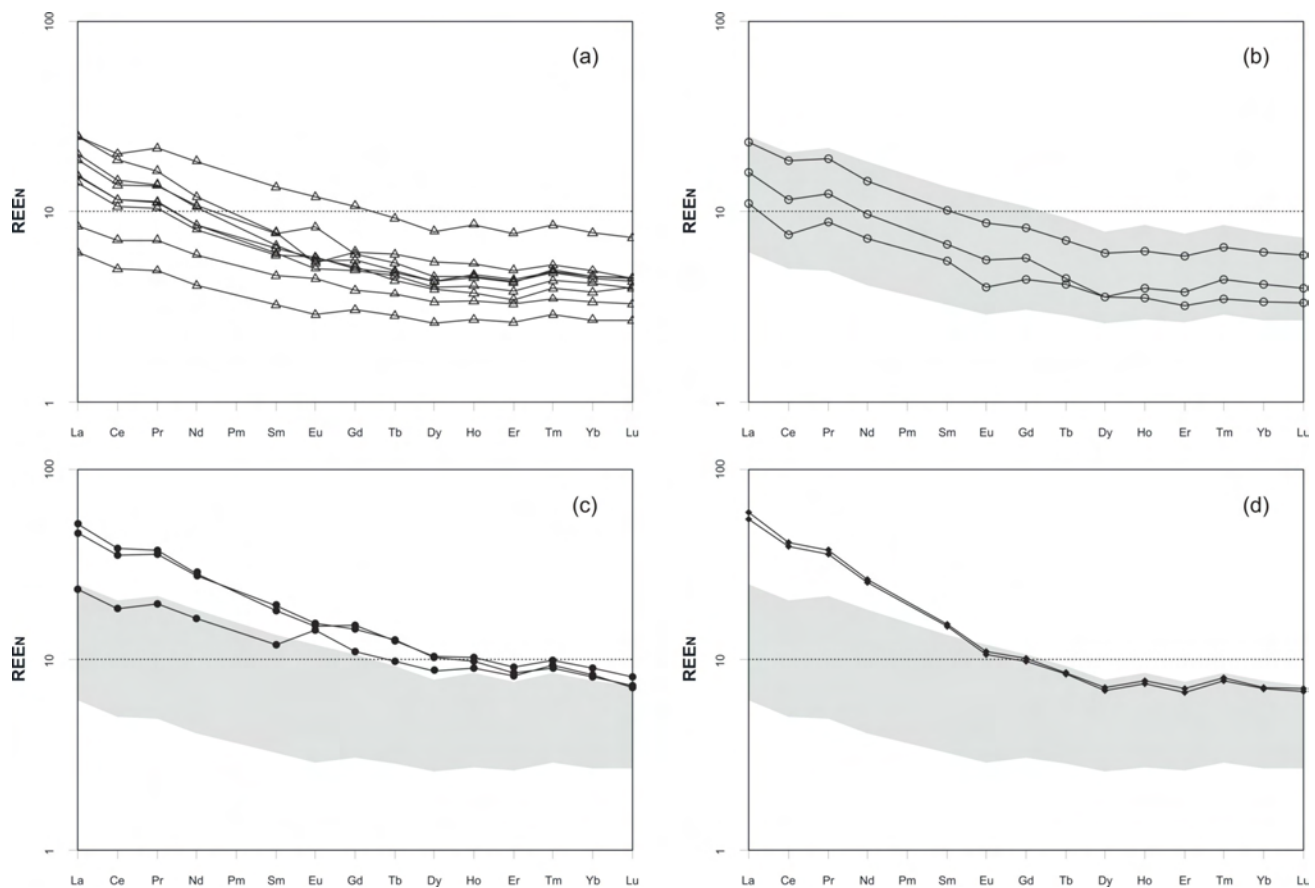


Figure 12. Chondrite-normalized rare-earth element plots for Lexington and Gidon Creek samples; a) dacite porphyry; b) crystal tuff; c) mafic tuff; and d) Gidon Creek porphyry. Shaded area in b) to d) is occupied by the dacite porphyry of Figure 12a. Normalizing values for REE (REE_N) after Nakamura (1974).

REFERENCES

- Andrew, K.P.E., Höy, T. and Drobe, J. (1990): Stratigraphy and tectonic setting of the Archibald and Elise Formations, Rossland Group, Beaver Creek area, southeastern British Columbia (82F/4E); in *Geological Fieldwork 1989, BC Ministry of Energy, Mines and Petroleum Resources*, Paper 1990-1, pages 19–27.
- Butler, S.P. (1997): Assessment Report on the Lexington Property 1996, Greenwood Mining Division, Britannia Gold Corp.; *BC Ministry of Energy, Mines and Petroleum Resources*, AR 24901, 27 pages.
- Cheney, E.S. (2004): The potential for volcanogenic massive sulfide deposits at the Morning Star mine Danville, Ferry County, Washington; Unpublished report for Brooklyn Mining and Exploration Company, LLC, 13 pages.
- Cheney, E.S., Rasmussen, M.G. and Miller, M.G. (1994): Major faults, stratigraphy, and identity of Quesnellia in Washington and adjacent British Columbia; *Washington Division of Geology and Earth Resources*, Bulletin 80, pages 49–71.
- Church, B.N. (1970): Lexington; in *Geology, Exploration, and Mining in British Columbia 1970, BC Ministry of Energy, Mines and Petroleum Resources*, pages 413–425.
- Church, B.N. (1986): Geological Setting and Mineralization in the Mount Attwood – Phoenix Area of the Greenwood Mining Camp; *BC Ministry of Energy, Mines and Petroleum Resources*, Paper 1986-2, 65 pages.
- Church, B.N. (1992): The Lexington Porphyry, Greenwood Mining Camp, southern British Columbia: Geochronology (82E/2E); in *Geological Fieldwork 1991, BC Ministry of Energy, Mines and Petroleum Resources*, Paper 1992-1, pages 295–297.
- Cowley, P.S. (2004): Assessment Report on the Lexington Property Diamond Drilling, Greenwood Mining Division, Gold City Industries Ltd.; *BC Ministry of Energy, Mines and Petroleum Resources*, AR 27393, 116 pages.
- Cox, K.G., Bell, J.D. and Pankhurst, R.J. (1979): The Interpretation of Igneous Rocks; *George Allen and Unwin.*, London, 450 pages.
- Dostal, J., Church, B.N. and Höy, T. (2001): Geological and geochemical evidence for variable magmatism and tectonics in the southern Canadian Cordillera: Paleozoic to Jurassic suites, Greenwood, southern British Columbia; *Canadian Journal of Earth Sciences*, volume 38, pages 75–90.
- Dunne, K.P.E. and Höy, T. (1992): Petrology of pre to syntectonic Early and Middle Jurassic intrusions in the Rossland Group, southeastern British Columbia (82F/SW); in *Geological Fieldwork 1991, BC Ministry of Energy, Mines and Petroleum Resources*, Paper 1992-1, pages 9–19.
- Fyles, J.T. (1990): Geology of the Greenwood – Grand Forks area, British Columbia, NTS 82E/1, 2; *BC Ministry of Energy, Mines and Petroleum Resources*, Open File 1990-25, 19 pages.
- Höy, T. and Andrew, K. (1989): The Rossland Group, Nelson map area, southeastern British Columbia (82F/6); in *Geological Fieldwork 1988, BC Ministry of Energy, Mines and Petroleum Resources*, Paper 1989-1, pages 33–43.

- Höy, T. and Dunne, K. (1997): Early Jurassic Rossland Group, Southern British Columbia: Part I Stratigraphy and Tectonics; *BC Ministry of Energy, Mines and Petroleum Resources, Bulletin 102*, 124 pages.
- Irvine, T.N. and Baragar, W.R.A. (1971): A guide to the chemical classification of the common volcanic rocks; *Canadian Journal of Earth Sciences*, volume 8, pages 523–548.
- Little, H.W. (1983): Geology of the Greenwood map area, British Columbia; *Geological Survey of Canada, Paper 79-29*, 37 pages.
- Merit Mining Corp. (2006): Greenwood Projects – Lexington Lone Star; *Merit Mining Corp.*, URL <<http://www.meritminingcorp.com/greenwood.htm#lexington>> [November 10, 2006].
- Nakamura, N. (1974): Determination of REE, Ba, Fe, Mg, Na and K in carbonaceous and ordinary chondrites; *Geochimica et Cosmochimica Acta*, volume 38, pages 757–775.
- Pearce, J.A., Harris, N.W. and Tindle, A.G. (1984): Trace element discrimination diagrams for the tectonic interpretation of granitic rocks; *Journal of Petrology*, volume 25, pages 956–983.
- Rasmussen, M.G. (2000): The Lamfoot Gold deposit, Ferry County, Washington (abstract); in “Republic Symposium 2000”, *Northwest Mining Association*, Dec 4-5, 2000.
- Seraphim, R.H., Church, B.N., and Shearer, J.T. (1995): The Lexington-Lone Star Copper-Gold Porphyry: An Early Jurassic Cratonic Linear System, Southern British Columbia; in *Porphyry Deposits of the Northwestern Cordillera of North America*, Schroeter, T.G., Editor; *Canadian Institute of Mining, Metallurgy and Petroleum, Special Volume 46*, pages 851–854.

Evaluation of Mineral Inventories and Mineral Exploration Deficit of the Interior Plateau Beetle Infested Zone (BIZ), South-Central British Columbia

by M.G. Mihalynuk

KEYWORDS: mountain pine beetle, Interior Plateau, geology, mineral inventory, mineral potential, mineral exploration, MINFILE, ARIS

INTRODUCTION

Mountain pine beetles are a natural disturbance agent within the forests of western North America, where they are known to range from British Columbia to northern Mexico (Amman and Logan, 1998). They were first described in South Dakota as the “pine destroying beetle of the Black Hills”, and measures were taken to control their spread as early as 1902 (Hopkins, 1905). Outbreaks of mountain pine beetle are a natural phenomenon. Recorded infestations in British Columbia date back to 1913 (Unger, 1993), and tree scar evidence for infestations dates back hundreds of years (Taylor and Erickson, 2003).

It is human interference with the normal succession of forest fires, a principal regulator of forest ecosystem health and creator of barriers to disease transmission (e.g. Hirsch *et al.*, 2001), that has rendered the pine forests of Interior British Columbia susceptible to an outbreak of mountain pine beetle of historically unprecedented scale.

In an area extending north from Kamloops to Smithers and east from the Coast Mountains to the Rocky Mountain Trench, pine is the most widespread commercial tree species, and pine beetle infestation was essentially continuous in 2004 (BC Ministry of Forests and Range, 2005a; Figure 1). We refer to this area as the Beetle Infested Zone (BIZ). The BC Ministry of Forests (MoF) predicts that only about 10% of the already diminished 2006 volume of pine will be left standing by 2016 (Eng *et al.*, 2006). Accelerated timber harvests have brought temporary economic prosperity to many forestry-dependent communities within the BIZ, but harvest levels will likely begin to decline by 2015 (BC Ministry of Forests and Range, 2005a). Anticipating an economic downturn in the forestry sector within the BIZ, the provincial government is supporting economic diversification throughout the region. Work presented here and by other reports in this volume, is part of that provincial effort (e.g. Andrews and Russell, 2007; Logan *et al.*, 2007; Mihalynuk *et al.*, 2007; Schiarizza and Macaulay, 2007).

Accelerated timber harvest, attendant overburden disturbance, needle loss and forest fires should yield unprecedented opportunities to discover never-before-seen bedrock outcrops within the BIZ. Cospatial with the BIZ is a

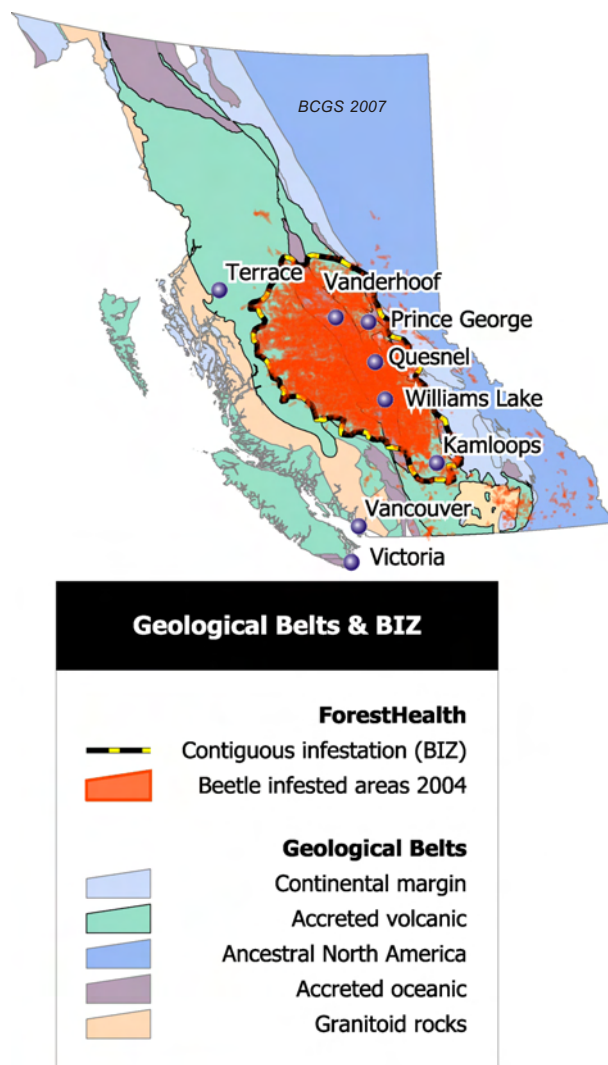


Figure 1. Location of the area of mountain pine beetle infestation, based on the BC Ministry of Forests and Range (2005) Forest Health Survey for 2004. The area of contiguous infestation, shown by the dashed outline, is herein referred to as the Beetle Infested Zone (BIZ).

geological province that has historically been avoided by mineral explorationists, mainly because of lack of outcrop and extensive veneers of Cenozoic volcanic deposits with no known economic mineralization. However, sparse exposures of basement rocks throughout the BIZ show that the pre-Cenozoic geological and metallogenic fabric of the province continue in the subsurface, and so too should the

This publication is also available, free of charge, as colour digital files in Adobe Acrobat® PDF format from the BC Ministry of Energy, Mines and Petroleum Resources website at http://www.em.gov.bc.ca/Mining/Geosurv/Publications/catalog/cat_fldwk.htm

rich mineral endowment both south and north of the BIZ (Fig 1). A principal objective of the BIZ Project is to demonstrate that application of conventional and nonconventional exploration techniques can be successfully applied to large tracts of the BIZ. Field-based results of the first season of the BIZ project are available as GeoFile 2007-5.

This report is concerned with estimating the value of past (Fig 2) mineral exploration expenditures, and measuring disparities in mineral production or inventories between geological belts outside the BIZ and those within the BIZ. Such disparities are herein attributed primarily to a relative lack of exploration within the BIZ.

ESTIMATES OF MINERAL ENDOWMENT

West of the ancestral North American continental margin, north-northwest-trending belts of ancient volcanic arcs form the principal geological fabric of British Columbia. Each belt is characterized by surprisingly consistent rock successions throughout the length of the province. Thus, the average mineral wealth demonstrated within the best exposed and most exhaustively explored parts of these belts can reasonably be expected within the least well exposed/ explored parts. In this manner, mineral resource production, inventory, exploration and probabilistic estimates

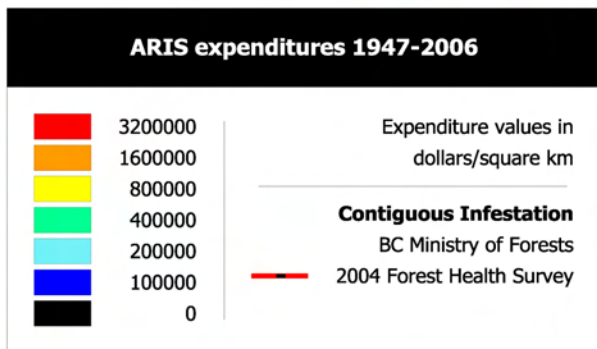
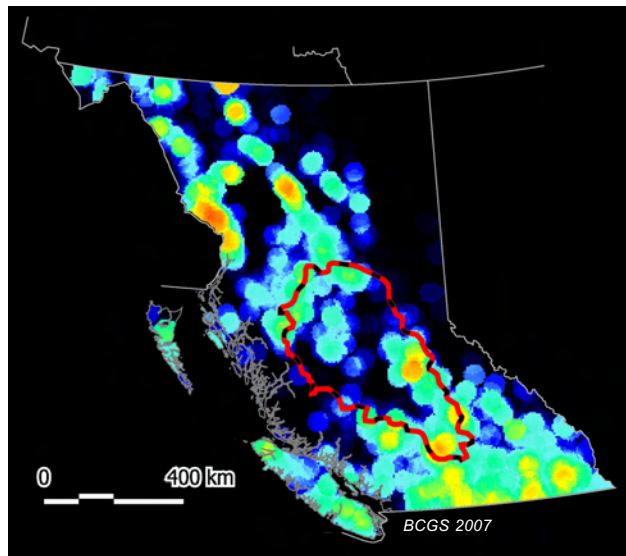


Figure 2. Contour plot showing the distribution of mineral exploration expenditures in British Columbia based on information captured within the Assessment Report Indexing System (ARIS) from its inception in 1947. The BIZ outline is shown for reference.

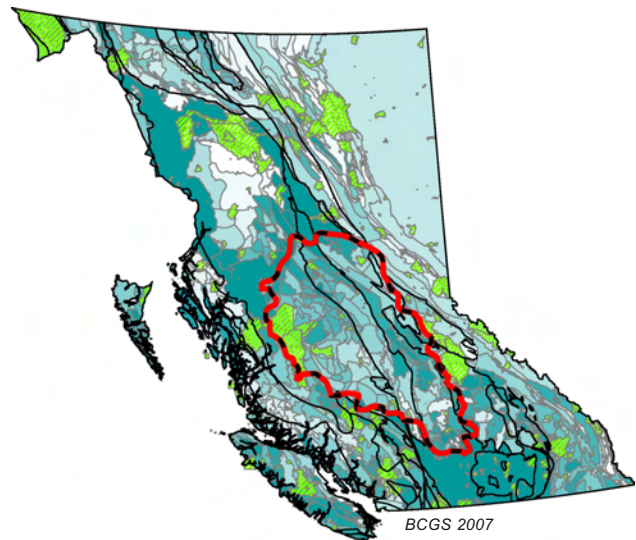


Figure 3. Mineral potential tracts and their relative ranking, based on the Mineral Resource Assessment (Level 1) results (*cf.* Kilby, 2004). Parklands and the BIZ are shown for reference. Much of the BIZ is underlain by tracts that have intermediate to high rankings.

made for well-exposed parts of the belts outside the BIZ can be compared to those within the BIZ, and deficits can be largely attributed to lack of exploration, mainly as a result of extensive cover by young volcanic rocks or glacial deposits. A summary of mineral endowment measurement criteria, and mineral exploration, inventory and production deficit estimates for the BIZ, is presented in Table 1.

Mineral Potential Project Data

Approximately 30 person-years of work between 1992 and 1997 were invested in the BC Geological Survey's Mineral Potential Project to help direct the establishment of park boundaries. This comprehensive assessment established British Columbia as the first province in Canada with a complete assessment of its mineral potential (Kilby, 2004). A decade later, these data continue to be useful in directing public policy, and they are used here as one method of estimating the undiscovered mineral wealth of the BIZ.

One of the first steps of the mineral potential evaluation was to divide the province into manageable land tracts of relatively uniform size defined principally on the basis of bedrock geology. Of the 794 mineral potential tracts thus defined, 150 fall entirely or largely within the BIZ (Fig 3). These tracts, taken to be representative of the BIZ, cover 158 000 km² — a good approximation of the 155 000 km² enclosed by the BIZ outline as determined from the BC Forest Health Survey (BC Ministry of Forests and Range, 2005a).

TABLE 1. COMPARISON OF METALLIC AND INDUSTRIAL MINERAL INVENTORIES AND MINERAL EXPLORATION WITHIN THE BIZ TO GEOLOGICAL BELTS ALONG STRIKE TO THE NORTH AND SOUTH

Estimation criteria	\$millions			\$/km ²
	Value	Average	Standard deviation	
BIZ (150 tracts, 158 000 km²):				
Assessment Reports BIZ (I 2.2%)*	280	0.047	0.23	1770
Assessment Reports BIZ (I 4.24%)#	430	0.073	0.34	2720
Metal Inventory BIZ	5470	36	120	34640
Industrial Minerals Inventory BIZ	3020	20	120	1910
Past Production BIZ	1610			10220
Exploration Efficacy Index (EEI) <i>((Inventory+\$Production)/\$Exploration)</i>	17			
South of BIZ (61 tracts, 48 000 km²):				
Assessment Reports south of BIZ (I 4.24%)	275	0.052	0.14	5730
Metal inventory south of BIZ	4680	77	200	97500
Industrial Mineral inventory south of BIZ	1640	27	110	34100
Past Production south of BIZ	2240			46600
EEI south of BIZ	31			
BIZ to Bowser Basin (40 tracts, 37 000 km²):				
Assessment Reports BIZ to Bowser (I 4.24%)	142	0.08	0.22	3840
Metal Inventory BIZ to Bowser	1960	49	96	53000
Industrial Mineral inventory BIZ to Bowser	102	2.6	9.3	2760
Past Production BIZ to Bowser	32			860
EEI BIZ to Bowser	15			
North of BIZ (125 tracts, 82000 km²):				
Assessment Reports north of BIZ (I 4.24%)	604	0.13	0.43	7370
Metal Inventory north of BIZ	7740	60	180	94400
Industrial Mineral inventory north of BIZ	280	2.2	17	3410
Past Production north of BIZ	910			11100
EEI north of BIZ	15			
BIZ deficits [(N+S)/2-BIZ] per km²:				
Exploration in BIZ (ARIS)				3830
Metal Inventory BIZ (Mineral Potential)				61310
Industrial Mineral inventory (Mineral Potential)				16850
Production				18630

Two estimates of inflation were used to adjust past expenditures: * an accepted modern inflation rate of 2.2%; # an inflation rate of 4.24% based on the calculated mean of the percentage change in the Consumer Price Indexes as provided by Statistics Canada for the years 1946 to 2006 (Figure 4). Assessment Reports with records of expenditures were required in BC starting in 1947.

Production and mineral inventory data used as part of the Mineral Potential Project were based on a 1986 compilation. Now 20 years out of date, the data remain useful from a comparative standpoint, even if the absolute numbers are no longer valid. Commodity prices used in the mineral potential evaluation were an average for the period 1981–1990 (*e.g.*, Au \$596/oz, Cu \$1.13/lb, Mo \$6/lb) and are comparable with commodity prices averaged over the past decade, although lower than prices for most of 2006.

Estimating undiscovered mineral resources is a difficult and contentious exercise. Part of the Mineral Potential Project involved computer simulation of undiscovered mineral resources guided by probabilistic estimates from mineral exploration experts. Numbers of undiscovered deposits thus determined were tabulated at various confidence levels. For example, in the Cariboo region, estimated metallic mineral resources yet to be discovered at 90, 50, 10 and 1% confidence levels (in millions of 1986 Canadian dollars) were 1912, 68 997, 886 029 and 14 894 274, respectively (Kilby, 2004; the Cariboo region, which under-

lies a large portion of the BIZ, is shown in 5). It is stressed that the utility of these probabilistic estimates is in ranking mineral potential tracts, not in determining the present in-ground value of undiscovered mineral resources. Nevertheless, as noted by Kilby (2004), a consistent result of the probabilistic assessment process is that, at the 50% confidence level, about three-quarters of the province's mineral endowment remains to be discovered.

Comparative Mineral Endowment

Despite considerable challenges for exploration within the BIZ, there are many examples of past exploration success. Historic producers, such as those of the Quesnel Trough copper belt (*e.g.*, Copper Mountain, Iron Mask, Mount Polley, along the axis of the eastern accreted volcanic belt, Fig 1), Equity Silver and large deposits with outlined resources that have yet to be mined (*e.g.*, Prosperity), are a testimony to the mineral endowment of the area.

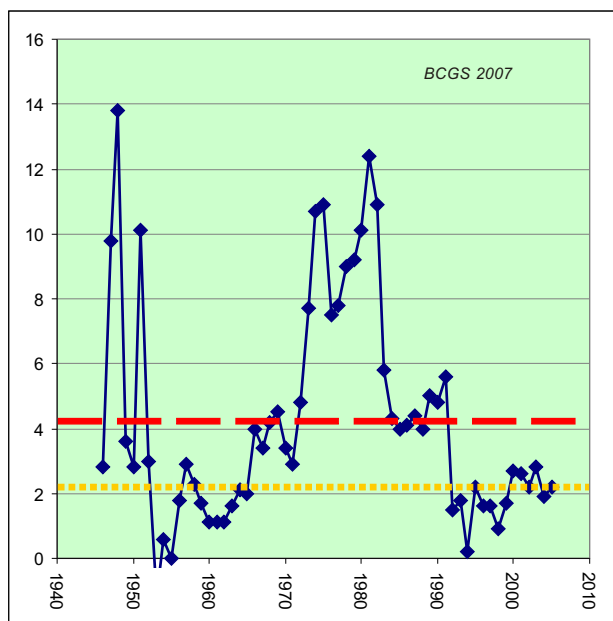


Figure 4. Annual change in Consumer Price Index as a monitor of inflation for the years 1946 to 2005. The average annual change in Consumer Price Index over this period is +4.24% (dashed red line). A commonly cited average rate of +2.2% is applicable to the last decade only (shown by the dotted yellow line). Source of data: Statistics Canada (2006).

Recognizing that geological belts continue from south to north of the BIZ, a qualitative visual estimate of undiscovered mineral wealth can be made by contouring the density of mineral occurrences, and comparing the area within the BIZ with areas along strike to the south and north. This can be easily accomplished using the province-wide MINFILE database of more than 12 000 mineral occurrences (MINFILE, 2006). For the purposes of presentation here, a grid (0.1° latitude by 0.2° degree longitude) was generated over the province and grid cells were coloured based on the number of MINFILE occurrences that they contain (Fig 5). An indication of the relative importance of MINFILE occurrences can be determined spatially by similarly contouring the distribution of mineral exploration expenditures (Fig 2). A recent data posting from the Assessment Report Indexing System (ARIS) is used (ARIS, 2006), with figures adjusted for an average inflation rate of 4.24% (Fig 4). Reporting mineral exploration activity in 'Assessment Reports' is one mechanism for maintaining mineral tenure within BC. A synoptic database of reports (available for download; ARIS, 2006), captures monetary expenditures since 1947. In 1997, it was estimated that only about 40% of mineral exploration expenditures in BC were recorded in ARIS (Wilcox, 1998)

In addition to the forgoing visual comparisons, quantitative analyses are presented here (Table 1), based on metallic and industrial mineral inventory and production figures from deposits within, north and south of the BIZ (MINFILE, 1995; see Fig 6 for areas covered). Mineral exploration expenditures recorded in ARIS since 1947 were compared for these same regions.

Results of Inventory and Exploration Expenditure Analysis

On a per square kilometre basis, mineral production values within the BIZ are \$10 220, whereas those to the south and north of it are \$46 600 and \$11 100, respectively (1986 Canadian dollars; Fig 5). Almost 400% more production has been recorded within the populated, relatively well-explored and well-exposed southern part of the province, as compared with rocks of the BIZ that lie along strike. Past production within the BIZ is comparable with that in correlative rocks to the north; however, metal inventories in the north are nearly 300% of those within the BIZ (\$94 400 versus \$34 640/km²), partly reflecting the difficulty of developing deposits within the remote north, but also underscoring the relative lack of exploration within the BIZ. For example, mineral exploration expenditures to the north along strike from the BIZ are nearly triple those within the BIZ. Exploration expenditures to the south are more than double those of the BIZ. The actual disparity is probably

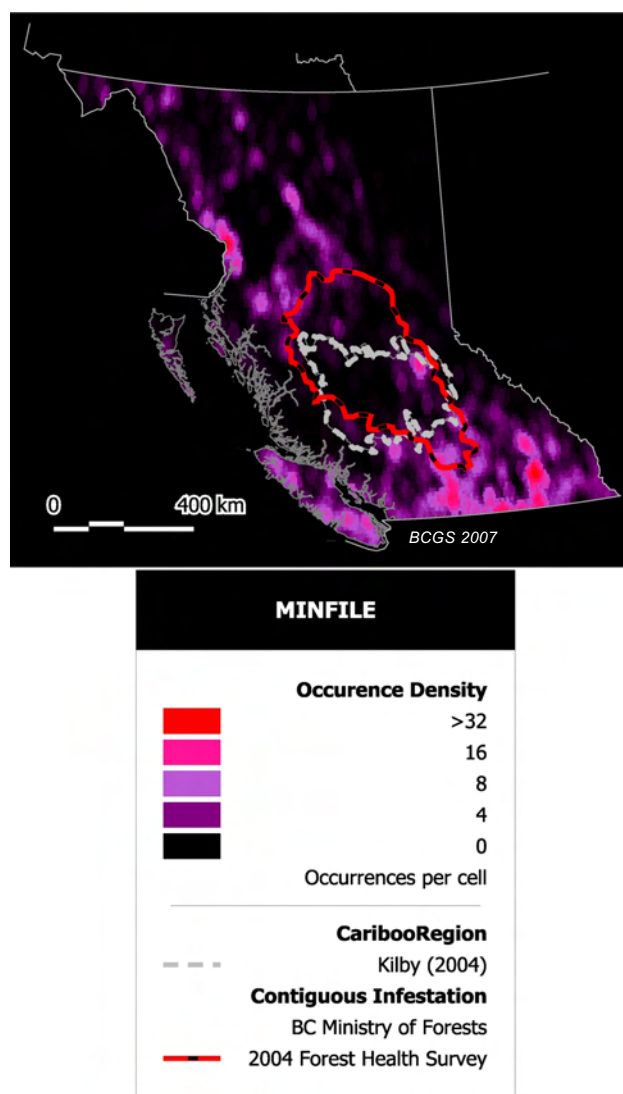


Figure 5. Number of mineral occurrences documented in MINFILE, shown as contoured density per 0.02 square degree grid cell. Also shown for reference is the Cariboo region, as defined in Kilby (2004), and the BIZ.

much greater because more of the exploration in the south predates the 1947 beginnings of expenditure capture by ARIS than is the case for the BIZ. In addition, perhaps as much as 60% of exploration work (*cf.* Wilcox, 1998), particularly regional work, is not filed for assessment and is therefore lost in this analysis.

An indication of how much exploration work in southern British Columbia predates ARIS can be estimated by comparing the ratio (Production + Inventories) / (ARIS expenditures) between regions. This ratio is essentially a measure of the efficacy of exploration. It is herein referred to as the Exploration Efficacy Index (EEI). Higher numbers indicate more inventory+production arising from each exploration dollar. South of the BIZ, the EEI is 31, versus 17 for the BIZ and 15 for areas to the north of the BIZ (Fig 6). Better infrastructure in the south can account for reduced exploration expenditures today. However, a lack of infrastructure 60 or more years ago (pre-1947) posed challenges in the south, as it now does in the central and northern parts of the province. It may be that mineral deposits were easier to find, and therefore investment in the first-pass mineral exploration was more fruitful, but most of the difference in EEI is herein attributed mainly to lack of capture of exploration expenditure data. If this is true, then an EEI of 17 to 20 for the south may be reasonable, and more accurate minimum exploration expenditures/km² would be at least 50% greater than those listed for 'South of the BIZ' (Table 1). Nevertheless, the conservative approach used herein considers only expenditures recorded in ARIS.

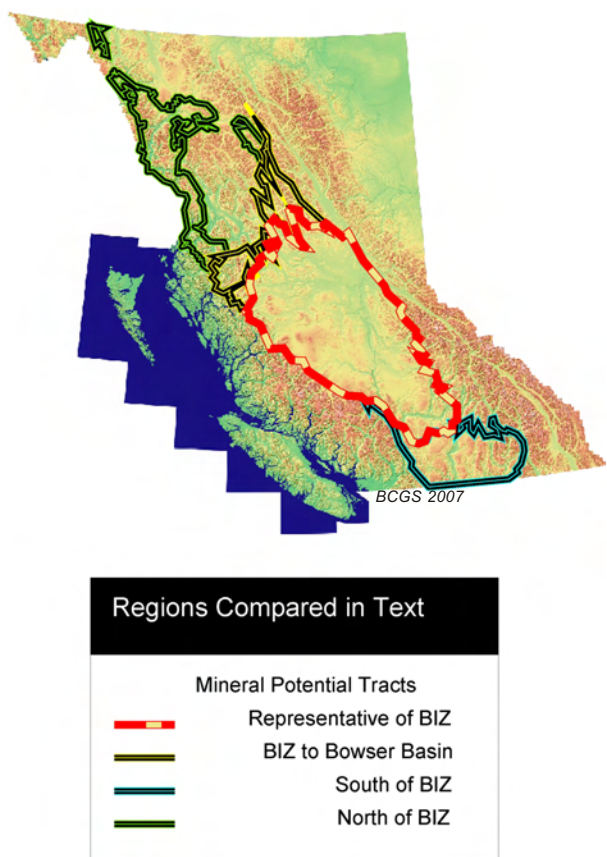


Figure 6. Regions compared within the analysis presented in this report. The area north of the BIZ is subdivided into south (yellow) and north (green) of the Bowser Basin. Major parks are excluded.

Exploration and inventory deficits within the BIZ can be crudely calculated by averaging the values from north and south of the BIZ and subtracting the values for the BIZ. Because this analysis includes pre-1947 data on mineral production, but not exploration expenditures, it gives only an indication of the minimum exploration expenditures required to find a density of deposits equivalent to the average outside the BIZ. For example, more than \$3800 of exploration per km² will be required to bring the level of exploration up to the recorded average level of exploration along strike outside the BIZ. This translates into a minimum of nearly \$600 million in exploration investment required in the BIZ to equal the average level of exploration in equivalent rocks to the north and south, as recorded by ARIS. Considering that maybe 40% of provincial mineral exploration expenditures are recorded in ARIS (likely less in the period between 1947 and 1997), a more accurate estimate of the current exploration expenditure deficit in the BIZ is probably about \$1.5 billion.

NEXT STEPS

Perhaps the greatest impediment to attracting significant mineral exploration investment in the BIZ is the geological uncertainty posed by the extent and thickness of cover successions. Work presented elsewhere in this volume (Andrews and Russell, 2007; Mihalynuk, 2007; Mihalynuk et al., 2007) suggests that the perceived thick blanket of cover may be exaggerated. For example, a first generation 3-D model of the principal cover succession indicates that most of it is less than 25 m thick (Mihalynuk, 2007). Future work aimed at refining the 3-D geometry of the cover succession, and its affect on geochemical and geophysical signals, will be instrumental in targeting the next \$1.5 billion invested in mineral exploration. Considering that an estimated three-quarters of the province's mineral wealth is yet to be discovered (Kilby, 2004), the mineral exploration prospects for the BIZ are bright indeed.

REFERENCES

- Amman, G.D. and Logan, J.A. (1998): Silvicultural control of mountain pine beetle: prescriptions and the influence of microclimate; *American Entomologist*, volume 44, pages 166–177.
- Andrews, G.D.M. and Russell, J.K. (2007): Mineral exploration potential beneath the Chilcotin Group (NTS 0920, P; 093A, B, C, F, G, J, K), south-central British Columbia: preliminary insights from volcanic facies analysis; in *Geological Fieldwork 2006, BC Ministry of Energy, Mines and Petroleum Resources*, Paper 2007-1 and *Geoscience BC*, Report 2007-1, pages 229–238.
- ARIS (2006): Assessment Report Indexing System; *BC Ministry of Energy, Mines and Petroleum Resources*, URL <http://www.em.gov.bc.ca/DL/BC_maps/MDBC/aris_dbf.zip> [September 2006].
- BC Ministry of Forests and Range (2005a): BC forest health survey data 2004; *BC Ministry of Forests and Range*, URL <http://www.for.gov.bc.ca/ftp/HFP/external/publish/Aerial_Overview/2004/> [February 2006].
- BC Ministry of Forests and Range (2005b): British Columbia's Mountain Pine Beetle Action Plan 2005–2010; *Province of British Columbia*, URL <http://www.for.gov.bc.ca/hfp/mountain_pine_beetle/actionplan/2005/actionplan.pdf> [December 2006].

- Eng, M., Fall, A., Hughes, J., Shore, T.L., Riel, B., Walton, A. and Hall, P. (2006): Provincial-level projection of the current mountain pine beetle outbreak: update of the projection of non-recovered losses for the reference management scenario based on the 2005 Provincial Aerial Overview of Forest Health and revisions to “the model” (BCMPB.v3); *BC Ministry of Forests and Range*, URL <<http://www.for.gov.bc.ca/hre/bcmpb/BCMPB.v3.BeetleProjection.Update.pdf>>, 7 pages [October 2006].
- Hirsch, K., Kafka, V., Tymstra, C., McAlpine, R., Hawkes, B., Stegehuis, H., Quintilio, S., Gauthier, S. and Peck, K. (2001): Fire-smart forest management: a pragmatic approach to sustainable forest management in fire-dominated ecosystems; *The Forestry Chronicle*, volume 77, pages 357–363.
- Hopkins, A.D. (1905): The Black Hills Beetle; *US Department of Agriculture, Bureau of Entomology*, Bulletin 56, 24 pages.
- Kilby, W.E. (2004): The British Columbia Mineral Potential Project 1992–1997; *BC Ministry of Energy and Mines*, Geofile 2004-2, 324 pages.
- Logan, J.M., Mihalynuk, M.G., Ullrich, T. and Friedman, R.M. (2007): U-Pb ages of intrusive rocks and $^{40}\text{Ar}/^{39}\text{Ar}$ plateau ages of copper-gold-silver mineralization associated with alkaline intrusive centres at Mount Polley and the Iron Mask batholith, southern and central British Columbia; in *Geological Fieldwork 2006, BC Ministry of Energy, Mines and Petroleum Resources*, Paper 2007-1 and *Geoscience BC*, Report 2007-1, pages 93–116.
- Mihalynuk, M.G. (2007): Neogene and Quaternary Chilcotin Group cover rocks in the Interior Plateau, south-central British Columbia: a preliminary 3-D thickness model; *BC Ministry of Energy, Mines and Petroleum Resources*, Paper 2007-1 and *Geoscience BC*, Report 2007-1, pages 143–148.
- Mihalynuk, M.G., Harker, L.L., Lett, R.E. and Grant, D.B. (2007): Results of reconnaissance surveys in the Interior Plateau Beetle Infested Zone; *BC Ministry of Energy, Mines and Petroleum Resources*, GeoFile 2007-5.
- MINFILE (1995): MINFILE reserves and resources inventory; *BC Ministry of Energy, Mines and Petroleum Resources*, Open File 1995-19.
- MINFILE (2006): MINFILEpc database, *BC Ministry of Energy, Mines and Petroleum Resources*, URL <<http://www.em.gov.bc.ca/Mining/Geolsurv/Minfile/minfpc.htm>> [October 2005].
- Read, P. B. (2000): Geology and industrial minerals of the Tertiary basins, south-central British Columbia; *BC Ministry of Energy, Mines and Petroleum Resources*, GeoFile 2000-3, 110 pages, URL <<http://www.em.gov.bc.ca/mining/Geolsurv/Publications/Geofiles/Gf2000-3/toc.htm>>, [October 2, 2006].
- Schiarizza, P. and Macaulay, J. (2007): Geology and mineral occurrences of the Hendrix Lake area (NTS 093A/02), south-central British Columbia; in *Geological Fieldwork 2006, BC Ministry of Energy, Mines and Petroleum Resources*, Paper 2007-1 and *Geoscience BC*, Report 2007-1, pages 179–202.
- Statistics Canada (2006): Consumer Price Index, historical summary; Statistics Canada, URL <<http://www40.statcan.ca/101/cst01/econ46a.htm>>, <<http://www40.statcan.ca/101/cst01/econ46b.htm>> and <<http://www40.statcan.ca/101/cst01/econ46c.htm>> [October 2006].
- Taylor, S. and Erickson, B. (2003): Historical pine beetle activity; *Canadian Forest Service, Pacific Forestry Centre*, URL <http://www.pfc.cfs.nrcan.gc.ca/entomology/mpb/historical/index_e.html> [October 2006].
- Unger, L.S. (1993): Mountain pine beetle; *Natural Resources Canada, Pacific Forestry Centre*, 8 pages.

Neogene and Quaternary Chilcotin Group Cover Rocks in the Interior Plateau, South-Central British Columbia: A Preliminary 3-D Thickness Model

by M.G. Mihalynuk

INTRODUCTION

Mineral exploration in the Interior Plateau region of British Columbia has been thwarted by lack of outcrop and a presumed 'great thickness' of Chilcotin Group cover. The plateau basalt of the Chilcotin Group has been considered a particularly severe impediment because it may mask underlying geochemical and geophysical signals. Thick cover also presents uncertainty for advanced exploration and development. If a mineral deposit was to be detected through thick basalt, would the extra exploration and development costs be prohibitive? What is the thickness of the overburden? Geological uncertainty is a principal source of exploration investment risk and, on the plateau, the principal geological unknown in many areas is depth of overburden.

To attract mineral exploration investment to underexplored parts of the Interior Plateau (*cf.* Mihalynuk, 2007), it is necessary to reduce investment risk. This paper is aimed at resolving uncertainty with respect to the cover thickness. It is an account of the methods and results of a first generation 3-D thickness model for Chilcotin Group cover over a large portion of the Interior Plateau.

The gently undulating plateau basalt flows that form the most conspicuous part of the Chilcotin Group range in age from Neogene¹ to Quaternary, *ca.* 16 to 1 Ma (Bevier, 1983; Mathews, 1989). These rocks are most extensive in NTS map sheets 092O and P, and 093B and C (Fig 1; Massey *et al.*, 2005). Accordingly, this area was chosen for the thickness model. Correlative rocks extend from the Okanagan Highlands, south of Vernon, to the Summit Lake area, north of Prince George (Mathews, 1989).

Most people are impressed by the thickness of the Chilcotin Group strata where they are best exposed along the incised flanks of major river valleys. However, these exposures may not be representative of the largest expanses of the Chilcotin Group. For example, thicknesses along the Fraser River may be representative of infilling of

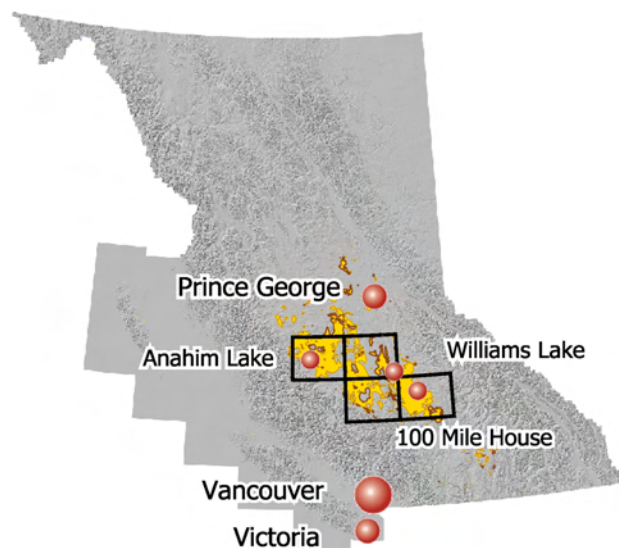


Figure 1. Provincial shaded relief map showing the location of the area considered for the Chilcotin thickness model. Map sheets, from northwest to southeast, are 093C, B; 092O, P. Chilcotin Group is highlighted in yellow.

a previous paleotopographic low. Immediately east of the Fraser River and south of the Highway 20 crossing, a narrow (less than approx. 200 m) basalt rampart clings to the pre-existing valley wall of Paleozoic strata (Fig 2). East of the Fraser River, K-Ar whole rock ages in this region average 4 Ma (N = 7), whereas those to the west average 16 Ma (N = 4; Mathews, 1989; Breitsprecher and Mortensen, 2004). In this same area, more than 180 m of glaciolacustrine strata have been incised by the Fraser River. Deposition of glaciolacustrine strata probably followed river damming by basalt flows (Mathews, 1989). An axis of glaciofluvial deposition near the Fraser River points to the precursor valley in Quaternary time, and the basalt ramparts built atop old valley walls point to an even older paleovalley (*cf.* Read, 2000; Mathews, 1989).

Neogene deformation has caused warping of the plateau basalt layers (Mathews, 1989). In addition, uplift of the Coast Ranges has been ongoing since at least Eocene time, with at least 2 km of uplift in the last 10 m.y. (Parrish, 1983). As a result, the base of the Chilcotin Group has been elevated to the west.

¹ Here we use the Neogene period and Quaternary period in the manner recommended by Clague (2006), with the base of the Quaternary at 2.588 Ma (including the Pleistocene and Gelasian). We have not adopted the recommendation of the International Commission on Stratigraphy to eliminate the Quaternary period, extending Neogene to the Present (e.g., Gradstein *et al.*, 2004).

This publication is also available, free of charge, as colour digital files in Adobe Acrobat® PDF format from the BC Ministry of Energy, Mines and Petroleum Resources website at http://www.em.gov.bc.ca/Mining/Geosurv/Publications/catalog/cat_fldwk.htm



Figure 2. Rampart of nearly horizontal Chilcotin Group strata built upon the ancient Fraser River valley wall (just above the middle photo horizon). Strata thicken rapidly towards the valley axis (towards viewer). Note light-coloured basement rocks cropping out above and below the Chilcotin Group. View is to the east across the Fraser River (which is not visible in the deep valley bottom).

CHILCOTIN THICKNESS MODEL

The regional thickness model for the Chilcotin Group was produced for 1:250 000 scale NTS sheets 092O and P, and 093B and C (Fig 1). Computational limitations necessitated splitting the area into two. For each half of the map area, the following six procedures were employed:

- 1) A digital elevation model (DEM) was produced from the existing digital 1:20 000 scale topographic base maps. Due to computational limitations, the DEM was generalized from 20 m to 100 m contour intervals (Fig 3).
- 2) Digital geology was gathered from the BC Geological Survey digital geology map (compiled at 1:100 000 scale to create a 1:250 000 scale product; Massey *et al.*, 2005). Boundary problems were rectified where appropriate.
- 3) Chilcotin Group basal contacts were spatially overlain on the digital 1:20 000 contour maps and elevation points generated at their intersections.
- 4) Intersection point elevation data was kriged using the 100 nearest neighbours to generate a Chilcotin basal contact surface in 3-D. Resolution of the 3-D surface is 0.01° pixels. An error surface can be generated to show how the distribution of point data affects the spatial uncertainty of the kriged surface.
- 5) The Chilcotin Group surface was subtracted from the DEM surface. The residual is a 3-D representation of the Chilcotin Group thickness (similar to Fig 4). An example of this process is shown in 2-D profiles in Figure 5 (profile location shown of Fig 4).
- 6) The two contoured thickness maps were reassembled to produce a product similar to Figure 4.

Four additional procedures were performed on the combined thickness maps:

- 1) The thickness data were converted to 0.01° gridded data.
- 2) Data points falling outside Chilcotin Group polygons were removed.
- 3) A 0.01° buffer was created around all Chilcotin Group polygons and broken into segments 0.01° long. Segment endpoints were assigned a zero value and these points added to the 0.01° grid of remaining thickness values.
- 4) The new grid of thickness values was kriged using 100 nearest neighbours and a resolution of 0.01°.
- 5) The resultant output was thematically formatted to produce a usable representation of the 3-D model (*e.g.*, Fig 4 legend).

MODEL HIGHLIGHTS

Thin Chilcotin Group is Widespread

Thickness distributions shown by the model indicate that, in more than 80% of the area covered by the Chilcotin Group, it is less than 25 m thick. According to the model, more than a third of the Chilcotin Group is less than 5 m thick. However, this figure is considered unreliable because the imprecise geological map data (1:250 000), as well as a maximum 20 m resolution of the digital elevation data, do not permit such precise thickness estimates.

Chilcotin Group Thickens towards Major Drainages

Increases in Chilcotin Group thickness towards major drainages are shown by the model. This is consistent with observations and inferences of previous workers (*e.g.*, Read, 2000) and contributors to this volume (Andrews and Russell, 2007). Good examples occur along the Fraser River west of Williams Lake, and along the Chilcotin River south of Alexis Creek. Best sections of Chilcotin Group — those exposed along major drainages — do appear to over-represent the thickness of the unit, creating a false impression of the exploration obstacle that they pose.

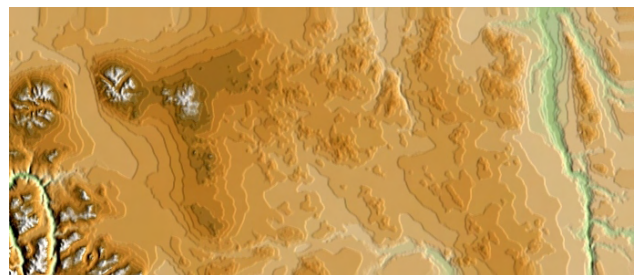


Figure 3. Digital elevation model for map sheets 093B (east half of figure) and C (west), derived from 20 m contour elevation data generalized to 100 m. Fraser River (east margin), Chilcotin River (south centre) and the three peralkaline Anahim Belt volcanoes of the Igachuz Range are prominent. Note steps in elevation model are emphasized in low-relief areas. Far Mountain is on the north side of the middle Anahim Belt volcano.

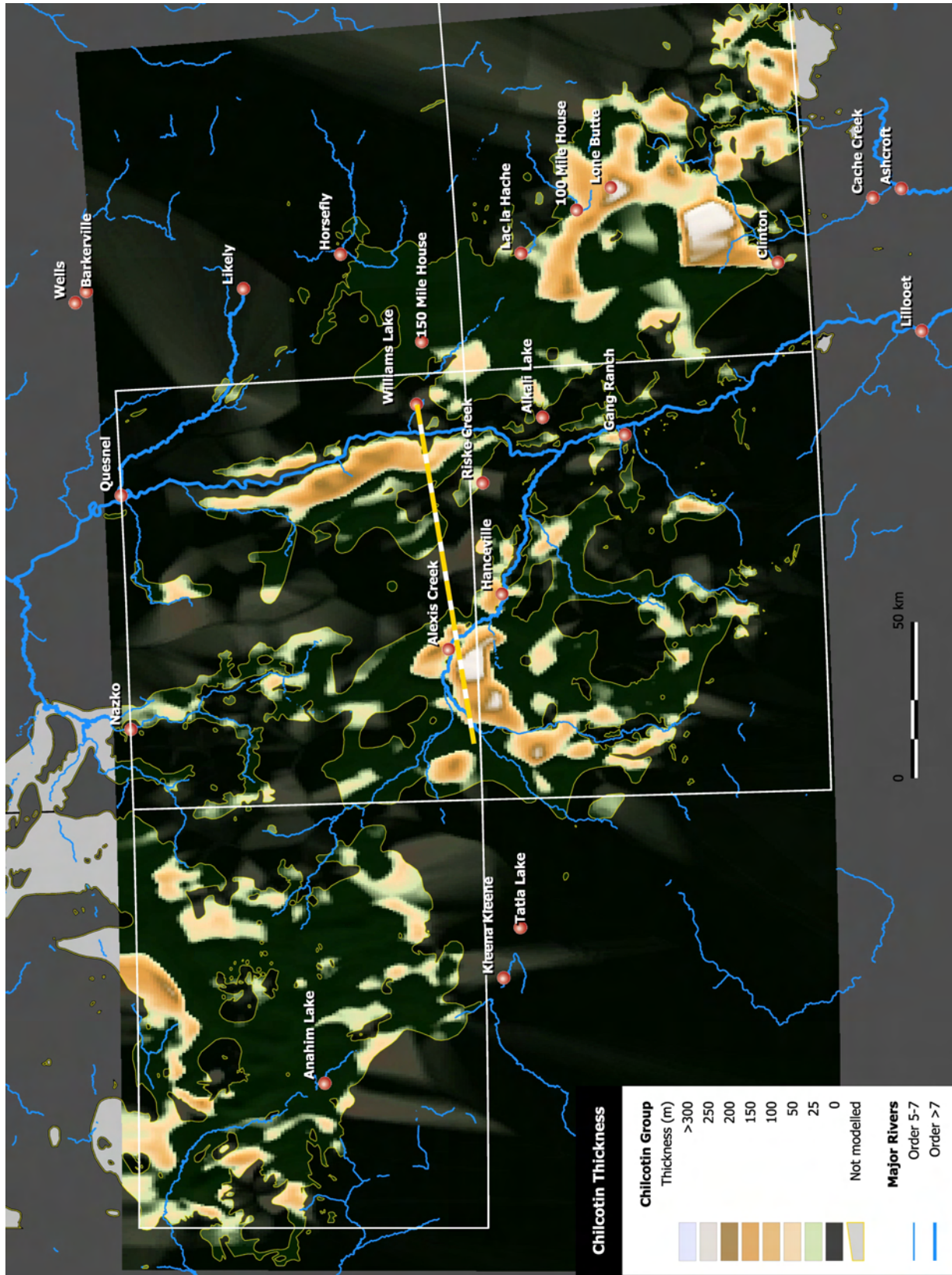


Figure 4. Chilcotin Group thickness model and section line for the profiles shown in Figure 5. Note that areas outside of the Chilcotin Group are shown as semitransparent so that the model shortcomings can be assessed. In these areas, some of the Chilcotin Group is shown by the model where none has been mapped (see text for discussion).

Major Thicknesses in Ilgachuz Range and 100 Mile House Areas

In addition to main river valleys, thicknesses of Chilcotin Group greater than 200 m are shown by the model in the Ilgachuz Range and near 100 Mile House. Peralkaline Anahim Group volcanic rocks in the Ilgachuz Range are mantled by the Chilcotin Group strata. The contact has significant topographic relief (400 m over 5 km) and possible flow structures on the north slope of Far Mountain. These features point to a centre of Chilcotin Group volcanism in the Ilgachuz Range (*cf.* Souther, 1986).

Atypical thicknesses of Chilcotin Group rocks are known in the 100 Mile House area, where they occur over an elevation range of 350 m according to (Mathews, 1989). Maximum thicknesses (>300 m) are shown by the model in the Lone Butte area, 13 km south-southeast of 100 Mile House, in concert with the observations of Mathews (1989).

MODEL LIMITATIONS

As is the case for most models, the quality of the input data and assumptions made in the generation of the model are key determinants of the quality of the model. Geological data used in this model do not include a measure of uncertainty (*e.g.*, defined, approximate or assumed contacts). Thus, all contacts were treated as defined at 1:250 000 scale. This is clearly not correct, and future models should take contact location uncertainty into consideration when generating an error surface. An example of an error surface is shown in Figure 5. It includes only that component of error that is introduced by the kriging process.

In some areas, the Chilcotin lavas were confined and ponded by paleotopographic highs. In such instances, the kriging algorithm used to determine the 3-D basal Chilcotin surface may under-represent the true thickness. In other areas, the contour surface clearly overestimates the thickness of Chilcotin basalt. One of the clearest and most drastic examples occurs about 20 km north of Hanceville, where the highest point in the area, Mount Alex Graham, is underlain by Eocene to Oligocene Endako Group volcanic rocks. However, the raw residual 3-D model shows the peak as flanked by Chilcotin Group. The probable reason for this error is that Mount Alex Graham was a paleotopographic feature that rose abruptly up from the plateau atop which the Chilcotin basalts were deposited. Basalt flows would have lapped up against the ancient flanks of Mount Alex Graham, but the model contours are biased by the kriging of the predominantly gently undulating Chilcotin Group base away from the peak.

A profile section was chosen (Fig 5, located on Fig 4) to demonstrate this problem and to highlight other features of the model. Additional estimates of lava thickness in the middle of the large expanses of Chilcotin basalt, and the mapping of small Chilcotin Group outliers atop expanses of older rocks, would greatly improve the accuracy of the model.

A second-order problem is those artifacts generated by DEM downsampling. These are seen in Figure 4 as a ‘tiger stripe’ pattern caused by the intersection of the relatively smoothly contoured basal Chilcotin contact surface with the step-like DEM (Fig 3).

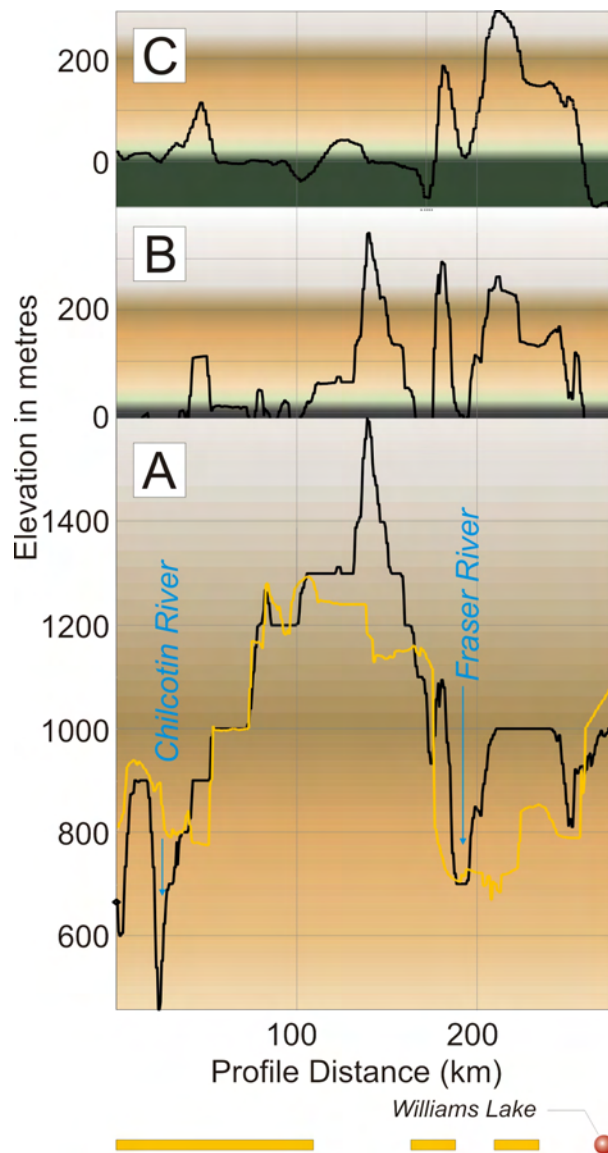


Figure 5. Profiles generated for the section line located in Figure 4: A) Base Chilcotin Group profile (yellow) is subtracted from the topography profile (black) to obtain the resultant thickness profile in (B). Height of land is Mount Alex Graham. Rekriging with a zero thickness buffer set 0.1° outside Chilcotin Group polygons yields the profile (C). See text for discussion. Distribution of Chilcotin Group along the section line as shown by Massey *et al.* (2005) is represented by the yellow bars at the base of the figure.

FUTURE THICKNESS MODELS

Next steps in revision of the model should include:

- 1) Addition of other sources of data that bear on the thickness of the Chilcotin Group, such as:
 - a) water-well bore information,
 - b) exploration oil-well cuttings,
 - c) seismic sections that image the base of the Chilcotin Group,
 - d) addition of future map data, and

- e) use of Forest Renewal BC surficial deposits maps to fine-tune the bedrock – glacial deposits thicknesses.
- 2) Extending the model to include Quaternary glacial deposits. This has already been done in some parts of the modelled region because the age range of the Chilcotin Group as defined by Mathews (1989) extends well into the Quaternary (e.g., 16–1 Ma).
- 3) Selective weeding of existing point elevation data and/or statistical weighting of high-quality data or outlier data of high importance.
- 4) Generation of a thickness model with a finer DEM in order to eliminate the 'tiger stripe' artifacts.
- 5) Field testing of the model by looking for basal Chilcotin Group contacts where predicted by the model.

Future Use of the Model in Mineral Exploration

Future iterations of the Chilcotin Group thickness model may attain levels of sophistication and accuracy that make it a useful tool for predictive mineral exploration. Integration of future thickness models with regional magnetic susceptibility data could enable removal of the Chilcotin Group magnetic response from the regional aeromagnetic survey, enhancing the magnetic fabric of basement rocks. In this way, future thickness models may permit the delineation of exploration targets beneath the Chilcotin Group — beneath a basalt blanket that is probably thinner than once believed.

REFERENCES

- Andrews, G.D.M. and Russell, J.K. (2007): Mineral exploration potential beneath the Chilcotin Group (NTS 920, P; 93A, B, C, F, G, J, K), south-central British Columbia: preliminary insights from volcanic facies analysis; in *Geological Fieldwork 2006, BC Ministry of Energy, Mines and Petroleum Resources*, Paper 2007-1 and *Geoscience BC*, Report 2007-1, pages 229–238.
- Bevier, M.L. (1983): Regional stratigraphy and age of Chilcotin Group basalts, British Columbia; *Canadian Journal of Earth Sciences*, volume 20, pages 515–524.
- Breitsprecher, K. and Mortensen, J.K. (2004): BCAGE 2004A – a database of isotopic age determinations for rock units from British Columbia (Release 2.0); *BC Ministry of Energy, Mines and Petroleum Resources*, URL <<http://www.em.gov.bc.ca/Mining/Geosurv/Publications/OpenFiles/OF2004-03/toc.htm>> [December 2006].
- Clague, J.J. (2006): Open letter by INQUA Executive Committee; *Quaternary Perspectives*, volume 16, pages 1–2.
- Gradstein, F., Ogg, J., Smith, A., Bleeker, W. and Lourens, L. (2004): A new geological time scale, with special reference to Precambrian and Neogene; *Episodes*, volume 27, pages 83–100.
- Massey, N.W.D., MacIntyre, D.G., Desjardins, P.J. and Cooney, R.T. (2005): Digital geology map of British Columbia: whole province; *BC Ministry of Energy, Mines and Petroleum Resources*, GeoFile 2005-1.
- Mathews, W.H. (1989): Neogene Chilcotin basalts in south-central British Columbia: geology, ages and geomorphic history; *Canadian Journal of Earth Sciences*, volume 26, pages 969–982.
- Mihalynuk, M.G. (2007): Evaluation of mineral inventories and mineral exploration deficit of the Interior Plateau beetle infested zone (BIZ), south-central British Columbia; in *Geological Fieldwork 2006, BC Ministry of Energy, Mines and Petroleum Resources*, Paper 2007-1 and *Geoscience BC*, Report 2007-1, pages 137–142.
- Parrish, R.R. (1983): Cenozoic thermal evolution and tectonics of the Coast Mountains of British Columbia. 1. Fission track dating, apparent uplift rates, and patterns of uplift; *Tectonics*, volume 2, pages 601–631.
- Read, P.B. (2000): Geology and industrial minerals of the Tertiary basins, south-central British Columbia; *BC Ministry of Energy, Mines and Petroleum Resources*, Geofile 2000-3, 110 pages, URL <www.em.gov.bc.ca/mining/Geosurv/Publications/Geofiles/Gf2000-3/toc.htm> [October 2006].
- Souther, J.G. (1986): The western Anahim Belt: root zone of a peralkaline magma system; *Canadian Journal of Earth Sciences*, volume 23, pages 895–908.

Terrace Regional Mapping Project Year 2: New Geological Insights and Exploration Targets (NTS 103I/16S, 10W), West-Central British Columbia

by J. Nelson and R. Kennedy¹

KEYWORDS: Terrace, northwest BC, regional geology, Stikinia, Cu-Mo porphyry, Telkwa Formation

INTRODUCTION

The 2006 field season was a continuation of regional geological mapping and mineral deposit studies in the area north of Terrace, extending north and west of the Usk map area, which was completed in 2005 (Fig 1; Nelson *et al.*, 2006a, b).

The area covered was the south half of the Doreen map sheet, NTS 103I/16, and the east half of the Terrace map sheet, NTS 103I/10.

The most important geological observations include

- the recognition and definition of a stratigraphic marker sequence at the top of the Hazelton Group, which corresponds in position, and possibly in age, to the rocks that host the Eskay Creek mine; and
- the establishment of stratigraphic offsets that constrain both normal motion and precursor thrust motion on the low-angle fault or faults that border the uplifted Kitselas metamorphic complex.

Key economic findings include

- a new zone of copper mineralization that was discovered over a significant area near the Borden Glacier on the north side of Mt Sir Robert; probably related to, but distinct from, previously known showings; and
- the discovery that the southern slopes of Mt Knauss have been affected by a large alteration system cored by a zone of porphyry-style molybdenum-copper mineralization (Womo, MINFILE 103I 122); this interesting area is currently staked but has had no recent exploration activity.

GEOLOGY

The Terrace, Usk and Doreen map areas are contiguous and the same geological issues arise throughout. Therefore, this treatment, although focused on geological units examined during 2006, also refers to the geology included in last year's map coverage (Nelson *et al.*, 2006a) for completeness. It should also be noted that our detailed mapping

succeeds regional work by G. Woodsworth and colleagues (Woodsworth *et al.*, 1985; Gareau *et al.*, 1997a, b; G. Woodsworth, 1:100 000 mapping, pers comm), which has provided an invaluable framework for subsequent study.

Tectonically, the area is divided into two distinct structural panels by gently to steeply east-dipping faults in the valley of the Skeena River, termed here the Skeena River fault zone. In the hangingwall of these faults, east of the Skeena River, is a stratigraphic sequence that ranges in age from Early Permian to Late Jurassic (Fig 2, 3).

From base to top, it includes the Permian Zymoetz Group (Nelson *et al.*, 2006a), overlain by extensive exposures of the mainly subaerial volcanic Howson facies of the Telkwa Formation, which is a thin but continuous marker unit of Middle (?) Jurassic clastic Smithers Formation, and chert-siliceous argillite-felsic tuff comparable to the 'pyjama beds' of the upper Hazelton Group in the Iskut area, and the Bowser Lake Group. This sequence is typical of much of Stikinia. The Telkwa and Smithers formations and the pyjama beds belong to the Early to Middle Jurassic Hazelton Group. Early Jurassic and older stratified rocks are intruded by the Early Jurassic Kleanza pluton. Between the Skeena River and the Kitsumkalum River valley, the footwall of the fault system comprises a somewhat different stratigraphic sequence of felsic and minor basaltic strata of the Early Jurassic Kitselas facies, overlain by a thin interval of more typical Telkwa varied volcanic units, the Smithers Formation, pyjama beds and the Bowser Lake Group. This panel is intruded by a strongly deformed granitoid suite of Paleocene age (the Kitsumkalum suite of Gareau *et al.*, 1997a, b). Undeformed Eocene granite, such as the Carpenter Creek and Newtown Creek plutons, cut the hangingwall and the footwall, as well as the faults that separate them. Metamorphic grades in the hangingwall panel range from zeolite facies to a narrow zone of greenschist along its base, whereas grades in the footwall panel increase from lower to upper greenschist toward the west.

The Kitsumkalum valley is part of a north-trending graben structure extending from Kitimat to the Nass valley. Within it, there are weakly metamorphosed stratified rocks of the Hazelton, Bowser Lake and Skeena groups, juxtaposed along steep faults against the Kitselas facies and deformed granitoid rocks in the mountains north of Terrace.

Stratified Units

TELKWA FORMATION EAST OF THE SKEENA RIVER

The upper part of the Early Jurassic Telkwa Formation extends north from exposures mapped in Legate Creek in 2005 (Fig 4; Nelson *et al.*, 2006a, b), into the area of Mt Sir Robert, Mt Quinlan and the upper reaches of Big Oliver Creek.

¹618 – 8th Ave NE, Calgary, Alberta

This publication is also available, free of charge, as colour digital files in Adobe Acrobat® PDF format from the BC Ministry of Energy, Mines and Petroleum Resources website at http://www.em.gov.bc.ca/Mining/Geosurv/Publications/catalog/cat_fldwk.htm

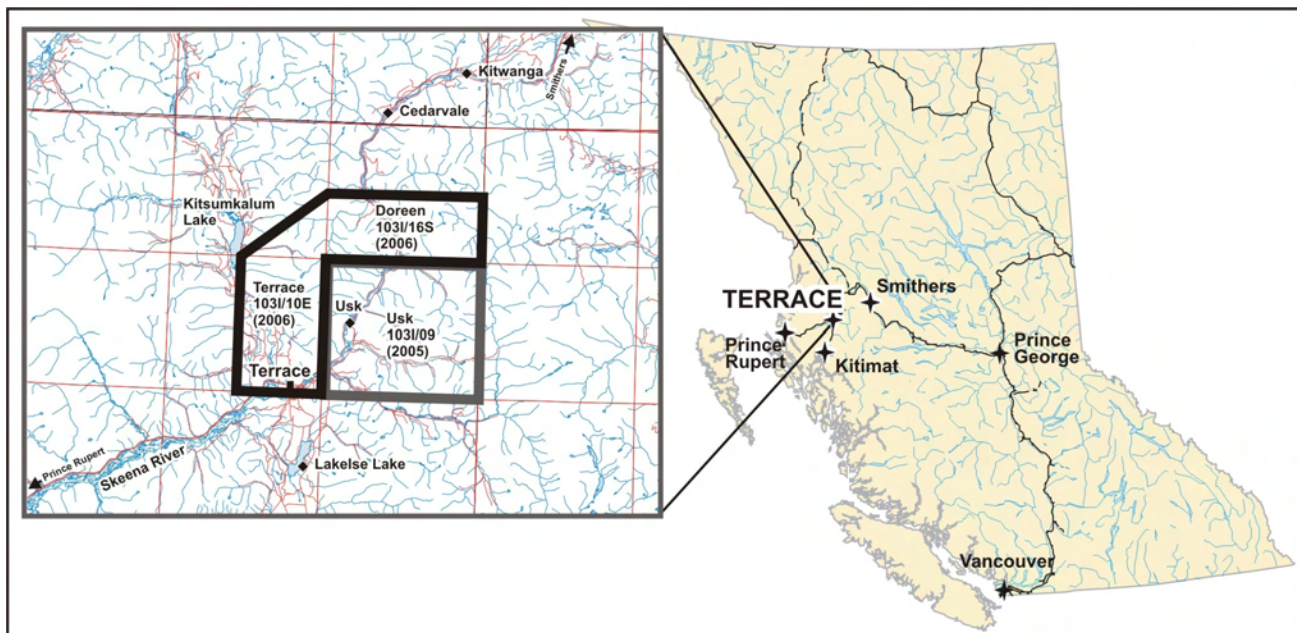


Figure 1. Location of the Terrace area in northwest BC, with current and 2005 mapping highlighted (shown in detail in Fig 2).

Farther south, it comprises flows and lesser tuff. Mt Sir Robert is composed mainly of andesitic rocks, while ridges to the south and west are underlain by more siliceous dacite. There is very little interbedding of intermediate and felsic compositions, perhaps because they were erupted from separate centres. The andesite on Mt Sir Robert is maroon to purple in colour and is generally aphanitic and often amygdaloidal. Amygdules in these flows are filled with calcite and sub-greenschist minerals such as prehnite±pumpellyite. Overall, the andesite is thickly bedded; bedding orientations can be determined by the occurrence of a minor, thinly bedded felsic strata as well as from the flattening of vesicles parallel to bed orientations. Dacitic rocks on the low ridge immediately north of Legate Creek are maroon to red and aphanitic to porphyritic. Most are coherent and probably make up a dome complex. Subsidiary welded tuff beds with strong eutaxitic fabrics provide local bedding control. Thickly bedded dacite flows and tuff also underlie the western slopes of Mt Quinlan and upper Big Oliver Creek.

The uppermost units of the Telkwa Formation, north and west of Mt Sir Robert, are brick red to maroon, rarely bright green, finely comminuted and, in part, laminated tuff that is at least partially of ignimbritic origin. Locally, thin limestone layers are intercalated with the tuff over an interval of 10 to 20 m. This tuffaceous sequence could be part of the red tuff member of the Smithers Formation (Tipper and Richards, 1976); however, it appears to be continuous with and related to dacite of the underlying Telkwa Formation rather than to the overlying, very different, clastic Smithers Formation. The stratigraphically highest unit in the Telkwa Formation is a distinctive, thickly bedded, very fine grained maroon tuff unit. Characteristically, it contains crudely planar concentrations of fist to cantaloupe-sized, ovoid to irregular, concentrically zoned clasts (Fig 5). It forms a continuous layer from the plateau north of Mt Sir Robert, to the west side of Mt Quinlan, a total of 10 km of strike length.

Stratified rocks around the lower portions of Little and Big Oliver Creek, and the northwestern part of the low

ridge north of Legate Creek, are separated from the Mt Sir Robert – Mt Quinlan section by a set of steep faults. In this area, the Hazelton Group is dominated by light grey dacite and/or rhyolite, predominantly coherent and monotonous, but with some lapilli and welded lapilli tuff. Dark green aphanitic basalt is also present. As discussed by Gareau *et al.* (1997a, b), the affinity of these rocks is uncertain. In terms of lithological composition — the predominance of very felsic compositions with minor mafic units — they are similar to the Kitselas facies farther south. However, they are only sporadically foliated, and greenschist-facies mineral development is very subtle. Also, they occupy a distinct structural panel from the Kitselas facies, which merges structurally into the upper Hazelton Group near Legate Creek (Fig 2). For these reasons, we consider them part of the main Hazelton Group, as suggested by Gareau *et al.* (1997b). If they are, then the suggested tie between the ca. 195 Ma Kitselas facies and the Telkwa Formation (Gareau *et al.*, 1997a, b) is considerably strengthened.

KITSELAS FACIES AND TELKWA FORMATION WEST OF THE SKEENA RIVER

Predominantly felsic volcanic rocks of the Kitselas facies occupy a broad region north of Terrace, spanning Kitselas Mountain, Mt Vanarsdoll, Lean-to Mountain and the high ridges in the headwaters of Hardscrabble Creek. On Kitselas Mountain, as previously described (Nelson *et al.*, 2006a), they are well-bedded pale grey to white rhyolite volcanoclastic units with some coherent flows or domes. Welded tuff with strong eutaxitic fabrics is locally well developed. Two prominent bands of dark green metabasalt strike east-northeast on the southern slope of Mt Vanarsdoll. They are the faulted equivalent of similar intervals on Kitselas Mountain, across a set of north-striking dextral faults with 500 to 1000 m offsets (Fig 2). The wider one is approximately 200 m thick. Although these rocks exhibit greenschist-facies alteration, original textures are well preserved. These include amygdaloidal and scoriaceous textures in flows, and fragmental textures in

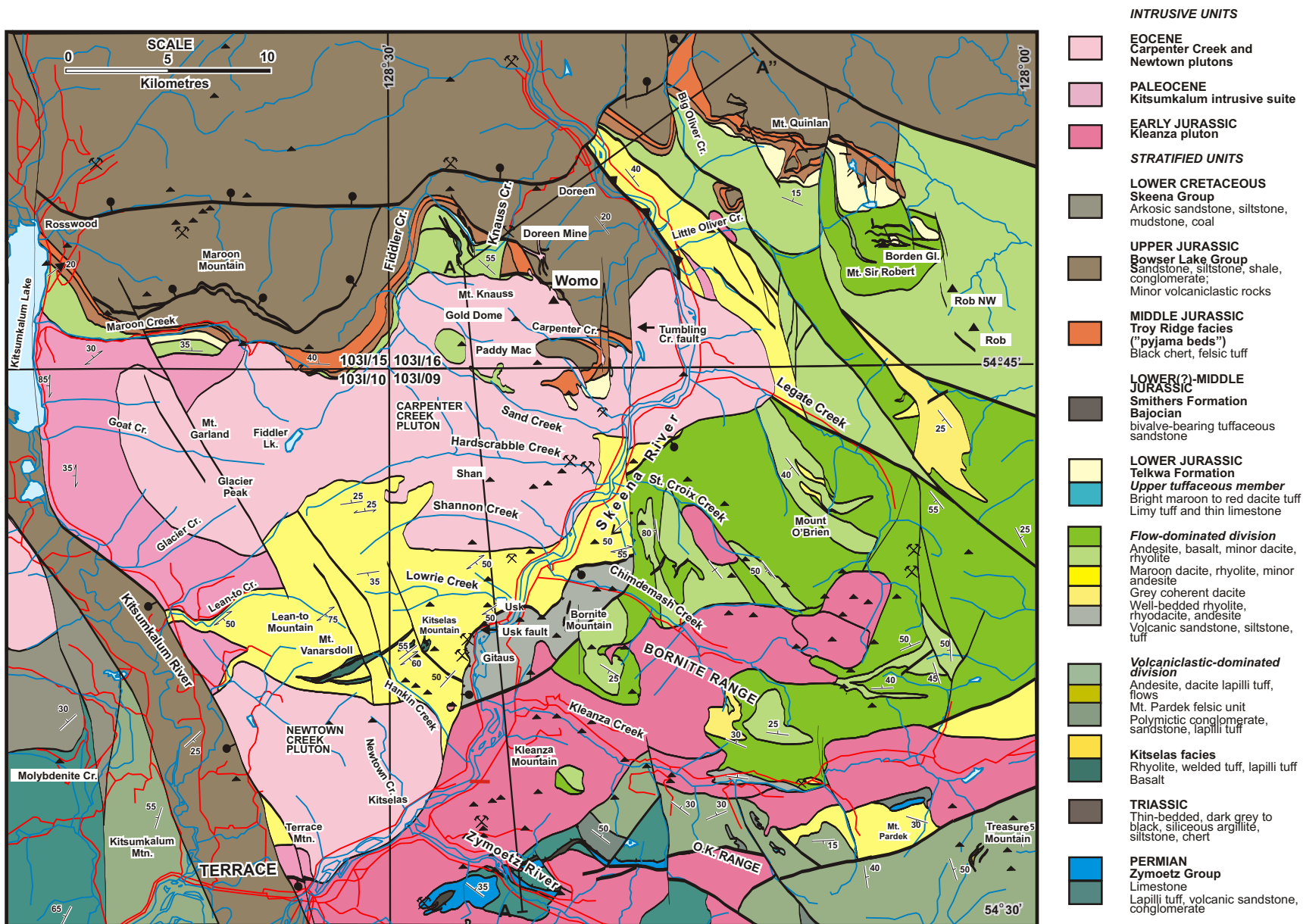


Figure 2. Geology of the Usk (NTS 1031/09), southern Doreen (NTS 1031/16) and eastern Terrace (NTS 1031/10) map areas, from field mapping in 2005 and 2006, compilation from 1:100 000 maps of G. Woodsworth (pers comm) and extrapolation of some faults and contacts.

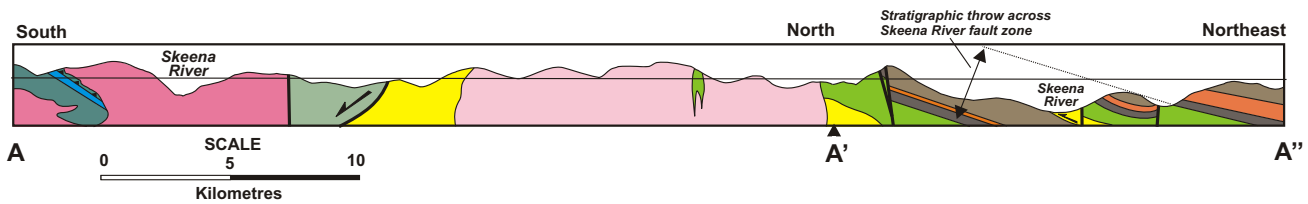


Figure 3. Cross-section of units in the Terrace area; A-A'-A'' on Fig 2; legend is the same as Fig 2.

basalt and mixed basalt-rhyolite tuff. One very small enclave on the eastern ridge of Lean-to Mountain consists of highly plagioclase-phyric, in part amygdaloidal, andesite. It is identical in texture to andesite in the upper Telkwa Formation near Mt O'Brien, even to the common clumping of tabular plagioclase into aggregates with ragged terminations. This provides further evidence of a linkage between the coeval, but for the most part compositionally distinct, Kitselas and Telkwa formations.

Overall, the Kitselas facies represents a very large felsic centre, measuring at least 15 km in the north-south dimension and 20 km east-west, which takes the place of the upper Telkwa andesite and dacite flows east of the Skeena River. It is unusual within the Telkwa for its size, uniformity and predominance of very felsic rocks; however, other smaller rhyolitic centres occur within the Telkwa Formation in the Usk area (Nelson *et al.*, 2006a, b).

Near the northern exposed limit of the Kitselas facies in the Hardscrabble Creek headwaters, where it is cut off by Eocene granite, layering dips primarily to the north, projecting below a section of variably metamorphosed Telkwa volcanic units that is, in turn, overlain by the Smithers Formation and the pyjama beds. The Telkwa rocks outcrop from near Carpenter Creek through Mt Knauss and the headwaters of Maroon Creek north of Fiddler Lake, and as far west as the eastern shore of Kitsumkalum Lake. Regional metamorphic grades increase from sub-greenschist in the east to upper greenschist near Kitsumkalum Lake, but primary compositions and textures are discernible throughout. Near Carpenter Creek, a very limited Telkwa section is truncated by Eocene granite. It consists of maroon to brick red, in part finely laminated tuff. These strata were assigned to the red tuff member of the Smithers Formation by Nelson

et al. (2006a, b), but based on observations near Mt Sir Robert, we now consider them to be the uppermost unit of the Telkwa Formation.

On eastern Mt Knauss, grey rhyolite with tiny, sparse feldspar phenocrysts is overlain by well-foliated dacite tuff and lesser basalt, a section that exhibits a degree of similarity to the Kitselas facies. The uppermost unit is a red tuff that contains planar concentrations of large, concentrically zoned clasts and is equivalent to the uppermost tuff unit east of the Skeena River. A more metamorphosed version of this unit occurs at the top of the Telkwa Formation in the headwaters of Maroon Creek. There, the clasts are replaced by concentrically zoned epidote-garnet-quartz-piedmontite(?) metadomains (Fig 6). Altogether, this unit has been recognized over a total of nearly 30 km of strike, not taking into account structural repetition across the Skeena River.

Farthest west, near Maroon Creek and along the highway east of Kitsumkalum Lake, the upper Telkwa Formation consists of green metabasalt and metadacite, generally coherent with lesser volcanoclastic textures.

SMITHERS FORMATION

The Smithers Formation lies stratigraphically between the Telkwa Formation and the pyjama beds in both the hangingwall and footwall of the fault system along the Skeena River. In the hangingwall, it is well exposed from north of Mt Sir Robert, south and west of Mt Quinlan, and in the low hills north of Big Oliver Creek. Its basal contact is sharp and paraconformable on maroon Telkwa tuff. The Smithers Formation is a uniform, well-bedded unit of light green tuffaceous volcanic-derived greywacke, with thin interbeds of tuffaceous siltstone. A high content of rhyolitic



Figure 4. Looking south across Legate Creek at the north face of Mt O'Brien, a spectacular exposure of the steeply southwest-dipping andesite of the Telkwa Formation.



Figure 5. Concentrically zoned clasts in uppermost tuff unit of the Telkwa Formation. Made of fine clastic layers, they may be cannibalized from unconsolidated ash deposits.

ash tuff gives a white cast to the weathered alpine exposures. Tiny feldspar grains are dispersed in the sand and locally white, subangular to subrounded rhyolitic pebbles occur. Curiously, no reddish dacitic or andesitic debris attributable to the underlying Telkwa Formation is present; this probably indicates a low relief environment. Fossiliferous beds and coquina, burrows and bioturbation are common. Black, petrified tree trunks, up to 30 cm in diameter, are also present in the area. Macrofossil species include large, smooth-shelled clams, trioniids, small ribbed bivalves, gastropods and rare ammonites. Some large clams are preserved open with their shells still attached. They supported colonies of small corals, gastropods and bryozoans, the open shell providing both shelter and a food source. The thoroughness of the bioturbation suggests that the Smithers Formation accumulated on a shallow seafloor (P. Mustard, pers comm, July 2006). The rhyolitic ash and sparse small volcanic lithic clasts were probably derived from active contemporary felsic centres farther to the south, for instance, in the Whitesail and Nechako regions of south-central Stikinia (L. Diakow, pers comm, August 2006; Diakow and Levson, 1997).

The age of the Smithers Formation, east of the Skeena River, is constrained at present by a single macrofossil collection of Aalenian age (G. Woodsworth and H.W. Tipper, unpublished data, 1985). Our collections made in 2006 have not yet been identified.

In the footwall sequence west of the Skeena River, the Smithers Formation lies paraconformably above the Telkwa Formation and below the pyjama beds from Carpenter Creek to Kitsumkalum Lake (Fig 2). A collection of bivalves from sandstone near Carpenter Creek was identified as of probable Early Bajocian age, similar to faunas in the Smithers Formation on Hudson's Bay Mountain and in the Whitesail area (T. Poulton *in Nelson et al.*, 2006a). Similar fossiliferous sandstone continues to the west across Mt Knauss. On the western side of Fiddler Creek, the metamorphic grade increases; fossils become streaks of coarse calcite, and bioturbation is recognized in uneven textures within the metasandstone. In its farthest western exposure where the highway cuts along Kalum Lake, the Smithers Formation is a glossy, pale green sericite-chlorite schist with epidote laminae replacing limy layers and spotty cor-



Figure 6. Epidote metadomains in greenschist-facies dacite, in the uppermost Telkwa Formation northeast of Fiddler Lake. These are interpreted as metamorphosed equivalents of concentrically zoned bombs (see Figure 5).

dierite perhaps nucleating in burrows. Its thick, regularly bedded character persists within the outcrops of these metamorphic rocks.

PYJAMA BEDS (TROY RIDGE FACIES)

This thin but distinctive formation lies between the Smithers Formation and the base of the Bowser Lake Group in the hangingwall and footwall panels both east and west of the Skeena River. It consists of black, rusty-weathering, ribbon-bedded chert and black siliceous argillite (Fig 7a). Its siliceous nature serves to separate it from the underlying greywacke of the Smithers Formation, although there is a transitional contact in which the uppermost Smithers Formation becomes more thinly bedded and more siliceous tens of metres below its upper contact. The pyjama beds are also distinct from the overlying, non-siliceous, fine-grained to coarse-grained clastic strata of the Bowser Lake Group. Most distinctive of this unit, although not observed everywhere within it, are pale pink to white, very thin felsic tuff laminations (Fig 7b). The black and white striping is comparable to the so-called 'pyjama beds' that lie at the top of the Hazelton Group in the Iskut region, for instance, at Troy Ridge (*cf.* Anderson and Thorkelsen, 1990). The Troy Ridge facies has been dated as Bajocian (*ca.* 175 Ma; K. Simpson and V. McNicoll, pers comm,



Figure 7. a) Ridge-top exposure of pyjama beds northeast of Fiddler Lake; b) close-up of pyjama beds in the saddle south of Maroon Mountain, showing their distinct and characteristic pale striping on millimetre to centimetre scales.

2005). It represents quiescent conditions at the end of the Hazelton arc cycle and is contemporaneous with the development of the Eskay Rift to the west.

The precise age of the pyjama beds in the Terrace area is not known. The unit is underlain by the Aalenian to Bajocian Smithers Formation and is overlain by the Bowser Lake Group, which locally contains fossil collections as old as Callovian (G. Woodsworth and H.W. Tipper, unpublished data, 1985). Thus it may be entirely coeval with the Troy Ridge facies, but could conceivably be as young as Early Callovian. A 2006 microfossil collection made near the top of this unit will be a useful indicator to confirm or weaken its correlation with the Troy Ridge facies.

In any event, geological mapping in the Terrace area during 2006 traced out a unit identical in character and stratigraphic position to the Troy Ridge facies, which outcrops over a 30 km strike length from the plateau north of Mt Sir Robert to the east side of Kalum Lake. It indicates that the same deep-water, quiescent environment existed in this region at the end of the Hazelton arc volcanism similar to the Iskut area, some 200 km north of Terrace. So far, no remnant of an Eskay-like rift facies with coarse clastic and bimodal volcanic deposits has been observed in this area; however, the rift to off-rift transition in the Iskut area is abrupt and similar rocks could be situated farther west.

BOWSER LAKE GROUP

The Terrace area lies along the southern margin of the Bowser Basin, the depocentre in which Late Jurassic to Early Cretaceous clastic strata of the Bowser Lake Group accumulated (Tipper and Richards, 1976). We recognize a variety of lithological subunits within the Bowser Lake Group, but structural complications and a lack of biostratigraphic control prevent an accurate time-stratigraphic subdivision.

The base of the Bowser Lake Group is well-defined and apparently conformable above the pyjama beds. Basal units vary from sequences of black carbonaceous siltstone to coarse sandstone and even conglomerate. This contact was the locus of strong structural disruption, and it is not clear to what degree the variability in the lowermost Bowser Lake Group reflects original facies, as opposed to different stratigraphic levels juxtaposed above a planar basal décollement.

In this area, most of the Bowser Lake Group consists of interbedded grey to black sandstone, siltstone and shale with minor limy clastic beds and dirty calcarenite. Macrofossils — bivalves, belemnites and ammonites — occur in uncommon but rich beds. Within the map area, Late Jurassic, Callovian and Oxfordian fauna have been identified (G. Woodsworth and H. Tipper, unpublished data, 1985). Coarser intervals of sandstone, grit and conglomerate are dominated by felsic volcanic sources. Rounded clasts of aphanitic, holocrystalline and porphyritic volcanic rocks, as well as sand-sized plagioclase grains, are the main reason the rocks weather pale green to white. The dominant volcanic source terrane in this area stands in strong contrast to the Bowser Lake Group in the Iskut area, and also farther upsection locally, in which northeasterly derived chert clasts from the Cache Creek Terrane are by far the most abundant. Tipper and Richards (1976) ascribe the early volcanic provenance to the uplift of the Skeena arch, a persistent east-trending structural high south of the Bowser Basin.

In one locality, east of Mt Quinlan, immature felsic volcanic breccia occurs within the Bowser Lake Group in several hundred metres of ridge exposures. They vary from jigsaw, puzzle-fit breccia to lapilli tuff comprising pebble to cobble-sized angular volcanic clasts in a clastic-volcaniclastic matrix. We interpret these as hyaloclastic deposits with local development of peperite. Volcanic deposits are known within the southern extent of the Bowser Lake Group in the Nechako area of central BC (Diakow and Levson, 1997). They represent a Late Jurassic renewal of volcanism to the south, after the mid-Jurassic demise of the Hazelton arc.

SKEENA GROUP

Clastic strata of the mid-Cretaceous Skeena Group only occur in the far western part of the Terrace map area, west of the Kitsumkalum River valley. These rocks are distinguishable from the Bowser Lake Group by the dominance of arkose as opposed to volcanic sandstone. They tend to be cream and buff-coloured, as opposed to the darker greys, greens and browns of the Bowser Lake Group. Crossbeds are common and coal is noted at several localities. In places, detrital white mica occurs within the Skeena Group sandstone.

Intrusive Units

EARLY JURASSIC KLEANZA SUITE

Intrusive bodies in the Terrace area belong to three suites of distinct age and structural setting. The oldest is the Early Jurassic Kleanza pluton, which occurs in the hangingwall of the Skeena River fault zone. This body has been dated at *ca.* 200 Ma (Gareau *et al.*, 1997a). It outcrops extensively along the Zymoetz River and Kleanza Creek in the Usk map area (Nelson *et al.*, 2006a, b). In the Terrace map area, it extends west across the Skeena River at the 'old bridge' northeast of Terrace and onto the lower slopes of Terrace Mountain (Fig 2). Overall, the Kleanza pluton shows a high degree of textural and compositional heterogeneity, with variants from gabbro to granite and fine-grained microdiorite to hornblende-plagioclase pegmatite. Its most westerly exposures, from the cliff at the base of Copper Mountain to Terrace Mountain, consist entirely of coarse-grained white to pink granite, with potassium feldspar megacrysts that range in size from a half centimetre to several centimetres. These pink megacrysts distinguish it from otherwise similar granite of the Carpenter Creek suite. The Kleanza granite does not exhibit penetrative deformation, although it is cut by discrete shear zones.

PALEOCENE KITSUMKALUM SUITE

Variably to strongly foliated, inhomogeneous granitoid occurs interlayered with Kitselas and Telkwa metavolcanic rocks between Maroon Creek on the east side of Kalum Lake, and Terrace Mountain on the northern outskirts of Terrace. This body has been dated at *ca.* 59 Ma (Gareau *et al.*, 1997a). Granite is the dominant rock type, but granodiorite and diorite are also present, the latter commonly as lenses and layers. Well-formed titanite crystals are one distinguishing feature of this suite of intrusive phases. Principally, however, the Kitsumkalum suite is identified based on the prevalence of ductile deformation fabrics within it. Unfortunately, the other plutons are cut by spaced shear zones; parts of the Kitsumkalum suite lack a homogeneous foliation. Thus, the distinction between this

and the other suites is not clear everywhere. Compared to Gareau *et al.* (1997a, b), we have considerably reduced its mapped extent (Fig 2). In particular, areas assigned to the Kitsumkalum suite near the town of Terrace and around Glacier Peak are underlain by undeformed granite that we assign to the younger Carpenter Creek suite (*see below*).

Minor occurrences of foliated granite occur within the structural base of the Telkwa Formation along the Skeena River in Kitselas Canyon and near Little Oliver Creek. Their foliated, greenschist-facies volcanic hosts are considered to have been affected by the same deformational event as the Kitselas complex in the footwall of the Skeena River fault zone.

EOCENE CARPENTER CREEK SUITE

Plutons of the post-kinematic Carpenter Creek suite are large, lobate bodies that crosscut the Kitselas facies, the Paleocene Kitsumkalum suite, the Skeena River fault zone and the Telkwa Formation in its hangingwall. The Carpenter Creek pluton has been dated as *ca.* 53 Ma (Gareau *et al.*, 1997a). The Carpenter Creek and Hardscrabble plutons occupy a large area between the Skeena River and Glacier Peak. They are actually two connected lobes of a single intrusion (Fig 2). A third body, the Newtown Creek pluton, outcrops in the hills north of Terrace. Like the others, it is coarse-grained, undeformed and intrudes rocks of the Kitselas complex that have been deformed in a ductile manner. Granite dominates these bodies, with lesser granodiorite; finer-grained porphyritic phases form local dike swarms.

Structure and Metamorphism

FRAMEWORK

The Terrace area is divided into three structural panels, defined by major faults along the east side of the Kitsumkalum valley and along the Skeena River (Fig 2). The Skeena River fault zone (SRFZ) is poorly exposed and largely obscured by Eocene plutons and later high-angle faults. The Usk fault (Nelson *et al.*, 2006a, b) is part of this system. The Usk fault dips gently to moderately to the east. Geological relationships across the SRFZ are suggestive of both early thrust movement and later top-to-the-east detachment. Faults along the east side of the Kitsumkalum valley are steep, with down-to-the-west normal and also dextral displacement. They postdate the gently dipping faults of the SRFZ and they cut the Eocene granite, as well as all older units.

The Kitsumkalum valley is a graben, bounded to the east by high-angle faults. It is mostly underlain by the unmetamorphosed Bowser Lake Group; Kitsumkalum Mountain west of Terrace is a small horst of Telkwa Formation. The height of land between Terrace, Kitsumkalum Lake and the Skeena River is an uplifted Paleocene metamorphic complex, the Kitselas complex, which comprises the Kitselas felsic volcanic facies of the Telkwa Formation, overlying upper Telkwa metavolcanic rocks, the Smithers Formation and pyjama beds, and the lowest part of the Bowser Lake Group near Maroon Creek. The hangingwall of the Skeena River fault zone east of the Skeena River is a single north-northeasterly dipping panel of generally unmetamorphosed Permian to Jurassic supracrustal rocks. This geological scenario was recognized by G. Woodsworth and his coworkers (Woodsworth *et al.*, 1985; Gareau *et al.*, 1997a, b; G. Woodsworth, pers comm, 2005,

2006). Here we corroborate and amplify the structural history of the area, focusing on the multistage development of the Kitselas complex.

EARLY DEVELOPMENT OF THE SKEENA RIVER FAULT ZONE

Correlation of the mainly felsic volcanic strata of the Kitselas facies within the Telkwa Formation east of the Skeena River raises the question of why the Kitselas facies to the west is at a distinctly higher metamorphic grade and state of ductile deformation than its correlative Telkwa facies to the east. In our mapping, we have shown that the much of the Telkwa and Smithers strata above the Kitselas facies, in the footwall of the SRFZ, have also attained greenschist grades and are characterized by layer-parallel foliations. Thus, the metamorphic and structural history of the entire panel west of the Skeena River differs from that to the east. Gareau *et al.* (1997a, b) describe the Kitselas metamorphic complex as a Paleocene core complex, bounded above by a low-angle detachment fault along the Skeena River. This is in accord with its comparatively high metamorphic grade compared to the panel structurally above it, as well as the presence within it of deformed Paleocene granitoid rocks.

Stratigraphic relationships across the Skeena River are, however, more suggestive of thrust motion than of normal relative motion. This can be seen in a gross sense, in that stratigraphic units as old as Permian, in the hangingwall, lie above the Early Jurassic and younger rocks in the footwall west of the Skeena River (Fig 2, 3). In detail, the projection of the Skeena River fault zone toward Doreen repeats Hazelton and Bowser Lake Group rocks: upper Telkwa rhyolite east of the river near Big and Little Oliver creeks lie structurally above east-dipping Bowser Lake strata to the west. The implied stratigraphic throw is about 3500 m, taking into account local vertical motion across high-angle faults (Fig 3, 8).

The hangingwall panel east of the Skeena River dips and youngs overall to the north-northeast. If the Skeena

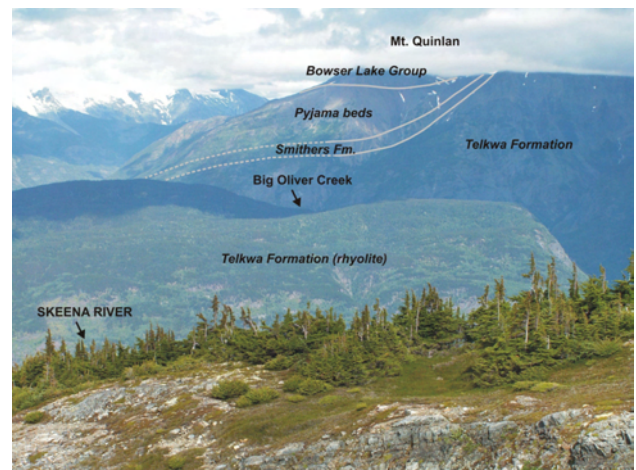


Figure 8. View northeast and downdip along Bowser Lake Group strata on the eastern flank of Mt. Knauss, across the Skeena River and into structurally higher Telkwa Formation and overlying units near Big Oliver Creek. This view corresponds to the northern end of the cross-section in Figure 3. The base of the Bowser Lake Group on Mt. Quinlan is about 3500 m structurally higher than it is west of the Skeena River. A thrust fault is inferred under the Skeena River valley (Fig 2, 3).

River fault zone is modelled as a frontal hangingwall ramp, then early thrust motion on it was probably to the north-northeast, perpendicular to the strike of the main units (Fig 2). Apparent horizontal displacement of the Smithers – pyjama bed marker is about 12 km (Fig 2).

Such a precursor thrusting event would explain the deeper crustal levels evidenced within the footwall, compared to the hangingwall of the SRFZ: rocks west of the Skeena River were buried beneath rocks to the east. The timing of this thrust imbrication is broadly constrained between Late Jurassic, the age of the affected Bowser Lake Group strata, and Paleocene, the age of the deformed granite of the core complex. In terms of regional events, Evenchick (2001) describes north-northeast shortening of the Bowser Basin in Middle to Late Cretaceous time. This is considered the most probable age for initial thrusting across the SRFZ.

LOW-ANGLE FAULTING AND RELATED FOLDING IN THE BOWSER LAKE GROUP

Compared to the Telkwa and Smithers Formations, which form a simple homoclinal package, strata of the Bowser Lake Group (BLG) are extensively imbricated along gently dipping planar faults. Structures of this type are particularly prominent around Mt Quinlan. There, the basal detachment is within the thinly bedded chert of the pyjama beds, which is, in places, repeated along with panels of the overlying BLG (Fig 2). A variety of features document the sense of motion. Folds within panels are overturned to the southwest; minor structures within fault zones show top-to-the-southwest sense of shear (220–240°) and steeply-dipping porphyritic granite dikes are consistently displaced towards the southwest (Fig 9). Farther to the west, Mihalynuk and Friedman (2005) describe top-to-the-south thrust faults within the BLG near Kalum Lake.

The sense of displacement in the BLG corresponds neither to the north-northeast thrust sense inferred for the SRFZ, nor to Paleocene-Eocene tops-to-the-east denudation of the Kitselas complex discussed below. Very strong southwest-vergent crustal compression affected the Coast Mountains west of Terrace in Late Cretaceous time (Andronicos *et al.*, 1999; Crawford *et al.*, 2000). The structures that we see in the BLG east of the Skeena River may represent the most easterly edge of this crustal-scale



Figure 9. Steeply northeast-dipping plagioclase-porphyritic dike displaced on top-to-the-southwest shears, south of Mt Quinlan.

deformational belt. In any event, the structural history of this area on the eastern flank of the Coast Mountains has been complex and is not yet well understood or constrained in time.

METAMORPHISM AND STRUCTURES WITHIN THE KITSELAS COMPLEX

With the exception of Smithers sandstone near Carpenter Creek, all stratified rocks below the pyjama beds between the Skeena River and the Kitsumkalum valley are regionally metamorphosed to greenschist facies. Diagnostic minerals in the predominant felsic metavolcanic rocks are lacking, but all of the mafic units contain actinolite-epidote-chlorite±garnet assemblages. Synkinematic cordierite is present in the Smithers Formation near Kalum Lake and andalusite is seen in the lowermost Bowser Lake Group near Maroon Creek. Some of the andalusite may be of contact metamorphic origin.

Two types of synmetamorphic planar fabrics were observed in Kitselas metavolcanic rocks. In the centre of the complex, foliation is axial planar to major northeasterly, upright, open folds. Nearer to the eastern and northern margins of the complex, layering is transposed into the foliation, dipping moderately to the northeast near the Skeena River and to the northeast and northwest along its northern side from the headwaters of Hardscrabble Creek to north of Maroon Creek. Lineations plunge northeasterly. Although it is tempting to relate them to top-to-the-northeast motion during denudation of the Kitselas complex, in the course of our work we have not located many shear-sense indicators in this area; it is equally possible that the lineations developed during earlier top-to-the-northeast thrust motion on the SRFZ.

The metamorphosed Telkwa and Smithers rocks in highway outcrops between Maroon Creek and the northern end of Kalum Lake show northwest-vergent recumbent folds (Fig 10a), and top-to-the-northwest shears are developed in the northern edge of the Kitsumkalum granite where it intrudes the Telkwa Formation near Maroon Creek (Fig 10b).

These structures may be related to denudation of the northern Kitselas complex on a separate, northwesterly-vergent fault located within the Bowser Lake Group. Low-angle detachments are apparent within it on the south face of Maroon Mountain and G. Woodsworth (pers comm, 2005) has located a possible detachment fault near the summit of this east-trending ridge. Such a fault would explain the rapid decline in metamorphic grade from the glossy, cordierite-bearing chlorite-sericite schist in the Smithers Formation to low-grade Bowser Lake Group strata north of Kalum Lake. On Figure 2, we also have located an inferred, top-to-the-north detachment fault from north of Maroon Mountain, through the lower Fiddler Creek drainage and across the Skeena River north of Big Oliver Creek, to account for discontinuities in structural trends as well as the decrease in grade.

LATE FAULTS

North to north-northwest-striking, steeply dipping to vertical faults occur throughout the area. The most prominent are those that define the western margin of the Kitselas complex. Fault strands exposed along the highway near Kalum Lake are thin zones of retrograde chlorite with downdip, or in some cases gently plunging, lineations. Deflection of foliations and shear bands indicate down-to-the-

west motion (Fig 11). Some slickensides reflect a dextral component of motion. Prominent linears in the hills north of Terrace probably correspond to subsidiary faults belonging to this set.

There are at least three prominent north-northwest faults that cut the Kitselas complex and the Hardscrabble pluton. The displacement of fold axial traces on two of these indicates dextral displacements on the order of 500 m to 1 km. The east-side-down Tumbling Creek fault extends north from the Usk map area (Nelson *et al.*, 2006a, b) into the hills near Carpenter Creek.

SUMMARY OF STRUCTURAL HISTORY

The Cretaceous to Eocene structural history of the Terrace area is complex, reflecting the major tectonic events that affected all of northwestern BC. The earliest event that we infer was the north-northeasterly imbrication of the Stikinian stratigraphic section, from Permian through to Late Jurassic, within the westerly hinterland of the Bowser fold and thrust belt. This was the earliest expression of the Skeena River fault zone. Although relative age constraints are not available, we tentatively relate south and southwest-

erly-vergent thrusting and folding in the Bowser Lake Group to the southwest-vergent thick-skinned deformation near Prince Rupert, described by Crawford *et al.* (2000). This event was complete by Paleocene time and built the tectonic welt that would collapse during core complex formation in the Eocene (Rusmore *et al.*, 2005). The Shames River shear zone and Shames River fault west of Terrace (Heah, 1991) represent easterly directed tectonic denudation at lower crustal levels during this time, while top-to-the-east detachment faulting on the SRFZ and top-to-the-northwest shears northeast of Kitsumkalum Lake exhumed the Kitselas complex from mid to upper crustal levels. Near the end of this event, steeper faults created the Kitsumkalum graben and displaced the SRFZ.

MINERALIZATION

Compared to the Usk map area, with its over 80 MINFILE occurrences, the southern Doreen and eastern Terrace map areas contain less-known mineral prospects. Our field study suggests that this may be in part due to a less thorough investigation, and we would like to highlight two particular areas that offer significant exploration possibilities. The first prospective area is on the northern slopes of Mt Sir Robert, where 2006 regional mapping has located a number of new copper showings in the upper part of the Telkwa Formation (Fig 2; Table 1, #27–#33; *see also* Nelson and Kennedy, in prep). This area displays a spectacular exposure of glacially scoured brick-red Telkwa volcanic rocks, cut by at least a dozen large (2–3 m wide) dikes, which are generally oriented in a linear east-west direction. The dikes range from felsic to intermediate in composition, suggesting multiple intrusive events.

These copper showings are numerous (Nelson and Kennedy, in prep) and extend over several kilometres to the northwest of the mineralization described by Carter (1996) on the northeastern side of the mountain, where similar copper mineralization was also encountered in 2006 (Table 1, #25, 26). Most of them are quartz-carbonate veins that contain malachite, chalcopyrite, azurite, pyrite and tetrahedrite (Fig 12). Although the individual veins are only a few centimetres thick, in places mineralization can be followed for tens of metres. Copper values in grab sam-

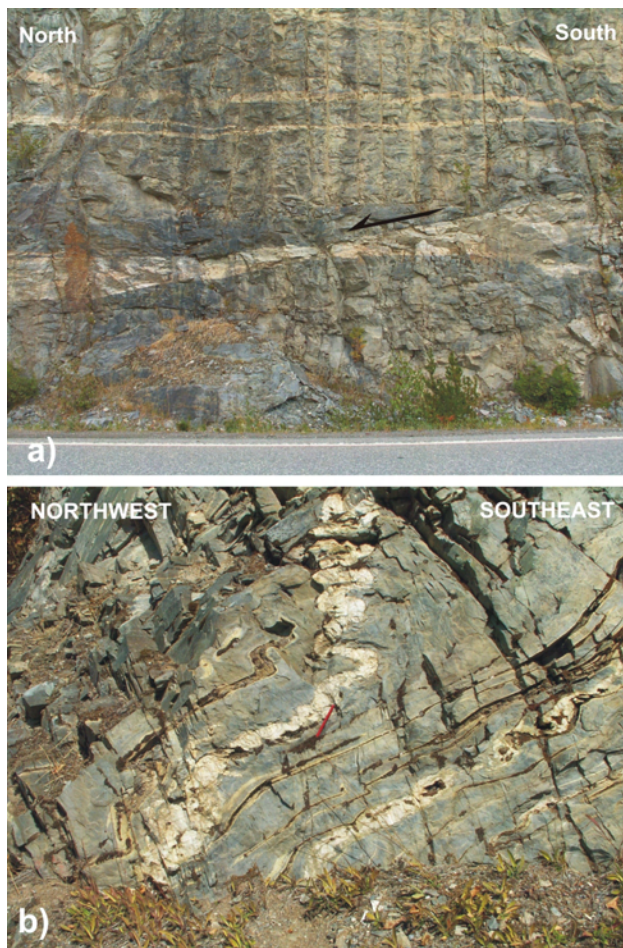


Figure 10. a) Northwest-vergent recumbent folds in metamorphosed Smithers Formation strata on the Nisga'a Highway near the north end of Kitsumkalum Lake. Minor fold axes trend northeasterly; b) gently-dipping shear band displaces a metre-thick apophysis of the Paleocene Kitsumkalum intrusion in a down-to-the-northwest sense; exposure north of Maroon Creek on the Nisga'a Highway.



Figure 11. Highway exposure, east of Kitsumkalum Lake, of down-to-the-west shear bands along the western margin of the Kitsumkalum intrusion.

TABLE 1 (CONTINUED)

#	Station number	UTM		MINFILE	Description	Element:	Mo	Cu	Pb	Zn	Ag	Mn	Fe	As	Au	Cd	Sb	Bi	W	Hg	Se	Te	
		Easting	Northing			Units:	(ppm)	(ppm)	(ppm)	(ppm)	(ppb)	(ppm)	(%)	(ppm)	(ppb)	(ppm)	(ppm)	(ppm)	(ppm)	(ppb)	(ppm)	(ppm)	(ppm)
Method:						ARMS	ARMS	ARMS	ARMS	ARMS	ARMS	ARMS	ARMS	ARMS	ARMS	ARMS	ARMS	ARMS	ARMS	ARMS	ARMS	ARMS	ARMS
Lab:						ACM	ACM	ACM	ACM	ACM	ACM	ACM	ACM	ACM	ACM	ACM	ACM	ACM	ACM	ACM	ACM	ACM	ACM
Detection limit:						0.01	0.01	0.01	0.1	2	1	0.01	0.1	0.1	0.1	0.01	0.02	0.02	0.2	5	0.1	0.02	
23	06RK15-02a	517239	6067596		1 m qz vein with mal, py, cpy part of larger set		10.81	725.47	1.93	53.6	1963	542	2.12	<.1	4.5	0.16	0.04	0.5	8	<5	0.2	0.08	
24	06RK15-02b	517239	6067596		another vein in set could continue 20 m under cover		9.52	952.28	3.02	90.5	1329	610	2.28	<.1	5	0.59	0.09	0.47	0.1	<5	0.2	0.19	
25	06RK18-02	559991	6070420	Rob (no number)	cpy, azurite, malachite from 2 veins		0.4	>10000	114.38	171.9	>100000	424	3.68	24.6	868.4	4.14	333.45	17.34	0.3	1295	63	0.52	
26	06RK19-05	561547	6068373	Rob (no number)	ROB vein (AR 24544)		0.85	3509.05	9.55	40.1	>100000	65	0.65	21.6	1.1	0.38	25.29	0.08	<.1	671	0.2	0.02	
27	06RK21-02	557786	6073276	Borden Gl. (new)	Cu staining in frags and spec hematite		0.28	1393.31	1.52	76.9	3290	1513	1.74	<.1	1	0.15	0.4	0.05	<.1	12	0.1	0.02	
28	06RK21-06a	558253	6074260	Borden Gl. (new)	A: vein of massive sulphides		6.89	352.3	11.33	19.3	2086	292	31.46	>10000	37	0.45	31.94	0.05	<.1	26802	6.2	0.05	
29	06RK21-06b	558253	6074260	Borden Gl. (new)	B: dissem through rhy		248.68	47.94	5.24	46.9	455	904	5.96	2552.6	0.7	0.28	10.31	0.05	0.2	4368	0.3	<.02	
30	06RK22-01	556792	6073665	Borden Gl. (new)	sulphides in veinlets and dissem		49.88	394.83	814.9	70.7	20013	746	1.83	19.2	121.8	1.13	0.4	6.46	<.1	58	1.4	0.41	
31	06RK22-03	556574	6073928	Borden Gl. (new)	Cu staining in 'blue' alteration zone		0.89	4525.88	3	70	12966	1386	1.72	4.3	222.6	0.65	0.16	0.07	<.1	30	0.2	0.5	
32	06RK22-09	556173	6073890	Borden Gl. (new)	very heavy sample of malachite tetrahedrite		0.18	>10000	11.03	57.4	>100000	1174	1.22	0.8	166.5	20.01	0.18	0.48	<.1	272	3.6	0.2	
33	06RK23-01	556854	6073358	Borden Gl. (new)	dissem sulphides and malachite in brecciated vein		5.21	5257.86	10.35	6.2	4375	334	0.74	6.3	21.1	36.62	0.62	0.47	<.1	114	1	0.81	
34	06RK24-03	558439	6073261	Borden Gl. (new)	cpy, malachite, bornite in veins		18.82	>10000	676.32	538.7	>100000	50	5.24	68.1	65	10.49	76.59	23.21	<.1	1660	1.9	0.51	
35	06RK30-01a	538545	6069759		A; from GPS location		5.4	59.05	217.02	25.4	35312	19	5.12	3.4	278.2	1.78	0.37	66.08	0.2	15	4.1	5.73	
36	06RK30-01b	538545	6069759		vein with cpy-galena		167.86	831.44	9976.23	44.3	28219	22	0.82	0.4	1258.7	2.32	10.88	15.39	76.3	29	5	0.98	
37	06RK31-04	538444	6070359	Gold Dome 1031 047	from adit		3.51	17.43	57.55	17.3	636	335	0.69	2.6	380	1.75	0.61	1.25	>100	9	0.1	0.14	
38	06RK31-07a	538139	6069997	Gold Dome 1031 047	float sample galena, cpy in quartz vein		78.66	2276.77	2195.22	266.9	60680	185	1.04	2.5	663.7	15.74	62.15	43.52	1.5	38	4.9	0.8	
39	06RK31-07b	538139	6069997	Gold Dome 1031 047	float sample galena, cpy in quartz vein		8.38	36.02	>10000	>10000	>100000	39	2.63	0.1	8084.2	>2000	126.89	20.79	11.8	9439	7.5	7.04	
40	06RK31-08	538243	6069974	Gold Dome 1031 047	float sample		59.02	4815.6	>10000	569.3	47171	23	1.35	0.4	1117.9	35.56	25.45	22.08	>100	128	6.5	1.13	
41	06RK31-09	538345	6069780	Gold Dome 1031 047	qtz vein in creek, shows cpy, malachite, and py		29.77	7895.49	2536.26	851.1	28728	585	2.42	0.9	4558.7	32.39	3.84	8.11	44.1	123	1.8	0.46	
42	06RK32-01	538421	6069573	Gold Dome 1031 047	vuggy qtz vein in granite with galena		215.07	29.05	4914.19	11.9	53877	30	1.02	0.1	9253	0.67	1.05	84.19	>100	23	5.6	2.13	
43	06RK32-02	538386	6069663	Gold Dome 1031 047	from felsic py bearing dike		1.61	33.57	63.32	73.6	281	555	1.74	0.4	6	2.34	0.24	0.22	1.2	<5	<.1	<.02	
44	06RK34-04	526184	6061166		qtz vein		4.66	32.98	28.47	49.3	414	408	3.78	0.9	11.5	0.15	0.1	1.27	2.3	7	1.2	0.22	
45	06RK36-05	530445	6056174		mix of rusty qtz vein and rusty country rock from gossan		16.15	12.55	86.41	26.1	1205	47	1.34	31.7	<.2	1.9	0.32	0.44	0.3	5	2.2	1.67	

ples range up to 5300 ppm (Table 1, #33), and Ag to >10 000 ppb (Table 1, #25, 26, 32). One sample from the Rob claims area contains 868 ppb Au (Table 1, #25). Malachite staining and disseminated chalcopyrite also occur in porphyritic dikes, with no apparent association with local veining. Mineralized veins are associated with minor brecciation and bluish (chlorite?) alteration in the surrounding Telkwa volcanic rocks. Two series of events are recognized to have facilitated the movement of mineralizing fluids. The first is the occurrence of dikes and breccia-forming vein systems. The intrusions both hosted the mineralization and provided heat and fluids to mobilize it into the country rocks. The second episode of mineralization occurred after the emplacement of the dikes and much of the veining in this area; it is expressed as fracture-hosted copper sulphide minerals associated with north-south dextral faulting. Mineralization of the second type is found in narrow valleys where the Telkwa is strongly altered to yellow or orange clay. These faults were never found to be more than 3 m wide. The concentration of mineralization decreases with distance from the individual fault planes. Where late fractures occur in dikes, there is an increase in mineralization. This may suggest that the highest concentration of mineralization occurs where intrusion and fault-related fluids intersect. The steep north-south faults on Mt Sir Robert are assumed to be related to the regional late faulting.

The second target of interest is a mineralized system on the southern slopes of Mt Knauss, north of Carpenter Creek. It is centred by the Womo Mo-porphyry showings (MINFILE 1031 122). This area was mapped and sampled in 1966 (Murphy and Richardson, 1966) and was the subject of a limited geochemical sampling program in 1981 (Livingston, 1980; Livingston and Carter, 1981). The recent increase in molybdenum prices provides an incentive to revisit this occurrence. In our brief traverses across it, we encountered a classic porphyry system located at the margin of the Carpenter Creek pluton. There is evidence of local shearing that involves late porphyritic phases of the granite, as well as the country rocks of the Bowser Lake Group. Conceivably, this structure could extend farther north to the area around the Doreen Mine and south to the high-grade veins at Paddy Mac and Gold Dome: they

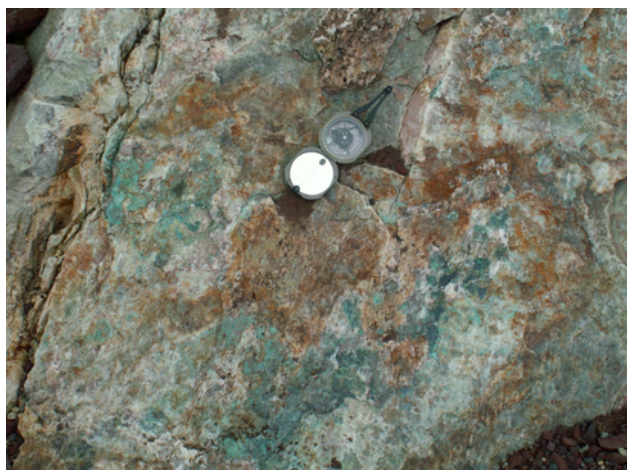


Figure 12. Malachite-stained, copper-rich quartz-carbonate vein north of Borden Glacier, one of many showings in this recently deglaciated area.

would represent the peripheral Au–Ag–base metal enrichments to the main porphyry system. In the core of the system along Rosette Creek (*see* Murphy and Richardson, 1966), we encountered a zone 200 by 1100 m of intense clay-sericite alteration with chalcopyrite and molybdenite in quartz vein stockworks (Fig 13a, b, c). Two vein grab samples from rubble in the stockwork zone contain 600 to



Figure 13. a) View of the Womo porphyry system along Rosette Creek, with pyritic hornfels in the foreground; b) example of stockwork quartz veining; c) molybdenite-chalcopyrite-bearing quartz vein.

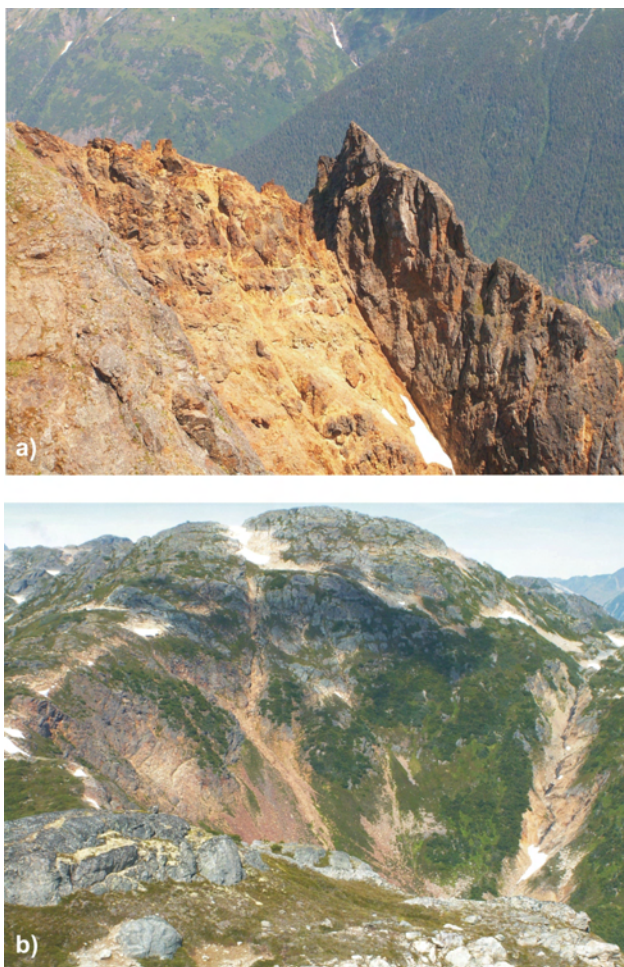


Figure 14. a) Strongly pyritic fault zone between Legate and Little Oliver creeks; b) large gossan in saddle between Hankin and Lean-to creeks.

1000 ppm Cu and 400 to 500 ppm Mo (Table 1, #17, 18). This system is open downslope in the steep, timbered gullies to the south. The core of the altered and mineralized system is partially surrounded to the northeast by a strong pyritic halo in the Bowser Lake clastic strata that measures 300 by 2000 m. This property is currently held by Knauss Creek Mines, who have been focusing their exploration efforts on the veins in Knauss Creek.

In addition to these groups of showings, there are some large pyritic gossans in the area that contrast with mineralization styles in the Usk map area. One is on the low ridge immediately north of Legate Creek. It is associated with steep north-striking faults (Fig 14a). Large patches of felsic volcanic rock are replaced by silica with up to 15% pyrite. Some of these were prospected, but others on cliffs and below the treeline remain unexamined. Two of four samples in this area (Table 1, #7–#10) contain anomalous Cu (to 1980 ppm) and Ag (to 3791 ppb). There is also a large, prominent, rusty pyritic gossan that lies across the height of land between Hankin and Lean-to creeks (Fig 14b). There is no record of assessment work on it; it remains an intriguing and unexplained possibility. Our single sample of it (Table 1, #20) is geochemically undistinguished; however, it in no way represents the potential of this large altered area.

CONCLUSIONS

The geology, structure and mineralization described for the Terrace area result from the conjunction of two fundamental provinces within the BC Cordillera. Stratigraphically, and in terms of its older (Early Jurassic) plutons, the area is part of the Stikine terrane. Structurally, it shows a strong influence of the eastern Coast Belt orogen. The Eocene, molybdenite-bearing plutons are related both to the eastern Coast Belt and to similar plutons of the Skeena arch.

In the 2006 mapping, we have traced out a continuous belt of uppermost Hazelton Group rocks, Smithers Formation and pyjama beds, for over 30 km of strike length. The pyjama beds are at least in part, time equivalent with the Eskay Rift facies in northwestern BC. We have also refined the definition and history of the Kitselas complex, an uplifted belt of metamorphosed Early Jurassic and younger strata that outcrops between the Skeena and Kitsumkalum rivers, north of Terrace. We propose that it was shaped by Cretaceous thrust imbrication followed by Paleocene to Eocene exhumation.

New copper mineralization discovered north of Mt Sir Robert marks a northern continuation of a copper-rich belt in the Telkwa Formation that extends north from Treasure Mountain through the Legate Creek area (see Nelson *et al.*, 2006 a, b). A significant zone of porphyry-style molybdenite and chalcopyrite mineralization on the Womo claims is part of a zone of molybdenite occurrences associated with the eastern side of the Carpenter Creek pluton. It includes the Shan property (MINFILE 1031 114), which was being drill tested by BCM Resources at time of writing (P. Wojdak, pers comm, 2006).

ACKNOWLEDGMENTS

Our geological assistants, Sarah Newman and Joel Angen of the University of Victoria, get rave reviews for their hard work, savvy and unflagging good cheer. Dan Parker of Kitselas kept our truck on the road and the boat right side up in the river. Lael McKeown of Terrace offered us hearth and hospitality without equal. Jean Black expedited flawlessly and Bill and Helene McRae were, as always, helpful and good company. We appreciated the expert piloting of Ian Swann and the staff of Quantum Helicopters — especially our good friend Randy Hildebrandt, who is gone away too soon.

REFERENCES

- Anderson, R.G. and Thorkelsen, D.J. (1990): Mesozoic stratigraphy and setting for some mineral deposits in Iskut River map area, northwestern British Columbia; in Current Research, *Geological Survey of Canada*, Paper 90-1F, pages 131–139.
- Andronicos, C.L., Hollister, L.S., Davidson, C. and Chardon, D. (1999): Kinematics and tectonic significance of transpressive structures in the Coast Plutonic Complex, British Columbia; *Journal of Structural Geology*, Volume 21, pages 229–243.
- Carter, N.C. (1996): Geochemical report on the Rob mineral claims, for R.T. Heard; *BC Ministry of Energy, Mines and Petroleum Resources*, AR24544, 14 pages.
- Crawford, M.L., Crawford, W.A. and Gehrels., G.E. (2000): Terrane assembly and structural relationships in the eastern Prince Rupert quadrangle, British Columbia; in *Tectonics of*

- the Coast Mountains, southeastern Alaska and British Columbia, Stowell, H.H. and McClelland, W.C., Editors, *Geological Society of America*, Special Paper 343, pages 1–22.
- Evenchick, C.A. (2001): Northeast-trending folds in the western Skeena fold belt, northern Canadian Cordillera: a record of Early Cretaceous sinistral plate convergence; *Journal of Structural Geology*, Volume 23, pages 1123–1140.
- Gareau, S.A., Friedman, R.M., Woodsworth, G.J. and Childe, F. (1997a): U-Pb ages from the northeastern quadrant of Terrace map area, west-central British Columbia; in Current Research, *Geological Survey of Canada*, Paper 1997-A/B, pages 31–40.
- Gareau, S.A., Woodsworth, G.J. and Rickli, M. (1997b): Regional geology of the northeastern quadrant of Terrace map area, west-central British Columbia; in Current Research, *Geological Survey of Canada*, Paper 1997-A/B, pages 47–55.
- Heah, T.S.T. (1991): Mesozoic ductile shear and Paleogene extension along the eastern margin of the Central Gneiss Complex, Coast Belt, Shames River area, near Terrace, British Columbia; MSc thesis, *The University of British Columbia*, 155 pages.
- Livingston, K.W. (1980): Prospecting report on geology, Womo claims, for Prism Resources Ltd.; *BC Ministry of Energy, Mines and Petroleum Resources*, AR8374, 8 pages.
- Livingston, K.W. and Carter, N.C. (1981): Geochemical Report on Womo 1 and 2, for JMT Services Ltd.; *BC Ministry of Energy, Mines and Petroleum Resources*, AR9524, 8 pages.
- Mihalynuk, M.G. and Friedman, R.M. (2005): Gold and base metal mineralization near Kitsumkalum Lake, north of Terrace, west-central British Columbia; in Geological Fieldwork 2004, *BC Ministry of Energy, Mines and Petroleum Resources*, Paper 2005-1, pages 67–82.
- MINFILE (2006): MINFILE BC mineral deposits database; *BC Ministry of Energy, Mines and Petroleum Resources*, URL <<http://www.em.gov.bc.ca/Mining/Geolsurv/Minfile/>> [December 2006].
- Murphy, D.J. and Richardson, P.W. (1966): Knauss Mountain claims; Dug group 54°N, 128°E, for Southwest Potash Corporation; *BC Ministry of Energy, Mines and Petroleum Resources*, AR798, 21 pages.
- Nelson, J.L., Barresi, T., Knight, E. and Boudreau, N. (2006a): Geology of the Usk map area (1931/09); *BC Ministry of Energy, Mines and Petroleum Resources*, Open File 2006-3, 1:50 000 scale.
- Nelson, J.L., Barresi, T., Knight, E. and Boudreau, N. (2006b): Geology and mineral potential of the Usk map area (1031/09) near Terrace, British Columbia; *BC Ministry of Energy, Mines and Petroleum Resources*, Geological Fieldwork 2005, Paper 2006-1, pages 117–134.
- Nelson, J.L. and Kennedy, R. (in prep): Geology of the Doreen south half (1031/16S) and Terrace east half (1031/10E) map areas, near Terrace, British Columbia; *BC Ministry of Energy, Mines and Petroleum Resources*, Open File, 1:50 000.
- Diakow, L.J. and Levson, V.M. (1997): Bedrock and surficial geology of the southern Nechako Plateau, central British Columbia (NTS 93F/2, 3, 6, 7); *BC Ministry of Energy, Mines and Petroleum Resources*, Geoscience Map 1997-2, 1:100 000 scale.
- Rusmore, M.E., Woodsworth, G.J. and Gehrels, G.E. (2005): Two-stage exhumation of midcrustal arc rocks, Coast Mountains, British Columbia; *Tectonics*, Volume 24, TC5013, doi:10.1029/2004TC001750.
- Tipper, H.W. and Richards, T.A. (1976): Jurassic stratigraphy and history of north-central British Columbia; *Geological Survey of Canada*, Bulletin 270, 73 pages.
- Woodsworth, G.J., Hill, M.L. and van der Heyden, P. (1985): Preliminary geology map of Terrace (NTS 1031, east half) map area, B.C., *Geological Survey of Canada* Open File 1136, scale 1:125 000.

Recent Revisions to the Early Mesozoic Stratigraphy of Northern Vancouver Island (NTS 102I; 092L) and Metallogenic Implications, British Columbia

by G.T. Nixon and A.J. Orr

KEYWORDS: Vancouver Group, Karmutsen Formation, Quatsino Formation, Parson Bay Formation, Bonanza Group, Bonanza island arc, LeMare Lake volcanics, Victoria Lake basalt, Pemberton Hills rhyolite, Vancouver Island, Wrangellia, picrite, regional geology, stratigraphy, metallogeny, volcanogenic massive sulphide, epithermal Au-Ag, Ni-Cu-PGE

INTRODUCTION

In order to improve our understanding of the mineral potential of northern Vancouver Island beyond the well-known intrusion-related Cu-Au-Ag(-Mo) porphyry deposits (*e.g.*, Hushamu, MINFILE 092L 240 and the former Island Copper mine, MINFILE 092L 158) and base and precious-metal skarns (*e.g.*, Merry Widow, MINFILE 092L 044), we need a better understanding of the stratigraphy of the Bonanza island arc so as to apply predictive models for mineral exploration that target specific stratigraphic metallogenetic. Epithermal precious-metal prospects are known (*e.g.*, Mount McIntosh – Hushamu, MINFILE 092L 240), but many more opportunities exist in the world-class, metallogenic supra-subduction zone and flood basalt environments presented on Vancouver Island.

A new stratigraphic framework for the Early Mesozoic stratigraphy of northern Vancouver Island was recently published in a series of Geoscience Maps (1:50 000 scale; Nixon *et al.*, 2006c–e). This paper provides a brief synopsis of our current view of the regional stratigraphy and attempts to highlight intervals in the stratigraphic column that are prospective for some important deposit types, not all of which are presently known on Vancouver Island.

REGIONAL GEOLOGY

The geology of Vancouver Island is characterized principally by Late Paleozoic to Early Mesozoic rocks belonging to the tectonostratigraphic terrane of Wrangellia (Jones *et al.*, 1977), which extends north through the Queen Charlotte Islands into southern Alaska (Wheeler and McFeely, 1991; Fig 1). Wrangellia was amalgamated with the Alexander Terrane in the Alaska panhandle to form the Insular Belt as early as the Late Carboniferous (Gardner *et al.*, 1988) and was accreted to inboard terranes of the Coast and

Intermontane Belts as late as mid-Cretaceous (Monger *et al.*, 1982) or as early as Middle Jurassic time (van der Heyden, 1991; Monger and Journeay, 1994).

At the latitude of northern Vancouver Island, Wrangellia is intruded to the east by granitoid rocks of the Coast Plutonic Complex and fault-bounded to the west by the Pacific Rim Terrane and metamorphosed rocks of the Westcoast Crystalline Complex (Wheeler and McFeely, 1991). Devonian to Early Permian island-arc volcanic, volcanoclastic and sedimentary rocks that form the basement of Wrangellia (Sicker and Buttle Lake groups; Massey, 1995a–c) are not exposed on northernmost Vancouver Island. The bedrock stratigraphy is dominated by the Triassic tripartite succession of Karmutsen flood basalt, Quatsino limestone and Parson Bay mixed carbonate-clastic (volcanic) sequence, which is diagnostic of Wrangellia (Jones *et al.*, 1977). The overlying Jurassic volcanic and sedimentary strata, together with coeval granitoid intrusions of the Island Plutonic Suite, comprise the main phase of magmatism of the Bonanza island arc (Northcote and Muller, 1972; DeBari *et al.*, 1999).

A major contractional event is marked by an angular unconformity underlying Jura-Cretaceous clastic sequences deposited on the eroded surface of the Bonanza Group. This episode of deformation is constrained by strata of Late Jurassic age (Oxfordian to Tithonian), locally underlying more widespread Cretaceous sedimentary rocks in the northern Vancouver Island – Queen Charlotte Islands region (Gamba, 1993; Haggart and Carter, 1993; Haggart, 1993).

The history of faulting on northern Vancouver Island is complex and embodies Cretaceous transpression and Tertiary extension. Major northwesterly trending, high-angle faults right-laterally displace (where possible to determine), downdrop and fold Jura-Cretaceous to early Late Cretaceous clastic rocks exposed in the Quatsino Sound area (Muller *et al.*, 1974; Nixon *et al.*, 1993a, 1994a, 1995a). These sequences are preserved as disparate fault-bounded remnants of the Cretaceous basins (Muller *et al.*, 1974; Jeletzky, 1976; Haggart, 1993). The relatively low relief and high heat flow of northernmost Vancouver Island reflect tectonism associated with the development of the Queen Charlotte Basin, a Tertiary transtensional province related to oblique convergence of the Pacific and Juan de Fuca plates with the North American Plate (Riddihough and Hyndman, 1991; Lewis *et al.*, 1997).

The present crustal architecture exhibits a dominant northwesterly trending structural grain manifested by the distribution of major lithostratigraphic units and granitoid plutons (Fig 1). Numerous fault-bounded blocks of homoclinal, Early Mesozoic strata generally dip westward

This publication is also available, free of charge, as colour digital files in Adobe Acrobat® PDF format from the BC Ministry of Energy, Mines and Petroleum Resources website at http://www.em.gov.bc.ca/Mining/Geosurv/Publications/catalog/cat_fldwk.htm

(Muller *et al.*, 1974). The northeasterly trending Brooks Peninsula fault zone appears to coincide with the southern limit of Neogene volcanism in the region and delineate the southern boundary of the Tertiary extensional regime in the Queen Charlotte Basin (Armstrong *et al.*, 1985; Lewis *et al.*, 1997).

PREVIOUS STRATIGRAPHIC NOMENCLATURE

The evolution of stratigraphic nomenclature for northern Vancouver Island is shown in Figure 2. The earliest recorded geological investigations were made by G.M.

Dawson, who introduced the name ‘Vancouver Series’ for all the volcanic and sedimentary rocks underlying the unconformity at the base of the Cretaceous succession (Dawson, 1887). Subsequently, Gunning (1930) adopted the term Vancouver Group to describe the conformable succession of Lower Mesozoic volcanic and sedimentary rocks in the Quatsino-Nimpkish area. He later subdivided the stratigraphy into three distinct units: the Quatsino limestone (Dolmage, 1919); the underlying Karmutsen volcanics named for extensive exposures overlooking the western shore of Nimpkish Lake in the Karmutsen Range; and the overlying sedimentary-volcanic succession of the Bonanza Group exposed on the upper slopes west of Bo-

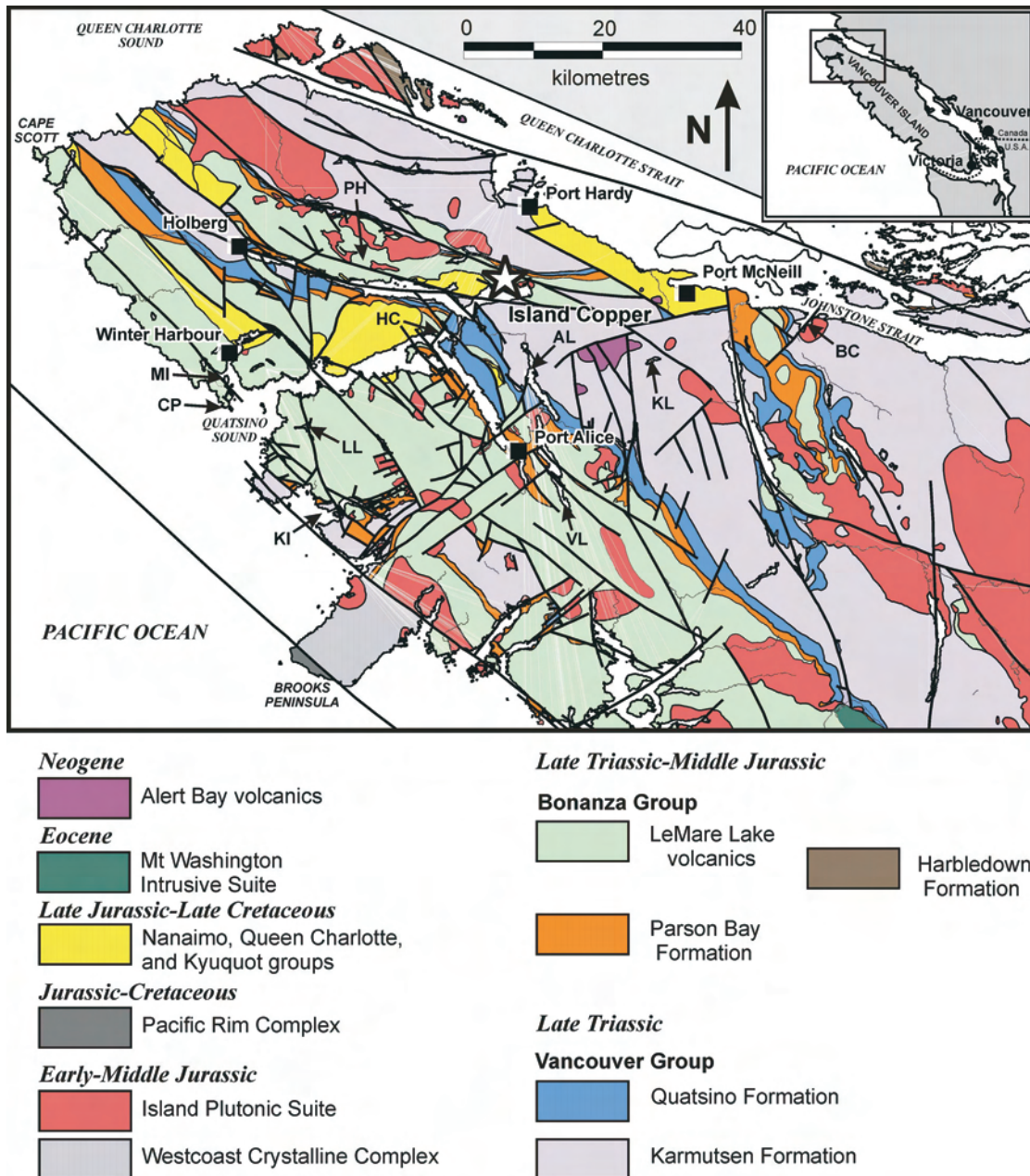


Figure 1. Regional geology of northern Vancouver Island (after Massey *et al.*, 2005). Abbreviations for localities mentioned in text: AL, Alice Lake; BC, Beaver Cove; CP, Cape Parkins; HC, Hecate Cove; KI, Klaskino Inlet; KL, Keogh Lake; LL, Le Mare Lake; MI, Mathews Island; PH, Pemberton Hills; VL, Victoria Lake.

nanza Lake (Gunning, 1932; Fig. 2). Based on sparse fossil evidence, the age of the Vancouver Group was considered to be Late Triassic to Early Jurassic. This tripartite succession was traced southward into the Zeballos region by Gunning (1933) and later by Hoadley (1953), who incorporated much of Gunning's earlier work in the Nimpkish and Woss areas (Gunning, 1938a–d). Hoadley (1953) more formally designated the Karmutsen volcanic rocks as the Karmutsen Group and was able to systematically map a lower sedimentary and upper volcanic division within the Bonanza Group, as previously recognized by Gunning (1932, 1933). This stratigraphic framework for the Vancouver Group was adopted by Muller and Carson (1969), who designated the Bonanza as a subgroup and the Karmutsen as a formation.

Between 1949 and the early 1970s, detailed geological investigations of coastal exposures in Quatsino Sound were conducted by J.A. Jeletzky, who established the basis for Mesozoic stratigraphy in the region from fossil collections (Jeletzky, 1950, 1954, 1969, 1970a, b, 1973, 1976). Following Gunning (1932) and Hoadley (1953), Jeletzky subdivided the Vancouver Group into the Karmutsen and Bonanza subgroups and divided the Bonanza into an upper volcanic and lower sedimentary division, which included the Quatsino Formation at its base (Fig 2). Above the Quatsino limestone, he recognized three mappable sedimentary units, from oldest to youngest: the informally named 'thinly bedded' and 'arenaceous' members, and the Sutton limestone situated at the top of the sedimentary division (where present) and correlative with the Sutton For-

mation at the type locality on Cowichan Lake (Tozer, 1967; Stanley, 1988). The overlying volcanic division of the Bonanza subgroup contained nine mappable units, only two of which were given formal status: the mixed volcanic-sedimentary succession of the Hecate Cove Formation at the base, named for the cove near Quatsino Narrows at the eastern end of Quatsino Sound; and the younger, predominantly argillaceous Mathews Island Formation near the entrance to the sound in Forward Inlet (Fig 1, 2).

Integrated lithostratigraphic, biostratigraphic and mineral deposit studies of the Alert Bay – Cape Scott map area (NTS 092L; 102I) by Muller and coworkers provided the first regional geological synthesis for northern Vancouver Island (Muller *et al.* 1974; Muller and Roddick, 1983). The entire Lower Mesozoic stratigraphy was referred to as the Vancouver Group and two new formations were introduced: the Late Triassic Parson Bay and Lower Jurassic Harbledown formations, as first distinguished by Crickmay (1928) on Harbledown Island, the type locality, in Queen Charlotte Strait (Fig 2). As used by Muller *et al.* (1974), the Parson Bay Formation is equivalent to the 'sedimentary division of the Bonanza subgroup' of Jeletzky (1973, 1976), but includes his Hecate Cove Formation and excludes the Quatsino limestone (Fig 2). The argillite-greywacke sequence of the Harbledown Formation is correlative with Bonanza volcanics of western Vancouver Island but in the Alert Bay – Cape Scott region has only been distinguished as a map unit at the type locality and on islands in Queen Charlotte Sound (Fig 1, 2). Muller *et al.* (1974) abandoned

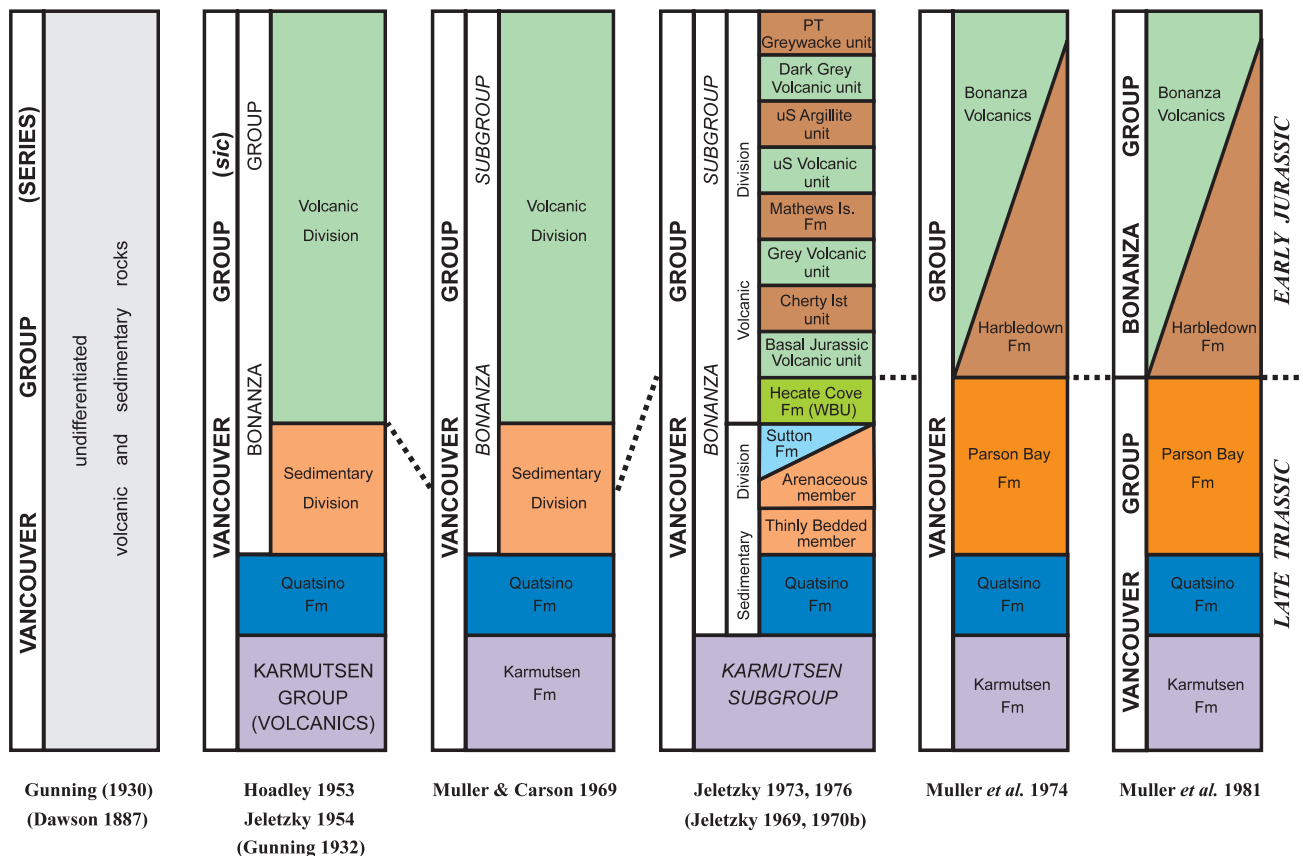


Figure 2. Evolution of Lower Mesozoic stratigraphic nomenclature for northern Vancouver Island. Alternative nomenclature and corresponding references shown in brackets. Abbreviations for Jeletzky's stratigraphy are as follows: WBU, water-laid breccia unit; uS, uppermost Sinemurian (early Early Jurassic); PT, Pliensbachian–Toarcian (late Early Jurassic).

the 'subgroup' and 'division' terminology and defined the 'Bonanza volcanics' as a single map unit comprising diverse volcanic rocks with minor intercalated sedimentary rocks, essentially equivalent to the 'Bonanza subgroup' and replacing the more complex stratigraphy erected by Jeletzky (1976). The base of the 'Bonanza volcanics' was taken as the lowest andesitic lava or volcanic breccia overlying sedimentary strata of the Late Triassic Parson Bay Formation in the west or the Early Jurassic Harbledown Formation in the east; and locally, this contact lies above the Sutton limestone. Subsequently, Muller *et al.* (1981), working in the Nootka Sound area, made revisions to the stratigraphy by restricting the Vancouver Group to the Karmutsen, Quatsino and Parson Bay formations, and reinstating the Bonanza Group, which now comprises the Harbledown Formation and the partly coeval 'Bonanza volcanics' (Fig 2).

REVISED LITHOSTRATIGRAPHY

Revisions to the Early Mesozoic lithostratigraphic nomenclature adopted in this report are shown in Figure 3 and are based on previously published and unpublished mapping, and geochronological and biostratigraphic data for the Quatsino Sound area (Nixon *et al.*, 1993a, b; 1994a, b; 1995a, b; 2000, 2006a–e; Friedman and Nixon, 1995; Archibald and Nixon, 1995). Absolute ages for stage boundaries are based on recent revisions to the geological time scale (Gradstein *et al.*, 2004; Furin *et al.*, 2006).

As shown in Figure 3, the Vancouver Group on northern Vancouver Island includes two lithostratigraphic units, the Late Triassic Quatsino and mid to Late Triassic Karmutsen formations. The basal unit of the Vancouver Group, the Middle (late Ladinian) to Late Triassic 'sediment-sill unit' of Muller *et al.* (1974), comprising siliceous black shale and siltstone (including the pelecypod-rich 'Daonella beds') intruded by super-abundant basaltic sills considered coeval with Karmutsen lava, is not exposed on this part of Vancouver Island. The overlying Bonanza Group now includes the Late Triassic Parson Bay Formation and two informal units of latest Triassic to Middle Jurassic (Bajocian) age: a mixed volcanoclastic-sedimentary rock sequence resting conformably on Parson Bay strata; and the overlying LeMare Lake volcanics. The latter unit is named for Le Mare Lake on the west coast near the entrance to Quatsino Sound (Mahatta Creek map sheet NTS 092L/05), where basaltic to rhyolitic lava, ash flow tuff and interbedded epiclastic deposits of the Bonanza Group are well exposed. The informal term 'LeMare Lake volcanics' replaces the 'Bonanza volcanics' of Muller *et al.* (1974, 1981; Fig 2) in order to potentially avoid confusion with the Bonanza Group as a whole and to conform to naming conventions specified in the North American Stratigraphic Code. Since the term 'Bonanza volcanics' is so well established in the literature, it may be usefully retained to describe all volcanic rocks within the Bonanza Group, including those within the Parson Bay Formation (described below).

The unnamed, latest Triassic – earliest Jurassic volcanoclastic-sedimentary unit of the Bonanza Group occupies a transition between predominantly marine deposition in the Parson Bay and widespread subaerial volcanism in LeMare Lake time, and appears to be partially correlative with the Early Jurassic Harbledown Formation (Muller *et al.*, 1974, 1981; Fig 2, 3). Following the early work of

Crickmay (1928) at the type locality in Parson Bay, Harbledown Island, Tipper (1977) found that ammonite zonation in the Harbledown Formation could only confirm late–early to latest Sinemurian strata, and noted that the Jurassic rocks were separated by a fault from the Late Triassic Parson Bay Formation. However, working farther south in the Bute Inlet area, Carlisle (1972) established a conformable contact between the Parson Bay and Harbledown formations. Based on ammonite fauna collected from an argillite-greywacke succession on Balaclava Island in the Queen Charlotte Sound, Muller *et al.* (1974) extended the Harbledown Formation into the Early Pliensbachian (Friebold and Tipper, 1970). Thus, these data indicate that the Harbledown Formation, as currently defined, is correlative with much of the lower part of the LeMare Lake volcanics and practically the entire stratigraphic succession erected by Jeletzky (1976; Fig 2).

STRATIGRAPHY

The principal mappable units of the Vancouver and Bonanza groups presently comprise both formal lithostratigraphic units and informal subunits, which require further investigation before their status can be determined. The latter units occur within the Karmutsen and Parson Bay formations and LeMare Lake volcanics, and are lithologically distinct from their hostrocks, except for picritic lava within the Karmutsen (Fig 3). Some of these subunits are regionally significant and may serve as local stratigraphic markers once confirmed by isotopic dating studies currently in progress. The main lithological and textural characteristics of the map units and their stratigraphic relationships, are summarized below.

Vancouver Group

The Vancouver Group in the Quatsino Sound area is represented by the mid to Late Triassic Karmutsen and overlying Quatsino formations.

KARMUTSEN FORMATION

Previous work by Carlisle (1972) in the Bute Inlet – Schoen Lake area established three subdivisions of regional significance within the Karmutsen flood basalt: a lower pillow lava sequence overlain by locally well-bedded pillow breccia, hyaloclastite ('aquagene' tuff) and reworked equivalents; in turn overlain by a succession of subaerial flows. In the Quatsino Sound area, layered flow sequences of the youngest Karmutsen subdivision predominate and the intermediate clastic division appears to be only weakly developed. The uppermost part of the basal pillow lava sequence underlies ground south of Port McNeill between the northern tips of Alice and Nimpkish lakes and toward the east coast in the poorly accessible, northeastern part of the Nimpkish map sheet (Nixon *et al.*, 2006a, b). The minimum true thickness of the entire basalt succession is estimated to exceed 6000 m (Muller *et al.*, 1974); evidence of low-grade metamorphism in the Karmutsen Formation, ranging from zeolite to prehnite-pumpellyite facies, is well documented (*e.g.*, Surdam, 1973; Kuniyoshi and Liou, 1976; Greenwood *et al.*, 1991).

Typical Karmutsen basalt is black to dark grey-green, commonly aphanitic or more rarely plagioclase-phyric, and generally amygdaloidal in some part of the flow unit. Contacts between individual flows are usually sharp and planar

to undulatory, and typically lack flow breccia or any evidence for significant erosion or paleosol development. Flow thicknesses are usually on the order of several metres, but range from 1 m or less to over 12 m where clearly discernible; flows up to 30 m thick were recorded by Muller *et al.* (1974). Primary columnar jointing, a characteristic feature of many continental flood basalt provinces, is notably lacking. Rarely, bulbous flow lobes, toes and ropy crusts of pahoehoe lava are well preserved. Certain lava exhibits pronounced flow foliations defined by zones of vesicle enrichment ranging from a few centimetres to >50 cm. These zones are almost invariably parallel to flow contacts and provide reliable structural markers in the absence of bedding. Locally conspicuous pipe vesicles are oriented perpendicular to flow contacts and vesicle layering, except where plastically deformed during the final stages of flow

emplacement. Amygdules are commonly filled with quartz, potassium feldspar, epidote, chlorite, carbonate, zeolite and clay minerals.

Pillow lava sequences are generally closely packed and locally contain interpillow hyaloclastite and interstitial quartz, zeolite, carbonate, epidote and chlorite. Rarely, near the top of the pillow basalt subdivision, compound flow units are exposed, comprising several metres of massive lava passing into pillowed flows directly below. Such features may represent an emergent event or simply reflect an increase in the rate of extrusion or local flow emplacement.

The pillow breccia is generally massive or indistinctly bedded and some contain dispersed whole pillows. Hyaloclastite deposits incorporate curvilinear, spalled pillow rinds, dispersed pillow fragments locally preserving

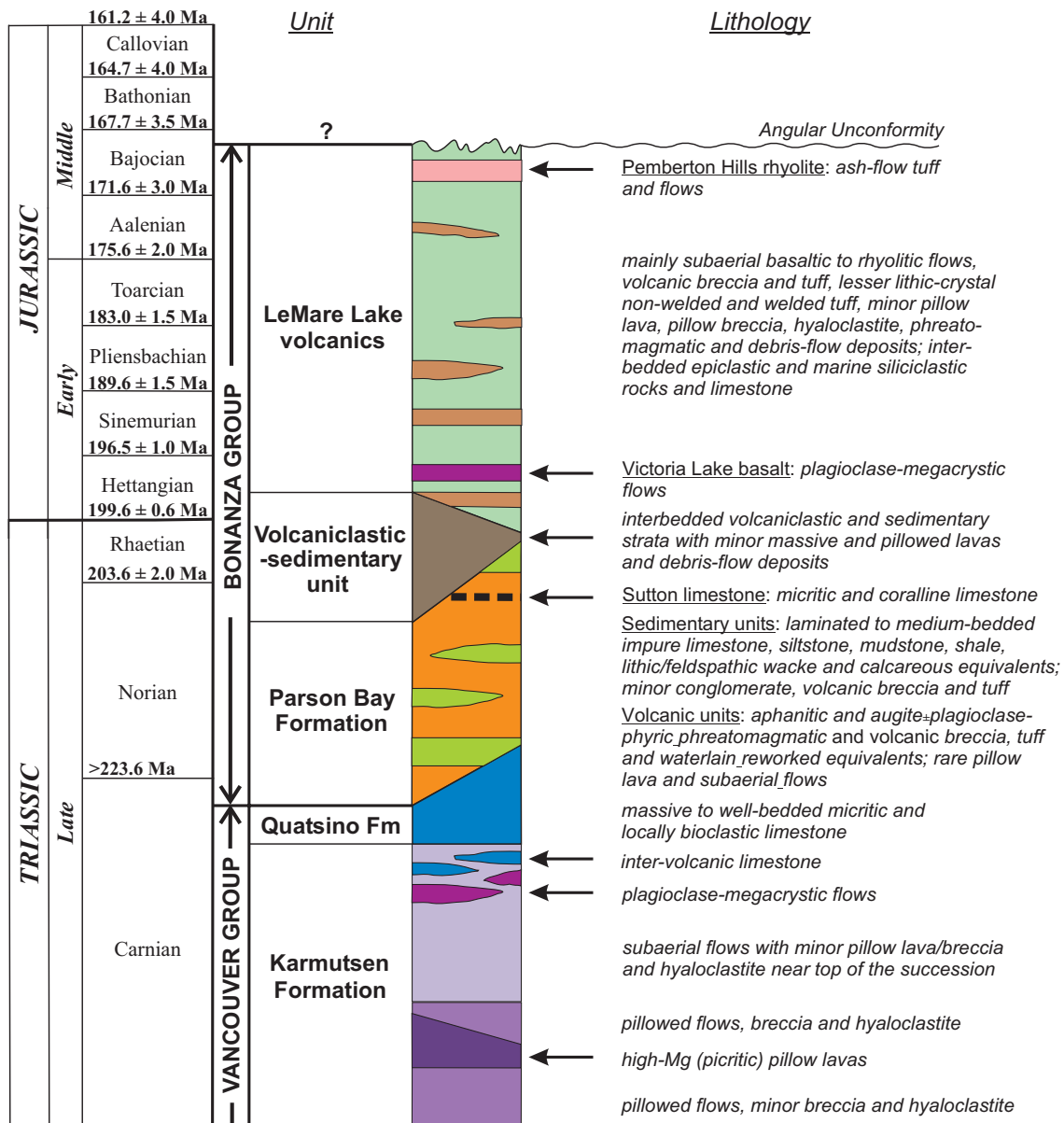


Figure 3. Schematic stratigraphy of northern Vancouver Island and revised nomenclature for Triassic-Jurassic lithostratigraphic units described in this report. The geological time scale is that of Gradstein *et al.* (2004), except for the Carnian-Norian Stage boundary, which is taken from Furin *et al.* (2006).

chilled margins and angular, lapilli-sized clasts set in a finely comminuted, grey-green to orange-brown (formerly palagonitized?) basaltic matrix.

Intra-Karmutsen Limestone

Discontinuous beds and lenses of grey limestone, and more rarely, fine-grained siliciclastic sedimentary rocks, occur near the top of the Karmutsen succession, not far below the base of the overlying Quatsino Formation. The intra-Karmutsen limestone is typically micritic, massive or poorly bedded, and generally does not exceed about 8 m in thickness. Rarely, this limestone contains oolitic beds and exhibits cross-stratification, providing clear evidence of intertidal and shallow marine deposition. Locally, the limestone is associated with thin units of pillow basalt. Other rare intervolcanic deposits include thin, laminated to medium-bedded, variably calcareous, intercalated sequences of mudstone, shale, siltstone and limestone. Similar, stratigraphically equivalent rock types, including *Halobia*-bearing shale, were described in detail by Carlisle and Suzuki (1974).

It is clear from their stratigraphic position that these intervolcanic sedimentary deposits were formed during the waning stages of Karmutsen volcanism. The limestone essentially represents the initial phase of deposition of Quatsino limestone prior to the cessation of volcanic activity, and the fine-grained clastic rocks are vestiges of erosive products deposited in low-energy environments. Thus, erosion, carbonate-clastic sedimentation and effusive volcanism were occurring concurrently, through to the initial stages of deposition of Quatsino limestone.

Plagioclase-Megacrystic Flows

Near the top of the subaerial succession, lava distinguished by its plagioclase megacrysts is locally intercalated with aphanitic and sparse porphyritic flows carrying plagioclase phenocrysts (<5 m). The plagioclase megacrysts (1–2 cm) form euhedral to subhedral laths and blocky grains, occupy 20 to 40 vol% of the rock, and are set in a compact to strongly amygdaloidal groundmass carrying smaller feldspar crystals. Locally, these lavas display trachytoid textures and zones of megacryst concentration oriented parallel to the flow fabric. It is important to note that these megacrystic flows are confined to the uppermost part of the Karmutsen Formation, and as such, serve as stratigraphic markers where outcrops of intra-Karmutsen or Quatsino limestone are sparse or absent altogether (Nixon *et al.*, 2006b).

Picritic Lavas

The first occurrence of picritic lava with high MgO content (up to ~20 wt%) in the Karmutsen Formation was recently reported by Greene *et al.* (2006). Currently known occurrences of picrite is confined to the uppermost part of the basal pillow basalt division (Fig 3). At Keogh Lake, the type locality situated 12 km south of Port McNeill, oblate to subrounded pillows measuring between about 0.25 and 1 m across form closely packed pillow sequences with virtually no interstitial clastic or mineral infillings. In other exposures, individual pillows may be much larger (up to 5 m), and secondary quartz, epidote and carbonate commonly occupy interstices between pillows and rarely infill semi-circular to oblate intrapillow cavities formed by partial lava drainage.

Macroscopically, the picrite is indistinguishable from normal Karmutsen basalt; they are slightly denser and characteristically non-magnetic, in contrast to the strongly magnetic character of the least-altered basalt. Chemical analysis and petrographic identification of olivine phenocrysts, which have been completely replaced by serpentine, talc, chlorite, opaque oxide and clay minerals, are the only true discriminants. Aside from their potential importance with respect to the petrogenesis of the Karmutsen flood basalt province, the picrite may have metallogenic significance with regard to the potential for Ni-Cu-PGE (platinum group element) mineralization in this part of Wrangellia (discussed below).

QUATSINO FORMATION

The contact between the Quatsino and Karmutsen formations has been described by Muller *et al.* (1974) as a paraconformity (*i.e.*, an uncertain unconformity in which no erosion surface is clearly discernible). The examination of this contact at various localities reveals either massive Quatsino limestone in sharp contact with basaltic flows, or a thin (<25 cm) intervening layer of black to orange-brown weathering, basaltic sandstone and siltstone, which is variably calcareous and clay altered. These clastic deposits are commonly discontinuous along strike, but provide clear evidence for a brief period of erosion of the lava shield prior to, and probably during, the primary stages of deposition of the Quatsino limestone. Thus, these initial carbonate-clastic deposits at the base of the Quatsino mirror those that formed prior to the cessation of volcanism as more restricted deposits of intra-Karmutsen limestone and marine siliciclastic material.

The lower part of the Quatsino Formation is typically a pale grey weathering, dark to medium grey, predominantly massive micritic limestone. Fossils are generally rare, although poorly preserved ammonites have been noted at several localities. The uppermost part of the Quatsino limestone is typically composed of thinly laminated to medium or thickly bedded micrite and rarely calcarenite, which locally contain laminae enriched in bioclastic debris. Dark grey to black chert concretions, layers and irregular replacements are locally conspicuous. Normally graded beds and rare crosslaminations in some sequences attest to deposition by turbidity currents. Transported shell fragments of note include gastropods up to 1 cm across, and thin-shelled pelecypods (mainly *Halobia* sp.) up to several centimetres in width. The top-most beds of the Quatsino Formation locally contain a diverse fossil assemblage, including both single and colonial corals, nautiloids and ammonites (Muller *et al.*, 1974; Jeletzky, 1976).

Previous workers noted that the thickness of Quatsino limestone varies from west to east across northern Vancouver Island: the unit is <40 m thick in Klaskino Inlet on the west coast, reaches a maximum thickness of almost 500 m in the central Alice Lake area and thins eastward to about 75 m in the vicinity of Beaver Cove (Muller and Rahmani, 1970). This variation in thickness corresponds to a difference in age. Based on ammonite and conodont faunas, the top of the Quatsino limestone in the thickest section near Alice Lake is late Early Norian in age, but on the east and west coasts, the limestone is entirely restricted to the Carnian (Muller *et al.*, 1974; Jeletzky, 1976; Nixon *et al.*, 2000; 2006a, b). Given the subaerial nature of the final phase of Karmutsen volcanism and the existence of a discontinuous veneer of basaltic detritus at the base of the

Quatsino limestone, it seems probable that the base of the Quatsino Formation is also diachronous.

Bonanza Group

The Late Triassic to Middle Jurassic Bonanza Group comprises the Parson Bay Formation at its base, an intermediate unnamed unit of interbedded volcanoclastic and sedimentary rocks, and the overlying LeMare Lake volcanics (Fig 3). As redefined herein, therefore, the Bonanza Group reverts to the original definition of Gunning (1932; Fig 2) and embodies a diverse assemblage of volcanic and epiclastic products related to the development and demise of the Bonanza island arc.

PARSON BAY FORMATION

The Parson Bay Formation may be described in terms of two mappable units: sedimentary units typically comprising fine-grained siliciclastic-carbonate sequences, which are usually predominant; and subordinate volcanic units, which includes flows and volcanoclastic deposits (*i.e.*, fragmental rocks of volcanic parentage, irrespective of origin). The volcanic units are restricted in lateral extent and occupy more than one stratigraphic position within the Parson Bay Formation (Fig 3). Their precise stratigraphic relationships are currently being investigated using conodont biostratigraphy and geochronology.

The contact between the Parson Bay Formation and underlying Quatsino limestone is conformable and typically gradational over widths of about 0.5 to 5 m. This thin to medium-bedded interval is generally marked by intercalations of pale grey-weathering Quatsino limestone and dark grey, impure (siliceous to sandy) limestone, calcareous mudstone and siltstone and minor, locally fossiliferous (*Halobia* sp.) black shale of the Parson Bay succession. The contact is placed at the first appearance of siliciclastic beds.

The thickness of the Parson Bay Formation is difficult to estimate due to its generally poor exposure, localized structural disruption by low-angle faults subparallel to bedding and intrusion by numerous dikes and sills coeval with the LeMare Lake volcanics. In measured sections presented by Muller and Rahmani (1970), the true thickness of the Parson Bay is estimated to be on the order of 300 m in the Klaskino section on the west coast, and 600 m in the central Alice Lake area. These thicknesses, however, include, in part or in whole, the Triassic-Jurassic volcanoclastic-sedimentary unit of this report (described below).

Sedimentary Rock Types

Typical Parson Bay sedimentary rock types include grey to black, thinly laminated to medium-bedded, impure micritic limestone and calcareous to non-calcareous mudstone, siltstone and shale. Minor interbeds include grey-brown to pale buff, fine to coarse-grained feldspathic sandstone, locally pebbly; grey-green lithic volcanic wacke; rare pebble to cobble conglomerate rich in volcanic clasts; and thin volcanoclastic breccia and debris-flow deposits. Rare ochre to pale grey weathering, clay-rich beds (<5 cm thick) may reflect degraded tuffaceous layers; black shale may be distinctly carbonaceous; and wavy laminations in certain limestone probably represent algal mats. Sedimentary structures observed in the sandy layers include normal, and rarely reverse, grading and rare bedding plane scours and dewatering features (load and flame struc-

tures). Debris flow deposits commonly occupy erosional channels, and structures resembling desiccation cracks were noted in mudstone at a single locality. Fissile black shale horizons may contain bedding planes crowded with thin-shelled pelecypods: *Halobia* sp. (Carnian to Middle Norian) in the lower part of the succession and *Monotis* sp. (Late Norian) in the upper part.

From the variety and distribution of sedimentary rock types forming the Parson Bay Formation, it is clear that depositional environments extended from predominantly shallow or moderate-depth marine to locally higher-energy intertidal and beach.

Volcanic Rock Types

The volcanic rock types of the Parson Bay Formation comprise mappable units of volcanoclastic breccia, massive flows and rare pillow lava. These volcanic rocks are particularly abundant and best exposed in the Quatsino – Port Alice area along Neroutsos Inlet and in Quatsino Sound, and have been traced south to the southern limit of the Alice Lake map sheet (Nixon *et al.*, 2006c–e). Although regionally significant, individual units have a limited lateral extent and thus stratigraphic correlation is hampered without adequate age control. Also, it is evident from field relationships that similar volcanic units occupy different stratigraphic positions within the Parson Bay Formation: some lie virtually on the contact with Quatsino limestone, whereas others occur near the top of the succession (Fig 3). Where contacts between volcanic and sedimentary rocks are exposed, they are generally conformable, or locally disconformable due to erosion, with little evidence for a significant hiatus in sedimentation.

The main characteristics and stratigraphic relationships among the volcanic and sedimentary components of the Parson Bay Formation may be best described with reference to the detailed work of Jeletzky (1976), who recognized Late Triassic (?Rhaetian) volcanism in the ‘Hecate Cove Formation’ (Fig 2). The diverse rock types comprising this formation were divided into three intercalated facies: 1) a characteristic assemblage of limestone breccia, water-laid volcanic breccia and mixed volcanic-sedimentary breccia (and associated volcanic conglomerate), in which clasts are supported by a fine-grained, impure limestone to calcareous mudstone-siltstone matrix; 2) well-bedded sequences of locally fossiliferous, variably tuffaceous limestone, calcareous argillite, wacke and water-laid tuff; and 3) coarse volcanic breccia, augite-porphyrific lava and volcanic conglomerate. He regarded the first two facies as predominantly marine and the third facies as nonmarine and resting with the regional unconformity on the deeply eroded remnants of the underlying sedimentary succession. The origin of the distinctive volcanic and sedimentary breccia in facies 1 were ascribed to explosive volcanism and concomitant syntectonic slumping accompanying the ‘Rhaetian Orogeny’.

Some of the best exposures of the Hecate Cove Formation were examined at the type locality just west of Hecate Cove and along the coast beyond (Jeletzky, 1976, sections 4 and 8; Fig 1). Dark reddish grey to greenish grey limestone sequences enclose breccia containing both lithified (angular to subrounded) and semi-consolidated (plastically deformed) clasts (most <15 cm across) of pale grey limestone dispersed in a dark grey-green, impure limestone matrix. Thin interbeds of volcanic breccia generally comprise angular to subangular, poorly sorted clasts (<2 cm) of aphan-

tic to augite±plagioclase-phyric basalt set in a fine-grained limy matrix. Hybrids of these two end-member breccia types also exist in this section. It is evident from the scattered occurrence of slump folds and the locally erosive base of these breccia units that they were emplaced as submarine debris flows, as inferred by Jeletzky (1976). As discussed below, these deposits were formed during the growth and emergence of small volcanic centres, and there is no evidence in the stratigraphic record for a major tectonic or erosional event in the latest Triassic, as previously contended by Muller *et al.* (1974).

Volcanic breccia of a different type is found in the middle to lower parts of the type section. These units form massive beds of dark grey-green, angular to subangular clasts (up to 20 cm across) of dense to amygdaloidal, aphanitic to porphyritic basalt set in a comminuted basaltic matrix rich in lapilli-sized fragments. The virtually monolithic, closed-framework textures, apparent lack of pillow fragments and hyaloclastite debris, presence of dense and vesicular, poorly sorted clasts and paucity of fine-grained constituents in the matrix implies either a direct pyroclastic airfall origin or limited epiclastic redistribution by near-vent mass wastage of basaltic ejecta and/or fragmented flow material. The textural features and close association of flows and breccia emplaced at the air-sea interface strongly suggest that phreatomagmatic activity was responsible for much of the fragmentation.

The lava flows associated with the latter deposits are generally massive and locally exhibit conspicuous flow breccia. Five types of basaltic lava have been recognized based on mineralogy and textures: augite-porphyritic, plagioclase-porphyritic, augite-plagioclase-porphyritic (the most common variety), augite-megacrystic and aphanitic (also common). The porphyritic lava carries euhedral to subhedral, blocky phenocrysts (<5 mm) that grade serially into an amygdaloidal, aphanitic groundmass. Euhedral augite megacrysts in hiatal-textured basalt flows reach up to 1.5 cm in length. The massive and locally oxidized nature of the flows, together with autobrecciated textures and lack of pillow lava/breccia, are consistent with subaerial emplacement, as suggested by Jeletzky (1976). Similar lava and associated breccia are found stratigraphically below the type section at the head of Hecate Cove and also occur above this section to the west (Berg Cove area) within the basal part of the overlying LeMare Lake volcanics (section 8, 'Basal Jurassic Volcanic Unit' of Jeletzky, 1976; Fig 2, 3).

Lithologically, the thinly bedded limestone and fine-grained siliciclastic rocks within the Hecate Cove succession belong to the Parson Bay Formation and were treated as such by Muller *et al.* (1974; Fig 2). Correlative sedimentary successions enclosing aphanitic to augite-plagioclase-phyric flows and water-laid volcanic-sedimentary breccia have been mapped across the inlet on the southern shores of Quatsino Sound and Drake Island where Early Norian to Rhaetian conodonts and bivalves have been recovered (Nixon *et al.*, 2006d). These sections also contain a pale grey weathering, micritic to locally coralline limestone near the top of the Parson Bay succession, which has been correlated with the Late Norian Sutton limestone of Cowichan Lake (Jeletzky, 1976; Muller *et al.*, 1974; Fig 3). This limestone has been identified farther south in slopes west of Neroutsos Inlet and possibly extends south beyond Alice Lake (*e.g.*, the coralline limestone unit at the top of the Alice Lake section; Muller and Rahmani, 1970), but ex-

posures are sparse and it does not form a regionally mappable unit.

Restricted occurrences of augite±plagioclase-phyric flows, volcanic breccia and related intrusions, and rare sequences of aphanitic pillow basalt, have been mapped locally around Neroutsos Inlet and south of Alice Lake (Nixon *et al.*, 2006c). In the latter area, local sequences of clast to matrix-supported aphanitic basaltic breccia, situated at or near the top of the Quatsino Formation, contain abundant, angular lapilli-sized fragments of limestone and appear to represent the variably remobilized products of vent-clearing, phreatomagmatic eruptions.

VOLCANICLASTIC-SEDIMENTARY UNIT

The volcaniclastic-sedimentary rock unit is transitional between the predominantly marine succession of the Parson Bay Formation and regionally extensive, subaerial volcanic sequences at the base of the LeMare Lake volcanics. A heterogeneous assemblage of laminated to thickly bedded sedimentary and volcaniclastic deposits are incorporated, but the unit is dominated by water-laid epiclastic detritus. The principal rock types are: dark grey to grey-green or buff, fine to coarse-grained lithic and feldspathic wacke locally exhibiting graded bedding, and rarely crosslaminations and channel features; finer-grained siliciclastic rocks including siltstone, mudstone and minor shale; impure limestone and calcareous equivalents of the clastic rocks described above; heterolithic and monolithic, clast and matrix-supported volcanic breccia, including rhyolitic to basaltic lapilli tuff, tuff breccia and reworked equivalents. Minor rock types include feldspathic arenite; heterolithic, and rarely monolithic, volcanic conglomerate and debris-flow breccia; and rare crystal-vitric airfall tuff and remobilized equivalents. Thin massive flows and pillow lava may occur locally, and the succession is cut by abundant dikes and sills related to the overlying volcanic rocks.

The basal contact with the Parson Bay Formation is conformable and arbitrarily placed, where clastic rocks, typically wacke, siltstone and fine volcanic breccia, first become dominant over carbonate rocks in the stratigraphy. It is a transitional contact which, because of the generally poor exposure of Parson Bay strata, is especially sensitive to the amount of outcrop. As such, this map unit may locally include typical Parson Bay rock types stratigraphically above the first significant interval of epiclastic material. The upper contact of this unit is more sharply defined and occurs where the predominantly epiclastic succession first passes into the thick sequence of lava flows and their associated breccia at the base of the LeMare Lake volcanics. Although poorly constrained by radiometric dates, both contacts appear to be diachronous (Fig 3).

LEMARE LAKE VOLCANICS

The LeMare Lake volcanics constitute thick sequences of intercalated volcanic and marine sedimentary strata and mark an episode of regionally extensive subaerial volcanism in the Bonanza Group. In fact, most of the western half of northern Vancouver Island is underlain by these rocks (Fig 1). As noted above, volcanic rocks at the base of the unit conformably overlie the shallow marine strata of the volcaniclastic-sedimentary unit, and the eroded top of the succession is marked by an angular unconformity overlain by Cretaceous clastic rocks. The thickness of the unit is difficult to estimate due to the faulting and the paucity of inter-

nal stratigraphic markers, except for two thin subunits (described below). A measured section presented by Muller *et al.* (1974), near Cape Parkins at the entrance to Quatsino Sound, gave an estimated thickness of some 2500 m, which is probably a minimum.

The age of the LeMare Lake volcanics is constrained by extensive fossil collections and, to a much lesser degree, geochronology, but is still inadequately known. The fragmentary fossil record indicates that, since the latest Triassic, marine sedimentation occurred intermittently between the mid-Hettangian and mid-Aalenian (*see* Nixon *et al.*, 2006c–e). The youngest U-Pb isotopic dates for the volcanic rocks are *ca.* 169 Ma (mid-Bajocian) obtained on the Pemberton Hills rhyolite and the oldest dates are approximately 199 to 202 Ma (Rhaetian-Hettangian) from rhyolite on the west coast and near Le Mare Lake (Friedman and Nixon, 1995; Fig 3). Volcanic stratigraphy lying between these extremes has not been dated, thus the interplay of arc volcanism and marine transgression through the Jurassic remains obscure. Therefore, the position of volcanic and sedimentary units within this part of the stratigraphic column shown in Figure 3 is somewhat conjectural.

The wide variety of rock types that characterize the LeMare Lake volcanics may be summarized as follows: black to grey-green or reddish grey, aphanitic to plagioclase-phyric, amygdaloidal flows of basaltic to andesitic composition; grey to pink and pale buff, dacitic to rhyolitic flows and flow-dome complexes with aphanitic to feldspar-phyric, flow-laminated textures, and localized, well-developed spherulitic devitrification; rhyodacitic to rhyolitic, welded to non-welded, lithic-crystal ash-flow tuff with angular to subrounded lapilli-sized volcanic and sedimentary clasts, strongly welded zones defined by collapsed eutaxitic pumice, and rare carbonized wood fragments; and basaltic to rhyolitic volcanic breccia of pyroclastic and autoclastic origin. Notable minor components are rhyolitic and basaltic airfall tuff; pyroclastic surge and explosion breccia of basaltic composition; and thin sequences of basaltic pillow lava, breccia and hyaloclastite.

The common non-marine to marine, generally well-bedded sedimentary rock types are: black to grey-green or reddish brown, variably calcareous siltstone, mudstone and shale, impure limestone (rarely oolitic), and epiclastic volcanic wacke and breccia. Heterolithic to monolithic conglomerate and debris-flow breccia, including lahars, are comparatively rare.

Victoria Lake Basalt

The Victoria Lake basalt is a distinctive plagioclase-megacrystic flow or multiple flow unit(s) found at or near the base of the LeMare Lake volcanics. It is named for Victoria Lake, where these flows are well exposed in roadcuts and along the shoreline. Although this lava is restricted in extent within any one area, it is a recurrent and widespread feature of the volcanic stratigraphy (Nixon *et al.*, 2006c–e).

The occurrence of ‘coarsely porphyritic’ flows in the LeMare Lake volcanics has been noted by previous workers. On the north shore of Quatsino Sound west of Hecate Cove (near Sherbourg Islands), Jeletzky (1976, section 8, unit 3) encountered these flows within a sequence of amygdaloidal lava and breccia that strongly resembles Karmutsen basalt, and assigned it to his ‘Basal Jurassic Volcanic Unit’ (Fig 2). At this locality, Victoria Lake megacrystic basalt is associated with aphanitic, amygdaloidal flows and flow breccia that rest on a densely welded,

lithic-crystal rhyolitic ash-flow tuff, in turn resting (contact not exposed) on pebble to cobble conglomerate (Jeletzky, 1976, section 8, near top of unit 4). These units lie near the base of the LeMare Lake volcanics, which is represented in Jeletzky’s type section by the contact between the ‘Basal Jurassic Volcanic Unit’ and his underlying ‘Hecate Cove Formation’, represented herein by a locally thick volcanic unit lying at the top of the Parson Bay Formation (Fig 3).

The Victoria Lake basalt is typically intercalated within the basal part of a much thicker sequence of aphanitic, variably amygdaloidal basaltic to andesitic lava, many of which are moderately to strongly magnetic, including the megacrystic member. The megacrystic flows may form a single unit or several distinct units within the local stratigraphic succession. The Karmutsen-like nature of this lavas is striking, even to the point of replication of its plagioclase-megacrystic textures.

The black to dark grey-green or reddish grey megacrystic lava is characterized by euhedral to subhedral, lath-shaped to blocky plagioclase crystals, commonly reaching 1 cm, and locally 2 cm, in length. Some megacrysts exhibit a pronounced flow orientation, which is useful as a structural indicator. The aphanitic to finely crystalline groundmass is dense to strongly amygdaloidal and the plagioclase population displays either hialal or seriate textures. Locally, at the base of the LeMare Lake succession, these flows are pillowed or fragmented and incorporated in laharic breccia. Rare intrusive equivalents may exhibit notably coarser groundmass textures involving subsophitic intergrowths of plagioclase and pyroxene.

The age of the Victoria Lake basalt is currently not well constrained. It is shown schematically in Figure 3 as Hettangian, but could range in age across the map area from Rhaetian to (Early?) Sinemurian. In the Cape Parkins section described by Muller *et al.* (1974), the Victoria Lake basalt appears to be correlative with plagioclase-megacrystic flows in unit 8, which is bracketed (assuming no fault disruption) by other units in the section containing ammonite fauna identified as Sinemurian.

Pemberton Hills Rhyolite

The Pemberton Hills rhyolite unit is situated north of Holberg Inlet and forms a southeasterly trending series of resistant knobs and ridges trending subparallel to the coastline from Mount McIntosh in the north through the Pemberton Hills. As noted above, this unit lies near the top of the LeMare Lake volcanics and is the youngest dated member of the Bonanza Group (mid-Bajocian). At its northern extremity, the unit is intruded by dioritic rocks of the Island Plutonic Suite, and to the south it disappears beneath the waters of Holberg Inlet about 15 km due west of the former Island Copper mine. The Pemberton Hills rhyolite is underlain by a succession of dark reddish grey to green-grey, aphanitic to pyroxene-plagioclase-phyric andesitic flows with minor interbeds of crystal-lithic and lapilli tuff, volcanic sandstone and epiclastic breccia. It is overlain by similar rock types, including hornblende-bearing andesite. Contacts between these map units are generally not exposed; however, at one locality, the lower contact of the rhyolite overlies an erosion surface.

Lithologically, the unit comprises mainly pale grey to buff or white-weathering, rhyolitic to rhyodacitic, crystal-lithic ash-flow tuff and viscous aphanitic lava that form the remnants of flow-dome complexes. Interbedded porphyritic andesite flows, heterolithic volcanic breccia and vitric

tuff are minor constituents. Textural features such as welding, flow laminations, flow folds and flow breccia are only rarely preserved due to regionally intense acid-sulphate leaching and silicification accompanying epithermal mineralization (described below).

MINERAL POTENTIAL

The mineral potential of stratigraphic metallotects on northern Vancouver Island does not appear to have attracted the same attention as the well-known base and precious-metal environments of the calcalkaline porphyry and skarn systems such as Island Copper (MINFILE 092L 158) and Merry Widow (MINFILE 092L 044), respectively, yet world-class metallogenic environments clearly exist in the Karmutsen flood basalt province and supra-subduction setting of the Bonanza volcanic arc. Recent advances in our understanding of the stratigraphy, as revealed by ongoing regional mapping and complementary biostratigraphic and geochronological studies, allow for a preliminary reconstruction of the Early Mesozoic evolution of this part of Wrangellia so as to bring into focus favourable stratigraphy in the search for new mineral deposits. The importance of stratigraphic controls on mineralization is perhaps best exemplified by intrusion-related deposits, where the prime environment for skarn mineralization occurs at the contact of Quatsino (and to a lesser extent intra-Karmutsen) limestone with granitoid of the Island Plutonic Suite (*e.g.*, Nixon *et al.*, 2006a, b).

Metallogenic Environments

The Early Mesozoic evolution of geological environments, as presently gleaned from the stratigraphic record, and a selection of important deposit types in relation to prospective stratigraphy are shown in Figure 4. A very generalized summary of the geological events that shaped northern Vancouver Island is offered below so as to properly place some prospective mineral deposit types described thereafter in their plate tectonic context.

TECTONOMAGMATIC SETTING

The voluminous Triassic flood basalt volcanism that built the Karmutsen oceanic plateau evolved from a wholly submarine phase to the construction of a low-profile lava shield near the end of the Carnian (Carlisle and Suzuki, 1974; Muller *et al.*, 1974; Jones *et al.*, 1977). As the plume-related hotspot thermally decayed, this plateau subsided and the ensuing marine transgression deposited, Quatsino limestone (Jones *et al.*, 1977; Richards *et al.*, 1991). As subsidence continued, fine siliciclastic detritus, marking the initial influx of Parson Bay sediments, began swamp carbonate deposition, beginning in the Carnian on the west and east coasts of Vancouver Island, and eventually covering the axial high (Alice Lake area) in the late Early Norian, as determined by macrofossils and conodont biostratigraphy (Muller *et al.*, 1974; Jeletzky, 1976; Nixon *et al.*, 2000, 2006a, b). The initial stages of deposition of Parson Bay siliciclastic rocks may well reflect distal detritus derived from an encroaching arc, a possibility first raised by Muller *et al.* (1974), but made in the context of an intra-oceanic arc-rift environment for the Karmutsen basalt, as opposed to the open oceanic hotspot setting currently envisaged (Richards *et al.*, 1991; Greene *et al.*, 2006). Evidence for proximal volcanic-arc sedimentation

in the Middle to Late Norian part of the Parson Bay Formation exists in the form of tuffaceous crystal-rich volcanic wacke and breccia, as well as rare debris-flow deposits with volcanic cobbles (Nixon *et al.*, 2000).

Incipient arc volcanism in Parson Bay time may have begun as early as the start of the Middle Norian in the Alice Lake area, judging by deposits of juvenile volcanoclastic breccia close to the Quatsino – Parson Bay contact. Early submarine phreatomagmatic and effusive basaltic volcanism in the Norian to Rhaetian, characterized by aphanitic and augite±plagioclase-phyric volcanic breccia and rare pillow lava, built small, isolated volcanic centres, some of which breached sea level on the emplacement of subaerial flows. Widespread subaerial volcanism commenced around the time of the Triassic-Jurassic boundary (Rhaetian to ?Early Sinemurian) and initiated the main phase of growth of the Bonanza arc. The nature of the volcanic products (LeMare Lake volcanics), which include significant volumes of basaltic to andesitic flows (Victoria Lake member and its associated aphanitic, amygdaloidal lava) and rhyolitic ignimbrite, are consistent with a more advanced stage of arc evolution on relatively mature crust. The Early to Middle Jurassic phase of arc development is poorly known but clearly involved marine transgressions punctuated by volcanic events. The Bonanza arc remained active until at least mid-Bajocian time, when rhyolitic tuff and flow-dome complexes were emplaced (Pemberton Hills rhyolite). The demise of Bonanza volcanic activity finally occurred sometime in the Middle to Late Jurassic and was followed by a significant period of tectonism and erosion prior to the deposition of continentally derived, marine to non-marine Jura-Cretaceous clastic rocks (Haggart, 1993).

Our current state of knowledge of the evolution of the Bonanza Group on northern Vancouver Island places the earliest arc volcanism in the Parson Bay Formation firmly within Late Norian, and probably Middle Norian time (Friedman and Nixon, 1995; Nixon *et al.*, 2000); and the cessation of volcanic activity in the Middle Jurassic (mid-Bajocian) at the earliest (Fig 3). The recognition of a nascent volcanic arc in the Late Triassic stratigraphy of the Bonanza Group significantly extends the record of arc magmatism previously documented for lower (Westcoast Crystalline Complex), middle (Island Plutonic Suite) and upper (Bonanza Group) crustal components of the arc (Debari *et al.*, 1999). The evolution of the Bonanza arc on northern Vancouver Island is the subject of current geochronological studies, but from the data at hand, arc volcanism on northern Vancouver Island, albeit episodic, spans on the order of 40 to 50 Ma, according to current time scales (Fig 3). The longevity of volcanic activity in the Bonanza Group compares favourably with the magmatic record of some of the best geochronologically calibrated island arcs in the circum-Pacific region, such as the Aleutians (~46 Ma, Jicha *et al.*, 2006). This time span is especially significant from a metallogenic perspective, when one considers that the Late Mesozoic to Cenozoic belts of ‘giant’ porphyry copper deposits and related epithermal systems in the Andes were emplaced during a protracted history of subduction and formed in distinct magmatic cycles lasting no more than ~15 m.y. per event (Camus, 2006).

EPITHERMAL PRECIOUS METALS

Epithermal precious and base-metal systems are an enticing exploration target, but may be difficult to discover

and economically evaluate; however, the prospect of finding even one 'Bonanza-type' orebody in this environment can make the search rewarding. One well-known example is El Indio, Chile, where ore reserves in narrow vein systems have been estimated at 140 t Au, 771 t Ag and 0.4 million tonnes Cu (Jannes *et al.*, 1990).

Epithermal mineralization on northern Vancouver Island is probably best known as a result of work conducted in the Mount McIntosh – Pemberton Hills area, a high-sulphidation or acid-sulphate base and precious-metal system (Panteleyev and Koyanagi, 1993, 1994; Koyanagi and Panteleyev, 1993; Nixon *et al.*, 1994a). Here, zones of advanced argillic and clay-silica alteration are associated with

weak Cu-Au-Ag mineralization and enveloped by propylitic alteration. The acid-sulphate alteration is hosted by crystal-lithic ash-flow tuff and flow-dome complexes of the Pemberton Hills rhyolite, and to a minor extent, adjacent andesite of the LeMare Lake volcanics and dioritic intrusions of the Island Plutonic Suite. These rocks have undergone pervasive silicification and localized acid leaching such that original textures may be completely obliterated. Finely crystalline pyrite is locally abundant in these zones. Panteleyev and Koyanagi (1994) describe irregular veins and stockworks of quartz, locally accompanied by alunite, zunyite, dickite, kaolinite, hematite and rutile. They also noted that pyrite occurs both in stockworks and as semi-

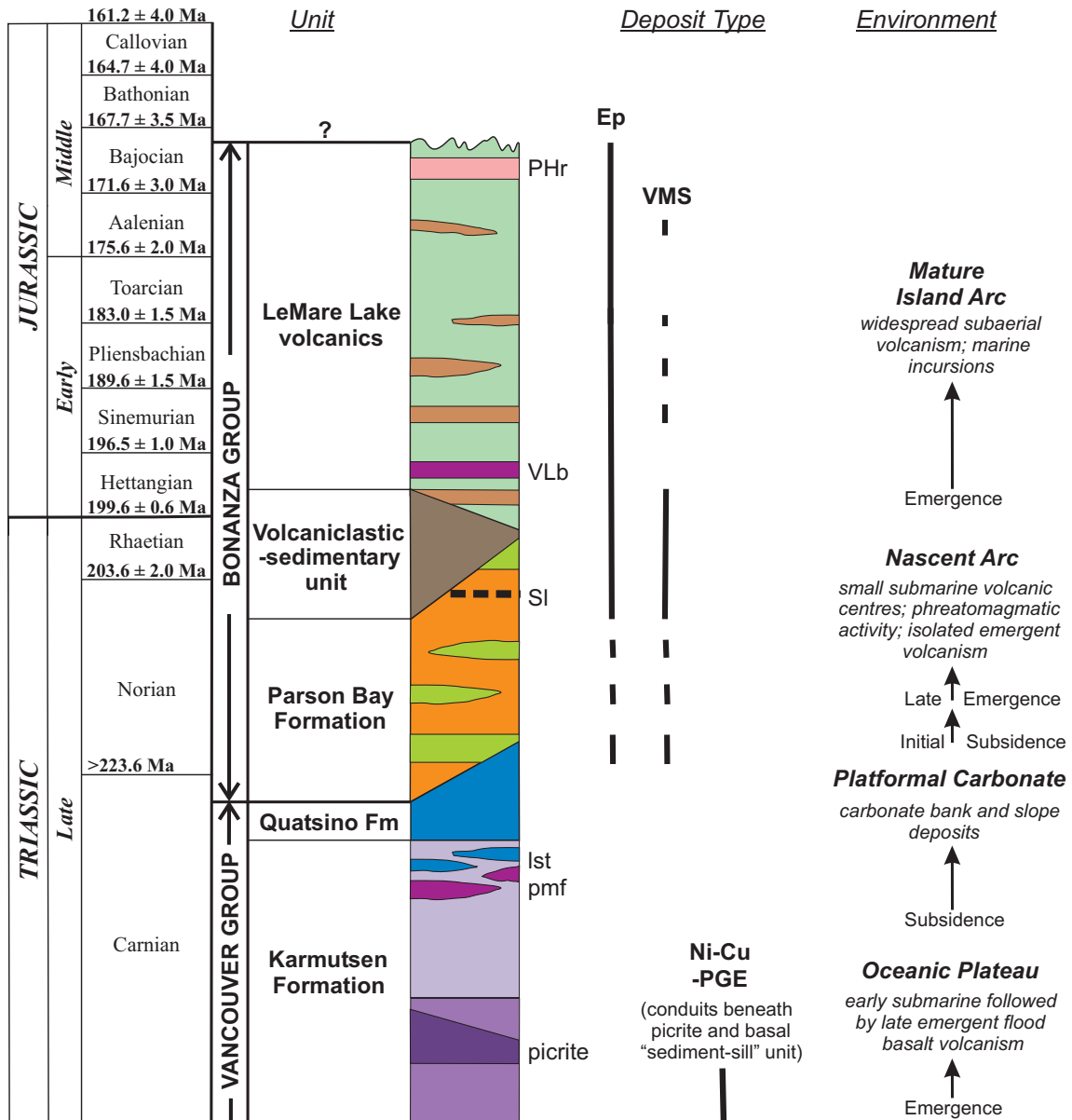


Figure 4. Tectonomagmatic evolution of northern Vancouver Island and environment of mineralization for selected mineral deposit types in relation to prospective stratigraphy as shown in Fig 3. Note that this diagram does not include the important porphyry copper and skarn mineralization. Abbreviations: PHr, Pemberton Hills rhyolite; VLb, Victoria Lake basalt; SI, Sutton limestone; Ist, intra-Karmutsen limestone; pmf, plagioclase-megacrystic flows; Ep, epithermal precious and base-metal deposits; VMS, volcanogenic massive sulphide deposits (Eskay and Kuroko-type); Ni-Cu-PGE, Noril'sk-Talnakh-type nickel-copper – platinum group element deposits.

massive to massive replacements in permeable clastic horizons within the rhyolite; and they discovered veins of pyrite-alunite containing rare native gold. Small amounts of copper minerals were identified as chalcocite, covellite and enargite. The occurrence of clasts of pyrite locally rimmed by marcasite was taken as evidence for repeated, synvolcanic mineralization in a near-surface, subaerial environment, and the source of magmatic-hydrothermal fluids was related to coeval intrusions of the Island Plutonic Suite at depth (Panteleyev and Koyanagi, 1994).

Taking the Mount McIntosh – Pemberton Hills epithermal system as a template for exploration, the most favourable metallotect is rhyolite within the LeMare Lake volcanics. Rhyolitic map units, comprising flows, flow-dome complexes and ash-flow tuff (welded and non-welded), have been distinguished where possible (Nixon *et al.*, 2006c–e). Our current knowledge of stratigraphic relationships would place many of these rhyolite units in the lower part of the LeMare Lake volcanics, below the Victoria Lake basalt. Since pervasive silicification attending acid-sulphate alteration promotes an inherent resistance to erosion and thereby positive relief, this tends to generate relatively large exploration targets for this class of deposit. Other favourable exploration factors include spatially related granitoid/porphyry intrusions and natural acidic drainages due to the high concentration of pyrite (Panteleyev and Koyanagi, 1994; Koyanagi and Panteleyev, 1993).

VOLCANOGENIC MASSIVE SULPHIDES

The Eskay Creek Au-Ag mine in northwestern BC is the world's highest-grade volcanogenic massive sulphide (VMS) deposit (MINFILE, 2006; 104B 008). It belongs to a relatively new class of shallow subaqueous hot spring VMS deposit, transitional toward subaerial epithermal Au-Ag deposits (Poulsen and Hannington, 1996; Barrett and Sherlock, 1996; Alldrick, 1995). The Eskay Creek deposit type is a polymetallic, precious-metal-rich sulphide and sulphosalt deposit with a total resource (past production + reserves + projected resources) of 2.34 million tonnes grading 51.3 g/t Au and 2326 g/t Ag (Roth, 2002).

The deposit is hosted by volcanic and sedimentary rocks of the Hazelton Group that belong to an Early to Middle Jurassic magmatic arc (McDonald *et al.*, 1996). The mineralization is hosted by rhyolitic to basaltic flows, volcanoclastic rocks and minor argillite; and ore horizons form laminated stratiform to massive layers and clastic, remobilized sulphide-sulphosalt beds associated with sulphide stockworks and breccia veins in the footwall (Roth, 2002). The geochemical signature of Eskay-type VMS deposits is transitional between typical volcanic-hosted base-metal massive sulphide minerals and precious-metal epithermal deposits (Massey *et al.*, 1999).

The most favourable stratigraphy for Eskay-type VMS in the Bonanza Group is where shallow marine sedimentary rocks are interbedded with, or pass laterally into, volcanic rocks, especially those packages containing rhyolitic rocks. Hence, the base of the LeMare Lake volcanic sequence, where marine deposits of the volcanoclastic-sedimentary unit pass upwards into subaerial basaltic to rhyolitic flows and volcanoclastic rocks, present a prime exploration target, as well as any transitions of similar nature within the LeMare Lake succession (Fig 4; see Nixon *et al.*, 2006c–e). It should be noted that these metallotects are also favourable for Kuroko-type VMS deposits, which appear to have

formed in deeper water (*e.g.*, the H-W deposit at the Myra Falls mine hosted by mid-Paleozoic volcanic arc rocks of the Sicker Group on Vancouver Island; MINFILE 092F 330; Massey, 1999). The shallow marine to emergent sequences of volcanic rocks within the Parson Bay Formation likewise present a prospective environment, but appear to have more limited potential due to the general lack of rhyolitic rock types. It is perhaps encouraging that a number of highly anomalous to anomalous RGS samples, screened for epithermal/Eskay-type VMS signatures, have been detected in the Bonanza Group along the northwest coastal regions of Vancouver Island (Massey *et al.*, 1999).

NI-CU-PGE

The recognition of picritic pillow basalt with MgO content ranging from 13 to 20 wt% in the Karmutsen Formation (Greene *et al.*, 2006) has important implications for the potential for Ni-Cu-PGE (platinum group element) mineralization on northern Vancouver Island.

World-class Ni-Cu-PGE deposits are well known in the Noril'sk-Talnakh region of Siberia where ultramafic intrusions associated with Permo-Triassic continental flood basalt hosts magmatic sulphide mineralization. The ore-bearing intrusions form transgressive sill-like bodies hosted by Devonian to Late Permian carbonate-clastic sequences, including evaporites and coal measures, directly underlying the flood basalt; and some of these bodies intrude the lower part of the overlying volcanic stratigraphy. As summarized by Naldrett (2004), the main ore horizons are hosted primarily by olivine-enriched, picritic (18–29 wt% MgO) and 'taxitic' (*i.e.*, variably textured; 9–16 wt% MgO) gabbrodolerite with interstitial and blebby disseminated sulphide minerals, mainly pyrrhotite, pentlandite, chalcopyrite and cubanite, and underlain by a layer of massive sulphide at the base of the intrusion. The massive sulphide minerals are somewhat enigmatic in that they commonly form apparently isolated bodies in the wallrocks and veins cutting both the lower intrusive contact and gabbrodolerite. Bulk ore compositions (*i.e.*, sulphide plus silicate gangue minerals) in disseminated ores average 2.3 to 3.3 g/t Pd, 0.5 to 1.1 g/t Pt, 0.4 to 0.7 wt% Ni and 0.9 to 1.2 wt% Cu; and in massive ores average 5.9 to 12.2 g/t Pd, 1.4 to 2.8% Pt, 4.6 to 5.2 wt% Ni and 2.9 to 4.8 wt% Cu.

In considering the origin of the Noril'sk-Talnakh deposits, Naldrett emphasized that a fortuitous combination of factors was necessary in order to produce such 'giant' ore deposits. Some critical aspects of his model are 1) an external source of sulphur (in this case, the combined assimilation of evaporites to supply oxidized sulphur and coal to act as a reductant); 2) a supply of hot picritic magma with the potential to thermally erode and assimilate country rocks; 3) arterial conduits that channelled sustained magma flow (recognized by anomalously well-developed peripheral zones of contact metamorphism); and 4) the presence of hydrodynamic traps in locally flared conduits that served to gravitationally concentrate the magmatic sulphide droplets.

The picritic pillow basalt of northern Vancouver Island demonstrates that this part of the Karmutsen flood basalt province received a supply of primitive magma from a mantle plume. Finding an external source of sulphur is more of a challenge, but the Middle Triassic shale and siltstone underlying the Karmutsen Formation may provide a suitable contaminant, especially if ascending magmas are close to saturation in sulphur. The later point is being ad-

dressed by J.S. Scoates and coworkers, whose preliminary investigations reveal that certain lava forming a chemical subtype of Karmutsen basalt with typical MgO content (8–10 wt%) and appreciable PGE abundances were erupted close to sulphide saturation (J.S. Scoates, pers comm, 2006). The intriguing observation of small concentrations of disseminated sulphide minerals (mainly pyrrhotite) near the lower contact of some Karmutsen sills intruding the basal ‘sediment-sill’ unit of Muller *et al.* (1974) is proof that certain magma batches did indeed reach sulphur saturation (Greene *et al.*, 2006). This demonstrates the potential for ore-forming processes near the base of the Karmutsen basalt, at least, but whether or not such processes have successfully produced significant Ni-Cu-PGE deposits in the Karmutsen of northern Vancouver island remains to be evaluated.

ACKNOWLEDGMENTS

We wish to thank Nick Massey for kindly enduring discussions on the geology of Vancouver Island, and James Scoates and Andrew Greene for providing preprints of on-going research results on the Karmutsen basalt. Critical comments by Nick Massey and editorial handling by Brian Grant are greatly appreciated.

REFERENCES

- Alldrick, D.J. (1995): Subaqueous hot spring Au-Ag (G07); in Selected British Columbia Mineral Deposit Profiles, Volume 1, *Metallics and Coal*, Lefebvre, D.V. and Ray, G.E., Editors, BC Ministry of Energy, Mines and Petroleum Resources, Open File 1995-20, pages 55–58.
- Archibald, D.A. and Nixon, G.T. (1995): $^{40}\text{Ar}/^{39}\text{Ar}$ geochronometry of igneous rocks in the Quatsino – Port McNeill map area, northern Vancouver Island (92L/12, 11); in Geological Fieldwork 1994, BC Ministry of Energy, Mines and Petroleum Resources, Paper 1995-1, pages 49–59.
- Armstrong, R.L., Muller, J.E., Harakal, J.E. and Muehlenbachs, K. (1985): The Neogene Alert Bay volcanic belt of northern Vancouver Island, Canada: descending-plate-edge volcanism in the arc-trench gap; *Journal of Volcanology and Geothermal Research*, Volume 26, pages 75–97.
- Barrett, T.J. and Sherlock, R.L. (1996): Geology, lithogeochemistry and volcanic setting of the Eskay Creek Au-Ag-Cu-Zn deposit, northwestern British Columbia; *Exploration and Mining Geology*, Volume 5, pages 339–368.
- Camus, F. (2006): The Andean porphyry copper systems; in Great Metallogenic Provinces of the World, *The University of British Columbia*, Mineral Deposit Research Unit Short course, Vancouver.
- Carlisle, D. (1972): Late Paleozoic to mid-Triassic sedimentary-volcanic sequence on northeastern Vancouver Island; in Report of Activities, November 1971 to March 1972, *Geological Survey of Canada*, Paper 72-1B, pages 24–30.
- Carlisle, D. and Suzuki, T. (1974): Emergent basalt and submergent carbonate-clastic sequences including the Upper Triassic Dillier and Welleri zones on Vancouver Island; *Canadian Journal of Earth Sciences*, Volume 11, pages 254–279.
- Crickmay, C.H. (1928): The stratigraphy of Parson Bay, British Columbia; *University of California*, Publications in Geological Sciences, Volume 18, pages 51–63.
- DeBari, S.M., Anderson, R.G. and Mortensen, J.K. (1999) Correlation amongst lower to upper crustal components in an island arc: the Jurassic Bonanza arc, Vancouver Island, Canada. *Canadian Journal of Earth Sciences*, Volume 36, pages 1371–1413.
- Dawson, G.M. (1887): Report on a geological examination of the northern part of Vancouver Island and adjacent coasts; *Geological Survey of Canada*, Annual Report 1886, Volume 2, Part B, pages 1–107.
- Dolmage, V. (1919): Quatsino Sound and certain mineral deposits of the west coast of Vancouver Island, BC; *Geological Survey of Canada*, Summary Report 1918, Part B, pages 30–38.
- Frebald, H. and Tipper, H.W. (1970): Status of the Jurassic of the Canadian Cordillera in British Columbia, Alberta and southern Yukon; *Canadian Journal of Earth Sciences*, Volume 7, pages 1–21.
- Friedman, R.M. and Nixon, G.T. (1995): U-Pb zircon dating of Jurassic porphyry Cu(-Au) and associated acid-sulphate systems, northern Vancouver Island, British Columbia; *Geological Association of Canada – Mineralogical Association of Canada Annual Meeting*, Victoria, BC, page A34.
- Furin, S., Preto, N., Rigo, M., Roghi, G., Gianolla, P., Crowley, J.L. and Bowring, S.A. (2006): High-precision U-Pb zircon age from the Triassic of Italy: implications for the Triassic time scale and the Carnian origin of calcareous nannoplankton and dinosaurs; *Geology*, Volume 34, pages 1009–1012.
- Gamba, C.A. (1993): Stratigraphy and sedimentology of the Upper Jurassic to Lower Cretaceous Longarm Formation, Queen Charlotte Islands, British Columbia; *Geological Survey of Canada*, Paper 93-1A, pages 139–148.
- Gardner, M.C., Bergman, S.C., Cushing, G.W., MacKevett, E.M. Jr., Plafker, G., Campbell, R.B., Dodds, C.J., McClelland, W.C. and Mueller, P.A. (1988): Pennsylvanian pluton stitching of Wrangellia and the Alexander Terrane, Wrangell Mountains, Alaska; *Geology*, Volume 16, pages 967–971.
- Gradstein, F.M., Ogg, J.G. and Smith, A.G. (2004): A geologic time scale 2004; *Cambridge University Press*, Cambridge, UK, 610 pages.
- Greene, A.R., Scoates, J.S., Nixon, G.T. and Weis, D. (2006): Picritic lavas and basal sills in the Karmutsen flood basalt province, northern Vancouver Island; in Geological Fieldwork 2005, BC Ministry of Energy, Mines and Petroleum Resources, Paper 2006-1, pages 39–51.
- Greenwood, H.J., Woodsworth, G.J., Read, P.B., Ghent, E.D. and Evenchick, C.A. (1991): Metamorphism, Chapter 16; in *Geology of the Cordilleran Orogen in Canada*, Gabrielse, H. and Yorath, C.J., editors, *Geological Survey of Canada*, Geology of Canada, Number 4, pages 533–570.
- Gunning, H.C. (1930): Geology and mineral deposits of Quatsino-Nimkish area, Vancouver Island; *Geological Survey of Canada*, Summary Report 1929, Part A, pages 94–143.
- Gunning, H.C. (1932): Preliminary report on the Nimkish Lake quadrangle, Vancouver Island, British Columbia; *Geological Survey of Canada*, Summary Report 1931, Part A, pages 22–35.
- Gunning, H.C. (1933): Zeballos River area, Vancouver Island, British Columbia; *Geological Survey of Canada*, Summary Report 1932, Part A, pages 29–50.
- Gunning, H.C. (1938a): Preliminary geological map, Nimkish, east half, British Columbia; *Geological Survey of Canada*, Paper 38-2.
- Gunning, H.C. (1938b): Preliminary geological map, Nimkish, west half, British Columbia; *Geological Survey of Canada*, Paper 38-3.
- Gunning, H.C. (1938c): Preliminary geological map, Nimkish, east half, British Columbia; *Geological Survey of Canada*, Paper 38-4.
- Gunning, H.C. (1938d): Preliminary geological map, Nimkish, west half, British Columbia; *Geological Survey of Canada*, Paper 38-5.

- Haggart, J.W. (1993): Latest Jurassic and Cretaceous paleogeography of the northern Insular Belt, British Columbia; in *Mesozoic Paleogeography of the Western United States*, Volume II, Book 71, Dunn, G. and McDougall, K., Editors, *Society of Economic Paleontologists and Mineralogists*, Pacific Section, pages 463–475.
- Haggart, J.W. and Carter, E.S. (1993): Cretaceous (Barremian-Aptian) radiolaria from Queen Charlotte Islands, British Columbia: newly recognized faunas and stratigraphic implications; *Geological Survey of Canada*, Paper 93-1E, pages 55–65.
- Hoadley, J.W. (1953): Geology and mineral deposits of Zeballos-Nimpkish area, Vancouver Island, British Columbia; *Geological Survey of Canada*, Memoir 272, 82 pages.
- Jannas, R.R., Beane, R.E., Ahler, B.A. and Brosnahan, D.R. (1990): Gold and copper mineralization in the El Indio deposit, Chile; in *Epithermal Gold Mineralization in the Circum-Pacific: Geology, Geochemistry, Origin and Exploration*, II; *Journal of Geochemical Exploration*, Volume 36, Number 1-3, pages 233–266.
- Jeletzky, J.A. (1950): Stratigraphy of the west coast of Vancouver Island between Kyuquot Sound and Esperanza Inlet, British Columbia; *Geological Survey of Canada*, Paper 50-37, 52 pages.
- Jeletzky, J.A. (1954): Tertiary rocks of the Hesquiat-Nootka area, west coast of Vancouver Island, British Columbia (with brief comments on adjacent Mesozoic formations); *Geological Survey of Canada*, Paper 53-17, 65 pages.
- Jeletzky, J.A. (1969): Mesozoic and Tertiary stratigraphy of northern Vancouver Island (92-E, 92-L, 102-I); *Geological Survey of Canada*, Paper 69-1, Part A, pages 126–134.
- Jeletzky, J.A. (1970a): Mesozoic stratigraphy of northern and eastern parts of Vancouver Island, British Columbia (92-E, F, L, 102-I); *Geological Survey of Canada*, Paper 70-1, Part A, pages 209–214.
- Jeletzky, J.A. (1970b): Some salient features of Early Mesozoic history of Insular Tectonic Belt, western British Columbia; *Geological Survey of Canada*, Paper 69-14, 26 pages.
- Jeletzky, J.A. (1973): Mesozoic and Tertiary rocks of Quatsino Sound, Vancouver Island; *Geological Survey of Canada*, Open File 148.
- Jeletzky, J.A. (1976): Mesozoic and ?Tertiary rocks of Quatsino Sound, Vancouver Island, British Columbia. *Geological Survey of Canada*, Bulletin 242, 243 pages.
- Jicha, B.R., Scholl, D.W., Singer, B.S., Yogodzinski, G.M. and Kay, S.M. (2006): Revised age of Aleutian island arc formation implies high rate of magma production; *Geology*, Volume 34, pages 661–664.
- Jones, D.L., Silberling, N.J. and Hillhouse, J. (1977): Wrangellia – a displaced terrane in northwestern North America. *Canadian Journal of Earth Sciences*, Volume 14, pages 2565–2577.
- Koyanagi, V.M. and Panteleyev, A. (1993): Natural acid-drainage in the Mount McIntosh – Pemberton Hills area, northern Vancouver Island (92L/12); in *Geological Fieldwork 1992*, *BC Ministry of Energy, Mines and Petroleum Resources*, Paper 1993-1, pages 445–450.
- Kuniyoshi, S. and Liou, J.G. (1976): Burial metamorphism of the Karmutsen volcanic rocks, northeastern Vancouver Island, British Columbia; *American Journal of Science*, Volume 276, pages 1096–1119.
- Lewis, T.J., Lowe, C. and Hamilton, T.S. (1997): Continental signature of a ridge-trench-triple junction: northern Vancouver Island; *Journal of Geophysical Research*, Volume 102, pages 7767–7781.
- Massey, N.W.D. (1999): Volcanogenic massive sulphide deposits in British Columbia; *BC Ministry of Energy, Mines and Petroleum Resources*, Open File 1999-2.
- Massey, N.W.D. (1995a): Geology and mineral resources of the Alberni-Nanaimo lakes sheet, Vancouver Island, 92F/1W, 92F/2E and part of 92F/7E; *BC Ministry of Energy, Mines and Petroleum Resources*, Paper 1992-2, 132 pages.
- Massey, N.W.D. (1995b): Geology and mineral resources of the Cowichan Lake sheet, Vancouver Island, 92C/16; *BC Ministry of Energy, Mines and Petroleum Resources*, Paper 1992-3, 112 pages.
- Massey, N.W.D. (1995c): Geology and mineral resources of the Duncan sheet, Vancouver Island, 92B/13; *BC Ministry of Energy, Mines and Petroleum Resources*, Paper 1992-4, 112 pages.
- Massey, N.W.D., Alldrick, D.J. and Lefebvre, D.V. (1999): Potential for subaqueous hot spring (Eskay Creek) deposits in British Columbia; *BC Ministry of Energy, Mines and Petroleum Resources*, Open File 1999-14.
- Massey, N.W.D., McIntyre, D.G., Desjardins, P.J. and Cooney, R.T. (2005): Digital geology map of British Columbia: whole province; *BC Ministry of Energy, Mines and Petroleum Resources*, Geofile 2005-1.
- McDonald, A.J., Lewis, P.D., Thompson, J.F.H., Nadaraju, G., Bartsch, R.D., Bridge, D.J., Rhys, D.A., Roth, T., Kaip, A., Godwin, C.I. and Sinclair, A.J. (1996): Metallogeny of an Early to Middle Jurassic arc, Iskut River area, northwestern British Columbia; *Economic Geology*, Volume 91, pages 1098–1114.
- MINFILE (2006): MINFILE BC mineral deposits database; *BC Ministry of Energy, Mines and Petroleum Resources*, URL <<http://www.em.gov.bc.ca/Mining/GeolSurv/Minfile/>> [December 2006].
- Monger, J.W.H. and Journeay, J.M. (1994): Basement geology and tectonic evolution of the Vancouver region; in *Geology and Geological Hazards of the Vancouver Region*, Southwestern British Columbia, Monger, J.W.H., Editor, *Geological Survey of Canada*, Bulletin 481, pages 3–25.
- Monger, J.W.H., Price, R.A. and Tempelman-Kluit, D.J. (1982): Tectonic accretion and the origin of the two major metamorphic and plutonic belts in the Canadian Cordillera. *Geology*, Volume 10, pages 70–75.
- Muller, J.E. and Carson, D.J.T. (1969): Geology and mineral deposits of Alberni map-area, British Columbia (92F); *Geological Survey of Canada*, Paper 68-50, 52 pages.
- Muller, J.E. and Rahmani, R.A. (1970): Upper Triassic sediments of northern Vancouver Island; *Geological Survey of Canada*, Paper 70-1B, pages 11–18.
- Muller, J.E. and Roddick, J.A. (1983): Alert Bay – Cape Scott; *Geological Survey of Canada*, Map 1552A, scale 1:250 000.
- Muller, J.E., Cameron, B.E.B. and Northcote, K.E. (1981): Geology and mineral deposits of Nootka Sound map-area, Vancouver Island, British Columbia. *Geological Survey of Canada*, Paper 80-16, 53 pages.
- Muller, J.E., Northcote, K.E. and Carlisle, D. (1974): Geology and mineral deposits of Alert Bay – Cape Scott map-area, Vancouver Island, British Columbia. *Geological Survey of Canada*, Paper 74-8, 77 pages.
- Naldrett, A.J. (2004): Magmatic Sulphide Deposits: Geology, Geochemistry and Exploration; *Springer-Verlag*, Berlin, 727 pages.
- Nixon, G.T., Hammack, J.L., Hamilton, J.V. and Jennings, H. (1993a): Preliminary geology of the Mahatta Creek area, northern Vancouver Island (92L/5); in *Geological Fieldwork 1992*, *BC Ministry of Energy, Mines and Petroleum Resources*, Paper 1993-1, pages 17–35.
- Nixon, G.T., Hammack, J.L., Hamilton, J.V. and Jennings, H. (1993b): Preliminary geology of the Mahatta Creek area (92L/5); *BC Ministry of Energy, Mines and Petroleum Resources*, Open File 1993-10, scale 1:50 000.

- Nixon, G.T., Hammack, J.L., Koyanagi, V.M., Payie, G.J., Panteleyev, A., Massey, N.W.D., Hamilton, J.V. and Haggart, J.W. (1994a): Preliminary geology of the Quatsino – Port McNeill map areas, northern Vancouver Island (92L/12, 11); in *Geological Fieldwork 1993, BC Ministry of Energy, Mines and Petroleum Resources*, Paper 1994-1, pages 63–85.
- Nixon, G.T., Hammack, J.L., Koyanagi, V.M., Payie, G.J., Panteleyev, A., Massey, N.W.D., Hamilton, J.V. and Haggart, J.W. (1994b): Preliminary geology of the Quatsino – Port McNeill map areas (92L/5); *BC Ministry of Energy, Mines and Petroleum Resources*, Open File 1994-26, 1:50 000.
- Nixon, G.T., Hammack, J.L., Payie, G.J. and Snyder L.D. (1995a): Quatsino – San Josef map area, northern Vancouver Island: geological overview (92L/12W, 102I/8, 9); in *Geological Fieldwork 1994, BC Ministry of Energy, Mines and Petroleum Resources*, Paper 1995-1, pages 9–21.
- Nixon, G.T., Hammack, J.L., Payie, G.J. and Snyder L.D. (1995b): Quatsino – San Josef map area (92L/12W, 102I/8, 9); *BC Ministry of Energy, Mines and Petroleum Resources*, Open File 1995-9, scale 1:50 000.
- Nixon, G.T., Friedman, R.M., Archibald, D.A., Orchard, M.J. and Tozer, T. (2000): A contribution to the geologic time scale: the Triassic-Jurassic boundary, northern Vancouver Island, Canada; *Geological Society of America*, Cordilleran Section, Annual Meeting, Vancouver, BC, Abstract Number 80179.
- Nixon, G.T., Kelman, M.C., Stevenson, D., Stokes, L.A. and Johnston, K.A. (2006a): Preliminary geology of the Nimpkish map area (NTS 92L/07), northern Vancouver Island; in *Geological Fieldwork 2005, BC Ministry of Energy, Mines and Petroleum Resources*, Paper 2006-1, pages 135–152.
- Nixon, G.T., Kelman, M.C., Stevenson, D., Stokes, L.A. and Johnston, K.A. (2006b): Preliminary geology of the Nimpkish map area, northern Vancouver Island (92L/07); *BC Ministry of Energy, Mines and Petroleum Resources*, Open File 2006-5, scale 1:50 000.
- Nixon, G.T., Snyder, L.D., Payie, G.J., Long, S., Finnie, A., Friedman, R.M., Archibald D.A., Orchard, M.J., Tozer, T., Poulton, T.P. and Haggart, J.W. (2006c): Geology of the Alice Lake area, northern Vancouver Island; *BC Ministry of Energy, Mines and Petroleum Resources*, Geoscience Map 2006-1, scale 1:50 000.
- Nixon, G.T., Hammack, J.L., Koyanagi, V.M., Payie, G.J., Haggart, J.W., Orchard, M.J., Tozer, T., Friedman, R.M., Archibald D.A., Palfy, J. and Cordey, F. (2006d): Geology of the Quatsino – Port McNeill area, northern Vancouver Island; *BC Ministry of Energy, Mines and Petroleum Resources*, Geoscience Map 2006-2, scale 1:50 000.
- Nixon, G.T., Hammack, J.L., Koyanagi, V.M., Payie, G.J., Snyder, L.D., Panteleyev, A., Massey, N.W.D., Archibald D.A., Haggart, J.W., Orchard, M.J., Friedman, R.M., Tozer, T., Tipper, H.W., Poulton, T.P., Palfy, J., Cordey, F and Barron, D.J. (2006e): Geology of the Holberg – Winter Harbour area, northern Vancouver Island; *BC Ministry of Energy, Mines and Petroleum Resources*, Geoscience Map 2006-3, scale 1:50 000.
- Northcote, K.E. and Muller, J.E. (1972): Volcanism, plutonism, and mineralization: Vancouver Island; *Canadian Institute of Mining, Metallurgy and Petroleum*, Bulletin 65, pages 49–57.
- Panteleyev, A. and Koyanagi, V.M. (1993): Advanced argillic alteration in Bonanza volcanic rocks, northern Vancouver Island – lithologic and permeability controls; in *Geological Fieldwork 1993, BC Ministry of Energy, Mines and Petroleum Resources*, Paper 1994-1, pages 101–110.
- Panteleyev, A. and Koyanagi, V.M. (1994): Advanced argillic alteration in Bonanza volcanic rocks, northern Vancouver Island – transitions between porphyry copper and epithermal environments; in *Geological Fieldwork 1992, BC Ministry of Energy, Mines and Petroleum Resources*, Paper 1993-1, pages 287–293.
- Poulsen, K.H. and Hannington M.D. (1996): Volcanic-associated massive sulphide gold; in *Geology of Canada Number 8*, Eckstrand, O.R., Sinclair, W.D. and Thorpe, R.I., Editors, *Geological Survey of Canada*, pages 183–196.
- Richards, M.A., Jones, D.L., Duncan, R.A. and DePaolo, D.J. (1991): A mantle plume initiation model for the Wrangellia flood basalt and other oceanic plateaus; *Science*, Volume 254, pages 263–267.
- Riddihough, R.P. and Hyndman, R.D. (1991): Modern plate tectonic regime of the continental margin of western Canada; in *Geology of the Cordilleran Orogen in Canada*, Gabrielse, H. and Yorath, C.J., Editors, *Geological Survey of Canada*, *Geology of Canada Number 4*, pages 435–455.
- Roth, T. (2002): Physical and chemical constraints on mineralization in the Eskay Creek deposit, northwestern British Columbia: evidence from petrography, mineral chemistry and sulphur isotopes; unpublished PhD thesis, *The University of British Columbia*, 401 pages.
- Stanley, G.D. Jr. (1988): An Upper Triassic reefal limestone, southern Vancouver Island, B.C.; in *Reefs: Canada and Adjacent Areas*, Geldsetzer, H.H.J., James, N.P. and Tebbutt, G.E., Editors, *Canadian Society of Petroleum Geologists*, *Memoir 13*, pages 766–776.
- Surdam, R.C. (1973): Low-grade metamorphism of tuffaceous rocks in the Karmutsen Group, Vancouver Island, British Columbia; *Geological Society of America Bulletin*, Volume 84, pages 1911–1922.
- Tipper, H.W. (1977): Jurassic studies in Queen Charlotte Islands, Harbledown Island, and Taseko Lakes area, British Columbia; *Geological Survey of Canada*, Report of Activities, Part A, Paper 77-1A, pages 251–254.
- Tozer, E.T. (1967): A standard for Triassic time; *Geological Survey of Canada*, Bulletin 156.
- van der Heyden, P. (1991): A Middle Jurassic to Early Tertiary Andean – Sierran arc model for the Coast Belt of British Columbia, *Tectonics*, Volume 11, pages 82–97.
- Wheeler, J.O. and McFeely, P. (1991): Tectonic Assemblage Map of the Canadian Cordillera and adjacent parts of the United States of America, *Geological Survey of Canada*, Map 1712A.

Geology and Mineral Occurrences of the Hendrix Lake Area (NTS 093A/02), South-Central British Columbia

by P. Schiarizza and J. Macauley¹

KEYWORDS: Quesnel Terrane, Slide Mountain Terrane, Kootenay Terrane, Nicola Group, Snowshoe Group, Takomkane batholith, Crooked amphibolite, molybdenum, tungsten, copper, gold

INTRODUCTION

The Takomkane project is a multiyear bedrock mapping program initiated by the British Columbia Geological Survey during the 2005 field season. This program is focused on Mesozoic arc volcanic and plutonic rocks of the Quesnel Terrane in the vicinity of the Takomkane batholith, which straddles the Bonaparte Lake (NTS 092P) and Quesnel Lake (NTS 093A) map sheets (Fig 1). Previous bedrock maps of the area are based on reconnaissance-scale mapping carried out by the Geological Survey of Canada in the 1960s. The purpose of the Takomkane project is to provide more detailed maps and an improved geological framework for interpreting mineral occurrences and geochemical anomalies, and for predicting favourable settings for future discoveries.

The first year of mapping for the Takomkane project covered about 1000 km² centred near Canim Lake, and tied in with 1:50 000 scale mapping carried out to the south during the 2000–2001 Bonaparte project (Fig 1). The results of the 2005 field program are summarized by Schiarizza and Boulton (2006a, b). Here, we present preliminary results from the second year of mapping for the Takomkane project, which was carried out by the authors from mid-June to early September 2006. The area mapped covers about 650 km² centred near Hendrix Lake, site of the former mining town that serviced the past-producing Boss Mountain molybdenum mine. It is situated within the Quesnel Highland physiographic province. Topography is generally subdued, although alpine ridges occur around Takomkane Mountain in the western part of the map area, and mountainous terrain along the eastern edge of the area is transitional into the high Cariboo Mountains to the east. The map area is transected by a north-south, all-season gravel road that connects with 100 Mile House to the southwest, and with Horsefly and Williams Lake to the northwest and west. Networks of secondary logging and Forest Service roads that branch from this main road provide access to most parts of the map area.

The Hendrix Lake map area is within the southern part of the Quesnel Lake sheet (NTS 093A), which is covered by a 1:125 000 scale map produced by R.B. Campbell (1978). The northeastern part of the map area borders the thesis study areas of K.V. Campbell (1971), Fillipone (1985), Carye (1986) and Bloodgood (1987, 1990), and the northern boundary of the area abuts the southern end of the Quesnel River – Horsefly map area described by Panteleyev *et al.* (1996). Detailed studies of the Boss Mountain molybdenum mine are presented by Soregaroli (1968), Soregaroli and Nelson (1976) and Macdonald *et al.* (1995). Descriptions of other mineral occurrences within the map area are found in assessment reports available through the BC Geological Survey's Assessment Report Indexing System (ARIS).

REGIONAL GEOLOGICAL SETTING

The regional setting of the Takomkane project area is summarized by Schiarizza and Boulton (2006a), and is only briefly reviewed here. The Quesnel Terrane, which underlies most of the project area, is characterized by Late Triassic to Early Jurassic volcanic, volcanoclastic and plutonic rocks that represent a magmatic arc that formed along or near the western North American continental margin (Mortimer, 1987; Struik, 1988a, b; Unterschutz *et al.*, 2002). These rocks form an important metallogenic province, particularly for porphyry deposits containing copper, gold and molybdenum. To the east, the Quesnel Terrane is faulted against Proterozoic and Paleozoic siliciclastic, carbonate and volcanic rocks of the Kootenay Terrane, and locally an intervening assemblage of mid to Late Paleozoic oceanic basalt and chert assigned to the Slide Mountain Terrane (Fig 1). The Kootenay Terrane probably represents an outboard facies of the ancestral North American miogeocline (Schiarizza and Preto, 1987; Colpron and Price, 1995), whereas the Slide Mountain Terrane is interpreted as the imbricated remnants of a Late Paleozoic marginal basin (Schiarizza, 1989; Roback *et al.*, 1994). Late Paleozoic through mid-Mesozoic oceanic rocks of the Cache Creek Terrane occur to the west of the Quesnel Terrane, and are interpreted as part of the accretion-subduction complex that was responsible for generating the Quesnel magmatic arc (Travers, 1978; Struik, 1988a). Younger rocks commonly found in the region include Cretaceous granitic stocks and batholiths, Eocene volcanic and sedimentary rocks, and flat-lying basalts of both Neogene and Quaternary age (Fig 1).

The structural geology of the Quesnel Terrane includes generally poorly understood faults that exerted controls on Late Triassic volcanic-sedimentary facies distributions and the localization of plutons and associated mineralization and alteration systems (Preto, 1977, 1979; Nelson and

¹University of Victoria, Victoria, BC

This publication is also available, free of charge, as colour digital files in Adobe Acrobat® PDF format from the BC Ministry of Energy, Mines and Petroleum Resources website at http://www.em.gov.bc.ca/Mining/GeolSurv/Publications/catalog/cat_fldwk.htm

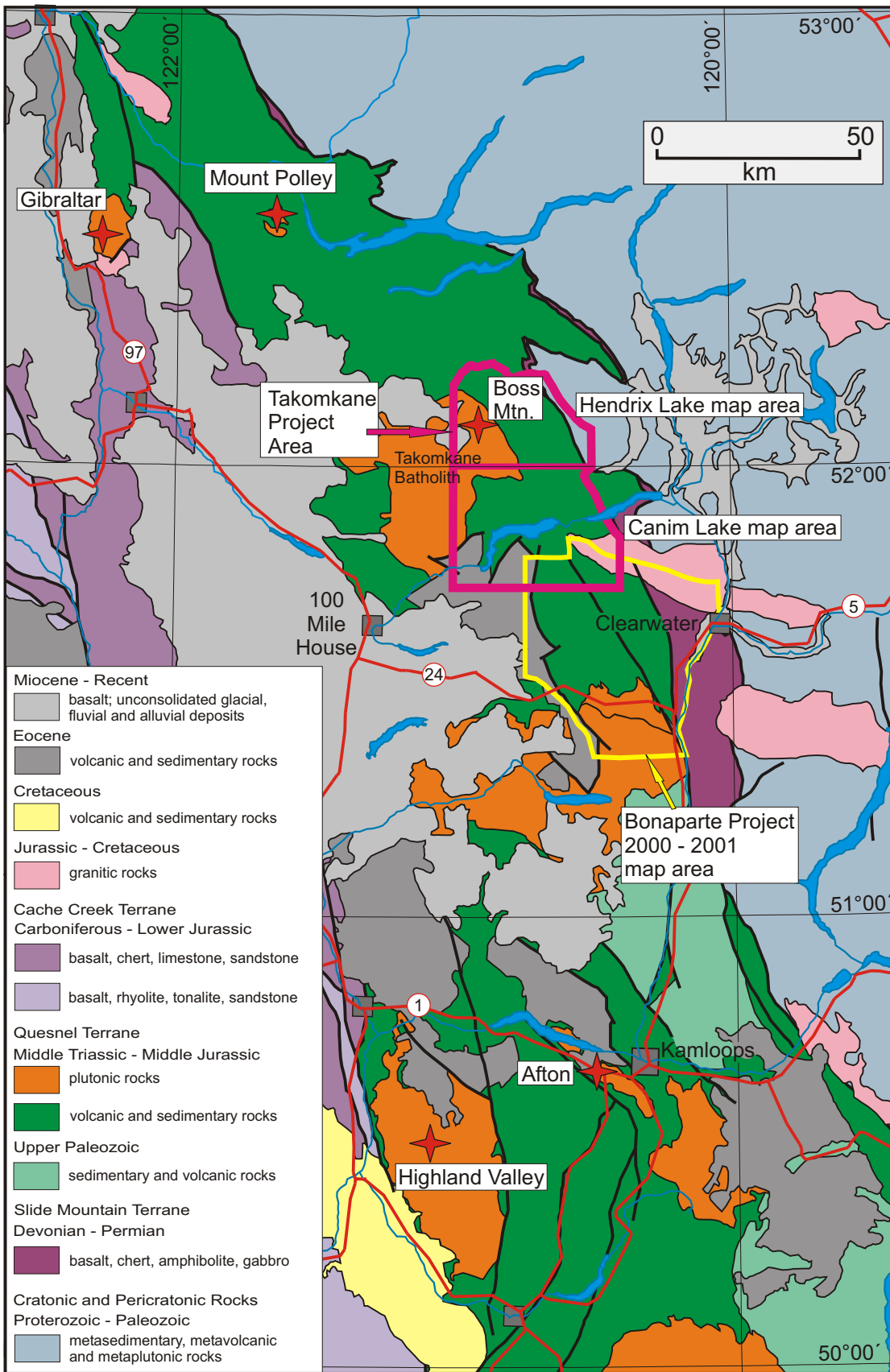


Figure 1. Regional geological setting of the Takomkane project area, showing the areas mapped in 2005 and 2006, the area mapped during the 2000–2001 Bonaparte project, and the locations of selected major mineral deposits.

Bellefontaine, 1996; Logan and Mihalynuk, 2005; Schiarizza and Tan, 2005). East-directed thrust faults and associated folds, of Permo-Triassic and/or Early Jurassic age, are documented within the eastern part of the Quesnel Terrane and the structurally underlying rocks of the Slide Mountain and Kootenay terranes (Struik, 1986, 1988b; Rees, 1987; Schiarizza, 1989; Ferri, 1997). Younger structures include west to southwest-verging folds, in part of early Middle Jurassic age, that deform the east-directed thrust faults (Ross *et al.*, 1985; Brown *et al.*, 1986; Rees, 1987; Schiarizza and Preto, 1987), and prominent systems of Eocene dextral strike-slip and extensional faults (Ewing, 1980; Panteleyev *et al.*, 1996; Schiarizza and Israel, 2001).

LITHOLOGICAL UNITS

The distribution of the main lithological units within the Hendrix Lake area is shown on Figure 2. The oldest rocks belong to the Proterozoic-Paleozoic Snowshoe Group of the Kootenay Terrane, which underlies the eastern part of the map area. These rocks are bounded to the west by a narrow belt of mafic schist assigned to the Crooked amphibolite of the Slide Mountain Terrane. East of the Crooked amphibolite, and underlying most of the map area, are Mesozoic rocks of the Quesnel Terrane. These include Middle to Late Triassic sedimentary and volcanoclastic rocks of the Nicola Group, as well as Late Triassic to Early Jurassic plutonic rocks of the Takomkane batholith. Ultramafic and mafic intrusive rocks exposed west and south of Hendrix Lake are also part of the Quesnel magmatic arc, whereas the Deception, Hendrix and Boss Mountain Mine stocks represent younger, mainly Cretaceous granitic suites that crosscut the terrane boundaries. The youngest rocks exposed in the area are small outliers of Quaternary basalt that are exposed on Takomkane Mountain and along Boss and Deception creeks.

Snowshoe Group

The Snowshoe Formation, named for the Snowshoe Plateau south of Barkerville, was defined by Holland (1954) as the uppermost formation of the Cariboo Group. Campbell *et al.* (1973) removed the formation from the Cariboo Group and suggested that it might be equivalent to the Proterozoic Kaza Group, which underlies the Cariboo Group in the Cariboo Mountains. The Snowshoe Formation was traced into the eastern part of the current study area by Campbell (1978), who mapped the formation in a wide, southeast-trending belt extending from the Snowshoe Plateau to Spanish and Deception creeks. The Snowshoe Formation was elevated to group status by Struik (1986, 1988c), who subdivided it into 14 informal units in the Cariboo Lake – Barkerville area and suggested that it ranged from Proterozoic to mid-Paleozoic in age. He assigned the Snowshoe Group to the Barkerville Terrane, which was interpreted as an outboard facies of the North American miogeocline (Struik, 1987, 1988a). Struik (1986) correlated the Snowshoe Group with Proterozoic to Paleozoic successions in the Kootenay Lake and Adams Lake areas, which are included in the Kootenay Terrane. Ferri and Schiarizza (2006) suggested revisions to Struik's (1988c) Snowshoe Group stratigraphy and regional correlations, but concurred with the general interpretation that it is a northern extension of Kootenay Terrane and an outboard facies of the North American miogeocline.

The Snowshoe Group was not studied in detail during the 2006 field season, but was examined in the Bassett Creek area at the northern end of the map area, and in the Deception Creek area to the south. Detailed descriptions of the group in part of the intervening area are provided by Fillipone (1985).

The Snowshoe Group, where examined during the present study, consists mainly of quartzite and pelitic schist, accompanied by minor amounts of marble and calcsilicate gneiss. The dominant rock type is light grey, brownish grey–weathering micaceous quartzite consisting of fine to medium-grained recrystallized quartz accompanied by scattered grains of feldspar and evenly distributed flakes of metamorphic biotite and muscovite. The quartzite commonly occurs as layers, from a few centimetres to several tens of centimetres thick, that are separated by thin partings or centimetre-thick layers of pelitic schist (Fig 3). The layering is parallel to the predominant metamorphic foliation and is accentuated by parallel lenses of vein quartz. The layers of pelitic schist consist of medium to coarse-grained, well-foliated quartz, muscovite, biotite and feldspar, with garnet porphyroblasts. Similar schist locally dominates intervals up to several tens of metres in thickness, where it is interlayered with subordinate amounts of micaceous quartzite (Fig 4). In the Bassett Creek area, pelitic schist becomes the dominant rock type at the eastern limit of our mapping. Fillipone (1985) showed a similar west to east transition from a quartzite-dominated to a schist-dominated succession. He also noted that staurolite appears as a component of the metamorphic assemblage just a few hundred metres east of the contact with the Crooked amphibolite.

Marble is a relatively minor component of the Snowshoe Group, but occurs locally as brown, tan or grey-weathered units, from less than a metre up to several tens of metres thick, intercalated with quartzite and pelitic schist. Layering in the marble is defined by colour variations in shades of light to medium grey, and is accentuated by parallel, centimetre-scale layers of dark grey quartz-biotite schist, and millimetre-scale lenses and stringers of rusty-weathered material containing quartz and muscovite. Well-layered, pale green to grey calcsilicate gneiss is another minor component of the Snowshoe Group, and commonly shows a spatial association with marble units. The mineralogy of the calcsilicate rocks includes quartz, garnet and fine-grained green minerals that may include amphibole, epidote and pyroxene.

The age of the Snowshoe Group within the Hendrix Lake area is unknown, but it is inferred to be Early Carboniferous or older because the succession is cut by foliated granitic rocks a short distance east of the area (Boss Mountain gneiss; Fillipone, 1985), and U-Pb analysis of zircons from these granitic rocks suggests a minimum emplacement age of 338.5 Ma (Mortensen *et al.*, 1987). The rocks exposed in the Hendrix Lake area are lithologically similar to successions assigned to units EBQ and EBH of the Eagle Bay assemblage, which crop out directly east of the Slide Mountain Terrane on the south margin of the Raft batholith (Schiarizza and Preto, 1987). These rocks were assigned an early Cambrian or older age based, in part, on the stratigraphic position of unit EBH beneath a succession that included Lower Cambrian *archaeocyathid*-bearing limestone. More recently, Thompson *et al.* (2006) suggested that all or parts of units EBQ and EBH might be Devonian in age, based on correlation with the lithologically similar

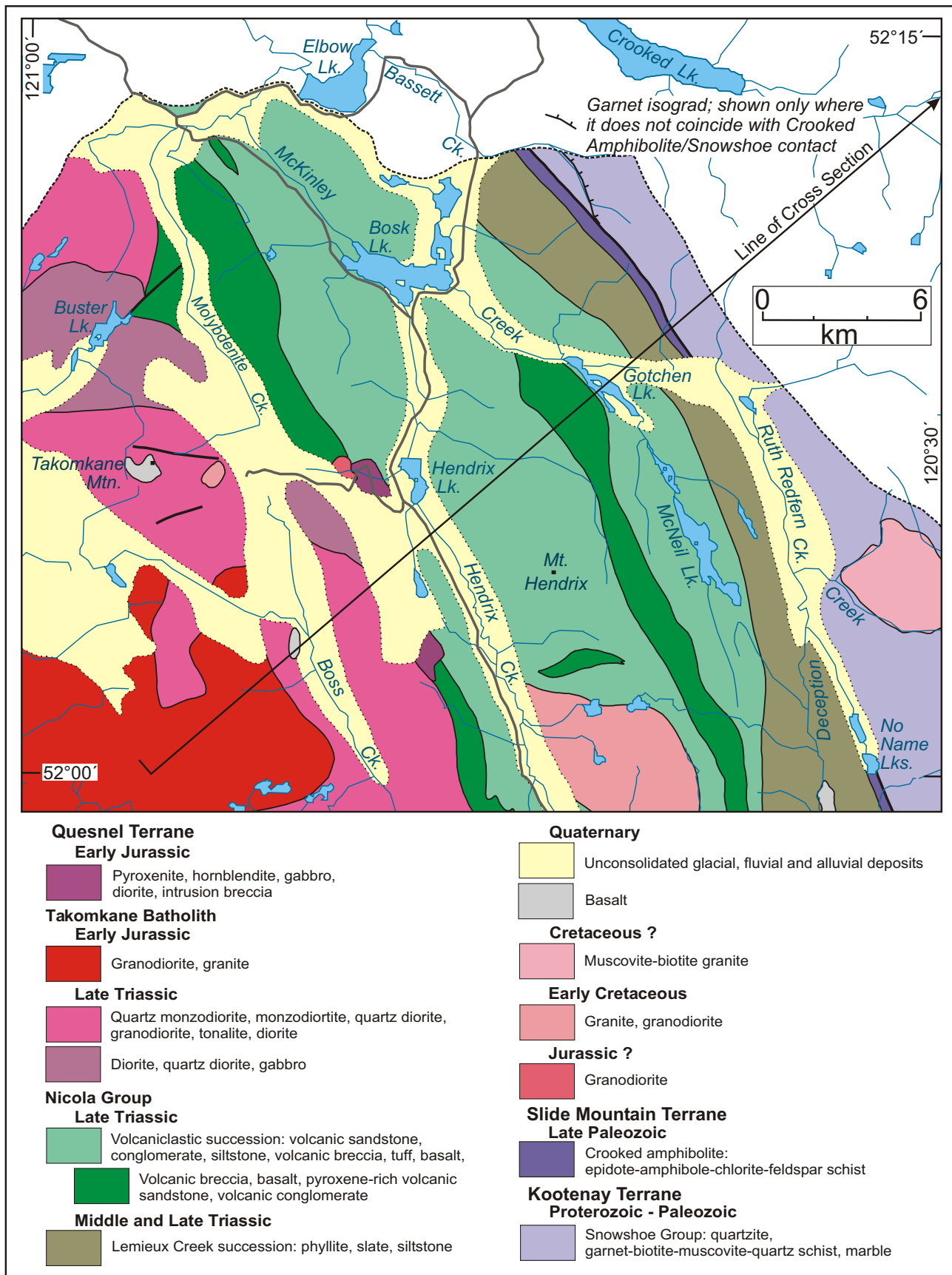


Figure 2. Generalized geology of the Hendrix Lake map area, based mainly on 2006 fieldwork.



Figure 3. Quartzite of the Snowshoe Group, Bassett Creek area.

Silver Creek Formation, which crops out farther to the southeast.

Crooked Amphibolite

The Crooked amphibolite comprises a narrow, discontinuous belt of foliated mafic and ultramafic rocks that defines the contact between the Kootenay and Quesnel terranes over a distance of more than 200 km, from the Hendrix Lake area northward to the vicinity of Prince George (Campbell, 1978; Struik, 1985, 1988c). These rocks were assigned to the Antler Formation of the Slide Mountain Group by K.V. Campbell (1971), R.B. Campbell (1978) and Struik (1982). The name 'Crooked amphibolite' was subsequently introduced by Struik, who considered the unit to be either the basal part of the Quesnel Terrane (Struik, 1985) or a part of the Slide Mountain Terrane (Struik, 1988c). The basal contact of the Crooked amphibolite is interpreted to be an east-directed thrust fault (Ross *et al.*, 1985; Brown *et al.*, 1986; Rees, 1987; Struik, 1988c). The upper contact, with Triassic sedimentary rocks of the Quesnel Terrane, has been interpreted as a sheared unconformity (Campbell, 1971; Rees, 1987; Struik, 1988c).

The Crooked amphibolite is locally well exposed in the northeastern part of the Hendrix Lake map area, and is represented by sparse subcrop in the southeastern corner of the area, south of No Name Lakes. It is not apparently exposed in much of the intervening area, due to an extensive blanket of till and alluvium adjacent to Ruth Redfern Creek. Where exposed, it forms a distinctive, dark green map unit that is easily distinguished from the grey rocks of the Snowshoe Group to the east, and the black rocks of the Lemieux Creek succession to the west. Where upper and lower contacts are well constrained, in the northeast corner of the map area, the Crooked amphibolite forms a layer about 500 m thick that is more or less concordant with the strong metamorphic foliation and transposed layering in bounding rocks of the Snowshoe Group and Lemieux Creek succession.

The Crooked amphibolite within the Hendrix Lake map area consists of medium to dark green, green-brown-weathered, epidote-actinolite-chlorite-feldspar schist. The moderate to strong metamorphic foliation is typically parallel to compositional layering (metamorphic segregation?) defined by dark, chlorite-rich lenses alternating with lighter coloured, relatively plagioclase-rich lenses. This



Figure 4. Garnetiferous schist of the Snowshoe Group, Bassett Creek area.

layering is developed on a scale of 2 to 10 mm, and is accentuated by parallel veins and stringers consisting of epidote, quartz and rusty carbonate. Biotite was observed rarely within the schist, and black hornblende occurs locally as randomly oriented needles within, but locally crosscutting, foliation surfaces. Most of the schist is fine to medium grained, but local sections are distinctly coarser grained, due to a large proportion of 2 to 6 mm grains and aggregates of epidote-altered plagioclase.

The composition of the Crooked amphibolite indicates a mafic igneous protolith. Hints of relict texture in the coarser grained sections suggest derivation from gabbroic rocks. The more common, finer grained schist might be a more highly sheared equivalent of the same rock type, or might be derived from a finer grained diabase or basalt protolith. Elsewhere, the Crooked amphibolite includes greenstone and mafic schist thought to be derived from basalt (including some with possible pillow forms), gabbroic rocks and serpentinized ultramafic rocks (Campbell, 1971; Rees, 1987; Struik, 1988c).

The main representatives of the Slide Mountain Terrane in the region are the Antler and Fennell formations, which comprise internally imbricated assemblages of mainly basalt, gabbro and chert that are in thrust contact with underlying rocks of the Kootenay Terrane. The Crooked amphibolite is included in the Slide Mountain Terrane because it shows a similar allochthonous relationship to the Kootenay Terrane and consists mainly of mafic rocks that have geochemical signatures similar to the ocean-floor tholeiite of the Fennell and Antler formations (Campbell, 1971; Rees, 1987). It is not in physical continuity with the Antler Formation, but seems to trace southward into the Fennell Formation (Fig 1). The Crooked amphibolite is not dated, but is inferred to be Late Paleozoic based on its correlation with the Late Devonian to Permian Antler and Fennell formations (Struik and Orchard, 1985; Schiarizza and Preto, 1987).

Nicola Group

The Nicola Group, originally named for exposures on the south side of Nicola Lake (Dawson, 1879), comprises a diverse assemblage of Middle and Late Triassic volcanic, volcanoclastic and sedimentary rocks that crop out over a

broad area in south-central British Columbia. The name is applied to Triassic rocks in the Takomkane project area following Campbell and Tipper (1971) and Panteleyev *et al.* (1996), although the Triassic rocks in the Quesnel Lake map sheet have also been referred to as Quesnel River Group (Campbell, 1978) or Takla Group (Rees, 1987). The former term has generally been superseded by Nicola Group, and the latter continues to be applied to Triassic rocks in central and northern British Columbia that correlate with the Nicola Group (*e.g.*, Nelson and Bellefontaine, 1996; Schiarizza and Tan, 2005).

The Nicola Group in the Hendrix Lake map area includes two major subdivisions: the Lemieux Creek succession, comprising Middle and Late Triassic sedimentary rocks in the eastern part of the group; and the volcanoclastic succession, an assemblage of volcanoclastic and volcanic rocks that crops out over a broad area to the west. Coarse volcanic breccia forms mappable units at several different stratigraphic levels within the volcanoclastic succession, and is assigned to breccia subunits. These subdivisions of the Nicola Group correlate directly with units mapped in the contiguous Canim Lake map area by Schiarizza and Boulton (2006a, b).

LEMIEUX CREEK SUCCESSION

The Lemieux Creek succession comprises dark grey to black phyllite, slate and siltstone, and forms the easternmost part of the Quesnel Terrane in the region. It has been traced as a continuous belt from the Hendrix Lake area southward to Little Fort, where it pinches out between strands of the Rock Island Lake and Lemieux Creek fault systems (Schiarizza and Israel, 2001; Schiarizza and Boulton, 2006a). Correlative rocks farther to the southeast are assigned to the Slocan Group (Thompson *et al.*, 2006). Rocks equivalent to the Lemieux Creek succession have been traced the length of the Quesnel Lake map sheet (unit uTra1 of Campbell, 1978; unit Tra of Bloodgood, 1990), and continue northward to near Prince George (unit Trp of Struik, 1985). Correlative rocks also occur in north-central British Columbia, where they are assigned to the Slate Creek succession of the Takla Group (Ferri and Melville, 1994; Nelson and Bellefontaine, 1996).

The Lemieux Creek succession is generally not well exposed, and is generally represented by small isolated exposures and subcrop. However, fairly continuous exposures are found in a logging cut northeast of Bosk Lake and along an east-flowing tributary to Deception Creek, west of No Name Lakes. Exposures northeast of McNeil Lake were not examined during the 2006 field season, but are included in the Lemieux Creek succession after Campbell (1978).

The Lemieux Creek succession within the Hendrix Lake map area consists mainly of dark grey to black, grey to rusty-weathered phyllite and slate, commonly containing small rusted-out porphyroblasts of siderite and/or pyrite. The strong phyllosilicate foliation is accentuated by parallel stringers of quartz a few millimetres wide. Thicker veins and lenses of quartz and quartz-carbonate are also common; most are parallel to cleavage, but some crosscut it at high angles. Transposed bedding is locally represented by cleavage-parallel laminae of light to medium grey siltstone, and less commonly by units of light grey platy quartzose siltstone up to 5 m thick.

The Lemieux Creek succession is not dated within the Hendrix Lake map area, but near Lemieux Creek, to the south, limestone-bearing intervals within the succession

have yielded macrofossils and conodonts of Middle and Late Triassic age (Campbell and Tipper, 1971; Schiarizza *et al.*, 2002a; M.J. Orchard, pers comm, 2001). Samples collected from correlative rocks to the north, near Quesnel Lake, have yielded Middle Triassic conodonts (Struik, 1988b, his pelite unit).

VOLCANICLASTIC SUCCESSION

The volcanoclastic succession of the Nicola Group forms a belt, 12 to 14 km wide, that is bounded by the Lemieux Creek succession to the east and the Takomkane batholith to the west. It consists mainly of volcanic sandstone, but also includes conglomerate, siltstone, volcanic breccia, basalt and minor amounts of silty limestone. Although it includes local siltstone intervals that are similar to rocks of the Lemieux Creek succession, the volcanoclastic succession is, for the most part, easily distinguished by the presence of sandstone and coarser rocks containing abundant pyroxene and feldspar. The contact between the volcanoclastic succession and the Lemieux Creek succession is not exposed, and is generally poorly constrained within the Hendrix Lake map area.

The volcanoclastic succession consists mainly of grey to green, fine to coarse-grained, commonly gritty volcanogenic sandstone (Fig 5). Mineral grains of pyroxene, feldspar and less common hornblende, together with lithic fragments containing these same minerals, are the dominant constituents. The sandstone is well bedded in places, but elsewhere forms massive units, up to several tens of metres thick, in which bedding is not apparent. In well-bedded sections, thin to thick sandstone beds commonly alternate with thin beds of green to grey siltstone, and locally display graded bedding, flame structures and rip-up clasts. Locally, thin-bedded to laminated siltstone forms intervals up to several metres thick with no sandstone interbeds. Sandstone and siltstone beds are locally calcareous, and beds of brown-weathered, laminated silty limestone occur rarely in the northwestern part of the map area.

Coarse-grained intervals, including pebble conglomerate, pebbly sandstone and volcanic breccia, are fairly common within the volcanoclastic succession, and dominate much of the interval in the vicinity of Mount Hendrix. Conglomerate and conglomeratic sandstone commonly occur as grey-green, medium to very thick beds intercalated



Figure 5. Volcanic sandstone and gritty sandstone of the Nicola volcanoclastic succession, northeast of Hendrix Lake.

with volcanic sandstone and siltstone. The matrix is typically sandy, and the angular to subrounded clasts are dominated by pyroxene-feldspar-phyric basaltic rocks, locally with minor proportions of siltstone, sandstone, limestone, hornblende-feldspar porphyry and diorite. However, a distinctive pebble conglomerate unit that was traced intermittently for about 6 km south and west of McNeil Lake has a dark grey, rusty-weathered, pyritic siltstone matrix and a heterogeneous clast population that includes abundant limestone, siltstone and sandstone, as well as pyroxene-feldspar porphyry, hornblende-feldspar porphyry and aphyric volcanic rocks. Massive volcanic breccia, as found in the mappable breccia subunits, is also common within the undivided portions of the volcanoclastic succession, where it forms units ranging from a few metres to a few tens of metres thick that are intercalated with volcanic sandstone and conglomerate.

Pyroxene-feldspar-phyric basaltic rocks are scattered throughout the volcanoclastic succession, but are not common. Some clearly form dikes and sills that intrude the clastic rocks, but some may be flows.

The Nicola volcanoclastic succession is not dated within the Hendrix Lake map area, but correlative rocks to the south locally contain Late Triassic macrofossils and conodonts (Campbell and Tipper, 1971; Schiarizza *et al.*, 2002a). Similar rocks to the north have yielded both Middle and Late Triassic fossils (Struik, 1988b; Panteleyev *et al.*, 1996). The succession is no younger than Late Triassic, because stratigraphic top indicators are consistently to the west and the western part of the succession is cut by the Boss Creek unit of the Takomkane batholith, which has yielded a latest Triassic U-Pb crystallization date.

Breccia Subunits

Mappable units dominated by coarse volcanic breccia containing fragments of mainly pyroxene-phyric basalt are assigned to breccia subunits within the volcanoclastic succession. Two major breccia subunits have been mapped, one in the eastern part of the volcanoclastic succession and one forming the westernmost exposures of the succession, adjacent to the Takomkane batholith. Smaller breccia subunits have been mapped north of the Hendrix stock and southeast of the confluence of Molybdenite and McKinley creeks (Fig 2). These breccia subunits are interpreted as relatively proximal accumulations of coarse volcanic material at several spatially and stratigraphically distinct sites within the volcanoclastic succession.

The breccia subunits are dominated by massive, unstratified, medium to dark green or grey-green, greenish brown to rusty brown-weathered volcanic breccia (Fig 6). Fragments are typically angular to subangular, and commonly range from a few centimetres to 10 cm in diameter, although much larger fragments occur locally. In most exposures, the fragments are dominantly or exclusively pyroxene and pyroxene-feldspar-phyric basalt, but show considerable textural variation based on size, abundance and feldspar versus pyroxene proportions in the phenocryst population, as well as degree of vesiculation and presence or absence of amygdules. The matrix is dominated by pyroxene and feldspar grains, and, in many exposures, the compositional similarity between clasts and matrix obscures the fragmental texture. Clasts of aphyric volcanic rock, hornblende-feldspar porphyry, hornblende-pyroxene-feldspar porphyry, diorite, pyroxenite, sandstone and siltstone occur locally. In a small area southwest of

Gotchen Lake, a part of the easternmost breccia subunit comprises clasts of ultramafic rock floating in a fine-grained, strongly indurated feldspathic matrix. The fragments range from less than 1 cm to more than 50 cm across, and consist mainly of clinopyroxenite, hornblende clinopyroxenite and hornblendite. The western breccia subunit likewise includes local sections containing fragments derived from an ultramafic-mafic intrusive complex just to the south of the Hendrix Lake map area (Schiarizza and Boulton, 2006a). These fragments were derived from erosion of, or extrusion through, ultramafic-mafic intrusive complexes similar to the Iron lake, Aqua Creek and Hendrix Lake complexes described later in this report. However, the ultramafic-mafic complexes currently exposed in the Takomkane project area are Early Jurassic in age, so are too young to have been the source for the fragments in these Triassic breccia units.

Minor components of the breccia subunits include thin to thick-bedded, pyroxene-rich sandstone, gritty sandstone and conglomerate, as well as massive units of pyroxene-feldspar porphyry probably derived from sills, dikes and flows. Chloritized amygdaloidal basalt with vague pillow structures was observed at one locality within the western breccia subunit, about 6 km south of Hendrix Lake. Hornfelsed and heavily chlorite-epidote-altered rocks of the western breccia subunit northeast of Buster Lake include some breccia, but are dominated by finer grained rocks that include gritty pyroxene-feldspar sandstone and sills of pyroxene-feldspar porphyry.

Intrusive Rocks

Intrusive rocks within the Takomkane project area include several Late Triassic to Early Jurassic suites that are part of the Quesnel magmatic arc, including the polyphase Takomkane batholith, as well as younger plutons of mainly Cretaceous age. Here, we describe the intrusive units found within the Hendrix Lake area, and also present preliminary isotopic dates for plutonic rocks mapped and sampled in the contiguous Canim Lake area during the 2005 field season. Figure 7, which summarizes the geology of the entire Takomkane project area, shows the locations of these dated samples.

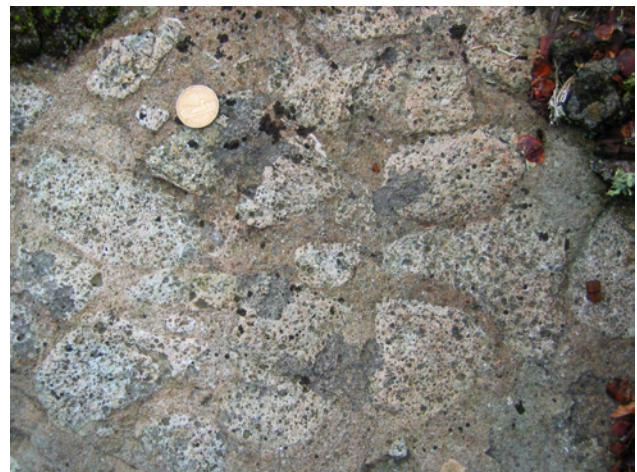
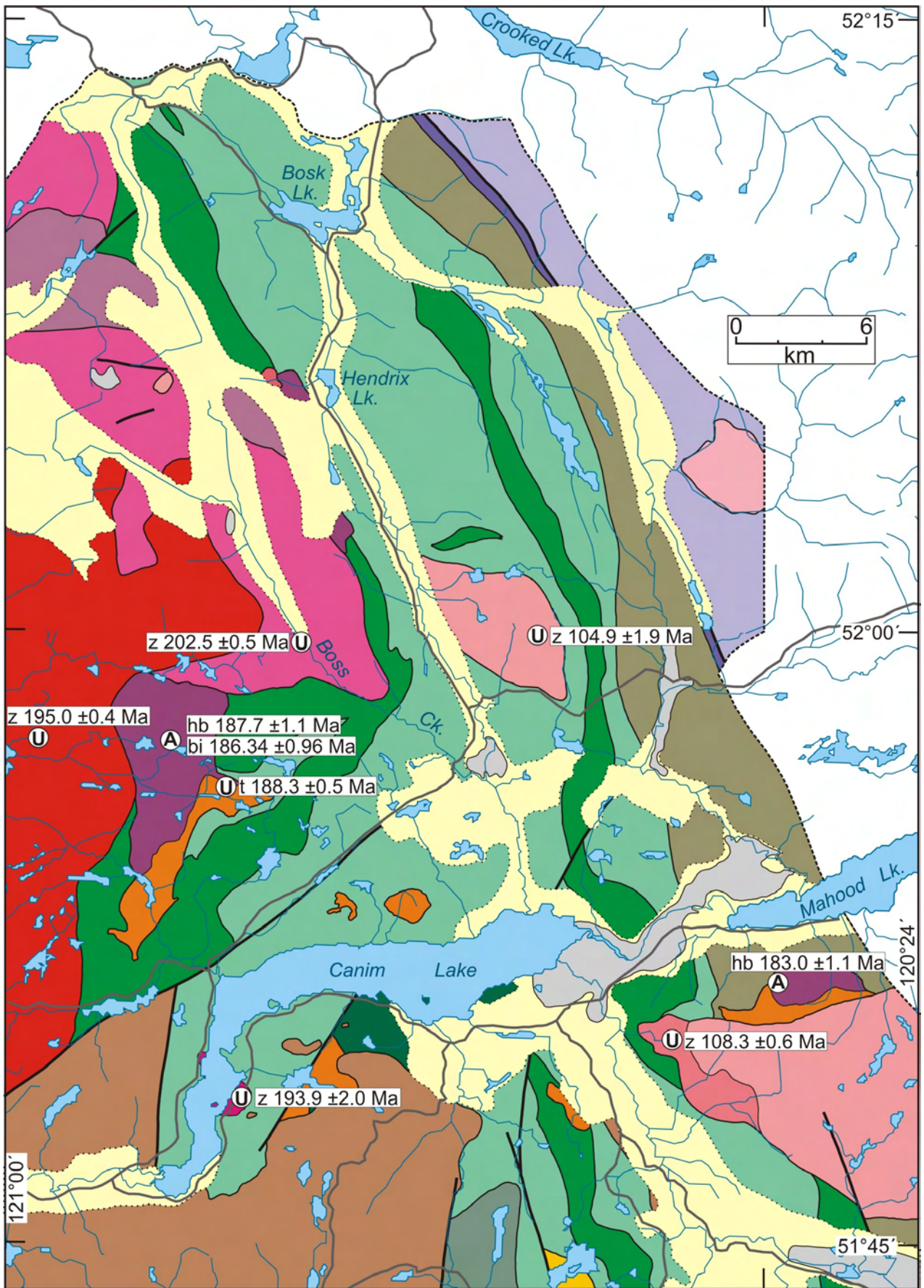


Figure 6. Volcanic breccia containing pyroxene-feldspar-phyric basalt fragments, eastern breccia subunit, west of McNeil Lake.



TAKOMKANE BATHOLITH

The Takomkane batholith is a large, Late Triassic – Early Jurassic granitic pluton that crops out in the northern Bonaparte Lake (NTS 092P) and southern Quesnel Lake (NTS 093A) map sheets (Fig 1). It cuts the Triassic Nicola Group, is itself cut by the Cretaceous Boss Mountain Mine stock, and is locally overlain by volcanic and sedimentary rocks of Eocene, Neogene and Quaternary age. The north-eastern part of the batholith crops out in the western part of the Hendrix Lake map area, where it cuts coarse volcanoclastic rocks assigned to the breccia subunit of the Nicola volcanoclastic succession and is subdivided into three lithological units. The two most extensive units, the Boss Creek and Schoolhouse Lake units, were traced northward from the Canim Lake map area, where they were first described by Schiarizza and Boulton (2006a, b). The third lithological division, comprising mainly dioritic rocks, is informally referred to as the Buster Lake unit. All units typ-

ically form massive, resistant outcrops. Textures are generally isotropic, but weak, steeply dipping foliations defined by the alignment of mafic minerals and clots were observed locally in all units. Weak to strong epidote-chlorite alteration is ubiquitous, and is commonly concentrated along northwest and northeast-striking fractures and joints.

Rocks assigned to the Boss Creek unit comprise much of the northeastern part of the Takomkane batholith (Fig 7). This unit consists mainly of light grey, medium to coarse-grained, equigranular rocks of predominantly quartz monzodiorite composition, but quartz and K-feldspar proportions (as estimated in the field) vary considerably, such that monzodiorite, granodiorite, quartz diorite, diorite and tonalite are also present. Mafic minerals commonly form 15 to 25% of the rock, and include varying proportions of clinopyroxene, hornblende and biotite. A porphyritic phase, comprising quartz monzodiorite to granodiorite containing phenocrysts of biotite and plagioclase, occurs locally at the Boss Mountain mine (Soregaroli and Nelson,

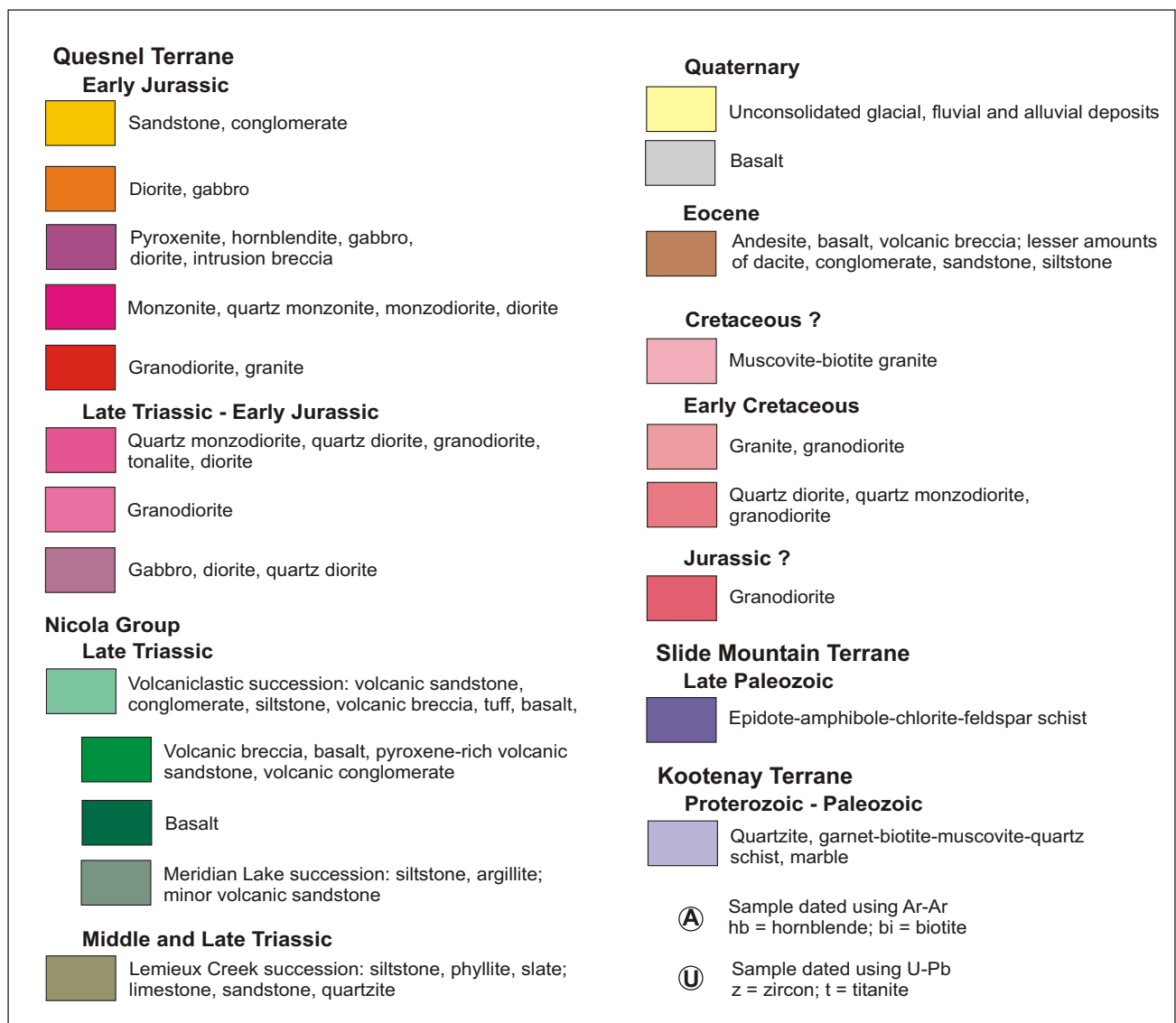


Figure 7. Simplified geology of the Takomkane project area, showing locations of isotopically dated samples collected during the 2005 field season.

1976). Zircons extracted from a sample of fairly typical quartz monzodiorite, collected from the unit on the west side of Boss Creek in 2005, have yielded a preliminary Late Triassic U-Pb date of 202.5 ± 0.5 Ma (Fig 7; R. Friedman, pers comm, 2006). The only other isotopic date reported for this unit is from a sample of quartz monzodiorite collected by R.B. Campbell about 550 m east-southeast of Takomkane Mountain. A biotite separate from this sample yielded a K-Ar date of 187 Ma (Lowdon, 1963). This cooling age was recalculated as 191 ± 15 Ma by Breitsprecher and Mortensen (2004) using International Union of Geological Science (IUGS) constants, but the date is considered unreliable because the biotite was altered and there was no correction for atmospheric argon.

The Buster Lake unit of the Takomkane batholith comprises dioritic rocks that crop out northwest and southeast of Buster Lake, as well as on a prominent knob about 4 km west of Hendrix Lake. It is enveloped by the Boss Creek unit to the north and south, and is in direct contact with the Nicola Group to the northwest. The Buster Lake unit consists mainly of medium greenish grey, coarse to medium-grained diorite, locally grading to quartz diorite. Mafic minerals typically form 25 to 50% of the rock, and consist mainly of clinopyroxene with minor amounts of biotite. Hornblende is prominent in some areas, but absent in others. Light grey leucocratic diorite to quartz diorite occurs locally as late-stage veins and/or matrix to intrusion breccia containing fragments of diorite. Rocks that are lithologically similar to the Buster Lake unit occur locally within the Late Triassic Boss Creek unit, and it is suspected that the two units are closely related. Alternatively, the Buster Lake unit might be more closely related to the Early Jurassic ultramafic-mafic complexes within the area.

The Schoolhouse Lake unit is a prominent component of the Takomkane batholith from its southern margin, west of Canim Lake, northward to Boss Creek. It forms the eastern margin of the batholith in the south, but farther north is enveloped by the Boss Creek unit to the east and north. Reconnaissance mapping suggests that it forms a major component of the southern part of the batholith for a considerable distance west of the Takomkane project area. The Schoolhouse Lake unit consists mainly of light grey to pinkish grey, coarse to medium-grained hornblende-biotite granodiorite to monzogranite. The texture is typically porphyritic, with pink orthoclase phenocrysts up to several centimetres in size. However, the rock is not porphyritic in some exposures, and grey plagioclase phenocrysts accompany the orthoclase in others. Mafic minerals typically form 10 to 20% of the rock, with hornblende predominating over biotite. The contact between the Schoolhouse Lake and Boss Creek units was not observed; however, at one locality where it is well constrained, both the phenocrysts and groundmass of the Schoolhouse Lake unit become finer grained as the contact is approached. This apparent chilled margin is consistent with preliminary isotopic dating, as a sample collected from the Schoolhouse Lake unit in 2005 yielded a U-Pb zircon date of 195.0 ± 0.4 Ma (Fig 7; R. Friedman, pers comm, 2006). This Early Jurassic date is similar to the U-Pb zircon date of 193.5 ± 0.6 Ma obtained by Whiteaker *et al.* (1998) from a sample collected at Ruth Lake, just 2 km west of the southern part of the Takomkane project area. The Ruth Lake sample is from granodiorite that was correlated with the Schoolhouse Lake unit by Schiarizza and Boulton (2006a).

SOUTH CANIM STOCK

The South Canim stock cuts volcanic sandstone and related rocks of the Nicola volcanoclastic succession along the southern part of Canim Lake. It consists mainly of light greenish grey to pinkish grey, medium to coarse-grained, hornblende-biotite monzonite, locally grading to quartz monzonite, monzodiorite and diorite. The stock was mapped as Cretaceous by Campbell and Tipper (1971), but Schiarizza and Boulton (2006a, b) suggested that it is more likely part of the Quesnel Terrane magmatic suite, and Late Triassic or Early Jurassic in age. A sample of quartz monzonite was collected from the stock during the 2005 field season and submitted for U-Pb dating of zircons. The zircons extracted from this sample yielded an Early Jurassic U-Pb laser-ablation date of 193.9 ± 2.0 Ma (Fig 7; R. Friedman, pers comm, 2006).

ULTRAMAFIC-MAFIC PLUTONIC COMPLEXES

Iron Lake Ultramafic-Mafic Complex

The Iron Lake complex comprises ultramafic and mafic plutonic rocks that crop out north of the west end of Canim Lake (Schiarizza and Boulton, 2006a, b). It intrudes the Nicola volcanoclastic succession, mainly the breccia subunit, along its east, south and southwest margins, but is juxtaposed against the Schoolhouse Lake and Boss Creek units of the Takomkane batholith across poorly exposed contacts to the northwest and north. At the scale of Figure 7, the Iron Lake complex is subdivided into an ultramafic unit and a mafic unit. The ultramafic unit consists mainly of clinopyroxenite and hornblende clinopyroxenite, but also includes olivine clinopyroxenite, wehrlite, hornblendite, gabbro, diorite and intrusion breccia (Schiarizza and Boulton, 2006a). The mafic unit consists mainly of medium to coarse-grained hornblende-pyroxene gabbro to monzogabbro, and medium to fine-grained hornblende diorite and microdiorite.

Melanocratic gabbro from the ultramafic unit of the Iron Lake complex yielded Ar/Ar plateau ages of 187.7 ± 1.1 Ma and 186.34 ± 0.96 Ma on hornblende and biotite separates, respectively (T. Ullrich, pers comm, 2006). Titanite from a diorite sample collected from the mafic unit of the complex has yielded a preliminary U-Pb concordia age of 188.3 ± 0.5 Ma (R. Friedman, pers comm, 2006). These Early Jurassic dates are significantly younger than the dates obtained from the Boss Creek and Schoolhouse Lake units, indicating that the Iron Lake complex is younger than the Takomkane batholith, and has presumably intruded the batholith as well as the Nicola Group.

Aqua Creek Ultramafic-Mafic Complex

The Aqua Creek complex comprises ultramafic and mafic plutonic rocks that crop out on the north side of the Raft batholith, south of the west end of Mahood Lake (Fig 7). These rocks intrude the Lemieux Creek succession of the Nicola Group, and are themselves cut by Early Cretaceous granodiorite of the Raft batholith. The Aqua Creek complex is lithologically very similar to the Iron Lake complex, and has likewise been subdivided into an ultramafic and a mafic unit. The ultramafic unit consists mainly of clinopyroxenite, hornblende clinopyroxenite, hornblendite, mafic gabbro and pegmatitic gabbro, whereas the mafic unit consists mainly of medium to coarse-grained

hornblende-pyroxene gabbro and medium-grained hornblende diorite.

Hornblende separated from a sample of pegmatitic gabbro collected from the ultramafic unit of the Aqua Creek complex in 2005 yielded an Early Jurassic Ar/Ar plateau age of 183.0 ± 1.1 Ma (T. Ullrich, pers comm, 2006). Uranium-lead laser-ablation dating of zircons extracted from diorite of the mafic unit is currently in progress.

Hendrix Lake Ultramafic-Mafic Complex

The Hendrix Lake complex is a newly recognized ultramafic-mafic pluton that is represented mainly by sparse exposures along and near the Boss Mountain Mine road, a short distance west of Hendrix Lake. These exposures include pyroxenite, melanocratic gabbro and diorite, as well as intrusion breccia comprising fragments of pyroxenite, hornblende and mafic gabbro within a diorite matrix (Fig 8). The south end of this intrusive complex may be represented by subcrop of similar diorite and intrusion breccia located in a logging cut 6 km south of Hendrix Lake. The intrusive rocks are not apparently exposed in the intervening area, but the two areas of exposure are linked by a prominent aeromagnetic high that suggests they represent the north and south ends, respectively, of a single, narrow ultramafic-mafic intrusion about 8 km long. This intrusion is suspected to be Early Jurassic in age, based on correlation with other ultramafic-mafic complexes in the area.

GRANODIORITE STOCK WEST OF HENDRIX LAKE

Light grey, medium-grained, equigranular hornblende-biotite granodiorite that crops out along and near the Boss Mountain Mine road forms a small stock that apparently cuts the Hendrix Lake ultramafic-mafic complex to the east and southeast, and the Nicola breccia subunit to the north. This stock was assigned a Jura-Cretaceous age by Campbell (1978), as were the Hendrix and Boss Mountain Mine stocks. However, the stock west of Hendrix Lake differs from the other two stocks, which are now known to be of Early Cretaceous age, in that hornblende is the dominant mafic phase. It is suspected that this stock is older than the Cretaceous stocks, perhaps correlative with the Middle Jurassic Ste Marie pluton, a hornblende granite that cuts



Figure 8. Intrusion breccia, Hendrix Lake ultramafic-mafic complex, west of Hendrix Lake.

Quesnel Terrane rocks southeast of Prince George (Struik *et al.*, 1992).

CRETACEOUS PLUTONS

Raft Batholith

The Raft batholith is an elongate granitic pluton that extends for about 70 km in a west-northwesterly direction and cuts across the boundaries between the Kootenay, Slide Mountain and Quesnel terranes (Fig 1). A significant portion of the western part of the batholith was mapped by Schiarizza *et al.* (2002a) and Schiarizza and Boulton (2006a). They found that it consists mainly of light grey, medium to coarse-grained biotite-hornblende granodiorite to monzogranite. However, a lithologically distinct unit at the west end of the batholith consists mainly of medium to fine-grained, equigranular hornblende-biotite quartz monzodiorite, locally grading to quartz diorite, diorite or granodiorite. A sample collected from the predominant granodiorite to monzogranite unit in 2001, about 10 km east of the Takomkane project area, yielded a concordia U-Pb zircon date of 105.5 ± 0.5 Ma (Schiarizza *et al.*, 2002b). A sample collected from the quartz monzodiorite unit at the west end of the batholith in 2005 yielded a slightly older U-Pb zircon date of 108.3 ± 0.6 Ma (Fig 7; R. Friedman, pers comm, 2006).

Hendrix Stock

The Hendrix stock is a granitic pluton that crops out east of Hendrix Creek and straddles the boundary between the Canim Lake and Hendrix Lake map areas. The stock has an elliptical shape in plan view, with a northwest-trending major axis about 9 km long. It intrudes the Nicola volcanoclastic succession to the south, east and north, but its western margin is obscured by Quaternary drift along Hendrix Creek. Hornfelsed country rocks along the north margin of the stock are locally mineralized at the Hen and Dyke showings.

The Hendrix stock consists mainly of light-grey, medium to coarse-grained, equigranular biotite-hornblende monzogranite to granodiorite, locally grading to tonalite along its margins. The stock was assigned a Cretaceous age by Campbell and Tipper (1971) and Schiarizza and Boulton (2006a, b). This interpretation has been confirmed by radiometric dating of zircons extracted from a sample collected from the western part of the stock in 2005. These zircons yielded a late Early Cretaceous U-Pb laser-ablation date of 104.9 ± 1.9 Ma (Fig 7; R. Friedman, pers comm, 2006).

Boss Mountain Mine Stock

The Boss Mountain Mine stock is an elliptical body of granite, about 1000 m long by 600 m wide, that intrudes older plutonic rocks of the Takomkane batholith 2 km east of Takomkane Mountain. The stock is spatially and genetically associated with molybdenum mineralization at the Boss Mountain mine, which lies within Takomkane rocks near the southwestern margin of the stock (Soregaroli, 1968; Soregaroli and Nelson, 1976). The stock is not well exposed at surface, but is represented locally by subcrop of brown-weathered, sericite-pyrite-chlorite-altered granitic rock northeast of the mine pits. The outline of the stock shown on Figure 2 is after Soregaroli (1968), and is in part projected from underground information.

The Boss Mountain Mine stock is pervasively altered, but descriptions and modal analyses presented by Soregaroli (1968) show that it consists mainly of porphyritic monzogranite, comprising phenocrysts of quartz, plagioclase and orthoclase within a medium to coarse-grained groundmass of quartz and orthoclase. Biotite and minor amounts of hornblende, zircon and apatite also occur as primary minerals. Secondary minerals include sericite, carbonate, pyrite, chlorite, rutile, epidote and zeolite. Where observed in underground workings, the contacts of the stock are sharp and are defined by a chilled margin about 2 m wide. A graphic intergrowth of quartz and orthoclase forms a narrow outer zone of the chilled margin and grades rapidly into an inner chill zone comprising quartz and plagioclase phenocrysts within a fine-grained groundmass of aplitic to granophyric quartz and orthoclase (Soregaroli, 1968; Soregaroli and Nelson, 1976).

The Boss Mountain Mine stock is not directly dated. However, three separate samples of hydrothermal biotite from the Boss Mountain mine yielded K-Ar dates of 98 ± 4 , 104 ± 4 and 105 ± 4 Ma, respectively (White *et al.*, 1968). Soregaroli and Nelson (1976) interpreted these dates as providing a general indication of the age of the stock, because the hydrothermal biotite is related to molybdenum mineralization, which was shown to be genetically related to the Boss Mountain Mine stock.

Deception Stock

The Deception stock is a small, two-mica granite pluton that cuts metasedimentary rocks of the Snowshoe Group north of Deception Creek, along the eastern boundary of the map area. The granite was first recognized by Helson (1982), who also noted its spatial association with tungsten soil anomalies. The Fox molybdenum-tungsten mineral showing was discovered along the south margin of the stock in 1999 (Ridley, 2000a), and the boundaries of the stock, which measures 4 to 5 km in diameter, were established during subsequent exploration in the area (Blann and Ridley, 2005b).

The Deception stock consists mainly of light grey, medium-grained, equigranular, biotite-muscovite granite that commonly contains small red garnets as an accessory phase. Dikes of leucocratic pegmatite and aplite occur locally within the granite and the adjacent country rock. Skarn alteration occurs along the southern margin of the stock, where it is associated with molybdenum-tungsten mineralization at the Fox occurrence, and also along the northeastern margin of the stock (Blann and Ridley, 2005b). The age of the stock is unknown, but a sample collected during the 2006 field season has been submitted for U-Pb dating of zircons. It is suspected that it is of mid-Cretaceous age, as two-mica granite bodies of this age occur elsewhere in the region, and commonly have associated molybdenum-tungsten mineralization (Logan, 2002).

Quaternary Volcanic Rocks

Quaternary alkali olivine basalt flows and related pyroclastic rocks are a prominent feature of Wells Gray Provincial Park to the east of the Hendrix Lake map area (Fig 1; Hickson and Souther, 1984). Similar basalt occurs as isolated occurrences to the west of the main volcanic field, within the northeastern part of the Bonaparte Lake map sheet and parts of the Quesnel Lake map sheet. These include, within the Hendrix Lake map area, a volcanic cen-

tre on Takomkane Mountain and remnants of flows located east of Boss Creek and along Deception Creek (Fig 2).

The volcanic rocks on Takomkane Mountain cover an area of about 1.5 km². The eastern part, including the twin peaks of the mountain (Fig 9), consists mainly of an eroded cinder cone, whereas the western part comprises a basalt flow that is about 5 m thick at its western extremity (Sutherland Brown, 1958; Soregaroli, 1968). Basalt also occurs locally along the northeast corner of the cinder cone, where it forms a steep wall, about 10 m high, at the edge of a small cirque. Sutherland Brown (1958) suggested that this reflects ponding of lava against a glacier that occupied the cirque at the time of eruption. For the most part, however, the Takomkane cone and lava flow lie above granitic rocks of the Takomkane batholith across a gently dipping contact. Sutherland Brown (1958) noted that the surface on which the volcano was built had already been glaciated, but the cone was partially eroded by subsequent glacial action, and both the cone and lava flow are locally overlain by granitic boulders inferred to be glacial erratics. He concluded that the Takomkane volcano erupted late in the Pleistocene epoch.

Basalt from the northeastern corner of the Takomkane volcano was studied by Fiesinger and Nicholls (1977). It comprises olivine microphenocrysts in a groundmass of augite, nepheline and magnetite, and is classified as a nephelinite. The basalt at this locality is host to a large number of mantle-derived peridotite xenoliths, and fewer granitic xenoliths derived from crustal rocks. The peridotite xenoliths, mainly spinel lherzolite, are commonly 2 to 15 cm across and rarely approach 50 cm in size (Fig 10; Soregaroli, 1968). They have received some attention as a potential source of peridot, the gem variety of olivine (Galloway, 1918; Reinecke, 1920), and a number of samples were submitted to Tiffany and Co., New York, for evaluation in 1915 or 1916. The ensuing report noted that, although the specimens were of a remarkably good colour, they were more or less flawed and therefore of little value as gem material (Galloway, 1918).

The remnants of a basalt flow on the west side of Boss Creek are represented by two small exposures along the

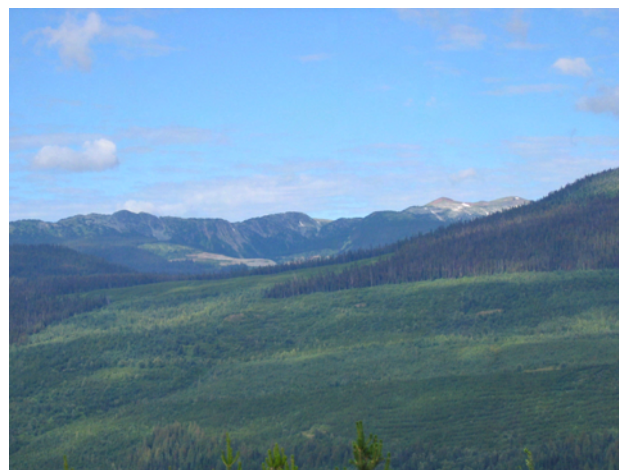


Figure 9. View westward to the eroded Quaternary cinder cone on Takomkane Mountain. Prominent ridge to the south is underlain by the Boss Creek unit of the Takomkane batholith. Workings of the past-producing Boss Mountain mine are partially obscured in the bowl beneath the ridge.



Figure 10. Lherzolite xenoliths within Quaternary basalt, east flank of Takomkane Mountain.

Boss Creek logging road, 8 km southeast of Takomkane Mountain. The grey basalt exposed here is weakly vesicular and contains abundant xenoliths, up to 6 cm in size, of peridotite, as well as sparse xenoliths of diorite and quartz diorite. Quaternary basalt, largely or entirely covered by alluvium, is also suspected to occur along part of Deception Creek, based on sparse exposures just south of the map area (Schiarizza and Boulton, 2006b). Campbell (1978) also mapped young basalt flows along Hendrix Creek. These flows were not located during the present study, but they may be present and largely covered by recent fluvial or alluvial deposits.

Soregaroli (1968) noted that basalt dikes, related to the Takomkane volcano, are common in the underground workings of the Boss Mountain molybdenum mine, where they occupy vertical fractures that strike north-northeast and east-southeast. Relatively fresh olivine basalt dikes were observed rarely elsewhere in the map area, and may be of similar age. A light grey, finely crystalline intrusive (?) rock observed in a single exposure about 1.3 km north of the Hendrix stock may also be related. It consists mainly of randomly oriented plagioclase laths, but also contains 1 to 5 mm grains and xenocrysts of olivine and lherzolite, and rare 1 to 2 cm xenoliths of gabbro, diorite and pyroxenite.

STRUCTURE AND METAMORPHISM

There is a major change in metamorphic grade and structural style from east to west across the Hendrix Lake map area. Penetratively deformed rocks of the Snowshoe Group are characterized by garnet-bearing assemblages in pelitic schist throughout most of the map area, and staurolite-bearing rocks occur locally in some eastern exposures (Fillipone, 1985). However, somewhat lower grade metamorphism was attained in a narrow wedge of westernmost Snowshoe rocks at the north end of the map area, where pelitic rocks are biotite-muscovite-quartz schist without garnet. The Crooked amphibolite displays penetrative fabrics comparable to those of the Snowshoe Group, but the metamorphic assemblage (typically chlorite-epidote-amphibole-plagioclase±biotite) cannot be directly compared to the Snowshoe Group because of their contrasting compositions. The Lemieux Creek succession also displays a strong penetrative fabric, comparable to the

Snowshoe Group and Crooked amphibolite, but the metamorphic assemblage is characterized by chlorite-muscovite without biotite, so is distinctly lower grade than nearby rocks of comparable composition within the Snowshoe Group. There is a distinctive change in structural style farther west, where rocks of the Nicola volcanoclastic succession do not generally display penetrative fabrics. However, slaty cleavage is developed locally, typically within finer grained sections of the volcanoclastic succession, so this change may be primarily a function of lithology. Metamorphic chlorite, actinolite and clinozoisite occur locally within the volcanoclastic succession, suggesting that there is not a significant metamorphic break between it and the Lemieux Creek succession.

Mesoscopic Structure

All rocks of the Snowshoe Group display a penetrative foliation, varying from a strong schistosity in pelitic schist to well-oriented, but dispersed, mica flakes in quartzite. This metamorphic foliation is parallel to compositional layering, defined typically as alternating quartzite and schist layers. Quartz veins and lenses are common, and are typically oriented parallel to the metamorphic foliation, although some veins crosscut the foliation. Thin quartzite layers and quartz veins within pelitic schist are locally boudinaged, and some quartz veins are isoclinally folded. Boudin necks and fold hinges typically plunge gently to the south. Only at one locality, in the northeastern part of the area, was the metamorphic foliation observed to be axial planar to a fold of lithological layering. There, an isoclinal fold pair outlined by compositional layering within micaceous quartzite plunges gently to the west-northwest and shows southward vergence. A vague mineral lineation, defined by quartz lenses and biotite aggregates, also plunges to the northwest in this area, but plunges to the southeast in the southern part of the belt. A more or less coaxial crenulation lineation likewise plunges to the northwest in the northern part of the area and to the southeast in the southern part. In the north, this crenulation lineation is locally associated with a weak crenulation cleavage that dips to the southwest at a steeper angle than the primary metamorphic foliation. A second, younger crenulation lineation was observed rarely, and plunges to the west or southwest.

The Crooked amphibolite is well exposed only in the northern part of the map area, where it displays a strong, northwest-dipping, penetrative metamorphic foliation that is parallel to the foliation within adjacent rocks of the Snowshoe Group. The foliation is defined mainly by platy chlorite grains and flattened grains and aggregates of feldspar and epidote. The metamorphic foliation is commonly accentuated by compositional layering, developed on a scale of a few millimetres to 1 cm, comprising dark chlorite-rich lenses interleaved with lenses of lighter coloured, relatively chlorite-poor material. It is also accentuated by parallel veins, stringers and lenses consisting of various combinations of epidote, quartz and rusty carbonate. At one locality, however, stringers and veins of quartz-epidote are folded into a northeast-verging, isoclinal, anticline-syncline pair, while chlorite defines an axial-planar foliation that cuts across the fold hinges. The main metamorphic foliation within the Crooked amphibolite is locally deformed by two sets of crenulations and associated folds, plunging northwest and west-southwest, as seen also in the adjacent Snowshoe Group.

The Lemieux Creek succession is characterized by slate and phyllite that display a well-developed cleavage. In the eastern part of the succession, this cleavage dips at moderate to steep angles to the west-southwest, and is parallel to the metamorphic foliation in the adjacent Crooked amphibolite. Farther west, the cleavage dips variably to the east-northeast or south-southwest, due in part to medium-scale folds that plunge gently to the southeast. The cleavage is parallel to compositional layering that is locally defined by quartzose siltstone units, and it is almost everywhere accentuated by parallel stringers of quartz a few millimetres wide. Locally, these quartz stringers are deformed into southeast-plunging folds that generally verge to the southwest. In the hinge zones of these folds, the predominant cleavage has the form of a crenulation cleavage that cuts an earlier phyllosilicate foliation that is parallel to the folded quartz stringers. It appears, therefore, that the predominant cleavage is actually a composite of two synmetamorphic foliation surfaces. This cleavage is locally deformed by a set of younger crenulations and open folds that plunges northwest or southeast, and rarely by a separate set of crenulations that plunges southwest. These younger structures are readily correlated with the two sets of crenulations observed in the Crooked amphibolite and Snowshoe Group.

Penetrative fabrics comparable to those in rock units to the east are generally not apparent within the Nicola volcanoclastic succession. A weak to moderately developed slaty or fracture cleavage, usually dipping steeply to the southwest or northeast, is developed locally, but outcrop-scale structures are more commonly represented by brittle faults and fractures. Bedding orientations are quite variable, but moderate to steep dips to the northeast or southwest are most common. Facing directions, where they could be established, are invariably to the southwest. Folds of bedding were observed at a few widely scattered localities and have highly variable orientations. There is no axial-planar foliation associated with any of the bedding folds observed within the volcanoclastic succession.

Map-Scale Structure

The main stratigraphic divisions within the Hendrix Lake map area are arranged as a succession of parallel, north-northwest-striking belts that are traced the full length of the area with no significant repetitions (Fig 2). Metamorphic foliations and transposed bedding in the Snowshoe Group, Crooked amphibolite and eastern part of the Lemieux Creek succession dip moderately to steeply toward the west-southwest. Foliation and bedding orientations within the western part of the Lemieux Creek succession and the adjacent volcanoclastic succession are more

variable, but generally dip steeply to the west-southwest or east-northeast. The most significant departure from these orientations is in the area north of the Hendrix stock, where bedding strikes east, parallel to the northern margin of the stock. Stratigraphic facing directions within the volcanoclastic succession are toward the west throughout most of the area, and are to the south in the east-striking zone north of the Hendrix stock.

As summarized above, the structural-stratigraphic succession within the map area is essentially a west-southwest facing homocline. As shown in Figure 11, this homocline comprises part of the west limb of the Boss Mountain anticline, a significant map-scale structure that folds the Kootenay, Slide Mountain and Quesnel terranes and their mutual boundaries (Fig 1). This anticline, and the adjacent Eureka Peak syncline, fold metamorphic isograds but are generally interpreted as late-stage folds within a significant metamorphic-structural event that clearly affected all rocks of the Snowshoe Group, Crooked amphibolite and Nicola Group (Campbell, 1971; Ross *et al.*, 1985; Phillipone and Ross, 1990). Peak metamorphic conditions were likely attained in the early Middle Jurassic, based on a 174 ± 4 Ma U-Pb date on metamorphic sphene from near Quesnel Lake (Mortensen *et al.*, 1987).

BASAL CONTACT OF THE CROOKED AMPHIBOLITE: THE EUREKA THRUST

The eastern contact of the Crooked amphibolite is well constrained over a length of several kilometres in the northeastern corner of the Hendrix Lake map area. The contact was not observed, but is locally defined by adjacent exposures of Snowshoe Group and Crooked amphibolite only a few metres apart. The rocks near the contact are strongly foliated and somewhat finer grained than is typical for these units, but mylonitic fabrics were not observed. Nevertheless, the contact is interpreted as an early east-directed thrust fault, following the more detailed studies of other workers in the region (*e.g.*, Ross *et al.*, 1985; Struik, 1986, 1988c; Rees, 1987). This fault is referred to as the Eureka thrust by Struik (1986, 1988c), and is equivalent to the Quesnel Lake shear zone of Rees (1987). It probably correlates with the basal thrust fault bounding an isolated klippe of ultramafic and mafic rocks, the Black Riders complex, that occurs structurally above the Snowshoe Group 10 km east of No Name Lakes (Montgomery, 1978).

The kinematic history of the Eureka thrust is best constrained by fabrics preserved in footwall orthogneiss and quartzofeldspathic metasedimentary rocks (Snowshoe Group) north of Quesnel Lake. There, Rees (1987) documented rotated feldspar megacrysts, S-C mylonitic fabrics and shear-band foliations that indicate a top-to-the-east

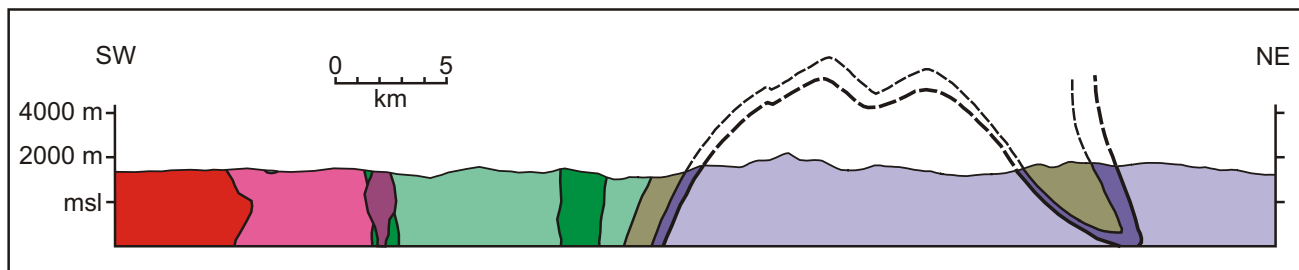


Figure 11. Schematic vertical cross-section along the line shown in Figure 2. The northeastern half of the section, beyond the limits of the Hendrix Lake map area, is from section C-D of Phillipone and Ross (1990).

sense of shear. He concluded that the shear fabrics formed under greenschist-facies conditions, and were in part overprinted by higher grade metamorphic assemblages associated with subsequent regional folding.

The Eureka thrust postdates the Crooked amphibolite and predates the regional folding event, of suspected early Middle Jurassic age (Mortensen *et al.*, 1987; Murphy *et al.*, 1995), that deforms the thrust contact. Rees (1987) suggested that the thrusting occurred in the Early Jurassic and that the Eureka thrust fault carried both the Crooked amphibolite and overlying Middle Triassic – Lower Jurassic rocks of the Quesnel Terrane eastward over the Kootenay Terrane. A different scenario is suggested by a study of a conglomerate unit that occurs within the basal part of the Quesnel Terrane a short distance above the Eureka thrust near Wingdam, east of Quesnel (McMullin, 1990 *et al.*). The conglomerate is mapped as Triassic by Struik (1988c) but is not dated. It contains clasts derived from the Kootenay Terrane and the Slide Mountain Terrane (Crooked amphibolite) that were deformed and foliated prior to their deposition as part of the conglomerate. This suggests that the Eureka thrust might be, at least in part, a Late Permian or Early Triassic structure that emplaced the Slide Mountain Terrane above the Kootenay Terrane, and that the Triassic rocks of the Quesnel Terrane depositionally overlapped these two older terranes after a period of erosion (McMullin *et al.*, 1990). Campbell (1971) also documented structural fabrics within the Crooked amphibolite that apparently predate deposition of Triassic rocks of the Quesnel Terrane, and Schiarizza (1989) suggested that east-directed thrusting and structural imbrication of the Fennell Formation, representing the Slide Mountain Terrane directly to the south, occurred in Permo-Triassic time. Our 2006 fieldwork provides no additional constraints on the age of the Eureka thrust, but we suspect, from relationships summarized above, that it formed in Permo-Triassic time, although it may have been reactivated during subsequent structural events.

BASAL CONTACT OF THE LEMIEUX CREEK SUCCESSION

The contact between the Crooked amphibolite and the Lemieux Creek succession is not exposed within the Hendrix Lake map area, but is fairly well constrained northeast of Bosk Lake, where it is more or less parallel to the strong, concordant, southwest-dipping foliations in the two map units. Campbell (1971) studied this contact in some detail and inferred that the Lemieux Creek succession had been deposited above the Crooked amphibolite across an unconformity, but that the contact had been variably sheared and transposed by subsequent Jurassic deformation. Rees (1987) and Struik (1988c) also interpreted this contact as a sheared unconformity, and this interpretation is accepted here, although Bloodgood (1990) and Panteleyev *et al.* (1996) mapped the contact as an east-directed thrust fault. Rees (1987) inferred that the Lemieux Creek succession and overlying volcanoclastic rocks were carried eastward with the Crooked amphibolite along an Early Jurassic Eureka thrust. As discussed in the previous section, McMullin *et al.* (1990) presented an alternative interpretation, suggesting that the Lemieux Creek succession was deposited above the Crooked amphibolite after it had already been emplaced above the Snowshoe Group on a Permo-Triassic Eureka thrust.

BASAL CONTACT OF THE VOLCANICLASTIC SUCCESSION

The contact between the Lemieux Creek and volcanoclastic successions of the Nicola Group is not exposed, nor even particularly well constrained, within the Hendrix Lake map area. The contact has been traced southward almost 70 km to Little Fort, although it is locally interrupted by the Raft batholith (Schiarizza *et al.*, 2002b, c; Schiarizza and Boulton, 2006b). Over this distance, it is partly defined by steeply dipping Eocene faults, but elsewhere it is not apparently faulted, although nowhere is it actually exposed. Relationships across the contact are not definitive, but permit the interpretation that it is an abruptly gradational contact across which the volcanoclastic succession stratigraphically overlies the Lemieux Creek succession (Schiarizza *et al.*, 2002a; Schiarizza and Boulton, 2006a). Rees (1987) likewise inferred a gradational stratigraphic contact between the two units north of Quesnel Lake, but suggested that, on a broader scale, the western volcanic facies probably interfingers with the eastern pelitic facies (his Fig 2.10). Struik (1988b) subsequently demonstrated, with conodont ages, that the two units are, in part, the same age, and also that the basal rocks of the volcanic unit on the north side of Quesnel Lake are older than some of the underlying rocks of the pelitic unit. He postulated that the two units represent a western volcanic facies and age-equivalent eastern pelitic facies that are currently juxtaposed across an east-directed Jurassic thrust fault of regional extent. The work of Bloodgood (1990) supports this interpretation, as she mapped the contact as a layer-parallel fault from Quesnel Lake southward to the area west of Crooked Lake. The poorly exposed contact provides no opportunity for confirming or rejecting this interpretation within the Hendrix Lake map area.

LATE FAULTS AND LINEAMENTS

Schiarizza and Israel (2001) mapped a system of Eocene dextral strike-slip faults from Little Fort northwestward to Canimred Creek. It is suspected that at least one major component of this system, the Rock Island Lake fault, extends across Canim Lake and into the Hendrix Lake map area, following a pronounced topographic lineament defined by lower Boss Creek and Hendrix Creek (Schiarizza and Boulton, 2006a). Faulting is not proven along this lineament in the Hendrix Lake map area, however, because bedrock is obscured by extensive drift cover. A parallel north-northwest-trending lineament is defined by upper Boss Creek and Molybdenite Creek. Soregaroli (1968) inferred that this drift-covered lineament was structurally controlled, and referred to it as the Molybdenite Creek fault. Although displacement is not proven along this zone, the distribution of map units defined by our 2006 fieldwork is consistent with dextral offset of the Buster Lake unit of the Takomkane batholith across the lineament.

Soregaroli (1968) mapped several northeast to east-northeast-striking faults in the area south of Takomkane Mountain, some showing apparent sinistral offsets of older structures and map units. He also mapped less conspicuous north-northeast-striking faults that postdated the east-northeast structures. A fault parallel to these latter structures is inferred to occupy the valley of Buster Lake, and coincides with an apparent dextral offset of the Takomkane-Nicola contact (Fig 2).

The Ten Mile Creek fault is a conspicuous structure that strikes east-southeast across the area north of the

Takomkane volcano and the Boss Mountain Mine stock (Soregaroli, 1968). A prominent system of faults with similar orientation occurs on the north margin of the Hendrix stock, and may follow a system of east-southeast-trending lineaments to Deception Creek (Ridley, 1997a), although there is no apparent displacement of lithological contacts within the Nicola Group in this area (Fig 2). Ridley (1997a) suggested that the fault system north of the Hendrix stock is equivalent to the Ten Mile Creek fault, and that the two segments have been offset by a dextral fault in the Hendrix Creek valley. This correlation is speculative but consistent with the interpretation that the Hendrix Creek linear is part of an Eocene fault system with dextral displacement (Schiarizza and Boulton, 2006a).

MINERAL OCCURRENCES

The known mineral occurrences within the Hendrix Lake map area are shown on Figure 12. The DL (MINFILE 093A 089) and Art (MINFILE 093A 200) showings, near the southern boundary of the map area, were described by Schiarizza and Boulton (2006a), so are not described here. Other showings include disseminated pyrite-chalcopyrite in the Buster Lake unit of the Takomkane batholith; mineralized veins in the Snowshoe Group and Lemieux Creek succession northeast of Bosk Lake; the past-producing Boss Mountain porphyry molybdenum deposit, associated with a small Cretaceous stock that cuts the Takomkane batholith east of Takomkane Mountain; mineralized veins and stockworks in the Takomkane batholith west of the Boss Mountain mine; gold-bearing hornfelsed rocks along the northern margin of the Hendrix stock; and molybdenum-tungsten mineralization along the southern margin of the Deception stock. Many of the known showings are not yet included in the MINFILE (2006) database, but are in the process of being entered into the system.

Gus (MINFILE 093A 020)

The Gus showing is located about 3.5 km southeast of Buster Lake, within the Buster Lake unit of the Takomkane batholith. It was discovered in 1970 during an exploration program for Exeter Mines Ltd. The mineralization is described as disseminated chalcopyrite and pyrite within porphyritic diorite (Allen, 1970). There is no additional information on file, and the showing was not located during our 2006 field program, although some old drill pads were located that may have been constructed by Exeter Mines Ltd. in 1971 (Blann and Ridley, 2005a).

Vein Occurrences Northeast of Bosk Lake

Quartz veins, some mineralized with pyrite and galena, are common within the Lemieux Creek succession, Crooked amphibolite and Snowshoe Group northeast of Bosk Lake. These veins were covered by the Cruiser claim group and explored with rock and soil geochemical surveys in 1989 (Bysouth, 1989; Barker and Bysouth, 1990). For the purposes of this discussion, a cluster of mineralized veins within the Snowshoe Group is referred to as the Bassett showing, whereas a more widespread area of veins within the Lemieux Creek succession, some with distinctly different character than the Bassett veins, is referred to as the Cruiser showing. Quartz veins are also present within

the intervening Crooked amphibolite, but they are not apparently mineralized.

BASSETT

The Bassett showing comprises a number of mineralized quartz veins within the Snowshoe Group, near its contact with the Crooked amphibolite. Mineralized veins, accompanied by nonmineralized veins, are exposed over a strike length of about 200 m within an interval of marble, quartzite and minor pelitic schist about 50 m wide. The veins are parallel, or at a low angle to, the strong foliation in the host rocks. Individual veins pinch and swell, but commonly range from a few centimetres to about 20 cm in thickness, although one poorly exposed vein within marble at the south end of the mineralized zone is at least 35 cm wide. The mineralized veins are generally cut by rusty hairline fractures and locally contain patches of ankerite and vugs containing subhedral crystals of quartz and carbonate. Mineralization comprises scattered grains and clots of galena and pyrite. Samples collected from three separate mineralized veins during the 2006 field season contained 1749 to 6450 ppm Pb, 51 to 888 ppm Mo and 1749 to 6449 ppb Ag, but did not contain significant amounts of Au (Table 1, samples 06PSC-282, 283, 284).

CRUISER

The Lemieux Creek succession in the area of the Cruiser showing is fairly well exposed over a width of about 2 km, mainly along roads and skid trails in an old logging cut. Quartz veins mineralized with galena and pyrite are scattered sparsely through this entire width (Bysouth, 1989) and are accompanied by a much larger number of nonmineralized veins. Some veins, particularly those in the east, are parallel to the strong southwest-dipping foliation within the enclosing phyllite. In the western part of the belt, however, mineralized and nonmineralized veins typically strike northeast to east-northeast, dip steeply to the southeast or northwest, and are hosted in grey-green, rusty-weathered alteration zones consisting of quartz, ankerite, sericite, mariposite and pyrite. In an area designated as the main prospect by Bysouth (1989), an isolated patch of pervasively altered rock is cut by several northeast-striking quartz veins, ranging from 25 to 50 cm wide. Contacts between the altered rock and nonaltered phyllite are not exposed in this area. Elsewhere, however, zones of similar alteration up to 3 m wide are approximately concordant with the foliation within the enclosing phyllite. Northeast-striking quartz veins within these alteration zones do not extend across the contacts into nonaltered phyllite.

The veins that cut pervasively altered rock at the main Cruiser showing comprise milky white quartz with vugs containing quartz and carbonate crystals, rare patches of rusty carbonate, and inclusions of altered wallrock. The veins are cut by rusty hairline fractures and contain sparsely scattered limonite-altered pyrite grains. A sample from the altered wallrock returned anomalous concentrations of Pb, Zn, Ag, Ni, Co, As and Sb (Table 1, sample 06PSC-73-1), whereas samples from two different veins did not yield significant base or precious metal values (samples 06PSC-73-2 and 3). A sample from a northeast-striking vein within a similar alteration zone, 500 m northwest of the main prospect, likewise did not yield significant base or precious metal values (Table 1, sample 06PSC-71). Thirteen samples from veins and alteration zones sampled by Bysouth

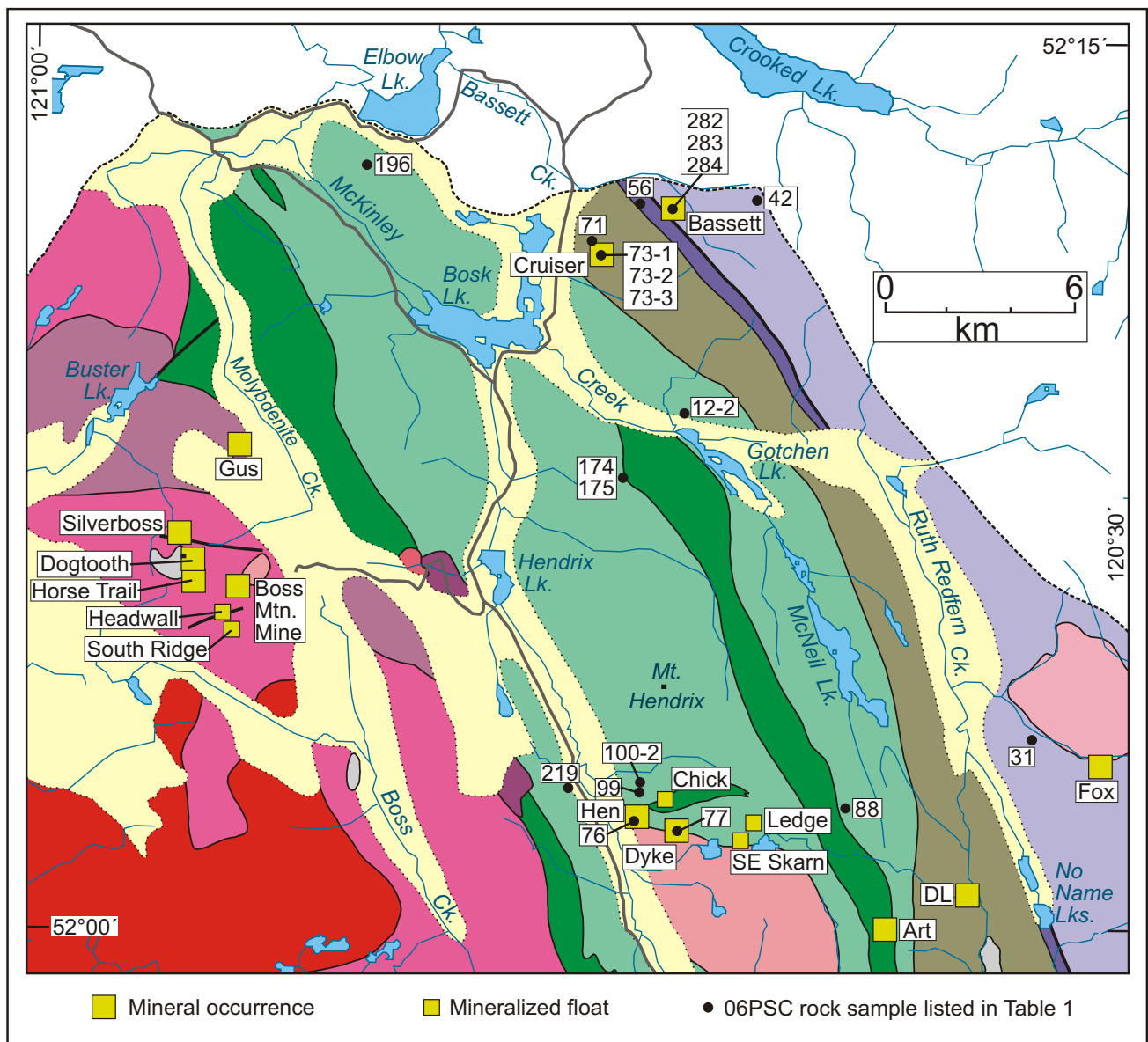


Figure 12. Locations of known mineral occurrences within the Hendrix Lake map area, and locations of rock samples listed in Table 1. See Figure 2 for legend.

(1989) returned Ag values ranging from 1.1 to 14.0 ppm, but did not yield anomalous Au concentrations.

Boss Mountain Molybdenum Mine (MINFILE 093A 001)

The past-producing Boss Mountain molybdenum mine is located on the east slopes of Takomkane Mountain, near the headwaters of Molybdenite Creek. The molybdenum mineralization was briefly described in the Annual Report of the BC Minister of Mines for 1917, when several hundred kilograms of ore were packed to Lac La Hache and subsequently shipped to Ottawa (Galloway, 1918). In the 1930s, the property was explored with surface trenches, open cuts and short adits by the Consolidated Mining and Smelting Company of Canada Ltd. In 1942, the British Columbia Department of Mines conducted 415 m of X-ray di-

amond-drilling (Eastwood, 1965). The property was acquired by H.H. Huestis and associates in 1955 and optioned to Climax Molybdenum Company, who conducted 11 277 m of diamond drilling before the option was dropped in 1960. Noranda Exploration Company Ltd. optioned the property in 1961 and brought it into production in 1965. The mine was in operation from 1965 to 1971, and again from 1974 to 1983. Production was from underground workings and two small open pits. In total, 15 546 034 kg of molybdenum were recovered from 7 588 072 t of ore milled. Current unclassified reserves are listed as 3 838 847 t grading 0.135% Mo (MINFILE, 2006).

The surface geology near the Boss Mountain mine pits was briefly examined during the 2006 field season, but most of the workings are inaccessible. However, detailed descriptions of the mineralization and local geology have been provided by Soregaroli (1968), Soregaroli and Nelson

TABLE 1. GEOCHEMICAL DATA FOR SELECTED ROCK SAMPLES COLLECTED DURING THE 2006 FIELD SEASON.

Element:	Mo	Cu	Pb	Zn	Ag	Ni	Co	As	Sb	Bi	Ba	Hg	Au**	Pt**	Pd**	
Units:	ppm	ppm	ppm	ppm	ppb	ppm	ppm	ppm	ppm	ppm	ppm	ppb	ppb	ppb	ppb	
Lab:	ACM	ACM	ACM	ACM	ACM	ACM	ACM	ACM	ACM	ACM	ACM	ACM	ACM	ACM	ACM	
Method:	ARMS	ARMS	ARMS	ARMS	ARMS	ARMS	ARMS	ARMS	ARMS	ARMS	ARMS	ARMS	FAIC	FAIC	FAIC	
Detection limit:	0.01	0.01	0.01	0.1	2	0.1	0.1	0.1	0.02	0.02	0.5	5	2	2	2	
Field no.	Rock type															
06PSC-12-2	Skarny rock	1.85	102.63	3.63	25	52	5.9	23.3	-0.1	0.19	0.08	56.2	11	16	8	4
06PSC-31	Rusty muscovite-biotite-quartz schist	1.44	41.09	12.67	107.4	110	40.1	16.5	-0.1	0.08	0.28	154.9	5	-2	5	2
06PSC-42	Quartz vein	0.32	9.62	5.54	13	73	2.9	1.8	0.1	0.15	2.4	7.7	8	-2	-3	7
06PSC-56	Silica-rusty carbonate-pyrite-altered rock	0.14	34.46	4.5	75.2	40	62.3	34	6.4	3.66	0.06	26.6	-5	-2	-3	-2
06PSC-71	Quartz vein	0.36	3.02	7.08	13.6	106	7.1	1.3	6	0.24	0.07	8.1	-5	5	4	3
06PSC-73-1	Quartz-ankerite-sericite-mariposite alteration	0.25	41.13	56.09	89.7	434	549.1	56.3	426.9	5.05	0.05	21.2	-5	2	8	4
06PSC-73-2	Quartz vein	0.19	3.97	3.87	9.4	193	13.5	1.6	16.2	0.39	0.02	5.1	5	-2	4	4
06PSC-73-3	Quartz vein	0.15	3.57	5.28	12.5	58	14.2	1.2	13.1	0.28	0.04	6.9	-5	2	3	-2
06PSC-76	Rusty pyritic hornfels	0.35	181.07	8.64	58.8	651	46.1	22.4	11.2	2.76	0.18	223.9	-5	13	8	11
06PSC-77	Rusty hornfels	4.9	152.45	4.04	10.9	1204	15.2	15.4	5.9	0.26	0.6	26.7	13	2121	-3	-2
06PSC-88	Pyritic siltstone	0.71	102.96	8.73	115.4	340	33.1	26	8.9	1.12	0.11	98.5	27	9	4	9
06PSC-99	Rusty fault rock	104.95	127.14	28.48	221.8	1234	45	14	7.7	14.94	0.14	29.2	34	77	9	14
06PSC-100-2	Quartz-pyrite-altered sandstone	1.3	108.65	3.74	36.3	316	14.6	13.8	3.9	4.18	0.16	215.3	-5	12	5	8
06PSC-174	Rusty pyritic rock in fault zone	4.07	79.88	9.15	169.5	306	26.1	15.5	17	3.85	0.07	63.6	117	9	7	9
06PSC-175	Rusty pyritic siltstone	15.58	97.15	8.36	65.7	188	33.3	16.6	4.3	1.65	0.07	59.5	24	4	-3	-2
06PSC-196	Rusty siltstone	2.71	132.19	3.89	93.1	161	17.2	14.9	9.8	0.58	0.17	90.1	40	4	7	13
06PSC-219	Pyritic sandstone	0.53	80.85	2.67	29.1	159	11.2	24	3.1	2.45	0.52	145.8	5	7	-3	-2
06PSC-282	Quartz vein; galena, pyrite	193.24	46.14	6449.6	7	2049	1.8	0.8	0.9	1.35	3.41	17.7	-5	10	-3	-2
06PSC-283	Quartz vein; galena, pyrite	887.73	29.23	2967.27	7.4	1143	3.7	2.4	0.2	0.7	2.46	249.3	10	4	-3	-2
06PSC-284	Quartz vein; galena, pyrite	50.9	12.87	1749.29	5	1320	2	0.6	0.4	0.22	4.38	10.5	6	4	4	4

Analysis of steel milled samples prepared by GSB

Abbreviations: ACM, Acme Analytical, Vancouver, BC; ARMS, aqua regia digestion with ICP-MS finish; FAIC, fire assay with ICP-ES finish

(1976) and Macdonald *et al.* (1995). The ore is hosted in quartz monzodiorite to granodiorite of the Boss Creek unit of the Takomkane batholith, but is related to a small mid-Cretaceous stock of monzogranite, the Boss Mountain Mine stock, that intrudes the batholith. Ore was mined from a system of sheeted quartz veins that forms a concentric zone centred on the southwestern margin of the stock, as well as from spatially associated subvertical breccia pipes. Soregaroli documented multiple episodes of alteration and mineralization associated with episodic diking, breccia formation, and fracture and vein development. He attributed the fracturing, brecciation, alteration and mineralization to multiple pulses of magmatic and hydrothermal pressure emanating from the Boss Mountain Mine stock. Three separate samples of hydrothermal biotite from the mine workings yielded K-Ar dates of 98 ± 4 , 104 ± 4 and 105 ± 4 Ma, respectively (White *et al.*, 1968). These dates are inferred to represent the age of mineralization and of the Boss Mountain Mine stock (Soregaroli and Nelson, 1976). Similar mid-Cretaceous ages have been obtained from the main monzogranite phase of the Raft batholith (Scharizza *et al.*, 2002b), and from the Tintlihohtan Lake stock about 20 km to the south (Soregaroli, 1979). Both of these plutons also host molybdenum mineralization.

Copper Showings near Takomkane Mountain

Mineralized quartz veins and stockworks are known over a fairly large area within the Takomkane batholith near Takomkane Mountain, mainly west and northwest of the Boss Mountain molybdenum mine. The mineralization consists mainly of pyrite and chalcopyrite, and commonly yields significant Au and Ag values. Mineralization was discovered north of Takomkane Mountain prior to 1917, and was briefly described by Galloway (1918) and

Reinecke (1920). Exeter Mines Ltd. staked claims around the known mineralization in 1969 and conducted an exploration program in 1970 that included geological mapping, soil sampling and a VLF-EM survey (Allen, 1970; Mark, 1970). Although no further assessment work was filed by Exeter, a cat trail from the Boss Mountain Mine road to the area of the main showings, old bulldozer trenches, and drillcore located at an old camp all show that some follow-up work was completed (Blann and Ridley, 2005a). The area of the main showings (Silverboss) was restaked by D. Ridley in 1993 and explored with small prospecting, mapping, and rock and soil geochemical programs in 1994, 1995 and 2000 (Ridley, 1994, 1995, 2000b). Additional geological and geochemical work was conducted during the 2004 field season, and the Silverboss claim group was optioned to Happy Creek Minerals Ltd. in December of that year (Blann and Ridley 2005a). Happy Creek Minerals Ltd. staked additional claims and carried out exploration programs on the Silverboss property in 2005 (Blann and Ridley, 2006) and 2006.

The mineralization on the Silverboss property is hosted by the Boss Creek unit of the Takomkane batholith, which ranges in composition from hornblende-biotite quartz monzodiorite to monzodiorite and granodiorite. Much of the *in situ* mineralization occurs in a zone, a little more than 1.5 km long, that extends from the Silverboss showing in the north to the Horse Trail zone in the south (Fig 12). The zone of mineralization may continue at least 2 km farther to the southeast, based on mineralized float samples located during reconnaissance prospecting south of the Boss Mountain mine (Headwall and South Ridge zones of Blann and Ridley, 2005a). The mineralized veins on the Silverboss property commonly occur along fractures and faults that strike either northeast or northwest. The known veins appear to form a partial envelope bounding the Boss Mountain mine workings to the south, west and

northwest. It is suspected that they are distal expressions of the same mineralizing system.

SILVERBOSS (MINFILE 093A 019)

The Silverboss showing is located about 600 m north of Takomkane Mountain. Mineralized quartz veins and lenses occur within a northeast-striking, steeply dipping shear zone, ranging from 1 to 10 m wide, that is exposed intermittently over a strike length of about 350 m (Allen, 1970; Ridley, 1994, 1995; Blann and Ridley, 2006). The mineralized structure is exposed mainly in old (mostly pre-1917) workings that include a water-filled shaft, a southwest-trending adit located 70 m northeast of the shaft, and numerous partially caved pits and trenches. The quartz veins are variably mineralized with pyrite and chalcopyrite, and locally contain arsenopyrite, pyrrhotite, galena, sphalerite, limonite, azurite and malachite (Galloway, 1918; Allen, 1970; Ridley, 1994). Individual veins range up to 30 cm in width and commonly contain vugs that are lined with quartz crystals, with or without sulphide minerals. The quartz monzodiorite within and adjacent to the shear zone is commonly altered with quartz, pyrite, chlorite, epidote and sericite. Chlorite-epidote-altered andesite dikes occur within and adjacent to the Silverboss shear zone, and locally have veins of vuggy quartz, sparsely mineralized with pyrite and chalcopyrite, along their margins (Ridley, 1995). Samples collected by Ridley (1994) show that mineralized material along the full length of the Silverboss structure contains significant concentrations of Au and Ag. The highest Au value came from a trench between the shaft and adit, where a grab sample from a well-mineralized quartz vein, 20 cm wide, contained 9.41 g/t Au, 514.8 g/t Ag and 1.34% Cu (Ridley, 1994, sample SB94-DR15). A 105 cm chip sample that included this vein, as well as sheared plutonic rock and several quartz stringers, returned 1.62 g/t Au, 63.2 g/t Ag and 1503 ppm Cu (sample SB94-DR13).

There are additional mineralized veins and shears documented in the vicinity of the Silverboss showing that are not within the main shear zone (Reinecke, 1920; Ridley, 1995, 2000a, b). One of these, referred to as the East Breccia zone (Ridley, 1995), is located on the east side of the ridge crest about 300 m east of the Silverboss shaft. There, an old blasted trench about 4 m wide forms a north-northwest-trending vertical slot in hornblende-biotite quartz monzodiorite. The east wall of the trench is coincident with the east margin of a zone of mineralized stockwork breccia that strikes 335° and dips about 80° to the east. The mineralized material is seen mainly as loose pieces on the floor of the trench, but some *in situ* mineralization remains along the east wall of the trench. The mineralization comprises a quartz stockwork that separates fragments of intensely chlorite-epidote-altered granitic rock, as well as some dark fragments that may have been derived from a mafic dike. The quartz is mineralized with pyrite, malachite-altered chalcopyrite and some specularite. A grab sample of mineralized breccia from the trench yielded 2.6% Cu, 42 ppm Ag and 1241 ppb Au (Ridley, 1995, sample TAK95-DR12).

DOGTOOTH ZONE

The Dogtooth zone (Blann and Ridley, 2006) is a northeast-striking mineralized shear zone located a short distance east of the Takomkane volcano, and about 950 m southeast of the Silverboss shaft. The shear zone is well exposed for about 35 m along an old (1917 vintage?) exploration trench, but is also recognized elsewhere, for a total

known strike length of about 150 m (Blann and Ridley, 2006). The zone strikes about 050°, is more or less vertical, and ranges from 1 to 5 m wide. The shear zone comprises strongly fractured, variably silicified and chlorite-epidote-sericite-altered quartz monzodiorite containing quartz veins and lenses ranging up to 20 cm in width. The quartz commonly contains vugs lined with limonite-coated quartz crystals, and crystals elsewhere are oriented perpendicular to vein walls to define comb or dogtooth textures. Sulphide minerals are not abundant, but limonite-altered pyrite and some chalcopyrite are present in places. Blann and Ridley (2006) reported that a grab sample collected across 1 m of veined and silicified rock in a pit at the southwest end of the old exploration trench returned 10.06 g/t Au, 26.0 g/t Ag and 643 ppm Cu (sample 185364). An adjacent sample across 2 m of sheared wallrock, containing quartz veins 3 cm and 14 cm wide, returned 4.7 g/t Au, 35.0 g/t Ag and 198 ppm Cu (sample 151704).

HORSE TRAIL ZONE

The Horse Trail zone, discovered by D. Ridley in 2004, is a series of mineralized quartz veins located about 1.5 km south-southeast of the Silverboss shaft. The discovery vein, adjacent to the old horse trail that connected the Boss Mountain molybdenum deposit to Lac La Hache, is about 8 cm wide, dips about 30° to the northeast and contains patches of chlorite, epidote, pyrite and chalcopyrite. The host quartz monzodiorite is altered with chlorite, epidote and tourmaline for 2 to 3 cm adjacent to the vein margins. A grab sample from this vein returned 4238 ppm Cu, 27.9 ppm Ag and 2413 ppb Au (Blann and Ridley, 2005a, sample 151679). Several other mineralized quartz veins occur within an exposure about 100 m south of the discovery vein. These veins range from 6 to 30 cm in width and typically dip steeply to the northeast. They contain epidote, tourmaline, pyrite and chalcopyrite, and some include vugs containing quartz crystals and rusted-out sulphide minerals. A 20 cm chip sample across one of these veins returned 5642 ppm Cu, 43.7 ppm Ag and 791.7 ppb Au (Blann and Ridley, 2005a, sample 151677).

HEADWALL AND SOUTH RIDGE ZONES

The Headwall and South Ridge zones are represented by float samples of vein material from a part of the Silverboss property that has been prospected only at reconnaissance scale (Blann and Ridley, 2005a). At the Headwall zone, vuggy and dogtooth-textured quartz contains pyrite and chalcopyrite. A sample of this material returned 549 ppm Cu, 51.3 ppm Ag and 723 ppb Au, and was also anomalous in Pb, As, Bi and W (Blann and Ridley, 2005a, sample 151797). At the South Ridge zone, narrow parallel quartz veins, 1 to 3 cm wide, contain pyrite, chalcopyrite and traces of molybdenite. A sample of this material returned 1926 ppm Cu, 68 ppm Mo, 17.4 ppm Ag and 149 ppb Au (Blann and Ridley, 2005a, sample 151674). Both the Headwall and the South Ridge samples were collected along east-northeast-striking faults that were mapped by Soregaroli (1968). He mapped a parallel fault 900 m north of the Headwall zone, and two float samples of pyritic quartz collected along this structure, 350 m southeast of the Horse Trail zone, returned 1.91 and 5.55 g/t Au (Blann and Ridley, 2006, samples 185374 and 185375).

Showings North of the Hendrix Stock

The Hen claims were first staked by D. Ridley in 1992, following his discovery of mineralized float on the 6300 logging road. Subsequent exploration led to the discovery of *in situ* mineralization at the Hen and Dyke showings, and additional discoveries of gold-bearing float or subcrop to the north and east (Fig 12; Chick, Ledge and Southeast Skarn showings of Ridley, 1997b). These widespread indications of mineralization prompted staking of a large group of claims, the Hen, Ledge and DL claim groups, that extended from Hendrix Creek eastward to the DL showing near Deception Creek (Ridley, 1997b). This swath of claims covers a prominent system of topographic linears that was interpreted to represent a major east-southeast-striking fault system, and shear zones associated with mineralization at the Hen showing were interpreted as part of this structural zone. The Hendrix stock is also an important mineralizing agent, since the known occurrences (except the DL showing at the east end) are in hornfelsed and skarn-altered rocks on the northern margin of the stock.

HEN

The Hen showing is within green to purplish grey hornfels on the north side of the 6300 logging road, about 1 km east of Hendrix Creek. The hornfels is derived mainly from volcanic sandstone of the Nicola volcanoclastic succession, although coarser volcanic breccia and mafic flow units occur locally. The northern contact of the Hendrix stock is inferred to be a short distance to the south, but is not exposed. The hornfels is cut by numerous east-striking fault and fracture systems that are commonly altered with quartz, actinolite, epidote, garnet, pyrite and pyrrhotite. The main Hen showing, discovered in 1994, is within a trench that exposes several tens of metres of sheared hornfels containing abundant pyrrhotite and veins of quartz and calcite. A zone containing pyrrhotite, arsenopyrite and abundant calcite veins returned 3.98 g/t Au over 2.1 m (Dunn and Ridley, 1994). Two diamond-drill holes angled to the south from north end of the trench intersected this mineralized zone at depth, and one of these holes intersected a separate zone of mineralization farther south, characterized by abundant calcite-quartz stringers, 5% pyrrhotite and up to 2% arsenopyrite. An 8 m core length of this zone averaged 0.86 g/t Au (Dunn and Ridley, 1994). A hole drilled in 1996 intersected gold mineralization that might represent the down-dip extension of the main mineralized zone discovered in 1994. This mineralization is more than 200 m below that exposed in the 1994 trench, and includes a 0.8 m length that returned 2.08 g/t Au (Ridley, 1997a).

DYKE

The Dyke showing is located on the north side of the 6300 logging road, about 1.3 km east-southeast of the Hen showing. It occurs within strongly hornfelsed rock about 30 m northeast of an exposure of biotite-hornblende tonalite that is inferred to form the north margin of the Hendrix stock. Most of the hornfels northeast of the tonalite comprises a medium grey, fine-grained mixture of quartz, biotite, amphibole and plagioclase, locally containing lenses and patches of calcsilicate rock that includes quartz, actinolite, epidote, garnet, biotite and pyrite. The Dyke showing comprises a 4.5 m zone of mainly rusty-weathered, grey-green silicified rock that contains 2 to 5% fine-grained disseminated sulphide minerals. The rusty zone includes some patches of grey nonsilicified hornfels, as well

as two narrow tonalite dikes that dip steeply to the north-northeast. The Dyke showing was discovered in 1997 when a grab sample returned 2640 ppb Au and 2.0 ppm Ag (Ridley, 1997b, sample HEN97-DR29). It was partially exposed by hand trenching in 1998, and a 2 m chip sample across the zone returned 1270 ppb Au and 0.6 ppm Ag (Ridley, 1998, sample HEN98-DR15). A grab sample collected from the rusty zone during our 2006 fieldwork returned 2121 ppb Au and 1.2 ppm Ag (Table 1, sample 06PSC-77).

Fox

The Fox molybdenum-tungsten showing is located in the southeastern part of the Hendrix Lake map area, within the Snowshoe Group on the southern margin of the Deception stock. The area north of the showing was covered by a geological and geochemical exploration program in 1982, which was implemented to follow up a regional geochemical survey that identified anomalous tungsten concentrations in heavy mineral samples in the Deception Creek drainage system (Helson, 1982). The Deception stock, consisting of garnet-bearing two-mica granite, was recognized at this time but not mapped in detail, and soil samples from around the eastern and northern margins of the stock were found to be slightly anomalous in tungsten. D. and C. Ridley located the southern contact of the Deception stock and adjacent skarn alteration in 1997, while prospecting along the newly constructed 7200 logging road. Further prospecting in 1999 led to the discovery of molybdenum-bearing skarn and staking of the Fox mineral claims (Ridley, 2000a). Subsequent work included grid construction, soil geochemical surveys, a ground magnetometer and VLF-EM geophysical survey, and additional prospecting and claim staking. The property was optioned to Happy Creek Minerals Ltd. in December 2004, and an exploration program comprising grid layout, soil and rock geochemical sampling, prospecting and geological mapping was carried out in 2005. This program led to the discovery of the Nightcrawler tungsten zone, 1 km east of the Discovery molybdenum zone (Blann and Ridley, 2005b).

The very sparse bedrock exposure in the vicinity of the Fox showing includes skarn, calcsilicate gneiss, quartz-biotite schist and quartzite, locally cut by aplitic, pegmatitic and granitic dikes. Layering and schistosity show gentle to moderate dips to the southwest. At the Discovery molybdenum zone, subcrop of garnet-epidote-pyroxene skarn, locally with distinct vesuvianite crystals, contains patches, fracture-fillings and disseminations of molybdenite. The Nightcrawler tungsten zone, about 1 km to the east, comprises some subcrop and outcrop, along with many large angular blocks, of scheelite-bearing skarn. Fine to coarse-grained scheelite, as fracture fillings and disseminations, is accompanied locally by traces of chalcopyrite, sphalerite and molybdenite (Blann and Ridley, 2005b). Samples from the Discovery zone have returned up to 4.9% Mo, while those from the Nightcrawler zone contain up to 3.16% W (Blann and Ridley, 2005b). The broad area that encompasses the two zones, more than 1 km long by several hundred metres wide, contains abundant mineralized float and several zones of anomalous tungsten and/or molybdenum in soils.

SUMMARY OF MAIN CONCLUSIONS

The Hendrix Lake map area is underlain mainly by Proterozoic-Paleozoic siliciclastic metasedimentary rocks of the Kootenay Terrane, Late Paleozoic mafic schist of the Slide Mountain Terrane and Middle Triassic to Early Jurassic sedimentary, volcanic and plutonic rocks of the Quesnel Terrane. Younger rocks include a small hornblende granodiorite stock of suspected Jurassic age, several granitic stocks of mid-Cretaceous age and minor amounts of Quaternary basalt.

The main stratigraphic assemblages in the area, representing the Kootenay, Slide Mountain and Quesnel terranes, form a west-southwest-facing homocline that constitutes part of the west limb of the Boss Mountain anticline, a significant map-scale fold that formed during the late stages of a regional structural-metamorphic event of mainly Early to Middle Jurassic age. Studies elsewhere in the region show that the Slide Mountain Terrane, represented by the Crooked amphibolite, was thrust eastward over the Kootenay Terrane, represented by the Snowshoe Group, prior to folding. The Quesnel Terrane, represented mainly by the Nicola Group, may have been deposited stratigraphically above the Slide Mountain Terrane, either before or after east-directed thrusting, but the contact has been the locus of shearing during subsequent structural events.

The Nicola Group in the Hendrix Lake map area includes two major subdivisions. The Lemieux Creek succession forms the eastern part of the group and consists mainly of dark grey phyllite, slate and siltstone. It is assigned a Middle to Late Triassic age based on correlation with dated rocks to the south and north. The volcanoclastic succession forms a wide outcrop belt to the west and consists of massive to well-bedded volcanic sandstone, siltstone and conglomerate, intercalated with pyroxene-rich volcanic breccia units and some mafic flows. It is Late Triassic and/or older because the upper part of the succession is cut by latest Triassic quartz monzodiorite of the Takomkane batholith. Fossils from correlative rocks to the north and south are mainly Late Triassic, but include some Middle Triassic forms near Quesnel Lake.

Intrusive rocks assigned to the Quesnel Terrane include the Takomkane batholith and the Hendrix Lake ultramafic-mafic plutonic complex. The Takomkane batholith comprises the Late Triassic Boss Creek unit of mainly quartz monzodiorite composition (U-Pb zircon age of 202.5 ± 0.5 Ma), undated diorite to quartz diorite of the Buster Lake unit, and Early Jurassic granodiorite to monzogranite of the Schoolhouse Lake unit (U-Pb zircon age of 195.0 ± 0.4 Ma). The poorly exposed Hendrix Lake ultramafic-mafic complex includes pyroxenite, gabbro, diorite and intrusion breccia. It is thought to be Early Jurassic, based on correlation with the lithologically similar Iron Lake and Aqua Creek complexes in the Canim Lake area (hornblende Ar/Ar plateau ages of 187.7 ± 1.1 Ma and 183.0 ± 1.1 Ma, respectively).

Quartz veins mineralized with galena and pyrite in the northeastern part of the area probably formed during Early to Middle Jurassic deformation and metamorphism. Many other mineral occurrences within the Hendrix Lake map area are associated with granitic stocks of mid-Cretaceous age. These include the past-producing Boss Mountain porphyry molybdenum deposit, molybdenum-tungsten skarn showings along the southern margin of the Deception

stock, and gold showings within hornfelsed rocks along the northern margin of the Hendrix stock. Precious-metal-bearing veins and stockworks near Takomkane Mountain, mineralized mainly with pyrite and chalcopyrite, might be distal expressions of the system that generated mineralization at the Boss Mountain mine.

ACKNOWLEDGMENTS

We thank Jean and Mike Peake of Eagle Creek for providing excellent accommodation and hospitality during our fieldwork. Lori Kennedy, Daniel Splawski and Elizabeth Kirkham cheerfully performed spot duty as field assistants, and Bruce Madu provided geological insights during a visit to the field area. We are particularly indebted to Dave Ridley for showing us around many of the mineral showings in the area. We also thank Richard Friedman and Thomas Ullrich for providing radiometric dates that are crucial to this study.

REFERENCES

- Allen, A.R. (1970): Geological survey, Big Timothy Mountain claims, Silver Boss, SB and Gus groups; *BC Ministry of Energy, Mines and Petroleum Resources*, Assessment Report 2513, 12 pages.
- Barker, G. and Bysouth, G. (1990): Geochemical survey on the Cruiser 1 claim group and the Cruiser 3 mineral claim, Cariboo Mining Division, 93A/2; *BC Ministry of Energy, Mines and Petroleum Resources*, Assessment Report 19 512, 5 pages.
- Blann, D. and Ridley, D. (2005a): Geological and geochemical report on the Silverboss property (SB 1-4 mineral claims), Cariboo Mining Division, 093A006/093A016; *BC Ministry of Energy, Mines and Petroleum Resources*, Assessment Report 27 755, 21 pages.
- Blann, D. and Ridley, D. (2005b): Geological and geochemical report on the Fox property, Cariboo Mining Division, 093A008; *BC Ministry of Energy, Mines and Petroleum Resources*, Assessment Report 27 886, 15 pages.
- Blann, D. and Ridley, D. (2006): Geological and geochemical report on the Silverboss property, Cariboo Mining Division, 093A006/093A016; *BC Ministry of Energy, Mines and Petroleum Resources*, Assessment Report 28 344, 25 pages.
- Bloodgood, M.A. (1987): Deformational history, stratigraphic correlations and geochemistry of eastern Quesnel Terrane rocks in the Crooked Lake area, central British Columbia, Canada; unpublished M.Sc. thesis, *University of British Columbia*, Vancouver, BC, 165 pages.
- Bloodgood, M.A. (1990): Geology of the Eureka Peak and Spanish Lake map areas, British Columbia; *BC Ministry of Energy, Mines and Petroleum Resources*, Paper 1990-3, 36 pages.
- Breitsprecher, K. and Mortensen, J.K. (2004): BCAGE 2004A – a database of isotopic age determinations for rock units from British Columbia; *BC Ministry of Energy, Mines and Petroleum Resources*, Open File 2004-3 (Release 3.0), 7757 records, 9.3 Mb.
- Brown, R.L., Journeay, J.M., Lane, L.S., Murphy, D.C. and Rees, C.J. (1986): Obduction, backfolding and piggyback thrusting in the metamorphic hinterland of the southeastern Canadian Cordillera; *Journal of Structural Geology*, volume 8, pages 255–268.
- Bysouth, G.D. (1989): Preliminary geochemical survey on the Cruiser 1 claim group, Cariboo Mining Division, 93A/2; *BC Ministry of Energy, Mines and Petroleum Resources*, Assessment Report 19 160, 6 pages.

- Campbell, K.V. (1971): Metamorphic petrology and structural geology of the Crooked Lake area, Cariboo Mountains, British Columbia; unpublished Ph.D. thesis, *University of Washington*, Seattle, WA, 192 pages.
- Campbell, R.B. (1978): Quesnel Lake, British Columbia; *Geological Survey of Canada*, Open File Map 574.
- Campbell, R.B., Mountjoy, E.W. and Young, F.G. (1973): Geology of McBride map-area, British Columbia; *Geological Survey of Canada*, Paper 72-35, 104 pages.
- Campbell, R.B. and Tipper, H.W. (1971): Bonaparte Lake map area, British Columbia; *Geological Survey of Canada*, Memoir 363, 100 pages.
- Carye, J.A. (1986): Structural geology of part of the Crooked Lake area, Quesnel Highlands, British Columbia; unpublished M.Sc. thesis, *University of British Columbia*, Vancouver, BC, 154 pages.
- Colpron, M. and Price, R.A. (1995): Tectonic significance of the Kootenay terrane, southeastern Canadian Cordillera: an alternative model; *Geology*, volume 23, pages 25–28.
- Dawson, G.M. (1879): Preliminary report on the physical and geological features of the southern portion of the interior of British Columbia; in Report of Progress, 1877–1878, Part B, *Geological Survey of Canada*, pages 1B–187B.
- Dunn, D.St.C. and Ridley, D.W. (1994): Report on a geological, geochemical, trenching and drilling program on the Hen group (Hen 5–19 mineral claims), Cariboo Mining Division, NTS 93A/2; *BC Ministry of Energy, Mines and Petroleum Resources*, Assessment Report 23 770, 8 pages.
- Eastwood, G.E.P. (1965): Boss Mountain; in Annual Report of the BC Minister of Mines for 1964; *BC Ministry of Energy, Mines and Petroleum Resources*, pages 65–80.
- Ewing, T.E. (1980): Paleogene tectonic evolution of the Pacific Northwest; *Journal of Geology*, volume 88, pages 619–638.
- Ferri, F. (1997): Nina Creek Group and Lay Range Assemblage, north-central British Columbia: remnants of late Paleozoic oceanic and arc terranes; *Canadian Journal of Earth Sciences*, volume 34, pages 854–874.
- Ferri, F. and Melville, D.M. (1994): Bedrock geology of the Germansen Landing – Manson Creek area, British Columbia (94N/9, 10, 15; 94C/2); *BC Ministry of Energy, Mines and Petroleum Resources*, Bulletin 91, 147 pages.
- Ferri, F. and Schiarizza, P. (2006): Re-interpretation of Snowshoe Group stratigraphy across a southwest-verging nappe structure and its implications for regional correlations within the Kootenay terrane; in Paleozoic Evolution and Metallogeny of Pericratonic Terranes at the Ancient Pacific Margin of North America, Canadian and Alaskan Cordillera, Colpron, M. and Nelson, J., Editors, *Geological Association of Canada*, Special Paper 45, pages 415–432.
- Fiesinger, D.W. and Nicholls, J. (1977): Petrography and petrology of Quaternary volcanic rocks, Quesnel Lake region, east-central British Columbia; in Volcanic Regimes in Canada, Baragar, W.R.A., Coleman, L.C. and Hall, J.M., Editors, *Geological Association of Canada*, Special Paper 16, pages 25–38.
- Fillipone, J.A. (1985): Structure and metamorphism at the western margin of the Omineca Belt near Boss Mountain, east-central British Columbia; unpublished M.Sc. thesis, *University of British Columbia*, Vancouver, BC, 150 pages.
- Fillipone, J.A. and Ross, J.V. (1990): Deformation of the western margin of the Omineca Belt near Crooked Lake, east-central British Columbia; *Canadian Journal of Earth Sciences*, volume 27, pages 414–425.
- Galloway, J.D. (1918): Timothy Mountain; in Annual Report of the Minister of Mines for 1917, *BC Ministry of Energy, Mines and Petroleum Resources*, pages F134–F136.
- Helson, J. (1982): Quesnel project, Jezebel claims group, geochemistry and geology, report #2, Cariboo Mining Division, NTS 93A/2; *BC Ministry of Energy, Mines and Petroleum Resources*, Assessment Report 10 641, 7 pages.
- Hickson, C.J. and Souther, J.G. (1984): Late Cenozoic volcanic rocks of the Clearwater – Wells Gray area, British Columbia; *Canadian Journal of Earth Sciences*, volume 21, pages 267–277.
- Holland, S.S. (1954): Geology of the Yanks Peak – Roundtop Mountain area, Cariboo District, British Columbia; *BC Ministry of Energy, Mines and Petroleum Resources*, Bulletin 34, 102 pages.
- Logan, J.M. (2002): Intrusion-related mineral occurrences of the Cretaceous Bayonne Magmatic Belt, southeast British Columbia; *BC Ministry of Energy, Mines and Petroleum Resources*, Geoscience Map 2002-1.
- Logan, J.M. and Mihalynuk, M.G. (2005): Porphyry Cu-Au deposits of the Iron Mask batholith, southeastern British Columbia; in Geological Fieldwork 2004, *BC Ministry of Energy, Mines and Petroleum Resources*, Paper 2005-1, pages 271–290.
- Lowdon, J.A. (1963): Isotopic ages; in Age Determinations and Geological Studies: Report 4, *Geological Survey of Canada*, Paper 63-17, pages 5–121.
- Macdonald, A.J., Spooner, E.T.C. and Lee, G. (1995): The Boss Mountain molybdenum deposit, central British Columbia; in Porphyry Deposits of the Northwestern Cordillera of North America, Schroeter, T.G., Editor, *Canadian Institute of Mining, Metallurgy and Petroleum*, Special Volume 46, pages 691–696.
- Mark, D.G. (1970): Geophysical-geochemical report, Silver Boss, SB and Gus claims, Hendrix Lake area, Cariboo Mining District, BC; *BC Ministry of Energy, Mines and Petroleum Resources*, Assessment Report 2785, 20 pages.
- McMullin, D.W.A., Greenwood, H.J. and Ross, J.V. (1990): Pebbles from Barkerville and Slide Mountain terranes in a Quesnel terrane conglomerate: evidence for pre-Jurassic deformation of the Barkerville and Slide Mountain terranes; *Geology*, volume 18, pages 962–965.
- MINFILE (2006): MINFILE BC mineral deposits database; *BC Ministry of Energy, Mines and Petroleum Resources*, URL <<http://www.em.gov.bc.ca/Mining/GeolSurv/Minfile/>> [December 2006].
- Montgomery, S.L. (1978): Structural and metamorphic history of the Lake Dunford map area, Cariboo Mountains, British Columbia: ophiolite obduction in the southeastern Canadian Cordillera; unpublished M.Sc. thesis, *Cornell University*, Ithaca, NY, 170 pages.
- Mortensen, J.K., Montgomery, J.R. and Phillipone, J. (1987): U-Pb zircon, monazite and sphene ages for granitic orthogneiss of the Barkerville terrane, east-central British Columbia; *Canadian Journal of Earth Sciences*, volume 24, pages 1261–1266.
- Mortimer, N. (1987): The Nicola Group: Late Triassic and Early Jurassic subduction-related volcanism in British Columbia; *Canadian Journal of Earth Sciences*, volume 24, pages 2521–2536.
- Murphy, D.C., van der Heyden, P., Parrish, R.R., Klepacki, D.W., McMillan, W., Struik, L.C. and Gabites, J. (1995): New geochronological constraints on Jurassic deformation of the western edge of North America, southeastern Canadian Cordillera; in Jurassic Magmatism and Tectonics of the North American Cordillera, Miller, D.M. and Busby, C., Editors, *Geological Society of America*, Special Paper 299, pages 159–171.
- Nelson, J.L. and Bellefontaine, K.A. (1996): The geology and mineral deposits of north-central Quesnellia; Tezzeron Lake to Discovery Creek, central British Columbia; *BC Ministry of Energy, Mines and Petroleum Resources*, Bulletin 99, 112 pages.

- Panteleyev, A., Bailey, D.G., Bloodgood, M.A. and Hancock, K.D. (1996): Geology and mineral deposits of the Quesnel River – Horsefly map area, central Quesnel Trough, British Columbia; *BC Ministry of Energy, Mines and Petroleum Resources*, Bulletin 97, 155 pages.
- Preto, V.A. (1977): The Nicola Group: Mesozoic volcanism related to rifting in southern British Columbia; in *Volcanic Regimes in Canada*, W.R.A. Baragar, L.C. Coleman and J.M. Hall, Editors, *Geological Association of Canada*, Special Paper 16, pages 39–57.
- Preto, V.A. (1979): Geology of the Nicola Group between Merritt and Princeton; *BC Ministry of Energy, Mines and Petroleum Resources*, Bulletin 69, 90 pages.
- Rees, C.J. (1987): The Intermontane-Omineca belt boundary in the Quesnel Lake area, east-central British Columbia: tectonic implications based on geology, structure and paleomagnetism; unpublished Ph.D. thesis, *Carleton University*, Ottawa, ON, 421 pages.
- Reinecke, L. (1920): Mineral deposits between Lillooet and Prince George, British Columbia; *Geological Survey of Canada*, Memoir 118, 129 pages.
- Ridley, D.W. (1994): Prospecting report on the Silverboss Group (S.B. 1–6 and Peridot 1–2 mineral claims), Cariboo Mining Division, NTS 93A/2W; *BC Ministry of Energy, Mines and Petroleum Resources*, Assessment Report 23 677, 14 pages.
- Ridley, D.W. (1995): Geological and geochemical report on the Silverboss Group (S.B. 1–6 and Peridot 1–2 mineral claims), Big Timothy (Takomkane) Mountain area, Cariboo Mining Division, NTS 93A/2W; *BC Ministry of Energy, Mines and Petroleum Resources*, Assessment Report 24 208, 19 pages.
- Ridley, D.W. (1997a): Geophysical and diamond drilling report on the Hen-Ledge-DL claim groups, Mt. Hendrix area, Cariboo Mining Division, NTS 93A/2E&W; *BC Ministry of Energy, Mines and Petroleum Resources*, Assessment Report 25 056, 14 pages.
- Ridley, D.W. (1997b): Geological and geochemical report on the Hen-Ledge-DL claim groups, Mt. Hendrix area, Cariboo Mining Division, NTS 93A/2E&W; *BC Ministry of Energy, Mines and Petroleum Resources*, Assessment Report 25 575, 22 pages.
- Ridley, D.W. (1998): Geological, geochemical and geophysical report on the Hen project (Hen 5–19, Ledge 1, Skarn 1–4 mineral claims), Mt. Hendrix area, Cariboo Mining Division, NTS 93A/2E&W; *BC Ministry of Energy, Mines and Petroleum Resources*, Assessment Report 25 876, 24 pages.
- Ridley, D.W. (2000a): Prospecting report on the Fox 1–4 two-post mineral claims, Deception Creek area, Cariboo Mining Division, NTS 93A/2E; *BC Ministry of Energy, Mines and Petroleum Resources*, Assessment Report 26 275, 7 pages.
- Ridley, D.W. (2000b): Geological and geochemical report on the Silverboss Group (S.B. 1–4; Peridot 2 mineral claims), Big Timothy (Takomkane) Mountain area, Cariboo Mining Division, NTS 93A/2W; *BC Ministry of Energy, Mines and Petroleum Resources*, Assessment Report 26 411, 12 pages.
- Roback, R.C., Sevigny, J.H. and Walker, N.W. (1994): Tectonic setting of the Slide Mountain terrane, southern British Columbia; *Tectonics*, volume 13, pages 1242–1258.
- Ross, J.V., Fillipone, J., Montgomery, J.R., Elsby, D.C. and Bloodgood, M. (1985): Geometry of a convergent zone, central British Columbia, Canada; *Tectonophysics*, volume 119, page 285–297.
- Schiarizza, P. (1989): Structural and stratigraphic relationships between the Fennell Formation and Eagle Bay Assemblage, western Omineca Belt, south-central British Columbia: implications for Paleozoic tectonics along the paleocontinental margin of western North America; unpublished M.Sc. thesis, *University of Calgary*, Calgary, AB, 343 pages.
- Schiarizza, P. and Boulton, A. (2006a): Geology and mineral occurrences of the Quesnel Terrane, Canim Lake area (NTS 092P/15), south-central British Columbia; in *Geological Fieldwork 2005*, *British Columbia Ministry of Energy, Mines and Petroleum Resources*, Paper 2006-1, pages 163–184.
- Schiarizza, P. and Boulton, A. (2006b): Geology of the Canim Lake area, NTS 92P/15; *British Columbia Ministry of Energy, Mines and Petroleum Resources*, Open File 2006-8, 1:50 000 scale.
- Schiarizza, P., Heffernan, S. and Zuber, J. (2002a): Geology of Quesnel and Slide Mountain terranes west of Clearwater, south-central British Columbia (92P/9, 10, 15, 16); in *Geological Fieldwork 2001*, *BC Ministry of Energy, Mines and Petroleum Resources*, Paper 2002-1, pages 83–108.
- Schiarizza, P., Heffernan, S., Israel, S. and Zuber J. (2002b): Geology of the Clearwater – Bowers Lake area, British Columbia (NTS 92P/9, 10, 15, 16); *BC Ministry of Energy, Mines and Petroleum Resources*, Open File 2002-15, 1:50 000 scale.
- Schiarizza, P. and Israel, S. (2001): Geology and mineral occurrences of the Nehalliston Plateau, south-central British Columbia (92P/7, 8, 9, 10); in *Geological Fieldwork 2000*, *BC Ministry of Energy, Mines and Petroleum Resources*, Paper 2001-1, pages 1–30.
- Schiarizza, P., Israel, S., Heffernan, S. and Zuber, J. (2002c): Geology of the Nehalliston Plateau (92P/7, 8, 9, 10); *BC Ministry of Energy, Mines and Petroleum Resources*, Open File 2002-4, 1:50 000 scale.
- Schiarizza, P. and Preto, V.A. (1987): Geology of the Adams Plateau – Clearwater – Vavenby area; *BC Ministry of Energy, Mines and Petroleum Resources*, Paper 1987-2, 88 pages.
- Schiarizza, P. and Tan, S.H. (2005): Geology and mineral occurrences of the Quesnel Terrane between the Mesilinka River and Wrede Creek (NTS 94D/8, 9), north-central British Columbia; in *Geological Fieldwork 2004*, *BC Ministry of Energy, Mines and Petroleum Resources*, Paper 2005-1, pages 109–130.
- Soregaroli, A.E. (1968): Geology of the Boss Mountain mine, British Columbia; unpublished Ph.D. thesis, *University of British Columbia*, Vancouver, BC, 198 pages.
- Soregaroli, A.E. (1979): K-Ar radiometric dates, Anticlimax molybdenum prospect; in *Age Determinations and Geological Studies, K-Ar Isotopic Ages: Report 14*, *Geological Survey of Canada*, Paper 79-2, page 17.
- Soregaroli, A.E. and Nelson, W.I. (1976): Boss Mountain; in *Porphyry Deposits of the Canadian Cordillera*, Sutherland Brown, A., Editor, *Canadian Institute of Mining and Metallurgy*, Special Volume 15, pages 432–443.
- Struik, L.C. (1982): Bedrock geology of Cariboo Lake (93A/14), Spectacle Lake (93H/3), Swift River (93A/13) and Wells (93H/4) map areas; *Geological Survey of Canada*, Open File 858.
- Struik, L.C. (1985): Pre-Cretaceous terranes and their thrust and strike-slip contacts, Prince George (east half) and McBride (west half), British Columbia; in *Current Research, Part A*, *Geological Survey of Canada*, Paper 85-1A, pages 267–272.
- Struik, L.C. (1986): Imbricated terranes of the Cariboo gold belt with correlations and implications for tectonics in southeastern British Columbia; *Canadian Journal of Earth Sciences*, volume 23, pages 1047–1061.
- Struik, L.C. (1987): The ancient western North American margin: an Alpine rift model for the east-central Canadian Cordillera; *Geological Survey of Canada*, Paper 87-15, 19 pages.
- Struik, L.C. (1988a): Crustal evolution of the eastern Canadian Cordillera; *Tectonics*, volume 7, pages 727–747.
- Struik, L.C. (1988b): Regional imbrication within Quesnel Terrane, central British Columbia, as suggested by conodont ages; *Canadian Journal of Earth Sciences*, volume 25, pages 1608–1617.

- Struik, L.C. (1988c): Structural geology of the Cariboo Gold Mining District, east-central British Columbia; *Geological Survey of Canada*, Memoir 421, 100 pages.
- Struik, L.C. and Orchard, M.J. (1985): Late Paleozoic conodonts from ribbon chert delineate imbricate thrusts within the Antler Formation of the Slide Mountain terrane, central British Columbia; *Geology*, volume 13, pages 794–798.
- Struik, L.C., Parrish, R.R. and Gerasimoff, M.D. (1992): Geology and age of the Naver and Ste Marie plutons, central British Columbia; in *Radiogenic Age and Isotopic Studies: Report 5, Geological Survey of Canada*, Paper 91-2, pages 155–162.
- Sutherland Brown, A. (1958): Boss Mountain; in *Annual Report of the Minister of Mines for 1957, BC Ministry of Energy, Mines and Petroleum Resources*, pages 18–22.
- Thompson, R.I., Glombick, P., Erdmer, P., Heaman, L.M., Lemieux, Y. and Daughtry, K.L. (2006): Evolution of the ancestral Pacific margin, southern Canadian Cordillera: insights from new geologic maps; in *Paleozoic Evolution and Metallogeny of Pericratonic Terranes at the Ancient Pacific Margin of North America, Canadian and Alaskan Cordillera*, Colpron, M. and Nelson, J., Editors, *Geological Association of Canada*, Special Paper 45, pages 433–482.
- Travers, W.B. (1978): Overtuned Nicola and Ashcroft strata and their relations to the Cache Creek Group, southwestern Intermontane Belt, British Columbia; *Canadian Journal of Earth Sciences*, volume 15, pages 99–116.
- Unterschutz, J.L.E., Creaser, R.A., Erdmer, P., Thompson, R.I. and Daughtry, K.L. (2002): North American margin origin of Quesnel terrane strata in the southern Canadian Cordillera: inferences from geochemical and Nd isotopic characteristics of Triassic metasedimentary rocks; *Geological Society of America Bulletin*, volume 114, pages 462–475.
- White, W.H., Harakal, J.E. and Carter, N.C. (1968): Potassium-argon ages of some ore deposits in British Columbia; *Canadian Institute of Mining and Metallurgy Bulletin*, volume 61, pages 1326–1334.
- Whiteaker, R.J., Mortensen, J.K. and Friedman, R.M. (1998): U-Pb geochronology, Pb isotopic signatures and geochemistry of an Early Jurassic alkalic porphyry system near Lac La Hache, BC; in *Geological Fieldwork 1997, BC Ministry of Energy, Mines and Petroleum Resources*, Paper 1998-1, pages 33-1–33-13.

Selected Industrial Minerals Trends in British Columbia, 2006

by G.J. Simandl

KEYWORDS: industrial minerals, aggregate, cement, trends, British Columbia

INVESTMENT CLIMATE

British Columbia has significant potential and opportunity for new industrial minerals exploration and development. Industrial minerals are less vulnerable than metals to abrupt commodity price swings related to global economic cycles. Nevertheless, such cycles do influence supply and demand for industrial minerals, including construction materials. The following discussion highlights some aspects relevant to successful development of industrial minerals deposits in the province. BC's infrastructure, its industrial minerals endowment, exploration and development trends, and initiatives, which could benefit developers, are reviewed, as well as current production levels and new development opportunities.

Decisions regarding coal-fired electrical generation and possible new developments surrounding offshore oil and gas resources may have important effects on the province's industrial minerals markets.

INFRASTRUCTURE

Industrial minerals are an increasingly significant component of international trade. BC is strategically located on the west coast of North America (Fig 1) with easy access, particularly to Pacific Rim countries. It has a well-developed transportation and industrial infrastructure in the southern third of the province, where population and industry are concentrated. It has several deepwater ports and well-maintained all-weather highway systems that permit efficient, long-distance trucking. Rail lines link BC's industrial centres to terminal points across Canada and the United States. The province has a significant and underdeveloped industrial minerals potential.

INDUSTRIAL MINERALS PRODUCTION AND UNTAPPED RESOURCES

BC's nonmetal production for 2006 is estimated at over \$676.3 million. This is considered a conservative projection based on 2005 estimates published by Natural Resources Canada in combination with 2006 growth rates and cost increases reported in the United States. Cement pro-



Figure 1. Strategic geographic location of British Columbia.

duction for 2006 is estimated at \$323.7 million, sand and aggregate at \$191.9 million, stone at \$78.3 million and all other industrial minerals combined for \$82.4 million. Natural Resources Canada does not provide a detailed breakdown due to confidentiality issues, but takes extra care to ensure nonduplication of the statistics, for example, limestone used for chemical applications will be part of the \$82.4 million and will not be counted also as crushed rock or cement raw material. In terms of sulphur production, there were 853 820 tonnes of sulphur produced in BC in 2005 at an estimated average price at the plant gate of \$41.26/t, therefore sulphur alone would have accounted for more than \$35.2 million of the 2005 nonmetal production. BC's sulphur production for 2006 will be similar to that of 2005 in terms of tonnage, but its dollar value will likely be lower reflecting a decrease in sulphur prices during 2006.

Apart from raw materials used for cement production, aggregate, crushed stone and sulphur, the most economically significant industrial minerals commodities produced in BC are magnesite, white calcium carbonate, limestone, silica, dimension stone and gypsum. Commodities produced in lesser quantities include jade (nephrite), magnetite, dolomite, barite, volcanic cinder, pumice, dimension stone (including flagstone and ornamental stones), clay and related high-alumina products used in applications other than cement, tufa, slag, fuller's earth and zeolites. There are

This publication is also available, free of charge, as colour digital files in Adobe Acrobat® PDF format from the BC Ministry of Energy, Mines and Petroleum Resources website at http://www.em.gov.bc.ca/Mining/Geosurv/Publications/catalog/cat_fldwk.htm



Figure 2. Selected industrial minerals mines in British Columbia.

more than 40 mines or quarries and at least 20 major sites where upgrading of industrial minerals into value-added products takes place (Simandl *et al.*, 2004). Although the value of industrial minerals pales in comparison to the value of BC's gas and coal production (Schroeter *et al.*, 2006), these minerals are essential for chemical, electronic, glass, pulp and paper, and refractory industries and coal processing. Selected industrial minerals mining operations, except for aggregate operations, are shown on Figure 2, and processing plants are depicted on Figure 3. Most operations are concentrated close to existing infrastructure and markets.

The most recent review of industrial minerals production in BC was produced by Simandl *et al.* (2004). Major sand and gravel operations are listed on the website of the British Columbia Aggregate Producers Association <http://www.gravelbc.ca/members/member_list.html>.

DEPOSITS AND GEOLOGICAL POTENTIAL

BC has excellent geological potential to host a variety of industrial minerals. There are over 40 industrial minerals

commodities recognized for the province (Simandl *et al.*, 2004) and there are over 2400 industrial minerals occurrences documented in the MINFILE database (MINFILE, 2006). MINFILE is available free of charge from the ministry website at <<http://www.em.gov.bc.ca/Mining/Geolsurv/Minfile/>>. The website also contains selected technical papers describing specific industrial minerals commodities and deposits (<http://www.em.gov.bc.ca/Mining/Geolsurv/IndustrialMinerals/default.htm>).

Deposit types directly applicable to BC have been listed and classified by Simandl *et al.* (1999). The same document also contains selected industrial minerals and gemstone descriptive deposit profiles.

INITIATIVES

The BC Geological Survey directly supports industrial minerals research and developments with its field programs, participation in meetings related to industrial minerals and other activities. In addition, there are a number of government initiatives available to industrial minerals developers, including the BC Mining Exploration Tax Credit Program, the federal government's flow-through share program and the Geoscience BC program. Geoscience BC (<http://www.geosciencebc.com>) funds

appropriate applied geoscience within the province and periodically invites proposals from the public, universities and industry. The BC Ministry of Energy, Mines and Petroleum Resources has a specialist available to assist in planning programs related to industrial minerals and developments.

EXISTING AND EMERGING TRENDS

The following material identifies some of the more significant trends affecting the province's industrial minerals industry.

China Syndrome

Until recently, China dominated industrial minerals export markets and kept consolidating its influence. China's strength is due to the combination of inexpensive labour and energy, lack of costly environmental restrictions, government encouragements driven by the need for hard currencies, and local availability of extensive natural resources. Over the last ten years, unprecedented industrial expansion has taken place in China driven by its access to

markets in industrialized countries and by rapid expansion of its own infrastructure and industrial capacity.

The strength of the Chinese economy is a driving force behind the price increases of iron ore and base metals, however, it also has effects on industrial minerals economics. For example, Chinese domestic demand for fluorite and hydrofluoric acid increased dramatically over the last two years and this led directly to reductions in Chinese fluorspar exports, presenting a market opportunity for western fluorite producers and opened the opportunity for developing new deposits outside of China. The Chinese government had also started to address the new and previously existing environmental challenges related to resource development and value-added processing. As a result, several small magnesium metal, magnesia, ferrosilicon and silicon metal producing plants in China were forced to close.

BC has important magnesite resources (Simandl, 2002b) but their development is still hampered by inexpensive magnesia and magnesium metal exports from China. China does not report reserves in accordance with Canada's National Instrument 43-101, and therefore the reported Chinese reserves are likely overestimated. Also, on the positive side, a number of magnesia-based construction materials are being introduced into the North American market and although most of these products are sourced in China, there is a possibility of new production out of BC.

BC also has important lump silica (quartzite) deposits, which used to supply the currently closed silicon metal and ferrosilicon producers in the United States. Should the Chinese influence in this domain decline over the next few years, BC's silica suppliers may benefit from the start-up of United States silicon metal and ferrosilicon operations.

Exports of Chinese raw talc were halted to avoid antidumping penalties and to help attract foreign investment needed for value-added processing. In the long-term, this may have a positive effect on the economic potential for BC's talc resources. Similar reasoning may apply to other commodities.

China's rapid growth can't continue indefinitely. As the country becomes more industrialized and the standard of living increases, availability of inexpensive energy resources which could be allocated to industry will shrink. The first manifestations that indicate that China has already reached this stage are surfacing. In November 2006, China introduced a 10% tax on selected silicon metal products. In addition, in late November 2006, there have been suggestions that China may start to implement a new export tax (5 and 15%) on magnesium and silicon in early 2007. The apparent objective of this tax is to reduce internal industrial energy requirements and to moderate exports of highly energy-intensive products.

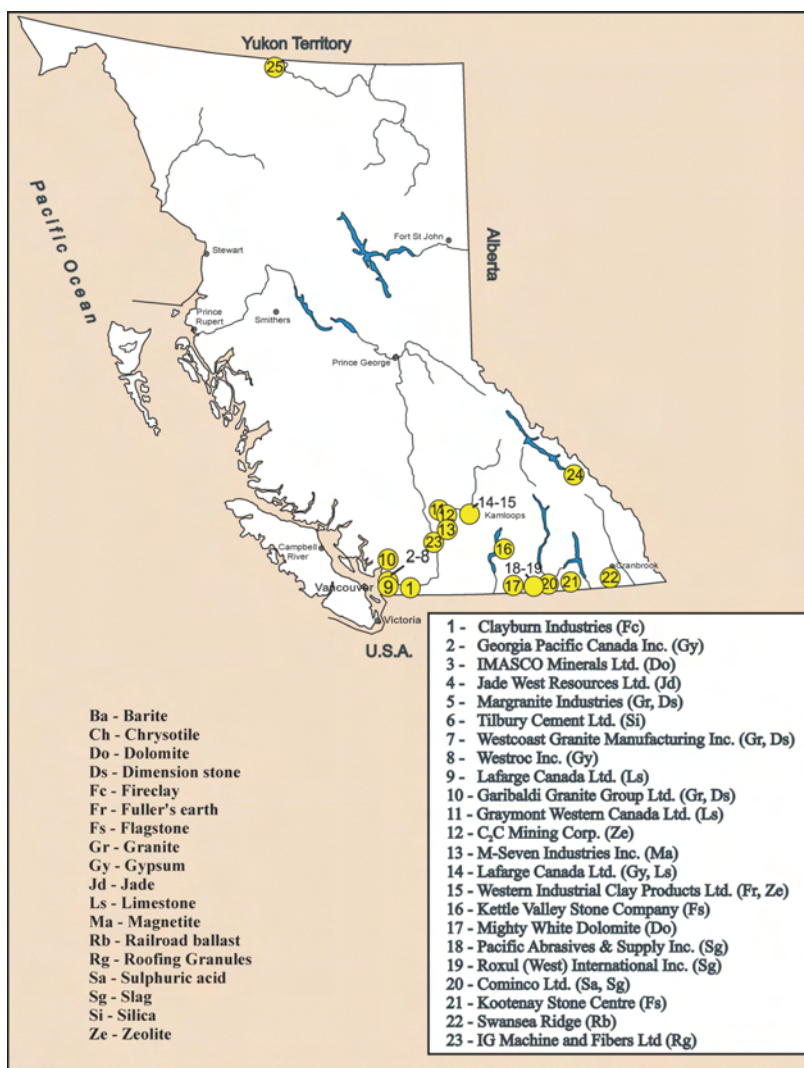


Figure 3. Selected industrial minerals processing plants in British Columbia.

Value-Added Processing

Another important trend, which propagated into BC in the 1990s, is the increase in value-added processing of industrial minerals. The process of turning raw materials into more highly sought after finished products results in a price per tonne increase of several times.

Examples from BC include the IG Machine & Fibers Ltd. (a subsidiary of IKO Industries Ltd.) roofing granule plant, located in the Ashcroft area of BC. This plant was constructed in 2001 with the intention to gradually ramp-up production. In mid-July 2002, it reached 50% of its capacity of 500 000 tonnes and currently it is running at over 70% of its designed capacity. While the raw material is a relatively common rock of basaltic composition, granules produced from that rock are exported to IKO's roof tile manufacturing plants all over western North America.

In addition, the rockwool (thermal insulation) plant located in Grand Forks is a focus of continuous investment by Roxul (West) International Inc. and recently reached full production capacity. Raw materials used by Roxul are low-cost industrial minerals such as dolomite, diorite rock and

even mine wastes such as slag, while the highly priced thermal insulation (end product) is exported internationally.

Green Minerals

New opportunities are arising in the field of ‘green’ minerals along the west coast. Green minerals are those that can be used in environmental clean-up, agriculture, waste disposal or otherwise to improve the environment. Depending on specifications, some of these deposits could supply material for linings and barriers in waste disposal applications. Use of lime, caustic magnesia, dolomitic lime and limestone for environmental rehabilitation and soil conditioning is slowly rising but it is partially balanced by a decline in demand from the pulp and paper industry within the province. Zeolites, bentonite, perlite and vermiculite are examples of other minerals with environmental applications (Simandl, 2003).

The Impact of Clean Coal Technology

Over the last 20 years, BC gradually changed from a large electricity exporter to a net electricity importer. BC currently produces approximately 27 million tonnes of coal annually, with a value of \$2 billion and most of it is exported (Schroeter *et al.*, 2006). Recent developments in clean coal technology (Australian Coal Association, 2006) make the use of coal in BC one of the possible options to make the province self-sufficient in electricity.

This year, BC Hydro awarded 38 contracts, aimed to add 7000 GW·h/a to its system by 2010. The contracts include 29 hydro, three wind, two biomass, two waste heat and two coal-biomass projects.

The proposed AESWapiti Energy Corporation’s coal-biomass project is near Tumbler Ridge with a projected capacity of 196 MW with total energy production of 702 GW·h/a. Compliance Power Corporation’s project (Princeton Power Project) is smaller, with a plant capacity of 56 MW and total energy production of 421 GW·h/a.

Flue gas released during electricity generation in a modern coal-fired plant goes through a complex system which extracts particulate emissions, produces fly ash and converts sulphur emissions into gypsum or similar products. Flue gas desulphurization (FGD) gypsum, bottom ash and fly ash are commonly recovered and used in the construction industry or other applications in the United States and Europe. Figure 4 illustrates the process and quantities of limestone, fly ash and gypsum involved (Pearson, 1998; Simandl, 2003). Fly ash could be an excellent and inexpensive raw material for cement, and FGD gypsum is a substitute for the natural gypsum used in wallboard and cement applications. In the future, in more advanced systems, sulphur may be recovered in its elemental form rather than as gypsum. If coal is used for electricity generation in BC, these artificial materials could significantly reduce the market for natural gypsum and some of the raw materials currently mined for making cement. On the positive side, calcium carbonate, lime or magnesia are needed to extract sulphur from the flue gas (Simandl, 2003), unless the flue gases are stored underground (Vormeij and Simandl, 2004).

Similarly, if the recently proposed gas-burning, electrical generating plant proposed for Red Deer, Alberta, goes into production, it may reduce demand for exports of BC’s natural gypsum to Alberta. If the objectives of the US

Department of Energy (2006) are achieved, by 2020 virtually 100% of products generated by clean, coal-fired, electrical plants will be used in industrial or construction applications. The same standards will likely apply in Canada.

CONSTRUCTION RAW MATERIALS

The construction industry in North America is booming and demand for construction materials is rising. Concrete, one of the most widely used construction materials, consists of a mixture of aggregate (crushed rock or natural), sand and cement.

Sand, Gravel and Crushed Rock

Over the last seven to twelve years, during the deep downturn in metal prices, several junior mining companies started to look at alternative exploration and development targets including industrial minerals. Some juniors concentrated their efforts on what was recognized as a looming shortage of aggregate materials and one of the most significant industrial minerals trends in BC, the export of crushed stone and natural aggregate to urban centres along the west coast of the United States and lower mainland of BC, was born. The report of the Aggregate Advisory Panel (2001) summarized and highlighted the need for long-term aggregate resource planning and added credibility to a number of aggregate projects promoted by junior mining companies looking for public financing. The demand for aggregates and crushed stone has further increased since 2001 and California and the lower mainland of BC still represent major markets. However, these markets may become very competitive. Currently, several junior companies are advancing their crushed stone and aggregate projects simultaneously and at the same time existing producers along coastal North America are increasing their capacity. It remains to be determined if in the short to mid-term, aggregate markets can support all of the proposed projects in various stages of development within BC, Mexico and elsewhere. Correction in the construction market, combined with an increased production capacity may have an adverse effect on aggregate and crushed stone prices and negatively affect the viability of some of these new projects.

Polaris Minerals Corporation, in cooperation with Namgis First Nation, is currently developing their Orca

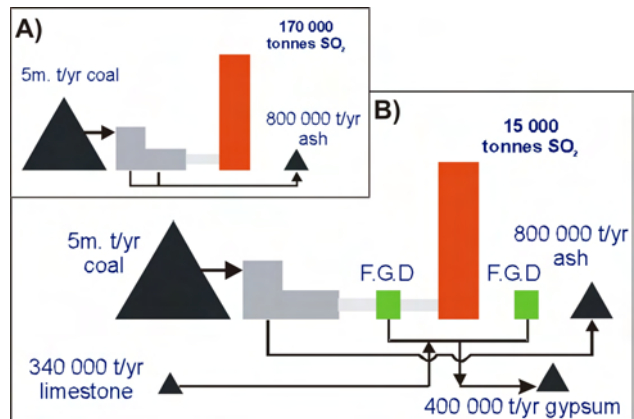


Figure 4. Flue gas desulphurization (FGD) concept (modified from Pearson, 1998; Simandl, 2003).

project located 3.8 km from Port McNeil. This aggregate deposit is believed to have reserves of 121 million tonnes and there is a planned production capacity of 6 million tonnes per year. The project requires US\$94.5 million development capital for the quarry and for the Richmond, California, terminal.

Ascot Resources Ltd. was granted a permit which allows it to begin development of its Swamp Point aggregate deposit located 50 km south of Stewart. Construction for the first phase of production started in October 2006. The company indicates that they have 18 years of reserves at a maximum capacity of 3.3 million tonnes per year. Reported capital cost of the project is \$27.5 million.

Currently there are at least 20 other aggregate sites in the permitting process in BC. These include both new projects as well as established producers increasing their reserves and production capacity.

Newcomers to the aggregate market have to compete with well established producers that work hard to keep a competitive advantage. For example, Texada Quarrying Ltd. is currently Canada's biggest aggregate operation. The company spent \$2.5 million in 2006 just on two large hauling trucks and an excavator. By 2007, Texada Quarrying plans to optimize its transloading capacity and to provide efficient service to clients such as Quinsam Coal Corporation and some of the sand and gravel operations. Canada's second largest aggregate producer, Construction Aggregates Ltd.'s Sechelt also invested to increase its productivity in 2005 and in 2006 it will spend \$4 million to double its primary source capacity and increase its screening capacity. The third example is the Construction Aggregates Ltd.'s Producers Pit, which supplies about 2.2 million tonnes of sand and gravel to the Victoria area. In 2005, this operation spent over \$2 million in new plant and mobile equipment in spite the fact that it is expected to close by 2007. The company plans to absorb up to 1 million tonnes of the lost production when Producers closes. Lehigh Northwest Cement Limited is also considering new projects.

The primary challenge for most industrial minerals investors in BC, and elsewhere, is identifying if there is a sufficient market to absorb new production. One scenario is that newcomers to the aggregate business, who will be continuously challenged by the established producers, is that they secure long-term contracts for a substantial proportion of their anticipated production, or form joint ventures with aggregate end-users.

Cement

Lafarge Canada Inc.'s plant in Richmond and Lehigh Northwest Cement Limited's plants in Delta are state-of-the-art cement operations in the lower mainland. Lafarge's plant has a reported capacity of 1.15 million tonnes of cement, but production for 2006 will most likely exceed that design capacity. According to the company, Lafarge Canada will be able to satisfy its clients in BC, however, some cement demand in Washington State, which was traditionally filled by the Richmond plant, will have to be replaced by imports from elsewhere.

The Kamloops cement plant of Lafarge Canada Inc. is forecast to mine over 300 000 tonnes of rock from the Harper Ranch quarry, and to produce about 220 000 tonnes of cement.

As it was the case over the last few years, Lehigh Northwest Cement Limited's plant in Delta, south of Vancouver, also operated at its maximum design capacity of 1.15 million tonnes of clinker per year. Ash Grove Cement announced early this year that it had acquired a 54 000 tonnes capacity import terminal from Goldendale Aluminum on the Willamette River in Portland, Oregon. The facility will be connected to the company's adjacent terminal on North Port Center Way, and combined storage capacity will be about 72 000 tonnes, enabling Ash Grove to supply as much as 800 000 tonnes of cement to customers in the greater northwest United States as well as some inland markets. The terminal will be serviced by ocean-going vessels and should be distributing cement by fall of this year.

Markets currently include at least eight varieties of grey Portland cement, white Portland cement and increasingly popular blended cements. Blended cements consist of Portland cement with one or more additives, such as ground granulated blast furnace slag (25–70% by weight), fly ash, natural pozzolans (15–40% by weight) and silica fume. In the past, blended cements were popular mainly in Europe and Asia, however, as environmental problems and energy concerns in North America rise, the popularity of the blended cements is increasing. Depending on specifications, cement may also contain interground limestone as an additive. The use of natural pozzolans, slag and fly ash, reduces energy consumption and greenhouse gas emissions and this trend is expected to continue.

As opposed to sand and gravel pits, cement plants require much larger venture capital to start, a greater technical expertise to run, and continuous research and development efforts are associated with evolving specifications and environmental regulations. There appears to be room for an increase in cement production capacity in BC, but such ventures may be of interest only to large, established and vertically integrated cement-producing companies. Expansion of production capacity elsewhere may well fill demand.

Fortunately, there is currently a strong international market demand for industrial minerals, particularly along the western seaboard of the United States. Access to low-cost transportation is key, and BC limestone and cement-grade silica producers are currently able to take advantage of markets along the west coast of North America.

Dimension Stone

In general, BC's strategic position on the west coast of North America favours the export of local industrial minerals. In terms of dimension stone, this coastal location acts as a double-edged sword. Raw or partially processed dimension stone is solid, dense and easy to handle. It is an ideal cargo for transoceanic ships where it is used as ballast. Some smaller BC dimension stone producers feel vulnerable to imports of inexpensive dimension stone from Asia and would like to restrict import of such low-cost product. Local stone importers and larger granite and marble processors and retailers consider the imports essential to provide their North American clients with a required variety of products. Margranite Industries in Surrey, Westcoast Granite Manufacturing Inc. in Delta, and Matrix Marble Corporation in Duncan are well-established BC stone processors. These companies rely to a large extent on imports for stone variety, but they also use local stones.

Margranite also processes nine granite varieties, from at least three of its quarries located in the East Anderson River, Beaverdell and Skagit Valley areas of BC. Matrix Marble Ltd., which is extracting blue and white marble from its Tahsis quarry in Tlupana Bay, just expanded its operation by installing the polishing line for their marble slabs, and will be selling Vancouver Island Marble in slabs 2 by 2.7 m (5.5 by 9 ft) in 1.9, 3.2 and 3.8 cm (¾, 1¼ and 1½ in) thicknesses.

Quadra Stone Company Ltd. relies extensively on the Fox Island granite, imported stones and variety of flagstone products. It also periodically produces a small tonnage of Cascade coral blocks from quarries near Beaverdell.

Bedrock Granite Sales & Stone Veneers primarily carries the Hardy Island granite, Haddington andesite and a variety of basalt and rhyolite products mined in the lower mainland. Kettle Valley Stone Company is renowned for its beige rhyodacitic tuff flagstone, ashlar and thin veneer, but it also mines and processes basalt with mantle-derived xenoliths and a number of landscape rock products of granite affinity.

Kettle Valley Stone Company and Kooteney Stone Center are the best known producers of locally derived flagstone. They started a trend that has strengthened since the last review of dimension stone in BC by Simandl and Gunning (2002). At least 15 new producers fitting this category were formed or emerged from obscurity over the last 10 years. Most of these producers are family-type operations with minimal capital, selling mostly to local markets. A few of the well-established or new operations with good financial backing, such as Golden Rock Products Inc., rapidly became mechanized and expanded their market share. Marketing over the internet and sales through stone distributors is a common practice.

Other significant producers are Huckleberry Stone Supply Ltd. of Burnaby and Mountain High Properties Ltd. of Pemberton which produce basalt from small quarries in the Whistler area. Rocky Mountain Tufa produced around 3500 tonnes of tufa, mainly for landscaping applications and an attractive red-purple slaty shale for flagstone applications. On Vancouver Island, K2 Stone Quarries Inc., San Juan Quarries Ltd. and Van Isle Slate produce and market flagstone.

Specialty fossiliferous limestone is test quarried in the Prince George area and a newly identified flagstone deposit consisting of attractive beige-yellow tuff, possibly partially zeolitized, was discovered by D. Sandberg about 10 km east of Beaverdell.

DRILLING MATERIALS

Oil prices reached record highs during early 2006 resulting in increased exploration and production drilling worldwide. In 2005, world production of barite was estimated at 7.8 million tonnes. Small barite operations in BC contributed about \$2.2 million in economic activity to the provincial economy. Assuming current trends hold, additional barite production from BC could be absorbed by the BC, Alberta and Alaska markets. Bentonite and zeolite are other minerals used by the oil and gas drilling industry that could benefit from this trend.

In the long-term, the BC offshore oil and gas exploration and development sector may become a substantial mar-

ket for local industrial minerals and heavy aggregate producers.

OTHER OPPORTUNITIES

Dolomite and magnetite resources along the coast of BC and potential markets for these minerals were described by Simandl (2006a, b). Magnesite resources were reviewed by Simandl (2002). There are numerous silica deposits documented in southeastern BC, however, large high-purity silica deposits, which could supply an expanding glass industry in the Pacific Northwest, are yet to be discovered along the BC coast.

ACKNOWLEDGMENTS

Early versions of this manuscript benefited from suggestions from Brian Grant and David Lefebure of BC Ministry of Energy, Mines and Petroleum Resources, and Suzanne Paradis of Natural Resources Canada. Laura Simandl from St. Margaret's School is thanked for her assistance. Victor Koyanagi and Bob Lane from the Prince George office, Bruce Madu and Mike Cathro from the Kamloops office, Dave Grieve from the Cranbrook office, Paul Wojdak from the Smithers office, Ian Webster from the Victoria office and Tom Schroeter from the Vancouver office of BC Ministry of Energy, Mines and Petroleum Resources helped to eliminate major omissions.

REFERENCES

- Aggregate Advisory Panel (2001): Managing aggregate, cornerstone of the economy; *Aggregate Advisory Panel*, URL <<http://www.em.gov.bc.ca/dl/AggregateReview/Report/FullReport.pdf>> [November 2006].
- Australian Coal Association (2006): Clean coal technologies – examples; *Australian Coal Association*, URL <<http://www.australiancoal.com.au/cleantech.htm>> [November 2006].
- Dunlop, S. and Simandl, G.J., Editors (2002): Industrial minerals in Canada; *Canadian Institute of Mining, Metallurgy and Petroleum*, Special Volume 53, 391 pages.
- MINFILE (2006): MINFILE BC mineral deposits database; *BC Ministry of Energy, Mines and Petroleum Resources*, URL <<http://www.em.gov.bc.ca/Mining/Geolsurv/Minfile/>> [November 2006].
- Pearson, K. (1998): Eco-minerals – opportunities on the green scene; *Industrial Minerals*, Number 370, pages 25–35.
- Schroeter, T., Cathro, M., Grieve, D., Lane, R., Pardy, J. and Wojdak, P. (2006): British Columbia mines and mineral exploration overview 2005; *BC Ministry of Energy, Mines and Petroleum Resources*, Information Circular 2006-1, 20 pages.
- Simandl, G.J. (2002a): Non metals mining – what the future will bring; sustainable mining in the 21st century; a workshop for geoscientists (extended abstract); organized by the *NUNA 2001 Committee on Sustainable Mineral Resources Development*, May 2–3, 2003, Vancouver, British Columbia, pages 17–18.
- Simandl, G.J. (2002b): The chemical characteristics and development potential of magnesite deposits in British Columbia, Canada; in *Industrial Minerals and Extractive Industry Geology*, Scott, P.W. and Bristow, C.M., Editors, *Geological Society*, London, pages 169–178.
- Simandl, G.J. (2003): Green minerals and market changes driven by environmental regulations; in *Proceedings of the 16th In-*

- dustrial Minerals International Congress, Taylor, L., Editor, Montreal, Canada, pages 153–161.
- Simandl, G.J. and Gunning, D.F. (2002): Dimension and ornamental stone in British Columbia; *in* Industrial Minerals in Canada, Dunlop, S. and Simandl, G.J., Editors, *Canadian Institute of Mining, Metallurgy and Petroleum*, Special Volume 53, pages 21–26.
- Simandl, G.J., Hora, Z.D. and Lefebure, D. (1999): Selected British Columbia mineral deposit profiles: industrial minerals and gemstones; *BC Ministry of Energy, Mines and Petroleum Resources*, Open File 1999-10, 137 pages.
- Simandl, G.J., Robinson, N.D. and Paradis, S. (2006a): Dolomite in BC: geology, current producers and possible development opportunities along the west coast; *in* Geological Fieldwork 2005, *BC Ministry of Energy, Mines and Petroleum Resources*, Paper 2006-1, and *Geoscience BC*, Report 2006-1, pages 197–207.
- Simandl, G.J., Robinson, N.D. and Paradis, S. (2006b): Iron (magnetite) ore resources in southwestern BC: soft niche or steel-hard market?; *in* Geological Fieldwork 2005, *BC Ministry of Energy, Mines and Petroleum Resources*, Paper 2006-1, and *Geoscience BC*, Report 2006-1, pages 209–230.
- Simandl, G.J., Robinson, N., Wojdak, P., Lane, B., Cathro, M. and Schroeter, T. (2004): Industrial minerals in British Columbia – review and opportunities; *in* Industrial Minerals with Emphasis on Western North America, *BC Ministry of Energy, Mines and Petroleum Resources*, Paper 2004-2, pages 5–14.
- United States Department of Energy, Electric Power Research Institute and the Coal Utilization Research Council (2006): Clean coal technology roadmap “CURC/EPRI/DOE Consensus Roadmap”; *DOE National Energy Technology Development Laboratory*, URL <<http://www.netl.doe.gov/technologies/coalpower/cctc/ccpi/pubs/CCT-Roadmap.pdf>> [November 2006].
- Voormeij, D.A. and Simandl, G.J. (2004): Geological, ocean and mineral CO₂ sequestration options: a technical review; *Geoscience Canada*, Volume 31, Number 1, pages 11–22.

Early Triassic Stuhini Group and Tertiary Sloko Group Magmatism (NTS 104K/10W), Northwestern British Columbia: New U-Pb Geochronological Results

by A.T. Simmons¹, R.M. Tosdal¹, H.J. Awmack², J.L. Wooden³ and R.M. Friedman¹

KEYWORDS: U-Pb geochronology, Early Triassic, Tertiary, Stikine Terrane, Stuhini Group, Sloko Group, geochemistry

INTRODUCTION

Upper Triassic volcanism represented by the Stuhini and Takla-Nicola groups is a major component of the Stikine and Quesnel terranes of the Canadian Cordillera. These two groups represent important arc-building products and host many of British Columbia's ore deposits. Despite their importance, the timing of volcanism and basic knowledge of their environment of formation remain poorly constrained. To date, there is only one known U-Pb age of 212.8 \pm 4.2–3.5 Ma (Logan *et al.*, 2000) from a rhyolitic unit within the Stuhini Group in the Iskut River area. Additionally, subvolcanic Stuhini Group intrusions have yielded U-Pb zircon ages of 216.7 \pm 4 Ma and 214 \pm 1 Ma from leucogabbro intrusions in northern British Columbia (Hart, 1995; Mihalynuk *et al.*, 1997). Other K-Ar ages have been reported, but these represent minimum ages (*e.g.*, Logan *et al.*, 2000).

In 2003, a research project initiated by the Mineral Deposit Research Unit (MDRU) at the University of British Columbia (UBC) investigated Late Cretaceous volcanoplutonic complexes in the Taku River area of the Stikine Terrane, northwestern British Columbia (Fig 1). A critical component of the study was also the Upper Triassic Stuhini Group and Lower to Middle Jurassic Laberge Group rocks, which are the country/hostrocks of these volcanoplutonic complexes. Work reported herein is drawn from fieldwork spanning 2003 through 2005 and from Simmons (2005). Funding for the project was derived in part from the Rocks to Riches Program, which was administered by the BC and Yukon Chamber of Mines (now the Association for Mineral Exploration BC) and from the Natural Sciences and Engineering Research Council of Canada (NSERC) through an Industrial Post-Graduate Fellowship and a Discovery Grant, the Society of Economic

Geologists, Equity Engineering Ltd., Rimfire Minerals Corporation and Cangold Limited.

During fieldwork from 2003 to 2005, approximately nine weeks of mapping and sampling were carried out over an area extending from the Bing prospect in the southeast to Mount Lester Jones in the northeast (Fig 2). Although the

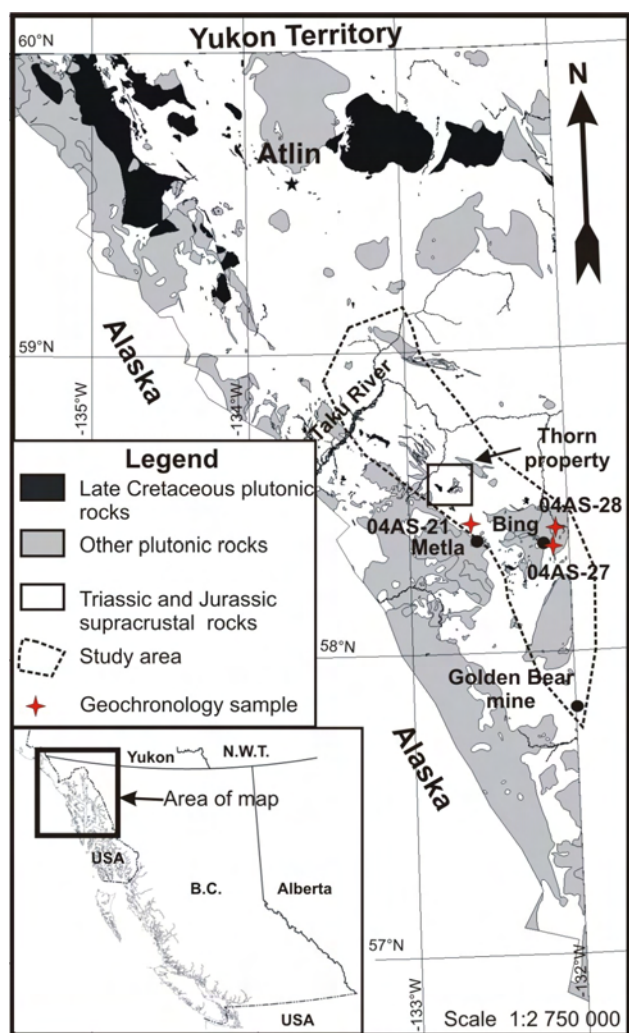


Figure 1. Location of 2003–2005 fieldwork, showing the distribution of pre-Cretaceous, Cretaceous and post-Cretaceous rocks. Additionally, locations of geochronology and geochemistry samples reported herein are given for data south of the Thorn property. Locations of mineral exploration prospects are shown for reference.

¹ Mineral Deposit Research Unit, Department of Earth and Ocean Sciences, University of British Columbia, Vancouver, BC

² Equity Engineering Ltd, Vancouver, BC

³ United States Geological Survey, Menlo Park, CA

This publication is also available, free of charge, as colour digital files in Adobe Acrobat® PDF format from the BC Ministry of Energy, Mines and Petroleum Resources website at http://www.em.gov.bc.ca/Mining/Geolsurv/Publications/catalog/cat_fldwk.htm

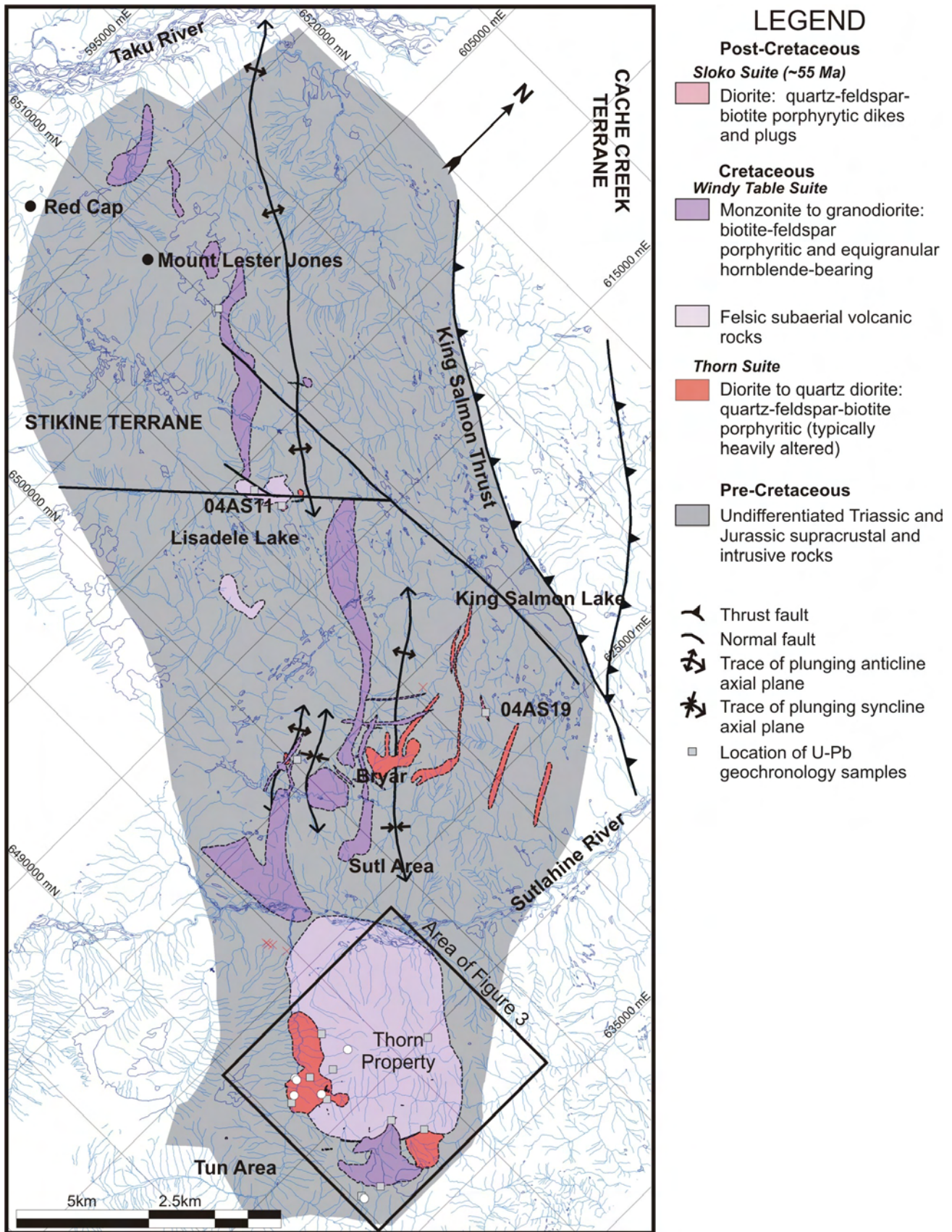


Figure 2. Regional geology of the study area, highlighting postaccretionary magmatic rocks with geochronology and geochemistry sample locations for data north of the Thorn property.

focus was mainly on Late Cretaceous rocks, significant effort was devoted to the relative timing of all rock types, including Stuhini Group, Sloko Group and other non-Cretaceous plutonic rocks, and the collection of samples suitably constrained for absolute timing using U-Pb methods on zircon. Geochronology was performed using both sensitive high (mass)-resolution ion microprobe – reverse geometry (SHRIMP-RG) and isotope dilution – thermal ionization mass spectrometry (ID-TIMS) at Stanford University and the University of British Columbia, respectively. Geochronological results for non-Cretaceous rocks are presented herein. Cretaceous geology and geochronology will be presented in future publications.

REGIONAL GEOLOGICAL CONTEXT

The Stikine, Cache Creek and Quesnel tectonostratigraphic terranes underlie the region, with Stikinia being the host terrane in the study area (Fig 1). The evolution of these terranes is a topic of much debate, with several different models currently existing; however, the model of Mihalynuk *et al.* (1994) is favoured here due to the proximity of this study to where the model was developed, which accounts for particular rock types present in the northern Cordillera. These terranes represent a continuous approximately 1400 km long island arc formed outboard of western ancestral North America along a northwest-trending subduction zone during and prior to the Late Carboniferous (Mihalynuk *et al.*, 1994). A Late Permian to Late Triassic reconfiguration of the subduction zone followed the initial stage of collapse of the Slide Mountain Basin during east-verging contraction (Nelson, 1993). The subduction zone was re-established outboard of Quesnellia and Stikinia by the Late Triassic, and the magmatic products are represented by the Stuhini and Nicola-Takla groups. Oroclinal bending of the terranes was also initiated during this time, in response to the collision of the Cache Creek plateau with Quesnellia and Stikinia (Mihalynuk *et al.*, 1994).

Extensive arc volcanism and plutonism dominated Stikinia and Quesnellia in the Late Triassic. Generally, the Triassic volcanic rock sequences are very similar, grading from subalkaline volcanic rocks (Stuhini and Nicola-Takla Groups, respectively) in the south to volcanoclastic sedimentary rocks (Lewes River Group and Nazcha Formation, respectively) in the north (Gabrielse, 1969). Arc-derived sedimentary rocks dominate the Late Triassic arc near the proposed oroclinal hinge, whereas arc volcanic rocks dominate elsewhere along the arc (Gabrielse, 1969). Monger *et al.* (1991) and Jackson (1992) provided evidence for the linkage of the Stikinia and Cache Creek terranes at this time, while the linkage between Cache Creek and Quesnellia (albeit in southern British Columbia) was provided by Monger (1984).

Clastic sedimentary rocks of the Lower to Middle Jurassic Laberge Group were deposited unconformably on the Late Triassic Stuhini Group throughout the region. Mihalynuk (1999) proposed that these sedimentary rocks recorded dissection of the Stuhini arc at the hinge zone of the oroclinal bend. South of the hinge zone, continued subduction under Stikinia and Quesnellia resulted in voluminous calcalkaline Hazelton Group volcanism. Nixon *et al.* (1993) established that Quesnellia was emplaced against the western margin of North America by 186 Ma. Locally, clastic sedimentary rocks are composed of detritus from older Laberge Group strata, indicating that rapid up-

lift occurred in limited areas. This basin cannibalization may represent the initial collapse leading to the Whitehorse Trough (Mihalynuk, 1999). Southwest-verging thrust faults play an important role in the development of the arc at this time. For example, the southwest-verging movement of the King Salmon thrust (Thorstad and Gabrielse, 1986) allowed for the emplacement of the Laberge Group and the formation of the clastic foredeep of the proto-Bowser Basin, which began in latest Toarcian to Aalenian time (Ricketts *et al.*, 1992; Mihalynuk, 1999).

Prior to the Middle Jurassic, the Stikine, Quesnel and Cache Creek terranes were discrete tectonic elements separated by subduction or collision zones. In the Middle Jurassic, Quesnellia was thrust over western North America, and the Cache Creek was thrust over Stikinia. Mihalynuk (1999) estimated shortening in excess of 50% in the Tagish Lake vicinity, approximately 100 km north of the study area. There, the Cache Creek and Stikine terranes were stitched together by 172 Ma by the undeformed Fourth of July batholith (Mihalynuk and Smith, 1992). Sedimentation in the Laberge Basin ceased by the latest Middle Jurassic and a period of tectonic quiescence followed, marking the beginning of a magmatic lull that lasted some 50 m.y.

By the Cretaceous, magmatism and strike-slip deformation dominated the tectonics of the northern Cordillera. Magmatism resumed in the latest Early Cretaceous with the onset of the Whitehorse Magmatic Epoch, which lasted from approximately 111 Ma (Hart, 1995) until 100 Ma (Mihalynuk, 1999). A series of felsic pyroclastic rocks and igneous intrusions, emplaced episodically during the Late Cretaceous, can be separated into two distinct periods: the Thorn suite (93–88 Ma) and Windy Table suite (86–80 Ma; Simmons *et al.*, 2005; Simmons, 2005).

Following another magmatic hiatus, magmatism resumed from 59 to 53 Ma (Mihalynuk, 1999) as part of the Sloko suite. These intermediate to felsic magmatic rocks are represented by voluminous eruptions of volcanic rocks with coeval semicircular granitic plutons, which mark the roots of Sloko-age volcanoes in the Coast Belt (Mihalynuk, 1999). Swarms of north-northeast to north-northwest-trending porphyritic quartz diorite dikes may have fed Sloko volcanic rocks.

GEOCHRONOLOGY METHODS

U-Pb Isotope Dilution Thermal Ionization Mass Spectrometry (ID-TIMS)

Zircon was separated from rock samples using conventional crushing, grinding and Wilfley table techniques, followed by final concentration using heavy liquids and magnetic separations. Mineral fractions for analysis were selected based on grain morphology, quality, size and magnetic susceptibility. All zircon fractions were air abraded prior to dissolution to minimize the effects of postcrystallization Pb loss, using the technique of Krogh (1982). All mineral separations, geochemical separations and mass spectrometry were done at the Pacific Centre for Isotopic and Geochemical Research in the Department of Earth and Ocean Sciences, University of British Columbia. Samples were dissolved in concentrated HF and HNO₃ in the presence of a mixed ²³³⁻²³⁵U-²⁰⁵Pb tracer. Separation and purification of Pb and U employed ion exchange column techniques modified slightly from those described by

Parrish *et al.* (1987). The Pb and U were eluted separately and loaded together on a single Re filament using a phosphoric acid – silica gel emitter. Isotopic ratios were measured using a modified single-collector VG-54R thermal ionization mass spectrometer equipped with a Daly photomultiplier. Measurements were done in peak-switching mode on the Daly detector. Analytical blanks for U and Pb were in the range 1 pg and 1 to 5 pg, respectively, during the course of this study. Fractionation of U was determined directly on individual runs using the $^{233-235}\text{U}$ tracer, and Pb isotopic ratios were corrected for a fractionation of 0.37%/amu for Faraday and Daly runs, respectively, based on replicate analyses of the NBS-981 Pb standard and the values recommended by Thirlwall (2000). All analytical errors were numerically propagated through the entire age calculation using the technique of Roddick (1987). Concordia intercept ages and associated errors were calculated using a modified version the York-II regression model (wherein the York-II errors are multiplied by the mean standard weighted deviate [MSWD]) and the algorithm of Ludwig (1980).

U-Pb Sensitive High-Resolution Ion Microprobe – Reverse Geometry (SHRIMP-RG) Zircon Geochronology

The samples were prepared at the University of British Columbia using the methods outlined for U-Pb TIMS analysis. The populations of zircons obtained from these samples were dated using the SHRIMP-RG at Stanford University, California. The SHRIMP-RG has a reverse geometry design and has improved mass resolution compared to conventional SHRIMP designs (Williams, 1998; Bacon *et al.*, 2000). Bacon *et al.* (2000) summarized the operational conditions for the SHRIMP-RG. Reviews on the ion microprobe technique and data interpretation are provided in Ireland and Williams (2003). Initial common Pb compositions were based on the measured ^{204}Pb and the model of Cumming and Richards (1975). Zircon and Pb isotope data were reduced using the SQUID (Ludwig, 2001) and Isoplot programs (Ludwig, 1999, 2003).

FIELD MAPPING STUDIES IN THE TAKU RIVER AREA

The study area is located on the western margin of the Stikine tectonostratigraphic terrane, where the Coast Belt meets the Intermontane Belt, as defined by Wheeler and McFeely (1987). Three distinct periods of magmatism postdate the amalgamation of Stikinia, Cache Creek and Quesnellia, and their accretion onto the western flank of North America. These magmatic bodies were emplaced into and deposited onto Upper Triassic subaqueous mafic

volcanic rocks and associated marine sedimentary rocks (Stuhini Group) and Lower to Middle Jurassic clastic sedimentary rocks (Laberge Group). Stuhini Group rocks are the oldest rocks mapped in the study area and are unconformably overlain by the Laberge Group at a shallow angle, east of the Outlaw zone on the Thorn property (Simmons *et al.*, 2005). The basement rocks were deformed during the amalgamation of Stikinia, Cache Creek and Quesnellia, and their subsequent accretion onto the western flank of North America. Deformation during this period is characterized by regional sub-greenschist metamorphism; north-west-trending, upright, open to closed folds; and north-west-trending thrust faults. The plutonic rocks of the Fourth of July suite intruded the basement rocks by 168 Ma and cut deformed Mesozoic rocks, indicating that amalgamation and accretion had ceased prior to these intrusions. North of the project area, in the Tagish Lake vicinity, Mihalynuk (1999) demonstrated that *ca.* 172 Ma plutons of the Fourth of July suite cut deformed Mesozoic rocks. Eocene Sloko suite magmatism is recognized in two locales within the study area, the Lisadele Lake and King Salmon Lake areas, as plagioclase-biotite-porphyratic dikes.

Late Cretaceous intrusive and volcanic rocks of the Thorn and Windy Table suites will be described in more detail elsewhere (A.T. Simmons *et al.*, work in progress).

A summary of the geochronology presented herein is given in Table 1.

Stuhini Group

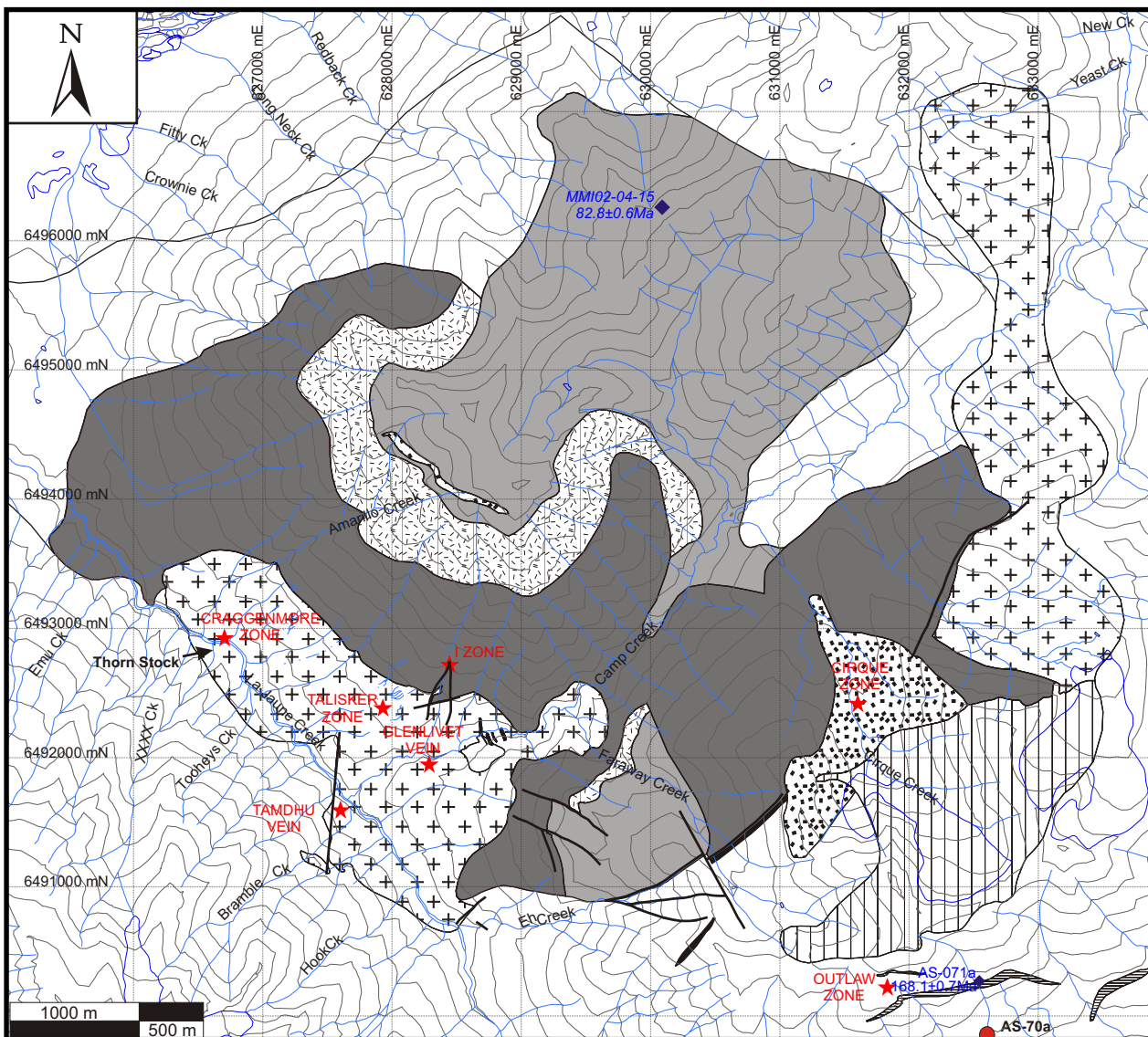
Strata of the Stuhini Group form a northwesterly-trending belt that extends through the entire study area from the vicinity of the Golden Bear mine to the Tulsequah area, where the rocks were named by Kerr (1948) after Stuhini Creek. These strata continue to the north through the Tagish Lake area (Mihalynuk, 1999) and are correlative with the Lewis River Group farther north (Wheeler, 1961; Hart *et al.*, 1989).

A wide range of rock types, including basic to intermediate subalkaline flows, pyroclastic rocks and related sedimentary rocks, characterize the Stuhini Group (Mihalynuk, 1999). The group is divided in the study area into a sequence dominated by submarine volcanic rocks and one dominated by clastic sedimentary rocks and lesser carbonate rocks. Near the Thorn property (Fig 3), submarine mafic volcanic strata are overlain by sedimentary strata (Baker, 2003; Simmons *et al.*, 2005) and are similar to the section described by Mihalynuk (1999) at Willison Bay, approximately 90 km north of the study area.

On the Thorn property, the Stuhini Group consists of submarine mafic volcanic rocks at the base, changing up the stratigraphic section to include increasing amounts of intercalated siltstone and conglomerate. South of the Thorn

TABLE 1. SUMMARY OF GEOCHRONOLOGY RESULTS PRESENTED IN THE PAPER.

Sample	UTM Zone 8 (NAD 83)		Method	Age (Ma)	Error (Ma) at 1 level	Sample description
	Easting ¹	Northing ¹				
04AS-21	636336	6479072	SHRIMP-RG U-Pb zircon	249.0	±6.4	Stuhini Group andesitic lapilli and crystal tuff
04AS-27	667318	6472437	SHRIMP-RG U-Pb zircon	214.2	±2.4	Stuhini Group subvolcanic intrusion-foliated gabbro
04AS-28	668843	6479202	SHRIMP-RG U-Pb zircon	219.2	±2.4	Stuhini Group subvolcanic granodiorite intrusion
AS-071a	632543	6490270	ID-TIMS U-Pb zircon	168.1	±0.7	Fourth of July suite rhyodacite dike
04AS-11	612037	6506538	SHRIMP-RG U-Pb zircon	56.3	±0.7	Sloko suite diorite porphyry
04AS-19	622970	6506461	SHRIMP-RG U-Pb zircon	55.5	±0.6	Sloko suite diorite porphyry



Explanation

Stratified Rocks Windy Table Suite

- Phase 3:** Dacitic lapilli and crystal tuff. Variable welding, grain size and fragment types throughout. Welding most dense near base and middle Phase 3 strata. Base of deposit dominantly ash, with lapilli-size fragments increasing upwards. Clast types include pumice, foreign wallrock, plant debris and flow-foliated rhyolite of Phase 2.
- Phase 2:** Fine-grained, rhyolitic, quartz-feldspar-biotite-phyric, flow-foliated units. Flow foliations defined by quartz and feldspar phenocrysts. Foliation may be intensely folded and, near the centre of the flow domes, foliation may be absent and phenocryst size increases.
- Phase 1:** Andesitic lapilli tuff with lesser horizons of reworked volcanoclastic sedimentary rocks and dacitic lapilli tuff petrographically similar to Phase 3. Andesitic units contain abundant broken feldspar crystals and rare pumice. Fragments are generally fine lapilli size.
- Undifferentiated Windy Table suite rocks.

Pre-Cretaceous Rocks

- Undifferentiated Upper Triassic submarine mafic volcanic and associated sedimentary rocks and Lower to Middle Jurassic calcareous clastic sedimentary rocks of the Stuhini and Laberge groups, respectively.

Intrusive Rocks Windy Table Suite

- Type 1:** Monzonite to granodiorite; crowded to matrix-supported feldspar, hornblende porphyry. Quartz is generally restricted to the matrix with feldspar, magnetite and lesser titanite and apatite and rare pyroxene.
- Type 2:** Quartz monzonite to monzogranite granophyric rocks. Appear equigranular in outcrop and contain hornblende, plagioclase and feldspar-quartz intergrowths. Lesser phases include biotite, magnetite and titanite.
- Type 4:** Rhyolitic, aphanitic, occasionally feldspar-phyric, flow-foliated dikes. Intrude around the periphery of the Thorn volcanic centre and are generally no wider than 3 m.

Thorn Suite

- Quartz diorite; crowded quartz-feldspar-biotite porphyry. Contains distinctive coarse-grained rounded quartz phenocrysts and coarse-grained euhedral biotite phenocrysts. Less porphyritic and may be flow-foliated near the margins.

Fourth of July Suite

- MJRIN: Rhyodacitic, aphanitic, 3-5 m wide, flow-foliated dykes. Rarely feldspar-phyric.

◆ U-Pb geochronology sample location. Labels in italics from Mihalynuk et al. (2003)

★ Mineralized zone location

— Surface trace of normal fault

● Geochemistry sample location

Figure 3. Geology of the Thorn property, showing locations of geochronology and geochemistry samples taken there.

property in the Little Trapper Lake area, an andesitic lapilli and crystal tuff, whose stratigraphic relation to Stuhini Group rocks on the Thorn property is not known, yielded a U-Pb SHRIMP-RG zircon age of 249 ± 6.4 Ma (Table 2, sample 04AS-21; Fig 1, 4a), based on the weighted mean of the spot analyzes. Spots AS21-2, AS21-5 and AS-21-6 are interpreted to have undergone postcrystallization Pb loss and are not considered in the statistical analysis. No correlation was noted between older and younger ages to core and rims of zircon grains. It is unclear if this age represents Paleozoic basement rocks similar to those of the Wann River orthogneiss (Currie, 1990) or if it represents Stuhini Group rocks with a slightly older age than the accepted range for the group.

The Stuhini Group locally contains significant quantities of intrusive rocks, commonly associated with pyroclastic rocks correlative in age (e.g., Willison Bay; Mihalynuk, 1999). South of the Thorn property in the Bing

area near the Sheslay River, two U-Pb zircon ages on subvolcanic intrusive rocks were obtained using SHRIMP-RG as part of this study. A strongly foliated gabbro containing large plagioclase crystals (2–15 mm) and interstitial hornblende yielded a U-Pb SHRIMP-RG zircon age of 214.2 ± 2.4 Ma (Table 2, sample 04AS-27; Fig 1, 4c). The zircons analyzed were extremely well behaved and did not yield multiple ages in spite of noted cores. Machine drift was encountered during this analysis, as seen in the weighted mean diagram, which shows a constantly decreasing age with each analysis. Spot AS27-5 is interpreted to have undergone postcrystallization Pb loss and was therefore not considered in the statistical analysis. Spots AS27-6 through 12 were used for statistical analysis because they form a more consistent weighted mean than spots AS27-1 through 4. Mihalynuk (1999) interpreted the foliated gabbroic rocks as subvolcanic intrusions. An equigranular granodiorite located approximately 5 km north of the foliated gabbro yielded a U-Pb SHRIMP-RG

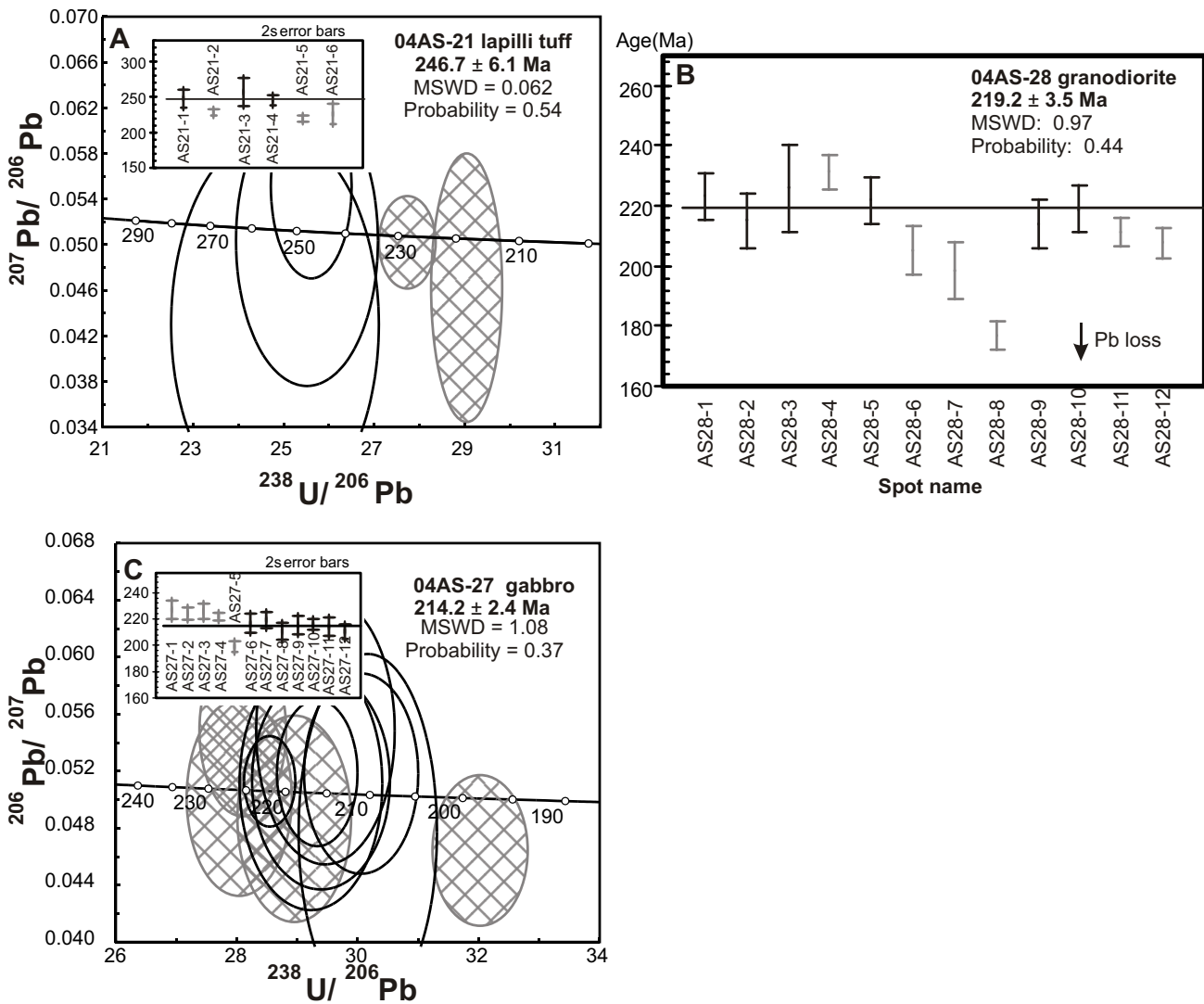


Figure 4. Weighted mean $^{206}\text{Pb}/^{238}\text{U}$ age plots for zircons from samples of intrusive and extrusive Stuhini Group rocks from the region surrounding the Thorn property. Ages are determined by weighted mean. Grey spot data are rejected due to either Pb loss or inheritance. Tera-Waserburg concordia plots are shown for comparison between concordia and weighted-mean ages. All errors are at 2σ levels. Tera-Waserburg plots are $^{207}\text{Pb}/^{206}\text{Pb}$ vs. $^{238}\text{U}/^{206}\text{Pb}$. 'Point data' represent individual ablated and ionized points from separate zircons on a grain mount.

TABLE 2. SENSITIVE HIGH-RESOLUTION ION MICROPROBE – REVERSE GEOMETRY (SHRIMP-RG) U-PB ZIRCON ANALYTICAL DATA FOR SAMPLES OF STUHINI GROUP ROCKS FROM THE STUDY AREA.

Sample spot	²⁰⁶ Pb ¹ (%)	U (ppm)	Th (ppm)	$\frac{^{232}\text{Th}}{^{238}\text{U}}$	²⁰⁶ Pb ² (ppm)	$\frac{^{206}\text{Pb}^2}{^{238}\text{U}}$	1 (%)	$\frac{^{207}\text{Pb}}{^{206}\text{Pb}^2}$	1 (%)	Apparent age $\frac{^{206}\text{Pb}}{^{238}\text{U}}$ ³	1 (Ma)
Unknown magmatic suite											
<i>Sample 04-AS21 (andesitic lapilli tuff):</i>											
AS21-1	-0.1	53	19	0.37	10.3	0.039089	2.51	0.0504	1.79	247.42	-6.34
AS21-2	0.09	921	308	0.35	3.3	0.035994	0.92	0.0502	28.48	227.76	-2.11
AS21-3	-1.04	28	12	0.47	16.1	0.040201	3.78	0.043	0.95	256.67	-9.82
AS21-4	0.5	151	104	0.71	6	0.038944	1.42	0.0551	5.05	245.07	-3.59
AS21-5	0.22	342	47	0.14	10.3	0.034581	1	0.0462	10.17	218.67	-2.26
AS21-6	-0.82	36	21	0.6	18.6	0.035379	3.01	0.0441	1.09	225.93	-7.1
Stuhini Group											
<i>Sample 04-AS28 (granodiorite):</i>											
AS28-1	-0.82	81	25	0.32	8.2	0.034867	1.71	0.044	2.42	222.73	-3.9
AS28-2	0.36	157	78	0.51	5.7	0.033951	2.16	0.0533	4.59	214.47	-4.66
AS28-3	0.09	53	15	0.3	11.4	0.035598	3.14	0.0514	1.62	225.28	-7.19
AS28-4	-0.22	181	83	0.47	6.2	0.036346	1.2	0.049	5.66	230.64	-2.86
AS28-5	-0.64	86	38	0.45	9.8	0.034686	1.74	0.0454	2.56	221.2	-4
AS28-6	-0.76	67	23	0.35	9.2	0.032001	1.91	0.0441	1.85	204.59	-4.01
AS28-7	-0.06	64	21	0.34	9.7	0.031169	2.32	0.0496	1.7	197.98	-4.69
AS28-8	0.12	105	33	0.32	6.2	0.027758	1.34	0.0505	2.51	176.3	-2.45
AS28-9	-0.73	84	22	0.27	8.4	0.033438	1.8	0.0445	2.4	213.56	-3.93
AS28-10	-0.17	132	69	0.54	6.3	0.034381	1.74	0.0491	3.91	218.28	-3.85
AS28-11	0.03	247	59	0.25	4.6	0.033255	1.05	0.0506	7.07	210.82	-2.28
AS28-12	0.03	181	41	0.24	5.4	0.032675	1.22	0.0505	5.09	207.2	-2.59
<i>Sample 04-AS27 (gabbro):</i>											
AS27-1	-0.54	144	40	0.29	4.41	0.035548	1.47	0.0399	13.8	226.37	-3.41
AS27-2	0.52	240	71	0.31	7.3	0.035465	1.05	0.0548	4.5	223.51	-2.43
AS27-3	-0.07	149	36	0.25	4.54	0.035564	1.28	0.0501	5.6	225.42	-2.96
AS27-4	0.09	722	125	0.18	21.67	0.034941	0.61	0.0513	2.5	221.21	-1.37
AS27-5	-0.45	356	67	0.19	9.54	0.031154	1.02	0.0465	4.6	198.65	-2.07
AS27-6	0.08	128	44	0.36	3.75	0.034126	1.65	0.0511	7.1	216.15	-3.66
AS27-7	-0.23	192	78	0.42	5.68	0.034425	1.33	0.0487	6.1	218.67	-2.99
AS27-8	0.33	195	96	0.51	5.57	0.033281	1.49	0.0477	10.7	210.36	-3.23
AS27-9	0.11	276	87	0.32	8.06	0.033933	1.59	0.0513	6.1	214.88	-3.47
AS27-10	0.18	420	236	0.58	12.26	0.034005	0.93	0.0519	4	215.19	-2.05
AS27-11	0.55	129	66	0.53	3.76	0.033849	1.59	0.0548	7	213.42	-3.51
AS27-12	0.19	161	55	0.35	4.6	0.033184	1.28	0.0518	5.5	210.06	-2.77

¹ common lead

² atomic ratios of radiogenic Pb

³ $\frac{^{206}\text{Pb}}{^{238}\text{U}}$ age using ^{207}Pb to correct for common lead

zircon age of 219.2 ± 3.5 Ma (Table 2, sample 04AS-28; Fig 1, 4b). Spots AS28-6, 7, 8, 11 and 12 are interpreted to have undergone postcrystallization Pb loss and were therefore not considered in the statistical analysis. Spot AS28-4 is interpreted as containing an inherited component, likely of Stuhini Group affinity, and was not considered in the statistical analysis. No correlation was noted between older and younger ages to crystal interiors and edges, respectively.

SINWA FORMATION

The upper part of the Stuhini Group contains the Sinwa Formation, which can be traced discontinuously throughout the study area (Souther, 1971; Fig 3). The Sinwa For-

mation ranges in thickness from 5 to 20 m and unconformably overlies Stuhini Group clastic sedimentary rocks on the Thorn property (Simmons, 2005).

It comprises two main rock types: lower limestone and upper clastic sedimentary rocks. Dolomitization, skarn development and recrystallization of limestone are widespread. Local boulder conglomerate units containing volcanic and intrusive rocks may correlate with the "Limestone Boulder Conglomerate" of Mihalynuk (1999), which separates Upper Triassic Stuhini Group strata from Pliensbachian argillite of the Laberge Group in the Moon Lake area, north of the study area.

Laberge Group

The Laberge Group is exposed over the entire length of the study area, extending from the vicinity of the Golden Bear mine in the south to the Yukon in the north (Fig 1). It is a major map unit in the study area. Souther (1971) estimated the thickness of the Laberge Group in the region to be 3100 m, although others have estimated it to be as much as 5000 m (*e.g.*, Bultman 1979). The Laberge Group comprises boulder to cobble conglomerate, immature sandstone and siltstone, wacke and argillite, all of which are generally calcareous. Correlation of individual sequences is difficult due to rapid lateral facies changes and lack of marker horizons. On the Thorn property, Laberge Group rocks overlie rocks of the Stuhini Group along a low-angle unconformably (Simmons *et al.*, 2005). These strata are thought to be an overlap assemblage linking terranes by the Early Jurassic (Wheeler *et al.*, 1991; Mihalynuk 1999).

Fourth of July Suite (Middle Jurassic)

Jurassic plutons are common in the Coast batholith to the northwest of the study area, where they in part form the Fourth of July plutonic suite of Mihalynuk (1999). They are sparsely observed southeast of the Taku River. During this study, several intrusions of the Fourth of July suite were recognized in one location on the Thorn property and dated at 168.1 ± 0.7 Ma (Table 3, sample AS-071a; Fig 3, 5) by TIMS U-Pb zircon geochronology. Four fractions were analyzed and all yielded concordant analyses. Fractions A and B give somewhat older ages than fractions C and D. The best estimate for age of crystallization of the sample is given by the total range of $^{206}\text{Pb}/^{238}\text{U}$ ages for the concordant and overlapping fractions A and B. Fractions C and D are interpreted to have experienced postcrystallization Pb loss. Intrusions of this age on the Thorn property are 3 to 5 m wide, fine-grained, aphanitic rhyodacite dikes (Fig 3). The 168.1 ± 0.7 Ma age from the rhyodacite dike is not a common age regionally for Jurassic magmatism. However, biotite cooling ages from the Fourth of July plutonic suite

can be as young as 164 Ma (*e.g.*, Roots and Parrish, 1988), which suggests the potential for plutonic rocks of similar age lying to the west of the study area. Fourth of July intrusions have important tectonic implications, as they apparently constrain the amalgamation and accretion of the Stikine, Cache Creek and Quesnel terranes.

Late Cretaceous Rocks

As the Late Cretaceous rocks will be discussed in more detail elsewhere (A.T. Simmons *et al.*, work in progress), these rocks are only briefly summarized here.

Following the accretion of the Stikine arc, a subduction zone was re-established west of the current location of Stikinia. Magmatism related to this subduction is recorded in three events at the Thorn property, beginning with the 93 to 88 Ma Thorn suite and followed by the 86 to 80 Ma Windy Table suite and the 58 to 54 Ma Sloko suite (Simmons, 2005). Together, the Thorn and Windy Table suites form the Late Cretaceous volcanoplutonic belt, which extends for at least 300 km from the Golden Bear mine to the BC-Yukon border (Simmons *et al.*, 2005).

Rocks of the Thorn suite are typified by the 'Thorn stock', which is a quartz-plagioclase-biotite-porphyrific quartz diorite. Large (>1 cm) euhedral biotite phenocrysts and rounded quartz phenocrysts are diagnostic of this rock type in the Late Cretaceous volcanoplutonic belt. The Windy Table suite is divided into intrusive and extrusive rocks. The extrusive rocks unconformably overlie the Thorn stock and cover the majority of the map area on the Thorn property (Simmons *et al.*, 2005). The volcanic strata form a volcanic sequence, greater than 5 km wide and 1600 m thick, that was deposited in a volcanic-tectonic depression. Rock types in the sequence include variably welded, dacitic to andesitic, crystal and lapilli tuffs with lesser volcanoclastic rocks and flow-foliated rhyolitic flow domes and shallow-level intrusions. Mihalynuk *et al.* (2003) reported a TIMS U-Pb zircon age of 82.8 ± 0.6 Ma near the top the volcanic sequence. There are several varieties of subvolcanic intrusions in the Windy Table suite, including

TABLE 3. ISOTOPE DILUTION – THERMAL IONIZATION MASS SPECTROMETRY (ID-TIMS) U-PB ZIRCON ANALYTICAL DATA FOR SAMPLES FROM THE THORN PROPERTY.

Sample fraction ¹	Weight (mg)	U ² (ppm)	Pb ³ (ppm)	$\frac{^{206}\text{Pb}^4}{^{204}\text{Pb}}$	Pb ⁵ (pg)	$^{208}\text{Pb}^3$ (%)	Isotopic ratios (error in % at 1 σ level) ⁶			Apparent age in Ma (error in % at 2 σ level) ⁶		
							$^{206}\text{Pb}/^{238}\text{U}$	$^{207}\text{Pb}/^{235}\text{U}$	$^{207}\text{Pb}/^{206}\text{Pb}$	$^{206}\text{Pb}/^{238}\text{U}$	$^{207}\text{Pb}/^{235}\text{U}$	$^{207}\text{Pb}/^{206}\text{Pb}$
Fourth of July suite												
<i>Sample AS-071a (rhyodacite dyke):</i>												
A	0.012	256	6.9	1406	4	11.8	0.02645 (0.14)	0.1807 (0.46)	0.04956 (0.41)	168.3 (0.5)	168.7 (1.4)	174 (19)
B	0.011	617	16.6	2372	5	11.7	0.02639 (0.12)	0.1799 (0.29)	0.04944 (0.22)	167.9 (0.4)	167.9 (0.9)	169 (10)
C	0.014	396	10.6	2632	3	12	0.02597 (0.11)	0.1770 (0.31)	0.04942 (0.26)	165.3 (0.4)	165.5 (1.0)	168 (12)
D	0.017	265	7	751	10	11.3	0.02598 (0.14)	0.1777 (0.44)	0.04960 (0.37)	165.3 (0.5)	166.1 (1.4)	176 (18)

¹ zircon fraction identifier

² U blank correction of 1 pg $\pm 20\%$; U fractionation corrections measured for each run with a double ^{233}U - ^{235}U spike (about 0.005/amu)

³ radiogenic Pb

⁴ measured ratio corrected for spike and Pb fractionation of 0.0037/amu $\pm 20\%$ (Daly collector), which was determined by repeated analysis of NBS Pb 981 standard

⁵ total common Pb in analysis based on blank isotopic composition

⁶ corrected for blank Pb, U and common Pb; common Pb corrections based on Stacey and Kramers (1975) model Pb at the age of the rock or the $^{207}\text{Pb}/^{206}\text{Pb}$ age of the rock

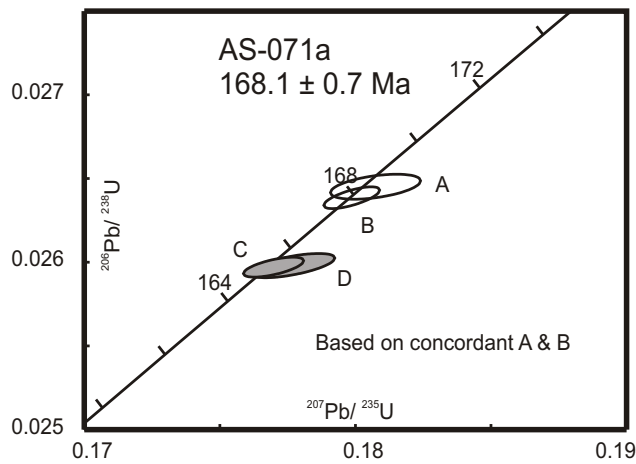


Figure 5. U-Pb concordia plot for a dike of the Fourth of July intrusive suite on the Thorn property. Zircon for this sample was analyzed by the isotope dilution – thermal ionization mass spectrometry (ID-TIMS) method. Empty ellipses and filled ellipses denote fractions used and rejected, respectively, for the age calculation.

variably porphyritic quartz monzonite to monzonite, plagioclase-megacrystic monzonite and flow-foliated rhyodacite dikes. These rocks are spatially, temporally and genetically related to veins at the Thorn property characterized by high-sulphidization mineral assemblages.

Sloko Suite Magmatism (58–54 Ma)

Souther (1971) mapped abundant early Tertiary, Sloko plutonic and volcanic rocks along the Late Cretaceous volcanoplutonic belt from the vicinity of the Golden Bear mine to the Tulsequah area. Between this study and that of Mihalynuk *et al.* (2003), only two locations are known where unequivocal Sloko plutonic rocks crop out. Both examples are plagioclase-biotite-porphyritic diorite in the Lisadele Lake area and the Sutl area, where they intrude into Laberge Group clastic sedimentary rocks. These rocks yielded SHRIMP U-Pb zircon ages of 56.3 ± 0.7 Ma and

55.5 ± 0.6 Ma, respectively (Fig 2, 6a, b; Table 4). For sample 04AS-11, no correlation was noted of older and younger ages to crystal interiors and edges, respectively. Spots 4AS11-1, 3, 5 and 12 are interpreted to have undergone postcrystallization Pb loss and were not considered in the statistical analysis. Spot 4AS11-2 is interpreted to contain an inherited component and was not considered in the statistical analysis. For sample 04AS-19, no correlation was noted of older and younger ages to crystal interiors and edges, respectively. Spots 4AS19-1, 2, 5 and 7 are interpreted to contain an inherited component and were not considered in the statistical analysis. The petrological similarity between this diorite and the Thorn stock makes it very difficult to unequivocally distinguish the two rock suites in the field. One criterion used was that Sloko suite rocks generally contain less quartz and are rarely unaltered.

GEOCHEMISTRY

Using major element geochemistry to classify rocks of the study area is problematic due to high degrees of acid leaching and alteration, which result in a net loss of CaO and Na₂O, and potential increases in K₂O, Al₂O₃ and SiO₂. Nonetheless, in order to build criteria for distinguishing these rocks from one another through varying degrees of alteration, representative rock units judged to be in their least altered states were analyzed. High degrees of variation in K₂O and Na₂O with respect to silica indicate that some of the major elements were, at least in part, mobile during postemplacement processes, such as alteration (*e.g.*, Fig 7c). However, trends that reflect fractionation processes are still present.

All rocks in this study are classified as relatively mafic units by the Zr/TiO₂ versus Nb/Y plot (Fig 7a). Stuhini Group rocks plot mainly as basaltic units, which is consistent with the known geochemistry of Stuhini Group volcanic rocks (*e.g.*, Mihalynuk, 1999). Two of the Stuhini Group rocks plot as ‘andesite/basalt’; both of these rocks are interpreted as subvolcanic Stuhini Group intrusions, one being a cumulate gabbroic rock and the other a quartz monzonite to granodiorite. Although there is a paucity of

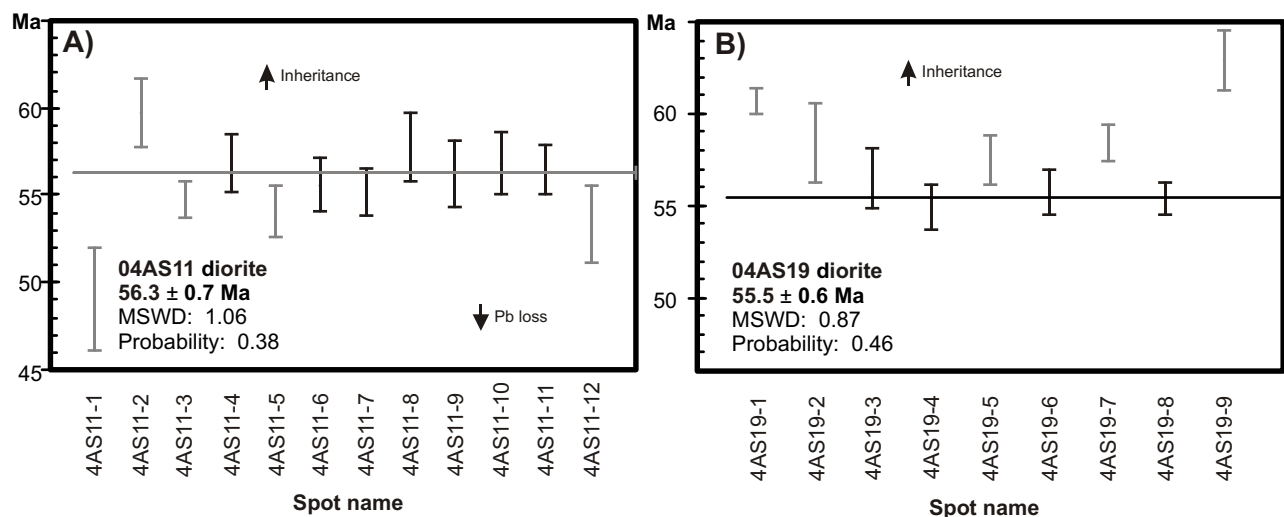


Figure 6. Weighted mean ²⁰⁶Pb/²³⁸U age plots for zircons from samples of intrusive rocks of the Sloko suite from the study area. Ages are determined by weighted mean. Grey spot data are rejected due to either Pb loss or inheritance. All errors are at 2σ levels. ‘Point data’ represent individual ablated and ionized points from separate zircons on a grain mount.

TABLE 4. SENSITIVE HIGH-RESOLUTION ION MICROPROBE – REVERSE GEOMETRY (SHRIMP-RG) U-PB ZIRCON ANALYTICAL DATA FOR SAMPLES OF SLOKO GROUP ROCKS FROM THE STUDY AREA.

Sample spot	²⁰⁶ Pb ¹ (%)	U (ppm)	Th (ppm)	²³² Th/ ²³⁸ U	²⁰⁶ Pb ² (ppm)	²⁰⁶ Pb ² / ²³⁸ U	1 (%)	²⁰⁷ Pb/ ²⁰⁶ Pb ²	1 (%)	Apparent age ²⁰⁶ Pb/ ²³⁸ U ³	1 (Ma)
Sloko suite											
<i>Sample 04AS11 (diorite porphyry):</i>											
4AS11-1	0.4	265	80	0.31	1.74	0.00753	3.1	0.037	20	49	-1.5
4AS11-2	0.47	206	67	0.34	1.66	0.00954	1.6	0.0675	5.7	59.64	-0.97
4AS11-3	0.15	658	360	0.56	4.82	0.008461	1	0.0422	7	54.65	-0.54
4AS11-4	0	587	236	0.42	4.44	0.00887	1.5	0.0497	6.2	56.72	-0.83
4AS11-5	0.58	319	123	0.4	2.31	0.00827	1.4	0.0341	12.7	53.94	-0.75
4AS11-6	0	289	106	0.38	2.15	0.00863	1.9	0.046	23.7	55.48	-0.77
4AS11-7	0.28	394	127	0.33	2.91	0.00851	1.3	0.0397	11.1	55.11	-0.67
4AS11-8	0.5	183	59	0.33	1.42	0.00881	2	0.0325	30.3	57.61	-0.98
4AS11-9	0	183	47	0.26	1.37	0.00864	2	0.0381	25.6	56.1	-0.95
4AS11-10	0.25	525	175	0.34	4	0.00886	1.5	0.0491	3.7	56.71	-0.88
4AS11-11	0.16	366	98	0.28	2.77	0.00878	1.3	0.0475	8.4	56.32	-0.7
4AS11-12	0	339	124	0.38	2.41	0.00819	2.2	0.0376	19.7	53.2	-1.1
<i>Sample 04AS19 (diorite porphyry):</i>											
4AS19-1	0.04	1053	410	0.4	8.56	0.009515	0.65	0.0518	5.7	60.69	-0.35
4AS19-2	0.72	131	52	0.41	1.03	0.00936	2.3	0.0683	18.5	58.4	-1.1
4AS19-3	0.78	219	69	0.32	1.67	0.00881	1.5	0.0476	10.5	56.49	-0.84
4AS19-4	0.53	312	151	0.5	2.31	0.00844	1.2	0.0365	16.7	54.89	-0.6
4AS19-5	0.29	283	84	0.31	2.19	0.009084	1.1	0.0578	6.2	57.51	-0.67
4AS19-6	1.04	313	143	0.47	2.36	0.00841	1.9	0.0216	62.9	55.72	-0.63
4AS19-7	0	464	262	0.58	3.63	0.009021	0.9	0.0403	9.1	58.4	-0.51
4AS19-8	0.05	679	230	0.35	5.04	0.008504	0.72	0.0355	7.3	55.39	-0.41
4AS19-9	1.01	239	80	0.35	2.03	0.00996	1.3	0.0602	6.7	62.87	-0.81

¹ common lead

² atomic ratios of radiogenic Pb

³ ²⁰⁶Pb/²³⁸U age using ²⁰⁷Pb to correct for common lead

data, intrusive rocks of the Sloko and Fourth of July suites plot as 'andesite/basalt'. These compositions are not surprising, given that the Sloko suite rock sampled is a coarse-grained diorite porphyry. However, this is somewhat surprising for the rocks of the Fourth of July suite, which are fine-grained flow-foliated rhyolitic dikes. The high SiO₂ concentration of this rock type suggests it was a late-stage intrusive rock that may have partially crystallized in vapour phase; this relatively evolved state may explain the differences in trace element concentrations (Fig 7a, b). All rocks are classified as medium-K calcalkaline series, with the exception of one sample from the Stuhini Group, a subvolcanic quartz monzonite to granodiorite intrusion, which plots in the high-K field (Fig 7b). Importantly, Stuhini Group basaltic rocks plot in medium-K field, which is key distinction from Stuhini Group basaltic rocks farther north in the Tagish Lake area, where Mihalynuk (1999) showed Stuhini Group basaltic rocks to be significantly K rich, plotting as absarokite. There is no known explanation for this difference along strike in the arc.

The Ba/La ratios of all magmatic rocks from the study area exceed 20 (Fig 7d), suggestive of an arc rather than a back-arc setting (e.g., Sasso and Clark, 1998; Bissig *et al.*, 2003). This environment is supported by the tectonic discrimination plots, which show that all samples plot as volcanic-arc granite (Fig 7e).

Stuhini Group and Fourth of July suite rocks also have relatively flat rare earth element (REE) patterns, the latter suite having higher overall concentrations of all REE and a negative Eu anomaly (Fig 7f). The Stuhini Group sample

(Table 5, AS-070a; Fig 7f) is from a subaqueous massive basaltic flow, which typically yields flat, relatively enriched REE patterns indicative of partial melting of the upper mantle. Mihalynuk (1999) suggested that Fourth of July suite magmas display similar chemistry to mature volcanic arcs (Fig 7f); sample AS-071a does not display similar chemistry. The high SiO₂ concentration of this rock suggests that it was a late-stage intrusive rock; this relatively evolved state may explain the differences in REE concentrations. Sloko suite intrusive rocks are geochemically distinct from Stuhini Group and Fourth of July suite rocks, having steeper REE patterns (Fig 7f).

DISCUSSION AND CONCLUSIONS

Stuhini Group rocks represent a major geological unit within the Stikine Terrane, yet very little is known about origin, timing and chemistry of these rocks, mainly due to a lack of significant studies in these rocks. Data presented herein are meant to add to the existing data publicly available in the hope that a significant dataset can be put together to unravel the mysteries of Stuhini Group magmatism. Mapping during this study is consistent with previous ideas that the Stuhini Group records a dynamic environment interpreted as two major arc-building events (e.g., Wheeler, 1961; Hart and Pelletier, 1989; Mihalynuk, 1999). Mihalynuk (1999) noted that evidence for the lower arc is observed at particular faults, in basal upper-arc conglomerate and as screens within late-arc subvolcanic Stuhini Group intrusions. Sample 04AS-21, taken south of the

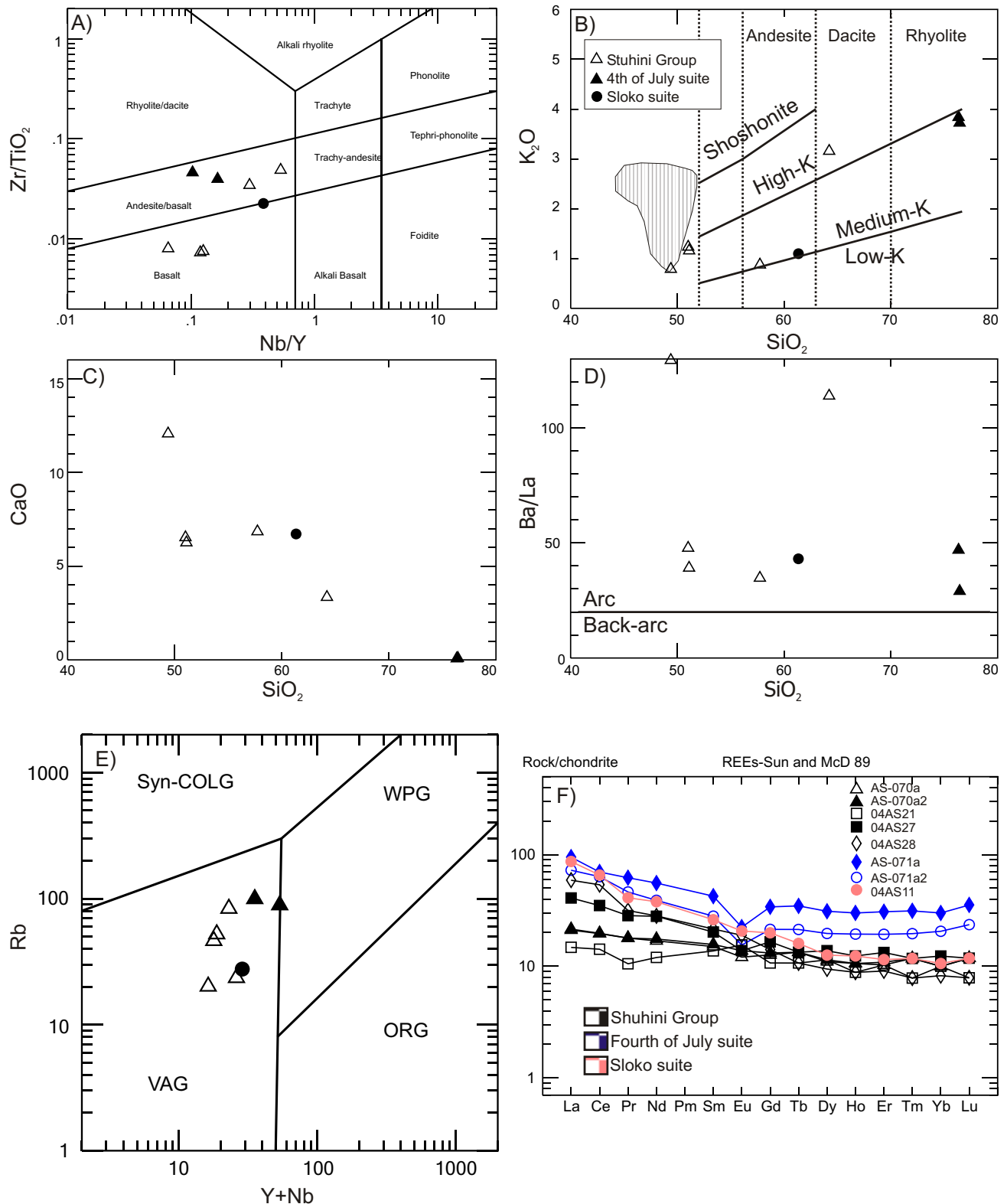


Figure 7. Various geochemical discrimination plots using major, trace and rare earth elements: A) Zr/TiO_2 versus Nb/Y from revised Winchester and Floyd (1977); from Pearce (1996); B) K_2O versus SiO_2 (after Gill, 1981); shaded area represents field for data collected by Mihalyuk (1999); C) CaO versus SiO_2 to show variation in major elements with minor changes in SiO_2 ; D) Ba/La versus SiO_2 for discrimination between arc and back-arc environments; E) Rb versus $Y+Nb$ tectonic discrimination plot (after Pearce *et al.*, 1984); F) REE spider plot (after Sun and McDonough, 1989). Abbreviations: syn-COLG, syn-collisional granite; WPG, within-plate granite; VAG, volcanic arc granite; ORG, ocean ridge granite.

TABLE 5. GEOCHEMICAL DATA FOR ALL ROCKS IN THIS STUDY.

Parameter	Sample:	Stuhini Group					Fouth of July suite		Sloko intrusive rocks
		AS070a	AS070a2	04AS27	04AS28	04AS21	AS071	AS071	04AS11
SiO ₂	wt%	47.31	47.21	56.8	63.5	49.4	73.55	73.68	58.1
TiO ₂	wt%	0.94	0.93	0.79	0.45	0.76	0.51	0.56	0.6
Al ₂ O ₃	wt%	17.58	17.6	18.7	17.85	15.64	14.75	14.9	16.35
Fe ₂ O ₃	wt%	10.56	10.43	4.24	3.74	12.12	2.55	2.5	5.69
FeO	wt%	6.29	6.21	2.52	2.23	-----	2.12	1.61	5.66
MnO	wt%	0.17	0.16	0.06	0.07	0.18	0.03	0.02	0.12
MgO	wt%	4.71	4.61	3.43	0.88	8.71	0.93	0.89	2.54
CaO	wt%	5.79	6.04	6.73	3.3	12.06	0.08	0.06	6.36
Cr ₂ O ₃	wt%	0.02	0.02	0.01	0.01	0.07	0.02	0.01	-----
Na ₂ O	wt%	4.15	4.12	6.29	5.56	0.03	0.09	0.06	3.26
K ₂ O	wt%	1.07	1.14	0.86	3.12	0.79	3.58	3.7	1.04
BaO	wt%	0.04	0.04	0.04	0.15	0.05	0.08	0.1	0.08
P ₂ O ₅	wt%	0.19	0.19	0.33	0.15	0.18	0.04	0.03	0.21
LOI	wt%	7.01	6.89	1.53	1.73	12.25	2.97	2.79	4.73
Total	wt%	99.58	99.41	99.9	100.5	100	99.19	99.29	99.4
Ba	ppm	199.5	239	337	1595	453	653	807	888
Co	ppm	33.5	32.5	11.5	8.7	49.2	3.7	3.8	14.6
Cr	ppm	120	120	60	100	510	190	110	50
Cs	ppm	12.7	17.5	1.2	2.6	1.8	12.1	5.9	2
Cu	ppm	132	132	47	15	130	6	-----	18
Ga	ppm	16	16	22	23	17	16	17	21
Hf	ppm	2	1	5	3	1	5	4	2
Mo	ppm	-----	-----	2	3	1	2	4	4
Nb	ppm	2	2	6	8	1	5	5	8
Ni	ppm	33	33	19	12	85	12	11	11
Pb	ppm	5	7	16	9	2.5	6	6	12
Rb	ppm	46.3	52.2	23.5	83.4	20.1	88.8	99.4	27.6
Sn	ppm	1	1	2	1	1	2	2	1
Sr	ppm	529	538	896	818	209	34.6	35.4	871
Ta	ppm	-----	-----	0.5	-----	0.25	-----	-----	0.6
Th	ppm	1	1	4	4	0.5	4	4	8
Tl	ppm	-----	-----	-----	-----	0.25	0.5	0.6	-----
U	ppm	0.7	0.6	2	1.7	0.25	1.1	1.1	4.3
V	ppm	366	353	201	80	329	50	54	146
W	ppm	1	1	4	2	8	1	2	2
Y	ppm	15.9	16.8	20.1	15	15.3	48.5	30.4	20.7
Zn	ppm	74	72	46	46	108	34	31	81
Zr	ppm	45.9	44.1	166	133	36.7	146.5	138	86.1
La	ppm	5.1	5	9.7	14	3.5	22.5	17.2	20.6
Ce	ppm	12.1	12	21.4	32.9	8.7	42.8	38.9	40.2
Pr	ppm	1.7	1.7	2.7	3	1	5.9	4.4	3.9
Nd	ppm	7.9	8.2	13.1	13.2	5.6	26	18.2	17.7
Sm	ppm	2.3	2.4	3.1	3.3	2.1	6.5	4.3	4
Eu	ppm	0.7	0.8	0.8	1.1	0.9	1.3	0.9	1.2
Gd	ppm	2.6	2.7	3.4	2.9	2.2	7	4.4	4.1
Tb	ppm	0.5	0.5	0.5	0.4	0.4	1.3	0.8	0.6
Dy	ppm	2.8	2.9	3.5	2.4	2.9	7.9	5	3.2
Ho	ppm	0.6	0.6	0.7	0.5	0.5	1.7	1.1	0.7
Er	ppm	1.7	1.8	2.2	1.5	1.7	5.1	3.2	1.9
Tm	ppm	0.3	0.3	0.3	0.2	0.2	0.8	0.5	0.3
Yb	ppm	1.7	1.7	2.1	1.4	1.7	5.1	3.5	1.8
Lu	ppm	0.3	0.3	0.3	0.2	0.2	0.9	0.6	0.3

Major oxide concentrations from XRF; all others by ICP-MS, from ALS Chemex, North Vancouver, BC

Thorn property in the Little Trapper Lake area, is an ande-site lapilli tuff that was previously mapped as Stuhini Group and yielded an age of 249 ±6.4 Ma. This rock, although poorly stratigraphically constrained, may represent

the earliest known volcanism related to early arc-building processes of the Stuhini Group. Alternatively, it may simply represent a previously unrecognized period of arc building. Magmatism during the late arc-building process

is recorded in samples 04AS-27 and 04AS-28, which yielded ages of 214.2 ± 2.4 and 219.2 ± 3.5 Ma, respectively. Both of these rocks are interpreted to be subvolcanic intrusive rocks related to late Stuhini Group volcanism. The geochemistry of Stuhini Group rocks from this study is somewhat distinct from those of previous studies to the north, for reasons that are presently unknown. Nonetheless, data from the study area are similar to those from rocks that reflect arc magmatism.

Other magmatic rocks of non-Cretaceous age in the study area include intrusive rocks of the Fourth of July and Sloko suites. Fourth of July suite rocks are spatially very limited and occur as very narrow dikes. These dikes cross-cut the upper stratigraphy of the Stuhini Group, as well as the clastic sedimentary rocks of the Lower to Middle Jurassic Laberge Group. Temporally, these rocks are slightly younger than those described in the Tagish Lake area, where the Fourth of July suite rocks intrude overlap assemblages and record the timing of amalgamation of the Stikine, Cache Creek and Quesnel terranes. Sloko suite rocks are distributed throughout the study area, with abundance increasing towards the west. These rocks represent a continental arc built in the earliest Eocene. Insufficient data are presently available to adequately characterize these rocks.

REFERENCES

- Bacon, C.R., Persing, J.M., Wooden, J.L. and Ireland, R.R. (2000): Late Pleistocene granodiorite beneath Crater Lake Caldera, Oregon, dated by ion microprobe; *Geology*, volume 28, pages 467–470.
- Baker, D.E.L. (2003): 2003 geological, geochemical and diamond drilling report on the Thorn property; *BC Ministry of Energy, Mines and Petroleum Resources*, Assessment Report 27120.
- Bissig, T., Clark, A.H., Lee, J.K.W. and von Quadt, A. (2003): Petrogenetic and metallogenic responses to Miocene slab flattening: new constraints from El Indio – Pascua Au-Ag-Cu belt, Chile/Argentina; *Mineralium Deposita*, volume 38, pages 844–862.
- Bultman, T.R. (1979): Geology and tectonic history of the Whitehorse Trough west of Atlin; unpublished PhD thesis, *Yale University*, 284 pages.
- Cumming, G.L. and Richards, J.R. (1975): Ore lead isotope ratios in a continuously changing Earth; *Earth and Planetary Science Letters*, volume 63, pages 155–171.
- Currie, L.D. (1990): Metamorphic rocks in the Florence Range, Coast Mountains, northwestern British Columbia (104M/8); in *Geological Fieldwork 1989*, *BC Ministry of Energy, Mines and Petroleum Resources*, Paper 1990-1, pages 197–203.
- Gabrielse, H. (1969): Geology of the Jennings River map-area, British Columbia (104-O); *Geological Survey of Canada*, Paper 68-55, 37 pages.
- Gill, J.B. (1981): Orogenic andesites and plate tectonics; *Springer-Verlag*, 390 pages.
- Hart, C.J.R. (1995): Magmatic and tectonic evolution of the Intermontane Superterrane and the Coast Plutonic Complex in southern Yukon Territory; unpublished MSc thesis, *University of British Columbia*, Vancouver, BC, 198 pages.
- Hart, C.J.R. and Pelletier, K.S. (1989): Geology of Carcross (105D/2) and part of Robinson (105D/7) map areas; *Indian and Northern Affairs Canada*, Open File 1989-1, 84 pages.
- Hart, C.J.R., Pelletier, K.S., Hunt, J. and Fingland, M. (1989): Geological map of Carcross (105D/2) and part of Robinson (105D/7) map areas; *Indian and Northern Affairs Canada*, Open File Map 1989-1.
- Ireland, T.R. and Williams, I.S. (2003): Considerations in zircon geochronology by SIMS; *Reviews in Mineralogy and Geochemistry*, volume 53, pages 215–241.
- Jackson, J.L. (1992): Tectonic analysis of the Nisling, northern Stikine and northern Cache Creek Terranes, Yukon and British Columbia; unpublished PhD thesis, *University of Arizona*, 200 pages.
- Kerr, F.A. (1948): Taku River map area, British Columbia; *Geological Survey of Canada*, Memoir 248.
- Krogh, T.E. (1982): Improved accuracy of U-Pb zircon ages by the creation of more concordant systems using an air abrasion technique; *Geochimica et Cosmochimica Acta*, volume 46, pages 637–649.
- Logan, J.M., Drobe, J.R. and McClelland, W.C. (2000): Geology of the Forrest Kerr – Mess Creek area, northwestern British Columbia (NTS 104B/10, 15 and 104G/2 and 7W), *BC Ministry of Energy Mines and Petroleum Resources*, Bulletin 104, 164 pages.
- Ludwig, K.R. (1980): Calculation of uncertainties of U-Pb isotopic data; *Earth and Planetary Science Letters*, volume 46, pages 212–220.
- Ludwig, K.R. (1999): ISOPLOT: a plotting and regression program for radiogenic-isotope data; *United States Geological Survey*, Open File 91-445, 41 pages.
- Ludwig, K.R. (2001): SQUID 1.00, a users manual; Berkeley Geochronology Center, Special Publication 2, 17 pages.
- Ludwig, K.R. (2003): ISOPLOT 3.00: a geochronological toolkit for Microsoft Excel; *Berkeley Geochronology Centre*, Special Publication 4.
- Mihalynuk, M.G. (1999): Geology and mineral resources of the Tagish Lake area, BC; *BC Ministry of Energy, Mines and Petroleum Resources*, Bulletin 105.
- Mihalynuk, M.G., Gabites, J.E., Orchard, M.J. and Tozer, E.T. (1997): Age of the Willison Bay pluton and overlying sediments: implications for the Carnian stage boundary; in *Geological Fieldwork 1996*, *BC Ministry of Energy, Mines and Petroleum Resources*, Paper 1997-1, pages 171–179.
- Mihalynuk, M.G., Mortensen, J., Friedman, R., Panteleyev, A. and Awmack, H.J. (2003): Cangold partnership: regional geologic setting and geochronology of high-sulphidation mineralization at the Thorn property, British Columbia; *BC Ministry of Energy, Mines and Petroleum Resources*, GeoFile 2003-10.
- Mihalynuk, M.G., Nelson, J. and Diakow, L. (1994): Cache Creek Terrane entrapment: oroclinal paradox within the Canadian Cordillera; *Tectonics*, volume 13, pages 575–595.
- Mihalynuk M.G. and Smith, M.T. (1992): Highlights of 1991 mapping in the Atlin-west map area (104N/12); in *Geological Fieldwork 1991*, *BC Ministry of Energy Mines and Petroleum Resources*, Paper 1992-1, pages 221–227.
- Monger, J.W.H. (1984): Cordilleran tectonics: a Canadian perspective; *Bulletin de la Société Géologique de France*, series 7, volume 26, pages 197–324.
- Monger, J.W.H., Wheeler, J.O., Tipper, H.W., Gabrielse, H., Harms, T., Struik, L.C., Campbell, R.B., Dodds, C.J., Gehrels, G.E. and O'Brien, J. (1991): Cordilleran terranes; in *Geology of the Cordilleran Orogen in Canada*, Gabrielse, H. and Yorath, C.J., Editors, *Geological Survey of Canada*, Geology of Canada, volume 4, pages 281–327.
- Nelson, J.L. (1993): The Sylvester Allochthon: Upper Paleozoic marginal-basin and island-arc terranes in northern British Columbia; *Canadian Journal of Earth Sciences*, volume 30, pages 631–643.
- Nixon, G.T., Archibald, D.A. and Heaman, L.M. (1993): ^{40}Ar - ^{39}Ar and U-Pb geochronometry of the Polaris Alaskan-type complex, British Columbia: precise timing of Quesnellia –

- North America interaction; *Geological Association of Canada – Mineralogical Society of Canada*, Joint Annual Meeting, Program and Abstracts, page A76.
- Parrish, R., Roddick, J.C., Loveridge, W.D. and Sullivan, R.W. (1987): Uranium-lead analytical techniques at the geochronology laboratory, Geological Survey of Canada; in *Radiogenic Age and Isotopic Studies: Report 1*, *Geological Survey of Canada*, Paper 87-2, pages 3–7.
- Pearce, J.A. (1996): A users guide to basalt discrimination diagrams; in *Trace element Geochemistry of Volcanic Rocks: Applications for Massive Sulphide Exploration*, *Geological Association of Canada*, Short Course Notes, volume 12, pages 79–113.
- Pearce, J.A., Harris, N.B.W. and Tindle, A.G. (1984): Trace element discrimination diagrams for the tectonic interpretation of granitic rocks; *Journal of Petrology*, volume 25, pages 956–983.
- Ricketts, D.B., Evenchick, C.A., Anderson, R.G. and Murphy D.C. (1992): Bowser Basin, northern British Columbia: constraints on the initial timing of subsidence and Stikinia – North America interactions; *Geology*, volume 20, pages 1119–1122.
- Roddick, J.C. (1987): Generalized numerical error analysis with application to geochronology and thermodynamics; *Geochimica et Cosmochimica Acta*, volume 51, pages 2129–2135.
- Roots, C.F. and Parrish, R. R., 1988, Age of the Mount Harper volcanic complex, southern Ogilvie Mountains, Yukon; in *Radiogenic Age and Isotopic Studies: Report 2*, *Geological Survey of Canada*, Paper 88-2, pages 29–36.
- Sasso, A.M. and Clark, A.H. (1998): The Farallón Negro Group, northwest Argentina: magmatic hydrothermal and tectonic evolution and implications for Cu-Au metallogeny in the Andean back-arc; *Society of Economic Geology Newsletters*, volume 34, pages 18–18.
- Simmons, A.T. (2005): Geological and geochronological framework and mineralization characterization of the Thorn property, and associated volcanoplutonic complexes of northwestern British Columbia, Canada; unpublished MSc thesis, *University of British Columbia*, Vancouver, BC, 168 pages.
- Simmons, A.T., Tosdal, R.M., Baker, D.E.L., Friedman, R.M. and Ullrich, T.D. (2005): Late Cretaceous volcano-plutonic arcs in northwestern British Columbia: implications for porphyry and epithermal deposits; in *Geological Fieldwork 2004, BC Ministry of Energy Mines and Petroleum Resources*, Paper 2005-1, pages 347–360.
- Souther, J.G. (1971): Geology and mineral deposits of the Tulsequah map-area, British Columbia; *Geological Survey of Canada*, Memoir 362, 84 pages.
- Stacey, J.S. and Kramers, J.D. (1975): Approximation of terrestrial lead evolution by a two-stage model; *Earth and Planetary Science Letters*, volume 26, pages 207–221.
- Sun, S.S. and McDonough, W.F. (1989): Chemical and isotopic systematics of oceanic basalts: implications for mantle composition and processes; in *Magmatism in the Ocean Basins*, *Geological Society of London*, Special Publication 42, pages 313–345.
- Thirlwall, M.F. (2000): Inter-laboratory and other errors in Pb isotope analyses investigated using a ^{207}Pb - ^{204}Pb double spike; *Chemical Geology*, volume 163, pages 299–322.
- Thorstad, L.E. and Gabrielse, H. (1986): The Upper Triassic Kutcho Formation, Cassiar Mountains, north-central British Columbia; *Geological Survey of Canada*, Paper 86-16, 53 pages.
- Wheeler, J.O. (1961): Whitehorse map-area, Yukon Territory (105D); *Geological Survey of Canada*, Memoir 312, 156 pages.
- Wheeler, J.O., Brookfield, A.J., Gabrielse, H., Monger, J.W.H., Tipper, H.W. and Woodsworth, G.J. (1991): Terrane map of the Canadian Cordillera; *Geological Survey of Canada*, Map 1713A, scale 1:2 000 000.
- Wheeler, J.O. and McFeely, P. (1987): Tectonic assemblage map of the Canadian Cordillera; *Geological Survey of Canada*, Open File 1565.
- Williams, I.S. (1998): U-Th-Pb geochronology by ion microprobe; in *Applications of Micro Analytical Techniques to Understanding Mineralizing Processes*, Volume 7, McKibben, M.A., Shanks, W.C., III and Ridley, W.I., Editors, *Reviews in Economic Geology*, pages 1–35.
- Winchester, J.A. and Floyd, P.A. (1977): Geochemical discrimination of different magma series and their differentiation products using immobile elements; *Chemical Geology*, volume 20, pages 325–343.

Geoscience BC Program Activities, 2006

Geoscience BC is pleased to present progress reports from projects funded during the spring and summer of 2006. These reports are also available as colour digital files in Adobe Acrobat PDF format from the British Columbia Ministry of Energy, Mines and Petroleum Resources website at http://www.em.gov.bc.ca/Mining/Geolsurv/Publications/catalog/cat_fldwk.htm

Geoscience BC is an industry-led, industry-focused, not-for-profit society that works in partnership with industry, academia, government, First Nations and communities to attract mineral and oil and gas investment to BC. Its mandate includes the collection, interpretation, and delivery of geoscience data and expertise, to promote investment in resource exploration and development in BC.

The Geoscience BC projects presented in *Geological Fieldwork 2006* include

- regional geochemical survey programs in central and northeastern BC;
- regional geophysical survey programs in central and northern BC;
- mapping and mineral potential studies on Vancouver Island and in central and southwestern BC;
- hydrocarbon potential studies for the Bowser, Sustut, Methow, and Nechako Basins; and
- an Advanced Spaceborne Thermal Emission and Reflection Radiometer (ASTER) imagery project.

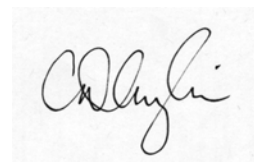
A number of the projects reported in the *Geological Fieldwork 2005* volume were completed during this past year, including three lake sediment and water geochemical surveys that cover the Anahim Lake and Nechako Plateau map sheets, as well as NTS areas 82N, 83C, 83D and 83E in southeastern BC. These surveys fill in some of the gaps in the regional geochemical database for British Columbia. In addition, two projects were undertaken to investigate new geochemical methodologies for detecting buried mineral deposits, and Phase I of a two phase ASTER imagery project, aimed at increasing the ASTER image database available through MapPlace, was completed.

Following completion of all projects, final data and reports can be downloaded from the Ministry of Energy, Mines and Petroleum (MEMPR) website at http://www.em.gov.bc.ca/Mining/Geolsurv/Publications/catalog/cat_gbc.htm or from MEMPR's digital MapPlace database.

These reports highlight the high-quality collaborative projects that are underway with a variety of partners, including graduate and undergraduate students. The results of these projects will enhance the geoscience database for the province of British Columbia and encourage new exploration for minerals, oil and gas. Increased claim staking and increased exploration expenditures have been recorded in response to data releases by Geoscience BC.

Geoscience BC encourages creative partnerships on all projects. The Bonaparte Lake geophysical survey was initiated by a proposal received from the Whispering Pines – Clinton Indian Band to carry out a multiparameter geophysical survey over their traditional territory. In partnership with the federal government's Targeted Geoscience Initiative and several companies, and with the support of the Indian Band, Geoscience BC engaged the federal government to contract and manage a combined aeromagnetic-radiometric geophysical survey of the eastern half of the Bonaparte Lake map sheet.

Geoscience BC would like to thank the authors of the Geoscience BC reports for their contribution towards enhancing the geological database of British Columbia through their participation in these projects, and for the timely reporting of preliminary results. Geoscience BC would like also to thank RnD Technical for their editorial and production services and the BC Geological Survey, in particular Brian Grant, for help and support in preparing the Geoscience BC publications and for publishing these papers in the *Geological Fieldwork* volume.



C.D. ('Lyn) Anglin, PhD
President & CEO
Geoscience BC
www.geosciencebc.com

Mineral Exploration Potential Beneath the Chilcotin Group (NTS 092O, P; 093A, B, C, F, G, J, K), South-Central British Columbia: Preliminary Insights from Volcanic Facies Analysis¹

by G.D.M. Andrews² and J.K. Russell²

KEYWORDS: *Chilcotin, Cariboo, basalt, pillow basalt, volcanic lithofacies, lava, exploration potential, hyaloclastite, paleotopography*

INTRODUCTION

Basalt of the Chilcotin Group (CG), situated in the Interior Plateau physiographic region of central British Columbia, covers an area of nearly 36 500 km². Its distribution is entirely within the region of BC that is most affected by mountain pine bark beetle (MPBB) infestation (Fig 1). The CG is immediately underlain by Paleozoic-Mesozoic basement rocks with high mineral potential (*e.g.*, Quesnel Trough) and Cretaceous-Eocene sedimentary rocks of the Nechako Basin with hydrocarbon potential. Previous workers (*e.g.*, Mathews, 1989) have suggested that the CG can reach thicknesses of approximately 200 m and average approximately 100 m. In addition, the CG is itself partially overlain by late Quaternary glacial deposits of variable (locally ≥ 200 m) and usually of unknown thickness (*e.g.*, Kerr and Levson, 1997).

The distribution of resources and prospects on the periphery of the CG (Fig 1) makes the potential for unexploited mineral resources extending beneath the CG and the Eocene volcanic cover compelling. However, there is currently little coherent information on the spatial distribution (*e.g.*, thicknesses), the lithostratigraphy (facies variations) and physical properties (density, porosity, magnetic susceptibility and conductivity) of the CG. The incompleteness of geoscience information for this unit is the single greatest impediment to successful exploration for resources beneath the CG, because the thickness of the cover (glacial sediments and basalt) is largely unknown, and the dearth of rock property data for the basalt limits interpretations of geophysical datasets. However, lithostratigraphy enables extrapolation of known geological relationships beneath areas of poor exposure, enabling greater understanding of the CG in a regional context.

This paper reports on results of volcanological field mapping of the lithofacies, thickness variations and base-

ment windows within the CG. The project was funded by Geoscience BC as a 'proof of concept' research program. The goal is to produce 3-D facies and thickness models for the CG that can be used to 1) extrapolate regional geology, metallogeny and structure beneath the CG cover; 2) find more windows to the basement and identify the geophysical signature of that basement geology; 3) delineate areas where the CG is thin and exploration drilling for 'blind' metallic deposits could be feasible; and 4) provide a 3-D representation of physical property variations to allow the signature of the CG to be accurately stripped from total-field geophysical datasets.

Early results from preliminary field investigations in the summer of 2006 include establishing the thickness and lateral thickness variations of the CG and characterizing the variations in lithofacies encountered. The stratigraphy of the CG was examined at 20 locations on the Cariboo, Chilcotin and Fraser plateaus during June, July and August 2006, during which time stratigraphic logs were constructed and a detailed sample suite collected.

GEOLOGICAL SETTING

The Neogene Chilcotin Group (CG) of south-central BC covers an area of approximately 36 500 km² (Fig 1). The region is characterized by moderately dissected, valley-incised plateaus that consist mainly of basaltic successions varying in thickness from 5 to 200 m. Estimates of total volume are as high as 3500 km³ (Bevier, 1983; Mathews, 1989), which would make the CG a medium-sized igneous province (Seth, *in press*). The CG ranges in age from 28 to 1 Ma and is broadly coeval with the voluminous Columbia River flood basalts of Oregon and Washington (*e.g.*, Hooper and Conrey, 1989). Characteristics they share include 1) flat to shallow dipping attitude, 2) massive to columnar jointed character, and 3) olivine-phyric basalt lavas with lesser volumes of pillow basalt and hyaloclastite. Rare intercalated felsic tephra has been collected from stratigraphic sections within the CG (*e.g.*, Bevier, 1983; Mathews, 1989).

ECONOMIC ISSUES

Stratigraphic units within Quesnellia host a high concentration of the most important metal reserves in BC, including the Afton, Gibraltar, Mount Polley and Highland Valley deposits, all of which occur adjacent to the margins of the CG (Fig 1). Exploration has traditionally focused on areas of basement exposed on the periphery of the CG because of the poorly constrained thickness and poorly known areal distribution of basalt lavas and glacial till.

¹ Geoscience BC contribution GBC019

² Volcanology and Petrology Laboratory, Department of Earth and Ocean Sciences, University of British Columbia, Vancouver, BC

This publication is also available, free of charge, as colour digital files in Adobe Acrobat® PDF format from the BC Ministry of Energy, Mines and Petroleum Resources website at http://www.em.gov.bc.ca/Mining/GeolSurv/Publications/catalog/cat_fldwk.htm

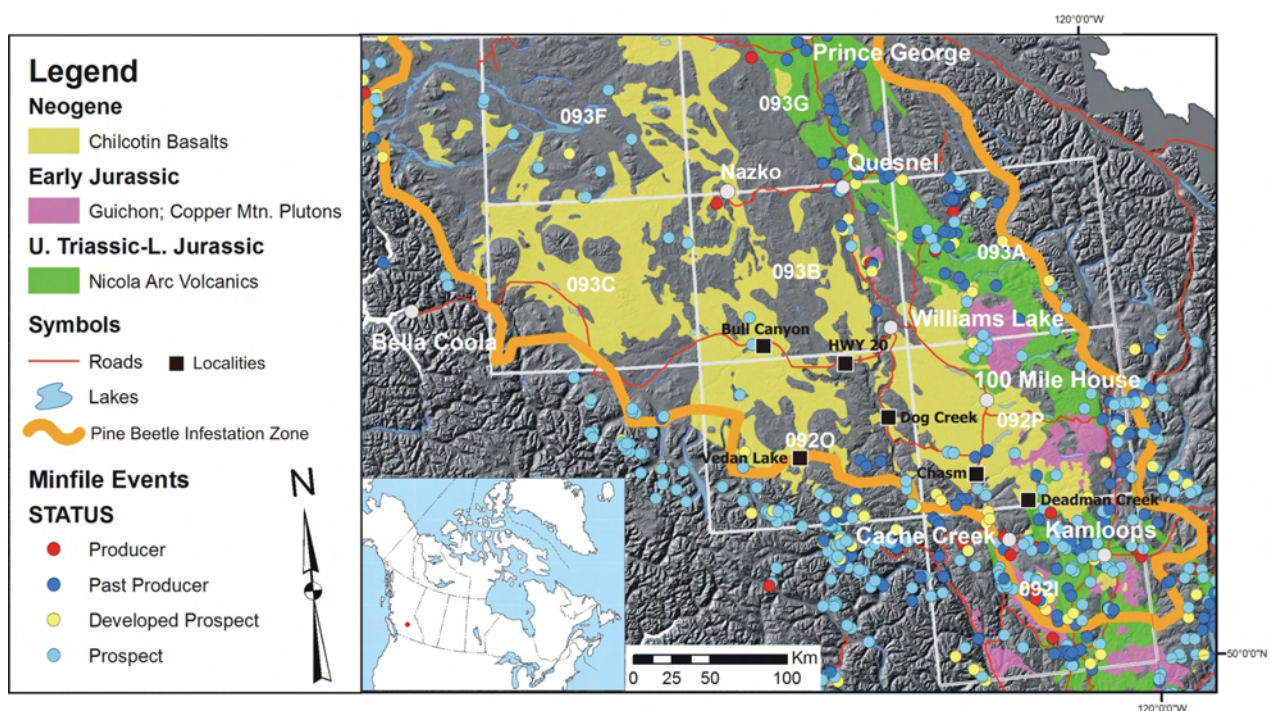


Figure 1. Shaded relief map of southern and central British Columbia, with important geological units highlighted (including the Chilcotin Group in yellow), the boundary of the mountain pine bark beetle infestation zone and the 1:250 000 NTS map sheet grid (NTS 092O, P; 093A, B, C, F, G, J, K). The economically important Nicola Group and intrusions hosted by it are shown. Key localities mentioned in the text are indicated by black squares.

However, it is highly probable that significant undiscovered mineral deposits are hosted by the basement rocks that underlie the CG, given the distribution of known ore deposits (Fig 1). Furthermore, the upper levels of hydrothermal-mineralization systems, where not eroded during the pre-Miocene (*e.g.*, Eocene unconformity), may have been protected from Holocene glaciation. Finally, burial of pre-CG drainages by basalt lavas offers the potential for discovery of new placer deposits (*e.g.*, Levson and Giles, 1995), especially given the proximity of the CG to the Cariboo goldfield.

The presence of the Chilcotin Group basalt cover makes exploration in this part of BC highly challenging, perhaps challenging enough to consider this a region of frontier exploration. However, rising global metal prices and constantly improving geophysical methods for mapping the subsurface ensure that the Chilcotin region remains within BC's exploration reserve. Furthermore, there is strong social interest in finding additional ore reserves (mines) in the MPBB area because of the near-future economic impact of the infestation. This environmental event is having, and will continue to have, a devastating effect on forestry-dependent communities in south-central BC (Fig 1). The MPBB infestation happens to be most intense in an area coincident with the distribution of the CG across the Cariboo, Chilcotin and Fraser plateaus. Stimulating renewed mineral exploration in the region is a short-term means of mitigating the economic impact of forestry decline; finding new ore reserves would provide longer term, sustained economic relief. Our contribution to this effort to renew mineral exploration in the region is to use mapping and modelling of the stratigraphy, volcanology and physical properties of the CG to remove the 'cover' and identify otherwise buried subsurface anomalies.

VOLCANIC STRATIGRAPHY OF THE CHILCOTIN GROUP

Fieldwork during 2006 was focused in the central portions of the CG, north of the Trans-Canada Highway, along Highways 20 and 97 (Fig 1). Previously documented and newly reported outcrop areas were examined across the study region (Farrell *et al.*, in press; Gordeev *et al.*, 2007). This paper summarizes and explores the broader scale implications of these studies.

Chasm-Style Lithofacies

CHASM PROVINCIAL PARK (NTS 092P)

A 7 km long canyon at Chasm Provincial Park exposes a thickness of more than 130 m of gently dipping, olivine-phyric basalt lavas at the southern margin of the Cariboo Plateau. The volcanic stratigraphy at Chasm is described in detail in Farrell *et al.* (in press). A layer-cake sequence of 13 laterally continuous lava horizons (Fig 2A) overlies a sequence of hyaloclastite pillow breccia (>15 m thick), capped by fluvial and lacustrine sedimentary rocks of the Lower Miocene Deadman Formation (Read, 1989). The lower succession appears to be laterally restricted to a paleochannel developed in the underlying Eocene Kamloops Group volcanoclastic breccia. The Eocene deposits represent the fill to an even earlier paleochannel developed in a basement of Permo-Triassic limestone of the Cache Creek Terrane. The topmost (and presumably youngest preserved) lava is dated at 9.2 ± 0.4 Ma (K-Ar; Mathews, 1989).

Chasm Provincial Park is the type section for a volcanic facies called 'Chasm type' (Farrell *et al.*, in press). The

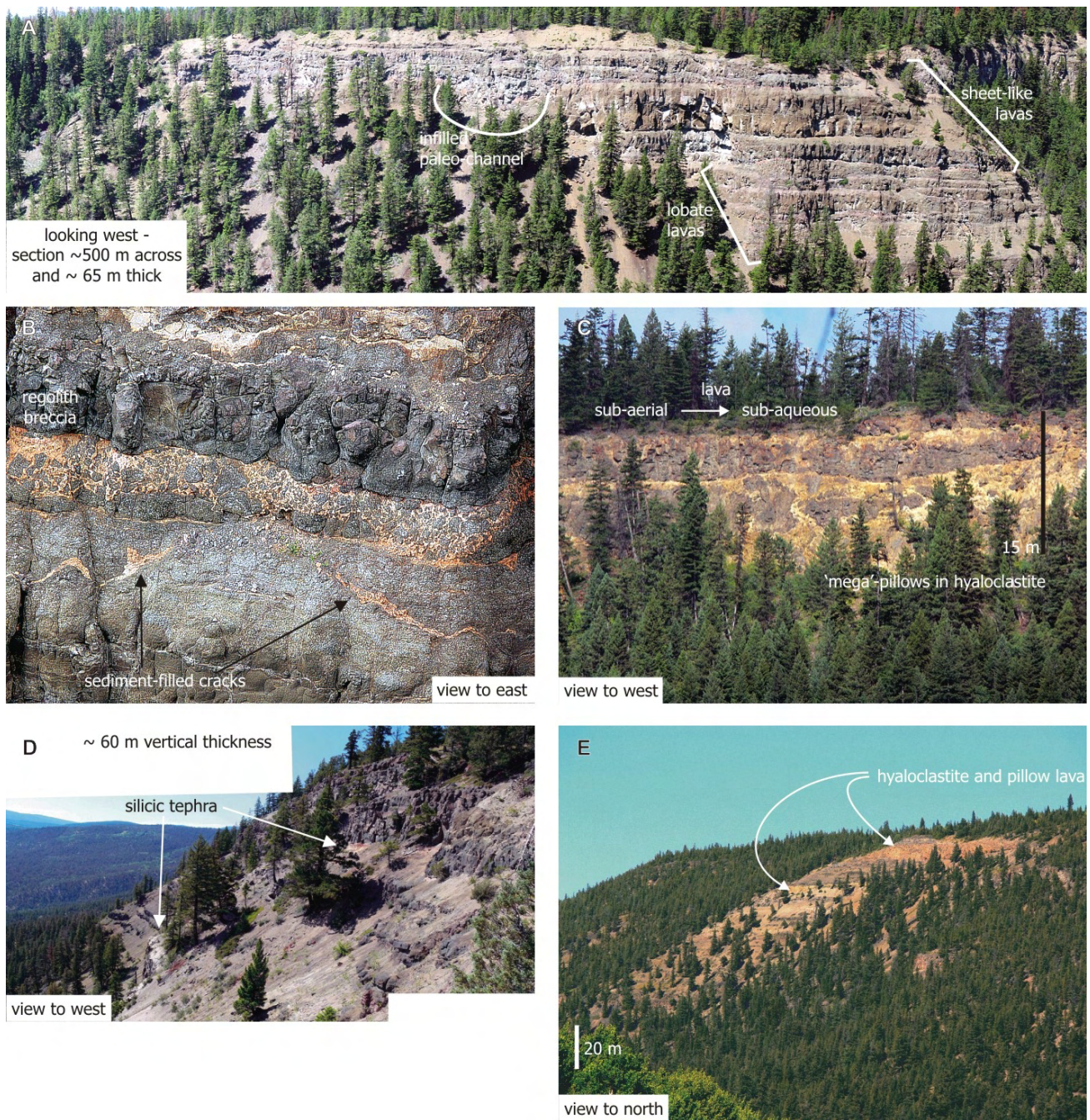


Figure 2: Chasm-style lithofacies: A) tiered subaerial lavas at Chasm separated by orange-red paleosols; the lower lavas are lobate in contrast to the laterally continuous, tabular lavas above; a prominent paleochannel is highlighted in the upper middle; B) close-up of the contact between two lavas depicting the red-black regolith breccia and infilled weathering cracks; C) lateral transition from coherent lava into hyaloclastite pillow breccia, Deadman Creek valley; D) intercalated felsic tephra with tiered lavas, Deadman Creek valley; E) tiered lavas and channel-confined hyaloclastite and pillow lavas, Vedan Lake.

Chasm-type lithofacies is characterized by relatively thick (≤ 15 m) massive basalt lavas (Fig 2A). Lavas at the base and top of the section tend to be laterally continuous (for > 5 km), whereas those in the centre of the section are typically lensoid (< 50 m across). All Chasm-type lavas are typically separated by baked red-brown paleosols and erosion surfaces with characteristic regolith breccia (Fig 2B). The regolith breccia consists of monolithic basalt breccia

formed *in situ* during soil formation. The vertical cracks filled by paleosol material and sediment are formed by *in situ* fracturing and plant roots (Fig 2B). Each lava has a characteristic internal stratigraphy of a thin (≤ 1 m) basal vesicular zone, a thick (≤ 10 m), columnar-jointed, nonvesicular central zone and an upper vesicular, amygdaloidal zone. Thin basal pillow horizons are typical of lavas lower in the section.

Chasm-type lavas are typically larger in volume than those observed elsewhere in the CG; however, they are similar in thickness and internal zonation to those commonly observed in flood basalt provinces elsewhere (e.g., Columbia River, Washington; Hooper and Conrey, 1989). We infer the presence of several paleosols and erosion surfaces between lavas to indicate there were significant repose periods (many thousands of years) between lava emplacements, when soil horizons and presumably vegetation and small rivers had time to become established. Therefore, the Chasm section may represent a considerable period of time from the deposition of basal hyaloclastite onwards; samples have been collected throughout the section for Ar/Ar dating of whole rock samples.

We have not encountered source vents for the lavas at Chasm, or elsewhere in the Chasm-style lithofacies; however, they are similar in age and composition to nearby gabbro plugs (Farquharson and Stipp, 1969), which may represent the eroded remains of small basaltic shield volcanoes from which the lavas were erupted.

DEADMAN CREEK VALLEY (NTS 092I, P)

Basalt lavas of the CG are exposed discontinuously for nearly 20 km along either side of Deadman Creek, at the southern margin of the Cariboo Plateau north of Kamloops Lake (Fig 1). Two successions were observed: 1) a widespread and thin (≤ 30 m thick) plateau-capping sequence of hyaloclastite and lava, and 2) a thick (~ 110 m) and spatially restricted sequence of multiple lavas separated by paleosols and intercalated tephra layers. The first succession (ca. 9.0 Ma, K-Ar; Mathews, 1989) is characterized by up to four moderately thick (≤ 10 m), laterally continuous, massive, columnar-jointed lavas overlying and interstratified with hyaloclastite pillow breccia (< 30 m thick; Fig 2C). Lava and hyaloclastite are seen to lie unconformably on fluvial and lacustrine sediments of the Lower Miocene Deadman Formation (Read, 1989) and volcanoclastic breccia of the Triassic Nicola Group. The Deadman Formation is restricted to paleochannels developed within the Nicola Group (no Eocene rocks are present), and it appears that the lenses of hyaloclastite are also controlled by the paleotopography.

The second succession occurs near Cultus Lake Ranch (ca. 8.2 Ma; Bevier, 1983) and is characterized by at least eight moderate to thick, laterally continuous, strongly weathered basalt lavas outcropping in a prominent south-facing bluff (Fig 2D). This section contains three felsic tephras interstratified between paleosols and overlying lavas (Bevier, 1983). Although the lavas in the section do not show evidence of lateral boundaries, their base is approximately 50 m below the present top of the basement in the adjacent valley sides, suggesting that they infill a broad paleochannel parallel to the present Deadman Creek valley.

Although it is not fully understood how the two successions in the Deadman Creek valley relate temporally or spatially, they are both Chasm-style lithofacies associations, characterized by thick lavas with multiple breaks in the stratigraphy, and both appear to be distributed along contemporary drainage systems.

CHILKO AND TASEKO RIVER VALLEY AREAS (NTS 092O)

Chasm-style lavas are exposed along the sides of Vedan and Elkin lakes (~ 150 m thick), Chilko Canyon (~ 40 m thick, ca. 6.8 Ma; Mathews, 1989) and Cardiff

Mountain (~ 70 m thick, ca. 6.6 Ma; Mathews, 1989), at the southern margin of the Chilcotin Plateau (Fig 1).

The sequence along Vedan and Elkin lakes comprises at least 11 poorly exposed, Chasm-style lavas (Fig 2E): vesicular and amygdaloidal bases and tops, massive columnar-jointed centres and well-developed paleosol horizons and regolith breccias (e.g., Fig 2B). An erosional unconformity (paleochannel) cuts through at least 15 m of Chasm-style lavas and is infilled by 1) a fluvial conglomerate containing metasedimentary clasts, possibly sourced from the adjacent Chilcotin and Pacific ranges, that are composed of Mesozoic and Upper Paleozoic rocks of the Tyaughton-Methow Basin and the Cadwallader-Methow Terrane (Schiarizza *et al.*, 2002); 2) fluvially reworked hyaloclastite containing rounded metasedimentary cobbles; 3) hyaloclastite pillow breccia; and 4) dense pillow lava. This sequence is overlain by more Chasm-style lavas that are, in turn, incised by a hyaloclastite-filled paleochannel. The lavas appear to be distributed along a broad paleovalley incised into basement metasedimentary rocks, therefore suggesting the re-establishment of fluvial drainage throughout the emplacement of the lavas, as evidenced by the fluvial conglomerate and reworked hyaloclastite.

Cardiff Mountain comprises at least three horizontal Chasm-style lavas overlying a basement of Mesozoic metasedimentary rocks and capped by a prominent 40 m high bluff, composed of a distinctive and different lava lithofacies. The uppermost lava preserves a superb example of entablature and colonnade jointing, and is nonvesicular throughout. Approximately six very strongly weathered, horizontal Chasm-style lavas are exposed along 500 m of Chilko Canyon; however, we do not yet understand its stratigraphic position or its relationship to paleotopography.

Bull Canyon–Style Lithofacies

CHILCOTIN RIVER VALLEY (NTS 092O; 093B)

Thick sequences of CG basalt (< 80 m) outcrop along the Chilcotin River valley and Highway 20 (Fig 1). These stratigraphic sections are volumetrically dominated by hyaloclastite, pillow lava and breccia, and minor peperite. These deposits are overlain by lesser thicknesses of flat-lying lavas identical to those of the Chasm-style lithofacies (e.g., Fig 3A). The Bull Canyon–style lithofacies is best exposed at Bull Canyon Provincial Park (Fig 1) and is fully described and interpreted by Gordee *et al.* (2007). The section exposed at this locality is characterized by intercalated vesicular lava, hyaloclastite, pillow lava, pillow breccia, and fluvial and/or lacustrine sedimentary rocks with peperite (Fig 3B, C). The subaqueous sequences are spatially confined to a paleochannel subparallel to the present-day Chilcotin River. As recognized by Gordee *et al.* (2007), the Bull Canyon–style lithofacies represents dominantly subaqueous depositional conditions. We suggest that the subaqueous succession results from the advance of subaerial lavas into water, where deltas of hyaloclastite are built outwards into deeper water at the front of an advancing lava. The drainage system re-established itself many times following disruption (including possible damming) by lava emplacement, as evidenced by the repeated sequences of hyaloclastite overlain by lava exposed in cliffs

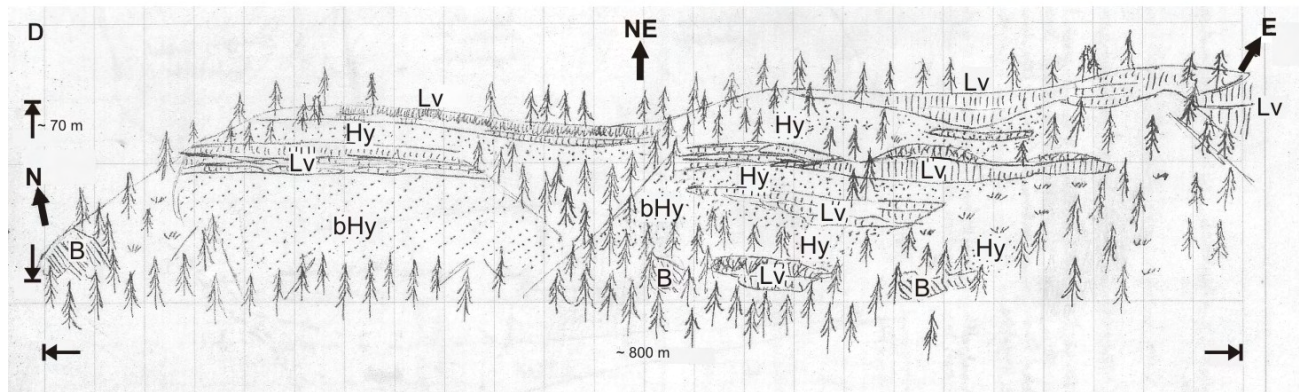
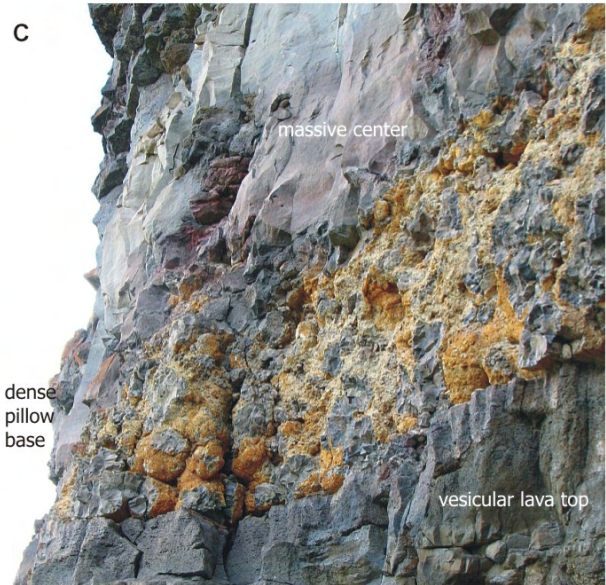
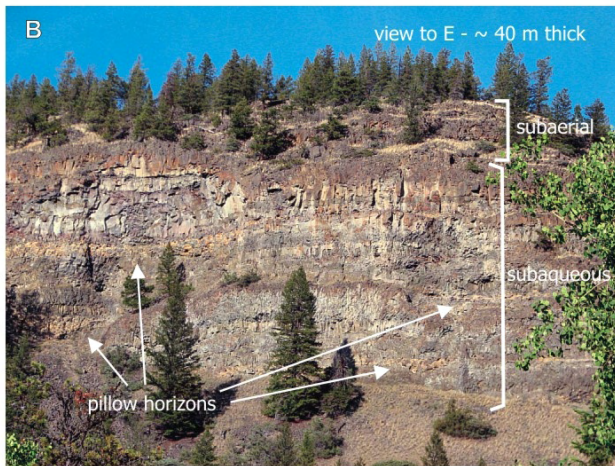


Figure 3: Bull Canyon–style lithofacies: A) subaerial lavas overlying foreset beds of hyaloclastite and hyaloclastite pillow breccia, near Hanceville; B) interstratified subaqueous lavas, pillow breccia and hyaloclastite, overlain by subaerial lavas, Bull Canyon; C) close-up of the densely packed pillow lava at the base of a lava, Bull Canyon; D) field sketch depicting the recurrence of significant depths of water during emplacement of at least four lavas, Anahim Flats Indian Reserve. Abbreviations: B, basement; Hy, hyaloclastite; bHy, bedded hyaloclastite; Lv, lava.

along Highway 20 (e.g., Anahim Flats Indian Reserve, Fig 3D).

Dog Creek–Style Lithofacies

FRASER RIVER (NTS 0920)

Exposures of subaerial CG basalt along the Fraser River Canyon display a distinctive lithofacies: the Dog Creek–style lithofacies, named after the valley where it is

best exposed (Farrell *et al.*, in press). These subaerial lava sequences are spatially restricted to valleys (Alkali Creek, Canoe Creek, Dog Creek and Harper Creek; Fig 1) along the margins of the present-day Fraser River valley. They appear to be considerably younger (<3 Ma; Mathews, 1989) than the lavas forming the Chasm-style lithofacies found in the surrounding area (e.g., Chasm Provincial Park). The lavas are laterally confined to long-lived paleodrainages (parallel to present-day valleys) cut into limestone of the Cache Creek Terrane.

All occurrences of Dog Creek–style lithofacies show evidence of contemporaneous rivers (a glacier and a glacier-fed stream; Mathews and Rouse, 1986) in the form of associated hyaloclastite deposits and sedimentary rocks. Excellent exposures along Dog Creek (>90 m thick) display two distinctive types of lava (Fig 4A): 1) thick (≤ 10 m) nonvesicular lavas exhibiting colonnade and entablature jointing and in narrow channels (Fig 4B); and 2) more voluminous, thin (≤ 3 m), lenticular, highly vesicular (highly inflated) lavas (Fig 4C). The thin lavas form laterally extensive, composite sheets of up to 50 stacked lavas without distinct intervening paleosols. The only breaks in lava emplacement recorded are short-lived channels filled by hyaloclastite and ‘thick’ lavas, and a glacial-sedimentary succession at the top of the section (Mathews and Rouse, 1986). The absence of paleosol horizons suggests sustained and rapid lava emplacement without significant repose periods. Furthermore, the presence of a volcanic bomb between two lavas (Fig 4D) and possible welded spatter (Farrell *et al.*, in press) suggest that the ‘thin’ lavas are proximal to their source.

DISCUSSION

Diverse Lava Morphologies and Types

Three lithofacies end-members, identified in early mapping at Chasm, Dog Creek and Bull Canyon, occur spatially and temporally throughout the CG. Characteristic features of the three lithofacies end-members are summarized/synthesized in Table 1 and Figure 5.

Chasm-style lavas exhibit many characteristics (Table 1) observed in flood basalt provinces elsewhere (*e.g.*, the Columbia River Province in Washington State and the Deccan Traps in India). They all exhibit thick (>5 m), subaerial and laterally extensive, large-volume tabular lavas (tens to hundreds of square kilometres). Each lava typically exhibits an internal stratification defined by zones of high and low vesicularity, significant columnar jointing and well-developed contacts between lavas (Fig 5). Therefore, such lavas are inferred to represent periodic (thousands to hundreds of thousands of years) emplacements of large magma volumes, at low mean effusion rates.

Large-volume (>1 km³) lava emplacement events are rare in recorded history (*e.g.*, Laki, 1783–1785), and theories for their emplacement have been controversial. Recent work, however, has started to provide some understanding of how large-volume lava fields are formed. Observations on the emplacement of small-volume Hawaiian pahoehoe lavas documented the pulsating inflation and deflation of the lava beneath a solid and insulating upper carapace. This has led to development of the SWELL hypothesis (standard way of emplacing large lavas; *e.g.*, Self *et al.*, 1998). By analogy with small inflated lavas, it is thought that large-volume lavas (*e.g.*, Chasm-style lavas) are produced by the gradual inflation of initially thin vesicular lava (<1 m thick) by through-flow of degassed (nonvesicular) magma that causes the characteristic vesicular zonation observed (vesicular upper and lower margins, and a columnar-jointed, nonvesicular interior). We infer Chasm-style lavas to have formed by this process.

The Bull Canyon–style lithofacies (Gordee *et al.*, 2007) is inferred to represent the subaqueous equivalent of the Chasm-style lithofacies. It is suggested that large volumes of lava were emplaced into active drainage systems (*e.g.*, rivers and lakes), intermittently filling them and finally burying them, and grading into subaerial lavas identical to those in the Chasm-style lithofacies (Fig 5). The diversity of subaqueous volcanoclastic deposits and lavas is attributed to interplay between rates of lava emplacement and the fluvial flux. For example, low lava fluxes, relative to the fluvial system, will produce hyaloclastite that is easily washed downstream. In contrast, where the lava effusion rates are equal to or exceed the fluvial flux, pillow lava and hyaloclastite will rapidly grade into massive lava that infills and buries the drainage system.

The Dog Creek–style lithofacies is inferred to be a different expression of subaerial basalt effusion, distinct from the widespread Chasm-style (Fig 5). Specifically, it is suggested that the succession at Dog Creek, and therefore that lithofacies, is proximal to the volcanic vent (*i.e.*, source). This interpretation is based on the presence of volcanic bombs and possible welded spatter textures. However, a vent has not been identified. The Dog Creek–style lithofacies was highly channellized in narrow paleovalleys that contained a long-lived river (*e.g.*, hyaloclastite and pillow lavas; Fig 5), which was fed by a glacier for some period of time (*e.g.*, proglacial sediments and till). It is inferred that the channel was intermittently filled and redirected by lavas; such lavas became overthickened and exhibit the entablature jointing thought to be characteristic of cooling lavas that have water flowing over their tops (*e.g.*, Long and Wood, 1986). The volumetrically dominant lavas are thin, highly vesicular (inflated) and do not exhibit well-developed contacts, suggesting that they were formed rapidly (high flux rate) and close to source (Table 1). These lavas are envisaged as being pahoehoe lavas, which typically form as rapidly growing ‘fields’ on the flanks of volcanoes.

Pre–Chilcotin Group Paleotopography

One of the main insights to result from the field program is that the pre–Chilcotin Group paleotopography is of critical importance to the distribution, style and thickness of the CG basalt cover. Without exception, the locations examined demonstrate the importance of paleodrainages in controlling the three-dimensional architecture of the CG. The field study shows that

- all sections of thickness greater than approximately 50 m are topographically restricted to (*e.g.*, Bull Canyon–style), or significantly thicker in (*e.g.*, Chasm-style), proven or inferred paleochannels;

TABLE 1. SUMMARY CHARACTERISTICS OF LITHOFACIES STYLES IN THE CHILCOTIN GROUP.

Parameter	Chasm-style	Bull Canyon-style	Dog Creek-style
Paleoenvironment	subaerial	subaqueous	subaerial
Areal distribution	plateau	valley-confined	valley-confined
Flow-unit thickness	5–10 m	<5 m	1 m
Flow-unit volume	large	small	small
Vesicularity	low	variable	very high
Eruption history	periodic	continuous	continuous
Eruption rate (integrated)	low	high to low	very high
Vent facies (proximal/distal)	?	?	proximal

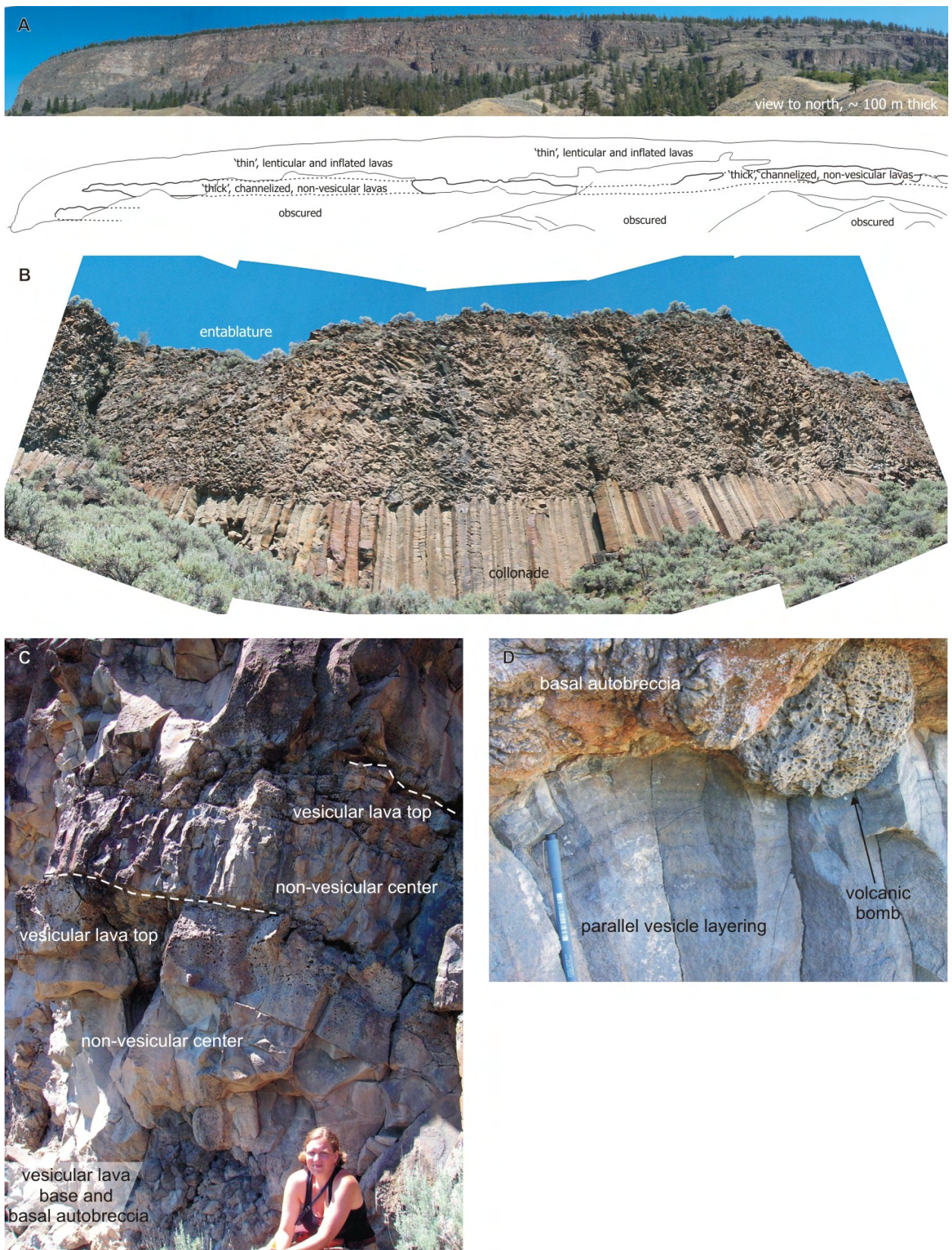


Figure 4: Dog Creek–style lithofacies: A) panorama and simplified internal stratigraphy in cliffs at Dog Creek that display two styles of lava (thin, lenticular and highly vesicular lavas and 30 m thick, channelized, nonvesicular lavas with characteristic colonnade and entablature jointing); B) colonnade and entablature jointing; C) internal layering typical of thin inflated pahoehoe lavas, defined by vesicular bases and upper surfaces, and massive centres; sitting person is 80 cm high; D) lava bomb on the upper surface of lavas indicates that they are proximal to a vent; pen is 15 cm long.

- most sections contain some of hyaloclastite, pillow lava or fluvial to lacustrine sedimentary deposits, indicative of interactions between lava emplacement and fluvial drainages (e.g., Dog Creek, Vedan lake); and
- clearly demonstrable paleochannels coincide with many present-day drainages (e.g., Dog Creek).

It is not surprising that many drainages appear to have re-established themselves and cut through the CG lavas, given the generally thin nature of the lavas (typically <100 m) compared to the relief of the present-day catchment areas (e.g., posteruption surfaces have ~500 m relief). Understanding the importance of topography for the distribution and nature of the CG has the potential to greatly improve our models for the architecture of this volcanic province and our ability to predict the thickness of basalt cover. The literature shows some of the thickest recorded sections of CG to be between 100 and 200 m (e.g., Bevier, 1983; Dostal *et al.*, 1996). This may have led to a paradigm that the CG forms a homogeneous tabular sheet that is everywhere greater than 100 m thick (Fig 6, scenario 1), even though Mathews (1989) demonstrated some sections to be within paleolows. If this paradigm is true, then the Chilcotin region must be considered as a frontier exploration region because of the technical challenges in identifying and testing targets in the deep (>100 m) subsurface.

However, our preliminary results suggest that the thickness of CG basalt is highly variable and that thickness variations are mainly a response to paleotopography. The implication is that the CG is, in fact, far from tabular in three dimensions. It is much more probable that the CG basalt distributions are irregular in extent and thickness (Fig 6, scenarios 2 and 3). Furthermore, the common coincidence of present-day drainage systems with pre and syn-CG drainages suggests that, where paleodrainages existed, there are now descendent drainages. One implication of this is that the areas between the present-day exposures of CG basalt are ‘paleoplateaus’ that feature relatively thin (0–30 m) basalt covers (Fig 6).

These suggestions are still speculative and are the focus of next year’s fieldwork.

SIGNIFICANCE FOR FUTURE MINERAL EXPLORATION

In light of our initial results, the exploration potential of the Chilcotin, Cariboo and Fraser plateaus should be re-evaluated. Previous evaluations assumed a more or less uniform and thick basalt cover that buried economically important rock types (Fig 6, scenario 1). The high-risk costs of blind-drilling through thick basalt and the subjectiveness of interpreting basalt-covered basement geology on the basis of geophysical datasets have ensured that the exploration potential of the CG has been ranked low.

However, our results may lead to an upgrading of the exploration potential by 1) improving knowledge of the three-dimensional distribution of the CG and 2) providing a georeferenced sample suite for physical property measurements. The former, which is the subject of this paper,

suggests that the three-dimensional distribution is very irregular and strongly influenced by paleotopography (Fig 6, scenarios 2 and 3). This allows for potential mineral deposits to be closer to the surface beneath a thinner basalt cover, and therefore easier and cheaper to investigate. Subsequent fieldwork may identify basement windows where basalt is totally absent. Our model for the architecture of the CG is to be supplemented by a comprehensive and georeferenced sample suite for which physical properties (magnetic susceptibility, density, porosity, electrical conductivity, etc.) are being measured. These results are intended to help constrain models derived from geophysical datasets.

We are optimistic that our results and future research will improve exploration potential beneath the CG and encourage other academic, government and industrial researchers to investigate the CG, ultimately with the goal of developing economic mineral deposits and increasing our knowledge of volcanism in BC.

CONCLUSIONS

Preliminary field investigations in the Cariboo-Chilcotin region of south-central British Columbia are revealing a diverse range of lithofacies types within the Neogene Chilcotin Group basalt. Stratigraphic sections throughout the region exhibit lithofacies architectures (e.g., thickness variations, lithofacies associations) consistent with lava emplacement into, and the burial of, mature paleochannels

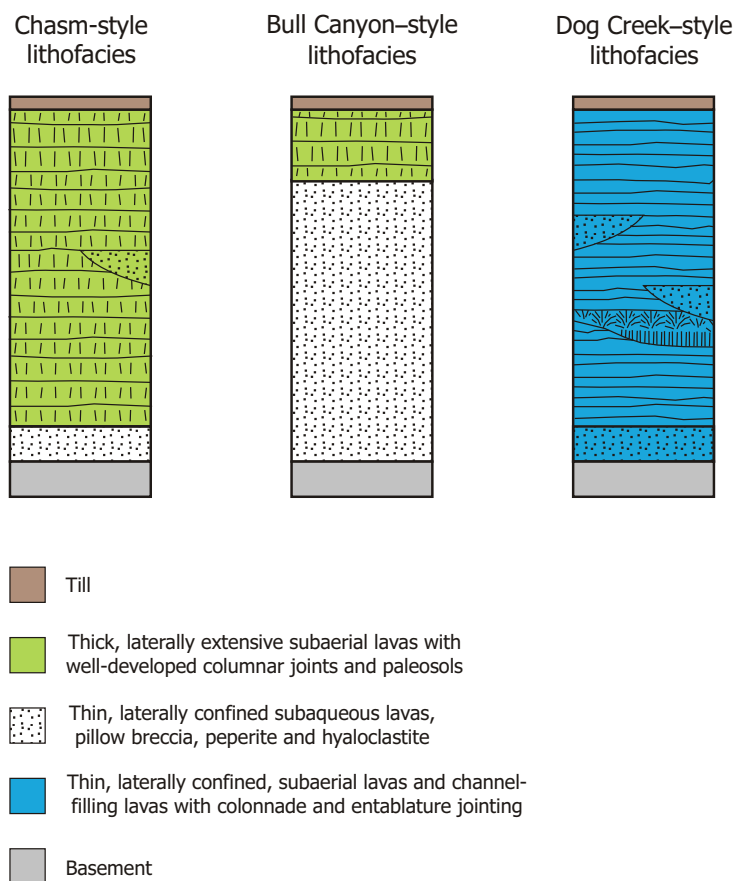
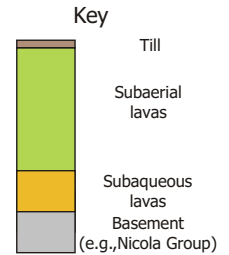
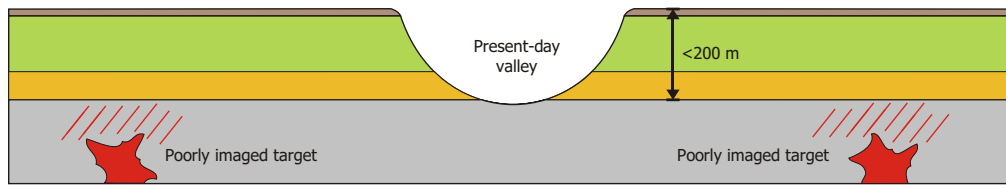
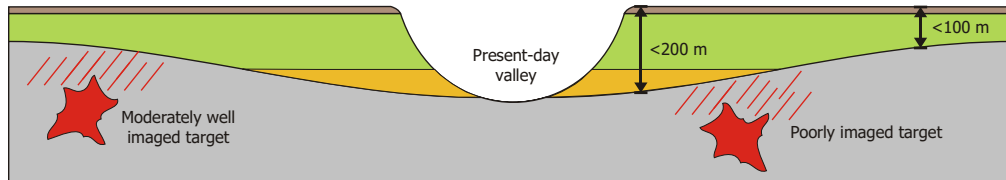


Figure 5: Schematic stratigraphic logs depicting the facies components (and their relative proportions) of the Chasm-style, Bull Canyon-style and Dog Creek-style lithofacies.

Scenario 1



Scenario 2



Scenario 3

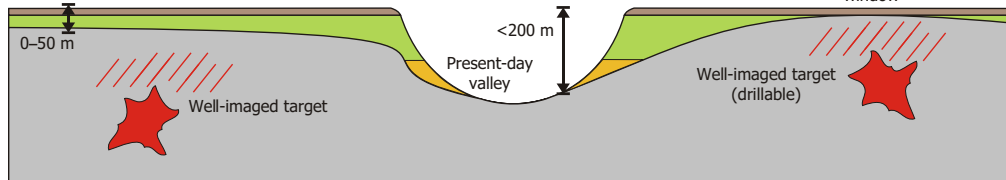


Figure 6: Schematic summary profiles through the Chilcotin Group, emphasizing the control of volcanic architecture on economic resource potential in the Nicola Group. Scenario 1: uniformly thick CG (low paleorelief), resulting in poor exploration potential due to deeply buried metallogenic bodies and attenuated geophysical signals. Scenario 2: broad paleovalleys infilled by CG (moderate paleorelief), resulting in poor to moderate exploration potential due to relatively thin CG cover over some mineral deposits. Scenario 3: narrow paleovalleys (high paleorelief), resulting in moderate to good exploration potential where some mineral deposits are very close to the surface beneath minimal or zero basalt cover, and are more clearly identified in geophysical surveys, soil geochemistry and economic test drilling. It is proposed that the distribution of the Chilcotin Group is a combination of scenarios 2 and 3, offering significantly better exploration prospects than previously thought. This is a simplified conceptual diagram that does not represent the possible presence of Eocene volcanic rocks (e.g., Kamloops Group) or Mesozoic sedimentary rocks (e.g., the Bowser Basin) that may occur between the CG and the basement.

with sustained rivers and bodies of standing water. Sections are typically dominated by locally thick subaqueous facies (e.g., pillow basalt, hyaloclastite, peperite), overlain by relatively thin subaerial plateau lavas. Differences in volcanic style and lithofacies architecture within the Chilcotin Group indicate that there is no single and unique type section that can be inferred as being representative of the entire group, and that previous regional-scale interpretations and conclusions must therefore be re-examined.

The following is a summary of results and conclusions:

- The Chilcotin Group is an irregularly distributed cover of basalt lavas and associated volcanoclastic deposits.
- The thickest sections (>50 m) are confined to paleodrainages; elsewhere, the CG is inferred to be relatively thin (<50 m).
- Three lithofacies end-members were identified; a proximal subaerial facies (Dog Creek-style), an areally extensive subaerial facies (Chasm-style) and its subaqueous equivalent (Bull Canyon-style).
- The Dog Creek and Bull Canyon-style lithofacies are confined to paleodrainages.
- The exploration potential of the CG is improved by recognition of its irregular three-dimensional

shape, allowing for thinner basalt cover over a wider area than previously thought.

ACKNOWLEDGMENTS

This research was funded by Geoscience BC under the project 'Mapping the Resource Potential Beneath the Chilcotin Flood Basalts (CFB): Volcanic Lithofacies Constraints on Geophysical Surveys'. We also acknowledge logistical support and assistance from the Geological Survey of Canada through the TGI-3 program and from the BC Geological Survey. We wish to thank Bob Anderson for his constructive review. Our work benefited from advice and helpful discussions with Kirstie Simpson, Stephen Williams, Sarah Gordee, Sarah Brown, R-E. Farrell, Paul Schiarizza and Cathy Hickson. Lastly, we thank the people of the Cariboo-Chilcotin region for their help and hospitality.

REFERENCES

- Bevier, M.L. (1983): Regional stratigraphy and age of Chilcotin Group basalts, south-central British Columbia; *Canadian Journal of Earth Sciences*, volume 20, pages 515–524.

- Dostal, J., Hamilton, T.S. and Church, B.N. (1996): The Chilcotin basalts, British Columbia: geochemistry, petrogenesis and tectonic significance; *Neues Jahrbuch für Mineralogie*, volume 170, pages 207–229.
- Farquharson, R.B. and Stipp J.J. (1969): Potassium-argon ages of dolerite plugs in the South Cariboo region, British Columbia; *Canadian Journal of Earth Sciences*, volume 6, pages 1468–1470.
- Farrell, R.-E., Andrews, G.D.M., Anderson, B., Russell, J.K. (in press): Internal stratigraphy of the Chilcotin Group basalts in and near the Bonaparte Lake map area (NTS 92P): the Chasm and Dog Creek–style lithofacies; *Geological Survey of Canada*, Current Research.
- Gordec, S., Andrews, G., Simpson, K.A. and Russell, J.K. (2007): Subaqueous, channel-confined volcanism within the Chilcotin Group, Bull Canyon Provincial Park (NTS 093B/03), south-central British Columbia; in *Geological Fieldwork 2006*, BC Ministry of Energy, Mines and Petroleum Resources, Paper 2007-1 and *Geoscience BC*, Paper 2007-1, pages 285–290.
- Hooper, P.R. and Conrey, R.M. (1989): A model for the tectonic setting of the Columbia River Basalt eruptions; *Geological Society of America*, Special Paper 239, pages 293–306.
- Kerr, D.E. and Levson, V.M. (1997): Drift prospecting activities in British Columbia: an overview with emphasis on the Interior Plateau; in *Interior Plateau Geoscience Project: Summary of Geological, Geochemical and Geophysical Studies*, BC Ministry of Energy, Mines and Petroleum Resources, Paper 1997-2, pages 159–172.
- Levson, V.M. and Giles, T.R. (1995): Buried-channel placers; in *Selected British Columbia Mineral Deposit Profiles*, Volume 1 – Metallics and Coal, Lefebure, D.V. and Ray, G.E., Editors, BC Ministry of Energy, Mines and Petroleum Resources, Open File Report 1995-20, pages 25–28.
- Long, P.E. and Wood, B.J. (1986): Structures, textures and cooling histories of Columbia River Basalt flows; *Geological Society of America Bulletin*, volume 97, pages 1144–1155.
- Mathews, W.H. (1989): Neogene Chilcotin basalts in south-central British Columbia; *Canadian Journal of Earth Sciences*, volume 26, pages 969–982.
- Mathews, W.H. and Rouse, G.E. (1986): An Early Pleistocene proglacial succession in south-central British Columbia; *Canadian Journal of Earth Sciences*, volume 23, pages 1796–1803.
- Read, P.B. (1989): Miocene stratigraphy and industrial minerals, Bonaparte to Deadman River area, southern British Columbia (92I/14, 15; 92P/2, 3); BC Ministry of Energy, Mines and Petroleum Resources, Paper 1989-1, pages 515–518.
- Schiarizza, P., Riddell, J., Gaba, R.G., Melville D.M., Umhoefer, P.J., Robinson, M.J., Jennings, B.K. and Hick, D. (2002): Geology of the Beece Creek – Nuit Mountain area, British Columbia (92N/8, 9, 10; 92O/5, 6, 12); BC Ministry of Energy, Mines and Petroleum Resources, Geoscience Map 2002-3, scale 1:100 000.
- Self, S., Keszthelyi, L. and Thordarson, T. (1998): The importance of pahoehoe; *Annual Reviews of Earth and Planetary Sciences*, volume 26, pages 81–110.
- Seth, H.C. (in press): ‘Large Igneous Provinces LIPs’: definition and a hierarchical classification; *Journal of Volcanology and Geothermal Research*.

New Models for Mineral Exploration in British Columbia: Is there a Continuum between Porphyry Molybdenum Deposits and Intrusion-Hosted Gold Deposits?¹

by G.B. Arehart², J.L. Smith² and R. Pinsent³

KEYWORDS: porphyry, molybdenum, isotope geochemistry, Atlin

INTRODUCTION

There has been very little research into, or exploration for, molybdenum deposits in Canada or elsewhere since the early 1980s, but that is likely to change, particularly if the price of molybdenum and tungsten stay at or anything near current levels. There are numerous poorly understood, relatively underexplored molybdenum deposits and occurrences in the Canadian Cordillera that are likely to be explored over the next several years, and it would be of great benefit to the exploration community if more was known about high and low-fluorine type molybdenum deposits in the province.

In addition, there are geochemical similarities (*e.g.*, redox state of the associated pluton; trace and major element chemistry of associated plutons; mineral and elemental assemblages such as high Bi, Te, W and low and peripheral Cu, Pb, Zn) between porphyry molybdenum deposits and 'intrusion-hosted' gold deposits (*e.g.*, Tombstone Belt; Fig 1), suggesting a possible genetic link. The Adanac molybdenum deposit belongs to an important class of occurrences within the Atlin gold camp. The Adanac deposit contains no gold itself, but placer gold is still being mined on the lower reaches of Ruby Creek below the deposit. Historically, it has always been assumed that the molybdenum deposit postdates gold mineralization, which occurs in quartz-carbonate-bearing shears in Cache Creek Group volcanic strata and as placers. However, isotopic work by Mihalynuk *et al.* (1992) suggests that this may not be the case. Mihalynuk's work on Feather Creek (pers comm, 2005) suggests that at least some of the placer gold in the Atlin area may have been derived from the Surprise Lake batholith. This is consistent with the presence of gold and tungsten-bearing quartz veins in the Boulder Creek drainage immediately south of the Adanac molybdenum deposit, because wolframite is commonly associated with porphyry

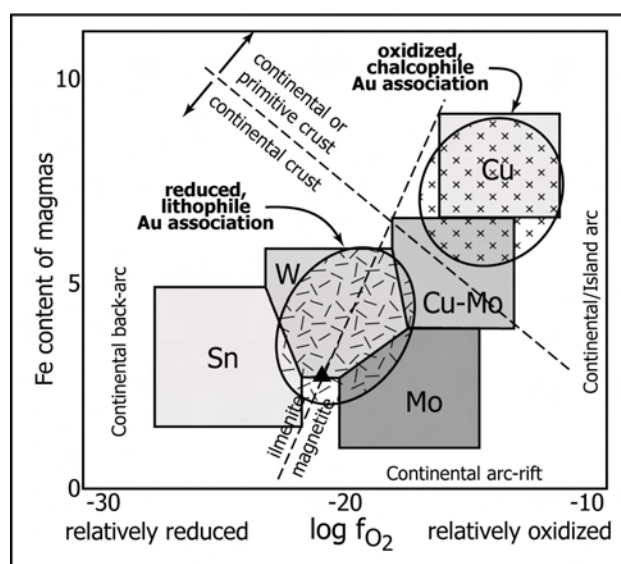


Figure 1. Plot of Fe content versus oxidation state for plutons and associated 'porphyry' mineral deposits (fields from Thompson *et al.*, 1999); note that Au is found in both oxidized (porphyry Cu) and reduced (porphyry Sn-W-Mo) environments; Surprise Lake batholith plots approximately at the solid triangle.

molybdenum deposits, peripheral to the molybdenite zone (Wallace *et al.*, 1967). Thus, the presence of gold in those wolframite veins raises the question of a potential linkage between gold-depleted molybdenum and gold-bearing tungsten 'intrusion-related' deposits. Understanding the association (or lack thereof) is an important step toward focusing further exploration in the province for both of these deposit types.

GEOLOGICAL BACKGROUND

The Adanac molybdenum deposit is located in the northwestern corner of British Columbia, near the town of Atlin (Fig 2). The geology of the Atlin area was mapped by Aitken (1959), and the regional setting of the deposit was discussed by Christopher and Pinsent (1982). The Atlin area (Fig 3) is underlain by deformed and weakly metamorphosed ophiolitic rocks of the Pennsylvanian and/or Permian Cache Creek Group (Monger, 1975). These rocks, which include serpentinite and basalt, as well as limestone, chert and shale, have long been thought to be the source of much of the placer gold found in the Atlin area. The sedimentary and volcanic rocks are cut by two younger batholiths: a Jurassic granodiorite to diorite intrusion

¹ Geoscience BC contribution GBC024

² Department of Geology, University of Nevada-Reno, MS-172, Reno, Nevada 89557

³ Adanac Molybdenum Corporation, 15782 Marine Drive, Suite 2A, Whiterock, BC V4B 1E6

This publication is also available, free of charge, as colour digital files in Adobe Acrobat® PDF format from the BC Ministry of Energy, Mines and Petroleum Resources website at http://www.em.gov.bc.ca/Mining/Geosurv/Publications/catalog/cat_fldwk.htm

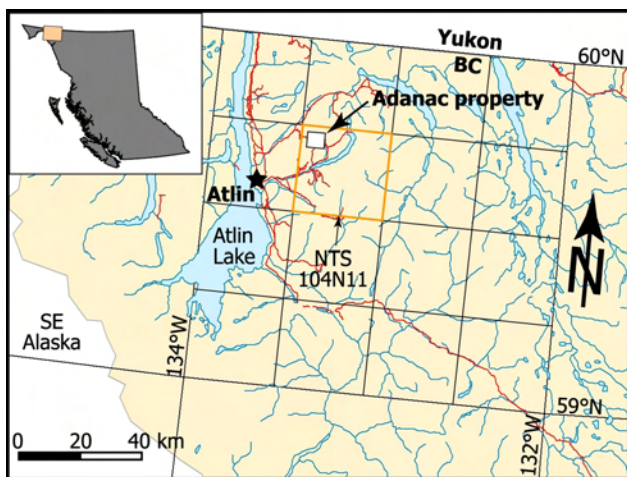


Figure 2. Location of the Adanac molybdenum deposit; white box is approximate location of Figure 3.

(Fourth of July batholith) north of Pine Creek and a Cretaceous granitic to quartz monzonitic intrusion (Surprise Lake batholith) north and south of Surprise Lake. The rocks are locally strongly faulted and the Adanac deposit is located near the intersection of two major syn to postmineral fault systems.

The deposit area was described by Sutherland Brown (1970), White *et al.* (1976), Christopher and Pinsent (1982), and Pinsent and Christopher (1995). The Adanac molybdenum deposit underlies the valley floor near the head of Ruby Creek. It is largely buried and has very little surface expression. There is little outcrop in the lower part of the valley and molybdenite is only rarely found in float and/or veins in outcrop in the bed of the creek. The geology underlying the valley floor is largely derived from drill data (Fig 4). Although the geology of the Adanac deposit is moderately well understood, it has had almost no detailed research. It appears to be a Climax-type high-fluorine alkalic stockwork deposit (Westra and Keith, 1982) with a single flat-lying to steeply dipping 'shell' of mineralization, as described by White *et al.* (1976) and Pinsent and Christopher (1995).

The deposit is near the western margin of the Surprise Lake batholith, a composite, highly evolved, uranium-rich granite. It is entirely within plutonic rock. There are three stages of intrusion: an early, generally coarse-grained stage that was deformed prior to intrusion of second-stage 'porphyry' domes, and a late, fine-grained phase that was injected through the previous two stages at about the same time as mineralization. The deposit itself is a disrupted, blanket-shaped deposit that formed late in the development of the plutonic suite. The deposit is partially controlled and offset by the Adera fault system, which trends approximately northeast and defines much of the southern boundary of the pre-ore Fourth of July batholith. The approximately north-trending Boulder Creek fault system appears to have localized emplacement of the late, third-stage porphyritic and aplitic plutonic rocks that are thought to have generated the majority of mineralization.

2006 SUMMER FIELD PROGRAM

The first phase of the study, comprising the development of a genetic and exploration model for the deposit type, including chemical, mineralogical and alteration zoning, was launched in the summer of 2006. Time was spent becoming familiar with deposit geology: background reading, field checking of old core logs and logging of new core from the drill program currently being carried out by Adanac Molybdenum Corporation. However, most of the summer focused on sampling. A total of 182 samples from core was collected along a series of cross-sections of the deposit shown in Figure 4. Thirty of these samples have been selected for petrographic analysis, the purpose of which is to shed light on major rock types (listed in Fig 4) and provide preliminary mineralogical and hydrothermal alteration data. Additional optical microscopy will be done as the project progresses.

Adanac Molybdenum Corporation had previously completed Mo percentage analysis in 10-foot (3 m) intervals on all drillholes and trace element analysis (excluding fluorine) on 5 of the 55 drill holes. Since the pulps from these analyses were still available, pulps from the drillholes on the cross-section in Figure 4 were composited according to similar lithology on intervals ranging from 30 to 50 feet (9–15 m). These composites are being analyzed for 41 trace elements plus fluorine by inductively coupled plasma mass spectrometry (ICP-MS). When the results become available, they will be used to generate the model of trace element zoning and alteration halos that is the ultimate goal of the first phase of this project.

Samples of a tungsten (huebnerite-wolframite) deposit that is located on the Adanac property and possibly related to the Adanac deposit (MINFILE 104N 053; MINFILE, 2006) were collected for comparison of fluid inclusions with those of the molybdenum deposit. Fluid inclusion measurements on these samples will provide clues as to whether the tungsten mineralization is directly related to the same hydrothermal system that deposited the molybdenum.

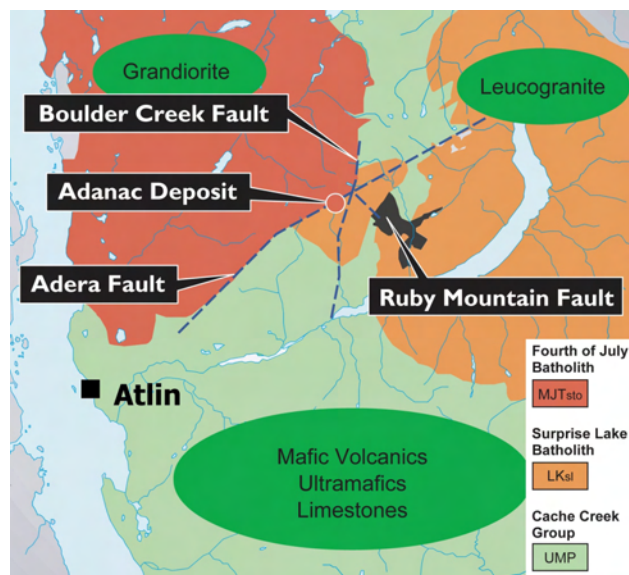


Figure 3. General geology of the Adanac deposit area (modified from Aitken, 1959).

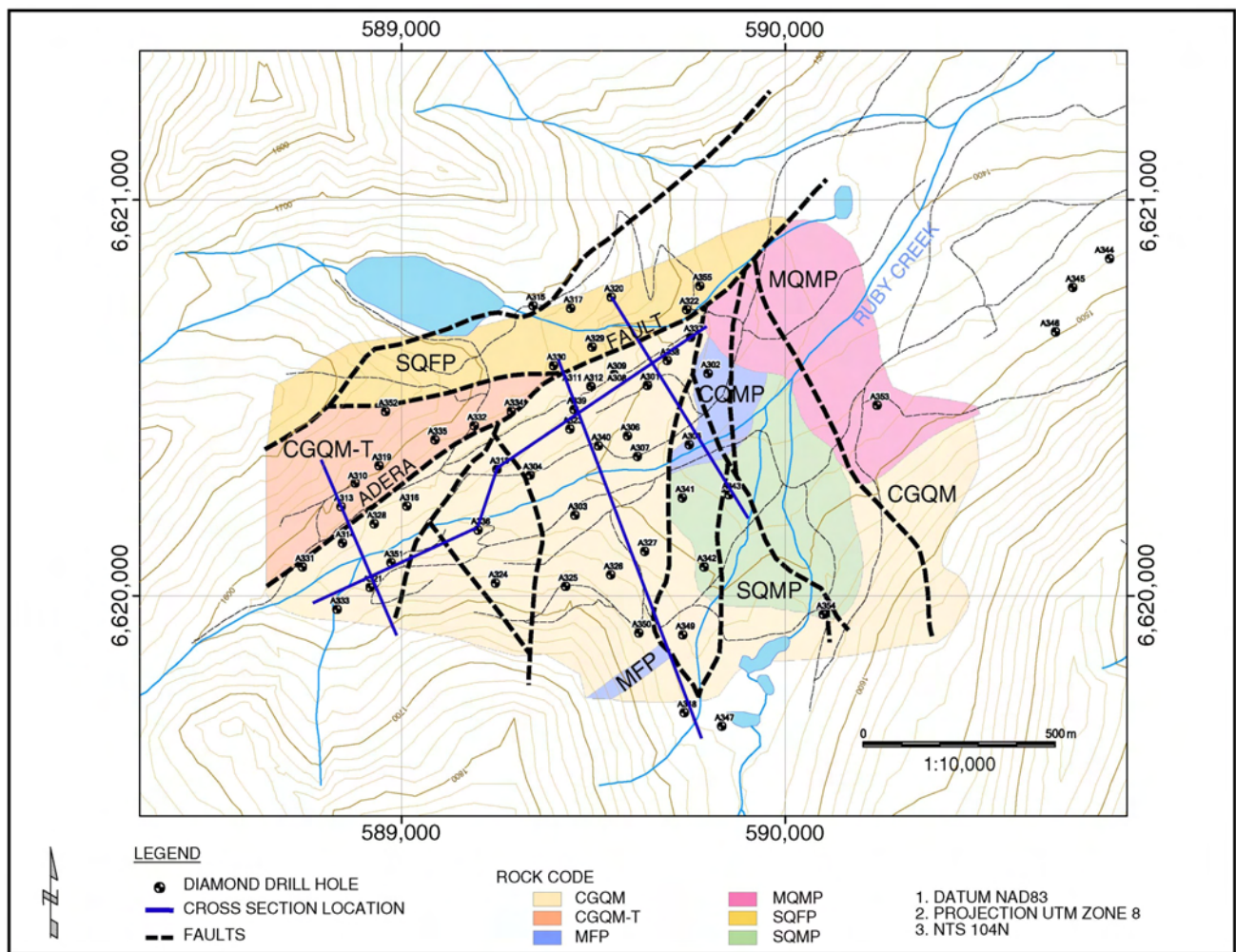


Figure 4. Surface geology of the Adanac molybdenum deposit (*modified from unpublished company reports*), showing a cross-section of diamond-drill holes from which samples were collected for geochemical analysis.

The second phase of the project is to compare this deposit with other molybdenum deposits in western North America, as well as with nontraditional molybdenum deposits, specifically intrusion-hosted gold deposits of the Tombstone Belt. To this end, fresh rock samples from the Surprise Lake pluton were collected in order to compare the chemistry of this pluton with that of other plutons in productive mineral belts. Oxidation state of these plutons will be investigated using magnetite/ilmenite by reflected-light microscopy and Fe^{2+}/Fe^{3+} geochemical analyses. This will help to place the pluton more clearly in the context of the geochemistry of porphyry intrusions (Fig 1). Isotope geochemistry (O and S isotope composition) will also be used to further constrain the origin of the plutons. At the deposit scale, stable isotopes can be used to constrain the origins of fluid components and for developing a model for fluid flow and water-rock interaction.

In addition, several samples of molybdenite were collected for Re-Os isotope geochronology. This will place a more precise date on the mineralization event. More important to the exploration community, however, is using that age in conjunction with Re-poor phases like pyrite to obtain an initial Re isotope composition for the molybdenite event. Comparison of the initial Re isotope composition of

the placer gold in Ruby Creek with that of the Mo system will allow a determination of whether there is a geochemical link between the gold and molybdenite. Proving or disproving this link will have very important ramifications for exploration strategies at a regional scale.

CONCLUSIONS

The first phase of fieldwork has been completed and a more complete model of mineralization at Adanac is being developed, including geological, geochemical and mineralogical patterns. These data will more clearly elucidate the similarities and differences between Adanac and other molybdenum and gold deposits in western North America.

ACKNOWLEDGMENTS

We thank Adanac Molybdenum Corporation for financial and logistical support. Additional financial support was provided by Geoscience BC. We appreciate constructive reviews by Rob Stevens and anonymous reviews by the staff of Geoscience BC.

REFERENCES

- Aitken, J.D. (1959): Atlin map area, British Columbia; *Geological Survey of Canada*, Memoir 307, 89 pages.
- Christopher, P.A. and Pinsent, R.H. (1982): Geology of the Ruby Creek – Boulder Creek area (Adanac molybdenum deposit); *BC Ministry of Energy, Mines and Petroleum Resources*, Preliminary Map 52, scale 1:12 000.
- Mihalynuk, M.G., Smith, M.T., Gabites, J.E. and Runkle, D. (1992): Age of emplacement and basement character of the Cache Creek terrane as constrained by new isotopic and geochemical data; *Canadian Journal of Earth Sciences*, volume 29, pages 2463–2477.
- MINFILE (2006): MINFILE BC mineral deposits database; *BC Ministry of Energy, Mines and Petroleum Resources*, URL <<http://www.em.gov.bc.ca/Mining/Geolsurv/Minfile/>> [November 2006].
- Monger, J.W.H. (1975): Upper Paleozoic rocks of the Atlin terrane; *Geological Survey of Canada*, Paper 74-47, 63 pages.
- Pinsent, R.H. and Christopher, P.A. (1995): Adanac (Ruby Creek) molybdenum deposit, northwestern British Columbia; *Canadian Institute of Mining and Metallurgy*, Special Volume 46, pages 712–717.
- Sutherland Brown, A. (1970): Adera; in *Geology, Exploration and Mining in British Columbia in 1969*; *BC Ministry of Energy, Mines and Petroleum Resources*, pages 29–35.
- Thompson, J.F.H., Sillitoe, R.H., Baker, T., Lang, J.R. and Mortensen, J.K. (1999): Intrusion related gold deposits associated with tungsten-tin provinces; *Mineralium Deposita*, volume 34, pages 323–334.
- Wallace, S.R., Muncaster, N.K., Jonson, D.C., Mackenzie, W.B., Bookstrom, A.A. and Surface, V.E. (1968): Multiple intrusion and mineralization at Climax, Colorado; in *Ore Deposits of the United States, 1933-1967*, *American Institute of Mining, Metallurgical and Petroleum Engineers*, pages 605–641.
- Westra, G. and Keith, S.B. (1981): Classification and genesis of stockwork molybdenum deposits; *Economic Geology*, volume 76, pages 844–873.
- White, W.H., Stewart, D.R. and Ganster, M.W. (1976): Adanac (Ruby Creek) porphyry molybdenum deposits of the calc-alkaline suite; *Canadian Institute of Mining and Metallurgy*, Special Volume 15, p. 476–483.

Preliminary Results from a Microseismic Noise Test Utilizing Passive Seismic Transmission Tomography, Nechako Basin (NTS 0920/11, 14), South-Central British Columbia¹

by M.E. Best² and J. Lakings³

KEYWORDS: microseismic, Nechako Basin, earthquakes, petroleum, seismic noise test

SUMMARY

Results of a reconnaissance microearthquake survey in the southern portion of the Nechako Basin are presented here. The data were acquired over a time period of approximately 24 hours in June 2006 and analyzed at the office of MicroSeismic, Inc. The analysis provided measurements of the background noise level and its diurnal variation. The very low background noise levels between 50 and 100 nm/s show that a surface seismic array is capable of detecting microearthquakes of local magnitude (M_l) approximately 0.0 and possibly down to approximately -0.5 as much as 30 km away. Earthquakes of this size are similar to small blasts at construction sites or mining quarries, and require a network of closely spaced, highly sensitive seismograph stations to detect and locate them. The high station density and the frequent occurrence of microearthquakes make these data ideally suited for mapping crustal structure in seismogenic belts. The initial results from the reconnaissance survey also located a magnitude 0.0 earthquake using a computer-aided search routine for microearthquake activity. This event was observed on all five of the geophone stations in the array and was approximately 30 km away from the centre of the array. Three-component geophones now occupy these same five sites and will remain there for approximately 8 weeks, in order to determine the amount of microseismic activity within this region.

INTRODUCTION

The Nechako Basin is one of several interior sedimentary basins in British Columbia. This basin is partially covered with basalt flows, which make it difficult to map the subsurface geology using traditional seismic methods. A few wells were drilled within the basin prior to 1980. The most significant exploration program, however, was carried out in the early 1980s by Canadian Hunter Exploration

Ltd. They conducted 2-D seismic (Fig 1) and gravity surveys, and drilled several wells. The quality of the seismic data was relatively poor due to surface and near-surface basalt flows. Nevertheless, several wells were drilled based on the seismic data. Sedimentary rocks were encountered in the wells, often with crystalline rocks. Economic accumulations of hydrocarbons were not encountered at that time; consequently, Canadian Hunter abandoned the play. No exploration activity has been carried out in the basin since that time.

In 2004, the BC Ministry of Energy, Mines and Petroleum Resources began a geological mapping program within the Nechako Basin (Hayes *et al.*, 2005), the objective of which is to provide new data that will encourage industry to re-examine the basin. They reprocessed several of Canadian Hunter's 2-D seismic lines using modern processing methods and investigated source-rock maturation levels in partnership with the Geological Survey of Canada (GSC). A detailed ground gravity and magnetic survey was carried out by Bemex Consulting International for the ministry along a 32 km line that crossed a large gravity low observed on the Canadian Hunter regional Bouguer gravity data (Best, 2004). During the 2005 and 2006 field seasons, the ministry conducted geological mapping and collected samples for density and magnetic susceptibility measurements (Ferri and Riddell, 2006).

Acquiring good-quality data from conventional 2-D seismic surveys in areas covered with basalt flows (e.g., the Columbia Plateau and parts of the Libyan desert) has always presented a challenge for the petroleum industry. The Nechako Basin is no exception, and this is one possible reason why there has been little exploration activity within the basin. Modern acquisition and processing methods may overcome some of the difficulties associated with acquiring traditional seismic data in basalt-covered regions of the world.

Alternative methods of acquiring 2-D and 3-D seismic information need to be investigated as well. This project proposes to use passive seismic transmission tomography (PSTT) as an alternative method for obtaining structural and lithological information within the Nechako Basin (e.g., Kapotis *et al.*, 2003; Mahony, 2003). The PSTT method utilizes the naturally occurring acoustic energy generated by microearthquakes in the upper few kilometres of the Earth as a seismic source. It employs conventional seismological methods to determine the hypocentres of these small-magnitude events, and then applies seismic tomographic techniques (Zhao *et al.*, 1992; Eberhart-Phillips, 1993; Thurber, 1993) to the data to produce 3-D, multicomponent velocity volumes through the area of interest. The PSTT energy source is located below the basalt and has to traverse the high-reflectivity zones only once,

¹ Geoscience BC contribution GBC028

² Bemex Consulting International, 3701 Wild Berry Bend, Victoria, BC

³ MicroSeismic, Inc., 175–800 Tully Road, Houston, TX

This publication is also available, free of charge, as colour digital files in Adobe Acrobat® PDF format from the BC Ministry of Energy, Mines and Petroleum Resources website at http://www.em.gov.bc.ca/Mining/Geolsurv/Publications/catalog/cat_fldwk.htm

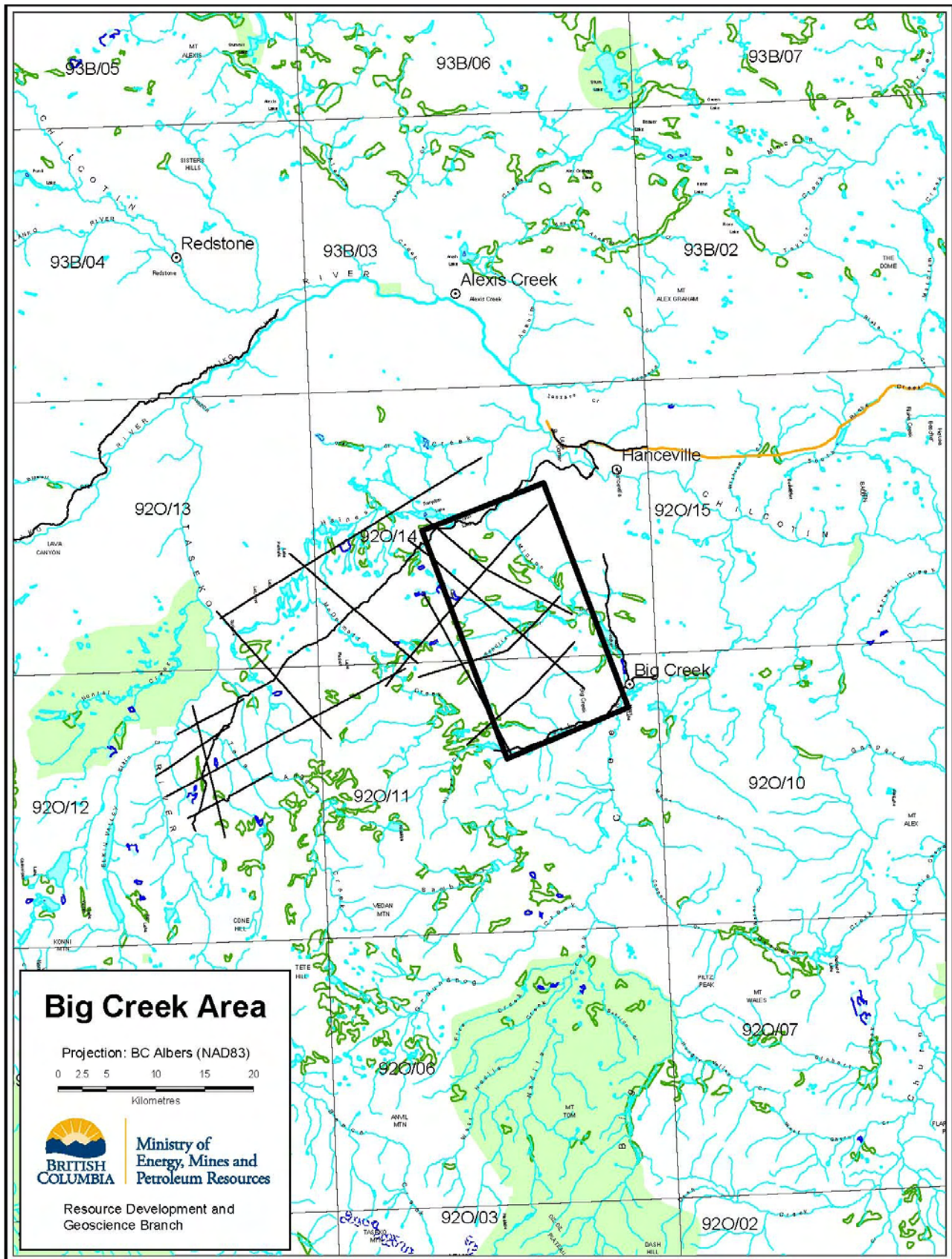


Figure 1: Approximate location of proposed passive seismic transmission tomography survey area (indicated by black rectangle); lighter black lines show locations of several 2-D seismic lines run by Canadian Hunter Exploration Ltd. in the early 1980s; map courtesy of BC Ministry of Energy, Mines and Petroleum Resources.

thus providing a less attenuated and more coherent signal than conventional sources placed directly on or above the basalt. The method provides a regional 3-D image of the Earth for the region of interest at a fraction of the cost of conventional 3-D surveys.

The focus of the fieldwork presently being carried out is to measure background noise levels and to estimate the amount of seismic activity in the rectangular area shown in Figure 1. This region was selected for the study because it contains several 2-D seismic lines shot by Canadian Hunter and a well that intersected sedimentary rocks. The recent detailed gravity and magnetic survey line described above (Best, 2004) and a regional gravity low are also located in this area (Fig 2). The large gravity low is intriguing, as it may be related to a sedimentary sub-basin within the Nechako Basin. The 2-D seismic quality, however, is too poor to determine if this is a sub-basin and, without more control, the gravity data alone cannot determine if the low is caused by sedimentary rocks or different volcanic rock units.

ACQUISITION

The surface noise in the Nechako Basin was sampled at five separate locations, four of which form the corners of the rectangular area in Figure 1, with the remaining station near the centre. The station locations were surveyed using hand-held Global Positioning System receivers. At each station, a Refraction Technology Inc. (REF TEK) RT-130 seismograph was used to record ground motion on three vertical 4.5 Hz geophones laid out over a 7.6 m interval. The stations were set up during the day and left to record for a period of approximately 24 hours (June 24–25, 2006). The data were sampled at a rate of 2000 μ s (2 ms) with a +32 dB gain. The units recorded the data using flash memory, which was later downloaded to a laptop computer. The data were converted to standard SEG-Y format for further processing and analysis.

ANALYSIS

The raw data were scanned using a trigger detection algorithm to find events that occurred on at least three stations. During the overnight recording period, one small microearthquake was detected on all five stations. The seismograms were converted to ground motion by deconvolving the instrument response. The amplitude spectra of the deconvolved traces were used to measure the frequency content of the signal and noise (Fig 3). The microearthquake had an M_l value of approximately 0.0 and the signal-to-noise ratio was 3:1 during the evening.

RESULTS

The Nechako Basin is seismically active and characterized by very low levels of background noise. The noise level hovers around ± 100 nm/s during the day, with occasional spikes to 1 μ m/s. During the evening, the noise drops off and is approximately half that during the daytime. These very low levels of background surface noise suggest that it will be possible to detect and time many of the numerous small microearthquakes in the area that are necessary for a successful PSTT project. This result is further supported by the small events (down to local magnitude of zero) reported

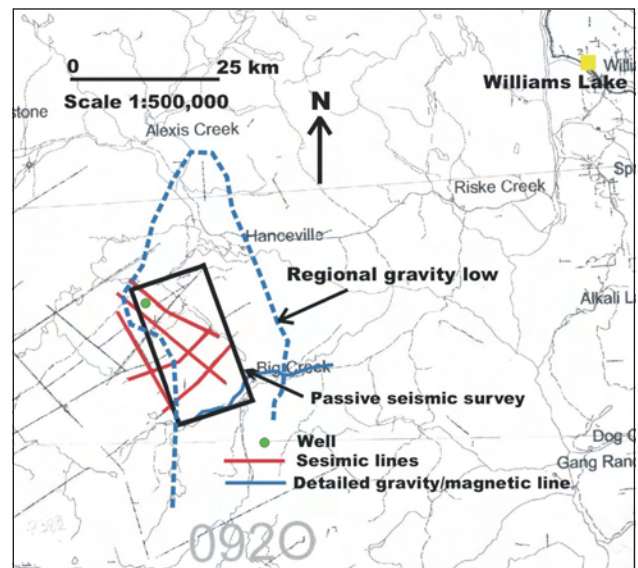


Figure 2: Locations of gravity low, exploration well drilled by Canadian Hunter Exploration Ltd. and recent gravity and magnetic survey carried out by Bemex Consulting International (Best, 2004).

for this area in the Geological Survey of Canada (GSC) earthquake catalogue. During the overnight recording period, an event with an M_l value of 0.0, approximately 30 km away, was recorded across the array, although it was too small to be reported by the GSC.

FUTURE WORK

The reconnaissance survey (phase I) of the project is now in progress. Five three-component seismometers, one being considered a spare, have been deployed for a period of approximately eight weeks at the sites that were tested for the noise analysis. The data will be used to constrain the strength, frequency and location of the background seismicity. With the generally very quiet recording conditions at the site, it was not necessary to deeply bury the geophones. The three-component seismometers were oriented and grouted in hand-augured holes that had been augured to a depth of approximately 1 m to ensure adequate coupling. This recording configuration will help to further refine the microearthquake detection threshold for this survey area and its economic implications.

The results of the phase I survey will determine if there is sufficient microseismic activity in the area to warrant a full-scale 3-D survey of the rectangular area shown in Figures 1 and 2.

ACKNOWLEDGMENTS

The authors would like to thank Geoscience BC and the BC Ministry of Energy, Mines and Petroleum Resources for joint funding of this project.

REFERENCES

- Best, M.E. (2004): Qualitative interpretation of potential field profiles: southern Nechako Basin; in Summary of Activities 2004, BC Ministry of Energy, Mines and Petroleum Resources, URL <<http://www.em.gov.bc.ca/subwebs/oil>>

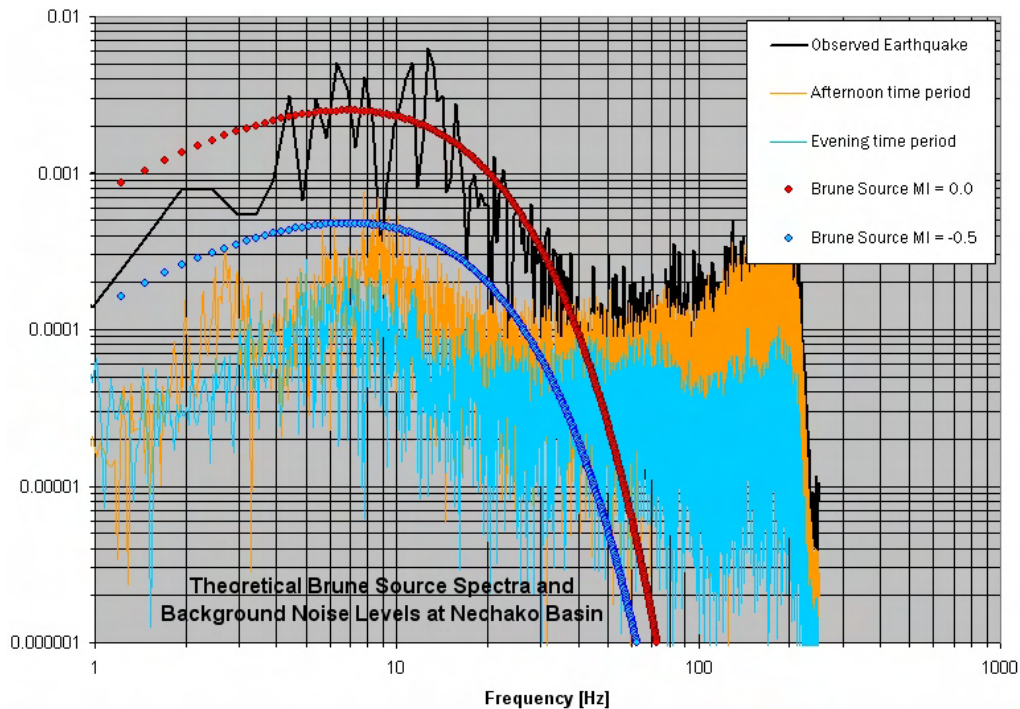


Figure 3: Amplitude spectra showing daytime and night-time noise levels and the amplitude spectrum of the observed earthquake; theoretical Brune source spectra for events with M_l values of 0.0 and 1.0 are also shown when the distance to the events is 30 km.

andgas/pub/reports/summary2004.htm> [November 2006], pages 73–77.

Eberhart-Phillips, D. (1993): Local earthquake tomography: earthquake source regions; in *Seismic Tomography Theory and Practice*, Iyer, H.M. and Hirahara, K., Editors, *Chapman & Hall*, London, United Kingdom, pages 613–643.

Ferri, F., and Riddell, J. (2006): The Nechako Basin project: new insights from the southern Nechako basin; in *Summary of Activities 2006, BC Ministry of Energy, Mines and Petroleum Resources*, URL <<http://www.em.gov.bc.ca/subwebs/oilandgas/pub/reports/summary2006.htm>> [November 2006], pages 89–124.

Hayes, M., Ferri, F., and Moril, S. (2005): Interior basins strategy; in *Summary of Activities 2004, BC Ministry of Energy, Mines and Petroleum Resources*, URL <<http://www.em.gov.bc.ca/subwebs/oilandgas/pub/reports/summary2004.htm>> [November 2006], pages 73–77.

www.em.gov.bc.ca/subwebs/oilandgas/pub/reports/summary2005.htm> [November 2006], pages 69–71.

Kapotis, S., Tselentis, G-Akis and Martakis, N. (2003): Case study in NW Greece of passive seismic tomography: a new tool for hydrocarbon exploration; *First Break*, volume 21, December, pages 37–42.

Mahony, J. (2003): No footprint seismic; *New Technology Magazine*, December, pages 10–12.

Thurber, C.H. (1993): Local earthquake tomography: velocities and V_p/V_s theory; in *Seismic Tomography Theory and Practice*, Iyer, H.M. and Hirahara, K., Editors, *Chapman & Hall*, London, United Kingdom, pages 563–583.

Zhao, D., Hasegawa, A. and Horiuchi, S. (1992): Tomographic inversion of P and S wave velocity structure in NE Japan; *Journal of Geophysical Research*, volume 97, pages 19909–19928.

Geochemistry of Mesozoic Intrusions, Quesnel and Stikine Terranes (NTS 082; 092; 093), South-Central British Columbia: Preliminary Characterization of Sampled Suites¹

by K. Breitsprecher², J.S. Scoates², R.G. Anderson³ and D. Weis²

KEYWORDS: geochemistry, isotopes, geochronology, Mesozoic, batholiths, porphyry, Quesnel Terrane, Stikine Terrane, Thuya, Takomkane, Okanagan, Topley, Endako, Nicola Group, Rossland Group, Takla Group, Jurassic, Triassic, Copper Mountain, Iron Mask

INTRODUCTION

The record of arc magmatism is widespread in the Canadian Cordillera (*e.g.*, Armstrong, 1988; Woodsworth *et al.*, 1991), particularly in the Quesnel and Stikine terranes, where plutonic rocks related to Mesozoic arcs host most of the porphyry-style mineral deposits in the Cordillera (Anderson, 1985; Woodsworth *et al.*, 1991; McMillan *et al.*, 1995; Fig 1). Isotopic characterization of arc rocks is a powerful tool for distinguishing source and contamination signatures of magmas, and has direct applications to developing economic and tectonic models for Mesozoic magmatism. Despite the importance of the plutonic hostrocks, there is a lack of reliable and complete geochemical and radiogenic isotope compositions for these intrusions in southern British Columbia. Previous geochemical studies have emphasized the volcanic units, particularly the Late Triassic to Jurassic (?) Nicola Group (Schau, 1970; Preto *et al.*, 1979; Mortimer, 1987; Smith *et al.*, 1995). Effective use of radiogenic isotope geochemistry requires knowledge of the absolute age of individual samples, and identification of temporal suites of intrusions from different regions. Poor age constraints on the Nicola Group and its complex structural style (Schau, 1970; Preto, 1979) have hindered widespread application of detailed studies (*e.g.*, Preto *et al.*, 1979; Mortimer, 1987; Smith *et al.*, 1995), particularly those involving Sr and Nd isotopes. Published Sr and Nd isotope compositions are available for a number of scattered intrusions (Ghosh, 1995), which provides an important basis for further geochemical study.

This study addresses the paucity of compositional information for Mesozoic igneous rocks of metallogenic importance in southern British Columbia (Fig 2). The work is

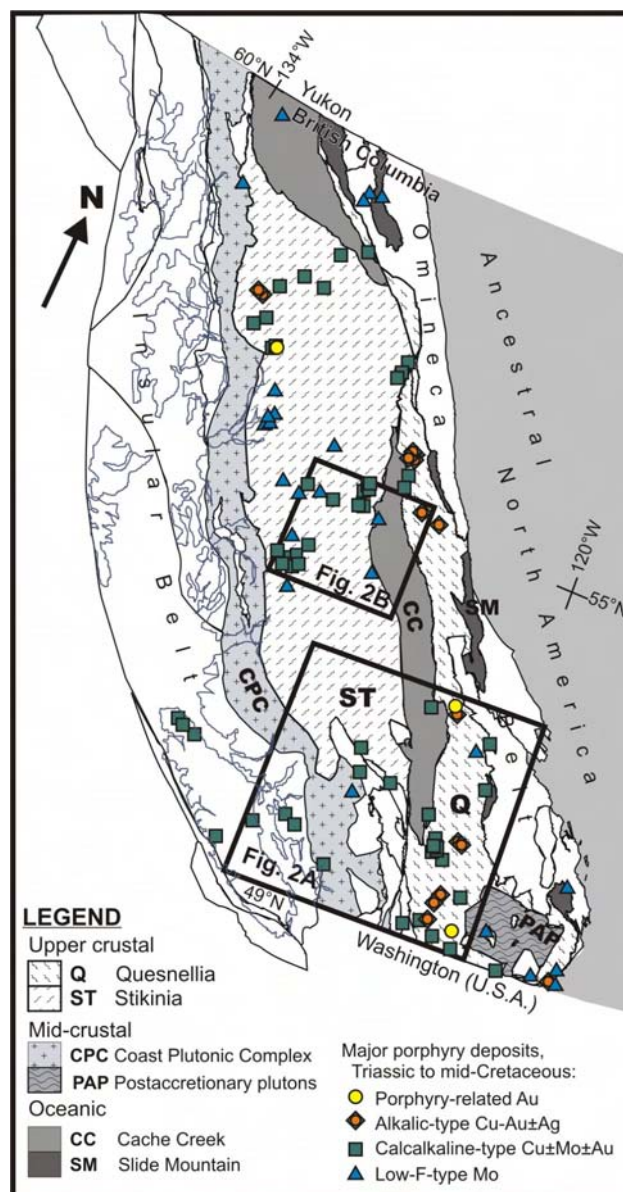


Figure 1. Major terranes of the Coast and Intermontane belts, and distribution of major Triassic to mid-Cretaceous porphyry-style deposits in the Canadian Cordillera; deposit information from MINFILE (2006) and CordMinAge 2006 (Madsen *et al.*, 2006); terrane polygons from MapPlace (2006).

¹ Geoscience BC contribution GBC037

² Pacific Centre for Geochemical and Isotopic Research, Department of Earth and Ocean Sciences, University of British Columbia, Vancouver, BC

³ Geological Survey of Canada, Vancouver, BC

This publication is also available, free of charge, as colour digital files in Adobe Acrobat® PDF format from the BC Ministry of Energy, Mines and Petroleum Resources website at http://www.em.gov.bc.ca/Mining/Geolsurv/Publications/catalog/cat_fldwk.htm

timely because 1) of recent improvements in mass spectrometry (e.g., Hf and Pb isotopes by multicollector inductively coupled plasma mass spectrometer); and 2) a significant number of reliable U-Pb zircon ages, which are critical for age corrections and the determination of initial isotopic ratios, have been reported from southern British Columbia since the previous geochemical studies were published. The purpose of this initial report is to provide an inventory and preliminary characterization for 57 new samples collected for high-precision geochemical analysis (major and trace element geochemistry, and Sr-Nd-Hf-Pb isotopic compositions). The primary objective is to provide compositional 'fingerprints' for mineralized suites, in order to characterize the 'mineralizer' phase(s) and to provide a basis for comparison of prospective suites identified in frontier exploration. The identification of variations in source or contamination with respect to geographic location and age in the Cordillera is potentially important in identifying the plutonic suites most likely responsible for the mineralizing event (e.g., McMillan *et al.*, 1995). If metal enrichment is related to source and/or processes of magma genesis of the host (mineralized) rocks, then definition of their petrology will lead to an improved understanding of the origins of the base metal endowments of the porphyry systems that characterize the southern Cordillera.

The Triassic and Early Jurassic rocks of Quesnellia and Stikinia have been interpreted to predate, or are coeval with, accretion of those terranes to the western edge of North America *ca.* 185 to 180 Ma (Monger *et al.*, 1982; Struik *et al.*, 2001; Monger and Price, 2002). New geochemical and isotopic compositions for arc rocks from the Quesnel Terrane, particularly the Hf and Pb isotopes, will be used to discern whether the pre-185 Ma lavas and plutonic rocks contain any component of radiogenic (Precambrian) crust. This will provide a test of an alternate hypothesis to the established accretionary-tectonism paradigm, which suggests an autochthonous (continental arc; Struik, 1988; Erdmer *et al.*, 2002; Thompson *et al.*, 2006)

rather than allochthonous (island arc; Monger *et al.*, 1982; Ghosh, 1995; Monger and Price, 2002) origin for the Quesnel Terrane.

GEOCHEMICAL SAMPLING

Fifty-seven new samples for geochemical investigation, as summarized at Table 1, were collected in the spring (TGI-3 area samples, Fig 2A) and summer (BIZ area samples, Fig 2A, B) of 2006. Magnetic susceptibility readings were recorded for the majority of the sampled outcrops, and the average of multiple measurements at each outcrop is reported in Table 1. The samples represent four time-slices of the evolution of the arc system (Fig 3A): latest Triassic (202 \pm 6/-4 Ma), Early Jurassic (190 \pm 4 Ma), Middle Jurassic (170 \pm 4 Ma) and Late Jurassic (150 \pm 5 Ma). The criteria for selecting the mean age of each time-slice was to target those suites with demonstrable economic merit (202 Ma, 193 Ma and 150 Ma suites) or tectonic relevance (170 Ma suite: provides baseline composition for postaccretionary magmatism). The intent of the time-slice approach is to minimize local effects such as crystal fractionation at any given igneous complex, in favour of providing a snapshot of compositions across the arc system. A given time-slice age is expanded to allow inclusion of rocks that are within error of the median error reported for a given suite (Table 1), which is done to ensure that truly cogenetic intrusions are not excluded from sampling of a suite on the basis of the error associated with a given age. Several Late Jurassic and mid-Cretaceous intrusive samples were collected in advance of an anticipated future phase of the project, which will test the possibility of a correlation between Stikinia and the Coast Plutonic Complex (e.g., Rusmore and Woodsworth, 1991; Israel and Kennedy, 2003). Such a correlation poses an intriguing alternative to the widely accepted tectonic model in which older phases of the Coast Plutonic Complex form the midcrustal counterpart to the Wrangell Terrane of the Insular Belt (Fig 1; e.g., Nelson, 1979; Monger *et al.*, 1982; Friedman *et al.*, 1995).

Most of the samples in this study are from the Quesnel Terrane. The Okanagan, Thuya and Takomkane batholiths are ideal targets, because they contain intrusive phases from more than one of the targeted time-slices that are apparently contained within a single crustal (fault) block. This will be an advantage when interpreting the geochemical results with respect to crustal assimilation or source, in a region that is fragmented by pervasive, large-scale, strike-slip deformation (e.g., Ewing, 1980; Struik, 1993; Irving *et al.*, 1996). For example, at the Okanagan batholith, samples from the Early Jurassic, Middle Jurassic and mid-Cretaceous intervals are not reportedly separated by major strike-slip faults, and thus their paleogeography with respect to one another is constrained. Thus, one assumption, namely that of emplacement into and assimilation by a common, albeit evolving, crustal assemblage, is removed at the interpretive stage.

In addition to the three major batholiths, samples were collected from intrusions of similar age that occur to the north and west of the Okanagan batholith. These include the latest Triassic Copper Mountain stock (Similco-Ingerbelle deposits; Preto, 1972; Preto *et al.*, 2004), the Allison Lake diorite (Axe deposit; Preto *et al.*, 1979) and the Cherry Creek phase of the Iron Mask batholith (Afton-Ajax deposits; Logan and Mihalynuk, 2004). The Quesnellia sample base is complemented by several sam-

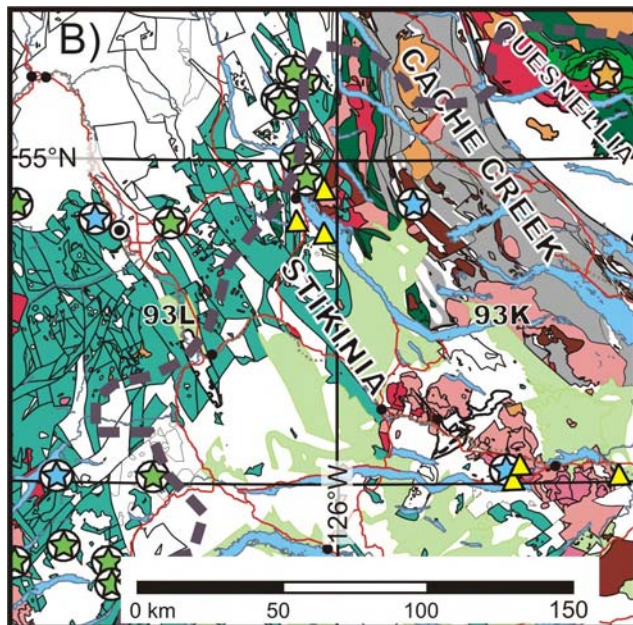


Figure 2B (caption on opposite page)

TABLE 1. SUMMARY, 2006 GEOCHEMICAL SAMPLING. SEE FIGURE 2 FOR SAMPLE LOCATIONS.

Sample no.	UTM: zone, E, N	Elev. (m)	NTS ref	Map unit	Rock description	Age, method ^{source} x-ref age o/c, proximity:	Mag. Susc.
Latest Triassic							
06KB013A	10 680376 5614658	832	92I/09	Iron Mask/ Cherry Crk	medium-grey weathering, reddish-pink, fine-grained fractured diorite	204.5 0.6, U(z), ¹	0.2
06KB014A	10 669347 5619598	467	92I/10	Iron Mask/ Cherry Crk	reddish-pink weathering, pinkish-grey, fine- grained, fractured hornblende monzodiorite	"	17.8
06KB020A	10 682440 5469869	1010	92H/07	Copper Mtn/ Voigt Stock	medium-grey weathering, dark-brown, fine-grained fractured hornblende diorite	202.7 +4.4/-0.5, U(z), ¹	2.9
06KB021A	10 681810 5469001	1059	92H/07	Copper Mtn/ Voigt Stock	light-grey weathering, medium-grey, medium-grained, massive hornblende monzodiorite	"	20.6
06KB025A	10 679300 5508479	920	92H/10	Allison Lake diorite	reddish-pink weathering, pinkish-grey, fine-grained fractured hornblende monzodiorite	204 10, K(b), ² NEW U-Pb in progress	n/a
06KB017A	10 701743 5530152	1614	92H/16	Nicola Group (east)	dark-grey weathering, medium-grey, fine-grained, veined augite plagioclase-phyric andesite	< 212 Ma	7.2
06KB023A	10 679459 5502199	877	92H/10	Nicola Group (east)	rusty weathering, dark-grey, aphanitic, fractured augite plagioclase-phyric basalt	< 212 Ma	24.6
06KB024A	10 679056 5508035	945	92H/10	Nicola Group (east)	light-grey weathering, greenish-grey, epidote-veined plagioclase-porphyrific, basaltic trachy-andesite	< 212 Ma	n/a
06KB053A	10 709567 5635368	1006	92I/16	Hefley Creek pluton	light-grey weathering, medium-grey, medium-grained pyritized hornblende quartz monzodiorite	208.1 6.1, U(z,t), ³ GR00-17, <5m	6.4
06KB044A	10 674757 5705921	1137	92P/08	North Thuya granodiorite	light-grey weathering, salt and pepper, coarse-grained, pyritized biotite hornblende quartz monzodiorite	201.3 2.3, U(z) ⁴ 01PSC-341, 2m	3.7
06KB039A	10 650533 5762839	1174	92P/15	Takomkane/ Boss Creek	cream weathering, medium-grey, medium-grained hornblende quartz monzodiorite	I.Tri U(z) (preliminary) ⁵ 05PSC-047, <1m	26.8
06KB045A	10 680201 5712047	1446	92P/09	Deer Lake stock	light-grey weathering, salt and pepper, coarse-grained hornblende-megacrystic epidotized hornblende diorite	197.8 1.4, U(z), ⁷ 01PSC-161, <1m	0.2
06KB050A	10 617454 5757942	1408	92P/14	Nicola Group	light-grey weathering, medium-grey, K-feldspar veined trachy-andesite with potassic alteration	203 4 U(z), ⁶ RW-95-97, 200m	38.3
06KB051A	10 616449 5757946	1408	92P/14	Takomkane/ satellite	orange weathering, dark-grey, fractured hornblende quartz monzodiorite	"	12.9
06KB030A	09 687693 6072806	739	93L/16	Topley (Stikine)	orange weathering, pinkish-grey, coarse-grained, foliated K-feldspar megacrystic hornblende granodiorite	210 2, A(h), ⁸	0.5
06KB033A	09 678716 6076754	786	93L/16	Takla Group (Stikine)	dark-grey weathering, medium-grey, augite plagioclase-porphyrific andesite	208 2, A(h), ⁸	-
Early Jurassic							
06KB006A	10 705082 5473992	553	92H/08	Okanagan/ Bromley	medium-grey weathering, salt and pepper, K-feldspar megacrystic biotite hornblende granodiorite	193 1 U(z), ⁹ MV-84-41, 400m	n/a
06KB002A	10 697857 5479121	586	92H/08	Okanagan/ Bromley	green-grey weathering, salt and pepper, K-feldspar porphyritic biotite hornblende granodiorite	"	0.0
06KB003A	10 694801 5480344	596	92H/08	Okanagan/ Bromley	medium-grey weathering, light-grey, medium-grained biotite hornblende granodiorite	"	0.7
06KB004A	10 690217 5481297	591	92H/08	Okanagan/ Bromley	medium-grey weathering, light-grey, biotite hornblende granodiorite	"	8.1
06KB018A	11 289090 5529561	1327	82E/13	Okanagan/ Pennask	pinkish-grey weathering, light-grey, coarse-grained, fractured biotite hornblende granodiorite	194 1 U(z), ⁹	8.6
06KB016A	10 701216 5529637	1581	92H/16	Okanagan/ Pennask	medium-grey weathering, light-grey, coarse-grained biotite hornblende quartz monzodiorite	"	6.8
06KB019A	11 300155 5498079	686	82E/12	Okanagan/ Pennask	medium-grey weathering, light-grey, coarse-grained biotite hornblende granodiorite	NEW U-Pb in progress	7.7
06KB054A	10 704003 5634909	1256	92I/16	Mt Fleet alk. complex	orange weathering, medium-pink, pyritized nepheline-megacrystic foid-bearing monzonite	186.9 1.7, U(z), ³ GR00-08	0.1
06KB055A	11 292240 5618517	898	82L/12	"Rossland" Group	rusty weathering, green-grey, fine-grained pyritized augite plagioclase-phyric andesite	< Early Jurassic ammonite ¹¹	0.3
06KB056A	11 291680 5618114	904	82L/12	"Rossland" Group	dark-grey weathering, green-grey, pyritized aphanitic augite plagioclase-phyric basalt	"	13.8
06KB057A	11 293269 5617923	840	82L/12	"Rossland" Group	medium-grey weathering, light-pink, coarse-grained biotite with potassic alteration, quartz veins and hematite	"	12.3
06KB058A	11 293633 5618252	795	82L/12	"Rossland" Group	grey-brown weathering, dark-grey, augite olivine (iddingsitized) phyric basalt	"	12.7
06KB049A	10 691744 5697853	1046	92P/08	Thuya granodiorite	light-grey weathering, salt and pepper, coarse-grained biotite hornblende quartz monzodiorite	192.7 0.9, U(z), ⁷ 00PSC-388, 25m	2.1
06KB047A	10 688400 5701994	1215	92P/08	Thuya/ Dum Lake	light-grey weathering, medium-grey, coarse-grained biotite hornblende quartz monzodiorite	eJ U(z), preliminary ⁵ 01PSC-296 200m	4.9
06KB040A	10 638838 5758074	923	92P/15	Takomkane/ Schoolhouse	cream weathering, light-pink, coarse-grained fractured biotite hornblende granodiorite	eJ U(z), preliminary ⁵ 05PSC-374, 100m	7.4
06KB043A	10 635702 5743233	865	92P/14	Takomkane granodiorite	light-pink weathering, medium-pink, coarse-grained, fractured biotite granodiorite	193.5 0.6, U(z), ⁶ RW95-122, 100m	8.7

TABLE 1 (CONTINUED)

Sample no.	UTM: zone, E, N	Elev. (m)	NTS ref	Map unit	Rock description	Age, method ^{source} x-ref age o/c, proximity:	Mag. Susc.
Early Jurassic (continued)							
06KB042A	10 644831 5758161	1027	92P/15	Takomkane/ Iron Lk u.m.	dark-grey (fresh and weathered) coarse-grained lineated pyroxene <i>hornblende</i>	eJ A(h,b) ^{5a} ; eJ U(z) ⁵ preliminary 05PSC-397	90.0
06KB041A	10 644560 5758541	1049	92P/15	Takomkane/ Iron Lk u.m.	dark-grey weathering, black, medium-grained brecciated <i>pyroxenite</i>	"	26.1
06KB048A	10 689368 5701087	1179	92P/08	Thuya / ultramafic	orange weathering, medium grey, medium-grained veined <i>pyroxenite</i>	?Early Jurassic	58.60
*05PSC-323	10 672101 5747556		92P/16	Aqua Creek ultramafic	<i>hornblende monzodiorite</i>	eJ A(h), preliminary ^{5a} 05PSC-323; identical	
*05PSC-373	10 648418 5741998		92P/15	South Canim stock	<i>hornblende-biotite quartz monzodiorite</i>	eJ U(z) preliminary ⁵ 05PSC-373; identical	
*05PSC-375	10 647472 5756215		92P/15	Takomkane/ Iron Lk u.m.	<i>hornblende diorite</i>	eJ U(t) preliminary ⁵ 05PSC- 375; identical	
06KB032A	09 687759 6087800	900	93L/16	Topley (Stikine)	cream weathering, orange, coarse-grained, massive <i>granodiorite</i>	193 2 A(b), ⁸ TO5, 100m	n/a
Middle Jurassic							
06KB005A	10 714114 5469284	521	92H/08	Okanagan/ Canim Cr stock	medium-pink weathering, salt and pepper, massive, biotite <i>hornblende quartz monzonite</i>	168.8 9.3 U(z), ¹² HD 80, 900m	12.8
06KB007A	10 688750 5497584	820	92H/09	Okanagan/ Osprey	light-grey weathering, dark-grey, coarse-grained K-feldspar megacrystic biotite <i>hornblende granodiorite</i>	?166 1 U(z), ⁹	14.8
06KB008A	10 696023 5506106	986	92H/09	Okanagan/ Osprey	light-grey weathering, light-pink, coarse-grained fractured <i>monzogranite</i>	NEW U-Pb in progress	8.0
06KB009A	10 700079 5510143	1097	92H/09	Okanagan/ Osprey	medium-grey weathering, light-grey, medium-grained, foliated <i>monzogranite</i>	"	6.1
06KB015A	10 695669 5528102	1568	92H/16	Okanagan/ Osprey	pinkish-grey (weathering and fresh), coarse-grained, K-feldspar megacrystic <i>monzogranite</i>	"	0.3
06KB026A	10 400157 5986305	739	93K/02	Stag Lake/ Sugarloaf (Stikine)	light-grey weathering, salt and pepper, heterogeneous (medium to coarse grained) <i>monzogranite</i>	171 1.7 A(b), ¹⁰	26.0
06KB052A	10 429471 5788933	1095	93C/01	Palmer granite (Stikine)	light-pink weathering, pinkish-grey, medium-grained miarolitic fractured <i>monzogranite</i>	ca. 169.9 U(z), ¹³ Palmer-RMF, 300m	8.9
Late Jurassic (156 144 Ma)							
06KB001A	10 672021 5443091	1034	92H/02	Eagle tonalite	pinkish-grey weathering, medium-grey, medium-grained foliated biotite biotite <i>granodiorite</i>	>157 4 U(z), ¹⁴	0.5
06KB012A	10 644301 5501350	-	92H/11	Eagle tonalite	light-grey weathering, salt and pepper, medium-grained, foliated biotite <i>granodiorite</i>	"	2.4
06KB038A	10 586883 5638843	798	92L/13	Mt Martley pluton	medium-grey weathering, salt and pepper, coarse-grained, equigranular <i>hornblende granodiorite</i>	155 1.6 U(z), ¹⁵ NM85-12A, 1500m	7.0
06KB028A	10 366717 5990717	913	93K/03	Endako/ Casey (Stikine)	cream weathering, orange, medium-grained equigranular <i>monzogranite</i>	145.1 0.2 U(z), ¹⁰	0.2
06KB029A	10 364143 5986058	735	93K/03	Endako/ Endako (Stikine)	cream weathering, orange, coarse grained K-feldspar megacrystic miarolitic <i>monzogranite</i>	148.4 1.5 A(b), ¹⁰	0.0
Age uncertain							
06KB035A	10 497445 5703038	1553	92O/06	Piltz Peak tonalite	light-grey weathering, salt and pepper, coarse-grained, massive <i>granodiorite</i>	Eocene? I.J? NEW U-Pb in progress	0.1
06KB036A	10 497538 5703542	1531	92O/06	Piltz Peak tonalite	medium-grey weathering, salt and pepper, coarse-grained, massive <i>granodiorite</i>	"	1.4
06KB022A	10 680572 5498160	887	92H/10	Summers Cr stock	medium-grey weathering, pinkish-grey, medium-grained, <i>granodiorite</i>	101 5.2, K(b), ² NEW U-Pb in progress	14.6
06KB046A	10 705296 5734144	430	92P/09	Raft batholith	rusty weathering, pinkish-grey coarse-grained K-feldspar megacrystic foliated <i>monzogranite</i>	105.5 0.5, U(z), ⁴ - or 168 +14/-12 U(z) ¹⁶	4.3
06KB034A	10 507909 5709920	1589	92O/10	Mt Alex pluton (Stikine)	medium-grey weathering, light-grey, medium-grained, <i>quartz</i> <i>monzodiorite</i>	NEW U-Pb in progress	0.2
06KB037A	10 501924 5719246	1381	92O/10	"	dark-grey weathering, rusty, coarse-grained <i>monzodiorite</i>	"	-

Notes:

05PSC-XXX samples collected by P. Schiarizza. All samples are from Quesnel Terrane, except where noted as Stikine .

Rock names in italic font are preliminary, based on visual estimates of mineral modes.

Abbreviations used for age method: A=Ar-Ar; K=K-Ar; U=U-Pb; b=biotite; h=hornblende; t=titanite; z=zircon.

Sources for age determinations are: 1 Mortensen et al., 1995; 2 Preto et al., 1979; 3 Friedman et al., 2002; 4 Schiarizza and Boulton, 2006a; 5 U-Pb dating in progress: R. Friedman and P. Schiarizza; 5a Ar-Ar dating in progress: T. Ullrich and P. Schiarizza; 6 Whiteaker et al., 1998; 7 Schiarizza et al., 2002a; 8 MacIntyre et al., 2001; 9 Parrish and Monger, 1992; 10 Villeneuve et al., 2001; 11 Beatty et al., 2006; 12 Ray and Dawson, 1994; 13 Friedman and Armstrong, 1989; 14 Greig et al., 1992; 15 Mortimer et al., 1990; 16 Calderwood et al., 1990.

Cooling ages are italicized, to distinguish them from igneous crystallization ages.

Samples from previously dated outcrops are listed with a cross-reference sample identification of the geochronology study, along with distance of the new sample from the reported co-ordinates for the dated outcrop in cases where the new sample was collected at or near to it.

UTM co-ordinate datum is NAD 83.

ples of volcanic rocks from the Nicola Group in the vicinity of the Okanagan batholith, and from volcanic rocks correlative with the Rossland Group northeast of Kamloops (Early Jurassic, reassigned from the Nicola Group; Beatty *et al.*, 2006). The Late Triassic to Early Jurassic Guichon batholith, which hosts major calcalkaline-type porphyry mineralization (Highland Valley, Bethsaida) is the subject

of a concurrent detailed study (J. Whalen and R. Anderson, Geological Survey of Canada) and was not sampled.

Minor sampling of Stikine intrusions is widespread, and generally occurs well north of Quesnel Terrane sampling. Significant variation in age distribution with latitude is evident within and between the two terranes (Fig 3B). In general, the Late Triassic and Early Jurassic suites are not well represented in southern Stikinia, and first appear at a latitude of approximately 54°N (Nechako area samples, Fig 2B), whereas all of the targeted suites are well represented and easily accessible in southernmost Quesnellia (southern British Columbia samples, Fig 2A). Middle to Late Jurassic igneous rocks are present and accessible in the Stikine 'Terrane' (postdates accretion) between latitudes 51 and 54°N, where they are exposed in windows through extensive cover of the Miocene Chilcotin Group lava flows. Late Jurassic to mid-Cretaceous (*ca.* 145–115 Ma) rocks are apparently absent in the Quesnel 'Terrane', and are spatially restricted in a relatively tight across-arc trend (present-day latitudes of 51.75–52.5°N) in the Stikine 'Terrane'. Present-day latitudinal patterns do not necessarily preserve the original distribution of magmatism amongst the two terranes, due to Cretaceous and Eocene dextral strike-slip deformation within and between them (*e.g.*, Ewing, 1980; Struik, 1993; Irving *et al.*, 1996).

PRELIMINARY CHARACTERIZATION OF SAMPLED SUITES

The major element compositions determined by X-ray fluorescence spectroscopy (XRF) have been completed for a subset of the new samples (06KB001A–06KB0025A), and major element classifications from normative mineralogy and other relevant petrological indices are summarized below. Two samples (013A and 025A) are strongly altered, with loss-on-ignition values >5 wt%, and are not included in the descriptions below.

Latest Triassic (202 ±6/–4 Ma): Alkalic 'Monzodiorite-Diorite' Suite

Late Triassic intrusions of southern Quesnellia form a belt of alkaline Cu-Au±Ag-type porphyry deposits from Copper Mountain in the south to Mount Polley in the north (Fig 2A). Samples from the Copper Mountain, Allison Lake and Iron Mask intrusions are microcrystalline, exhibit varying degrees of potassic alteration and typically contain abundant hornblende needles. The Allison Lake diorite phase is undated; a new geochronology sample (06KB025A) is in progress for U-Pb dating (Geochronology Laboratory, Geological Survey of Canada, Ottawa). The microcrystalline intrusive samples (Copper Mountain, Iron Mask) are silica-undersaturated (normative olivine) calcalkaline monzodiorite (Fig 4A, B), with an intermediate but tightly restricted range in Mg# (0.49–0.51; Fig 4C), where $Mg\# = Mg / (Mg + Fe^{2+})$. The Nicola Group volcanic rocks are basalt, basaltic trachyandesite and andesite, and are variably alkaline and silica undersaturated (olivine normative) or calcalkaline and silica oversaturated, with a wider range of Mg# (0.45–0.64). All samples of this suite are metaluminous (Fig 4D) and potassic ($[Na_2O - K_2O] < 2 wt\%$). Magnetic susceptibility (ms) in these rocks varies widely from weakly magnetic ($ms = +4$) to magnetic ($ms = +25$), and appears to be inversely correlated with degree of alteration and outcrop fracturing (*i.e.*, depth and volume of

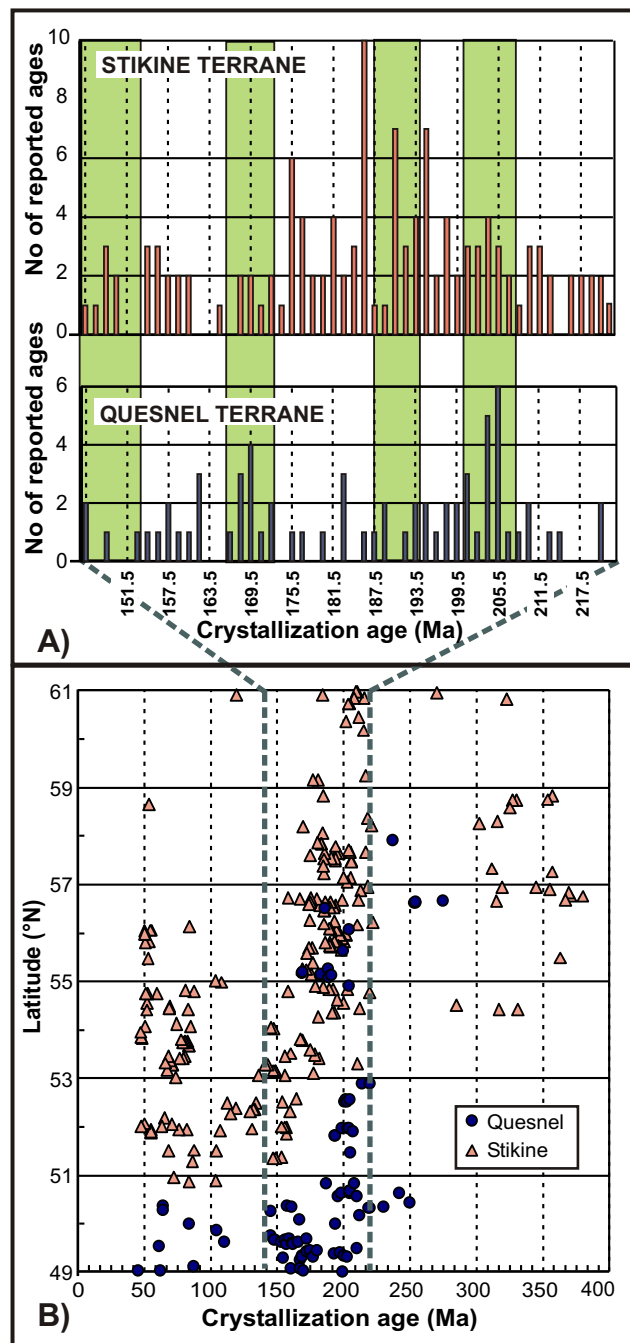


Figure 3. A) Histogram of reliable age determinations for igneous rocks of the Quesnel and Stikine terranes; shaded bands indicate time-slices targeted for geochemistry in this study. B) Latitudinal distribution of igneous rocks of the Quesnel and Stikine terranes. Source: BCAGE 2004 (Breitsprecher and Mortensen, 2004), query criteria = A-rated (= 'reliable'; analytical quality criteria as specified in BCAGE 2004 documentation), U-Pb, crystallization.

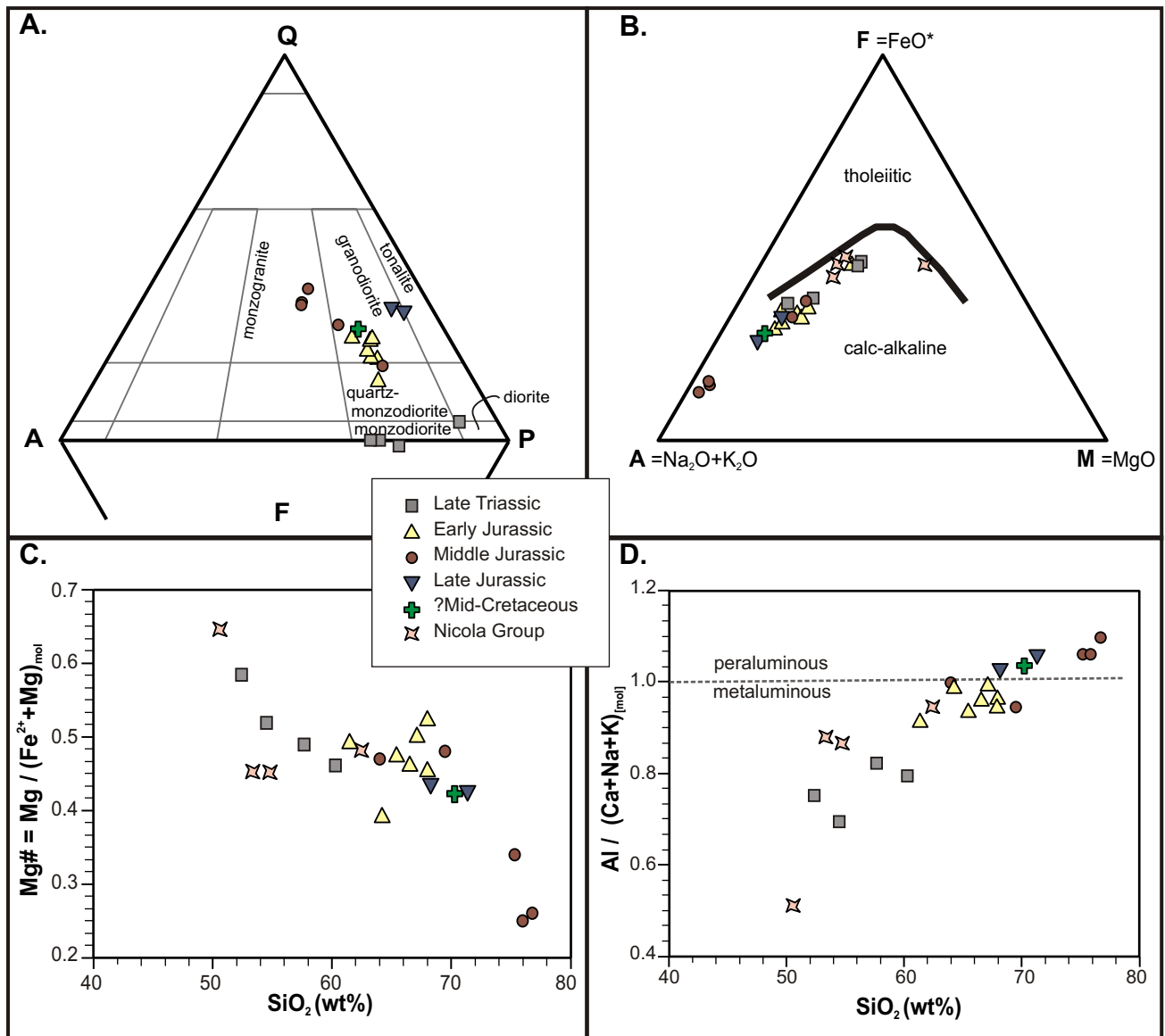


Figure 4. Major element classification of samples 06KB001A to 025A: A) QAPF diagram, based on CIPW normative mineralogy in wt%; B) AFM diagram (after Irvine and Baragar, 1971); C) Mg# versus SiO₂; D) alumina saturation versus SiO₂.

intact rock on which the magnetic susceptibility meter can act).

Observations for the more northerly samples indicate broad similarities to the characteristics outlined above for the southerly samples, although they include slightly more siliceous rocks and exhibit a wider range of textures. The Heffley Lake pluton, northeast of Kamloops, is a medium-grained quartz monzodiorite with well-developed pyrite crystals up to 2 mm in diameter. Samples from the Thuya and Takomkane batholiths are medium to coarse-grained quartz monzodiorite to hornblende-megacrystic recrystallized diorite. Magnetic susceptibility for samples from all three localities varies from weakly magnetic to magnetic (ms = +4 to +38). Potassium feldspar-epidote and/or pyrite alteration are common features in the majority of sampled outcrops of this suite. Correlative samples from Stikinia, collected on the west side of Babine Lake near Topley Landing (Fig 2B), include a coarse-grained K-feld-

spar megacrystic granodiorite of the Topley intrusive suite (MacIntyre *et al.*, 2001) and two samples (flow top and flow bottom) of augite and plagioclase-porphyrific andesite of the Takla Group volcanic rocks.

Early Jurassic (190 ± 4 Ma): 'Hornblende-Biotite Granodiorite' Suite

In the Quesnel Terrane, Early Jurassic magmatism is typified by large (>900 km²), hornblende and biotite-bearing granodioritic intrusions. Seven samples were collected from the Pennask and Bromley batholiths of the Okanagan complex (Monger, 1989; Monger and McMillan, 1989) to provide a robust geochemical dataset for type intrusions of this age. The samples from the Pennask and Bromley plutons are calcalkaline biotite-hornblende granodiorite (Fig 4A, B) with the exception of sample 06KB016A, which is from the Pennask pluton within 100 m of its con-

tact with Nicola Group andesite. At that locality, the outcrop grades from 30 to 10 vol% andesitic xenoliths over an interval of approximately 250 m (Fig. 5); crustal assimilation may explain the anomalous composition. Biotite typically occurs as large (up to 6 mm), well-formed, relatively unaltered books, and hornblende and biotite together account for 10 to 15 vol% of the rock. All samples from the Okanagan complex and vicinity are silica oversaturated (normative quartz 15–25%), metaluminous and potassic, with whole-rock Mg# ranging from 0.45 to 0.53 (Fig. 4C, D). At the Okanagan batholith, Early Jurassic rocks have relatively restricted magnetic susceptibility readings ($ms = +7$ to $+9$).

Farther north, Early Jurassic intrusive phases from the Thuya and Takomkane batholiths are volumetrically dominated by biotite and hornblende-bearing granodiorite to quartz monzodiorite bodies, with a wide range of other rock types locally present (Schiarizza *et al.*, 2002 a–c; Schiarizza and Boulton, 2006a, b). Sampled rock types from the lower portion of this time-slice (194–190 Ma) include biotite-hornblende-bearing granodiorite and quartz monzodiorite (Table 1). Magnetic susceptibility is typically low to moderate ($ms = +0.1$ to $+14$). Sampled rock types from the upper portion of the time-slice (190–186 Ma) include nepheline-megacrystic syenite of the Mount Fleet alkalic complex (sample 06KB054A) from north of Kamloops, and hornblende diorite and pyroxenite from the mafic-ultramafic units at the Thuya and Takomkane complexes (Table 1). The ultramafic outcrops are extremely magnetic ($ms > +90$). Volcanic rocks include basalt from the Lions Head succession of the Rossland Group, collected northeast of Kamloops (Beatty *et al.*, 2006). A sample of granodiorite of the Topley intrusive suite (MacIntyre *et al.*, 2001) from the east side of Babine Lake (Fig 2B) represents correlative magmatism in the Stikine Terrane.

Middle Jurassic (170 ±4 Ma): ‘K-Feldspar Megacrystic Monzogranite’ Suite

In the southern part of the Quesnel study region, Middle Jurassic magmatism is represented by the Osprey pluton. A previous geochronological study did not provide definitive results (Parrish and Monger, 1992); a new geochronology sample (06KB008A) is in progress for dating by the U-Pb method (Geochronology Laboratory, Geological Survey of Canada, Ottawa). On the basis of conflicting K-Ar and Rb-Sr age determinations, the phase immediately east of the Osprey pluton has been variably assigned as either Pennask (Early Jurassic) or Osprey (Middle Jurassic); a new geochronology sample from this easterly phase (06KB019A) has been collected for U-Pb analysis. The Osprey pluton samples are K-feldspar megacrystic monzogranite, except for 06KB007A (granodiorite), which was sampled near the western contact with the Summers Creek stock. The Cahill Creek satellite stock sample (06KB005A), collected just east of the town of Hedley, is a medium-grained biotite-hornblende quartz monzodiorite (Fig 4A). These latter two samples are metaluminous and have intermediate Mg# not inconsistent with the previous magmatic suites (0.47–0.48), whereas those closer to the Osprey core are peraluminous and have significantly lower Mg# (0.25–0.34; Fig 4C, D). The suite is moderately magnetic ($ms = +6$ to $+15$).

Farther north, K-feldspar megacrystic monzogranite of the Raft batholith (06KB046A), which is geographically



Figure 5. Partly digested elongate xenoliths of Nicola Group basalt in Pennask granodiorite, at the northeastern contact of the pluton on Highway 97C (UTM Zone 10, 701215E, 5529637N).

situated between the Thuya and Takomkane batholiths, was collected from the west side of the Clearwater River, northwest of the town of Clearwater. Correlative samples from the Stikine Terrane include monzogranite of the Sugarloaf phase, Stag Lake suite (Villeneuve *et al.*, 2001), collected south of the town of Fraser Lake, and monzogranite of the Palmer granite (Friedman and Armstrong, 1989), collected north of Chilanko Forks.

Late Jurassic (150 ±5 Ma): ‘Hornblende-Biotite Tonalite’ Suite

In the study area, Late Jurassic intrusions have typically been classified by previous workers as ‘tonalite’ (Greig *et al.*, 1992). The samples collected from this suite (Eagle tonalite, Piltz Peak tonalite, Mount Martley pluton) are granodiorite on the basis of their CIPW normative mineralogy, but are shifted towards the tonalite field on a QAPF diagram relative to the Early Jurassic suite (Fig 4A). Potassium-feldspar staining reveals small amounts of potassic feldspar within these rocks, either as secondary fracture fill or as primary phases. The Eagle ‘tonalite’ is sodic and peraluminous, and has intermediate to evolved Mg# (0.43–0.44). The suite is weakly magnetic ($ms = +0.1$ to $+2.4$), with the exception of the moderately magnetic Mount Martley pluton ($ms = +7.0$). Two monzogranite samples from the Endako suite of the Stikine Terrane complement the sample subset; they are characterized by distinctively dark orange K-feldspar relative to samples from any suite of the Quesnel Terrane.

Mid-Cretaceous

Several samples of mid-Cretaceous age were included in the sampling program in anticipation of a future phase of the project. A sample of granite from the Summers Creek stock, which intrudes the southwestern part of the Osprey pluton north of Princeton, is peraluminous and potassic, and has a Mg# of 0.42. The age of the stock is constrained by a K-Ar biotite cooling age of 101 ± 5.2 Ma (Preto *et al.*, 1979); a new geochronology sample (06KB022A) was collected for dating by the U-Pb method. In the Stikine 'Terrane', the undated Mount Alex pluton is inferred to be of mid-Cretaceous age (Massey *et al.*, 2005). Two geochemistry samples were collected, and additional material for one (06KB034A) was collected for dating by the U-Pb method.

FURTHER WORK

The samples in this study have been collected primarily based on their economic importance as hosts to metallogenic porphyry-style deposits and on their tectonic relevance. Geochemical analysis to be undertaken includes 1) major element determination (XRF) for samples 06KB026A to 06KB058A, which is in progress (Applied Analytical Geochemistry Laboratory, Memorial University of Newfoundland); 2) trace element determination (including the rare earth elements) by high-resolution inductively coupled plasma mass spectrometry, using a Finnigan™ Element2 instrument (Pacific Centre for Isotopic and Geochemical Research (PCIGR) at the University of British Columbia); and 3) determination of radiogenic isotopic compositions (Rb-Sr, Sm-Nd, Pb-Pb and Lu-Hf) for a subset of 40 samples (PCIGR). Six new geochronology samples are planned; two are in progress at the Geochronology Laboratory, Geological Survey of Canada (Ottawa). The application of radiogenic isotope systematics will lead to a better understanding of middle Mesozoic magmatism and tectonics in southern British Columbia. In addition, it is anticipated that this study will result in the geochemical mapping of crustal domains, based on the large areal extent of sampling and the inclusion of at least two known major crustal domains or terranes.

ACKNOWLEDGMENTS

We thank Pam King for the XRF analyses at the Memorial University of Newfoundland. Voluntary field assistance by Robin McQuinn, Kirsti Medig, Frederico Henriques and Caroline-Emmanuelle Morisset is greatly appreciated. Sample material for the 05PSC-XXX samples was provided by Paul Schiarizza. Discussions with Rich Friedman and Bert Struik helped to improve the sample-target planning. Significant financial support from both Geoscience BC and the Geological Survey of Canada (TGI-3, 2005 program) for fieldwork and analytical costs is crucial to achieving the project objectives, and we are grateful for this support. The senior author is supported by the Natural Sciences and Engineering Research Council of Canada (NSERC; PGS-A).

REFERENCES

Anderson, R.G. (1985): An overview of some Mesozoic and Tertiary plutonic suites and their associated mineralization in

the northern Canadian Cordillera; *in* Recent Advances in the Geology of Granite-related Mineral Deposits, Taylor, R.P. and Strong, D.F., Editors, *Canadian Institute of Mining and Metallurgy*, Special Volume 39, pages 96–113.

- Armstrong, R.L. (1988): Mesozoic and early Cenozoic magmatic evolution of the Canadian Cordillera; *in* Processes in Continental Lithospheric Deformation, Clark, S.P., Burchfiel, B.C. and Suppe, J., Editors, *Geological Society of America*, Special Paper 218, pages 55–91.
- BC Geological Survey (2006): MapPlace GIS internet mapping system; *BC Ministry of Energy, Mines and Petroleum Resources*, MapPlace website, URL <<http://www.MapPlace.ca>> [November 2006].
- Beatty, T.W., Orchard, M.J. and Mustard, P.S. (2006): Geology and tectonic history of the Quesnel terrane in the area of Kamloops, British Columbia; *in* Paleozoic Evolution and Metallogeny of Pericratonic Terranes at the Ancient Pacific Margin of North America, Canadian and Alaskan Cordillera, Colpron, M. and Nelson, J.L., Editors, *Geological Association of Canada*, Special Paper 45, pages 483–504.
- Breitsprecher, K. and Mortensen, J.K., Compilers (2004): BCAGE 2004: a database of isotopic age determinations for rock units from British Columbia; *BC Ministry of Energy, Mines and Petroleum Resources*, Open File 2004-3, 7763 records, 9.1 Mb.
- Calderwood, A.R., van der Heyden, P. and Armstrong, R.L. (1990): Geochronometry of the Thuya, Takomkane, Raft, and Baldy batholiths, south-central British Columbia; *Geological Association of Canada – Mineralogical Association of Canada – Canadian Geophysical Union*, Joint Annual Meeting, Program with Abstracts, volume 15, page 19.
- Erdmer, P.E., Moore, J.M., Heaman, L., Thompson, R.I., Daughtry, K.L. and Creaser, R.A. (2002): Extending the ancient margin outboard in the Canadian Cordillera: record of Proterozoic crust and Paleocene regional metamorphism in the Nicola horst, southern British Columbia; *Canadian Journal of Earth Sciences*, volume 39, pages 1605–1623.
- Ewing, T.E. (1980): Paleogene tectonic evolution of the Pacific Northwest; *Journal of Geology*, volume 88, pages 619–639.
- Friedman, R.M. and Armstrong, R.L. (1989): U-Pb dating of Permian, Jurassic, and Eocene granitic rocks between the Coast Plutonic complex and Fraser–Pinchi fault systems (51 degrees–54 degrees N), BC; *Geological Society of America*, Abstracts with Programs, volume 21 (5), page 81.
- Friedman, R.M., Mahoney, J.B., and Cui, Y. (1995): Magmatic evolution of the southern Coast Belt: constraints from Nd-Sr isotopic systematics and geochronology of the southern Coast Plutonic Complex; *Canadian Journal of Earth Sciences*, volume 32, pages 1681–1698.
- Friedman, R., Ray, G. and Webster, I. (2002): U-Pb zircon and titanite dating of intrusive rocks in the Heffley Lake area, south-central British Columbia; *in* Geological Fieldwork 2001, *BC Ministry of Energy, Mines and Petroleum Resources*, Paper 2002-1, pages 109–118.
- Ghosh, D.K. (1995): Nd-Sr isotopic constraints on the interactions of the Intermontane Superterrane with the western edge of North America in the southern Canadian Cordillera; *Canadian Journal of Earth Sciences*, volume 32, pages 1740–1758.
- Greig, C.J., Armstrong, R.L., Harakal, J.E., Runkle, D. and van der Heyden, P. (1992): Geochronometry of the Eagle plutonic complex and the Coquihalla area, southwestern British Columbia; *Canadian Journal of Earth Sciences*, volume 29, pages 812–829.
- Irvine, T.N. and Baragar, W.R.A. (1971): A guide to the chemical classification of the common volcanic rocks; *Canadian Journal of Earth Sciences*, volume 7, pages 523–547.
- Irving, E., Wynne, P.J., Thorkelson, D.J. and Schiarizza, P. (1996): Large (1000 to 4000 km) northward movements of tectonic

- domains in the northern Cordillera, 83 to 45 Ma; *Journal of Geophysical Research*, volume 101B, pages 17 901–17 916.
- Israel, S.A. and Kennedy, L.A. (2003): Geology of the Atnarko metamorphic complex, southern Tweedsmuir Park, west-central British Columbia; *Geological Survey of Canada, Current Research 2003-A3*, 8 pages.
- Logan, J.M. and Mihalynuk, M.G. (2004): Porphyry Cu-Au deposits of the Iron Mask batholith, southeastern British Columbia; in *Geological Fieldwork 2004, BC Ministry of Energy, Mines and Petroleum Resources*, Paper 2005-1, pages 271–290.
- MacIntyre, D.E., Villeneuve, M.E. and Schiarizza, P. (2001): Timing and tectonic setting of Stikine Terrane magmatism, Babine – Takla lakes area, central British Columbia; *Canadian Journal of Earth Sciences*, volume 38, pages 579–601.
- Madsen, J.K., Breitsprecher, K. and Anderson, R.G., Compilers (2006): CordMinAge 2006: Isotopic ages for significant mineral deposits of the Canadian Cordillera; *Geological Survey of Canada*, Open File 4969, Release 1.1, 1.9 Mb.
- Massey, N.W.D., MacIntyre, D.G., Desjardins, P.J. and Cooney, R.T. (2005): Geology of British Columbia; *BC Ministry of Energy, Mines and Petroleum Resources*, Geoscience Map 2005-3, scale 1:1 000 000.
- McMillan, W.J., Thompson, J.F.H., Hart, C.J.R. and Johnston, S.T. (1995): Regional geological and tectonic setting of porphyry deposits in British Columbia and Yukon Territory; in *Porphyry Deposits of the Northwestern Cordillera of North America*, Schroeter, T.G., Editor, *Canadian Institute of Mining, Metallurgy and Petroleum*, Special Volume 46, pages 40–57.
- MINFILE (2006): MINFILE BC mineral deposits database; *BC Ministry of Energy, Mines and Petroleum Resources*, URL <<http://www.em.gov.bc.ca/Mining/Geosurv/Minfile/>> [November 2006].
- Monger, J.W.H. (1989): Geology, Hope, British Columbia (92H); *Geological Survey of Canada*, Map 41-1989, sheet 1, scale 1:250 000.
- Monger, J.W.H. and McMillan, W.J. (1989): Geology, Ashcroft, British Columbia (92I); *Geological Survey of Canada*, Map 42-1989, sheet 1, scale 1:250 000.
- Monger, J.W.H. and Price, R. (2002): The Canadian Cordillera: geology and tectonic evolution; *Canadian Society of Exploration Geophysicists (CSEG) Recorder*, February, pages 17–36.
- Monger, J.W.H., Price, R. and Tempelman-Kluit, D.J. (1982): Tectonic accretion and the origin of the two major metamorphic and plutonic belts in the Canadian Cordillera; *Geology*, volume 10, pages 70–75.
- Mortensen, J.K., Ghosh, D.K. and Ferri, F. (1995): U-Pb geochronology of intrusive rocks associated with copper-gold porphyry deposits in the Canadian Cordillera; in *Porphyry Deposits of the Northwestern Cordillera of North America*, *Canadian Institute of Mining, Metallurgy and Petroleum*, Special Volume 46, pages 142–158.
- Mortimer, N. (1987): The Nicola Group: Late Triassic and Early Jurassic subduction-related volcanism in British Columbia; *Canadian Journal of Earth Sciences*, volume 24, pages 2521–2536.
- Mortimer, N., van der Heyden, P., Armstrong, R.L. and Harakal, J. (1990): U-Pb and K-Ar dates related to the timing of magmatism and deformation in the Cache Creek Terrane and Quesnellia, southern British Columbia; *Canadian Journal of Earth Sciences*, volume 27, pages 117–123.
- Nelson, J. (1979): The western margin of the Coast Plutonic Complex on Hardwicke and West Thurlow Islands, British Columbia; *Canadian Journal of Earth Sciences*, volume 16, pages 1166–1175.
- Parrish, R.R. and Monger, J.W.H. (1992): New U-Pb dates from southwestern British Columbia; in *Radiogenic Age and Isotopic Studies: Report 5, Geological Survey of Canada*, Paper 91-2, pages 87–108.
- Preto, V.A. (1972): Geology of Copper Mountain; *BC Ministry of Energy, Mines and Petroleum Resources*, Bulletin 59, 87 pages.
- Preto, V.A. (1979): Geology of the Nicola Group between Merritt and Princeton; *BC Ministry of Energy, Mines and Petroleum Resources*, Bulletin 69, 90 pages.
- Preto, V.A., Osatenko, M.J., McMillan, W.J. and Armstrong, R.L. (1979): Isotopic dates and strontium isotopic ratios for plutonic and volcanic rocks in the Quesnel Trough and Nicola Belt, south-central British Columbia; *Canadian Journal of Earth Sciences*, volume 16, pages 1658–1672.
- Preto, V.A., Nixon, G.T. and Macdonald, E.A.M. (2004): Alkaline Cu-Au porphyry systems in British Columbia: Copper Mountain; *BC Ministry of Energy, Mines and Petroleum Resources*, Geoscience Map 2004-3, scale 1:15 000.
- Ray, G.E. and Dawson, G.L. (1994): The geology and mineral deposits of the Hedley gold skarn district, southern British Columbia; *BC Ministry of Energy, Mines and Petroleum Resources*, Bulletin 87, 156 pages.
- Rusmore, M.E. and Woodsworth, G.J. (1991): Distribution and tectonic significance of Upper Triassic terranes in the eastern Coast Mountains and adjacent Intermontane Belt, British Columbia; *Canadian Journal of Earth Sciences*, volume 28, pages 532–541.
- Schau, M.P. (1970): Stratigraphy and structure of the type area of the Upper Triassic Nicola Group in south-central British Columbia; in *Structure of the Southern Canadian Cordillera*, Wheeler, J.O., Editor, *Geological Association of Canada*, Special Paper 6, pages 123–135.
- Schiarizza, P., and Boulton, A. (2006a): Geology and mineral occurrences of the Quesnel Terrane, Canim Lake area (NTS 092P/15), south-central British Columbia; in *Geological Fieldwork 2005, BC Ministry of Energy, Mines and Petroleum Resources*, Paper 2006-1, pages 163–184.
- Schiarizza, P. and Boulton, A. (2006b): Geology of the Canim Lake area (NTS 92P/15); *BC Ministry of Energy, Mines and Petroleum Resources*, Open File 2006-8, scale 1:50 000.
- Schiarizza, P., Heffernan, S. and Zuber, J. (2002a): Geology of Quesnel and Slide Mountain terranes west of Clearwater, south-central British Columbia (92P/9, 10, 15, 16); in *Geological Fieldwork 2001, BC Ministry of Energy, Mines and Petroleum Resources*, Paper 2002-1, pages 83–108.
- Schiarizza, P., Heffernan, S., Israel, S. and Zuber, J. (2002b): Geology of the Clearwater – Bowers Lake area (NTS 92P/9, 10, 15, 16); *BC Ministry of Energy, Mines and Petroleum Resources*, Open File 2002-15, scale 1:50 000.
- Schiarizza, P., Israel, S., Heffernan, S. and Zuber, J. (2002c): Geology of the Nehalliston Plateau (NTS 92P/7, 8, 9, 10); *BC Ministry of Energy, Mines and Petroleum Resources*, Open File 2002-4, scale 1:50 000.
- Smith, A.D., Brandon, A.D. and St. John Lambert, R. (1995): Nd-Sr isotope systematics of Nicola Group volcanic rocks, Quesnel terrane; *Canadian Journal of Earth Sciences*, volume 32, pages 437–446.
- Struik, L.C. (1988): Crustal evolution of the eastern Canadian Cordillera; *Tectonics*, volume 7, page 727–747.
- Struik, L.C. (1993): Intersecting intracontinental Tertiary transform fault systems in the North American Cordillera; *Canadian Journal of Earth Sciences*, volume 30, pages 1262–1274.
- Struik, L.C., Schiarizza, P., Orchard, M.J., Cordey, F., Sano, H., MacIntyre, D.G., Lapierre, H. and Tardy, M. (2001): Imbricate architecture of the upper Paleozoic to Jurassic oceanic

- Cache Creek Terrane, central British Columbia; *Canadian Journal of Earth Sciences*, volume 38, pages 495–514.
- Thompson, R.I., Glombick, P., Erdmer, P., Heaman, L.M., Lemieux, Y. and Daughtry, K.L. (2006): Evolution of the ancestral Pacific margin, southern Canadian Cordillera: insights from new geologic mapping; in *Paleozoic Evolution and Metallogeny of Pericratonic Terranes at the Ancient Pacific Margin of North America*, Canadian and Alaskan Cordillera, Colpron, M. and Nelson, J.L., Editors, *Geological Association of Canada*, Special Paper 45, pages 433–482.
- Villeneuve, M., Whalen, J.B., Anderson, R.G. and Struik, L.C. (2001): The Endako batholith: episodic plutonism culminating in formation of the Endako porphyry molybdenite deposit, north-central British Columbia; *Economic Geology*, volume 96, pages 171–196.
- Whiteaker, R.J., Mortensen, J.K. and Friedman, R.M. (1998): U-Pb geochronology, Pb isotopic signatures and geochemistry of an Early Jurassic alkalic porphyry system near Lac la Hache, BC; in *Geological Fieldwork 1997*, BC Ministry of Energy, Mines and Petroleum Resources, Paper 1998-1, pages 33.1–33.13.
- Woodsworth, G.W., Anderson, R.G. and Armstrong, R.L. (1991): Plutonic regimes; in *Geology of the Cordilleran Orogen in Canada*, Gabrielse, H. and Yorath, C.J., Editors, *Geological Society of America*, The Geology of North America, volume G-2, pages 491–531.

Toward an Integrated Model for Alkalic Porphyry Copper Deposits in British Columbia (NTS 093A, N; 104G)¹

by C.M. Chamberlain², M. Jackson², C.P. Jago², H.E. Pass³, K.A. Simpson⁴, D.R. Cooke³ and R.M. Tosdal²

KEYWORDS: Mount Polley, Mount Milligan, Galore Creek, alkalic, porphyry, magmatic-hydrothermal breccia, hydrothermal alteration

INTRODUCTION

Recent discoveries have raised awareness of the economic importance of the alkalic class of porphyry and epithermal deposits, and have provided opportunities to better define the characteristics of these somewhat anomalous but potentially metal-rich mineral systems. Alkalic systems include some of the world's highest grade porphyry gold resources (e.g., Ridgeway, New South Wales, 53 Mt grading 2.5 g/t Au (4.26 million oz) and 0.77% Cu; Cadia Far East, New South Wales, 290 Mt grading 0.98 g/t Au (9.13 million oz) and 0.36% Cu), and some of the largest gold accumulations in epithermal settings (e.g., Lihir, Papua New Guinea, 44.7 million oz Au). Jensen and Barton (2000) have provided the most comprehensive review to date of alkalic mineral deposits (Fig 1), and descriptions of these deposits in British Columbia are available in Shroeter (1995).

Alkalic porphyry Cu deposits have features that distinguish them from the subalkalic porphyry systems. Although the alkalic porphyry deposits are known in various mineral provinces around the world, particularly in BC and eastern Australia, the quality of individual deposit descriptions in the public domain varies markedly. Thus, there are considerable gaps in knowledge regarding this important deposit type. Filling the knowledge gaps is the aim of a collaborative project between the Mineral Deposit Research Unit at the University of British Columbia, the Centre for Excellence in Ore Deposit Research at the University of Tasmania (Australia), Amarc Resources Ltd., AngloGold Ashanti Limited, Barrick Gold Corporation, Imperial Metals Corporation, Lysander Minerals Corporation, Newcrest Mining Limited, Newmont Mining Corporation, Novagold Resources Inc. and Teck Cominco Limited. Additional fi-

nancial support derives from grants from the Natural Sciences and Engineering Research Council of Canada (NSERC) and Geoscience BC. This project seeks to build an integrated model for these deposits, including the characteristics of various alteration styles that can develop in either a shallow or deep-level alkalic igneous setting. This paper reports the early stages of the collaborative research on the alkalic porphyry deposits in BC.

British Columbia is the type area for alkalic porphyry deposits and is therefore the focus for any study of such systems. Furthermore, it is locally a data-rich environment with basic descriptions of many of the deposits (e.g., Schroeter, 1995) and detailed studies of a few (summarized in Lang *et al.*, 1995b). This project builds upon this database with new studies at the Mount Polley, Mount Milligan, Galore Creek and Lorraine deposits (Fig 2). The project also draws upon the recently published work on alkalic porphyry Cu-Au systems in New South Wales (e.g., Lickfold *et al.*, 2003; Wilson *et al.*, 2003; Cooke *et al.*, in press). Collectively, the new studies in BC were selected to span the apparent depth range of the porphyry systems, from high-level breccia-hosted bodies (Mount Polley) to deeper level intrusive-centred sulphide accumulations (Mount Milligan or Lorraine). In order to build a coherent model for alkalic porphyry systems, the integration of detailed structural, paragenetic, alteration zonation and geochemical information are essential. This paper presents a review of alkalic mineral deposits and preliminary results from the first year of a three-year study into the BC systems.

THE ALKALIC PORPHYRY ENVIRONMENT

Alkalic Au-Cu porphyry deposits are known in a few mineral provinces worldwide. The best known are from the Mesozoic arc of British Columbia and the Late Ordovician Lachlan Fold Belt of New South Wales (Australia). Other isolated alkalic systems include Dinkidi (Philippines) and Skouries (Greece). Alkalic porphyry deposits are locally high grade and associated with small-volume pipe-like intrusions that may have areal extents of only a few hundred square metres. They thus present difficult exploration targets. Furthermore, the alkalic porphyry systems lack advanced argillic alteration assemblages (possibly excluding Dinkidi), and there is no evidence of a connection to high sulphidization epithermal deposits, despite the local presence of high sulphidization alteration systems in New South Wales that are of the same general age as the alkalic porphyry deposits (Cooke *et al.*, in press). Phyllic alteration in the alkalic porphyry systems is typically restricted to fault zones that penetrate late in the hydrothermal system. Supergene enrichment zones will be, at best, poorly devel-

¹ Geoscience BC contribution GBC040

² Mineral Deposit Research Unit, University of British Columbia, Vancouver, BC

³ Australian Research Council Centre for Excellence in Ore Deposit Research, University of Tasmania, Hobart, Tasmania, Australia

⁴ Geological Survey of Canada, Vancouver, BC

This publication is also available, free of charge, as colour digital files in Adobe Acrobat® PDF format from the BC Ministry of Energy, Mines and Petroleum Resources website at http://www.em.gov.bc.ca/Mining/Geosurv/Publications/catalog/cat_fldwk.htm

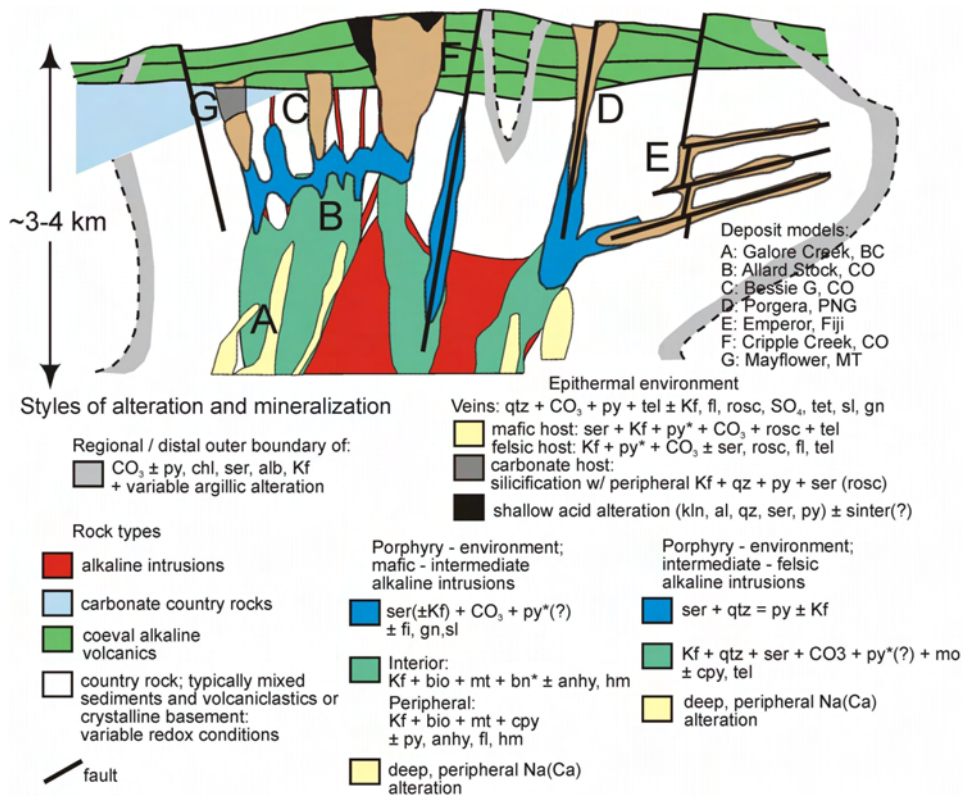


Figure 1. Schematic model of alkalic igneous complexes and associated ore deposit and alteration patterns (redrafted from Jensen and Barton, 2000).

oped due to the low sulphide contents of the alteration assemblages. The incipient nature of the peripheral hypogene alteration assemblages makes identifying the focus for fluid flow difficult when more than several hundred metres away from the mineralized centre. Skarns can occur in systems that contain carbonate hostrocks. Other manifestations of hydrothermal activity peripheral to alkalic

porphyry deposits are poorly documented and their exploration significance has not been assessed rigorously.

An empirical relationship has been postulated between alkalic epithermal and porphyry deposits, but it remains unproven (Jensen and Barton, 2000; Cooke *et al.*, in press; Fig 1). With the exception of Cowal in New South Wales (Australia), no significant alkalic epithermal deposits are known

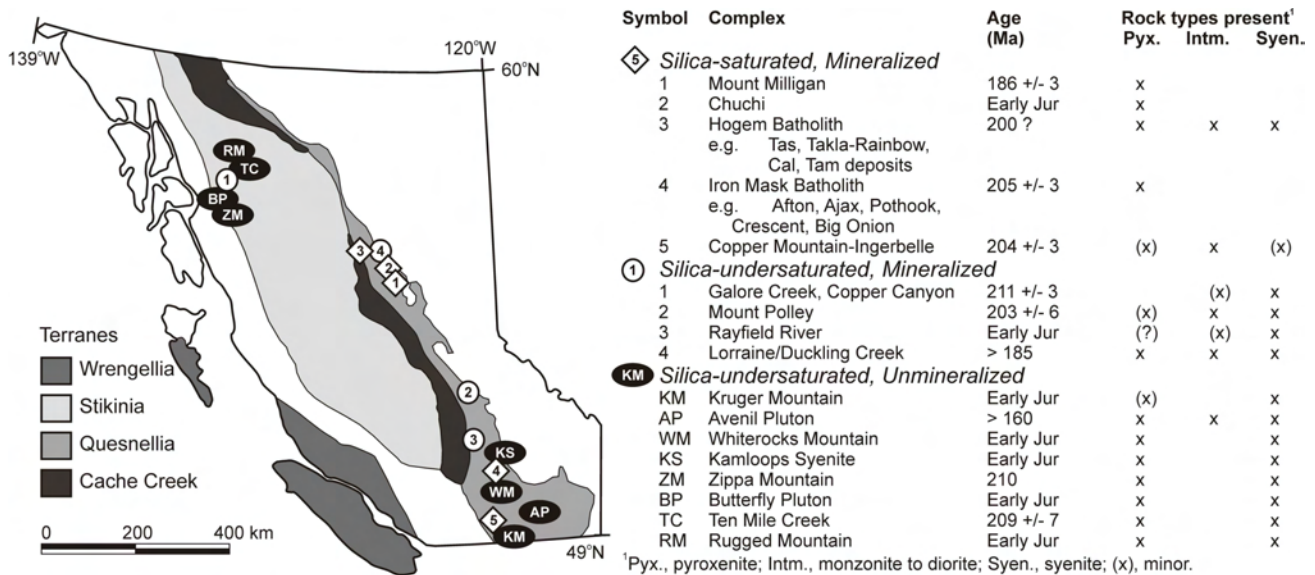


Figure 2. Location of early Mesozoic alkalic intrusive complexes and mineralized intrusions of British Columbia (Lang *et al.*, 1995a).

from the major alkalic porphyry belts of western New South Wales and British Columbia. One explanation for the negative relationship may be the depth of erosion, and hence a general lack of preservation of the shallower parts of alkalic magmatic-hydrothermal systems.

Alkalic Igneous Framework in British Columbia

Lang *et al.* (1995a) defined two suites of alkalic intrusions, silica saturated and silica undersaturated, associated with porphyry Cu-Au systems in British Columbia (Fig 2). Both suites are Triassic to Early Jurassic in age (Mortensen *et al.*, 1995) and represent the youngest intrusions in the Quesnel and Stikine terranes prior to the resumption of 'normal' calcalkaline arc volcanic rocks represented by the Early Jurassic Rossland Group and Ashcroft Formation in Quesnellia and the Hazelton Group in Stikinia. The alkalic deposits thus formed during a transition in the convergent margin evolution, a time that is thought to be conducive to the formation of porphyry Cu-type deposits (Tosdal, 2004).

The silica-undersaturated complexes are characterized by pyroxenite and syenite, and are locally zoned (Lueck and Russell, 1994). Potentially related volcanic rocks are only recognized in a few locations. The plutons have varying proportions of aegirine-augite, K-feldspar, biotite, melanite, titanite and apatite, with local hornblende, magnetite, plagioclase and vishnevitte-cancrinite. The accessory phase melanitic garnet (Ti-bearing andradite) is a distinguishing feature, and occurs as both a primary igneous phase and a hydrothermal alteration phase. Mineral chemical differences can distinguish the two paragenetic sequences (Lueck and Russell, 1994). Silica-saturated complexes, which are known only in Quesnellia, are dominated by diorite and monzonite. Pyroxenite and syenite are rare. Augite, biotite, magnetite, plagioclase, K-feldspar and apatite are the major mineral phases, whereas hornblende and titanite are less common. Quartz is rare.

Of the known major alkalic porphyry Cu-Au systems in BC (Copper Mountain, Chuchi, Ajax, Iron Mask, Mount Polley, Galore Creek, Copper Canyon, Mount Milligan, Red Chris; Fig 2), there are five mineralized centres associated with silica-saturated complexes and four with silica-undersaturated complexes (Lang *et al.*, 1995a). There are also other alkalic complexes that do not have known porphyry Cu-Au mineralized rock, and these are apparently indistinguishable, at first glance, from those that contain Cu-Au-bearing sulphide minerals. Lueck and Russell (1994) proposed that the presence or absence of hornblende and magnetite in silica-undersaturated rocks is a diagnostic feature of mineralized versus barren, respectively, silica-undersaturated igneous complexes. No criteria have been proposed to distinguish the productive from the barren silica-saturated complexes. Regardless of the overall composition of the alkalic systems, the gross-scale petrological similarity between barren and mineralized intrusive complexes is a very common feature of the high-level plutonic and volcanic environment, and one that has been the subject of numerous geological investigations over the years.

Considerable effort has been devoted to defining criteria to distinguish potentially mineralized from barren igneous complexes, but usually with limited success. However, within the calcalkaline environment, it has become evident,

although not universally proven, that certain element trends typify igneous complexes containing rock mineralized with precious and base metals (Kay *et al.*, 1999). The elemental characteristics are essentially some of the diagnostic features of island arc rocks of 'adakitic' compositions. These characteristics are: enrichment in Sr, Na and Eu; depletion in Y and heavy rare earth elements; $\text{SiO}_2 > 56 \text{ wt}\%$; $\text{Al}_2\text{O}_3 > 15 \text{ wt}\%$; $\text{Na}_2\text{O} > 3.5 \text{ wt}\%$; $\text{Sr} > 400 \text{ ppm}$; $\text{Y} < 18 \text{ ppm}$; $\text{Yb} > 1.9 \text{ ppm}$; $\text{La/Yb} \sim 20$; and $\text{Sr/Y} \sim 40$ (Drummond and Denfant, 1990). The enrichment of Na is not seen in many of the adakitic complexes associated with porphyry Cu systems. The recognition of an igneous chemical association of many porphyry Cu deposits in calcalkaline environments has occurred since the last serious research effort on the alkalic igneous complexes in BC (Lang *et al.*, 1995a), although recent work by Logan (2005) and Logan and Mihalynuk (2005a, b) has begun to evaluate the igneous complexes on a regional basis. Some constraints are offered by recent work in eastern Australia, where the porphyry Cu-Au deposits are associated with K-enriched ($\text{K/Na} > 1$) alkalic and shoshonitic complexes that show additional enrichment in large-ion lithophile elements, abundances of low-mantle-compatibility elements and marked depletions in Ti, Nb and Ta (Blevin, 2002; Holliday *et al.*, 2002).

ALKALIC PORPHYRY DEPOSITS IN BC: ARCHITECTURE, IGNEOUS GEOCHEMISTRY AND HYDROTHERMAL ALTERATION

In order to build a coherent model for alkalic porphyry systems, the integration of detailed geological architecture, paragenesis, alteration zonation and geochemical information is essential. A review of the initial results based on fieldwork and laboratory studies from the Mount Polley, Mount Milligan and Galore Creek alkalic Cu-Au porphyry deposits is presented herein; these studies build upon previous studies (*e.g.*, Enns *et al.*, 1995; Fraser *et al.*, 1995; Lang *et al.*, 1995; Sketchley *et al.*, 1995; DeLong, 1996; Logan and Mihalynuk, 2005a; Logan, 2005).

Mount Polley

The Mount Polley Cu-Au mining district in central British Columbia consists of at least six discrete porphyry Cu-Au-Ag deposits and prospects associated with monzonitic intrusions emplaced into the alkaline island arc rocks of the Quesnel Terrane (Fig 2). Located 56 km northeast of Williams Lake, the district consists of the Cariboo, Springer and Bell zones, which have been previously mined, and the Northeast zone, which is currently being developed. Other sulphide occurrences on the property are known but have yet to be mined. Overall, the various deposits and prospects constitute a reserve of 41 Mt of ore grading 0.44% Cu and 0.28 g/t Au, with varying amounts of Ag (Imperial Metals Corporation, 2006). The Northeast zone orebody, the focus of investigation here, contains 9.1 Mt of ore grading 0.88% Cu, 2.9 g/t Au and 6.4 g/t Ag, with approximately 80% of the ore hosted in breccia and the remainder hosted in pre-mineral, equigranular, nepheline-normative monzonite.

Differences in Cu/Au ratio, Ag content, Mo content, alteration, hostrock (breccia-hosted versus non-breccia-hosted ore) and intrusive texture, coupled with the north-

ward tilting of post-mineral Early Jurassic strata on the north, all suggest that the current outcrop at Mount Polley represents an oblique cross-section through a series of spatially related but slightly different porphyry-style deposits (Fraser *et al.*, 1995; Logan and Mihalynuk, 2005a) that potentially formed at different crustal depths (Panteleyev *et al.*, 1996). The Northeast zone is considered to reflect the shallowest structural level presently known, and thus potentially provides a link between deeper level porphyry and shallower levels in the upper crust typical of epithermal environments.

INTRUSIVE ROCK SEQUENCE

The Northeast zone contains breccia-hosted sulphide minerals that cut equigranular monzonite of the host Mount Polley intrusive complex. A complex series of intrusive rocks is associated with the breccia (Fig 3). Based on detailed core logging of a representative section through the Northeast zone (section 18; Fig 4), the intrusive phases are divided into three broad categories: pre-breccia intrusions, syn-mineral intrusions and post-mineral intrusions. Chalcopyrite, bornite and pyrite are the principal sulphide minerals that cement the breccias, although other silicate, carbonate and oxide phases and rock-flour matrix locally form infill to breccia clasts.

An equigranular monzonite forms the most volumetrically significant member of the Mount Polley intrusive complex, is the dominant clast type of the breccia, and represents the major pre-breccia intrusive unit in the Northeast zone. It is equigranular and fine to medium grained, with less than 10% mafic minerals. Potassium-feldspar (~70%) and plagioclase (~20%) are the dominant minerals. Internal to the body, fine-grained margins, inferred to represent chilled contacts, (*i.e.*, equigranular monzonite chilled against equigranular monzonite), suggest that this unit is not a single intrusive body but rather a swarm of coalesced dikes or stocks. The pre-mineral equigranular monzonite hosts xenoliths ranging from diorite to monzodiorite (Fig 5a), and of the host marine mafic volcanic rocks.

Megacrystic K-feldspar-phyric monzonite porphyry represents the volumetrically most important syn-mineral and syn-breccia intrusions. Within the deposit, the megacrystic monzonite porphyry is present as breccia clasts. Outside the breccia body, the megacrystic porphyry is present as discrete dikes intruding the host pre-mineral equigranular monzonite. Within the breccia, many megacrystic monzonite porphyry clasts have distinct fluidal shapes, suggesting a close timing of intrusion and brecciation (Fig 5b). More commonly, clasts are rounded to angular. Abundance of megacrystic porphyry clasts varies from absent to as much as 60 to 70% of the breccia. Diagnostic K-feldspar phenocrysts, which vary from 0.5 to 2 cm in length, form 20 to 30% of the porphyry. The phenocrysts are set in a fine-grained to aphanitic groundmass consisting of subequal plagioclase and K-feldspar. Mafic minerals, dominantly hornblende, form less than 5% of the rock.

Equigranular augite monzonite forms a second, volumetrically less abundant syn-mineral dike suite. This monzonite intrudes the mineralized breccia (Fig 5c) and is

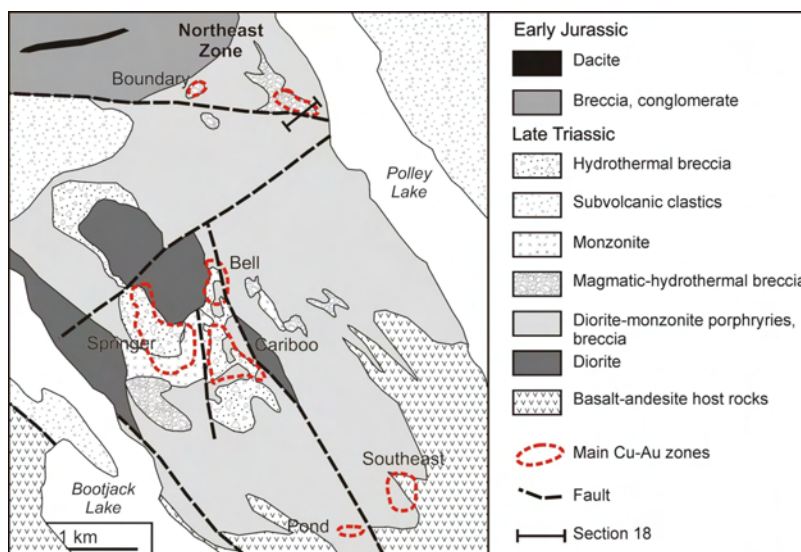


Figure 3. Simplified geology and location of mineralized zones at Mount Polley (Rees *et al.*, 2005).

locally cut by narrow (<1 mm) veins of chalcopyrite, bornite and magnetite that cross the contact into the host mineralized breccia. These relationships indicate that the equigranular monzonite intruded after brecciation but prior to a younger but less intense and spatially more restricted stage of sulphide mineralization.

Post-mineral dikes are compositionally and texturally distinct. They intrude mineralized breccia and late mineralized but post-breccia equigranular augite monzonite. Based on crosscutting intrusive relations, as well as mineralogy and inferred composition, the post-mineral dikes are divided into five families. These are, in order of decreasing age: K-feldspar-phyric monzonite porphyry (Fig 5d), K-feldspar and plagioclase-phyric monzonite porphyry, hornblende and biotite equigranular monzonite, plagioclase-phyric microporphyry, and mafic dikes. Among the post-mineral K-feldspar-phyric dikes, there is a general trend characterized by decreasing phenocryst size and abundance with time: the older dikes of the family contain up to 30% K-feldspar phenocrysts 2 to 5 mm in size, whereas the youngest have <5% K-feldspar phenocrysts 1 to 3 mm in size.

HYDROTHERMAL PARAGENESIS AND MINERAL CHEMISTRY

Sulphide minerals in the Northeast zone are principally cement to breccia clasts with less common replacement of rock-flour matrix or veins cutting clasts. Pyrite, chalcopyrite and bornite dominate, with trace amounts of galena and primary chalcocite (Fig 6a, b). Secondary covellite is also present. Chalcopyrite and bornite form a core to the orebody (Fig 7), and are surrounded by chalcopyrite and finally chalcopyrite accompanied by increasing pyrite towards the margins. As illustrated in Figure 7, based on a cross-section through section 18 (geology shown in Fig 4), the bornite and chalcopyrite zone is up to 30 m wide, the chalcopyrite zone is up to 150 m wide and the pyritic halo is at least 300 m wide. In the high-grade core, bornite frequently forms millimetre-scale rims on chalcopyrite.

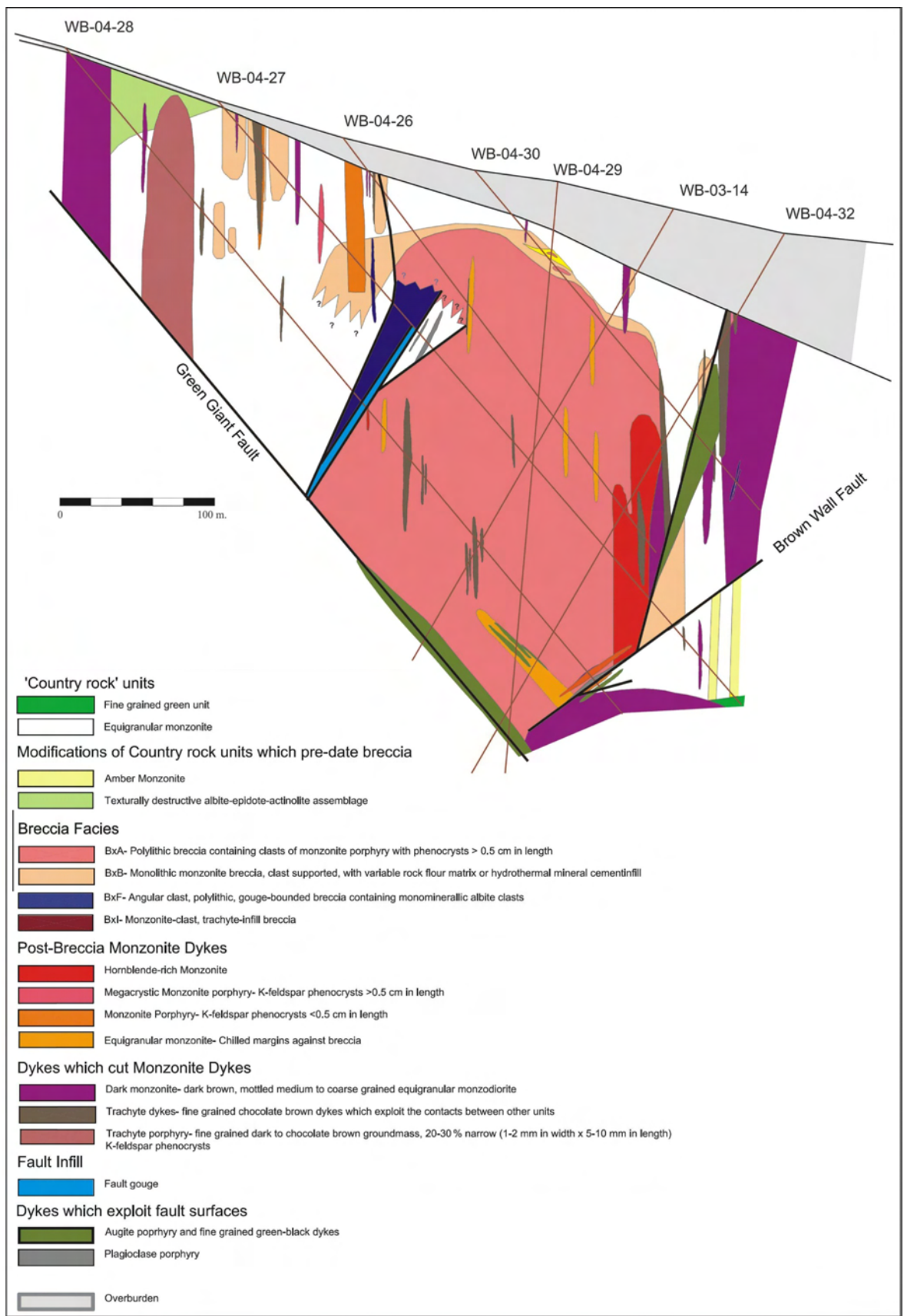


Figure 4. Cross-section along section 18, showing distribution of igneous rocks and breccia in the Northeast zone, Mount Polley.

Trace element chemistry shows that bornite and galena are elevated in Ag, whereas magnetite is elevated in Zn. Gold was not identified in any abundance in any sulphide minerals analyzed. Chalcopyrite is characterized by a trace element zonation, with Se and Bi elevated in the core of section 18 and decreasing in concentration outward. Deyell and Tosdal (2005, augmented in this study) showed that $\delta^{34}\text{S}_{\text{CDT}}$ values in chalcopyrite, pyrite and bornite range from -0.55 to -7.10% . The most negative sulphide values are from pyrite near the core of the deposit, but also near the top of the deposit and farther outboard from the core of the deposit (Fig 7). Both sulphide and sulphate $\delta^{34}\text{S}_{\text{CDT}}$ values are consistent with an oxidizing fluid source. At least two stages of early carbonate, one main stage, and multiple stages of late carbonate and anhydrite veins are also present (Fig 6c).

Mount Milligan

Mount Milligan, located 155 km northwest of Prince George, is the youngest alkalic-type porphyry Cu-Au deposit in BC. Total resources, as reported by Placer Dome Inc. (December 31, 2005), are 205.9 Mt grading 0.6 g/t Au (3.7 million oz) and 0.247% Cu (1.12 billion lbs).

The Mount Milligan area is moderately to steeply tilted (dipping $\sim 45^\circ\text{W}$), based on the dip of the host sequences as well as the geometry of the stocks and derivative sills, specifically the MBX stock and Rainbow dike (Fig 8, 9). Implicit in this geometry is that the bottom of each vertical drillhole has a more peripheral location relative to the stock than the top, so that outward gradational and zonal changes in alteration for a particular hole occur at depth. Consequently, due to the present structural orientation of the

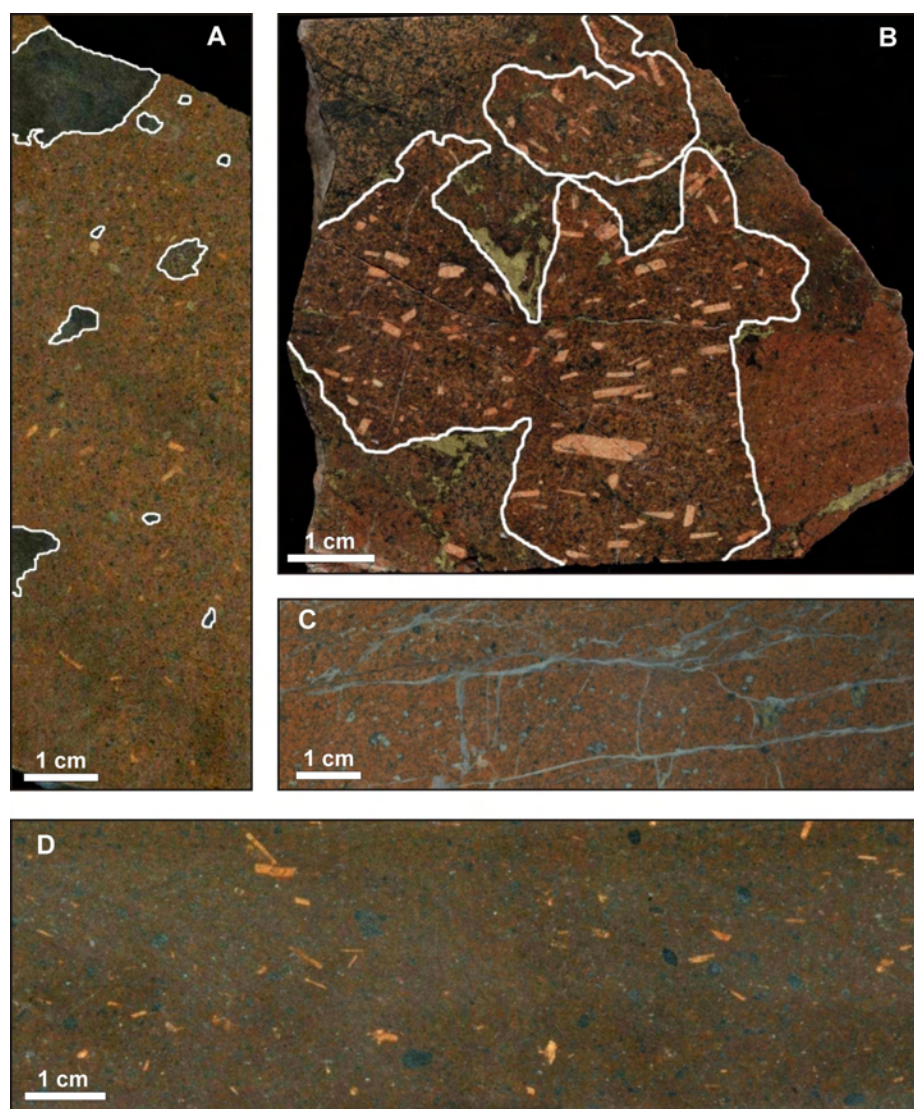


Figure 5. Representative intrusive rock in the Northeast zone of Mount Polley: A) pre-mineral equigranular monzonite; B) fluidal clast of megacrystic K-feldspar-phyric monzonite porphyry that is syn-breccia and syn-mineral; C) late syn-mineral equigranular monzonite; and D) post-mineral K-feldspar-phyric monzonite.

orebody, there is the opportunity to simultaneously track lateral and vertical physicochemical changes within the deposit. In addition, a fault separates a Au-rich but Cu-poor zone of the deposit (66 zone) from the Cu-enriched part of the deposit (MBX zone). Accordingly, the down-faulted segment preserves a part of the hydrothermal system that has been eroded elsewhere in the deposit, and provides a glimpse of the upper parts of the hydrothermal system. As a result, Mount Milligan provides a unique opportunity to define the lateral and vertical characteristics of mineralization and alteration, and broad-scale geochemical zonation with

respect to the regional architecture, building upon the previous work presented in Sketchley *et al.* (1995). Current research at this site is focused on defining the paragenesis of the deposit through a detailed examination of alteration, sulphide mineral distribution and broad-scale geochemical zonation with respect to the regional architecture.

In order to constrain the lateral and vertical changes in alteration and mineralization, a hinged cross-section (Fig 9) through the MBX stock and then southeast through the 'MBX' (Cu and Au-rich) and '66' (Cu-poor, Au-rich) zones was relogged. This section crosses the Rainbow

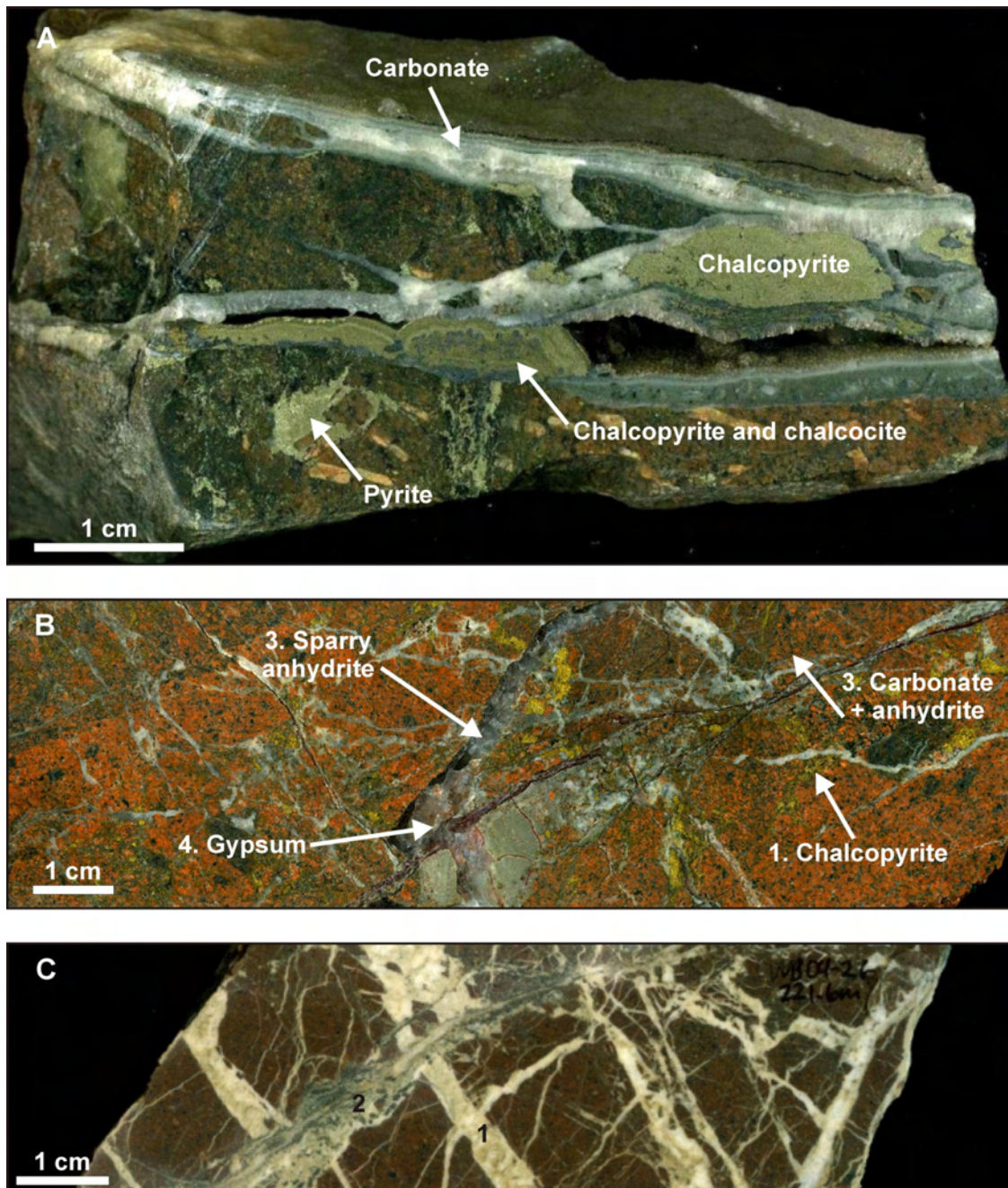


Figure 6. Examples of mineralized rocks in the Northeast zone of Mount Polley: A) main-stage Cu-sulphide mineralization and associated carbonate veins; B) chalcopyrite cut by late-stage carbonate, anhydrite and gypsum; and C) post-sulphide carbonate veins (1), in turn cut by younger carbonate veins (2).

fault, which is currently mapped with a northeasterly trend extending from the Divide fault to the Great Eastern fault, so that it truncates the Rainbow dike at its southernmost extent and separates the MBX and 66 zones. Formerly, the Rainbow fault was mapped as running north-south, parallel to bedding along the east side the Rainbow dike (Sketchley *et al.*, 1995). The revised fault geometry is significant because it implies that the transition in alteration and mineralization from the MBX to the 66 zone is not continuous. Furthermore, it is apparent that the moderately south-dipping fault has juxtaposed two different parts of the hydrothermal system. Accordingly, alteration and vein stages from the upper segments of 66-zone drillholes on the hangingwall of the Rainbow fault represent a portion of the deposit that has been eroded from the footwall.

HYDROTHERMAL ALTERATION ZONATION

By comparing the distribution of sulphide and alteration minerals sequentially from the stock outward, a generalized zone of strong potassic alteration (secondary orthoclase and biotite) between the MBX stock and the Rainbow dike (along the hangingwall of the dike) is interpreted to be the result of focusing of hot, magmatic-hydrothermal fluids. Lower temperature, propylitic alteration (chlorite-epidote-calcite-albite) typically occurs below the

footwall of the monzonitic Rainbow dike where it overprints potassic alteration in volcanic hostrocks. The propylitic zone becomes shallower with distance away from the stock, suggesting an upward, concentrically zoned pattern to the alteration zones.

Bedded volcanic units with high permeability are strongly potassically altered, suggesting some lateral channellizing of high-temperature magmatic fluids. The net effect of the channellized flow is propylitically altered rocks, representative of lower temperature fluids or the interaction of orthomagmatic and meteoric fluids, sandwiched between zones of strong potassic alteration near the monzonite intrusion, and in high permeability rocks at depth (180–200 m). Overall, the alteration pattern reveals more complexity to the fluid flow than implied by the gross-scale concentric alteration pattern. Clearly, structure and lithology are major contributing factors defining the deposit paragenesis, as well as the distribution of alteration assemblages.

Mineral mapping using a short-wave infrared (SWIR) instrument demonstrates that an approximately 100 m wide potassic zone adjacent to the stock is surrounded by an approximately 60 m wide sodic-calcic zone, which grades upward into a chlorite-sericite assemblage. Late-stage alteration (illite-montmorillonite-sericite) is superposed on the

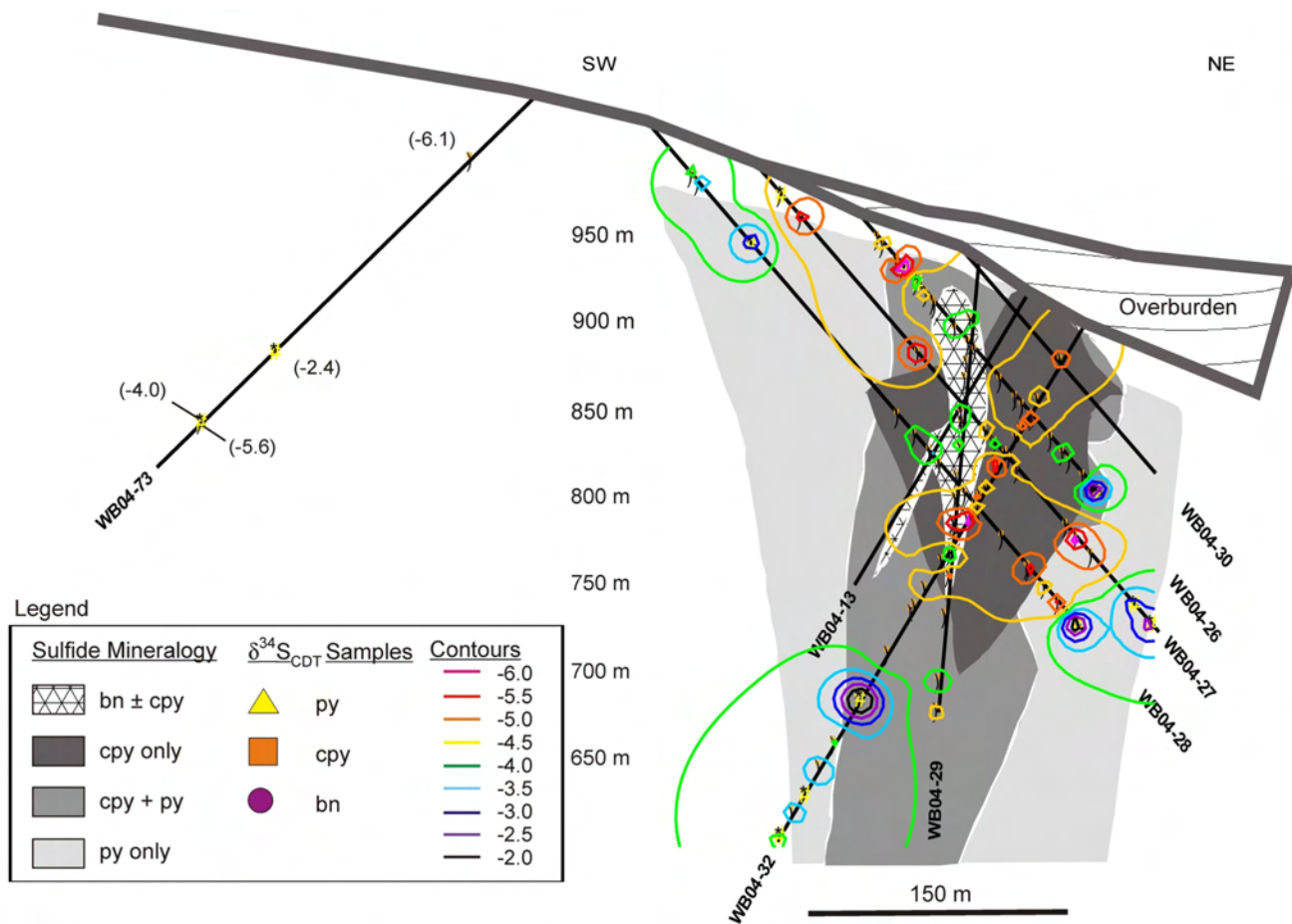


Figure 7. Distribution of sulphide minerals and contoured sulphur isotope ($\delta^{34}\text{S}_{\text{CDT}}$) data across section 18. Contours are based on results from all sulphide minerals of Deyell and Tosdal (2005), supplemented by new data. $\delta^{34}\text{S}_{\text{CDT}}$ samples with numbers in brackets have been provided for completeness; these values were not included in contours. Sulphide mineralogy from Deyell and Tosdal (2005). Abbreviations: bn, bornite; cpy, chalcopyrite; py, pyrite.

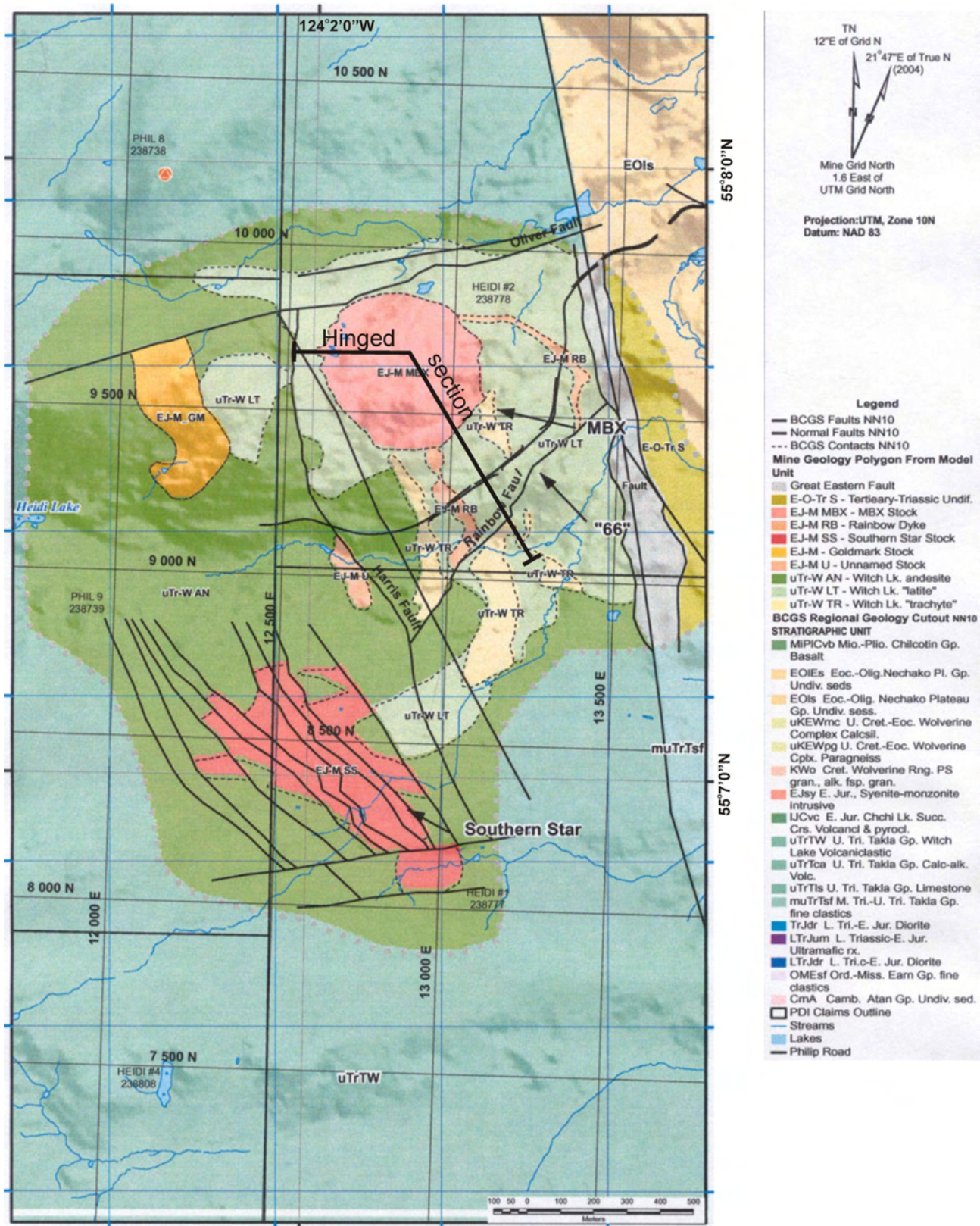


Figure 8. Location and simplified geology of Mount Milligan deposit.

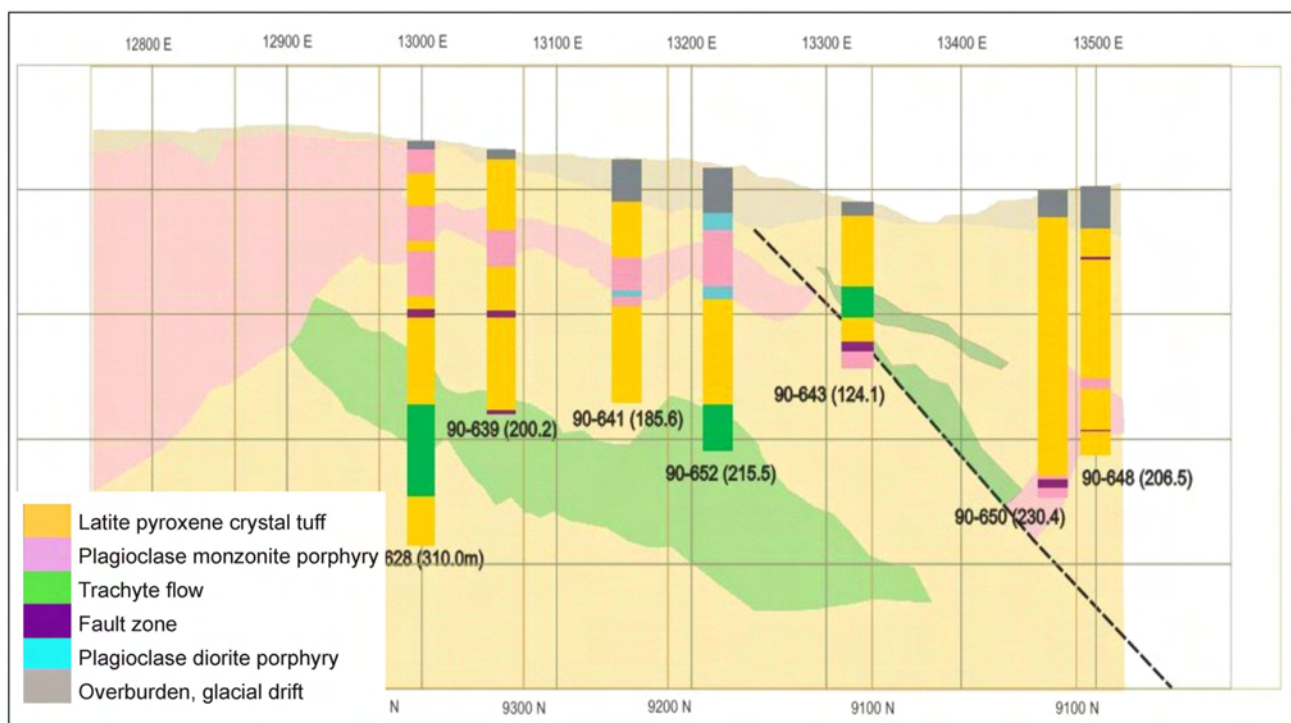


Figure 9. Compiled cross-section of the Mount Milligan deposit; see Figure 8 for location.

potassic zone and along the Rainbow dike, suggesting prolonged fluid channelization due to higher permeability and/or hostrock fracturing.

Analysis of $\delta^{34}\text{S}_{\text{CDT}}$ values in association with the sulphide from which they were obtained was undertaken to determine if $\delta^{34}\text{S}_{\text{CDT}}$ values correlated with particular mineralization events, such as early versus late veins, and disseminated sulphide minerals (Fig 10). There appears to be a distinct difference between Au-deficient, late pyrite-magnetite-chlorite veins/clots ($\delta^{34}\text{S}_{\text{CDT}}$ values ranging from -1 to 0%) and sulphide minerals from earlier veins and disseminations. Although, differences in $\delta^{34}\text{S}_{\text{CDT}}$ values among earlier sulphidization events are unclear, there may be a difference between potassic and propylitic sulphide events, with early veins (most with a chalcopyrite component) and disseminations having $\delta^{34}\text{S}_{\text{CDT}}$ values between -3 and -2% , and pyrite veins with propylitic halos and lesser chalcopyrite ranging between -2.2 and -1.5% . In terms of metal concentrations, near-zero $\delta^{34}\text{S}$ values are Au-Cu deficient. The range of Cu/ $\delta^{34}\text{S}$ ratios is widest near the MBX stock and generally decreases with distance. The same pattern is observed with Au/ $\delta^{34}\text{S}$ ratios, although there is a jump in Au values and Au/ $\delta^{34}\text{S}$, potentially indicating a second mineralization event involving Au transported as a bisulphide versus chloride complex. Generally, there appear to be at least three phases of mineralization with distinct ranges of $\delta^{34}\text{S}$ values.

Galore Creek

Galore Creek is the most important example of the silica-undersaturated class of alkalic porphyry Cu-Au deposits (Lang *et al.*, 1995). The property is underlain mainly by marine volcanic and sedimentary rocks of the Middle to

Upper Triassic Stuhini Group (Fig 11). These rocks are intruded by an alkali syenite complex composed of multiple intrusions emplaced into volcanic rocks of similar composition. To date, 12 Au-Ag-Cu mineralized zones have been identified (Fig 12). Overall, the mineralized zones extend more than 5 km in length and 2 km in width. The mineralization is hosted predominantly in highly altered volcanic rocks and, to a lesser degree, in syenite intrusions. The largest zone of mineralization, the Central zone, and the flanking North and South gold zones, host high-grade Cu-Au, have marked spatial variation in Au/Cu ratio, and are unique among the alkalic porphyry Cu-Au deposits in the high abundance of garnet within the alteration parageneses (Enns *et al.*, 1995). The temporal and spatial evolution of hydrothermal fluids in this deposit is therefore of interest in elucidating the characteristics that governed the formation of the deposit.

HYDROTHERMAL ALTERATION ZONATION PATTERNS

Five broad styles of alteration are manifested as alteration assemblages at Galore Creek, and are summarized in Figure 13.

Calcsilicate Alteration

A calcsilicate assemblage dominated by diopside and pale brown garnet replaces one or more fragmental horizons in the footwall of the pre-mineralization porphyry stock. This assemblage is considered to constitute prograde skarn and is metal poor unless overprinted by hydrothermal biotite. In the Central zone, crosscutting relationships with the K-silicate assemblage and lack of mineralization indicate that this alteration is early in the sequence.

Potassium-Silicate Alteration

Potassium-silicate alteration dominates and affects the host volcanic rocks, pre and syn-mineral porphyries and, to a minor extent, post-mineral porphyries (see Enns *et al.* (1995) for a thorough review of the intrusive history). The

most intense K-silicate alteration in pre-mineral porphyry consists of K-feldspar, biotite, magnetite and anhydrite, with associated bornite and chalcopyrite. Potassium-silicate alteration is notably weaker in syn-mineral porphyry, although biotitization of a rock-flour matrix breccia is locally intense.

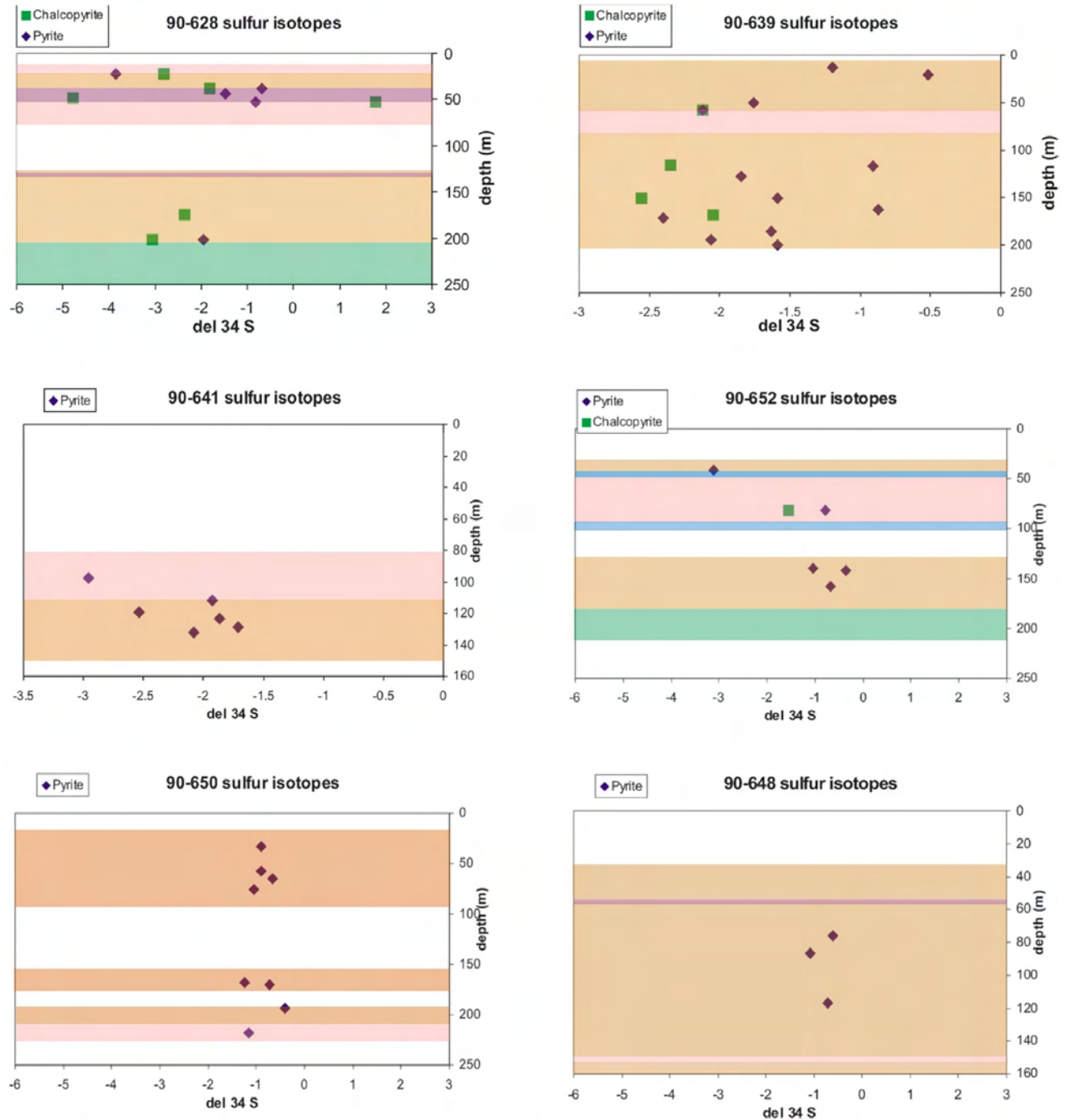


Figure 10. Sulphur isotope ($\delta^{34}\text{S}$) values versus depth and lithology for the six Mount Milligan drillholes sampled (Jago, 2006). Legend: blue diamonds, pyrite; green squares, chalcopyrite; pink shading, Rainbow dike (or MBX Main stock at ~20 m depth in 90-628); brown shading, 'latite'; green shading, 'trachyte'; purple shading, fault zone; blue shading, monzodiorite porphyry dike (suggesting that the Rainbow dike is a potassically altered monzodiorite dike versus a true 'monzonite'). Note the decrease in the range of values outward from the centre of the system, and the overall shift to near-zero values. The widest range of values in 90-628 is situated within the faulted rock on the hangingwall of the Rainbow Dike, indicating prolonged fluid channelization.

Figure 11. Simplified geology of the Galore region (adapted from Enns et al., 1995).

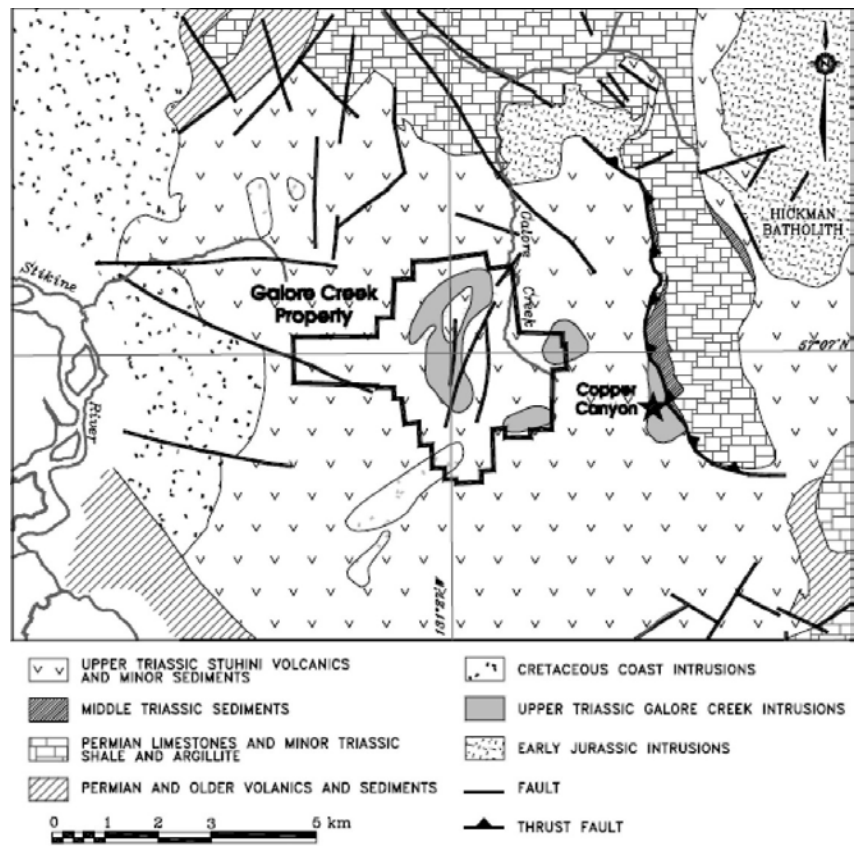
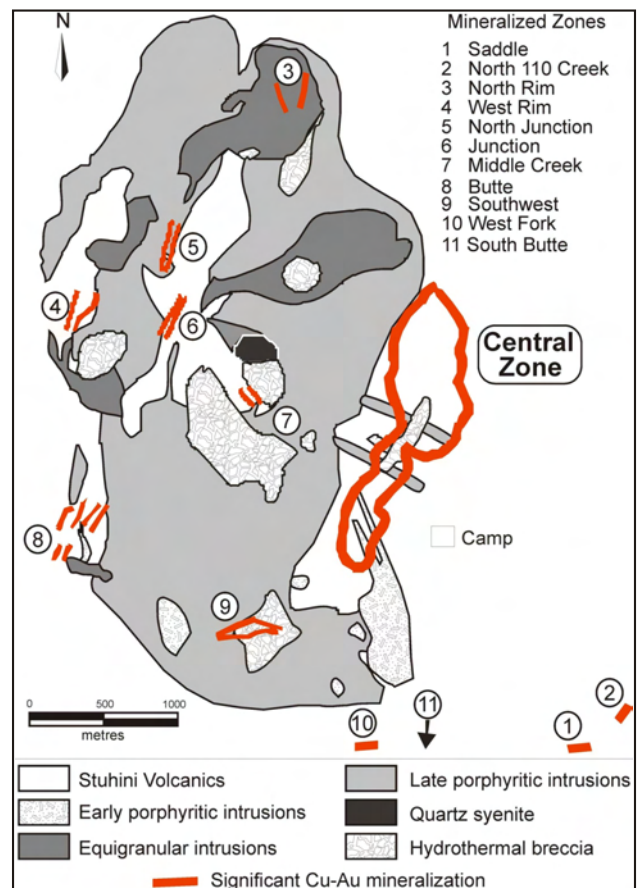


Figure 12. Summary map illustrating mapped geology of the Galore Creek deposits (after Enns et al., 1995).



Within the core of the Central zone, there occurs an associated 'Ca-K-silicate' assemblage, characterized by the addition of a dark brown garnet with locally occurring diopside, epidote and plagioclase. This assemblage appears to be localized where the high-temperature K-silicate altering fluids encountered calcic mafic rocks from which they derived Ca and precipitated garnet. Decreasing Ca in the alteration from the core region to the north and south of the Central zone is accompanied by generally increasing magnetite and early hematite.

Intermediate Argillic Alteration

Intermediate argillic alteration, composed of green sericite, carbonate and minor chlorite, appears most intense in the upper parts of the pre-mineral intrusion and usually overprints K-silicate alteration. Older magnetite is altered to hematite. Sericite affects all volcanic units as well as the pre-mineral and, to a lesser extent, post-mineral porphyry dikes. The paragenetic relationship of the alteration assemblages suggests that the intermediate argillic alteration was largely peripheral to the main centres of Cu and Au mineralization. Intermediate argillically altered rocks are intruded by post-mineral porphyry bodies.

Sericite-Anhydrite-Carbonate (SAC) Alteration

Sericite-anhydrite-carbonate alteration overprints early alteration phases and is locally extensive at the outer margins of the Central zone. In the southern part of the Central zone, it is accompanied by late hematite. In the northern part of the Central zone, it is marked by increasing pyrite±hematite and decreasing bornite-chalcopyrite, suggesting that Cu was remobilized during this alteration. In the core of the Central zone, sericite-anhydrite-carbonate alteration is poorly developed and patchy in occurrence.

Propylitic Alteration

An epidote-chlorite assemblage, locally accompanied by garnet, is present in post-mineral megacrystic porphyry bodies and penetrated for a few metres into their wallrocks.

MINERALIZATION

Sulphide minerals are closely associated with intense, pervasive K-silicate alteration as replacement, disseminated and fracture-controlled chalcopyrite with locally abundant bornite. Higher Au values are normally associated with bornite, which is better developed in the North and South gold lenses, relative to the Cu-enriched core of the Central zone. The Central zone is elongated in a north-northwesterly (015°) direction and dips steeply to the west. It is 1700 m in length and 200 to 500 m wide, and has been traced to a depth of 450 m through drilling, remaining open below that. In the west and south, mineralized rock is truncated by post-mineral megacrystic porphyry dikes.

Intense sericite-anhydrite-carbonate alteration has obliterated sulphide-mineralized rock in the northwestern part of the Central zone. In the north, mineralized volcanic

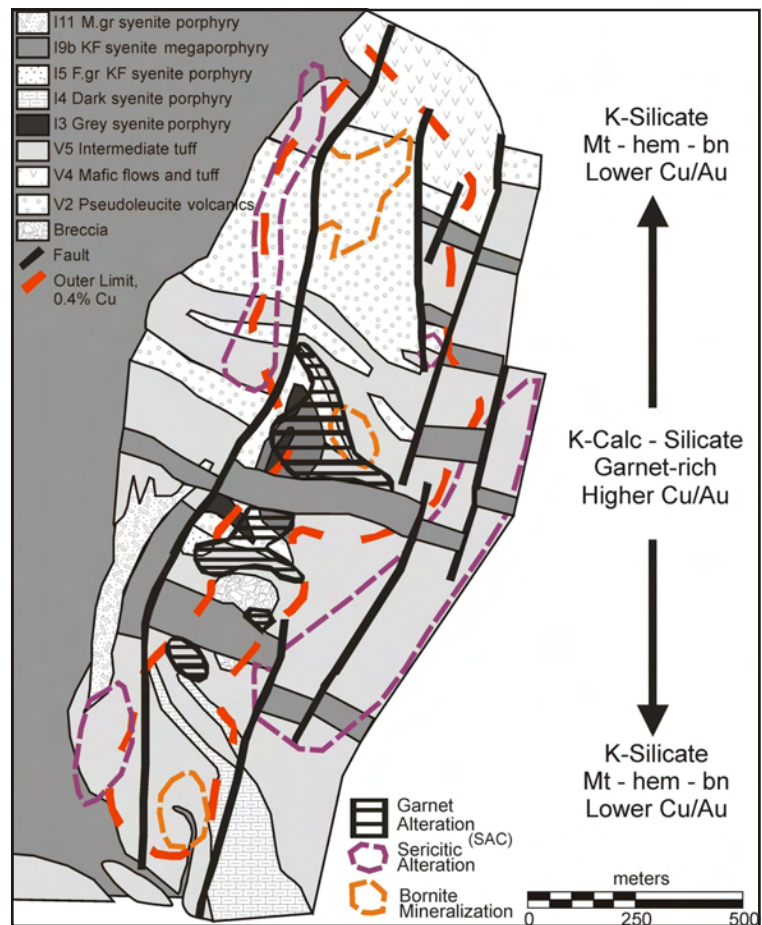


Figure 13. Distribution of the principal styles of alteration shown in relation to the Galore Creek geology, including gross metal ratios (after Enns et al., 1995).

rocks end abruptly against a thick sequence of barren epiclastic sedimentary and volcanic rocks. The Central zone has considerable internal variation in sulphide minerals and alteration mineral assemblages. Hydrothermal alteration assemblages change from Ca-K-silicate in the core to intense K-silicate assemblages toward the north and south parts of the zone. In terms of Au-Ag-Cu replacement, the most favourable volcanic rocks are pseudoleucite-bearing rocks in the north and crystal tuff in the south. Augite-bearing volcanic and volcanoclastic rocks in the north have low to moderate Cu grades. Gold values are highest in the northern and southern portions of the Central zone, where significant disseminated bornite, magnetite and hematite are present. Lower Au grades correlate with an intense Ca-K-silicate altered core. Chalcopyrite is the most important Cu mineral and occurs as replacements, disseminations and fracture fillings throughout the zone. Pyrite increases in abundance to the east of the Central zone, reaching concentrations of up to 5%. Minor supergene Cu is present, primarily as malachite, azurite and chrysocolla on fractures within 60 m of the surface.

GARNET PARAGENESIS AS A GUIDE TO THE EVOLUTION OF THE GALORE CREEK PORPHYRY DEPOSIT

Galore Creek is unique among the alkalic porphyry Cu-Au deposits in the abundance of garnet-rich alteration.

Garnet coexists with biotite, K-feldspar, anhydrite and apatite in the core of the Central zone, where it replaces early porphyry dikes and adjacent volcanic wallrocks. This alteration grades outwards into a conventional K-silicate assemblage of biotite, K-feldspar, magnetite and apatite. Garnet is characterized by growth zones marked by prominent colour variations, entrapment of primary fluid inclusions and episodic coprecipitation with, or replacement by, anhydrite. Fluid inclusion characteristics and chemical cycling are consistent with the formation of alteration and mineralization by release of magmatic fluids early in the igneous sequence at Galore Creek. Extended garnet growth at the high temperatures indicated by fluid inclusions suggests that the hostrocks sat and 'stewed' in a hydrothermal fluid-dominated system. The composition of the fluids, dominated by NaCl, KCl and CaCl₂, is consistent with the alteration assemblage K-feldspar, biotite, apatite, anhydrite, garnet and anhydrite. It also suggests that the alteration was occurring in a fluid-buffered system in which the hostrock composition had little control over the ultimate style or composition of alteration and possibly the ore assemblage.

FUTURE WORK

Ongoing integration of detailed structural, geochemical and geochronological information is essential to the development of an improved alkalic porphyry deposit model. While this work is in the initial stages, the overall goal of the project is to build a view of the structural and geological architecture, alteration zonation patterns and mineral chemistry at each of the study sites. Current studies will be augmented by a new study initiated at the Lorraine deposit. This latter deposit has perhaps some of the most abnormal characteristics of the alkalic porphyry systems, and suggests that sulphide mineral deposition bridged the transition from magmatic-segregation to magmatic-hydrothermal deposits. The Lorraine deposits also appear to represent the deepest possible level of formation in the alkalic porphyry environment. Defining the hydrothermal features of each deposit, combined with available data from deposits around the world, will thus provide the basis for establishing the characteristics of the intrusion-centred systems at a range of inferred deposit depths.

ACKNOWLEDGMENTS

We thank the Imperial Metals Corporation, Novagold Resources Inc., Placer Dome Inc. (now Barrick Gold Corporation), Terrane Minerals Corp., Teck Cominco Limited, and Eastfield Resources Ltd. for logistical support for project members in the field. We also thank the sponsoring companies, the Natural Sciences and Engineering Council of Canada (NSERC) and Geoscience BC for their financial support of the project.

REFERENCES

- Blevin, P.L. (2002): The petrographic and compositional character of variably K-enriched magmatic suites associated with Ordovician porphyry Cu-Au mineralization in the Lachlan Fold Belt, Australia; *Mineralium Deposita*, volume 37, pages 87–99.
- Cooke D.R., Wilson A.J., House M.J., Wolfe R.C., Walshe J.L., Lickfold V. and Crawford A.J. (in press): Alkalic porphyry Au-Cu and associated mineral deposits of the Ordovician to Early Silurian Macquarie Arc, NSW; *Australian Journal of Earth Sciences*.
- DeLong, R.C. (1996): Geology, alteration, mineralization and metal zonation of the Mt. Milligan porphyry copper-gold deposits; unpublished MSc thesis, *University of British Columbia*, Vancouver, BC, 121 pages.
- Deyell, C.L. and Tosdal, R.M. (2005): Alkalic Cu-Au deposits of British Columbia: sulfur isotope zonation as a guide to mineral exploration; in *Geological Fieldwork 2004, British Columbia Ministry of Energy, Mines and Petroleum Resources*, Paper 2005-1, pages 191–208.
- Drummond, M. S. and Denfant, M.J. (1990): A model for trondhjemite-tonalite-dacite genesis and crustal growth via slab melting; *Journal of Geophysical Research*, volume 95, pages 503–521.
- Enns, S.G., Thompson, J.F.H., Stanley, C.R. and Yarrow, E.W. (1995): The Galore Creek porphyry copper-gold deposits, NW British Columbia; in *Porphyry Deposits of the Northern Canadian Cordillera*, Schroeter, T.G., Editor, *Canadian Institute of Mining and Metallurgy and Petroleum*, Special Volume 46, pages 630–644.
- Fraser, T.M., Stanley, C.R., Nikic, Z.T., Pesalj, R. and Gorc, D. (1995): The Mount Polley alkalic porphyry copper-gold deposit, south-central British Columbia; in *Porphyry Deposits of the Northwestern Cordillera of North America*, Schroeter, T.G., Editor, *Canadian Institute of Mining, Metallurgy and Petroleum*, Special Volume 46, pages 609–622.
- Holliday, J.R., Wilson, A.J., Blevin, P.L., Tedder, I.J., Dunham, P.D. and Pfitzner, M. (2002): Porphyry gold-copper mineralization in the Cadia district, eastern Lachlan Fold Belt, New South Wales, and its relationship to shoshonitic magmatism; *Mineralium Deposita*, volume 37, pages 100–116.
- Imperial Metals Corporation (2006): Mount Polley property and mine operations: updated reserve/resource table, January 23, 2006; Imperial Metals Corporation, URL <<http://www.imperialmetals.com/s/MountPolleyTables.asp>> [November 2006].
- Jensen, E.P. and Barton, M.D. (2000): Gold deposits related to alkaline magmatism; *Reviews in Economic Geology*, volume 13, pages 279–314.
- Kay S.M., Mpodozis C. and Coira B. (1999): Neogene magmatism, tectonism, and mineral deposits of the Central Andes (22° to 33° latitude); *Society of Economic Geologists*, Special Publication 7, pages 27–59.
- Lang, J.R., Lueck, B., Mortensen, J.K., Russell, J.K., Stanley, C.R. and Thompson, J.M. (1995a): Triassic-Jurassic silica-undersaturated and silica-saturated alkalic intrusions in the Cordillera of British Columbia: implications for arc magmatism; *Geology*, volume 23, pages 451–454.
- Lang J.R., Stanley C.R., Thompson J.F.H. and Dunne K.P.E. (1995b): Na-K-Ca magmatic-hydrothermal alteration in alkalic porphyry Cu-Au deposits, British Columbia; *Mineralogical Association of Canada*, Short Course 23, pages 339–336.
- Lickfold, V., Cooke, D.R., Smith, S.G. and Ullrich, T.D. (2003): Endeavor copper-gold porphyry deposits, North Parkes, New South Wales: intrusive history and fluid evolution; *Economic Geology*, volume 98, pages 1607–1636.
- Logan, J.M. (2005): Alkaline magmatism and porphyry Cu-Au deposits at Galore Creek, northwestern British Columbia; in *Geological Fieldwork 2004, British Columbia Ministry of Energy, Mines and Petroleum Resources*, Paper 2005-1, pages 237–248.
- Logan, J.M. and Mihalynuk, M.G. (2005a): Regional geology and setting of the Cariboo, Bell, Springer and Northeast porphyry Cu-Au zones at Mount Polley, south-central British Columbia; in *Geological Fieldwork 2004, British Columbia*

- Ministry of Energy, Mines and Petroleum Resources*, Paper 2005-1, pages 249–270.
- Logan, J.M. and Mihalynuk, M.G. (2005b): Porphyry Cu-Au deposits of the Iron Mask Batholith, southeastern British Columbia; in *Geological Fieldwork 2004, British Columbia Ministry of Energy, Mines and Petroleum Resources*, Paper 2005-1, pages 271–290.
- Lueck, B.A. and Russell, J.K. (1994): Silica-undersaturated, zoned alkaline intrusions within the British Columbia Cordillera; in *Geological Fieldwork 1993, BC Ministry of Energy and Mines and Petroleum Resources*, Paper 1994-1, pages 311–315.
- Mortensen, J.K., Ghosh, D.K. and Ferri, F. (1995): U-Pb geochronology of intrusive rocks associated with copper-gold porphyry deposits in the Canadian Cordillera; in *Porphyry Deposits of the Northwestern Cordillera of North America*, Schroeter, T.G., Editor, *Canadian Institute of Mining, Metallurgy and Petroleum*, Special Volume 46, pages 142–158.
- Panteleyev, A., Bailey, D.G., Bloodgood, M.A. and Hancock, K.D. (1996): Geology and mineral deposits of the Quesnel River – Horsefly map area, central Quesnel Trough, British Columbia (NTS 93A/5, 6, 7, 11, 13; 93B/9, 16; 93G/1; 93H/4); *BC Ministry of Energy and Mines and Petroleum Resources*, Bulletin 97, 156 pages.
- Rees, C., Bjornson, L., Blackwell, J., Ferreira, L., McAndless, P., Robertson, S., Roste, G., Stuble, T. and Taylor, C. (2005): Geological report on the Mount Polley property and summary of exploration in 2003–2004; *Imperial Metals Corporation*, unpublished internal report, 211 pages.
- Schroeter, T.G., Editor (1995): *Porphyry Deposits of the Northwestern Cordillera of North America*; *Canadian Institute of Mining, Metallurgy and Petroleum*, Special Volume 46, 888 pages.
- Sketchley, D.A., Rebagliati C.M. and DeLong, C. (1995): Geology, alteration and zoning patterns of the Mt. Milligan copper-gold deposits; in *Porphyry Deposits of the Northwestern Cordillera of North America*, Schroeter, T.G., Editor, *Canadian Institute of Mining, Metallurgy and Petroleum*, Special Volume 46, pages 650–665.
- Tosdal, R.M. (2004): Tectonics of porphyry copper and epithermal deposits as constrained by vein geometry; in *24 Carat Gold Workshop*, Cooke, D.R., Deyell, C., and Pongratz, J., Editors, *Australian Research Council Centre of Excellence in Ore Deposits (CODES)*, University of Tasmania, Hobart, Tasmania, Special Publication 5, pages 41–44.
- Wilson, A., Cooke, D.R. and Harper, B.L. (2003): The Ridgeway gold-copper deposit: a high-grade alkalic porphyry deposit in the Lachlan Fold Belt, NSW, Australia; *Economic Geology*, volume 98, pages 1637–1656.

Stratigraphic Record of Initiation of Sedimentation in the Bowser Basin (NTS 104A, H), Northwestern British Columbia¹

by J-F. Gagnon², W. Loogman², J.W.F. Waldron², F. Cordey³ and C.A. Evenchick⁴

KEYWORDS: sedimentology, stratigraphy, hydrocarbon, Bowser Lake Group, Hazelton Group, Spatsizi Formation

INTRODUCTION

The Bowser Basin is a sedimentary basin located over the Stikine Terrane in the Intermontane Belt of northwestern British Columbia (Fig 1). In this area, the Stikine Terrane is overlain by Early Jurassic sedimentary rocks of the upper Hazelton Group (Troy Ridge facies of the Salmon River Formation in Anderson [1993]; Spatsizi Formation in Thomson *et al.* [1986]) and then by a thick succession (approximately 6 km) of Middle Jurassic to Early Cretaceous sedimentary rocks mainly assigned to the Bowser Lake Group (Evenchick and Thorkelson, 2005). The fill of the Bowser Basin was deposited over the arc volcanic rocks and associated volcanoclastic rocks of the lower Hazelton Group. A broad variety of sedimentary environments characterized the Bowser Basin, ranging from basin-floor turbidites at the base through marginal-marine clastic rocks to nonmarine redbeds in the uppermost parts of the succession.

Recent thermal maturity investigations have shown the existence of an effective petroleum system in the Bowser Basin (Evenchick *et al.*, 2002; Osadetz *et al.*, 2003; Stasiuk *et al.*, 2005). Black shales of the Spatsizi Formation have returned total organic carbon content up to 6%, and these values might have been two to four times greater before the expulsion of organic material (Ferri and Boddy, 2005). This suggests that under the proper conditions, organic shales of the Spatsizi Formation would have acted as excellent source rocks. However, variable thermal maturation levels throughout the basin and the lack of information regarding the linkage of source rocks of the upper Hazelton Group and potential reservoir rocks of the Bowser Lake Group create uncertainty in terms of exploration risks.

The aim of this study is to understand the conditions that led to a change in the deposition style in the Middle Jurassic from a volcanic arc-dominated environment to a sub-

siding sedimentary basin. For that purpose, study areas were selected based on known exposures that exhibit the transition from the Hazelton Group into the Bowser Lake Group in structurally undisturbed sections. Three areas are described in this report, Todagin Mountain, Mount Will and Oweegee Dome (Fig 1). Systematic measurements of detailed stratigraphic sections were conducted in the field to document the onset of sedimentation in the Bowser Basin.

STRATIGRAPHY OF THE LOWER HAZELTON GROUP

The lowest stratigraphic unit observed in the vicinity of Todagin Mountain consists of a mixture of greenish grey to maroon volcanoclastic rocks and light grey trachyandesitic volcanic flows. This dominantly intermediate volcanic suite and associated plutons, which unconformably overlie the Triassic Stuhini Group, was mapped as andesite breccias and derived epiclastic rocks by Ash *et al.* (1997). Five individual intrusive bodies from this suite returned U-Pb zircon dates from 205 to 198 Ma, suggesting a Hettangian to Sinemurian age (Friedman and Ash, 1997). The lavas identified in this study are mostly aphanitic and contain calcite-filled amygdules. Small intrusive bodies of leucocratic monzogranite are also present to a lesser extent. Poorly sorted reworked tuff, containing abundant subrounded lithic fragments, is interbedded with welded lapilli tuff and recessive bands of very fine grained crystal tuff. The presence of flattened pumice (fiamme) in medium-grained lapilli tuff along with light beige euhedral feldspar crystals in a matrix of fine-grained air-fall tuff suggests that explosive volcanism was the predominant mode of deposition at that time. Hematite is a common mineral amongst these pyroclastic rocks, suggesting that they mostly accumulated in an oxidizing subaerial environment.

In the Mount Will district, the lower Hazelton Group consists of a bimodal assemblage termed the Cold Fish volcanics by Thorkelson (1992). According to Thorkelson (1992), this unit can be divided into a felsic suite of high-silica rhyolite and a mafic suite of basalt, andesite and dacite. The upper 100 m of this succession were examined approximately 10 km southwest of Gladys Lake. Maroon to green, very poorly sorted epiclastic and indurated lapilli tuffs conformably overlie a thick unit of oxidized rhyolite. The recessive volcanoclastic interval is capped by approximately 30 m of densely welded ignimbrite characterized by large open vugs, fiamme, lava particles and angular volcanic fragments. This indurated felsic ash flow constitutes the last major pulse of explosive volcanism in the region before the establishment of sedimentary conditions.

The volcanic arc rocks of the lower Hazelton Group around Oweegee Dome consist of fine layers of fissile dust

¹Geoscience BC contribution GBC023

²Department of Earth and Atmospheric Sciences, University of Alberta, Edmonton, AB (jfgagnon@ualberta.ca)

³Sciences de la Terre, Université Claude Bernard Lyon 1, Villeurbanne, France

⁴Geological Survey of Canada, Vancouver, BC

This publication is also available, free of charge, as colour digital files in Adobe Acrobat® PDF format from the BC Ministry of Energy, Mines and Petroleum Resources website at http://www.em.gov.bc.ca/Mining/GeolSurv/Publications/catalog/cat_fldwk.htm

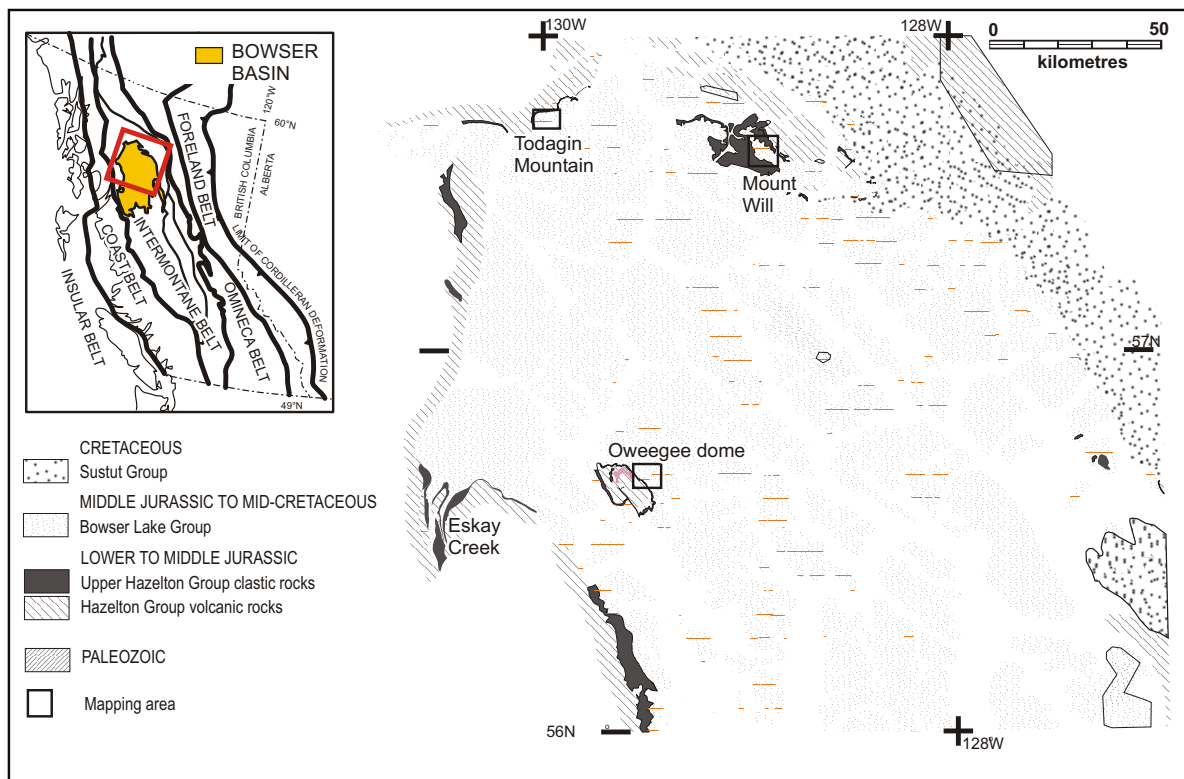


Figure 1. Simplified geology of the northern two-thirds of the Bowser Basin showing areas of detailed study in 2006, northwest BC. Inset shows the location of the Bowser Basin in relation to principal tectonic belts of the Canadian Cordilleran Orogen.

tuff interbedded with well-stratified maroon and green volcanic sandstone, pebble to cobble conglomerate, debris flows and minor andesitic volcanic flows. These units are overlain by a thick unit of felsic porphyritic rhyolite that was dated at 199 ± 2 Ma by Greig and Gehrels (1995).

STRATIGRAPHY OF THE UPPER HAZELTON GROUP

Rocks assigned to the upper part of the Hazelton Group are exposed in a southwest-trending section west of Todayin Mountain (Evenchick and Green, 2004). The upper Hazelton Group consists of a bimodal volcanic suite with multiple fine-grained sedimentary intercalations. A detailed stratigraphic column representing the section is presented in Figure 2. Thick units of columnar basalt constitute most of the section. Thin intervals of marine clastic sedimentary rocks contain numerous ammonites of the Frebaldi zone, which suggest a Pliensbachian age (Evenchick *et al.*, 2001; T. Poulton, pers comm, 2006). The stratigraphic section contains an angular discordance at 264 m (Fig 2) where a recessive unit of altered basalt is unconformably overlain by crosslaminated limestone and oxidized basalt debris. A thin layer of dacitic lapilli tuff 50 cm above this unconformity yielded a U-Pb zircon age of 185.6 ± 0.6 Ma (Palfy *et al.*, 2000) which confirms the Pliensbachian age obtained from paleontological data. The top of the succession is characterized by a thick unit of vesicular marine pillow basalt and hyaloclastite indicating deposition in a submarine environment (Fig 3).

Sedimentary rocks assigned to the Spatsizi Formation are exposed in the Mount Will district (Evenchick and Thorkelson, 2005), located approximately 10 km northeast

of Joan Lake, where Thomson *et al.* (1986) carried out earlier stratigraphic work. The lowest stratigraphic unit of the Spatsizi Formation at Mount Will is characterized by brownish to light grey arkosic sandstone deposited on top of welded ignimbrite. The high proportion of altered volcanogenic clasts in the sandstone indicates recycling of locally derived extrusive rocks of the underlying Cold Fish volcanics. Even though no angular discordance was observed, the contact with the underlying ignimbrite is erosional and probably corresponds to an unconformity. Fine to medium-grained subrounded lithic fragments and feldspar grains are moderately sorted and sedimentary structures such as ripple crosslaminations and planar crossbedding are common. The basal sandstone unit contains multiple calcareous intervals ranging from 35 to 55 cm thick with a broad variety of marine fossils (ammonites, corals, belemnites and bivalves; Fig 4). Large pieces of fossil wood and plant fragments found in thinly laminated siltstone and very fine grained sandstone indicate that a significant quantity of terrestrial debris was transported to the basin. The abundance and high diversity of bioturbation suggest that paleoenvironmental conditions, such as oxygen content, temperature and salinity, were relatively stable. The presence of symmetric wave-generated ripples is consistent with a depositional environment above the fair-weather wave base in an open, shallow-marine setting. Upsection, there is a significant increase in silt and clay content, and the sandstone beds are usually thinner. Concretionary beds of limestone are associated with the coarser grained rock units whereas rounded calcareous concretions are mostly found in shale. Trace fossils and bivalves are omnipresent in those rocks suggesting that the depositional environment was still within the photic zone.

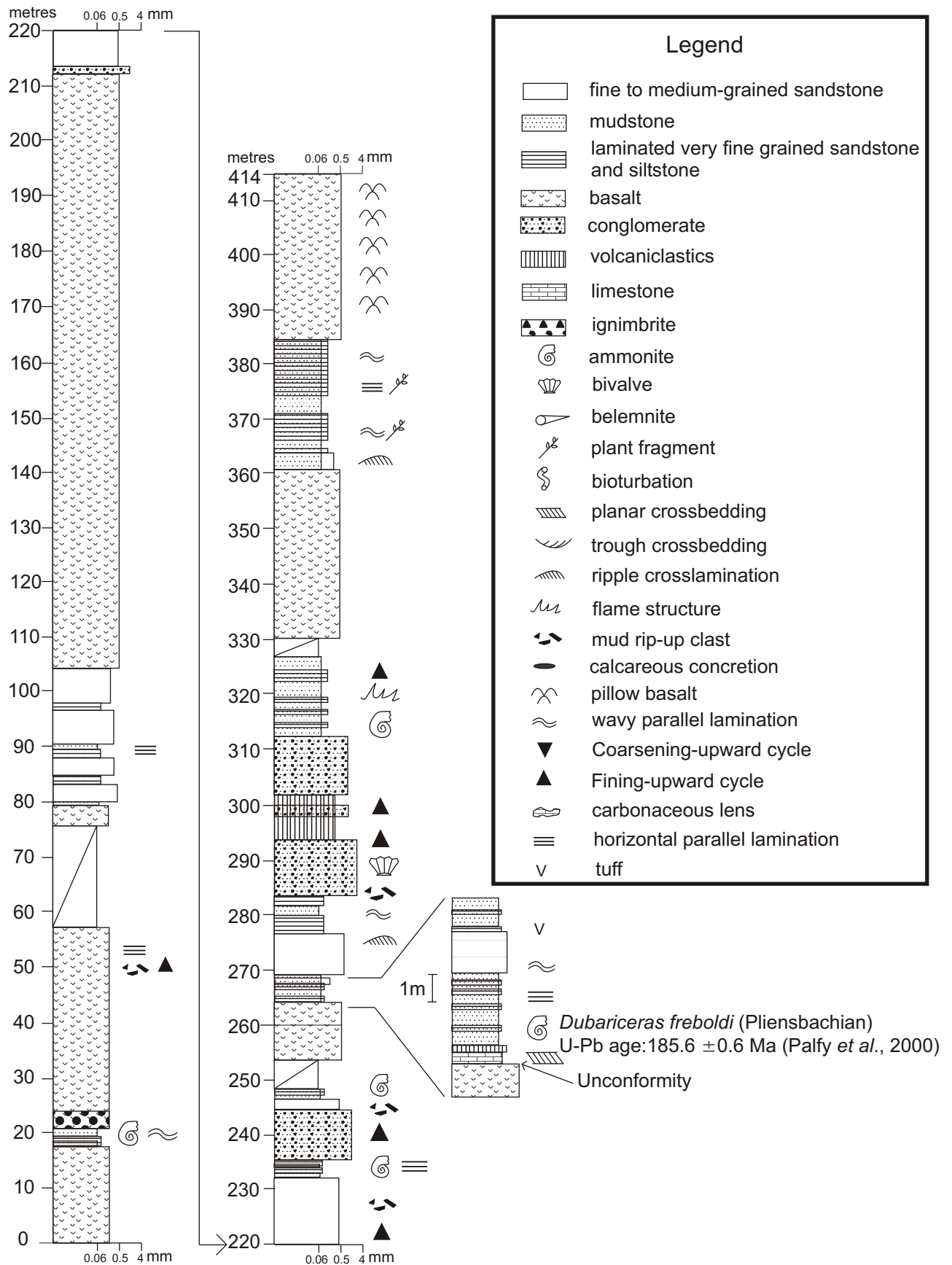


Figure 2. Detailed stratigraphic section showing interbedded volcanic rocks and marine sedimentary rocks of the upper Hazelton Group, Todagin Mountain area, BC.

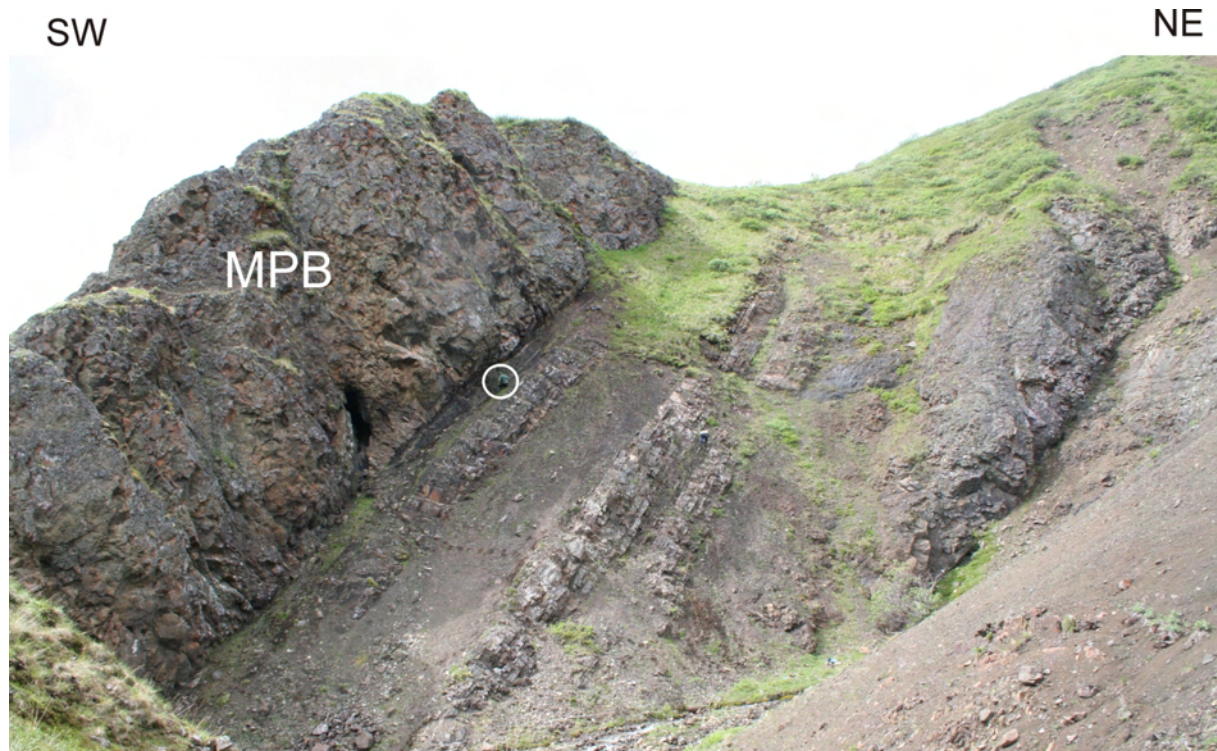


Figure 3. Upper part of the detailed section (335–414 m) measured west of Todagin Mountain, BC, showing thinly laminated siltstone and shale overlain by marine pillow basalt (MPB). See person for scale.



Figure 4. Well-preserved ammonite fossil of the Spatsizi Formation, Mount Will area, BC.

The fossiliferous shallow-marine succession is overlain by 140 m of interbedded black siliceous mudstone and pale orange tuffaceous siltstone (Fig 5). This unit was originally classified as the Quock Formation of the Spatsizi Group by Thomson *et al.* (1986) and later lowered to member status within the Spatsizi Formation by Evenchick and Thorkelson (2005). In the regions surrounding the Bowser Basin, correlative rocks are attributed to the informal name of pyjama beds because of the alternation of pale orange and black weathered layers that give them a striped appearance (Fig 6). Ammonite faunal assemblages at the base of the succession indicate an early Bajocian age (Thomson *et al.*, 1986). In the measured sections, the siliceous shales are generally blocky and indurated. The siliceous mudstone contains abundant radiolarian microfossils, which suggest deposition from suspension in a low energy environment.

Even though Thomson *et al.* (1986) considered the volcanic ash to be the primary source of silica in the rocks, observations of the pyjama beds in thin sections suggest that introduction of silica content to the system via remobilization of silica from radiolarian tests was significant. Recessive fine-grained tuff bands vary from 1 to 5 cm in thickness and attest to distal volcanism. Chlorite and plagioclase are the most common mineral phases in the crystal tuffs. The rarity of trace fossils along with high organic content can probably be related to oxygen-deficient conditions in a deeper water environment. However, the occurrence of thin to medium-bedded limestone in the section signifies that sediments accumulated above the carbonate compensation depth.

On the eastern edge of Oweegeee Dome, a 270 m succession with sedimentary characteristics similar to the Quock Member was observed above andesitic and volcanoclastic rocks of the lower Hazelton Group. There, the lower and upper Hazelton Group are separated by an angular unconformity (Greig, 1991; Waldron *et al.*, 2006). In this area of the basin, the thinly interbedded siliceous radiolarian mudstones and ash tuffs have been classified as the Troy Ridge facies of the Salmon River Formation (Anderson, 1993; Greig, 1991). The pyjama beds, identified around Oweegeee Dome, are thinly interbedded with occasional wavy parallel laminations and convolute slump structures. Carbonate content is common in the recessive coarser tuffaceous bands whereas the mudstone is blockier and completely cemented by silica. Well-preserved radiolarian samples in black siliceous mudstone have yielded an early Bajocian to early Bathonian age for the upper part of the section, which seems slightly older than the Bathonian to Callovian age obtained in the same area by Evenchick *et al.* (2001). The preliminary results are presented in Table 1. Near the top of the section, the tuff bands

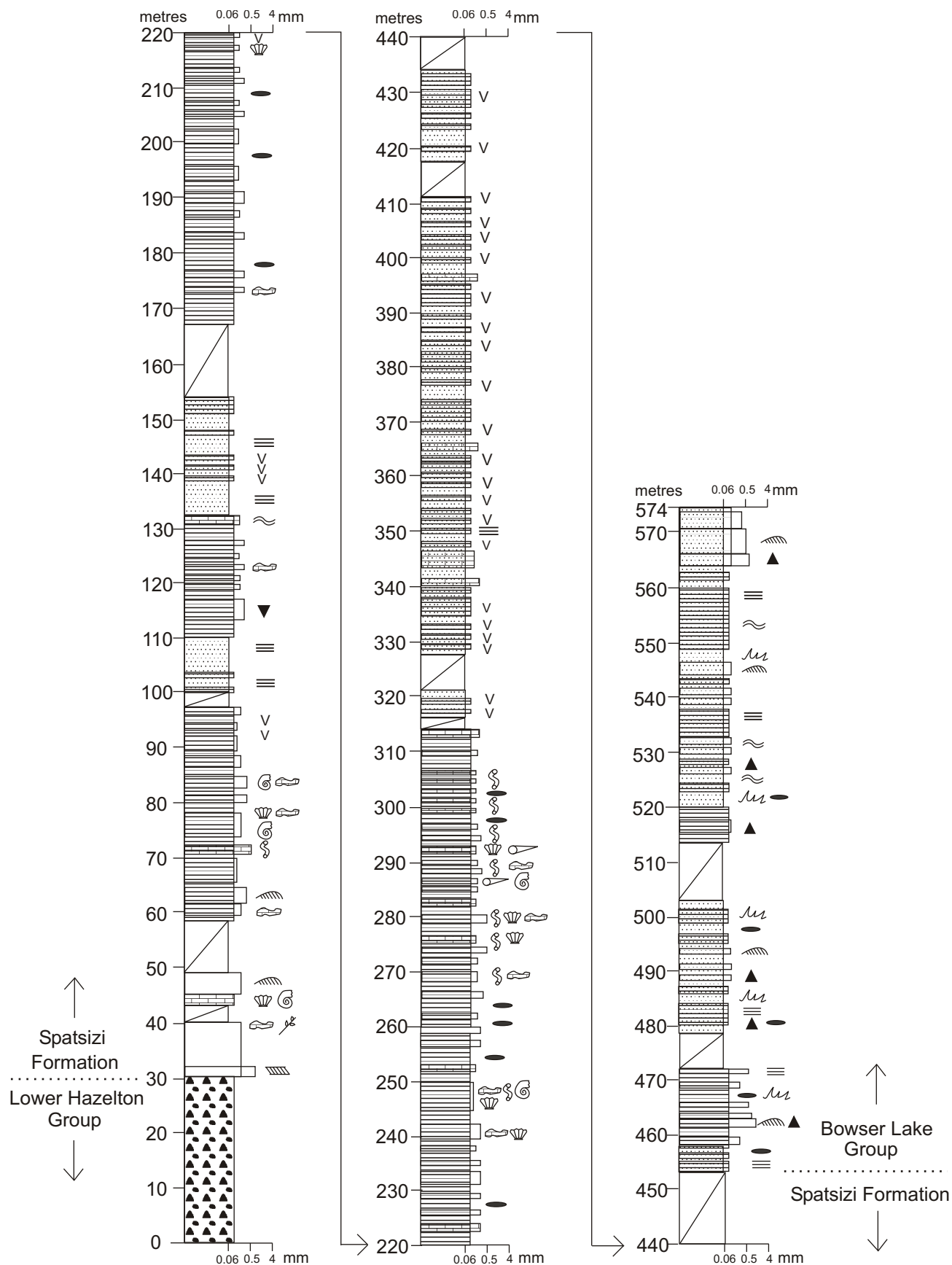


Figure 5. Detailed stratigraphic section showing uppermost volcanic unit of the lower Hazelton Group, marine sedimentary rocks of the Spatsizi Formation and the contact with the overlying Bowser Lake Group, Mount Will area, BC. See Figure 2 for legend.

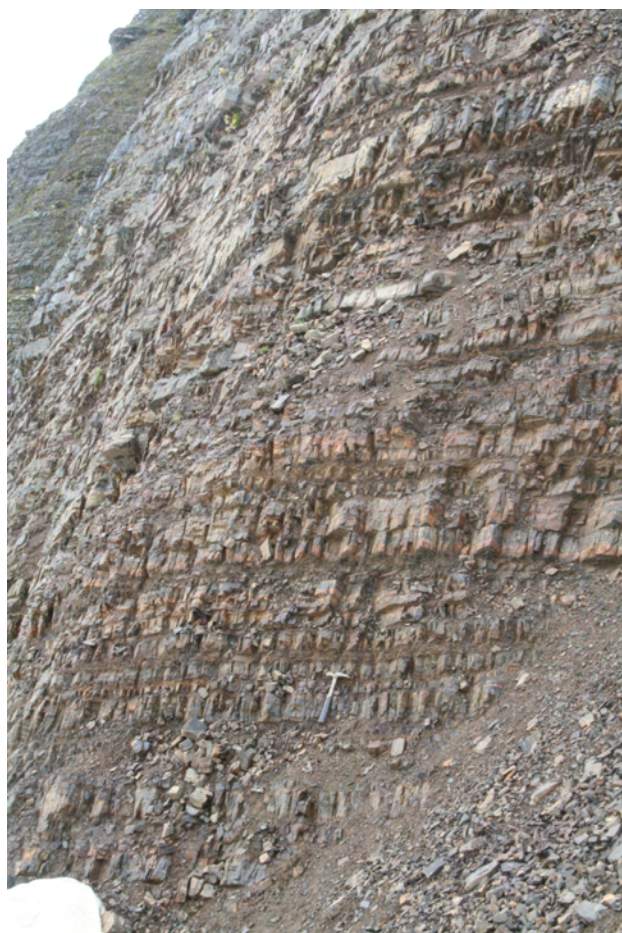


Figure 6. Thinly interbedded resistant siliceous mudstone and recessive tuffaceous siltstone (pyjama beds) of the Quock Member, Mount Will area, BC. See hammer for scale.

become thinner and are less abundant. The transition into the overlying turbidites of the Bowser Lake Group appears concordant and gradational.

STRATIGRAPHY OF THE BOWSER LAKE GROUP

The basal unit of the Bowser Lake Group in the vicinity of Mount Will consists of thinly laminated very fine

grained sandstone with pale orange weathering and dark grey siltstone with shale intervals. It was classified as the Todagin assemblage of the Bowser Lake Group by Evenchick and Thorkelson (2005) and is interpreted to represent a prodelta slope setting. Pebble to cobble chert-rich conglomerate units are also found in the prodelta slope lithofacies assemblage. The thickness of these coarse-grained packages is highly variable and can reach up to 50 m. They are characterized by sharp erosive bases that show scouring into underlying fine-grained rocks. Measurements on flutes and groove casts indicate paleocurrent directions towards the southeast. Near Todagin Mountain, Green (1991) interpreted similar conglomerate bodies as channelized deposits in incised canyons and gullies in a slope environment. Overbank sand deposits with trough crossbedding and planar crosslamination are also common on the edge of the main channel axes. Centimetre-scale calcareous concretions are abundant in the fine-grained rock units and are usually associated with diagenetic pyrite. Differential compaction indicates concretionary growth early in the diagenetic processes when pores were still filled with water. Soft-sediment deformation features such as load structures, sedimentary dikes and syndepositional folds and faults are common features in the Todagin assemblage. These are interpreted to represent high fluid pressure combined with rapid sediment accumulation rates that created instability in the sediment pile and resulted in slope failure.

Sedimentary facies at the base of the Bowser Lake Group near Oweege Dome are slightly different from those observed in the northern part of the basin. Thick beds of massive well-sorted sandstone interbedded with calcareous fissile shales are found above the pyjama beds. The impressive lateral extent of the sandbodies along with graded beds and partial Bouma sequences suggest that these sediments were deposited as deepwater turbidites in submarine-fan complexes. Sharp erosive bases, convolute laminations and flame structures are common. The absence of bioturbation features and shelly fossils is interpreted to represent a hostile environment where sedimentation influx was too high to sustain biogenic activity on the basin floor.

These turbidite deposits, assigned to the Ritchie-Alger assemblage by Evenchick *et al.* (2006), rapidly grade up into shallower sedimentary facies of the Muskaboo Creek assemblage (Evenchick *et al.*, 2006). An uninterrupted stratigraphic section displaying multiple sequences was measured along an east-trending ridge east of Oweege

TABLE 1. SUMMARY OF THE RADIOLARIAN FAUNA IDENTIFIED IN PYJAMA BEDS EAST OF OWEEGEE DOME. SAMPLE INDICATED AN EARLY BAJOCIAN TO EARLY BATHONIAN AGE NEAR THE TOP OF THE UNIT (BASED ON ZONATIONS FROM CARTER *ET AL.* [1988] AND BAUMGARTNER *ET AL.* [1995]).

Sample KA031A	Sample KA032B
<i>Emiluvia chica</i> s.l. Foreman	<i>Podobursa</i> sp.
<i>Higumastra</i> sp.	<i>Paronaella</i> sp.
<i>Hsuum</i> sp.	<i>Parvicingula</i> sp. D Carter
<i>Orbiculiforma</i> sp.	<i>Orbiculiforma</i> sp.
<i>Napora</i> sp.	
<i>Parvicingula</i> sp. cf. <i>dhimenaensis</i> s.l. Baumgartner	
<i>Parvicingula</i> sp. cf. <i>schoolhousensis</i> gr. Pessagno & Whalen	
<i>Perispyridium</i> sp.	
<i>Tetratrabs izeensis</i> Yeh	

Dome (Fig 7, 8). Alternating packages of fine to medium-grained sandstone and silty shale are interpreted to represent fluctuations of relative sea-level, this being the primary control on the mode of sedimentation. Coarsening-upward cycles in calcareous coquina beds found at the bases of the sandy intervals contain mud rip-up clasts derived from each underlying shale unit. The cyclicity of these deposits suggests that a shelf environment was periodically subjected to storm-induced high energy conditions that transported skeletal material away from the place of growth. The sandstone intervals vary from 35 to 100 m in thickness and contain abundant trace fossils, bivalves and ripple crosslaminations. They are capped by maximum flooding surfaces above which are laminated shale and siltstone, which accumulated from suspension during relative highstands.

DISCUSSION

Units of the lower Hazelton Group observed in all the study areas seem to indicate that these rocks mostly accumulated in an oxidizing, subaerial environment. The transition from the lower to the upper Hazelton is abrupt and marked by a regional erosional surface. Above this unconformity, the deposition style of the Spatsizi Formation and equivalents is quite variable on the basin scale, depending on the paleotopography and the distance from active volcanic centres. In volcano-sedimentary successions, the ratio of volcanoclastic rocks to marine sedimentary rocks is a function of proximity to the eruptive centre. For instance, the Pliensbachian to Bajocian fine-grained sedimentary rocks at Todagin Mountain are interbedded with thick intervals of marine pillow basalt and hyaloclastite, whereas calcareous fossiliferous sandstone and siltstone of the same age in the Mount Will district show only minor volcanic input.

Basal sedimentary rocks of the Spatsizi Formation are heavily bioturbated, fossil rich and contain multiple sedimentary structures such as symmetrical wave ripples and planar crosslaminations, which attest to a shallow marine clastic-shelf environment. Upsection, the percentage of fine-grained sedimentary rocks increases gradually and shelly fossils are rare. This is interpreted to represent a progressively deepening environment where clastic sediments accumulated via turbiditic input. Laminated siliceous mudstones and calcareous tuffaceous siltstones (pyjama beds) were found in every measured stratigraphic section. Detailed mapping conducted in this study revealed strong similarities between rocks of the Troy Ridge facies and the pyjama beds of the Quock Member, as noted in previous work (Greig, 1991; Anderson, 1993; Ferri and Boddy,

2005). In the sections at Oweege Dome and Mount Will, calcareous beds are present throughout the unit and the proportion of rust-coloured volcanic ash gradually decreases near the top. Furthermore, radiolarian samples extracted from black siliceous mudstone suggest a early Bajocian to early Bathonian age for the upper part of the Oweege section (Table 1). These results are consistent with previous ages obtained from ammonites by Thomson *et al.* (1986) for the Quock Member in the Joan Lake area. The transition from the pyjama beds of the upper Hazelton Group to the overlying clastic deepwater sedimentary rocks of the Bowser Lake Group is subtle and covered in most sections. The absence of vein material in the float and consistent bedding measurements on either side of the contact indicate that the latter is likely to be concordant with no structural offset.

An unusually thin succession of deepwater sedimentary rocks was observed around Oweege Dome. Sand-rich turbidites of the Ritchie-Alger assemblage rapidly grade up into shallow-marine clastic-shelf deposits of the Muskaboo Creek assemblage (Evenchick *et al.*, 2006). This is interpreted to be the result of deposition over an uneven topography, where Oweege Dome constituted a structural high in the Bowser Basin. The abundance of soft-sediment deformation, erosive bases and sedimentary dikes in the Todagin and Ritchie-Alger assemblages are attributed to high sedimentation rates in a deepwater environment. This marks a drastic change from the underlying pyjama bed units where coarse clastic input was almost nonexistent.

The occurrence of organic radiolarian mudstones above structural highs such as Oweege Dome suggests that these potential source rocks have been deposited and preserved throughout the entire basin. Thick and laterally extensive sandbodies deposited on the edge of the Middle Jurassic clastic shelf during relative lowstands might constitute excellent reservoir rocks for petroleum exploration.

Based on the observations made in the measured stratigraphic sections, it appears that continuous sedimentation took place in a tectonically active, shallow marine basin on Stikinia from the early Pliensbachian to early Bajocian. Depending on the relative position of active volcanoes, the sediments incorporated more or less volcanic input and were deposited along with subaqueous and subaerial bimodal volcanic flows. Rapid lateral facies change and the variability of sediment thickness in the upper Hazelton Group are attributed to active normal faulting during an extensional back-arc stage that isolated multiple sub-basins. A significant decrease of volcanism during the Aalenian and Bajocian is attributed to the cessation of subduction of oceanic crust under Stikinia and to the final accretion of volcanic-arc rocks with the Cache Creek Terrane. Following the end of magmatism, thermal relax-

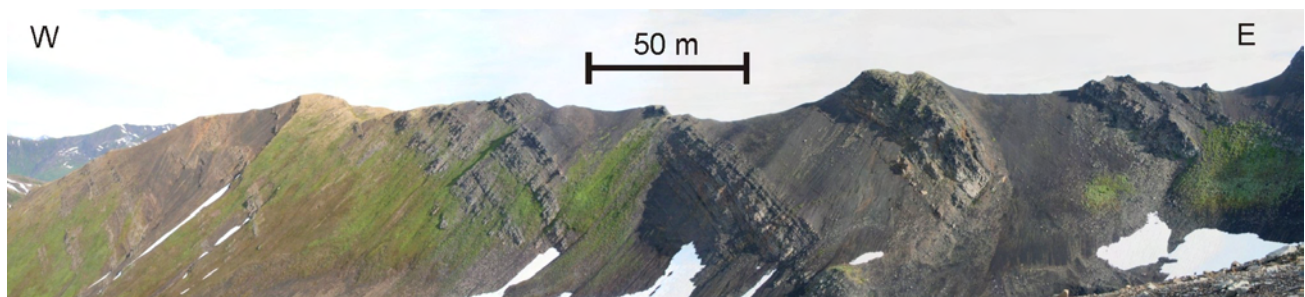


Figure 7. Panorama view of the detailed measured stratigraphic section west of Oweege Dome, BC.

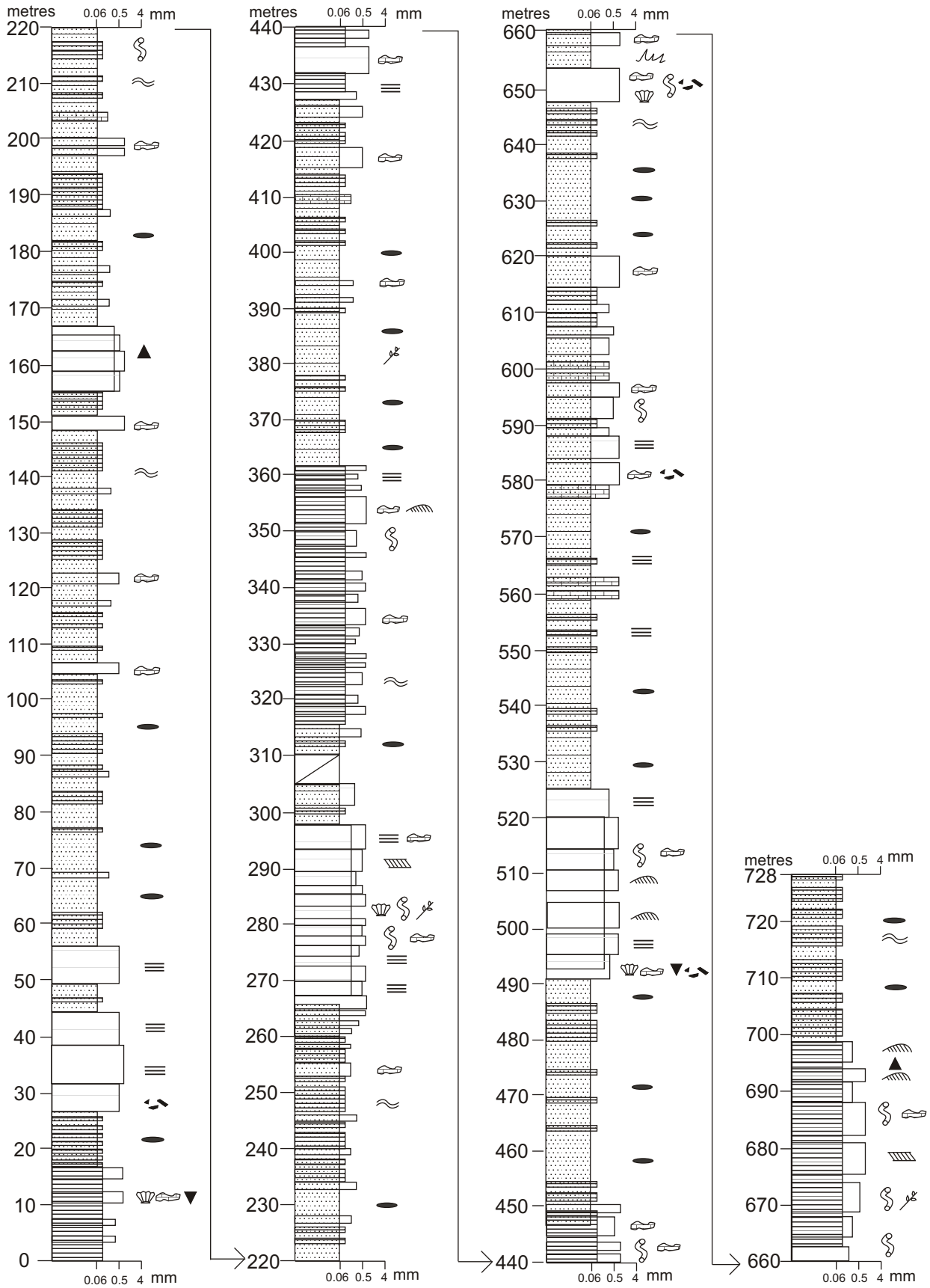


Figure 8. Detailed stratigraphic section showing alternating sandstone and shale intervals of the Muskaboo Creek assemblage of the Bowser Lake Group, BC. See Figure 2 for legend.

ation of the crust combined with eustatic sea-level rise generated new accommodation space in the basin where condensed sections of fine-grained deepwater sediments were deposited. Obduction of the Cache Creek Terrane along the King Salmon thrust fault (Evenchick and Thorkelson, 2005) generated a new source of chert-rich sediments that were shed in the basin via turbiditic input and fan-deltas corresponding to the deposition of the Bowser Lake Group.

ACKNOWLEDGMENTS

The authors would like to thank Geoscience BC for supporting this research through a grant to the Geological Survey of Canada. Additional field expenses were supported by Natural Sciences and Engineering Research Council of Canada (NSERC) Discovery Grant A8508 held by J.W.F. Waldron. Helicopter support was provided by Prism and Pacific Western Helicopters. Heidi Tomes and Cordell Bloomberg are thanked for their remarkable work in the field. Fieldwork in the Gladys Ecological Reserve was made possible by BC Parks through a Research & Education Park Use Permit. Sabina Silver and Eskay Creek Mine were hospitable in allowing us to use their site. Murray Gingras provided helpful comments on an earlier version of the manuscript.

REFERENCES

- Anderson, R.G. (1993): A Mesozoic stratigraphic and plutonic framework for northwestern Stikinia (Iskut River area), northwestern British Columbia, Canada; *in* Mesozoic Paleogeography of the Western United States-II, Dunne, G. and McDougall, K., Editors, *Society of Economic Paleontologists and Mineralogists*, Pacific Section, Volume 71, pages 477–494.
- Ash, C.H., Macdonald, R.W.J. and Friedman, R.M. (1997): Stratigraphy of the Tatogga Lake area northwestern British Columbia (104H/12&13, 104G/9&16); *in* Geological Fieldwork 1996, Lefebvre, D.V., McMillan W.J. and McArthur, J.G., Editors, *BC Ministry of Energy, Mines and Petroleum Resources*, Report 1997-1, pages 283–290.
- Baumgartner, P.O., Bartolini, A., Carter, E.S., Conti, M., Cortese, G., Danelian, T., De Wever, P., Dumitrica, P., Dumitrica-Jud, R., Gorican, S., Guex, J., Hull, D.M., Kito, N., Marcucci, M., Matsuoka, A., Murchev, B., O'Dogherty, L., Savary, J., Vishnevskaya, V., Widz, D., and Yao, A. (1995): Middle Jurassic to Early Cretaceous radiolarian biochronology of Tethys based on unitary associations; *in* Middle Jurassic to Lower Cretaceous Radiolaria of Tethys: Occurrences, Systematics, Biochronology, Baumgartner, P.O., *et al.*, Editors, *Mémoires de Géologie*, Lausanne, Volume 23, pages 1013–1043.
- Carter, E.S., Cameron, B.E.B. and Smith, P.L. (1988): Lower and Middle Jurassic radiolarian biostratigraphy and systematic paleontology, Queen Charlotte Islands, British Columbia; *Geological Survey of Canada*, Bulletin 386, 109 pages.
- Evenchick, C.A. and Green, G.M. (2004): Geology, Kluea Lake, British Columbia, NTS 104H/12; *Geological Survey of Canada*, "A" Series Map, 2028A, scale 1:50 000.
- Evenchick, C.A., Hayes, M.C., Buddell, K.A. and Osadetz, K.G. (2002): Vitrinite and bitumen reflectance data and preliminary organic maturity model for the northern two-thirds of the Bowser and Sustut basins, north-central British Columbia; *Geological Survey of Canada*, Open File 4343.
- Evenchick, C.A., Mustard, P.S., McMechan, M.E., Ferri, F., Ritcey, D.H. and Smith, G.T. (2006): Compilation of geology of Bowser and Sustut basins draped on shaded relief map, north-central British Columbia; *Geological Survey of Canada*, Open File 5313, scale 1:500 000.
- Evenchick, C.A., Poulton, T.P., Tipper, H.W. and Braidek, I. (2001): Fossils and facies analysis of the northern two-thirds of the Bowser Basin, British Columbia; *Geological Survey of Canada*, Open File 3956, 103 pages.
- Evenchick, C.A. and Thorkelson, D.J. (2005): Geology of the Spatsizi River map area, north-central British Columbia; *Geological Survey of Canada*, Bulletin 577, 276 pages.
- Ferri, F. and Boddy, M. (2005): Geochemistry of Early to Middle Jurassic organic-rich shales, intermontane basins, British Columbia; *in* Summary of Activities 2005, *BC Ministry of Energy, Mines and Petroleum Resources*, URL <<http://www.em.gov.bc.ca/subwebs/oilandgas/pub/reports.htm>>, pages 132–151.
- Friedman, R.M. and Ash, C.H. (1997): U-Pb age of intrusions related to porphyry Cu-Au mineralization in the Tatogga Lake area, northwestern British Columbia (104H/12NW, 104G/9NE); *in* Geological Fieldwork 1996, Lefebvre, D.V., McMillan W.J. and McArthur, J.G., Editors, *BC Ministry of Energy, Mines and Petroleum Resources*, Report 1997-1, pages 291–297.
- Green, G.M. (1991): Detailed sedimentology of the Bowser Lake Group, northern Bowser Basin, British Columbia; *Geological Survey of Canada*, Current Research Paper 91-1A, pages 187–195.
- Greig, C.J. (1991): Stratigraphic and structural relations along the west-central margin of the Bowser Basin, Oweege and Kinskuch areas, northwestern British Columbia; *Geological Survey of Canada*, Current Research Paper 91-1A, pages 197–205.
- Greig, C.J. and Gehrels, G.E. (1995): U-Pb zircon geochronology of Lower Jurassic and Paleozoic Stikinian strata and Tertiary intrusions, northwestern British Columbia; *Canadian Journal of Earth Sciences*, Volume 32, pages 1155–1171.
- Osadetz, K.G., Evenchick, C.A., Ferri, F., Stasiuk, L.D. and Wilson, N.S.F. (2003): Indications for effective petroleum systems in the Bowser and Sustut basins, north-central British Columbia; *in* Geological Fieldwork 2002, *BC Ministry of Energy, Mines and Petroleum Resources*, Paper 2003-1, pages 257–264.
- Palfy, J., Mortensen, J.K., Smith, P.L., Friedman, R.M., McNicoll, V.J. and Villeneuve, M. (2000): New U-Pb zircon ages integrated with ammonite biochronology from the Jurassic of the Canadian Cordillera; *Canadian Journal of Earth Sciences*, Volume 37, pages 549–567.
- Stasiuk, L.D., Evenchick, C.A., Osadetz, K.G., Ferri, F., Ritcey, D., Mustard, P.S. and McMechan, M.E. (2005): Regional thermal maturation and petroleum stage assessment using vitrinite reflectance, Bowser and Sustut basins, north-central British Columbia; *Geological Survey of Canada*, Open File 4945, 13 pages.
- Thomson, R.C., Smith, P.L. and Tipper, H.W. (1986): Lower to Middle Jurassic (Pliensbachian to Bajocian) stratigraphy of the northern Spatsizi area, north-central British Columbia; *Canadian Journal of Earth Sciences*, Volume 23, pages 1963–1973.
- Thorkelson, D.J. (1992): Volcanic and tectonic evolution of the Hazelton Group in Spatsizi River (104H) map area, north-central British Columbia; unpublished PhD thesis, *Carleton University*, 361 pages.
- Waldron, J.W.F., Gagnon, J.-F., Loogman, W. and Evenchick, C.A. (2006): Initiation and deformation of the Jurassic-Cretaceous Bowser Basin: implications for hydrocarbon exploration; *in* Geological Fieldwork 2005, *BC Ministry of Energy, Mines and Petroleum Resources*, Paper 2006-1 and *Geoscience BC*, Paper 2006-1, pages 349–360.

Subaqueous Channel-Confined Volcanism within the Chilcotin Group, Bull Canyon Provincial Park (NTS 093B/03), South-Central British Columbia¹

by S. Gordee², G. Andrews³, K.A. Simpson⁴ and J.K. Russell³

KEYWORDS: volcanology, basalt, lava, Chilcotin, volcanic stratigraphy, volcanic facies, hyaloclastite, subaqueous, subaerial, paleodrainage

stratigraphic succession for eruption style, distribution and thickness of the CG and pre-CG paleotopography.

INTRODUCTION

The Chilcotin Group (CG) is situated in the Interior Plateau of south-central British Columbia and overlies an area of ~36 500 km² (Fig 1; NTS map sheets 092O, P and 093A, B, C, F, G, J and K). The CG mainly comprises flat to shallowly dipping massive to columnar-jointed, olivine-phyric basalt lava with lesser volumes of pillow basalt and hyaloclastite (Mathews, 1989). The basalt ranges in age from 25 to 3 Ma and is broadly coeval with the voluminous Columbia River flood basalt of Oregon and Washington (*e.g.*, Hooper and Conrey, 1989). The CG basalt is typically 5 to <200 m thick and estimates of the total volume are as high as 3 500 km³; this volume would make the CG a medium-sized igneous province (Seth, *in press*). Previous studies have concentrated on reconnaissance-scale fieldwork and geochemical studies (*e.g.*, Mathews, 1964, 1989; Bevier, 1983; Dostal *et al.*, 1996; Anderson *et al.*, 2001).

The work presented here is part of a larger research program for field mapping of the volcanic lithofacies and thicknesses of the CG basalt. The goal of the larger project is to create a 3-D model for facies and thickness variations across the Chilcotin volcanic province that can be used to delineate areas where the CG is thin and exploration drilling for 'blind' metallic deposits becomes feasible. As part of that research program, reports are done on field mapping in and adjacent to Bull Canyon Provincial Park (Fig 1, 2). At this locality, 120 m of CG basalt is exposed, including deposits representing subaqueous and subaerial eruption environments. The intention of this work is to 1) describe and interpret the volcanic stratigraphy and lithofacies exposed at this location; 2) introduce this stratigraphic section as a type section (Bull Canyon-style) for comparing against other sections of CG (*cf.* Andrews and Russell, 2007; Farrell *et al.*, 2007); and 3) explore the implications of this

GEOLOGICAL SETTING AND LOCATION OF THE STUDY AREA

The study area is located in Bull Canyon, approximately 8 km west of Alexis Creek along the Bella Coola – Chilcotin Highway 20 (Alexis Creek map sheet 093B/3; Fig 1, 2). The area was most recently mapped and described by Tipper (1959). In general, the bedrock geology of the south-central Quesnel map area consists of accreted Mesozoic arc terranes (Stikine and Cadwallader terranes; Wheeler and McFeely, 1991), unconformably overlain by early Cenozoic felsic volcanoclastic rocks (*e.g.*, Eocene Kamloops Group), which are themselves unconformably overlain by flat-laying plateau basalt of the Neogene CG.

Lavas of the CG form a series of laterally semicontinuous cliffs along the northern margin of the Chilcotin River where it has incised through the Chilcotin Plateau, from Hanceville (~15 km southeast of Alexis Creek) to the confluence of the Chilcotin and Chilanko Rivers (~20 km west of Alexis Creek). In general, the bluffs comprise basalt lava that dips gently (<5°) to the east and southeast and are at least 15 to 20 m thick. Thicknesses are a minimum because the bases of the cliffs are commonly buried by talus and the upper surfaces have been glaciated and are buried by till. Substantially thicker sections (<150 m) occur along the Chilcotin River valley, where basaltic lava overlies or is interleaved with pillow breccia and hyaloclastite deposits (*e.g.*, Hanceville, Anahim Flats Indian Reserve and Bull Canyon; Andrews and Russell, 2007).

In the area between Alexis Creek and Bull Canyon, basaltic rocks of the CG bury an uneven paleotopographic surface cut into Early Cenozoic (possibly Eocene Kamloops Group) felsic volcanoclastic rocks. The older felsic volcanoclastic rocks rest unconformably on metasedimentary basement. The Bull Canyon is formed where the Chilcotin River is diverted south and east around a paleotopographic high comprising more resistant basement rocks. The diversion produces a 90° bend in the river channel and provides a three-dimensional exposure through the entire succession of CG basalt exposed here (Fig 2, 3, 4). The following section presents a series of stratigraphic sections from the Bull Canyon area based on mapping completed north of the Chilcotin River during the summer of 2006.

¹ Geoscience BC contribution GBC034

² Centre for Ore Deposits and Exploration Studies, University of Tasmania, Hobart, Australia

³ Volcanology and Petrology Laboratory, Earth and Ocean Sciences, University of British Columbia, Vancouver, BC

⁴ Geological Survey of Canada, Vancouver, BC

This publication is also available, free of charge, as colour digital files in Adobe Acrobat® PDF format from the BC Ministry of Energy, Mines and Petroleum Resources website at http://www.em.gov.bc.ca/Mining/GeolSurv/Publications/catalog/cat_fldwk.htm

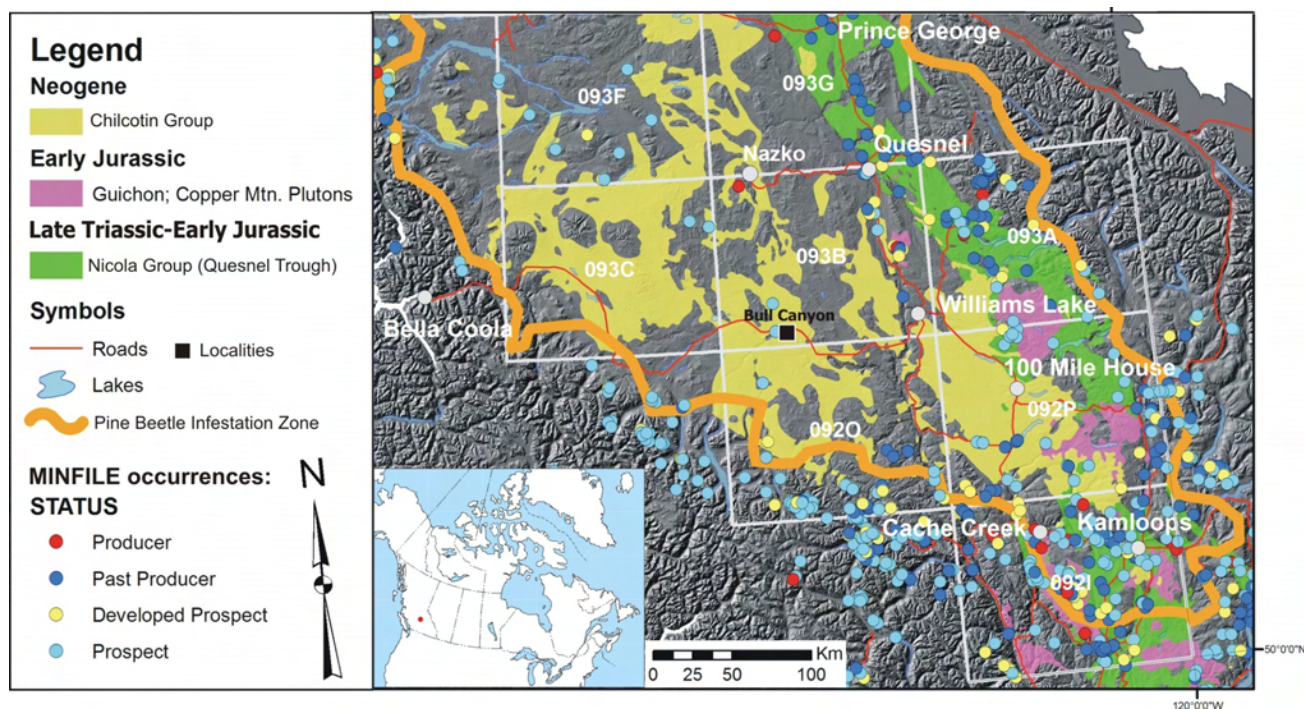


Figure 1. Shaded-relief digital elevation model showing the location of the study area (Bull Canyon) within the Quesnel (093B) 1:250 000 NTS map sheet in west-central BC. The map also shows 1) distributions of geological units (Chilcotin Group basalt and plutonic and meta-volcanic rocks of the Quesnel Trough); 2) areal limits of mountain pine beetle infestation; and 3) distributions of mineral occurrences, prospects and mines (MINFILE, 2006). Inset shows the location of the Quesnel map sheet.

LITHOFACIES DESCRIPTIONS, DISTRIBUTIONS AND ASSOCIATIONS

The following lithofacies descriptions are specific to the units illustrated in Figure 3 and to the interpreted facies associations summarized in Figures 4 and 5. The volcanic facies exposed in Bull Canyon have been organized into the following two principal mappable units (Fig 4): 1) a lower pillow-dominated basalt that is the type example of the Bull Canyon-style lithofacies association and 2) an upper co-

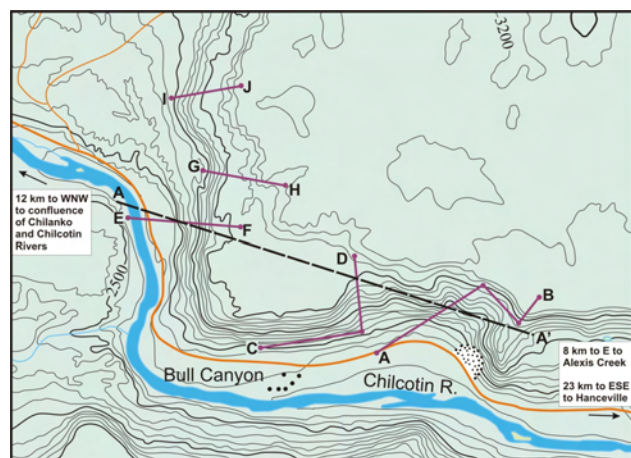


Figure 2. Topography (elevations in feet) of the Bull Canyon area showing, the distribution of exposures of CG basalt within Bull Canyon (black circles), locations and orientations of stratigraphic sections used for graphic logs and cross-sections and the locations of geographic features discussed in the text.

herent basalt. Results of detailed graphic logs are summarized in the schematic stratigraphic columns shown in Figure 5.

Bull Canyon-Type Lithofacies: Pillow-Dominated Basalt (unit pB)

The pillow-dominated basalt unit is best exposed along the tallest and steepest southwest-facing wall of the Bull Canyon massif (Fig 3), where it unconformably overlies older felsic volcanoclastic rocks that may belong to the Kamloops Group. Unit pB constitutes much of the cliff, whereas exposures to the north and east are thinner and less continuous. The pB unit contains several subaqueous volcanic and volcanoclastic lithofacies (Fig 5) including, from most to least volumetrically abundant 1) close-packed basaltic pillow facies (cpB), 2) basaltic pillow-fragment breccia and basalt breccia facies (bpB), 3) hyaloclastite (HpB), and 4) a peperitic facies (PpB).

CLOSE-PACKED BASALTIC PILLOW FACIES (cpB)

This facies is, volumetrically, the most abundant in the pB unit and consists of repeated successions of close-packed basaltic pillows (Fig 6a, 6b). Individual pillowed facies are lensoid in shape, range from about 2 to 10 m in thickness, are apparently thin and become increasingly discontinuous at progressively higher stratigraphic intervals of the pB unit. The pillows are spherical to elongate where sections along the main Bull Canyon cliff face are oriented roughly parallel to the elongation direction of interconnected lava lobes (*cf.* McPhie *et al.*, 1993). The pillows are moulded around mutual contacts and display a wide variety

of textures common to pillowed lava formations (Fig 6b, 6c), including (but not limited to) multiple rind structures, spreading cracks, gas cavities, concentric vesicle trains and radial pipe vesicles. Prismatic joints are common. Interpillow sediment comprises a mixture of massive to thinly-laminated mudstone or pillow fragments.

Several localities along the main Bull Canyon cliff face display basaltic pillows surrounding more massive zones of basaltic lava with radial columnar jointing (Fig 3, 6a). This association is possible evidence of the propagation of lava tubes within the cpB facies (McPhie *et al.*, 1993). Highly vesicular domains within individual pillows and abundant multiple rind structures of this facies suggest that basaltic lava was deposited in very shallow water (*e.g.*, Kano, 1991).



Figure 3. Field photograph showing a panorama of the west-southwest face of the main Bull Canyon massif, north of Highway 20. The bluff is approximately 500 m high.

BASALTIC PILLOW FRAGMENT BRECCIA AND BASALT BRECCIA FACIES (bpB)

The cpB facies in the main Bull Canyon section grades laterally over ≤ 50 m into pillow breccia and reworked pillow basalt breccia (bpB), respectively (Fig 6c, 6e). Individual exposures of these facies are thin (< 3 m) and lensoid in shape. The components of the bpB facies are identical to the interpillow fragmental matrix found in the close-packed pillow facies, except that the bpB facies becomes progressively and proportionally enriched in the matrix relative to coherent pillows.

The bpB facies contains a small proportion (1–2%) of *in situ* pillows, isolated pillows and pillow fragments, presumably derived from the cpB facies. The bpB facies also contains ‘rag-shaped’ vesicular clasts of basalt that have large gas cavities. These clasts possibly formed on the margins of a subaqueous, pillow-forming lava. Poorly formed pillows and lava rags could have been torn from its margins and fed immediately into a rapidly moving and depositing current. The basalt breccia facies is massive to crudely medium to thickly bedded and crudely normally graded. The facies is monomictic, clast supported, lacks a fine matrix and clasts are blocky and angular. These characteristics, together with the association with the aforementioned facies, support the interpretation that this facies derives from a single source: the progressive disintegration of basaltic pillows in a subaqueous environment.

HYALOCLASTITE FACIES (HpB)

Discontinuous lenses of hyaloclastite facies are very common in association with successions of pillow basalt. Apparently regular, columnar-jointed lava, upon closer inspection, comprises a clast-supported, matrix-free, jigsaw-fit, monomict basalt volcanoclastic deposit. Clasts range from ~ 2 mm to ~ 20 mm in size and have curvilinear margins. A significant proportion of angular basalt clasts within the basalt breccia facies (bpB) probably derive from this facies.

PEPERITE FACIES (PpB)

The peperitic facies (PpB) is well developed within the pillow basalt unit in horizons where there is significant

mudstone. The PpB facies consists of jigsaw-fit, monomict basalt clasts with curvilinear margins and an evenly distributed mudstone matrix (Fig 6d). Some interstitial mudstone is hornfelsed. The PpB facies occurs at the base of single basalt units and is interpreted to have formed where basaltic lava flows interacted and were quench-fragmented by wet, unconsolidated mud overlying earlier flows. This facies commonly grades vertically and laterally into columnar-jointed basalt or close-packed basalt pillows.

Coherent Basalt (unit cB)

The uppermost mappable unit comprises a relatively thin (≤ 30 m) and laterally continuous aphyric basalt lava (cB) that features well-developed, widely-spaced columnar joints. The cB unit outcrops along the northern margin of the Chilcotin River valley and is best exposed in the areas north and east of the main Bull Canyon locality. This unit is the equivalent of the Chasm-style lithofacies (Farrell *et al.*, 2007) typical of subaerial lavas throughout the CG (Andrews and Russell, 2007).

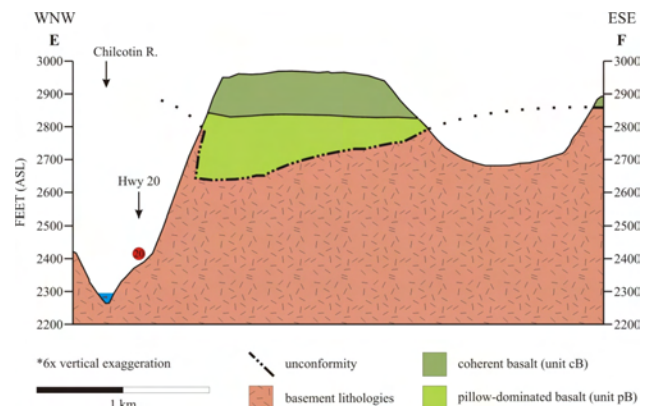


Figure 4. Cross-section illustrating the general stratigraphic relationships between Chilcotin Group basalt and the basement rocks (*e.g.*, Kamloops Group (?)) in the Bull Canyon study area. The location of the cross-section is shown as E-F in Figure 2. The cross-section orientation was chosen to emphasize the relief on the contact due to the original paleochannel filled in by Chilcotin Group basalt.

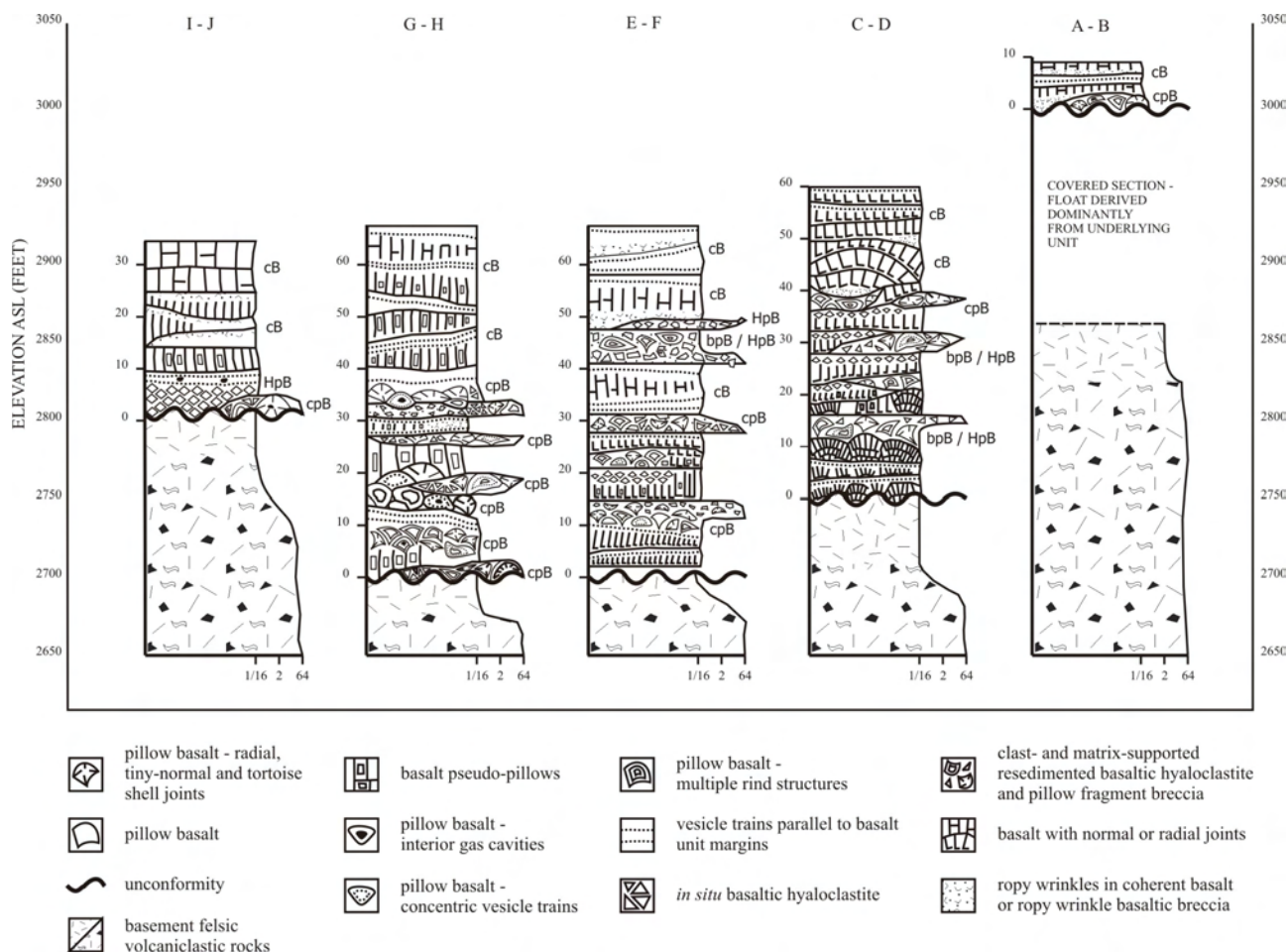


Figure 5. Stratigraphic sections of Chilcotin Basalt sequences summarizing graphic logs of the section exposed in Bull Canyon, west-central BC. Locations of stratigraphic sections are shown in Figure 2. The upper limit of each stratigraphic column corresponds to the highest elevation of continuous rock exposure but does not necessarily represent the top of the stratigraphic section, which is locally found at an elevation of 3200 ft (975 m).

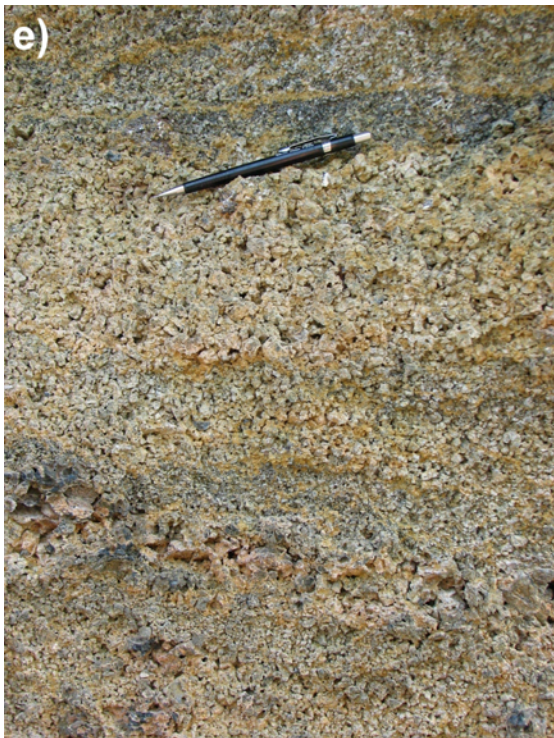
DISCUSSION

Careful examination of the specific elevations of the basal unconformity between the Chilcotin Group and underlying basement felsic volcaniclastic rocks in Bull Canyon delineates an uneven paleotopographic surface (Fig 4, 5). More specifically, in three dimensions, the morphology of the feature is that of a paleochannel with a moderately steep north paleowall and very steep east paleowall. The southern wall of the paleochannel appears to coincide with the present-day southern bank of the Chilcotin River (Fig 4) and was apparently steep as well. The paleochannel is greater than 1 km wide and has an approximate northeast orientation (Fig 2, 4). Outside of the paleocanyon, outcrops of thin (<15 m thick), coherent basalt lava rest unconformably on top of pre-Chilcotin Group rocks. This relationship defines the margins of the paleochannel and constrains its width to ≤ 1.5 km.

The pillow basalt unit (pB) is concentrated within this paleodepression and is interpreted to record the emplacement of basalt lava flows into a locally deep and water-filled channel. The flows probably dammed up the local paleodrainage system, which periodically ruptured, generating the currents necessary to rapidly erode pillow basalt (cpB), peperite (PpB) and hyaloclastite (HpB) facies, and

transport and deposit material to form pillow fragments and basalt breccia facies (bpB). Widespread, thin, coherent and sheet-like lava flows (cB) of the upper basalt unit cap the infilled paleochannel, having apparently been emplaced over a relatively flat, subaerial paleotopographic surface.

Figure 6. Field photographs of volcanic units exposed in the walls of Bull Canyon: a) outcrop (~10 m across) comprising pillowed basalt (pB) underlain by lava tubes and overlain by massive basalt (cB); b) detailed image of closely packed pillows (cpB) featuring small-scale (centimetre) radial columnar joints and concentric structure parallel to the outer surface, defined by banding; hammer is 35 cm long; c) pillow fragment breccia (bpB) within a more coherent pillow basalt unit; grey domains are more-or-less intact basaltic pillows; orange-brown patches comprise clast-supported, monomict, basalt breccia resulting from the disintegration of basaltic pillows and pseudopillows (HpB); d) peperitic basalt breccia (PpB) formed by the entrainment of wet, poorly consolidated mudstone (grey) into massive to pillowed basalt; pencil is 15 cm long; e) moderately well-bedded, clast-supported, monomict, angular volcaniclastic deposit of palagonitized hyaloclastite; pencil is 15 cm long; f) vertical exposure (5 m) of massive basalt stratigraphically above pillow basalt and hyaloclastite (partly obscured by grass); the unit grades downward and laterally from coherent basalt with well-developed, regularly oriented columnar joints (right) into a less-coherent, irregular, fragmented breccia (left and centre).



CONCLUSIONS

Similar subaqueous-subaerial facies associations have been observed elsewhere in the Chilcotin and Fraser plateaus (Bevier, 1983; Mathews, 1989; Farrell *et al.*, 2007; Andrews and Russell, 2007): 1) along the Fraser Canyon from Soda Creek south to Canoe Creek (NTS 092O, 093A and 093B); 2) elsewhere along the Chilcotin, Chilco, Chilanko and Taseko Rivers (092N, 092O and 093B); 3) at Chasm Provincial Park (092P); and 4) along Upper Deadman Creek (092P). The authors consider the section exposed at Bull Canyon to be the type locality for the subaqueous Bull Canyon-style lithofacies in the CG. These initial observations, together with those in the Bull Canyon area, potentially have major implications for the emplacement of the CG: 1) subaqueous-subaerial facies transitions over a wide area indicate that the early stages of volcanism were strongly controlled by significant paleotopography; 2) within paleochannels, the CG is the thickest (≤ 150 m); away from paleochannels, however, the Chilcotin Group lavas are typically much thinner (≤ 20 m); 3) paleodrainages were long-lived, as suggested by the gradual transition from subaqueous to subaerial lithofacies; and 4) the lack of major paleosol horizons or erosion surfaces within many sections, including at Bull Canyon, suggests a short duration of volcanism in individual areas.

This study provides some of the primary evidence used by Andrews and Russell (2007), to support their assertion that the exploration potential of the Chilcotin Group should be re-evaluated in light of an improved understanding of the three-dimensional architecture of the CG. Specifically, the recognition of the Bull Canyon-style lithofacies highlights the importance of pre-CG paleotopography (paleochannels) on the overall architecture of the CG, and the thickness distribution that is key to interpreting geophysical exploration data.

ACKNOWLEDGMENTS

This research was funded by Geoscience BC for the project 'Mapping the Resource Potential Beneath the Chilcotin Flood Basalts (CFB): Volcanic Lithofacies Constraints on Geophysical Surveys'. We also acknowledge logistical support and assistance from the Geological Survey of Canada through the TGI-3 program and from the BC Geological Survey. We are especially appreciative of the assistance afforded by Stephen Williams (GSC Vancouver). We also wish to thank the BC Parks Service, the residents of Alexis Creek and the Tletinqox-tin First Nation. Bob Anderson provided a thoughtful and thorough review of this manuscript.

REFERENCES

- Anderson, R.G., Resnik, J., Russell, J.K., Woodsworth, G.J., Villeneuve, M.E. and Grainger, N.C. (2001): The Cheslatta Lake suite: Miocene mafic alkaline magmatism in central BC; *Canadian Journal of Earth Sciences*, volume 38, pages 697–717.
- Andrews, G.D.M. and Russell, J.K. (2007): Mineral exploration potential beneath the Chilcotin Group (NTS 092O, P; 093A, B, C, F, G, J, K), south-central British Columbia: preliminary insights from volcanic facies analysis; in *Geological Fieldwork 2006, BC Ministry of Energy, Mines and Petroleum Resources*, Paper 2007-1 and *Geoscience BC*, Report 2007-1, pages 229–238.
- Bevier, M.L. (1983): Regional stratigraphy and age of Chilcotin Group basalts, south-central BC; *Canadian Journal of Earth Sciences*, volume 20, pages 515–524.
- Dostal, J., Hamilton, T.S. and Church, B.N. (1996): The Chilcotin basalts, BC; *Neues Jahrbuch für Mineralogie*, volume 170, pages 207–229.
- Farrell, R.-E., Andrews, G.D.M., Anderson, B., Russell, J.K. (2007): Internal architecture of the Chilcotin Flood Basalts: Preliminary Results from the Bonaparte Lake area (NTS map sheet 92P). *Geological Survey of Canada Current Research*.
- Hooper, P.R. and Conrey, R.M. (1989): A model for the tectonic setting of the Columbia River Basalt eruptions; *Geological Society of America Special Paper* 239, pages 293–306.
- Kano, K. (1991): Miocene pillowed sills in the Shimane Peninsula, SW Japan; *Journal of Volcanology and Geothermal Research*, volume 48, pages 359–366.
- Mathews, W.H. (1964): K-Ar age determinations of Cenozoic volcanic rocks from BC; *Geological Society of America, Bulletin* 75, pages 465–468.
- Mathews, W.H. (1989): Neogene Chilcotin basalts in south-central BC; *Canadian Journal of Earth Sciences*, volume 26, pages 969–982.
- McPhie, J., Doyle, M. and Allen, R.L. (1993): Volcanic textures: a guide to the interpretation of textures in volcanic rocks; *University of Tasmania, Centre for Ore Deposit and Exploration Studies*, Hobart, Tasmania, 196 pages.
- MINFILE (2006): MINFILE BC mineral deposits database; *BC Ministry of Energy, Mines and Petroleum Resources*, URL <<http://www.em.gov.bc.ca/Mining/GeolSurv/Minfile/>> [November 2006].
- Seth, H.C. (*in press*): 'Large Igneous Provinces LIPs': definition and a hierarchical classification; *Journal of Volcanology and Geothermal Research*.
- Tipper, H.W. (1959): Geology of the Quesnel area, Cariboo District, BC; *Geological Survey of Canada*, Map 12-1959.
- Wheeler, J.O. and McFeeley, P. (1991): Tectonic assemblage map of the Canadian Cordillera and adjacent part of the United States of America; *Geological Survey of Canada*, Map 1712A, scale 1:2 000 000.

Geochronological and Regional Metallogenic Investigations in the Bralorne – Bridge River Mining District (Parts of NTS 092D, J, I, O), Southwestern British Columbia: Project Rationale¹

by C.J.R. Hart² and R.J. Goldfarb³

KEYWORDS: regional metallogeny, gold deposit models, geochronology, stable isotope geochemistry, orogenic gold, epizonal

INTRODUCTION

Orogenic gold deposits are characterized by structurally controlled, low-sulphide quartz veins that formed proximal to deep-crustal faults in greenschist-facies metamorphic terranes. These deposits, previously referred to as mesothermal, greenstone-hosted, shear-hosted and turbidite-hosted deposits, have a wide range of associated mineralization styles and associated metals that are dependent upon the depth (pressure) and temperature at which they formed in the crust, as well as the character of the hostrocks. Whereas the vertical extent of an orogenic lode gold deposit is known to span several kilometres at an individual mine, the range of possible formation depths for these deposits extends from the deep hypozonal (15–20 km) to the shallow epizonal (2–5 km) environments (Groves *et al.*, 1998). This recognition led to the development of the continuum model (Colvine, 1989; Groves, 1993; Groves *et al.*, 1998), whereby a diverse range of deposits is accommodated within a single deposit model, with features specific to their temperature and depth of formation. For example, a range of Alaskan orogenic gold deposits with variable mineralogical assemblages and structural styles (Goldfarb *et al.*, 1997, 2005) would include those of the hypozonal Alaska-Juneau deposit (15 km), mesothermal Chugach Terrane deposits (5–10 km) and epizonal Donlin Creek deposit (2–3 km), all of which are classified by the orogenic deposit model.

The Bralorne – Bridge River mineral district in southwestern British Columbia (Fig 1) hosts a variety of mineral deposit types and styles, with the Bralorne-Pioneer orogenic gold vein systems being historically the most significant in economic terms. These deposits generated more than 128 t (4.1 million oz) of gold from high-grade ores (19.9 g/t; 0.58 oz/T), between 1897 and 1971 (Church, 1996), making them the largest lode gold producers in BC.

However, although orogenic gold deposits almost always occur in districts with numerous significant producers, only a very small amount of gold (approximately 715 kg; 23,000 oz) was produced from other deposits (Wayside, Congress, Minto) in the district, despite almost 60 known occurrences. Furthermore, many of the mineral occurrences in the district are characterized by antimony and mercury mineralization, which historically led to their consideration as less attractive gold exploration targets.

The distribution of gold-dominant, stibnite-dominant and mercury-dominant mineral occurrences in the Bralorne – Bridge River area has been recognized to form a general zonation from west to east (Pearson, 1975; Woodsworth *et al.*, 1977). Limited, and often imprecise, isotopic dating of the mineralization also indicates a younging trend from west to east (Schiarrizza *et al.*, 1997, Fig 35). These data and observations have resulted in the development of contradictory regional metallogenic models that variably involve: a single protracted mineralizing event; three different mineralizing events; three different structural episodes; zoning influenced by distance away from the Coast Plutonic Complex; and mineralization directly related to specific magmatic events, such as emplacement of the Bendor plutonic suite or albitite dikes (e.g., McCann, 1922; Cairnes, 1937; Woodsworth *et al.*, 1977; Leitch *et al.*, 1991; Church, 1996; Schiarrizza *et al.*, 1997; Church and Jones, 1999). Most significantly, vein systems in the district have at different times been classified according to different deposit models, such as mesothermal (orogenic), intrusion-related, ophiolite-related and epithermal (e.g., Cairnes, 1937; Woodsworth *et al.*, 1977; Leitch *et al.*, 1989; Ash, 2001).

We would argue that this ambiguity is largely the effect of 1) imprecise and inaccurate dating of mineralization at Bralorne and other occurrences within this important district; and 2) lack of recognition that shallower, mercury and antimony-rich epizonal ores may be the tops to important orogenic gold vein systems. This is supported by oxygen isotope data from Maheux (1989), which suggests metal precipitation from one main fluid type throughout the district rather than the presence of unrelated, shallow meteoric hydrothermal cells that may have been responsible for relatively young epithermal deposits. Without better age data, it is difficult to relate mineralization to any single specific magmatic, structural or tectonic event with confidence. Consequently, it prevents establishment of a district-scale metallogenic model, which is a key component for better exploration targeting. As a result, a Geoscience BC project was established to provide improved geochronological and metallogenic models upon which to base exploration programs. At this preliminary stage of the project, we present further justification for the project and anticipated outcomes from samples collected in the summer of 2006.

¹ Geoscience BC contribution GBC038

² Centre for Exploration Targeting, University of Western Australia, Crawley, WA, Australia

³ United States Geological Survey, Denver, CO

This publication is also available, free of charge, as colour digital files in Adobe Acrobat® PDF format from the BC Ministry of Energy, Mines and Petroleum Resources website at http://www.em.gov.bc.ca/Mining/Geosurv/Publications/catalog/cat_fldwk.htm

LOCATION

The project area is the region north of Pemberton, mostly between the towns of Gold Bridge and Lillooet in the Bridge River and Yalakom River valleys in southwestern British Columbia (Fig 1). The project area is mostly in the Taseko Lakes and Pemberton map areas, which are covered by 1:50 000 NTS map sheets 92O/01, 02, 03; 92J/09, 10, 11, 14, 15, 16; 92I/12, 13; and 92D/04. Map areas 92O and 92I have been identified as a priority for Geoscience BC proposals because of the mountain pine beetle infestation.

REGIONAL GEOLOGY

The project area is within the southeastern Coast Belt near its transition to the Intermontane Belt and is recognized as a region of structural complexity and intense deformation. Tectonically, the region is largely underlain by 1) the Mississippian to Middle Jurassic accretionary complexes of oceanic rock assemblages of the Bridge River Terrane in the west; 2) the intervening Late Triassic to Early Jurassic Cadwallader Terrane island arc volcanic rocks and mostly marine, clastic strata of a marginal basin; and 3) the Shulaps ultramafic complex in the east, which was obducted over rocks of the Cadwallader Terrane in the mid-Cretaceous (Schiarizza *et al.*, 1997). Together, these assemblages are variably overlain by clastic, mostly nonmarine successions belonging to the Jurassic-Cretaceous Tyaughton Basin.

The western margin of the area is defined by the eastern limit of the Coast Plutonic Complex, and its eastern limit by the Yalakom fault. Magmatically, the region has been intruded and overlain by a wide range of Cretaceous and Tertiary plutonic and volcanic rocks and their hypabyssal equivalents. Significant among these are the Late Cretaceous Bendor plutonic suite in the west and the Eocene Rexmount porphyry bodies in the east. Structurally, the region has been affected by the mid-Cretaceous contractional and oblique-sinistral Bralorne-Eldorado fault system and the westerly-directed Shulaps thrust belt (in the east). Early Late Cretaceous sinistral movements on the Eldorado fault and the Castle Pass fault system are likely coeval with deposition of most of the Bralorne ores (Schiarizza *et al.*, 1997). Younger, northwest-trending dextral displacements reactivated many of the older faults and were dominant in the east, particularly along the Marshall Creek and Yalakom faults, and are considered to have controlled mineralization that is located proximal to the faults in these areas.

PREVIOUS WORK

A considerable amount of excellent research has been completed in the region, providing a broad understanding of the relevant deposit geology and geochemistry. A solid geological foundation for the Bridge River area was provided by Schiarizza *et al.* (1997), building upon numerous studies in the region mentioned in the references. In addition

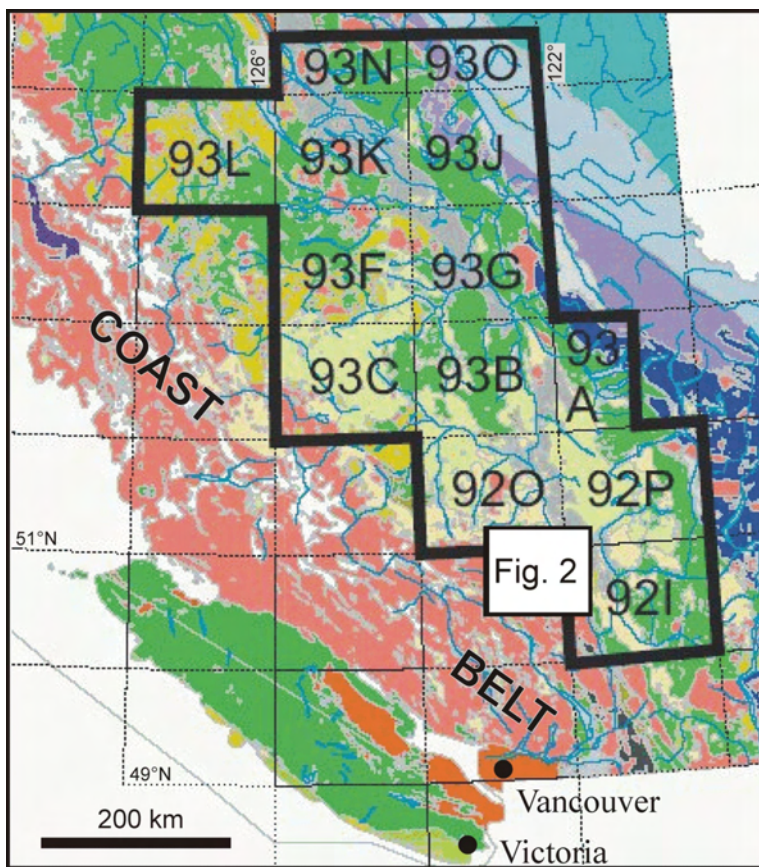


Figure 1. Location of project area (Fig 2) in southwestern British Columbia. Location of greatest infestation of mountain pine beetle outlined in black.

tion to the numerous early studies on Bralorne-Pioneer and related mineral occurrences (McCann, 1922; Dolmage, 1934; Cairnes, 1937; Joubin, 1948), more recent broad-based contributions (Church, 1987, 1995; Church *et al.*, 1988; Church and Pettipas, 1989; Church and Jones, 1999) have been particularly important. Contemporary isotope geochemistry and geochronology studies, although solely specific to Bralorne-Pioneer deposit, have been completed by Leitch (1990), Leitch *et al.* (1989, 1991) and Ash (2001), and detailed fluid inclusion and stable isotope geochemistry studies were carried out on many mineral occurrences in the district by Maheux (1989).

METALLOGENIC MODELS

Throughout the Bralorne – Bridge River district, there is a variety of well-described mineral occurrence types (Fig 2). In addition to low-sulphide (orogenic) gold-quartz veins, there are numerous small stibnite, mercury, tungsten and polymetallic vein occurrences that have been mainly interpreted as being related to proximal intrusions or as being of epithermal origin. These mineral occurrences tend not to be the focus of aggressive exploration for associated gold resources. If gold enrichments exist in these various occurrences, such anomalies are typically small in magnitude and erratic in distribution, and overall gold deposition was likely related to boiling zones of limited vertical extent. This has discouraged aggressive gold exploration over much of the area, except for those veins proximal to the

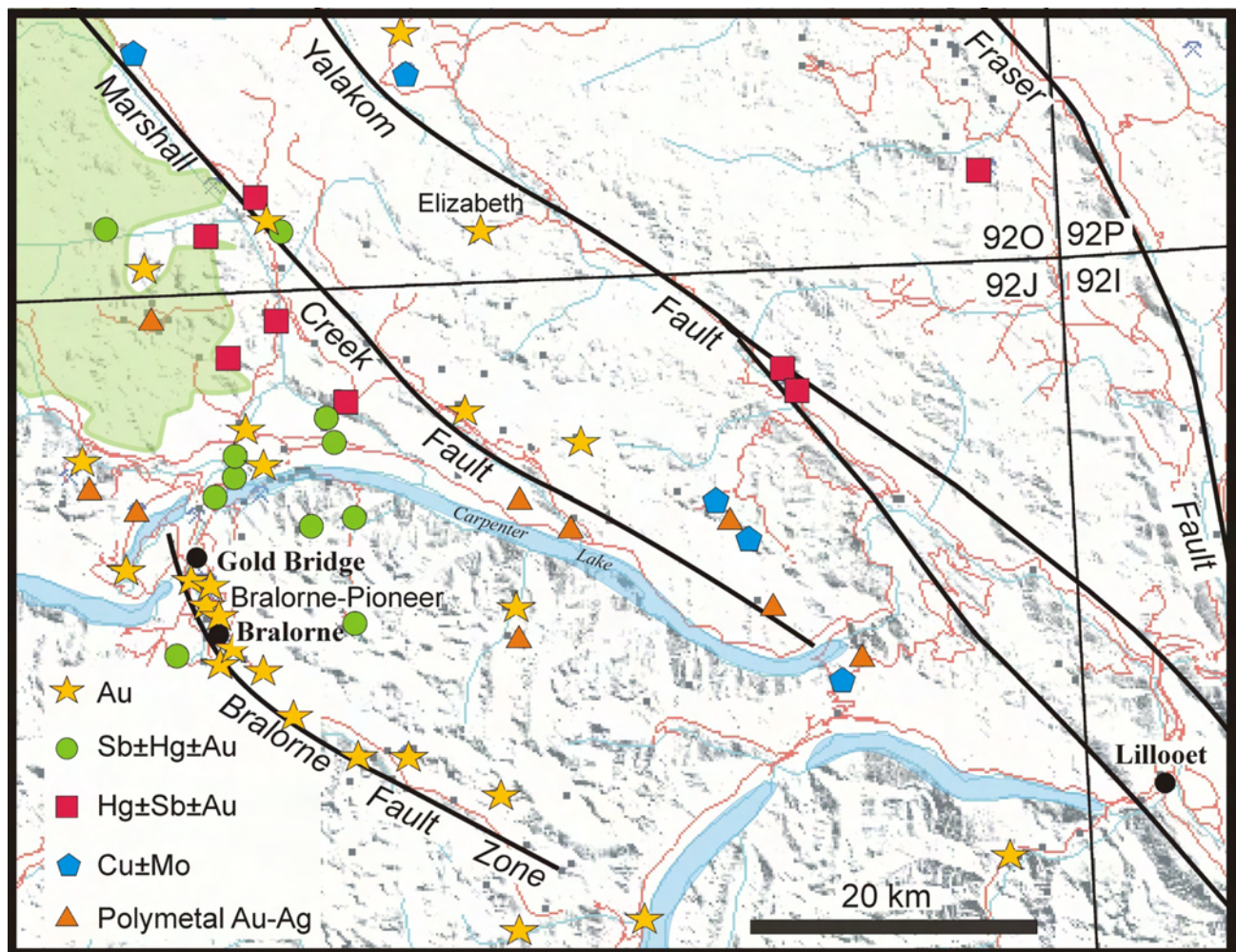


Figure 2. Study area, featuring the regional distribution of differing mineral deposit types in the Bralorne – Bridge River district and the major structural features. Shaded area in the northwest is the Spruce Lake Protected Area.

Bralorne-Pioneer gold system in the southern part of the district.

Building on the regional metal trends recognized by Pearson (1975), Woodsworth *et al.* (1977) emphasized a relationship between metal precipitation and the emplacement and cooling of the Coast Plutonic Complex (CPC). Similarly, an easterly decrease in K-Ar ages for mineral occurrences led Leitch *et al.* (1989) to suggest a model emphasizing the importance of proximity and cooling of *ca.* 80 to 59 Ma igneous rocks that form the eastern margin of the CPC. Further dating modified the model, whereby pulses of heat from the CPC resulted in several generations of mineralization, which decrease in age and formation P-T outward from the CPC (Leitch *et al.*, 1991). Additional work at Bralorne further emphasized a relationship with *ca.* 90 Ma albite porphyry dikes (Leitch *et al.*, 1991). In almost all cases, however, efforts have been toward partitioning the deposit types throughout the district into unrelated deposit groups or ore-forming events. For example, Schiarizza *et al.* (1997) recognized that each metal zone is associated with a different fault system; specifically, the gold deposits are associated with the Bralorne-Eldorado fault system, the stibnite mineralization is associated with the Castle Pass fault system, and the mercury mineraliza-

tion is associated with the Marshall Creek and Yalakom – Relay Creek fault systems. Each of these three structural systems is considered to have been active at different times, thus further partitioning the district based on poorly defined geochronology.

Several intrusion-related models have been put forth to account for the generation of metallic mineralization in this district. Both the historic and some of the most recent models placed a large genetic emphasis on the role of magmatic rocks. Depending on the study, the CPC, the Bendor batholith, albitite dikes or the felsic porphyry bodies have been considered as potential causative mineralization agents.

Despite district-wide geochronology, Maheux (1989) was the one worker to suggest, based on oxygen and hydrogen isotope data, that all the different deposit types may be defined by a single model and that the classic epithermal model was not appropriate. He used the isotope data from numerous occurrences to develop a model that relied upon the deep circulation of a “unique meteoric” fluid as being responsible for the various ore systems throughout the entire district. He suggested that the variability of the ores in the Bridge River camp was suggestive of patterns seen in world-class ore camps in the Jiagnan orogen of southeast-

ern China, the eastern Cordillera of South America, the Lachlan fold belt of southeastern Australia, and the Otago region of South Island, New Zealand.

GEOCHRONOLOGY

The timing of mineralization and the relationships with various magmatic units have often been based on age determinations of hosting and crosscutting rocks. The age of mineralization at Bralorne, for example, was constrained to between *ca.* 91 and 86 Ma by Leitch (1990), based on U-Pb and K-Ar dates on pre and postmineral dikes. This overlaps, within the range of analytical error, an 85 Ma K-Ar date on an altered intrusion near a mineralized vein on the Cosmopolitan property at the Bralorne deposit (Church, 1995). In contrast, Pearson (1977) reported a K-Ar white mica alteration age from Bralorne as *ca.* 64 Ma. Leitch *et al.* (1991) argued that it was likely a reset age due to the nearby CPC stocks.

Dikes at the Minto and Congress prospects yielded K-Ar dates of *ca.* 69 to 67 Ma (Harrop and Sinclair, 1986), which often are assumed to be the mineralization ages. This has, therefore, suggested to many workers that a series of mineralizing events over tens of millions of years may have characterized the Bridge River district. In the northern part to the district, Leitch *et al.* (1991) reported a K-Ar sericite date of *ca.* 58 Ma for the Lucky Gem deposit. A K-Ar date on hydrothermal fuchsite at Minto of *ca.* 45 Ma (Pearson, 1977) likely represents post-ore resetting.

In summary, most previous age determinations in the district were made using the K-Ar method. The reliability of this method cannot be independently assessed, but is often questioned because of the high susceptibility of a rock or mineral to argon loss at some time after crystallization. This is particularly likely for this part of BC, which has a complex thermal history. Utilization of the better Ar/Ar method would provide more interpretable data, if suitable samples for such a dating procedure can be found at many of the Bridge River mineral occurrences. Ash (2001) attempted to use this method for hydrothermal fuchsite in veined and altered diabase from the Pioneer mine dump. Unfortunately, problems associated with the evaluation of material that was too fine grained (*i.e.*, recoil) yielded a poor analysis and a result equivalent to a conventional K-Ar-type age at *ca.* 79 Ma. A couple of additional chrome-bearing illite samples from the Bralorne system gave Ar/Ar dates of *ca.* 80 to 70 Ma, but, as pointed out by Ash (2001), these dates may relate to thermal overprinting of an early fuchsite generation. Thus, this initial Ar/Ar attempt at dating Bralorne and Pioneer still emphasizes many problems in the geochronological picture and also conflicts with the constraints stressed by Leitch and co-workers. To the northwest, a *ca.* 70 ± 5 Ma Ar/Ar age on the diorite that hosts the Elizabeth and Yalakom prospects (Schiarrizza *et al.*, 1997) places a relatively young maximum age on these gold systems and yielded a large (10 m.y.) error window.

PROJECT RATIONALE

Previous metallogenic models for the region variably included 1) ore fluids sourced from different magmatic suites or from the CPC, 2) episodic pulses of heat from the CPC, or 3) different structural events. Without precise age determinations from the deposits and magmatic rocks, such assertions are impossible to make with confidence. Initial

interpretations of generally similar stable isotopic data from veins throughout the district (Maheux, 1989), in combination with an understanding of the continuum model for orogenic gold deposits, potentially indicate that mineralization at Bralorne-Pioneer and throughout most of the district simply represents different structural levels of a single hydrothermal event. For example, although antimony and mercury deposits are often interpreted to be upper parts of small epithermal systems, hot spring deposits in California have fluid, isotopic and trace element chemistries similar to typical Mother Lode orogenic gold deposits, both consistent with a deep-crustal fluid source. In addition, the huge Donlin Creek gold deposit, originally a small stibnite prospect, is now recognized as an epizonal or shallow-crustal orogenic gold deposit (Goldfarb *et al.*, 2004), with heavy oxygen and light sulphur data indicating a fluid evolved through metamorphic devolatilization of the host flysch basin.

Within the diversity of mineralization in the Bridge River region, specific geological aspects, such as age, structural setting, crustal level and hydrothermal fluid types, can be used to assess prospectivity by associating appropriate deposit models, thus enabling more effective exploration targeting. In simple language, "Which occurrences are worthy of aggressive exploration efforts?" Although most indications of mineralization ages in the district are broadly Late Cretaceous, the existing age dataset is not sufficiently precise to allow district-wide comparisons between deposits, or with magmatism such as the Bendor plutonic suite. Additionally, most published dates are by the K-Ar method and are likely variably reset by younger thermal events; this is clearly evident from the abundance of contradictory age relationships in the literature on the district. The existing district geological data themselves are good: mapping is thorough, there is a wealth of deposit geological and mineralogical information, and adequate fluid and stable isotope data exist. To date, however, these data are not well compiled in a comprehensive manner, typically lacking appropriate interpretations and application to regional geology. This situation provides part of the justification for this project.

PROJECT OBJECTIVES

The main objective of this project is to comprehensively assess the nature and timing of mineralization in the Bralorne – Bridge River district, in order to construct a contemporary regional-scale exploration model.

The project will

- 1) obtain new and more precise geochronological control for both the world-class Bralorne-Pioneer deposits and many other gold, stibnite and mercury occurrences in the district;
- 2) determine the most appropriate deposit models for the varied deposit types of the district; and
- 3) provide a regional metallogenic model and suggestions for improved exploration targeting and success within the district.

METHODS

We plan to utilize two main methods for collection of new data to assess the regional metallogeny of the Bralorne – Bridge River mineral district: geochronology and ore-fluid geochemistry.

Three different geochronological dating methods will be variably employed on alteration, gangue minerals and, potentially, ore minerals, and these data will be combined with recognized crosscutting relationships. The Ar/Ar method will be most commonly used to date the timing of mineralization from different mineral occurrences across the region in order to assess their timing of formation. However, many of the lower temperature occurrences may not form minerals (*i.e.*, micas) that are appropriate or easily dated by this method. These will be constrained by dating hosting or crosscutting rock phases where possible, by both Ar/Ar and SHRIMP U-Pb. In addition, we will attempt to date the sulphide minerals themselves, particularly arsenopyrite, using the innovative Re-Os dating method with the participation of R. Creaser at the University of Alberta. This last method assumes that the host minerals contain enough Re, which is critical when dating such young events.

Ore geochemistry is an effective method of indicating the nature of the ore-forming fluids, their chemistry, origin and the processes involved in generating ore deposits. Most deposits from the region have a reasonable amount of existing geochemical data, such as fluid inclusion P-T-X measurements, and stable and lead isotope analyses. However, except for those from Bralorne (Leitch *et al.*, 1991), much of the other data remain unpublished. We intend to compile the salient published and unpublished data, and collect new data that will be assessed and interpreted. From this, we will provide a modern interpretation of the regional metallogeny upon which to base exploration models. Preliminary work indicates that quartz from the lower temperature stibnite veins precipitated from fluids with oxygen isotopic values similar to those of higher temperature gold-only veins at Bralorne-Pioneer. This observation alone is critical, as it means that the low-temperature veins are likely the upper parts of orogenic lode gold systems, and that they were not formed from shallow meteoric fluids associated with unrelated epithermal deposit types.

ANTICIPATED OUTCOMES

As the result of this project we will

- 1) determine the timing of mineralization at Bralorne and other deposits and occurrences across the entire district;
- 2) determine the timing of magmatic events, such as the Bendor plutons;
- 3) assess the nature of the fluids that formed deposits throughout the district; and
- 4) re-evaluate and determine the most appropriate ore deposit models for the region's MINFILE (2006) occurrences.

Fieldwork has been completed, samples and observations have been obtained from approximately 12 significant occurrences and deposits, and materials have been submitted for geochronology, fluid inclusion and stable isotope study.

ACKNOWLEDGMENTS

Funding from this project comes from Geoscience BC, with support from the University of Western Australia and the United States Geological Survey. Information and ad-

vice from Ned Reid and Aaron Pettipas of Bralorne Gold Mines Ltd. (formerly Bralorne-Pioneer Mines Ltd.), as well as from Ted Illidge of Gold Bridge, are appreciated. The staff at the Gold Bridge Hotel are thanked for their hospitality.

REFERENCES

- Ash, C.H. (2001): Ophiolite-related gold quartz veins in the North American Cordillera; *BC Ministry of Energy, Mines and Petroleum Resources*, Bulletin 108, 140 pages.
- Cairnes, C.E. (1937): Geology and mineral deposits of the Bridge River mining camp, BC; *Geological Survey of Canada*, Memoir 213, 140 pages.
- Church, B.N. (1987): Geology and mineralization of the Bridge River mining camp; in *Geological Fieldwork 1986*, *BC Ministry of Energy, Mines and Petroleum Resources*, Paper 1987-1, pages 23–29.
- Church, B.N. (1996): Bridge River mining camp geology and mineral deposits; *BC Ministry of Energy, Mines and Petroleum Resources*, Paper 1995-3, 159 pages.
- Church, B.N., Gaba, R.G., Hanna, M.J. and James, D.A.R. (1988): Geological reconnaissance in the Bridge River mining camp (92J/15, 16, 10; 92O/02); in *Geological Fieldwork 1987*, *BC Ministry of Energy, Mines and Petroleum Resources*, Paper 1988-1, pages 93–100.
- Church, B.N. and Jones, L.D. (1999): Metallogeny of the Bridge River mining camp (092J/10, 15, 092O/02); *BC Ministry of Energy, Mines and Petroleum Resources*, MINFILE digital data, URL <<http://www.em.gov.bc.ca/mining/geolsurv/minfile/mapareas/bridge.htm>> [November 2006].
- Church, B.N. and Pettipas A.R. (1989): Research and exploration in the Bridge River mining camp (92J/15, 16); in *Geological Fieldwork 1988*, *BC Ministry of Energy, Mines and Petroleum Resources*, Paper 1989-1, pages 105–114.
- Colvine, A.C. (1989): An empirical model for the formation of Archean gold deposits — products of final cratonization of the Superior Province, Canada; *Economic Geology Monograph*, volume 6, pages 37–53.
- Dolmage, V. (1934): The Cariboo and Bridge River gold fields, British Columbia; *Canadian Institute of Mining and Metallurgy Transactions*, 1934, pages 405–430.
- Goldfarb, R.J., Ayuso, R., Miller, M.L., Ebert, S.W., Marsh, E.E., Petsel, S.A., Miller, L.D., Bradley, D., Johnson, C. and McClelland, W. (2004): The Late Cretaceous Donlin Creek deposit, southwestern Alaska — controls on epizonal formation; *Economic Geology*, volume 99, pages 643–671.
- Goldfarb, R.J., Baker, T., Dubé, B., Groves, D.I., Hart, C.J.R. and Gosselin, P. (2005): Distribution, character, and genesis of gold deposits in metamorphic terranes; in *Economic Geology 100th Anniversary Volume*, Hedenquist, J.W., Thompson, J.F.H., Goldfarb, R.J., and Richards, J.P., Editors, *Economic Geology*, 100th Anniversary Volume, pages 407–450.
- Goldfarb, R.J., Miller, L.D., Leach, D.L. and Snee, L.W. (1997): Gold deposits in metamorphic rocks in Alaska; *Economic Geology Monograph*, volume 9, pages 151–190.
- Groves, D.I. (1993): The crustal continuum model for late-Archean lode-gold deposits of the Yilgarn block, Western Australia; *Mineralium Deposita*, volume 28, pages 366–374.
- Groves, D.I., Goldfarb, R.J., Gebre-Mariam, M., Hagemann, S.G. and Robert, F. (1998): Orogenic gold deposits: a proposed classification in the context of their crustal distribution and relationship to other gold deposit types; *Ore Geology Reviews*, volume 13, pages 2–27.

- Harrop, J.C. and Sinclair, A.J. (1986): A re-evaluation of production data, Bridge River – Bralorne Camp (92J); in *Geological Fieldwork, 1985, BC Ministry of Energy, Mines and Petroleum Resources*, Paper 1986-1, pages 303–310.
- Joubin, F.R. (1948): Bralorne and Pioneer Mines; in *Structural Geology of Canadian Ore Deposits, Canadian Institute of Mining and Metallurgy*, Jubilee Volume, pages 168–177.
- Leitch, C.H.B. (1990): Bralorne: a mesothermal, shield-type vein gold deposit of Cretaceous age in southwestern British Columbia; *Canadian Institute of Mining, Metallurgy, and Petroleum Bulletin*, volume 83, number 941, pages 53–80.
- Leitch, C.H.B., Dawson, K.M. and Godwin C.I. (1989): Early late Cretaceous, Early Tertiary gold mineralization: a galena lead isotope study of the Bridge River mining camp, southwestern British Columbia; *Economic Geology*, volume 84, pages 2226–2236.
- Leitch, C.H.B., van der Heyden, P., Godwin, C.I., Armstrong, R.L. and Harakal J.E. (1991): Geochronometry of the Bridge River mining camp, southwestern British Columbia; *Canadian Journal of Earth Sciences*, volume 28, pages 195–208.
- Maheux, P.J. (1989): A fluid inclusion and light stable isotope study of antimony-associated gold mineralization in the Bridge River District, British Columbia, Canada; unpublished MSc thesis, *University of Alberta*, Edmonton, Alberta, 160 pages.
- McCann, W.S. (1922): The Bridge River area; *Geological Survey of Canada*, Memoir 130, 150 pages.
- MINFILE (2006): MINFILE BC mineral deposits database; *BC Ministry of Energy, Mines and Petroleum Resources*, URL <<http://www.em.gov.bc.ca/Mining/Geolsurv/Minfile/>> [November 2006].
- Pearson, D.E. (1975): Bridge River map-area; in *Geological Fieldwork, 1974, BC Ministry of Energy, Mines and Petroleum Resources*, Paper 1975-2, pages 35–39.
- Pearson, D.E. (1977): Mineralization in the Bridge River Camp, BC; in *Geology in British Columbia, 1975, BC Ministry of Energy, Mines and Petroleum Resources*, pages G57–G63.
- Schiarizza, P., Gaba, R.G., Glover, J.K., Garver, J.I. and Umhoefer, P.J. (1997): Geology and mineral occurrences of the Taseko – Bridge River area; *BC Ministry of Energy, Mines and Petroleum Resources*, Bulletin 100, 291 pages.
- Woodsworth, G.J., Pearson, D.E. and Sinclair, A.J. (1977): Metal distribution patterns across the eastern flank of the Coast Plutonic Complex, south-central British Columbia; *Economic Geology*, volume 72, pages 170–183.

Mineralization, Alteration and Structure of the Taseko Lakes Region (NTS 0920/04), Southwestern British Columbia: Preliminary Analysis¹

by L. Hollis², S.K. Blevings², C.M. Chamberlain², K.A. Hickey² and L.A. Kennedy²

KEYWORDS: Coast Belt, Cu-Mo porphyry, Taseko Lakes, Tchaikazan fault

INTRODUCTION

This two-year research project will investigate the characteristics of the volcanoplutonic architecture and associated porphyry-epithermal mineralization in the Taseko Lakes region, located in southwestern British Columbia (Fig 1). The study will integrate detailed geological, structural and alteration mapping, petrology, isotope geochemistry and geochronological analyses, with the aim of developing a conceptual geological model for the structural and economic evolution of the area to assist in the application of predictive exploration. Parts of the field area were previously mapped by McLaren (1990) and Israel and Kennedy (2001). This paper focuses on the structural and economic geology of the area.

The paper presents preliminary field observations concentrating on four main areas within the Taseko Lakes region: the Hub, which is a suspected Cu-Mo porphyry system; the Northwest Copper showing, which is an areally extensive, suspected epithermal Cu-Au showing; the Twin Creeks area, where anomalous Cu, Mo and Au values have been identified from prospecting and stream sediment samples (McLaren, 1990); and the Tchaikazan fault.

REGIONAL GEOLOGICAL SETTING

The project area is located within the Coast Belt, along the boundary between the southeast Coast Belt and southwest Coast Belt (Monger and Journeay, 1994; Fig 1, 2). The southeast Coast Belt includes rocks of the Bridge River accretionary complex, the Cadwallader arc terrane and overlying clastic rocks of the Tyaughton-Methow Basin. The southwest Coast Belt consists mainly of Middle Jurassic to mid-Cretaceous plutonic rocks, as well as Early Cretaceous volcanic and associated rocks of the Gambier Group. This geographic area is located at the eastern limit of the Coast Plutonic Complex, and it is along this boundary that many Cu-Mo-Au showings are located in the southern Coast Belt (McLaren, 1990).

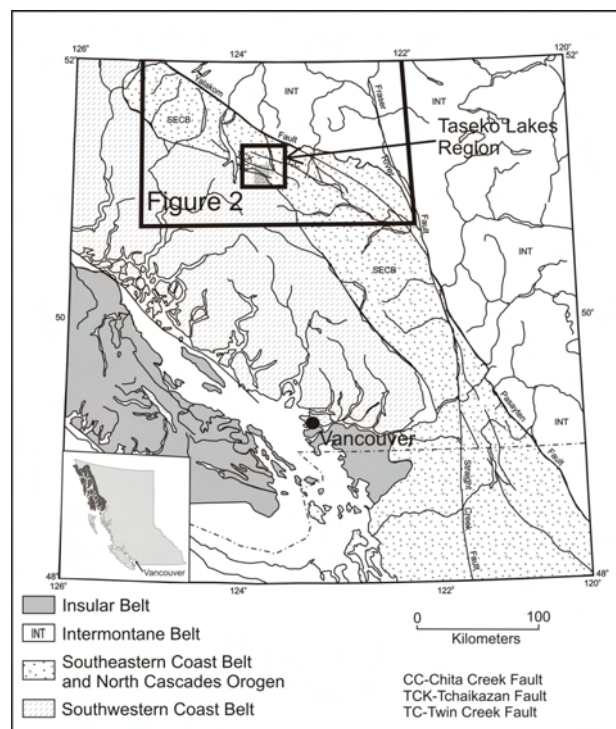


Figure 1. Orogenic belts of southwestern British Columbia (modified from Israel and Kennedy, 2001), showing the location of the Taseko Lakes region.

The Tchaikazan fault is a major strike-slip fault that strikes southeast through the field area (Fig 2, 3; Umhoefer et al., 1994). The bedrock to the northeast of the Tchaikazan fault is mainly clastic sedimentary rock from the Tyaughton-Methow Basin, including the Relay Mountain, Jackass Mountain and Taylor Creek groups (Fig 2). The bedrock to the southwest of the Tchaikazan fault forms the East Waddington thrust belt, which is a northeast-verging fold and thrust belt that deforms Triassic to Cretaceous volcanic and clastic sedimentary rock (Fig 2; Rusmore and Woodsworth, 1991; Umhoefer et al., 1994; Mustard and van der Heyden, 1994; van der Heyden et al., 1994; Schiarizza et al., 1997; Rusmore et al., 2000). The Powell Creek Formation, a Late Cretaceous package of volcanic and volcanoclastic rock that is abundant in the field area, occurs on both sides of the Tchaikazan fault. Mid-Cretaceous contraction of the southeast Coast Belt resulted in mostly southwest-verging thrust faults (Journeay and Friedman, 1993); however, in the field area, most thrust faults verge to the northeast and are correlated with the East Waddington Fold and Thrust Belt (Rusmore and Woodsworth, 1994). A system of regional-scale dextral strike-slip faults devel-

¹ Geoscience BC contribution GBC025

² Department of Earth and Ocean Sciences, 6339 Stores Road, University of British Columbia, Vancouver, BC V6T 1Z4

This publication is also available, free of charge, as colour digital files in Adobe Acrobat® PDF format from the BC Ministry of Energy, Mines and Petroleum Resources website at http://www.em.gov.bc.ca/Mining/Geosurv/Publications/catalog/cat_fldwk.htm

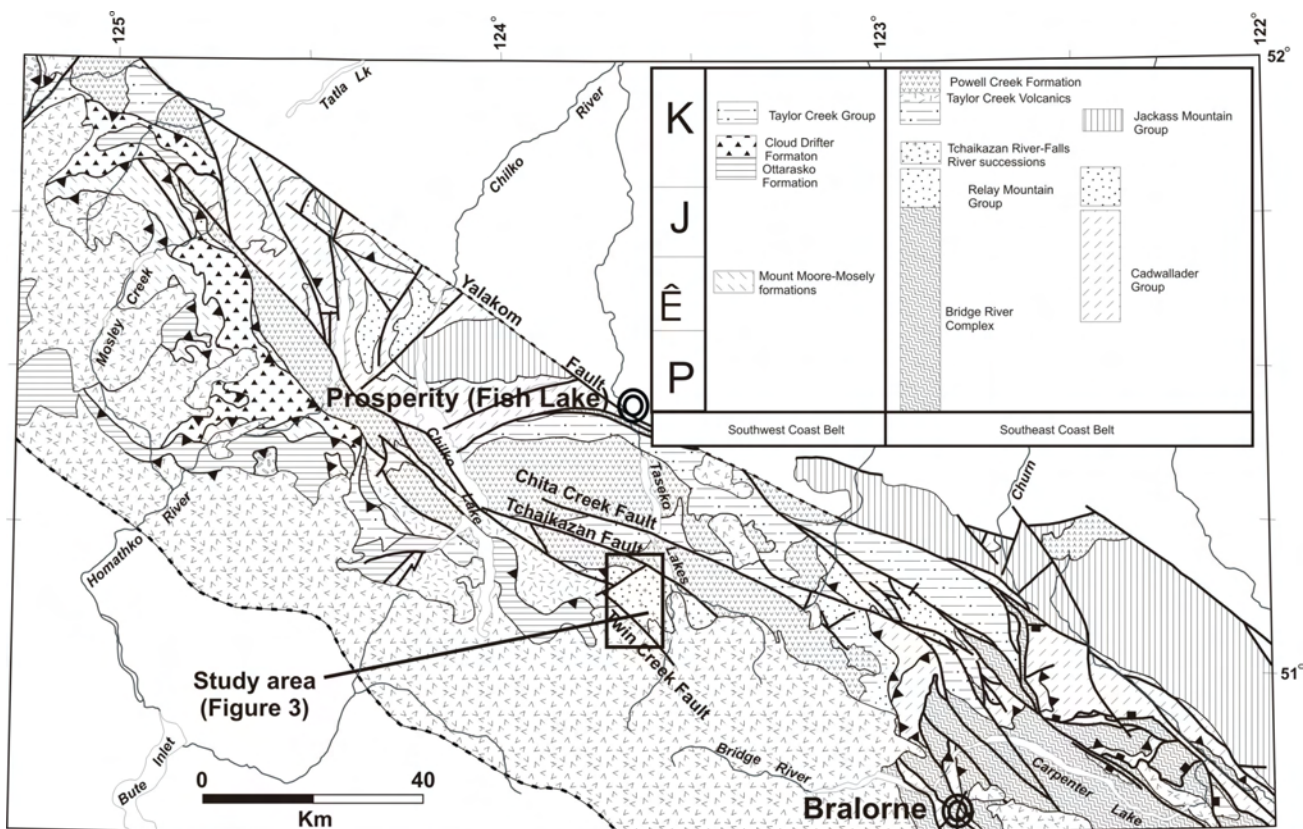


Figure 2. Regional geology of the southeast Coast Belt (modified from P. Schiarizza, unpublished data), showing the locations of the nearby Bralorne and Prosperity mineral deposits.

oped in the southeast Coast Belt from latest Cretaceous to Eocene time (Umhoefer and Schiarizza, 1996; Schiarizza *et al.*, 1997). These faults include the Tchaikazan, Twin Creek, Chita Creek and Yalakom faults (Fig. 2, 3), and they appear to cut all other structures in the area. In total, these structures are believed to have accommodated as much as several hundred kilometres of offset (Umhoefer and Schiarizza, 1996). Sinistral faults occur locally and are demonstrably older than the Eocene dextral faults (Israel *et al.*, in press). It is not yet known if these faults predate mid-Late Cretaceous contraction or if they are kinematically linked to the Cretaceous thrusts.

LITHOLOGICAL UNITS

Paleozoic Rocks

TWIN CREEKS SUCCESSION

The lone unit of Paleozoic rock in the study area is the Twin Creeks succession. The unit occurs as a few fault lenses within the Twin Creeks area (Fig 4) and is composed mainly of marine sedimentary rock of Permian age. These rocks consist of siltstone turbidite sequences and arkosic and grey sandstone. In areas proximal to faults, the unit appears heavily oxidized and rusty in colour. The minimum age for the succession, based on a U-Pb zircon date from a crosscutting aplite dike, is 251 ± 16 Ma (Israel and Kennedy, 2001).

MESOZOIC ROCKS

The majority of the study area is underlain by several rock units of Cretaceous age. These units, from oldest to youngest, include the Tchaikazan River succession, Falls River succession, Taylor Creek Group and Powell Creek Formation (Israel and Kennedy, 2001; Israel *et al.*, in press). The Tchaikazan and Falls River successions consists mainly of intermediate submarine volcanic rock and relatively fine grained marine sedimentary rock. The Powell Creek Formation is composed of subaerial purple andesitic flows and volcaniclastic rocks.

TCHAIKAZAN RIVER SUCCESSION

The Tchaikazan River succession is the most areally extensive unit in the Twin Creeks region (Fig 4). It consists of a sediment-dominated facies and a volcanic-dominated facies. The sedimentary facies consists of clastic marine sedimentary rocks of varying grain size interbedded with minor andesitic flows. The volcanic facies comprises intermediate volcanic conglomerate and breccia, clastic marine sedimentary rock and andesite flows. These flows consist of porphyritic, massive and amygdale-rich units. These facies grade into one another, making the distinction between them at times somewhat arbitrary. Fossil evidence suggests an age as old as 140 Ma (Berriasian) for the Tchaikazan succession, whereas U-Pb dates from abraded zircon fractions from a crosscutting intrusion (McLaren, 1990; Israel and Kennedy, 2001) suggest an age older than 102 ± 2 Ma, which is consistent with fossil evidence.

FALLS RIVER SUCCESSION

The Falls River succession is another areally extensive unit in the Twin Creeks area. It contains slightly more volcanic rock than the Tchaikazan River succession and generally consists of andesitic flows, volcanic conglomerate and minor medium to fine-grained clastic sedimentary rock. Many of the andesitic flows are clast rich and grade into conglomerate and breccia units. Possible peperite occurs on the contacts between andesitic flows and sedimentary rock. Uranium-lead zircon dating of a partially welded tuff within the unit has given the Falls River succession an age of 102 to 110 Ma (Israel and Kennedy, 2001). The age is further constrained to be older than 103 ± 0.5 Ma, based on a U-Pb zircon date from the crosscutting Mount McLeod batholith (Israel and Kennedy, 2001).

TAYLOR CREEK GROUP

The Taylor Creek Group occurs in the area north of the Tchaikazan fault, in the mapped areas of the Northwest Copper showing (Fig 5) and in the Tchaikazan River valley (Fig 6). It consists of marine sedimentary rock, varying from interbeds of sandstone and siltstone (Fig 5D) to well-bedded grey sandstone, which are predominantly Albian (113–97.5 Ma) in age (Garver, 1992). The sandstone-siltstone interbeds likely represent turbidite sequences. The Taylor Creek Group is cut by the Tchaikazan Rapids pluton, establishing that the unit is older than 76 Ma (Israel and Kennedy, 2001).

POWELL CREEK FORMATION

The Powell Creek Formation is well exposed throughout the northwestern part of the field area, particularly in the Northwest Copper area (Fig 5, 7). Abundant exposures of purple and red, massive andesite flows, together with resedimented volcanic breccia, form much of the area (Fig 7A). The formation is deeply weathered and good, continuous stratigraphic sections are separated by hundreds of metres of weathered debris (Israel, 2001).

The volcanoclastic rocks vary from tuffaceous horizons to massive, angular, intermediate volcanic breccia. Figure 7 shows the detailed stratigraphy of a 340 m section (measured as accurately as possible perpendicular to dip) of well-exposed andesite flows and massive volcanoclastic rocks trending southeast. Volcanic breccia units range in thickness from 15 cm to 30 m. Typically maroon/purple and polymictic with subrounded clasts, they have highly undulating and often erosive bases (Fig 7B). Andesite is the dominant clast composition within these brecciated units. Clast size is variable; basal parts are often dominated by centimetre-scale clasts (Fig 7C), whereas clast size increases toward the top of the section, where lahar-style deposits are common. Red, massive andesite flows are dominantly plagioclase phyric (Fig 7D) and moderately propylitically altered. Highly fractured/quenched flow tops form sharp stratigraphic boundaries with overlying volca-

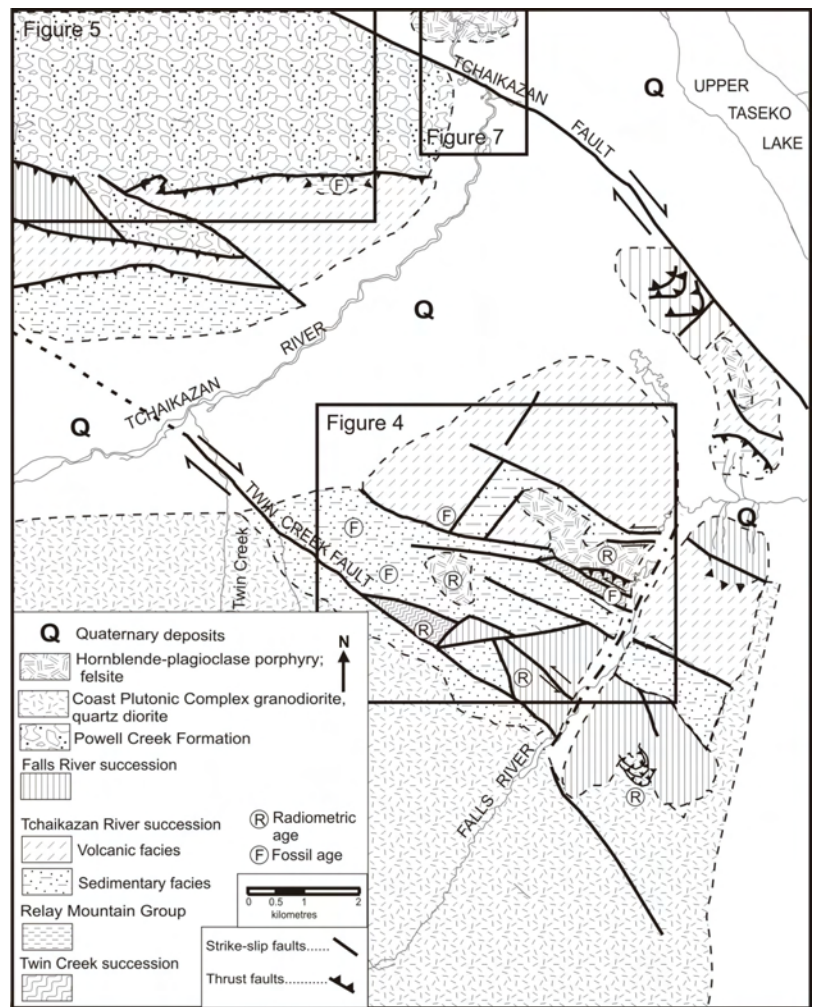


Figure 3. Geology of the Taseko Lakes region (modified from Israel *et al.*, in press), showing the locations of the Twin Creeks (Figure 4), Northwest Copper (Figure 5) and Tchaikazan River valley (Figure 6) areas.

nic breccia. Way-up structures are rare, but fining of volcanoclastic flow units is the most useful tool in the determination of stratigraphic top for the unit.

Several generations of highly altered plagioclase porphyry dikes are located within the Northwest Copper area. They show varying orientations and dips, and it has been proposed by Israel and Kennedy (2001), because of an aeromagnetic anomaly, that they are linked to a deeper seated pluton beneath the Powell Creek Formation.

Intrusive Rocks

MOUNT MCLEOD BATHOLITH

The most extensive igneous body in the area is the Mount McLeod batholith, which occurs in the southernmost part of the Twin Creeks area. All plutonic rocks in the area are, by definition, part of the Coast Plutonic Complex. It comprises medium to coarse-grained, hornblende-rich granodiorite. Areas of the batholith contain decimetre-scale enclaves of finer grained material of similar composition. Previous U-Pb dating on the batholith has given ages of 101.1 ± 0.3 Ma from titanite constraints to 103.8 ± 0.5 Ma from $^{238}\text{U}/^{206}\text{Pb}$ zircon ages (Israel and Kennedy, 2001).

GRIZZLY CABIN PLUTON

The Grizzly Cabin pluton outcrops as an ellipse-shaped intrusion. Parts of the intrusion show irregular intermingling of heterogeneous rock types (Fig 4E), whereas other areas show a single homogeneous phase. The homogeneous zones comprise medium to fine-grained hornblende-biotite quartz diorite, whereas the heterogeneous areas show segregation of medium to fine-grained hornblende diorite and quartz monzodiorite. The intrusion cuts all other visible rock units and has been previously U-Pb dated, from three abraded zircon fractions, to about 102 to 99 Ma. Another zircon fraction recorded the crystallization age of the rock at 101.5 Ma (Israel and Kennedy, 2001).

TCHAIKAZAN RAPIDS PLUTON

The Tchaikazan Rapids pluton dominates the mapped area to the north of the Tchaikazan fault. The pluton is a plagioclase-hornblende porphyry with plagioclase pheno-

crysts up to 2 cm in size. Much of the pluton has undergone significant clay alteration. It cuts the Taylor Creek Group, which is the only rock unit that it contacts, but is itself cut by the Tchaikazan fault. From previous U-Pb dating, the intrusion has a minimum crystallization age of 76 Ma (Israel and Kennedy, 2001).

STRUCTURAL GEOLOGY

The Taseko Lakes region has undergone at least three separate phases of deformation: sinistral/reverse slip faults, mid to Late Cretaceous compressional deformation, and dextral strike-slip faults. This section will focus on three areas mapped in detail: Twin Creeks, Tchaikazan River valley and Northwest Copper. The purpose of the detailed mapping was to determine the geometry and kinematics of the structures and to deduce their role, if any, in localizing or offsetting mineralization.

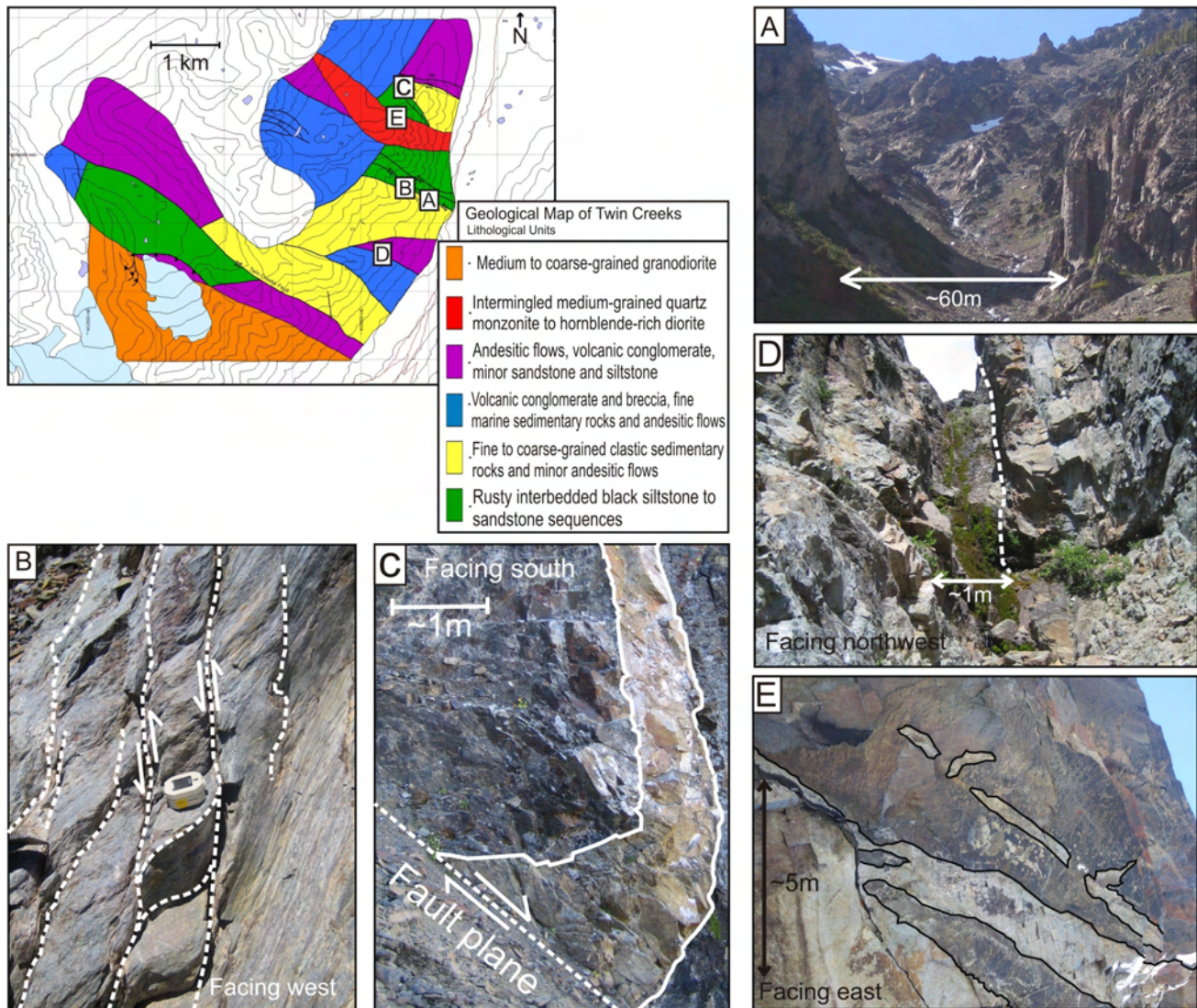


Figure 4. Geology of the Twin Creeks region, showing locations of photographs: A) sinistral/reverse shear zone; B) deflected foliations giving a sinistral shear sense with respect to the shear zone; (C) dike that has undergone drag folding, giving dextral movement sense next to fault zone; D) suspected dextral fault zone running parallel to the Twin Creeks fault; and E) intermingling of quartz monzodiorite (light grey) and diorite (dark grey) from within the Grizzly Cabin pluton.

Twin Creeks Area

Several northwest-striking and nearly vertical shear zones occur in the Twin Creeks area (Fig 4A). The fault zones are discontinuous along strike, as they are crosscut by later structures. These later crosscutting faults tend to have northeast orientations and unknown senses of movement. Many of them are inferred and were inaccessible during this field season. The shear zones are generally wide, ranging from 10 to 60 m in thickness. Very well developed shear fabrics, with sigmoidal asymmetry providing a

sinistral shear sense, are common (Fig 4B) and slickenside lineations indicate a component of reverse movement. Siltstone units appear to accommodate most strain, with the more competent andesite units containing only a weak shear fabric (Fig 4B).

Chloritization and silicification of the rocks proximal to these sinistral faults is common. Minor pyrite and arsenopyrite are rarely associated with these faults. An Ar/Ar cooling age of illite, collected from a sinistral fault fabric, is 89 Ma (Israel *et al.*, in press). This is similar to the age of

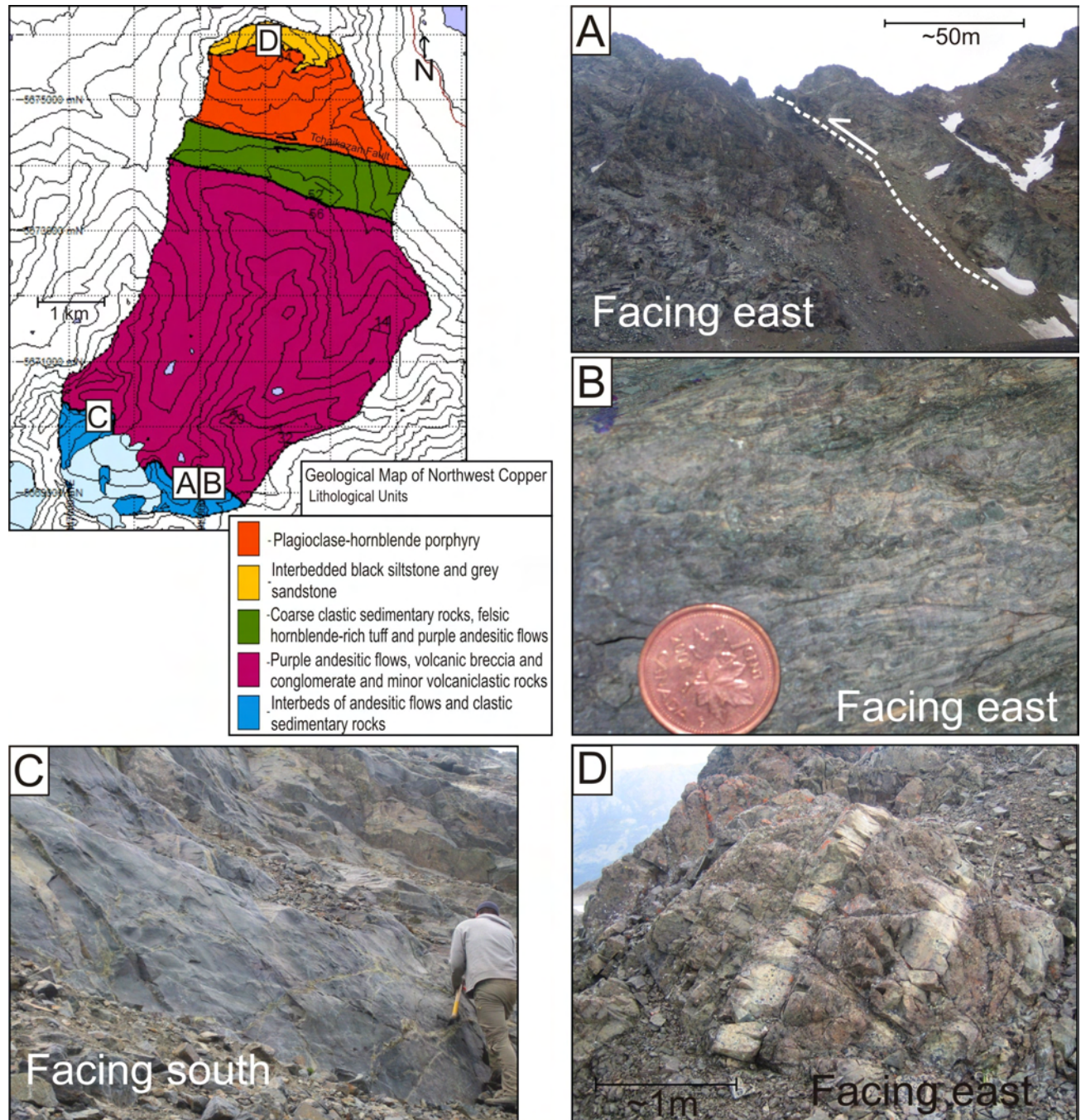


Figure 5. Geology of the Northwest Copper area, showing locations of photographs: A) north-verging thrust fault; B) significantly chloritized mylonite sample from the fault shown in (A); C) dense quartz-epidote veining in andesite located in the hanging wall of the thrust fault shown in (A); and D) siltstone and sandstone interbeds of the Taylor Creek Group, north of the Tchaikazan fault.

other significant sinistral faults in the region, particularly a system of reverse-sinistral faults, located approximately 50 km southeast of the area (Fig 2), that hosts the Bralorne gold veins and has been constrained to between 91 and 86 Ma in age (Leitch *et al.*, 1991).

Smaller scale dextral-slip faults are also present throughout the Twin Creeks area (Fig 4C). They are characterized by smaller zones of damaged fault zone material, consisting generally of highly fractured and foliated clastic sedimentary rocks (<10 m thickness). Other smaller dextral faults in the region show little deformation in the surround-

ing wallrock and are characterized more by slickensided surfaces and the narrow linear gullies in which they are found (Fig 4D). The majority of these smaller scale dextral faults strike southeast, similar to the Tchaikazan fault.

Northwest Copper

North to northeast-verging thrust faults occur in the Northwest Copper area (Fig 5A). The best exposed thrust fault in the area hosts mylonite that has undergone significant chlorite and epidote alteration (Fig 5B). The mylonite forms a zone approximately 1 to 2 m thick and was likely

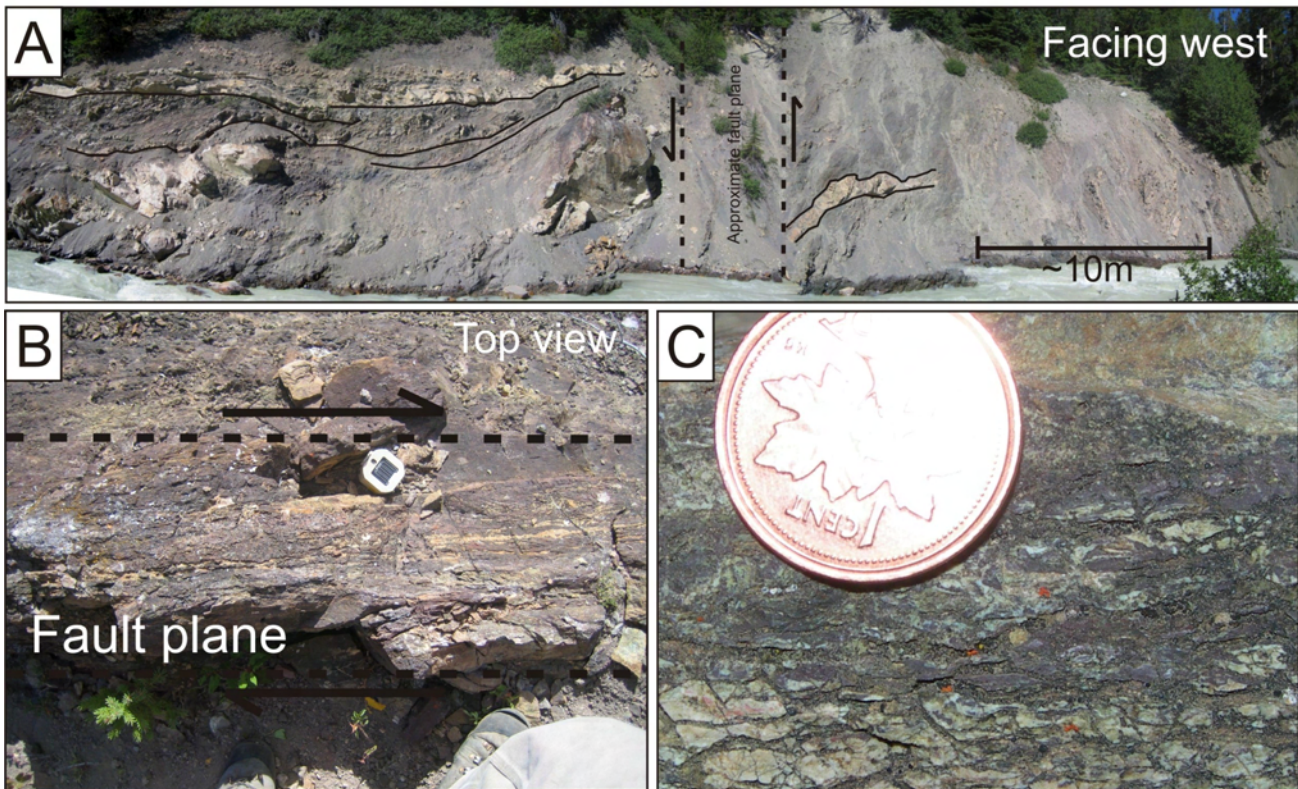
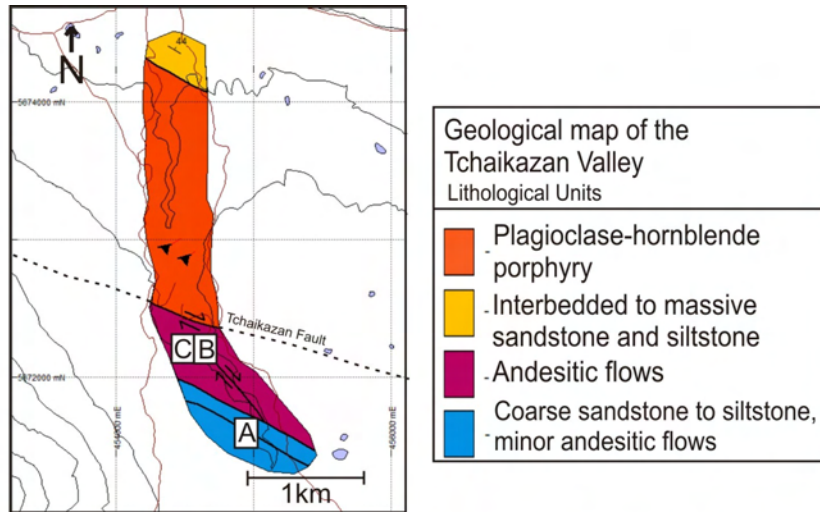


Figure 6. Geology of the Tchaikazan River valley area, showing locations of photographs: A) major fault zone representing either the Tchaikazan fault or a smaller parallel structure; B) small dextral fault interpreted as antithetic to the Tchaikazan fault; and C) well-bedded, fresh grey sandstone.

formed in andesitic rocks of the Powell Creek Formation. Asymmetric shear fabrics within the mylonite indicate a top-to-the-northeast shear sense (*i.e.*, contractional). The hangingwall above the mylonite is believed to be the Tchaikazan River succession, which is located stratigraphically below the Powell Creek Formation. The hangingwall immediately above the fault is densely epidote veined and hosts some sulphide minerals, such as pyrite, arsenopyrite and possibly some chalcopyrite. These sulphide minerals occur within the epidote veins as well as in small (<10 cm) alteration halos surrounding the veins (Fig 5C). These were the only exposures of mylonite observed in the area: all other faults were much more brittle in nature, hosting fault gouge and cataclasite rather than mylonite. Compressional deformation in the region is correlated with the East Waddington thrust belt (EWTB; Rusmore and Woodsworth, 1994).

Tchaikazan River Valley

Dextral strike-slip faults occur in the area on a variety of scales and cut all other structures. Movement along the faults occurred largely during the Eocene (Schiarizza *et al.*, 1997; Israel and Kennedy, 2001). The Tchaikazan fault is

the largest dextral fault in the field area. Outcrop is rare but it is exposed in the Tchaikazan River valley as thick zones (>50 m) of damaged wallrock. The fault zones comprise clastic sedimentary rocks that have been highly deformed and sheared to form gouge layers as well as cataclasite, and enclaves of relatively undeformed country rock (Fig 6A). Smaller antithetic faults are associated with the main faults. These smaller faults (<1 m wide) have suspected dextral movements inferred from asymmetric kinematic indicators from within the fault (Fig 6B, C).

The EWTB formed during a period of compressional deformation in the mid-Cretaceous, from approximately 87 to 84 Ma (Umhoefer *et al.*, 1994). The Tchaikazan and Twin Creek faults may be correlated with other regional dextral faults, including the Chita Creek and Yalakom faults to the north, that together would form a fault system known as the Yalakom fault system. This system is believed to have evolved together as a left-stepping system and has accommodated approximately 120 to 130 km of dextral offset (Schiarizza *et al.*, 1997). The Tchaikazan fault has accommodated approximately 7 to 8 km of dextral offset (Mustard and van der Heyden, 1997). Schiarizza *et al.* (1997) suggested a sinistral component to the Tchaikazan fault prior to the more recent dextral movement, based on

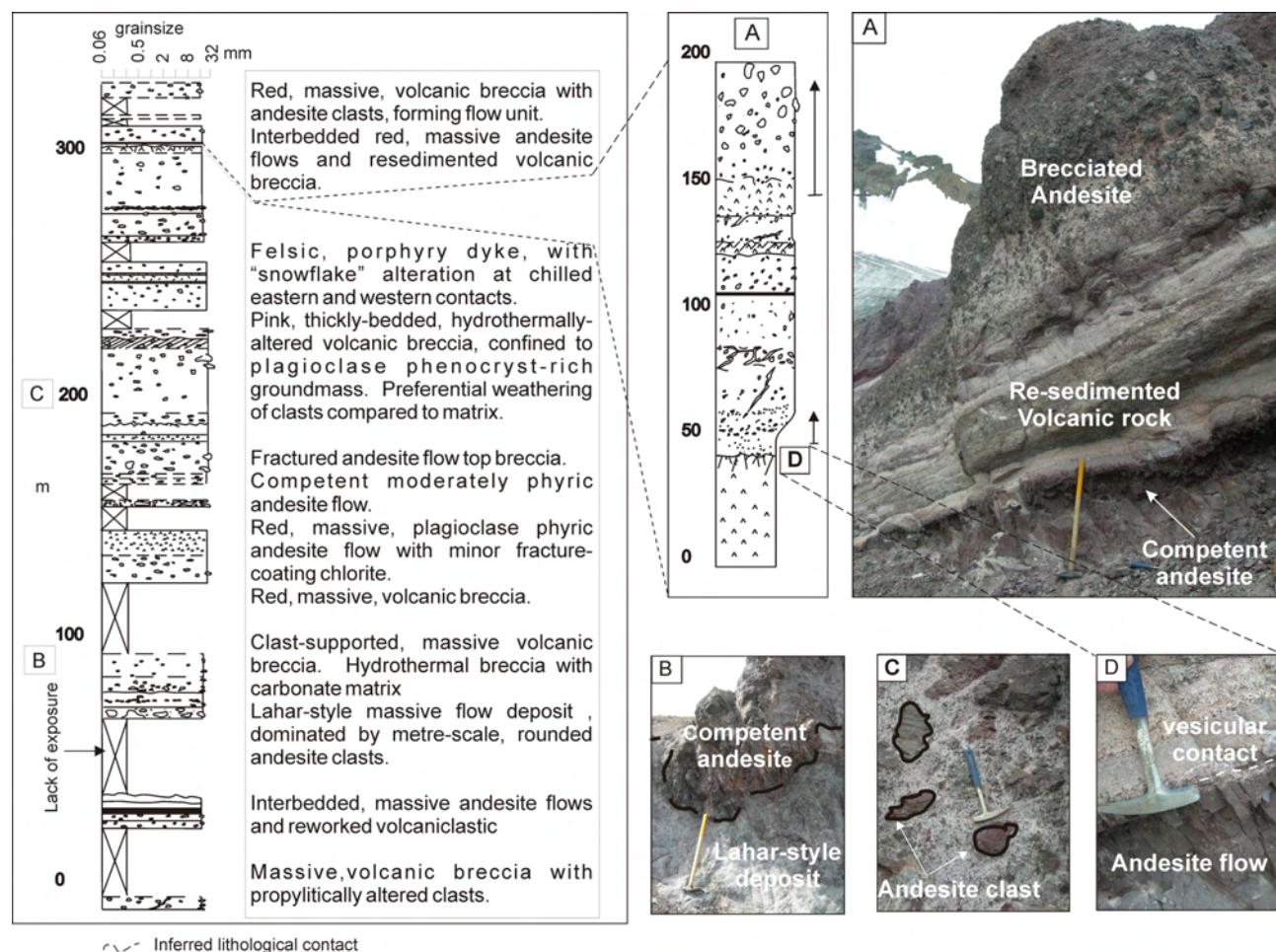


Figure 7. Schematic stratigraphic column of a 340 m measured section from the Northwest Copper area (left): A) detailed stratigraphic representation of 2.9 m of volcanic and reworked volcanic rocks; B) contact between a competent andesite flow (above) and a lahar-style deposit (below); C) brecciated andesite flow with large competent clasts in a fine-grained matrix; and D) vesicular contact between a competent andesite flow and a reworked volcanic flow.

apparent sinistral offset of Lower Jurassic sedimentary rock to the west of the study area. The relative timing of this truncation has been given by a batholith (the Dickson-McLure) that apparently plugs the Tchaikazan fault and has a K-Ar age of 86 Ma (Schiarizza *et al.*, 1997).

MINERALIZATION

Mineralization in the study area is characterized by a number of porphyry and suspected epithermal deposits. This study has focused on two such deposits within the region, the Hub and Northwest Copper (Fig 3). The primary focus of this year's fieldwork was detailed geological trench mapping in areas of the Hub at a scale of 1:100. Figure 8 shows a representative trench map from the Hub area, illustrating lithology and its relationship to mineralization and alteration. Approximately 300 m of exposure was mapped using the Anaconda method of trench mapping. The Anaconda method is a method of mapping geological trenches that utilizes detailed mapping techniques in order to accurately record lithological information and structural and crosscutting relationships, as well as hydrothermal veining, mineralization and alteration.

Hub Showing

H. Warren from the University of British Columbia first identified the Hub showing in the 1940s. The area is dominated by the interaction of two main rock types, granodiorite and a magnetite±biotite-cemented breccia, both of which act as hosts to mineralization. The Hub is located approximately 4 km southeast of the Northwest Copper showing and is also at a much lower elevation. One of the key questions to be answered regarding these two areas is whether the Hub represents a deep-seated porphyry system. And if so, is the Northwest Copper showing the shallow epithermal-style mineralization related to this plutonic environment? The Hub outcrop forms a southeast-trending exposure that parallels the Tchaikazan River. Granodiorite forms the primary igneous phase and contains large, hexagonal biotite crystals that are readily identifiable with the naked eye (Fig 8F). The granodiorite is not dated, but its relationship with several crosscutting feldspar porphyry dikes allows a relative timing of intrusive events to be interpreted. The granodiorite displays a complex intrusive relationship, interfingering with the second most abundant lithology, a dark grey-black, magnetite±biotite-cemented

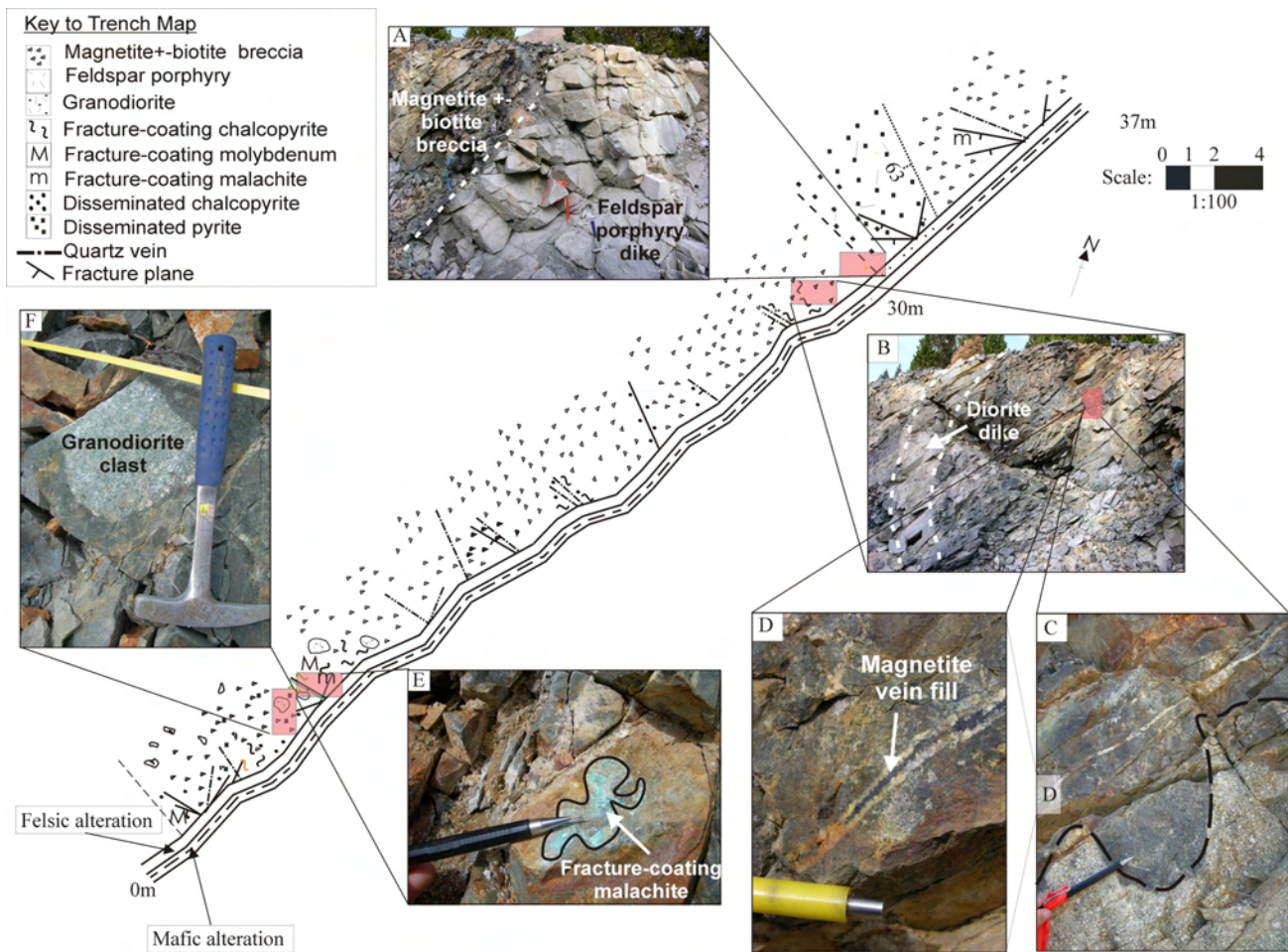


Figure 8. Geology of the Hub trench area, showing locations of photographs: A) lithological contact between magnetite±biotite-cemented breccia and feldspar porphyry dike; B) lithological contact between diorite dike and magnetite±biotite-cemented breccia; C) undulating contact between magnetite breccia and granodiorite; D) quartz vein with magnetite central vein fill; E) fracture-coating malachite on fracture plane; and F) granodiorite clast included within magnetite±biotite-cemented host rock.

breccia. Together, these rock types account for more than 90% of the observed outcrop (Fig 8B, C).

Several felsic dikes crosscut both the granodiorite and the magnetite breccia. These include an intermediate plagioclase-phyric dike with abundant biotite and a late, quartz-feldspar porphyry dike (Fig 8A, B). Part of the future work will be to ascertain whether the magnetite breccia is a replacement or forms as a breccia infill. The granodiorite and magnetite±biotite-cemented breccia are cut by 1.5 cm thick quartz veins that are filled with aphanitic magnetite (Fig 8D).

Mineralization is consistently focused on randomly oriented fracture planes, where fracture-coating chalcopyrite±pyrite is the dominant form of sulphide and often occurs in association with malachite (Fig 8E). The late feldspar porphyry dike contains up to 7% disseminated pyrite and is the most mineralized lithology observed toward the south (Fig 8A). Mineralization is interpreted to increase in concentration to the north, where molybdenite and chalcopyrite are found in association with centimetre-scale quartz veins. These veins show a relative history of emplacement: intrusion of granodiorite, magnetite±biotite-cemented breccia, quartz veins and finally emplacement of the quartz-feldspar porphyry dike.

Northwest Copper Showing

The Northwest Copper showing hosts numerous subcropping quartz-carbonate veins, most of which are not mineralized but may form part of the hypothesized epithermal system.

A 30 m wide, irregular subcropping zone of secondary copper mineralization, consisting of malachite and azurite, occurs at one of the north-northeast-trending ridges (informally known as Ravioli ridge). Associated with these oxides is considerable secondary silica replacement of the host rocks, which could be interpreted as the result of mobilization of silica and subsequent formation of copper minerals in oxidized zones. Associated with this zone is an 8 m wide zone of silicified vein material containing magnetite infillings. To the southwest, dark green, propylitically altered andesite of the Powell Creek Formation hosts minor disseminated pyrite. Copper oxide mineralization (usually malachite) is distributed sporadically in centimetre-scale coatings throughout the Powell Creek Formation. The malachite mineralization is associated with the highest density of quartz-carbonate veining and is typically associated with maroon, plagioclase-phyric andesite flows.

DISCUSSION AND FUTURE WORK

The economic potential for copper in the area was first identified in the early 1930s and, since then, several prospects have been identified, including the Late Cretaceous Prosperity deposit (formerly known as the Fish Lake deposit), Taseko Empress and Chita showings. The Prosperity deposit is a low-grade Cu-Au resource located approximately 30 km north of field area (Caira *et al.*, 1995). It is hosted in quartz diorite and Early Cretaceous andesite, which are typically associated with quartz-feldspar porphyry dikes (Caira *et al.*, 1995).

The Prosperity deposit displays many similarities to the study area, including the presence of potassically altered rock (characterized by replacement of mafic minerals

by biotite), the development of propylitic and phyllic alteration zones, and possibly a similar age of mineralization.

The Twin Creek area hosts several mineral occurrences previously identified by McLaren (1990). Anomalous Cu, Mo and Au values have been identified from prospecting and stream sediment samples. Many of the anomalous Au values have been found proximal to the Twin Creek fault. Whether the mineralization has any relation to the fault has yet to be determined and is a topic of ongoing research.

Continuing research will include extensive U-Pb and Ar/Ar dating of rock units and fault zone materials, in order to better constrain dates of both deformation and mineralization. For example, what is the role of deformation in localizing and/or offsetting mineralization in the field area? Detailed studies of rock types, mineralization and alteration assemblages in both mineralized areas and fault zones will be carried out in an attempt to determine any relationship that exists between fault zone fluids and mineralizing fluids. Samples from fault zones will also be further studied, in order to better understand the kinematics of fault movement and the physical conditions of deformation.

ACKNOWLEDGMENTS

The authors would like to thank Galore Resources Inc. and Geoscience BC for their support in funding the project.

REFERENCES

- Caira, N.M., Findlay, A., DeLong, C. and Rebagliati, C.M. (1995): Fish Lake copper-gold deposit, central British Columbia; unpublished company report, *Taseko Mines Limited*.
- Garver, J.L. (1992): Provenance of Albian-Cenomanian rocks of the Methow and Tyaughton basins, southern British Columbia: a mid-Cretaceous link between North America and the Insular Terrane; *Canadian Journal of Earth Sciences*, volume 29, pages 1274–1295.
- Israel, S. and Kennedy, L. (2001): Structural and stratigraphic relationships within the Tchaikazan River area, southwestern British Columbia: implications for the tectonic evolution of the southern Coast Belt; unpublished MSc thesis, *University of British Columbia*, Vancouver, BC.
- Israel, S., Schiarizza, P., Kennedy, L.A., Friedman, R.M. and Villeneuve, M. (in press): Evidence for Early to Late Cretaceous, sinistral deformation in the Tchaikazan River area, southwestern British Columbia: implications for the evolution of the southeastern Coast Belt; in Evidence for Major Lateral Displacements in the North American Cordillera, Haggart, J.W., Enkin, R.J. and Monger, J.W.H., Editors, *Geological Association of Canada*, Special Paper 46.
- Journeay, J.M. and Friedman, R.M. (1993): The Coast Belt thrust system: evidence of Late Cretaceous shortening in southwestern British Columbia; *Tectonics*, volume 12, pages 756–775.
- Leitch, C.H.B., van der Heyden, P., Godwin, C.L., Armstrong, R.L. and Harakel, J.E. (1991): Geochronometry of the Bridge River camp, southwestern British Columbia; *Canadian Journal of Earth Sciences*, volume 28, pages 195–208.
- McLaren, G.P. (1990): A mineral resource assessment of the Chilko Lake planning area; *BC Ministry of Energy, Mines and Petroleum Resources*, Bulletin 81, 117 pages.
- Monger, J.H.W. and Journeay, J.M. (1994): Guide to the geology and tectonic evolution of the southern Coast Mountains; *Geological Survey of Canada*, Open File 2490, 81 pages.

- Mustard, P.S. and van der Heyden, P. (1994): Stratigraphy and sedimentology of the Tatla Lake – Bussel Creek map areas, west-central British Columbia; in Current Research 1994-A, *Geological Survey of Canada*, pages 95-104.
- Mustard, P.S. and van der Heyden, P. (1997): Geology of Tatla Lake (92N/15) and the east half of Bussel Creek (92N/14) map areas; in Interior Plateau Geoscience Project: Summary of Geological, Geochemical and Geophysical Studies, Diakow, L.J. and Newell, J.M., Editors, *Geological Survey of Canada*, Open File 3448, pages 103-118.
- Rusmore, M.E. and Woodsworth, G.J. (1991): Distribution and tectonic significance of Upper Triassic terranes in the eastern Coast Mountains and adjacent Intermontane Belt, British Columbia; *Canadian Journal of Earth Sciences*, volume 28, pages 532-541.
- Rusmore, M.E. and Woodsworth, G.J. (1994): Evolution of the eastern Waddington Thrust Belt and its relation to the mid-Cretaceous Coast Mountains arc, western British Columbia; *Tectonics*, volume 13, pages 1052-1067.
- Rusmore, M.E., Woodsworth, G.J. and Gehrels, G.E. (2000): Late Cretaceous evolution of the eastern Coast Mountains, Bella Coola, British Columbia; in Stowell, H.H., and McClelland, W.C., Editors, Tectonics of the Coast Mountains, Southeastern Alaska and British Columbia, *Geological Society of America*, Special Paper 343.
- Schiarizza, P., Gaba, R.G., Glover, J.K., Garver, J.I. and Umhoefer, P.J. (1997): Geology and mineral occurrences of the Taseko – Bridge River area; *BC Ministry of Energy, Mines and Petroleum Resources*, Bulletin 100, 291 pages.
- Umhoefer, P.J., Rushmore, M.E. and Woodsworth, G.J. (1994): Contrasting tectonostatigraphy and structure in the Coast Belt near Chilko Lake, British Columbia: unrelated terranes or an arc – back-arc transect?; *Canadian Journal of Earth Sciences*, volume 31, pages 1700-1713.
- Umhoefer, P.J., and Schiarizza, P. (1996): Latest Cretaceous to Early Tertiary dextral strike-slip faulting on the southeastern Yalakom fault system, southeastern Coast Belt, British Columbia; *Geological Society of America Bulletin*, volume 108, pages 768-785.
- van der Heyden, P., Mustard, P. and Friedman, R. M. (1994): Northern continuation of the Eastern Waddington thrust belt and Tyaughton trough, Tatla Lake – Bussel Creek map areas, west-central British Columbia; in Current Research 1994-A, *Geological Survey of Canada*, pages 87-94.

Mountain Pine Beetle Infestation Area (Parts of NTS 082, 092, 093), Central British Columbia: Regional Geochemical Data Repository Project¹

by W. Jackaman²

KEYWORDS: mountain pine beetle, mineral exploration, geochemistry, multi-element, multimedia, GIS, database

INTRODUCTION

A large area in central British Columbia has been infested by the mountain pine beetle (MPB), parts of this area have been the focus of several federal and provincial geoscience initiatives over the last 25 years (Fig 1; Struik *et al.*, 2002). Results of this work have produced a large collection of publicly available multimedia regional geochemical information. Previous projects include regional-scale stream sediment and water surveys (Lett, 2005), lake sediment and water surveys (Cook *et al.*, 1997, 1998, 1999; Jackaman, 2006; Jackaman, in press), till programs (Levson and Giles, 1997; Levson *et al.*, 2001; Plouffe *et al.*, 2001; Levson, 2002; Lett *et al.*, 2006; Paulen and Lett, 2006), biogeochemistry studies (Dunn, 1997; Cook and Dunn, 2006) plus numerous associated research activities. To date, over 22 000 regional sites have been sampled in parts of the 150 000 km² MPB infestation area (Fig 2). Survey results include in excess of 750 000 analytical determinations for a wide range of metals and pathfinder elements.

The MPB Infestation Area Regional Geochemical Data Repository Project will produce a GIS database of existing regional geochemical data and associated geospatial information. The resulting digital framework will improve access to the information for the mineral exploration industry, assist in the planning of detailed surveys and targeted studies, identify gaps in geochemical data that can be profiled for future attention, and provide long-term data management advantages.

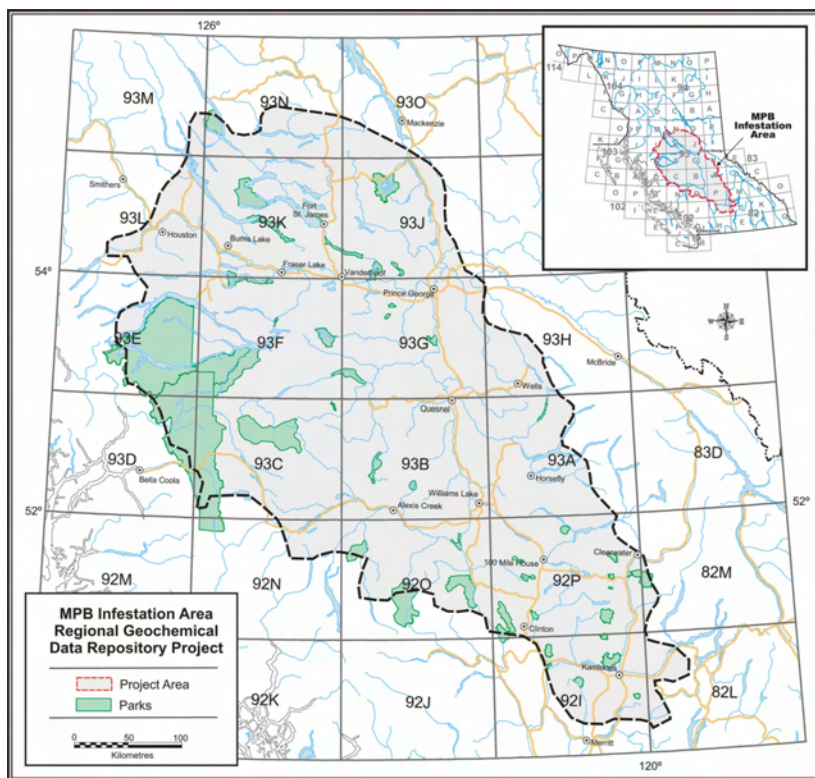


Figure 1. Location of study area, central BC.

PROJECT DESCRIPTION AND METHODOLOGY

The primary goal of this project is to consolidate this diverse data landscape into a functional data repository. The resulting framework will include valuable regional geochemical data and associated geospatial information that can be easily accessed and incorporated into a wide range of exploration and research activities. The repository will provide immediate benefits of data access, delivery and functionality.

Within the study area, in excess of 22 000 multimedia regional geochemical sample sites have been identified. Although this data is publicly available there is no central repository that provides comprehensive access to the information and associated geospatial datasets. To accomplish this task various actions are being taken. These include repository framework development and implementation; data acquisition and documentation; data compilation, profiling and quality assessment; and data manipulation and presentation.

¹Geoscience BC contribution GBC029

²Consultant, Sooke, BC

This publication is also available, free of charge, as colour digital files in Adobe Acrobat® PDF format from the BC Ministry of Energy, Mines and Petroleum Resources website at http://www.em.gov.bc.ca/Mining/Geosurv/Publications/catalog/cat_fldwk.htm

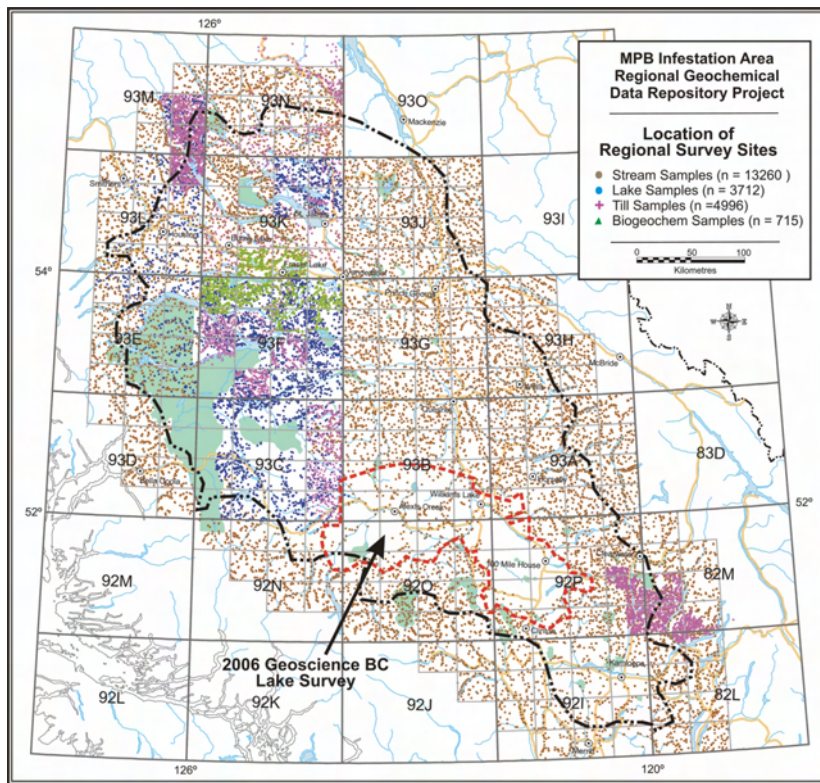


Figure 2. Location of various regional geochemical sample sites in the study area, central BC.

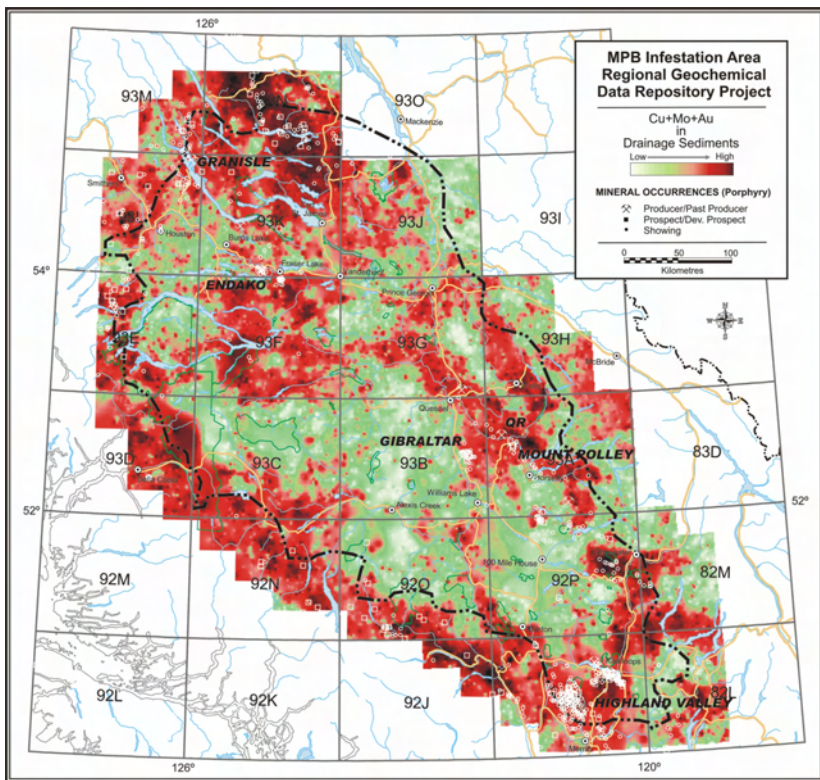


Figure 3. Distribution of Cu+Mo+Au in drainage sediment samples in the study area, overlain by known porphyry mineral occurrences (MINFILE, 2006), central BC.

The initial stage of the project is to establish a digital framework that will provide easy access to the repository and improved functionality of the multifaceted geochemical information. This structure must meet the needs of a client base with a wide range of computer expertise and also be compatible with common GIS applications. In addition, future repository updates and amendments must be easily accomplished.

Secondly, potential data source agencies and data custodians have been contacted to establish access to the most recent versions of their datasets. This will provide an opportunity to acquire and generate a complete and accurate inventory and understanding of the information and its attributes including data history, features and limiting factors.

Once the collected information has been assembled into the digital framework, quality assurance checks will be conducted to ensure data is accurate and complete. At this point, attribute relationships can be defined between datasets and initial data manipulations can proceed. The merging of the geochemical data with digital topographic and other geospatial base maps within a GIS environment will enable the production of a wide range of regional thematic maps of the study area. For example, Figure 3 represents the distribution of Cu+Mo+Au in 16 000 drainage sediment samples. Overlying the contoured geochemical map image are known porphyry occurrences that were extracted from the provincial mineral inventory (MINFILE, 2006) database.

DATA DELIVERY

To demonstrate the utility of the collection, a number of thematic maps will be produced in a style similar to a geochemical atlas. The initial series of maps plus the first version of raw geochemical data, statistical summaries and associated geospatial data coverage will be presented on a CD and distributed at the Cordilleran Roundup in Vancouver, BC, in 2007. The compilation will also be made available on the ministry's MapPlace website (BC Geological Survey, 2006).

ACKNOWLEDGMENTS

The author wishes to acknowledge Geoscience BC for project support, the contributions being made by the various data custodians and Ray Lett for his editorial comments.

REFERENCES

- BC Geological Survey (2006): MapPlace GIS internet mapping system; *BC Ministry of Energy, Mines and Petroleum Resources*, MapPlace website, URL <<http://www.MapPlace.ca>>.
- Cook, S.J. and Dunn, C.E. (2006): Preliminary results of the Cordilleran geochemistry project: a comparative assessment of soil geochemical methods for detecting buried mineral deposits, 3Ts Au-Ag prospect (NTS 93F/3), central British Columbia; in *Geological Fieldwork 2005, BC Ministry of Energy, Mines and Petroleum Resources*, Paper 2006-1 and *Geoscience BC*, Report 2006-1, pages 237–257.
- Cook, S.J., Jackaman, W., Lett, R.E.W., McCurdy, M.W. and Day, S.J. (1999): Regional lake water geochemistry of parts of the Nechako Plateau, central British Columbia (93F/2, 3; 93K/9, 10, 15, 16; 93L/9, 16; 93M/1, 2, 7, 8); *BC Ministry of Energy, Mines and Petroleum Resources*, Open File 1999-5.
- Cook, S.J., Jackaman, W., McCurdy, M.W., Day, S.J. and Friske, P.W.B. (1997): Regional lake sediment and water geochemistry of part of the Fort Fraser map area, British Columbia (93K/9, 10, 15, 16); *BC Ministry of Energy, Mines and Petroleum Resources*, Open File 1996-15.
- Cook, S.J., Lett, R.E.W., Levson, V.M., Jackaman, W., Coneys, A.M. and Wyatt, G.J. (1998): Regional lake sediment and water geochemistry of the Babine porphyry belt, central British Columbia (93L/9, 16; 93M/1, 2, 7, 8); *BC Ministry of Energy, Mines and Petroleum Resources*, Open File 1997-17.
- Dunn, C.E. (1997): Biogeochemical surveys in the Interior Plateau of British Columbia; in *Interior Plateau Geoscience Project: Summary of Geological, Geochemical and Geophysical Studies*, Diakow, L.J. and Newell, J.M., Editors, *Geological Survey of Canada*, Open File 3448 and *BC Ministry of Energy, Mines and Petroleum Resources*, Paper 1997-2, pages 205–218.
- Jackaman, W. (2006): Regional drainage sediment and water geochemistry of part of the Nechako River and Anahim Lake map areas (NTS 93C and 93F); *Geoscience BC*, Report 2006-4.
- Jackaman, W. (in press): South Nechako Basin and Cariboo Basin Lake sediment geochemical survey (parts of NTS map sheets 92O, 92P, 93A and 93B); *Geoscience BC*.
- Lett, R.E.W. (2005): Regional geochemical survey database on CD; *BC Ministry of Energy, Mines and Petroleum Resources*, Geofile 2005-17.
- Lett, R.E.W., Cook, S.J. and Levson, V. (2006): Till geochemistry of the Chilanko Forks, Chezacut, Clusko River and Toil Mountain map areas, British Columbia (NTS 93C/1, 8, 9 and 16); *BC Ministry of Energy, Mines and Petroleum Resources*, Geofile 2006-01.
- Levson, V.M. (2002). Quaternary geology and till geochemistry of the Babine porphyry copper belt, British Columbia (NTS 93 L/9,16,M/1,2,7,8); *BC Ministry of Energy, Mines and Petroleum Resources*, Bulletin 110, 278 pages.
- Levson, V.M. and Giles, T.R. (1997): Quaternary geology and till geochemistry studies in the Nechako and Fraser plateaus, central British Columbia (NTS 93C/1, 8, 9, 10; F/2, 3, 7; L/16; M/1); in *Interior Plateau Geoscience Project: Summary of Geological, Geochemical and Geophysical Studies*, Diakow, L.J. and Newell, J.M., Editors, *Geological Survey of Canada*, Open File 3448 and *BC Ministry of Energy, Mines and Petroleum Resources*, Paper 1997-2, pages 121–147.
- Levson, V.M., Mate, D., Stumpf, A.J. and Stewart, A. (2001): Till geochemistry of the Tetachuck Lake and Marilla map areas (NTS 93 F/5 and F/12); *BC Ministry of Energy, Mines and Petroleum Resources*, Open File 2001-15.
- MINFILE (2006): MINFILE BC mineral deposits database; *BC Ministry of Energy, Mines and Petroleum Resources*, URL <<http://www.em.gov.bc.ca/Mining/Geosurv/Minfile/>> [November 2006].
- Paulen, R.C. and Lett, R.E.W. (2006): Till geochemistry: a viable tool for polymetallic mineral exploration in British Columbia's southern interior; *BC Ministry of Energy, Mines and Petroleum Resources*, Geofile 2005-18.
- Plouffe, A., Levson, V.M. and Mate, D.J. (2001): Till geochemistry of the Nechako River map area (NTS 93F), central British Columbia; *Geological Survey of Canada*, Open File 4166, 66 pages.
- Struik, L.C., MacIntyre, D. and Hastings, N.L. (2002): Geochemistry data, Nechako NATMAP project; *Geological Survey of Canada*, Open File 4356 and *BC Ministry of Energy, Mines and Petroleum Resources*, Paper 2001-9, 1 CD-ROM.

South Nechako Basin and Cariboo Basin Lake Sediment Geochemical Survey (Parts of NTS 092N, O, P; 093A, B), Central British Columbia¹

by W. Jackaman² and J.S. Balfour³

KEYWORDS: Nechako Basin, Cariboo Basin, mineral exploration, geochemistry, multi-element, lake sediment, lake water, epithermal, gold, molybdenum, copper, porphyry deposit

INTRODUCTION

Within the mountain pine beetle (MPB) infestation area of central British Columbia there has been a significant gap in regional geochemical survey (RGS) coverage (Fig 1). Although this 18 000 km² region was included in previous RGS stream sediment programs, subdued topography and poor drainage limited the availability of suitable stream sample sites. In fact, large parts of the surveyed areas have not been sampled. As a result, sampling had been limited to 385 stream sites and the average sample density was only one site every 47 km². In order to expand the first level sample density of this region, a total of 1370 lakes were sampled as part of the 2006 south Nechako Basin and Cariboo Basin lake sediment and water geochemical survey.

The results of this survey will provide access to new regional lake sediment and water geochemical information in an underexplored and geologically poorly understood region of the MPB infestation area. The work will significantly enhance existing geochemical information, and complement other ongoing geoscience initiatives and future projects. It also provides immediate economic opportunities to local service providers and potential long-term benefits from increased mineral and oil and gas exploration.

SURVEY AREA DESCRIPTION

Within the MPB infestation zone, the 2006 survey covers approximately 18 000 km² of the Nechako Basin, the

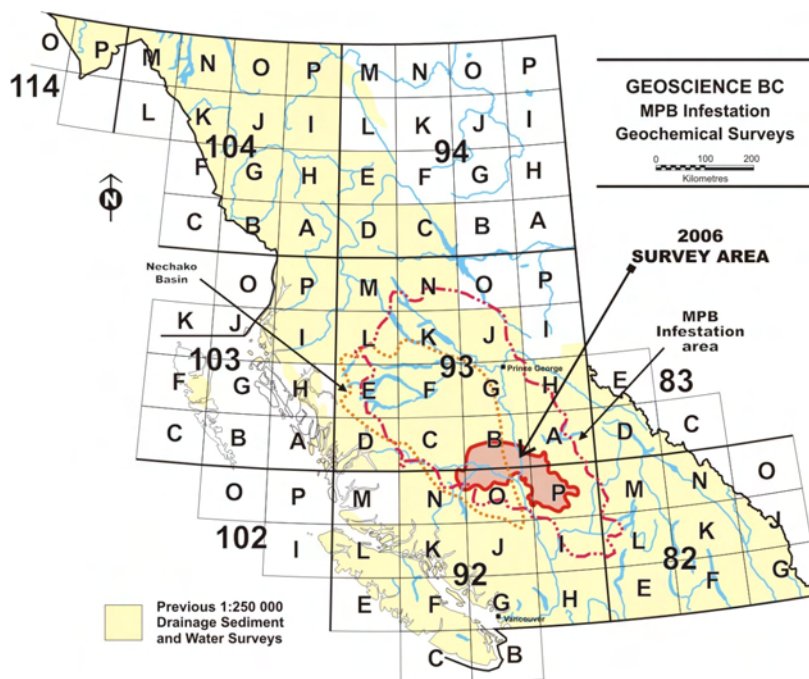


Figure 1. Location of survey area, central BC.

Fraser River Basin and the Cariboo Basin (Fig 2). Straddling highways 20 and 97, the project area extends southeast from Puntzi Lake to 70 Mile House and includes the larger communities of Williams Lake and 100 Mile House. The relatively subdued topography varies from exposed grasslands to rolling hills covered with pine and spruce forests. Opportunely, the upland surfaces of the plateau are dotted with over 11 000 lakes and ponds, including 6500 potential sample sites, ranging in size from 4000 to 400 000 m² (Fig 3).

Extensive Tertiary to recent volcanic flows and thick glacial deposits cover much of the survey area. Underlying this material are Middle Jurassic to Tertiary marine and nonmarine sedimentary and lesser volcanic rocks. East of the project area, Late Triassic to Early Jurassic Cache Creek Group and Permian to Triassic Quesnel Terrane rocks can be found.

Within the survey area, the MINFILE database (MINFILE, 2006) lists only 12 metallic mineral occurrences. The most notable is a Cu±Mo±Au porphyry prospect named Newton (MINFILE 092O 050). Adjacent to the region are several significant porphyry deposits such as producing mines Mount Polley (MINFILE 093A 008) and Gibraltar (MINFILE 093B 012) plus developed prospects

¹Geoscience BC contribution GBC030

²Consultant, Sooke, BC

³Consultant, Cranbrook, BC

This publication is also available, free of charge, as colour digital files in Adobe Acrobat® PDF format from the BC Ministry of Energy, Mines and Petroleum Resources website at http://www.em.gov.bc.ca/Mining/Geolsurv/Publications/catalog/cat_fldwk.htm

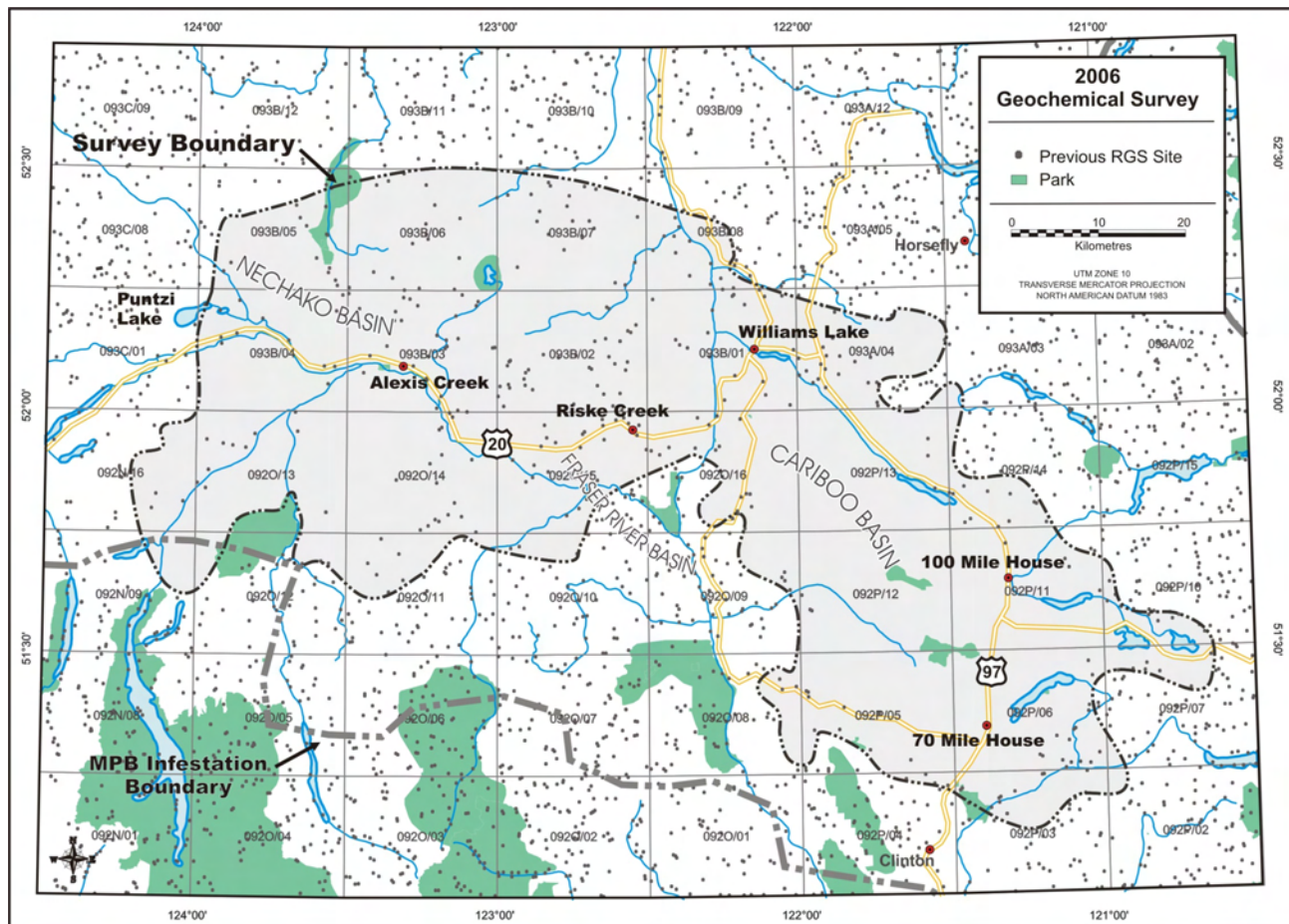


Figure 2. Detailed location map showing south Nechako Basin and Cariboo Basin survey area, central BC.

Prosperity (MINFILE 092O 041) and Frasersgold (MINFILE 093A 150). Other local targets include polymetallic veins represented by the Pellaire developed prospect (MINFILE 092O 045) and epithermal precious metal deposits such as the Blackdome mine (MINFILE 092O 053) and skarn mineralization found at the Spout Lake developed prospect (MINFILE 092P 120).

sediment and water samples were routinely collected in each analytical block of 20 samples.

SURVEY METHODS AND SPECIFICATIONS

Methods and specifications are based on standard lake sediment geochemical survey strategies used elsewhere in Canada for the National Geochemical Reconnaissance (NGR) program (Friske, 1991), as well as prior orientation studies and regional lake sediment surveys completed in BC (Cook, 1997; Jackaman, 2006).

Helicopter-supported sample collection was carried out in August 2006, during which 1445 lake sediment and water samples were systematically collected from 1370 sites. Average sample site density was one site per 13 km² over the 18 000 km² survey area. Field duplicate



Figure 3. Typical lake sample site located in southeastern Nechako Basin, central BC. The extent of mountain pine beetle kill can be seen by the number of orange to brown trees.

Lake sites were accessed using a float-equipped Bell Jet Ranger helicopter. The sampling crews collected sediment material with a torpedo-style sampler, and water samples were saved in 250 mL bottles. Samples were successfully collected from most of the lakes targeted in the survey area. However, some of the smaller ponds were not sampled due to poor sampling conditions, and samples were not collected from several very large and deep lakes. In general, lake bottom samples sent for analysis represent a 35 cm section of material obtained from below the water-sediment interface. Samples typically consisted of organic gels with varying amounts of inorganic sediment and organic matter. Field observations and site locations were recorded for each site.

After drying, each sample will be pulverized in a ceramic ring mill to approximately -150 mesh (100 µm), and two analytical splits are extracted from the material. To monitor and assess accuracy and precision of analytical results, control reference material and analytical duplicate samples are routinely inserted into each block of 20 sedi-

ment samples. The sediment samples will be analyzed for base and precious metals, pathfinder elements and rare earth elements by instrumental neutron activation analysis (INAA) and inductively coupled plasma mass spectrometry (ICP-MS). Loss-on-ignition and fluorine will also be determined for sediment material. Fluoride, conductivity and pH will be determined for the water samples. A complete list of elements and analytical detection limits is provided in Tables 1 and 2.

RELEASE DETAILS

Reconnaissance-scale drainage sediment and water surveys are recognized as an important mineral exploration tool. Results from these types of activities are directly responsible for follow-up mineral exploration that is valued in the millions of dollars and has been credited with the discovery of numerous mineral prospects. Results from the 2006 survey will stimulate mineral exploration by presenting new geochemical information for an underexplored area that is considered to have a high potential for future discoveries.

Survey results will be compiled into a traditional RGS-style data package that will include survey descriptions and

TABLE 1. DETECTION LIMITS FOR SEDIMENT SAMPLES ANALYZED BY INDUCTIVELY COUPLED PLASMA MASS SPECTROMETRY (ICP-MS).

Element	Detection	
	limit	Units
aluminum	Al	0.01 %
antimony	Sb	0.02 ppm
arsenic	As	0.1 ppm
barium	Ba	0.5 ppm
bismuth	Bi	0.02 ppm
cadmium	Cd	0.01 ppm
calcium	Ca	0.01 %
chromium	Cr	0.5 ppm
cobalt	Co	0.1 ppm
copper	Cu	0.01 ppm
gallium	Ga	0.2 ppm
iron	Fe	0.01 %
lanthanum	La	0.5 ppm
lead	Pb	0.01 ppm
magnesium	Mg	0.01 %
manganese	Mn	1 ppm
mercury	Hg	5 ppb
molybdenum	Mo	0.01 ppm
nickel	Ni	0.1 ppm
phosphorus	P	0.001 %
potassium	K	0.01 %
scandium	Sc	0.1 ppm
selenium	Se	0.1 ppm
silver	Ag	2 ppb
sodium	Na	0.001 %
strontium	Sr	0.5 ppm
sulphur	S	0.02 %
tellurium	Te	0.02 ppm
thallium	Tl	0.02 ppm
thorium	Th	0.1 ppm
titanium	Ti	0.001 %
tungsten	W	0.1 ppm
uranium	U	0.1 ppm
vanadium	V	2 ppm
zinc	Zn	0.1 ppm

TABLE 2. DETECTION LIMITS FOR SEDIMENT SAMPLES ANALYZED BY INSTRUMENTAL NEUTRON ACTIVATION ANALYSIS (INAA), LOSS-ON-IGNITION (LOI) AND FLUORINE (F), AND FLUORIDE, CONDUCTIVITY AND PH OF WATER SAMPLES.

Analytical parameter	Detection	
	limit	Units
antimony	Sb	0.1 ppm
arsenic	As	0.5 ppm
barium	Ba	50 ppm
bromine	Br	0.5 ppm
cerium	Ce	5 ppm
cesium	Cs	0.5 ppm
chromium	Cr	20 ppm
cobalt	Co	5 ppm
europium	Eu	1 ppm
gold	Au	2 ppb
hafnium	Hf	1 ppm
iron	Fe	0.2 %
lanthanum	La	2 ppm
lutetium	Lu	0.2 ppm
rubidium	Rb	5 ppm
samarium	Sm	0.1 ppm
scandium	Sc	0.2 ppm
sodium	Na	0.02 %
tantalum	Ta	0.5 ppm
terbium	Tb	0.5 ppm
thorium	Th	0.2 ppm
tungsten	W	1 ppm
uranium	U	0.2 ppm
ytterbium	Yb	2 ppm
sample weight	Wt	0.01 g
fluorine	F	10 ppm
loss-on-ignition	LOI	0.1 %
pH	pH	
conductivity	CND	0.01 uS

details regarding methods; analytical and field data listings; summary statistics; sample location maps; and maps for individual elements. The publications will be released as PDF files on a CD and will include all raw digital data files used in the production process. The package will be made available to the public in the spring of 2007. At this time, the digital data will be available on the ministry's MapPlace website (BC Geological Survey, 2006).

ACKNOWLEDGMENTS

The authors wish to acknowledge John Faulkner for his excellent helicopter flying abilities; Laura Mitchell, Steven Reichheld, Erik Jackaman and Emma Jackaman for their tireless contributions both on the ground and in the air; the many support services located in and around the Riske Creek, Puntzi Lake and 100 Mile House communities that contributed to the completion of the survey. Ray Lett is thanked for his editorial comments and suggestions.

REFERENCES

- BC Geological Survey (2006): MapPlace GIS internet mapping system; *BC Ministry of Energy, Mines and Petroleum Resources*, MapPlace website, URL <<http://www.MapPlace.ca>>.
- Cook, S.J. (1997): Regional and property-scale application of lake sediment geochemistry in the search for buried mineral deposits in the southern Nechako Plateau area, British Columbia; in Interior Plateau Geoscience Project: Summary of Geological, Geochemical and Geophysical Studies, Diakow, L.J. and Newell, J.M., Editors, *Geological Survey of Canada*, Open File 3448 and *BC Ministry of Energy, Mines and Petroleum Resources*, Paper 1997-2, pages 175–203.
- Friske, P.W.B. (1991): The application of lake sediment geochemistry in mineral exploration; in Exploration Geochemistry Workshop, *Geological Survey of Canada*, Open File 2390, pages 4.1–4.20.
- Jackaman, W. (2006): Regional drainage sediment and water geochemistry of part of the Nechako River and Anahim Lake map areas (NTS 93C and 93F); *Geoscience BC*, Report 2006-4.
- MINFILE (2006): MINFILE BC mineral deposits database; *BC Ministry of Energy, Mines and Petroleum Resources*, URL <<http://www.em.gov.bc.ca/Mining/Geolsurv/Minfile/>> [November 2006].

ASTER Multispectral Satellite Imagery and Product Coverage, British Columbia – Phase 2¹

by W.E. Kilby² and C.E. Kilby²

KEYWORDS: MapPlace, ASTER, KML/KMZ, image analysis

INTRODUCTION

The second phase of the ASTER Imagery for British Columbia Project, sponsored by Geoscience BC, has included increasing the quantity of Advanced Spaceborne Thermal Emission and Reflection Radiometer (ASTER) imagery available through the BC Ministry of Energy, Mines and Petroleum Resources' MapPlace website (BC Geological Survey, 2006). One hundred new images have been added to the collection for a total of 239 (Kilby *et al.*, 2004; Kilby, 2005; Kilby and Kilby, 2006) and they are available for analysis through the MapPlace's Image Analysis Toolbox (IAT). The new imagery fills in gaps between previously obtained imagery and adds coverage in areas where coverage was previously available. Every effort was made to use the latest imagery possible with a number of the images being collected in the summer of 2006. A number of adjustments have been made in the type and quality of the derivative products associated with the ASTER imagery.

The preparation of the ASTER imagery for analysis through the IAT has remained the same as described in Kilby and Kilby (2006). This includes orthorectification and atmospheric correction. The two virtual reality files have been removed from the product suite for the 100 images added during this project. The Keyhole Markup Language (KML/KMZ) file product has been improved to provide simpler delivery with better results. This modification has been made for all the ASTER imagery on the website. In response to user requests, the static mineral map images are now available for download. The static image mask described in Kilby and Kilby (2006) has been replaced by an interactive masking tool in the IAT.

The IAT now provides online image analysis capabilities for 239 ASTER images covering most of the province. The northeast portion of the province still remains sparsely covered due to the relatively low value of ASTER imagery to mineral exploration in this region. Other popular web tools such as Google Earth (Google, 2006) have made some of the earlier IAT products such as the virtual reality files somewhat redundant and they have been discontinued. The increased popularity of the KML format for spatial data de-

livery and viewing has spurred the enhancement of the KML files provided by the site.

This project provides access to a recent provincial-scale detailed dataset of multispectral imagery that can be freely downloaded or used online in conjunction with the MapPlace to identify alteration zones, geological features and new exposures. The tools in the IAT can be used to generate map images of alteration zones in areas of good exposure or prospect for alteration minerals in isolated outcrops and roadcuts.

IMAGE ANALYSIS TOOLBOX ENHANCEMENTS

Image Coverage and Processing

One hundred new ASTER images were purchased as part of this project. Two previous projects had added 139 images to the IAT. ASTER imagery for this project was obtained from the Land Processes Distributed Active Archive Center operated by the United States Geological Survey (USGS) and the National Aeronautics and Space Administration (NASA) for US\$80 per image. Selection criteria for the new imagery were 1) new area coverage, 2) minimal snow and cloud cover and 3) currency of images. Figure 1 shows the distribution of the newly added imagery and the previously existing imagery on the IAT.

The new ASTER imagery was processed in the same manner as previous years. The image data was orthorectified and atmospherically corrected. Orthorectification was performed using the AsterDTM (SulSoft, 2006) add-on to the ENVI image analysis program (ITT, 2006). The orthorectified images were then manually adjusted to fit the TRIM (Terrain Resource Inventory and Mapping) 1:20 000 scale digital base map data displayed on MapPlace. Positional problems exist with the TRIM base in some areas and some positional errors are possible with ASTER. For consistency, the ASTER images were migrated to the TRIM base.

Atmospheric corrections were performed on the VNIR (Visible and Near Infrared) and SWIR (Short Wave Infrared) bands in all the images using the ACORN5 (Atmospheric CORrection Now) program (ImSpec LLC, 2006). This program performs a pixel-by-pixel correction of the image values by removing the effect of water vapour and other gases in the atmosphere using the MOTRAN4 technology. ASTER imagery does not contain enough information to calculate the amount of water vapour found within an image, so an estimated value of 15 mm of atmospheric water was used for all images. The ground elevation is required as input to accurately estimate the thickness of atmosphere above the target area. Each image was examined and

¹Geoscience BC contribution GBC020

²Cal Data Ltd., Kelowna, BC

This publication is also available, free of charge, as colour digital files in Adobe Acrobat® PDF format from the BC Ministry of Energy, Mines and Petroleum Resources website at http://www.em.gov.bc.ca/Mining/Geosurv/Publications/catalog/cat_fldwk.htm

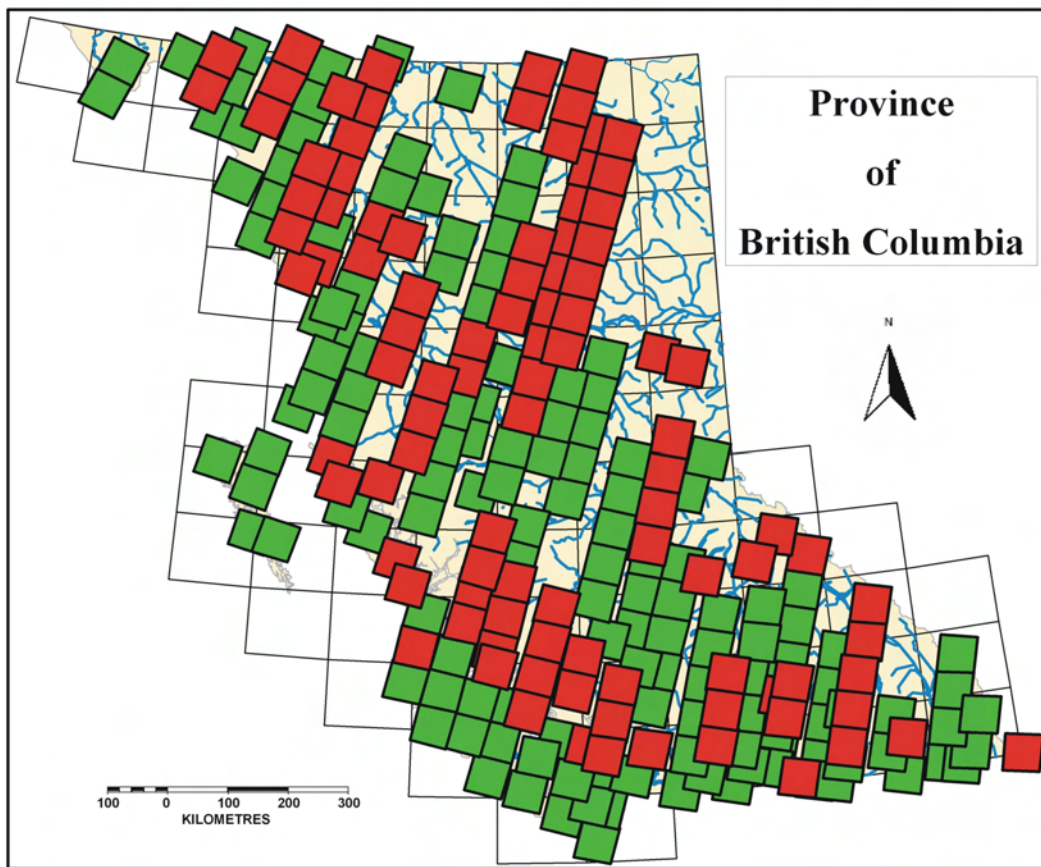


Figure 1. Display of ASTER image footprints in BC. Images added during this project are displayed in dark red and previously available images are displayed in green.

the elevation value for most of the rock exposure was used for this calculation. The atmospheric correction changes the image values from radiance to relative reflectance.

Interactive Masking Tool

The original method used to mask unwanted image pixels out of IAT calculations (Kilby and Kilby, 2006) was precalculated and had limited flexibility given the many possible analysis scenarios. For example, a single mask that included the removal of water pixels from an analysis is of little value to someone interested in looking at the water but not the vegetation or clouds. A new set of interactive masking tools have been added that allows users to apply flexible parameters to deal with variability between images and analysis targets. Figure 2 shows the layout of the masking tool available for all the ASTER analysis tools.

A mask can be built up from three components: vegetation, water and white stuff (snow, ice and clouds). The default values in the input boxes can be changed by users as they see fit. The mask is applied by checking the Apply box prior to digitizing an area of interest on the image. The masked area will appear black and not be included in any of the calculations. The vegetation value is based on the NDVI (Normalized Difference Vegetation Index) value of the pixels that range from 0 to 1. The higher this value the more vegetation (chlorophyll) must be measured in a pixel before it is masked out. Both the white stuff and water parameters use band 3 values to decide if a pixel is to be masked out. The water component masks out all pixels with

band 3 values lower than the entered value and the white stuff component masks out all pixels with band 3 values greater than the entered value. Users are encouraged to ex-

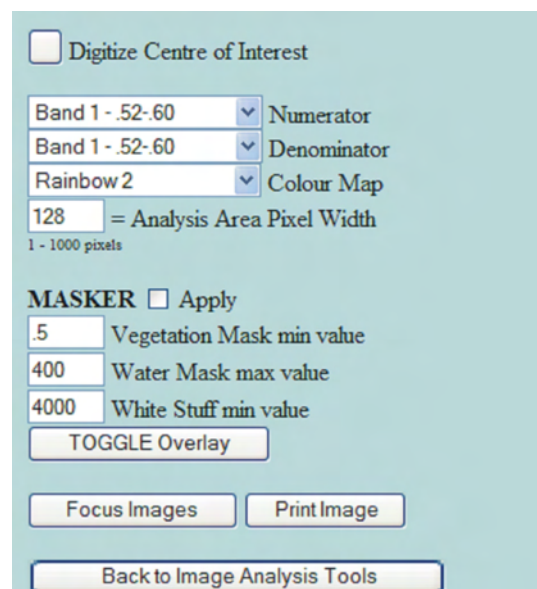


Figure 2. Masking tool layout as it appears in all tools used to analyze ASTER images in the Image Analysis Toolbox (IAT). In this case, the Two-Band Ratio tool is shown. The user can change the initial default values and check the Apply box to activate the tool.

periment with values to produce a black mask of recognizable areas, such as vegetation, water, snow and ice, and apply the mask to a specific area of interest.

Alteration Image Download

Four mineral alteration images were prepared for each ASTER image and made available within the IAT. Shortly after an earlier release of this information, users requested the download of these files for use in their own software. As a result, these files are now included on the download page. The images are in portable network graphics (PNG) format with an associated world geo-location file (PGW) and are in UTM projection. The masked-out portions of these images have been made transparent. The four images map the band ratios that have proven useful in identifying siliceous rocks, iron oxides, sericite and illite, and alunite and kaolinite. The band combinations (J.A. Zamudio, pers comm, 2005) used to calculate each of these images are

- siliceous rocks $(B10+B11+B12)/3/B13$
- sericite and illite $(B5+B7)/B6$
- alunite and kaolinite $(B4+B6)/B5$
- iron oxides $B2/B1$

Virtual Reality Removal

Virtual reality files (WRL format) were produced for the first 139 images loaded on the site. The purpose of these images was to allow users, with the appropriate viewers, to interactively fly around the 3-D terrain models. However, with the availability of easy-to-use viewers such as Google Earth, there is no longer a need for these files. ASTER-related images and products can be draped directly over the Google Earth terrain by the user, making for a very interactive viewing option. In some areas, the Google Earth terrain is not as detailed as the ASTER-derived DEM, but this is likely to change as more detailed elevation data is released.

Keyhole Markup Language (KML/KMZ) Data

The KML format has recently become very popular for distributing spatial data due largely to the success of the Google Earth KML viewer (Fig 3). A number of other viewers and GIS products now can utilize data in KML/KMZ format. KMZ format is essentially a compressed version of the KML file with a few additional capabilities. The KMZ files provided through the Google Earth

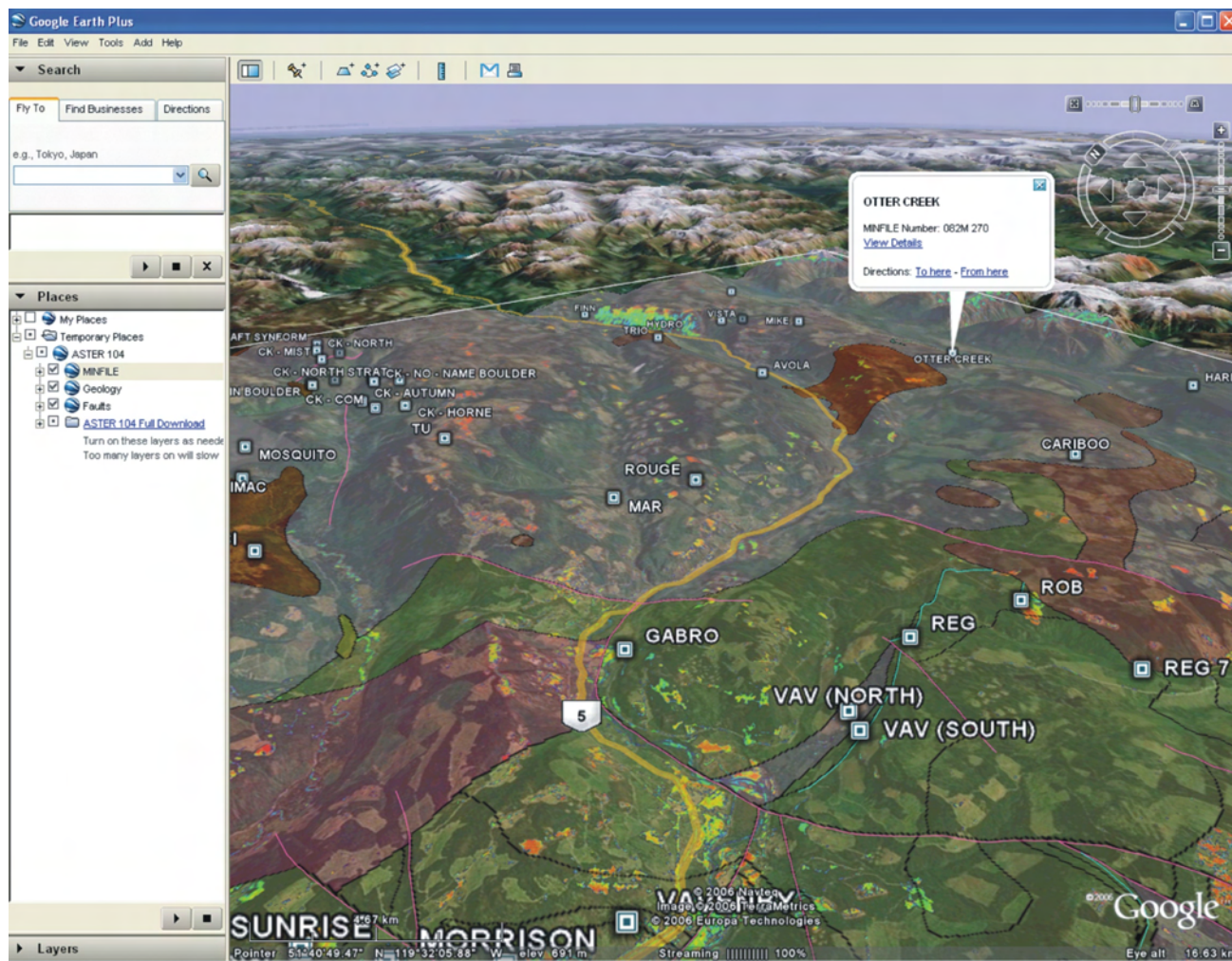


Figure 3. Example of a Google Earth view of a Keyhole Markup Language (KML/KMZ) file for a single ASTER image. Shown in the view are the geology polygons with about 50% transparency, fault lines, iron oxide mineral alteration image and MINFILE points (MINFILE, 2006).

link on the IAT have been modified to simplify their delivery and improve the resultant views.

The original six ASTER-related image overlays and the ASTER image footprint are still included in the KMZ file. These include

- a near-natural colour image
- an anaglyph image
- a siliceous rock image
- a sericite and illite image
- an alunite and kaolinite image
- an iron oxide image
- the imagery and spatial data from Google Earth.

Previously, some geology and mineral occurrence (MINFILE, 2006) information was included from the MapPlace. The delivery of this information was based on WMS (Web Map Service) technology. The result of this form of delivery was very coarse raster linework that required refreshing from the server every time the view moved. The geology consisted of fault lines and formation contacts. The MINFILE data was displayed with poor quality labelling. The WMS style of data delivery in the KMZ files has been dropped in this project in preference for including the actual linework for the faults and geology polygons (Massey *et al.*, 2005; Fig 3). As a result, the initial download may take a little longer but the resultant display is far superior. The MINFILE locations are also displayed in a more dynamic form with links to occurrence details, similar to those found on the MapPlace and MINFILE websites. Viewers such as Google Earth, WorldWind and ArcGIS Explorer or GIS systems such as Manifold and FME can read the geology and MINFILE information delivered in this format.

ACKNOWLEDGMENTS

This project was made possible by a grant from Geoscience BC. The BC Ministry of Energy, Mines and Petroleum Resources provided support in the form of internet hosting of the project products on the MapPlace website (www.MapPlace.ca).

The authors would like to thank Larry Jones and Pat Desjardins for their thorough review of this paper and useful suggestions.

REFERENCES

- BC Geological Survey (2006): MapPlace GIS internet mapping system; *BC Ministry of Energy, Mines and Petroleum Resources*, MapPlace website, URL <<http://www.MapPlace.ca>> [November 2006].
- Google (2006): Google Earth, global internet viewer of imagery and vector information; *Google*, URL <earth.google.com> [October 2006].
- ImSpec LLC (2006): ACORN5, atmospheric correction software; *ImSpec LLC*, URL <www.imspec.com> [October 2006].
- ITT (2006): ENVI, image analysis software package; *ITT*, Version 4.3, URL <www.ittvis.com> [October 2006].
- Kilby, W.E. (2005): MapPlace.ca image analysis toolbox – phase 2; in *Geological Fieldwork 2004*, *BC Ministry of Energy, Mines and Petroleum Resources*, Paper 2005-1, pages 231–235.
- Kilby, W.E. and Kilby, C.E. (2006): ASTER imagery for BC – an online exploration resource; in *Geological Fieldwork 2005*, *BC Ministry of Energy, Mines and Petroleum Resources*, Paper 2006-1 and *Geoscience BC*, Report 2006-1, pages 287–294.
- Kilby, W.E., Kliparchuk, K. and McIntosh, A. (2004): Image analysis toolbox and enhanced satellite imagery integrated into the MapPlace; in *Geological Fieldwork 2003*, *BC Ministry of Energy, Mines and Petroleum Resources*, Paper 2004-1, pages 209–215.
- Massey, N.W.D., MacIntyre, D.G., Desjardins, P.J. and Cooney, R.T. (2005): Digital geology map of British Columbia: whole province; *BC Ministry of Energy, Mines and Petroleum Resources*, GeoFile 2005-1.
- MINFILE (2006): MINFILE BC mineral deposits database; *BC Ministry of Energy, Mines and Petroleum Resources*, URL <<http://www.em.gov.bc.ca/Mining/Geolsurv/Minfile/>> [November 2006].
- SulSoft (2006): AsterDTM, ASTER orthorectification software; *SulSoft*, Version 2.2, URL <www.envi.com.br/asterdtm/english/index.htm> [October 2006].

Ultramafic Rock Occurrences in the Jurassic Bonanza Arc near Port Renfrew (NTS 092C/09, 10, 15, 16), Southern Vancouver Island¹

by J. Larocque² and D. Canil²

KEYWORDS: Wrangellia, Vancouver Island, mapping, arc, plutons, ultramafic rocks

INTRODUCTION

Igneous rocks of Jurassic age on Vancouver Island, British Columbia represent an obliquely tilted section of island arc crust called the Bonanza arc. The structural depth of rocks exposed is currently uncertain. Recently, several isolated bodies of ultramafic rock were recognized by G. Pearson, a local prospector, within what are presumed to be the deeper levels of the arc in the area of Port Renfrew. Ultramafic rock outcrops, in many cases, correspond to strong anomalies in the regional aeromagnetic pattern, as well as soil anomalies for nickel and chromium in nearby streams. The extent to which ultramafic rocks are present in the Bonanza arc is potentially very significant, as they may be prospective for nickel and platinum group elements. During the summer of 2006, a field study was conducted as part of the first author's MSc thesis, in order to ascertain the extent of the ultramafic bodies, to determine their relationship to other rocks of the Bonanza arc and to address their economic potential.

FIELD AREA

The field area (Fig 1) is located approximately a two-hour drive northwest of Victoria, BC. The field area is bordered by the San Juan River in the south, Cowichan Lake in the north, Lake Nitinat and the Nitinat River to the west and northwest and the Fleet River to the east. Access to the area is provided by a network of variably maintained logging roads. Many of the roads that once accessed some of the more elevated, remote areas are badly overgrown. Overall, rock exposures are mainly concentrated along active logging roads. Exposure is best in elevated areas that have recently been logged.

REGIONAL GEOLOGY

Most of Vancouver Island is underlain by rocks of Wrangellia as originally defined by Jones *et al.* (1977). The



Figure 1. Southern Vancouver Island, showing the field area of the present study (as outlined above). The grid outlines NTS sheets 092C, 092F, 092G and 092B (clockwise from lower left).

Sicker Group forms the basement to Wrangellia on Vancouver Island, and consists of mafic and felsic volcanic and volcanoclastic rocks, overlain by epiclastic and carbonate sediments of the Permian Buttle Lake Group (Massey and Friday, 1987). The Sicker Group is interpreted as an island arc that was active from Devonian to Permian time (Greene *et al.*, 2005). Overlying the Sicker Group are the Triassic Karmutsen basalt, a thick (~2500 m) sequence of subaqueous pillow lava, overlain by a few hundred metres of pillow breccia, which are themselves topped by another thick (~3000 m) sequence of subaerial sheet flows (Nixon *et al.*, 1993). The Karmutsen flood basalts may be an emergent ocean island built upon the extinct Sicker island arc (Greene *et al.*, 2005). Conformably overlying the Karmutsen basalt is a thin (<75 m) sequence of micritic limestone called the Quatsino Formation, which is itself conformably overlain by the Parsons Bay Formation, a 35 m thick sequence of thinly bedded argillaceous mudstone, limestone, siltstone and sandstone (Massey and Friday, 1987; Nixon *et al.*, 1995). The Jurassic Bonanza arc intrudes, as well as unconformably overlies, older units of Wrangellia.

Jurassic Bonanza Arc

In the field area, rocks of the Bonanza arc are separated from the Jurassic-Cretaceous Pacific Rim Terrane to the south by the San Juan fault and from the Sicker Group to the north by the Cowichan fault. The Jurassic-aged rocks of

¹Geoscience BC contribution GBC 033

²School of Earth and Ocean Sciences, University of Victoria, Victoria, BC

This publication is also available, free of charge, as colour digital files in Adobe Acrobat® PDF format from the BC Ministry of Energy, Mines and Petroleum Resources website at http://www.em.gov.bc.ca/Mining/GeolSurv/Publications/catalog/cat_fldwk.htm

Wrangellia on Vancouver Island have been recognized as the products of island arc magmatism, based on petrology and geochemistry (Isachsen, 1987; DeBari *et al.*, 1999). From base to top, these units include the West Coast Crystalline Complex, the Island Plutonic suite and the Bonanza Group volcanic rocks. Rocks in the field area have undergone zeolite to locally greenschist facies metamorphism, but the original igneous lithologies are used in their descriptions.

WEST COAST CRYSTALLINE COMPLEX

The West Coast Crystalline Complex has been interpreted as the deepest-preserved level of the Jurassic arc, based on its intrusive relationship with country rock that most often belongs to the Sicker Group (DeBari *et al.*, 1999). Sicker Group rocks, however, were not encountered anywhere in the field area south of Cowichan Lake. Plutonic margins in the West Coast Crystalline Complex tend to be concordant with the country rocks (DeBari *et al.*, 1999).

The complex is dominated by melanocratic to leucocratic quartz diorite and gabbro containing varying amounts of hornblende, biotite, orthopyroxene and clinopyroxene. Grain sizes vary locally from fine grained to pegmatitic. As noted by DeBari *et al.* (1999), West Coast Crystalline Complex diorite commonly contains inclusions of finer-grained mafic rock that range from well-defined, angular shapes to faint, wispy lenticular bodies. As well as sporadic granitoid intrusions, outcrops of diabase are found locally in the West Coast Crystalline Complex in the field area, southwest of the Gordon River. Directly to the north, two distinct bands of light grey marble occur as septa in the diorite. Similar marble outcrops are found in the eastern part of the field area, although these are more irregular in outcrop pattern. Minor magnetite-rich skarn bodies, with variably-developed diopside-garnet assemblages, are found at the contact with the marble. Due to the metamorphosed nature of these carbonate rocks, they are suggested to represent fragments and/or faulted slices of the Buttle Lake Formation, as opposed to recrystallized Quatsino limestone. Most significantly, the West Coast Crystalline Complex contains bodies of ultramafic rock, which are further described below.

Foliations within the West Coast Crystalline Complex, defined by planar fabric of hornblende, biotite or plagioclase, strike northwest and dip 60 to 75° degrees to the southwest. Roughly in the middle of the field area, a large area of Karmutsen basalt is juxtaposed with the West Coast Crystalline Complex along a shear zone with the same attitude as the pervasive foliation in the diorite. Shear zones defined by mylonite horizons within the West Coast Crystalline Complex have a similar orientation in the westernmost parts of the field area. The common orientation and sense of shear (tops to the northeast) for all these shear zones suggest that the West Coast Crystalline Complex is a series of east-verging thrust-faulted panels, the easternmost one of which has been thrust onto the overlying Karmutsen basalt.

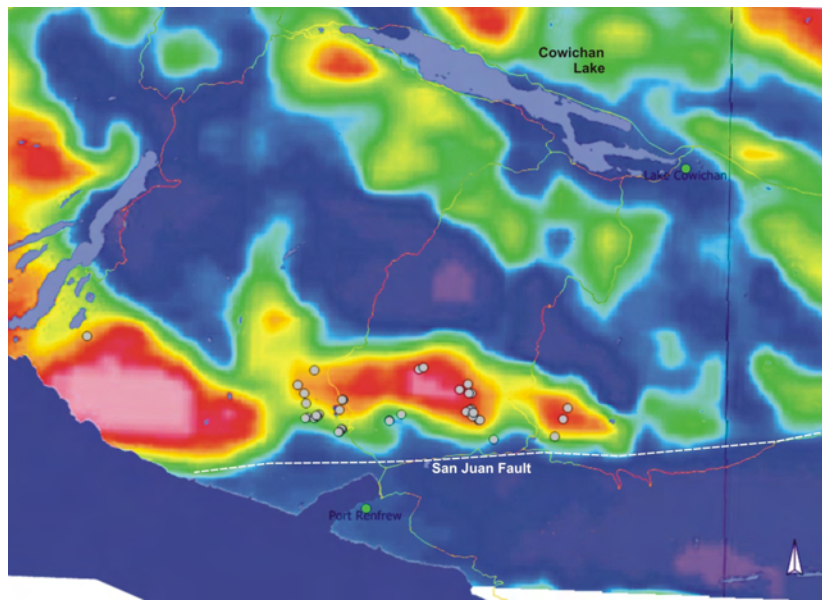


Figure 2. Regional aeromagnetic anomaly map of the field area (BC Geological Survey, 2006). Circles show locations of ultramafic-cumulate gabbro in outcrop.

Regional-scale aeromagnetic data available for southern Vancouver Island (Fig 2) shows a prominent magnetic high, running parallel to, and extending north from the San Juan fault. At this resolution, the magnetic anomaly appears to roughly correspond with areas underlain by West Coast Crystalline Complex rocks, but deviations from this general trend exist.

ISLAND PLUTONIC SUITE

The Island Plutonic suite occurs as a roughly north-west-southeast aligned series of plutons ranging from quartz diorite to alkali feldspar granite. As noted by DeBari *et al.* (1999), the Island Plutonic suite most commonly intrudes the Triassic Karmutsen basalt and is distinguished from plutons of similar composition of the West Coast Crystalline Complex by lacking any foliation (Muller *et al.*, 1981). Except where faulted, the contact between the Island Plutonic suite and the West Coast Crystalline Complex is not well defined. In the field area, rocks of the Island Plutonic suite occur mainly in the northern and eastern parts of the field area, separated from the West Coast Crystalline Complex to the southwest by intervals of Karmutsen basalt and Quatsino limestone.

BONANZA GROUP VOLCANIC ROCKS

The Bonanza Group volcanic rocks are only very weakly metamorphosed, displaying assemblages indicative of the zeolite facies (Massey and Friday, 1987) and vary from aphanitic basalt, through plagioclase, pyroxene and/or hornblende-phyric andesite to minor dacite. In addition to massive flows, the Jurassic volcanic rocks are also encountered as pillowed flows and flow breccia. Lesser pyroclastic deposits have been noted, with rhythmic banding of aphanitic felsic and mafic ash flows and fall deposits. The lateral extent and continuity of these deposits is obscured by vegetation and overburden. Similar rocks were noted by Nixon *et al.* (1995) in the Quatsino Sound region of northern Vancouver Island.

ULTRAMAFIC ROCKS

Previous Occurrences

Isachsen (1987) reports the occurrence of isolated bodies of gabbro and peridotite, containing up to 35% orthopyroxene and olivine, along Lemmens Inlet on Meares Island, northeast of Tofino. These bodies are associated with Isachsen's Westcoast amphibolite, Westcoast diorite and Westcoast migmatite subunits of the West Coast Crystalline Complex. Their nonfoliated nature and low grade of metamorphism led Isachsen to believe that they were younger than the West Coast Crystalline Complex rocks into which they intruded.

Contact Relationships

Ultramafic rocks occur as discrete bodies within the West Coast Crystalline Complex diorite, ranging in size from 1 m to several tens of metres. Although obscured by overburden, there is some lateral continuity of mineralogically distinct ultramafic bodies over distances of up to 1 km. Contact relationships between the ultramafic bodies and the West Coast Crystalline Complex diorite are quite variable. Smaller bodies, which tend to be more olivine-rich, have either abrupt, undeformed contacts with their host (Fig 3), or are present as sheared pods. Larger bodies, which are generally more gabbroic, grade into the melano and leucocratic diorites of the West Coast Crystalline Complex. In several locations, the association of olivine pyroxenite and pegmatitic hornblende diorite has been noted (Fig 4). Areas of the West Coast Crystalline Complex that host ultramafic rocks appear to correspond with the extreme magnetic highs (see Fig 2). The ultramafic bodies were first discovered using an aeromagnetic survey from 1972 (G. Pearson, *pers comm*, 2006). If the regional magnetic signal is controlled by the presence of ultramafic rock, there may be a significant amount of these rocks hidden within the West Coast Crystalline Complex.

Sample Descriptions

In outcrop, the ultramafic bodies are notoriously difficult to recognize, owing to their strongly weathered charac-



Figure 3. Sharp contact between ultramafic body and West Coast Crystalline Complex diorite.



Figure 4. Olivine pyroxenite (far right, black) in association with pegmatite diorite (middle) and leucodiorite (left).

ter. Often, a weathered outcrop containing peridotite can initially be mistaken as dark soil. The majority of the outcrop is commonly in an advanced stage of chemical weathering, with small patches of well-preserved rock dispersed throughout (Fig 5, 6). Peridotite and olivine pyroxenite outcrops weather to dun or chocolate brown and have fresh surfaces that are dark grey to black, often with large oikocrysts of amphibole and pyroxene enclosing subhedral olivine (Fig 7). The gabbroic outcrops weather to a dark brown or dun colour and are better preserved than their olivine-rich counterparts.

In thin section, the peridotite and olivine pyroxenite consist of variably serpentinized cumulus olivine with inclusions of euhedral spinel, poikilitically enclosed by either orthopyroxene, amphibole, or more rarely, clinopyroxene. Orthopyroxene and clinopyroxene coexist in several samples. Weakly to strongly altered plagioclase is present as an intercumulus phase in some samples. In these samples, olivine is never directly in contact with plagioclase and is always mantled by a corona of pyroxene (Fig 8).

Where present, amphibole appears as the result of reaction with pyroxene, along grain boundaries or along exsolution lamellae. The amphibole is of igneous origin as a deuteric alteration of anhydrous minerals during ad-



Figure 5. Outcrop of mica peridotite. The majority of the outcrop has weathered to soil.



Figure 6. Peridotite sample with chemically altered outcrop in the background.

vanced crystallization of hydrous magma (*e.g.*, Beard *et al.*, 2005). Moreover, we would not expect the preservation of fresh olivine if these rocks were hydrated (to form amphibole) by metamorphism (*e.g.*, Fig. 9). Igneous phlogopite is also present as a minor phase in some samples.

Cumulate gabbro and gabbroonorite display cumulus plagioclase, \pm orthopyroxene, clinopyroxene and, in one case, olivine. Much of the postcumulus clinopyroxene has been replaced by amphibole (Fig 10). Plagioclase in these samples is invariably less altered than in the peridotite and olivine pyroxenite samples.

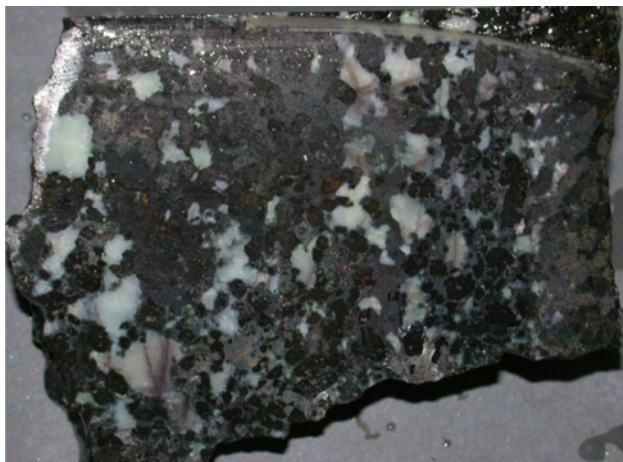


Figure 7. Cut slab of feldspathic olivine pyroxenite. Sample is approximately 10 cm across.

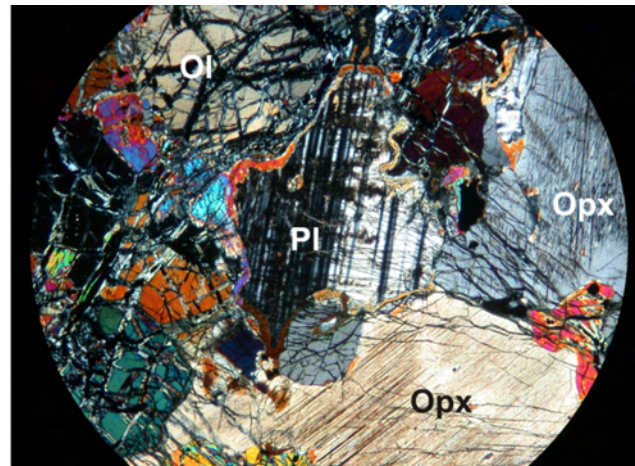


Figure 8. Photomicrograph showing intercumulus plagioclase (Pl) with cumulus olivine (Ol) and orthopyroxene (Opx) oikocrysts. Field of view is 2 mm across.

Magnetite with minor ilmenite exsolution is the dominant opaque phase in the ultramafic samples. It occurs as minor disseminated grains in the peridotite and olivine pyroxenite, and as both a euhedral and intercumulus phase in the gabbroic rocks (Fig 11). A euhedral, dark grey mineral with low reflectivity is present in peridotite and olivine pyroxenite samples, possibly chromite. Minor amounts of chalcopyrite are noted in most samples. Rare inclusions of round, white, high-reflectivity grains in olivine are noted, possibly pentlandite (Fig 12).

DISCUSSION

Ultramafic rocks occur in several different tectonic settings in the Canadian Cordillera, including ophiolite rocks, Alaskan-type intrusions and cumulates associated with calcalkaline intrusions in arc terranes (Nixon, 2003). The hydrous, calcalkaline nature of the parent magma that produced the ultramafic cumulates in the Bonanza arc, as attested to by the presence of primary amphibole, phlogopite and magnetite, is inconsistent with an ophiolite association. Furthermore, there is no spatial association of

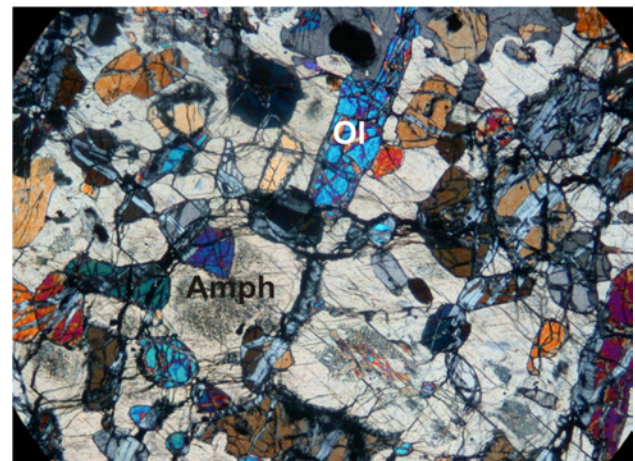


Figure 9. Photomicrograph of fresh cumulus olivine (Ol) enclosed by primary amphibole (Amph). Field of view is approximately 4 mm across.

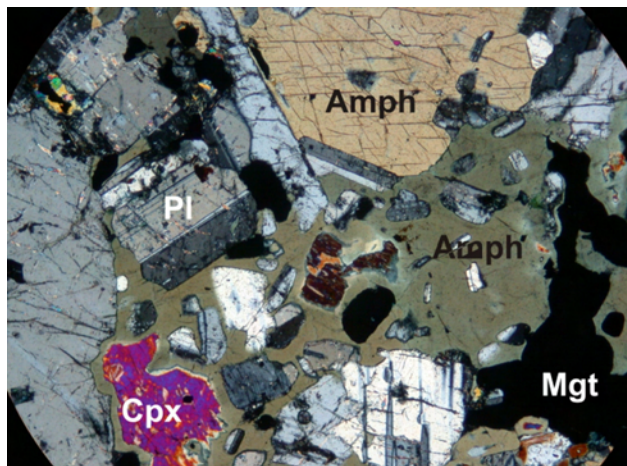


Figure 10. Photomicrograph of cumulate gabbro, with fresh cumulus plagioclase (Pl), amphibole (Amph), relict clinopyroxene (Cpx) and oxides (Mgt). Field of view is approximately 4 mm across.

mantle tectonite, pillow lava or sheeted dikes with the ultramafic bodies or their hostrocks.

Several lines of evidence also show that the ultramafic bodies are not of Alaskan-type affinity. First and foremost, orthopyroxene is a common phase in many samples, an observation that is inconsistent with Alaskan-type ultramafic occurrences (Taylor, 1967). Unlike the Alaskan-type situation, the parent magma from which the ultramafic bodies separated must have been silica saturated. In addition to the mineralogical evidence, field relations also argue against an Alaskan-type origin — the peridotite and olivine pyroxenite bodies lack any concentric zoning and occur as blocks and lozenges in diorite.

Strikingly similar petrography and field relations to the ultramafic rocks of the current study are known from the Giant Mascot deposit of southern BC. Nickel-copper-platinum group element sulphide ores at Giant Mascot are hosted by ultramafic rocks, including peridotite, pyroxenite and feldspathic pyroxenite (Metcalf *et al.*, 2002). As in the current study, the Giant Mascot rocks contain cumulus spinel and olivine, poikilitically enclosed by orthopyroxene and amphibole (Metcalf *et al.*, 2002).

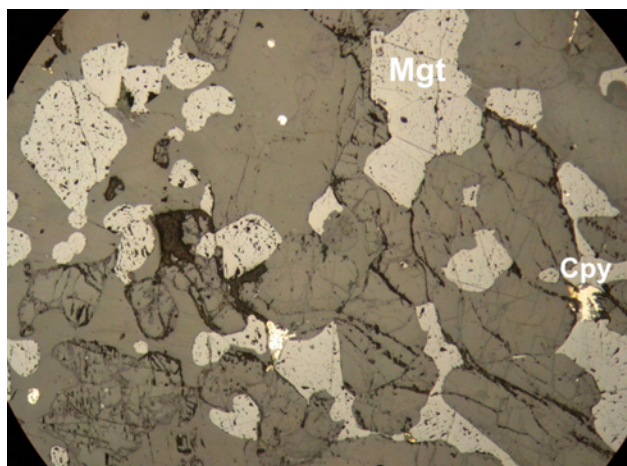


Figure 11. Photomicrograph showing euhedral and intercumulus magnetite (Mgt), with minor chalcopyrite (Cpy) in cumulate gabbro. Field of view is approximately 2 mm across.

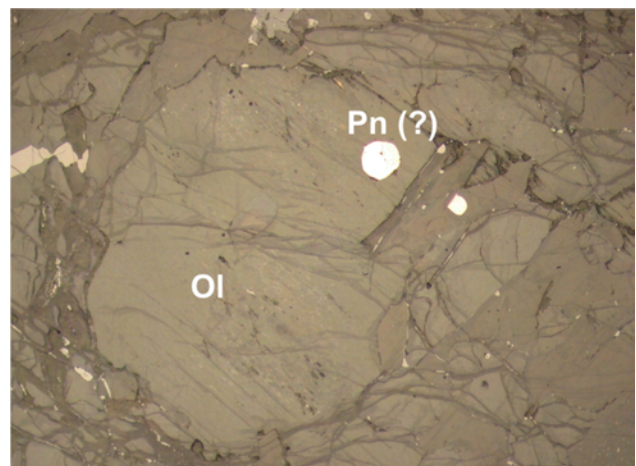


Figure 12. Photomicrograph of pentlandite (?; Pn) inclusion in olivine (Ol). Field of view is approximately 1.5 mm across.

Based on spinel chemistry, the Giant Mascot cumulates have been interpreted as fragments of the root zone to the tholeiitic Karmutsen basalt that were sampled by the Spuzzum diorite (Nixon, 2003). The hydrous nature of the cumulates is explained by Metcalfe *et al.* (2002) as the result of anatexis of metapelitic wallrock, causing dehydration and thereby introducing water into the magma. Although chemical data is pending for the current study, it is difficult to reconcile the presence of primary magnetite and amphibole in the Bonanza ultramafic rocks with the tholeiitic nature or the anatectic processes evident in the Giant Mascot rocks. In the Port Renfrew area, the presence of fresh olivine in amphibole oikocrysts rules out a metasomatic origin for the latter and there is no field evidence for the assimilation of hydrous or pelitic country rock.

Peridotite and pyroxenite are noted to occur in association with gabbronorite towards the middle and base of crust in exhumed island arc terranes in the Cordillera and elsewhere (*e.g.*, Burns, 1985; Takahashi *et al.*, 2006). For example, an oblique section of arc crust exposed in the Kohistan Terrane of northern Pakistan contains peridotite, anorthosite, troctolite and olivine gabbro cumulates, within a larger body of granoblastic diorite and gabbronorite. (Takahashi *et al.*, 2006).

The Bonanza arc and its setting are very similar to the Talkeetna arc in south-central Alaska and it has been proposed that the two are of similar age and can be correlated along strike (DeBari *et al.*, 1999). In the Talkeetna arc, ultramafic cumulates are present in large but sporadic occurrences at the base of the arc crust section, in contact with mantle harzburgite and dunite (Burns, 1985; DeBari and Coleman, 1989). The ultramafic cumulates in the Talkeetna arc section are thought to be genetically linked to the more evolved magmatic rocks of the arc (DeBari and Sleep, 1991). In the Tonsina assemblage, a part of the Talkeetna arc, peridotite and pyroxenite bodies occur in association with cumulate garnet-bearing gabbro, which grades into cumulate gabbronorite containing Fe and Ti oxides (DeBari and Coleman, 1989). Plagioclase is present as a late postcumulus phase and never coexists with olivine (DeBari and Coleman, 1989; DeBari and Sleep, 1991). While amphibole is present in the peridotite and pyroxenite primarily in the form of reaction rims on pyroxene, it appears to be a major postcumulus phase in the overlying

gabbroic cumulates (DeBari and Coleman, 1989). These petrographic relationships are strikingly similar to ultramafic cumulates from our field area. We suggest that the ultramafic rocks found within the West Coast Crystalline Complex represent cumulates from a primitive (parent?) Bonanza arc magma. There may be a melt-residue relationship between the West Coast Crystalline Complex diorite and the ultramafic cumulates, the latter having been entrained in the former during emplacement.

FUTURE DIRECTIONS AND ECONOMIC POTENTIAL

Whole rock geochemical analysis for major and selected trace elements will further elucidate the origin of the ultramafic and related plutonic rocks in the Port Renfrew area. In addition, geochronological investigations are underway to constrain the age of rocks that host the ultramafic bodies, as well as to constrain the igneous history of this portion of the Bonanza arc. All of the ultramafic samples collected have been sent for assay. In addition, the Ni concentration of olivine will be investigated in peridotite and olivine pyroxenite samples to test if they were in equilibrium with Ni-sulphide. This may shed light on the prospectivity of the ultramafic bodies for Ni-Cu or PGE sulphide, both in the Port Renfrew field area and elsewhere in the West Coast Crystalline Complex.

The majority of the ultramafic bodies are no more than a few tens of metres wide. Although it is discontinuous at the surface, the ultramafic outcrops tend to be distributed in patches throughout the West Coast Crystalline Complex. Geophysical investigations may reveal continuity between these or other ultramafic bodies at depth. No significant concentrations of economic minerals were noted in outcrop, hand sample or thin section, apart from minor Cu and Ni sulphide minerals. Nonetheless, the West Coast Crystalline Complex is exposed along most of western Vancouver Island and the findings of Isachsen (1987) on Meares Island suggest that ultramafic bodies are likely to be present elsewhere throughout the West Coast Crystalline Complex on Vancouver Island, possibly associated with concentrations of Ni-Cu sulphide minerals.

ACKNOWLEDGMENTS

This work was jointly funded by Geoscience BC and Emerald Fields Resources to whom we are indebted for their support. Holly Steenkamp is thanked for field assistance. In Port Renfrew, special thanks go to Tom Mawson for his hospitality and Gary Pearson for much guidance, cheer and logistical help.

REFERENCES

- BC Geological Survey (2006): MapPlace GIS internet mapping system; *BC Ministry of Energy, Mines and Petroleum Resources*, MapPlace website, URL <<http://www.MapPlace.ca>> [November 2006].
- Beard, J.S., Ragland, P.C. and Crawford, M.L. (2005): Using incongruent equilibrium hydration reactions to model latter-stage crystallization in plutons: examples from the Bell Island tonalite, Alaska; *Journal of Geology*, volume 113, pages 589–599.
- Burns, L. (1985): The Border Ranges ultramafic and mafic complex, south-central Alaska: cumulate fractionates of island arc volcanics; *Canadian Journal of Earth Sciences*, volume 22, pages 1020–1038.
- DeBari, S., Anderson, R.G. and Mortensen, J.K. (1999): Correlation among lower to upper crustal components in an island arc: the Jurassic Bonanza arc, Vancouver Island, Canada; *Canadian Journal of Earth Sciences*, volume 36, pages 1371–1413.
- DeBari, S.M. and Coleman, R.G. (1989): Examination of the deep levels of an island arc: evidence from the Tonsina ultramafic-mafic assemblage, Tonsina, Alaska; *Journal of Geophysical Research*, volume 94, pages 4373–4391.
- DeBari, S.M. and Sleep, N.H. (1991): High-Mg, low-Al bulk composition of the Talkeetna island arc, Alaska: Implications for primary magmas and the nature of arc crust; *Geological Society of America Bulletin*, volume 103, pages 37–47.
- Greene, A.R., Scoates, J.S. and Weis, D. (2005): Wrangellia Terrane on Vancouver Island, British Columbia: distribution of flood basalts with implications for potential Ni-Cu-PGE mineralization in southwestern British Columbia; in *Geological Fieldwork 2004, BC Ministry of Energy, Mines and Petroleum Resources*, Paper 2005-1, pages 209–220.
- Isachsen, C.E. (1987): Geology, geochemistry, and cooling history of the Westcoast Crystalline Complex and related rocks, Meares Island and vicinity, Vancouver Island, British Columbia; *Canadian Journal of Earth Sciences*, volume 24, pages 2047–2064.
- Jones, D.L., Silberling, N.J. and Hillhouse, J. (1977): Wrangellia—a displaced terrane in northwestern North America; *Canadian Journal of Earth Sciences*, volume 14, pages 2565–2577.
- Massey, N.W.D. and Friday, S.J. (1987): Geology of the Cowichan Lake area, Vancouver Island (92C/16); in *Geological Fieldwork 1987, BC Ministry of Energy, Mines and Petroleum Resources*, Paper 2003-1, pages 223–229.
- Metcalfe, P., McClaren, M., Gabites, J. and Houle, J. (2002): Ni-Cu-PGE deposits in the Pacific Nickel Complex, southwestern BC: a profile for magmatic Ni-Cu-PGE mineralization in a transpressional magmatic arc; in *Exploration and Mining in British Columbia 2002, BC Ministry of Energy, Mines and Petroleum Resources*, pages 65–79.
- Muller, J.E., Cameron, B.E.B. and Northcote, K.E. (1981): Geology and mineral deposits of Nootka Sound map-area, Vancouver Island, British Columbia; *Geological Survey of Canada*, Paper 80-16, 53 pages.
- Nixon, G.T. (2003): Use of spinel in mineral exploration: the enigmatic Giant Mascot Ni-Cu-PGE deposit – possible ties to Wrangellia and metallogenic significance; in *Geological Fieldwork 2002, BC Ministry of Energy, Mines and Petroleum Resources*, Paper 2003-1, pages 115–128.
- Nixon, G.T., Hammack, J.L., Hamilton, J. and Jennings, H. (1993): Preliminary geology of the Mahatta Creek area, northern Vancouver Island (92L/5); in *Geological Fieldwork 1992, BC Ministry of Energy, Mines and Petroleum Resources*, Paper 1993-1, pages 17–35.
- Nixon, G.T., Hammack, J.L., Payie, G.J., Snyder, L.D., Archibald, D.A. and Barron, D.J. (1995): Quatsino-San Josef map area, northern Vancouver Island: Geological overview (92L/12W, 1021/8, 9); in *Geological Fieldwork 1994, BC Ministry of Energy, Mines and Petroleum Resources*, Paper 1995-1, pages 9–21.
- Takahashi, Y., Mikoshiba, M.U., Takahashi, Y., Kauser, A.B., Khan, T. and Kubo, K. (2006): Geochemical modelling of the Chilas Complex in the Kohistan Terrane, northern Pakistan; *Journal of Asian Earth Sciences*, doi: 10.1016/j.jseas.2006.04.007
- Taylor, H.P. (1967): The zoned ultramafic complexes of southeastern Alaska; in *Ultramafic and related rocks*, Wyllie, P.J., Editor, *John Wiley and Sons*, pages 97–121.

Structural Overprinting in the Northwestern Skeena Fold Belt (NTS 104B, H), Northwestern British Columbia¹

by W. Loogman², J-F. Gagnon², J.W.F. Waldron³ and C.A. Evenchick³

KEYWORDS: Skeena Fold Belt, folds, faults, overprinting

INTRODUCTION

The Skeena Fold Belt, as defined by Evenchick (1991a), is located in northwestern British Columbia, in the Stikine Terrane of the Intermontane Belt of the Canadian Cordillera (Fig 1). The distribution of the Skeena Fold Belt roughly mirrors the location of the Mesozoic Bowser Basin, and the fold belt is predominantly developed in the Middle Jurassic – Early Cretaceous Bowser Lake Group of the Bowser Basin. The Early Jurassic Hazelton Group and the Late Cretaceous Sustut Group are also affected by folding and thrust faulting. Two regional fold trends are present within the Skeena Fold Belt: northwest-trending folds are dominant in the eastern two-thirds of the fold belt, and northeast-trending folds are present in the western third (Fig 1). Locally, these fold trends are found outside their dominant domains and overprint each other (Evenchick, 1991a; Evenchick, 2001). It is the aim of this study to evaluate overprinted structures and their timing relationships. Fieldwork was conducted in 2006 as a follow-up to fieldwork carried out in the summer of 2005 and reported on by Waldron *et al.* (2006). This work accompanies that reported by Gagnon *et al.* (2007).

In an effort to aid in hydrocarbon exploration within the Bowser Basin, recent studies of its petroleum potential by the Geological Survey of Canada and BC Ministry of Energy, Mines and Petroleum Resources (Osadetz *et al.*, 2003; Evenchick *et al.*, 2003) have focused on updating the thermal maturity models of Bustin and Moffat (1989), which predicted unfavourably high heat flow to much of the Bowser Basin, and on developing models for assessing the effectiveness of petroleum systems. In addition to conventional petroleum, there is potential for coalbed methane and conventional coal. Mineral potential exists in volcanic rocks on the flanks of the basin (Fig 1), as shown by the high-grade stratiform volcanogenic massive sulphide (VMS) Au-Ag deposits at Eskay Creek (Roth *et al.*, 1999).

¹ Geoscience BC contribution GBC022

² Department of Earth Sciences, University of Alberta, Edmonton, AB T6G 2E3

³ Geological Survey of Canada, 605 Robson Street, Vancouver, BC V6B 5J3

This publication is also available, free of charge, as colour digital files in Adobe Acrobat® PDF format from the BC Ministry of Energy, Mines and Petroleum Resources website at http://www.em.gov.bc.ca/Mining/GeolSurv/Publications/catalog/cat_fldwk.htm

Understanding the structural history of the region will contribute to exploration and evaluation of these resources.

REGIONAL STRATIGRAPHIC FRAMEWORK

The mapped regions of the Skeena Fold Belt expose rocks of the Middle Jurassic – Early Cretaceous Bowser Lake Group, including the Ritchie-Alger, Eaglenest and Skelhorne lithofacies assemblages, described in Evenchick and Thorkelson (2005). The lack of regionally correlative boundaries in the Bowser Lake Group makes the use of formal formation/group designations difficult. Synchronous deposition of shallow and deep marine facies occurred; the Bowser Lake Group reflects an overall progradational depositional history.

The Ritchie-Alger assemblage comprises sandstone, siltstone and shale, with rare chert-rich conglomerate. Sheet-like intervals of fine to medium-grained sandstone, separated by shale intervals that are metres thick, have been interpreted to relate to submarine fan deposition (Evenchick and Thorkelson, 2005). Evidence of turbidite accumulation within the submarine fan complexes includes normal grading, groove casts, dewatering structures and Bouma cycles. The Ritchie-Alger assemblage is estimated to reach thicknesses of 1800 m in the western third of the Bowser Basin (Evenchick and Thorkelson, 2005).

The Skelhorne lithofacies assemblage comprises more than 1000 m of siltstone, sandstone and conglomerate (Evenchick and Thorkelson, 2005). Common medium to thick-bedded coarsening-upward cycles, marine and plant fossils, wave-generated ripples and bioturbation are interpreted to record a moderate-energy deltaic depositional environment (Evenchick and Thorkelson, 2005). The Skelhorne assemblage is most common in the west-central part of the Bowser Basin.

The Eaglenest lithofacies assemblage comprises a high percentage (up to 80%) of rusty- weathering conglomerate and sandstone, with minor siltstone and shale, and reaches thicknesses of 1000 m (Evenchick and Thorkelson, 2005). Conglomerate clasts are well-rounded and well-sorted pebbles composed predominantly of chert. Plant fossils, including substantial silicified trees, are abundant, whereas marine fossils are rare. The abundance of conglomerate, coarsening-upward cycles and tree fossils all suggest a high-energy deltaic depositional environment (Evenchick and Thorkelson, 2005).

EXISTING STRUCTURAL FRAMEWORK

The Skeena Fold Belt overlies the Stikine Terrane of the Intermontane Belt (Evenchick, 1991a). The Skeena

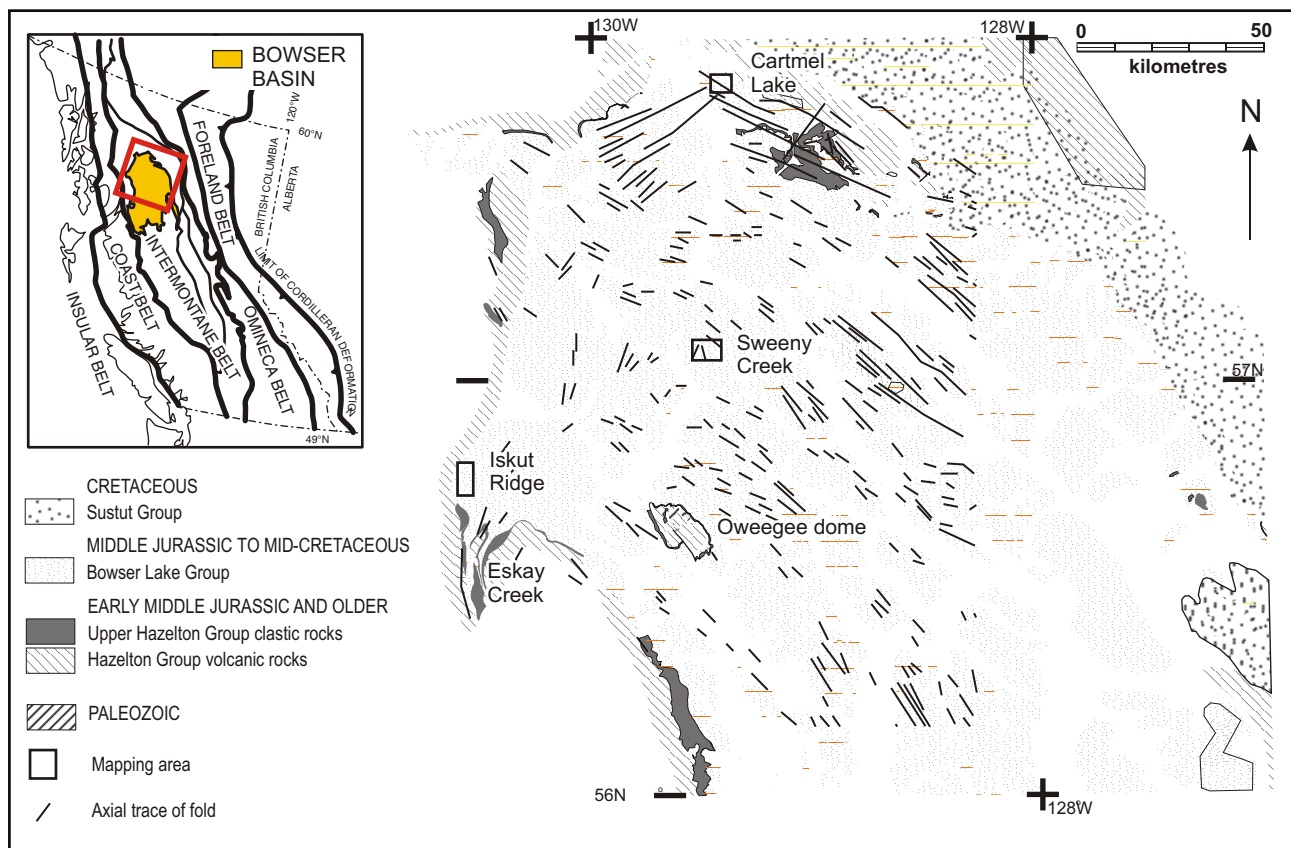


Figure 1. Simplified regional geology of the northwestern Skeena Fold Belt (compiled from Evenchick, 1991a; Bone, 2002; Evenchick and Thorkelson, 2005; Waldron *et al.*, 2006), showing fold axial traces and study areas referred to in the text; inset shows location of figure within the Canadian Cordillera.

Fold Belt was formed between the Albian and early Tertiary (Evenchick, 1991a; Evenchick and Thorkelson, 2005). The fold belt has been interpreted as a fold-and-thrust belt rooted in the Coast Mountains (Evenchick, 1991b). Evenchick (2001) suggested that oblique northwest-southeast shortening occurred first, affecting the western Bowser Basin, and was followed by a long period of northeast-southwest shortening that generated northwest-trending folds, parallel to the surface strike of the Canadian Cordillera. On the basis of work conducted in the Groundhog coalfield, Moffat and Bustin (1993) proposed three periods of shortening: initial northeast-southwest shortening, then northwest-southeast shortening and lastly northeast-southwest shortening. Bone (2002) examined a basal fold-interference pattern identified by Evenchick (1991a), formed by intersection of two similar-scale synclines, confirming the presence of type I fold interference (Ramsay, 1967); interference of this type can produce domes favourable to petroleum accumulation.

2006 FIELD MAPPING

During the 2006 field season, six areas were mapped at 1:25 000 scale from helicopter-positioned fly camps (Fig 1). Results from three of these areas are reported on here. The Iskut ridge area was selected due to its proximity to the Eskay Creek area, an area known to have multiple generations of folds (Read *et al.*, 1989; Lewis, 1992; Waldron *et al.*, 2006). The Cartmel Lake area was selected as an area dominated by northwest-trending folds with pos-

sible overprinting of northeast-trending folds, recognized by Evenchick and Green (2004). The Sweeny Creek area was chosen for its convergence of fold trends, as shown by Evenchick (2004).

Iskut Ridge

A small ridge, east of the Iskut River and north of Palmiere Creek at the western margin of the Bowser Basin, is herein referred to as 'Iskut ridge' (Fig 1). All rock units observed in this area are assigned to the Ritchie-Alger lithofacies assemblage (Evenchick *et al.*, 2004). Structure in the Iskut ridge area is dominated by north and north-northeast-trending folds traceable throughout much of the map area (Fig 2). North-trending folds are rounded and open to tight. Mappable deflections in north-trending axial traces occur near southeast-trending minor folds. Minor folds are open to tight, and commonly plunge steeply (~60°) southeast.

Equal-area projections of poles to bedding (Fig 3a) show a diffuse girdle distribution with an eigenvector 1 plunging steeply toward the southeast. These data suggest small-scale folding about a southeast-plunging axis, in contrast to map-scale relationships that indicate north-trending folds as the dominant structure. Cleavage is ubiquitous within fine units of the turbidite succession and sporadic in coarser sandstone. Pencil lineations are widespread, defined by intersection of steep bedding and steep cleavage. Cleavage data shown in Figure 3b lie in two clusters: a dominant steeply dipping cleavage that strikes northwest,

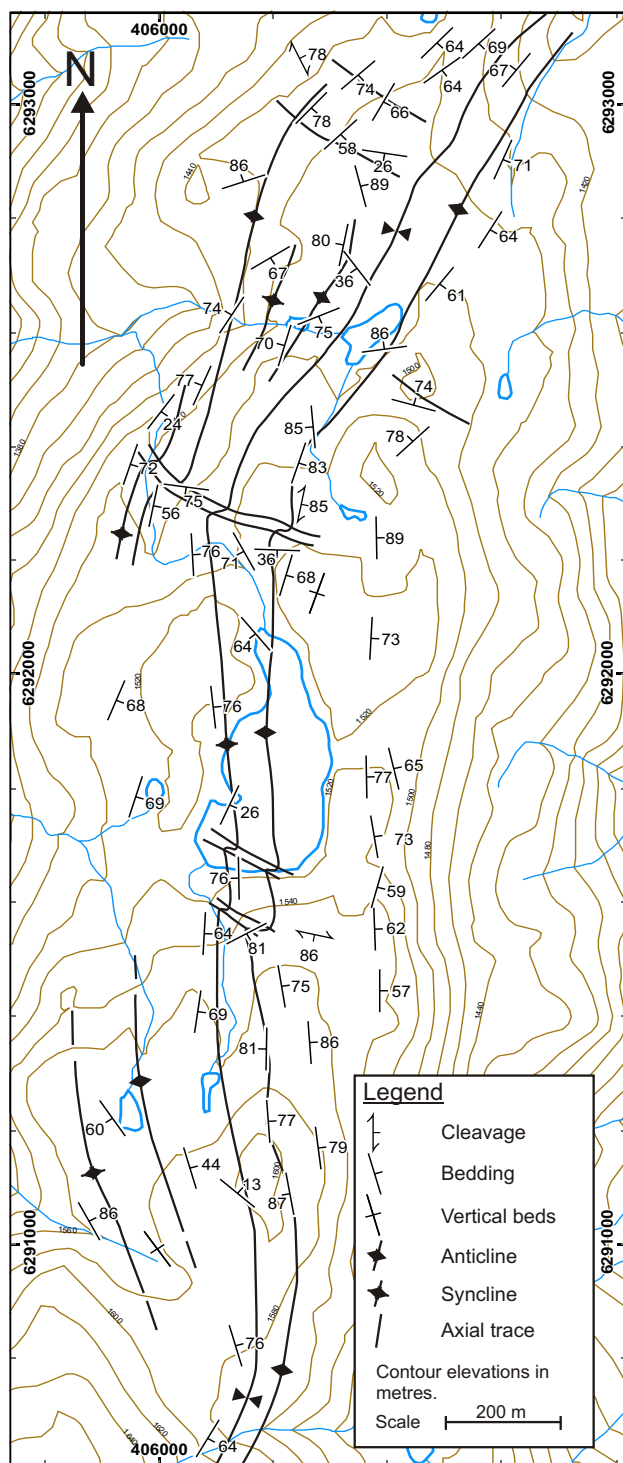


Figure 2. Structure of the Iskut Ridge area, showing bedding orientations and mapped axial traces.

and a lesser steep cleavage that strikes northeast. In outcrop, cleavage appears to be a spaced pressure-solution fabric. Slaty cleavage characterized by penetrative mineral alignment is rare. Oriented samples were collected and will be used for future petrographic analyses of cleavage. Because of the scarcity of mineral alignment, overprinted cleavage does not display crenulation. The clusters of

cleavage poles in Figure 3b are attributed to superposition of two episodes of shortening. There is no girdle distribution, such as might be expected if an earlier cleavage were refolded by later shortening. This is likely because extension directions during both deformation episodes were nearly parallel and approximately vertical. Mapped deflections of north-south axial traces by southeast-trending folds (Fig 2) indicate that the north to north-northeast-striking folds formed first and were subsequently overprinted by relatively minor southeast-trending folds. This is consistent with overall folding of bedding about a southeast-plunging axis (Fig 3a), suggesting that minor folds are part of a larger structure.

Equal-area plots of bedding-cleavage intersection lineations in Figure 3c show a scattered cluster centred on a northwest-trending axis. The scatter is attributed to the relative scarcity of northeast-striking cleavage in comparison to northwest-striking cleavage.

Faults are relatively rare in this area compared with the rest of the western Skeena Fold Belt. Brittle structures observed include *en échelon* veins at a number of locations. There are a number of 'S' and 'Z' asymmetric veins interpreted to record sinistral and dextral movement, respectively. In some cases, both asymmetries can be observed at a single locality (Fig 4, 5). The presence of *en échelon* veins suggests a component of brittle strain, possibly related to the nearby Forrest Kerr fault (Read *et al.*, 1989) and faults interpreted by Logan *et al.* (2000).

Cartmel Lake

An area exposing rocks of the Eaglenest assemblage approximately 3 km southwest of Cartmel Lake was selected for study of previously recognized overprinted folds (Evenchick and Green, 2004). The topography is dominated by cliff-forming conglomerate beds in which a near-vertical rough cleavage dominates the exposed surfaces.

The structure at Cartmel Lake is dominated by three major folds that trend southeast (Fig 6). At map scale, a gently dipping surface in the northern section of the map area truncates bedding at a low angle and is interpreted as a *décollement*. A fault in the southern section of the map area truncates bedding in a similar fashion and is interpreted as a continuation of the same *décollement* (Fig 6). Bedding cut-offs indicate that this detachment climbs upsection to the southeast. Associated outcrop-scale folds face and verge southeast. A northeast-trending map-scale fold at the southern extremity of the area is presumed to be related to the same deformation that produced the southeast-verging detachment. Map-scale southeast-trending folds can be traced through the detachment without offset, implying that it must have been folded.

Numerous steep northwest-striking faults, traceable over less than a kilometre, offset cliff-forming conglomerate in a dextral sense, with offsets ranging from metres to tens of metres (Fig 6). Slickenline lineations indicate dextral strike-slip motion. Rare sinistral faults of similar size and scale, but traceable over just a few metres, are present. These faults offset the mapped trace of the low-angle *décollement* by similar amounts. The sinistral faults may be conjugate to dextral faults, as suggested by their clockwise orientation relative to the dextral faults and similar offset of strata. The orientations of the conjugate faults suggest an approximate north-south shortening direction.

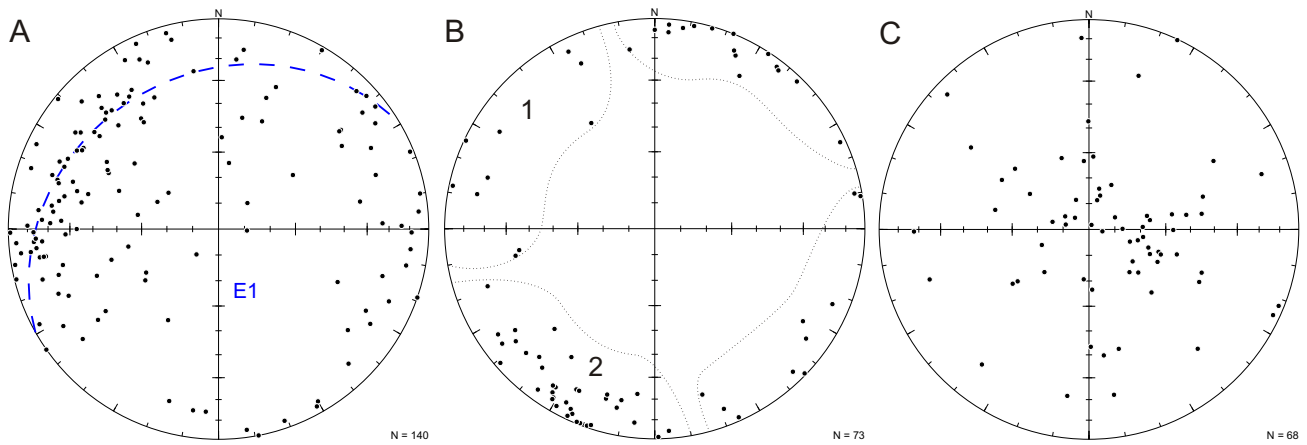


Figure 3. Lower-hemisphere equal-area projection of structural data collected in the Iskut ridge area: A) poles to bedding; E1, eigenvector 1; dashed line shows principal E1 girdle plane; B) poles to cleavage, dotted lines outline interpreted distributions of cleavage clusters 1 and 2; C) bedding-cleavage intersection lineations.

Spaced cleavage is well developed in conglomerate of the Cartmel Lake area, with some outcrops showing three distinct cleavage sets. The high percentage (75–90%) of coarse-grained rock types within the Eaglenest lithofacies assemblage may account for the common occurrence of cleavage within conglomerate; lithology is relatively homogeneous and therefore strain is not partitioned to finer grained rock types. The cleavage distribution is unusual compared to other Bowser Lake Group assemblages that have a bulk fine-grained composition and only rarely develop cleavage in coarse rock types. Cleaved conglomerate shows smooth weathering surfaces instead of the ‘bumpy’ weathering pattern of pebble conglomerate elsewhere in

the basin, as cleavage planes cut through pebbles. Despite deformation of pebbles, significant porosity is observed to have been retained between the clasts. Equal-area plots of cleavage poles in Figure 7b show a widely scattered distribution, consistent with multiple phases of deformation. Equal-area plots of bedding poles in Figure 7a show a diffuse girdle normal to an east-southeast-trending, shallowly plunging eigenvector 1, consistent with mapping showing folding of the low-angle detachment by northwest-trending folds.

Sweeny Creek

The area around the headwaters of Sweeny Creek was mapped, expanding mapping of the Tumeka Creek study area reported in Waldron *et al.* (2006). Rock units in this area belong to the Skelhorne assemblage of the Bowser Lake Group (Evenchick, 2004). Prior mapping in the Sweeny Creek area revealed north-northeast and north-northwest-trending folds converging without intersection,

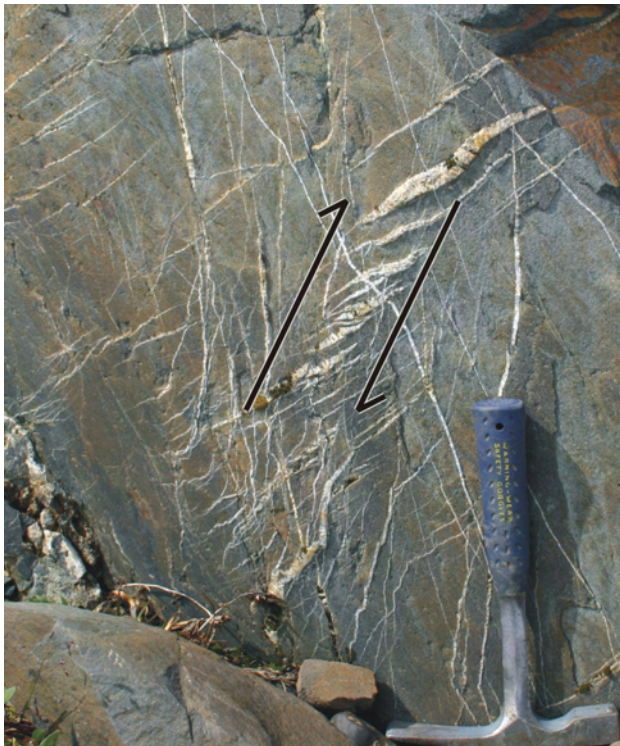


Figure 4. Z-asymmetric *en échelon* quartz veins, indicating dextral and reverse sense of shear; arrows indicate interpreted sense of shear; view towards the west-northwest.

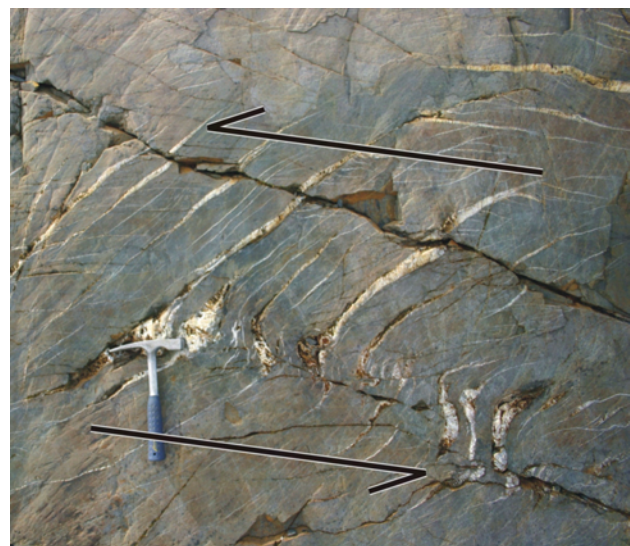


Figure 5. S-asymmetric *en échelon* quartz veins, indicating sinistral and reverse sense of shear; arrows indicate interpreted sense of shear; view towards the west-southwest.

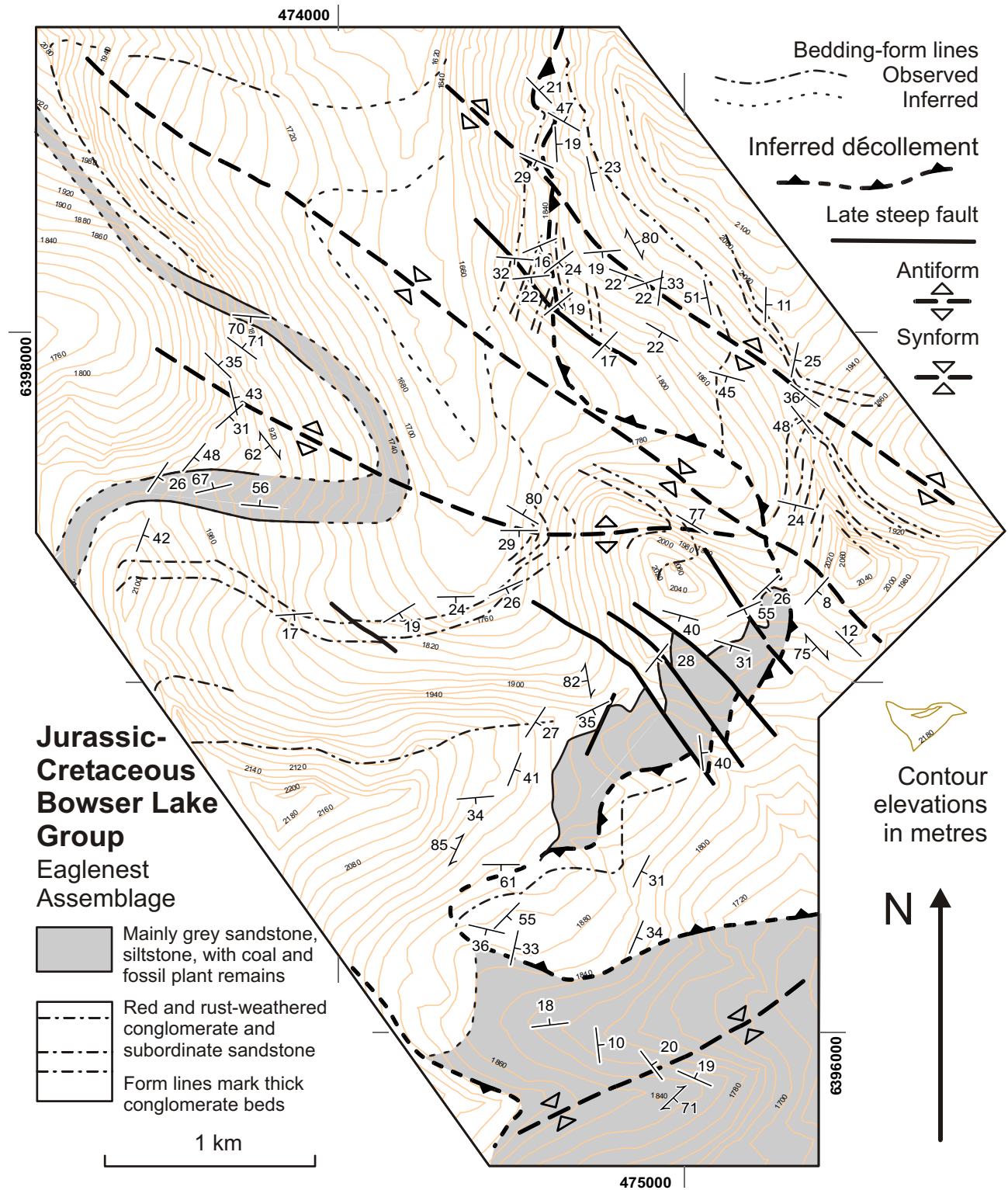


Figure 6. Structure of the Cartmel Lake area; note distribution of early *décollement* and later folds.

within an area dominated by northwest-trending folds (Evenchick, 2004). Folds mapped in the Sweeny Creek area have variable orientations, plunging between north-northwest and north-northeast. Figure 8 shows axial traces that converge with each other but do not crosscut. The map pattern suggests that these folds are of the same generation

and are part of a larger system of conical folds. Map relationships also show that all north to northeast folds appear to increase in plunge toward the northeast. All bedding in the northern part of the study area dips to the northeast; regionally, the structures in this area are part of the southwest limb of a gentle northwest-trending syncline, with a wave-

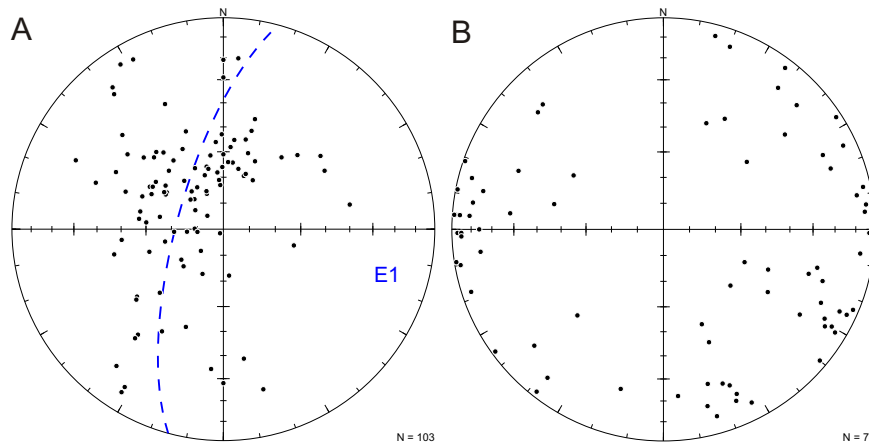


Figure 7. Lower-hemisphere equal-area projection of structural data collected in the Cartmel Lake area: A) poles to bedding; E1, eigenvector 1; dashed line shows principal E1 girdle plane; B) poles to cleavage.

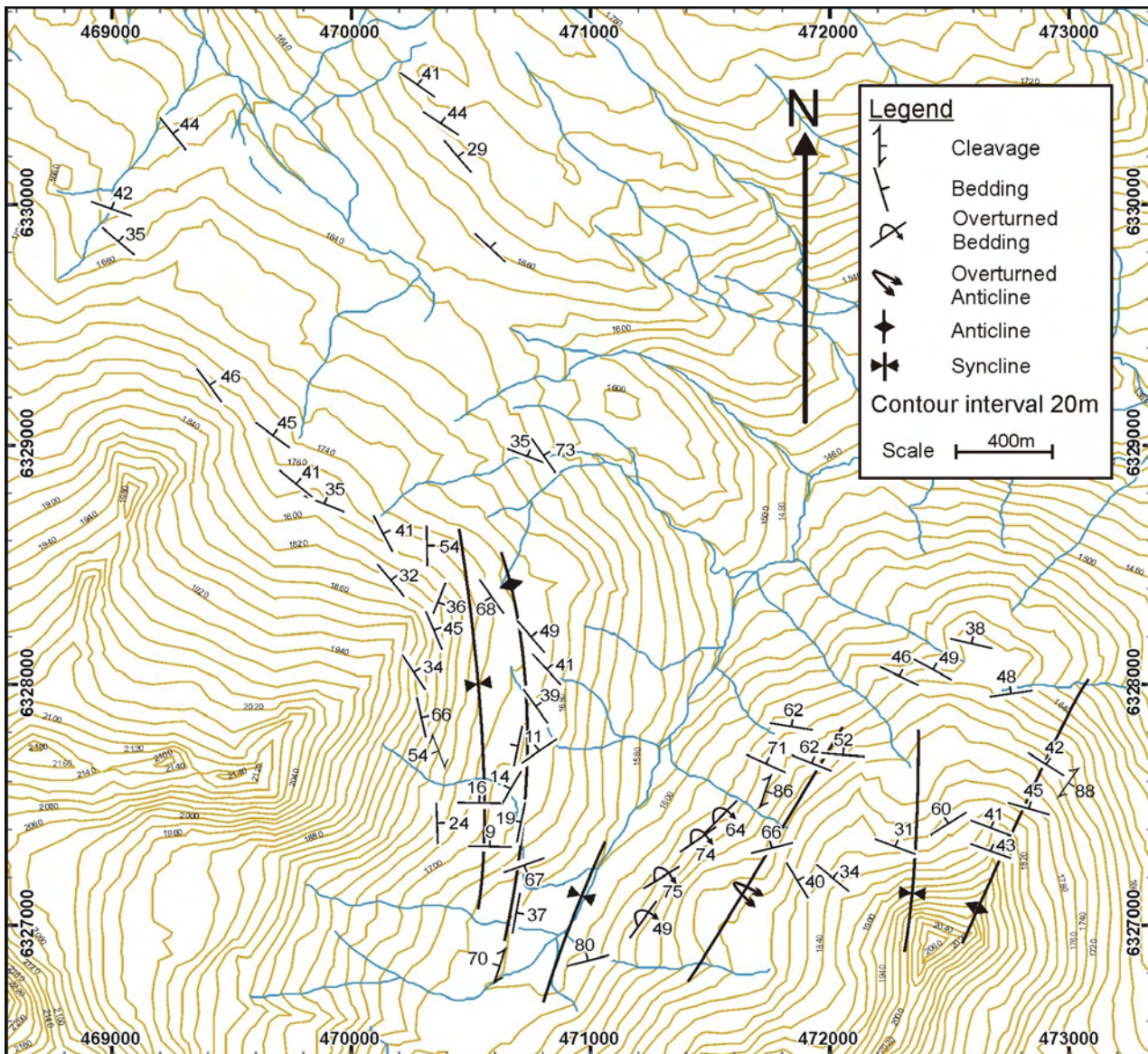


Figure 8. Structure of the Sweeny Creek area, showing orientations of structures and axial traces.

length on approximately the 5 km scale, observed to the north of Sweeny Creek. The syncline is interpreted to have increased the plunge of north-trending folds.

DISCUSSION

All three areas mapped show overprinting of structures. At Iskut ridge, a major north to north-northeast-trending fold is refolded by smaller, southeast-trending structures. The Cartmel Lake area is characterized by overprinting of northwest-trending folds on an earlier detachment; folds associated with the earlier detachment show northeast trends. The Cartmel Lake area may record the importance of detachments in the deformation history of the area, as suggested by Evenchick (1991b). Overprinting is less clearly displayed at Sweeny Creek, but progressive down-plunge steepening of northeast-trending folds is consistent with refolding by folds with northwest trends. Thus, structures in all three areas are consistent with early, generally northwest-southeast shortening, followed by northeast-southwest shortening.

The development of type I dome-and-basin interference patterns is dependent upon overprinting of folds at a high angle. Large domes prospective for petroleum accumulation result from in-phase interference of anticlines of similar amplitude. Where structures of different wavelengths or amplitudes interfere, the resulting patterns are more complex. Fold amplitudes, wavelengths and intersection angles are variable in the Skeena Fold Belt. At Iskut ridge, the early north to north-northeast folds are map scale, and folds with southeast trends are relatively minor structures. If present in the subsurface, such a structural pattern could serve as an array of small petroleum traps, as southeast-trending folds could trap petroleum located in early folds. At Sweeny Creek, there is a northwest-trending kilometre-scale syncline and the north-trending folds have wavelengths on the hundred metre scale. Down-plunge steepening of early folds by a northwest-trending fold of this type could drive subsurface petroleum migration to the south, forming a broad pool with several pockets within early folds. The Cartmel Lake area includes multiple sets of spaced pressure-solution cleavage within conglomerate that dissolves pebbles but does not obliterate porosity in the matrix. At Cartmel Lake, early folds are likely associated with *décollements*. Locating such structures in the subsurface would provide insights on the location of potential petroleum traps.

ACKNOWLEDGMENTS

The authors thank Geoscience BC for continuing to support this research. Additional field costs were supported by Natural Sciences and Engineering Research Council of Canada (NSERC) Discovery Grant A8508 to J. Waldron. H. Tomes and C. Bloomberg provided excellent assistance in the field. Helicopter support was provided by Quantum, Prism and Pacific Western Helicopters. Research at Cartmel Lake was made possible through a research permit from the Spatsizi Plateau Wilderness Provincial Park. Sabina Silver Corporation and the Eskay Creek mine were very hospitable in allowing us to visit their sites. Helpful review by Philippe Erdmer and Rob Stevens improved the manuscript.

REFERENCES

- Bone, K.E. (2002): Relative timing and significance of folding in the western Skeena Fold Belt, northwestern Bowser Basin, British Columbia: interpretation of structural and seismic reflection data; unpublished MSc thesis, *University of British Columbia*, Vancouver, BC, 171 pages.
- Bustin, R.M. and Moffat, I.W. (1989): Semianthracite, anthracite and meta-anthracite in the central Canadian Cordillera: their geology, characteristics and coalification history; in *Coal: Classification, Coalification, Mineralogy, Trace-element Chemistry, and Oil and Gas Potential*, Lyons P.C. and Alpern, B., Editors, *International Journal of Coal Geology*, volume 13, pages 303–326.
- Evenchick, C.A. (1991a): Geometry, evolution, and tectonic framework of the Skeena Fold Belt, north central British Columbia; *Tectonics*, volume 10, pages 527–546.
- Evenchick, C.A. (1991b): Structural relationships of the Skeena Fold Belt west of the Bowser Basin, northwest British Columbia; *Canadian Journal of Earth Sciences*, volume 28, pages 973–983.
- Evenchick, C.A. (2001): Northeast-trending folds in the western Skeena Fold Belt, northern Canadian Cordillera: a record of Early Cretaceous sinistral plate convergence; *Journal of Structural Geology*, volume 23, pages 1123–1140.
- Evenchick, C.A. (2004): Geology, Sweeny Creek, British Columbia; *Geological Survey of Canada*, Map 2037A, scale 1:50 000.
- Evenchick, C.A., Ferri, F., Mustard, P.S., McMechan, M., Osadetz, K., Stasiuk, L., Wilson, N.S.F., Enkin, R.J., Hadlari, T. and McNicoll, V.J. (2003): Recent results and activities of the Integrated Petroleum Resource Potential and Geoscience Studies of the Bowser and Sustut Basins Project, British Columbia; *Geological Survey of Canada*, Current Research 2003-A13, 11 pages.
- Evenchick, C.A. and Green, G.M. (2004): Geology, Eaglenest Creek, British Columbia; *Geological Survey of Canada*, Map 2029A, scale 1:50 000.
- Evenchick, C.A., Mustard, P.S., Woodsworth, G.J. and Ferri, F. (2004): Compilation of geology of Bowser and Sustut basins draped on shaded relief map, north-central British Columbia; *Geological Survey of Canada*, Open File 4638, scale 1:500 000.
- Evenchick, C.A. and Thorkelson, D.J. (2005): Geology of the Spatsizi River map area, north-central British Columbia; *Geological Survey of Canada*, Bulletin 577, 276 pages.
- Gagnon, J-F., Loogman, W., Waldron, J.W.F., Cordey, F. and Evenchick, C.A. (2007): Stratigraphic record of initiation of sedimentation in the Bowser Basin, northwestern British Columbia; *BC Ministry of Energy, Mines and Petroleum Resources*, Geological Fieldwork, Paper 2007-1 and *Geoscience BC*, Report 2007-1, pages 275–284.
- Lewis, P.D. (1992): Structural geology of the Prout Plateau region, Iskut River map area, British Columbia (104B/9); in *Geological Fieldwork 1991*, *BC Ministry of Energy, Mines and Petroleum Resources*, Paper 1992-1, pages 521–527.
- Logan, J.M., Drobe, J.R. and McClelland, W.C. (2000): Geology of the Forrest Kerr – Mess Creek Area, northwestern British Columbia, NTS 104B/10, 15, 104G/2, 7W; *BC Ministry of Energy, Mines and Petroleum Resources*, Bulletin 104, 164 pages.
- Moffat, I.W. and Bustin, R.M. (1993): Deformational history of the Groundhog coalfield, northeastern Bowser Basin, British Columbia; styles, superposition and tectonic implications; *Bulletin of Canadian Petroleum Geology*, volume 41, pages 1–16.
- Osadetz, K.G., Evenchick, C.A., Ferri, F., Stasiuk, L.D. and Wilson, N.S.F. (2003): Indications for effective petroleum systems in Bowser and Sustut Basins, north-central British

- Columbia; in *Geological Fieldwork 2002, BC Ministry of Energy, Mines and Petroleum Resources*, Paper 2003-1, pages 257–264.
- Ramsay, J.G. (1967): *Folding and Fracturing of Rocks*; McGraw-Hill, New York, 567 pages.
- Read, P.B., Brown, R.L., Psutka, J.F., Moore, J.M., Journeay, M., Lane, L.S., Orchard, J.J. (1989): Geology, More and Forrest Kerr creeks (parts of 104B/10, 15, 16, and 104G/1, 2); *Geological Survey of Canada*, Open File 2094, scale 1:50 000.
- Roth, T., Thompson, J.F.H. and Barrett, T.J. (1999): The precious metal-rich Eskay Creek deposit, northwestern British Columbia; Chapter 15 in *Volcanic-Associated Massive Sulfide Deposits: Processes and Examples in Modern and Ancient Settings*, Barrie, C.T. and Hannington, M.D., Editors, *Reviews in Economic Geology*, volume 8, pages 357–373.
- Waldron, J.W.F., Gagnon, J-F., Loogman, W. and Evenchick, C.A. (2006): Initiation and deformation of the Jurassic Cretaceous Bowser Basin: implications for hydrocarbon exploration in north-central BC; in *Geological Fieldwork 2005, BC Ministry of Energy, Mines and Petroleum Resources*, Paper 2006-1 and *Geoscience BC*, Report 2006-1, pages 347–360.

Geology and Mineral Deposits of the Skeena Arch, West-Central British Columbia (Parts of NTS 093E, L, M; 094D; 103I, P): Update on a Geoscience BC Digital Data Compilation Project¹

by D. MacIntyre²

KEYWORDS: Skeena Arch, mineral deposits, geology, metallogeny, MapPlace, digital data, GIS

INTRODUCTION

The Skeena Arch is a northeast-trending belt of uplifted Jurassic and older rocks that transects central British Columbia. This uplift is believed to have formed in the Middle Jurassic and resulted in separation of the Bowser and Nechako basins (Yorath, 1991). Rocks exposed along the Skeena Arch represent a long-lived magmatic arc that has produced a diverse range of mineral deposits in a wide variety of geological settings. This area represents some of the most richly endowed terrain in British Columbia and has been the site of mineral exploration for the past 125 years. Since 1985, the BC Geological Survey and the Geological Survey of Canada have been involved in regional mapping projects along the Skeena Arch, first as part of the Whitesail and Smithers projects (*e.g.*, MacIntyre *et al.*, 1989) and more recently as part of the Interior Plateau (Diakow *et al.*, 1997) and Nechako NATMAP (MacIntyre, 1998, 2001a, b; MacIntyre and Villeneuve, 2001; MacIntyre *et al.*, 1996a, b, 1997, 1998) projects. This work has resulted in a much better understanding of the geological evolution of the arch, particularly during the metallogenically important Jurassic through Cretaceous time periods. Although there are gaps in the map coverage, a large part of the project area (80%) has now been mapped in detail. These data were originally compiled at 1:100 000 scale as part of the Mineral Potential Project (MacIntyre *et al.*, 1994) and revised and updated as part of the Digital Geology of BC Project (Massey *et al.*, 2005).

The Skeena Arch project will provide a means of accessing new and existing geoscience data through an interactive map on MapPlace, a website hosted by the BC Ministry of Energy, Mines and Petroleum Resources. This report describes how the site can be used in the exploration for new mineral resources along the trend of the Skeena Arch. The site will provide four significant components, to be published as GeoFiles: an interactive MapPlace map with layer groups designed to highlight specific metallogenic

targets, such as porphyry Cu-Mo deposits; downloadable data in shape-file format for use in most GIS systems, such as ArcView[®] and ArcExplorer[®]; Manifold[®] map files for use in Manifold[®] GIS; and KML files for use in viewers such as the free Google[™] Earth application.

LOCATION OF THE PROJECT AREA

The area covered by the Skeena Arch project is shown in Figure 1. The area includes all of the Hazelton (093M), Smithers (093L) and Whitesail (093E) NTS map sheets, and the south half of McConnell Creek (094D), east half of Terrace (103I) and southeast corner of Nass River (103P).

GEOLOGY AND MINERAL DEPOSITS OF THE SKEENA ARCH

The geology and mineral deposits of the Skeena Arch have been described in a previous report (MacIntyre, 2006). This information is repeated here in abbreviated form for completeness of this report.

The Skeena Arch project area lies within the Intermontane Belt, which at this latitude includes the Stikine (Stikinia) volcanic arc terrane and a small part of the oceanic Cache Creek Terrane. The Stikine Terrane comprises Carboniferous to Middle Jurassic island arc volcanic and sedimentary rocks and related plutonic suites (Schiarizza and MacIntyre, 1999). The Stikine Terrane is believed to have evolved in the eastern Pacific of the Northern Hemisphere and moved northward to dock with ancestral North America sometime during the Middle Jurassic (Monger *et al.*, 1972; Monger and Nokleberg, 1996). The Stikine Terrane is well exposed along the Skeena Arch. North of the Skeena Arch, the Stikine Terrane is overlain by postaccretion, Late Jurassic to Early Cretaceous, marine and nonmarine sedimentary rocks of the Bowser Basin. The southern part of the Skeena Arch is overlapped by Late Cretaceous and Eocene continental volcanic arc and related sedimentary rocks of the Ootsa Lake and Endako groups.

The project area spans the zone of westward-directed thrust faulting that marks the boundary between the Stikine and Cache Creek terranes (Struik *et al.*, 2001). This structural imbrication occurred prior to 165 Ma (Schiarizza and MacIntyre, 1999), as indicated by isotopic ages for postkinematic plutons that cut both terranes. Folds and thrust faults related to this imbrication are offset by a complex pattern of high-angle faults. This pattern of faulting is not unique to the boundary between the Stikine and Cache Creek terranes, as it is observed throughout the Smithers and Hazelton map sheets (Tipper and Richards, 1976a, b; Richards 1980, 1990). Most of these faults formed during

¹ Geoscience BC contribution GBC042

² Consulting Geologist, D.G. MacIntyre & Associates Ltd., Victoria, BC

This publication is also available, free of charge, as colour digital files in Adobe Acrobat[®] PDF format from the BC Ministry of Energy, Mines and Petroleum Resources website at http://www.em.gov.bc.ca/Mining/GeolSurv/Publications/catalog/cat_fldwk.htm

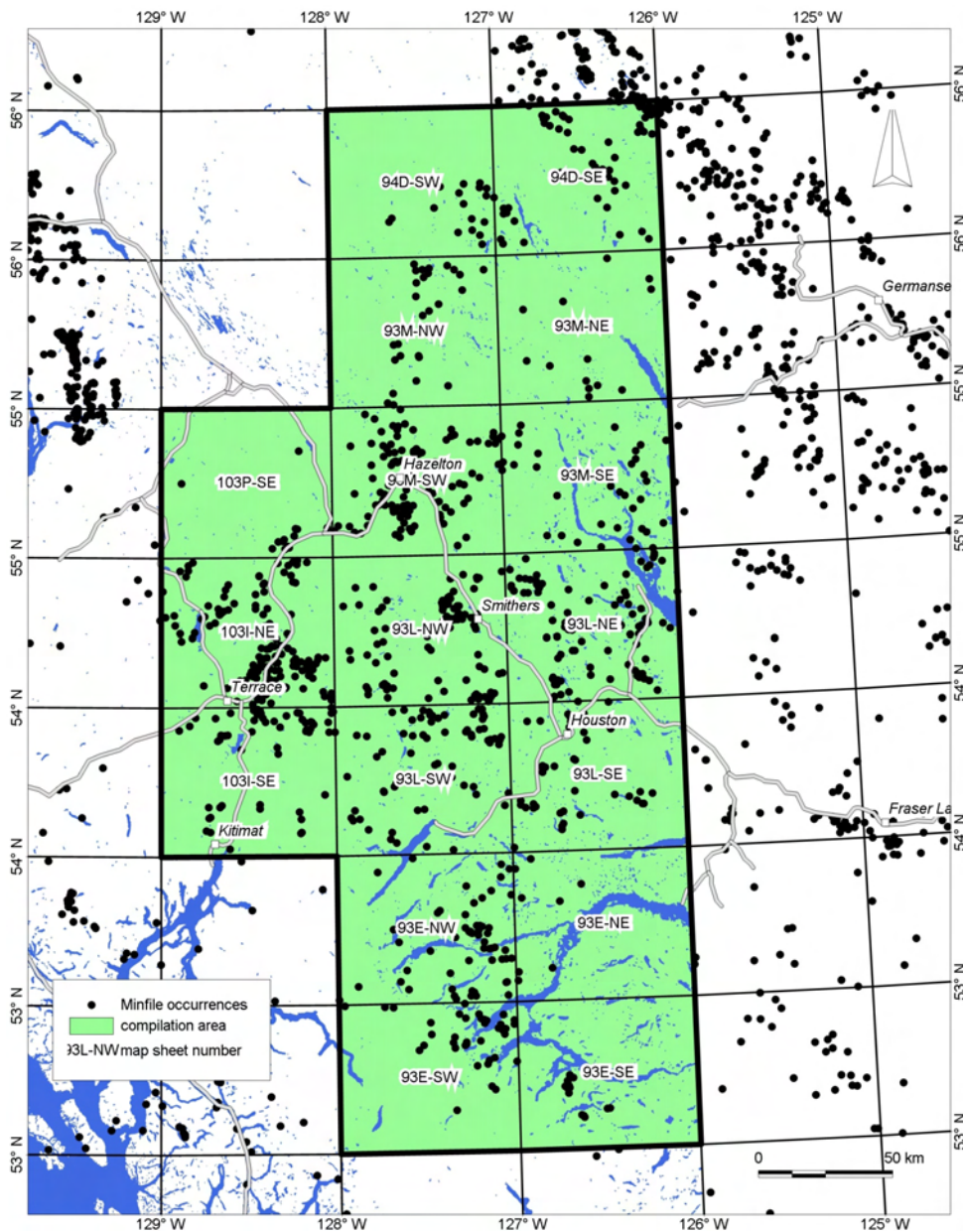


Figure 1. Location of the Skeena Arch project area and MINFILE (2006) occurrences.

Late Cretaceous to Eocene or younger block-faulting events (MacIntyre *et al.*, 1997, 1998). In most parts of the project area, Stikine Terrane rocks display broad, open fold patterns. The occurrence of a penetrative cleavage and metamorphic grade higher than lower greenschist facies is rare.

The geology of the Skeena Arch project area is based on a recent compilation completed by the BC Geological Survey (Massey *et al.*, 2005). Most of the project area is underlain by the Stikine Terrane, which here includes the Carboniferous to Permian Asitka Group island arc metavolcanic rocks and limestone; Middle to Late Triassic augitephyric basalt, andesite and related island arc marine sedimentary rocks of the Takla Group; and Early to Middle Jurassic andesitic volcanic, volcanoclastic and related marine sedimentary rocks of the Hazelton Group island arc to con-

tinental arc assemblage (Thorkelson *et al.*, 1995; Richards, 1980, 1990). The stratified rocks are cut by the granodiorite and quartz diorite of the Late Triassic to Early Jurassic Topley intrusive suite and the newly recognized Early to Middle Jurassic Spike Peak intrusive suite (MacIntyre *et al.*, 2001), which are probably comagmatic with the Takla and Hazelton volcanic arc successions.

In the northwest corner of the project area, the Stikine Terrane is overlain by marine to nonmarine clastic sedimentary strata of the Late Jurassic Bowser Lake and Early Cretaceous Skeena groups. These rocks were deposited in a fluvial-deltaic to nearshore shelf environment along the southeastern margin of the Bowser Basin (Bassett, 1991; Bassett and Kleinspehn, 1996; Evenchick, 1999). A detailed discussion of these overlap assemblages is presented in MacIntyre (1998).

In the western half of the project area, Late Cretaceous to Early Eocene porphyritic andesite, basalt, rhyolite and related pyroclastic and volcanoclastic continental arc rocks unconformably overlie both folded and uplifted rocks of the Stikine Terrane and Late Jurassic to Early Cretaceous sedimentary rocks of the Bowser Basin. The younger volcanic rocks are preserved in grabens or as erosional remnants on ridge tops. The Late Cretaceous rocks include porphyritic andesite flows and lahars of the Kasalka Group and coeval granodiorite and quartz diorite plutons of the Bulkley plutonic suite (Carter, 1981; MacIntyre, 1985). In the vicinity of Babine Lake, the Stikine Terrane is unconformably overlain by porphyritic andesite flows of the Early Eocene Newman Formation and cut by porphyritic granodiorite to quartz monzonite plutons of the Babine plutonic suite. In the southern part of the project area, small porphyritic quartz monzonite and related felsic intrusions form the Nanika plutonic suite. Important porphyry copper deposits are associated with the Bulkley, Babine and Nanika intrusive rocks (Carter, 1976, 1981; MacIntyre and Villeneuve, 2001; Carter *et al.*, 1995).

In the east and southeast parts of the project area, the Stikine and Cache Creek terranes are unconformably overlain by Early Eocene basalt and rhyolite flows and related pyroclastic rocks of the Endako and Ootsa Lake groups (Grainger and Anderson, 1999; Grainger *et al.*, 2001) and Miocene basalt flows of the Chilcotin Group. These younger rocks have also been block faulted and tilted during an Eocene or younger extensional tectonic event.

The Skeena Arch project area is richly endowed with metallic mineral deposits, with over 800 occurrences listed in the BC Geological Survey's MINFILE (2006) database. The different deposit types that have been recognized include polymetallic veins (268), subvolcanic Cu-Ag-Au-(As-Sb) mineralization (153), porphyry Cu±Mo±Au (140), volcanic red-bed copper (86), porphyry Mo (66), intrusion-related Au pyrrhotite veins (38) and copper skarns (20). Most of these deposits are related to the Late Cretaceous Bulkley and Eocene Babine and Nanika plutonic suites. These intrusions are part of a long-lived magmatic arc that forms the core of the Skeena Arch.

In recent years, potential for the discovery of Eskay Creek-type volcanogenic massive sulphide deposits has been recognized. The most prospective targets are Middle Jurassic submarine volcanic rocks of the Hazelton Group (Massey, 1999; Massey *et al.*, 1999) and mid-Cretaceous bimodal volcanic rocks of the Rocky Ridge Formation (MacIntyre, 2001a, b).

There is currently only one deposit in production in the project area: the Huckleberry porphyry Cu-Mo deposit at Tahtsa Lake, 90 km south of the town of Houston. Two other deposits are in the advanced stages of feasibility studies: the Davidson (aka Glacier Gulch or Yorke-Hardy) porphyry Mo deposit at Smithers and the Morrison porphyry Cu deposit at Babine Lake.

ACCESSING AND VIEWING DATA FOR THE SKEENA ARCH AREA

As mentioned previously, data for the Skeena Arch project are now available on the BC Ministry of Energy, Mines and Petroleum Resources MapPlace (2006) website. To locate the data and view the map, select the Thematic Maps hyperlink and scroll down to the section entitled 'De-

tailed Geology Maps', where the Skeena Arch project is listed. Selecting the *more details* hyperlink at the end of the brief project description will open another page that gives an overview of the project and provides links to data downloadable as ESRI[®] shape files, Manifold[®] GIS map files and KML files for Google[™] Earth. Shape files are provided in both geographic (longitude-latitude) and UTM projections. Unlike the main BC Geological Survey Geology Map, which is in BC Albers projection, the Skeena Arch map is in Zone 9 UTM projection. It was felt that this projection would be more useful for those who wish to print maps from the website and plot their own data using UTM co-ordinates captured from a GPS unit. The map is built using the Autodesk[®] MapGuide[™] application.

The Skeena Arch map can be launched either by clicking on the map image or Skeena Arch hyperlink on the Thematic Maps page, or by clicking on the image on the More Details page. Clicking on this map will launch the Mapguide viewer, thus enabling interactive display of the data layers that constitute the Skeena Arch map. The different components of the metallogenic map are arranged in the Skeena Arch Metallogeny layer group, which can be activated or deactivated by checking the box next to the layer group name. By default this layer group is set to 'On', with the MINFILE, Faults, Bedrock Geology and Project Area layers selected for display when the map is launched (Fig 2).

The Skeena Arch map includes most of the layer groups that make up the main MapPlace geology maps, although some layers have been deleted because they are not relevant to the Skeena Arch project area or because they present data that are not of sufficient detail to be useful in displaying metallogenic themes for the project area. Also, some layers have been rearranged for simplicity of use. This is particularly true of the topographic layers, which have been put into layer groups so that features like lakes, rivers, etc. can be turned on or off by simply selecting or de-selecting the layer group they are in. As mentioned above, the display of layers within a topographic layer group is scale dependent, so the layers that are displayed will depend on the scale of the map. For example, topographic contours will be displayed at increasing detail as the user zooms into an area, with the most detailed being the 20 m contours from the TRIM contour layer. Key geological layer groups, such as geology, mineral potential, mineral titles, mineral inventory and regional geochemistry, are all included as part of the Skeena Arch map.

A key component of the Skeena Arch Metallogeny map is the ability to display different deposit types by turning their corresponding layers on or off. Layers have been created for the deposit types shown in Table 1, which make up 93% of the metallic mineral occurrences in the project

TABLE 1. MAIN DEPOSIT TYPES IN THE SKEENA ARCH PROJECT AREA.

Deposit type	Profile code	No of occurrences
Volcanic red-bed Cu	D03	86
Intrusion-related Au pyrrhotite veins	I02	38
Polymetallic Ag-Pb-Zn Au veins	I05	268
Cu skarns	K01	20
Subvolcanic Cu-Ag-Au-(As-Sb)	L01	153
Porphyry Cu Mo Au	L04	140
Porphyry Mo (low-F-type)	L05	66

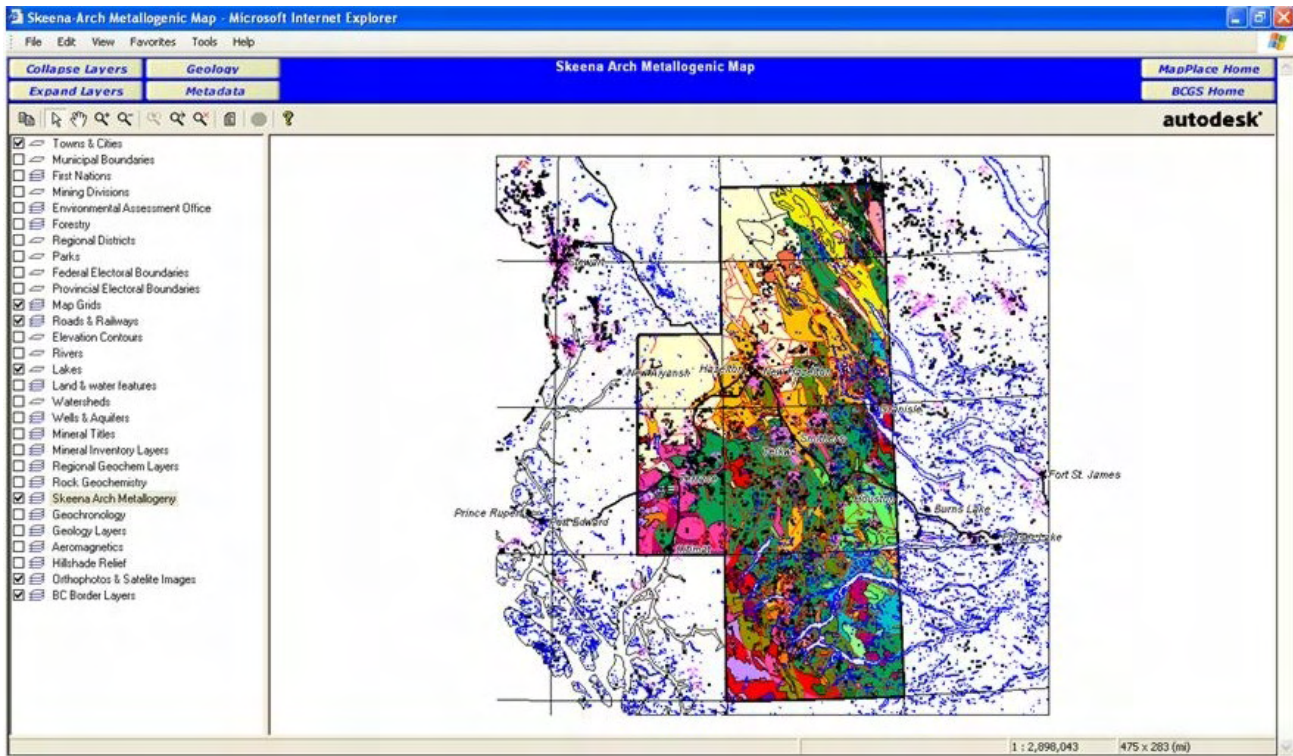


Figure 2. Screen capture of the default map for the Skeena Arch site, showing bedrock geology within the project area.

area. These layers are designed to be used in conjunction with the main MINFILE layer, which provides direct access to information on individual occurrences in the MINFILE database.

In addition to creation of layers for specific MINFILE deposit types, 95th percentile threshold values for Regional Geochemical Survey data within the project area have been calculated. Separate layers showing the locations of anomalous samples for Cu, Mo, Au, Ag, Hg, As, Sb, Pb and Zn have also been created. Recalculated threshold values are shown in Table 2.

Porphyry Molybdenum Example

The following example illustrates how the Skeena Arch map can be used to produce metallogenic maps for a specific deposit type, in this case porphyry molybdenum occurrences. This particular deposit type is currently of interest to exploration companies because of high Mo commodity prices. A number of properties in the area, including the Red Bird, Lucky Ship and Davidson (formerly Yorke-Hardy and Glacier Gulch) deposits, are currently the sites of active exploration programs. As shown in Table 1, there are 66 MINFILE occurrences in the project area that have been classified as porphyry Mo. This particular deposit type is characterized by the presence of molybdenite-bearing quartz vein stockworks and fractures that are spatially and genetically associated with high-level to subvolcanic felsic to intermediate intrusive complexes. In the project area, deposits of this type are associated with intrusions that are Late Cretaceous (*e.g.*, Bulkley plutonic suite) or Eocene (*e.g.*, Nanika and Babine plutonic suites) in age. Intrusive phases that are associated with Mo mineralization are typically medium to fine-grained biotite-quartz-feldspar-

phyric intrusions that range from quartz monzonite to granite in composition. Multiple stages of fracture and vein-controlled Mo mineralization are typically found near an intrusive contact, either within the intrusion itself or in surrounding hornfelsed country rocks. Molybdenite is the pri-

TABLE 2. RECALCULATED REGIONAL GEOCHEMICAL SURVEY (RGS) THRESHOLD VALUES AT THE 95TH PERCENTILE FOR THE SKEENA ARCH PROJECT AREA.

Element	Method	95 th percentile threshold value	
Ag	AAS	0.40	ppm
As	AASH	37.00	ppm
As	NA	44.00	ppm
Au	FA	6.00	ppb
Au	NA	15.00	ppb
Cu	AAS	80.00	ppm
Hg	AASF	120.00	ppb
Mo	AAS	4.00	ppm
Mo	NA	4.00	ppm
Pb	AAS	19.00	ppm
Sb	AASH	2.00	ppm
Sb	NA	3.40	ppm
W	NA	3.00	ppm
Zn	AAS	175.00	ppm

Abbreviations: AAS, atomic absorption spectrophotometry; AASF, flameless atomic absorption spectrophotometry; AASH, hybrid-generation atomic absorption spectrophotometry; FA, fire assay; NA, neutron activation

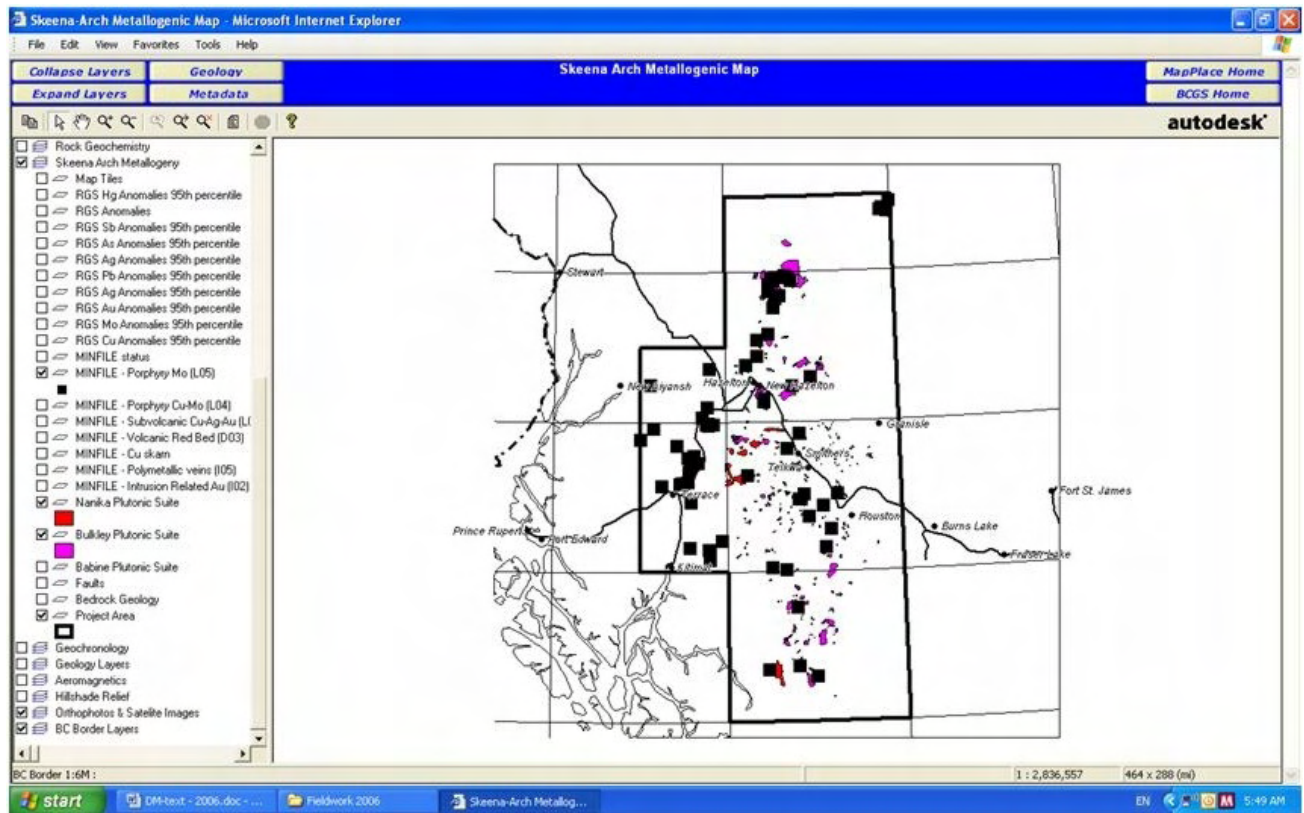


Figure 3. Screen capture of the Skeena Arch metallogenic map, showing the distribution of porphyry Mo occurrences in the project area.

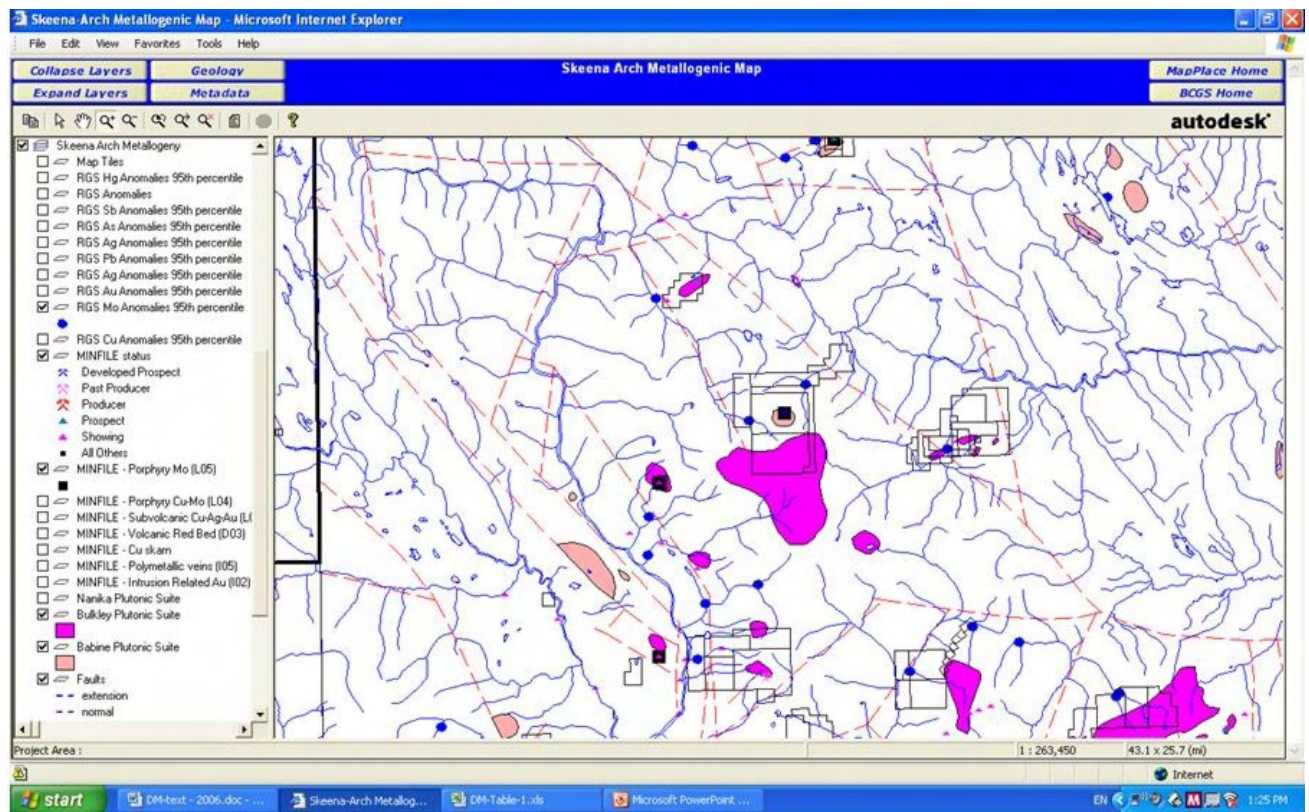


Figure 4. Screen capture of the Skeena Arch metallogenic map, showing porphyry Mo occurrences and related intrusions in the Mount Thomlinson area.

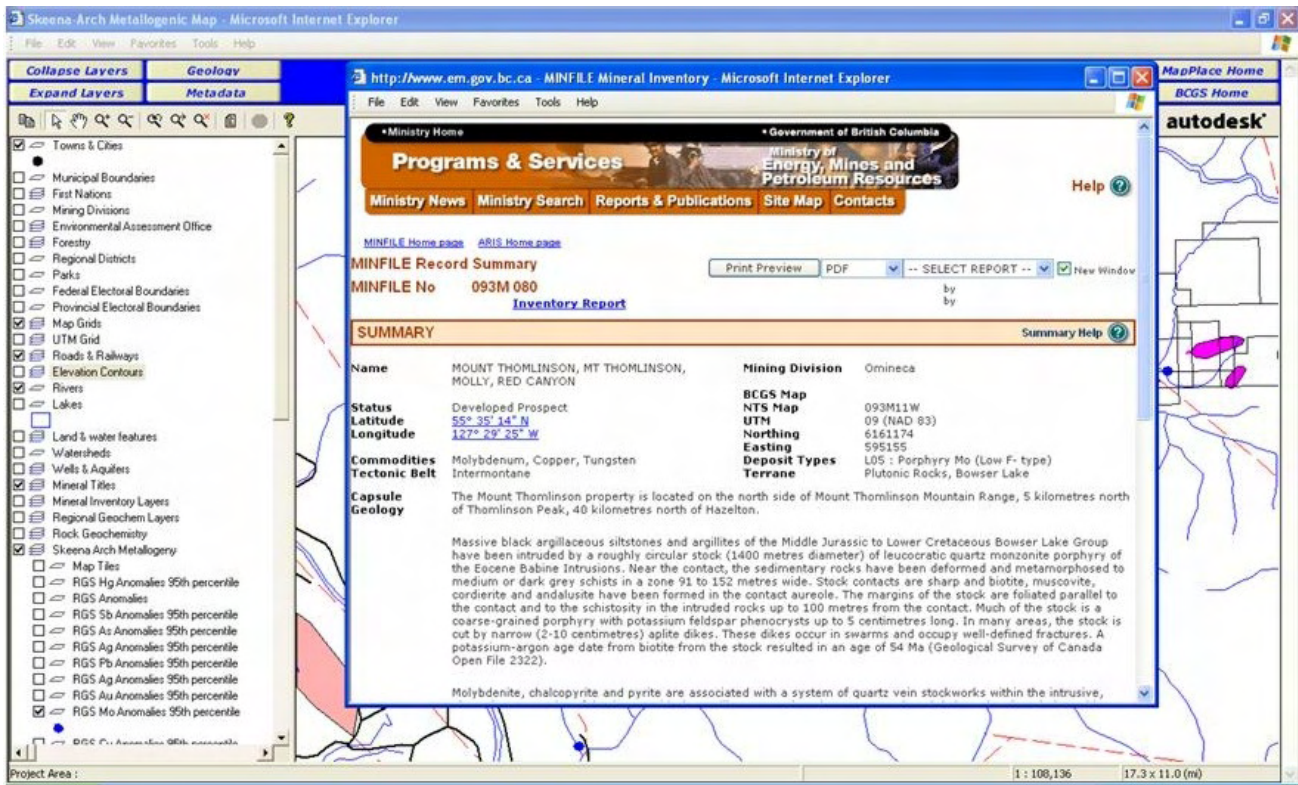


Figure 5. Screen capture showing MINFILE information for the Mount Thomlinson occurrence; MINFILE database is accessed by clicking on the location markers that are displayed when the MINFILE status layer is on.

Mt. Thomlinson Area - Porphyry Mo targets

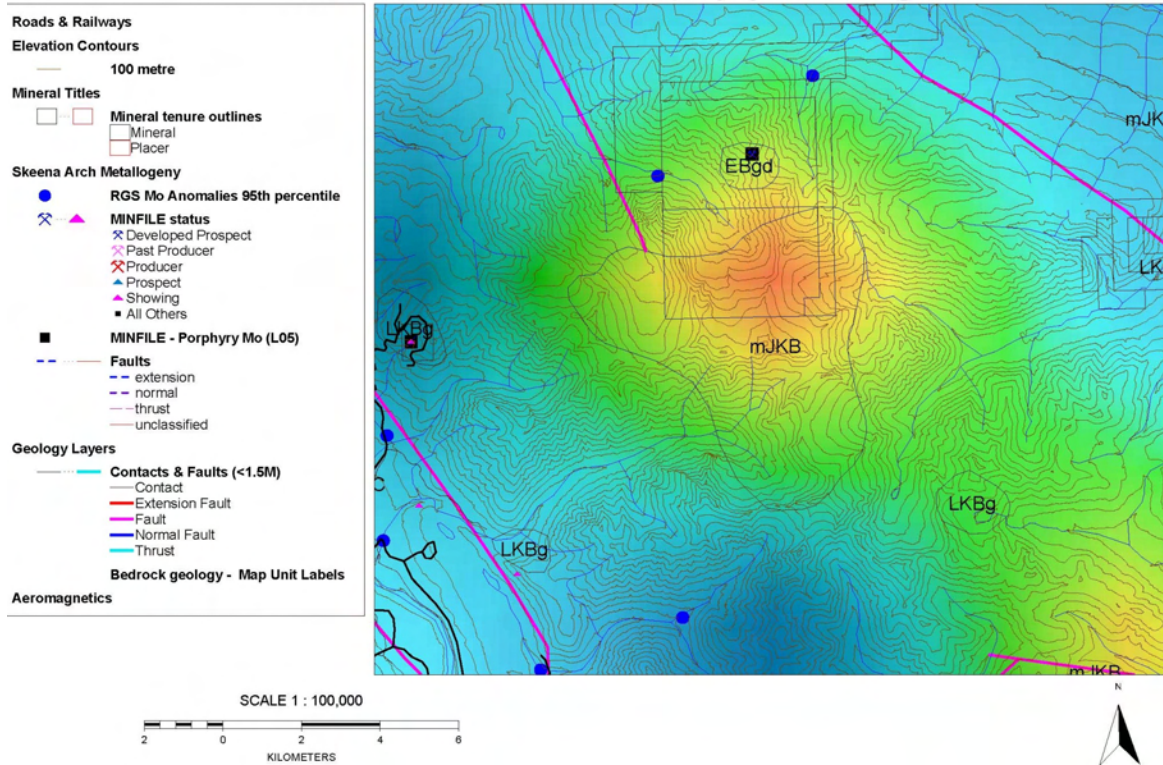


Figure 6. Custom printout generated from the Skeena Arch map, showing MINFILE occurrences, Mo geochemical anomalies, mineral tenure outlines and geological contacts and aeromagnetic anomalies in the Mount Thomlinson area.

mary sulphide mineral, but chalcopyrite may also be present in subordinate amounts. Alteration assemblages associated with Mo mineralization include K-feldspar, biotite, quartz, sericite and pyrite. As would be expected, the primary geochemical signature for porphyry Mo deposits in regional stream sediments is Mo, with F, Cu, W, Pb, Zn and Ag also locally elevated.

As a starting point, a user interested in the distribution of porphyry Mo occurrences in the Skeena Arch project area would turn on the MINFILE porphyry Mo layer. As shown in Figure 3, this will display all MINFILE occurrences whose primary classification is Porphyry Mo (Deposit Profile L05). To get more detailed information for a particular area, the user would then zoom into that area and turn on additional layers, such as Regional Geochemical Survey (RGS) Mo anomalies and the layers for associated plutonic rocks (e.g., the Babine and Bulkley intrusions). They could also show up-to-date mineral tenures in the area by turning on the Mineral Tenure layer group. An example of such a map for the Mount Thomlinson area north of Hazelton is shown in Figure 4. Note that, by left double-clicking on the marker for individual MINFILE occurrences, the user can access the MINFILE database and acquire information about the mineral occurrence selected (Fig 5). Within the MINFILE database are links to assessment reports that are available in PDF format through the Assessment Report Indexing System (ARIS).

In a few minutes, the user has a map of the area of interest that can be printed at any scale and a complete list of information on the mineral occurrences in the area. One of the strengths of the Mapguide system is that it provides the user with the ability to create custom map printouts at any scale. An example of a printout, again using the Mount Thomlinson area example, is shown in Figure 6. This map has 100 m contours, with geological contacts and map unit labels superimposed on an aeromagnetic map of the area. This map shows that intrusions in the area that have associated Mo mineralization are possibly related to a larger intrusive body at depth, corresponding to the extent of a large aeromagnetic anomaly. In addition, there are a number of RGS Mo anomalies that are unexplained by the distribution of known occurrences, suggesting there may be potential for new discoveries in the area.

SUMMARY

Geoscience information for the Skeena Arch project has now been posted to the BC Ministry of Energy, Mines and Petroleum Resources MapPlace (2006) website for download and viewing. The site provides four significant components, published as GeoFile 2007-3: an interactive MapPlace map with layer groups designed to highlight specific metallogenic targets such as porphyry Cu-Mo deposits; downloadable data in shape file format for use in most GIS systems, such as ArcView or ArcExplorer; Manifold map files for use in Manifold GIS; and KML files for use in viewers such as Google Earth. A new set of digital 1:100 000 scale maps will also be made available for the project area early in 2007.

ACKNOWLEDGMENTS

The author would like to acknowledge the financial support provided by Geoscience BC for this project. In addition, the British Columbia Ministry of Energy, Mines and

Petroleum Resources has provided support by providing their award-winning MapPlace website as a host for the Skeena Arch map.

REFERENCES

- Bassett, K.N. (1991): Preliminary results of the sedimentology of the Skeena Group in west-central British Columbia; in Current Research, Part A, *Geological Survey of Canada*, Paper 91-1A, pages 131–141.
- Bassett, K.N. and Kleinspehn, K.L. (1996): Mid-Cretaceous transension in the Canadian Cordillera: evidence from the Rocky Ridge volcanics of the Skeena Group; *Tectonics*, volume 15, pages 727–746.
- BC Geological Survey (2006): MapPlace GIS internet mapping system; *BC Ministry of Energy, Mines and Petroleum Resources*, MapPlace website, URL <<http://www.MapPlace.ca>> [November 2006].
- Carter, N.C. (1976): Regional setting of porphyry deposits in west-central British Columbia; in *Porphyry Deposits of the Canadian Cordillera*, Sutherland Brown, A., Editor, *Canadian Institute of Mining and Metallurgy*, Special Volume 15, pages 227–238.
- Carter, N.C. (1981): Porphyry copper and molybdenum deposits, west-central British Columbia; *BC Ministry of Energy, Mines and Petroleum Resources*, Bulletin 64.
- Carter, N.C., Dirom, G.E. and Ogryzlo, P.L. (1995): Porphyry copper-gold deposits, Babine Lake area, west-central British Columbia; in *Porphyry Deposits of the Northwestern Cordillera of North America*, Schroeter, T.G., Editor, *Canadian Institute of Mining, Metallurgy and Petroleum*, Special Volume 46, pages 247–255.
- Diakow, L.J., Webster, I.C.L., Richards, T.A. and Tipper, H.W. (1997): Geology of the Fawnie and Nechako Ranges, southern Nechako Plateau, central British Columbia (93F/2, 3, 6, 7); in *Interior Plateau Geoscience Project: Summary of Geological, Geochemical and Geophysical Studies*, Diakow, L.J. and Newell, J.M., Editors, *BC Ministry of Energy, Mines and Petroleum Resources*, Paper 1997-2, *Geological Survey of Canada*, Open File 3448, pages 7–30.
- Evenchick, C.A. (1999): Depositional and structural histories of the northern two-thirds of the Bowser Basin – Skeena Fold Belt, northern British Columbia: records of terrane interactions; in *Terrane Paths 99*, Circum-Pacific Terrane Conference, Evenchick, C.A., Woodsworth, G.J. and Jongens, R., Editors, *Geological Survey of Canada – Geological Association of Canada*, Abstracts and Program, pages 30–32.
- Grainger, N.C. and Anderson, R.G. (1999): Geology of the Eocene Ootsa Lake Group in northern Nechako River and southern Fort Fraser map area, central British Columbia; in *Current Research 1999-A*, *Geological Survey of Canada*, pages 139–148.
- Grainger, N.C., Villeneuve, M.E., Heaman, L.M. and Anderson, R.G. (2001): New U-Pb and Ar/Ar isotopic age constraints on the timing of Eocene magmatism, Fort Fraser and Nechako River Map areas, central British Columbia; *Canadian Journal of Earth Sciences*, volume 38, number 4, pages 679–696.
- MacIntyre, D.G. (1985): Geology and mineral deposits of the Tahta Lake district, west-central British Columbia; *BC Ministry of Energy, Mines and Petroleum Resources*, Bulletin 75.
- MacIntyre, D.G. (1998): Babine Porphyry District Project: bed-rock geology of the Nakinilerak Lake map sheet (93M/8), British Columbia; in *Geological Fieldwork 1997*, *BC Ministry of Energy, Mines and Petroleum Resources*, Paper 1998-1, pages 2-1–2-18.

- MacIntyre, D.G. (2001a): Geological compilation of the Babine porphyry copper district, BC; *BC Ministry of Energy, Mines and Petroleum Resources*, Open File Map 2001-3.
- MacIntyre, D.G. (2001b): The Mid-Cretaceous Rocky Ridge Formation — a new target for subaqueous hot-spring deposits (Eskay Creek-type) in central British Columbia; in *Geological Fieldwork 2000, BC Ministry of Energy, Mines and Petroleum Resources*, Paper 2001-1, pages 253–268.
- MacIntyre, D.G. (2006): Geology and mineral deposits of the Skeena Arch, west-central British Columbia: a Geoscience BC digital data compilation project; in *Geological Fieldwork 2005, BC Ministry of Energy, Mines and Petroleum Resources*, Paper 2006-1, pages 303–312.
- MacIntyre, D.G., Ash C. and Britton, J. (1994): Nass-Skeena (93/E, L, M; 94/D; 103/G, H, I, J, P; 104/A, B); *BC Ministry of Energy, Mines and Petroleum Resources*, Open File 1994-14.
- MacIntyre, D.G., Desjardins, P. and Tercier, P. (1989): Jurassic stratigraphic relationships in the Babine and Telkwa ranges; in *Geological Fieldwork 1988, BC Ministry of Energy, Mines and Petroleum Resources*, Paper 1989-1, pages 195–208.
- MacIntyre, D.G. and Villeneuve, M.E. (2001): Geochronology and tectonic setting of mid-Cretaceous to Eocene magmatism, Babine porphyry copper district, central British Columbia; *Canadian Journal of Earth Sciences*, volume 38, pages 639–655.
- MacIntyre, D.G., Villeneuve, M.E. and Schiarizza, P. (2001): Timing and tectonic setting of Stikine Terrane magmatism, Babine-Takla lakes area, central British Columbia; *Canadian Journal of Earth Sciences*, volume 38, pages 579–601.
- MacIntyre, D.G., Webster, I.C.L. and Bellefontaine, K. (1996a): Babine Porphyry District Project: bedrock geology of the Fulton Lake map area (NTS 93L16); in *Geological Fieldwork 1995, BC Ministry of Energy, Mines and Petroleum Resources*, Paper 1996-1, pages 11–35.
- MacIntyre, D.G., Webster, I.C.L. and Bellefontaine, K. (1996b): Geology of the Fulton Lake map sheet (93L/16); *BC Ministry of Energy, Mines and Petroleum Resources*, Open File Map 1996-29.
- MacIntyre, D., Webster, I. and Desjardins, P. (1998): Bedrock geology of the Old Fort Mountain map area, north-central BC; *BC Ministry of Energy, Mines and Petroleum Resources*, Open File Map 1997-10.
- MacIntyre, D.G., Webster, I.C.L. and Villeneuve, M. (1997): Babine Porphyry District Project: bedrock geology of the Old Fort Mountain area (93M/1), British Columbia; in *Geological Fieldwork 1996, BC Ministry of Energy, Mines and Petroleum Resources*, Paper 1997-1, pages 47–67.
- Massey, N.W.D. (1999): Volcanogenic massive sulphide deposits in British Columbia; *BC Ministry of Energy, Mines and Petroleum Resources*, Open File 1999-2.
- Massey, N.W.D., Alldrick, D.J. and Lefebure, D.V.L. (1999): Potential for subaqueous hot-spring (Eskay Creek) deposits in British Columbia; *BC Ministry of Energy, Mines and Petroleum Resources*, Open File 1999-14.
- Massey, N.W.D., MacIntyre, D.G., Haggart, J.W., Desjardins, P.J., Wagner, C.L. and Cooney, R.T. (2005): Digital map of British Columbia: tile NN8-9 North Coast and Queen Charlotte Islands/Haida Gwaii; *BC Ministry of Energy, Mines and Petroleum Resources*, GeoFile 2005-5.
- MINFILE (2006): MINFILE BC mineral deposits database; *BC Ministry of Energy, Mines and Petroleum Resources*, URL <<http://www.em.gov.bc.ca/Mining/Geosurv/Minfile/>> [November 2006].
- Monger, J.W.H., Gabrielse, H. and Souther, J.A. (1972): Evolution of the Canadian Cordillera: a plate tectonic model; *American Journal of Science*, volume 272, pages 577–602.
- Monger, J.W.H. and Nokleberg, W.J. (1996): Evolution of the northern North American Cordillera: generation, fragmentation, displacement and accretion of successive North American plate-margin arcs; in *Geology and Ore Deposits of the American Cordillera*, Coyner, A.R. and Fahey, P.L., Editors, *Geological Society of Nevada*, Symposium Proceedings, Reno-Sparks, Nevada, April 1995, pages 1133–1152.
- Richards, T.A. (1980): Geology of the Hazelton map area (93M); *Geological Survey of Canada*, Open File 720.
- Richards, T.A. (1990). Geology of the Hazelton map area (93M); *Geological Survey of Canada*, Open File 2322.
- Schiarizza, P. and MacIntyre, D.G. (1999): Geology of the Babine Lake – Takla Lake area, central British Columbia; in *Geological Fieldwork 1998, BC Ministry of Energy, Mines and Petroleum Resources*, Paper 1999-1, pages 33–68.
- Sinclair, W.D. (1995): Porphyry Mo (low-F-type); in *Selected British Columbia Mineral Deposit Profiles, Volume 1 — Metallics and Coal*, Lefebure, D.V. and Ray, G.E., Editors, *BC Ministry of Energy, Mines and Petroleum Resources*, Open File 1995-20, pages 93–96.
- Struik, L.C., Schiarizza, P., Orchard, M.J., Cordey, F., Sano, H., MacIntyre, D.G., Lapierre, H. and Tardy, M. (2001): Imbricate architecture of the upper Paleozoic to Jurassic oceanic Cache Creek Terrane, central British Columbia; *Canadian Journal of Earth Sciences*, volume 38, number 4, pages 495–514.
- Thorkelson, D.J., Mortensen, J.K., Marsden, H. and Taylor, R.P. (1995): Age and tectonic setting of Early Jurassic episodic volcanism along the northeastern margin of the Hazelton Trough, northern British Columbia; in *Jurassic Magmatism and Tectonics of the North American Cordillera*, Miller, D.M. and Busby, C., Editors, *Geological Society of America*, Special Paper 299, pages 83–94.
- Tipper, H.W. and Richards, T.A. (1976a): Geology of the Smithers area; *Geological Survey of Canada*, Open File Map 351.
- Tipper, H.W. and Richards, T.A. (1976b): Jurassic stratigraphy and history of north-central British Columbia; *Geological Survey of Canada*, Bulletin 270, 73 pages.
- Yorath, C.J. (1991): Upper Jurassic to Paleogene assemblages; Chapter 9 in *Geology of the Cordilleran Orogen of Canada*, Gabrielse, H. and Yorath, C.J., Editors, *Geological Survey of Canada*, Geology of Canada, number 4, p. 329–371 (also *Geological Society of America*, *The Geology of North America*, volume G-2).

New Geological Mapping and Implications for Mineralization Potential in the Southern and Western Whitesail Lake Map Area (NTS 093E), Southwestern British Columbia¹

by J.B. Mahoney², J.W. Haggart³, R.L. Hooper², L.D. Snyder², G.J. Woodsworth³ and R.M. Friedman⁴

KEYWORDS: Hazelton Group, Whitesail Lake, layered mafic intrusion, Central Gneiss Complex, Gamsby complex

INTRODUCTION

This investigation focuses on detailed bedrock mapping and economic mineralization potential in the southern and western Whitesail Lake map area (NTS 093E; Fig 1). Fieldwork in 2006 targeted the western and southwestern portions of the map area, specifically NTS 093E/04, 05, 06, 11 and 12. Mapping in these areas provides linkage to work completed in the southern portion of the Whitesail Lake map area under the Rocks to Riches Program (Mahoney *et al.*, 2005; Gordee *et al.*, 2005), and attempts to tie in with pre-existing mapping in the central portion of the map area (Fig 2). The primary objective of this investigation is to provide a comprehensive evaluation of potential for economic mineralization in the southern and western Whitesail Lake map area.

Objectives and Scope

The western and southwestern Whitesail Lake (NTS 093E) 1:250 000 map area straddles the transition zone between the Coast and Intermontane morphogeological belts, and is underlain by igneous and metamorphic rocks of the Coast Plutonic Complex on the west and Jurassic and Cretaceous volcanosedimentary successions of southwestern Stikinia on the east (Fig 1, 2). This boundary was examined to the south under the Bella Coola Targeted Geoscience Initiative (TGI; 2000–2004), which focused on constraining the geological evolution of the region and assessing the economic potential of Mesozoic volcanic assemblages and plutonic belts in the area (Haggart *et al.*, 2006). The geological framework established by the Bella Coola TGI was extended to the north, into the southern Whitesail Lake map

area (NTS 093E/02, 03), under the Rocks To Riches Program in 2004. The geological setting and economic mineralization potential of Jurassic and Cretaceous stratified volcanosedimentary successions in the central portion of the Whitesail Lake map area have been documented previously by the British Columbia Geological Survey (1987–1990), and mapping conducted under the present project has been designed to link into this existing geological framework (Diakow and Mihalyuk, 1987; Diakow and Koyanagi, 1988; Diakow and Drobe, 1989; Diakow, 1990).

The current investigation focuses on 1:50 000 scale mapping and economic mineral assessment in the western and southwestern portions of the Whitesail Lake map area (093E/04, 05, 12 and parts of 093E/06 and 11). This project, sponsored by Geoscience BC, involves a combined research team from the University of Wisconsin – Eau Claire, the Geological Survey of Canada and the University of British Columbia. It seeks to improve our understanding of the geological evolution and economic mineral potential of the west-central portion of the Coast Mountains of British Columbia (53–54°N).

The primary focus of mapping during the 2006 field season was the western and southwestern portions of the Whitesail Lake map area, including portions of the Kitlope Lake (093E/04), Tsaytis River (093E/05), Chikamin Mountain (093E/06), Troitsa Peak (093E/11) and Tahtsa Peak (093E/12) 1:50 000 map areas (Fig 1–3). This region is underlain by Triassic, Jurassic and Cretaceous volcanic and sedimentary successions on the western edge of Stikinia, which have volcanogenic massive sulphide potential, and by Jurassic to Eocene plutonic bodies along the eastern margin of the Coast Plutonic Complex, which are known hosts for a variety of porphyry deposits (Woodsworth, 1980; Dawson *et al.*, 1991; Diakow *et al.*, 2002). This report briefly describes the geology of this region, based on detailed bedrock mapping during the 2006 field season (Fig 3). This investigation will integrate regional bedrock mapping, stratigraphic and structural analyses, geochronology, plutonic and volcanic geochemistry, isotopic analyses and mineral assays into a comprehensive assessment of the geological framework and economic mineral potential of the region.

Geological Setting

The geology of the western and southwestern Whitesail Lake map area can be described in terms of three northwest-trending lithological belts of sedimentary and metamorphic rocks that are intruded by plutons of primarily Jurassic, Cretaceous and Cenozoic ages. These lithological belts include, from east to west 1) unmetamor-

¹ Geoscience BC contribution GBC039

² Department of Geology, University of Wisconsin, Eau Claire, WI (mahonej@uwec.edu)

³ Geological Survey of Canada, Vancouver, BC

⁴ Pacific Centre for Isotopic and Geochemical Research, University of British Columbia, Vancouver, BC

This publication is also available, free of charge, as colour digital files in Adobe Acrobat® PDF format from the BC Ministry of Energy, Mines and Petroleum Resources website at http://www.em.gov.bc.ca/Mining/Geolsurv/Publications/catalog/cat_fldwk.htm

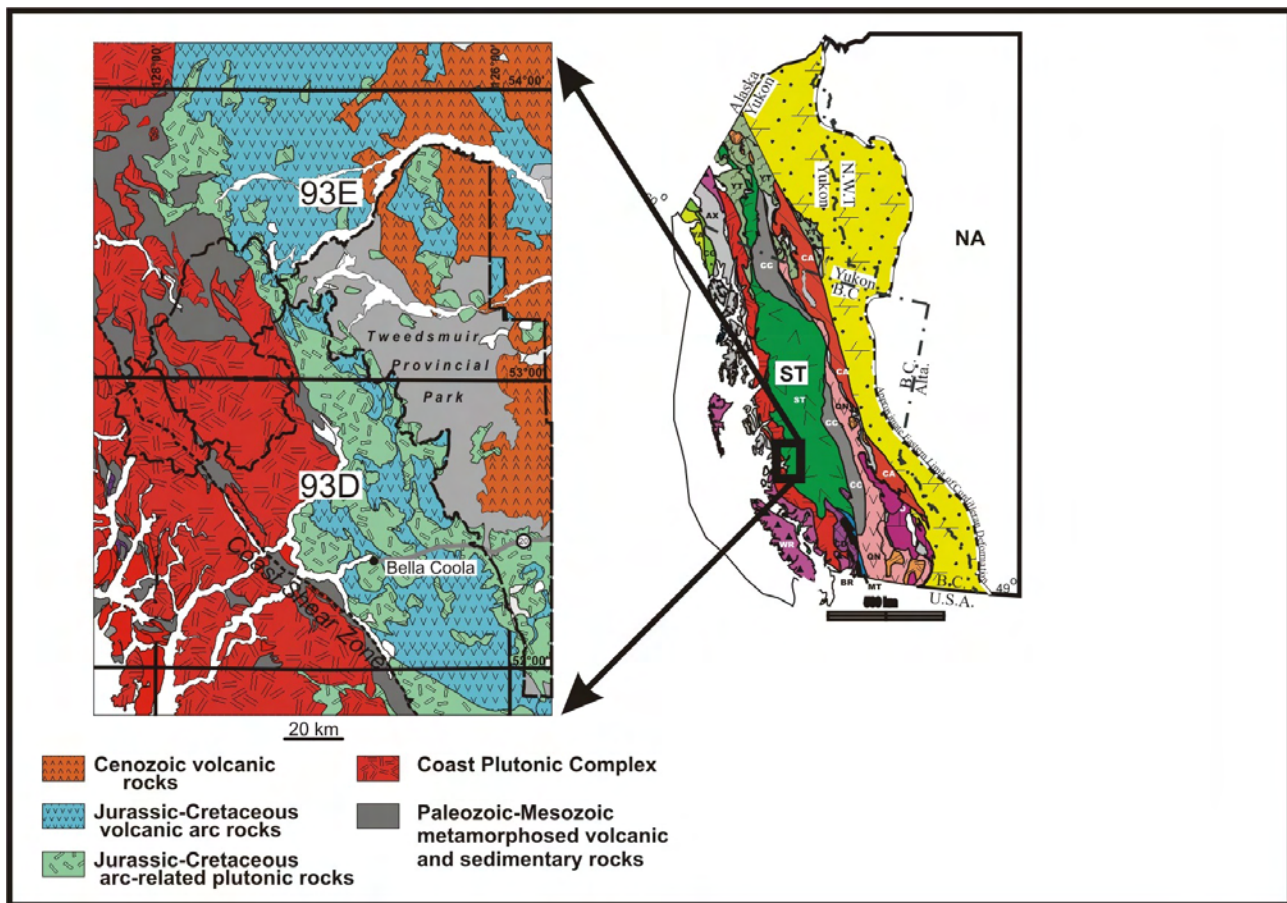


Figure 1. General geological setting of NTS 93D (Bella Coola) and 93E (Whitesail Lake) 1:250 000 map areas; inset is a schematic terrane map of the Canadian Cordillera, modified from Wheeler and McFeely (1991).

posed to weakly metamorphosed supracrustal stratigraphic successions, including the Lower to Middle Jurassic Hazelton Group (and its weakly metamorphosed equivalents), Upper Jurassic sedimentary rocks, Lower Cretaceous Skeena Group, and Upper Cretaceous Kasalka volcanic rocks; 2) upper greenschist to upper amphibolite facies volcanic, sedimentary and plutonic rocks of the Triassic to Lower Jurassic (?) Gamsby complex; and, 3) high-grade metamorphic rocks of the Central Gneiss Complex. These lithological packages are described sequentially below, from east to west.

EASTERN LITHOLOGICAL BELT

HAZELTON GROUP (UNIT Jh)

The western and southern Whitesail Lake map area contains some of the southernmost exposures of the Lower to Middle Jurassic Hazelton Group (Woodsworth, 1980;

Figure 2. Geographic distribution of existing 1:50 000 geological maps in the Whitesail Lake map area, and the extent of mapping (red) conducted under the Geoscience BC program. Blue areas were mapped by BC Geological Survey teams (ca. 1985–1990; letters keyed to reference list); yellow area is thesis map of van der Heyden (1982); light purple area was mapped by Bella Coola Targeted Geoscience Initiative project in Bella Coola area (NTS 93D; 2001–2003), and NTS 93E/02 and 03 were mapped under the Rocks to Riches Program (2004).

Gordec *et al.*, 2005). The stratigraphy, geochronology and geochemistry of the Hazelton Group in the southern Whitesail Lake map area (NTS 93E/02, 03) were documented during a regional assessment of potential Eskey

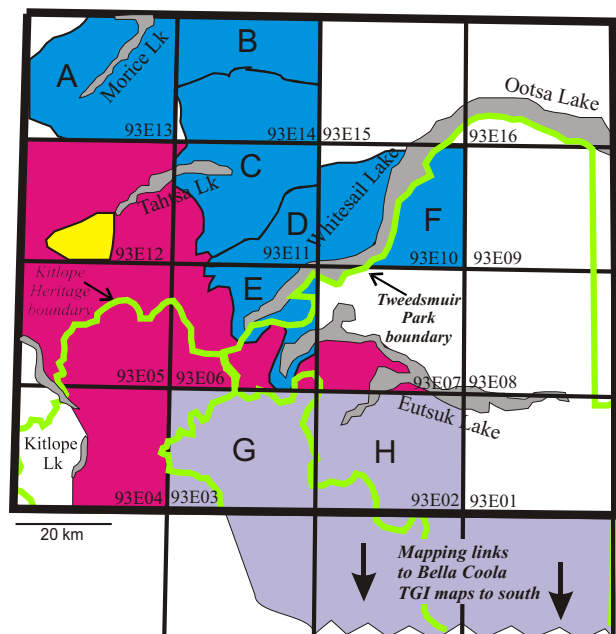


TABLE 1. GEOCHRONOLOGICAL SAMPLE LOCATIONS, SOUTHERN AND WESTERN WHITESAIL LAKE AREA.

Map ID	Sample number	Easting	Northing	Map unit	Rock type	Location	Mean $^{206}\text{Pb}/^{238}\text{U}$	Method	Purpose
1	147aJBM04	633145	5807159	Eqm	Biotite-quartz monzonite	Red Bird Mtn	53.0 ± 0.3	TIMS	Dates Mo porphyry
2	HFB-05-94	609910	5913716	IJg	Granodiorite	Mt Irma N	146.3 ± 1.6	LA	Constrains TJmv + Js age
3	05-wv-50	597396	5905702	Jlm	Quartz diorite	Black Dome	187.5 ± 1.8	LA	Constrains Jlm age
4	HFB-05-52	614950	5900950	TJmv	Rhyolite breccia	Ear Lake N	170.28 ± 0.97	LA	Constrains TJmv protolith
5	05-RH-11	584274	5904955	TJgc	Metatonalite	NW Black Dome	206.0 ± 1.7	LA	Constrains TJgc protolith
6	HFB-05-53	603590	5901475	Jt	Hornblende quartz diorite	Tenaiko range	123.9 ± 1.6	LA	Dates Tenaiko suite
7	60JBM05	584601	5898393	Jt (?)	Epidote-biotite granodiorite	Tysatis Peak	125.50 ± 0.65	LA	Dates upper plate of the detachment

Abbreviations: LA, laser-ablation inductively coupled plasma mass spectrometry; TIMS, thermal ionization mass spectrometry

Creek-type volcanogenic massive sulphide mineralization (Gordec, 2005; Gordec *et al.*, 2005; Mahoney *et al.*, 2005). In that area, the Hazelton Group comprises a thick (>4 km), bimodal volcanic succession of basaltic and basaltic andesite flows and associated volcanogenic strata, interbedded with and overlain by rhyolitic tuff, lapilli tuff, tuff-breccia, tuffaceous sedimentary rocks and associated rhyolitic domes (Gordec, 2005; Gordec *et al.*, 2005). The stratigraphic position and composition of Middle Jurassic strata in the southern Whitesail Lake map area are very similar to the strata hosting the Eskay Creek VMS deposit. Although the strata were deposited in an actively extending environment favourable for the formation of VMS deposits, it is apparent that, in this region, these rocks were deposited in a shallow-marine setting that did not promote formation of such deposits (Gordec, 2005).

Structural, stratigraphic, geochronological and biostratigraphic data indicate that Hazelton Group strata in the Whitesail Lake map area occur in eastward-younging, gently east-dipping structural panels that become progressively older to the west, with deeper levels of the volcanic system exposed adjacent to the Coast Plutonic Complex (Gordec *et al.*, 2005; Mahoney *et al.*, 2005; Haggart *et al.*, 2006). In the southern and western portions of the map area, rocks assigned to the Hazelton Group occur in a discontinuous, northwesterly-trending structural panel east of the Central Gneiss Complex and associated metavolcanic rocks and west of extensive exposures of Cretaceous sedimentary and volcanic strata (Fig 3). Rocks herein mapped as Hazelton Group have previously assigned to the Lower Cretaceous Gambier Group (Woodsworth, 1980; Diakow, 2006). Lithological and stratigraphic similarities with rocks mapped as Hazelton Group (Gordec, 2005; Gordec *et al.*, 2005) to the south and new age constraints on crosscutting plutons (*see* description of Sias pluton, below) support inclusion of these strata in the Hazelton Group. The Hazelton Group comprises a thick succession of mafic volcanic flows, breccia, tuff-breccia and lapilli tuff, with lesser dark, thin-bedded, fine-grained argillite, siltstone and sandstone. Rhyolitic lapilli tuff, tuff and domes occur locally, but represent less than 20% of the main outcrop belt. Sedimentary strata intercalated with andesitic flows south of Price Peak yielded a poorly preserved ammonite and bivalve fossil assemblage of Late Pliensbachian to Toarcian

age (Haggart, 2005), and U-Pb geochronology on other localities is in progress.

CHATSQUOT LAYERED MAFIC INTRUSION (UNIT Jlm)

Chatsquot Mountain and adjacent ridges contain spectacular exposures of a layered mafic intrusion (Jlm) that forms an important component of the regional volcanic stratigraphy. Compositional banding consists of variable proportions of olivine, pyroxene, plagioclase and magnetite, and ranges in composition from ultramafic magnetite-olivine websterite to anorthositic gabbro. The prominent foliation in the rock parallels the compositional layering and results in a distinctly layered appearance. Typical compositional layers are less than 1 m thick, with clinopyroxene-rich gabbro (80% clinopyroxene) alternating with more plagioclase-rich layers that distinctly weather to a lighter colour. Subordinate ultramafic layers include apparent cumulate layers of magnetite-olivine-rich rocks that weather to a distinctive rusty brown with knobby surfaces. Along the ridge northeast of Chatsquot Mountain, unit Jlm is cut by numerous andesite porphyry dikes that locally exceed unit Jlm in volume and form intrusion breccia units. Unit Jlm extends from Chatsquot Mountain to the southern end of the Mount Gamsby ridge, and also caps the high peaks near Black Dome, where the layered mafic intrusion appears as a large screen within the Tenaiko intrusive suite (Fig 3).

The age of the Chatsquot layered mafic intrusion (LMI) is unclear. Two geochronological samples from anorthosite on Chatsquot Mountain and Gamsby Ridge were barren of zircons. A sample of undeformed quartz diorite collected from a succession of layered mafic intrusive rocks north of Black Dome yields a 187.5 ± 1.8 Ma U-Pb zircon age. The quartz diorite is structurally concordant with layers within the LMI, and may represent a late-stage differentiate from the layered mafic system or, conversely, could be a younger sill. Therefore, this age is considered to provide a minimum age for the Chatsquot LMI.

JURASSIC (?) ARGILLITE AND SANDSTONE (UNIT Js)

A north to northeast-dipping, locally overturned panel of argillite, siltstone and sandstone underlies Lindquist

Peak, east of Mount Irma (Fig 3). The overall succession may be up to 2.5 km thick and consists of alternating units of argillite and sandstone, although portions of the section may be thrust repeated. Similar lithological facies comprise six sedimentary units, which include, in ascending order 1) a basal mixed sandstone and argillite package; 2) a massive, strongly foliated argillite package; 3) a dominantly massive sandstone package, with minor shale interbeds; 4) a dominantly argillaceous package, with minor interstratified sandstone; 5) a massive sandstone package, similar to unit 3; and 6) an upper mixed argillite and sandstone package.

Sedimentary structures include climbing ripple cross-stratification, flaser bedding and abundant bioturbation. Sandstone interbeds are locally micaceous. Wood fragments are abundant and bivalve moulds occur as shell lag deposits in a fine-grained, calcareous-cemented facies. The composition and sedimentary structures in this unit contrast strongly with those of volcanogenic strata of the Hazelton Group, and these rocks have been inferred to represent the base of the Jurassic–Cretaceous Bowser Lake Group in this region (Mahoney *et al.*, 2006). This stratigraphic assignment is supported by a new 146.3 ± 1.6 Ma U–Pb zircon age on a crosscutting pluton (Fig 4, Table 1), which requires these strata to be Late Jurassic or older.

TRIASSIC (?) – JURASSIC METAVOLCANIC ROCKS (UNIT TJmv)

A succession of variably metamorphosed, mafic to silicic volcanic and volcanoclastic rocks, including andesitic to basaltic flows, tuff-breccia and tuff, with lesser argillite, is exposed west and south of Lindquist Lake. The metavolcanic rocks range from unfoliated to slightly foliated, thick bedded to massive, andesitic to rhyolitic lapilli tuff and tuff-breccia to strongly foliated tuff, sandstone and siltstone. The metamorphic grade varies from lower greenschist to upper greenschist, and chloritic schist (\pm epidote) dominates the package. A diagnostic characteristic of this package is that it contains readily identifiable volcanic textures with variable degrees of foliation, reflecting a strong rheological control during deformation. These rocks form a thrust panel structurally above unmetamorphosed Jurassic sedimentary rocks to the east (unit Js), and structurally beneath higher grade metavolcanic and metasedimentary rocks of the Gamsby complex (TJgc) to the west. These rocks occur along strike from unmetamorphosed to sub-greenschist Hazelton Group volcanic rocks, and a metamorphosed rhyolite breccia within the succession yielded a U–Pb zircon age of 170.3 ± 0.97 Ma (Fig 4, Table 1), which is interpreted to constrain the age of the protolith, in part. The structural position, composition and age constraints suggest these rocks are metamorphosed equivalents of the Lower to Middle Jurassic Hazelton Group, based on their dominantly volcanic character and paucity of carbonate interbeds. The rocks appear to represent a metamorphic and structural transition between the more highly deformed and higher grade Gamsby complex and the Hazelton Group. It is therefore possible that the TJmv package includes Triassic (?) metavolcanic and metasedimentary components.

MOUNT NEY VOLCANIC ROCKS (?) (UNIT Kv)

East of Tsah Mountain, sparse outcrops containing fine-grained, dark green to black basalt flows with fresh,

dark green augite phenocrysts and localized pillow structures overlie Jurassic Hazelton Group tuff-breccia and fine-grained volcanoclastic strata. These strata appear, in turn, to be overlain by feldspathic arenite and argillite of the Lower Cretaceous Skeena Group. Contacts in this area are not well exposed, but the overall stratigraphic succession appears to be a disconformable one. Lithological similarity and stratigraphic position suggest these rocks belong to unit IKv of MacIntyre (1985). Similar exposures are found just north of the Tahtsa Lake road, several kilometres southeast of Rhine Ridge and just east of the east end of Tahtsa Lake. Diakow (2006) informally referred to these strata as the Mount Ney volcanic rocks.

SKEENA GROUP (UNIT Ks)

A thick sequence of lithic feldspathic arenite and argillite is found in the northeastern part of the study area, the Rhine Ridge area and regions to the north, as well as the low country on the south side of Tahtsa Lake. Most of the succession dips very gently to the east. The base of the succession is not seen, although it appears to rest conformably (?) on the Mount Ney volcanic rocks approximately 5 km east of Tsah Mountain. The basal contact is interpreted to continue southward along strike to cross Tahtsa Lake where the Skeena Group appears to rest on Hazelton Group volcanic rocks. The unit is possibly overlain unconformably (?) by gently dipping to flat-lying Kasalka Group volcanic rocks on Rocky Ridge, although the precise nature of the contact, and whether or not it represents an unconformity, has not been established.

South of Tahtsa Lake, the lower part of the Skeena Group consists of approximately 350 m of mostly massive, fine to medium-grained feldspathic arenite. Individual sandstone beds within this lower part of the succession are up to several metres thick, locally show faint parallel laminations, and are intercalated with thinner, parallel-laminated mudstone or siltstone. Thin pebble lag horizons, including rounded to subangular, poorly sorted volcanic clasts and chert grains up to several centimetres in diameter, are noted uncommonly within the succession. The upper part of the Skeena Group is approximately 450 m in thickness, and consists of argillite with lesser sandstone beds of similar composition to those in the lower part of the succession. Wood fragments (up to several tens of centimetres in length) and leaf impressions are locally abundant.

In the Rhine Ridge area, the base of the section is not exposed, but the lower part of the succession consists of thick-bedded, fine to medium-grained sandstone with locally abundant ripple marks. Strata at this level of the section contain fossils assigned to the trigoniid bivalve *Myophorella (Steinmanella)* sp. (at UTM 608272E, 5955896N; Zone 9, NAD1983; identification by J.W. Haggart, specimens uncollected), suggesting a Valanginian (?) to Aptian age (Saul, 1978). The lower portion of the section is overlain by an argillitic section similar to that south of Tahtsa Lake, although this portion of the succession is significantly thinner in this area. Skeena Group rocks are considered to represent a range of shallow-marine to nonmarine depositional environments.

KASALKA GROUP (UNIT Kk)

North of Tahtsa Lake, the Upper Cretaceous Kasalka Group unconformably (?) overlies well-bedded arenite and argillite of the Skeena Group (Ks) and, to the south, forms a carapace on the Eocene Bollum stock (Fig 3; MacIntyre,

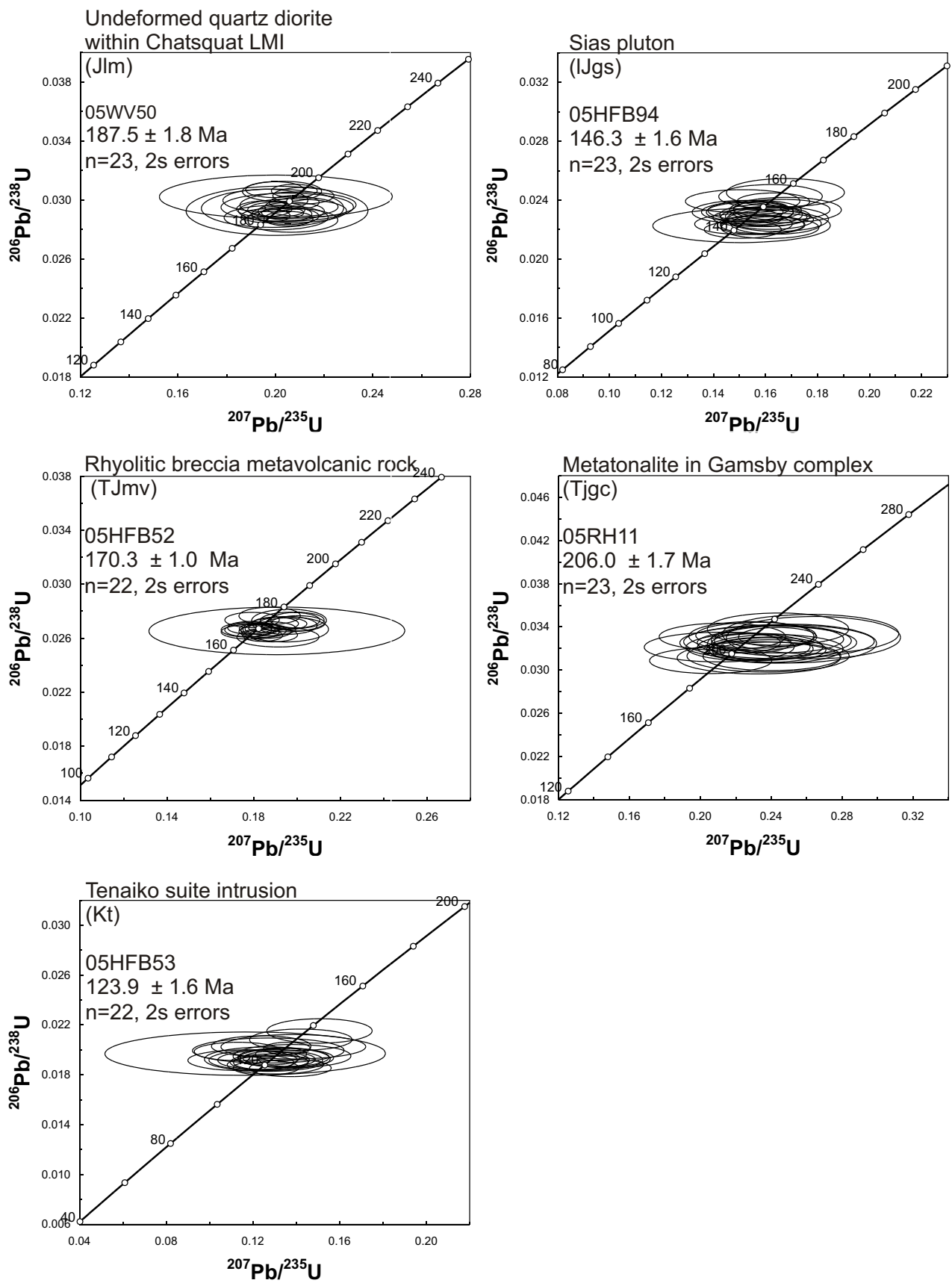


Figure 4. Standard concordia diagrams with U-Pb zircon data by laser ablation ICP-MS plotted at the 2 σ confidence level; all interpreted ages are based on weighted averages of $^{206}\text{Pb}/^{238}\text{U}$ dates, also reported with 2 σ errors; see text for discussion.

1985). On the western side of the outcrop belt, the base of the Kasalka Group is locally a spectacular buttress unconformity (?) displaying up to 10 m of relief between basal Kasalka Group boulder conglomerate containing 20 to 30% plutonic boulders (up to 1 m in diameter) and the underlying medium grey feldspathic arenite and dark grey argillite of the Skeena Group. To the east, the Kasalka Group – Skeena Group contact is far less prominent, represented by a basal felsic pebble conglomerate (<80% felsite pebbles) containing sparse Skeena Group rip-up clasts interbedded with feldspathic arenite and overlying the Skeena Group with less than a meter of erosional relief. The basal 200 m of the Kasalka Group consist of light grey-green felsic pebble conglomerate to dark red siltstone interbedded with dark red, primarily matrix-supported, pebble to cobble volcanic conglomerate that locally contains minor basalt flows. The proportion of primary basalt and basaltic andesite in the unit increases dramatically to the south near Mount Bollum. The Kasalka Group is easily distinguished from older Hazelton Group volcanic rocks by its essentially unaltered mineralogy and more heterogeneous conglomerate clast assemblage. A vertical feeder to the Kasalka Group extrusive volcanic rocks is seen intruding Hazelton Group andesitic volcanic rocks and volcanic sedimentary rocks on the northwest-trending ridge approximately 5 km east of Tsah Mountain. The feeder is roughly circular and approximately 150 m in diameter, and contains angular and fresh andesitic breccia fragments.

CENTRAL LITHOLOGICAL BELT

Gamsby Complex (Unit TJgc)

The central portion of the map area is underlain by a belt of imbricate structural panels of amphibolite, chloritic mafic metavolcanic rocks, and strongly foliated diorite, tonalite and granodiorite assigned to the Permian (?) to Jurassic Gamsby complex (Woodsworth, 1980). The Gamsby complex ranges in metamorphic grade from greenschist to lower amphibolite, locally to upper amphibolite, and there is a distinct decrease in metamorphic grade from west to east in this succession of metaplutonic and metavolcanic rocks (van der Heyden, 1982). This belt of rocks is flanked on the east by unmetamorphosed to weakly metamorphosed stratigraphic successions and on the west by the

high-grade Central Gneiss Complex (Fig 3). The increased metamorphic grade and significantly higher proportion of metaplutonic rocks distinguish this succession from lower grade rocks to the east, and the presence of abundant chlorite distinguishes it from the Central Gneiss Complex to the west.

The Gamsby complex is composed primarily of strongly foliated chloritic schist, carbonaceous pelite, non-descript mafic to intermediate metavolcanic rocks, rhyolitic metatuff and lapilli tuff, with lesser quartzofeldspathic gneiss, amphibolite and micaceous schist. Felsic and intermediate dikes are common. Blue-grey, thin-bedded recrystallized carbonate forms a locally distinctive component (up to 30%; Fig 5). These rocks are complexly interleaved with pre and syndeformational metatonalite to granodiorite. Protomylonite and mylonite zones are common throughout the succession. Abundant quartz veining is common locally.

The unit is pervasively foliated, dominated by a very consistent, well-developed, northwest-trending foliation with locally abundant, tight to isoclinal, mesoscopic (5–25 cm amplitude) folds (Fig 5). Fold hinges are generally not dismembered, and fold limbs can be traced for several metres through a folded succession. These structures fold an earlier foliation, suggesting a polydeformational history.

The Gamsby complex is internally imbricated, with structural panels that interleave volcanic and plutonic rocks of different metamorphic grades. The Gamsby complex presumably represents a structural level intermediate between the Central Gneiss Complex to the west and lower grade rocks to the east. It forms the hangingwall of a major low-angle detachment structure that separates it from the underlying Central Gneiss Complex. On its eastern margin, the Gamsby complex is in thrust fault contact with lower grade rocks of the eastern belt. North of Tahtsa Peak, one of these west-dipping thrust faults places the Gamsby complex over the less deformed Tahtsa complex, and the fault is intruded by the Cretaceous Horetzky dike (Woodsworth, 1980; Stuart, 1960). The Gamsby complex therefore records evidence of pre-Cretaceous contractional deformation, which is overprinted by extension related to the uplift of the Central Gneiss Complex in Paleocene time (van der Heyden, 1982; Rusmore *et al.*, 2005).



Figure 5. A) Folded carbonate rocks in the Triassic–Jurassic Gamsby complex on ridge west of the Tsayitis River; carbonate interbeds have been sampled for micropaleontology. B) Foliated chloritic schist and discontinuous quartz segregations typical of the Gamsby complex.

The Gamsby complex contains a significant volume of metavolcanic and metaplutonic rocks, suggesting a probable volcanic arc setting. Geochemical analyses of metavolcanic rocks indicate a tholeiitic and calcalkaline volcanic arc origin (van der Heyden, 1982). The age of the volcanic protolith is probably Late Triassic to Early Jurassic, based on a 206.0 ± 1.6 Ma U-Pb zircon age on a predeformational metatonalite east of Tsaytis Peak, and a poorly constrained *ca.* 210 Ma U-Pb age on a metarhyolite within the succession (van der Heyden, 1982). Additional geochronology is in progress. The abundance of carbonate lenses and beds within the complex also suggests a Triassic or Paleozoic age, at least in part.

WESTERN LITHOLOGICAL BELT

Central Gneiss Complex (Unit Tcgc)

The western lithological belt is defined by a distinctive sequence of strongly deformed upper amphibolite to granulite-facies quartzofeldspathic gneiss of the Central Gneiss Complex (Fig 3). The Central Gneiss Complex is a broad belt of high-grade metamorphic rocks that extends up the eastern edge of the Coast Plutonic Complex from about 53° to 56° N (Rusmore *et al.*, 2005). In the western Whitesail Lake map area, the Central Gneiss Complex is dominated by orthogneiss, including complexly interleaved quartzofeldspathic gneiss, hornblende-biotite tonalitic gneiss, amphibolitic gneiss and lesser amphibolite. Constituent minerals are very fresh and consist primarily of quartz, plagioclase, hornblende and biotite, with locally abundant garnet and epidote. Crosscutting foliated and nonfoliated biotite tonalite dikes are abundant, and migmatite zones are common. The complex is cut by numerous mylonitic shear zones. Ductile deformation fabrics, primarily mesoscale (0.5–1.5 m amplitude) tight to isoclinal folds and associated axial-planar foliation are common. Plutonic and metaplutonic rocks are widespread, including locally abundant foliated biotite tonalite, and syn to postdeformational K-feldspar-megacrystic granite and titanite-bearing granodiorite to tonalite.

PLUTONIC ASSEMBLAGES

Plutonic rocks are common throughout the western Whitesail Lake map area, and include Jurassic and Cretaceous diorite, granodiorite and tonalite, and Paleogene granodiorite and tonalite. There is no consistent age progression in the region, although Jurassic and Cretaceous plutons are concentrated between the western margin of the unmetamorphosed stratigraphic assemblages and the eastern edge of the Central Gneiss Complex, and Cenozoic plutons are most common in, but not restricted to, the Central Gneiss Complex. Plutons in the southwestern portion of the Whitesail Lake map area were described in Mahoney *et al.* (2006), so the following description focuses on the major plutonic bodies in the Tsaytis River (NTS 093E/5) and Tahtsa Lake (NTS 093E/12) 1:50 000 map areas.

Tahtsa Complex (Unit TJtc)

The name ‘Tahtsa complex’ was used by Stuart (1960) for a heterogeneous igneous complex of hornblende diorite and quartz diorite cut by quartz monzonite stocks and both granodiorite and mafic sills and dikes. The Tahtsa complex

underlies a broad area west and north of the west end of Tahtsa Lake (Fig 3). The western margin of the complex is a low-angle, west-dipping thrust fault that places the Gamsby complex in the hangingwall over the Tahtsa complex in the footwall. The Tahtsa complex is in fault contact with the Hazelton Group along its eastern margin (Fig 3).

The Tahtsa complex is a heterogeneous assemblage of moderately foliated to nonfoliated, texturally variable, fine to coarse-grained hornblende diorite to quartz diorite (Fig 6). The complex is texturally and compositionally variable, with nonsystematic variations in grain size, mineral content, xenolith abundance, crosscutting dikes/dikelets and varying degrees of foliation. Importantly, the Tahtsa complex is not as pervasively deformed as the adjacent Gamsby complex. The rocks contain abundant xenoliths and screens of recrystallized pyroxene-bearing basaltic andesite and andesite, and are cut by abundant fine-grained felsic, intermediate and mafic dikes. The complex is intruded by numerous pods and stocks of undeformed coarse-grained granite. Rocks of the Tahtsa complex are predominantly lower greenschist grade, and locally upper greenschist to lower amphibolite grade.

The age of the Tahtsa complex is poorly constrained. It is cut by the Cretaceous (*ca.* 73 Ma) Horetzky dike (van der Heyden, 1982) and contains abundant metavolcanic screens that could represent stopped blocks of the Hazelton Group or Gamsby complex. Compositional similarities and spatial relations suggest the Tahtsa complex could be subvolcanic to the Hazelton Group, and therefore Early Jurassic in age. Geochronological analysis is underway.

Sias Pluton (Unit IJgs)

The Sias pluton is a homogeneous, medium to coarse-grained biotite-hornblende granodiorite to granite exposed near Sias Mountain. The pluton intrudes volcanic rocks of the Hazelton Group on its northern and western edges, and intrudes Triassic–Jurassic metavolcanic rocks (unit TJmy) and Jurassic (?) sedimentary rocks (unit J (?)s) along its southern boundary. It is itself intruded along its southwestern margin by mirolitic granite of the Gamsby River stock (Mahoney *et al.*, 2006). The pluton has a characteristically mottled green and pink colouration with distinctly green-tinted plagioclase, mottled green mafic minerals and dark



Figure 6. Heterolithic intrusive breccia and diorite and granodiorite dikes, showing multiple crosscutting relationships, typical of Tahtsa complex rocks.

pink potassium feldspar. This colour results from the presence of extensively chloritized biotite and hornblende, saussuritized plagioclase and dark pink interstitial and phenocrystic K-feldspar. Quartz, K-feldspar, chlorite and epidote veining is common. The body contains abundant hydrothermal breccia features, consisting of veins and pods of brecciated pluton fragments in a matrix of chlorite±epidote.

The Sias pluton is very similar to rocks of the Stick Pass plutonic suite mapped in the Bella Coola region to the south (Haggart *et al.*, 2006). This correlation is supported by a new 146.3 ± 1.6 Ma U-Pb zircon date from the southern portion of the pluton (Fig 4, Table 1).

Tenaiko Suite (Unit Kt)

A heterogeneous assemblage of hornblende diorite to quartz diorite forms an extensive intrusive complex into the Gamsby complex, Chatsquot layered mafic intrusion and Hazelton Group between Mount Gamsby and Mount Irma in the southwestern portion of the Whitesail Lake map area. The Tenaiko suite is a compositionally and texturally heterogeneous intrusive suite that ranges from a coarse-grained pyroxene-hornblende gabbro to medium to coarse-grained hornblende diorite to quartz diorite with lesser hornblende granodiorite. The suite is characterized by complex intrusive relations with adjacent metavolcanic rocks and layered mafic intrusions, and contains locally abundant mafic and ultramafic xenoliths and metavolcanic screens, ranging from a few centimetres to tens of metres in length. The density of the inclusions is variable, ranging from isolated mafic xenoliths to dense intrusion breccia with distinctive interlocking jigsaw clast boundaries. Intrusive boundaries are highly irregular, with felsic stringers and dikelets invading adjacent country rock. The intrusive rocks are complexly foliated, locally displaying magmatic foliation surrounding entrained, structurally deformed metavolcanic screens and locally displaying syndeformational folds and postdeformational tectonic foliations.

The Tenaiko suite intrudes the Lower to Middle Jurassic Hazelton Group along its southern margin, is intruded by Paleogene granitoid plutons along its eastern margin and is cut by the Central Gneiss detachment fault along its western margin. The age of the suite is constrained by a new U-Pb zircon age of 123.9 ± 1.6 Ma (Fig 4, Table 1), an Early Cretaceous age that is in agreement with a poorly constrained *ca.* 129 Ma U-Pb age on an unfoliated quartz diorite sample from the same body (van der Heyden, 1989).

Horetzky Dike (Unit Kgd)

The Horetzky dike was the name given by Stuart (1960) to a northeast-trending, elongate, medium-grained diorite and quartz diorite stock that occupies the drainage of Horetzky Creek (Fig 3). Other nearby bodies of similar composition are included within this unit. The principal body is medium grey in colour and is characterized by medium-grained, fresh, subhedral to euhedral hornblende; light grey to white subhedral plagioclase; and grey interstitial quartz. The mineralogy of the dike was described in detail by Stuart (1960). The dike is undeformed and has an unusual northeast-trending orientation that cuts northwest-trending contractional structures within the Tahtsa and Gamsby complexes. The age of the dike therefore provides a crucial constraint on contractional deformation in the re-

gion. Woodsworth (as reported in Diakow, 2006) obtained a 73.5 ± 2.2 Ar/Ar biotite age on the Horetzky dike, which may or may not constrain the emplacement age. Uranium-lead zircon geochronology is underway.

Paleocene-Eocene Plutonic Rocks

KITLOPE PLUTON (UNIT Egk)

The Kitlope pluton is a massive, homogeneous biotite granite to granodiorite that intrudes the Central Gneiss Complex southeast of Kitlope Lake. The unit is characteristically medium to coarse grained and equigranular, but locally includes K-feldspar-porphyrific biotite granite with clean fresh books of biotite, white to pink K-feldspar, euhedral white plagioclase and large, anhedral quartz blebs. Oxidation of biotite leads to a distinct yellow weathering rind. The intrusive contact is generally sharp, with a locally well-developed intrusion breccia along the boundary. The Kitlope pluton clearly truncates the Central Gneiss detachment fault north of the Kitlope River drainage. Preliminary geochronological data suggest an Eocene age (M. Rusmore, pers comm to GJW, 2006).

TSAYTIS PLUTON (UNIT Egt)

The Tsaytis pluton was described by van der Heyden (1989) as a set of foliated tonalite sills, with foliation defined by aligned mafic minerals and stretched xenoliths along the pluton margins. Mapping east of Gardner Canal in the western portion of the Tsaytis River (093E/05) demonstrates that the Tsaytis pluton is composed primarily of syn to postkinematic K-feldspar-megacrystic biotite granite. The majority of the pluton is undeformed biotite granite that clearly truncates foliation within the Central Gneiss Complex but is locally foliated along the margins of the pluton. The pluton is elongate parallel to the dominant foliation trend in the Central Gneiss Complex, which suggests at least partial structural control on emplacement.

The unit is medium to coarse grained, characterized by fresh K-feldspar megacrysts (1–4 cm) within a matrix of brown euhedral biotite, white subhedral plagioclase feldspar and grey anhedral quartz. Intrusive contacts are generally sharp, but well-developed intrusion breccia is evident locally. The age of the pluton is not constrained, but must be Eocene or younger, based on the known age of the Central Gneiss Complex (Rusmore *et al.*, 2005). Van der Heyden (1989) reported a *ca.* 55 Ma U-Pb age, but it is unclear if this date is from the main K-feldspar-megacrystic phase of the pluton.

STRUCTURAL FEATURES

Central Gneiss Detachment

In the western Whitesail Lake map area, upper amphibolite to granulite facies rocks of the Central Gneiss Complex are separated from greenschist to lower amphibolite grade rocks of the Gamsby complex and Tenaiko suite by a low-angle, east-dipping detachment fault (Fig 7). In the lower plate, the Central Gneiss Complex is characterized by widespread quartzofeldspathic gneiss with well-developed foliation and abundant isoclinal folds, interleaved with fresh foliated to nonfoliated biotite tonalite. The majority of the upper plate contains chloritic, mafic to intermediate metavolcanic rocks and variably foliated diorite,

tonalite and granodiorite of the Gamsby complex. The upper plate contains several imbricated structural panels of greenschist facies chloritic metavolcanic rocks, lower amphibolite facies metavolcanic rocks and metatonalite. The structural panels are apparently separated by steep, west-dipping faults of unknown displacement. These faults locally juxtapose amphibolitic metavolcanic rocks and metatonalite against greenschist facies metavolcanic-metaplutonic rocks; in other cases, the metamorphic transition appears more gradational.

These structurally interleaved panels increase in metamorphic grade from east to west, and the highest grade portion of the Gamsby complex in the hangingwall is commonly adjacent to the Central Gneiss Complex in the footwall, making the detachment fault difficult to locate precisely in the field. Locally, the detachment fault is readily recognized by a significant change in metamorphic grade, and by the abundance of chloritic rocks in the upper plate and the absence of chlorite in the lower plate. Elsewhere, the detachment fault does not appear to be a discrete structure, but rather a zone of interleaved panels of upper and lower plate rocks. The detachment fault is a very low angle structure, and may be partly crenulated, as suggested by the presence of at least one fenster east of the main detachment, where rocks of the lower plate project through, and are surrounded by, lower grade rocks of the upper plate (Fig 3).

Contractional Structures

In the southwestern portion of the Whitesail Lake map area, northeast of Chatsquot Mountain, various structural levels within the Hazelton Group are complexly imbricated in a stack of northeast-vergent thrust sheets (Mahoney *et al.*, 2006). A system of easterly-vergent imbricate thrust panels within the Gamsby complex was described by van der Heyden (1982). Mapping in the western Whitesail Lake map area documents a series of northwest-trending, east-vergent thrust faults that imbricate the Gamsby complex, Tahtsa complex, Tenaiko suite, Triassic–Jurassic metavolcanic rocks and the Hazelton Group. In general, there is a decrease in metamorphic grade from west to east, and the thrust system consists of imbricated panels of higher grade rocks structurally overlying lower grade rocks. This inverted metamorphic gradient was described by van der Heyden (1982), but a critical observation is that this east-vergent thrust system is restricted to the hangingwall of the Central Gneiss detachment. Geological mapping and structural analysis document distinctly different structural styles between lower plate and upper plate rocks, with the Central Gneiss Complex displaying a relatively uniform, northwest-trending fold-axis orientation, which contrasts markedly with the much more widely distributed orientations characteristic of folds in the Gamsby complex (Fig 8). The distinct difference in structural style suggests that the region has been subject to at least two structural episodes, an interpretation that is supported by mapping that demon-

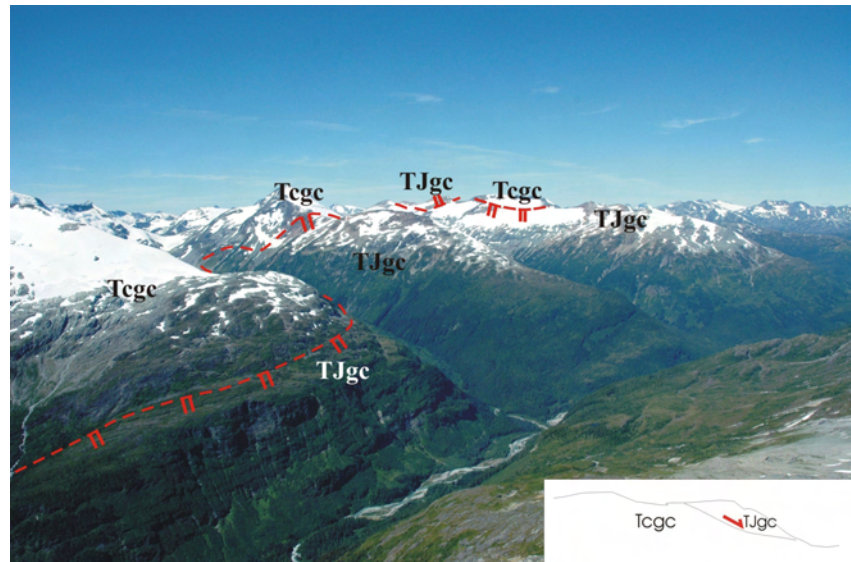


Figure 7. View to the west from the ridge east of the Tsaytis River drainage, highlighting the trace of the Central Gneiss detachment fault. Inset is a schematic cross-section, illustrating the relationship between the Gamsby complex (TJgc) and the Central Gneiss Complex (Tcgc).

strates west-dipping faults that imbricate the Gamsby complex are cut by the unfoliated *ca.* 73 Ma Horetzky dike (Stuart, 1960; van der Heyden, 1989), whereas the Central Gneiss Complex includes pervasively foliated rocks as young as Paleocene (Rusmore *et al.*, 2005). We suggest the Gamsby complex was deformed in a pre-late Cretaceous deformational event, and the Central Gneiss Complex was produced by Paleocene deformation before their juxtaposition by thrust faults.

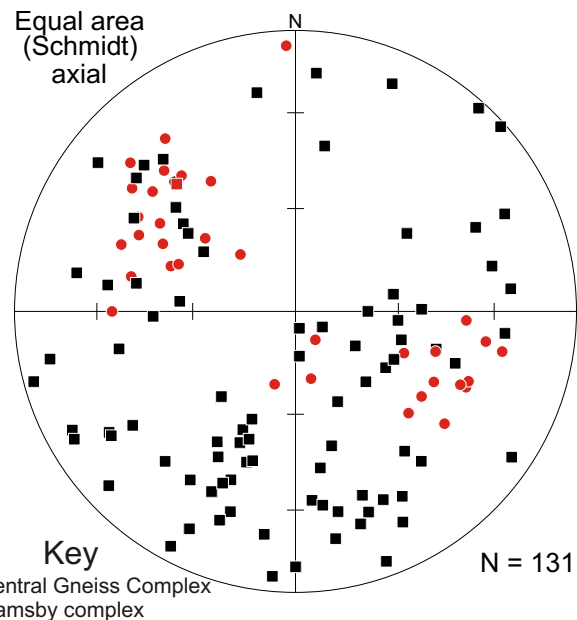


Figure 8. Stereonet of fold-axis orientations in the Gamsby complex (TJgc) and the Central Gneiss Complex (Tcgc) in the Tsaytis River (NTS 093E/05) and Tahtsa Peak (NTS 093E/12) 1:50 000 map areas.

Transcurrent Shear Zones

Several high-angle shear zones transect the area and cut all pre-Paleocene rock units. One of the larger shear zones parallels the Kimsquit River valley, extending north from the northern end of Dean Channel through Whitecone Peak and the western flank of Crawford Peak, where it is apparently truncated by a northeast-trending normal fault (Fig 3). The shear zone is characterized by pervasive near-vertical fracture planes and locally intense foliation development, manifested by mineral realignment and the stretching and reorientation of xenoliths and metamorphic screens. East of Crawford Peak, graphitic phyllite, chloritic schist and clastic metasedimentary and metavolcanic rocks are incorporated into the shear zone, and dextral transpression is indicated by the orientation of kink bands and vergence of isoclinal folds with moderately plunging (30–35°) fold axes (Mahoney *et al.*, 2005). A second prominent shear zone extends from Chatsquot Mountain northwest toward Black Dome. This shear system is approximately 1 to 1.5 km wide and consists of chloritic schist, micaceous schist, local actinolitic schist, foliated hornblende diorite and granodiorite, and pods of pyroxene gabbro that are crosscut by syndeformational andesitic to basaltic dikes. The shear zone is characterized by northwest-trending foliation containing prominent, moderately northwest-plunging intersection and mineral-elongation lineations. The shear zone is flanked on both sides by the Tenaiko suite, suggesting a lack of major offset along the system. The shear zone is truncated at its southern end by a high-angle normal fault that separates it from the Chatsquot layered mafic intrusion. The presence of high-angle shear zones at both ends of the thrust system suggests that the thrust system may represent a contractional step-over at a restraining bend along a dextral transpressional system (Mahoney *et al.*, 2005, 2006).

The northern portion of the map area contains several significant northwest-trending, generally steeply east-dipping normal faults that juxtapose different structural and metamorphic levels. Many of these high-angle structures appear to be brittle faults, but several display penetrative fabrics and may have accommodated strike-slip translation of unknown magnitude.

ECONOMIC POTENTIAL

The primary objective of this investigation is a comprehensive evaluation of the economic mineralization potential in the western and southwestern Whitesail Lake map area. Known mineral occurrences (MINFILE, 2006), stream sediment geochemistry (Lefebvre and Gunning, 1988) and regional bedrock mapping suggest that the area may hold potential for volcanogenic massive sulphide, Cu±Mo±Au porphyry and Ni-Cu-Cr-PGE (platinum group element) mineralization. Detailed geological mapping and systematic geochemistry, geochronology, petrology and economic mineral evaluation studies are assessing the distribution of, and controls on, potential economic mineralization in the region. Bedrock geological mapping and preliminary geochemical data suggest that there are several potential targets of economic importance.

Volcanogenic Massive Sulphide Deposits Within the Hazelton Group

Lower to Middle Jurassic strata of the Hazelton Group in the southern Whitesail Lake map area are strikingly simi-

lar to strata hosting the Eskay Creek volcanogenic massive sulphide (VMS) deposit in northern British Columbia. Detailed mapping, volcanic facies analysis, geochronology and geochemistry of Hazelton Group strata demonstrate the lithological, age, compositional and stratigraphic similarities between these rocks and Eskay Creek strata, and document predominantly shallow-water deposition in an extensional volcanic arc environment (Gordee, 2005). The similarities between these strata and those in the Eskay Creek area suggest that the Hazelton Group in the Whitesail Lake map area is also prospective for VMS mineralization. Despite these similarities, no direct evidence of VMS-style mineralization has been discovered beyond stratiform pyritic horizons, and it is likely that the shallow-marine depositional setting of Hazelton Group rocks in the southern Whitesail Lake map area was not favourable for deposition of volcanogenic massive sulphides (Gordee, 2005).

Rhyolitic volcanic rocks of the Hazelton Group in the southern Whitesail Lake map area are near the top of a homoclinal, eastward-dipping stratigraphic sequence that becomes progressively older to the west, with deeper levels of the volcanic system exposed in the southwestern and western portions of the study area. Here, rocks assigned to the Hazelton Group contain a higher proportion of mafic volcanic flows and associated breccia, tuff-breccia, lapilli tuff, and tuff, as well as intervals of dark, thin-bedded, fine-grained argillite, siltstone and sandstone. Rhyolitic tuff-breccia, lapilli tuff, tuff and domes form a minor, yet ubiquitous, portion of the section. Hazelton Group rocks contain locally abundant sulphide-bearing (pyrite, minor chalcopyrite) quartz-siderite veins, particularly adjacent to crosscutting plutons, and commonly contain disseminated pyrite associated with rhyolitic tuff and dikes. In addition, the Hazelton Group probably represents, in part, the protolith for the Triassic–Jurassic metavolcanic sequence and the Gamsby complex, and these units may therefore have potential for both VMS and postdepositional vein-type mineralization.

Chatsquot Layered Mafic Intrusion

The Chatsquot layered mafic intrusion has previously been inferred to have potential for significant Cu-Ni sulphide and PGE mineralization (Mahoney *et al.*, 2006). Pyroxene-rich compositional layers (clinopyroxene gabbro) locally contain visible coarse-grained chalcopyrite (or Cu-Ni sulphide) mineralization, which occurs as disseminated stratiform sulphides and sulphide veins. Preliminary geochemical results from unmineralized gabbro bodies indicate elevated metal values (*e.g.*, >0.35% Cu, >600 ppm Ni, >0.20% Cr). Although initial PGE assays are not particularly encouraging, additional detailed stratigraphic and geochemical analysis may be beneficial.

Cu±Mo±Au Porphyry Mineralization

Paleocene and Eocene plutonic rocks in the southwestern Whitesail Lake map area are generally coarse-grained, locally porphyritic granitic rocks that were apparently emplaced at relatively shallow levels. Intrusive contacts with adjacent country rock are generally sharp, although extensive (tens of metres) zones of locally mineralized intrusive breccia occur locally, and there is evidence of sulphide (primarily Cu and Mo) remobilization along some intrusive boundaries (Mahoney *et al.*, 2006). Geochemical and geochronological studies of these plutons are under-

way, and assay samples collected from alteration zones adjacent to pluton margins have been submitted.

Fault-Controlled Mineralization

The Central Gneiss detachment fault represents an important surface for potential economic mineralization. The high-grade gneiss and associated foliated to nonfoliated plutonic and metaplutonic rocks of the Central Gneiss Complex in the footwall do not contain economic mineralization, apparently due to the high temperature of formation. However, low-grade metamorphic rocks in the hangingwall are cut by several generations of faults and shear zones, which locally display structurally controlled, sulphide-bearing (pyrite, chalcopyrite) vein mineralization. Chloritic schist and metavolcanic rocks of the Triassic–Jurassic metavolcanic rocks (unit TJmv) and the Gamsby complex are cut by both brittle and ductile structures with associated quartz-siderite veins, which locally display both disseminated and vein pyrite-chalcopyrite mineralization (Fig 9). Dioritic plutonic rocks of the Tahtsa complex are cut by discrete brittle faults that host similar mineralization. Fault-parallel, tan to pink quartz-siderite veins with locally abundant pyrite and chalcopyrite are common; siderite veins are commonly cut by quartz-rich veins and display open space, comb and cockscomb textures containing coarse (4–5 mm) euhedral pyrite. These structures are readily identified by ubiquitous iron staining and locally well-developed malachite staining, and small gossans are common in the area, particularly adjacent to crosscutting plutons. Initial assay results indicate locally elevated metal values in the metavolcanic package (unit TJmv; >20.7% Cu, >2.7 ppm Au, >270 ppm Ag; Fig 9) and the Tahtsa complex (>1.7% Pb, >0.12% Ag, >0.8% Zn). Additional assays from these units and the Gamsby complex are underway.

Just south of Mount Irma, an approximately 1 km wide, low-angle, southwest-dipping shear zone deforms Triassic–Jurassic metavolcanic rocks trending southwards to Lindquist Pass. Metavolcanic rocks consist primarily of feldspar-phyric meta-andesite, andesite breccia and basalt, with lesser associated metadiorite. The metavolcanic package northeast of this zone is relatively undeformed, whereas rocks to the southwest are strongly foliated, schistose and chloritic, with locally extensive epidote stockwork and clots, and siliceous veining. The shear zone is the locus of numerous quartz and biotite-phyric rhyolitic dikes, swarms and plugs, oriented subparallel to the shear zone fabric; dikes are inferred to be of Eocene age. A few dikes also intrude the relatively undeformed metavolcanic rocks exposed northeast of the shear zone. Dikes vary in width from several tens of decimetres up to several tens of metres and commonly brecciate associated country rock; several dikes are traceable for 1 to 2 km. The rhyolitic intrusive activity is associated with prominent sulphide mineralization, developed in siliceous quartz-rich veins within the shear zone and also disseminated in adjacent country rock (Park and Peacock MINFILE occurrences). Quartz veins show pervasive pyrite-chalcopyrite-malachite-bornite mineralization (Fig 9). Pyrite is typically angular and coarse (2–3 mm), and developed in open framework within quartz veins; associated bornite is also localized in quartz veins, and is typically fine to medium-grained (1–2 mm). Geochemical assays are in process.

ACKNOWLEDGMENTS

This project would not have been possible without the dedication and expertise of Danny Hodson of Rainbow West Helicopters. Adam Kjos, Kate Maclaurin, Brandon

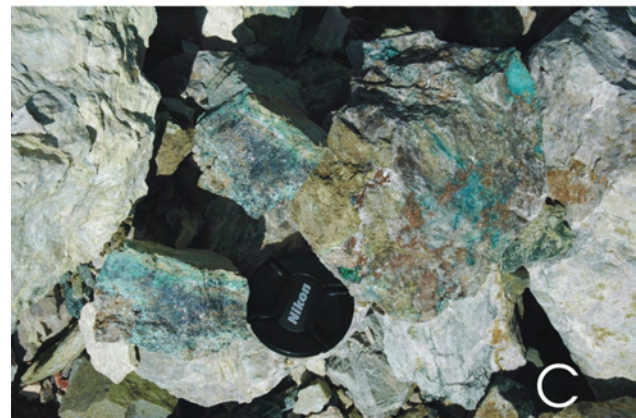
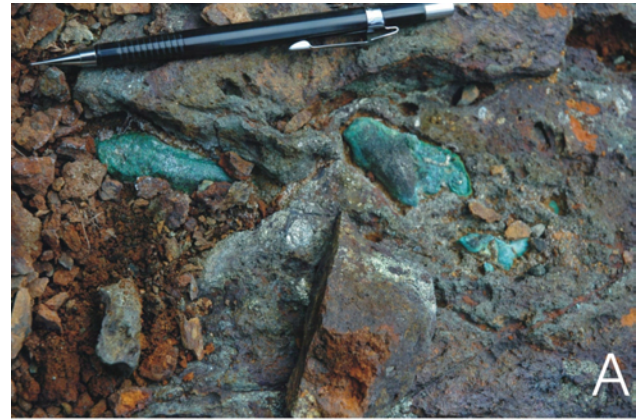


Figure 9. A) Mineralized shear zone within unit TJmv; fault gouge contains thick (2–3 cm) veins of massive pyrite and lesser chalcopyrite (foreground); breccia clasts within fault zone are pervasively copper stained. B) massive (30–35 cm) hydrothermal quartz vein with copper staining along margins cutting chloritic schist of the Gamsby complex; these quartz veins locally brecciate country rock and contain disseminated pyrite±chalcopyrite. C) Pyrite-chalcopyrite-malachite-bornite mineralization in quartz veins within shear zone in unit TJmv, near Mount Irma.

Barber and Mark Nelson provided excellent field assistance despite frequently adverse weather conditions. Adam Kjos and Kate Maclaurin assisted with geochemical laboratory analyses and figure preparation. Assistance with U-Pb dating was provided by H. Lin and R. Lishansky at the Pacific Centre for Isotopic and Geochemical Research, University of British Columbia. C. van Staal is thanked for an informal review of the paper. Funding for this investigation was provided by Geoscience BC, the Geological Survey of Canada, the University of British Columbia and the University of Wisconsin – Eau Claire.

REFERENCES

- Dawson, K.M., Panteleyev, A., Sutherland Brown, A. and Woodsworth, G.J. (1991): Regional metallogeny; Chapter 19 in *Geology of the Cordilleran Orogen in Canada*, Gabrielse, H. and Yorath, C.J., Editors, *Geological Survey of Canada*, Geology of Canada, no 4, pages 707–768.
- Diakow, L.J. (1990): Geology of Nanika Lake map area (93E/13); in *Geological Fieldwork 1989*, *BC Ministry of Energy, Mines and Petroleum Resources*, Paper 1990-1, pages 83–89. [BCGS map area A on Fig 2]
- Diakow, L.J., Compiler (2006): Geology of the Tahtsa Ranges between Eutsuk Lake and Morice Lake, Whitesail Lake map area, west-central British Columbia (parts of NTS 93E/5, 6, 7, 9, 10, 11, 12, 13, 14 and 15); *BC Ministry of Energy, Mines and Petroleum Resources*, Geoscience Map 2006-5, 1:150 000 scale.
- Diakow, L.J. and Drobe, J. (1989): Geology and mineral occurrences in north Newcombe Lake map sheet, NTS 093E/14; *BC Ministry of Energy, Mines and Petroleum Resources*, Open File Map 1989-1, 1 sheet, scale 1:50 000. [BCGS map area B on Fig 2]
- Diakow, L.J. and Koyanagi, V.M. (1988): Geology of Chikamin Mountain map area, NTS 093E/6; *BC Ministry of Energy, Mines and Petroleum Resources*, Open File Map 1988-2, 1 sheet, scale 1:50 000. [BCGS map area E on Fig 2]
- Diakow, L.J., Mahoney, J. B., Gleason, T.G., Hrudey, M.G., Struik, L.C. and Johnson, A.D. (2002): Middle Jurassic stratigraphy hosting volcanogenic massive sulphide mineralization in the eastern Bella Coola map area (NTS 093/D), southwest British Columbia; in *Geological Fieldwork 2001*, *BC Ministry of Energy, Mines and Petroleum Resources*, Paper 2002-1, pages 119–134.
- Diakow, L.J. and Mihalynuk, M. (1987): Geology of Whitesail Reach and Troitsa Lake area, NTS 93E/10W and 93E/11E; *BC Ministry of Energy, Mines and Petroleum Resources*, Open File Map 1987/4, 1 sheet, scale 1:50 000. [BCGS map area D on Fig 2]
- Gordee, S.M. (2005): Volcanostratigraphy, age, and geologic setting of the Lower–Middle Jurassic upper Hazelton Group, west-central British Columbia; unpublished MSc thesis, University of British Columbia, Vancouver, BC, 161 pages.
- Gordee, S.M., Mortensen, J.K., Mahoney, J.B. and Hooper, R.L. (2005): Volcanostratigraphy, litho-geochemistry and U-Pb geochronology of the upper Hazelton Group, west-central British Columbia: implications for Eskay Creek – type VMS mineralization in southwest Stikinia; in *Geological Fieldwork 2004*, *BC Ministry of Energy, Mines and Petroleum Resources*, Paper 2005-1, pages 311–322.
- Haggart, J.W. (2005): Report on Jurassic fossils from Whitesail Lake map area (93E), British Columbia; *Geological Survey of Canada*, unpublished Paleontological Report JWH-2005-01, 2 pages.
- Haggart, J.W., Diakow, L.J., Mahoney, J.B., Struik, L.C., Woodsworth, G.J., Gordee, S.M. and Rusmore, M. (2006): Geology, Bella Coola area (93D/01, /07, /08, /10, /15 and parts of D/02, D/03, /06, /09, /11, /14, /16 and 92M/15 and /16), British Columbia; *Geological Survey of Canada*, Open File 5385 and *BC Ministry of Energy, Mines and Petroleum Resources*, Geoscience Map 2006-7, scale 1:100 000.
- Lefebvre, D.V. and Gunning, M.H. (1988): Regional geochemical stream sediment survey results for Smithers (93L) and Whitesail Lake (93E) map sheet; in *Exploration in British Columbia, 1987*, *BC Ministry of Energy, Mines and Petroleum Resources*, pages B127–B148.
- MacIntyre, D.G. (1985) Geology and mineral deposits of the Tahtsa Lake District, west central British Columbia; in *Bulletin - Ministry of Energy, Mines and Petroleum Resources*, vol.75, 82 pages
- Mahoney, J.B., Haggart, J.W., Hooper, R.L., Snyder, L.D. and Woodsworth, G.J. (2006): Geological setting and mineralization potential of the southwestern Whitesail Lake map area (NTS 93E), western BC: preliminary assessment; in *Geological Fieldwork 2005*, *BC Ministry of Energy, Mines and Petroleum Resources*, Paper 2006-1, pages 313–322
- Mahoney, J.B., Hooper, R.L., Gordee, S.M., Haggart, J.W. and Mortensen, J.K. (2005): Initial evaluation of bedrock geology and economic mineralization potential of southern Whitesail Lake map area (92E/02, 03), west-central British Columbia; in *Geological Fieldwork 2004*, *BC Ministry of Energy, Mines and Petroleum Resources*, Paper 2005-1, pages 291–299.
- MINFILE (2006): MINFILE BC mineral deposits database; *BC Ministry of Energy, Mines and Petroleum Resources*, URL <<http://www.em.gov.bc.ca/Mining/Geolsurv/Minfile/>> [Nov 2006].
- Rusmore, M.E., Woodsworth, G.J. and Gehrels, G.E. (2005): Two-stage exhumation of midcrustal arc rocks, Coast Mountains, British Columbia; *Tectonics*, volume 24, TC5013, doi:10.1029/2004TC001750.
- Saul, L.R. (1978): The North Pacific Cretaceous trigoniid genus *Yaadia*; *University of California*, Publications in Geological Sciences, volume 119, 65 pages, 12 plates.
- Stuart, R.A. (1960): Geology of the Kemano-Tahtsa area; *BC Ministry of Energy, Mines and Petroleum Resources*, Bulletin 42, 52 pages.
- van der Heyden, P. (1982): Tectonic and stratigraphic relations between the Coast Plutonic Complex and Intermontane belt, west-central Whitesail Lake map area, British Columbia; unpublished MSc thesis, *University of British Columbia*, Vancouver, BC, 172 pages.
- van der Heyden, P. (1989): U-Pb and K-Ar geochronometry of the Coast Plutonic Complex, 53°N to 54°N, British Columbia, and implications for the Insular-Intermontane Superterrane boundary; unpublished PhD thesis, University of British Columbia, Vancouver, BC, 392 pages.
- Wheeler, J.O. and McFeely, P., Compilers (1991): Tectonic assemblage map of the Canadian Cordillera and adjacent parts of the United States of America; *Geological Survey of Canada*, Map 1712A, 2 sheets, scale 1:2 000 000.
- Woodsworth, G.J. (1980): Geology of Whitesail Lake (93 E) map-area, BC; *Geological Survey of Canada*, Open File 708, 1 sheet, scale 1:250 000.

Geology and Mineral Potential Update for the Muchalat-Hesquiatic Region (NTS 092E, F, K, I), Vancouver Island¹

by D. Marshall², E. Street², T. Ullrich³, G. Xue², S. Close² and K. Fecova²

KEYWORDS: ore deposits, layered ultramafic rocks, porphyry copper mineralization, Jurassic Island intrusive suite, metamorphism, Westcoast Crystalline Complex, geochemistry, Nootka Sound

INTRODUCTION

This report provides an update on results previously reported (Marshall *et al.*, 2006) and is based on fieldwork undertaken during the summer of 2006. The overall study area comprises the Nootka Sound region (Fig 1). This report provides an updated geological map (Fig 2) and details on the mineralogy and chemistry of two specific rock units within the area and their mineral potential: copper-porphyry potential within the Jurassic Island intrusive suite (JI) and platinum group metals (PGM) potential within a newly discovered magnetite-rich layer within the lower Jurassic, layered ultramafic phase (lJum) of the JI. The regional and detailed geology are described in Muller *et al.* (1981) and Marshall *et al.* (2006). The regional tectonic setting is described in Yorath *et al.* (1999).

LOWER JURASSIC LAYERED ULTRAMAFIC ROCKS

The layered ultramafic rocks occur sporadically within the Island intrusive suite (Muller *et al.*, 1981; DeBari *et al.*, 1999). These rocks outcrop mostly in the drainage courses flowing into the Conuma River and it seems appropriate that these layered rocks should be named the Conuma phase of the Island intrusive suite. The best exposures of these rocks are at the top of the Conuma Main Forestry Road and along Norwood Creek. In some cases, the unit can be traced over a few hundred metres. The unit weathers somewhat recessively compared to the main diorite-granodiorite phases of the Island intrusive suite, and thus it is best exposed in roadcuts.



Figure 1. Location map of the study area, Vancouver Island, BC.

The Conuma phase comprises two main rock types (Fig 3). The first is a gabbro to hornblende-diorite. This rock type varies locally but in general is composed of 60% hornblende, 40% plagioclase and minor phlogopite. Most of the pyroxene within these rocks has been metamorphosed to hornblende and phlogopite. It weathers light brown and is altered locally to epidote and serpentine along fractures. Some zones of intense alteration have malachite staining. The second rock type is metaperidotite. The metaperidotite weathers the typical tan colour of ultramafic rocks. In general, the pyroxenite shows slight alteration but most of the primary mineralogy is preserved. There are minor amounts of igneous hornblende, although some hornblende appears to be metasomatic or metamorphic in origin. Orthopyroxene and olivine are easily visible in thin section (Fig 4) and are relatively fresh. The olivine in these rocks is slightly altered to serpentine along fractures but is generally quite well preserved. The rock is composed of approximately 40% olivine, 45% orthopyroxene, 10% hornblende and 5% plagioclase feldspar. Assuming all the hornblende is retrograded from pyroxene, the rock was probably an olivine-websterite prior to metamorphism. Magnetite (Fig 5, 6) is common within these rocks with magnetite abundances varying locally up to 5%. Melt inclusions within the olivine generally host small magnetite crystals indicating that magnetite was present and in equilibrium with the olivine during crystallization. Thus there is potential for magnetite layers within the Conuma phase.

¹Geoscience BC contribution GBC021

²Earth Sciences, Simon Fraser University, Burnaby, BC, V5A 1S6

³Pacific Centre for Isotopic and Geochemical Research, Earth and Ocean Sciences, University of British Columbia, Vancouver, BC, V6T 1Z4

This publication is also available, free of charge, as colour digital files in Adobe Acrobat® PDF format from the BC Ministry of Energy, Mines and Petroleum Resources website at http://www.em.gov.bc.ca/Mining/Geolsurv/Publications/catalog/cat_fldwk.htm

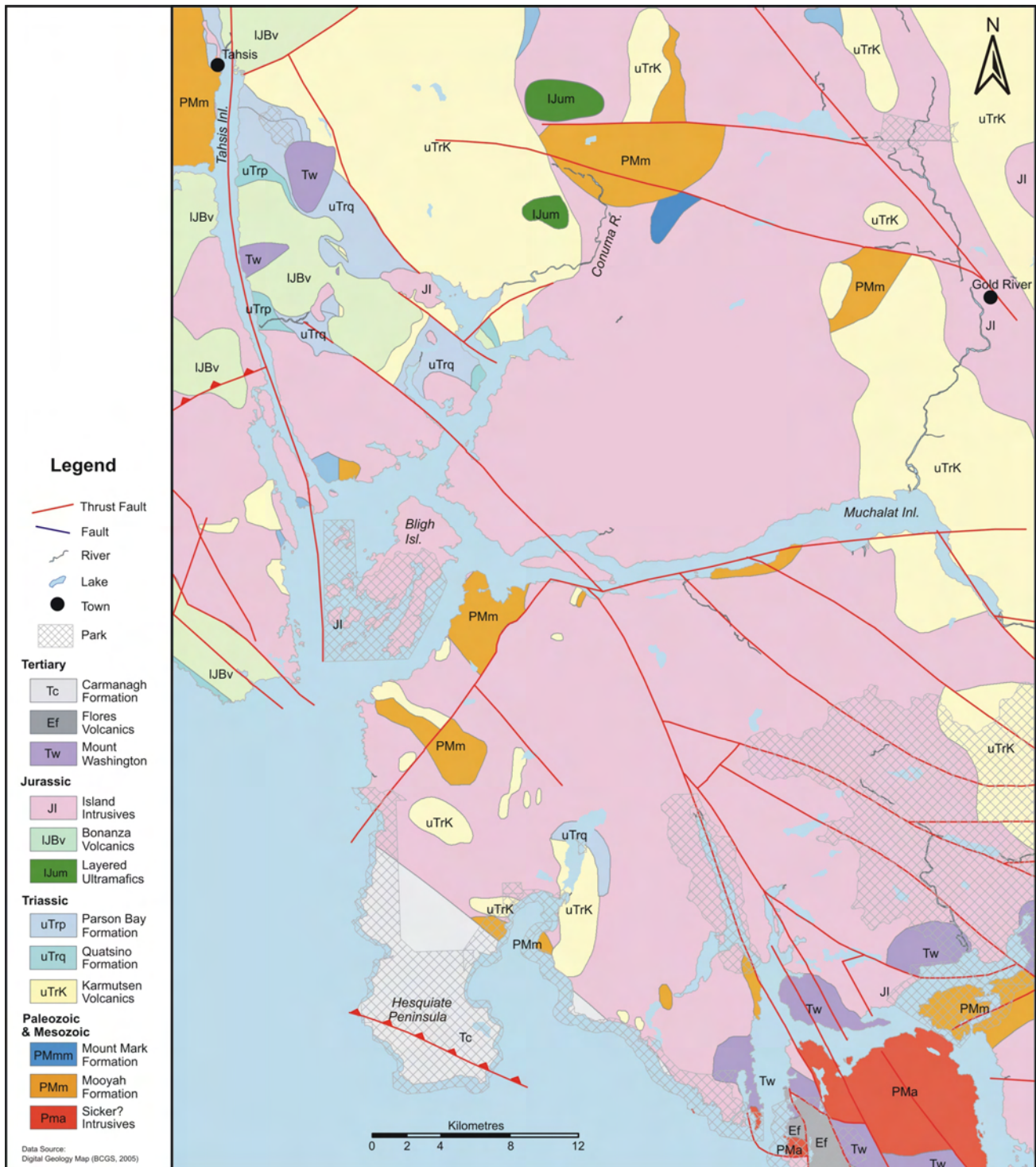


Figure 2. Preliminary geological map for the study area, Vancouver Island, BC (after Muller *et al.*, 1981; Marshall *et al.*, 2006).

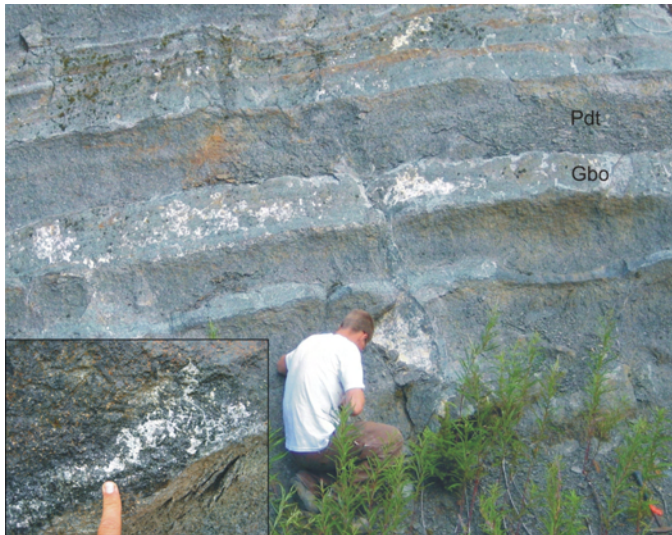


Figure 3. Outcrop photograph of the layered ultramafic rocks of the Conuma phase, showing dark green metagabbro (Gbo) and recessive-weathering black to rusty tan metaperidotite (Pdt) layers, Vancouver Island, BC. Inset photo: close-up of the layering from the same phase at a different locality. Also note the small amount of ductile deformation in the metaperidotite layer and the lack of deformation in the more competent metagabbro layers.

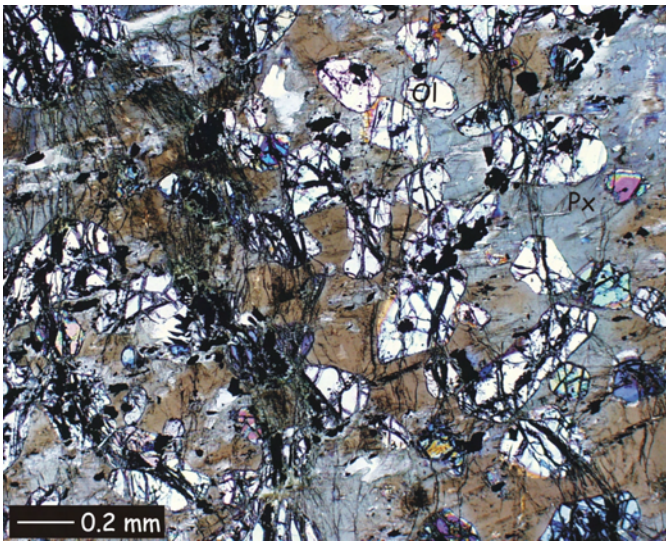


Figure 4. Photomicrograph showing the relatively fresh orthopyroxene (Px) and olivine (Ol) within the metaperidotite. The high-relief highly birefringent olivine displays minor alteration to serpentine along fractures. The pleochroic brown to grey orthopyroxene is relatively fresh but may be slightly altered to amphibole locally. Photograph taken in plane-polarized transmitted light. Sample DM05-212A.

Hornblende from the Conuma phase has been dated by Ar-Ar geochronology. The primary igneous hornblende yields an excellent lower Jurassic plateau age of 189.9 ± 2.1 Ma comprising 85% of the ^{39}Ar (Fig 7). A second amphibole from this same rock unit yielded a similar age. Plagioclase grains yielded a very disturbed Ar-Ar spectrum with no interpretable age data.

Although the preliminary platinum group elements (PGE) analyses results (Table 1) are less than exciting, the potential remains for PGE mineralization associated with

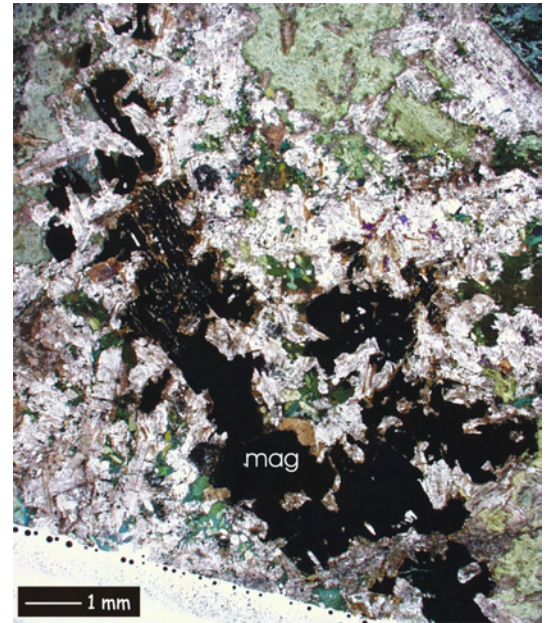


Figure 5. Photomicrograph showing a magnetite (mag)-rich portion within the Conuma phase. Photograph taken in plane-polarized transmitted light.

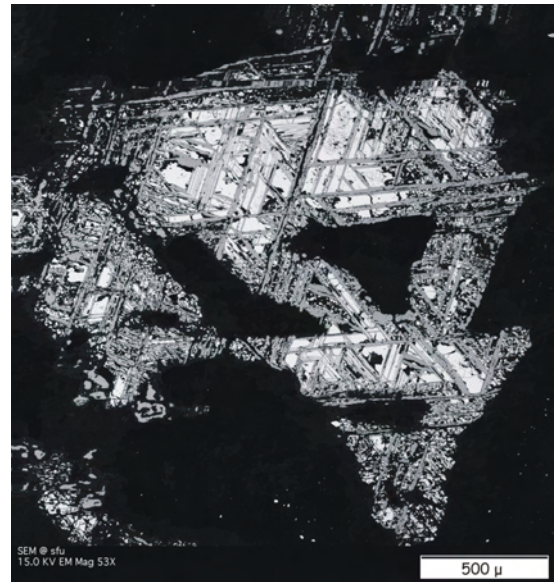


Figure 6. Backscattered electron image of the intergrown magnetite and ilmenite from the magnetite-rich layers of the Conuma phase of the Island intrusive suite.

magnetite in layered intrusions, such as those documented by Sá *et al.* (2005) and Maier *et al.* (2003) in Brazil and South Africa, respectively.

PORPHYRY-STYLE MINERALIZATION WITHIN THE ISLAND INTRUSIVE SUITE

The Island intrusive suite has been an exploration target for porphyry copper mineralization since the mid 1900s

TABLE 1. REPRESENTATIVE GEOCHEMICAL VALUES FROM GRAB SAMPLES OF THE PORPHYRY-STYLE AND LAYERED ULTRAMAFIC MINERALIZATION TARGETS.

Sample no.	Lithology	Au (ppm)	Pt (ppm)	Pd (ppm)	Cu (ppm)	Ni (ppm)	Pb (ppm)	Zn (ppm)	Ag (ppm)	As (ppm)	S (wt.%)	Co (ppm)	Cr (ppm)
DM06-32A	Ultramafic	<0.3	<0.3	0.3	168	16	2	48	0.1	5	0.04	17	20
DM06-56	Porphyry copper	-	-	-	31800	2	11	102	113	4	0.92	3	4
DM06-57	Porphyry copper	-	-	-	9040	7	2	65	4	2	0.57	10	11

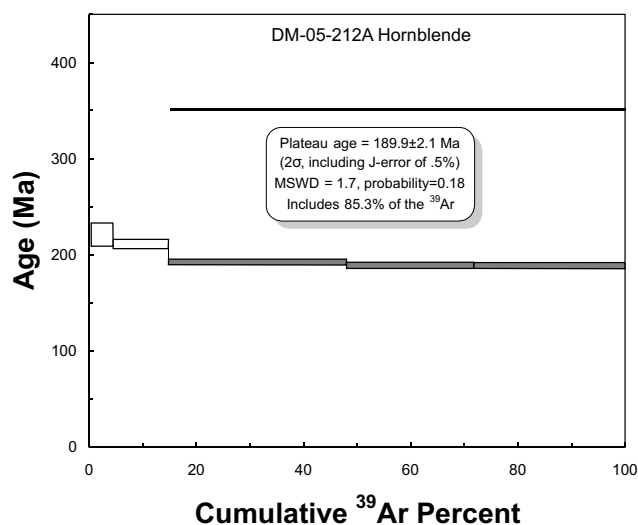


Figure 7. Ar-Ar spectrum for hornblende from the amphibole of the lower Jurassic ultramafic phase (LJum). Filled steps were used for the plateau calculations, open steps were rejected. Step heights are reported at the 2σ level.

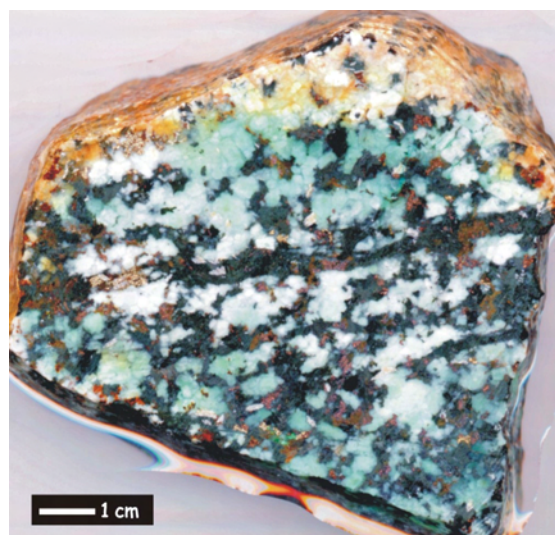


Figure 8. Scanned slab of copper-rich diorite. The original diorite of the Island intrusive suite is cut and altered by stockwork-like veins of amphibole, bornite and chalcopyrite. There is also abundant disseminated bornite and chalcopyrite. The light green stain in this sample is chrysocolla. Bulk rock analysis of this sample returned 2.5 ppm Au, 182 ppm Ag and 5% Cu.

(*cf.* Northcote and Robinson, 1972; Leitch *et al.*, 1995). This summer a float, found in a recently constructed roadbed, had chrysocolla stain. In addition to chrysocolla, the sample also contained visible chalcopyrite and bornite (Fig 8). The outcrop at this locality was the same rock type but did not have the same copper stain. Samples were taken from the roadbed and a search was initiated to find the outcrop. Another outcrop of the same rock type with copper stain was found further along the road.

The copper minerals are hosted within a hornblende-diorite of the Island intrusive suite. The diorite is fairly typical of the large batholithic intrusions in the area, displaying an equigranular texture and a composition of approximately 80% plagioclase feldspar and 20% amphibole. Superimposed on the primary igneous mineralogy is a hydrothermal overprint resulting in anastomosing veins containing amphibole, chlorite and copper-bearing minerals. Chalcopyrite, bornite, covellite, chrysocolla and malachite are visible on cut slabs of the vein material and disseminated throughout the rock (Fig 9).

OTHER POTENTIAL MINERALIZATION STYLES

The Nootka region is host to some arc-type volcanic rocks. Preliminary geochemistry and the presence of the overlying Mooyah Formation indicate that some of the

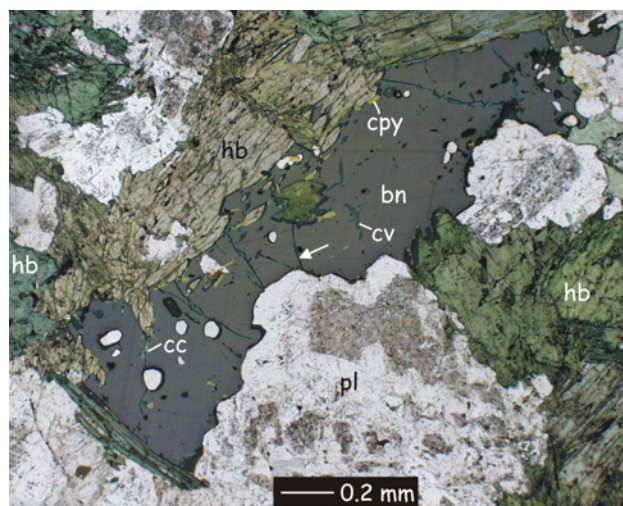


Figure 9. Photomicrograph of the copper-rich samples shown in Figure 8. Bornite (bn) is the most abundant copper-bearing mineral. Chalcopyrite (cpy) is in equilibrium with the bornite, both of which are being replaced by covellite (cv) and chalcocite (cc). Silicate matrix comprises plagioclase feldspar (pl) and hornblende (hb). Also note the late veinlets (arrow) of hematite and silicates. Photograph taken in plane-polarized reflected light.

subsurface volcanic rocks are most likely Sicker Group volcanic rock equivalents and correlative to the rocks hosting the Myra Falls mine as described by Barrett and Sherlock (1996) and Jones *et al.* (2005). The volcanic rocks at one locality (Marshall *et al.*, 2006) are highly gossanous and contain abundant mineralized veins up to 15 cm wide comparable to typical volcanogenic massive sulphide (VMS) stockwork mineralization.

The area is also prospective for gold mineralization similar to the intrusion-related deposits in the Zeballos camp (Stevenson, 1938, 1939, 1950; Hansen and Sinclair, 1984; Marshall *et al.*, 2005). The Zeballos mineralization is related to the emplacement of the Tertiary Mount Washington intrusive rocks. A large intrusion of this type has been identified in Shelter Inlet (Marshall *et al.*, 2006) and there is still much unexplored ground in the region.

The Silverado and Indian Chief mines within the study area are reported as having skarn-type mineralization. The Silverado is predominantly a Zn skarn with minor Ag, Au and Cu mineralization. Preliminary conodont studies indicate that the carbonate rocks at the Silverado are Triassic (M. Orchard, pers comm, 2006). Additionally, the Ford Fe skarn north of Zeballos is hosted within Triassic carbonate rocks. This is a magnetite skarn and is related to the emplacement of Jurassic Island intrusions. There are some localities in the study area that have similar geology, most notably in the area around Hesquiat Lake (MINFILE 092E 013; MINFILE, 2006).

PRE-TERTIARY FAULTS

A focus of mapping in the Muchalat-Hesquiat region is placing the Westcoast Crystalline Complex (WCC) within the context of the existing Vancouver Island stratigraphy (Yorath *et al.*, 1999) and setting this part of Vancouver Island in a more modern plate-tectonic framework. To this end, some time was devoted to documenting major vertical and/or lateral movement on some of the large north-trending faults. The most remarkable of these is the Tahsis fault that runs all the way down Tahsis Inlet and separates the eastern coast of Nootka Island from Vancouver Island. In the area around Tahsis, the entire sequence of Triassic Karmutsen volcanic rocks is missing on the west side of the fault. This corresponds to a vertical offset in excess of 6 km (Surdam, 1968). This is also evidenced by an abrupt change in grade from upper greenschist in the Nootka Island rocks (Close, 2006) to lower or sub-greenschist on the east side of the fault (Marshall *et al.*, 2006). Movement on these faults must have occurred prior to the Tertiary as the Tertiary Carmanah sedimentary rocks are observed on both sides of the southern trace of the Tahsis fault.

ACKNOWLEDGMENTS

The authors would like to thank Geoscience BC, Simon Fraser University, Natural Sciences and Engineering Research Council of Canada, Interfor, Western Forest Products and Peter Buckland (Cougar Annie's Garden) for financial aid and/or help in the field and/or access to properties. Nick Massey from the BC Geological Survey is gratefully acknowledged for very useful discussions.

REFERENCES

- Barrett, T.J. and Sherlock, R.L. (1996): Volcanic stratigraphy, litho-geochemistry, and seafloor setting of the H-W massive sulfide deposit, Myra Falls, Vancouver Island, British Columbia; *Exploration and Mining Geology*, Volume 5, pages 421–458.
- BC Geological Survey (2005): Geology and mineral deposits of northern Vancouver Island, (NTS 102I, 092L); *BC Ministry of Energy, Mines and Petroleum Resources*, MapPlace website, URL <<http://webmap.em.gov.bc.ca/mapplace/minpot/bcgs.cfm>>.
- Close, S. (2006): Geology and tectonics of the Nootka Island region, British Columbia; unpublished MSc thesis, *Simon Fraser University*, 137 pages.
- DeBari, S.M., Anderson, R.G. and Mortensen, J.K. (1999): Correlation among lower to upper crustal components in an island arc: the Jurassic Bonanza arc, Vancouver Island, Canada; *Canadian Journal of Earth Sciences*, Volume 36, pages 1371–1413.
- Hansen, M.C. and Sinclair, A.J. (1984): A preliminary assessment of Zeballos mining camp (92L); in *Geological Fieldwork, 1983*, *BC Ministry of Energy, Mines and Petroleum Resources*, pages 219–232.
- Jones, S., Herrmann, W. and Gemmel, B. (2005): Short wavelength infrared spectral characteristics of the HW horizon: implications for exploration in the Myra Falls volcanic-hosted massive sulfide camp, Vancouver Island, British Columbia, Canada; *Economic Geology*, Volume 100, pages 273–294.
- Leitch, C., Ross, K., Fleming, J. and Dawson, K. (1995): Preliminary studies of hydrothermal alteration events at the Island copper deposit, northern Vancouver Island, British Columbia; in *Current Research, Geological Survey of Canada*, 1995-A, pages 51–59.
- Maier, W., Barnes, S.J., Gartz, V. and Andrews, G. (2003): Pt-Pd reefs in magnetitites of the Stella layered intrusion, South Africa; a world of new exploration opportunities for platinum group elements; *Geology*, Volume 31, pages 885–888.
- Marshall, D., Lesiczka, M., Xue, G., Close, S. and Fecova, K. (2006): An update on the mineral deposit potential of the Nootka Sound region; in *Geological Fieldwork 2005*, *BC Ministry of Energy, Mines and Petroleum Resources*, Paper 2006-1 and *Geoscience BC*, Report 2006-1, pages 323–330.
- Marshall, D., Podstawskyj, N. and Aichmeier, A. (2005): Gold mineralization and geology in the Zeballos area, Nootka Sound, British Columbia; in *Geological Fieldwork 2004*, *BC Ministry of Energy, Mines and Petroleum Resources*, pages 301–310.
- MINFILE (2006): MINFILE BC mineral deposits database; *BC Ministry of Energy, Mines and Petroleum Resources*, URL <<http://www.em.gov.bc.ca/Mining/Geolsurv/Minfile/>> [November 2006].
- Muller, J.E., Cameron, B.E.B. and Northcote, K.E. (1981): Geology and mineral deposits of the Nootka Sound map-area, Vancouver Island, British Columbia; *Geological Survey of Canada*, Paper 80-16, 53 pages.
- Northcote, K. and Robinson, W. (1972): Island copper mine; in *Geology, Exploration and Mining in BC 1972*, *BC Ministry of Energy, Mines and Petroleum Resources*, pages 293–303.
- Sá, J., Barnes, S.J., Prichard, H.M. and Fisher, P.C. (2005): The distribution of base metals and platinum-group elements in magnetitite and its host rocks in the Rio Jacaré intrusion, northeastern Brazil; *Economic Geology*, Volume 100, pages 333–348.
- Stevenson, J.S. (1938): Lode-gold deposits of the Zeballos area, west coast of Vancouver Island, British Columbia; *BC Ministry of Energy, Mines and Petroleum Resources*, Miscellaneous Report 1938-1, 23 pages.

- Stevenson, J.S. (1939): Geology and ore deposits of the Zeballos area, British Columbia; *Transactions of the Canadian Institute of Mining and Metallurgy and of the Mining Society of Nova Scotia*, Volume 42.
- Stevenson, J.S. (1950): Geology and mineral deposits of the Zeballos mining camp; *BC Ministry of Energy, Mines and Petroleum Resources*, Bulletin 27, 145 pages.
- Surdam, R. (1968): The stratigraphy and volcanic history of the Karmutsen Group, Vancouver Island, British Columbia; *Geology*, Volume 7, pages 15–26.
- Yorath, C.J., Sutherland Brown, A. and Massey, N.W.D. (1999): LITHOPROBE, southern Vancouver Island, British Columbia: geology; *Geological Survey of Canada*, Bulletin 498, 145 pages.

Indicator Mineral Content and Geochemistry of Stream and Glacial Sediments from the Etsho Plateau Region (NTS 094I, P) as an Aid to Kimberlite and Base Metal Exploration, Northeast British Columbia¹

by M.W. McCurdy², I.R. Smith³, A. Plouffe², J. Bednarski⁴, S.J.A. Day², P.W.B. Friske², R.J. McNeil², I.M. Kjarsgaard⁵, T. Ferbey, V.M. Levson, A.S. Hickin, M. Trommelen and T.E. Demchuk⁶

KEYWORDS: kimberlite, indicator minerals, heavy minerals, mineral exploration, G3, G9, G11, G12, garnet, Cr-pyrope, Cr-diopside, Cr-spinel, ilmenite, chromite, olivine, glacial sediment, streamwater, stream sediments, base metal, sphalerite, geochemistry

INTRODUCTION

A two-year reconnaissance-scale stream and glacial sediment sampling project, funded by Geoscience BC and the Geological Survey of Canada, was implemented by the Geological Survey of Canada in 2005 with the objective of evaluating the potential for diamond-bearing kimberlite, gold, base metal and other economic commodities in northeast BC (Plouffe *et al.*, 2006b). The intended benefit of the project is to promote future investments for mineral exploration and to reduce the risk associated with such activity. This project was created following the announcement of the occurrence of kimberlite indicator minerals (KIM) in glacial sediments from northeast BC (Levson *et al.*, 2004; Simandl, 2005), which sparked interest in the exploration of kimberlites in northeast BC. This project includes participants from the Geological Survey of Canada (GSC) and the BC Ministry of Energy, Mines and Petroleum Resources (MEMPR). The GSC, under the Northern Resources Development Program, and the Alberta Energy and Utilities Board/Alberta Geological Survey (EUB/AGS) are funding a project with similar objectives in northwest Alberta. A more detailed overview of the BC project was presented by Plouffe *et al.* (2006b).

The first year of the project (2005) involved reconnaissance-scale sampling of stream and glacial sediments (Plouffe *et al.*, 2006b). Samples were processed for heavy minerals during the winter of 2006. In the second and last year of the project, additional stream sediment sam-

pling was completed during the fall along three east-west transects located between Fort St. John and Fort Nelson. The objective of this paper is to present the preliminary results of the 2005 sampling program and the progress made during 2006. Final results will be released in a future publication (GSC Open File Report), which will include an integrated interpretation of the 2005 and 2006 stream and glacial sediment mineralogy and geochemistry. All data produced from this project will be provided in a format that allows it to be integrated into the MEMPR MapPlace website (BC Geological Survey, 2006).

PHYSIOGRAPHY

A description of the physiography, bedrock and surficial geology of the area was provided by Plouffe *et al.* (2006b) and is only briefly summarized here. The study area is generally flat to gently rolling with an average elevation below 600 m asl with the exception of the Etsho Plateau, which stands at an average elevation of 900 m asl. Streams are generally poorly developed because of the flat terrain, except around the Etsho Plateau where they are incised into glacial sediment and bedrock.

GEOLOGY OF THE STUDY AREA

Archean and Proterozoic basement rocks overlain by a succession of nearly horizontal Paleozoic and Mesozoic sedimentary rocks underlie northeast BC. Rocks of the Cretaceous Shaftesbury (dominantly shale) and Dunvegan (dominantly sandstone) formations outcrop in a limited number of places within the region. Given the age of the youngest sedimentary rocks in the region, any kimberlites older than the Cretaceous would not be exposed to glacial or fluvial erosion and would not contribute indicator minerals directly to the surficial sediments. Therefore, the methodology applied in this project limits any discoveries to kimberlites younger than or contemporaneous with the Cretaceous host rocks.

The Laurentide ice sheet advanced over northeast BC during the Late Wisconsinan glaciation leaving behind a thick cover of glacial sediments including sand and gravel-rich glaciofluvial sediments, clay-rich till and glaciolacustrine sediments. Exposures in borrow pits and well-log records indicate great thicknesses of till and other glacial sediments (>20 m) in many parts of the low-lying areas surrounding the Etsho Plateau. Around the periphery of the plateau, till thicknesses are much less, in some places forming only a veneer (<1 m thick) overlying shale bedrock. On

¹Geoscience BC contribution GBC037

²Geological Survey of Canada, Ottawa, ON

³Geological Survey of Canada, Calgary, AB

⁴Geological Survey of Canada, Sidney, BC

⁵Consulting Mineralogist, Ottawa, ON

⁶University of Victoria, Victoria, BC

This publication is also available, free of charge, as colour digital files in Adobe Acrobat® PDF format from the BC Ministry of Energy, Mines and Petroleum Resources website at http://www.em.gov.bc.ca/Mining/GeolSurv/Publications/catalog/cat_fldwk.htm

top of the plateau, till thicknesses are in the order of 5 to 10 m. Several surficial geology maps which depict ice-flow direction and surficial sediment distribution have been published (Bednarski, 2005a, b; Smith, in press a–d). At glacial maximum, ice generally flowed west to southwest as indicated by the orientation of drumlins, flutings, crag-and-tails and till clast fabrics. Deglaciation of the region occurred around 11 500 to 11 000 radiocarbon years before present with the highest point, Etsho Plateau, being deglaciated first (Dyke *et al.*, 2003; Dyke, 2004). In his reconstruction of the ice front configuration during ice retreat, Mathews (1980) depicted the ice-free Etsho Plateau surrounded by lobes of ice to the north and south; the southern one was referred to as the Fort Nelson lobe. Meltwater flowing from the retreating ice eroded significant meltwater channels and deposited glaciofluvial sand and gravel, which have been a focus of the glacial sediment sampling program. Glaciofluvial sediments provide a broader regional sampling of the bedrock mineralogy, as compared to till. Such deposits are, however, rare and geographically restricted in the field area, thus the glacial sediment sampling program also includes bulk till samples, and samples from discrete sand and gravel units observed within thicker till sections. These sand and gravel units are associated with glacial deformation processes, including the thrusting and stacking of till sheets. They form as a result of winnowing of finer material by water flow either at the base of a glacier, or along shear planes within the till, and are thus analogous to glaciofluvial deposits. A large proportion of the area is overlain by organic deposits (fens and bogs), which greatly impeded any systematic and spatially integrated sampling of glacial sediments.

New Potential for Base Metal Exploration

Approximately 180 km east-southeast of the Etsho Plateau in the Zama Lake, Alberta region, a new potential for base metal exploration was revealed by the identification of a sphalerite dispersal train in till (Plouffe *et al.*, 2006a). The sphalerite was identified in the sand-sized fraction of a number of till samples, which contain up to 1000 grains of sphalerite and trace amounts of galena. The anomaly overlies bedrock of the Shaftesbury Formation and is in close proximity to the Great Slave Lake Shear Zone (GSLSZ), a major structural break trending southwest and extending from Great Slave Lake to northeast BC (Gehrels and Ross, 1998). The Pine Point Mississippi Valley-type deposit, on the south shore of Great Slave Lake, occurs along the GSLSZ approximately 330 km northeast of the anomaly. Plouffe *et al.* (2006a) suggest that the till anomaly is

derived from an undiscovered bedrock source as opposed to representing long distance glacial transport from the Pine Point region. The potential for zinc mineralization in northeast BC might also exist given that the bedrock geology of northwest Alberta is similar.

METHODOLOGY

Stream Sediment and Water Sample Collection

Trucks and a helicopter were used to collect stream sediment and water for geochemical and KIM analyses. Stream sediment sampling was focused on the best-developed streams. At 49 sites (Fig 1), a 125 ml water sample and approximately 2 kg of silt and clay were collected

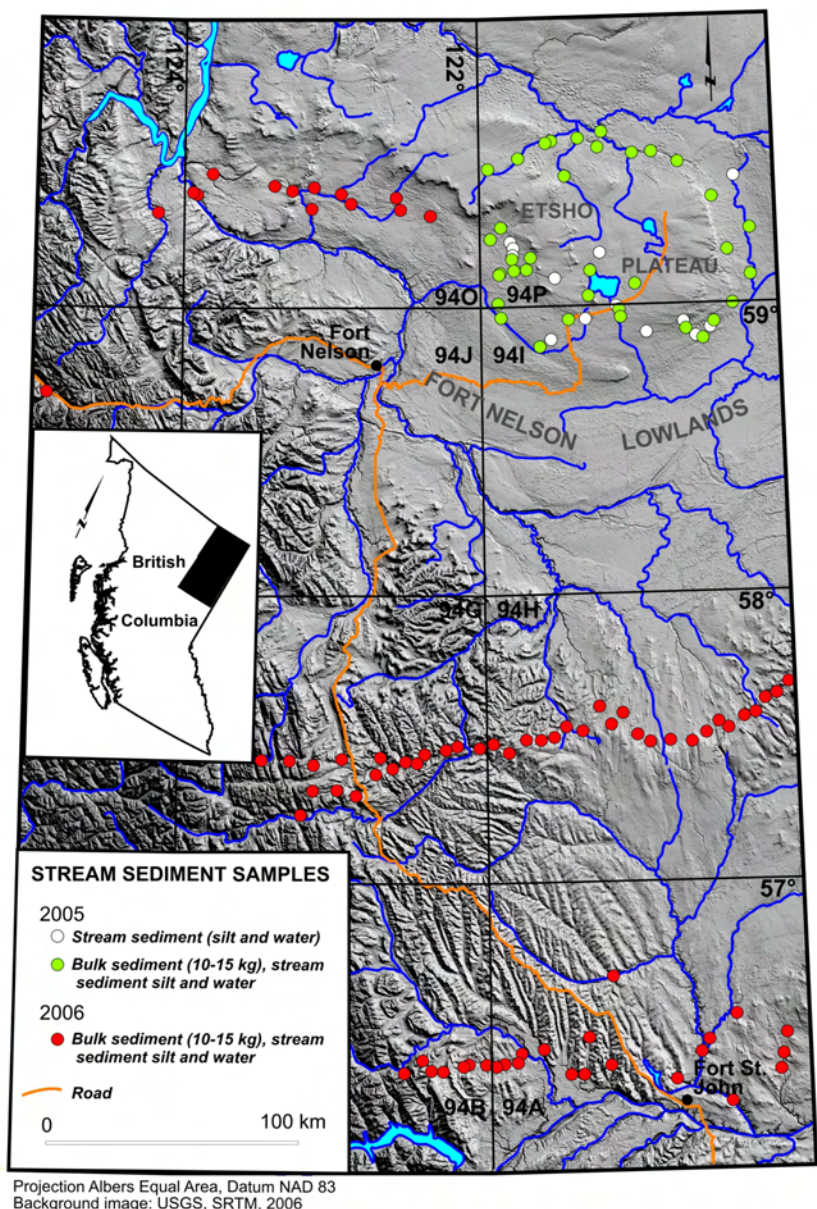


Figure 1. Location of stream sediment and water samples collected in northeast BC in 2005 and 2006.

from the active part of the stream channel. At 36 of these sites (Fig 1), coarse sediment (ideally from the upstream end of midchannel bars) was wet-sieved through a 12-mesh (1.68 mm) screen to obtain a sample weighing between 10 and 15 kg for additional geochemical and mineralogical, including KIM, analysis. Site locations were recorded with a global positioning system (GPS) receiver, field observations were noted and sites were flagged. For a more detailed description of sample collection, see McCurdy *et al.* (2006). Preliminary results of these analyses are presented below.

To extend the coverage of stream sediment baseline data for northeast BC, three east-west stream sediment sample transects were completed with truck and helicopter support across the zone where the Laurentide ice sheet, Cordilleran ice and Rocky Mountain montane glaciers were thought to be in contact during the late Wisconsinan (Mathews, 1980). Completed in the fall of 2006, silt, water, pebbles and bulk sediment samples were collected from a total of 79 sites (Fig 1). Geochemical data from sediments, water and heavy mineral concentrates in addition to mineralogical information from heavy mineral concentrates and pebbles will be published in 2007.

Glacial Sediment Sample Collection

Trucks, all-terrain vehicles and helicopters were used to collect glacial sediment for geochemical analysis. At 140 sites approximately 4 kg of till were collected below the depth of the oxidized soil horizon from roadcuts, hand-dug pits, borrow pits and auger holes. At 17 of these sites, bulk samples weighing approximately 25 kg were collected for KIM analysis. An additional 26 bulk samples of primarily glaciofluvial sediment were collected for KIM analysis. One sample of crushed bedrock (Dunvegan Formation sandstone) was collected for KIM analysis. Site locations were recorded with a global positioning system (GPS) receiver, field observations were noted and sites were flagged. For a more detailed description of sample collection, see Plouffe *et al.* (2006b).

Sample Processing and Analysis

Bulk glacial and stream sediment samples were shipped to Overburden Drilling Management Limited (ODM), Ottawa, Ontario, for heavy mineral separation using a combination of a shaking table and heavy liquids (specific gravity 3.2) to separate the nonferromagnetic heavy mineral fraction. The heavy mineral concentrate (HMC) was picked for KIM and other indicators such as gold in the same laboratory. Gold grains, KIM and other heavy minerals were identified in the 0.25 to 2 mm fraction under binocular microscopes by staff mineralogists at ODM. Based on the total volume of visible gold grains identified in each sample and the total weight, an estimate of the gold concentration of the HMC, in parts per billion, was calculated by ODM. Visual identification of mineral grains was made mainly on the basis of colour, crystal habit, lustre and alteration. A scanning electron microscope was used to confirm the identity of some grains. One sample of bulk till spiked with a known number of KIM was included in the samples sent to the laboratory to monitor the quality of the visual identification.

Microprobe analyses of KIM grains derived from glacial sediments were conducted using the CAMECA

Camebax electron microprobe at Carleton University, Ottawa, Ontario. Kimberlite indicator grains derived from the heavy mineral fraction of stream sediments were analyzed at the GSC using a CAMECA SX-50 electron microprobe. Selected results are presented and discussed herein; a complete analytical report will be published in 2007 as a GSC Open File Report.

Stream and glacial sediment samples (2 and 4 kg) were shipped to Acme Analytical Laboratories Ltd., Vancouver, BC, for preparation and geochemical analysis. Inductively coupled plasma mass spectrometry (ICP-MS) and instrumental neutron activation analysis (INAA) were conducted on the silt and clay-sized fraction (-250 mesh or <0.063 mm) of the till samples only. The -80 mesh (<177 μm) fraction of the stream sediments and the <0.25 mm fraction of the heavy mineral concentrates were analyzed by ICP-MS at Acme Analytical Laboratories Ltd. Instrumental neutron activation analysis was carried out at Becquerel Laboratories Inc., Toronto, Ontario. Analytical quality was monitored with additional standard and duplicate samples inserted into the sample suite following sample preparation.

Water samples collected at stream sediment sites were filtered and acidified with nitric acid within 24 hours of collection. An unacidified, unfiltered subsample was used to determine pH and conductivity at this time. Samples were shipped to the GSC for analysis by ICP-MS and inductively coupled plasma emission spectroscopy (ICP-ES).

RESULTS AND DISCUSSION

KIM in Glacial and Stream Sediments

Of the 44 glacial sediment samples submitted for analysis, 23 samples yielded between one and three KIM in the 0.25 to 0.5 mm fraction (Table 1; Fig 2). Most of the KIM were recovered from glaciofluvial sand and gravel deposits and only 2 out of 15 till samples contained a single KIM grain (one Mg-ilmenite and one peridotitic garnet). Concentrations of KIM were low in all samples (a total of 36 individual KIM were identified in the entire sample set), as was mineralogical diversity – only four samples had more than one type of KIM. Peridotitic (Cr-pyrope) garnet (20) was the most common KIM, followed by chromite (8) and lesser amounts of Cr-diopside (4) and Mg-ilmenite (4). With the exception of one ilmenite grain retrieved from the 0.5 to 1.0 mm fraction of sample SUV05329, all of the KIM identified were found in the smallest sand-size fraction, 0.25 to 0.5 mm. No KIM were recovered from the bedrock sample (TFE05-6).

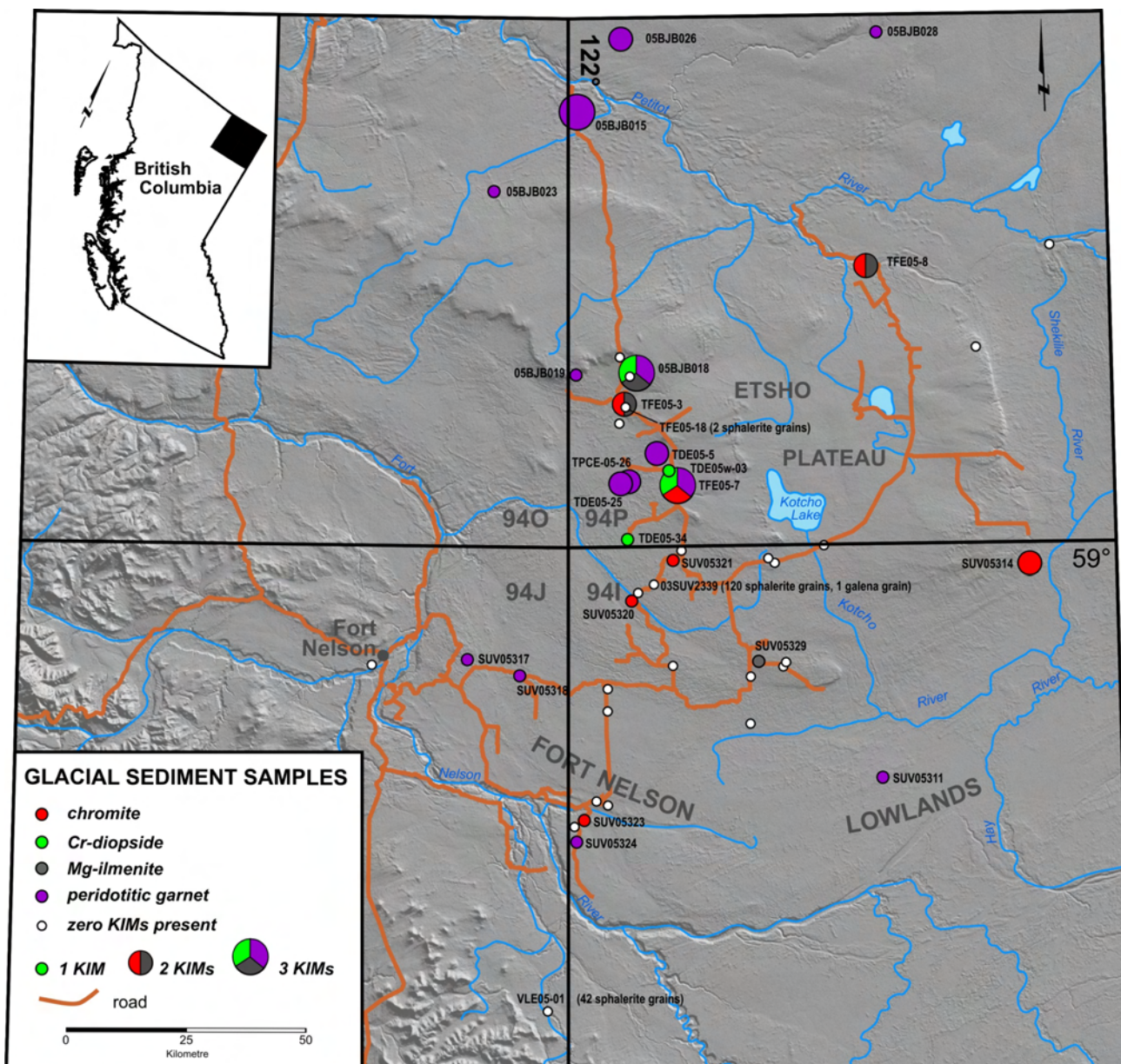
The Cr-pyrope garnets contain between 2.66 and 11.61 wt.% Cr_2O_3 . Most are classified as G9 garnets from lherzolite xenoliths, except for four G12 garnets high in CaO, which are from wehrlite, and one moderately Ti-rich (0.40 wt.% TiO_2) G11 garnet, which could be classified as a garnet from sheared and/or metasomatized lherzolite (Table 1). One pyrope from sample SUV05311 falls on the Gurney's (1984) 85% line separating subcalcic harzburgitic garnets from fertile peridotitic garnets – all other garnets fall above the 85% line. No subcalcic harzburgitic garnets were found.

Microprobe analysis of the Cr-diopside grains yielded Cr_2O_3 concentrations between 0.65 and 1.17 wt.%, which are fairly moderate compared to other mantle Cr-diopsides.

TABLE 1. GLACIAL SEDIMENT SAMPLE LOCATIONS AND KIMBERLITE INDICATOR MINERAL (KIM) DATA, NORTHEAST BC. ALL KIM GRAINS WERE RETRIEVED FROM THE 0.25 TO 0.5 MM FRACTION EXCEPT FOR ONE MAGNESIUM-ILMENITE GRAIN IN THE 0.5 TO 1.0 MM FRACTION OF SAMPLE SUV05329.

Sample no.	Sample type	Easting (NAD83)	Northing (NAD83)	Sample		Kimberlite indicator minerals (confirmed by probe analysis)						Total
				weight (g)	Material	Peridotitic garnet	Eclogitic garnet (G3)	Cr- diopside	Olivine	Chromite	Mg- ilmenite	
AH05082208	glaciofluvial	495542	6345782	16.8	sand, gravel							0
AH05090315	glaciofluvial	526846	6285837	16.2	sand, gravel							0
AH05090801	glaciofluvial	673984	6114298	17.7	sand, gravel							0
05BJB003	glaciofluvial	642388	6582953	27.8	sand, gravel							0
05BJB008	glaciofluvial	657605	6606064	22.4	sand, gravel							0
05BJB015	glaciofluvial	558510	6631336	29.1	sand	3						3
05BJB018	glaciofluvial	571458	6577012	25.6	sand	1		1			1	3
05BJB019	glaciofluvial	558408	6576514	26.8	sand	1						1
05BJB023	glaciofluvial	542323	6611531	15.9	sand, gravel	1 (G12)						1
05BJB026	glaciofluvial	566397	6647091	19.5	sand, gravel	2 (G9,G12)						2
05BJB028	glaciofluvial	620082	6649890	18.4	sand, gravel	1						1
TDE05-5	glaciofluvial	575001	6559192	28.0	sand	2 (G9,G12)						2
TDE05-18	till	568431	6570801	25.1	till							0
TDE05-25	glaciofluvial	570268	6554421	25.1	sand, gravel	2 (G9,G11)						2
TDE05-29	glaciofluvial	570642	6576584	19.3	sand, gravel							0
TDE05-34	glaciofluvial	569289	6541614	21.7	sand, gravel			1				1
TDE-05w-03	glaciofluvial	577988	6557173	25.4	sand, gravel			1				1
TFE05-3	glaciofluvial	568376	6570926	17.3	sand, gravel					1	1	2
TFE05-5	till	567670	6580969	25.3	till							0
TFE05-6	bedrock	567986	6566251	12.5	crushed rock							0
TFE05-7	glaciofluvial	579115	6554073	17.4	sand, gravel	1		1		1		3
TFE05-8	glaciofluvial	618526	6601001	21.5	sand, gravel					1	1	2
TFE05-9	till	609589	6541386	21.0	till							0
TPCE-05-26	glaciofluvial	569294	6553872	19.4	sand, gravel	2 (G9,G12)						2
SUV05311	till	623127	6493387	30.6	sand	1						1
SUV05314	fluvial, Tertiary	654056	6539077	16.8	sand, gravel					2		2
SUV05317	till	537106	6516768	23.2	sand, gravel	1						1
SUV05318	till	548627	6513265	25.8	sand, gravel	1						1
SUV05319	till	579208	6516097	23.6	till							0
SUV05320	till	571489	6529518	24.1	sand, gravel					1		1
SUV05321	glaciofluvial	579560	6538956	25.1	sand, gravel					1		1
SUV05322	till	564840	6487053	19.0	sand, gravel							0
SUV05323	till	561225	6483879	24.1	sand, gravel					1		1
SUV05324	till	559889	6478976	24.6	till	1						1
SUV05325	till	595816	6514514	24.4	till							0
SUV05326	till	600606	6538407	21.8	till							0
SUV05328	till	604594	6517488	25.7	till							0
SUV05329	till	597854	6516988	14.7	till						1	1
03SUV2338	till	565925	6507214	32.5	till							0
03SUV2339	till	575154	6533261	27.9	till							0
03SUV2341	till	595709	6504607	26.7	till							0
03SUV2343	till	605130	6517808	22.6	till							0
03SUV2344	till	599821	6538389	25.8	till							0
VLE-05-01	fluvial, modern	554596	6443457	23.4	till							0

¹Total sample weight of the <2 mm fraction processed



Projection Albers Equal Area, Datum NAD 83
Background image: RADARSAT, USGS, 2004

Figure 2. Kimberlite indicator mineral (KIM), confirmed by electron microprobe, and sphalerite and galena concentrations from heavy mineral separates of bulk (approximately 26 kg) glacial sediment samples, northeast BC. All peridotitic garnets are classified as G9 garnets, unless otherwise indicated.

When plotted using Nimis (1998) criteria, three of the Cr-diopside grains are discriminated as being from garnet peridotite (samples TDE05-34, TDE05w-03, TFE05-7), while the fourth (sample O5BJB018) is from spinel-peridotite assemblages.

Most of the oxide grains were chromites with one Cr-spinel in sample SUV05314, and one hercynite ((Fe,Mg)Al₂O₄) in sample TFE05-3. Interestingly, sample SUV05314 chromite is interpreted to represent a Tertiary fluvial outlier, largely composed of quartzite erratics of montane provenance. None of the oxide grains identified fall within the diamond intergrowth or inclusion fields of Fipke *et al.* (1995).

Of four ilmenite grains identified, only three were Mg-ilmenites (samples SUV05329, TFE05-3, TFE05-8), containing between 5.84 to 12.08 wt.% MgO and between 0.78 to 2.22 wt.% Cr₂O₃. These grains plot within the compositional range of kimberlitic megacryst ilmenite.

No fresh olivine grains were found in any of the samples. Olivine easily succumbs to alteration when it is exposed to chemical weathering for a long period of time, and thus does not travel well in glacial or fluvial sediments (Ehlers and Blatt, 1982). Garnet, Cr-diopside and spinel compositions indicate that garnet and spinel-peridotite, specifically lherzolite and wehrlite, xenoliths were sampled by the kimberlite(s) that have been eroded and depos-

TABLE 2. BULK STREAM SEDIMENT SAMPLE LOCATIONS AND KIMBERLITE INDICATOR MINERAL DATA. PERIDOTITIC GARNET IS LHERZOLITIC (G9), UNLESS OTHERWISE INDICATED. NUMBERS IN BRACKETS INDICATE GRAINS IN THE 0.5 TO 1.0 MM FRACTION. ONE GRAIN, AN OLIVINE AT SITE 094P051034, IS IN THE 1.0 TO 2.0 MM FRACTION. ALL OTHER GRAINS ARE IN THE 0.25 TO 0.5 MM FRACTION.

Sample no.	Easting (NAD83)	Northing (NAD83)	Sample weight (kg)	<2.0 mm table concentrate (g)	Kimberlite indicator minerals (confirmed by probe analysis)						Total
					Peridotitic garnet	Eclogitic garnet (G3)	Cr-diopside	Olivine	Chromite	Mg-ilmenite	
094I051003	647349	6536003	10.6	806.1	0	1	0	0	3 (3)	0	4
094I051005	643192	6529531	11.1	927.4	1	0	0	0	1	0	2
094I051006	636540	6533138	14.5	1575	2 (G9,G12)	0	1	1 (1)	5	2 (1)	11
094I051009	610799	6540231	9.8	906.9	1 (G11)	0	1	0	0	0	2
094I051011	611309	6537325	1.7	931.1	0	0	0	0	2	0	2
094I051013	591243	6536148	7.9	863.9	0	0	2	0	1	0	3
094I051015	580239	6525552	10.9	1514.9	4 (1)	0	0	0	1	0	5
094I051016	565271	6536580	9.3	1093.2	0	0	0	0	1	0	1
094I051017	654556	6543119	9.1	892.6	1	0	1	0	0	0	2
094P051006	569388	6559214	11.2	826.6	0	0	0	0	0	0	0
094P051007	564922	6553818	6.9	606.3	0	0	1	0	1	1	3
094P051008	564431	6553144	10.5	1199.8	2	0	1	0	2	1 (1)	6
094P051009	570215	6554817	11.0	1024.8	1	0	0	0	0	0	1
094P051010	576618	6559853	8.0	1143.2	0	0	0	0	0	0	0
094P051011	575049	6555203	10.9	1367.9	1	0	1	0	2	1	5
094P051012	564125	6542029	8.7	1174.3	0	0	0	0	1 (1)	1 (1)	2
094P051013	561033	6566895	13.1	1361.2	0	0	0	0	0	0	0
094P051014	565041	6571435	11.9	1780.2	1 (1)	0	0	0	1	0	2
094P051015	560027	6593946	15.0	1713	1	0	0	0	2	0	3
094P051016	571624	6598150	8.5	1251.4	2	0	1	0	1	1	5
094P051020	599561	6555248	10.1	1049.7	0	0	0	0	0	1 (1)	1
094P051022	598889	6545501	11.9	1361.7	1	1	0	1 (1)	0	0	3
094P051023	589594	6591531	11.4	1496.2	1 (G11)	0	2	0	1	0	4
094P051024	584389	6605039	8.9	1232.2	0	1 (1)	1 (1)	1 (1)	1 (1)	1 (1)	5
094P051025	594628	6606255	14.7	1578.6	0	0	2	0	3 (2)	2	7
094P051026	602210	6602842	9.1	1028.2	0	0	2	0	0	1 (1)	3
094P051027	603688	6608825	15.4	1221.5	0	0	1	0	0	0	1
094P051028	615566	6600765	13.7	1703.7	1	0	1	0	0	0	2
094P051030	582156	6604214	10.4	895.4	1 (G11)	0	0	0	0	0	1
094P051031	622976	6601386	9.1	1239	0	0	0	0	3 (1)	0	3
094P051032	633158	6597549	8.7	1163	0	0	0	0	5 (2)	4 (3)	9
094P051034	646292	6584199	12.6	1667.8	0	0	0	1	0	0	1
094P051035	661007	6572141	10.3	1199.7	0	0	1	0	0	0	1
094P051037	652374	6563796	8.4	620.9	0	0	0	0	0	0	0
094P051038	661394	6554199	9.4	1176.9	0	0	2	0	4 (2)	1 (1)	7
094P051039	616867	6550299	10.9	1161.7	2	0	0	0	0	0	2

ited in association with the regional glacial sediment samples. However, no grains from diamond-bearing assemblages such as eclogite or subcalic harzburgite were found.

KIM in stream sediments were visually identified from the heavy mineral concentrates of 34 out of 36 samples collected around the margins of the Etsho Plateau. Identified KIM include peridotitic garnet, eclogitic garnet, Cr-diopside, olivine, chromite and Mg-ilmenite (Table 2). Note that results are not normalized to a standard heavy mineral concentrate weight. Total abundance of confirmed KIM varies from one grain (seven sites) to eleven grains.

The distribution of KIM, identified as such by electron microprobe, are shown in Figure 3. Using the classification scheme of Grütter *et al.* (2004), three garnets were classified as eclogitic (G3) garnets. Eclogitic garnets are extremely important pathfinder minerals in diamond exploration (Grütter, 2004). A further 19 were classified as Cr-pyrope garnets derived from lherzolite (G9 garnets).

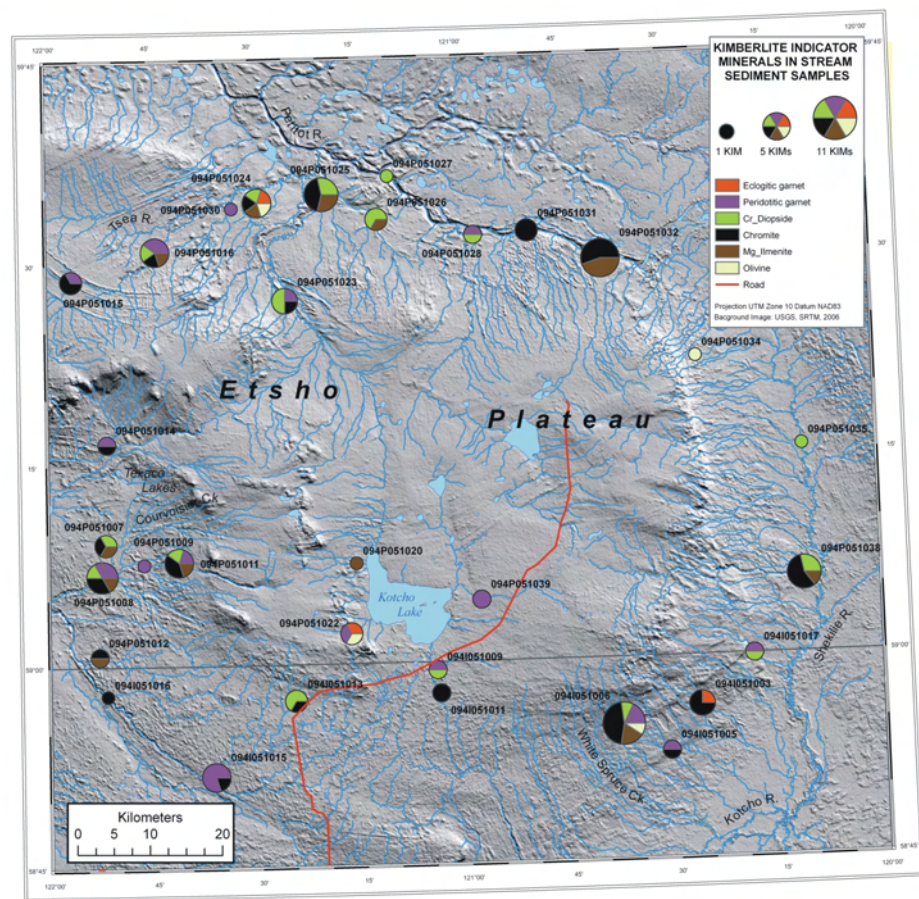


Figure 3. Kimberlite indicator mineral results, confirmed by electron microprobe, from bulk (10–15 kg) stream sediment samples, northeast BC. All peridotitic garnets are classified as G9 garnets, unless otherwise indicated.

BASE METAL POTENTIAL: GEOCHEMISTRY AND INDICATOR MINERALS FROM GLACIAL SEDIMENTS

A summary of the geochemical results for selected elements in the <0.063 mm fraction of glacial sediments is presented in Table 3. No localized anomalous distribution or

concentration of any one, or combined suite of elements was detected in a preliminary examination of the results. However, the Zn and Pb geochemical maps suggest relatively moderate elevated concentrations over the Etsho Plateau, falling off to the west in the direction of ice flow (Fig 4). In the region of the aforementioned sphalerite dispersal train in Alberta, 180 km east of the Etsho Plateau, Zn con-

TABLE 3. SUMMARY OF GEOCHEMICAL DATA FOR SELECTED PRECIOUS AND BASE METALS, IN THE SILT AND CLAY-SIZED FRACTION (–250 MESH, <0.063 MM) OF GLACIAL SEDIMENT SAMPLES, NORTHEAST BC. MEASURED BY INDUCTIVELY COUPLED PLASMA MASS SPECTROMETRY AND EMISSION SPECTROSCOPY (ICP-MS AND ES) WITH AQUA REGIA DIGESTION. DISTRIBUTION OF SAMPLES IS SHOWN IN FIGURE 2.

	ICP-ES and MS with aqua regia digestion								INAA						
	Ag (ppb)	Cu (ppm)	Mo (ppm)	Ni (ppm)	Pb (ppm)	S (%)	U (ppm)	Zn (ppm)	As (ppm)	Au (ppb)	Ba (ppm)	Co (ppm)	Fe (%)	Sb (ppm)	U (ppm)
No. of samples	142	142	142	142	142	142	142	142	139	139	139	139	139	139	139
Minimum	26.0	6.1	0.12	9.5	5.5	<0.01	0.3	23.1	2.0	-2	250	3.0	0.8	-0.1	0.9
Maximum	1315.0	170.8	12.30	205.8	197.1	1.42	6.2	355.5	27.8	16	4090	28.0	4.5	2.5	9.2
Median	217.5	29.3	2.49	31.6	14.2	0.03	1.9	112.1	12.9	-2	740	11.0	3.0	1.0	4.1
75 percentile	250.8	31.6	3.53	35.3	15.8	0.15	2.4	120.8	14.7	-2	820	12.0	3.3	1.3	4.7
90 percentile	282.8	34.7	4.91	40.8	18.3	0.66	2.8	132.5	16.4	6	1042	14.2	3.5	1.6	5.1
95 percentile	341.9	37.3	5.65	44.5	19.4	0.76	3.1	145.3	17.5	8	1142	16.1	3.6	1.7	5.8

Abbreviations: ICP-ES and MS, inductively coupled plasma emission spectroscopy and mass spectrometry; INAA, instrumental neutron activation analysis

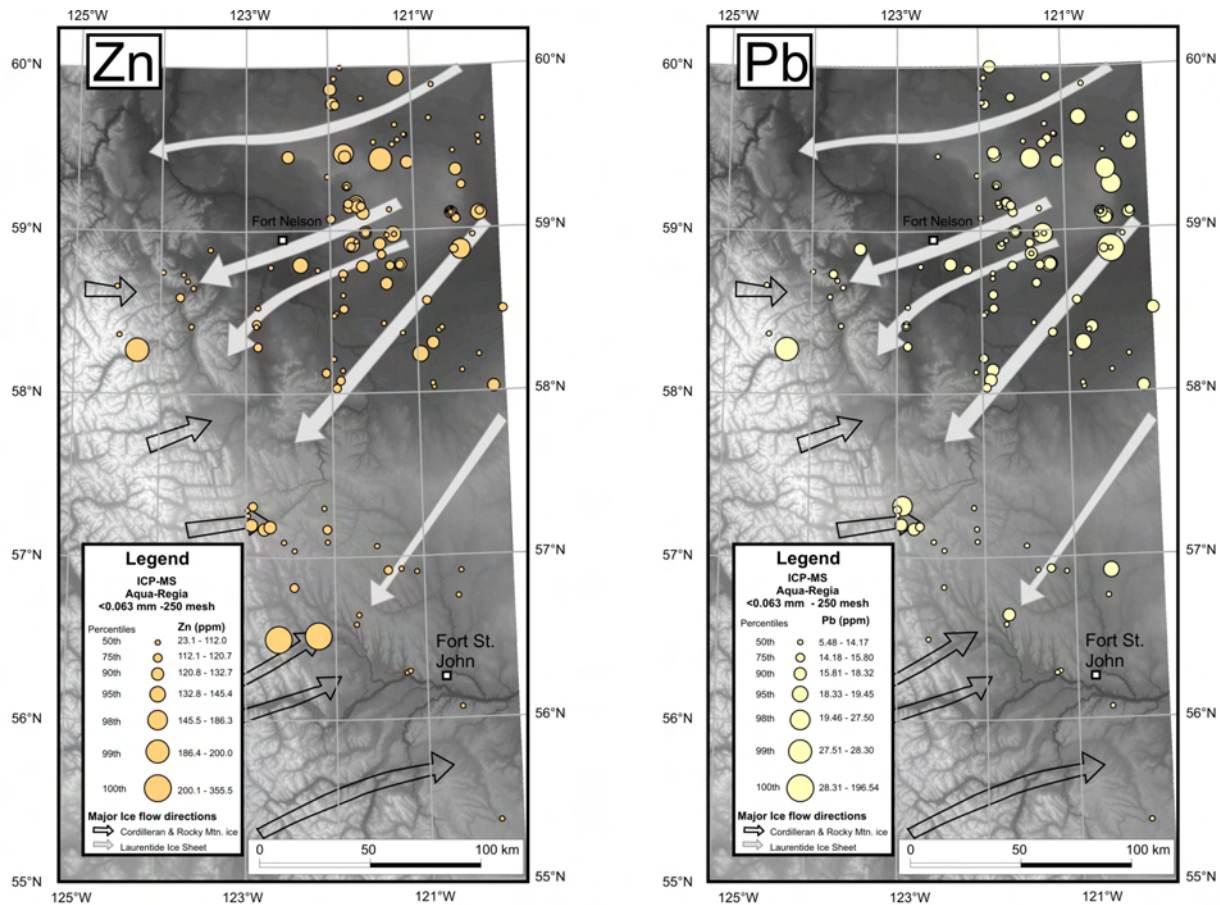


Figure 4. Lead (Pb) and zinc (Zn) concentrations in the silt and clay-sized fraction (~ 250 mesh, <0.063 mm), as measured by inductively coupled plasma mass spectrometry (ICP-MS) with aqua regia digestion, northeast BC.

centrations in the silt and clay-sized fraction of glacial sediments were also not high, ranging from 169 to 231 ppm (Plouffe *et al.*, 2006a). Similarly, even with the presence of trace amounts of galena in the same region, lead concentrations were low, varying from 17 to 25 ppm.

Similar Pb and Zn concentrations were observed in the glacial sediment samples from the Etsho Plateau. Sphalerite grains, however, were found in one fluvial and two till sediment samples (03SUV2339, till, 120 grains; VLE05-01, fluvial, 42 grains; TDE05-18, till, 2 grains) and one till sample yielded a galena grain (03SUV2339). None of these samples have yielded anomalous Zn or Pb concentrations. These results suggest that base metal mineralization might be present in northeast BC and that heavy mineral concentrates recovered from the sand-sized fraction of glacial sediments are more effective than geochemical analysis of the fine fraction (~ 250 mesh, <0.063 mm) to detect concealed mineralization. The effectiveness of the geochemical analysis of the sand-sized fraction at detecting mineralization remains to be tested.

STREAM SEDIMENT GEOCHEMISTRY

The relative mobility of elements in surface environments is affected by climate and physiography, as well as biological, anthropogenic and geological factors (Plant and Raiswell, 1994). Stream sediment and water surveys were carried out from 2001 to 2004 (Friske *et al.*, 2003;

McCurdy *et al.*, 2006) in an area east of the survey area, in the Buffalo Head Hills of northwest Alberta. A useful comparison can be made between data from the Buffalo Head Hills survey and the present survey around the perimeter of the Etsho Plateau. The two areas are similar in nature, with similar geology, glacial history, physiography, vegetation and surficial geology. Table 4 compares mean and median concentrations in the silt fraction for selected metals from the two datasets. Generally, values are similar. Median and mean values of Ag in Buffalo Head Hills stream sediments are lower than comparable values around the Etsho Plateau and may be affected by slightly more alkaline streamwater in the Buffalo Head Hills. The average pH of streams draining the Buffalo Head Hills is 7.65 (Friske *et al.*, 2003; McCurdy *et al.*, 2006), whereas the average pH of streams draining the Etsho Plateau is 7.19. The geochemical mobility of Ag is reduced in neutral to alkaline waters (Plant and Raiswell, 1994). Because the main purpose of the stream sediment survey was to establish the potential for diamond-bearing rock in northeast BC, samples were mainly taken from second and third-order streams, from which elemental concentrations of most elements would be expected to be diluted from input from large areas of drainage basins. However, geochemistry of the silt does suggest moderate potential for follow-up work in three areas, west of Shekile River, Courvoisier Creek and Tsea River. West of the Shekile River a number of sites contain elevated concentrations of Zn and Pb (Fig 5a, b). In this area, Ag, Cd,

TABLE 4. COMPARISON OF MEAN AND MEDIAN VALUES OF SELECTED ELEMENTS IN STREAM SEDIMENT (SILT) FROM THE ETSHO PLATEAU, NORTHEAST BC AND BUFFALO HEAD HILLS, NORTH-CENTRAL ALBERTA (FRISKE ET AL., 2003; MCCURDY ET AL., 2006). ALL VALUES ARE PPM UNLESS OTHERWISE INDICATED.

Element (analysis)	Etsho Plateau (n=49)		Buffalo Head Hills (n=470)	
	Mean	Median	Mean	Median
Ag (ICP-MS)	117 ppb	104 ppb	84 ppb	77 ppb
As (INAA)	8.7	8.7	10.9	10
Ba (INAA)	720	710	878	810
Co (INAA)	10	10	10	9
Cu (ICP-MS)	12.6	11.08	12.18	10.52
Fe (INAA)	2.90%	2.80%	3.00%	2.80%
Hg (ICP-MS)	38 ppb	34 ppb	47 ppb	39 ppb
Mn (ICP-MS)	431	331	718	440
Mo (ICP-MS)	1.51	1.26	0.99	0.67
Ni (ICP-MS)	17.3	15.8	16.7	14.7
Pb (ICP-MS)	8.38	8.23	8.29	7.81
Sb (INAA)	0.6	0.6	0.7	0.6
U (INAA)	4.1	3.6	3.2	3
Zn (ICP-MS)	80	76.6	61.9	57.6

Abbreviations: ICP-MS, inductively coupled plasma mass spectrometry; INAA, instrumental neutron activation analysis

Co±As and Sb are also elevated relative to the whole dataset. Similar patterns of distribution are noted in the drainage basins of Courvoisier Creek and the Tsea River (Fig 5a, b).

In addition to the silt samples, geochemical analyses were conducted on the heavy mineral concentrates of the <0.25 mm fraction. The geochemical results for the heavy mineral concentrates are presented using a descriptive terminology defined as follows: the median value for a given element is considered as background and anomalies are considered weak (2–3 times the median value), moderate (3.1–5 times the median value), strong (5.1–10 times the median value) or very strong (>10 times the median value).

Median values for selected elements are similar in the Buffalo Head Hills and the Etsho Plateau except for Zn and Pb; both exhibit higher median and mean values over the Etsho Plateau compared to the Buffalo Head Hills (Table 5). In addition, the Ag median value is more elevated over the Etsho Plateau in comparison to the Buffalo Head Hills.

Zinc values are elevated generally around the north-west margins of the Etsho Plateau (Fig 6a). Throughout the drainage basin of the Tsea River, Zn values are anomalous, with a strongly anomalous value of 1295 ppm (ap-

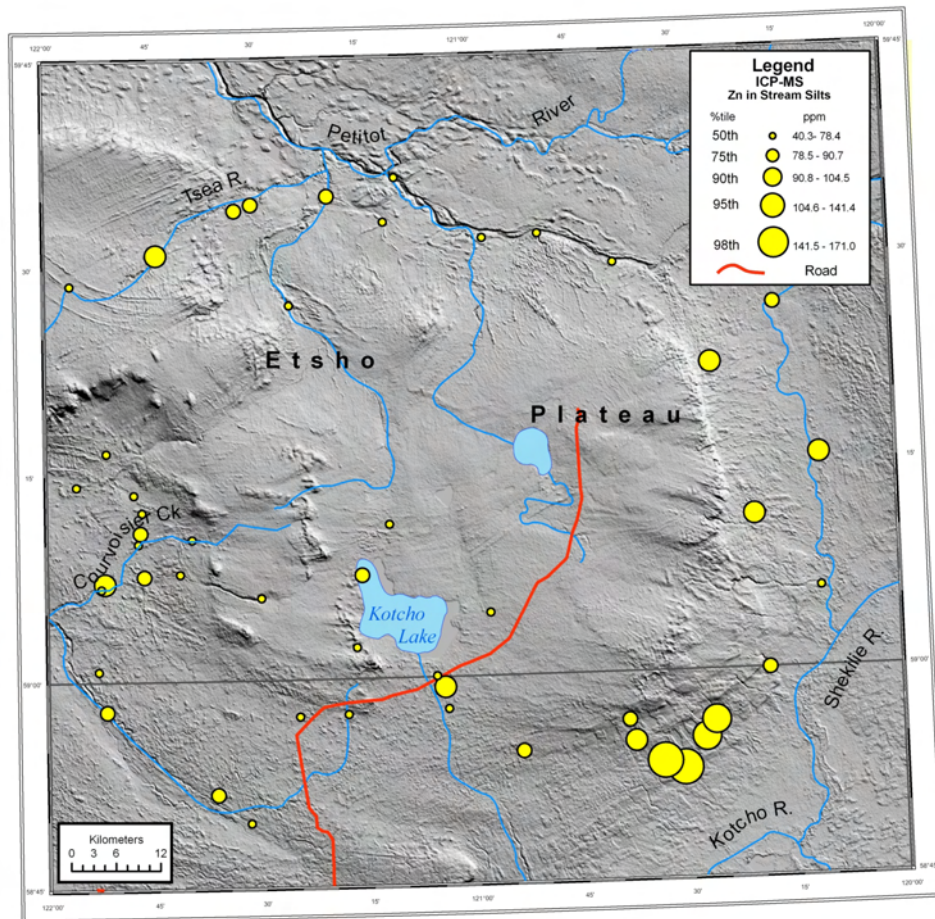


Figure 5a. Zinc concentrations in stream silts (<177 μm), determined by inductively coupled plasma mass spectrometry (ICP-MS) with aqua regia digestion, northeast BC.

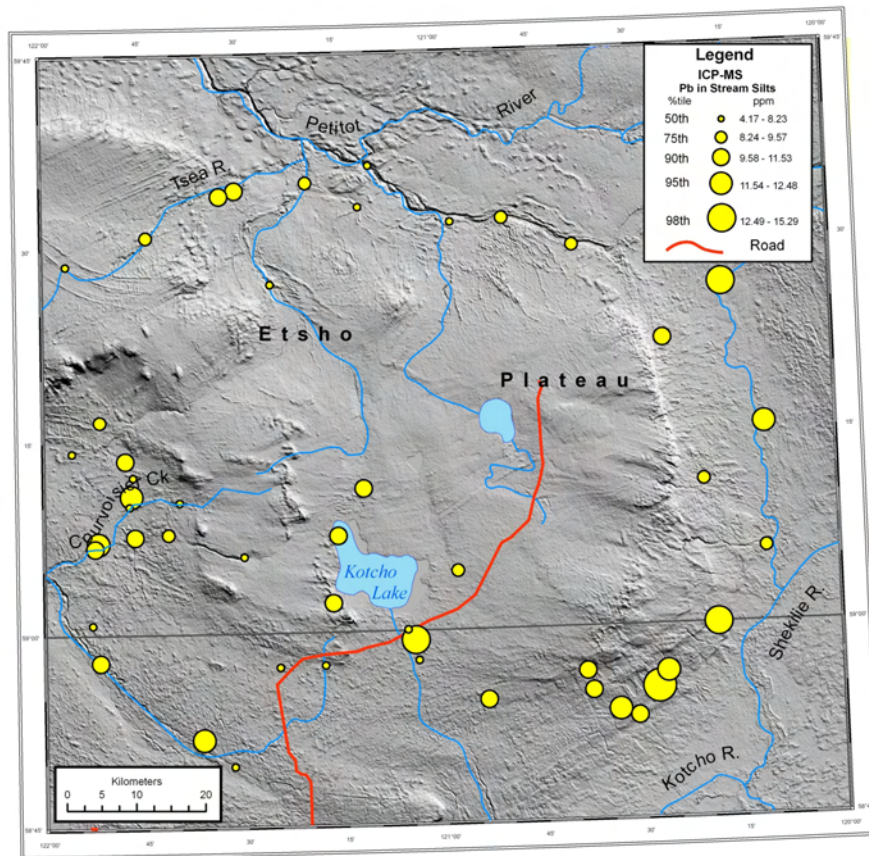


Figure 5b. Lead concentrations in stream silts (<177 μm), determined by inductively coupled plasma mass spectrometry (ICP-MS) with aqua regia digestion, northeast BC.

TABLE 5. COMPARISON OF MEAN AND MEDIAN VALUES OF SELECTED ELEMENTS IN THE <0.25 MM FRACTION OF HEAVY MINERAL CONCENTRATES FROM THE ETSHO PLATEAU, NORTHEAST BC AND BUFFALO HEAD HILLS, NORTH-CENTRAL ALBERTA (FRISKE *ET AL.*, 2003; MCCURDY *ET AL.*, 2006). ALL VALUES ARE PPM UNLESS OTHERWISE INDICATED.

Element (analysis)	Etsho Plateau (n=36)		Buffalo Head Hills (n=267)	
	Mean	Median	Mean	Median
Ag (ICP-MS)	176 ppb	103 ppb	271 ppb	76 ppb
As (INAA)	18.5	23.8	34.4	17
Ba (INAA)	14293	13750	21601	18250
Co (INAA)	38	38	36	35
Cu (ICP-MS)	19.25	14.83	16.8	9.73
Fe (INAA)	27.30%	27.30%	24.70%	25.00%
Hg (ICP-MS)	57 ppb	36 ppb	155 ppb	42 ppb
Mn (ICP-MS)	989	935	1389	1239
Mo (ICP-MS)	3.22	2.4	3.52	1.71
Ni (ICP-MS)	13.2	10.1	17.6	9.6
Pb (ICP-MS)	36.09	37.35	27.13	26.2
Sb (INAA)	1.9	1.8	1.8	1.2
U (INAA)	24.6	25.8	21	21
Zn (ICP-MS)	351.2	182.4	124.8	63.3

Abbreviations: ICP-MS, inductively coupled plasma mass spectrometry; INAA, instrumental neutron activation analysis

proximately seven times the median value of 182 ppm) on the upper reaches of the Tsea River (092P051016). Zinc values are also elevated south of Kotcho Lake. Both Ag and Pb (Fig 6b) exhibit similar patterns of distribution, suggesting the possibility of proximity to a number of different sedimentary-hosted mineralization types. In addition, sphalerite grains were identified visually and confirmed by scanning electron microscope in samples from the Tsea River drainage basin. Barium values are relatively high throughout the survey area.

CONCLUSIONS

KIM have been recovered from glacial (mostly glacio-fluvial sand and gravel) and stream sediments from the Etsho Plateau of northeast BC. The distribution of KIM in both sample media does not suggest a specific source region over the Etsho Plateau. Therefore, it is still unclear if the KIM are locally derived from concealed kimberlite(s) or represent material from the east and northeast that has been glacially transported long distances and reworked by fluvial processes.

The potential for Pb-Zn-Ag mineralization might be present in the Etsho Plateau region given the elevated concentration of these metals in the heavy mineral concentrates of stream sediments and the presence of sphalerite grains in two till samples from this region.

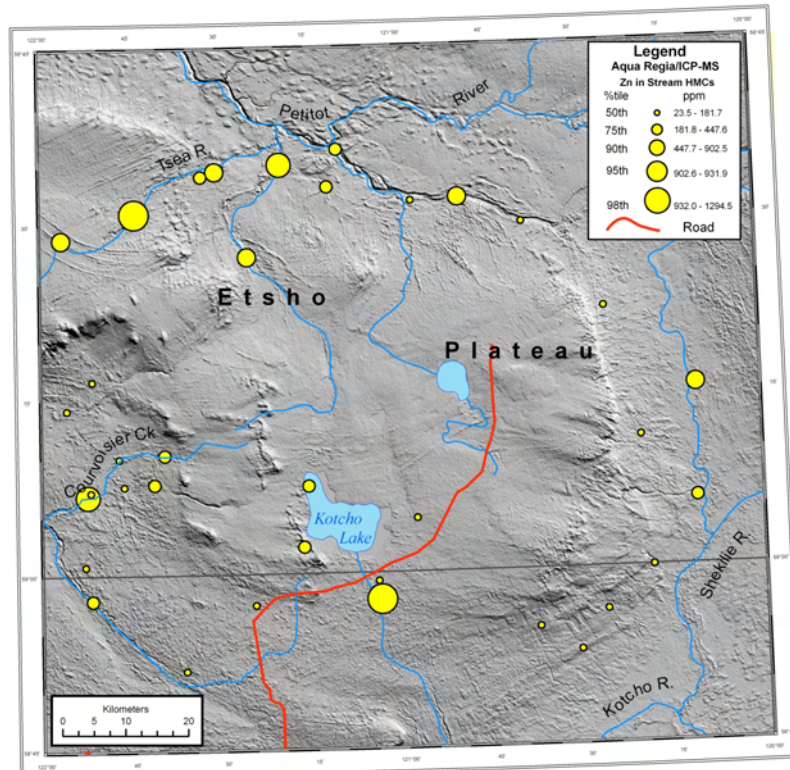


Figure 6a. Zinc (Zn) concentrations in the <0.25 mm fraction of heavy mineral concentrates (HMC), determined by inductively coupled plasma mass spectrometry (ICP-MS) with aqua regia digestion, northeast BC.

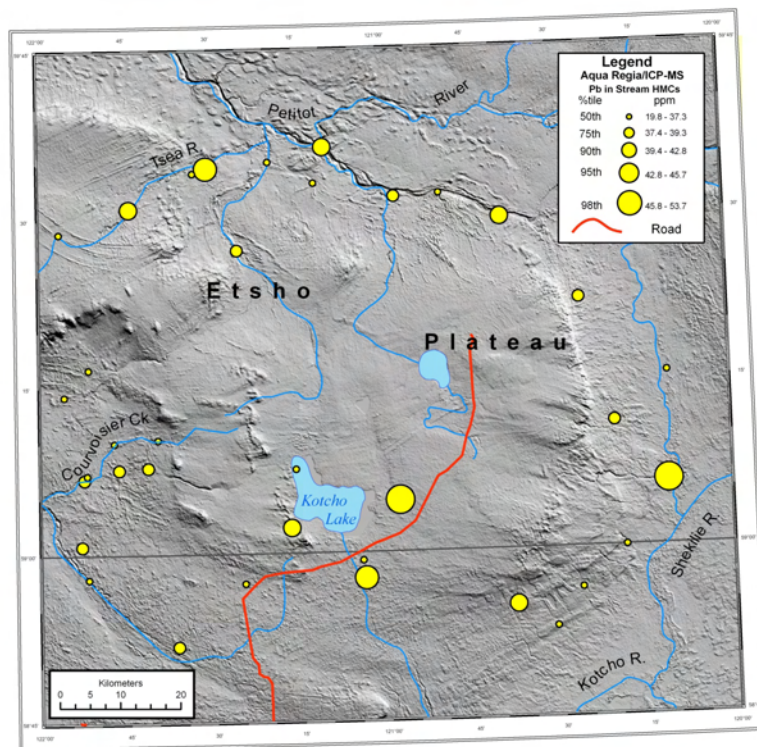


Figure 6b. Lead (Pb) concentrations in the <0.25 mm fraction of heavy mineral concentrates (HMC), determined by inductively coupled plasma mass spectrometry (ICP-MS) with aqua regia digestion, northeast BC.

ACKNOWLEDGMENTS

For the glacial sediment survey, Jamie Andrews from Land and Water British Columbia and Kirsten Brown provided field assistance. Highland Helicopters and Vancouver Island Helicopters provided charter helicopter services. Accommodation and services provided by Kleido Construction Camp 102 were greatly appreciated.

A helicopter for stream sediment and water collection was chartered from Canadian Helicopters based in Fort Nelson. Accommodation and services provided by Kleido Construction Camp 102 were greatly appreciated.

This report benefited considerably from the constructive review by M. Beth McClenaghan, Geological Survey of Canada.

REFERENCES

- BC Geological Survey (2006): MapPlace GIS internet mapping system; *BC Ministry of Energy, Mines and Petroleum Resources*, MapPlace website, URL <<http://www.MapPlace.ca>> [November 2006].
- Bednarski, J.M. (2005a): Surficial geology, Estsine Lake, British Columbia (NTS 94P/13); *Geological Survey of Canada*, Open File 4825, scale 1:50 000.
- Bednarski, J.M. (2005b): Surficial geology, Gote Creek, British Columbia (NTS 94P/12); *Geological Survey of Canada*, Open File 4846, scale 1:50 000.
- Dyke, A.S. (2004): An outline of North American deglaciation with emphasis on central and northern Canada; in *Quaternary Glaciations - Extent and Chronology, Part II*, Ehlers, J. and Gibbard, P.L., Editors, *Elsevier*, Amsterdam, pages 373–424.
- Dyke, A.S., Moore, A. and Robertson, L. (2003): Deglaciation of North America; *Geological Survey of Canada*, Open File 1574, CD-ROM.
- Ehlers, E.G. and Blatt, H. (1982): Petrology – Igneous, Sedimentary and Metamorphic; *W.H. Freeman and Company*, 732 pages.
- Fipke, C.E., Gurney, J.J. and Moore, R.O. (1995): Diamond exploration techniques emphasizing indicator mineral geochemistry and Canadian examples; *Geological Survey of Canada*, Bulletin 423, 86 pages.
- Friske, P.W.B., Prior, G.J., McNeil, R.J., McCurdy, M.W. and Day, S.J.A. (2003): National Geochemical Reconnaissance (NGR) stream sediment and water survey in the Buffalo Head Hills area (parts of NTS 84B, 84C, 84F and 84G) including analytical, mineralogical and kimberlite indicator mineral data from silts, heavy mineral concentrates and waters; *Alberta Energy and Utilities Board/Alberta Geological Survey*, Special Report 66 and *Geological Survey of Canada*, Open File 1790, 539 pages.
- Gehrels, G.E. and Ross, G.M. (1998): Detrital zircon geochronology of Neoproterozoic to Permian miogeoclinal strata in British Columbia and Alberta; *Canadian Journal of Earth Sciences*, Volume 35, pages 1380–1401.
- Grütter, H.S., Gurney, J.J., Menzies, A.H. and Winter, F. (2004): An updated classification scheme for mantle-derived garnet, for use by diamond explorers; *Lithos*, Volume 77, pages 841–857.
- Gurney, J.J. (1984): A correlation between garnets and diamonds in kimberlites; in *Kimberlite Occurrence and Origin: A Basis for Conceptual Models in Exploration*, *Geology Department and University Extension, University of Western Australia*, Publication Number 8, pages 143–166.
- Levson, V.M., Ferbey, T., Kerr, B., Johnsen, T., Bednarski, J.M., Smith, R., Blackwell, J. and Jonnes, S. (2004): Quaternary geology and aggregate mapping in northeast BC: applications for oil and gas exploration and development; in *Summary of Activities 2004, BC Ministry of Energy, Mines and Petroleum Resources*, URL <<http://www.em.gov.bc.ca/subwebs/oilandgas/pub/reports.htm>>, page 12 [November 2006].
- Mathews, W.H. (1980): Retreat of the last ice sheets in northeastern British Columbia and adjacent Alberta; *Geological Survey of Canada*, Bulletin 331, 22 pages.
- McCurdy, M.W., Prior, G.J., Friske, P.W.B., McNeil, R.J., Day, S.J.A., Nicholl, T.J. (2006): Geochemical, mineralogical and kimberlite indicator mineral electron microprobe data from silts, heavy mineral concentrates and waters from a National Geochemical Reconnaissance stream sediment and water survey in the northern and southwestern Buffalo Head Hills, northern Alberta (parts of 84B, 84C, 84F and 84G); *Alberta Energy and Utilities Board/Alberta Geological Survey*, Special Report 76 and *Geological Survey of Canada*, Open File 5057.
- Nimis, P. (1988): Evaluation of diamond potential from the composition of peridotitic chromian diopside; *European Journal of Mineralogy*, Volume 10, pages 505–519.
- Plant, J.A. and Raiswell, R.W. (1994): Modifications to the geochemical signatures of ore deposits and their associated rocks in different surface environments; in *Drainage Geochemistry*, Hale, M. and Plant, J.A., Editors, *Handbook of Exploration Geochemistry*, Volume 6, Elsevier Science B.V., pages 73–109.
- Plouffe, A., Paulen, R.C. and Smith, I.R. (2006a): Indicator mineral content and geochemistry of glacial sediments from northwest Alberta (NTS 84L, M): new opportunities for mineral exploration; *Geological Survey of Canada*, Open File 5121 and *Alberta Energy and Utilities Board*, Special Report 77, CD-ROM.
- Plouffe, A., Smith, I.R., McCurdy, M.W., Friske, P.W.B., Ferbey, T., Bednarski, J., Levson, V. M., Demchuk, T.E., Trommelen, M.S., Day, S. and Hickin, A.S. (2006b): Glacial and stream sediments sampling in support of kimberlite exploration in northeastern British Columbia; in *Geological Fieldwork 2005, BC Ministry of Energy, Mines and Petroleum Resources*, Paper 2006-1 and *Geoscience BC*, Report 2006-1, pages 337–342.
- Simandl, G.J. (2005): Diamond potential - new advances in British Columbia; *British Columbia and Yukon Chamber of Mines*, Mineral Exploration Roundup 2005, Vancouver, BC, Abstract Volume, page 10.
- Smith, I.R. (in press a): Surficial geology, Gunnell Creek, British Columbia (NTS 94I/13); *Geological Survey of Canada*, Open File 5305 and *BC Ministry of Energy, Mines and Petroleum Resources*, Surficial Geology Map 2006-3, scale 1:50 000.
- Smith, I.R. (in press b): Surficial geology, Kyklo Creek, British Columbia (NTS 94I/11); *Geological Survey of Canada*, Open File 5307 and *BC Ministry of Energy, Mines and Petroleum Resources*, Surficial Geology Map 2006-1, scale 1:50 000.
- Smith, I.R. (in press c): Surficial geology, Lichen Creek, British Columbia (NTS 94I/14); *Geological Survey of Canada*, Open File 5309 and *BC Ministry of Energy, Mines and Petroleum Resources*, Surficial Geology Map 2006-4, scale 1:50 000.
- Smith, I.R. (in press d): Surficial geology, Nogah Creek, British Columbia (NTS 94I/12); *Geological Survey of Canada*, Open File 5306 and *BC Ministry of Energy, Mines and Petroleum Resources*, Surficial Geology Map 2006-2, scale 1:50 000.

Aeromagnetic Survey over the Jennings River Map Area (NTS 1040), Northern British Columbia¹

by W.F. Miles², R. Dumont² and C. Lowe³

KEYWORDS: geophysics, aeromagnetic, magnetic anomaly, Jennings River, volcanogenic massive sulphide, porphyry, skarn

INTRODUCTION

A high-resolution aeromagnetic survey has been completed over the 1:250 000 Jennings River map area (Fig 1; NTS 1040), northern British Columbia, has been completed. Funding for the survey was provided by Geoscience BC and project management was undertaken by the Geological Survey of Canada (GSC). The survey was flown under contract by Goldak Airborne Surveys, Saskatoon. The survey provides aeromagnetic coverage where none previously existed. The aim of the project is to spark new private sector investment in resource exploration. This objective falls within the mandate of Geoscience BC, as well as the scope of the Northern Resource Development Program of Natural Resources Canada's Earth Science Sector.

PURPOSE AND SCOPE

The Jennings River map area in northern BC is considered prospective for a number of mineral deposit types, including carbonate-hosted Ag-Pb-Zn deposits, porphyry deposits (Mo and W) and skarn deposits (Cu and Mo). In addition, the possibility of volcanogenic massive sulphide occurrences is indicated by belts containing felsic rock contemporaneous with such deposits in the neighbouring Yukon. Despite these positive factors, exploration in the region has been limited. This can be attributed, in part, to the extensive Quaternary cover, the lack of public domain geophysical data and the status of geological mapping. Although regional bedrock maps were produced for the northern half of the map area in the past decade or so (Mihalynuk *et al.*, 2000, 2001; Nelson and Bradford, 1993; Nelson *et al.*, 2000, 2001), mapping in the southern half of the map area dates from the 1960s and is reconnaissance in scale (Gabrielse, 1969).

Aeromagnetic surveys provide a rapid, cost-effective means of preliminary geological evaluation of large tracts of bedrock and are basic resource exploration infrastruc-

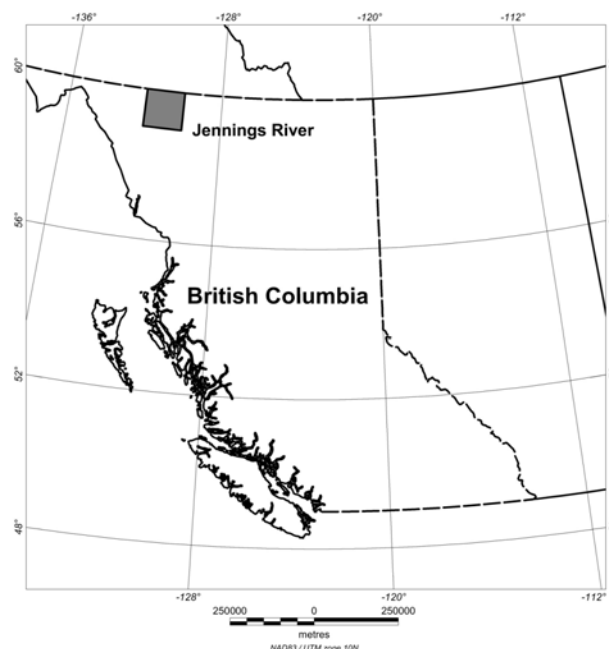


Figure 1. Location of the Jennings River map area in northern BC.

ture. The data acquired by these surveys provide information on lithology and the extent of regional rock units, help delineate fault and diking patterns and allow for the estimation of source depths. In regions of poor exposure, aeromagnetic data would be valuable for extrapolating mapped geology beneath areas of cover. Therefore, it is expected that the new data acquired in the Jennings River area will significantly advance the understanding of the geological and mineral resource potential of the area.

METHOD

A Request for Proposals was generated by the Geological Survey of Canada for completion of the aeromagnetic survey. The contract was awarded to Goldak Airborne Surveys of Saskatoon. Surveying began on May 15, 2006 and concluded on June 22, 2006. Two Piper PA-31 NavajoTM aircraft performed the survey, which consisted of 33 752 line km, covering all of NTS 1040. The traverse flight-line spacing was 500 m with an N45°E orientation. The control-line spacing was 2000 m with an orientation of N135°E. The survey altitude was a nominal mean terrain clearance of 150 m on a predetermined smooth draped surface. Magnetometer calibration was performed at the Meanook, Alberta test site. The magnetic data were recorded at 10 Hz using a split-beam line cesium vapour mag-

¹Geoscience BC contribution GBC026

²Geological Survey of Canada, Ottawa, ON

³Geological Survey of Canada, Sidney, BC

This publication is also available, free of charge, as colour digital files in Adobe Acrobat[®] PDF format from the BC Ministry of Energy, Mines and Petroleum Resources website at http://www.em.gov.bc.ca/Mining/Geosurv/Publications/catalog/cat_fldwk.htm

netometer with a sensitivity of 0.01 nT, mounted on board the aircraft. The maximum tolerance for diurnal variation was 3.0 nT per minute. Flight-path information was recovered using a post-flight differential Global Positioning System.

The Regional Geophysics Section of GSC Central Canada Division performed project management, including quality assurance and quality control, for the survey. The scientific authority for the survey performed an inspection of the contractor's site as the survey began. Quality control was performed on the data as they were acquired. The data were tie-line levelled and determined to be acceptable for archiving in the Canadian Aeromagnetic Database. The processing of the data is now underway with a target completion date of December 2007, at which time the data will be available for public release.

RESULTS

Project plans call for the joint publication of sixteen 1:50 000 total field magnetic anomaly and vertical derivative maps (GSC Open Files 5351-5382 and Geoscience BC Maps 2006-3-1 to 2006-3-16 and 2006-4-1 to 2006-4-16) in late January 2007. Vertical derivative images enhance short wavelength components (shallow sources) in a dataset at the expense of longer wavelength components (deep sources) and can provide important insights into the near-surface geology.

Additionally, the digital profile and gridded data will be made available online and at no cost via the Geoscience Data Repository for Aeromagnetic Data (http://gdr.nrcan.gc.ca/aeromag/index_e.php). Bitmap images and PDFs of the maps will be available online and at no cost via the Geoscience Data Repository's MIRAGE application (http://gdr.nrcan.gc.ca/mirage/index_e.php). Bitmap images and gridded datasets will also be available on the BC Ministry of Energy, Mines and Petroleum Resources' MapPlace (<http://www.em.gov.bc.ca/mining/Geolsurv/MapPlace/>).

An interpretation of the aeromagnetic data by the Geological Survey of Canada will be undertaken and the findings will be published in Spring 2007.

REFERENCES

- Dumont, R., Potvin, J. and Kiss, F. (2007): Residual total magnetic field, Jennings River Aeromagnetic Survey (NTS 104O/1-16), British Columbia; *Geological Survey of Canada*, Open File 5351-5366 and Geoscience BC Map 2006-3-1-16, scale 1:50 000.
- Dumont, R., Potvin, J. and Kiss, F. (2007): First vertical derivative of the magnetic field, Jennings River Aeromagnetic Survey (NTS 104O/1-16), British Columbia; *Geological Survey of Canada*, Open File 5367-5382 and Geoscience BC Map 2006-4-1-16, scale 1:50 000.
- Gabrielse, H. (1969): Geology of Jennings River map area, British Columbia (104 O); *Geological Survey of Canada*, Paper 68-55, 37 pages.
- Mihalynuk, M.G., Nelson, J.L., Gleeson, T., Roots, C. and de Keijzer, M. (2000): Geology of Smart River area 104O/13 (1:50 000 scale); *BC Ministry of Energy, Mines and Petroleum Resources*, Open File 2000-6.
- Mihalynuk, M.G., Harms, T.A., Roots, C.F., Nelson, J.L., de Keijzer, M., Friedman, R.M. and Gleeson, T.P. (2001): Geology, Teh Creek map area, 104 O/12, British Columbia; *BC Ministry of Energy, Mines and Petroleum Resources*, Open File 2001-17.
- Nelson, J.L. and Bradford, J.A. (1993): Geology of the Midway-Cassiar area, northern British Columbia (104O, P); *BC Ministry of Energy, Mines and Petroleum Resources*, Bulletin 83, 94 pages.
- Nelson, J., Harms, T.A., Zantvoort, W., Gleeson, T. and Wahl, K. (2000): Geology of the southeastern Dorsey Terrane, 104O/7, 8, 9, 10; *BC Ministry of Energy, Mines and Petroleum Resources*, Open File 2000-4.
- Nelson, J.L., Harms, T.A., Roots, C.F., Friedman, R. and de Keijzer, M. (2001): Geology of north-central Jennings River map area, 104O/14E, 15; *BC Ministry of Energy, Mines and Petroleum Resources*, Open File 2001-6.

Airborne Gamma-Ray Spectrometric and Magnetic Surveys over the Bonaparte Lake Area (NTS 092P), South-Central British Columbia¹

by W.F. Miles², R.B.K. Shives², J. Carson², J. Buckle², R. Dumont² and M. Coyle²

KEYWORDS: geophysics, spectrometric, radiometric, aeromagnetic, magnetic, copper porphyry, skarn

INTRODUCTION

Airborne gamma-ray spectrometric and magnetic geophysical surveying is underway over the Bonaparte Lake area, British Columbia, in the eastern half of NTS 092P (Fig 1). The survey is funded by Geoscience BC, Natural Resources Canada's Targeted Geoscience Initiative (TGI3), Candorado Operating Company Ltd., G W R Resources Inc. and Amarc Resources Ltd. Surveying consists of a fixed-wing component over the flatter western portion and a helicopter-borne component over the more rugged eastern portion (Fig 1) of the survey area. The aim of the project is to encourage new private sector investment in resource exploration, to aid in the assessment and development of targets for mineral exploration and to support future bedrock and surficial geological mapping. These objectives fall within the mandate of Geoscience BC, as well as the scope of the TGI3 Program.

PURPOSE AND SCOPE

The Bonaparte Lake area in south-central BC (Fig 1) is prospective for a number of mineral deposit types, particularly copper porphyry. However, an extensive Quaternary cover, Tertiary volcanic cover and a lack of public domain geophysical data have resulted in limited exploration in the region.

Airborne gamma-ray spectrometry provides a physical measurement that contributes to geochemical mapping of the top 30 cm of the earth's surface. The technique provides bedrock and overburden mapping assistance by fingerprinting the radioactive element signatures inherent in all rocks and soils. Where the normal signatures are disrupted by mineralizing processes, anomalies provide direct exploration vectors.

Aeromagnetic surveys provide structural and lithological information from rocks located at surface down to considerable depths. In the area of the proposed surveys, the technique allows the determination of mag-



Figure 1. Location of the Bonaparte Lake area, south-central BC.

netic source depths, key to understanding lithology and mineral potential under the extensive cover sequences.

When these two techniques are integrated into a single-pass airborne survey, they provide complementary information that serves as a long-standing geophysical-geochemical framework, supporting new geological and practical mineral exploration models for a wide variety of commodities. For example, similar surveys recently conducted in areas adjacent to the proposed surveys have improved geological understanding and exploration for porphyry Cu-Au, skarn and other deposit types.

METHOD

Requests for Proposals were generated by the Geological Survey of Canada (GSC) on behalf of the survey partners for completion of the surveys. The contracts were awarded to Sander Geophysics Limited of Ottawa (fixed-wing) and Fugro Airborne Surveys of Toronto (helicopter). Surveying began on September 15, 2006.

The fixed-wing survey (Fig 2) was flown with a Britten-Norman Islander™ (C-GSGX) and consists of 13 968 line km covering the survey area. The traverse flight-line spacing was 400 m, except in the Rayfield and Amarc blocks (Fig 2, areas B and C of the fixed-wing area)

¹ Geoscience BC contribution GBC027

² Geological Survey of Canada, Ottawa, ON

This publication is also available, free of charge, as colour digital files in Adobe Acrobat® PDF format from the BC Ministry of Energy, Mines and Petroleum Resources website at http://www.em.gov.bc.ca/Mining/GeolSurv/Publications/catalog/cat_fldwk.htm

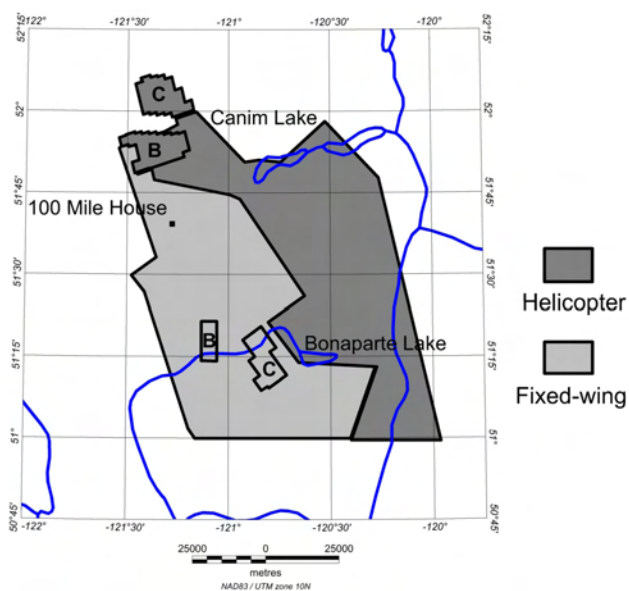


Figure 2. Bonaparte Lake survey boundaries.

where the line spacing was 200 m. All traverse lines have a N55°E orientation. The control line spacing was 2400 m, oriented perpendicular to the traverse lines. The survey altitude was a nominal mean terrain clearance of 125 m on a predetermined smooth draped surface. Gamma-ray spectrometric data were recorded at 1.0 second intervals using a 256-channel Exploranium™ GR820 spectrometry system with 50.4 L of downward-looking crystals and 8.4 L of upward-looking sodium iodide detectors. The magnetic data were recorded at 10 Hz using a Scintrex™ split-beam line cesium vapour magnetometer, with a sensitivity of 0.01 nT, mounted in a stinger attached to the aircraft. Magnetometer calibration was performed at the GSC Calibration Range in Bourget, Ontario. The maximum tolerance for diurnal variation was 2.0 nT per minute. Flight-path information was recovered using post-flight differential Global Positioning System. Surveying was not completed at the time of writing.

The helicopter-borne survey (Fig 2) was flown with a Eurocopter™ AS350B2 helicopter and consists of 14 780 line km. The traverse line spacing was 420 m, except in the Rail block (Fig 2, area B of the helicopter area) where the line spacing was 210 m and in the Murphy block (Fig 2,

area C of the helicopter area) where the line spacing was 250 m. The traverse line orientation was N70°E with control line oriented N165°E. The survey altitude was a nominal mean terrain clearance of 125 m. The magnetometer system was mounted in a stinger attached to the helicopter skids. The spectrometric system had smaller detector volumes than the fixed-wing system with 33.6 L of downward-looking crystals and 4.2 L of upward-looking crystals. Magnetometer calibration was performed at the GSC Calibration Range in Meanook, Alberta. The maximum tolerance for diurnal variation was 2.0 nT per minute. Flight-path information was recovered using a post-flight differential Global Positioning System. Surveying was not completed at the time of writing.

The Regional Geophysics Section and the Radiation Geophysics Section of GSC Central Canada Division performed project management, including quality assurance and quality control, for the survey. The scientific authorities for the surveys performed inspections of the contractors on-site as the survey began. Quality control was performed as the data were acquired. The magnetic data will be tie-line levelled and, once accepted by the scientific authority, will be archived in the Canadian Aeromagnetic Database. The spectrometric data will be processed and compiled by the contractors to the standards of the National Gamma-Ray Spectrometry Program (NATGAM). Measured and computed data include two magnetic parameters (residual total magnetic field and the first vertical derivative of the magnetic field) and eight spectrometric parameters (ternary, total count, K, eU, eTh, and ratios eU/eTh, eU/K, and eTh/K).

RESULTS

The data will be published jointly as GSC Open Files and Geoscience BC Maps by April 1, 2007. The digital profile and gridded data will be made available online and at no cost via the Geoscience Data Repository for Aeromagnetic Data (http://gdr.nrcan.gc.ca/aeromag/index_e.php) and the Geoscience Data Repository for Radioactivity Data (http://gdr.nrcan.gc.ca/gamma/index_e.php). Bitmap images and PDFs of the maps will be available online and at no cost via the Geoscience Data Repository's MIRAGE application (http://gdr.nrcan.gc.ca/mirage/index_e.php). Bitmap images and gridded datasets will also be available on the Government of British Columbia's MapPlace (<http://www.em.gov.bc.ca/mining/Geolsurv/MapPlace/>).

Stratigraphic Analysis of Cretaceous Strata Flanking the Southern Nechako Basin (Parts of NTS 092M, O; 093B), British Columbia: Constraining Basin Architecture and Reservoir Potential¹

by P.S. Mustard² and J.B. Mahoney³

KEYWORDS: sedimentology, stratigraphy, provenance, Jackass Mountain Group, Nechako, Methow, Cretaceous

INTRODUCTION

The Nechako Basin (Fig 1) is part of the Interior Plateau physiographic region of British Columbia and has been variously defined in terms of extent and age (Ferri and Riddell, 2006). Accurate assessment of the petroleum potential of the Nechako Basin hinges on a comprehensive understanding of the basin architecture developed within Cretaceous strata, which represent the most prospective targets in the subsurface. Modelling the subsurface distribution of these Cretaceous strata requires detailed stratigraphic analysis of coeval, laterally adjacent strata exposed along the basin margins. The age and general lithological character of strata in the subsurface of the Nechako Basin are broadly known from industry drillholes and examination of isolated outcrops of Cretaceous strata exposed beneath extensive Neogene volcanic cover (reviewed in Ferri and Riddell [2006], also see Fig 1 for the location of many of these drillholes). However, regional facies patterns and basin architecture are poorly understood, and even the stratigraphic affinities of subsurface strata are unclear. For example, Hunt (1992) identifies some subsurface strata as possible Jackass Mountain Group, a generally marine succession which is exposed along the southern margins of the Nechako Basin, whereas Hannigan *et al.* (1994) assigns these rocks to the Skeena 'Assemblage' (more commonly termed the Skeena Group), a generally nonmarine succession which is exposed along the northern margins of the Nechako Basin. This confusion illustrates the poorly known nature of the subsurface strata in this region. For a more thorough discussion of stratigraphic problems, see Ferri and Riddell (2006).

At the southern end of the Nechako Basin, Lower Cretaceous Jackass Mountain Group (JMG) strata are unconformably overlain by Neogene volcanic rocks (Fig 2). They are generally classified as part of the Methow Basin but are

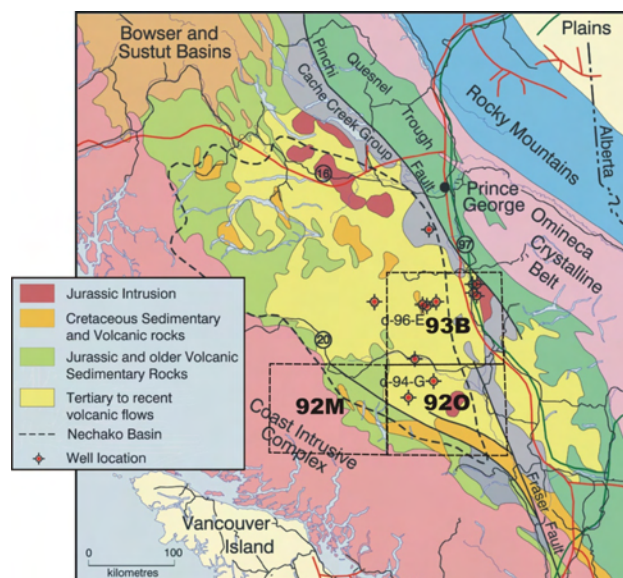


Figure 1. Regional geological location map with boundaries of relevant 1:250 000 map areas, BC (modified from BC Ministry of Energy, Mines and Petroleum Resources, 2002).

clearly the surface expressions of strata that continue northward into the subsurface beneath the Tertiary rocks, which form most of the exposed strata of the Nechako Basin (Hickson *et al.*, 1994; J.B. Mahoney *et al.*, in progress). The JMG and associated strata include thick (thousands of metres), laterally extensive (tens of kilometres) marine sandstone successions that overlie and interfinger with marine mudstone. However, the three-dimensional architecture of the stratigraphy is very poorly constrained, and therefore the subsurface facies distribution is unknown. Previous studies have interpreted them as the deposits of large submarine fan deposystems (*e.g.*, Kleinspehn, 1982, 1985). However, these previous studies were primarily first order stratigraphic assessments, commonly associated with government regional mapping projects, and preceded a large number of studies that, over the last 15 years, have greatly enhanced the understanding of submarine fan sedimentation models (*e.g.*, Bouma, 2000).

THIS STUDY

The intent of the three-year study is to conduct a regional analysis of lateral and vertical variations in Early Cretaceous stratigraphic character along the southern margin of the Nechako Basin, which will be integrated with

¹Geoscience BC contribution GBC037

²Department of Earth Sciences, Simon Fraser University, Burnaby, BC

³Department of Geology, University of Wisconsin, Eau Claire, Wisconsin

This publication is also available, free of charge, as colour digital files in Adobe Acrobat® PDF format from the BC Ministry of Energy, Mines and Petroleum Resources website at http://www.em.gov.bc.ca/Mining/GeolSurv/Publications/catalog/cat_fldwk.htm

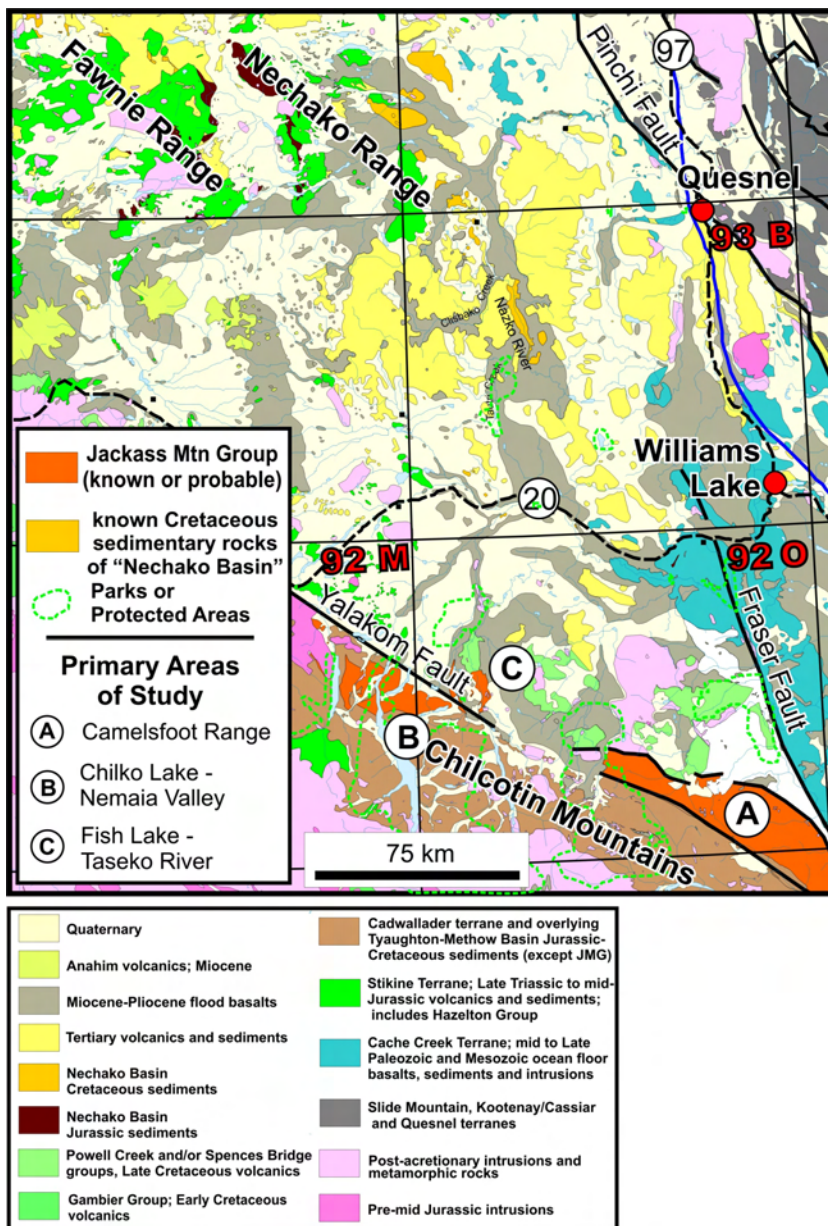


Figure 2. Regional geological framework and location of major areas of study, BC (modified from Ferri and Riddell, 2006; Riddell, 2006).

analysis of the isolated exposures within the basin to provide constraints on temporal and spatial variations in the subsurface. This study builds on earlier studies, but with more detailed sedimentology and stratigraphic analysis, petrological analysis (with porosity/permeability estimates), provenance studies (detrital mica and zircon, Nd analysis of fine-grained units, geochemistry of conglomerate clasts), biostratigraphic studies and hydrocarbon reservoir rock potential. The emphasis on the Jackass Mountain Group reflects the authors' contention that this is probably the best candidate for a major reservoir system in the subsurface of the Nechako Basin. This study suggests that the JMG are the closest surface analogue and most likely directly correlative to the Skeena 'Assemblage' of the subsurface, which is interpreted by Hannigan *et al.* (1994)

to contain "the most significant petroleum plays in this assessment".

Field reconnaissance examination in late August 2006 identified the main focus areas for detailed analysis of Lower Cretaceous sedimentary successions in the southern part of the Nechako Basin and along its southern margins. Two MSc students will conduct thesis research as part of this project. One MSc investigation will include detailed examinations of well exposed sections of the JMG in the Camelsfoot Range (Fig 2, locality A). The JMG is well exposed on several ridges in this area (Fig 3) and volumetrically the most significant unit in the central and eastern Camelsfoot Range (Hickson *et al.*, 1994; Schiarizza *et al.*, 1997; J.B. Mahoney *et al.*, in progress). It forms the central part of an approximately 150 km long, southward-tapering wedge of mainly medium to coarse-grained sandstone and polymictic conglomerate exposed between the Yalakom and Fraser fault systems. It is part of a broad, asymmetric synclinorium; the base of the unit is exposed in steeply dipping beds on the western limb, east of the Yalakom River, and the upper part is exposed in moderately west-dipping beds in the eastern limb. Multiple stratigraphic sections will be measured with detailed examination of the facies associations and architecture on the ridges between section locations. Extensive sampling of rock types keyed to stratigraphic position will facilitate detailed petrological, organic maturation, and porosity/permeability analyses (done mostly in conjunction with ongoing regional studies of these parameters by F. Ferri of the BC Geological Survey as outlined in Ferri and Riddell [2006]). Traditional sedimentological measurements (paleocurrents, facies types and descriptions, conglomerate clast compositions, stratigraphic thickness variations and cyclicity and other sedimentological parameters) will be supplemented with

sampling for isotopic provenance studies. It is hoped that new fossil localities will add to biostratigraphic information available for these units.

A second MSc student will conduct a similar detailed stratigraphic study of JMG and related strata in the Chilko Lake - Nemaia Valley area (Fig 2, locality B). JMG and other Jurassic and Cretaceous sedimentary successions are well exposed in this area, especially on Nemaia Mountain and surrounding ridges (Fig 4; Schiarizza *et al.*, 2002). These strata occur immediately southwest of the Yalakom fault and traditionally are considered part of the Tyaughton Basin, which Garver (1992) described as a sub-basin separate from the Methow Basin, with different sedimentation patterns and source areas. However, restoration of the approximately 115 km of dextral offset on the Yalakom fault restores the JMG of the Camelsfoot Range directly adjacent

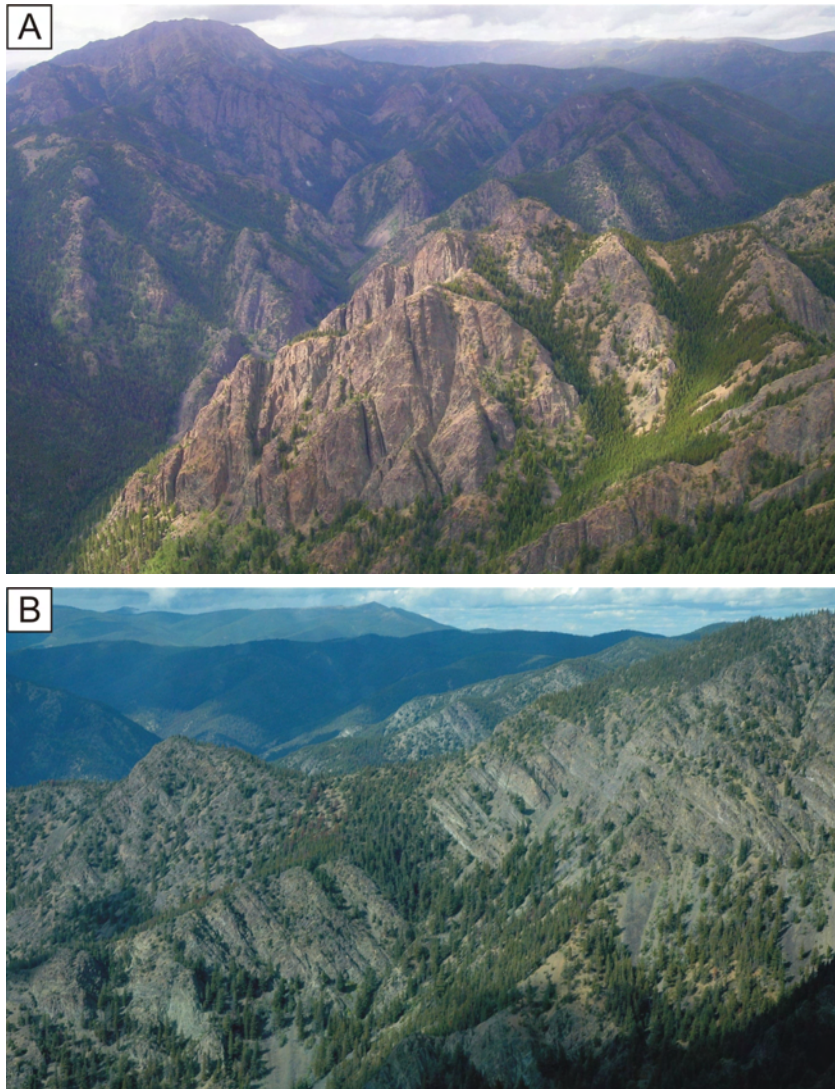


Figure 3. Exposures of Jackass Mountain Group in the Camelsfoot Range, BC: A) looking northwest toward Yalakom Mountain (upper left of photo), showing several kilometre thick successions dominated by thick-bedded sandstone turbidites, B) looking east from Yalakom Mountain area at eastern Camelsfoot Range ridges showing extensive sandstone and mudstone submarine fan facies associations of the steeply south-dipping Jackass Mountain Group (JMG) strata.

to the Chilko Lake – Nemaia Valley exposures, suggesting original depositional continuity. Detailed stratigraphy and provenance analysis of Cretaceous strata in both areas will document lateral and vertical depositional patterns and source regions, which will permit evaluation of the sub-basin hypothesis of Garver (1991) and provide new and more detailed information to constrain the nature of the JMG along the southern margin of the Nechako Basin.

In addition to the detailed MSc project studies, the authors have begun a regional study of these Cretaceous strata. Examination of Lower Cretaceous strata in well exposed areas (potentially all identified areas of Cretaceous strata on Fig 2) will permit regional evaluation of lateral variations in the stratigraphic successions. Paleocurrent and provenance data will be collected, including systematic sampling for isotope geochemistry, conglomerate clast geochemistry, and sandstone petrology. Detailed stratigraphic sections will be integrated with sections provided by the MSc projects to provide a regional stratigraphic framework. For example, locality C (Fig 2) is the site of several different areas of known lower Cretaceous sedimentary rock exposures. Regional mapping projects have included descriptions of these exposures, the most detailed descriptions were by Schiarizza and Riddell (1997), who refer to these strata by various locality names (Chaunigan Lake, Vick Lake, Fish Lake, Elkin Creek). Much of these strata have been tentatively correlated with either Relay Mountain Group or JMG strata, both by Schiarizza and Riddell (1997) and Schiarizza *et al.* (2002) and on the new Geological Survey of Canada geology map for map area

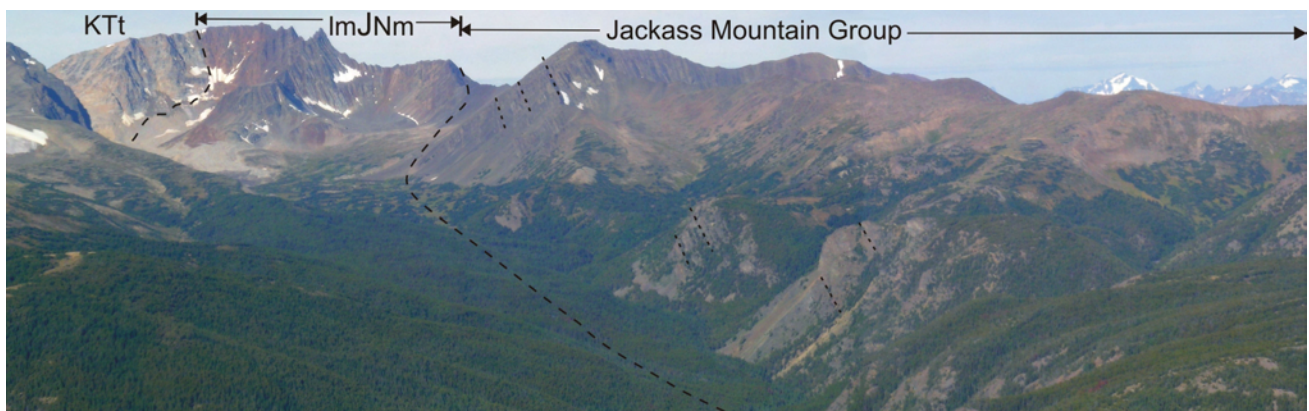


Figure 4. Looking west at Nemaia Range ridges, showing extensive steeply northeast-dipping Jackass Mountain Group (JMG) strata, unconformably overlying Jurassic strata informally named Nemaia formation by Schiarizza (2002, labelled ImJNm on photo). KTt is an unnamed and undated pluton, probably Cretaceous or Tertiary (Schiarizza, 2002). Dashed lines within JMG indicate the general dip of strata, with tops to the northeast.

092O (J.B. Mahoney *et al.*, in progress). As part of this project, these areas will be re-examined and evaluated for their relationship to other Cretaceous units and their role in overall basin development.

SUMMARY

Detailed lateral and vertical stratigraphic studies will provide a basis for assessment of the stratigraphy, sedimentology, provenance and potential reservoir suitability of the Jackass Mountain Group and associated Cretaceous strata of the southern Nechako Basin. These focused studies, combined with regional examinations of Cretaceous strata in this area, will allow the development of a model of basin evolution during the Early Cretaceous in terms of large-scale depositional systems and patterns of sedimentation, which in turn will allow prediction of the types of sedimentation and thus stratigraphy that should occur in subsurface areas of the southern Nechako Basin. Ultimately this new data will permit evaluation of previous models of the Nechako and related Methow, Tyaughton (and possibly Skeena) basins during the Cretaceous, both in terms of temporal variations in tectonic controls on basin evolution and evidence for the importance and extent, if any, of separate sub-basins. An understanding of these critical stratigraphic relationships and a more detailed understanding of the sedimentology and basin deposystems during the Early Cretaceous are fundamental to the success of hydrocarbon exploration in the Nechako Basin.

ACKNOWLEDGMENTS

Fil Ferri and Janet Riddell are thanked for constructive reviews and for permission to use figures from previous publications in this article. Rob Stevens is thanked for final review of the manuscript. Discussions both in the field and office with Fil Ferri and Janet Riddell have been essential to defining the scope and nature of this study. Funding is provided primarily from Geoscience BC Grant 2006-014, with additional financial support from Simon Fraser University to P. Mustard and the University of Wisconsin, Eau Claire, to B. Mahoney.

REFERENCES

- BC Ministry of Energy, Mines and Petroleum Resources (2002): Nechako Basin: oil and gas opportunities in central British Columbia; *BC Ministry of Energy, Mines and Petroleum Resources*, information brochure.
- Bouma, A.H. (2000): Fine-grained, mud-rich turbidite systems: model and comparisons with coarse-grained, sand-rich

systems; in *Fine-Grained Turbidite Systems*, Bouma, A.H. and Stone, C.G., Editors, *American Association of Petroleum Geologists, Memoir 72 / Society for Sedimentary Geology (SEPM)*, Special Publication 68, pages 9–68.

- Ferri, F. and Riddell, J. (2006): The Nechako Basin project: new insights from the southern Nechako Basin; in *Summary of Activities 2006, BC Ministry of Energy, Mines and Petroleum Resources*, URL <<http://www.em.gov.bc.ca/subwebs/oilandgas/pub/reports.htm>>, pages 89–124.
- Garver, J.I. (1992): Provenance of Albian-Cenomanian rocks of the Methow and Tyaughton basins, southern British Columbia: a mid-Cretaceous link between North America and the Insular terranes; *Canadian Journal of Earth Sciences*, Volume 29, pages 1274–1295.
- Hannigan, P., Lee, P.J., Osadetz, K.J., Dietrich, J.R. and Olsen-Heise, K. (1994): Oil and gas resource potential of the Nechako-Chilcotin area of British Columbia; *Geological Survey of Canada*, Geofile 2001-6, 167 pages, 5 maps.
- Hickson, C.J., Mahoney, J.B. and Read, P. (1994): Geology of Big Bar map area: facies distribution in the Jackass Mountain Group; in *Current Research, Part A, Geological Survey of Canada*, Paper 94-1A, pages 143–150.
- Hunt, J.A. (1992): Stratigraphy, maturation, and source rock potential of Cretaceous strata in the Chilcotin-Nechako region of British Columbia; unpublished MSc thesis, *University of British Columbia*, 447 pages.
- Kleinspehn, K.L. (1982): Cretaceous sedimentation and tectonics, Tyaughton-Methow Basin, southwestern British Columbia; unpublished PhD thesis, *Princeton University*, 184 pages.
- Kleinspehn, K.L. (1985): Cretaceous sedimentation and tectonics, Tyaughton-Methow Basin, southwest British Columbia; *Canadian Journal of Earth Sciences*, Volume 22, pages 154–174.
- Riddell, J.M., Compiler (2006): Geology of the southern Nechako Basin, NTS 92N, 92O, 93B, 93C, 93F, 93G; *BC Ministry of Energy, Mines and Petroleum Resources*, Petroleum Geology Map 2006-1.
- Schiarizza, P., Gaba, R.G., Glover, J.K., Garver, J.I. and Umhoefer, P.J. (1997): Geology and mineral occurrences of the Taseko-Bridge River area; *BC Ministry of Energy, Mines and Petroleum Resources*, Bulletin 100, 291 pages.
- Schiarizza, P. and Riddell, J. (1997): Geology of the Tatlayoko Lake – Beece Creek area; in *Interior Plateau Geoscience Project: Summary of Geological, Geochemical and Geophysical Studies*, *BC Ministry of Energy, Mines and Petroleum Resources*, Paper 1997-2 and *Geological Survey of Canada*, Open File 3448, pages 63–101.
- Schiarizza, P., Riddell, J., Gaba, R.G., Melville, D.M., Umhoefer, P.J., Robinson, M.J., Jennings, B.K. and Hick, D. (2002): Geology of the Beece Creek – Nui Mountain area, BC (NTS 92N/8, 9, 10; 92O/5, 6, 12); *BC Ministry of Energy, Mines and Petroleum Resources*, Geoscience Map 2002-3.

Geological Setting of Volcanogenic Massive Sulphide Occurrences in the Middle Paleozoic Sicker Group of the Southeastern Cowichan Lake Uplift (NTS 092B/13), Southern Vancouver Island¹

by T. Ruks² and J.K. Mortensen²

KEYWORDS: Sicker Group, Paleozoic, Vancouver Island, Cowichan Lake uplift, VMS deposit, stratigraphy, U-Pb zircon geochronology, litho geochemistry

INTRODUCTION

Volcanogenic strata of the mid-Paleozoic Sicker Group on Vancouver Island (Fig 1) host the world-class Myra Falls volcanogenic massive sulphide (VMS) deposit (combined production and proven and probable reserves in excess of 30 million tonnes of Zn-Cu-(Au-Ag) ore), as well as numerous other VMS deposits and occurrences, especially in the Big Sicker Mountain area in the southeastern part of the Cowichan Lake uplift (Fig 1). Three of these deposits, the Lenora, Tyee and Richard III (MINFILE occurrences 092B 001, 002, 003) have seen limited historical production, and the Lara deposit (MINFILE occurrence 092B 129), farther to the northwest, also contains a significant drill-indicated resource. Geological mapping (Massey and Friday, 1987) suggests that the Big Sicker Mountain area is underlain mainly by deformed mafic to felsic volcanic and volcanoclastic rocks of the Nitinat and McLaughlin Ridge formations and high level intrusions of the Saltspring intrusive suite, as well as abundant gabbroic dikes and sills of the Triassic Mount Hall gabbro. Logging activity in the Big Sicker Mountain area over the past decade has provided abundant new outcrops and prompted a re-examination of the geological setting of VMS mineralization and of the potential for new discoveries in this area. This report presents a preliminary version of a revised geological map of the Big Sicker Mountain area, as well as new litho geochemical and U-Pb zircon geochronology results that bear on the geological setting of VMS mineralization in the southeastern Cowichan Lake uplift, as well as the potential for new discoveries in the area.

Reconnaissance sampling for litho geochemistry, U-Pb zircon dating and Pb isotopic studies in the Big Sicker Mountain area was carried out in 2005 (Mortensen, 2005), and a total of two weeks of geological mapping was done in October 2006.

¹ Geoscience BC contribution GBC035

² Mineral Deposit Research Unit, Department of Earth and Ocean Sciences, University of British Columbia, Vancouver BC V6T 1Z4 (tyler_ruks@hotmail.com)

This publication is also available, free of charge, as colour digital files in Adobe Acrobat® PDF format from the BC Ministry of Energy, Mines and Petroleum Resources website at http://www.em.gov.bc.ca/Mining/Geolsurv/Publications/catalog/cat_fldwk.htm

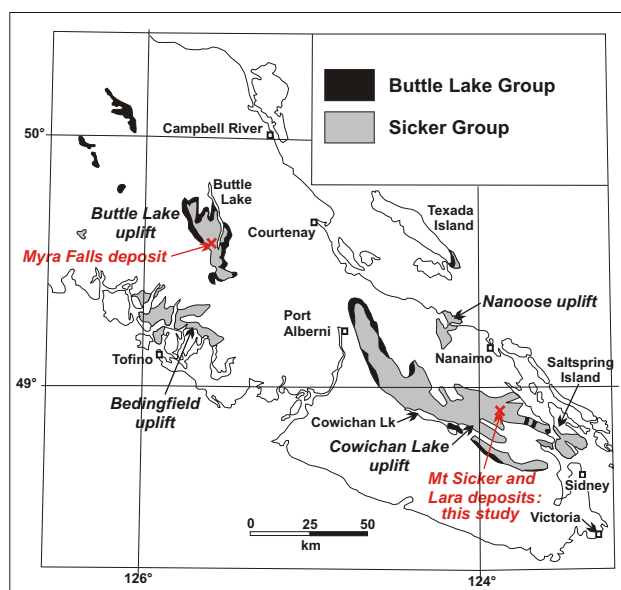


Figure 1. Distribution of Paleozoic strata of the Sicker and Buttle Lake groups on Vancouver Island and the Gulf Islands.

REGIONAL GEOLOGY OF THE SICKER GROUP

The mid-Paleozoic Sicker Group on southern and central Vancouver Island represents the stratigraphically lowest portion of the Wrangellia Terrane. Equivalents of the Sicker Group are not present elsewhere in Wrangellia farther to the north in northwestern British Columbia, southwestern Yukon and southern Alaska, where the oldest rock units are the Skolai Group, which is no older than Pennsylvanian (*e.g.*, Katvala, 2006). This and other differences between the Wrangellian stratigraphy on Vancouver Island and that in more northerly exposures emphasizes the lack of understanding regarding much of Wrangellia (*e.g.*, Katvala, 2006) and the need for studies such as this. The Cowichan Lake uplift on Vancouver Island and adjacent portions of the Gulf Islands, which is the focus of this study, is the largest of four structural uplifts that expose the Sicker and overlying late Paleozoic Buttle Lake groups (Fig 1).

Previous detailed studies of the Sicker Group have focused mainly on the stratigraphic setting of VMS mineralization at the Myra Falls deposits in the Buttle Lake uplift (Fig 1; *e.g.*, Juras, 1987; Barrett and Sherlock, 1996). Regional mapping of the Cowichan Lake uplift by Massey and Friday (1987, 1989) and Yorath *et al.* (1999) led to an inter-

preted stratigraphic framework that may be applicable to the entire Sicker Group (Fig. 2). This stratigraphic framework, however, is based on mapping in only one of the four main uplifts of Sicker Group rocks, and is supported by a very limited amount of biostratigraphic and isotopic age data (e.g., Brandon *et al.*, 1986). Major along and across-strike facies changes and geochemical variations are to be expected in submarine volcanic sequences such as the one that forms the Sicker Group; hence, the regional applicability of the proposed stratigraphic framework of Yorath *et al.* (1999) must be tested with detailed mapping and litho-geochemical and U-Pb dating studies. This is critical for regional exploration for VMS deposits within the Sicker Group. For example, the question of whether VMS deposits and occurrences in the Cowichan Lake uplift are all of the same age, and how their hostrocks are directly correlative with those that host the Myra Falls deposit, are of obvious importance.

The Sicker Group within the Cowichan Lake uplift is presently interpreted to represent three distinct and regionally mappable volcanic and volcanoclastic assemblages that together are thought to record the evolution of an oceanic magmatic arc (Massey, 1995a, b, c; Yorath *et al.*, 1999). The Duck Lake Formation, at the base of the section, consists of dominantly tholeiitic basalt, which passes upward into calcalkaline lava. The lowermost Duck Lake Formation yields mainly normal mid-ocean-ridge basalt (N-MORB) geochemical signatures (Massey, 1995a) and is interpreted to represent the oceanic crust basement on which the Sicker arc was built. The upper portions of the Duck Lake Formation yield tholeiitic to calcalkaline compositions and may represent primitive arc rocks. The Duck Lake Formation is overlain by the Nitinat Formation, which comprises mafic, submarine, volcanic and volcanoclastic rocks with dominantly calcalkaline compositions and trace element signatures typical of volcanic arc settings. These rocks are interpreted to represent an early stage of arc development. The andesitic to mainly dacitic and rhyolitic McLaughlin Ridge Formation that overlies the Nitinat and hosts the Myra Falls deposit reflects a more evolved stage of arc activity. Eruption of Nitinat volcanic and volcanoclastic rocks appears to have occurred from several widely scattered centres, whereas the McLaughlin Ridge Formation within the Cowichan Lake uplift is thought to represent eruption from one or more major volcanic edifices. The abundance of proximal felsic volcanoclastic

rocks and the presence of voluminous comagmatic felsic intrusions (Saltspring intrusions) in the Saltspring Island and Duncan area (Fig 1) indicates that one of these major volcanic centres was located in this area. Plant material and trace fossils indicate that at least a minor amount of the McLaughlin Ridge volcanism occurred in a subaerial setting. Deposition of the overlying Fourth Lake Formation of the Buttle Lake Group followed the cessation of Sicker arc magmatism, and scarce mafic volcanic rocks contained within the Fourth Lake Formation yield enriched tholeiitic rather than the calcalkaline compositions that characterize the McLaughlin Ridge. Massey (1995a) speculated that the Buttle Lake Group may represent a marginal-basin assemblage that developed on top of the Sicker arc.

Studies of the Sicker and Buttle Lake groups on southern Saltspring Island at the southeastern end of the Cowichan Lake uplift by Sluggett (2003) and Sluggett and Mortensen (2003) provided new U-Pb zircon age constraints on both felsic volcanic rocks of the McLaughlin Ridge Formation and several bodies of Saltspring intrusions. This work demonstrates that two distinct episodes of felsic magmatism occurred in this portion of the Cowichan Lake uplift. One sample of felsic volcanic rocks from the McLaughlin Ridge Formation and three samples of Saltspring intrusions yielded U-Pb ages in the range 356.5 to 359.1 Ma. A somewhat older U-Pb age of 369.7 Ma was obtained from a separate body of the Saltspring intrusions at Burgoyne Bay on the southwest side of Saltspring Island, indicating that magmatism represented by the McLaughlin Ridge Formation and associated Saltspring intrusions occurred over a time span of at least 15 m.y. There is insufficient age control available at this point to determine whether the magmatism was continuous or episodic during this time period. Litho-geochemical data reported by Sluggett (2003) for samples of the McLaughlin Ridge and Nitinat formations on Saltspring Island, together with data previously reported by Massey (1995a, b, c), provide a geochemical framework with which to compare the new results from the Big Sicker Mountain study area.

RESULTS OF NEW MAPPING IN THE BIG SICKER MOUNTAIN AREA

Field Geology

Preliminary mapping of an area of Big Sicker Mountain covering approximately 25 km² was conducted over 12 days in October 2006 (Fig 3). The mapping concentrated primarily in the area of the past-producing Lenora, Richard III and Tye VMS deposits, and nearby MINFILE (2006) occurrences. Bedrock outcrop on Big Sicker Mountain is generally poor and is mainly restricted to logging-road cuts and slashes. As a result, contact locations between major rock types are mostly inferred.

The oldest rocks in the Big Sicker Mountain area are mafic volcanic rocks assigned to the Nitinat Formation (Massey and Friday, 1987). During the course of 2006 mapping, rocks of the Nitinat Formation were encountered only in a small area along the western flanks of Little Sicker Mountain (Fig 3). They consist of dark green, dominantly aphyric basalt with abundant ovoid epidote-quartz alteration patches up to 4 to 5 cm in diameter (Fig 4a). Sulphide mineralization is observed in one outcrop of Nitinat Formation, and consists of pyrite stringers up to 5 cm in width hosted in a vertically dipping fault zone approximately 2 m

Muller, 1977 (Vancouver Island)		Juras, 1987 (Buttle Lake Uplift)		Yorath et al., 1999 (Alberni area)	
Sicker Gp		Buttle Lake Gp	Henshaw Fm	Buttle Lake Gp	St. Mary Lk Fm
	Buttle Lk Fm		Mt Mark Fm		Mt Mark Fm
	sediment sill unit				Fourth Lk Fm
	Myra Fm	Sicker Gp	Flower Ridge Fm	Sicker Gp	McLaughlin Ridge Fm
	Nitinat Fm		Thelwood Fm		Nitinat Fm
			Myra Fm		
			Price Fm		Duck Lk Fm

Figure 2. Stratigraphic nomenclature for the Sicker and Buttle Lake groups on Vancouver Island.

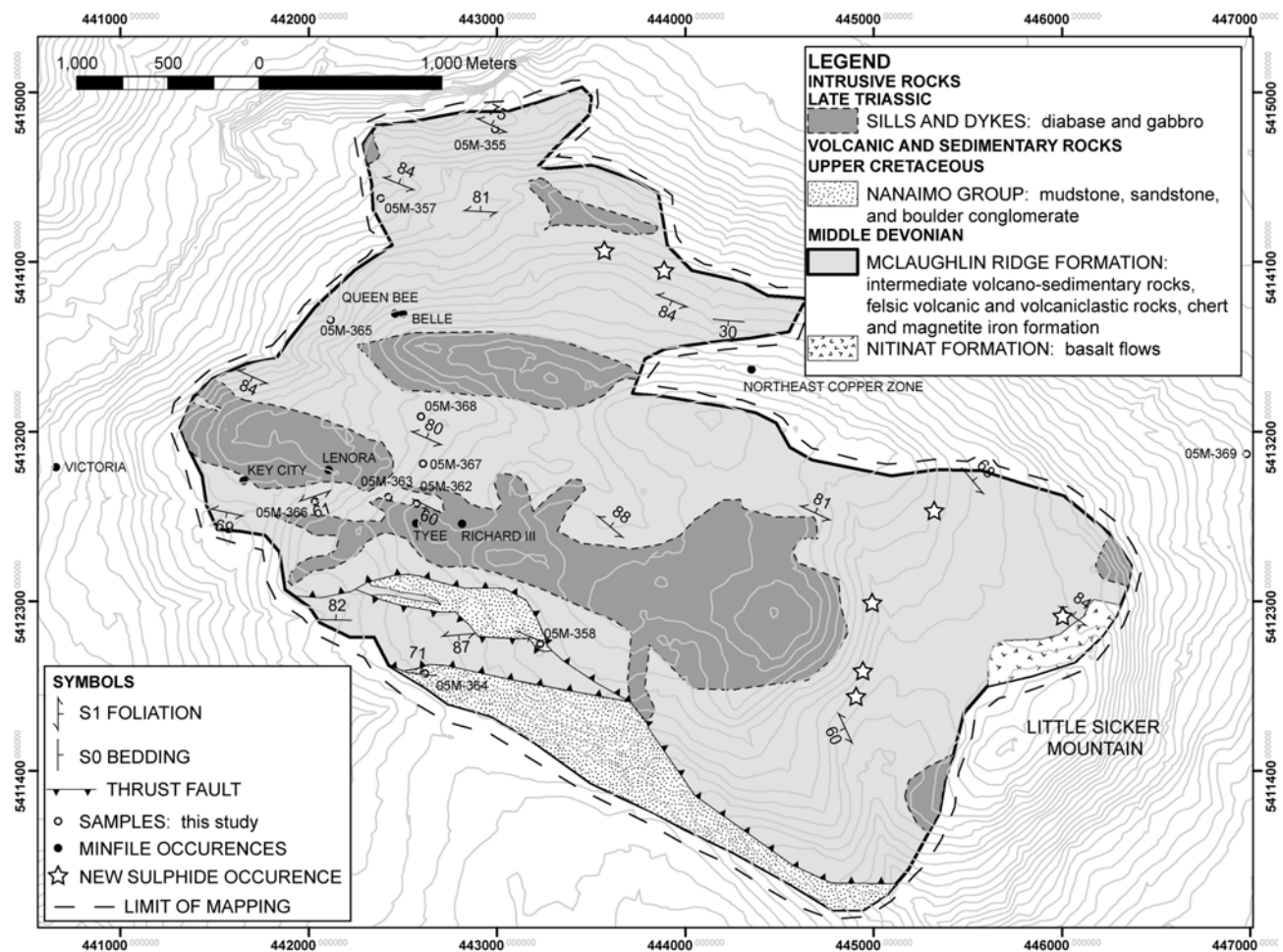


Figure 3. Preliminary revised geology of the Big Sicker Mountain area, based on fieldwork conducted for this study.

in width (Fig 4b). This outcrop appears to have been trenched for mineral exploration purposes.

Rocks of the McLaughlin Ridge Formation sit stratigraphically above those of the Nitinat Formation (Massey and Friday, 1987) and consist of intermediate volcanosedimentary rocks, felsic volcanic and volcanoclastic rocks, and, to a lesser degree, mudstone, chert and magnetite iron formation. Mafic to intermediate volcanosedimentary rocks are most prevalent along the northern to northeastern boundary of the map area. These rocks consist of thinly bedded to laminated, dark green, variably chlorite, sericite and silica-altered siltstone to fine sandstone, and more massive, medium-grained, feldspar-bearing sandstone or sandy tuff (Fig 5). Felsic rocks of the McLaughlin Ridge Formation include predominantly rhyolitic to dacitic ash, quartz-feldspar crystal tuff, aphyric flows, quartz-feldspar porphyry and, to a lesser extent, tuff-breccia (Fig 6).

Sericite and quartz alteration is commonly very strong in the felsic volcanic rocks. This, together with a well-developed foliation, makes it difficult to distinguish between those that formed from lavas (*i.e.*, a porphyry or flow) versus those that are crystal-bearing volcanoclastic rocks (*i.e.*, a crystal tuff). Dark grey to black, variably graphitic mudstone has only been observed locally within the vicinity of the main deposits (Fig 7a). Chert is not abundant and

has been identified thus far only in a restricted area in the northern and south-southwesternmost parts of the study area (Fig 7b). In the southwestern part of the field area, laminated chert is associated with dacitic tuff, jasper and a localized magnetite iron formation (Fig 7c).

Triassic gabbro and diabase intrude rocks of the Sicker Group (Fig 8), are very prevalent throughout the field area (Fig 3), and are of variable thickness. Drillhole MTS-81 (Wells, 1990), located approximately 1 km southeast of the Richard III shaft in the vicinity of the BC Tel communication towers, encountered a gabbro thickness of >100 m before intersecting rocks of the Sicker Group at depth. However, the Richard III and Tyee shafts are sunk in gabbro, and are assumed to intersect rocks of the Sicker Group at a shallower depth, suggesting a westward thinning of these intrusions. The intrusive textures are quite variable from outcrop to outcrop, most likely due to localized shearing; however, the most common lithology is holocrystalline hornblende and plagioclase gabbro (Fig 8), consisting of variably chlorite-altered cumulus hornblende phenocrysts, up to 4 mm in size, in a matrix of intercumulus plagioclase.

Upper Cretaceous rocks of the Nanaimo Group lie unconformably on those of the Sicker Group (Massey and Friday, 1987) and crop out solely in the southernmost part of the field area. However, in the field area, the contact between the Sicker Group and Nanaimo Group marks the po-

sition of the Fulford fault and associated splays. In the field area, Nanaimo Group rocks consist largely of mudstone, shale, arkosic medium-grained sandstone and boulder conglomerate. The latter rock type contains abundant volcanic and gabbroic rock clasts that appear to have been derived from underlying Sicker Group and Triassic gabbro.

Structure

The most prominent fabric in the Big Sicker Mountain area is, on average, east to southeast-striking with a near-

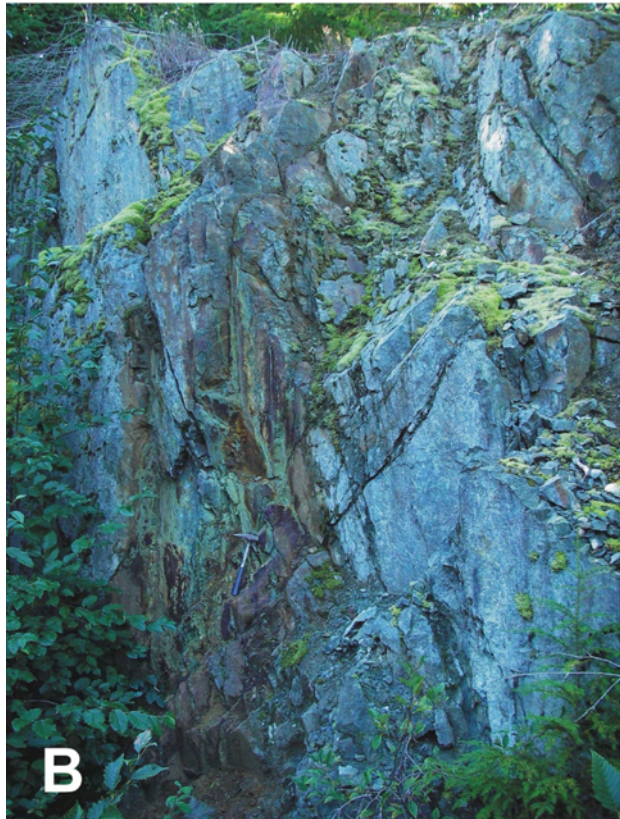


Figure 4. Intermediate to mafic volcanic rocks of the Nitinat Formation: A) aphyric basaltic andesite with ovoid quartz-epidote patches; B) pyrite-stringer-bearing fault in basaltic andesite flow (?); note hammer for scale in lower central part of photo.

vertical dip, and represents both bedding and a bedding-parallel foliation herein termed S1 (Fig 9a). As mentioned before, due to extensive alteration in rocks of the McLaughlin Ridge Formation, it is commonly difficult to differentiate between those that originated as bedded volcanoclastic rocks and those that were originally massive flows or sills. Hence, some of the fabrics recorded as foliations may be bedding measurements. Small-scale (sub-metre wavelength), steeply plunging S and Z-shaped folds deform the primary layering in the volcanosedimentary package throughout the map area and are probably parasitic folds related to a larger F1 structure (Fig 9b). Second phase (D2) kinking of D1 structures occurs in several localities. Third phase (D3) structures consist of small-scale, shallowly plunging folds (2–3 cm wavelength) that were only observed in one locality (Fig 9a). The most prominent faults in the area are dominantly east striking, with near-vertical dips. In one such locality, shear-sense indicators in faulted dacite tuff of the McLaughlin Ridge Formation suggest a strong component of north-side-up motion (Fig 9c).



Figure 5. Intermediate volcanosedimentary rocks of the McLaughlin Ridge Formation (?) from the northern (A) and north-eastern (B) parts of the field area.

MINERALIZATION

Sulphide mineralization is widespread throughout the field area, and consists mainly of pyrite±chalcopyrite stringers and small pods/lenses associated with areas of intense sericite+silica alteration. Many of these sulphide occurrences are close to MINFILE (2006) occurrences, but some are not. For example, several zones of sulphide min-

eralization, consisting of pyrite±chalcopyrite stringers and patches up to 15 cm wide, occur in silicified and sericitized felsic volcanic rocks (tuff and quartz-feldspar porphyry) approximately 3 to 3.5 km east, along strike, from the known deposits (Fig 10).

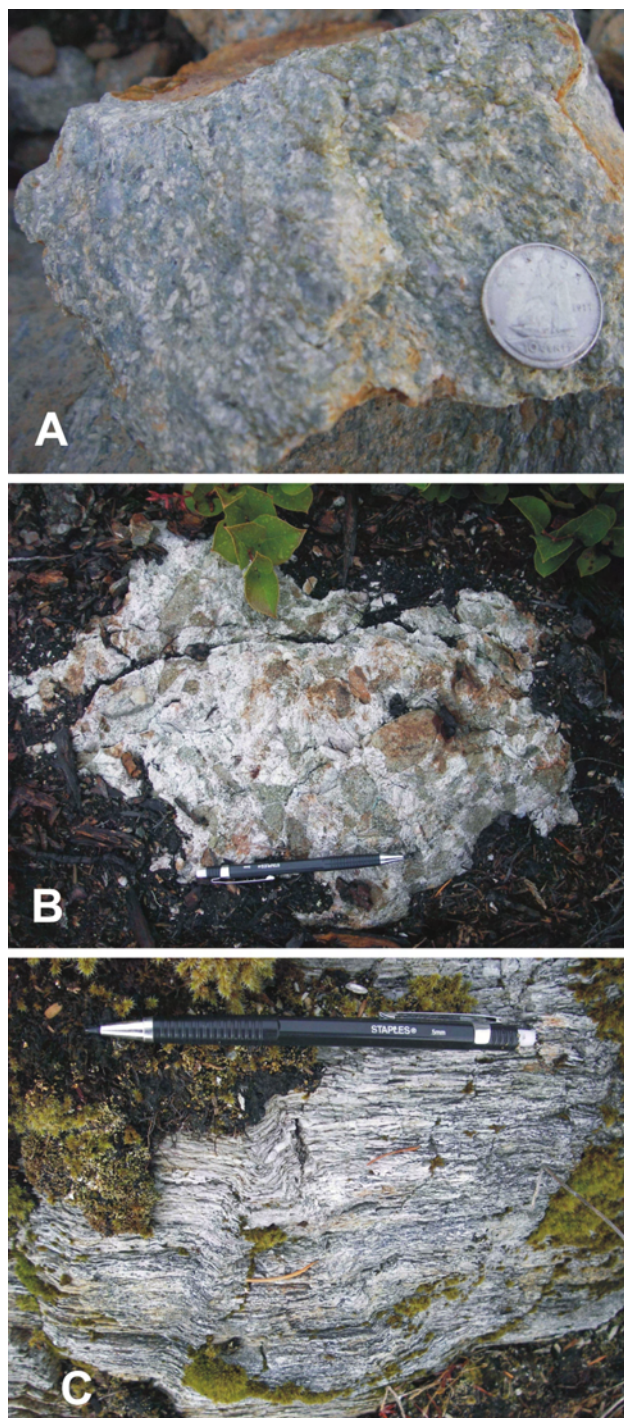


Figure 6. Felsic rocks of the McLaughlin Ridge Formation include A) rhyodacite porphyry, B) heterolithic tuff-breccia, and C) rhyodacite crystal tuff.

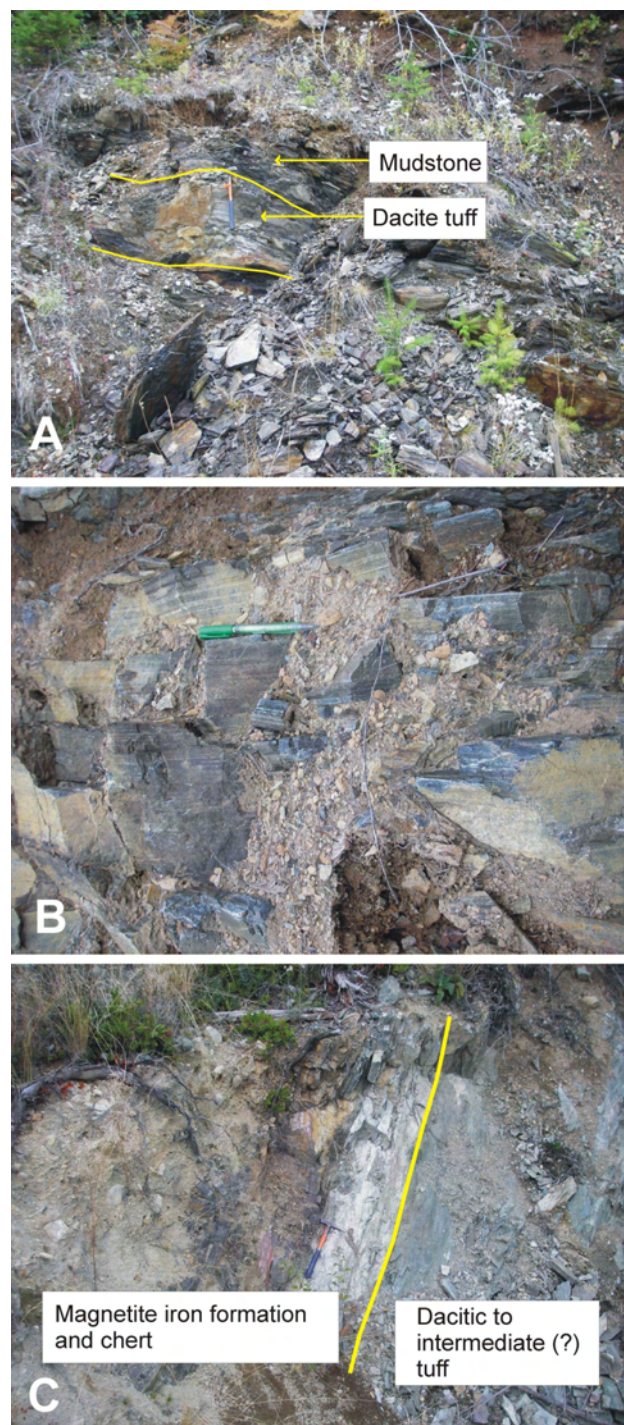


Figure 7. Rocks of the McLaughlin Ridge Formation: A) laminated mudstone interbedded with dacitic tuff; B) laminated chert; C) magnetite iron formation that forms a restricted layer (approximately 0.5–1 m thick) interbedded with laminated chert and dacitic to intermediate (?) tuff.

Also in the northeastern part of the map area (Fig 3), approximately 1.6 km northeast of the Lenora-Tyee deposits and approximately 900 m northeast of the Queen Bee MINFILE occurrence, abundant pyrite stringers up to 2 to 3 cm thick are associated with zones of intense silicification and sericitization of intermediate volcanosedimentary rocks. These occurrences are not documented in MINFILE, and do not show signs of significant exploration activity. Mineralization associated with the main workings is best documented in the vicinity of the Lenora deposit, where polymetallic massive sulphide mineralization was accessed via an adit trending 163°. This adit was excavated in highly silicified and sericitized felsic volcanic rocks with abundant silicified mudstone and/or chert (Fig 11). Here, sulphide mineralization consists of extensive foliation/bedding-parallel pyrite±chalcopyrite stringers and patches up to 15 cm wide, often associated with malachite staining.

Mineralization was not observed at the Richard III and Tyee workings, as the shafts used to access these deposits are sunk in gabbro. However, this suggests that the thickness of postmineral Triassic gabbro in many locations throughout the field area is not substantial enough to negate the potential for large VMS deposits.

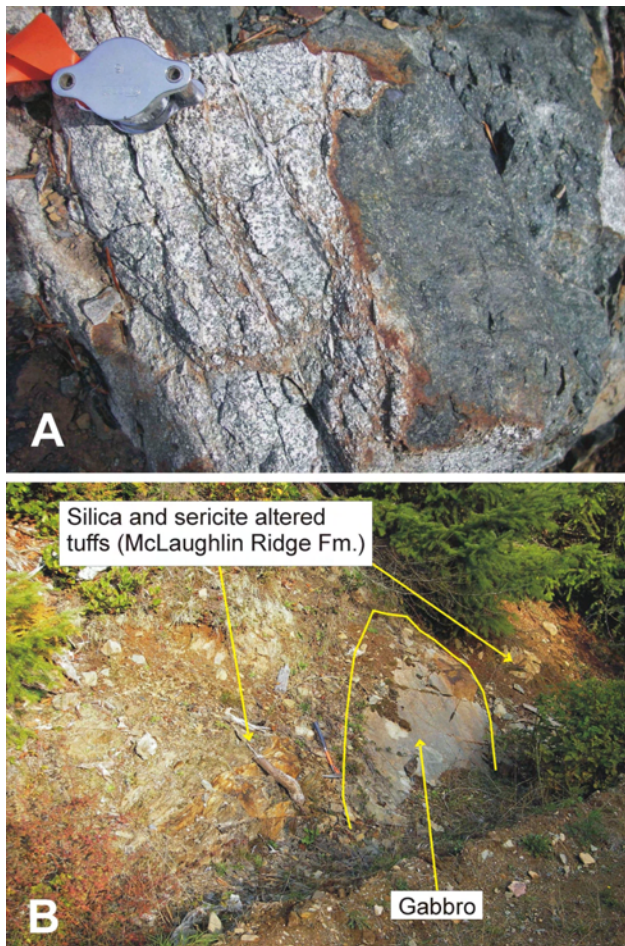


Figure 8. Triassic gabbros of the Big Sicker Mountain area: A) hornblende and plagioclase-bearing gabbro; B) gabbro crosscutting altered and gossanous volcanosedimentary rocks of the McLaughlin Ridge Formation

U-PB GEOCHRONOLOGY

Uranium-lead dating of zircons by laser-ablation inductively coupled plasma mass spectrometry (ICP-MS) is being used to constrain ages of eruption and/or intrusion of

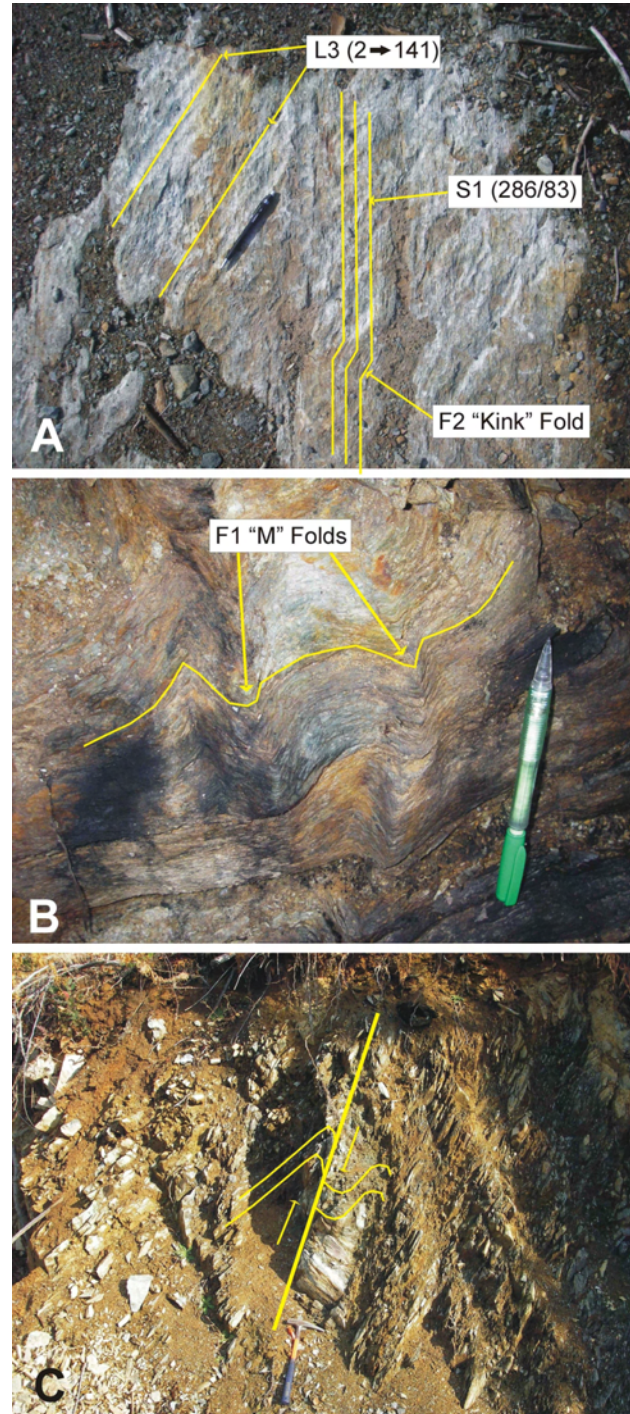


Figure 9. Structural geology of the Big Sicker Mountain area: A) east-striking S1 fabric in dacitic tuff is deformed by F2 kink folds; both of these structures are deformed by shallowly plunging F3 folds; B) steeply plunging F1 'M' folds in sericite and silica-altered rhyodacite tuff; C) north-side-up displacement in fault zone, indicated by drag folding in faulted dacitic tuff.

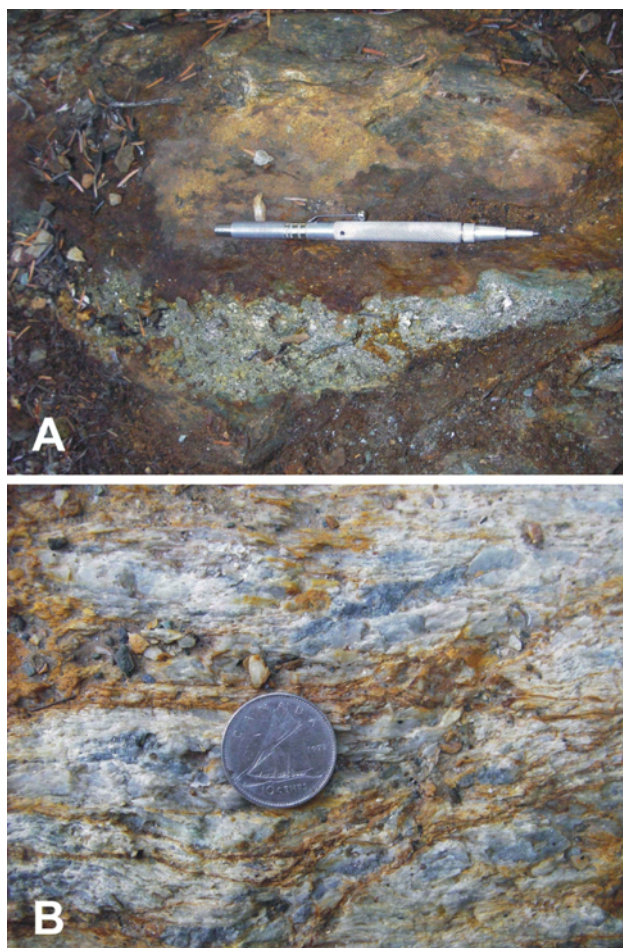


Figure 10. Selected new sulphide occurrences: A) 1 to 2% pyrite±chalcopyrite stringers (up to 15 cm wide) hosted in quartz-feldspar porphyry, eastern part of map area; B) strongly silica+sericite-altered volcanosedimentary rock with up to 3% disseminated and stringer pyrite, northeastern part of map area.

igneous rock units and to construct a chronostratigraphic framework for magmatism in the Sicker Group. This paper includes preliminary U-Pb zircon ages for six volcanic units in the southeastern Cowichan Lake uplift. Zircons were recovered from samples weighing approximately 10 kg using conventional crushing, grinding, wet shaking table, heavy liquids and magnetic methods. Selected grains were mounted in thermal-setting epoxy; the grain mounts were carefully ground down until the interior of the individual grains were exposed. The ground surfaces were then brought to a high polish using sequentially finer diamond pastes. The surfaces of the mounts were then washed with dilute nitric acid for ten minutes and rinsed with ultrapure water. Analyses were done in the Pacific Centre for Isotopic and Geochemical Research (PCIGR) facility at the University of British Columbia (UBC), using a New Wave™ 213 nm Nd-YAG laser coupled to a Thermo Finnigan™ Element2 high-resolution ICP-MS. Ablation took place within a New Wave ‘Supercell’ ablation chamber that is designed to

achieve very high efficiency entrainment of aerosols into the carrier gas. Helium was used as the carrier gas for all experiments, and gas flow rates, together with other parameters such as torch position, were optimized prior to beginning a series of analyses. A 25 µm spot with 60% laser power was used, making line scans rather than spot analyses in order to avoid within-run elemental fraction. Each analysis consists of a 7 second background measurement (laser off), followed by an approximately 28 second data acquisition period with the laser firing. A typical analytical session consists of four analyses of the standard zircon, followed by four analyses of unknown zircons, two standard analyses, four unknown analyses, etc., and finally four standard analyses. Data were reduced using the GLITTER software, marketed by the Geochemical Evolution and Metallogeny of Continents (GEMOC) group at Macquarie University, which automatically subtracts background measurements, propagates all analytical errors and calculates isotopic ratios and ages. Final ages for relatively young (Phanerozoic) zircons are typically based on a weighted average of the calculated $^{206}\text{Pb}/^{238}\text{U}$ ages for 10 to 20 individual analyses. Final interpretation and plotting of the analytical results employed the Isoplot software written by K.R. Ludwig.

Zircons recovered from all of the Sicker Group volcanic rocks form stubby, subhedral to euhedral pinkish prisms with vague internal growth zoning but no visible inherited cores. Approximately 25 grains were mounted from each sample and 12 to 20 individual analyses were carried out for each sample. The results are plotted in Figure 12, which shows a compilation of the calculated $^{206}\text{Pb}/^{238}\text{U}$ ages for individual analyses with a calculated weighted-average age.

Sample 05M-366 is from strongly foliated, sparsely quartz-phyric lapilli tuff collected 5 m north of the Lenora adit. Sixteen individual analyses were done and there is considerable scatter in the data (Fig 12a). One of the analyses gives a $^{206}\text{Pb}/^{238}\text{U}$ age of 403 Ma and is rejected as probably a xenocrystic grain incorporated into the tuff. A

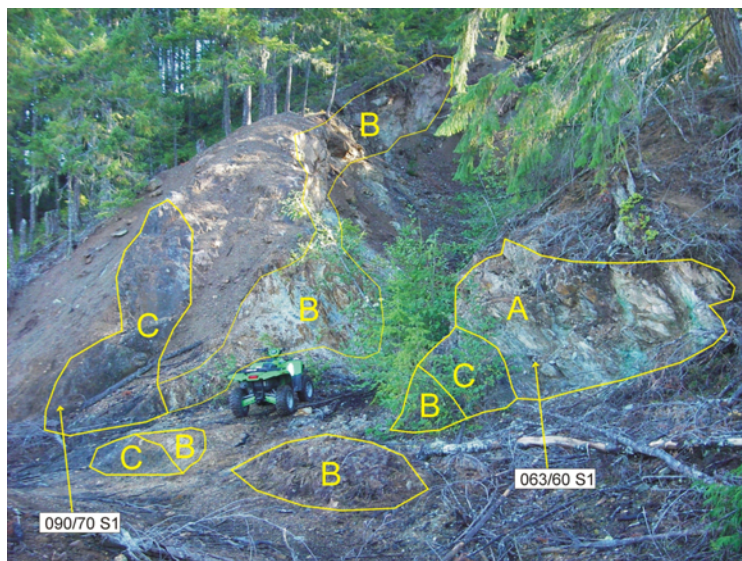


Figure 11. Geology of the Lenora adit area. Lithological units include A) rhyodacite crystal tuff (?) with abundant malachite staining and pyrite+chalcopyrite stringers up to 10 cm in size; B) variably silica-altered, black graphitic mudstone; and C) strongly sericite+silica-altered tuff (?) with abundant pyrite stringers.

weighted average of the remaining 15 analyses is 369.1 ± 6.5 Ma. Note that the high mean standard weighted deviate (MSWD) of 10.7 reflects the large amount of scatter in the data. The calculated weighted average is considered to

give an approximate age for eruption of the lapilli tuff unit that partly hosts the Lenora VMS deposit.

Sample 05M-393 is a strongly welded quartz and feldspar-phyric lapilli tuff at the main adit on the Lara property.

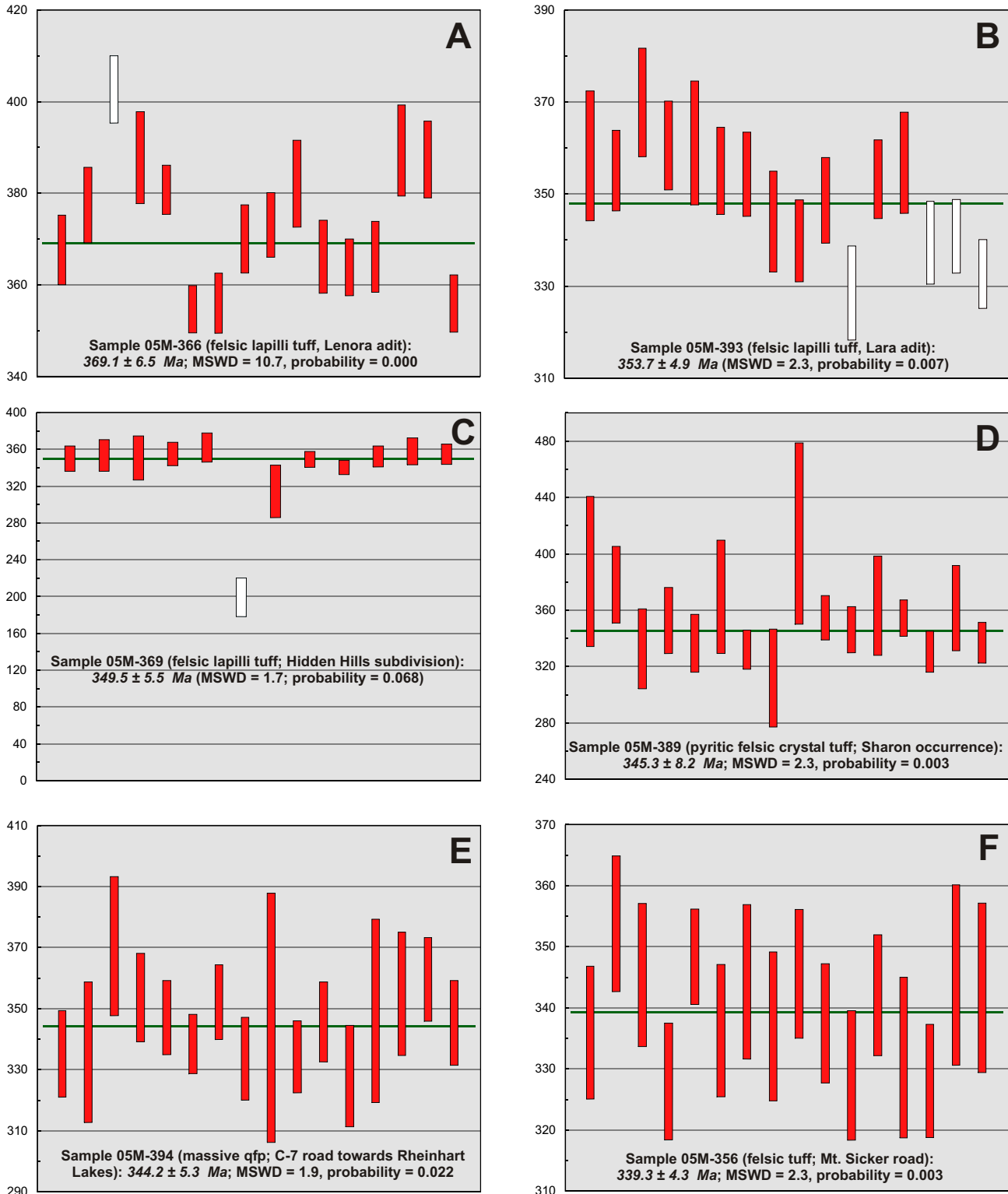


Figure 12. Calculated $^{206}\text{Pb}/^{238}\text{U}$ (zircon) ages for felsic volcanic rocks of the Sicker Group collected from the Cowichan Lake uplift during the course of this study.

Twelve of a total of sixteen individual analyses give a weighted average $^{206}\text{Pb}/^{238}\text{U}$ age of 353.7 ± 4.9 Ma (Fig 12b), which is interpreted as the crystallization age for this felsic unit. The four remaining analyses appear to reflect minor postcrystallization Pb loss.

Sample 05M-369 is a moderately to strongly foliated, pyritic, quartz-phyric felsic lapilli tuff from a road exposure in the Hidden Hills subdivision, immediately east of the study area. Eleven of twelve individual analyses (Fig 12c) give a weighted average $^{206}\text{Pb}/^{238}\text{U}$ age of 349.5 ± 5.5 Ma, which is interpreted as the crystallization age for this unit. One analysis gives a much younger $^{206}\text{Pb}/^{238}\text{U}$ age and is interpreted to have suffered postcrystallization Pb loss.

Sample 05M-389 is a strongly foliated, pyritic quartz-muscovite schist with scattered quartz eyes from the Sharon occurrence that is interpreted to be a deformed quartz-phyric crystal tuff. A weighted average $^{206}\text{Pb}/^{238}\text{U}$ age of 345.3 ± 8.2 Ma for this sample, based on sixteen individual analyses (no rejects; Fig 12d), is interpreted as the crystallization age of the hostrocks for the Sharon mineralization.

Sample 05M-394 is a massive quartz-feldspar porphyry exposed along the C-7 road towards Rheinhart Lake, northwest of the Lara deposit. A weighted average $^{206}\text{Pb}/^{238}\text{U}$ age of 344.2 ± 5.3 Ma was obtained for this sample, based on sixteen individual analyses (no rejects; Fig 12e), and is interpreted as the crystallization age for the porphyry body.

Sample 05M-356 was collected from a roadcut on the south side of the Mount Sicker road. It is a weakly to strongly foliated, quartz-phyric lapilli tuff. Sixteen individual analyses (no rejects) give a weighted average $^{206}\text{Pb}/^{238}\text{U}$ age of 339.3 ± 4.3 Ma, which is interpreted as the crystallization age of this unit.

The range of ages obtained for felsic extrusive rocks and high-level felsic intrusions in this part of the Cowichan Lake uplift was unexpected. Only one other well-constrained age is presently available for any of the Sicker Group units in the Big Sicker Mountain area: a U-Pb zircon age of 362 ± 2 Ma reported by Parrish and McNicoll (1992) for a quartz-feldspar porphyry body of the Saltspring intrusive suite along the Island Highway on the east side of Big Sicker Mountain. The preliminary age of 369.1 ± 6.5 Ma reported here for felsic lapilli tuff that partly hosts the Lenora VMS orebody (sample 05M-366 above) is within uncertainty of both the porphyry body dated by Parrish and McNicoll (1992) and a separate body of Saltspring intrusions in the Burgoyne Bay area on western Saltspring Island that was dated at 369.7 ± 1.9 Ma (Sluggett, 2003; Sluggett and Mortensen, work in progress). Two other samples of Saltspring intrusions from near Erskine Point and Lake Stowell on Saltspring Island, which were dated by Sluggett (2003) and Sluggett and Mortensen (work in progress), gave U-Pb ages of 359.1 ± 1.4 and 356.5 ± 1.7 Ma, respectively, and a sample of felsic tuff of the McLaughlin Ridge Formation near Isabella Point in the southwest part of Saltspring Island gave a U-Pb age of 354.1 ± 1.2 Ma.

Previous work had therefore already demonstrated a significant age range for McLaughlin Ridge and Saltspring intrusive suite magmatism. The new data from this study, however, indicate that felsic magmatism lasted from ca. 370 Ma until at least as young as 339 Ma. More importantly, these data suggest that VMS mineralization of at least two

separate ages is present in the southeastern part of the Cowichan Lake uplift. Mineralization at the Lenora deposit is hosted by felsic tuff (and interlayered sedimentary rocks) with a depositional age of ca. 369 Ma, whereas hostrocks for the Lara deposit give an age of 353.7 Ma. Felsic tuff that hosts bands of stratabound, possibly syngenetic sulphide minerals at the Sharon occurrence and in the vicinity of the Hidden Hills subdivision on the east side of Big Sicker Mountain are even younger, at 345.3 and 349.5 Ma, respectively. There are as yet no reliable crystallization ages for felsic volcanic rocks that host VMS mineralization at the Myra Falls deposit in the Buttle Lake uplift. Sampling of the Myra Falls hostrocks for U-Pb dating to facilitate comparison with the ages of VMS mineralization in the southeastern Cowichan Lake uplift is planned for the fall of 2006.

LITHOGEOCHEMISTRY OF IGNEOUS ROCKS IN THE BIG SICKER MOUNTAIN AREA

Sixteen samples of Sicker Group igneous rocks from the southeastern part of the Cowichan Lake uplift (from Rheinhart Lake on the northwest to southern Saltspring Island on the southeast) were analyzed for major, trace and rare earth elements in order to better characterize the petrochemistry of the various igneous units in the area. These analyses were conducted at ALS Chemex, using a combination of x-ray fluorescence (XRF) and ICP-MS methods. Data are presented in a series of plots in Figure 13, along with data from an additional 11 samples of Sicker Group rock units on Saltspring Island that were reported by Sluggett (2003). The two data sets compare very closely and the following observations are based on the combined dataset.

On a Zr/TiO₂ versus Nb/Y plot (Fig 13a; Winchester and Floyd, 1977), volcanic and volcanoclastic rocks of the Nitinat Formation fall in the subalkaline basalt and basaltic andesite fields. On a V versus Ti plot (Fig 13b; Shervais, 1982), the samples lie in the island arc tholeiite field. Samples of the Saltspring intrusive suite plot as subalkaline and rhyodacite/dacite to rhyolite in composition on a Zr/TiO₂ versus Nb/Y plot (Fig 13a; Winchester and Floyd, 1977), and are of volcanic arc affinity on a Nb versus Y tectonic discrimination diagram (Fig 13c; Pearce *et al.*, 1984). On a Zr/TiO₂ versus Nb/Y plot (Fig 13a; Winchester and Floyd, 1977), McLaughlin Ridge samples span the subalkaline rhyodacite/dacite to rhyolite compositional fields (except for one andesitic sample), and are of volcanic arc affinity on a Nb versus Y tectonic discrimination diagram (Fig 13c; Pearce *et al.*, 1984). A sample of dark green, chlorite-rich volcanosedimentary rock from the north end of the map area (05M-355) plots as subalkaline andesite on a Zr/TiO₂ versus Nb/Y diagram (Fig 13a; Winchester and Floyd, 1977), and as an island arc tholeiite on a V versus Ti diagram (Fig 13b; Shervais, 1982). A primitive mantle normalized multi-element diagram (Fig 13d; Sun and McDonough, 1989) for all samples shows weak to moderate light rare earth element (LREE) enrichment and negative Nb and Ti anomalies, typical for rocks generated in a volcanic arc setting.

Although samples from the McLaughlin Ridge Formation partially overlap with the roughly coeval and probably comagmatic Saltspring intrusive suite (Fig 13), they show

considerably more scatter and include one andesitic outlier. This outlier may be the result of a volcanoclastic origin involving a mafic epiclastic component reworked from underlying Nitinat Formation, or a pulse of intermediate volcanism in the McLaughlin Ridge Formation. This scenario also applies to the intermediate tuff collected from the north end of the property (05M-355). Although this unit lacks the clinopyroxene phenocrysts that are characteristic of Nitinat Formation mafic units, the composition of this single sample is very similar to that of Nitinat units. If this unit is actually Nitinat rather than McLaughlin Ridge Formation, it would help constrain where the local base of the McLaughlin Ridge is and hence provide a useful stratigraphic marker in the vicinity of the known VMS deposits.

VOLCANOGENIC MASSIVE SULPHIDE MINERALIZATION IN THE BIG SICKER MOUNTAIN AREA

The southeastern portion of the Cowichan Lake uplift is one of two exposures of the Sicker Group where volcanogenic massive sulphide (VMS) mineralization is known to occur, the other being the Myra Falls area in the Buttle Lake uplift (Fig 1). Most known VMS occurrences in the Sicker Group are of the Kuroko type (or 'bimodal felsic type', as defined by Franklin *et al.*, 2005) and are hosted by felsic volcanic and volcanoclastic rocks of the McLaughlin Ridge Formation or equivalents. However, examples of manganeseiferous and/or pyritic chert horizons that may be exhalative in origin are also locally present in

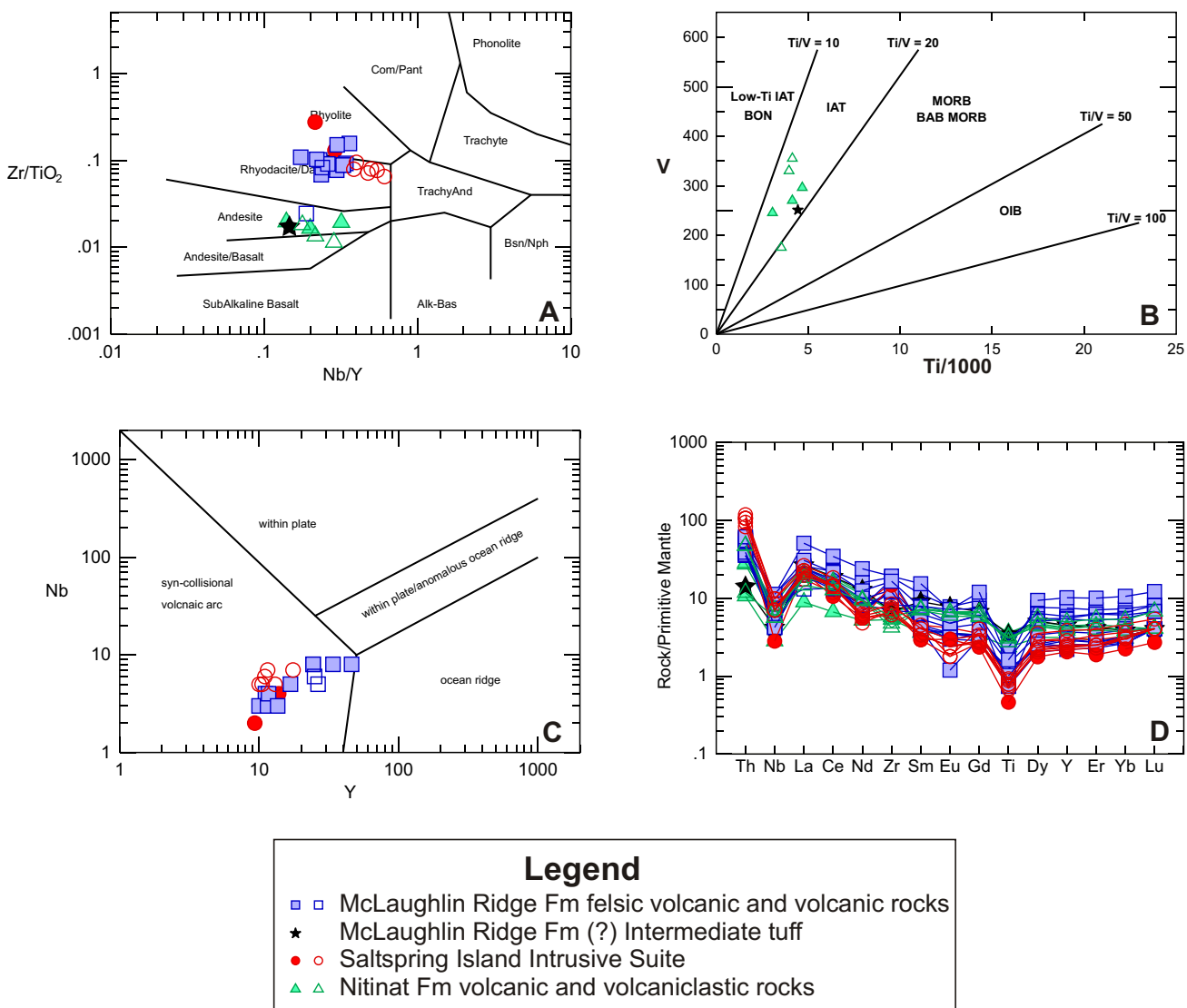


Figure 13. Lithochemical plots for Sicker Group igneous rock units in the southeastern part of the Cowichan Lake uplift. Solid symbols are from this study; open symbols are from Sluggett (2003). Petrochemical fields defined from the following sources: A) Zr/TiO₂ versus Nb/Y plot (Winchester and Floyd, 1977); B) V versus Ti (Shervais, 1982); C) Nb versus Y tectonic discrimination diagram (Pearce *et al.*, 1984); D) multi-element diagram normalized to primitive mantle (Sun and McDonough, 1989). Abbreviations: BAB, back-arc basin; IAT, island-arc tholeiite; BON, boninite; MORB, mid-ocean-ridge basalt; OIB, ocean-island basalt.

the upper Duck Lake Formation and the lowermost Fourth Lake Formation (*e.g.*, Massey and Friday, 1989; this study). Three VMS deposits have been mined historically in the Big Sicker Mountain area: the Lenora, Tyee and Richard III (MINFILE occurrences 092B 001–003, respectively; Fig 1). Production data reported in the MINFILE (2006) mineral inventory indicate that, between 1898 and 1909, a total of 229 221 t of ore were mined from these three deposits, with recovered grades of 4.0% Cu, 4.8 g/t Au and 100 g/t Ag. The three deposits were mined as a single operation (the Twin J mine) between 1942 and 1952; during that period, a total of 48 082 t of ore with a recovered grade of 7.6% Cu, 3.4% Pb, 1.0 g/t Au and 41.7 g/t Au were mined. Exploration of the Big Sicker Mountain area has been carried out sporadically since the early 1960s. The most recent estimate of existing resources, based on work between 1967 and 1970, is 317 485 tonnes grading 1.6% Cu, 0.7% Pb, 6.6% Zn, 4.1 g/t Au and 140.5 g/t Ag (The Northern Miner, 1969). Exploration by Minnova Incorporated in the late 1990s (Wells, 1990) included some diamond-drilling in the vicinity of the old mines but did not lead to a revised resource estimate. Stratiform and stratabound mineralization in the Lenora, Tyee and Richard III deposits is hosted mainly in cherty felsic tuff and fine-grained carbonaceous clastic rocks. Two main ore types are present: 1) polymetallic baritic ore with variable amounts of fine-grained pyrite, sphalerite, chalcopyrite and galena, and 2) quartz-rich ore consisting mainly of quartz and chalcopyrite. Ore at the Lenora deposit forms two lenticular orebodies that are contained within folded sedimentary strata.

Several other mineral occurrences that are interpreted to be syngenetic in origin have also been explored historically through adits, trenching and limited drilling in the Big Sicker Mountain area. These include the Key City (MINFILE occurrence 092B 087), immediately north-northwest of the Lenora adit; the Queen Bee (MINFILE occurrence 092B 088), approximately 1 km north of the Lenora adit; and the Northeast Copper (MINFILE occurrence 092B 099), approximately 2 km east-northeast of the Lenora adit (Fig 2). Sulphide mineralization in these occurrences comprises mainly disseminated pyrite (\pm pyrrhotite), chalcopyrite and locally sphalerite in schistose andesitic to rhyolitic volcanic rocks and/or associated carbonaceous sedimentary rocks, or in bands of cherty tuff.

The Lara deposit (MINFILE occurrence 092B-129) is a polymetallic VMS deposit hosted within the same package of Sicker Group stratigraphy and located approximately 10 km along strike to the northwest from Big Sicker Mountain. The main hostrocks are steeply dipping, intermediate to felsic volcanic and volcanoclastic strata of the McLaughlin Ridge Formation. A resource of approximately 500 000 t averaging 1.0% Cu, 1.2% Pb, 5.9% Zn, 4.3 g/t Au and 90 g/t Ag in two separate mineralized bodies has been reported (George Cross News Letter Ltd., 1992; Laramide Resources Ltd., 2006). Three distinct styles of mineralization are recognized at the Lara: a massive sulphide facies, a banded and laminated facies and a stringer facies. Mineralization occurs in three main bodies, and has been traced for a total strike length of at least 2 km and a down-dip extent of at least 440 m.

The Sharon occurrence (MINFILE occurrence 092B 040), located approximately 3.5 km northwest of Big Sicker Mountain (between the Mount Sicker and Lara deposits), has also been tested by three short adits as well as

drilling and trenching. Hostrocks in the area comprise pyritic quartz-muscovite and chlorite-muscovite schists that locally preserve textures indicating a mainly lapilli tuff protolith. Small bodies of weakly foliated quartz-feldspar porphyry are also present. The Sharon is mainly a copper occurrence, with zones of disseminated to semimassive recrystallized pyrite and minor chalcopyrite in bands of strongly foliated and transposed metavolcanic rocks.

The authors are using Pb isotopic analyses of sulphide minerals from various deposits and showings within the Sicker Group in the Cowichan Lake uplift to differentiate between syngenetic mineralization and younger epigenetic mineralization. Previous studies by Godwin *et al.* (1988) and Andrew and Godwin (1989) provide an excellent compositional database for both VMS and epigenetic occurrences hosted by Sicker Group strata on southern and central Vancouver Island, including data from the Mount Sicker and Lara deposits (Fig 3). Lead isotope analyses are presently being carried out on sulphide minerals from a suite of mineralized samples from throughout the southeastern Cowichan Lake uplift, including banded sulphide minerals at the Sharon occurrence (MINFILE occurrence 092B 040), pyrite from thin conformable bands of pyrite (with minor base metal enrichment; A. Francis, pers comm, 2005) within quartz-feldspar-phyrlic lapilli tuff in the Hidden Hills subdivision, and several new, possibly syngenetic occurrences that were discovered during the 2006 field work. The aim of this part of the study is to evaluate the total extent of syngenetic mineralization in the Big Sicker Mountain area and to distinguish which, if any, of the occurrences are younger and unrelated to submarine VMS processes. These new data will make it possible to fit all of the definite syngenetic occurrences in the Big Sicker Mountain area into their correct stratigraphic context and evaluate the true lateral and vertical extent of VMS mineralization in the area. This approach will subsequently be extended to cover the entire Cowichan Lake uplift.

IMPLICATIONS FOR VMS POTENTIAL IN THE BIG SICKER MOUNTAIN AREA

Evaluating the remaining potential within the vicinity of the existing Lenora, Tyee and Richard III mines, and potential for new, as yet undiscovered mineralization elsewhere in the Big Sicker Mountain area, is complicated by the difficulty in correlating stratigraphy from one area to another due to the lack of good marker horizons, and also by complexity imposed by postmineral folding and faulting. In addition, the three-dimensional extent of the Triassic gabbro bodies must be ascertained in order to determine the volume of prospective McLaughlin Ridge Formation that exists in the subsurface. Furthermore, the presence of numerous proven or probable syngenetic mineral occurrences scattered throughout the study area, including the Key City, Queen Bee and Northeast Copper occurrences (MINFILE occurrences 092B 087, 088 and 099, respectively), together with unnamed stratiform sulphide minerals in the Hidden Hills subdivision and newly discovered occurrences in the northern and eastern parts of the map area, demonstrate that VMS mineralization is widely developed within this package of Sicker Group strata. The authors have not yet been able to establish definitively the direction of stratigraphic younging within the McLaughlin Ridge Formation in the Big Sicker Mountain area. This is critical, because some of the styles of mineralization, espe-

cially the quartz-copper ores, could be interpreted to represent stringer or vent zone mineralization beneath as yet undiscovered stratiform ore lenses.

PLANNED FUTURE WORK

Work planned for the 2007 field season in the immediate Big Sicker Mountain area will focus on unravelling the structural and stratigraphic complexity through ongoing surface mapping, as well as integration of all available surface and subsurface information from previous exploration and mining activity in that area into a detailed three-dimensional model for the area. In particular, an attempt will be made to place all known stratiform and/or stratabound mineralization in the area into a volcanological framework for this part of the Cowichan Lake uplift. Studies will also be extended farther to the northwest in the Cowichan Lake uplift, as far as Rheinart Lake, to encompass the other main areas of known VMS mineralization. In parallel with the geological mapping and synthesis work, the authors will also carry out additional litho-geochemical studies and U-Pb dating, as well as focused geological mapping in key areas elsewhere in the Cowichan Lake uplift.

ACKNOWLEDGMENTS

This project is funded by a Geoscience BC grant, as well as a Natural Sciences and Engineering Research Council of Canada (NSERC) Discovery Grant to the junior author. We thank Nick Massey for discussions and insights into the geology of the Sicker Group, and Dick Tosdal for having provided a critical review of this manuscript. We also thank several prospectors, consultants and explorationists working on Vancouver Island, especially Allen Francis, Jacques Houle, Herb McMaster and Sy Tresierra, for sharing their time and knowledge of Sicker geology and mineralization with us.

REFERENCES

Andrew, A. and Godwin, C.I. (1989): Lead- and strontium-isotope geochemistry of Paleozoic Sicker Group and Jurassic Bonanza Group volcanic rocks and Island intrusions, Vancouver Island, British Columbia; *Canadian Journal of Earth Sciences*, volume 26, pages 894–907.

Barrett, T.J. and Sherlock, R.L. (1996): Volcanic stratigraphy, litho-geochemistry and seafloor setting of the H-W massive sulfide deposit, Myra Falls, Vancouver Island, British Columbia; *Exploration and Mining Geology*, volume 5, pages 421–458.

Brandon, M.T., Orchard, M.J., Parrish, R.R., Sutherland Brown, A. and Yorath, C.J. (1986): Fossil ages and isotopic dates from the Paleozoic Sicker Group and associated intrusive rocks, Vancouver Island, British Columbia; in *Current Research, Part A, Geological Survey of Canada*, Paper 86-1A, pages 683–696.

Franklin, J.M., Gibson, H.L., Jonasson, I.R. and Galley, A.G. (2005): Volcanogenic massive sulphide deposits; in *Economic Geology 100th Anniversary Volume*, Hedenquist, J.W., Thompson, J.F.H., Goldfarb, R.J. and Richards, J.P., Editors, *Economic Geology*, pages 523–560.

George Cross News Letter Ltd. (1992): [title unknown]; *George Cross News Letter*, number 188, September 29, 1992.

Godwin, C.I., Gabites, J.E. and Andrew, A. (1988): Leadtable: a galena lead isotope database for the Canadian Cordillera;

BC Ministry of Energy, Mines and Petroleum Resources, Paper 1988-4, 214 pages.

Juras, S.J. (1987): Geology of the polymetallic volcanogenic Buttle Lake Camp, with emphasis on the Price Hillside, central Vancouver Island, British Columbia, Canada; unpublished PhD thesis, *University of British Columbia*, Vancouver, BC, 279 pages.

Katvala, E.C. (2006): Reexamining the stratigraphic and paleontologic definition of Wrangellia; *Geological Society of America*, Abstracts with Program, volume 38, page 24.

Laramide Resources Ltd. (2006): Lara Project: Vancouver Island, British Columbia; *Laramide Resources Ltd.*, project description, URL <http://www.laramide.com/proj_lara.html> [November 2006].

Massey, N.W.D. (1995a): Geology and mineral resources of the Duncan sheet, Vancouver Island, 92B/13; *BC Ministry of Energy, Mines and Petroleum Resources*, Paper 1992-4.

Massey, N.W.D. (1995b): Geology and mineral resources of the Alberni-Nanaimo Lakes sheet, Vancouver Island, 92F/1W, 92F/2E and part of 92F/7E; *BC Ministry of Energy, Mines and Petroleum Resources*, Paper 1992-2.

Massey, N.W.D. (1995c): Geology and mineral resources of the Cowichan Lake sheet, Vancouver Island, 92C/16; *BC Ministry of Energy, Mines and Petroleum Resources*, Paper 1992-3.

Massey, N.W.D. and Friday, S.J. (1987): Geology of the Chemainus River – Duncan area, Vancouver Island (92C/16, 92B/13); *BC Ministry of Energy, Mines and Petroleum Resources*, Paper 1988-1, pages 81–91.

Massey, N.W.D. and Friday, S.J. (1989): Geology of the Alberni-Nanaimo Lakes area, Vancouver Island (92F/1W, 92F/2E and part of 92F/7); *BC Ministry of Energy, Mines and Petroleum Resources*, Open File 1987-2.

MINFILE (2006): MINFILE BC mineral deposits database; *BC Ministry of Energy, Mines and Petroleum Resources*, URL <<http://www.em.gov.bc.ca/Mining/GeolSurv/Minfile/>> [November 2006].

Mortensen, J.K. (2005): Stratigraphic and paleotectonic studies of the Middle Paleozoic Sicker Group and contained VMS occurrences, Vancouver Island, British Columbia; in *Geological Fieldwork 2005*, *BC Ministry of Energy, Mines and Petroleum Resources*, Paper 2006-1, pages 331–336.

Muller, J.E. (1977): Evolution of the Pacific margin, Vancouver Island and adjacent regions; *Canadian Journal of Earth Sciences*, volume 14, pages 2062–2085.

The Northern Miner Ltd. (1969): [title unknown]; *The Northern Miner*, September 25, 1969.

Parrish, R.R. and McNicoll, V.J. (1992): U-Pb age determinations from the southern Vancouver Island area, British Columbia; in *Radiogenic Age and Isotopic Studies: Report 5, Geological Survey of Canada*, Paper 91-2, pages 79–86.

Pearce, J.A., Harris, N.B.W. and Tindle, A.G. (1984): Trace element discrimination diagrams for the tectonic interpretation of granitic rocks; *Journal of Petrology*, volume 25, pages 956–983.

Shervais, J. W. (1982): Ti-V plots and the petrogenesis of modern and ophiolitic lavas; *Earth and Planetary Science Letters*, volume 59, pages 101–118.

Sluggett, C.L. (2003): Uranium-lead age and geochemical constraints on Paleozoic and Early Mesozoic magmatism in Wrangellia Terrane, Saltspring Island, British Columbia; unpublished BSc thesis, *University of British Columbia*, Vancouver, BC, 56 pages.

Sluggett, C.L. and Mortensen, J.K. (2003): U-Pb age and geochemical constraints on the paleotectonic evolution of the Paleozoic Sicker Group on Saltspring Island, southwestern British Columbia; *Geological Association of Canada – Min-*

- erological Association of Canada, Joint Annual Meeting, Program with Abstracts, volume 28.*
- Sun, S.S. and McDonough, W.F. (1989): Chemical and isotopic systematics of oceanic basalts: implications for mantle composition and processes; *in* Magmatism in Ocean Basins, Saunders, A.D. and Norry, M.J., Editors, *Geological Society of London*, pages 313–345.
- Wells, G.S. (1990): Diamond drilling report, Mount Sicker property; *BC Ministry of Energy, Mines and Petroleum Resources*, Assessment Report 19754, 15 pages.
- Winchester, J.A. and Floyd, P.A. (1977): Geochemical discrimination of different magma series and their differentiation products using immobile elements; *Chemical Geology*, volume 20, pages 325–343.
- Yorath, C.J., Sutherland Brown, A. and Massey, N.W.D. (1999): LITHOPROBE, southern Vancouver Island, British Columbia: geology; *Geological Survey of Canada, Bulletin 498*, 145 pages.

Utility of Magnetotelluric Data in Unravelling the Stratigraphic-Structural Framework of the Nechako Basin (NTS 092N; 093C, B, G, H), South-Central British Columbia, from a Re-Analysis of 20-Year-Old Data¹

by J.E. Spratt², J. Craven³, A.G. Jones², F. Ferri and J. Riddell

KEYWORDS: magnetotelluric data, electromagnetic data, Nechako Basin

INTRODUCTION

The Canadian Cordillera, where the Juan de Fuca oceanic plate is currently being subducted beneath the North American continent, is comprised of oceanic and island arc terranes accreted to the western edge of ancestral North America since the Neoproterozoic (Gabrielse and Yorath, 1991; Monger *et al.*, 1972; Monger and Price, 1979; Monger *et al.*, 1982). The Mesozoic Nechako Basin, located within the Intermontane Belt of the Canadian Cordillera, includes overlapping sedimentary sequences deposited in response to this terrane amalgamation. Regional transcurrent faulting and associated east-west extension, beginning in the Late Cretaceous, was accompanied by the extrusion of basaltic lava in Eocene and Miocene times that forms a variably thick sheet, averaging 100 m in thickness and possibly extending up to 1 km thick in isolated places, covering much of the basin. The main geological elements within the southern Nechako area include Miocene flood basalt, Tertiary volcanic and sedimentary rocks, Cretaceous sedimentary rocks and Jurassic sedimentary rocks (Fig 1). Understanding the distribution and structure of these sedimentary rocks at depth is vital for assessing possible resources. An assessment of the hydrocarbon potential based on existing geological information and well data, performed by the Geological Survey of Canada in 1994, suggested that the Nechako Basin may contain as much as a trillion cubic metres of gas and a billion cubic metres of oil (Hannigan *et al.*, 1994). The thick volcanic cover limits the transmission of reflection seismic waves and has made it difficult to determine the physical boundaries of the basin, impeding exploration.

Magnetotelluric (MT) data can distinguish between lithological units, as flood basalt and igneous basement rocks typically have electrical resistivity values of >1000 ohm-m, whereas sedimentary rocks are more conductive with values of 1 to 1000 ohm-m. In the 1980s, the

University of Alberta recorded MT data across the Nechako Basin between 52° and 53° latitude using short period automatic MT system (SPAM) instruments that recorded data in the frequency range of 0.016 to 130 Hz (Fig 1; Majorowicz and Gough, 1991). These data, along with other geophysical information, have been re-examined using modern analysis techniques to assess the usefulness of undertaking MT in the Nechako region and to determine specific data acquisition techniques for future MT surveys that will provide higher-resolution crustal imaging.

Initial analysis of the data collected in the 1980s (Fig 1) revealed structure that was obtained from the phase pseudosections along a profile consisting of 26 sites. Depth estimates were based on a one-dimensional inversion of six of these sites (Majorowicz and Gough, 1991). The data revealed an anomalously conductive upper crust (10–300 ohm-m) in the eastern half of the profile and was attributed to the presence of saline water in pore spaces and fractures. The western half of the profile showed the presence of an eastward-dipping resistive feature. The resistive body has been interpreted to represent granodiorite or other crystalline rocks of the Coast Belt that extends beneath a thin layer of basalt (Gough and Majorowicz, 1992; Majorowicz and Gough, 1994; Jones and Gough, 1995; Ledo and Jones, 2001).

Since the early 1990s, considerable advancements in processing software and techniques, as well as modelling and interpretations packages, have significantly improved our abilities to analyze and interpret MT data. Many of these new techniques, including strike analysis, distortion decompositions and modern 2-D modelling inversions, have been applied to the MT data collected in the 1980s. The results of these analyses and an examination of the resolving power of MT based on borehole logs have improved our understanding of the data limitations and enhanced our knowledge of the resolution of the 2-D models in the area, particularly at crustal depths within the Nechako sedimentary basin. Our studies indicate that future MT studies can reveal substantially more shallow information related to the basin itself.

MAGNETOTELLURIC DATA ANALYSIS

The magnetotelluric (MT) method involves measuring natural variations in the Earth's electric and magnetic fields in order to provide information on the electrical conductivity structure of the subsurface (*e.g.*, Jones, 1992). The measurement of mutually perpendicular components of the electric and magnetic fields at the surface of the Earth allows us to calculate MT response curves, phase lags and ap-

¹Geoscience BC contribution GBC032; Geological Survey of Canada contribution 20060441

²Dublin Institute for Advanced Studies, Dublin, Ireland

³Geological Survey of Canada, Ottawa, ON

This publication is also available, free of charge, as colour digital files in Adobe Acrobat® PDF format from the BC Ministry of Energy, Mines and Petroleum Resources website at http://www.em.gov.bc.ca/Mining/Geolsurv/Publications/catalog/cat_fldwk.htm

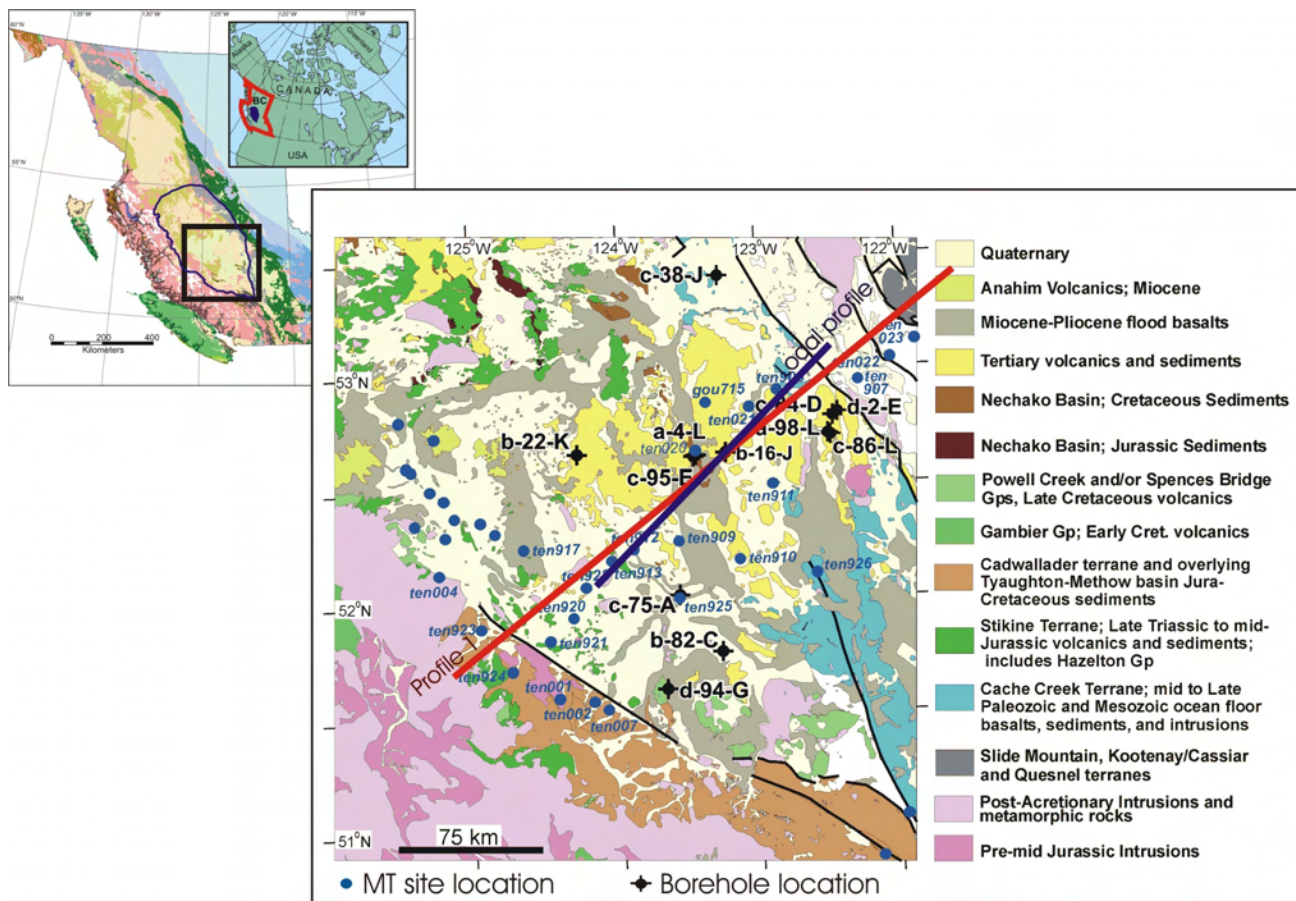


Figure 1. Geology of the Nechako region. The blue dots show the location of magnetotelluric sites recorded in the 1980s. The red and blue lines indicate the orientation of two-dimensional MT models generated for these data. The black dots indicate the location of borehole wells. Modified from Ferri and Riddell (2006).

parent resistivities at various frequencies for each site recorded. Since the depth of investigation of these fields is directly related to the frequency of the measurement and the resistivity of the material, estimates of the phase and apparent resistivities provide a rough guide to the true spatial variation of resistivity beneath each site. For example, if apparent resistivities rise as the frequency drops, that is an indication that the true resistivity is increasing with depth. To arrive at a more realistic depth image of the subsurface resistivity distribution, a model must be generated with synthetic or calculated responses that match the measured data within measurement error. The choice of an algorithm to calculate the synthetic data is strongly dependent on the complexity of the subsurface resistivity distribution. In turn, the complexity of the resistivity distribution is a function of a number of factors, including lithological variations, structural fabrics, rock porosity and salinity of groundwater within pore spaces. It is common in geological situations to have predominantly two-dimensional distributions (*i.e.*, the electrical conductivity is invariant in one direction, the strike direction) and therefore most of the modelling algorithms in use today assume a two-dimensional structure.

Because orthogonal components of the electric and magnetic fields are measured, four response curves can be formulated to define the four elements of the 2 by 2 MT tensor. The tensor contains the information to discern the complexity of the Earth's electrical distribution. In a two-dimensional

Earth, two of the elements are zero and two are not. The two non-zero elements are referred to as the Transverse Electric (TE) and Transverse Magnetic (TM) modes of electromagnetic (EM) field propagation. The four components of the tensor are non-zero in three-dimensional environments. The two modes of electromagnetic field propagation demonstrate equivalent phase lags when the structure is one-dimensional or layered. Mathematical decomposition analysis on the tensor data is typically undertaken to determine if it is appropriate to use two-dimensional modelling algorithms and to assign the preferred geo-electric strike direction for the sites along a profile (Groom and Bailey, 1989). The results of decompositions also provide the TE and TM-mode response curves that most accurately reflect the two-dimensional structure. Two-dimensional modelling of these data will then determine the most reasonable resistivity structure of the subsurface beneath a profile. The analysis begins by re-examining the data, using modern tensor decompositions, to determine if two-dimensional algorithms are appropriate.

Decomposition Analysis

Single-site and multisite Groom-Bailey (1989) decompositions, using the method of McNeice and Jones (2001), were applied to the MT sites along the profile and showed much of the data to be one-dimensional as maxi-

imum phase differences between the two modes were below 10° , particularly at frequencies above 1 s (Fig 2). For the few sites with a strong two-dimensionality, and that exhibited larger phase differences, the preferred geo-electric strike angle was determined to be -35° degrees, *i.e.*, north-northwest, approximately parallel to the geologically mapped strike of the belts. The models generated in the McNeice-Jones decomposition analysis show that the data fit well within 3.5%, equivalent to a 2° error floor in phase. This geo-electric strike angle is consistent throughout the dataset and appears to correlate well with structures revealed in the gravity data (Fig 3) indicating that the strike is likely to be dominated by regional large-scale two-dimensional structures.

Preliminary Borehole Comparisons

Several boreholes have been drilled within the southern Nechako Basin region since the 1960s and resistivity well log data were acquired for some of them (Fig 4). Most

MT sites are too far away from the wells to be useful in comparing measured and modelled responses; however, well log a-4-L is located close to MT site ten020 and can be used for this comparison. Synthetic apparent resistivity and phase curves were calculated using the Geotools MT interpretation package from long normal and deep induction logs measured at well a-4-L (Fig 5a). From these synthetic curves, as well as measured curves from the data recorded at site ten020, one-dimensional models were generated (Fig 5b). The 1-D models for both sets of curves, synthetic (from the borehole data) and measured (at the MT site), are generally quite similar with just two major differences: 1) the starting resistivity value is nearly one order of magnitude higher in the MT data compared to the synthetic well data; and 2) the different resistivity layers appear to be downshifted, that is, that the boundaries between the layers occur at deeper depths in the 1-D model for the MT site. Contrary to the assumptions made by Majorowicz and Gough (1991) — that there was little static-shift effect on the data — these differences indicate that there is most

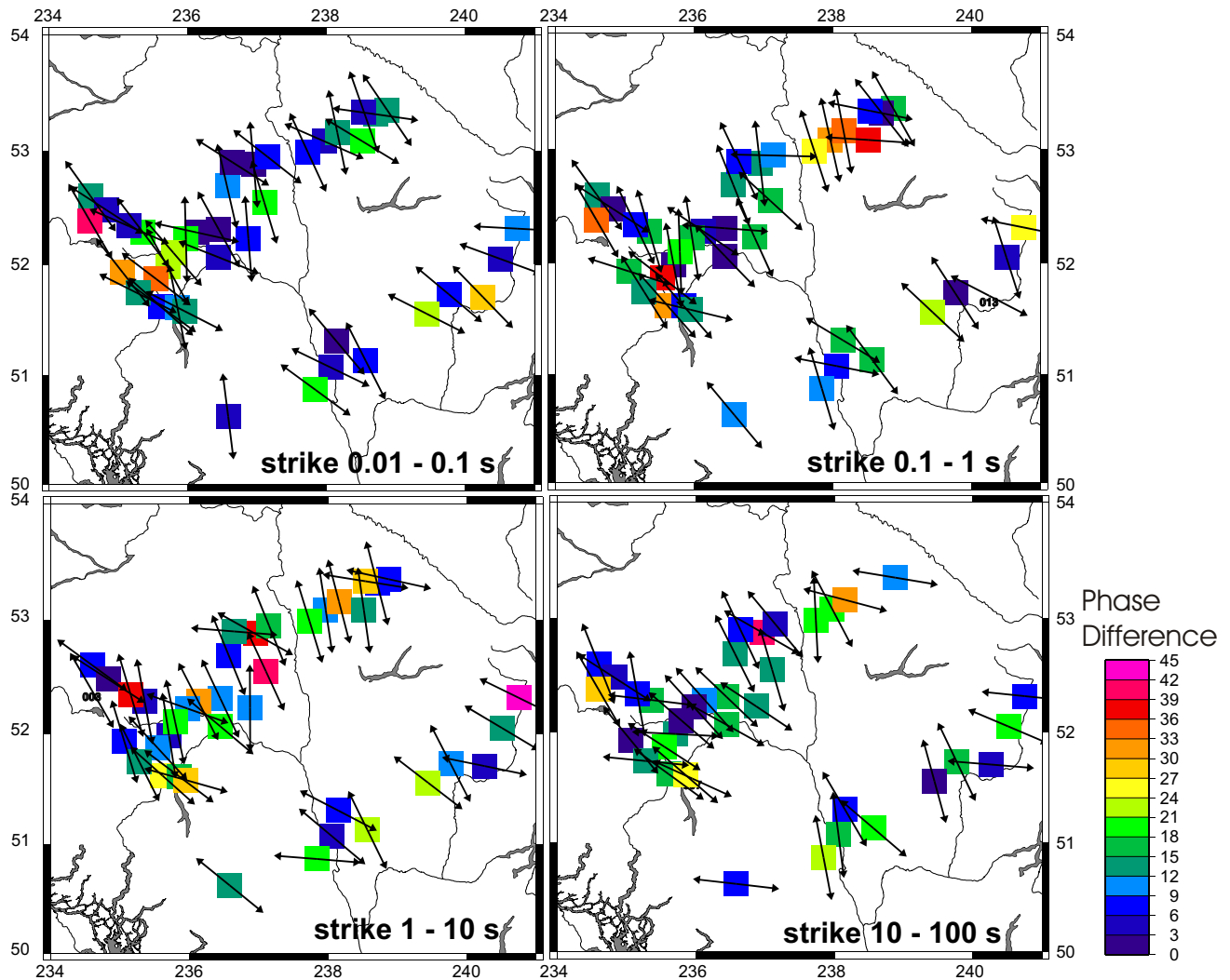


Figure 2. Maps showing the geo-electric strike directions determined from Groom and Bailey (1989) galvanic decomposition models for each site at four different period bands between 0.01 and 100 s. The colours represent the maximum phase difference between the Transverse Electric (TE) and Transverse Magnetic (TM) modes. Each band samples progressively deeper into the crust and represents the best-fit two-dimensional strike of the electrical units in the subsurface. Small phase differences are indicative of one-dimensional or layered geometries in the subsurface.

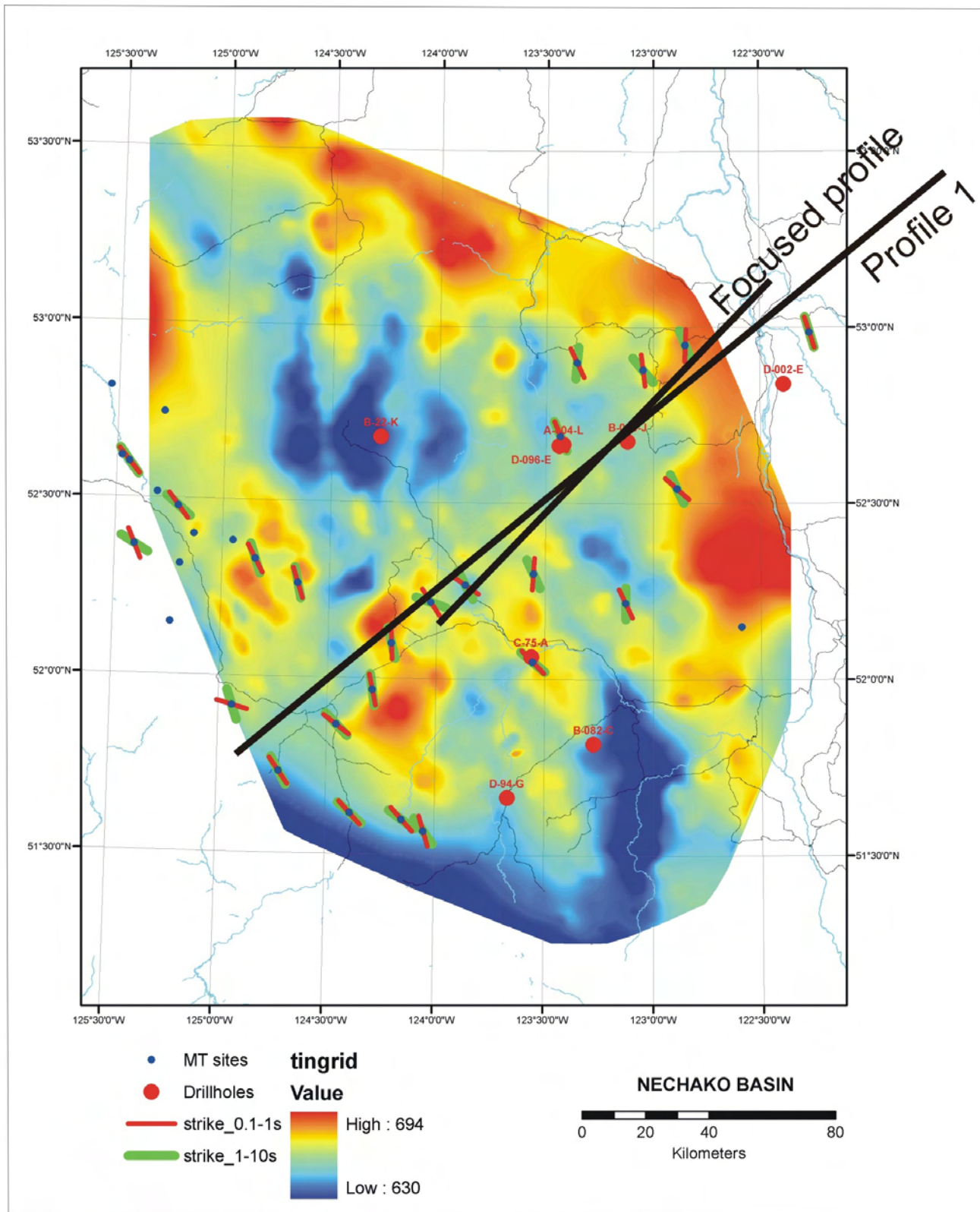


Figure 3. Bouguer gravity for the Nechako region and strike directions obtained using multifrequency McNeice-Jones decompositions for period bands 0.1 to 1 s and 1 to 10 s. The black lines mark the profile traces of the MT models. *Modified from Ferri and Riddell (2006).*

likely a significant effect of static shift on the measured MT data and these effects need to be accounted for in further models. The similarities suggest that the MT data is capable of imaging the shallow conductivity layers observed in the well. The differences indicate that there is a need for additional measures to be taken in future MT data acquisition in this region in order to get an accurate depth estimate for these layers. For example, the model obtained from the data (Fig 5b) is entirely featureless at depths shallower than 100 m, suggesting that the frequency bandwidth utilized by the SPAM system (up to 130 Hz) is insufficient to explore at shallow depths. High-frequency audio-magnetotelluric (AMT) soundings up to 10 000 Hz would help to constrain the resistivity structure at shallow depths and other methods, such as time-domain electromagnetic, borehole resistivity logs or electrical rock property measurements performed in a laboratory, could be used to correct for this static-shift effect.

DATA MODELLING

Two-dimensional models along Profile 1 (Fig 1) were determined for the decomposition-corrected MT responses at a geo-electric strike angle of -35° of both the Transverse Magnetic (TM) and Transverse Electric (TE) modes, as well as the TE mode only. Since the nature of MT models is non-unique, careful steps need to be undertaken to ensure that the model generated is the best representation of the structure of the Earth. A trade-off is required between the smoothness of the model between cells, the tau value (τ), and the fit of the model to the data, the RMS (root mean squared) misfit value. Inverse modelling using Rodi and Mackie's (2001) code, as implemented in Geosystem's WinGlink software package, was run for 100 iterations for models with varying smoothness parameters (τ). Higher values of τ increase the smoothness and therefore the fidelity of the model, but degrade the fit of the model as represented by the RMS. From the L-curve trading-off fit (RMS) against τ , the best trade-off was determined to be at $\tau = 3$ (Fig 6). In order to account for static-shift effects, the data were inverted to preferentially fit the phase data, with high error floors (25%) set for the apparent resistivities. The data were also inverted with error floors for both the phase and apparent resistivities equivalent to 2° (as determined acceptable from the distortion analysis) and after 100 iterations, a static-shift correction was applied to the model parameters. The structures of the different models and the associated conductivity values were very similar and the final model generated achieves an RMS misfit of 2.4. Pseudosections allow a visual comparison between the calculated forward response of the apparent resistivities and phases, and the original data (Fig 7). These show that there is a reasonable fit at most sites along the profile, particularly at shallow depths.

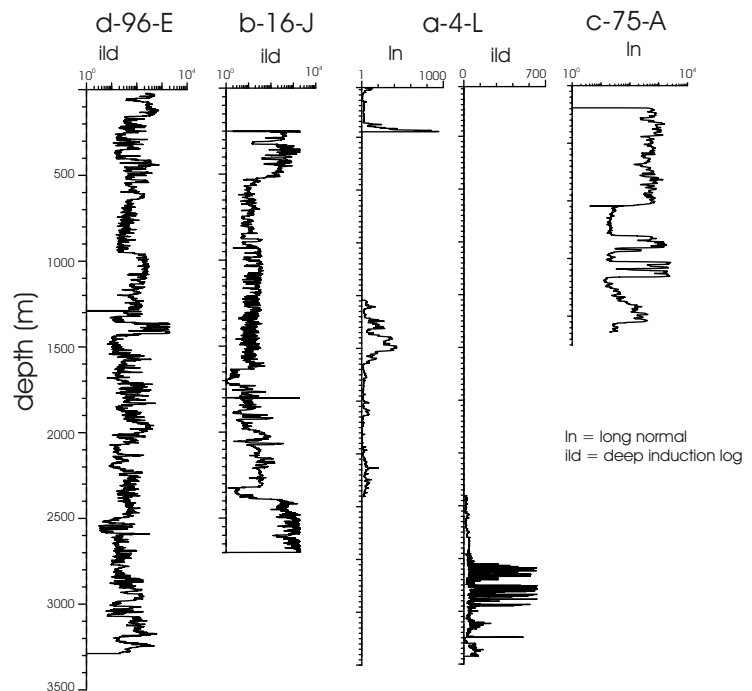


Figure 4. Resistivity data measured at four of the wells in the southern Nechako region.

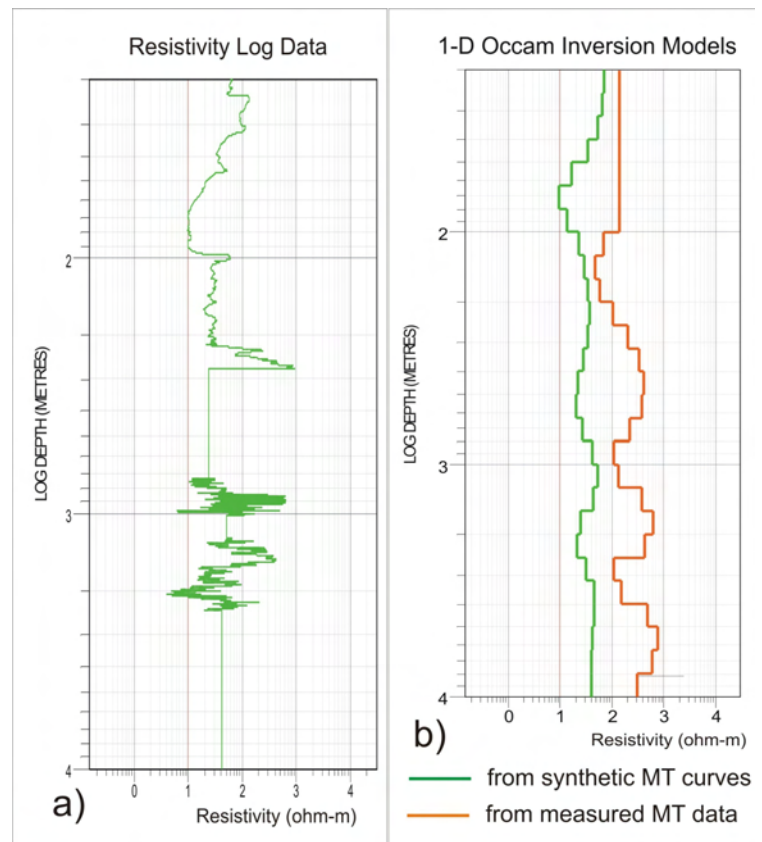


Figure 5. a) Resistivity log data recorded at well a-4-L re-plotted in log domain; b) one-dimensional models of synthetic data from borehole log a-4-L and magnetotelluric (MT) site ten020 at the same location.

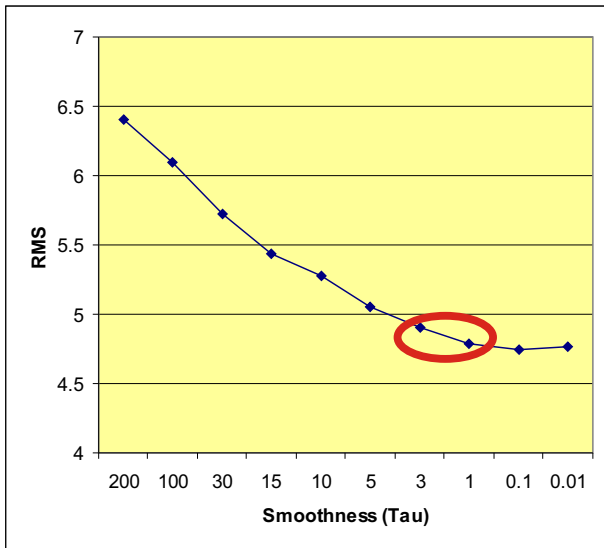


Figure 6. Trade-off plot shows the relationship between the root mean squared (RMS) misfit value and the smoothness modelling parameter, tau (τ). The red circle shows the region where the model has the highest τ (smoothest model) and the best fit (smallest RMS).

Main Model Features

The model shows distinct variations in the conductivity structure along the profile and reveals a moderately conductive layer (40 ohm-m) that varies in depth up to ~5 km (Fig 8). There is a good correlation between the gravity lows, which are assumed to represent sedimentary sequences, and the high conductivity layer (<100 ohm-m) where it thickens between sites 922 and 908 in the 2-D model along Profile 1 (Fig 8). Where the MT model shows resistive structure near the surface at both ends of the profile, there are gravity highs that have been interpreted to represent volcanic basement. This indicates consistency between the two datasets and suggests that the MT data are capable of distinguishing the different lithological units at depth and defining the boundary of the Nechako Basin.

Model Focused on Shallow Basin Structure

A new model was generated for the eastern edge of the Nechako Basin using the high-frequency data only (1–130 Hz) in order to determine how sensitive the data are to the shallow structures in this region. This model shows significant conductivity changes at shallow depths along the profile (Fig 9). A comparison of calculated modelled responses to the observed data is shown in Figure 10. To the

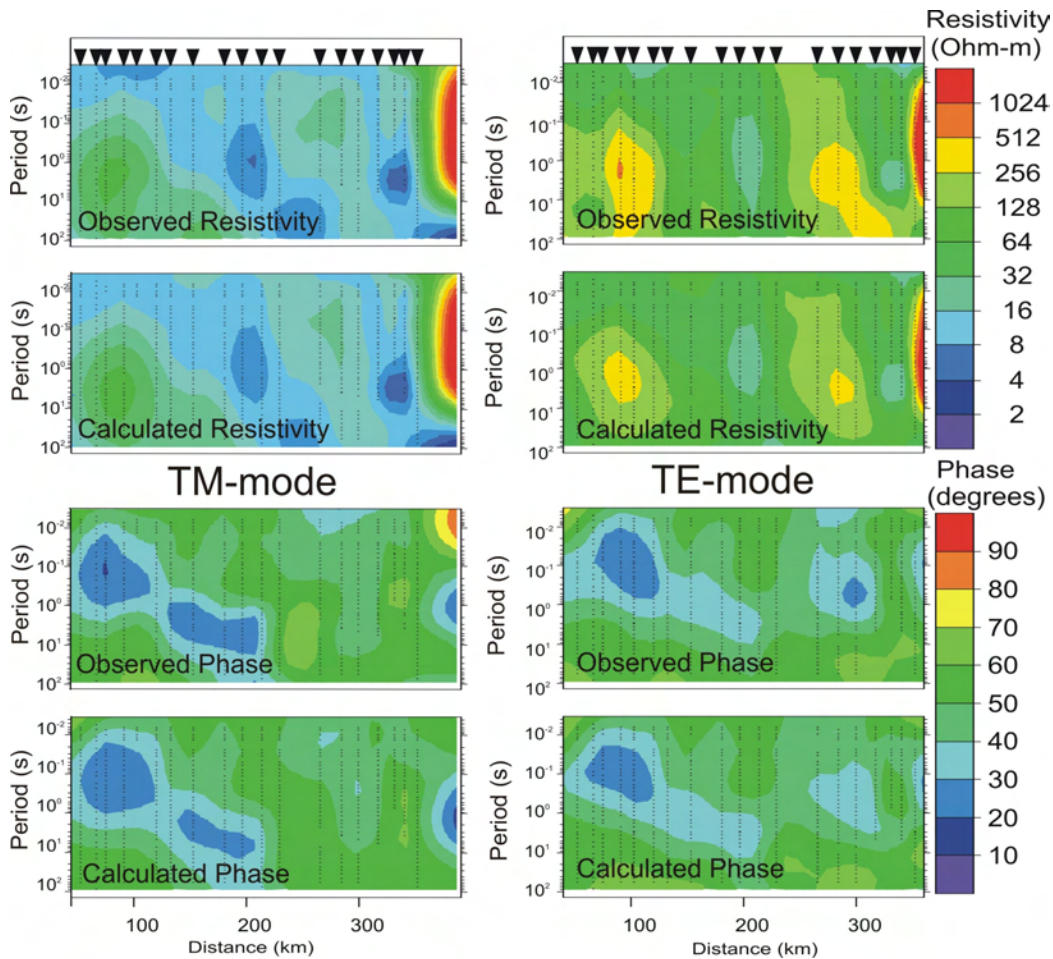


Figure 7. Plots of the measured data and the model forward responses of the apparent resistivities and phases for both Transverse Magnetic (TM) and Transverse Electric (TE) modes of the two-dimensional model shown in Figure 8.

southwest, there is a conductive (~100 ohm-m) region overlying resistive (>1000 ohm-m) material; Majorowicz and Gough (1991) interpreted this to represent sedimentary rocks in Nechako Basin overlying granitic intrusions. To the northeast, the conductive region becomes resistive

across the boundary between the Nechako Basin and the Cache Creek Terrane (Fig 1, 9). The model also shows two very conductive features (<10 ohm-m) that correlate with the surface-mapped Tertiary volcanic and sedimentary rocks (Fig 1).

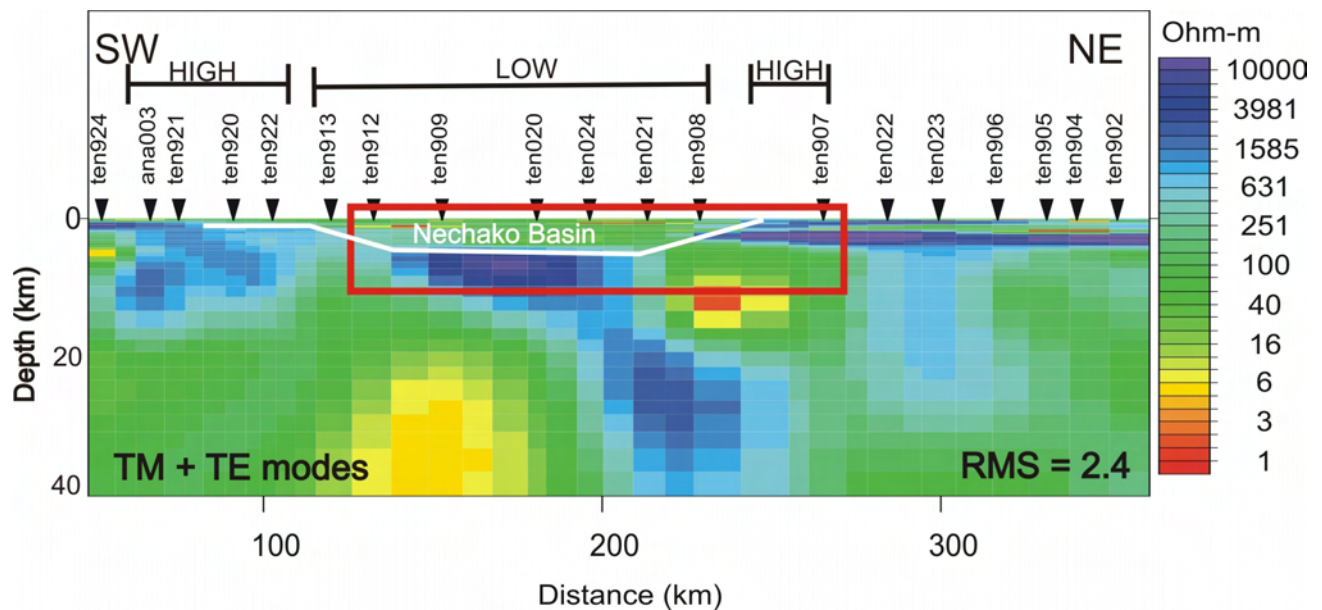


Figure 8. Two-dimensional resistivity model obtained from MT data across the Nechako Basin. The model was generated using both Transverse Electric (TE) and Transverse Magnetic (TM) mode distortion-decomposed apparent resistivity and phase data, and a root mean squared (RMS) misfit of 2.4 was achieved. The red box indicates the region of localized modelling shown in Figure 9. The black bars above the model illustrate the regions of high and low gravity data, as seen in Figure 3.

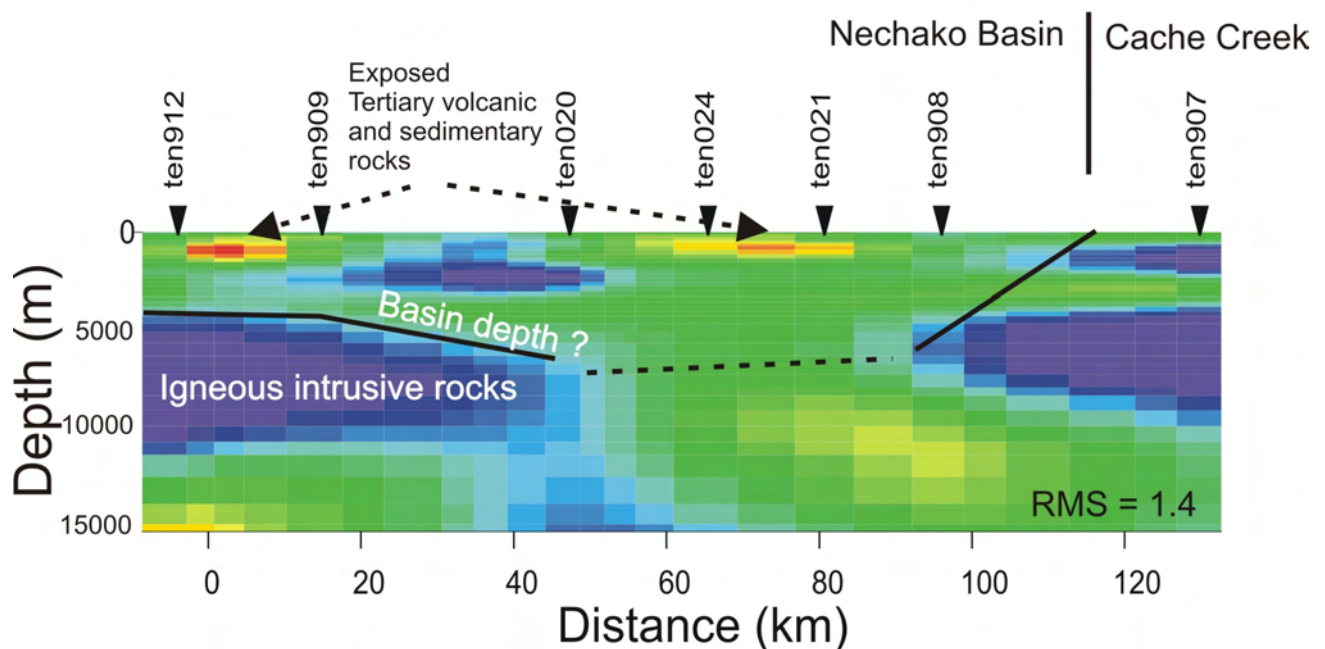


Figure 9. A two-dimensional model focusing on the shallow structures crossing the eastern boundary of the Nechako Basin. The model was generated using high-frequency data (1–130 Hz) for both the Transverse Electric (TE) and Transverse Magnetic (TM) modes and a root mean squared (RMS) misfit of 1.4 was achieved.

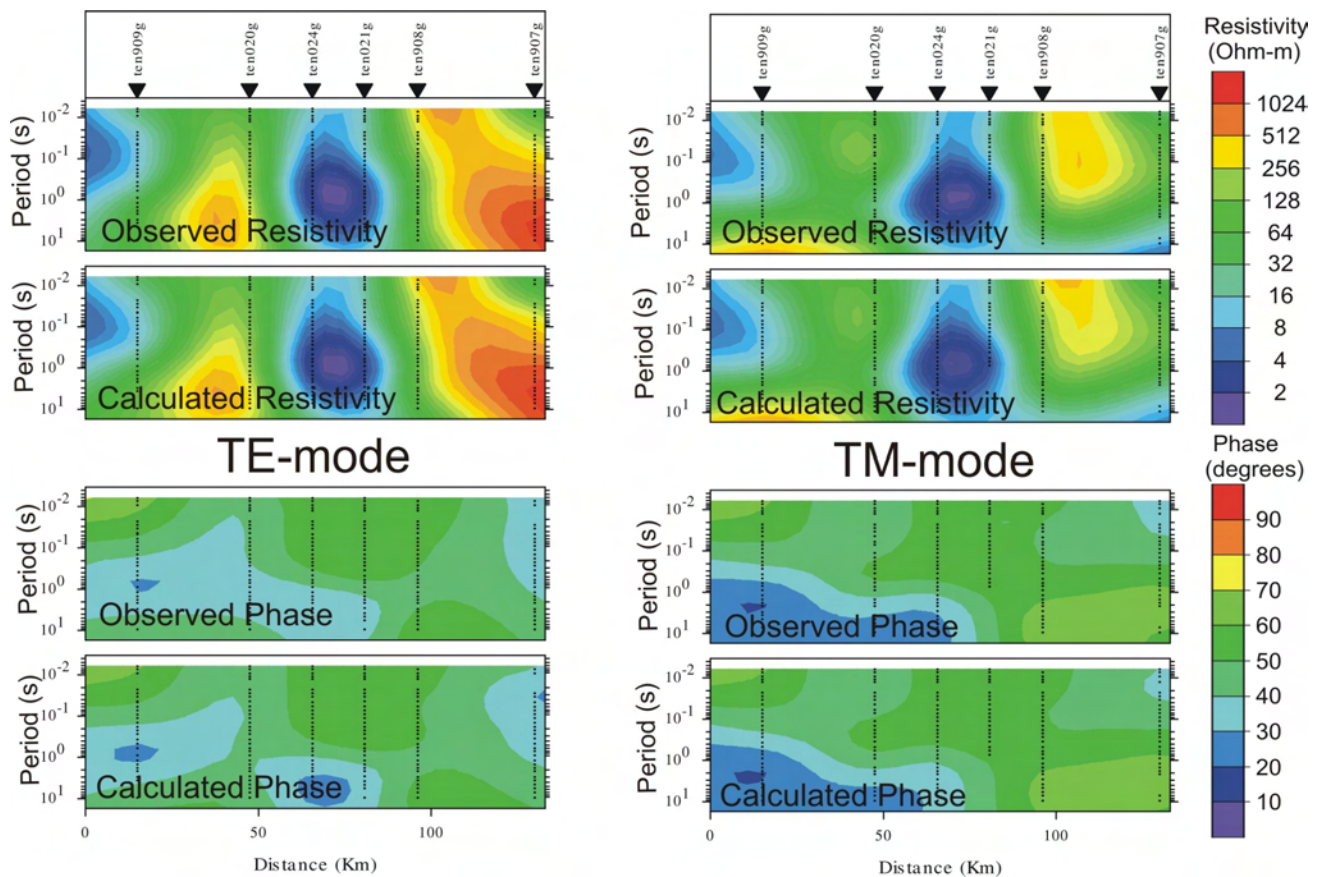


Figure 10. Plots of the observed data and the data calculated from the model forward responses of the apparent resistivities and phases for both Transverse Magnetic (TM) and Transverse Electric (TE) modes of the two-dimensional model shown in Figure 9.

Hypothesis testing of these shallow conductors was undertaken by replacing the high conductivity values with a higher resistivity value (~200 ohm-m, similar to the surrounding values) and running a forward response. The RMS values increased dramatically (from 1.4 to 8.2) and a comparison of the calculated versus measured pseudosections of both the TM and TE modes, in both the apparent resistivities and phases, showed distinct differences. This indicates that the shallow conductive structures are required by the measured data and are not artifacts of the inversion algorithm and that, although currently sparse, the MT data is capable of discerning shallow structure within the Nechako basin. The SPAM MT systems used for acquisition of the measured data recorded a maximum frequency of 130 Hz (0.007 s). Modern audio-magnetotelluric (AMT) instruments can reliably acquire data to 10 000 Hz (0.0001 s). With a dense site spacing, additional AMT and broadband MT data acquisition would be useful in determining the shallow structure within the Nechako Basin and would allow the basin boundaries to be clearly identified.

CONCLUSIONS

Magnetotelluric data collected two decades ago are capable of penetrating the Cenozoic volcanic rocks and imaging the shallow features of the Nechako Basin. The two-dimensional models show a good correlation between along-strike conductivity variations and mapped geological units as well as observed gravity anomalies. A comparison with

measured borehole resistivities allows us to quantify static-shift effects and indicates the need to account for these effects in the interpretation of the existing data. Additional MT data acquisition using modern high frequency (AMT) and broadband instrumentation would be a highly cost-effective method to determine the thicknesses and boundaries of the Nechako basin. This information is key for advancing our understanding of the region's resource potential.

ACKNOWLEDGMENTS

Helpful reviews by R. Stevens and C. Lowe are gratefully acknowledged. Borehole data was provided by Jonathon Mwenifumbo of the Geological Survey of Canada. The project has received financial support from Geoscience BC and the BC Ministry of Energy, Mines and Petroleum Resources.

REFERENCES

- Ferri, F. and Riddell, J. (2006): The Nechako Basin Project: new insights from the southern Nechako Basin; *in* Summary of Activities 2006, *BC Ministry of Energy, Mines and Petroleum Resources*, pages 89–124.
- Gabrielse, J. and Yorath, C.J., Editors (1991): Geology of the Cordilleran Orogen in Canada; *in* Geology of Canada, number 4, *Geological Survey of Canada* and *in* Geology of North America, volume G-2, *Geological Society of America*.

- Gough, D.I. and Majorowicz, J.A. (1992): Magnetotelluric soundings, structure and fluids in the southern Canadian Cordillera; *Canadian Journal of Earth Sciences*, volume 29, pages 609–620.
- Groom, R.W. and Bailey, R.C. (1989): Decomposition of magnetotelluric impedance tensors in the presence of local three-dimensional galvanic distortion; *Journal of Geophysical Research*, volume 94, pages 1913–1925.
- Hannigan, P., Lee, P.J., Osadetz, K.G., Dietrich, J.R. and Olsen-Heise, K. (1994): Oil and gas resource potential of the Nechako-Chilcotin area of British Columbia, *BC Ministry of Energy, Mines and Petroleum Resources*, Geofile 2001-6, 38 pages.
- Jones, A.G. (1992): Electrical conductivity of the continental lower crust; in *Continental Lower Crust*, Fountain, D.M., Arculus, R.J. and Kay, R.W., Editors, *Elsevier*, pages 81–143.
- Jones, A.G. and Gough, D.I. (1995): Electromagnetic images of crustal structures in southern and central Canadian Cordillera; *Canadian Journal of Earth Sciences*, volume 32, pages 1541–1563.
- McNeice, G. and Jones, A.G. (2001): Multi-site, multi-frequency tensor decomposition of magnetotelluric data; *Geophysics*, volume 66, pages 158–173.
- Ledo, J. and Jones, A.G. (2001): Regional electrical resistivity structure of the southern Canadian Cordillera and its physical interpretation; *Journal of Geophysical Research*, volume 106, pages 30755–30769.
- Majorowicz, J.A. and Gough, D.I. (1991): Crustal structures from MT soundings in the Canadian Cordillera; *Earth and Planetary Science Letters*, volume 102, pages 444–454.
- Majorowicz, J.A. and Gough, D.I. (1994): A model of conductive structure in the Canadian Cordillera; *Geophysical Journal International*, volume 117, pages 301–312.
- Monger, J.W.H. and Price, R.A. (1979): Geodynamic evolution of the Canadian Cordillera — progress and problems; *Canadian Journal of Earth Sciences*, volume 16, pages 770–791.
- Monger, J.W.H., Price, R.A. and Tempelman-Kluit, D. (1982): Tectonic accretion of two major metamorphic and plutonic belts in the Canadian Cordillera; *Geology*, volume 10, pages 70–75.
- Monger, J.W.H., Souther, J.G. and Gabrielse, H. (1972): Evolution of the Canadian Cordillera — a plate tectonic model; *American Journal of Science*, volume 272, pages 557–602.
- Rodi, W. and Mackie, R.L. (2001): Nonlinear conjugate gradients algorithm for 2-D magnetotelluric inversion; *Geophysics*, volume 66, pages 174–187.

